DE GRUYTER

Astrid Sigel, Helmut Sigel, Eva Freisinger, Roland K. O. Sigel (Eds.)

METALLO-DRUGS: DEVELOPMENT AND ACTION OF ANTICANCER AGENTS

METAL IONS IN LIFE SCIENCES 18

Astrid Sigel, Helmut Sigel, Eva Freisinger, Roland K.O. Sigel
Metal Ions in Life Sciences 18

Metal Ions in Life Sciences

Edited by
Astrid Sigel, Helmut Sigel, Eva Freisinger
and Roland K.O. Sigel

Volume 18

Metallo-Drugs: Development and Action of Anticancer Agents

DE GRUYTER

Editors

Astrid Sigel and Helmut Sigel
Department of Chemistry
Inorganic Chemistry
University of Basel
Spitalstrasse 51
CH-4056 Basel
Switzerland
<astrid.sigel@unibas.ch>
<helmut.sigel@unibas.ch>

Eva Freisinger and Roland K. O. Sigel
Department of Chemistry
University of Zürich
Winterthurerstrasse 190
CH-8057 Zürich
Switzerland
<freisinger@chem.uzh.ch>
<roland.sigel@chem.uzh.ch>

ISBN 978-3-11-046984-4
e-ISBN (PDF) 978-3-11-047073-4
e-ISBN (EPUB) 978-3-11-046990-5
Set-ISBN 978-3-11-047074-1
ISSN 1559-0836
e-ISSN 1868-0402
DOI: 10.1515/9783110470734

Library of Congress Cataloging-in-Publication Data
A CIP catalog record for this book has been applied for at the Library of Congress.

Bibliographic information published by the Deutsche Nationalbibliothek
The Deutsche Nationalbibliothek lists this publication in the Deutsche Nationalbibliografie; detailed bibliographic data are available on the Internet at http://dnb.dnb.de.

Cover illustration: The figure on the dust cover shows *cis*-$[(NH_3)_2Pt(Cl)]^+$ coordinated to the imidazole residue of histidine-105 from human serum albumin. This figure is an expanded version of Figure 3(A) in Chapter 13; it was prepared by Christian Hartinger and coworkers based on PDB ID 4S1Y and modified for the cover by Fabio Steffen and Roland Sigel from the University of Zürich.

Typesetting: Meta Systems Publishing & Printservices GmbH, Wustermark, Germany
Printing and binding: CPI books GmbH, Leck
♾ Printed on acid-free paper
Printed in Germany

For further volumes: www.mils-WdG.com
www.degruyter.com

About the Editors

Astrid Sigel (University of Basel) has studied languages; she was an editor of the *Metal Ions in Biological Systems* series (until Volume 44) and also of the "Handbook on Toxicity of Inorganic Compounds" (1988), the "Handbook on Metals in Clinical and Analytical Chemistry" (1994; both with H. G. Seiler), and on the "Handbook on Metalloproteins" (2001; with Ivano Bertini). She is also an editor of the *MILS* series from Volume 1 on and she co-authored about 40 papers on topics in Bioinorganic Chemistry.

Helmut Sigel is Emeritus Professor (2003) of Inorganic Chemistry at the University of Basel, Switzerland, and a previous editor of the *MIBS* series until Volume 44. He served on various editorial and advisory boards, published over 350 articles on metal ion complexes of nucleotides, coenzymes, and other ligands of biological relevance, and lectured worldwide. He was named Protagonist in Chemistry (2002) by *ICA* (issue 339); among further honors are the P. Ray Award (Indian Chemical Society, of which he is also an Honorary Fellow), the Alfred Werner Prize (Swiss Chemical Society), a Doctor of Science honoris causa degree (Kalyani University, India), appointments as Visiting Professor (e.g., Austria, China, Japan, Kuwait, UK) and Endowed Lectureships; he is also a Honorary Member of SBIC (Society of Biological Inorganic Chemistry).

After participating in the edition of three Handbooks (see above at A.S.) and 44 volumes in the previous series *Metal Ions in Biological Systems* as well as in the first 18 volumes (including this one) of our new series *Metal Ions in Life Sciences*, it is time to step down as an Editor. However, I am very pleased to hand over the burden to Eva Freisinger, my daughter-in-law. I am very fortunate that a most competent bioinorganic colleague is replacing myself. Hence, I welcome Eva as an Editor of the *MILS* series and wish her much success and satisfaction in her new editorial job.

H.S.

Eva Freisinger is an independent group leader at the Department of Chemistry at the University of Zürich, Switzerland. She obtained her doctoral degree (2000) from the University of Dortmund, Germany, working with Bernhard Lippert. Thereafter she spent three years as a postdoc at SUNY Stony Brook, USA, with Caroline Kisker. Since 2003 she performs independent research at the University

of Zürich where she held a Förderungsprofessur of the Swiss National Science Foundation from 2008 to 2014. In 2014 she received her *Habilitation* in Bioinorganic Chemistry. Her research is focused on the study of plant metallothioneins and the sequence-specific modification of nucleic acids. She serves on a number of Advisory Boards for international conference series; since 2014 she is the Secretary of the European Bioinorganic Chemistry Conferences (EuroBICs). She is one of the Editors of the Bioinorganic Chemistry section of the *International Journal of Molecular Sciences* (IJMS) and now also of the *MILS* series from Volumes 18 on.

Roland K. O. Sigel is Full Professor (2016) of Chemistry at the University of Zürich, Switzerland. In the same year he became Vice Dean of Studies (BSc/MSc) and in 2017 Dean of the Faculty of Science. From 2003 to 2008 he was endowed with a Förderungsprofessur of the Swiss National Science Foundation and he is the recipient of an ERC Starting Grant 2010. He received his doctoral degree summa cum laude (1999) from the University of Dortmund, Germany, working with Bernhard Lippert. Thereafter he spent nearly three years at Columbia University, New York, USA, with Anna Marie Pyle (now Yale University). During the six years abroad he received several prestigious fellowships from various sources, and he was awarded the EuroBIC Medal in 2008 and the Alfred Werner Prize (SCS) in 2009. His research focuses on the structural and functional role of metal ions in ribozymes, especially group II introns, regulatory RNAs, and on related topics. He was also an editor of Volumes 43 and 44 of the *MIBS* series and of the *MILS* series from Volume 1 on.

Historical Development and Perspectives of the Series *Metal Ions in Life Sciences*[*]

It is an old wisdom that metals are indispensable for life. Indeed, several of them, like sodium, potassium, and calcium, are easily discovered in living matter. However, the role of metals and their impact on life remained largely hidden until inorganic chemistry and coordination chemistry experienced a pronounced revival in the 1950s. The experimental and theoretical tools created in this period and their application to biochemical problems led to the development of the field or discipline now known as *Bioinorganic Chemistry*, *Inorganic Biochemistry*, or more recently also often addressed as *Biological Inorganic Chemistry.*

By 1970 *Bioinorganic Chemistry* was established and further promoted by the book series *Metal Ions in Biological Systems* founded in 1973 (edited by H. S., who was soon joined by A. S.) and published by Marcel Dekker, Inc., New York, for more than 30 years. After this company ceased to be a family endeavor and its acquisition by another company, we decided, after having edited 44 volumes of the *MIBS* series (the last two together with R. K. O. S.) to launch a new and broader minded series to cover today's needs in the *Life Sciences.* Therefore, the Sigels new series is entitled

Metal Ions in Life Sciences.

After publication of 16 volumes (since 2006) with various publishers during the past 10 years, we are happy to join forces (from Volume 17 on) in this still growing endeavor with Walter de Gruyter GmbH, Berlin, Germany, a most experienced Publisher in the *Sciences.*

The development of *Biological Inorganic Chemistry* during the past 40 years was and still is driven by several factors; among these are (i) attempts to reveal the interplay between metal ions and hormones or vitamins, etc., (ii) efforts regarding the understanding of accumulation, transport, metabolism and toxicity of metal ions, (iii) the development and application of metal-based drugs,

---

[*] Reproduced with some alterations by permission of John Wiley & Sons, Ltd., Chichester, UK (copyright 2006) from pages v and vi of Volume 1 of the series *Metal Ions in Life Sciences* (MILS-1).

(iv) biomimetic syntheses with the aim to understand biological processes as well as to create efficient catalysts, (v) the determination of high-resolution structures of proteins, nucleic acids, and other biomolecules, (vi) the utilization of powerful spectroscopic tools allowing studies of structures and dynamics, and (vii), more recently, the widespread use of macromolecular engineering to create new biologically relevant structures at will. All this and more is reflected in the volumes of the series *Metal Ions in Life Sciences.*

The importance of metal ions to the vital functions of living organisms, hence, to their health and well-being, is nowadays well accepted. However, in spite of all the progress made, we are still only at the brink of understanding these processes. Therefore, the series *Metal Ions in Life Sciences* links coordination chemistry and biochemistry in their widest sense. Despite the evident expectation that a great deal of future outstanding discoveries will be made in the interdisciplinary areas of science, there are still "language" barriers between the historically separate spheres of chemistry, biology, medicine, and physics. Thus, it is one of the aims of this series to catalyze mutual "understanding".

It is our hope that *Metal Ions in Life Sciences* continues to prove a stimulus for new activities in the fascinating "field" of *Biological Inorganic Chemistry.* If so, it will well serve its purpose and be a rewarding result for the efforts spent by the authors.

Astrid Sigel and Helmut Sigel
Department of Chemistry, Inorganic Chemistry
University of Basel, CH-4056 Basel, Switzerland

Roland K. O. Sigel
Department of Chemistry
University of Zürich, CH-8057 Zürich, Switzerland

October 2005
and September 2016

Preface to Volume 18

Metallo-Drugs: Development and Action of Anticancer Agents

Platinum-based anticancer drugs are among the most widely used of all chemotherapeutic cancer treatments. Three FDA-approved platinum(II) anticancer drugs, i.e., cisplatin, carboplatin, and oxaliplatin, have been in the clinic for many years to treat testicular, ovarian, cervical, head and neck, colorectal, and other cancers. These breakthroughs are the result of the serendipitous discovery of the anticancer activity of cisplatin, *cis*-diamminodichloroplatinum(II), more than 50 years ago. Meanwhile an understanding of its medicinal properties has developed, allowing for improved treatment regimens reducing somewhat the side effects, including nephrotoxicity, myelosuppression, peripheral neuropathy, ototoxicity, and nausea. All this and more is covered in *Chapter 1* which focuses on *Cisplatin and Oxaliplatin*.

Polynuclear Platinum Complexes (PPCs) were developed to combat cisplatin-resistant cancers. PPCs represent a discrete structural class of DNA-binding agents: The use of at least two platinum-coordinating units makes multifunctional binding modes possible. Proof of principle of this hypothesis was achieved by the advance to the clinic (Phase II trials) of triplatin, a charged trinuclear, bifunctional, DNA-binding agent with two terminal arms, $–NH_2$-Pt$(NH_3)_2$Cl. *Chapter 2* emphasizes the structural diversity and reactivity of PPCs.

Another approach to avoid resistance and side effects centers on octahedral and kinetically inert *Pt(IV) Prodrugs* (*Chapter 3*) They can be reduced in cancer cells to active square-planar Pt(II) complexes, e.g., by intracellular reducing agents such as glutathione or by photoexcitation. The additional axial ligands in Pt(IV) complexes, which are released on reduction, allow bioactive molecules to be delivered, which can act synergistically with the Pt(II) species in killing the cancer cells. Pt(IV) complexes are likely to be stable under the highly acidic conditions in the stomach and therefore suitable for oral administration.

Metal Ions in Life Sciences, Volume 18 Edited by Astrid Sigel, Helmut Sigel, Eva Freisinger, and Roland K. O. Sigel

https://doi.org/10.1515/9783110470734-202

Chapter 4 introduces the concept of *Metalloglycomics*, that is, the interaction of metal ions with biologically relevant oligosaccharides, in particular glycosaminoglycans (GAGs) such as heparin and heparan sulfate. Their structure and conformation and the role of various metal ions during their interaction with proteins and enzymes are reviewed. Cleavage of heparan sulfate proteoglycans by heparanase modulates tumor-related events. Heparan sulfate is identified as a ligand receptor for polynuclear platinum complexes defining a new mechanism of cellular accumulation.

The structure of the ruthenium(III) drug candidates KP1019 and NAMI-A is deceptively similar, i.e., *trans*-$RuCl_4(X,Y)^-$, as discussed in *Chapter 5*, yet, surprisingly they have markedly different macroscopic pharmacological activities: KP1019 behaves rather as a classical antitumor compound (with the advantage of being active also against platinum(II)-resistant tumors), whereas NAMI-A has a more unconventional activity that affects metastases and not the primary tumor. The complicated *in vivo* chemistry (no clearly identified target) is affecting negatively their further clinical development after initial progress (Phase II).

Organometallic ruthenium-arene complexes (*Chapter 6*) have risen to prominence as a pharmacophore due to the success of other ruthenium drug candidates in clinical trials. Ru(arene) complexes are almost exclusively octahedral, low-spin d^6 Ru(II) species. Mononuclear Ru(arene) complexes have therapeutic properties against cancer *in vitro* and *in vivo*, therefore researchers began exploiting these potentially therapeutic entities for higher-order multinuclear Ru(arene) complexes.

The *Medicinal Chemistry of Gold Anticancer Metallodrugs* is described in *Chapter 7*. Since ancient times gold and its complexes have been used as therapeutics against different diseases. In modern medicine gold drugs are applied for the treatment of rheumatoid arthritis, but recently they also serve as antiparasitic, antibacterial, and antiviral agents. The exciting findings on gold(I) and gold(III) complexes as antitumor agents are summarized and warrant the discussion of the relevant aspects of their modes of action.

Titanium(IV) complexes represent attractive alternatives to Pt(II)-based anticancer drugs because of their low toxicity (*Chapter 8*). The pioneering compounds titanocene dichloride and budotitane were the first to enter clinical trials. Yet, despite the high efficacy and low toxicity observed *in vivo*, they failed, mainly because of formulation complications, their rapid hydrolysis, the difficulty of isolating and identifying the particular active species and the precise cellular target. The following generation of phenolato-based complexes came three decades later and exhibited high activity and improved stability, with no signs of toxicity to the treated animals. The mechanistic insights gained so far include the interaction with DNA and the induction of apoptosis; hence, these Ti(IV) complexes are highly promising for future clinical development.

Vanadium compounds have been known for long to have beneficial therapeutic properties (*Chapter 9*), but it was not until 1965 when it was discovered that these effects could be extended to treating cancer due to the similarities in some metabolic pathways that are utilized by both diabetes and cancer. The links between these diseases emerged through epidemiological investigations which

suggest that the incidence of pancreatic, liver, and endometrial cancers are associated with diabetes though the links are not yet fully understood.

The antineoplastic activity of gallium nitrate, $Ga(NO_3)_2$, was recognized over three decades ago and several clinical trials (Phase I and II) have confirmed this in patients with lymphoma and bladder cancer (*Chapter 10*). Ga(III) shares chemical characteristics with Fe(III) and these enable it to interact with iron-binding proteins and to disrupt iron-dependent tumor cell growth. Beyond the first generation of gallium(III) salts (parenterally administered) a new generation of complexes such as tris(8-quinolinato)gallium(III) with oral bioavailability, has emerged and is now evaluated in the clinic while other ligands for Ga(III) are in preclinical development.

Non-covalent Metallo-Drugs: Using Shape to Target DNA and RNA Junctions and Other Nucleic Acid Structures is the title of *Chapter 11*. This *shape specificity* contrasts with the most effective class of anticancer drugs in clinical use, the Pt(II) agents, which act by binding to duplex B-DNA in a *sequence-specific* manner, but duplex B-DNA is not DNA in its active form. The chapter describes how large cationic metallo-supramolecular structures can be used to bind to less common, yet active, nucleic acid structures like Y-shaped forks and 4-way junctions, and thus, possibly display high cytotoxicity and inhibit cancer.

Chapter 12 deals with *Nucleic Acid Quadruplexes and Metallo-Drugs*. Guanine-rich sequences of DNA can readily fold into tetra-stranded helical assemblies, known as G-quadruplexes (G4). It has been proposed that these structures play important roles in transcription, translation, replication, and telomere maintenance. Therefore they receive attention as potential drug targets for small molecules including metal complexes. Indeed, G4s have been identified as potential drug targets, in particular for cancer.

Anticancer platinum-based drugs are widely used in the treatment of a variety of tumoric diseases. They target DNA and thereby induce apoptosis in cancer cells. Their reactivities with other biomolecules have often been associated with side effects during chemotherapy. The development of metal compounds that target proteins rather than DNA has the potential to overcome or to reduce these disadvantages. New compounds on track toward clinical application are highlighted in *Chapter 13, Antitumor Metallodrugs that Target Proteins*.

Chapter 14, entitled *Metallointercalators and Metalloinsertors* deals with their structural requirements for DNA recognition and anticancer activity. The focus is on the non-covalent recognition of the highly structured DNA surface by substitutionally inert metal complexes (mostly of Ru(II) and Rh(III) with low-spin $4d^6$) capable of either *sliding in* between the normal base pairs (metallointercalators) or *flipping out* thermodynamically destabilized mispaired nucleobases (metalloinsertors). New structural insights enable the development of novel DNA binding modes and thus, new anticancer drug candidates.

The last three chapters of this volume deal with essential metal ions. First, *Iron and Its Role in Cancer Defence: A Double-Edged Sword* is discussed (*Chapter 15*). Iron is vital for many biological functions including electron transport, DNA synthesis, detoxification, and erythropoiesis. Interactions between Fe(II/III) and O_2 can result in the generation of reactive oxygen species. Excess iron may cause

oxidative damage resulting in cell death, but DNA damage may also lead to permanent mutations. Hence, iron is carcinogenic and may initiate tumor formation and growth; however, Fe(II/III) can also contribute to cancer defence by initiating specific forms of cell death, which will benefit cancer treatment. Furthermore, Fe-binding and Fe-regulatory proteins, such as heme oxygenase-1, ferritin, and iron-sulfur clusters can display antitumor properties in certain cancer types. Consequently, very specific and selective drugs that target Fe metabolism in tumors are promising candidates for the prevention and therapy of cancer.

Copper is another essential micronutrient required for fundamental biological processes in all organisms (*Chapter 16*). It is a redox-active metal able to shift between reduced (Cu^{+}) and oxidized (Cu^{2+}) states. Free copper ions can generate highly reactive oxygen species (ROS) and damage lipids, proteins, nucleic acids, and other biomolecules. Hence, copper homeostasis is tightly regulated to ensure sufficient copper for cuproprotein biosynthesis, while limiting oxidative stress and toxicity. Over the last century copper complexes have been developed as antimicrobials and for treating special diseases which now also include cancer because copper has been recognized as a limiting factor for multiple aspects of cancer progression including growth, angiogenesis, and metastasis. Consequently, 'old copper complexes' (e.g., tetrathiomolybdate and clioquinol) have been repurposed for cancer therapy and have demonstrated anticancer activity *in vitro* and in preclinical models. Likewise, with tailer-made copper complexes considerable progress has been made in understanding their pharmacological requirements and human clinical trials continue.

Zinc(II) is gaining momentum as a potential target for cancer therapy since it has been recognized as a second messenger (*Chapter 17*). It is able to activate many signalling pathways within a few minutes by an *extra*cellular stimulus which leads to the release of zinc(II) from *intra*cellular stores.This zinc(II) release inhibits tyrosine phosphatases preventing the inactivation of tyrosine kinases, etc. These signalling pathways are commonly considered the main driving force in aberrant cancer growth. These insights position zinc(II) signalling as a particularly important new target to prevent aggressive cancer growth.

To conclude, this volume, devoted to *Metallo-Drugs: Development and Action of Anticancer Agents*, is rich on specific information. *MILS-18* updates our knowledge not only on platinum(II) and related platinum complexes, but it provides also deep insights on the new research frontiers dealing with the next generation of anticancer drugs. It is a *must* for all researchers working in medicinal chemistry and beyond as well as for teachers giving courses on this topic.

Astrid Sigel
Helmut Sigel
Eva Freisinger
Roland K. O. Sigel

Contents

ABOUT THE EDITORS — **v**

HISTORICAL DEVELOPMENT
AND PERSPECTIVES OF THE SERIES — **vii**

PREFACE TO VOLUME 18 — **ix**

CONTRIBUTORS TO VOLUME 18 — **xix**

TITLES OF VOLUMES 1–44 IN THE
METAL IONS IN BIOLOGICAL SYSTEMS SERIES — **xxiii**

CONTENTS OF VOLUMES IN THE
METAL IONS IN LIFE SCIENCES SERIES — **xxv**

Imogen A. Riddell and Stephen J. Lippard
1 CISPLATIN AND OXALIPLATIN: OUR CURRENT
UNDERSTANDING OF THEIR ACTIONS — **1**
Abstract — **2**
1. Introduction — **2**
2. Cellular Uptake and Efflux/Membrane Transport — **6**
3. Covalent Adducts Generated with Platinum Agents — **13**
4. Cellular Processing of Platinum DNA Adducts — **18**
5. Signal Transduction Pathways Activated by Platinum DNA Damage — **25**
6. Undesired Consequences of Platinum-Based Chemotherapy — **30**
7. Concluding Remarks and Future Directions — **33**

Acknowledgments — **34**
Abbreviations and Definitions — **34**
References — **35**

Viktor Brabec, Jana Kasparkova, Vijay Menon, and Nicholas P. Farrell
2 POLYNUCLEAR PLATINUM COMPLEXES. STRUCTURAL
DIVERSITY AND DNA BINDING — **43**
Abstract — **44**
1. Introduction — **44**

2. Dinuclear Bifunctional Platinum(II) Complexes with Alkanediamine Linkers — **46**
3. Polyamine-Linked Bifunctional Dinuclear Platinum(II) Complexes — **49**
4. DNA-Protein Crosslinking — **53**
5. Dinuclear Platinum(II) Complexes Stabilizing G-DNA Quadruplexes — **53**
6. Structural Variation in Dinuclear Platinum(II) Complexes — **55**
7. Trinuclear Platinum(II) Complexes — **56**
8. Conclusions and Outlook — **62**

Acknowledgments — **63**
Abbreviations and Definitions — **63**
References — **64**

V. Venkatesh and Peter J. Sadler

3 PLATINUM(IV) PRODRUGS — **69**
Abstract — **70**
1. Introduction — **70**
2. Interactions with Biomolecules — **77**
3. Design Features for Anticancer Complexes — **80**
4. Photoactivatable Complexes — **88**
5. Nano Materials for Drug Delivery — **92**
6. Concluding Remarks — **101**

Acknowledgments — **102**
Abbreviations — **102**
References — **103**

Nicholas P. Farrell, Anil K. Gorle, Erica J. Peterson, and Susan J. Berners-Price

4 METALLOGLYCOMICS — **109**
Abstract — **110**
1. Introduction. Metalloglycomics, Heparin, and Heparan Sulfate — **110**
2. Structure and Conformation of Heparin and Heparan Sulfate — **112**
3. Interaction of Metal Ions with Glycosaminoglycans — **118**
4. Interaction of Coordination Compounds with Glycosaminoglycans — **121**
5. Consequences of High-Affinity Heparan Sulfate Binding — **128**
6. Use of Metal Complexes in Heparin Analysis — **134**
7. Conclusions and Outlook — **135**

Acknowledgments — **135**
Abbreviations and Definitions — **135**
References — **136**

Enzo Alessio and Luigi Messori

5 THE DECEPTIVELY SIMILAR RUTHENIUM(III) DRUG CANDIDATES KP1019 AND NAMI-A HAVE DIFFERENT ACTIONS. WHAT DID WE LEARN IN THE PAST 30 YEARS? — **141**
Abstract — **142**
1. Introduction — **142**
2. Comparison of NAMI-A and KP1019 — **145**
3. Conclusions and Outlook — **164**
Acknowledgments — **165**
Abbreviations and Definitions — **165**
References — **166**

Maria V. Babak and Wee Han Ang

6 MULTINUCLEAR ORGANOMETALLIC RUTHENIUM-ARENE COMPLEXES FOR CANCER THERAPY — **171**
Abstract — **172**
1. Introduction — **172**
2. Homoleptic Dinuclear Complexes — **174**
3. Homoleptic Trinuclear and Tetranuclear Complexes — **178**
4. Polynuclear Ruthenium-Arene Cages — **181**
5. Heteronuclear Ruthenium-Arene Complexes — **186**
6. Conclusions — **192**
Acknowledgments — **193**
Abbreviations — **193**
References — **194**

Angela Casini, Raymond Wai-Yin Sun, and Ingo Ott

7 MEDICINAL CHEMISTRY OF GOLD ANTICANCER METALLODRUGS — **199**
Abstract — **200**
1. Introduction — **200**
2. Current Status of Registered Gold Drugs — **200**
3. Gold(I) Anticancer Drugs — **202**
4. Gold(III) Anticancer Drugs — **205**
5. Biological Functions of Gold Complexes — **208**
6. General Conclusions — **213**
Acknowlegments — **213**
Abbreviations and Definitions — **214**
References — **214**

Edit Y. Tshuva and Maya Miller

8 COORDINATION COMPLEXES OF TITANIUM(IV) FOR ANTICANCER THERAPY — **219**
Abstract — **219**
1. Introduction — **220**
2. Cyclopentadienyl-Based Complexes — **221**

3. Budotitane and Related Diketonato Complexes — **227**
4. Complexes of Phenolato Ligands — **230**
5. Conlusions and Outlook — **237**
Acknowledgments — **240**
Abbreviations and Definitions — **240**
References — **240**

Debbie C. Crans, Lining Yang, Allison Haase, and Xiaogai Yang
9 HEALTH BENEFITS OF VANADIUM AND ITS POTENTIAL AS AN ANTICANCER AGENT — **251**
Abstract — **252**
1. Introduction: Vanadium-Containing Compounds Induce Biological Actions — **252**
2. Applications of Vanadium Compounds in Human Studies — **254**
3. Biological Chemistry of Vanadium — **258**
4. The Anticancer Effects of Vanadium Compounds — **262**
5. Vanadium-Containing Drugs in Context of Other Diseases — **265**
6. Vanadium-Based Drugs and Additives and Their Formulation — **267**
7. Conclusions and Outlook — **272**
Acknowledgments — **273**
Abbreviations — **273**
References — **274**

Christopher R. Chitambar
10 GALLIUM COMPLEXES AS ANTICANCER DRUGS — **281**
Abstract — **282**
1. History — **282**
2. Chemistry — **283**
3. Gallium-Based Agents in Clinical Use. Pharmacology and Efficacy — **283**
4. Cellular Handling of Gallium — **288**
5. Antineoplastic Mechanism of Clinically Used Gallium Compounds — **290**
6. Gallium Compounds in Preclinical Development — **294**
7. Summary and Outlook — **296**
Acknowledgments — **297**
Abbreviations — **297**
References — **297**

Lucia Cardo and Michael J. Hannon
11 NON-COVALENT METALLO-DRUGS: USING SHAPE TO TARGET DNA AND RNA JUNCTIONS AND OTHER NUCLEIC ACID STRUCTURES — **303**
Abstract — **304**
1. Introduction — **304**
2. Metallo-Cylinders — **304**

3. Other Supramolecular Designs and Their Targets — **310**
4. Concluding Remarks and Future Directions — **319**
Acknowledgments — **320**
Abbreviations and Definitions — **320**
References — **321**

Ramon Vilar
12 NUCLEIC ACID QUADRUPLEXES AND METALLO-DRUGS — **325**
Abstract — **325**
1. Introduction — **326**
2. G-Quadruplexes and Their Biological Roles — **327**
3. Metal Complexes as G-Quadruplex Binders — **328**
4. Metal-Based Optical Probes for G-Quadruplexes — **338**
5. Biological Activity of Metal-Based G-Quadruplex Binders — **340**
6. Concluding Remarks and Future Directions — **344**
Acknowledgments — **344**
Abbreviations — **344**
References — **345**

Matthew P. Sullivan, Hannah U. Holtkamp, and Christian G. Hartinger
13 ANTITUMOR METALLODRUGS THAT TARGET PROTEINS — **351**
Abstract — **352**
1. Introduction — **352**
2. Anticancer Metallodrugs that Target Carrier Proteins — **354**
3. Selected Cancer-Related Proteins as Targets — **362**
4. Non-Conventional Protein Targets for Anticancer Metallodrugs — **373**
5. Modern Bioanalytical Methods — **375**
6. Concluding Remarks and Future Directions — **376**
Acknowledgments — **377**
Abbreviations — **377**
References — **379**

Ulrich Schatzschneider
14 METALLOINTERCALATORS AND METALLOINSERTORS: STRUCTURAL REQUIREMENTS FOR DNA RECOGNITION AND ANTICANCER ACTIVITY — **387**
Abstract — **388**
1. Introduction — **388**
2. The Basics: Nucleic Acid Structure and Enzymatic Processing — **389**
3. Analytical Methods to Study Metal Complex-DNA Interactions — **394**
4. Metallointercalators — **396**
5. Metalloinsertors — **413**
6. Concluding Remarks and Future Directions — **426**
Abbreviations and Definitions — **427**
References — **430**

Frank Thévenod

15 IRON AND ITS ROLE IN CANCER DEFENSE: A DOUBLE-EDGED SWORD — **437**
Abstract — **438**
1. Introduction — **438**
2. Short Overview of Systemic and Cellular Iron Homeostasis — **439**
3. Iron and Cancer Formation: "A Predominant Feature" — **441**
4. Iron and Cancer Defense: "Long Live the Difference" — **444**
5. General Conclusions — **456**

Acknowledgments — **456**
Abbreviations and Definitions — **456**
References — **458**

Delphine Denoyer, Sharnel A. S. Clatworthy, and Michael A. Cater

16 COPPER COMPLEXES IN CANCER THERAPY — **469**
Abstract — **470**
1. Introduction — **470**
2. Repurposing Old Copper Complexes for Cancer Treatment — **477**
3. Emerging Classes of Copper Complexes for Cancer Treatment — **489**
4. General Conlusions — **496**

Acknowledgments — **497**
Abbreviations — **497**
References — **498**

Silvia Ziliotto, Olivia Ogle, and Kathryn M. Taylor

17 TARGETING ZINC(II) SIGNALLING TO PREVENT CANCER — **507**
Abstract — **507**
1. Introduction — **508**
2. Zinc Handling in Cells — **508**
3. Zinc in Cancer — **513**
4. Zinc Signalling in Cancer — **518**
5. Targeting Zinc Signalling Mechanisms in Cancer — **520**
6. General Conclusions — **523**

Acknowledgments — **523**
Abbreviations and Definitions — **524**
References — **524**

SUBJECT INDEX — **531**

Contributors to Volume 18

Numbers in parentheses indicate the pages on which the authors' contributions begin.

Enzo Alessio Department of Chemical and Pharmaceutical Sciences, University of Trieste, Via L. Giorgieri 1, I-34127 Trieste, Italy <alessi@units.it> (141)

Wee Han Ang Department of Chemistry, National University of Singapore, Block S15, Level 5, 3 Science Drive 2, Singapore 117543 <chmawh@nus.edu.sg> (171)

Maria V. Babak Department of Chemistry, National University of Singapore, Block S15, Level 5, 3 Science Drive 2, Singapore 117543 <phamari@nus.edu.sg> (171)

Viktor Brabec Institute of Biophysics, Academy of Sciences of the Czech Republic, Královopolská 135, CZ-61265 Brno, Czech Republic <brabec@ibp.cz> (43)

Sue Berners-Price Institute for Glycomics, Griffith University, Gold Coast Campus, Southport, QLD 4222, Australia <s.berners-price@griffith.edu.au> (109)

Lucia Cardo School of Chemistry, University of Birmingham, Edgbaston, Birmingham, B15 2TT, UK <l.cardo@bham.ac.uk> (303)

Angela Casini School of Chemistry, Cardiff University, Park Place, Cardiff, CF10 3AT, UK <casinia@cardiff.ac.uk> (199)

Michael A. Cater Centre for Cellular and Molecular Biology, School of Life and Environmental Sciences, Deakin University, Burwood, VIC 3125, Australia, Department of Pathology, The University of Melbourne, Parkville, Victoria, Australia <mcater@unimelb.edu.au> and Rural Clinical School, The University of New South Wales, Port Macquerie, New South Wales, Australia <m.cater@unsw.edu.au> (469)

Christopher R. Chitambar Department of Medicine, Hematology and Oncology Division, Medical College of Wisconsin and Froedtert Clinical Cancer Center, 9200 W. Wisconsin Avenue, Milwaukee, WI 53226, USA <cchitamb@mcw.edu> <chitambr@mcw.edu> (281)

Sharnel A. S. Clatworthy Centre for Cellular and Molecular Biology, School of Life and Environmental Sciences, Deakin University, Burwood, Victoria, Australia (469)

Debbie C. Crans Department of Chemistry and Cell and Molecular Biology, Colorado State University, Fort Collins, CO 80523, USA <debbie.crans@colostate.edu> (251)

Delphine Denoyer Centre for Cellular and Molecular Biology, School of Life and Environmental Sciences, Deakin University, Burwood, Victoria, Australia <d.denoyer@deakin.edu.au> (469)

Nicholas P. Farrell Department of Chemistry, Virginia Commonwealth University, 1001 West Main Street, P.O.B. 842006, Richmond, VA 23284–2006, USA <npfarrell@vcu.edu> (43, 109)

Anil K. Gorle Institute for Glycomics, Griffith University, Gold Coast Campus, Southport, QLD 4222, Australia (109)

Allison Haase Department of Chemistry and Cell and Molecular Biology, Colorado State University, Fort Collins, CO 80523, USA (251)

Michael J. Hannon School of Chemistry, University of Birmingham, Edgbaston, Birmingham, B15 2TT, UK <m.j.hannon@bham.ac.uk> (303)

Christian G. Hartinger School of Chemical Sciences, University of Auckland, Private Bag 92019, NZ-1142 Auckland, New Zealand <c.hartinger@auckland.ac.nz> (351)

Hannah U. Holtkamp School of Chemical Sciences, University of Auckland, Private Bag 92019, NZ-1142 Auckland, New Zealand (351)

Jana Kasparkova Institute of Biophysics, Academy of Sciences of the Czech Republic, Královopolská 135, CZ-61265 Brno, Czech Republic (43)

Stephen J. Lippard Department of Chemistry, Massachusetts Institute of Technology, 77 Massachusetts Avenue, Cambridge, MA 02139-4307, USA <lippard@mit.edu> (1)

Vijay Menon Department of Chemistry, Virginia Commonwealth University, 1001 West Main Street, P.O.B. 842006, Richmond, VA 23284-2006, USA (43)

Luigi Messori Department of Chemistry 'Ugo Schiff', University of Florence, Via della Lastruccia 3–13, I-50019 Sesto Fiorentino, Italy <luigi.messori@unifi.it> (141)

Maya Miller Institute of Chemistry, The Hebrew University of Jerusalem, Jerusalem 91904, Israel (219)

Olivia Ogle School of Pharmacy and Pharmaceutical Sciences, College of Biomedical and Life Sciences, Cardiff University, Redwood Building, King Edward VIIth Avenue, Cardiff, CF10 3NB, UK (507)

Ingo Ott Institute of Medicinal and Pharmaceutical Chemistry, Technical University Braunschweig, Beethovenstr. 55, D-38106 Braunschweig, Germany <ingo.ott@tu-bs.de> (199)

Erica J. Peterson Department of Chemistry, Virginia Commonwealth University, 1001 West Main Street, P.O.B. 842006, Richmond, VA 23284–2006, USA (109)

Imogen A. Riddell Department of Chemistry, Massachusetts Institute of Technology, 77 Massachusetts Avenue, Cambridge, MA 02139–4307, USA (1)

Peter J. Sadler Department of Chemistry, University of Warwick, Coventry CV4 7AL, UK <p.j.sadler@warwick.ac.uk> (69)

Ulrich Schatzschneider Institut für Anorganische Chemie, Julius-Maximilians-Universität Würzburg, Am Hubland, D-97074 Würzburg, Germany <ulrich.schatzschneider@uni-wuerzburg.de> (387)

Matthew P. Sullivan School of Chemical Sciences, University of Auckland, Private Bag 92019, NZ-1142 Auckland, New Zealand (351)

Raymond Wai-Yin Sun Guangzhou Lee & Man Technology Co. Ltd., Guangzhou, Guangdong, P. R. China and Department of Chemistry, Shantou University, 243 Daxue Road, Shantou, Guangdong 515063, P. R. China <rwysun@leemanchemical.com> (199)

Kathryn M. Taylor School of Pharmacy and Pharmaceutical Sciences, College of Biomedical and Life Sciences, Cardiff University, Redwood Building, King Edward VIIth Avenue, Cardiff, CF10 3NB, UK <taylorkm@cardiff.ac.uk> (507)

Frank Thévenod ZBAF (Centre for Biomedical Education and Research), Department of Medicine, Faculty of Health, Private University of Witten/Herdecke, Stockumer Str. 12, D-58453 Witten, Germany <frank.thevenod@uni-wh.de> (437)

Edit Y. Tshuva Institute of Chemistry, The Hebrew University of Jerusalem, Jerusalem 91904, Israel <edit.tshuva@mail.huji.ac.il> (219)

V. Venkatesh Department of Chemistry, University of Warwick, Coventry CV4 7AL, UK <venka7@gmail.com> (69)

Ramon Vilar Department of Chemistry, RCS1–315, Imperial College London, South Kensington Campus, London, SW7 2AZ, UK <r.vilar@imperial.ac.uk> (325)

Lining Yang Department of Chemistry and Cell and Molecular Biology, Colorado State University, Fort Collins, CO 80523, USA and College of Pharmacy, Xi'an Medical University, Xi'an, Shaanxi 710021, China (251)

Xiaogai Yang Department of Chemical Biology, School of Pharmaceutical Sciences, Peking University, Beijing 100191, China (251)

Silvia Ziliotto School of Pharmacy and Pharmaceutical Sciences, College of Biomedical and Life Sciences, Cardiff University, Redwood Building, King Edward VIIth Avenue, Cardiff, CF10 3NB, UK (507)

Titles of Volumes 1–44 in the *Metal Ions in Biological Systems* Series

edited by the SIGELs
and published by Dekker/Taylor & Francis (1973–2005)

Volume 1: **Simple Complexes**
Volume 2: **Mixed-Ligand Complexes**
Volume 3: **High Molecular Complexes**
Volume 4: **Metal Ions as Probes**
Volume 5: **Reactivity of Coordination Compounds**
Volume 6: **Biological Action of Metal Ions**
Volume 7: **Iron in Model and Natural Compounds**
Volume 8: **Nucleotides and Derivatives: Their Ligating Ambivalency**
Volume 9: **Amino Acids and Derivatives as Ambivalent Ligands**
Volume 10: **Carcinogenicity and Metal Ions**
Volume 11: **Metal Complexes as Anticancer Agents**
Volume 12: **Properties of Copper**
Volume 13: **Copper Proteins**
Volume 14: **Inorganic Drugs in Deficiency and Disease**
Volume 15: **Zinc and Its Role in Biology and Nutrition**
Volume 16: **Methods Involving Metal Ions and Complexes in Clinical Chemistry**
Volume 17: **Calcium and Its Role in Biology**
Volume 18: **Circulation of Metals in the Environment**
Volume 19: **Antibiotics and Their Complexes**
Volume 20: **Concepts on Metal Ion Toxicity**
Volume 21: **Applications of Nuclear Magnetic Resonance to Paramagnetic Species**
Volume 22: **ENDOR, EPR, and Electron Spin Echo for Probing Coordination Spheres**
Volume 23: **Nickel and Its Role in Biology**
Volume 24: **Aluminum and Its Role in Biology**
Volume 25: **Interrelations Among Metal Ions, Enzymes, and Gene Expression**
Volume 26: **Compendium on Magnesium and Its Role in Biology, Nutrition, and Physiology**
Volume 27: **Electron Transfer Reactions in Metalloproteins**

Volume 28: **Degradation of Environmental Pollutants by Microorganisms and Their Metalloenzymes**
Volume 29: **Biological Properties of Metal Alkyl Derivatives**
Volume 30: **Metalloenzymes Involving Amino Acid-Residue and Related Radicals**
Volume 31: **Vanadium and Its Role for Life**
Volume 32: **Interactions of Metal Ions with Nucleotides, Nucleic Acids, and Their Constituents**
Volume 33: **Probing Nucleic Acids by Metal Ion Complexes of Small Molecules**
Volume 34: **Mercury and Its Effects on Environment and Biology**
Volume 35: **Iron Transport and Storage in Microorganisms, Plants, and Animals**
Volume 36: **Interrelations Between Free Radicals and Metal Ions in Life Processes**
Volume 37: **Manganese and Its Role in Biological Processes**
Volume 38: **Probing of Proteins by Metal Ions and Their Low-Molecular-Weight Complexes**
Volume 39: **Molybdenum and Tungsten. Their Roles in Biological Processes**
Volume 40: **The Lanthanides and Their Interrelations with Biosystems**
Volume 41: **Metal Ions and Their Complexes in Medication**
Volume 42: **Metal Complexes in Tumor Diagnosis and as Anticancer Agents**
Volume 43: **Biogeochemical Cycles of Elements**
Volume 44: **Biogeochemistry, Availability, and Transport of Metals in the Environment**

Contents of Volumes in the *Metal Ions in Life Sciences* Series

edited by the SIGELs

Volumes 1–4
published by John Wiley & Sons, Ltd., Chichester, UK (2006–2008)
<http://www.Wiley.com/go/mils>
<http://www.wiley.com/WileyCDA/Section/id-300350.html>

Volumes 5–9
published by the Royal Society of Chemistry, Cambridge, UK (2009–2011)
since 2015 by Walter de Gruyter GmbH, Berlin, Germany
<http://www.bioinorganic-chemistry.org/mils> <http://www.mils-WdG.com>

Volumes 10–16
published by Springer Science & Business Media BV, Dordrecht,
The Netherlands (2012–2014; MILS-10 to MILS-14)
and by Springer International Publishing AG, Cham, Switzerland
(2015–2016; MILS-15 and MILS-16)
<http://www.bioinorganic-chemistry.org/mils>

and from Volume 17 on
published by Walter de Gruyter GmbH, Berlin, Germany
<http://www.mils-WdG.com>

Volume 1: Neurodegenerative Diseases and Metal Ions

1. The Role of Metal Ions in Neurology. An Introduction
   Dorothea Strozyk and Ashley I. Bush
2. Protein Folding, Misfolding, and Disease
   Jennifer C. Lee, Judy E. Kim, Ekaterina V. Pletneva, Jasmin Faraone-Mennella, Harry B. Gray, and Jay R. Winkler
3. Metal Ion Binding Properties of Proteins Related to Neurodegeneration
   Henryk Kozlowski, Marek Luczkowski, Daniela Valensin, and Gianni Valensin

4. Metallic Prions: Mining the Core of Transmissible Spongiform Encephalopathies
David R. Brown
5. The Role of Metal Ions in the Amyloid Precursor Protein and in Alzheimer's Disease
Thomas A. Bayer and Gerd Multhaup
6. The Role of Iron in the Pathogenesis of Parkinson's Disease
Manfred Gerlach, Kay L. Double, Mario E. Götz, Moussa B. H. Youdim, and Peter Riederer
7. *In Vivo* Assessment of Iron in Huntington's Disease and Other Age-Related Neurodegenerative Brain Diseases
George Bartzokis, Po H. Lu, Todd A. Tishler, and Susan Perlman
8. Copper-Zinc Superoxide Dismutase and Familial Amyotrophic Lateral Sclerosis
Lisa J. Whitson and P. John Hart
9. The Malfunctioning of Copper Transport in Wilson and Menkes Diseases
Bibudhendra Sarkar
10. Iron and Its Role in Neurodegenerative Diseases
Roberta J. Ward and Robert R. Crichton
11. The Chemical Interplay between Catecholamines and Metal Ions in Neurological Diseases
Wolfgang Linert, Guy N. L. Jameson, Reginald F. Jameson, and Kurt A. Jellinger
12. Zinc Metalloneurochemistry: Physiology, Pathology, and Probes
Christopher J. Chang and Stephen J. Lippard
13. The Role of Aluminum in Neurotoxic and Neurodegenerative Processes
Tamás Kiss, Krisztina Gajda-Schrantz, and Paolo F. Zatta
14. Neurotoxicity of Cadmium, Lead, and Mercury
Hana R. Pohl, Henry G. Abadin, and John F. Risher
15. Neurodegerative Diseases and Metal Ions. A Concluding Overview
Dorothea Strozyk and Ashley I. Bush

Subject Index

Volume 2: Nickel and Its Surprising Impact in Nature

1. Biogeochemistry of Nickel and Its Release into the Environment
Tiina M. Nieminen, Liisa Ukonmaanaho, Nicole Rausch, and William Shotyk
2. Nickel in the Environment and Its Role in the Metabolism of Plants and Cyanobacteria
Hendrik Küpper and Peter M. H. Kroneck

3. Nickel Ion Complexes of Amino Acids and Peptides
Teresa Kowalik-Jankowska, Henryk Kozlowski, Etelka Farkas, and Imre Sóvágó
4. Complex Formation of Nickel(II) and Related Metal Ions with Sugar Residues, Nucleobases, Phosphates, Nucleotides, and Nucleic Acids
Roland K. O. Sigel and Helmut Sigel
5. Synthetic Models for the Active Sites of Nickel-Containing Enzymes
Jarl Ivar van der Vlugt and Franc Meyer
6. Urease: Recent Insights in the Role of Nickel
Stefano Ciurli
7. Nickel Iron Hydrogenases
Wolfgang Lubitz, Maurice van Gastel, and Wolfgang Gärtner
8. Methyl-Coenzyme M Reductase and Its Nickel Corphin Coenzyme F_{430} in Methanogenic Archaea
Bernhard Jaun and Rudolf K. Thauer
9. Acetyl-Coenzyme A Synthases and Nickel-Containing Carbon Monoxide Dehydrogenases
Paul A. Lindahl and David E. Graham
10. Nickel Superoxide Dismutase
Peter A. Bryngelson and Michael J. Maroney
11. Biochemistry of the Nickel-Dependent Glyoxylase I Enzymes
Nicole Sukdeo, Elisabeth Daub, and John F. Honek
12. Nickel in Acireductone Dioxygenase
Thomas C. Pochapsky, Tingting Ju, Marina Dang, Rachel Beaulieu, Gina Pagani, and Bo OuYang
13. The Nickel-Regulated Peptidyl-Prolyl *cis*/*trans* Isomerase SlyD
Frank Erdmann and Gunter Fischer
14. Chaperones of Nickel Metabolism
Soledad Quiroz, Jong K. Kim, Scott B. Mulrooney, and Robert P. Hausinger
15. The Role of Nickel in Environmental Adaptation of the Gastric Pathogen *Helicobacter pylori*
Florian D. Ernst, Arnoud H. M. van Vliet, Manfred Kist, Johannes G. Kusters, and Stefan Bereswill
16. Nickel-Dependent Gene Expression
Konstantin Salnikow and Kazimierz S. Kasprzak
17. Nickel Toxicity and Carcinogenesis
Kazimierz S. Kasprzak and Konstantin Salnikow

Subject Index

Volume 3: The Ubiquitous Roles of Cytochrome P450 Proteins

1. Diversities and Similarities of P450 Systems: An Introduction
Mary A. Schuler and Stephen G. Sligar

2. Structural and Functional Mimics of Cytochromes P450
Wolf-D. Woggon
3. Structures of P450 Proteins and Their Molecular Phylogeny
Thomas L. Poulos and Yergalem T. Meharenna
4. Aquatic P450 Species
Mark J. Snyder
5. The Electrochemistry of Cytochrome P450
Alan M. Bond, Barry D. Fleming, and Lisandra L. Martin
6. P450 Electron Transfer Reactions
Andrew K. Udit, Stephen M. Contakes, and Harry B. Gray
7. Leakage in Cytochrome P450 Reactions in Relation to Protein Structural Properties
Christiane Jung
8. Cytochromes P450. Structural Basis for Binding and Catalysis
Konstanze von König and Ilme Schlichting
9. Beyond Heme-Thiolate Interactions: Roles of the Secondary Coordination Sphere in P450 Systems
Yi Lu and Thomas D. Pfister
10. Interactions of Cytochrome P450 with Nitric Oxide and Related Ligands
Andrew W. Munro, Kirsty J. McLean, and Hazel M. Girvan
11. Cytochrome P450-Catalyzed Hydroxylations and Epoxidations
Roshan Perera, Shengxi Jin, Masanori Sono, and John H. Dawson
12. Cytochrome P450 and Steroid Hormone Biosynthesis
Rita Bernhardt and Michael R. Waterman
13. Carbon-Carbon Bond Cleavage by P450 Systems
James J. De Voss and Max J. Cryle
14. Design and Engineering of Cytochrome P450 Systems
Stephen G. Bell, Nicola Hoskins, Christopher J. C. Whitehouse, and Luet L. Wong
15. Chemical Defense and Exploitation. Biotransformation of Xenobiotics by Cytochrome P450 Enzymes
Elizabeth M. J. Gillam and Dominic J. B. Hunter
16. Drug Metabolism as Catalyzed by Human Cytochrome P450 Systems
F. Peter Guengerich
17. Cytochrome P450 Enzymes: Observations from the Clinic
Peggy L. Carver

Subject Index

Volume 4: Biomineralization. From Nature to Application

1. Crystals and Life: An Introduction
Arthur Veis

2. What Genes and Genomes Tell Us about Calcium Carbonate Biomineralization
Fred H. Wilt and Christopher E. Killian

3. The Role of Enzymes in Biomineralization Processes
Ingrid M. Weiss and Frédéric Marin

4. Metal–Bacteria Interactions at Both the Planktonic Cell and Biofilm Levels
Ryan C. Hunter and Terry J. Beveridge

5. Biomineralization of Calcium Carbonate. The Interplay with Biosubstrates
Amir Berman

6. Sulfate-Containing Biominerals
Fabienne Bosselmann and Matthias Epple

7. Oxalate Biominerals
Enrique J. Baran and Paula V. Monje

8. Molecular Processes of Biosilicification in Diatoms
Aubrey K. Davis and Mark Hildebrand

9. Heavy Metals in the Jaws of Invertebrates
Helga C. Lichtenegger, Henrik Birkedal, and J. Herbert Waite

10. Ferritin. Biomineralization of Iron
Elizabeth C. Theil, Xiaofeng S. Liu, and Manolis Matzapetakis

11. Magnetism and Molecular Biology of Magnetic Iron Minerals in Bacteria
Richard B. Frankel, Sabrina Schübbe, and Dennis A. Bazylinski

12. Biominerals. Recorders of the Past?
Danielle Fortin, Sean R. Langley, and Susan Glasauer

13. Dynamics of Biomineralization and Biodemineralization
Lijun Wang and George H. Nancollas

14. Mechanism of Mineralization of Collagen-Based Connective Tissues
Adele L. Boskey

15. Mammalian Enamel Formation
Janet Moradian-Oldak and Michael L. Paine

16. Mechanical Design of Biomineralized Tissues. Bone and Other Hierarchical Materials
Peter Fratzl

17. Bioinspired Growth of Mineralized Tissue
Darilis Suárez-González and William L. Murphy

18. Polymer-Controlled Biomimetic Mineralization of Novel Inorganic Materials
Helmut Cölfen and Markus Antonietti

Subject Index

Volume 5: Metallothioneins and Related Chelators

1. Metallothioneins. Historical Development and Overview
Monica Nordberg and Gunnar F. Nordberg
2. Regulation of Metallothionein Gene Expression
Kuppusamy Balamurugan and Walter Schaffner
3. Bacterial Metallothioneins
Claudia A. Blindauer
4. Metallothioneins in Yeast and Fungi
Benedikt Dolderer, Hans-Jürgen Hartmann, and Ulrich Weser
5. Metallothioneins in Plants
Eva Freisinger
6. Metallothioneins in Diptera
Silvia Atrian
7. Earthworm and Nematode Metallothioneins
Stephen R. Stürzenbaum
8. Metallothioneins in Aquatic Organisms: Fish, Crustaceans, Molluscs, and Echinoderms
Laura Vergani
9. Metal Detoxification in Freshwater Animals. Roles of Metallothioneins
Peter G. C. Campbell and Landis Hare
10. Structure and Function of Vertebrate Metallothioneins
Juan Hidalgo, Roger Chung, Milena Penkowa, and Milan Vašák
11. Metallothionein-3, Zinc, and Copper in the Central Nervous System
Milan Vašák and Gabriele Meloni
12. Metallothionein Toxicology: Metal Ion Trafficking and Cellular Protection
David H. Petering, Susan Krezoski, and Niloofar M. Tabatabai
13. Metallothionein in Inorganic Carcinogenesis
Michael P. Waalkes and Jie Liu
14. Thioredoxins and Glutaredoxins. Functions and Metal Ion Interactions
Christopher Horst Lillig and Carsten Berndt
15. Metal Ion-Binding Properties of Phytochelatins and Related Ligands
Aurélie Devez, Eric Achterberg, and Martha Gledhill

Subject Index

Volume 6: Metal-Carbon Bonds in Enzymes and Cofactors

1. Organometallic Chemistry of B_{12} Coenzymes
Bernhard Kräutler
2. Cobalamin- and Corrinoid-Dependent Enzymes
Rowena G. Matthews

3. Nickel-Alkyl Bond Formation in the Active Site of Methyl-Coenzyme M Reductase
Bernhard Jaun and Rudolf K. Thauer
4. Nickel-Carbon Bonds in Acetyl-Coenzyme A Synthases/Carbon Monoxide Dehydrogenases
Paul A. Lindahl
5. Structure and Function of [NiFe]-Hydrogenases
Juan C. Fontecilla-Camps
6. Carbon Monoxide and Cyanide Ligands in the Active Site of [FeFe]-Hydrogenases
John W. Peters
7. Carbon Monoxide as Intrinsic Ligand to Iron in the Active Site of [Fe]-Hydrogenase
Seigo Shima, Rudolf K. Thauer, and Ulrich Ermler
8. The Dual Role of Heme as Cofactor and Substrate in the Biosynthesis of Carbon Monoxide
Mario Rivera and Juan C. Rodriguez
9. Copper-Carbon Bonds in Mechanistic and Structural Probing of Proteins as well as in Situations where Copper Is a Catalytic or Receptor Site
Heather R. Lucas and Kenneth D. Karlin
10. Interaction of Cyanide with Enzymes Containing Vanadium and Manganese, Non-Heme Iron, and Zinc
Martha E. Sosa-Torres and Peter M. H. Kroneck
11. The Reaction Mechanism of the Molybdenum Hydroxylase Xanthine Oxidoreductase: Evidence against the Formation of Intermediates Having Metal-Carbon Bonds
Russ Hille
12. Computational Studies of Bioorganometallic Enzymes and Cofactors
Matthew D. Liptak, Katherine M. Van Heuvelen, and Thomas C. Brunold

Subject Index

Author Index of *MIBS*-1 to *MIBS*-44 and *MILS*-1 to *MILS*-6

Volume 7: Organometallics in Environment and Toxicology

1. Roles of Organometal(loid) Compounds in Environmental Cycles
John S. Thayer
2. Analysis of Organometal(loid) Compounds in Environmental and Biological Samples
Christopher F. Harrington, Daniel S. Vidler, and Richard O. Jenkins
3. Evidence for Organometallic Intermediates in Bacterial Methane Formation Involving the Nickel Coenzyme F_{430}
Mishtu Dey, Xianghui Li, Yuzhen Zhou, and Stephen W. Ragsdale

4. Organotins. Formation, Use, Speciation, and Toxicology
Tamas Gajda and Attila Jancsó
5. Alkyllead Compounds and Their Environmental Toxicology
Henry G. Abadin and Hana R. Pohl
6. Organoarsenicals: Distribution and Transformation in the Environment
Kenneth J. Reimer, Iris Koch, and William R. Cullen
7. Organoarsenicals. Uptake, Metabolism, and Toxicity
Elke Dopp, Andrew D. Kligerman, and Roland A. Diaz-Bone
8. Alkyl Derivatives of Antimony in the Environment
Montserrat Filella
9. Alkyl Derivatives of Bismuth in Environmental and Biological Media
Montserrat Filella
10. Formation, Occurrence and Significance of Organoselenium and Organotellurium Compounds in the Environment
Dirk Wallschläger and Jörg Feldmann
11. Organomercurials. Their Formation and Pathways in the Environment
Holger Hintelmann
12. Toxicology of Alkylmercury Compounds
Michael Aschner, Natalia Onishchenko, and Sandra Ceccatelli
13. Environmental Bioindication, Biomonitoring, and Bioremediation of Organometal(loid)s
John S. Thayer
14. Methylated Metal(loid) Species in Humans
Alfred V. Hirner and Albert W. Rettenmeier

Subject Index

Volume 8: Metal Ions in Toxicology: Effects, Interactions, Interdependencies

1. Understanding Combined Effects for Metal Co-Exposure in Ecotoxicology
Rolf Altenburger
2. Human Risk Assessment of Heavy Metals: Principles and Applications
Jean-Lou C. M. Dorne, George E. N. Kass, Luisa R. Bordajandi, Billy Amzal, Ulla Bertelsen, Anna F. Castoldi, Claudia Heppner, Mari Eskola, Stefan Fabiansson, Pietro Ferrari, Elena Scaravelli, Eugenia Dogliotti, Peter Fuerst, Alan R. Boobis, and Philippe Verger
3. Mixtures and Their Risk Assessment in Toxicology
Moiz M. Mumtaz, Hugh Hansen, and Hana R. Pohl
4. Metal Ions Affecting the Pulmonary and Cardiovascular Systems
Massimo Corradi and Antonio Mutti
5. Metal Ions Affecting the Gastrointestinal System Including the Liver
Declan P. Naughton, Tamás Nepusz, and Andrea Petroczi

6. Metal Ions Affecting the Kidney
Bruce A. Fowler
7. Metal Ions Affecting the Hematological System
Nickolette Roney, Henry G. Abadin, Bruce Fowler, and Hana R. Pohl
8. Metal Ions Affecting the Immune System
Irina Lehmann, Ulrich Sack, and Jörg Lehmann
9. Metal Ions Affecting the Skin and Eyes
Alan B. G. Lansdown
10. Metal Ions Affecting the Neurological System
Hana R. Pohl, Nickolette Roney, and Henry G. Abadin
11. Metal Ions Affecting Reproduction and Development
Pietro Apostoli and Simona Catalani
12. Are Cadmium and Other Heavy Metal Compounds Acting as Endocrine Disrupters?
Andreas Kortenkamp
13. Genotoxicity of Metal Ions: Chemical Insights
Woijciech Bal, Anna Maria Protas, and Kazimierz S. Kasprzak
14. Metal Ions in Human Cancer Development
Erik J. Tokar, Lamia Benbrahim-Tallaa, and Michael P. Waalkes

Subject Index

Volume 9: Structural and Catalytic Roles of Metal Ions in RNA

1. Metal Ion Binding to RNA
Pascal Auffinger, Neena Grover, and Eric Westhof
2. Methods to Detect and Characterize Metal Ion Binding Sites in RNA
Michèle C. Erat and Roland K. O. Sigel
3. Importance of Diffuse Metal Ion Binding to RNA
Zhi-Jie Tan and Shi-Jie Chen
4. RNA Quadruplexes
Kangkan Halder and Jörg S. Hartig
5. The Roles of Metal Ions in Regulation by Riboswitches
Adrian Ferré-D'Amaré and Wade C. Winkler
6. Metal Ions: Supporting Actors in the Playbook of Small Ribozymes
Alexander E. Johnson-Buck, Sarah E. McDowell, and Nils G. Walter
7. Multiple Roles of Metal Ions in Large Ribozymes
Daniela Donghi and Joachim Schnabl
8. The Spliceosome and Its Metal Ions
Samuel E. Butcher
9. The Ribosome: A Molecular Machine Powered by RNA
Krista Trappl and Norbert Polacek

10. Metal Ion Requirements in Artificial Ribozymes that Catalyze Aminoacylations and Redox Reactions
Hiroaki Suga, Kazuki Futai, and Koichiro Jin

11. Metal Ion Binding and Function in Natural and Artificial Small RNA Enzymes from a Structural Perspective
Joseph E. Wedekind

12. Binding of Kinetically Inert Metal Ions to RNA: The Case of Platinum(II)
Erich G. Chapman, Alethia A. Hostetter, Maire F. Osborn, Amanda L. Miller, and Victoria J. DeRose

Subject Index

Volume 10: Interplay between Metal Ions and Nucleic Acids

1. Characterization of Metal Ion-Nucleic Acid Interactions in Solution
Maria Pechlaner and Roland K. O. Sigel

2. Nucleic Acid-Metal Ion Interactions in the Solid State
Katsuyuki Aoki and Kazutaka Murayama

3. Metal Ion-Promoted Conformational Changes of Oligonucleotides
Bernhard Spingler

4. G-Quadruplexes and Metal Ions
Nancy H. Campbell and Stephen Neidle

5. Metal Ion-Mediated DNA-Protein Interactions
Barbara Zambelli, Francesco Musiani, and Stefano Ciurli

6. Spectroscopic Investigations of Lanthanide Ion Binding to Nucleic Acids
Janet R. Morrow and Christopher M. Andolina

7. Oxidative DNA Damage Mediated by Transition Metal Ions and Their Complexes
Geneviève Pratviel

8. Metal Ion-Dependent DNAzymes and Their Applications as Biosensors
Tian Lan and Yi Lu

9. Enantioselective Catalysis at the DNA Scaffold
Almudena García-Fernández and Gerard Roelfes

10. Alternative DNA Base Pairing through Metal Coordination
Guido H. Clever and Mitsuhiko Shionoya

11. Metal-Mediated Base Pairs in Nucleic Acids with Purine- and Pyrimidine-Derived Nucleosides
Dominik A. Megger, Nicole Megger, and Jens Müller

12. Metal Complex Derivatives of Peptide Nucleic Acids (PNA)
Roland Krämer and Andrij Mokhir

Subject Index

Volume 11: Cadmium: From Toxicity to Essentiality

1. The Bioinorganic Chemistry of Cadmium in the Context of Its Toxicity
Wolfgang Maret and Jean-Marc Moulis
2. Biogeochemistry of Cadmium and Its Release to the Environment
Jay T. Cullen and Maria T. Maldonado
3. Speciation of Cadmium in the Environment
Francesco Crea, Claudia Foti, Demetrio Milea, and Silvio Sammartano
4. Determination of Cadmium in Biological Samples
Katrin Klotz, Wobbeke Weistenhöfer, and Hans Drexler
5. Imaging and Sensing of Cadmium in Cells
Masayasu Taki
6. Use of ^{113}Cd NMR to Probe the Native Metal Binding Sites in Metalloproteins: An Overview
Ian M. Armitage, Torbjörn Drakenberg, and Brian Reilly
7. Solid State Structures of Cadmium Complexes with Relevance for Biological Systems
Rosa Carballo, Alfonso Castiñeiras, Alicia Domínguez-Martín, Isabel García Santos, and Juan Niclós-Gutierrez
8. Complex Formation of Cadmium(II) with Sugar Residues, Nucleobases, Phosphates, Nucleotides, and Nucleic Acids
Roland K. O. Sigel, Miriam Skilandat, Astrid Sigel, Bert P. Operschall, and Helmut Sigel
9. Cadmium(II) Complexes of Amino Acids and Peptides
Imre Sóvágó and Katalin Várnagy
10. Natural and Artificial Proteins Containing Cadmium
Anna F. Peacock and Vincent L. Pecoraro
11. Cadmium in Metallothioneins
Eva Freisinger and Milan Vašák
12. Cadmium-Accumulating Plants
Hendrik Küpper and Barbara Leitenmaier
13. Cadmium Toxicity in Plants
Elisa Andresen and Hendrik Küpper
14. Toxicology of Cadmium and Its Damage to Mammalian Organs
Frank Thévenod and Wing-Kee Lee
15. Cadmium and Cancer
Andrea Hartwig
16. Cadmium in Marine Phytoplankton
Yan Xu and François M. M. Morel

Subject Index

Volume 12: Metallomics and the Cell
Guest Editor: Lucia Banci

1. Metallomics and the Cell: Some Definitions and General Comments
Lucia Banci and Ivano Bertini
2. Technologies for Detecting Metals in Single Cells
James E. Penner-Hahn
3. Sodium/Potassium Homeostasis in the Cell
Michael J. V. Clausen and Hanna Poulsen
4. Magnesium Homeostasis in Mammalian Cells
Andrea M. P. Romani
5. Intracellular Calcium Homeostasis and Signaling
Marisa Brini, Tito Calì, Denis Ottolini, and Ernesto Carafoli
6. Manganese Homeostasis and Transport
Jerome Roth, Silvia Ponzoni, and Michael Aschner
7. Control of Iron Metabolism in Bacteria
Simon Andrews, Ian Norton, Arvindkumar S. Salunkhe, Helen Goodluck, Wafaa S. M. Aly, Hanna Mourad-Agha, and Pierre Cornelis
8. The Iron Metallome in Eukaryotic Organisms
Adrienne C. Dlouhy and Caryn E. Outten
9. Heme Uptake and Metabolism in Bacteria
David R. Benson and Mario Rivera
10. Cobalt and Corrinoid Transport and Biochemistry
Valentin Cracan and Ruma Banerjee
11. Nickel Metallomics: General Themes Guiding Nickel Homeostasis
Andrew M. Sydor and Deborah B. Zamble
12. The Copper Metallome in Prokaryotic Cells
Christopher Rensing and Sylvia Franke McDevitt
13. The Copper Metallome in Eukaryotic Cells
Katherine E. Vest, Hayaa F. Hashemi, and Paul A. Cobine
14. Zinc and the Zinc Proteome
Wolfgang Maret
15. Metabolism of Molybdenum
Ralf R. Mendel
16. Comparative Genomics Analysis of the Metallomes
Vadim N. Gladyshev and Yan Zhang

Subject Index

Volume 13: Interrelations between Essential Metal Ions and Human Diseases

1. Metal Ions and Infectious Diseases. An Overview from the Clinic
Peggy L. Carver

2. Sodium and Potassium in Health and Disease
Hana R. Pohl, John S. Wheeler, and H. Edward Murray
3. Magnesium in Health and Disease
Andrea M. P. Romani
4. Calcium in Health and Disease
Marisa Brini, Denis Ottolini, Tito Calì, and Ernesto Carafoli
5. Vanadium. Its Role for Humans
Dieter Rehder
6. Chromium. Is It Essential, Pharmacologically Relevant, or Toxic?
John B. Vincent
7. Manganese in Health and Disease
Daiana Silva Avila, Robson Luiz Puntel, and Michael Aschner
8. Iron: Effect of Overload and Deficiency
Robert C. Hider and Xiaole Kong
9. Cobalt: Its Role in Health and Disease
Kazuhiro Yamada
10. Nickel and Human Health
Barbara Zambelli and Stefano Ciurli
11. Copper: Effects of Deficiency and Overload
Ivo Scheiber, Ralf Dringen, and Julian F. B. Mercer
12. Zinc and Human Disease
Wolfgang Maret
13. Molybdenum in Human Health and Disease
Guenter Schwarz and Abdel A. Belaidi
14. Silicon: The Health Benefits of a Metalloid
Keith R. Martin
15. Arsenic. Can this Toxic Metalloid Sustain Life?
Dean E. Wilcox
16. Selenium. Role of the Essential Metalloid in Health
Suguru Kurokawa and Marla J. Berry

Subject Index

Volume 14: The Metal-Driven Biogeochemistry of Gaseous Compounds in the Environment
Guest Editors: Peter M. H. Kroneck and Martha E. Sosa-Torres

1. The Early Earth Atmosphere and Early Life Catalysts
Sandra I. Ramírez Jiménez
2. Living on Acetylene. A Primordial Energy Source
Felix ten Brink

3. Carbon Monoxide. Toxic Gas and Fuel for Anaerobes and Aerobes: Carbon Monoxide Dehydrogenases
Jae-Hun Jeoung, Jochen Fesseler, Sebastian Goetzl, and Holger Dobbek
4. Investigations of the Efficient Electrocatalytic Interconversions of Carbon Dioxide and Carbon Monoxide by Nickel-Containing Carbon Monoxide Dehydrogenases
Vincent C.-C. Wang, Stephen W. Ragsdale, and Fraser A. Armstrong
5. Understanding and Harnessing Hydrogenases. Biological Dihydrogen Catalysts
Alison Parkin
6. Biochemistry of Methyl-Coenzyme M Reductase: The Nickel Metalloenzyme that Catalyzes the Final Step in Synthesis and the First Step in Anaerobic Oxidation of the Greenhouse Gas Methane
Stephen W. Ragsdale
7. Cleaving the N,N Triple Bond: The Transformation of Dinitrogen to Ammonia by Nitrogenases
Chi Chung Lee, Markus W. Ribbe, and Yilin Hu
8. No Laughing Matter: The Unmaking of the Greenhouse Gas Dinitrogen Monoxide by Nitrous Oxide Reductase
Lisa K. Schneider, Anja Wüst, Anja Pomowski, Lin Zhang, and Oliver Einsle
9. The Production of Ammonia by Multiheme Cytochromes *c*
Jörg Simon and Peter M. H. Kroneck
10. Hydrogen Sulfide: A Toxic Gas Produced by Dissimilatory Sulfate and Sulfur Reduction and Consumed by Microbial Oxidation
Larry L. Barton, Marie-Laure Fardeau, and Guy D. Fauque
11. Transformations of Dimethylsulfide
Ulrike Kappler and Hendrik Schäfer

Subject Index

Volume 15: Sustaining Life on Planet Earth: Metalloenzymes Mastering Dioxygen and Other Chewy Gases
Guest Editors: Peter M. H. Kroneck and Martha E. Sosa-Torres

1. The Magic of Dioxygen
Martha E. Sosa Torres, Juan P. Saucedo-Vázquez, and Peter M. H. Kroneck
2. Light-Dependent Production of Dioxygen in Photosynthesis
Junko Yano, Jan Kern, Vittal K. Yachandra, Håkan Nilsson, Sergey Koroidov, and Johannes Messinger
3. Production of Dioxygen in the Dark: Dismutases of Oxyanions
Jennifer L. DuBois and Sunil Ojha

4. Respiratory Conservation of Energy with Dioxygen: Cytochrome *c* Oxidase
Shinya Yoshikawa, Atsuhiro Shimada, and Kyoko Shinzawa-Itoh
5. Transition Metal Complexes and the Activation of Dioxygen
Gereon M. Yee and William B. Tolman
6. Methane Monooxygenase: Functionalizing Methane at Iron and Copper
Matthew H. Sazinsky and Stephen J. Lippard
7. Metal Enzymes in "Impossible" Microorganisms Catalyzing the Anaerobic Oxidation of Ammonium and Methane
Joachim Reimann, Mike S. M. Jetten, and Jan T. Keltjens

Subject Index

Volume 16: The Alkali Metal Ions: Their Roles for Life

1. Bioinorganic Chemistry of the Alkali Metal Ions
Youngsam Kim, Thuy Tien Nguyen, and David G. Churchill
2. Determination of Alkali Ions in Biological and Environmental Samples
Peter C. Hauser
3. Solid State Structures of Alkali Metal Ion Complexes Formed by Low-Molecular-Weight Ligands of Biological Relevance
Katsuyuki Aoki, Kazutaka Murayama, and Ning-Hai Hu
4. Discriminating Properties of Alkali Metal Ions towards the Constituents of Proteins and Nucleic Acids. Conclusions from Gas-Phase and Theoretical Studies
Mary T. Rodgers and Peter B. Armentrout
5. Alkali-Metal Ion Complexes with Phosphates, Nucleotides, Amino Acids, and Related Ligands of Biological Relevance. Their Properties in Solution
Francesco Crea, Concetta De Stefano, Claudia Foti, Gabriele Lando, Demetrio Milea, and Silvio Sammartano
6. Sodium and Potassium Interactions with Nucleic Acids
Pascal Auffinger, Luigi D'Ascenzo, and Eric Ennifar
7. Role of Alkali Metal Ions in G-Quadruplex Nucleic Acid Structure and Stability
Eric Largy, Jean-Louis Mergny, and Valérie Gabelica
8. Sodium and Potassium Ions in Proteins and in Enzyme Catalysis
Milan Vašak and Joachim Schnabl
9. Roles and Transport of Sodium and Potassium in Plants
Manuel Nieves-Cordones, Fouad Razzaq Al Shiblawi, and Hervé Sentenac
10. Potassium *versus* Sodium Selectivity in Monovalent Ion Channel Selectivity Filters
Carmay Lim and Todor Dudev

11. Sodium as Coupling Cation in Respiratory Energy Conversion
Günter Fritz and Julia Steuber
12. Sodium-Proton (Na^+/H^+) Antiporters: Properties and Roles in Health and Disease
Etana Padan and Meytal Landau
13. Proton-Potassium (H^+/K^+) ATPases: Properties and Roles in Health and Disease
Hideki Sakai, Takuto Fujii, and Noriaki Takeguchi
14. Bioinspired Artificial Sodium and Potassium Channels
Nuria Vázquez-Rodríguez, Alberto Fuertes, Manuel Amorín, and Juan R. Granja
15. Lithium in Medicine: Mechanisms of Action
Duarte Mota de Freitas, Brian D. Leverson, and Jesse L. Goossens
16. Sodium and Potassium Relating to Parkinson's Disease and Traumatic Brain Injury
Yonghwang Ha, Jeong A. Jeong, Youngsam Kim, and David G. Churchill

Subject Index

Volume 17: Lead: Its Effects on Environment and Health

1. The Bioinorganic Chemistry of Lead in the Context of Its Toxicity
Wolfgang Maret
2. Biogeochemistry of Lead. Its Release to the Environment and Chemical Speciation
Jay T. Cullen and Jason McAlister
3. Analytical Methods for the Determination of Lead in the Environment
Peter C. Hauser
4. Smart Capsules for Lead Removal from Industrial Wastewater
Bartosz Tylkowski and Renata Jastrząb
5. Lead Speciation in Microorganisms
Theodora J. Stewart
6. Human Biomonitoring of Lead Exposure
Katrin Klotz and Thomas Göen
7. Solid State Structures of Lead Complexes with Relevance for Biological Systems
Katsuyuki Aoki, Kazutaka Murayama, and Ning-Hai Hu
8. Lead(II) Complexes of Amino Acids, Peptides, and Other Related Ligands of Biological Interest
Etelka Farkas and Péter Buglyó
9. Lead(II) Binding in Metallothioneins
Daisy L. Wong, Maureen E. Merrifield-MacRae, and Martin J. Stillman

10. Lead(II) Binding in Natural and Artificial Proteins
Virginia Cangelosi, Leela Ruckthong, and Vincent L. Pecoraro

11. Complex Formation of Lead(II) with Nucleotides and Their Constituents
Astrid Sigel, Bert P. Operschall, and Helmut Sigel

12. The Role of Lead(II) in Nucleic Acids
Joana Palou-Mir, Miquel Barceló-Oliver, and Roland K. O. Sigel

13. Historical View on Lead: Guidelines and Regulations
Hana R. Pohl, Susan Z. Ingber, and Henry G. Abadin

14. Environmental Impact of Alkyl Lead(IV) Derivatives
Montserrat Filella and Josep Bone

15. Lead Toxicity in Plants
Hendrik Küpper

16. Toxicology of Lead and Its Damage to Mammalian Organs
Samuel Caito, Ana Carolina B. Almeida Lopes, Monica M. B. Paoliello, and Michael Aschner

Subject Index

Volume 18: Metallo-Drugs: Development and Action of Anticancer and Antitumor Agents
(this book)

Volume 19: Essential Metals in Medicine: Therapeutic Use and Toxicity of Metal Ions in the Clinic (tentative)
Guest Editor: Peggy L. Carver

1. Introduction to Therapeutic Use of Metal Ions in the Clinic
Peggy L. Carver

2. "Small Molecules": The Past or the Future in Drug Innovation?
Bernard Meunier

3. Iron Chelation for Iron Overload in Thalassemia
Guido Crisponi, Valeria M. Nurchi, and Joanna I. Lachowicz

4. Infections Associated with Iron Administration
Manfred Nairz and Guenter Weiss

5. Iron Oxide Nanoparticle Formulations for Supplementation
Amy B. Pai

6. Ironing Out the Brain
Roberta J. Ward and Robert R. Crichton

7. Manganese
Michael Aschner

8. Copper Depletion as a Therapeutic Strategy in Cancer
Jay Lopez, Divya Ramchandani, and Linda T. Vahdat

9. Developing Vanadium as an Antidiabetic Drug: A Practical and Clinical Perspective
Debbie C. Crans, Eric Pohlen, Chris Orvig, and Barry I. Posner
10. Chromium Supplemantation: Both Non-Essential and a Long-Term Health Risk?
Aviva Levina and Peter A. Lay
11. Cobalt-Schiff Base Complexes: Preclinical Research and Potential Therapeutic Uses
Elizabeth A. Bajema, Kaleigh Roberts, and Thomas J. Meade
12. Metal Compounds in the Development of Antiparasitic Agents: Rational Design from Basic Chemistry to the Clinic
Dinorah Gambino and Lucía Otero
13. Building a Trojan Horse: Sideophore-Drug Conjugates for the Diagnosis and Treatment of Infectious Diseases
Elzbieta Gumienna-Kontecka and Peggy L. Carver
14. Chemical and Clinical Aspects of Metal-Containing Antidotes for Poisoning by Cyanide
Sigrídur G. Suman and Johanna M. Gretarsdottir

Comments and suggestions with regard to contents, topics, and the like for future volumes of the series are welcome.

1

Cisplatin and Oxaliplatin: Our Current Understanding of Their Actions

Imogen A. Riddell and Stephen J. Lippard
Department of Chemistry, Massachusetts Institute of Technology, Cambridge, MA 02139, USA
<lippard@mit.edu>

ABSTRACT 2
1. INTRODUCTION 2
2. CELLULAR UPTAKE AND EFFLUX/MEMBRANE TRANSPORT 6
   2.1. Overview of Platinum Transport Processes 6
   2.2. Copper Transporters 7
      2.2.1. Copper Import Transporters 1 and 2 8
      2.2.2. P-Type Export Transporters 9
   2.3. Polyspecific Organic Cation Transporters 10
      2.3.1. SLC22A1-3 Transporters 11
      2.3.2. Multidrug and Toxin Extrusion Antiporters 12
3. COVALENT ADDUCTS GENERATED WITH PLATINUM AGENTS 13
   3.1. Cytosolic Transformations of Platinum Drugs 13
   3.2. Speciation of DNA-Platinum Adducts 15
   3.3. Effects on Chromatin 17
4. CELLULAR PROCESSING OF PLATINUM DNA ADDUCTS 18
   4.1. Inhibition of DNA Synthesis 18
   4.2. Transcription Inhibition 19
   4.3. Repair of Platinum Lesions 19
      4.3.1. Nucleotide Excision Repair 19
      4.3.2. Recombination Repair 21
      4.3.3 Fanconi's Anemia 21
      4.3.4. Mismatch Repair 22
      4.3.5. Base Excision Repair 22
   4.4. Protein Binding to Platinated DNA 23

Metal Ions in Life Sciences, Volume 18 Edited by Astrid Sigel, Helmut Sigel, Eva Freisinger, and Roland K. O. Sigel

https://doi.org/10.1515/9783110470734-001

5. SIGNAL TRANSDUCTION PATHWAYS ACTIVATED BY PLATINUM DNA DAMAGE 25
5.1. Overview of Signal Transduction 25
5.1.1. DNA Damage Sensors 26
5.1.2. Signal Transducers 26
5.2. Checkpoint Kinases 27
5.3. MAPK Proteins (ERK/JNK/p38) 27
5.4. Tumor Suppressor Protein p53 29
5.5. Oxaliplatin Does Not Induce a DNA Damage Response 29
6. UNDESIRED CONSEQUENCES OF PLATINUM-BASED CHEMOTHERAPY 30
6.1. Toxicity 30
6.2. Multifactorial Resistance 32
6.3. Cancer Stem Cell Enrichment 32
6.4. Mutagenicity 33
7. CONCLUDING REMARKS AND FUTURE DIRECTIONS 33
ACKNOWLEDGMENTS 34
ABBREVIATIONS AND DEFINITIONS 34
REFERENCES 35

Abstract: Following the serendipitous discovery of the anticancer activity of cisplatin over 50 years ago, a deep understanding of the chemical and biochemical transformations giving rise to its medicinal properties has developed allowing for improved treatment regimens and rational design of second and third generation drugs. This chapter begins with a brief historical review detailing initial results that led to the worldwide clinical approval of cisplatin and development of the field of metal anticancer agents. Later sections summarize our understanding of key mechanistic features including drug uptake, formation of covalent adducts with DNA, recognition and repair of Pt-DNA adducts, and the DNA damage response, with respect to cisplatin and oxaliplatin. The final section highlights known shortcomings of classical platinum anticancer agents, including problems with toxicity and mutagenicity, and the development of resistance and enrichment of cancer stem cells brought about through treatment. Instances where specific differences in the response or mechanism of action of cisplatin versus oxaliplatin have been demonstrated are discussed in the text. In this manner the chapter provides a broad overview of our current understanding of the mechanism of action of platinum anticancer agents, providing a framework for improving the rational design of better Pt-based anticancer agents.

Keywords: anticancer · DNA damage response · DNA repair · mechanistic understanding · platinum

1. INTRODUCTION

Following Barnett (Barney) Rosenberg's appointment to Michigan State University in 1961 he began to investigate the possibility that cell division might be affected by electric fields having noted that the arrangement of the mitotic spindle in dividing cells resembled that of iron filings within a magnetic field [1, 2]. Initial experiments performed with *Escherichia coli* (*E. coli*) bacterial cells grown in ammonium chloride-buffered solutions stimulated with platinum electrodes

showed distinctive changes in morphology [3]. Elongation of the bacterial cells was ultimately determined to arise from inhibition of cellular division while cell growth was maintained, allowing filamentous strands to grow up to 300 times their normal length. Further studies determined that it was not the electric field, but platinum compounds generated at 1–10 ppm concentrations under the experimental conditions, that brought about the morphological changes [4, 5]. Subsequent experiments probing the effect of *cis*-dichlorodiammineplatinum(II) (cisplatin or CDDP) and *cis*-tetrachlorodiammineplatinum(IV) on sarcoma 180 and leukemia L1210 mouse models confirmed the potent anticancer activity of cisplatin and led to a collaboration with the National Cancer Institute (NCI) [6]. The NCI had over the previous 15 years screened approximately 140,000 compounds to assess their anticancer activity [5], however, inorganic compounds had ceased to be of interest to the community and only a handful of the compounds evaluated contained metals.

Despite the predisposition against metal compounds as chemotherapeutic agents at the time, cisplatin displayed broad-spectrum activity against transplantable, carcinogenically-induced, and virally-generated tumors. In addition, experiments revealed that even highly advanced stage tumors could be treated successfully with cisplatin [5] and, appropriately, the clinical development of cisplatin was fast-tracked with initial clinical trials being run in 1971 [7, 8] and Platinol, the trade name for cisplatin, was brought to the market by Bristol Laboratories (later Bristol-Myers Squibb) in 1978. Initially, Food and Drug Administration (FDA) approval was given for the treatment of advanced testicular, ovarian, and bladder cancers. Since then, however, the spectrum of cancers for which cisplatin has received approval was significantly extended to include cervix, head and neck, esophageal, and small cell lung cancers as well as some pediatric malignancies among many others.

Although it was clear from preclinical studies [9] onwards that cisplatin was a very potent anticancer agent with broad-spectrum activity, it suffered from certain toxic side effects. Preclinical studies indicted platinum concentration in the excretory organs and that it could persist in the body for up to four months after treatment. Nephrotoxicity reported in beagle dogs continued to be a major concern throughout Phase I studies. However, the discovery that high-volume fluid hydration [10] and forced diuresis could prevent renal damage combined with unprecedented cures of testicular germ cell tumors ensured continued development of the drug candidate [2]. Similarly potent antiemetics including the 5HT3 antagonists [11–13] were developed to overcome acute and delayed emesis as a result of cisplatin treatment.

In addition to research for the development of protective compounds able to ameliorate the undesired side effects of cisplatin, another key area of research was the discovery of less toxic cisplatin analogs. Several second-generation compounds containing dicarboxylate leaving groups in place of the more labile chloride ions of the parent compound cisplatin were investigated in the 1980s based on the hypothesis that platinum(II) diammine compounds containing more stable leaving groups would retain the desired anticancer properties while imparting lower toxicity and more predictable pharmokinetics [2, 14]. This hypothesis

turned out to be correct for carboplatin, which was granted FDA approval in 1989, and is now widely used in clinics primarily in the treatment of ovarian cancer and where patients have recurrent, platinum-resistant disease. Research indicated that the adducts formed by carboplatin are identical to those of cisplatin, but the rate of adduct formation is 10-fold slower, which necessitates 20- to 40-fold higher concentrations of carboplatin to produce the same number of adducts [15]. Four other analogs, namely, enloplatin (1,1-cyclobutane dicarboxylato-O′,O′ tetrahydro-4H pyran-4,4-dimethylamine-N′,N′ platinum(II)), zeniplatin (2,2-bis aminomethyl-1,3-propandiol-N-N′ 1,1-cyclobutane dicarboxylate-O′,O′ platinum(II)), NK-121/C1–973 (*cis*-1,1-cyclobutane dicarboxylato(2R)-2-methyl-1,4-butanediamine platinum(II)), and miboplatin (R-2-amino methyl pyrrolidine 1,1-cyclobutane dicarboxylate platinum(II)) also entered clinical trials in the 1980s [12, 16], but with the exception of miboplatin they all suffered from loss of anticancer activity and/or dose-limiting toxicity. In contrast, miboplatin performed well, and reached Phase III clinical trials in Japan. Ultimately, however, miboplatin was abandoned despite its good anticancer activity, for it showed no clear advantage over cisplatin [12].

In addition to lowering toxicity, significant research has been invested into improving the spectrum of activity of platinum anticancer agents, with oxaliplatin (*trans*-L-diaminocyclohexane oxalate platinum(II)) emerging as the prominent third-generation drug. Oxaliplatin was originally proposed as a potential anticancer agent in the late 1970s [17] but did not receive FDA approval until 2002 [18]. Early murine leukemia studies indicated that oxaliplatin performed better than cisplatin while showing reduced side effects [12]. Moreover, *in vitro* screening of oxaliplatin against the NCI-60 human cancer cell panel [19] indicated that oxaliplatin might provide a suitable treatment for cancers including colon cancer that do not respond to cisplatin treatment. Following four large Phase III trials in the early 2000s that demonstrated the potential of oxaliplatin treatment in combination with 5-fluorouracil and leucovorin for the treatment of metastatic colon cancer [14], oxaliplatin was given FDA approval. Prior to oxaliplatin approval it was widely accepted that colon cancer did not respond to treatment with platinum agents, with response rates reported as low as 19 % [20] and 22 % [21], respectively, following cisplatin treatment. In contrast, colorectal cancer response rates were significantly improved, with oxaliplatin-based chemotherapy raising this value to 50 % [22].

In addition to cisplatin, carboplatin, and oxaliplatin, which have received worldwide approval, nedaplatin (diammine[hydroxyacetato-O,O′]platinum(II)) was approved for treatment in Japan, lobaplatin ([2-hydroxypropanoato-O1,O2][1,2-cyclobutanedimethanamine-N,N′]platinum(II)) for treatment in China, and heptaplatin ([propanedioato-O,O′][2-(1-methylethyl)-1,3-dioxolane-4,5-dimethanamine-N,N′]platinum(II)) for treatment in the Republic of Korea (Figure 1).

With the advent of platinum drugs and altered behavioral patterns, cancer prognosis improved significantly over the last fifty years. Approval of cisplatin and subsequent optimization in treatment regimes for platinum drugs, combined with an increased understanding of the factors that promote cancer, have ultimately reduced cancer incidence and provided cures. In particular, successes in

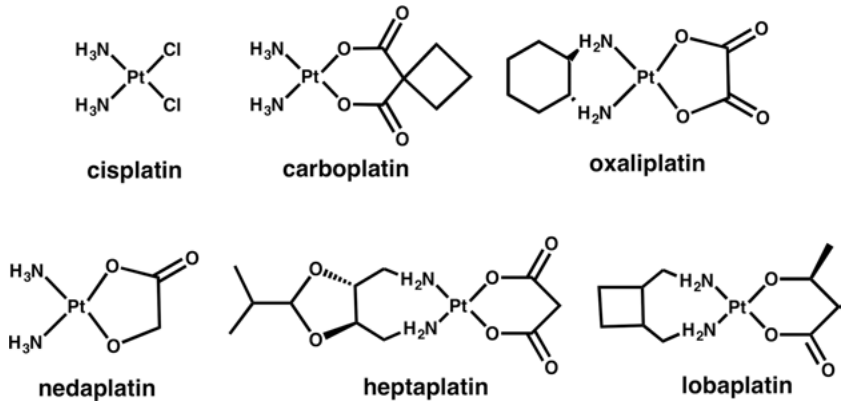

Figure 1. Platinum drugs that have received clinical approval for cancer treatment in at least one country. Cisplatin, carboplatin, and oxaliplatin have all received worldwide approval, while nedaplatin is approved in Japan, heptaplatin in the Republic of Korea, and lobaplatin in China.

treatment of testicular cancer and lung cancer across this period are clearly identified from cancer statistics [23]. Prior to approval of cisplatin, testicular cancer was only curable in its earliest stages through a combination of aggressive surgery and radiation, but for patients in the later stage of the disease a diagnosis was almost always fatal [8]. In stark contrast, cisplatin treatment offers an overall 90 % cure rate, which, when coupled with public education campaigns highlighting the importance of early detection, has resulted in a sharp decline in cancer-related deaths in men. Similarly, public education campaigns and governmental policies restricting the sale of tobacco have significantly lessened the incidence of lung cancer. The American Cancer Institute reports cancer-related deaths in the US have decreased by 23 % since 1991, a value that corresponds to 1.7 millions deaths being averted since 2012 [23]. Continued research to identify improved anticancer agents able to target resistant cancer cell lines, or combat recurrent disease in combination with increased understanding of the mechanistic actions of platinum agents offers the possibility to further improve these statistics. In particular, as we move into the era of personalized medicine, detailed mechanistic studies are expected to be invaluable in guiding clinicians to the best treatment regimens, optimized to take advantage of an individual's biochemistry and/or genetics.

The present chapter provides a broad summary of our current knowledge of the mechanisms of action of cisplatin and oxaliplatin, detailing mechanisms by which platinum agents pass through cell membranes (Section 2), form covalent adducts with biological nucleophiles (Section 3), and are processed by cellular machinery (Sections 4 and 5). Finally, we conclude by highlighting specific challenges that the medicinal inorganic community is yet to overcome. For many of these challenges non-classical anticancer agents, including monofunctional, multi-nuclear, or non-platinum based anticancer agents that are discussed in later

chapters of this book have been postulated to further exceed the potency of the approved platinum drugs.

2. CELLULAR UPTAKE AND EFFLUX/MEMBRANE TRANSPORT

2.1. Overview of Platinum Transport Processes

The anticancer activity of both cisplatin and oxaliplatin arises from the ability of these complexes to generate covalent adducts with nuclear DNA, which ultimately triggers cell death [24]. In order to generate platinum-DNA adducts, the platinum agents must avoid deactivation in the bloodstream and be internalized by the cell. Once inside the cell platinum agents will undergo aquation due to the reduced concentration of chloride ions in the cytosol compared with the extracellular chloride concentration, and then, following localization in the nucleus, bind covalently at the most nucleophilic sites on DNA. Cellular uptake thus serves as a critical step in the mechanism of action of platinum anticancer agents. Of equal importance is the ability of cells to effectively export platinum agents, with platinum efflux being a demonstrated mechanism by which cells can become resistant to platinum-based chemotherapy [25]; export also mediates toxic side effects associated with platinum-based chemotherapy [26].

Both active and passive processes have been implicated in platinum agent membrane transport [27] (Figure 2), the difference being that active transport employs a receptor that utilizes energy to convey the platinum agent, whereas passive transport occurs without the need for energy input. Passive diffusion refers to processes by which platinum agents diffuse through the lipid membrane to enter cells and requires neither energy input nor a transporter for platinum uptake [28].

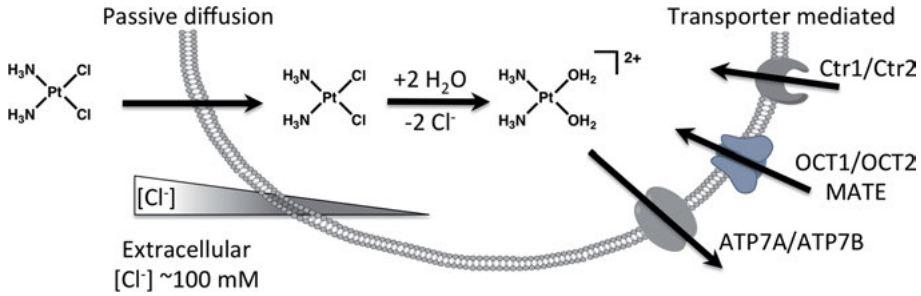

Figure 2. Summary of the proposed platinum transport processes including passive diffusion driven by reduced intracellular chloride concentration, and the postulated transporter-mediated processes including uptake by copper transporters Ctr1 and Ctr2 and the polyspecific organic cation transporters OCT1, OCT2, and MATE, and export via P-type ATPases ATP7A and ATP7B.

Early research examining the cellular accumulation of cisplatin and its analogs concluded that passive diffusion was the main route by which cisplatin accumulates in cells [29]. Support for passive uptake of cisplatin was provided by the observations that (i) cellular uptake depended linearly on cisplatin concentration and (ii) that structural analogs of cisplatin did not inhibit uptake, as expected if active transport were implicated. More recently the possibility that passive diffusion might be operative for cisplatin uptake was reinvestigated, providing compelling evidence that protein-mediated uptake is not an absolute requirement for cisplatin accumulation [30]. These observations, combined with the growing skepticism surrounding mechanisms of active transport, call into question whether passive transport is the dominant mechanism for cellular uptake of cisplatin.

To test the hypothesis that cisplatin is internalized through passive diffusion, the permeability coefficient, P_d, of cisplatin was monitored as a function of the chloride concentration of the medium using unilamellar DOPC vesicles. Here, P_d is defined by Equation (1):

$$P_d = \frac{k_{obs} r}{3} \tag{1}$$

where k_{obs} is the rate of cisplatin uptake, measured by stopped-flow spectroscopy, and r is the average vesicle radius, as measured by dynamic light scattering. These studies showed a gradual increase in P_d as a function of chloride concentration up to approximately 100 μM, at which point the system was saturated, consistent with passive diffusion of cisplatin into the vesicles. The authors argue that the internalization and accumulation of cisplatin in cells through passive diffusion is not surprising given the speciation of cisplatin intra- and extracellularly. Outside of the cell cisplatin has an overall neutral charge and is therefore not subjected to the large Born energy barrier that prevents many small, hydrophilic ions from crossing the plasma membrane. However, once internalized, cisplatin will form a mixture of mono- and dicationic species that will have to pay a large energy penalty (100–300 $kJmol^{-1}$) to passively diffuse out of the cell. These differential energy requirements for passive diffusion of cisplatin into and out of the cell are believed to account for the cellular accumulation observed for cisplatin [30].

Extensive research into active transporters expressed on the cell surface has also been undertaken and a detailed discussion of the role of the copper transporters, organic cation transporters, and multidrug and toxin extrusion protein is given below. Unlike passive diffusion, utilizing membrane transporters for drug uptake offers opportunities for selective targeting of tumor cells and reduced toxic side effects in instances where the transporter is preferentially expressed in specific tissues.

2.2. Copper Transporters

The copper transporters Ctr1, Ctr2, ATP7A, and ATP7B as well as the copper chaperone ATOX1 have all been implicated in the regulation of cisplatin in mammalian cells [31, 32]; however, the mechanism by which these transporters

interact with cisplatin remains unknown. Therefore, speculation as to which of the transporters is the most influential and indeed, whether or not these transporters actually play a critical role in import and export of cisplatin and its analogs, remains unknown [33]. Furthermore, recent findings support the hypothesis that reduction of cellular copper sensitizes cells to cisplatin treatment [34], adding to the debate around whether copper transporters facilitate cisplatin transport across the membrane.

2.2.1. Copper Import Transporters 1 and 2

The copper transporter proteins 1 and 2, (Ctr1; *SLC31A1* and Ctr2; *SLC31A2*, respectively), share considerable structure homology while varying in their amino acid sequences, with only 41 % conserved residues [32]. They are surface receptors generated from homotrimers of the monomer unit. Their primary function is copper homeostasis, providing a mechanism by which copper can enter cells, but in recent years they have received attention as a transporter for cisplatin.

Initial studies in yeast correlated intracellular platinum concentrations with yCtr1 expression levels [35, 36]. Subsequent work confirmed an equivalent correlation between human Ctr1 expression and cisplatin uptake, when hCtr1 was forcibly overexpressed [37]. Several research groups have also reported reduced Ctr1 expression in cisplatin resistant cell lines [38, 39] and downregulation of Ctr1 in response to cisplatin treatment [40]. Reports that the Ctr1 transporter is internalized in response to cisplatin treatment [41] led to the suggestion that resistance may arise from reduced cisplatin uptake by Ctr1 transporters. A recent clinical study also identified two single nucleotide polymorphisms present in the Ctr1 genes of patients with non-small cell lung cancer who did not respond well to platinum chemotherapy [42].

However, as Ivy and Kaplin [33] point out, all of these data are 'correlative and not causative' and there is a growing body of evidence that supports Ctr1 being unable to import cisplatin into a cell. Recently [33], experiments that were initially put forward as evidence of passive diffusion of cisplatin into cells confirmed that uptake does not saturate at biologically relevant concentrations. This result indicates that cisplatin uptake is most likely not protein-mediated. In the same publication the authors also evaluated cisplatin and copper uptake in HEK cells expressing hCtr1 under the influence of a tetracycline-sensitive promotor. There was growth in the presence of tetracycline that increased the copper uptake by 8- to 10-fold, but cisplatin uptake was unchanged irrespective of whether or not tetracycline was present. Similarly, by comparing Ctr1 (+/+) and Ctr1(–/–) mouse embryonic fibroblasts (MEFs), the authors saw no difference in the rate of cisplatin uptake and no difference in uptake in Ctr1(+/+) MEFs when copper was added, indicating that copper does not compete with cisplatin for the mechanism of uptake. Recently, work using the CRISPR-Cas9 genome editing system to systematically knockout CTR1, CTR2, ATOX1 or CCS from HEK-293T cells [43] revealed that, following knockdown, none of the cell lines exhibited greater cisplatin sensitivity than the variance in the parental populations. The results indicate that neither Ctr1 nor Ctr2 is implicated in the mechanism of cisplatin uptake.

Structural modification of Ctr1 has also provided insight into the potential mechanism by which the copper transporter may interact with cisplatin. Deletion of the N-terminal extracellular domain of hCTR1 reduced cisplatin uptake while completely eliminating copper uptake [44]. Modification of Met150, Met154 or His139, the three residues involved in the transchelation mechanism invoked for copper uptake, disabled copper uptake but increased cisplatin accumulation [45]. These results together with the limited pore size of Ctr1 (estimated to be 8 Å), smaller than the estimated radius of cisplatin (9.57 Å), suggest that if Ctr1 is involved in cisplatin uptake the mechanism by which cisplatin is internalized by Ctr1 must be significantly different from that of copper [33].

Less is known about the function of mammalian Ctr2 than Ctr1, but due to structural similarity between the transporters the effect of Ctr2 on cisplatin uptake was evaluated [46, 47]. Ctr2 binds copper albeit with a lower affinity than Ctr1 (K_m ~1.7 μM versus ~6–10 μM, respectively), but the differential localization of Ctr1 and Ctr2 indicates that they may play different roles in copper homeostasis and interact differentially with cisplatin [32]. Ctr1 is localized exclusively to the membrane, whereas Ctr2 is found in late endosomes, lysomes, and the nucleus. Initial studies indicated that, unlike Ctr1, knockdown of Ctr2 enhances platinum uptake and the platinum sensitivity of cells [46]. Following Ctr2 knockdown in MEFs, cisplatin and carboplatin uptake increased by 2- to 3-fold, independent of Ctr1 expression levels. The increased platinum concentration was attributed to an initial influx of platinum and not from decreased efflux of platinum agents from the cells or increased concentration of platinum in intracellular vesicles. Similar results were observed in mouse xenograft models. When Ctr2 was knocked down, there was a 9.1-fold increase in platinum at the tumor site relative to the parent cell line [48]. However, in the most recent paper where Ctr2 was knocked out by using CRISPR-Cas9, the same authors acknowledge that the 2- to 5-fold changes in cisplatin sensitivity do not exceed the variance observed in the parental populations, thereby negating a role for Ctr2 in cisplatin uptake [43]. Further work is required to establish a relevance of Ctr1 and Ctr2 expression in cancer treatment, either as a prognostic marker or as a harbinger of successful treatment.

2.2.2. P-Type Export Transporters

The p-type proteins, ATP7A and ATP7B, function primarily to sequester and extrude excess copper. These transporters share 65 % amino acid sequence and homologous structures comprising eight transmembrane domains [27] and a conserved CxxC domain [49], but are differentiated by their tissue expression and interaction with platinum agents. ATP7A is expressed preferentially in the intestine, choroid plexus in smooth muscle cells, vascular endothelial cells, aorta, and cerebrovascular endothelial cells, whereas ATP7B is primarily expressed in liver and brain [26].

Both p-type proteins have been linked with cisplatin resistance, although the mechanism by which resistance occurs appears to differ subtly. Both transporters mediate platinum sequestration in intracellular vesicles, but cells expressing

ATP7B appear to promote trafficking and extracellular efflux of the platinum to a far greater extent than those expressing ATP7A. Cells expressing ATP7A typically show increased intracellular platinum accumulation despite having high cisplatin and oxaliplatin resistance [50]. In contrast, overexpression of ATP7B has been correlated with reduced cisplatin uptake and an increased rate of platinum efflux [51]. Employing fluorescently tagged ATP7B and a fluorescein-labeled cisplatin analog, it was observed that intracellular platinum and ATP7B colocalize within vesicles that subsequently move toward the cell surface [50].

In particular, ATP7B has been more closely linked with cisplatin resistance than either Ctr1 or ATP7A [52]. Therapeutically, a strong correlation exists between patients having a poor outcome for oxaliplatin treatment of colorectal cancer and those displaying increased levels of ATP7B [53]. Recent studies evaluating co-delivery of an ATP7B silencing siRNA alongside cisplatin [53] have shown great promise, increasing the human oral squamous cell line OSC-19-R sensitivity by 10.6-fold over cells not transfected with siRNA [52]. The dual therapy reduces cancer cell proliferation and angiogenesis while increasing tumor cell apoptosis.

2.3. Polyspecific Organic Cation Transporters

The organic cation transporters (OCT1-3; *SLC22A1-3*) and multidrug and toxin extrusion antiporters (MATE; *SLC47*) are termed polyspecific because they transport a broad range of compounds, both endogenous and exogenous, having different sizes and molecular structures. By contrast, the majority of membrane transporters are metabolite- or nutrient-specific and are termed oligospecific [54–56].

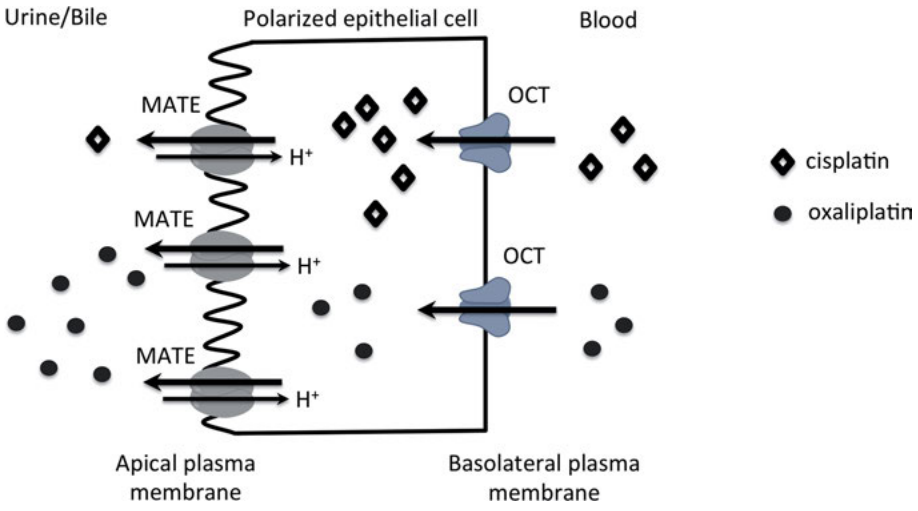

Figure 3. Vectorial movement of platinum agents from the blood to urine or bile, through the basolateral then apical membrane of a polarized epithelial cell. The differential uptake of cisplatin and oxaliplatin by OCTs and MATEs is highlighted.

Both OCTs and MATEs are highly expressed in excretory organs where they work sequentially to move organic cations from the blood to either the bile in the liver or to urine in the kidneys [54]. In the initial step, OCTs transfer substrates through the basolateral membrane of polarized epithelial cells before they interact with MATEs localized in the apical plasma membrane (Figure 3).

Given the wide variety of substrates transported by polyspecific transporters, large variations in the binding affinity and rate of transport for different species are expected and, critically, not all substrates transported by OCTs are good substrates for MATEs. This differential binding (Figure 3) is intimately linked with drug toxicity and provides a strong rationale for why some platinum agents and not others are nephrotoxic [26, 54].

2.3.1. SLC22A1-3 Transporters

The organic cation transporters, OCT1-3, are expressed in different locations and it is important to note for translational purposes that variations in distribution between human and rodent orthologs have been reported [57]. hOCT1 is preferentially expressed in the liver, hOCT2 in the kidney and brain, specifically in dopamine-rich regions of the pyramidal cells of the cerebral cortex and the hippocampus, and hOCT3 in a broad range of tissues including brain, heart, liver, skeletal muscle, placenta, and kidney [56]. Despite their differential expression, all OCTs function as bidirectional transporters for small hydrophobic compounds ~60–350 Da in size [55]. Research indicates that both cisplatin and oxaliplatin are substrates for hOCTs, and because the mechanism of transport relies on both an electrical and concentration gradient [54], the intracellular platinum concentration may exceed the extracellular platinum concentration.

Renal tubular epithelial cell toxicity was linked with cisplatin nephrotoxicity for many years; however, the molecular mechanisms of action giving rise to this toxicity did not become apparent until the discovery of OCT1 in 1994 [58]. Subsequent studies with OCT1/2 knockout mice confirmed the role of OCTs in excretion of organic cations [59]. Direct evidence for the role of OCTs in cisplatin uptake came in 2005 when two groups [60, 61] transfected HEK293 cells with rat and human orthologs of OCT2, respectively, and observed increased cellular uptake of platinum, correlating with increased cell death. Subsequent studies employing inhibitors of OCT2 [62] and OCT2 knockout mice [63] confirmed the initial observations that OCT2 is a key determinant of cisplatin-induced nephrotoxicity. Clinical data also support use of cimetidine, a known OCT2 substrate, as a protective agent for the kidneys of patients undergoing cisplatin treatment [64, 65].

Following the observation that OCT2 is expressed in the outer hair cells and the stria vascularis cells of the cochlea [66], the role of OCTs in ototoxicity has also been investigated. Reduced or completely eliminated ototoxicity was observed following genetic deletion of OCT1 and OCT2 [63], and co-treatment of cisplatin with cimetidine in mice [66] confirmed the conclusion that cisplatin uptake by OCTs is linked with both nephro- and ototoxicity.

In contrast to cisplatin, oxaliplatin exhibits low nephrotoxicity. Therefore, based on the hypothesis above it might be expected that oxaliplatin is not trans-

ported by OCTs. Indeed, when carboplatin and nedaplatin, widely regarded to have low nephrotoxicity, were evaluated for uptake in OCTs, no evidence for their transport was recorded [67]. Oxaliplatin, however, interacts strongly with hOCT2 as demonstrated through cell studies [67, 68] and visual inspection of renal slices having collapsed non-perfused lumens [69]. The nephrotoxic patterns of these slices resemble those of cisplatin and, therefore, the hypothesis was drawn that platinum uptake via OCTs is non-toxic when coupled with an effective efflux transporter [67]; this transporter was later identified as the hMATE transporter (see below, Section 2.3.2).

Variations in OCT substrate specificity and the implications thereof are highlighted by uptake data for hOCT3. The observation that oxaliplatin but not cisplatin is a substrate for hOCT3, which is expressed among other locations in the intestine, led researchers to postulate that the cytotoxicity of oxaliplatin against colon cancer cells arises at least in part from the expression of hOCT3 in this location [67]. Moreover, recent studies have indicated a correlation between hOCT3 expression in cancerous versus non-cancerous colon and rectal tissues, with a 9.7-fold higher mRNA level being reported for patient-derived colon cancer tissues over their non-cancerous counterparts [70].

2.3.2. Multidrug and Toxin Extrusion Antiporters

As noted above hMATEs including hMATE1 and hMATE2-K are widely accepted to be efflux transporters that protect cells by transferring organic cations to the bile and urine. Experiments in mice with genetic deletion of hMATE support this postulate through increased incidence of nephrotoxicity [71]. As with the OCTs, MATE tissue distribution varies between species with hMATE1 being highly expressed in the kidney, liver, heart, skeletal muscle, and other locations, whereas hMATE2-K is kidney-specific [56].

Contradictory results have been reported for the uptake of cisplatin by hMATE1, in part due to the H^+/organic cation antiporter nature of the transporter, which requires pretreatment of cells with ammonium chloride to activate the H^+ gradient across the plasma membrane [26]. However, good substrate specificity has been demonstrated for MATE2-K, with oxaliplatin being readily taken up by this transporter while cisplatin is not [67]. This specificity, combined with hMATE2-K localization in the kidneys, has led to the hypothesis that the differential nephrotoxicity of oxaliplatin and cisplatin arises from their interaction with hOCT2 and hMATE2-K, facilitating their passage into the waste stream. If, like cisplatin, a platinum complex interacts with only the import transporter hOCT2 it will most likely exhibit toxic side effects due to renal accumulation [72] (Figure 3).

3. COVALENT ADDUCTS GENERATED WITH PLATINUM AGENTS

3.1. Cytosolic Transformations of Platinum Drugs

It is widely accepted that when platinum agents pass into a cell they readily undergo aquation in response to the significant decrease in chloride concentration between the extracellular blood plasma (~100 mM) and the intracellular cytosol [24, 25, 30]. The chloride ion concentration within a cell is typically reported at 4 mM based on application of the Nernst equation to passive diffusion of chloride across the plasma membrane in muscle and nerve cells [73], however, direct measurements within a range of cells including cancer cells reveal actual intracellular chloride concentrations in the 12–55 mM range [73]. Diffusion of aquated, cationic platinum complexes out of the cell is unfavorable, and instead they react with a variety of cellular components, including DNA, RNA, proteins, phospholipids, and thiol complexes, via competing pathways [74–77]. The thermodynamics and kinetics of many of these pathways have been extensively studied as platinum speciation is intimately linked with the efficacy and toxicity of platinum agents.

For cisplatin it has been shown that the neutral parent complex *cis*-$[Pt(NH_3)_2Cl_2]$ (**1**; Figure 4) fails to react directly with typical nitrogen and oxygen donor biological nucleophiles; however, complexes activated by replacement of chloride ligands with labile water ligands ($t_{1/2}$ ~2 h) are 10–70 × more reactive than their parent starting material and react indiscriminately with biological nucleophiles [73, 77]. The rate of reaction for complex **2** with biological nucleophiles ($t_{1/2}$ ~0.1 h) occurs on a sufficiently fast timeframe that **4** is not observed in appreciable concentrations *in vivo* [74].

In addition to aquation, deprotonation of coordinated water molecules may occur to generate the hydroxo complexes *cis*-$[Pt(NH_3)_2Cl(OH)]$ (**3**) and *cis*-$[Pt(NH_3)_2(OH)_2]$ (**6**) that are considerably less reactive than their corresponding aqua species **2** and **4** owing to the relative inertness of the Pt–OH bond. Furthermore, formation of hydroxide-bridged oligomers [74] of the form $[\{Pt(NH_3)_2(\mu\text{-}OH)\}_n]^{n+}$ have been reported under specific conditions. The extent of deprotonation of the aqua ligands (K_a) is governed by its pK_a and the pH of the aqueous solution. Recent studies employing ^{15}N-edited ^{1}H and [^{1}H,^{15}N] heteronuclear multiple quantum interference NMR spectroscopy [78] provide the most accurate measurements of the pK_a values for cisplatin. In particular, this methodology overcomes complications associated with fitting potentiometric curves comprising multiple overlapping events and reduction in signal due to formation of hydroxo bridged dimers. pK_a values of 6.41 for *cis*-$[PtCl(H_2O)(NH_3)_2]^+$ and 5.37 and 7.21 for *cis*-$[Pt(H_2O)_2(NH_3)_2]^+$, were reported, in agreement with previous reports.

Single crystal X-ray diffraction [79, 80] and ^{195}Pt NMR spectroscopic studies [81] support the formation of the dimers, trimers, and higher oligomers when the pH of the solution is within two pK_a units of the Pt–OH_2 bond (pK_a ± 2). Formation of hydroxide-bridged dimers is undesired because they remove active

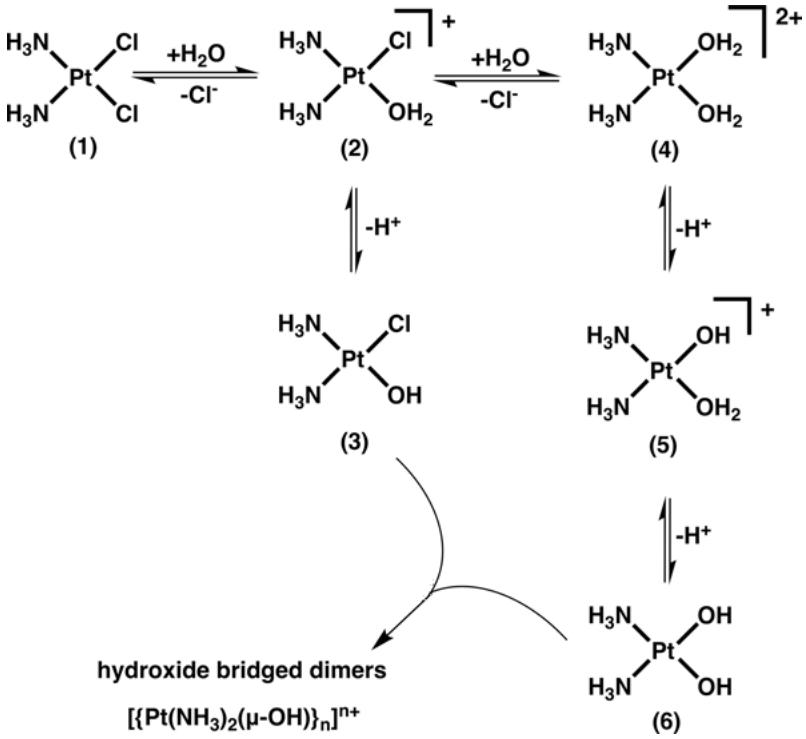

Figure 4. Structures and equilibria of species derived from cisplatin in aqueous solution.

drug from solution and may modulate toxicity [82]. Detailed studies indicate that, if the mononuclear diammineplatinum(II) complex is injected into a patient, the platinum concentration *in vivo* will be sufficiently low to prevent oligomer formation. However, should a hydroxo-bridged oligomer be injected it would most likely persist [74, 83, 84], highlighting the importance of properly storing and administering the drug.

Cisplatin may also react with other biological nucleophiles including sulfur atom donor species [76] and carbonate [85]. The high affinity of thiolate anions for platinum complexes has been cited as a major cause of platinum drug resistance [25], with increased intracellular glutathione and overexpression of glutathione S-transferase [86, 87] being correlated strongly with resistance. Experimental evidence indicates that sulfur nucleophiles react directly with cisplatin without the need for activation via aquation [88]. Furthermore, recent research has indicated that Pt-guanosine adducts may be generated more rapidly in the presence of sulfur nucleophiles [89], but the importance of this reaction pathway in platinum treatment regimens has yet to be determined.

Like cisplatin, oxaliplatin forms adducts with a variety of biological nucleophiles following aquation. *In vivo*, biotransformation studies were performed where the plasma ultrafiltrate of five patients who received oxaliplatin by infusion at 130 mg/m^2 for 2 h was analyzed, and the $[Pt(DACH)(Cl)(OH_2)]^+$

(DACH = *trans-R,R*-1,2-diaminocyclohexane) derivative was identified as the major species (31–100 %) by HPLC. Methionine (8–24 %), diaqua (2–26 %), monochlorocreatinine (2–11 %), and glutathione (1 %) adducts were also tentatively identified [90].

3.2. Speciation of DNA-Platinum Adducts

Within the cell, cisplatin forms adducts with both nuclear and mitochondrial DNA [91]. Aside from its localization, mitochondrial DNA differs from nuclear DNA in its lack of histones and slower kinetics of cisplatin intrastrand cross-link repair [92] (discussed below). A larger percentage of Pt-DNA adducts [93] (4- to 6-fold [94]) have been reported for mitochondrial DNA over nuclear DNA, and this difference has been attributed to higher initial binding rates and inefficient removal of the major adducts by repair processes [95].

Most research has focused on the ability of cisplatin to modify nuclear DNA, and it is widely accepted that platinum reaching the nucleus without being deactivated primarily forms covalent adducts at the N^7 position of the purine bases [91, 96]. The monoaqua adduct of cisplatin ($t_{1/2}$ = ~2 hours) reacts rapidly to generate covalent adducts with the N^7 positions on adenine and guanine bases ($t_{1/2}$ = 0.1 h), after which the second chloride ligand is aquated to facilitate formation of a bifunctional cross-link [24, 77]. Cross-links are designated as 1,2- or 1,3-intra- or interstrand cross-links, where the numeric designation specifies whether two modified nucleotides are adjacent to each other (1,2-d(GpG)) or separated by an unmodified nucleotide N (1,3-d(GpNpG)). For intrastrand cross-links both modified nucleotides are on the same strand of the DNA, whereas interstrand cross-links have one modified nucleotide on each strand of duplex DNA. Numerous enzymatic degradation and acid hydrolysis experiments have been performed to elucidate the distribution of Pt-DNA adducts with nuclear DNA. The consensus is that approximately 60–65 % of Pt-DNA adducts are 1,2-intrastrand d(GpG) links, 25–30 % are 1,2-intrastrand d(ApG) links, 5–10 % are 1,3-intrastrand d(GpNpG) linkages, and 1–3 % of Pt-DNA adducts are interstrand cross-links (ICLs) [97, 98]. Comparable Pt-DNA adduct profiles are reported for oxaliplatin [99].

Each platinum adduct distorts and unwinds the structure of double-stranded DNA to which it is bound in a unique manner [100]. Single crystal X-ray structures (Figure 5) of platinum adducts of double-stranded DNA have provided insight into the structural basis of DNA processing events that are influenced by platinum binding. Analysis of the solid state structure of the major cisplatin 1,2-d(GpG) intrastrand cross-link [101] (Figure 5A) reveals that the Pt adduct forms hydrogen bonds with the DNA backbone on the 5′ side of the lesion and unwinds the duplex DNA by ~25°. In the solid state, a global bend of 35–40° in the DNA occurs, whereas NMR data [102, 103] suggest that, in solution, this bend angle may be significantly increased, up to 60–70°. The 1,3-d(GpNpG) minor adduct [104] (Figure 5B) is globally bent by about 30°, but the region around the platinated nucleotide is more severely distorted. In contrast to both the intrastrand

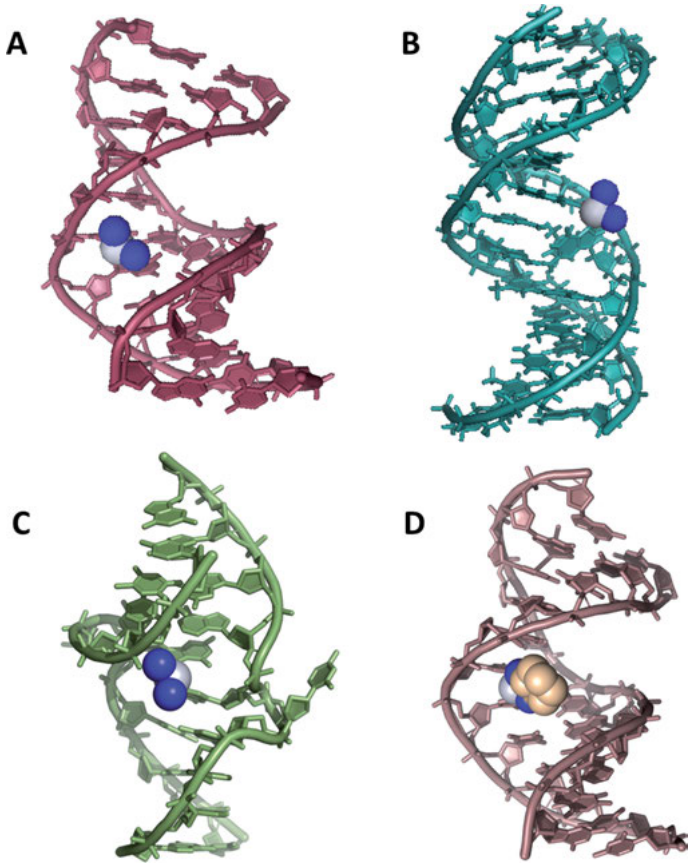

Figure 5. X-ray crystal structures of platinum lesions on duplex DNA. (**A**) 1,2-d(GpG) cisplatin lesion (1AIO [101]); (**B**) 1,3-d(GpG) cisplatin lesion (1DA4 [104]); (**C**) interstrand cisplatin lesion (1A2E [105]); (**D**) 1,2-d(GpG) oxaliplatin lesion (1IHH [106]). Cisplatin and oxaliplatin are shown in space-filling representation; platinum(grey), nitrogen(blue), and carbon (beige).

cross-links, crystal structures of a cisplatin interstrand cross-link [105] (Figure 5C) reveal that the duplex is bent at a 47° angle toward the minor instead of the major groove, and that the duplex is unwound by 110° overall. Finally, analysis of the crystal structure of the oxaliplatin adduct on duplex DNA [106] (Figure 5D) highlights the effects of exchanging a *cis*-diammine(II) [80] moiety for a *cis*-{Pt(DACH)}$^{2+}$ group, mainly involving a change in hydrogen bonding around the lesions. In contrast to cisplatin, structural characterization of oxaliplatin DNA adducts supports hydrogen bond formation between the platinum adduct and the DNA backbone on the 3′ side of the cross-link [107]. Only the biologically active *R,R*-isomer, and not the *S,S*-isomer, can generate 3′ hydrogen bonds. This conformational difference between cisplatin and oxaliplatin adducts is proposed

to interfere with the recognition of the damaged DNA by cellular components, contributing to the differential properties of the two drug molecules [100].

3.3. Effects on Chromatin

DNA in the nucleus is packaged as nucleosomes, which consist of a core of eight histone proteins $(H_{2a}H_{2b}H_3H_4)_2$ around which genomic DNA (146 bp duplex) is wrapped in a shallow, left-handed helix. The nucleosomes are separated by strings of linker DNA (typically 10–50 bp [108]) that are not tightly bound to proteins. Because the positioning of the genome on the nucleosome influences gene expression [109], and it has been proposed that platination of nucleosomal DNA may alter its positioning [110], several groups have investigated chromatin modification by cisplatin and related platinum agents.

Early studies [111] confirmed that the formation of cisplatin adducts with DNA occurred to a similar extent in the presence and absence of core proteins, with an average of ~45 platinum atoms per core particle being reported upon saturation after 40 hours. Additionally, in contrast to the *trans* isomer (*trans*-dichlorodiammineplatinum(II)), no significant histone-histone or histone-DNA cross-links were observed. Later studies sought to evaluate whether cisplatin preferentially formed covalent adducts with linker versus nucleosomal DNA [112–114], and it was concluded that platinum adducts preferentially form in the linker region [113]. Measurement of the rate of platinum adduct formation with chromatin, core particle, and DNA as a function of platinum concentration indicated that the platinum/chromatin ratio was equivalent to the platinum/free DNA ratio and differed significantly from the platinum/core particle ratio, which was significantly less. Subsequent experiments with chromatin extracted from human cells [115] and reconstituted chromatin [114] confirmed that DNA within the core particles was protected from cisplatin damage through direct visualization of the platination sites using a polymerase stop assay. Experiments also showed that direct platination of histones prevents nucleosome core particle formation, but platination of nuclear DNA prior to nucleosome formation does not affect core formation [114].

Given that most (75–90 %) nuclear DNA is wrapped around nucleosomes [116], significant research has been performed to elucidate the effect of platination on the translational and rotational settings of the nucleosome core particles. Experiments [108] in which nucleosome core particles were directly treated with cisplatin and oxaliplatin indicate that lesions formed on assembled core particles do not significantly affect their positioning but instead are generated at intrinsically preferred sites. Complementary experiments [117, 118] in which site-specifically platinated DNA was assembled with histone proteins indicate that platination overrides the predefined rotational setting of the nucleosomes. In both cases [108, 117, 118] the platinum lesions were directed inward, facing the histone octamer core, thus shielding their recognition and repair by DNA damage recognition proteins [119] (see Section 4.3.1). Additionally, platination of nucleosomal DNA reduces the dynamic nature of the nucleosome [108].

4. CELLULAR PROCESSING OF PLATINUM DNA ADDUCTS

4.1. Inhibition of DNA Synthesis

Based on prior observations that the organic anticancer agent hydroxyurea causes *E.coli* to elongate and inhibits division of mammalian cells and DNA synthesis, it was postulated that cisplatin might also block DNA synthesis [96]. Quantitation of the rate of incorporation of ^{3}H-thymidine, ^{3}H-uridine, and ^{3}H-L-leucine in the presence of cisplatin confirmed that, at concentrations of ≤5 μM, DNA synthesis was selectively inhibited by cisplatin in AV_3 cells, whereas at concentrations of >25 μM, DNA, RNA, and protein synthesis were all blocked [96]. Subsequent experiments evaluated the roles of purified, individual DNA polymerases in processing both intra- and interstrand cross-links, revealing that DNA replication polymerases are inhibited by bifunctional lesions ~90 % of the time [24, 98, 120]. In contrast to these results, several studies indicated that DNA synthesis continues to occur in cells that fail to divide following treatment with cisplatin [121], suggesting that a cellular mechanism for bypassing Pt-DNA lesions may be operative. This mechanism is now known to be translesion synthesis (TLS), and the efficiency and fidelity with which cells are able to bypass DNA-platinum lesions is linked with drug sensitivity, resistance, and mutagenicity.

Specialized TLS polymerases [122] have evolved in mammalian cells to incorporate nucleotides opposite damaged nucleotides on the template strand, including members of the Y family of polymerases (η, ι, κ, and Rev1) and DNA polymerase ζ [123, 124]. For TLS, polymerase switching must occur, where the replication polymerase is displaced by the TLS polymerase. This process is signaled by mono-ubiquitination of proliferating cell nuclear antigen (PCNA) at Lys-164. Once ubiquitinated, PCNA has a higher affinity for the Y-family polymerases, all of which share a novel ubiquitin binding motif that localizes TLS polymerases at the site of the blocked replication machinery. Following recruitment of the TLS polymerase three distinct steps occur to bypass a bifunctional lesion such as a 1,2-d(GpG) adduct, namely, (i) insertion of a nucleotide opposite the 3′-G, (ii) insertion of a nucleotide opposite the 5′-G, and (iii) extension onward from the 5′-G. Each of these steps has distinct kinetics that depend on the specific polymerase and the nature of the lesion [123, 125]. Differences in the solution geometry of cisplatin- and oxaliplatin-DNA adducts account for the differential TLS efficiency and fidelity observed for these two species, with polymerase η and β bypassing oxaliplatin lesions more readily than cisplatin lesions [99, 126]. *In vivo* studies subsequently revealed that Pol η or κ incorporate the correct or incorrect nucleotide, respectively, opposite a 1,2-d(GpG) cisplatin intrastrand cross-link, while the extension step is performed by Pol ζ. Pol ζ is an error-prone polymerase that, in the absence of other polymerases, performs TLS past cisplatin adducts with low efficiency [99, 127].

Recent studies have also discovered a role for TLS polymerases in the repair of ICLs. In general, ICL bypass consists of three steps. The first is an unhooking step where incisions are made at either side of the damaged nucleotide on one strand of the DNA. This process is followed by TLS past the unhooked ICL,

which restores one of two strands and provides an intact template to complete the repair process [128]. Difficulties studying this process at a mechanistic level persist, however, owing to the combined effects of multiple ICL repair pathways, potential redundancy between polymerases, and the limited options currently available to study these pathways [129].

4.2. Transcription Inhibition

As for DNA polymerases, RNA polymerases that transcribe mRNA encoded on DNA are efficiently blocked by bifunctional platinum adducts. Early studies exploring the mechanism of action of cisplatin revealed that cell death was proceeded by G2/M arrest [121], indicating that, under physiologically relevant conditions, sufficient DNA synthesis occurred to satisfy progression of the cell cycle through the S phase. More detailed studies correlated the cellular sensitivity of Chinese hamster ovary cells both proficient and deficient in DNA repair with G2 arrest following cisplatin treatment. These experiments confirmed that cisplatin affected the extent of DNA synthesis but importantly was not linked to the sensitivity of the cell line [130].

Taken together, the results are consistent with the hypothesis that transcription inhibition is the main mechanism by which cisplatin exerts its action, arresting the cell cycle at G2/M, resulting in cellular failure to transcribe the genes necessary to enter mitosis. More detailed experiments performed with site-specifically modified Pt-DNA adducts indicate transcription by RNA polymerase II (Pol II) and *E. coli* polymerase (RNAP) to be blocked by 1,2-d(GpG) and 1,2-d(ApG) adducts on the template strand but only slightly inhibited when the adduct is on the nontemplate strand [131]. To date a vast body of research into transcription inhibition has been reported with Pol II, the mammalian polymerase involved in transcription of the majority of eukaryotic genes. Inhibition of RNA polymerase I (Pol I), which is involved in transcription of rRNA, has received considerably less attention but is speculated to be operative via a comparable mechanism [24, 132]. Pol I transcribes far more DNA overall than Pol II and its inhibition may be responsible for ribosome biogenesis stress (see below, Section 5.5), the mechanism to which the anticancer properties of oxaliplatin were recently attributed [133].

In addition to failing to transcribe the requisite genes, once stalled, the polymerases act as damage recognition sentinals that may either instigate repair pathways or mediate cell death, as discussed in the following sections. Normal cells have multiple different repair pathways, and often more than one pathway is operative in the removal of a lesion.

4.3. Repair of Platinum Lesions

4.3.1. Nucleotide Excision Repair

Nucleotide excision repair (NER) is a programmed cellular repair mechanism for removal of DNA lesions and the primary mechanism by which cisplatin-DNA

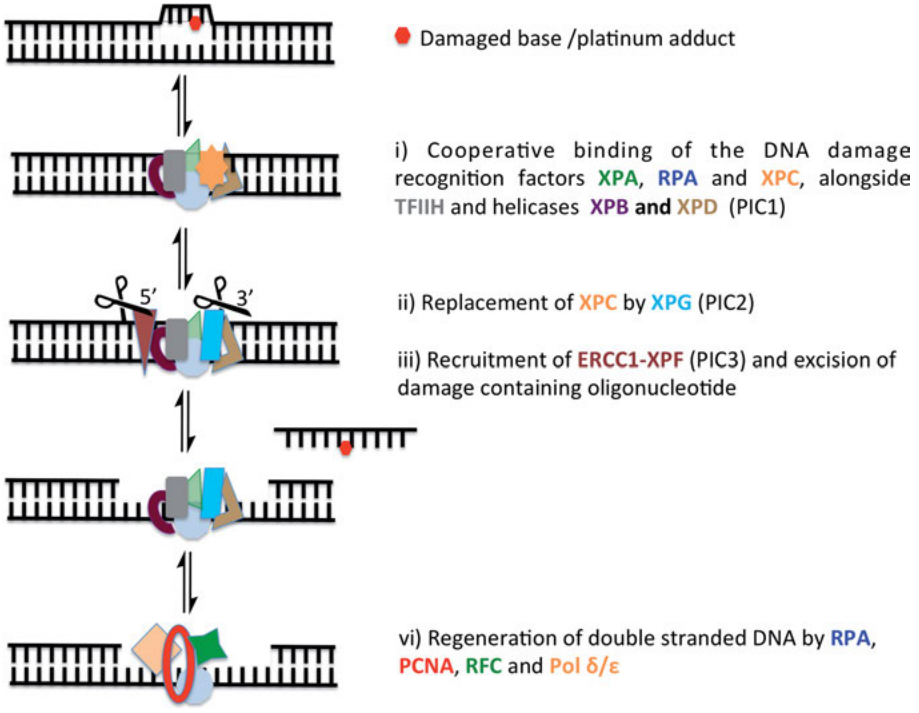

Figure 6. Schematic representation of the NER pathway and the multiple proteins involved in recognition and excision of the platinum lesion followed by regeneration of the double-stranded DNA.

1,2-intrastrand cross-links are removed [24]. *In vitro* experiments indicate that intrastrand adducts of oxaliplatin are repaired in a similar manner [134], revealing that the carrier ligand does not influence the repair mechanism. However, interstrand cross-links generated by cisplatin are not substrates for NER [135].

NER is a complex, multistep process [136] (Figure 6) that requires six repair factors: RPA, XPA, XPC, TFIIH, XPG, and XPF·ERCC1. The initial step is an ATP-independent recognition process that is believed to involve indirect readout of the damage through sensing abnormal DNA backbone conformations. In this step RPA, XPA, and XPC-TFIIH bind cooperatively in a random order at the site of the damage-generating pre-incision complex 1 (PIC1). The DNA is then unwound by up to 20 base pairs and a kinetic proofreading step takes place, ensuring that only damaged DNA undergoes NER. Once DNA is unwound, XPG binds the damaged site with high affinity displacing XPC to generate PIC2. Finally, XPF·ERCC1 is recruited to the damage site and generates dual incisions around the damaged nucleotide (PIC3) liberating a 24–32 nucleotide oligomer containing the damaged site. The excised platinum oligomer is expected to undergo degradation in the nucleus, like other small oligomers, but the fate of the platinum remains unknown [24]. DNA polymerases δ and ε fill the gapped re-

gion left following excision of the damaged strand before ligation of the ends regenerates double-stranded DNA.

Xeroderma pigmentosum (XP) cells lacking one of more components of the NER pathway are 5- to 10-fold more sensitive to cisplatin treatment than normal cells [24, 137], confirming the role of NER in processing platinum lesions. Complementary data indicate a correlation between increased expression of NER genes and cisplatin resistance.

As discussed in Section 3.3, platinum lesions on nuclear DNA effect the positioning of genomic DNA in nucleosomes, with lesions being preferentially oriented toward the histone core proteins, thus shielding damage recognition and repair by NER proteins [119]. *In vivo*, NER is further modulated by post-translational modification of the histones [119].

4.3.2. Recombination Repair

Recombination repair (RR) operates by two pathways, homologous recombination (HR) and non-homologous end joining (NHEJ) [24, 136]. Like NER-deficient cells, cells deficient in RR are sensitive to cisplatin treatment. Furthermore, cells deficient in both NER and RR are more sensitive to cisplatin than either deficient cell line alone [138]. DNA recombination is most commonly implicated in the repair of interstrand cross-links [139].

As with all repair mechanisms the first stage is damage recognition. Following double-stranded break recognition, nucleolytic processing generates single-stranded DNA with free 3′-ends facilitating Rad51-mediated strand invasion forming a Holliday junction. Subsequent DNA synthesis, ligation, and resolution of the Holliday junction regenerates double-stranded DNA with high fidelity, with information lost from the broken double-stranded DNA being regenerated from the homologous duplex. In contrast, NHEJ is an error-prone repair pathway that ligates the two duplex termini regardless of whether they come from the same or a different chromosome [136, 139]. Experiments support HR as an important repair mechanism for cisplatin lesions, whereas knockout of the NHEJ pathway does not significantly affect the cisplatin sensitivity of cells [140].

4.3.3 Fanconi's Anemia

Fanconi's Anemia (FA) is a rare autosomal disease arising from deregulation of replication-dependent removal of interstrand cross-links [141]. It is generally believed that the FA pathway has evolved in eukaryotes to deal with the difficulties associated with repairing ICLs where both strands of a DNA duplex are damaged. Patients with Fanconi's Anemia are thus unable to efficiently remove ICLs and are therefore hypersensitive to cisplatin and other anticancer agents operative through formation of ICLs [142].

The FA pathway utilizes elements of the HR, NER, and TLS pathways in the repair processes and its activity is closely regulated. The pathway is only operative in the S phase of the cell cycle and is turned off following repair of DNA

damage [141, 143]. The current mechanism for DNA repair by FA proteins is incomplete but is believed to be instigated by ATR activation and ubiquitination of FANCD2, which then co-localizes with repair proteins at the site of DNA damage. Subsequently, endonucleases generate double-strand breaks that uncouple the two sister chromatids. The structure-specific nucleases ERCC1-XPF and MUS81-EME1 have been linked with ICL repair, and cells lacking these proteins are sensitive to cross-linking agents. Following formation of the double-strand break it is speculated that the cross-link is unhooked to generate a single nucleotide lesion that can be processed like a monofunctional adduct by NER and TLS proteins. Finally, following replication through the site of DNA damage, HR proteins are implicated in regeneration of the replication fork [141].

4.3.4. Mismatch Repair

The mismatch repair (MMR) pathway is involved in recognition and repair of base-base mismatches and insertion and deletion loops generated where one partnerless nucleotide in double-stranded DNA is partially extrahelical [144]. MMR has been linked with repair of both intra- and interstrand platinum cross-links, but mismatch repair proteins do not recognize oxaliplatin cross-links [145]. Furthermore, several studies have demonstrated correlations between cisplatin-resistant cell lines and MMR defects, having both intrinsic and acquired resistance [24, 144, 146, 147].

Current research indicates that hMSH2, which forms heterodimers hMutSα and -β with MSH6 and MSH3, respectively, binds with high affinity (K_d ~67 nM [148]) to 1,2-d(GpG) intrastrand cross-links but poorly with 1,3-d(GpTpG) cisplatin adducts [149]. MutSβ also binds ICLs generated with cisplatin [150]. Preferential recognition of cisplatin over oxaliplatin, *trans*-diamminedichloroplatinum(II), and $[Pt(dien)Cl]^+$ adducts has also been reported [148, 149]. Following damage recognition, MutLα, a heterodimer of MSH1 and postmeiotic segregation increased 2 (PMS2), is recruited to the site of action and a relatively stable ATP-dependent ternary complex is generated with the damaged DNA. Additionally, the PCNA sliding clamp, DNA polymerase δ, exonuclease 1, and DNA ligase are required to complete the MMR process [24]. MMR proteins also play an important role in signaling DNA-damage induced apoptosis [151], effecting phosphorylation of p53, and activating the stress-activated kinase, JNK, as discussed in Section 5 in greater detail.

4.3.5. Base Excision Repair

Base excision repair (BER) has evolved to repair damaged bases that result in minimal distortion of the DNA duplex [152], and recent evidence supports an additional role for BER in cross-link repair [153]. Data supporting dysregulation of BER proteins in cisplatin-resistant cancers [154] has led researchers to investigate its role in the development of cisplatin resistance. Results [153] obtained with BER-defective MEFs in the presence and absence of a small molecule

inhibitor of APE1, a critical enzyme in the BER pathway, support the involvement of BER in ICL repair while showing that BER does not affect intrastrand cross-link processing. In contrast, minimal changes in sensitivity of the BER-deficient/inhibited cells compared with wild-type cells occurs when they were treated with oxaliplatin, indicating a specific role for cisplatin.

Two BER pathways have been reported – short and long patch pathways [136]. Damage recognition and excision are initiated in each pathway by DNA glycosylases that bind the damaged DNA, compressing it and flipping the damaged base out of the helix into the active site of the enzyme. Cleavage of the damaged base generates an abasic site on the DNA, and subsequent removal of the abasic sugar generates a one-nucleotide gap, which is filled by DNA Pol β, APE1, and DNA ligase III-XRCC1 in mammalian cells. Alternatively, the long patch pathway requires APE1 to make an incision on the 5′-side of the abasic site, followed by a 3′-incision made by FEN1 endonuclease. This cut liberates a 2–10 nucleotide long excision product and DNA Pol δ/ε and PCNA then synthesize a new patch that is ligated by DNA ligase I to regenerate the double-stranded DNA.

4.4. Protein Binding to Platinated DNA

In addition to specific repair proteins highlighted in the preceding sections several other mammalian proteins recognize and bind to platinated DNA [24, 100, 155]. The best studied of these are the high-mobility group (HMG) domain proteins (Figure 7). High mobility group box (HMGB) proteins 1–4 share considerable structural homology, and all contain two tandem HMG domains, capable of recognizing and binding with high affinity to bent and distorted duplex DNA.

HMGB1 is a 30 kDa protein comprising two HMG domains appended with an acidic tail that is not essential for DNA binding. Owing to its high intercellular concentration, short residence time on DNA, and affinity for bent DNA, HMGB1 has a high probability of encountering platinum adducts; it has therefore long been postulated to be involved in cisplatin sensitization [24, 156, 157]. However, experimental results aiming to correlate HMGB1 expression levels with cisplatin sensitivity [158], or to introduce foreign HMGB1 to modulate cisplatin sensitivity, have proved inconclusive [24]. Recent results from our laboratory [159, 160] support the initial hypothesis that HMGB binding to cisplatin-damaged DNA prevents NER via a repair shielding mechanism, thereby sensitizing cells to cisplatin treatment. Critically, however, formation of a disulfide bond between Cys22 and Cys44 in the second HMG domain must be prevented if cisplatin sensitization is to be achieved. Experiments performed with HMGB4, a variant of the HMG box protein that contains a tyrosine residue in place of Cys22 and therefore is not affected by the intracellular redox potential, unambiguously allowed correlation of HMGB4 expression with cisplatin sensitivity. Supporting these results are clinical observations that link the exceptionally high cure rates of testicular germ cell tumors (TGCTs) with the preferential expression of HMGB4 in testes. Finally, a two-fold increase in cisplatin sensitivity was demonstrated for cisplatin-resistant

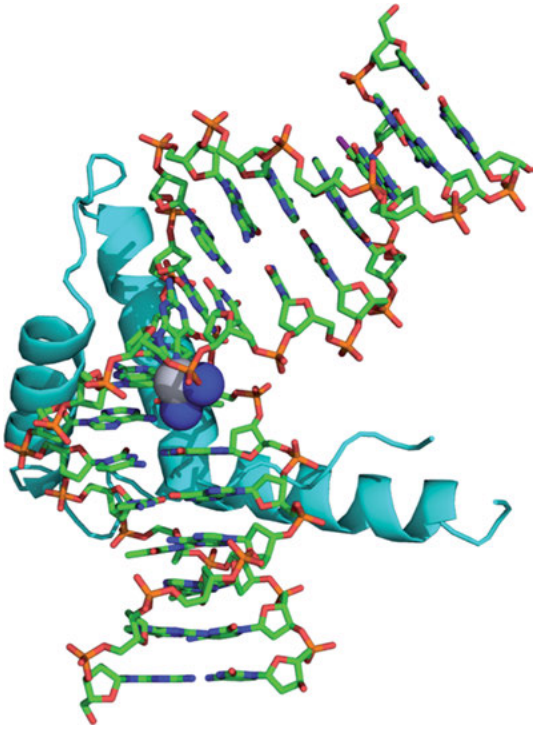

Figure 7. X-ray structure of HMGB1 bound to duplex DNA containing a cisplatin 1,2-d(GpG) intrastrand cross-link (1CKT [224]; see also [159]). Cisplatin is shown as a space-filling model with platinum in gray and nitrogen in blue, and HMGB1 is represented as cyan ribbon.

breast cancer cells MDA-MB-231 following transfection of HMGB4 cDNA and subsequent HMGB4 expression in the cell line.

Several non-HMGB proteins contain one or more HMG domains, including the structure-specific recognition protein SSRP1 and the ribosomal RNA transcription factor hUBF (human upstream binding factor). SSRP1 is an 81 kDa protein containing one HMG domain that forms a heterodimer with Spt16/Cdc68 [24]. The heterodimer FACT (facilitates chromatin transcription) is a chromatin modulator that binds cisplatin DNA adducts. The isolated HMG domain of SSRP1 also binds damaged DNA, whereas the full SSRP1 complex alone does not [161]. hUBF contains six HMG domains [100] and binds cisplatin-damaged DNA with high specificity and the strongest reported affinity ($K_d = 60$ pM [162]). The binding affinity of hUBF for its natural substrate, the rRNA promotor, and cisplatin-damaged DNA are comparable, leading the authors to propose transcription hijacking [100, 162] as an alternative means by which protein binding to cisplatin-damaged DNA may sensitize cells to treatment. At saturated levels of hUBF and platinum concentrations below those reported in cancer patients, complexation of hUBF

with the rRNA promotor was completely inhibited. Such dysregulation of rRNA synthesis is likely to have a negative effect on a cell's welfare.

The TATA-binding protein (TBP) also binds cisplatin-damaged DNA with a preference for 1,2-d(GpG) intrastrand over 1,3-d(GpG) cross-links [163]. The binding affinity and kinetics of TBP to the TATA box are similar to that observed for TBP binding to cisplatin-damaged DNA and increased by 20-fold in the presence of HMGB1, leading to speculation that a TBP-HMGB1 complex interacts with platinated DNA. TBP binding to damaged DNA results in transcription inhibition through reduced interaction of the TBP with the TATA box and to reduced transcription factor recruitment [24].

YB-1 is a transcription factor that binds to an inverted CCAAT box sequence called the Y-box [164]. It also binds preferentially to platinated DNA sequences including 1,2-d(GpG), 1,2-d(ApG), and 1,3-d(GpTpG). YB-1 also physically interacts with many cellular proteins including PCNA, MSH2, and DNA polymerase δ, many of which are elements of various repair pathways suggesting a possible role for YB-1 in modulation of DNA damage repair [24].

The 104 amino acid protein poly(ADP-ribose)polymerase 1 (PARP-1) is a platinum damage response protein that binds to cisplatin 1,2-d(GpG) and 1,3-d(GpTpG) modified DNA in both its activated and unactivated forms [165]. PARP-1 also binds DNA adducts generated with oxaliplatin and the monofunctional platinum agent pyriplatin ($[Pt(NH_3)_2(pyridine)Cl]^+$) indicating that the protein binding event occurs in response to the presence of a foreign substance on DNA rather than a specific structural distortion [165]. PARP-1 has been associated with BER [166] and induces apoptosis through formation of poly(ADP-ribose) polymers that signal release of apoptosis-inducing factors from mitochondria [167]. In response to DNA damage PARP is heavily upregulated [165], resulting in NAD^+ depletion and ultimately cell death via necrosis as a result of glycolysis shutdown. Recently, the concept of synthetic lethality has given rise to the development of PARP inhibitors for treatment of patients with defective BRCA genes [166, 168].

Tumor suppressor protein p53 contains two DNA-binding domains, both of which are required for binding to platinated DNA [169]. However, the C-terminal domain is more critical for preferential binding of damaged over undamaged DNA [24, 170]. Purified, active p53 binds 1,2-d(GpG) intrastrand cross-links (K_d = 150 nM) but has no affinity for 1,3-d(GpG) cross-links, ICLs, or monofunctional adducts [171]. Like PARP, p53 interacts with damage recognition elements in DNA repair pathways and also enhances HMGB1 binding [172], thereby modulating repair of adducts.

5. SIGNAL TRANSDUCTION PATHWAYS ACTIVATED BY PLATINUM DNA DAMAGE

5.1. Overview of Signal Transduction

Before DNA damage can be repaired it must first be identified and the information communicated to damage response proteins within the cell. Once the DNA

damage response (DDR) has been initiated the cell cycle check points, Chk1 and Chk2, become activated, halting cell cycle progression and providing the opportunity for the cell to repair the damage before cell cycle re-entry (checkpoint recovery) [136, 173, 174]. Cell cycle check points are thus implicated in control and activation of DNA repair pathways, in addition to composition of telomeric chromatin, localization of DNA repair proteins, and in some cells induction of apoptosis [173]. Cell cycle arrest may occur at the G1, intra-S, or G2 phase of the cell cycle [136]. If the cell is unable to efficiently repair the damage it will remain arrested or undergo apoptosis, preventing genetically unstable cells from progressing through replication. The cytotoxicity of classical platinum agents thus relies not only on their ability to inhibit DNA and RNA synthesis but also on the inability of cells to sense and signal repair of platinum lesions.

5.1.1. DNA Damage Sensors

Until recently little was known about proteins involved in detecting DNA damage [173], but a growing body of evidence supports the role of the so-called 9-1-1 complex [175] in combination with Rad17 and the proximal kinases ataxia-telangiectasia mutated (ATM) and ATM- and Rad3-related kinases (ATR) [176]. The 9-1-1 complex is a heterotrimeric, toroidal clamp, comprising Rad9, Hus1, and Rad1 proteins, that shares structural and mechanistic features with the better known PCNA [177]. Following genotoxic stress induced through replication inhibition as well as other mechanisms the 9-1-1 complex is loaded onto the chromatin by the clamp loader Rad17-replication factor C (RFC) [178, 179]. Independently but simultaneously, ATM-Rad3 related kinases-ATR-interacting protein (ATR-ATRIP) binds to the damaged DNA. Finally recruitment of TopBP1, which bridges between the 9-1-1 complex and ATRIP-ATR, facilitates ATR-mediated Chk1 phosphorylation and activation [180]. Whereas ATR can phosphorylate some substrates in the absence of Rad9, TopBP1 localization depends on the Rad9 tail and is therefore essential for Chk1 phosphorylation.

5.1.2. Signal Transducers

Following recognition of damage by the cell, information is transferred via a series of signal transducers to effectors that instigate repair of damaged DNA or halt cell cycle progression [173]. Several sequential steps are therefore required to execute the function of the DNA damage response pathway, and these steps must occur within a timeframe fast enough to prevent transition of damaged cells into the next phase of the cell cycle [181]. Additionally, the damage signal must be durable enough to persist as long as the damage. Distinct mechanisms are therefore implicated in the induction and maintenance of checkpoint responses.

5.2. Checkpoint Kinases

In addition to regulating cell cycle, checkpoint kinases Chk1 and Chk2 are DNA damage kinases activated by ATR and ATM, respectively [182]. ATR and ATM are protein kinases structurally related to the phosphatidylinositol-3-OH kinases (PI(3)K) family. Broadly, ATM is activated in response to double-strand breaks whereas ATR responds to breaks created by a variety of agents including stalled replication forks caused by bulky base adducts. Secondary activation of ATR is also observed during the processing of double-strand breaks, which generates single-stranded lesions [181].

The role of Chk1, which is expressed in the S and G2 phases of the cell cycle, is conserved from yeast to humans [181] and involves ATR-mediated phosphorylation of claspin complexed Chk1 at Ser317 and Ser345 [182, 183]. Chk1 is encoded on the CHEK1 gene and is essential for genome integrity, with early studies confirming the embryonic lethality of Chk1 knockout mice [184, 185]. Following the initial ATR-promoted phosphorylation steps, Chk1 dissociates from chromatin and autophosphorylation of Chk1 Ser296 generates a docking site for 14-3-3γ that in turn promotes Chk1 phosphorylation of Cdc25A at Ser76, which in turn signals proteasomal degradation [181–183]. Transitions between different phases of the cell cycle are governed by the cyclin-dependent kinases (Cdks) in combination with a variety of cyclins. Negative regulation of Cdks is achieved through phosphorylation at Thr14 and Tyr15 by the Wee1 and Myt1 kinases, while dephosphorylation by Cdc25 kinases activates Cdks. Cell cycle arrest thus occurs as a result of unregulated phosphorylation of Cdk2 or Cdk1 [181], bringing about G1 or G2 checkpoint arrest, respectively.

In contrast to Chk1, studies with Chk2-knockout mice have confirmed that Chk2 is redundant in higher eukaryotic systems [183], leading to the hypothesis that Chk1 is the main checkpoint inhibitor and Chk2 may be a supportive kinase. Chk2 functions in a similar manner to Chk1, inhibiting Cdc25 phosphatases following ATM-mediated Chk2 Thr68 phosphorylation and subsequent autophosphorylation events [181].

5.3. MAPK Proteins (ERK/JNK/p38)

The mitogen-activated protein kinase (MAPK) cascade has also been implicated in signal transduction following recognition of cisplatin-induced DNA lesions [186]. The major MAPK family members [187] include the extracellular signal-regulating kinases (ERK), the c-Jun N-terminal kinases (JNKs, also known as the stress-activated protein kinases), and the p38 kinases [28, 174]. In healthy cells MAPKs are responsible for signal transduction from the cell surface to the nucleus, thereby modulating gene expression and controlling cell proliferation, differentiation, and death [186]. Activation of MAPK in response to cisplatin is cell-dependent and may induce, suppress, or have no role in apoptosis [186]. MAPK cascades will be activated not only in response to platinum-DNA lesions but also to platinum adducts generated with other biological nucleophiles [186].

MAPKs have thus been implicated in both induction of apoptosis and the development of resistance to platinum agents, but the exact role of each of these kinases is controversial owing to complex, cell-specific responses.

In addition to activation by endogenous growth factors and mitogens, ERK is activated in response to cisplatin treatment [188, 189]. Following dual phosphorylation by MAPK kinase (MAPKK) and MAPKK kinase (MAPKKK), ERK phosphorylates p53, thereby upregulating p21, GADD45, and Mdm2 and effecting cell cycle regulation [28]. Data supporting ERK activation both contributing to and preventing cisplatin-induced apoptosis [190] have been reported for a variety of cell lines.

Like ERK, p38 proteins respond to a wide variety of stimuli including inflammatory cytokines and environmental stress, and they have been implicated in cisplatin-induced apoptosis [191]. Activation of p38 sensitizes cells to cisplatin whereas inactivation of p38 makes cells cisplatin-resistant [28, 191]. As with Chk1, ATM, and ATR may under certain circumstances activate p38. Once activated, p38 can then go on to phosphorylate the downstream MAP kinase-activated protein kinase 2 (MAPKAP kinase 2; MK2), which can induce a checkpoint response through phosphorylation of Cdc25 in an analogous manner to Chk1. Checkpoint maintenance is regulated through stabilization of Gadd45a mRNA that further potentiates MK2 activation [182]. Additionally, p38 kinases and the downstream kinase, mitogen- and stress-activated protein kinase 1 (MSK1), are involved in cisplatin-induced phosphorylation of histones [192].

JNKs have been implicated in both cell proliferation and apoptosis, as determined by the duration of JNK activation [174, 193]. Sustained activation of JNK correlates with apoptosis induction, whereas acute and transient activation of JNK signals cell survival. Most of the factors that activate p38 also activate JNK and, like p38, JNK is activated through phosphorylation of Thr and Tyr residues by MKK. Apoptosis is then controlled by modulating the activity of pro-apoptotic proteins via phosphorylation and increased expression of pro-apoptotic genes such as TNF-alpha, Bak, and Fas-L [193]. Initial observations for the role of JNK in cisplatin induced apoptosis found that JNK-defective cells are cisplatin-resistant[194]. Since then others have provided evidence to support the hypothesis that the JNK pathway is involved in cisplatin-induced apoptosis [174].

A considerable amount of research has thus been performed to determine the role of the MAP kinases, but much remains to be done if their complex roles in cisplatin-induced apoptosis and resistance are to be fully elucidated. As noted above, in many instances activation of the MAPKs may be triggered by different events and cause multiple different cellular responses, sometimes in parallel. More recently the role of ras oncogenes, which are upstream regulators of ERK and JNK, has received attention [195]. The ras superfamily consists of H-, K-, and N-ras G proteins that function as molecular switches [196]. When bound to GTP ras activates ERK, and the upstream kinases MEK and raf, which ultimately signal p53 phosphorylation following signal transduction. However, when in the GDP-bound state, ras is unable to induce signal transduction [196]. Ras overexpression and mutation has been implicated in cisplatin resistance.

5.4. Tumor Suppressor Protein p53

The status of p53 is closely linked with the ability of a cell to tolerate DNA damage and hence a patient's prognosis and likelihood of developing resistance [197, 198]. Roughly half of all human cancers exhibit a mutation in the *TP53* gene [195], approximately 75 % of which are missense mutations that prevent p53-induced apoptosis and often result in aggressive tumor growth [199].

In normal cells, p53 is regulated by the E3 ubiquitin ligase Mdm2, which both tags p53 for ubiquitin proteasomal degradation and binds directly to p53 transactivation domains 1 and 2 (TAD1 and 2) [199]. Thus the concentration of p53 is maintained at a low steady state around 10^3–10^4 molecules per cell [200]. Following activation in response to diverse stress signals including DNA damage, p53 undergoes ATM and/or ATR phosphorylation, leading to its stabilization [28]. A growing body of evidence supports p53 having both a potent transcriptional activation domain and the ability to indirectly modify gene transcription [199]. Wild-type and several mutants of p53 can directly bind cisplatin-modified DNA [169, 170, 201].

Cisplatin-induced cell death is regulated by p53 via several pathways including degradation of the FLICE-like inhibitory protein (FLIP), overexpression of the phosphatase and tension homolog (PTEN), and inhibition of AMP-kinase. Additionally, binding of p53 to Bcl-xL counteracts the antiapoptotic function of this protein [28].

5.5. Oxaliplatin Does Not Induce a DNA Damage Response

Recent experimental evidence has identified key differences in the way cisplatin and oxaliplatin induce cell death [133]. Oxaliplatin, unlike cisplatin, does not induce a DNA damage response but instead kills cells by ribosomal biogenesis stress, providing a fundamental explanation for the differential side-effects and spectrum of activity reported for these classical platinum anticancer agents. Initial observations, made using an RNAi platform [202] indicated that, unlike cisplatin and carboplatin that classify as DNA cross-linkers, oxaliplatin exhibits a distinctive mechanism of action consistent with that of the monofunctional agent, phenanthriplatin. Oxaliplatin and phenanthriplatin are mechanistically closer to the transcription/translation inhibitors rapamycin and actinomycin D. Further studies indicated that oxaliplatin treatment results in fewer double strand breaks on DNA than formed by other platinum agents and confirmed a relative lack of sensitivity to the silencing of genes involved in HR and those implicated in repair of ICLs within DT40 cells, by comparison to the properties of cisplatin. In support of the conclusion that oxaliplatin induces cell death through ribosome biogenesis stress is the fact that pre-rRNA was upregulated following treatment with this agent when measured at time points greater than thirty minutes, while RNA Pol II transcripts remained stable. Moreover, knock down of RplII, an essential component of the ribosome, rendered Eu-Myc p19Arf-/- lymphoma and A549 human lung adenocarcinoma cells oxaliplatin-resistant. Ribosome biogene-

sis stress induces overexpression of RplII subunits that bind to Mdm2 and prevent it from interacting with p53. Western blot analysis of p53 expression supported diminution of p53 upon oxaliplatin treatment.

Finally, using The Cancer Genome Atlas the authors compared gene expression for colorectal cancer, which responds well to oxaliplatin treatment, to that for ovarian cancer, for which cisplatin and carboplatin are the preferred treatment. The greatest differences in expression levels between colorectal and ovarian cancers were observed for ribosomal genes. Notably, expression of ribosomal genes in colorectal cancer was significantly upregulated by comparison to equivalent ovarian cancer genes, thus establishing clinical relevance for the different mechanisms of cisplatin and oxaliplatin cell killing [133].

6. UNDESIRED CONSEQUENCES OF PLATINUM-BASED CHEMOTHERAPY

6.1. Toxicity

One of the limitations associated with platinum based-chemotherapy is the development of dose-limiting toxicities that prevent continuation of treatment. Several systematic toxicities are commonly encountered including gastrointestinal, oto-, nephro-, hepato-, and neurotoxicities as well as myelosuppression [203, 204]. Broadly, toxicity occurs as a result of drug accumulation at non-cancerous sites. Typically, the sites involve rapidly growing cells such as those found in the lining of the gasterointestinal tract, bone marrow, and hair cells [203], although it is unclear whether this classification applies to platinum drugs. Research is ongoing into the precise origin of each of these toxicities in the hope that a better understanding of the mechanism by which each drug becomes toxic will allow development of treatment regimens or next generation drugs specifically designed to minimize toxic side effects. Our laboratory has made significant contributions to this effort, in recent years elucidating the role and thus potential clinical implications for HMGB4 in improving the efficacy of cisplatin [159], and initiating development of novel platinum drug delivery constructs, one of which, BTP-114, is currently undergoing clinical trials. Preclinical trials with BTP-114, a cisplatin derivative, have demonstrated reduced toxicity in addition to a 13-fold increase in platinum loading in lung and ovarian cancer tumor models compared to cisplatin.

Neurotoxicity commonly referred to as peripheral neuropathy is dose-limiting in both cisplatin and oxaliplatin treatment, but there is evidence for dissimilar mechanisms of action for the two platinum-induced neuropathies [205]. Peripheral neuropathy is reported to occur in around 85 % of patients [206] receiving cisplatin at a cumulative dose greater than 300 mg/m^2 and, whereas oxaliplatin is generally less toxic than cisplatin, it still generates a high incidence of peripheral neuropathy that is further classified as either acute or chronic in nature depending on its presentation immediately following treatment or after high cumulative doses, respectively. Clinically, peripheral neuropathy is characterized by the ini-

tial development of paraesthesia (tingling) and dysaesthesias of the toes and fingers, which extends with time to a 'glove and stocking' distribution [26, 207]. The pain induced is severe and may affect a patient's functional abilities as well as lowering the quality of life. Factors that affect the onset of peripheral neuropathy in response to chemotherapy include a patient's age and pre-existing medical conditions as well as the drug-dose intensity, cumulative dose, and therapy duration [207]. Strategies to limit neurotoxicity include the co-administration of thiols, particular glutathione (GSH) [207], or vitamin E together with the platinum agent [207]. Contradictory reports of the success of glutathione treatment for peripheral neuropathy have been reported, and there are concerns at the observation that GSH expression correlates with platinum resistance [195] that have diminished the interest in this approach in recent years. In contrast, clinical data support alleviation of peripheral neuropathy for patients treated with a calcium and magnesium infusion on the day of oxaliplatin treatment, without loss of oxaliplatin anticancer activity [204]. The non-pharmacological approach of 'stop and go' treatment has also demonstrated similar response rates and progression-free survival compared to the classical oxaliplatin continuous treatment model. In 'stop and go' treatment a patient is treated with oxaliplatin up to the point where they exhibit peripheral neuropathy. The treatment is then discontinued, and only when the effects of peripheral neuropathy have worn off is the patient again treated with oxaliplatin. In this manner the long term and accumulating effects of oxaliplatin are managed [204]. Recently, research has linked acute oxaliplatin-induced neuropathy with impairment of voltage-gated sodium channels [205, 208]. In particular, increased sodium influx due to prolonged opening of the sodium channels is implicated in the presentation of unwanted neuropathological side effects.

Nephrotoxicity is commonly encountered in cisplatin treatment and it has been estimated that 28–36 % of patients who receive an initial dose of 50–100 mg/m^2 develop acute renal failure [203], from which most patients fail to fully recover. Similarly, ototoxicity, which includes hearing loss, ear pain, and tinnitus is a common dose-dependent side effect of cisplatin [26, 209]. In contrast, reports of nephrotoxicity and ototoxocity are rare following oxaliplatin treatment [210]. The origins of oto- and nephrotoxicity have been briefly highlighted in Section 2.3 and involve the differential transport of platinum agents by membrane transporters [26, 72]. Early studies indicated that hydration with saline or saline infused with mannitol- or furosemide induces diuresis effectively reducing the nephrotoxicity of cisplatin to the point where it is no longer dose-limiting [203, 211]. More recently exogenous thiol treatment, particularly with the pro-drug amifostine (S-2(3-amino-propylamino)ethylphosphorothioic acid), has been proposed as a means to further reduce nephro- and ototoxicity in addition to previously mentioned neurotoxicity [203, 206].

Gastrointestinal symptoms including vomiting and hepatotoxicity [212] are also observed with both cisplatin and oxaliplatin treatment. Neither is considered limiting as gastrointestinal conditions are effectively treated with 5HT3 antagonists [13] and hepatotoxicity remains a secondary concern to nephrotoxicity.

6.2. Multifactorial Resistance

In addition to dose-limiting toxicities, acquired and intrinsic cellular resistance to platinum agents limits their efficacy as anticancer agents. The multistep mechanism of action required for platinum anticancer agents to bring about a desired therapeutic response is matched at each stage by multiple resistance mechanisms. Intracellular accumulation of platinum is modulated by membrane transporters that alter both influx and efflux, and the number of platinum-DNA lesions is minimized by deactivation of platinum agents in the cytoplasm and increased repair of the adducts [25]. In general, cellular resistance arises when several mechanisms are operative simultaneously, a phenomenon termed multifactorial resistance [195].

Reduced cisplatin accumulation has been reported for several cisplatin resistant cell lines in comparison to the parental line [213]. However, resistance is often mediated by more than one mechanism, and a direct correlation between reduced cisplatin accumulation and resistance is rarely observed [195]. Moreover, continuing controversy surrounding the mechanism of transport for platinum agents further confounds attempts to determine whether reduced accumulation is due to reduced cellular uptake, increased efflux, or both [195, 213].

In contrast, more consistent data are available for identifying the role of thiols in resistance, with the concentration of several biological thiols being correlated with resistance both *in vitro* and in the clinic [195, 213]. In particular, several cisplatin-resistant cell lines have elevated concentrations of GSH, including a testicular tumor cell line that is normally cisplatin-sensitive but which acquired cisplatin resistance *in vitro* [214]. Similarly, increased concentrations of cysteine-containing metallothioneins have been identified in cisplatin-resistant tumor models [25, 215].

Another factor operative in platinum resistance is the ability of cells to tolerate or repair platinum lesions on DNA. Downregulation or mutation of the MMR proteins hMLH1 or hMSH6 increases replicative bypass by 3- to 6-fold past cisplatin lesions, but the same defects have little effect on the extent of bypass across oxaliplatin lesions [25], indicating that cisplatin lesions are better tolerated by MMR-deficient cell lines. Moreover, cisplatin-resistant cells deficient in MMR often have abrogated p53 function, which is implicated in the downregulation of hMSH2 [195]. When operative, the contribution of increased repair is low, but nonetheless clinically significant, and typically gives rise to 1.5- to 2-fold resistance [25]. Increased repair of platinum-DNA lesions is linked with increased NER protein expression, specifically, increased mRNA levels of ERCC1 and XPA have been reported for samples taken from patients exhibiting acquired resistance to cisplatin [195]. This result correlates with data supporting low levels of these proteins in testicular tumor cells known to be sensitive to cisplatin [195].

6.3. Cancer Stem Cell Enrichment

Some researchers now believe that cancer stem cells (CSC), which make up as little as 1 % of the tumor population [216], may be responsible for the develop-

ment of resistance and tumor recurrence following chemotherapy [217–219]. It is postulated that conventional chemotherapeutic agents, which are targeted to bulk tumor cells, spare CSCs, thereby enriching the population of resistant CSCs. Research into CSC treatment is still in its infancy, and much work has yet to be done to fully understand the properties of CSCs, develop tools required to study this distinct subpopulation of cancer cells [218], and ultimately discover new anticancer agents capable of effectively targeting CSC, specifically without affecting normal stem cells.

6.4. Mutagenicity

In addition, to concerns related to resistance, toxicity, and cancer stem cell enrichment, the mutagenic potential of platinum anticancer agents must also be noted. Early mouse models indicated that, at therapeutic doses, cisplatin was carcinogenic and that treatment may induce secondary tumor formation [220]. Subsequent research has investigated the mutagenicity of cisplatin and other platinum agents in a variety of cell types, and assessed the relative mutagenicity of different cisplatin lesions [221]. It is known [222, 223] that the major 1,2-d(GpG) cisplatin intrastrand cross-link was the most lethal among 1,2-d(GpG), 1,2-d(ApG), and 1,3-d(GpTpG) adducts investigated and therefore could account for most of the cytotoxicity displayed by cisplatin. The 1,2-d(GpG) link is also considerably less mutagenic than the 1,2-d(ApG) link, with relative mutation frequencies of 1.4 % for 1,2-d(GpG) and 6 % for 1,2-d(ApG). No specific mutations were reported for the 1,3-d(GpTpG) cross-links.

7. CONCLUDING REMARKS AND FUTURE DIRECTIONS

The value of metallo-drugs as anticancer agents has been firmly established in the half century that has passed since the seminal discovery of cisplatin as a potent anticancer agent. The mechanism of action that governs the activity of the classical bifunctional platinum agents, including cisplatin and oxaliplatin, has been extensively studied during this time, allowing scientists to appreciate the many factors that dictate the efficacy of new drug candidates.

More recently, non-classical anticancer agents that differ from the traditional classical agents in their metal identity or coordination preference have been developed in a bid to overcome some of the remaining limitations with the currently approved platinum drugs. In particular, non-classical anticancer agents, including pro-drugs such as BTP-114 discussed above, polynuclear metal complexes, and drugs based on non-platinum metals including gold and ruthenium, discussed in detail in later chapters of this book, may have improved efficacy and cellular uptake over classical platinum(II) agents, while at the same time showing reduced incidence of drug resistance, tumor recurrence, and toxic side-effects.

ACKNOWLEDGMENTS

This work was supported by a National Cancer Institute Grant (CA034992) awarded to SJL.

ABBREVIATIONS AND DEFINITIONS

9-1-1	Rad9, Hus1, and Rad1
ATM	ataxia-telangiectasia mutated
ATOX1	copper chaperone
ATP	adenosine 5′-triphosphate
ATR(ATRIP)	ATM-Rad3 related kinases-ATR-interacting protein
BER	base excision repair
bp	base pair
Cdks	cyclin-dependent kinases
chk1/2	cell cycle checkpoint 1/2
cisplatin/CDDP	*cis*-dichlorodiammineplatinum(II)
CSC	cancer stem cell
Ctr1/2	copper transporter 1/2
DACH	*trans-R,R*-1,2-diaminocyclohexane
DDR	DNA damage response
dien	diethylenetriamine = 1.4.7-triazaheptane
E. coli	*Escherichia coli*
enloplatin	1,1-cyclobutane dicarboxylato-O′,O′ tetrahydro-4H pyran-4,4-dimethylamine-N′,N′ platinum(II)
ERCC	excision repair cross complementing
ERK	extracellular signal regulating kinases
FA	Fanconi's Anemia
FACT	facilitates chromatin transcription
FDA	US Food and Drug Administration
FLIP	FLICE-like inhibitory protein
GSH	glutathione
HMG(B)	high mobility group (box)
HPLC	high performance liquid chromatography
HR	homologous recombination
ICL	interstrand cross-link
JNK	c-Jun N-terminal kinases
lobaplatin	[2-hydroxypropanoato-O1,O2][1,2-cyclobutanedimethanamine-N,N′]platinum(II)
MAP(K)	mitogen activated protein (kinase)
MAPKAP kinase 2	MAP kinase-activated protein kinase 2
(h)MATE	(human) multidrug and toxin extrusion antiporters
MMR	mismatch repair
heptaplatin	[propanedioato-O,O′][2-(1-methylethyl)-1,3-dioxolane-4,5-dimethanamine-N,N′]platinum(II)

miboplatin	*R*-2-amino methyl pyrrolidine 1,1-cyclobutane dicarboxylate platinum(II)
MEF	mouse embryonic fibroblasts
MSK1	mitogen- and stress-activated protein kinase 1
NCI	National Cancer Institute
nedaplatin	diammine[hydroxyacetato-O,O′]platinum(II)
NER	nucleotide excision repair
NHEJ	non-homologous end joining
NK-121/CI-973	*cis*-1,1-cyclobutane dicarboxylato(2R)-2-methyl-1,4-butanediamine platinum(II)
OCT	organic cation transporter
(h/y)OCT1/2/3	(human/yeast) organic cation transporter 1/2/3
oxaliplatin	*trans*-L-diaminocyclohexane oxalate platinum(II)
PARP	poly(ADP-ribose)polymerase 1
PCNA	proliferating cell nuclear antigen
PIC1/2/3	preincision complex 1/2/3
PI(3)K	phosphatidylinositol-3-OH kinases
PMS2	postmeiotic segregation increased 2
Pol	polymerase
PTEN	phosphatase and tension homolog
RR	recombination repair
(r/m)RNA	(ribosomal/messenger) ribonucleic acid
siRNA	small interfering RNA
SSRP1	structure specific recognition protein
$t_{1/2}$	half-life
TAD1/2	transactivation domains 1/2
TBP	TATA-binding protein
TLS	translesion synthesis
(h)UBF	(human)upstream binding factor
XP	xeroderma pigmentosum
zeniplatin	2,2-bis aminomethyl-1,3-propandiol-N-N′ 1,1-cyclobutane dicarboxylate-O′,O′platinum(II)

REFERENCES

1. R. A. Alderden, M. D. Hall, T. W. Hambley, *J. Chem. Edu.* **2006**, *83*, 728–734.
2. F. M. Muggia, A. Bonetti, J. D. Hoeschele, M. Rozencweig, S. B. Howell, *J. Clin. Oncol.* **2015**, *33*, 4219–4226.
3. B. Rosenberg, L. Van Camp, T. Krigas, *Nature* **1965**, *205*, 698–699.
4. B. Rosenberg, L. Van Camp, E. B. Grimley, A. J. Thomson, *J. Biol. Chem.* **1967**, *242*, 1347–1352.
5. B. Rosenberg, *Platin. Met. Rev.* **1971**, *15*, 42–51.
6. B. Rosenberg, L. Van Camp, J. E. Trosko, V. H. Mansour, *Nature* **1969**, *222*, 385–386.
7. D. J. Higby, H. J. Wallace, D. J. Albert, J. F. Holland, *Cancer* **1974**, *33*, 1219–1225.
8. N. Hanna, L. H. Einhorn, *J. Clin. Oncol.* **2014**, *32*, 3085–3092.
9. M. Rozencweig, D. D. Von Hoff, M. Slavik, F. M. Muggia, *Ann. Intern. Med.* **1977**, *86*, 803–812.

10. E. Cvitkovic, J. Spaulding, V. Bethune, J. Martin, W. F. Whitmore, *Cancer* **1977**, *39*, 1357–1361.
11. C. F. J. Barnard, *Platin. Met. Rev.* **1989**, *33*, 162–167.
12. D. Lebwohl, R. Canetta, *Eur. J. Cancer* **1998**, *34*, 1522–1534.
13. L. X. Cubeddu, I. S. Hoffmann, N. T. Fuenmayor, A. L. Finn, *New Eng. J. Med.* **1990**, *322*, 810–816.
14. L. Kelland, *Nat. Rev. Cancer* **2007**, *7*, 573–584.
15. R. J. Knox, F. Friedlos, D. A. Lydall, J. J. Roberts, *Cancer Res.* **1986**, *46*, 1972–1979.
16. L. R. Kelland, S. J. Clarke, M. J. McKeage, *Platin. Met. Rev.* **1992**, *36*, 178–189.
17. Y. Kidani, K. Inagaki, M. Iigo, A. Hoshi, K. Kuretani, *J. Med. Chem.* **1978**, *21*, 1315–1318.
18. N. J. Wheate, S. Walker, G. E. Craig, R. Oun, *Dalton Trans.* **2010**, *39*, 8113–8127.
19. O. Rixe, W. Ortuzar, M. Alvarez, R. Parker, E. Reed, K. Paull, T. Fojo, *Biochem. Pharmacol.* **1996**, *52*, 1855–1865.
20. J. L. Grem, N. McAtee, F. Balis, R. Murphy, D. Venzon, B. Kramer, B. Goldspiel, M. Begley, C. J. Allegra, *Cancer* **1993**, *72*, 663–668.
21. P. J. Loehrer, S. Turner, P. Kubilis, S. Hui, J. Correa, R. Ansari, D. Stephens, R. Woodburn, S. Meyer, *J. Clin. Oncol.* **1988**, *6*, 642–648.
22. A. de Gramont, A. Figer, M. Seymour, M. Homerin, A. Hmissi, J. Cassidy, C. Boni, H. Cortes-Funes, A. Cervantes, G. Freyer, D. Papamichael, N. Le Bail, C. Louvet, D. Hendler, F. de Braud, C. Wilson, F. Morvan, A. Bonetti, *J. Clin. Oncol.* **2000**, *18*, 2938–2947.
23. R. L. Siegel, K. D. Miller, A. Jemal, *Cancer J. Clin.* **2016**, *66*, 7–30.
24. Y. Jung, S. J. Lippard, *Chem. Rev.* **2007**, *107*, 1387–1407.
25. M. Kartalou, J. M. Essigmann, *Mutat. Res.* **2001**, *478*, 23–43.
26. G. Ciarimboli, *Scientifica* **2012**, *2012*, 18, 473829.
27. M. D. Hall, M. Okabe, D.-W. Shen, X.-J. Liang, M. M. Gottesman, *Annu. Rev. Pharmacol. Toxicol.* **2008**, *48*, 495–535.
28. A. Basu, S. Krishnamurthy, *J. Nucleic Acids* **2010**, *2010*, 16; doi: 10.4061/*2010*/201367.
29. S. P. Binks, M. Dobrota, *Biochem. Pharmacol.* **1990**, *40*, 1329–1336.
30. N. D. Eljack, H.-Y. M. Ma, J. Drucker, C. Shen, T. W. Hambley, E. J. New, T. Friedrich, R. J. Clarke, *Metallomics* **2014**, *6*, 2126–2133.
31. R. Safaei, *Cancer Lett.* **2006**, *234*, 34–39.
32. P. Abada, S. B. Howell, *Met. Based Drugs* **2010**, *9*; doi: 10.1155/2010/317581.
33. K. D. Ivy, J. H. Kaplan, *Mol. Pharmacol.* **2013**, *83*, 1237–1246.
34. S. Ishida, F. McCormick, K. Smith-McCune, D. Hanahan, *Cancer Cell* **2010**, *17*, 574–583.
35. S. Ishida, J. Lee, D. J. Thiele, I. Herskowitz, *Proc. Natl. Acad. Sci. USA* **2002**, *99*, 14298–14302.
36. X. Lin, T. Okuda, A. Holzer, S. B. Howell, *Mol. Pharmacol.* **2002**, *62*, 1154–1159.
37. I.-S. Song, N. Savaraj, Z. H. Siddik, P. Liu, Y. Wei, C. J. Wu, M. T. Kuo, *Mol. Cancer Ther.* **2004**, *3*, 1543–1549.
38. J. Zisowsky, S. Koegel, S. Leyers, K. Devarakonda, M. U. Kassack, M. Osmak, U. Jaehde, *Biochem. Pharmacol.* **2007**, *73*, 298–307.
39. Z. D. Liang, Y. Long, W.-B. Tsai, S. Fu, R. Kurzrock, M. Gagea-Iurascu, F. Zhang, H. H. W. Chen, B. T. Hennessy, G. B. Mills, N. Savaraj, M. T. Kuo, *Mol. Cancer Ther.* **2012**, *11*, 2483–2494.
40. A. K. Holzer, K. Katano, L. W. J. Klomp, S. B. Howell, *Clin. Cancer Res.* **2004**, *10*, 6744–6749.
41. A. K. Holzer, S. B. Howell, *Cancer Res.* **2006**, *66*, 10944–10952.
42. X. Xu, L. Duan, B. Zhou, R. Ma, H. Zhou, Z. Liu, *Clin. Exp. Pharmacol. Physiol.* **2012**, *39*, 786–792.

43. K. M. Bompiani, C.-Y. Tsai, F. P. Achatz, J. K. Liebig, S. B. Howell, *Metallomics* **2016**, *8*, 951–962.
44. C. A. Larson, P. L. Adams, D. D. Jandial, B. G. Blair, R. Safaei, S. B. Howell, *Biochem. Pharmacol.* **2010**, *80*, 448–454.
45. C. A. Larson, P. L. Adams, B. G. Blair, R. Safaei, S. B. Howell, *Mol. Pharmacol.* **2010**, *78*, 333–359.
46. B. G. Blair, C. A. Larson, R. Safaei, S. B. Howell, *Clin Cancer Res.* **2009**, *15*, 4312–4321.
47. C. P. Huang, M. Fofana, J. Chan, C. J. Chang, S. B. Howell, *Metallomics* **2014**, *6*, 654–661.
48. B. G. Blair, C. A. Larson, P. L. Adams, P. B. Abada, C. E. Pesce, R. Safaei, S. B. Howell, *Mol. Pharmacol.* **2011**, *79*, 157–166.
49. V. Calandrini, F. Arnesano, A. Galliani, T. H. Nguyen, E. Ippoliti, P. Carloni, G. Natile, *Dalton Trans.* **2014**, *43*, 12085–12094.
50. K. Katano, R. Safaei, G. Samimi, A. Holzer, M. Tomioka, M. Goodman, S. B. Howell, *Clin. Cancer Res.* **2004**, *10*, 4578–4588.
51. M. Komatsu, T. Sumizawa, M. Mutoh, Z.-S. Chen, K. Terada, T. Furukawa, X.-L. Yang, H. Gao, N. Miura, T. Sugiyama, S. Akiyama, *Cancer Res.* **2000**, *60*, 1312–1316.
52. K. Yoshizawa, S. Nozaki, H. Kitahara, T. Ohara, K. Kato, S. Kawashiri, E. Yamamoto, *Oncol. Rep.* **2007**, *18*, 987–991.
53. E. Martinez-Balibrea, A. Martínez-Cardús, E. Musulén, A. Ginés, J. L. Manzano, E. Aranda, C. Plasencia, N. Neamati, A. Abad, *Int. J. Cancer* **2009**, *124*, 2905–2910.
54. S. Harrach, G. Ciarimboli, *Front. Pharmacol.* **2015**, *6*, 85; doi: 10.3389/fphar.2015.00085.
55. J. W. Jonker, A. H. Schinkel, *J. Pharm. Exp. Ther.* **2004**, *308*, 2–9.
56. H. Koepsell, K. Lips, C. Volk, *Pharmaceut. Res.* **2007**, *24*, 1227–1251.
57. E. Schlatter, P. Klassen, V. Massmann, S. K. Holle, D. Guckel, B. Edemir, H. Pavenstädt, G. Ciarimboli, *Pflügers Arch., EJP* **2014**, *466*, 1581–1589.
58. D. Gründemann, V. Gorboulev, S. Gambaryan, M. Veyhl, H. Koepsell, *Nature* **1994**, *372*, 549–552.
59. J. W. Jonker, E. Wagenaar, S. van Eijl, A. H. Schinkel, *Mol. Cell. Biol.* **2003**, *23*, 7902–7908.
60. A. Yonezawa, S. Masuda, K. Nishihara, I. Yano, T. Katsura, K.-i. Inui, *Biochem. Pharmacol.* **2005**, *70*, 1823–1831.
61. G. Ciarimboli, T. Ludwig, D. Lang, H. Pavenstädt, H. Koepsell, H.-J. Piechota, J. Haier, U. Jaehde, J. Zisowsky, E. Schlatter, *Am. J. Path.*, *167*, 1477–1484.
62. H. Katsuda, M. Yamashita, H. Katsura, J. Yu, Y. Waki, N. Nagata, Y. Sai, K. Miyamoto, *Biol. Pharm. Bull.* **2010**, *33*, 1867–1871.
63. K. K. Filipski, R. H. Mathijssen, T. S. Mikkelsen, A. H. Schinkel, A. Sparreboom, *Clin. Pharmacol. Ther.* **2009**, *86*, 396–402.
64. D. Th. Sleijfer, J. J. G. Offerman, N. H. Mulder, M. Verweij, G. K. van der Hem, H. S. Koops, S. Meijer, *Cancer* **1987**, *60*, 2823–2828.
65. J. Zhang, W. Zhou, *Food Chem.Toxicol.* **2012**, *50*, 2289–2293.
66. G. Ciarimboli, D. Deuster, A. Knief, M. Sperling, M. Holtkamp, B. Edemir, H. Pavenstädt, C. Lanvers-Kaminsky, A. am Zehnhoff-Dinnesen, A. H. Schinkel, H. Koepsell, H. Jürgens, E. Schlatter, *Am. J. Path.* **2010**, *176*, 1169–1180.
67. A. Yonezawa, S. Masuda, S. Yokoo, T. Katsura, K.-i. Inui, *J. Pharm. Exp. Ther.* **2006**, *319*, 879–886.
68. S. Zhang, K. S. Lovejoy, J. E. Shima, L. L. Lagpacan, Y. Shu, A. Lapuk, Y. Chen, T. Komori, J. W. Gray, X. Chen, S. J. Lippard, K. M. Giacomini, *Cancer Res.* **2006**, *66*, 8847–8857.

69. T. Kanou, J. Uozumi, K. Soejima, Y. Tokuda, Z. Masaki, *Clin. Exp. Nephrol.* **2004**, *8*, 310–315.
70. S. Yokoo, S. Masuda, A. Yonezawa, T. Terada, T. Katsura, K.-i. Inui, *Drug Metab. Dispos.* **2008**, *36*, 2299–2306.
71. T. Nakamura, A. Yonezawa, S. Hashimoto, T. Katsura, K.-i. Inui, *Biochem. Pharmacol.* **2010**, *80*, 1762–1767.
72. A. Yonezawa, K.-i. Inui, *Biochem. Pharmacol.* **2011**, *81*, 563–568.
73. M. Jennerwein, P. A. Andrews, *Drug Metab. Dispos.* 1995, *23*, 178–184.74. S. J. Berners-Price, T. G. Appleton, in *Platinum-Based Drugs in Cancer Therapy*, Eds L. R. Kelland, N. P. Farrell, Humana Press, Totowa, NJ, 2000, pp. 3–35.
75. O. Pinato, C. Musetti, C. Sissi, *Metallomics* **2014**, *6*, 380–395.
76. P. C. Dedon, R. F. Borch, *Biochem. Pharmacol.* **1987**, *36*, 1955–1964.
77. D. P. Bancroft, C. A. Lepre, S. J. Lippard, *J. Am. Chem. Soc.* **1990**, *112*, 6860–6871.
78. S. J. Berners-Price, T. A. Frenkiel, U. Frey, J. D. Ranford, P. J. Sadler, *J. Chem. Soc., Chem. Commun.* **1992**, 789–791.
79. R. Faggiani, B. Lippert, C. J. L. Lock, B. Rosenberg, *Inorg. Chem.* **1977**, *16*, 1192–1196.
80. R. Faggiani, B. Lippert, C. J. L. Lock, B. Rosenberg, *J. Am. Chem. Soc.* **1977**, *99*, 777–781.
81. B. Rosenberg, *Biochimie* **1978**, *60*, 859–867.
82. D. S. Gill, B. Rosenberg, *J. Am. Chem. Soc.* **1982**, *104*, 4598–4604.
83. T. G. Appleton, R. D. Berry, C. A. Davis, J. R. Hall, H. A. Kimlin, *Inorg. Chem.* **1984**, *23*, 3514–3521.
84. M. C. Lim, R. B. Martin, *J. Inorg. Nucl. Chem.* **1976**, *38*, 1911–1914.
85. R. C. Todd, K. S. Lovejoy, S. J. Lippard, *J. Am. Chem. Soc.* **2007**, *129*, 6370–6371.
86. K. Zhang, M. Chew, E. B. Yang, K. P. Wong, P. Mack, *Mol. Pharmacol.* **2001**, *59*, 837–843.
87. D. M. Townsend, K. D. Tew, *Oncogene* **2003**, *22*, 7369–7375.
88. O. Heudi, A. Cailleux, P. Allain, *J. Inorg. Biochem.* **1998**, *71*, 61–69.
89. K. J. Barnham, M. I. Djuran, P. del Socorro Murdoch, J. D. Ranford, P. J. Sadler, *Dalton Trans.* **1995**, 3721–3726.
90. M. A. Graham, G. F. Lockwood, D. Greenslade, S. Brienza, M. Bayssas, E. Gamelin, *Clin. Cancer Res.* **2000**, *6*, 1205–1218.
91. E. R. Jamieson, S. J. Lippard, *Chem. Rev.* **1999**, *99*, 2467–2498.
92. S. P. LeDoux, G. L. Wilson, E. J. Beecham, T. Stevnsner, K. Wassermann, V. A. Bohr, *Carcinogenesis* **1992**, *13*, 1967–1973.
93. X. Shu, X. Xiong, J. Song, C. He, C. Yi, *Angew. Chem. Int. Ed.* 2016, *55*, 14246–14249.
94. O. A. Olivero, C. Semino, A. Kassim, D. M. Lopez-Larraza, M. C. Poirier, *Mutat. Res. Lett.* **1995**, *346*, 221–230.
95. O. A. Olivero, P. K. Chang, D. M. Lopez-Larraza, M. Cristina Semino-Mora, M. C. Poirier, *Mutat. Res.* **1997**, *391*, 79–86.
96. H. C. Harder, B. Rosenberg, *Int. J. Cancer* **1970**, *6*, 207–216.
97. M. Kartalou, J. M. Essigmann, *Mutat. Res.* **2001**, *478*, 1–21.
98. S. E. Sherman, S. J. Lippard, *Chem. Rev.* **1987**, *87*, 1153–1181.
99. S. G. Chaney, S. L. Campbell, E. Bassett, Y. Wu, *Crit. Rev. Oncol. Hematol.* **2005**, *53*, 3–11.
100. R. C. Todd, S. J. Lippard, *Metallomics* **2009**, *1*, 280–291.
101. P. M. Takahara, A. C. Rosenzweig, C. A. Frederick, S. J. Lippard, *Nature* **1995**, *377*, 649–652.
102. D. Yang, S. S. G. E. van Boom, J. Reedijk, J. H. van Boom, A. H.–J. Wang, *Biochem.* **1995**, *34*, 12912–12920.

103. A. Gelasco, S. J. Lippard, *Biochem.* **1998**, *37*, 9230–9239.
104. C. J. Van Garderen, L. P. A. Van Houte, *Eur. J. Biochem.* 1994, *225*, 1169–1179.
105. F. Coste, J.-M. Malinge, L. Serre, W. Shepard, M. Roth, M. Leng, C. Zelwer, *Nucleic Acids Res.* **1999**, *27*, 1837–1846.
106. B. Spingler, D. A. Whittington, S. J. Lippard, *Inorg. Chem.* 2001, *40*, 5596–5602.
107. Y. Wu, P. Pradhan, J. Havener, G. Boysen, J. A. Swenberg, S. L. Campbell, S. G. Chaney, *J. Mol. Biol.* **2004**, *341*, 1251–1269.
108. B. Wu, C. A. Davey, *Chem. Biol.* **2008**, *15*, 1023–1028.
109. I. Ioshikhes, A. Bolshoy, K. Derenshteyn, M. Borodovsky, E. N. Trifonov, *J. Mol. Biol.* **1996**, *262*, 129–139.
110. A. J. Danford, D. Wang, Q. Wang, T. D. Tullius, S. J. Lippard, *Proc. Natl. Acad. Sci. USA* **2005**, *102*, 12311–12316.
111. S. J. Lippard, J. D. Hoeschele, *Proc, Natl Acad. Sci. USA* **1979**, *76*, 6091–6095.
112. M. Foka, J. Paoletti, *Biochem. Pharmacol.* **1986**, *35*, 3283–3291.
113. J. J. Hayes, W. M. Scovell, *Biochim. Biophysi. Acta* **1991**, *1088*, 413–418.
114. A. M. Galea, V. Murray, *Biochim. Biophys. Acta* **2002**, *1579*, 142–152.
115. N. P. Davies, L. C. Hardman, V. Murray, *Nucleic Acids Res.* **2000**, *28*, 2954–2958.
116. E. Segal, Y. Fondufe-Mittendorf, L. Chen, A. Thåström, Y. Field, I. K. Moore, J.-P. Z. Wang, J. Widom, *Nature* **2006**, *442*, 772–778.
117. M. Ober, S. J. Lippard, *J. Am. Chem. Soc.* **2007**, *129*, 6278–6286.
118. M. Ober, S. J. Lippard, *J. Am. Chem. Soc.* **2008**, *130*, 2851–2861.
119. D. Wang, R. Hara, G. Singh, A. Sancar, S. J. Lippard, *Biochem.* **2003**, *42*, 6747–6753.
120. K. M. Comess, J. N. Burstyn, J. M. Essigmann, S. J. Lippard, *Biochem.* **1992**, *31*, 3975–3990.
121. C. M. Sorenson, A. Eastman, *Cancer Res.* **1988**, *48*, 4484–4488.
122. S. Prakash, R. E. Johnson, L. Prakash, *Annu. Rev. Biochem.* **2005**, *74*, 317–353.
123. J. K. Hicks, C. L. Chute, M. T. Paulsen, R. L. Ragland, N. G. Howlett, Q. Guéranger, T. W. Glover, C. E. Canman, *Mol. Cell. Biol.* **2010**, *30*, 1217–1230.
124. A. Vaisman, S. E. Lim, S. M. Patrick, W. C. Copeland, D. C. Hinkle, J. J. Turchi, S. G. Chaney, *Biochem.* **1999**, *38*, 11026–11039.
125. A. R. Lehmann, A. Niimi, T. Ogi, S. Brown, S. Sabbioneda, J. F. Wing, P. L. Kannouche, C. M. Green, *DNA Repair* **2007**, *6*, 891–899.
126. S. G. Chaney, S. L. Campbell, B. Temple, E. Bassett, Y. Wu, M. Faldu, *J. Inorg. Biochem.* **2004**, *98*, 1551–1559.
127. P. A. Knobel, T. M. Marti, *Cancer Cell Int.* **2011**, *11*, 39–39.
128. T. V. Ho, A. Guainazzi, S. B. Derkunt, M. Enoiu, O. D. Schärer, *Nucleic Acids Res.* **2011**, *39*, 7455–7464.
129. U. Roy, O. D. Schärer, *DNA Repair* **2016**, *44*, 33–41.
130. C. M. Sorenson, A. Eastman, *Cancer Res.* **1988**, *48*, 6703–6707.
131. Y. Corda, C. Job, M.-F. Anin, M. Leng, D. Job, *Biochem.* **1991**, *30*, 222–230.
132. R. Hara, C. P. Selby, M. Liu, D. H. Price, A. Sancar, *J. Biol. Chem.* **1999**, *274*, 24779–24786.
133. P. M. Bruno, Y. Liu, G. Y. Park, J. Murai, C. E. Koch, T. J. Eisen, J. R. Pritchard, Y. Pommier, S. J. Lippard, M. T. Hemann, *Nat. Med.* **2017**, *23*, 461–471.
134. J. T. Reardon, A. Vaisman, S. G. Chaney, A. Sancar, *Cancer Res.* **1999**, *59*, 3968–3971.
135. D. B. Zamble, D. Mu, J. T. Reardon, A. Sancar, S. J. Lippard, *Biochem.* **1996**, *35*, 10004–10013.
136. A. Sancar, L. A. Lindsey-Boltz, K. Ünsal-Kaçmaz, S. Linn, *Annu. Rev. Biochem.* **2004**, *73*, 39–85.
137. T. Furuta, T. Ueda, G. Aune, A. Sarasin, K. H. Kraemer, Y. Pommier, *Cancer Res.* **2002**, *62*, 4899–4902.

138. Z. Z. Zdraveski, J. A. Mello, M. G. Marinus, J. M. Essigmann, *Chem. Biol.* **2000**, *7*, 39–50.
139. D. M. Noll, T. M. Mason, P. S. Miller, *Chem. Rev.* **2006**, *106*, 277–301.
140. G. P. Raaphorst, J.-M. Leblanc, L. F. Li, *Anticancer Res.* **2005**, *25*, 53–58.
141. G.-L. Moldovan, A. D. D'Andrea, *Annu. Rev. Genet.* 2009, *43*, 223–249.
142. A. D. D'Andrea, M. Grompe, *Nat. Rev. Cancer* **2003**, *3*, 23–34.
143. B. Haynes, N. Saadat, B. Myung, M. P. V. Shekhar, *Mutat. Res.* **2015**, *763*, 258–266.
144. J. Jiricny, *Nat. Rev. Mol. Cell. Biol.* **2006**, *7*, 335–346.
145. A. Sawant, A. Kothandapani, A. Zhitkovich, R. W. Sobol, S. M. Patrick, *DNA Repair* **2015**, *35*, 126–136.
146. D. Fink, S. Nebel, S. Aebi, H. Zheng, B. Cenni, A. Nehmé, R. D. Christen, S. B. Howell, *Cancer Res.* **1996**, *56*, 4881–4886.
147. D. Fink, S. Aebi, S. B. Howell, *Clin. Cancer Res.* **1998**, *4*, 1–6.
148. J. A. Mello, S. Acharya, R. Fishel, J. M. Essigmann, *Chem. Biol.* **1996**, *3*, 579–589.
149. D. R. Duckett, J. T. Drummond, A. I. H. Murchie, J. T. Reardon, A. Sancar, D. M. J. Lilley, P. Modrich, *Proc. Natl. Acad. Sci. USA* **1996**, *93*, 6443–6447.
150. G. Zhu, S. J. Lippard, *Biochem.* **2009**, *48*, 4916–4925.
151. Z. Li, A. H. Pearlman, P. Hsieh, *DNA Repair* **2016**, *38*, 94–101.
152. H. E. Krokan, M. Bjørås, *Cold Spring Harb. Perspect. Biol.* **2013**, *5*, a012583; doi: 10.1101/cshperspect.a012583.
153. A. Kothandapani, V. S. M. N. Dangeti, A. R. Brown, L. A. Banze, X.-H. Wang, R. W. Sobol, S. M. Patrick, *J. Biol. Chem.* **2011**, *286*, 14564–14574.
154. D. Wang, D.-B. Xiang, X.-q. Yang, L.-S. Chen, M.-X. Li, Z.-Y. Zhong, Y.-S. Zhang, *Lung Cancer* **2009**, *66*, 298–304.
155. J. Zlatanova, J. Yaneva, S. H. Leuba, *FASEB J.* **1998**, *12*, 791–799.
156. W. M. Scovell, N. Muirhead, L. R. Kroos, *Biochem. Biophys. Res. Commun.* **1987**, *142*, 826–835.
157. S. L. Bruhn, P. M. Pil, J. M. Essigmann, D. E. Housman, S. J. Lippard, *Proc. Natl. Acad. Sci. USA* **1992**, *89*, 2307–2311.
158. M. Wei, O. Burenkova, S. J. Lippard, *J. Biol. Chem.* **2003**, *278*, 1769–1773.
159. S. G. Awuah, I. A. Riddell, S. J. Lippard, *Proc. Natl. Acad. Sci. USA* **2017**, *114*, 950–955.
160. S. Park, S. J. Lippard, *Biochemistry* **2012**, *51*, 6728–6737.
161. A. T. Yarnell, S. Oh, D. Reinberg, S. J. Lippard, *J. Biol. Chem.* **2001**, *276*, 25736–25741.
162. D. K. Treiber, X. Zhai, H. M. Jantzen, J. M. Essigmann, *Proc. Natl Acad. Sci. USA* **1994**, *91*, 5672–5676.
163. F. Coin, P. Frit, B. Viollet, B. Salles, J.-M. Egly, *Mol. Cell. Biol.* **1998**, *18*, 3907–3914.
164. T. Ohga, K. Koike, M. Ono, Y. Makino, Y. Itagaki, M. Tanimoto, M. Kuwano, K. Kohno, *Cancer Res.* **1996**, *56*, 4224–4228.
165. G. Zhu, P. Chang, S. J. Lippard, *Biochem.* **2010**, *49*, 6177–6183.
166. H. Farmer, N. McCabe, C. J. Lord, A. N. J. Tutt, D. A. Johnson, T. B. Richardson, M. Santarosa, K. J. Dillon, I. Hickson, C. Knights, N. M. B. Martin, S. P. Jackson, G. C. M. Smith, A. Ashworth, *Nature* **2005**, *434*, 917–921.
167. V. Schreiber, F. Dantzer, J.-C. Amé, G. de Murcia, *Nat. Rev. Mol. Cell Biol.* **2006**, *7*, 517–528.
168. J. Michels, I. Vitale, L. Galluzzi, J. Adam, K. A. Olaussen, O. Kepp, L. Senovilla, I. Talhaoui, J. Guegan, D. P. Enot, M. Talbot, A. Robin, P. Girard, C. Oréar, D. Lissa, A. Q. Sukkurwala, P. Garcia, P. Behnam-Motlagh, K. Kohno, G. S. Wu, C. Brenner, P. Dessen, M. Saparbaev, J.-C. Soria, M. Castedo, G. Kroemer, *Cancer Res.* **2013**, *73*, 2271–2280.
169. C. C. Wetzel, S. J. Berberich, *Biochim. Biophys. Acta* **2001**, *1517*, 392–397.

170. H. Pivoňková, M. Brázdová, J. Kašpárková, V. Brabec, M. Fojta, *Biochem. Biophys. Res. Commun.* **2006**, *339*, 477–484.
171. J. Kasparkova, S. Pospisilova, V. Brabec, *J. Biol. Chem.* **2001**, *276*, 16064–16069.
172. T. Imamura, H. Izumi, G. Nagatani, T. Ise, M. Nomoto, Y. Iwamoto, K. Kohno, *J. Biol. Chem.* **2001**, *276*, 7534–7540.
173. B.-B. S. Zhou, S. J. Elledge, *Nature* **2000**, *408*, 433–439.
174. D. Wang, S. J. Lippard, *Nat. Rev. Drug Discov.* **2005**, *4*, 307–320.
175. P. Roos-Mattjus, B. T. Vroman, M. A. Burtelow, M. Rauen, A. K. Eapen, L. M. Karnitz, *J. Biol. Chem.* **2002**, *277*, 43809–43812.
176. A. Maréchal, L. Zou, *Cold Spring Harb. Perspect. Biol.* **2013**, *5*, a012716; doi: 10.1101/cshperspect.a012716.
177. M. Xu, L. Bai, Y. Gong, W. Xie, H. Hang, T. Jiang, *J. Biol. Chem.* **2009**, *284*, 20457–20461.
178. E. R. Parrilla-Castellar, S. J. H. Arlander, L. Karnitz, *DNA Repair* **2004**, *3*, 1009–1014.
179. M. Toueille, N. El-Andaloussi, I. Frouin, R. Freire, D. Funk, I. Shevelev, E. Friedrich-Heineken, G. Villani, M. O. Hottiger, U. Hübscher, *Nucleic Acids Res.* **2004**, *32*, 3316–3324.
180. S. Delacroix, J. M. Wagner, M. Kobayashi, K.-i. Yamamoto, L. M. Karnitz, *Genes Dev.* **2007**, *21*, 1472–1477.
181. R. H. Medema, L. Macurek, *Oncogene* **2012**, *31*, 2601–2613.
182. J. Benada, L. Macurek, *Biomolecules* **2015**, *5*, 1912–1937.
183. B.-B. S. Zhou, J. Bartek, *Nat. Rev. Cancer* **2004**, *4*, 216–225.
184. H. Takai, K. Tominaga, N. Motoyama, Y. A. Minamishima, H. Nagahama, T. Tsukiyama, K. Ikeda, K. Nakayama, M. Nakanishi, K.-i. Nakayama, *Genes Dev.* **2000**, *14*, 1439–1447.
185. C. S. Sørensen, R. G. Syljuåsen, *Nucleic Acids Res.* **2012**, *40*, 477–486.
186. A. Brozovic, M. Osmak, *Cancer Lett.* **2007**, *251*, 1–16.
187. J. M. Kyriakis, J. Avruch, *Physiol. Rev.* **2001**, *81*, 807–869.
188. X. Wang, J. L. Martindale, N. J. Holbrook, *J. Biol. Chem.* **2000**, *275*, 39435–39443.
189. Y. K. Kim, H. J. Kim, C. H. Kwon, J. H. Kim, J. S. Woo, J. S. Jung, J. M. Kim, *J. App. Toxicol.* **2005**, *25*, 374–382.
190. S. Lee, S. Yoon, D.-H. Kim, *Gynecol. Oncol.* **2007**, *104*, 338–344.
191. J. H. Losa, C. P. Cobo, J. G. Viniegra, V. J. S.-A. Lobo, S. Ramon y Cajal, R. Sánchez-Prieto, *Oncogene* **2003**, *22*, 3998–4006.
192. D. Wang, S. J. Lippard, *J. Biol. Chem.* **2004**, *279*, 20622–20625.
193. D. N. Dhanasekaran, E. P. Reddy, *Oncogene* **2008**, *27*, 6245–6251.
194. B. W. Zanke, K. Boudreau, E. Rubie, E. Winnett, L. A. Tibbles, L. Zon, J. Kyriakis, F.-F. Liu, J. R. Woodgett, *Curr. Biol.* **1996**, *6*, 606–613.
195. Z. H. Siddik, *Oncogene* 2003, *22*, 7265–7279.
196. W. Dempke, W. Voigt, A. Grothey, B. T. Hill, H.-J. Schmoll, *Anticancer Drugs* **2000**, *11*, 225–236.
197. J. M. Nigro, S. J. Baker, A. C. Preisinger, J. M. Jessup, R. Hosteller, K. Cleary, S. H. Bigner, N. Davidson, S. Baylin, P. Devilee, T. Glover, F. S. Collins, A. Weston, R. Modali, C. C. Harris, B. Vogelstein, *Nature* **1989**, *342*, 705–708.
198. M. Hollstein, D. Sidransky, B. Vogelstein, C. C. Harris, *Science* **1991**, *253*, 49–53.
199. G. L. Y. Zhang, *Annu. Rev. Cancer Biol.* **2017**, *1*, null.
200. C. C. Harris, *J. Natl. Cancer Inst.* **1996**, *88*, 1442–1455.
201. T. Saha, R. K. Kar, G. Sa, *Prog. Biophys. Mol. Bio.* **2015**, *117*, 250–263.
202. H. Jiang, J. R. Pritchard, R. T. Williams, D. A. Lauffenburger, M. T. Hemann, *Nat. Chem. Biol.* **2011**, *7*, 92–100.
203. K. Barabas, R. Milner, D. Lurie, C. Adin, *Vet. Comp. Oncol.* **2008**, *6*, 1–18.

204. P. M. Hoff, E. D. Saad, F. Costa, A. K. Coutinho, R. Caponero, G. Prolla, R. C. Gansl, *Clin. Colorectal Cancer* **2012**, *11*, 93–100.
205. H. Adelsberger, S. Quasthoff, J. Grosskreutz, A. Lepier, F. Eckel, C. Lersch, *Eur. J. Pharmacol.* **2000**, *406*, 25–32.
206. R. S. Go, A. A. Adjei, *J. Clin. Oncol.* **1999**, *17*, 409–409.
207. S. Wolf, D. Barton, L. Kottschade, A. Grothey, C. Loprinzi, *Eur. J. Cancer* **2008**, *44*, 1507–1515.
208. S. B. Park, C. S.-Y. Lin, A. V. Krishnan, D. Goldstein, M. L. Friedlander, M. C. Kiernan, *PLOS ONE* **2011**, *6*, e18469; doi: doi:10.1371/journal.pone.0018469.
209. K. U. Wensing, G. Ciarimboli, *Anticancer Res.* **2013**, *33*, 4183–4188.
210. E. Raymond, S. G. Chaney, A. Taamma, E. Cvitkovic, *Ann. Oncol.* **1998**, *9*, 1053–1071.
211. V. Pinzani, F. Bressolle, I. J. Haug, M. Galtier, J. P. Blayac, P. Balmès, *Cancer Chemother. Pharmacol.* **1994**, *35*, 1–9.
212. D. McWhirter, N. Kitteringham, R. P. Jones, H. Malik, K. Park, D. Palmer, *Crit. Rev. Oncol. Hematol.* **2013**, *88*, 404–415.
213. L. R. Kelland, *Crit. Rev. Oncol. Hematol.* **1993**, *15*, 191–219.
214. J. R. W. Masters, R. Thomas, A. G. Hall, L. Hogarth, E. C. Matheson, A. R. Cattan, H. Lohrer, *Eur. J. Cancer* **1996**, *32*, 1248–1253.
215. K. Kasahara, Y. Fujiwara, K. Nishio, T. Ohmori, Y. Sugimoto, K. Komiya, T. Matsuda, N. Saijo, *Cancer Res.* **1991**, *51*, 3237–3243.
216. F.-S. Liu, *Taiwan. J. Obstet. Gynecol.* **2009**, *48*, 239–244.
217. J. E. Visvader, G. J. Lindeman, *Nat. Rev. Cancer* **2008**, *8*, 755–768.
218. A. Wiechert, C. Saygin, P. S. Thiagarajan, V. S. Rao, J. S. Hale, N. Gupta, M. Hitomi, A. B. Nagaraj, A. DiFeo, J. D. Lathia, O. Reizes, *Oncotarget* **2016**, *7*, 30511–30522.
219. A. Vassilopoulos, C. Xiao, C. Chisholm, W. Chen, X. Xu, T. J. Lahusen, C. Bewley, C.-X. Deng, *J. Biol. Chem.* **2014**, *289*, 24202–24214.
220. W. R. Leopold, E. C. Miller, J. A. Miller, *Cancer Res.* **1979**, *39*, 913–918.
221. B. J. S. Sanderson, L. R. Ferguson, W. A. Denny, *Mutat. Res.* **1996**, *355*, 59–70.
222. L. J. N. Bradley, K. J. Yarema, S. J. Lippard, J. M. Essigmann, *Biochem.* **1993**, *32*, 982–988.
223. K. J. Yarema, S. J. Lippard, J. M. Essigmann, *Nucleic Acids Res.* **1995**, *23*, 4066–4072.
224. U. M. Ohndorf, M. A. Rould, Q. He, C. O. Pabo, S. J. Lippard, *Nature* **1999**, *399*, 708–712.

2

Polynuclear Platinum Complexes. Structural Diversity and DNA Binding

Viktor Brabec, [1] ***Jana Kasparkova,*** [1]
Vijay Menon, [2] ***and Nicholas P. Farrell*** [2]

[1]Institute of Biophysics, Czech Academy of Sciences,
Kralovopolska 135, CZ-612 65 Brno, Czech Republic
<brabec@ibp.cz>

[2]Department of Chemistry, Virginia Commonwealth University,
Richmond, VA 23284–2006, USA
<npfarrell@vcu.edu>

ABSTRACT 44
1. INTRODUCTION 44
2. DINUCLEAR BIFUNCTIONAL PLATINUM(II) COMPLEXES WITH ALKANEDIAMINE LINKERS 46
   2.1. {Pt,Pt} Interstrand Crosslinks 46
   2.2. {Pt,Pt} Intrastrand Crosslinks 48
   2.3. Conformational Changes in DNA 48
   2.4. Protein Recognition 48
3. POLYAMINE-LINKED BIFUNCTIONAL DINUCLEAR PLATINUM(II) COMPLEXES 49
   3.1. Consequences of DNA Binding of Dinuclear Polyamine-Linked Complexes 50
   3.2. Interduplex Crosslinking 51
   3.3. Susceptibility to Metabolic Decomposition and Structural Variations 51
   3.4. Macrocyclic Polyamine-Linked Complexes 52
4. DNA-PROTEIN CROSSLINKING 53
5. DINUCLEAR PLATINUM(II) COMPLEXES STABILIZING G-DNA QUADRUPLEXES 53

Metal Ions in Life Sciences, Volume 18 Edited by Astrid Sigel, Helmut Sigel, Eva Freisinger, and Roland K. O. Sigel

https://doi.org/10.1515/9783110470734-002

Met. Ions Life Sci. **2018**, *18*, 43–68

6. STRUCTURAL VARIATION IN DINUCLEAR PLATINUM(II) COMPLEXES 55
6.1. Azole- and Azine-Bridged Dinuclear Bifunctional Pt(II) Complexes 55
6.2. Miscellaneous Dinuclear Platinum(II) Complexes 56
7. TRINUCLEAR PLATINUM(II) COMPLEXES 56
7.1. The Trinuclear Bifunctional Platinum(II) Complex Triplatin (BBR3464) 56
7.2. Directional Isomers 57
7.3. Walking on Double-Helical DNA and Linkage Isomerization 59
7.4. Interactions of DNA Modified by Triplatin by Damaged-DNA Binding Proteins 60
7.4.1. Recognition by HMG-Domain Proteins and DNA Repair 60
7.4.2. Recognition by the Tumor Suppressor Protein p53 60
7.4.3. Recognition by the Nuclear Transcription Factor κB 61
7.4.4. DNA Structural Conformational Changes, Protein Recognition, and Cell Cycle Effects 61
8. CONCLUSIONS AND OUTLOOK 62
ACKNOWLEDGMENTS 63
ABBREVIATIONS AND DEFINITIONS 63
REFERENCES 64

Abstract: Polynuclear platinum complexes (PPCs) represent a discrete structural class of DNA-binding agents with excellent antitumor properties. The use of at least two platinum coordinating units automatically means that multifunctional DNA binding modes are possible. The structural variability inherent in a polynuclear platinum structure can be harnessed to produce discrete modes of DNA binding, with conformational changes distinct from and indeed inaccessible to, the mononuclear agents such as cisplatin. Since our original contributions in this field a wide variety of dinuclear complexes especially have been prepared, their DNA binding studied, and potential relevance to cytotoxicity examined. This chapter focuses on how DNA structure and reactivity is modulated through interactions with PPCs with emphasis on novel aspects of such structure and reactivity. How these major changes are further reflected in damaged DNA-protein binding and cellular effects are reviewed. We further review, for the first time, the great structural diversity achieved in PPC complex design and summarize their major DNA binding effects.

Keywords: DNA conformations · DNA-protein crosslinking · polynuclear platinums · structural diversity

1. INTRODUCTION

The acceptance of DNA as cellular target of cisplatin (*cis*-$[PtCl_2(NH_3)_2]$; *cis*-DDP) and its congeners has led to significant understanding on the factors affecting platinum complex-DNA adduct structure and how these can be modulated by suitable complex design. DNA as a cellular target for platinum metal-based anticancer drugs remains an active area of research including the search for (i) new, more specific or more potent analogs of existing drugs; (ii) agents to

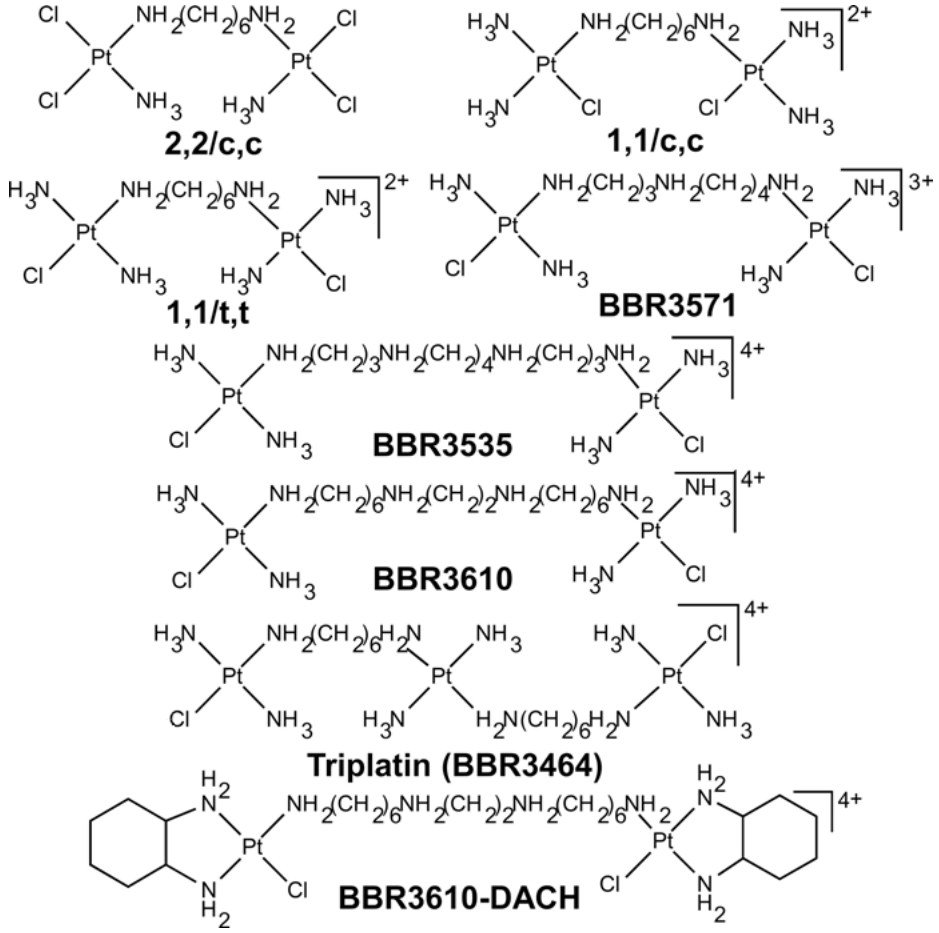

Figure 1. Structures of principal alkanediamine-linked polynuclear platinum complexes (PPCs). Triplatin is BBR3464; 1,1/t,t is BBR3005; 1,1/t,t refers to two monofunctional Pt units where the Pt-Cl is *trans* to the diamine bridge, etc.

induce, interfere with, or preferentially interact with, unusual or "non-B DNA" structures such as Z-DNA, Holliday junctions, and G-quadruplexes; and (iii) agents capable of interacting at the level of DNA-protein complexes, such as telomerase and topoisomerase.

Polynuclear platinum complexes (PPCs) represent a discrete class of platinum-based anticancer agents whose development was based on the concepts that alteration of DNA adduct structure in comparison to those formed by cisplatin and congeners would induce differential downstream effects with respect to protein recognition and cellular signaling pathways (Figure 1). Tolerance of DNA adducts, a property linked in part to the development of cellular resistance to cisplatin, may be considered to be altered through formation of different adduct structures by circumventing the cellular processes associated with cisplatin-DNA adduct rec-

ognition and repair [1–3]. In this way logical approaches to design drugs effective against cisplatin-resistant cancers can be envisaged. Proof of principle for this hypothesis was achieved by the advance to the clinic of Triplatin (BBR3464, $[\{trans\text{-}PtCl(NH_3)_2\}_2\mu\text{-}\{trans\text{-}Pt(NH_3)_2(H_2N(CH_2)_6NH_2)_2\}]^{4+}$), a charged trinuclear bifunctional DNA-binding agent (Figure 1). The pharmacology and antitumor activity of Triplatin and dinuclear analogs have been reviewed [4–6].

The polynuclear platinum structure as shown in Figure 1 inherently leads to a very diverse array of complexes by varying the nature and geometry of the coordination sphere as well as the nature of the linker. The major studies have been on alkanediamine-linked dinuclear and trinuclear complexes but many researchers have now modified this basic structure. DNA represents a rich template for coordination chemistry and, in this review, we will emphasise how research in the polynuclear field has delineated specific DNA modifications, structures and reactivity patterns not readily available to mononuclear complexes. The majority of complexes have good cytotoxicity and in general are collaterally sensitive to cisplatin – these aspects will not be covered in detail, but References are provided.

2. DINUCLEAR BIFUNCTIONAL PLATINUM(II) COMPLEXES WITH ALKANEDIAMINE LINKERS

The predominant DNA adducts in all cases of dinuclear bifunctional Pt(II) complexes are long-range {Pt,Pt} inter- and intrastrand crosslinks (CLs) and DNA-protein crosslinks may also be formed (Figure 2). In $[\{PtCl(NH_3)_2\}_2(H_2N(CH_2)_nNH_2)]^{2+}$ the leaving chloride ligands are either *cis* (1,1/c,c) or *trans* (1,1/t,t) to the diamine bridge (Figure 1). Both geometries display *in vivo* antitumor activity comparable with that of cisplatin but importantly they retain activity in acquired cisplatin-resistant cell lines [1, 4, 5]. This situation represents a fundamental difference between mononuclear and dinuclear platinum chemistry and biology – in the mononuclear case cisplatin is antitumor-active, while transplatin is not.

2.1. {Pt,Pt} Interstrand Crosslinks

{Pt,Pt} interstrand CLs are preferentially formed between N7-platinated G residues and are oriented in the $5' \rightarrow 5'$ direction. Besides 1,2 interstrand CLs (between G residues in neighboring base pairs), 1,3 or 1,4 CLs are also possible where the platination sites are separated by one or 2 base pairs, respectively. Geometry affects the relative proportion of interstrand CLs with the efficiency of formation being much higher for the 1,1/c,c over the 1,1/t,t isomer [7–9]. The 1,1/t,t complex preferentially forms interstrand CLs even when the specific sequence contains the possibility to form a 1,2-intrastrand adduct [10]. The 1,2 CLs are formed with a pronouncedly slower rate than the longer-range 1,3 or 1,4 CLs

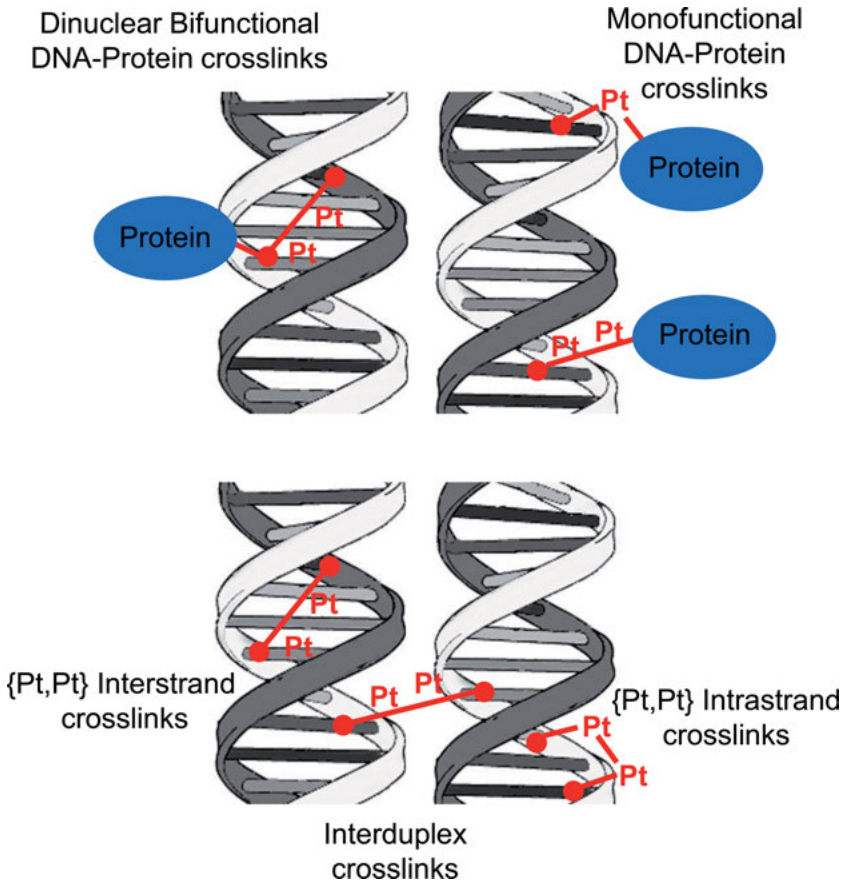

Figure 2. Schematic of major DNA and DNA-protein adducts accessible to PPCs. The {Pt,Pt} crosslinks may be long-range where the platinating sites are separated by up to 4 intervening base pairs (see text).

[11]. The conformational distortions induced in DNA by the 1,3- or 1,4-interstrand CLs of 1,1/t,t show that these lesions result only in a very small directional bending of the helix axis (~10°) and duplex unwinding (9°) and are thus conformationally flexible [11].

The structure of the alkanediamine linker in the dinuclear Pt(II) complexes can control the substitution process with small nucleophiles [12]. DNA reactions proceed primarily *via* formation of the monoaqua monochloro species in the rate-limiting step [13]. Aquation and subsequent formation of the monofunctional adducts of 1,1/t,t is preceded by preassociation with the polyanionic DNA surface through electrostatic interactions and hydrogen bonding [9, 13]. Transformation of monofunctional to bifunctional adducts proceeds *via* the aquated intermediate and this closure is markedly faster than that found for the major 1,2-intrastrand CL formed from the diaqua form of cisplatin [9]. The rate of aquation

of 1,1/t,t is enhanced in the presence of single-stranded over double-stranded DNA showing that the nature of template DNA may affect substrate specificity [14]. Notably, 1,1/c,c is hydrolyzed less readily than 1,1/t,t and there is no evidence for the preassociation of 1,1/c,c [15].

2.2. {Pt,Pt} Intrastrand Crosslinks

The 1,1/t,t isomer forms minor 1,2-GG intrastrand CLs producing a flexible, nondirectional bend in DNA [16] which noticeably reduces thermal and thermodynamic stability of the duplex more than the equivalent mononuclear cisplatin adduct [17]. {Pt,Pt} intrastrand CLs have not been observed in DNA modified by 1,1/c,c [7, 8]. NMR studies have shown restricted rotation around the Pt-3′-G bond in single-stranded r(GpG), d(GpG), and d(TGGT) adducts and this steric hindrance may be responsible for the inability to form the 1,2-GG intrastrand CLs with sterically more demanding double-helical DNA [18].

2.3. Conformational Changes in DNA

On a global level, both dinuclear platinums induce the B→Z transition in poly(dG-dC) · poly(dG-dC) and Pt-DNA bond formation is not an absolute necessity for the Z-DNA induction, but the {Pt,Pt} interstrand crosslink may be important in 'locking' the Z-conformation [8, 19]. This is a general property and the polyamine-linked dinuclear complexes (Section 3) are also very effective in inducing irreversible conformational changes including the B→A transition [20].

The structural changes on site-specific oligonucleotides have been summarized [21]. The {Pt,Pt} 1,4-interstrand crosslink of 1,1/t,t-modified $(5'\text{-AT}\mathbf{G}\text{TA}\mathbf{C}\text{AT})_2$ shows that both A and G purine residues adopt a *syn* conformation of the nucleoside unit – a pre-requisite for induction of the left-handed conformation [22]. The structure of this adduct closely resembles that formed by the trinuclear compound Triplatin (BBR3464) (see below, Section 7). The combined biophysical features – bifunctional DNA binding through two monofunctional Pt units and changes to the sugar residues in an extended sequence – may explain the conformational flexibility noted, significantly different to the rigid bending of cisplatin [11, 21].

2.4. Protein Recognition

DNA interstrand crosslinks pose a special challenge to repair enzymes because they involve both strands of DNA and therefore cannot be repaired using the information in the complementary strand for resynthesis [23]. High-mobility-group (HMG)-domain proteins play a role in sensitizing cells to cisplatin [23, 24]. An important structural motif recognized by HMG-domain proteins on DNA

modified by cisplatin is a stable, directional bend of the helix axis. One possible consequence of binding of HMG-domain proteins to cisplatin-modified DNA is the shielding of damaged DNA from intracellular nucleotide excision repair (NER) [25]. The conformational flexibility of the major {Pt,Pt} crosslinks results in very weak or no recognition of their DNA adducts by HMGB1 proteins [11]. The {Pt,Pt} interstrand adducts may, however, present a block to DNA or RNA polymerase [9, 26].

With respect to intrastrand crosslinks, the affinity of HMG-domain proteins to the duplex containing 1,2-GG intrastrand CL of cisplatin is sequence-dependent and is reduced with increasing thermodynamic destabilization of the duplex [27]. The weak affinity of the minor 1,2-GG intrastrand CL of 1,1/t,t to HMG-domain proteins is consistent with the observation that this lesion reduces the thermal and thermodynamic stability of DNA markedly more than the same lesion of cisplatin [16, 17]. Consistent with the weak recognition by HMGB1 proteins, effective removal of {Pt,Pt} intrastrand adducts by NER has been observed [28].

The major {Pt,Pt} interstrand CLs are repaired much less easily than the {Pt,Pt} intrastrand CLs and are not removed in an *in vitro* assay using mammalian and rodent cell-free extracts capable of removing the intrastrand CLs [11, 29]. Hence, the {Pt,Pt} interstrand adducts do not have to be shielded by damaged DNA recognition proteins, such as those containing HMG domains, to prevent their repair. Clearly, the mechanism of antitumor activity of bifunctional dinuclear Pt(II) complexes does not involve recognition by HMG-domain proteins as a crucial step, in contrast to the proposals for cisplatin and its direct analogs. This critical ability to dictate a biological effect is reasonably attributed to the design and formation of a structurally unique set of Pt-DNA adducts accessible only to the dinuclear structure.

3. POLYAMINE-LINKED BIFUNCTIONAL DINUCLEAR PLATINUM(II) COMPLEXES

An important subset of bifunctional dinuclear platinum complexes are those where the platinum units are linked through natural and synthetic polyamines, adding extra charge to the overall structure (Figure 1) [30]. Their promising preclinical activity has been summarized [5, 6, 31, 32]. The design of BBR3610 mimics the charge and the distances between platinating centers in the trinuclear Triplatin (BBR3464). The BBR3610-DACH (DACH = 1,2-diaminocyclohexane) compound is the first dinuclear analog of oxaliplatin. The DNA binding mode of these dinuclear Pt(II) complexes, including sequence preference, type of the major adducts, and resulting conformational alterations, is not very different from that of the alkanediamine-linked analogs. The kinetics of binding of the spermine and spermidine compounds corresponds to their relatively high charge (2+ to 4+). The preference for the formation of {Pt,Pt} interstrand CLs, however, does not follow a charge-based pattern nor the length of the polyamine chain (Table 1) [33, 34]. The presence of the central positively-charged moiety reduces the interstrand crosslinking efficiency – synthesis of the central

N-blocked spermidine derivative (BBR3571) such as in [{*trans*-$PtCl(NH_3)_2$}$_2${μ-BOC-spermidine}]$^{2+}$ (BOC = *t*-BuOCO), [35], results in markedly less crosslinking than the parent protonated compound [33]. Both the spermidine and spermine-linked compounds are very effective inducers of irreversible B → Z and B → A transitions in DNA [20].

Table 1. Summary of the DNA-binding characteristics of selected polynuclear platinum compounds.[a]

	unwinding angle/adduct (°)	interstrand CL/adduct (%)
1,1/t,t n = 6	10–14	70–90
BBR3571	12.3	40
BBR3535	15.4	57
Triplatin (BBR3464)	14	20
BBR3610	14	23
BBR3610-DACH	13	26
Cisplatin	13	6

[a] See [33, 34]. All compounds have *trans*-oriented platinating groups (Figure 1).

3.1. Consequences of DNA Binding of Dinuclear Polyamine-Linked Complexes

The major adducts of BBR3610 and BBR3610-DACH are removed from DNA by DNA repair systems with a markedly lower efficiency than the adducts of cisplatin [34]. The increased length of the linker allows for formation of longer-range {Pt,Pt} intrastrand CLs in comparison to the 1,2-adducts formed by 1,1/t,t. The ability of {Pt,Pt} intrastrand CLs of BBR3610 and BBR3610-DACH to thermodynamically destabilize DNA depends on the number of base pairs separating the platinated bases and the greatest destabilization is observed for the long-range CL in which the platinated sites are separated by four base pairs [36]. The extent of destabilization correlates with the extent of conformational distortions induced. The efficiency of excinucleases to remove these CLs from DNA also depends on their length; the trend is identical to that observed for the ability to thermodynamically destabilize the duplex.

A second example of how DNA downstream effects may be "fine-controlled" by the nature of the linking diamine/polyamine chain is seen in the inhibition of DNA replication by the site-specific {Pt,Pt} 1,2-intrastrand crosslinks of BBR3571 [37]. The interaction of DNA polymerases with a Pt-DNA adduct is an important determinant of the propensity of a given adduct to be cytotoxic, mutagenic, or ultimately, of no long-term consequence. The 1,2-GG intrastrand CL of BBR3571 inhibits DNA translesion synthesis markedly more efficiently than the equivalent adduct of cisplatin [37]. This result has been explained by the bulkier adduct of the dinuclear complex and by the flexibility induced in DNA which can make the productive binding of this adduct at the polymerase site more difficult.

3.2. Interduplex Crosslinking

The properties of DNA globally modified by polynuclear complexes are highlighted by markedly enhanced intraduplex {Pt,Pt} interstrand crosslinking (Figure 2). In general, DNA interstrand crosslinking requires close proximity of binding sites in the two DNA strands. This requirement may be easily fulfilled in the case of formation of the intraduplex DNA interstrand CLs by bifunctional Pt(II) complexes because binding *via* one leaving group inevitably leaves the other close to other binding sites in the same duplex. However, if the reactive sites of the bifunctional crosslinking agents are sufficiently distant, then binding to adjacent duplexes may occur. Thus, bifunctional Pt(II) compounds might also be effective interduplex crosslinkers in cases when two fragments of double-helical DNA molecules are forced to lie together, for instance, during recombination, at replication forks or sites of topoisomerase action, or more generally in cellular environmental conditions. Under molecular crowding conditions mimicking environmental conditions in the cellular nucleus the spermine-linked BBR3535 fulfills the requirements placed on interduplex DNA crosslinkers considerably better than mononuclear cisplatin or transplatin [38]. Platinating sites in 1,1/t,t-spermine are markedly more distant (2.7 nm) than those in cisplatin (0.28 nm) and moreover, the *trans* geometry of leaving ligands in the dinuclear complex may allow the spermine linker to direct the reactive sites in opposite directions, which may facilitate binding to adjacent duplexes.

The structural features promoting interduplex CLs may, in fact, be quite varied when we consider polynuclear platinum complexes. The trinuclear tridentate $[Pt_3Cl_3(hptab)]^{3+}$ (hptab = *N*,*N*,*N′*,*N′*,*N″*,*N″*-hexakis(2-pyridylmethyl)-1,3,5-tris-(aminomethyl)benzene) forms mainly trifunctional {Pt,Pt,Pt} intrastrand CLs in the absence of proteins and molecular crowding agents, where all Pt(II) centers are coordinated to G residues [39–41]. In the presence of a molecular crowding agent two DNA duplexes are bound in high yield [41]. The increased functionality of the complex also allows for observation of DNA-protein crosslinks in high yield (see Section 4). These examples suggest concepts for the systematic design of polynuclear agents capable of forming interduplex DNA-DNA crosslinks.

3.3. Susceptibility to Metabolic Decomposition and Structural Variations

Decomposition of the PPC structure occurs when the substitution-labile ligand is *trans* to the linker because replacement of the Pt–Cl bond by a *trans*-labilizing sulfur donor results in breaking the Pt-amine (linker) bond [42, 43]. The kinetic data for these reactions indicate that aquation is not a rate-limiting step for reactions with sulfur nucleophiles. This metabolic effect is deactivating and also diminishes the capacity to form long-range CLs. On the other hand, the *cis* geometry as in $[\{cis\text{-}PtCl(NH_3)_2\}_2\text{-}\mu\text{-}Y]^{n+}$ should preserve the main features of antitu-

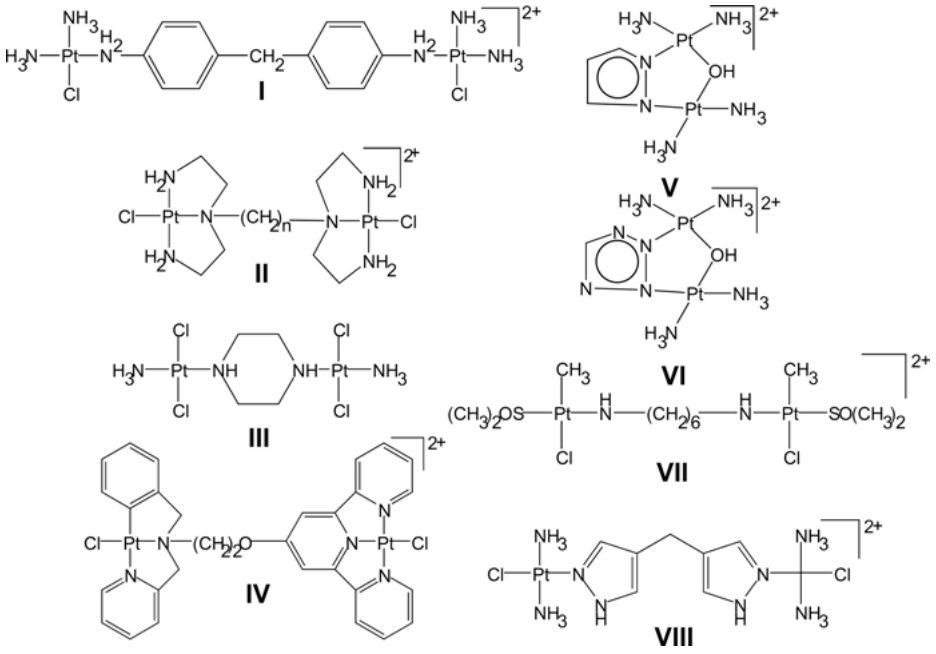

Figure 3. Structures of various dinuclear platinum(II) complexes discussed in the text for their DNA binding properties.

mor polynuclear Pt(II) complexes but with enhanced stability to metabolic deactivation [44, 45].

A unique 11-member chelate ring contains a glutathione-bridged Pt-μ-GS-Pt structure [44]. The BBR3610-DACH compound was synthesized for this reason and shows enhanced metabolic stability over BBR3610 [46]. A second example of enhanced stability to metabolic deactivation is afforded by use of a semi-rigid linker in the compound $[\{cis\text{-}Pt(NH_3)_2Cl\}]_2(\mu\text{-}4,4'\text{-methylenedianiline})]^{2+}$ (**I**, Figure 3), [47–49]. The DNA adducts of **I** demonstrated for the first time for PPCs a strong specific recognition and binding of HMG-domain proteins to modified DNA [49]. Dinuclear *trans*-oriented Pt(II) complexes may remain stable in the presence of sulfur-containing compounds as observed for long chain $[\{trans\text{-}PtCl(dien)\}_2\text{-}\mu\text{-}(CH_2)_n]^{2+}$ (n = 7,10,12, dien = diethylenetriamine) (**II**, Figure 3) [50]. DNA conformational changes are also dependent on the linking chain length [50].

3.4. Macrocyclic Polyamine-Linked Complexes

The compound $[Pt_2(DTBPA)Cl_2]$ (DTBPA = 2,2′-(4,11-dimethyl-1,4,8,11-tetraaza-cyclotetradecane-1,8-diyl)bis-(N-(2-(pyridin-2-yl)ethyl)acetamide)), which combines a modified macrocyclic polyamine (cyclam) and two pyridine moieties,

shows only moderate affinity to DNA possibly due to the steric hindrance of the cyclam ring which affects the DNA-binding of the two Pt(II) centers but it does unwind the DNA double helix [51, 52]. The analogue $[Pt_2(TPXA)Cl_2]Cl_2$ (TPXA = *N*,*N*,*N'*,*N'*-tetra(2-pyridylmethyl)-*m*-xylylene diamine), in which the Pt(II) centers are now bridged by a bulky aromatic linker, forms 1,4-{Pt,Pt} intrastrand rather than 1,3-intra- and interstrand CLs which exert more perturbation on the tertiary structure of negatively supercoiled DNA than cisplatin [52, 53].

4. DNA-PROTEIN CROSSLINKING

The presence of two or more Pt centers automatically leads to the possibility of "higher-order" tri- and tetrafunctional DNA binding when *cis*-$[PtCl_2(amine)_2]$ units are used as in the canonical 2,2/c,c (Figure 1). Dinuclear tri- and tetrafunctional platinum complexes form very efficient coordinative ternary DNA-protein CLs to a range of proteins including components of the UVrABC repair system and the Klenow fragment [54–56]. The protein binding is effected from a first formed {Pt,Pt} interstrand CL, thus significantly differentiating the structures from mononuclear DNA-protein adducts, where by definition only monofunctional Pt-DNA binding is possible. The bulky DNA–protein CLs represent a more distinct and persisting structural motif recognized by the components of downstream cellular systems processing DNA damage in a considerably different manner than the DNA adducts of mononuclear platinum drugs.

An interesting implication is that the formation of DNA-protein crosslinks by tri- or tetrafunctional dinuclear Pt(II) complexes is related to their different cytotoxicity profile in comparison with the dinuclear bifunctional analogues [4, 5]. Use of a rigid linker in the tetrafunctional [{*trans*-$PtCl_2(NH_3)$}$_2$(μ-piperazine)], (**III**, Figure 3), also allows for observation of DNA-protein CLs while {Pt,Pt} interstrand crosslinking is diminished relative to the alkanediamine-linked 1,1/c,c or 1,1/t,t [57].

5. DINUCLEAR PLATINUM(II) COMPLEXES STABILIZING G-DNA QUADRUPLEXES

Certain guanine (G)-rich nucleic acid sequences can form four-stranded structures which can adopt a wide diversity of structures and topologies (Figure 4) [58]. These structures have many interesting biological roles including roles in telomeres, DNA replication, gene regulation, transcription, and translation. These properties make them appealing therapeutic targets so that the identification of small molecules that demonstrate selectivity for biologically relevant G-quadruplexes is an active area in drug discovery.

G-quadruplexes have been shown to be a target for several dinuclear Pt(II) complexes as exemplified by $[\{trans\text{-}PtCl(NH_3)_2\}_2\text{-}\mu\text{-}H_2N(CH_2)_nNH_2]^{2+}$ (n = 2 or 6) [59]. The folding of $AG_3(T_2AG_3)_3$ in either Na^+ (antiparallel) or K^+ (par-

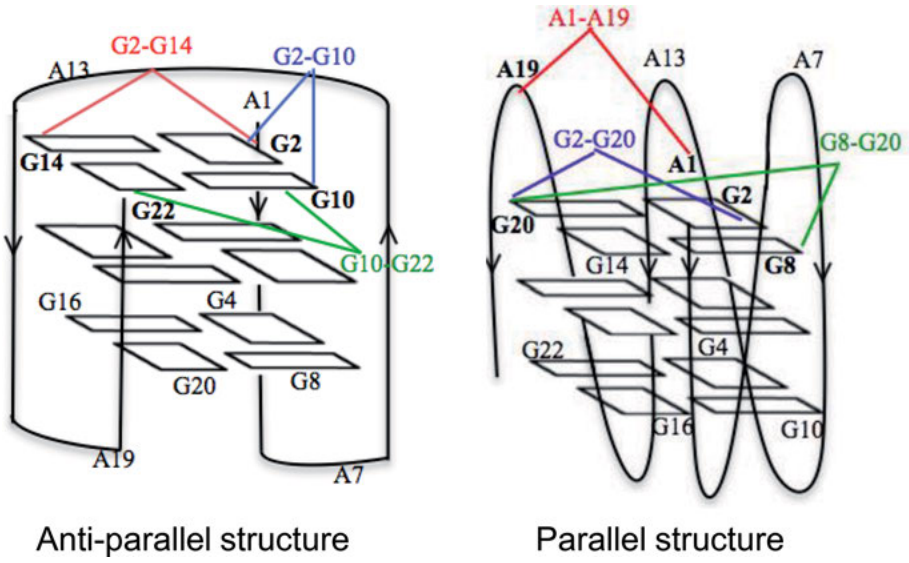

Figure 4. The parallel and antiparallel structures of the G-quadruplex $AG_3(T_2AG_3)_3$. Note the bifunctional platination sites in the same quadruplex. Adapted with permission from [59]; copyright 2005 American Chemical Society.

allel) forms and the complexes showed that the parallel structure exists whatever the cation and confirmed the existence of the antiparallel structure in the presence of both cations. The unique {Pt,Pt} CLs are formed between Gs belonging to the same quartet (Figure 4). Molecular dynamics rationalized these findings, where it was shown that the guanines were flexible allowing reversible migration to form the top G-quartet, thereby making the N7 atoms accessible to platination [59]. Many planar ligands have been used to stack with the G-quartets.

The dinuclear terpyridine-based Pt(II) complex (**IV**, Figure 3) interacts *via* π-π stacking and with the DNA phosphate backbone *via* direct coordination or electrostatic interactions [60]. The complex induces the formation of quadruplex DNA (largely the antiparallel conformation) even in the absence of potassium ions and with good selectivity (up to 100-fold) over duplex DNA. Another type of Pt(II) complex stabilizing DNA quadruplexes is represented by symmetric dinuclear terpyridine-Pt(II) units – in general $[\{Pt(terpy\}_2\mu\text{-}Y]^{4+}$ where Y is a flexible thiol bridging ligand or 4,4'-trimethylene-dipyridine ligand [61]. These substitution-inert complexes markedly increase the melting temperature of various G-DNA quadruplex motifs and maintain this binding in up to a 600-fold excess of double-helical DNA. The isomeric dinuclear cations, $[\{Pt(2,2'\text{-}bpy)\}_2(tppz)]^{4+}$ (tppz = tetrakis(pyridine-2-yl)pyrazine), differ in their overall shape and display different affinities toward duplex DNA and human telomeric quadruplex DNA [62].

Trinuclear Pt(II) complexes are also effective and selective G-quadruplex binders and good telomerase inhibitors. Two propeller-shaped, trigeminal-ligand-

containing, flexible trinuclear Pt(II) cations, $[\{Pt(dien)\}_3(ptp)]^{6+}$ and $[\{Pt(dpa)\}_3(ptp)]^{6+}$ (dpa = bis-(2-pyridylmethyl)amine; ptp = 6′-(pyridin-3-yl)-3,2′: 4′,3″-terpyridine), exhibit higher affinity for human telomeric and c-myc promoter G4 sequences than duplex DNA [63]. Both complexes are good telomerase inhibitors, with IC_{50} values in the micromolar range.

6. STRUCTURAL VARIATION IN DINUCLEAR PLATINUM(II) COMPLEXES

6.1. Azole- and Azine-Bridged Dinuclear Bifunctional Pt(II) Complexes

A consistent theme in platinum complex drug development is the design of agents capable of pharmacological inhibition of DNA repair [1, 2, 24, 64]. An interesting series in this respect is the set of dinuclear Pt(II) complexes where two *cis*-$\{Pt(NH_3)_2\}$ units are bridged by various azole-based bridging ligands such as $[\{cis\text{-}Pt(NH_3)_2\}_2(\mu\text{-OH})(\mu\text{-pyrazolato})](NO_3)_2$ (1,1/c,c-prz), $[\{cis\text{-}Pt(NH_3)_2\}_2(\mu\text{-OH})(\mu\text{-tri- or tetraazolato})](NO_3)_2$ (**V** and **VI**, Figure 3) [65–68]. The μ-hydroxo acts as a leaving group in these complexes, and the rigid bridging azolates keep the appropriate distance between the two Pt atoms to enable binding of two neighboring G residues in double-helical DNA. Complex **V** forms in DNA duplexes major 1,2-GG intrastrand CLs but the distortion induced is significantly less pronounced than that induced by similar CLs from cisplatin and concomitantly, the thermodynamic stability of the modified DNA duplex is lessened considerably [69, 70]. As a corollary, the dinuclear adducts, although formally similar to those formed by cisplatin, are weak substrates for HMGB1 protein recognition and represent poor substrates for DNA repair through a "cisplatin-like" mechanism [70]. Notably, **V** and **VI** cause irreversible compaction of DNA through an intermediate state in which coil and compact parts coexist in a single DNA molecule, a feature different from that of typical condensing agents [71, 72].

In contrast to the azole-bridged dinuclear bifunctional Pt(II) complexes, the benzotriazolate (Btaz)-bridged one, $[\{cis\text{-}PtCl(NH_3)_2\}_2(\text{l-Btaz-H})]Cl$, utilizes the rigid aromatic ring as a linker with non-bridging chloride ions as leaving groups [73]. Monofunctional DNA adducts of this dinuclear complex are converted to more toxic bifunctional CLs considerably more slowly in comparison with cisplatin, or the 1,1/t,t or 1,1/c,c [73]. The compound is weakly antitumor-active but susceptible to metabolic deactivation. Use of the rigid aromatic rings of azines as bridging ligands affords compounds such as $([\{cis\text{-}PtCl(NH_3)_2\}_2(\mu\text{-Y})]^{2+}$ (Y = pyrazine, pyrimidine or pyridazine) [74, 75]. The complexes with the least steric hindrance and those with more delocalized ligands capable of additional DNA intercalations such as base stacking are the most cytotoxic. Finally, a series of pyrazine-bridged dinuclear Pt(II) complexes with general formulas $[\{PtCl(L)\}_2(\mu\text{-prz})]^{2+}$ (L = chelating diamines such as ethylenediamine, en; (±)-1,2-propylenediamine; isobutylenediamine; *trans*-(±)-1,2-diaminocyclohexane;

1,3-propylenediamine; 2,2-dimethyl-1,3-propylenediamine) and one pyridazine (pydz)-bridged complex, $[\{PtCl(en)\}]_2(\mu\text{-pydz})]^{2+}$, effectively interact with DNA in cell-free media [76].

6.2. Miscellaneous Dinuclear Platinum(II) Complexes

Additional DNA-binding modes may be incorporated into dinuclear Pt(II) complexes by use of intercalating moieties such as acridines and anthraquinones in the linker [77, 78]. Another group of antitumor dinuclear Pt(II) compounds that bind DNA and also interact *via* intercalation comprise the complexes $[\{PtCl(bpy)\}_2(\mu\text{-L-H})_2]$ and $[\{PtCl(phen)\}_2(\mu\text{-L-H})_2]$ (bpy = 2,2′-bipyridine, phen = 1,10-phenanthroline, and L = 2,2′-azanediyldibenzoic dianion or 1,3-benzothiazol-2-amine) dibridged by H_2L ligands [79, 80]. The results performed in cell-free media have shown that the DNA binding mode of the complexes involve their intercalative DNA interaction and that these complexes can cleave DNA.

A series of organometallic dinuclear Pt(II) complexes was synthesized with the aim to tune the electronic and steric properties of the Pt centers so that the bifunctional dinuclear Pt(II) compounds could act by different mechanistic pathways in comparison with classical 1,1/c,c [81, 82]. Modifications of DNA by $[\{Pt(CH_3)Cl((CH_3)_2SO)\}_2(\mu\text{-}H_2N(CH_2)_6NH_2)]$ (**VII**, Figure 3), show a DNA binding mode different from that of the formally equivalent 1,1/c,c, with mostly monofunctional adducts. The minor {Pt,Pt} interstrand CLs (2 %) are capable of terminating RNA synthesis *in vitro* while the major monofunctional adducts are not.

The dinuclear $[\{trans\text{-}PtCl(NH_3)_2\}_2\mu\text{-dpzm}]^{2+}$ (dzpm = 4,4′-dipyrazolylmethane) (**VIII**, Figure 3) forms {Pt,Pt} intrastrand and interstrand crosslinks in double-stranded DNA, but with a distinct preference for AA or AG sites [83, 84]. Use of modified pyridine groups such as isonicotinamide or substituted isonicotinamide as linker results in dinuclear compounds formally similar to picoplatin (*cis*-$[PtCl_2(NH_3)(2\text{-mepyridine})]$ [85, 86].

Finally, dinuclear boron-containing bifunctional and tetrafunctional Pt(II)-amine complexes, in which two Pt(II) moieties are bridged by 1,7-carborane [carborane = dicarba-*closo*-dodecaborane(12)], $[\{trans\text{-}PtCl(NH_3)_2\}_2\mu\text{-}1,7\text{-}NH_2(CH_2)_3CB_{10}H_{10}\text{-}C(CH_2)_3NH_2]^{2+}$ (1,1/t,t-carborane) and $[\{cis\text{-}PtCl_2(NH_3)\}_2\mu\text{-}1,7\text{-}NH_2(CH_2)_3\text{-}CB_{10}H_{10}C(CH_2)_3NH_2]$ (2,2/c,c-carborane), were synthesized as potential DNA targeting agents in boron neutron capture therapy (BNCT) [87].

7. TRINUCLEAR PLATINUM(II) COMPLEXES

7.1. The Trinuclear Bifunctional Platinum(II) Complex Triplatin (BBR3464)

The synthetic pathways developed for alkanediamine-linked dinuclear compounds automatically lead the way to trinuclear compounds and a cisplatin

synthon can be developed using three sequential *cis*-$[PtCl_2(amine)_2$ units [88]. The most studied compound is Triplatin (BBR3464) $[\{trans\text{-}PtCl(NH_3)_2\}_2\mu\text{-}\{trans\text{-}Pt(NH_3)_2(H_2N(CH_2)_6NH_2)_2\}]^{4+}$, a trinuclear, bifunctional DNA binding agent with an overall 4+ charge where the bridging between the two platinating units is formally made by the $[\{trans\text{-}Pt(NH_3)_2\}\mu\text{-}\{H_2N(CH_2)_6NH_2\}_2$] unit (Figure 1). The drug advanced to Phase II clinical trials where durable responses in cisplatin-resistant ovarian cancer were noted. The drug did not advance further due to a combination of pharmacokinetics involving loss of the trinuclear structure (albeit with overall reactivity similar to cisplatin if we consider that <5 % of administered cisplatin is considered to get to DNA) and pharmaceutical company takeovers.

The trinuclear compound and the dinuclear polyamine-linked species are formally equivalent with both linking units containing a charged moiety capable of hydrogen-bonding and electrostatic interactions with DNA, and both series can be seen as logical extensions of the "original" alkanediamine-linked series. It may be noted that the polyamine-linked dinuclear compounds are as similarly potent as Triplatin. Several reviews on various aspects of the pre-clinical and clinical studies on Triplatin, including DNA binding studies, have been published [1, 2, 5, 6, 21, 89]. It is the purpose in this chapter to highlight the contributions that Triplatin-DNA studies have made to delineation of novel DNA structure and reactivity.

The high charge on Triplatin facilitates rapid binding to DNA with a $t_{1/2}$ of ~40 min, significantly faster than the neutral cisplatin [90]. Triplatin forms {Pt,Pt} long-range interstrand CLs in natural DNA in a considerably higher amount (~20 %) than cisplatin (Table 1) [90]. Changing the geometry of the central unit from *trans* to *cis*, as in $[\{trans\text{-}PtCl(NH_3)_2\}_2\mu\text{-}cis\text{-}Pt(NH_3)_2\{H_2N(CH_2)_6NH_2\}_2]^{4+}$ (BBR3499, 1,0,1/t,c,t) results in enhanced {Pt,Pt} interstrand crosslinks with reduced sequence specificity and slower binding to DNA [91]. The BBR3499-DNA adducts distort DNA conformation and are repaired by cell-free extracts considerably better than the adducts of BBR3464 [91]. DNA molecules aggregate and compact upon treatment with Triplatin, as revealed by high-resolution atomic force microscopy, reasonably attributed the combination of charge and formation of the long-range CLs [92].

7.2. Directional Isomers

The {Pt,Pt} interstrand crosslinks of Triplatin occur in both the 5′-5′ and 3′-3′ sense, forming "directional isomers" (Figure 5) [93, 94]. The directionality is dependent on the nature of the crosslink. The 1,2-interstrand CL forms preferentially the 3′-3′ direction (in an antiparallel manner), the 1,4-interstrand CL forms in both directions in approximately equal proportions, whereas the 1,6-interstrand CL forms in preferentially the 5′-5′ direction [89, 93]. The kinetics of formation of 1,2- and 1,4-interstrand CLs were found to be similar and faster than that for the analogous 1,6-interstrand CL [93, 94]. The kinetics of binding follows the trend seen for the dinuclear alkanediamine-bridged 1,1/t,t compound

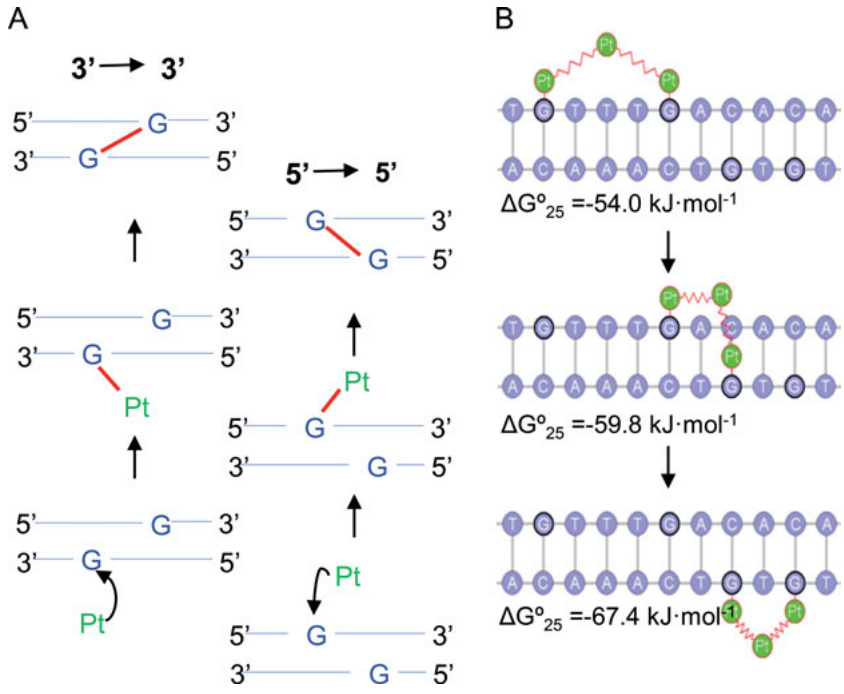

Figure 5. **A**. A scheme for the formation of novel 5′-5′ and 3′-3′ directional isomers on DNA. **B**. The "walking" of {Pt,Pt} DNA adducts is induced by different thermodynamic destabilization of the double helix by structurally different adducts.

with aquation followed by monofunctional binding and then closure to the bifunctional crosslink [95].

In examining the factors affecting the formation of directional isomers by $\{^{1}H,^{15}N\}$ HSQC NMR spectroscopy, differences occur at the monofunctional binding step. In the 5′-5′ case, pre-association with initial hydrogen-bonding and electrostatic interactions with DNA are observed in the minor grove [96]. Two distinct pathways for the terminal $\{PtN_3Cl\}$ groups to approach and bind the guanine N7 in the major groove with the central linker anchored in the minor groove were inferred. To achieve platination of the guanine residues the central linker remains in the minor groove but triplatin must diffuse off the DNA for covalent binding to occur. Unlike the 5′-5′ case a number of 3′-3′ crosslinked adducts are observed [97].

Molecular dynamics simulations showed a highly distorted structure with considerable base fraying and widening of the minor groove [96]. In contrast to the 1,4-situation the 3′-3′ 1,2-interstrand crosslink is formed preferentially in the sequence d(A**CG**TATA**CG**T)$_2$ where two simultaneous adducts are formed between the adjacent guanines, the first examples of a structurally characterized 3′-3′ adduct [98]. The structure is quite distinct from the analogous cisplatin 1,2-interstrand $(GC)_2$ adduct and from the 5′-5′ 1,2-Cl formed by [{*trans*-

$(PtCl(NH_3)_2\}_2\mu\text{-}H_2(CH_2)_4NH_2]^{2+}$ [89, 98, 99]. The ability to form directional isomers is a property shared with BBR3571, but not 1,1/t,t, suggesting that the presence of charge in the central moiety, implying pre-association, is a key factor in dictating this property.

Both directional {Pt,Pt} 1,4-interstrand CLs formed by Triplatin exist as two distinct non-interconvertible conformers [100]. Analysis of the conformers by differential scanning calorimetry, chemical probes of DNA conformation, and minor groove binder Hoechst 33258 have demonstrated that each of the four conformers affects DNA in a distinctly different way and adopts a different conformation and are distinct from those of the short-range adducts of cisplatin [100]. The properties of these site-specific adducts of Triplatin, such as conformational distortions, are also distinctly different from those of the short-range adducts of mononuclear cisplatin [93, 101]. The structural distortions on site-specific {Pt,Pt} CLs of Triplatin have been summarized [21].

7.3. Walking on Double-Helical DNA and Linkage Isomerization

In studying the properties of site-specific long-range CLs of Triplatin, some CLs of this platinum compound were found unstable [102]. The inherent steric effects around the Pt center of the mononuclear bifunctional adduct are replaced by the steric constraints of the conformational change as a whole. Since specific Triplatin adducts distort DNA conformation differently, it is reasonable to expect that the energetic signatures of these dissimilar adducts are different. Under physiological conditions the Pt-G(N7) bonds are reactive leading to linkage isomerization reactions on the double-helical DNA substrate. Upon incubation of DNA duplexes containing a single, site-specific intrastrand CL between G residues the coordination bonds between Pt and the N7 of one of the G residues within the intrastrand adduct are cleaved leading to the formation of interstrand CLs (linking both strands of DNA). These interstrand CLs react further to form intrastrand CL in the strand complementary to that in which original intrastrand CL was formed. This successive rearrangement may proceed in the way that the molecule of Triplatin originally coordinated to one strand of DNA can spontaneously translocate from this strand to its complementary counterpart *via* intermediate interstrand CL (Figure 5), which may evoke walking of this platinum complex on DNA molecules.

Differential scanning calorimetry of duplexes containing single, site-specific CLs of Triplatin revealed that one of the driving forces that leads to the lability of DNA CLs of Triplatin is a difference between the thermodynamic destabilization induced by the CL and by the adduct into which it could isomerize [102]. Thus, one of the driving forces that leads to the lability of DNA CLs of Triplatin is a difference between the thermodynamic destabilization induced by the CL and by the adduct into which it could isomerize.

7.4. Interactions of DNA Modified by Triplatin by Damaged-DNA Binding Proteins

Binding of cellular damaged DNA-binding proteins to DNA modified by platinum complexes plays an important role in initial phases of the mechanism of cytotoxic action of platinum drugs [23–25]. Thus, due to its ability to modify DNA in a unique manner, Triplatin could distinctly evoke different pathways of cellular response to DNA damage such as triggering of the apoptotic pathway.

7.4.1. Recognition by HMG-Domain Proteins and DNA Repair

In contrast to distortions induced by major CLs of cisplatin, the CLs of Triplatin do not extensively unwind and rigidly bend DNA so that they are not substrates for damaged DNA-binding proteins, such as HMG-domain proteins [93, 94]. Thus, the antitumor effects of BBR3464 do not involve a shielding or hijacking mechanism as the effects of cisplatin (*vide supra*). On the other hand, while intrastrand adducts of Triplatin are readily removed from DNA by the NER systems, the interstrand CLs are not.

7.4.2. Recognition by the Tumor Suppressor Protein p53

The DNA binding activity of the p53 protein is crucial for its tumor suppressor function. The active protein p53 is a nuclear phosphoprotein that consists of 393 amino acids and contains four major functional domains [102]. Active p53 binds as a tetramer to ~50 different response elements that occur naturally in the human genome and shows functionality [103]. Free DNA in the segments corresponding to the consensus sequence is already intrinsically bent toward the major groove [104, 105]. The interactions of active and latent p53 proteins with DNA fragments and oligodeoxyribonucleotide duplexes modified by Triplatin in a cell-free medium has been examined and the results have been compared with those describing interactions of these proteins with DNA modified by cisplatin [106].

The results indicate that structurally different DNA adducts of Triplatin and cisplatin exhibit a different efficiency to affect the binding affinity of the modified DNA to p53 protein. It has been suggested that different structural perturbations induced in DNA by the adducts of Triplatin and cisplatin produce differential response to p53 protein activation and recognition. Triplatin retains significant activity in human tumor cell lines and xenografts refractory or poorly responsive to cisplatin and displays high activity in human tumor cell lines characterized by both wild-type and mutant p53 gene. In contrast, on average, cells with mutant p53 are more resistant to the effect of cisplatin. The results support the hypothesis that the mechanism of antitumor activity of Triplatin may also be associated with its efficiency to affect the binding affinity of platinated DNA to active p53 protein. Thus, a "molecular approach" to control downstream effects such as protein recognition and pathways of apoptosis induction may consist in design of structurally unique DNA adducts as cell signals.

7.4.3. Recognition by the Nuclear Transcription Factor κB

Multiple signaling pathways have been linked to tumor resistance to mononuclear cisplatin, among them also activation of nuclear transcription factor kappaB (NF-κB) [107]. Interestingly, suppression of apoptosis or necrosis is an important NF-κB function [108, 109]. Binding of NF-κB proteins to their consensus sequences in DNA (κB sites) is the key biochemical activity responsible for the biological functions of NF-κB [110, 111].

Structurally different DNA adducts of Triplatin, cisplatin, and transplatin exhibit a different efficiency to affect the affinity of the platinated DNA (κB sites) to NF-κB proteins [112]. Triplatin-DNA adducts exhibited the highest efficiency to inhibit binding of NF-κB protein to its κB very likely connected with the enhanced extent of the conformational perturbations induced in DNA.

7.4.4. DNA Structural Conformational Changes, Protein Recognition, and Cell Cycle Effects

A major question for all this work is to ask how are the structural modifications and modulations of DNA adduct-protein recognition reflected in changes in cell cycle and signaling pathways. Real changes could affect signaling pathways and thus be truly complementary to other clinically used anticancer drugs, beyond the cisplatin class. An interesting example comes from the PPC work (Figure 6).

Mismatch repair is an important determinant in the efficacy of cisplatin treatment [113]. HCT116 cells deficient in the mismatch repair protein, MLH1, which was shown earlier to be resistant to cisplatin, were not resistant to Triplatin, indicating that Triplatin overrides one of the main factors contributing toward cisplatin resistance, in this case the mismatch repair status of the cells [114]. In both melphalan-sensitive and resistant OAW42 ovarian cancer cells, Triplatin induced a persistent G2/M phase cell cycle arrest as compared to cisplatin, which caused an initial S phase accumulation followed by a G2/M arrest that was later resolved [115].

In another study, A431 cells (human cervix squamous carcinoma) and its cisplatin-resistant counterpart, A431/Pt on treatment with Triplatin showed a varying degree of cellular effects which mainly included upregulation of genes like E2F1 (A431/Pt), antimetastatic factors (Nm23-H2 in A431 cells, Nm23-H1 and SAP102 in A431/Pt cells, and CD9 in both A431 and A431/Pt cells) and downregulation of pro-metastatic factors (e.g., Axl and VEGF in A431 cells and IL0–1b in A431/Pt cells) [116]. Further, Triplatin treatment showed a G2/M phase arrest in both A431 and A431/Pt cells although it was a much stronger effect in the former. Cytoflow analysis indicated a high proportion of sub-G1 cells in Triplatin-treated A431/Pt cells. In this context, a comparative study of U2OS cells showed a persistent increase in S phase cells following cisplatin treatment whereas Triplatin treatment showed a persistent accumulation of cells in the G2/M phase with some cells still retained in the G1 phase [117].

BBR3610 exhibits low-dose toxicity in colon cancer cells that harbored either wild-type p53 (HCT116) or mutant p53 (DLD1) suggesting that the cellular ef-

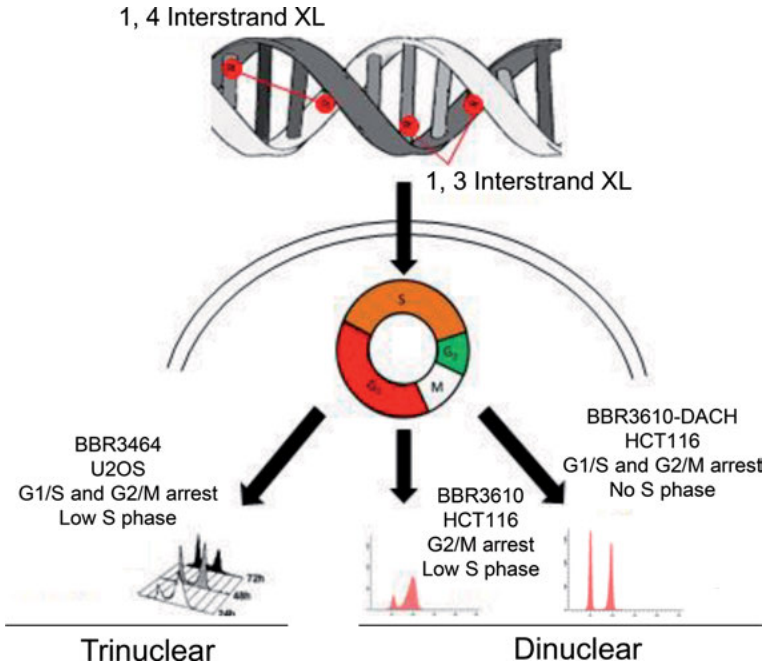

Figure 6. Differential cell-cycle effects caused by Triplatin, BBr3610, and BBR3610-DACH showing different downstream consequences of {Pt,Pt} interstrand crosslinking.

fects of BBR3610 were p53-independent [32]. BBR3610 induces G2/M arrest, early autophagy, and late apoptosis in glioma cells [118]. One of the hallmarks of cancer development is a deregulated cell cycle progression. Cells exposed to DNA-damaging agents trigger various cell cycle checkpoints, subsequently leading to G1/S or G2/M cell cycle arrest. Similar to cisplatin, BBR3464 and BBR3610 block DNA synthesis, cause S phase accumulation, and eventually this leads to G2/M arrest. However, BBR3610-DACH showed a paradigm shift, causing both a G1/S and G2/M arrest with complete depletion of S phase [119]. Both BBR3610 and BBR3610-DACH formed approximately the same number of interstrand CLs but their downstream cell cycle effects are different. This aspect of Pt-DNA conformational changes, by structurally distinct complexes, in general, requires further exploration.

8. CONCLUSIONS AND OUTLOOK

The major structural alterations in DNA such as irreversible conformational changes, stabilization of G-quadruplexes, high efficiency of DNA-protein adduct formation, the observation of directional isomers and the 'walking' of adducts on DNA are all effected by the design and structure of polynuclear platinum complexes. Many of these features are not accessible to mononuclear complexes.

The high charge of many of the PPCs suggests that pre-association plays important roles in dictating many of these properties. Substitution-inert or "non-covalent" complexes, which have also a wide variety of effects on DNA, are beyond the scope of this chapter but have been reviewed recently [89, 120]. Since the early publications on the straight chain alkanediamine-linked dinuclear complexes, various researchers have adapted the basic structure to obtain a wide variety of complexes and DNA binding modes and, eventually, antitumor activity equivalent to the original series. Triplatin remains the only "non-classical" platinum complex to enter human clinical trials. This chapter shows the rich diversity of PPCs and the potential for further clinical development, based on the strategy to produce DNA adducts structurally dissimilar to those of cisplatin and oxaliplatin.

ACKNOWLEDGMENTS

NPF acknowledges support through The National Institutes of Health (RO1 CA78754) and The Massey Cancer Center (P30 CA016059). VB acknowledges support from the Czech Science Foundation (grant 17–094365).

ABBREVIATIONS AND DEFINITIONS

BOC	*t*-BuOCO
bpy	2,2′-bipyridine
Btaz	benzotriazolate
cisplatin	*cis*-$PtCl_2(NH_3)_2$, *cis*-DDP
CLs	crosslinks
DACH	1,2-diaminocyclohexane
dien	diethylenetriamine = bis-(2-aminoethyl)amine
dpa	bis-(2-pyridylmethyl)amine
DTBPA	2,2′-(4,11-dimethyl-1,4,8,11-tetraaza-cyclotetradecane-1,8-diyl)bis-(N-(2-(pyridin-2-yl)ethyl)acetamide
dzpm	4,4′-dipyrazolylmethane
GS	glutathione
HMG	high-mobility-group
hptab	*N*,*N*,*N*′,*N*′,*N*″,*N*″-hexakis(2-pyridylmethyl)-1,3,5-tris(aminomethyl)benzene)
HSQC	heteronuclear single quantum coherence
IC_{50}	half maximal inhibitory concentration
L	2,2′-azanediyldibenzoic dianion or 1,3-benzothiazol-2-amine
NER	nucleotide excision repair
phen	1,10-phenanthroline
PPCs	polynuclear platinum complexes

prz	pyrazine
ptp	6′-(pyridin-3-yl)-3,2′:4′,3″-terpyridine
pydz	pyridazine
tppz	tetrakis(pyridine-2-yl)pyrazine
TPXA	*N*,*N*,*N*′,*N*′-tetra(2-pyridylmethyl)-*m*-xylylene diamine
Triplatin	BBR3464, $[\{trans\text{-}PtCl(NH_3)_2\}_2\mu\text{-}\{trans\text{-}Pt(NH_3)_2(H_2N(CH_2)_6NH_2)_2\}]^{4+}$

REFERENCES

1. N. Farrell, *Metal Ions in Biological Systems*, Eds. A. Sigel, H. Sigel, Marcel Dekker, Inc., New York, Basel, 2004, Vol. 42, pp 251–296.
2. V. Brabec, *Prog. Nuc. Acid Res. Mol. Biol.* **2002,** *71*, 1–68.
3. V. Brabec, J. Kasparkova, *Drug Resistance Updates* **2005**, *8*, 131–146.
4. N. Farrell, Y. Qu, U. Bierbach, M. Valsecchi, E. Menta, in *Cisplatin. Chemistry and Biochemistry of a Leading Anticancer Drug*, Ed. B. Lippert, Wiley-VCH, Zurich, Weinheim, 1999, pp 479–496.
5. N. P. Farrell, in *Platinum-based Drugs in Cancer Therapy*, Eds. L. R. Kelland, N. P. Farrell, Humana Press Inc., Totowa/NJ, 2000, pp 321–338.
6. N. Farrell, *Drugs of The Future* **2012**, *37*, 795–806.
7. J. Kasparkova, O. Novakova, O. Vrana, N. Farrell, V. Brabec, *Biochemistry* **1999,** *38*, 10997–11005.
8. N. Farrell, T. G. Appleton, Y. Qu, J. D. Roberts, A. P. S. Fontes, K. A Skov, P. Wu, Y. Zou, *Biochemistry* **1995,** *34*, 15480–15486.
9. R. Zaludova, A. Zakovska, J. Kasparkova, Z. Balcarova, V. Kleinwächter, O. Vrana, N. Farrell, V. Brabec, *Eur. J. Biochem.* **1997,** *246*, 508–517.
10. S. J. Berners-Price, M. S. Davies, J. W. Cox, D. S. Thomas, N. Farrell, *Chem. Eur. J.* **2003,** *9*, 713–725.
11. J. Kasparkova, N. Farrell, V. Brabec, *J. Biol. Chem.* **2000,** *275*, 15789–15798.
12. E. Selimović, J. Bogojeski, *Int. J. Chem. Kinetics* **2015,** *47*, 327–333.
13. J. W. Cox, S. Berners-Price, M. S. Davies, Y. Qu, N. Farrell, *J. Am. Chem. Soc.* **2001,** *123*, 1316–1326.
14. M. S. Davies, S. J. Berners-Price, J. W. Cox, N. P. Farrell, *Chem. Commun.* **2003,** 122–123.
15. J. Zhang, D. Thomas, M. Davies, S. Berners-Price, N. Farrell, *J. Biol. Inorg. Chem.* **2005**, *10*, 1–15.
16. J. Kasparkova, K. J. Mellish, Y. Qu, V. Brabec, N. Farrell, *Biochemistry* **1996,** *35*, 16705–16713.
17. C. Hofr, N. Farrell, V. Brabec, *Nuc. Acids Res.* **2001,** *29*, 2034–2040.
18. K. J. Mellish, Y. Qu, N. Scarsdale, N. Farrell, *Nuc. Acids Res.* **1997,** *25*, 1265–1271.
19. A. Johnson, Y. Qu, B. Vanhouten, N. Farrell, *Nuc. Acids Res.* **1992,** *20*, 1697–1703.
20. T. D. McGregor, W. Bousfield, Y. Qu, N. Farrell, *J. Inorg. Biochem.* **2002,** *91*, 212–219.
21. J. B. Mangrum, N. P. Farrell, *Chem. Commun.* 2010, 46, 6640–6650.
22. Y. Qu, N. J. Scarsdale, M. C. Tran, N. Farrell, *J. Inorg. Biochem.* **2004,** *98*, 1585–1590.
23. M. Kartalou, J. M. Essigmann, *Mutation Res.* **2001,** *478*, 1–21.
24. T. C. Johnstone, K. Suntharalingam, S. J. Lippard, *Chem. Rev.* **2016,** *116*, 3436–3486.
25. Y. Jung, S. J. Lippard, *Chem. Rev.* **2007,** *107*, 1387–1407.
26. Y. Zou, B. Van Houten, N. Farrell, *Biochemistry* **1994,** *33*, 5404–5410.

27. N. Poklar, D. S. Pilch, S. J. Lippard, E. A. Redding, S. U. Dunham, K. J. Breslauer, *Proc. Natl. Acad. Sci. USA* **1996,** *93*, 7606–7611.
28. M. Missura, T. Buterin, R. Hindges, U. Hubscher, J. Kasparkova, V. Brabec, H. Naegeli, *EMBO J.* **2001,** *20*, 3554–3564.
29. V. Brabec, in *Platinum-based Drugs in Cancer Therapy*, Eds. L. R. Kelland, N. P. Farrell, Humana Press Inc., Totowa/NJ, 2000; pp 37–61.
30. H. Rauter, R. Di Domenico, E. Menta, A. Oliva, Y. Qu, N. Farrell, *Inorg. Chem*. **1997**, *36*, 3919–3927.
31. C. Billecke, S. Finniss, L. Tahash, C. Miller, T. Mikkelsen, N. P. Farrell, O. Boegler, *Neuro-Oncology* **2006,** *8*, 215–226.
32. C. Mitchell, P. Kabolizadeh, J. Ryan, J. D. Roberts, A. Yacoub, D. T. Curiel, P. B. Fisher, M. P. Hagan, N. P. Farrell, S. Grant, P. Dent, *Mol. Pharmacol.* **2007,** *72*, 704–714.
33. T. D. McGregor, A. Hegmans, J. Kasparkova, K. Neplechova, O. Novakova, H. Penazova, O. Vrana, V. Brabec, N. Farrell, *J. Biol. Inorg. Chem.* **2002,** *7*, 397–404.
34. L. Zerzankova, T. Suchankova, O. Vrana, N. P. Farrell, V. Brabec, J. Kasparkova, *Biochem. Pharmacol.* **2010,** *79*, 112–121.
35. A. Hegmans, J. Kasparkova, O. Vrana, V. Brabec, N. P. Farrell, *J. Med. Chem*. **2008**, *51*, 2254–2260.
36. J. Florian, J. Kasparkova, N. Farrell, V. Brabec, *J. Biol. Inorg. Chem.* **2012,** *17*, 187–196.
37. B. Moriarity, O. Novakova, N. Farrell, V. Brabec, J. Kasparkova, *Arch. Biochem.Biophys.* **2007,** *459*, 264–272.
38. T. Muchova, S. Quintal, N. Farrell, V. Brabec, J. Kasparkova, *J. Biol. Inorg. Chem.* **2012,** *17*, 239–245.
39. Y. Zhao, W. He, P. Shi, J. Zhu, L. Qiu, L. Linb, Z. Guo, *Dalton Trans.* **2006**, 2617–2619.
40. Y. Zhu, Y. Wang, G. Chen, *Nucl. Acids. Res.* **2009,** *37*, 5930–5942.
41. R. Olivova, J. Kasparkova, O. Vrana, M. Vojtiskova, T. Suchankova, O. Novakova, W. He, Z. Guo, V. Brabec, *Mol. Pharmaceutics* **2011,** *8*, 2368–2378.
42. M. E. Oehlsen, Y. Qu, N. Farrell, *Inorg. Chem.* **2003,** *42*, 5498 –5506.
43. N. Summa, J. Maigut, R. Puchta, R. van Eldik, *Inorg. Chem.* **2007,** *46*, 2094–2104.
44. M. E. Oehlsen, A. Hegmans, Y. Qu, N. Farrell, *Inorg. Chem*. **2005**, *44*, 3004–3006.
45. M. E. Oehlsen, A. Hegmans, Y. Qu, N. Farrell, *J. Biol. Inorg. Chem*. **2005**, *10*, 433–442.
46. J. W. Williams, Y. Qu, G. H. Bulluss, E. Alvorado, N. P. Farrell, *Inorg. Chem.* **2007,** *46*, 5820–5822.
47. D. Fan, X. Yang, X. Wang, S. Zhang, J. Mao, J. Ding, L. Lin, Z. Guo, *J. Biol. Inorg. Chem.* **2007,** *12*, 655–665.
48. L. Zerzankova, T. Suchankova, O. Vrana, N. P. Farrell, V. Brabec, J. Kasparkova, *Biochem. Pharmacol.* **2010,** *79*, 112–121.
49. L. Zerzankova, H. Kostrhunova, M. Vojtiskova, O. Novakova, T. Suchankova, M. Lin, Z. Guo, J. Kasparkova, V. Brabec, *Biochem. Pharmacol.* **2010,** *80*, 344–351.
50. J. Pracharova, O. Novakova, J. Kasparkova, D. Gibson, V. Brabec, *Pure Appl. Chem.* **2013,** *85*, 343–354.
51. Z. H. Xu, Y. M. Zhang, Z. Q. Xue, X. L. Yang, Z. Y. Wu, Z. J. Guo, *Inorg. Chim. Acta* **2009,** *362*, 2347–2352.
52. H. W. Yue, B. Yang, Y. Wang, G. J. Chen, *Int. J. Mol. Sci.* **2013,** *14*, 19556–19586.
53. J. Zhu, Y. Zhao, Y. Zhu, Z. Wu, M. Lin, W. He, Y. Wang, G. Chen, L. Dong, J. Zhang, Y. Lu, Z. Guo, *Chem. Eur. J.* **2009,** *15*, 5245–5253.
54. Y. Qu, H. Rauter, A. P. S. Fontes, R. Bandarage, L. R. Kelland, N. Farrell, *J. Med. Chem.* **2000,** *43*, 3189–3192.

55. M. Kloster, H. Kostrhunova, R. Zaludova, J. Malina, J. Kasparkova, V. Brabec, N. Farrell, *Biochemistry* **2004,** *43*, 7776–7786.
56. B. van Houten, S. Illenye, Y. Qu, N. Farrell, *Biochemistry* **1993,** *32*, 11794–11801.
57. V. Brabec, P. Christofis, M. Slamova, H. Kostrhunova, O. Novakova, Y. Najajreh, D. Gibson, J. Kasparkova, *Biochem. Pharmacol.* **2007,** *73*, 1887–1900.
58. S. Neidle, *J. Med. Chem.* **2016,** *59*, 5987–6011.
59. I. Ourliac-Garnier, M. A. Elizondo-Riojas, S. Redon, N. Farrell, S. Bombard, *Biochemistry* **2005,** *44*, 10620–10634.
60. K. Suntharalingam, A. J. P. White, R. Vilar, *Inorg. Chem.* **2010,** *49*, 8371–8380.
61. D. L. Ang, B. W. J. Harper, L. Cubo, O. Mendoza, R. Vilar, J. Aldrich-Wright, *Chem. Eur. J.* **2016,** *22*, 2317–2325.
62. P. von Grebe, K. Suntharalingam, R. Vilar, P. J. Sanz Miguel, S. Herres-Pawlis. B. Lippert, *Chem. Eur. J.* **2013,** *19*, 11429–11438.
63. C.-X. Xu, Y. Shen, Q. Hu, Y. X. Zheng, Q. Cao,P. Z. Qin, Y. Zhao, L. N. Ji, Z. W. Mao *Chem. Asian J.* **2014,** *9*, 2519–2526.
64. C. A. Rabikz, M. E. Dolan, *Cancer Treatment Rev.* **2007,** *33*, 9–23.
65. S. Komeda, *Metallomics* **2011,** *3*, 650–655.
66. S. Teletchéa, S. Komeda, J.-M. Teuben, M. A. Elizondo-Riojas, J. Reedijk, J. Kozelka, *Chem. Eur. J.* **2006,** *12*, 3741–3753.
67. K. Spiegel, A. Magistrato, P. Carloni, J. Reedijk, M. L. Klein, *J. Phys. Chem. B* **2007,** *111*, 11873–11876.
68. S. Komeda, Y.-L. Lin, M. Chikuma, *ChemMedChem* **2011,** *6*, 987 – 990.
69. J. Mlcouskova, J. Malina, V. Novohradsky, J. Kasparkova, S. Komeda, V. Brabec, *Biochim. Biophys. Acta* **2012,** *1820*, 1502–1511.
70. J. Mlcouskova, J. Kasparkova, T. Suchankova, S. Komeda, V. Brabec, *J. Inorg. Biochem.* **2012,** *114*, 15–23.
71. N. Kida, Y. Katsuda, Y. Yoshikawa, S. Komeda, T. Sato, Y. Saito, M. Chikuma, M. Suzuki, T. Imanaka, K. Yoshikawa, *J. Biol. Inorg. Chem* **2010,** *15*, 701–707.
72. Y. Yoshikawa, S. Komeda, M. Uemura, T. Kanbe, M. Chikuma, K. Yoshikawa, T. Imanaka, *Inorg. Chem.* **2011,** *50*, 11729–11735.
73. R. Olivova, J. Stepankova, T. Muchova, V. Novohradsky, O. Novakova, O. Vrana, J. Kasparkova, V. Brabec, *Inorg. Chim. Acta* **2012,** *393*, 204–211.
74. S. Komeda, G. V. Kalayda, M. Lutz, A. L. Spek, Y. Yamanaka, T. Sato, M. Chikuma, J. Reedijk, *J. Med. Chem.* **2003,** *46*, 1210–1219.
75. G. V. Kalayda, S. Komeda, K. Ikeda, T. Sato, M. Chikuma, J. Reedijk, *Eur. J. Inorg. Chem.* **2003,** *24*, 4347–4355.
76. L. Senerovic, M. D. Zivkovic, A. Veselinovic, A. Pavic, M. I. Djuran, S. Rajkovic, J. Nikodinovic-Runic, *J. Med. Chem.* **2015,** *58*, 1442–1451.
77. B. A. J. Jansen, P. Wielaard, G. V. Kalayda, M. Ferrari, C. Molenaar, H. J. Tanke, J. Brouwer, J. Reedijk, *J. Biol. Inorg. Chem* **2004,** *9*, 403–413.
78. H. -L. Chan, D.-M. Ma, M. Yang, C.-M Che, *J. Biol. Inorg. Chem.* **2003,** *8*, 761–769.
79. E. J. Gao, M. C. Zhu, H. X. Yin, L. Liu, Q. Wu, Y. G. Sun, *J. Inorg. Biochem.* **2008,** *102*, 1958–1964.
80. E. Gao, L. Liu, M. Zhu, Y. Huang, F. Guan, X. Gao, M. Zhang, L. Wang, W. Zhang, Y. Sun, *Inorg. Chem.* **2011,** *50*, 4732–4741.
81. G. Cafeo, C. Lo Passo, L. Monsu Scolaro, I. Pernice, R. Romeo, *Inorg. Chim. Acta* **1998,** *275–276*, 141–149.
82. V. Marini, J. Kasparkova, O. Novakova, L. M. Scolaro, R. Romeo, V. Brabec, *J. Biol. Inorg. Chem.* **2002,** *7*, 725–734.
83. N. J. Wheate, B. J. Evison, A. J. Herlt, D. R. Phillips, J. G. Collins, *Dalton Trans.* **2003,** 3486–3492.

84. N. J. Wheate, G. M. Abbott, R. J. Tate, C. J. Clements, R. Edrada-Ebel, B. F. Johnston, *J. Inorg. Biochem.* **2009,** *103*, 448–454.
85. B. W. Johnson, V. Murray, M. D. Temple, *BMC Cancer* **2016,** *16*, 333–349.
86. S. D. Brown, K. D. Trotter, O. B. Sutcliffe, J. A. Plumb, B. Waddell, N. E. B. Briggs, N. J. Wheate, *Dalton Trans.* **2012,** *41*, 11330–11339.
87. S. L. Woodhouse, L. M. Rendina, *Chem. Commun.* **2001,** 2464–2465.
88. Y. Qu, T. G. Appleton, J. D. Hoeschele, N. P. Farrell, *Inorg. Chem.* **1993**, *32*, 2591–2593.
89. N. P. Farrell, *Chem. Soc. Rev.* **2015***, 44,* 8773–8785.
90. V. Brabec, J. Kasparkova, O. Vrana, O. Novakova, J. W. Cox, Y. Qu, N. Farrell, *Biochemistry* **1999,** *38*, 6781–6790.
91. J. Kasparkova, O. Vrana, N. Farrell, V. Brabec, *J. Inorg. Biochem.* **2004,** *98*, 1560–1569.
92. T. Banerjee, P. Dubey, R. Mukhopadhyay, *Biochimie* **2010,** *92*, 846–851.
93. J. Kasparkova, J. Zehnulova, N. Farrell, V. Brabec, *J. Biol. Chem.* **2002,** *277*, 48076–48086.
94. J. Zehnulova, J. Kasparkova, N. Farrell, V. Brabec, *J. Biol. Chem.* **2001,** *276*, 22191–22199.
95. M. S. Davies, D. S. Thomas, A. Hegmans, S. J. Berners-Price, N. Farrell, *Inorg. Chem.* **2002,** *41*, 1101–1109.
96. A. Hegmans, S. J. Berners-Price, M. S. Davies, D. Thomas, A. Humphreys, N. Farrell, *J. Am. Chem. Soc.* **2004,** *126*, 2166–2180.
97. R. Ruhayel, J. Moniodis, X. Yang, J. Kasparkova, V. Brabec, S. J. Berners-Price, N. Farrell, *Chem. Eur. J.* **2009,** *15*, 9365–9374.
98. Y. Qu, M.-C. Tran, N. P. Farrell, *J. Biol Inorg. Chem*. **2009**, *14*, 969–977.
99. D., Yang, S. van Boom, J. Reedijk, J. van Boom, N. Farrell, A. H.-J. Wang, *Nature Struct. Biol.*, **1995**, *2*, 577–581.
100. J. Malina, N. P. Farrell, V. Brabec, *Chem. Asian J.* **2011,** *6*, 1566–1574.
101. J. Malina, J. Kasparkova, N. P. Farrell, V. Brabec, *Nuc. Acids Res.* **2011**, *39*, 720–728.
102. P. May, E. May, *Oncogene* **1999,** *18*, 7621–7636.
103. T. Tokino, S. Thiagalingam, W. S. Eldeiry, T. Waldman, K. W. Kinzler, B. Vogelstein, *Hum. Mol. Genet.* **1994,** *3*, 1537–1542.
104. A. K. Nagaich, V. B. Zhurkin, S. R. Durell, R. L. Jernigan, E. Appella, R. E. Harrington, *Proc. Natl. Acad. Sci. USA* **1999,** *96*, 1875–1880.
105. A. Lebrun, R. Lavery, H. Weinstein, *Protein Eng.* **2001,** *14*, 233–243.
106. J. Kasparkova, M. Fojta, N. Farrell, V. Brabec, *Nucleic Acids Res.* **2004,** *32*, 5546–5552.
107. S. Oiso, R. Ikeda, K. Nakamura, Y. Takeda, S. I. Akiyama, H. Kariyazono, *Oncol. Rep.* **2012,** *28*, 27–32.
108. J.-L Luo, H. Kamata, M. Karin, *J. Clin. Immunol.* **2005,** *25*, 541–550.
109. J. Dutta, Y. Fan, N. Gupta, G. Fan, C. Gelinas, *Oncogene* **2006,** *25*, 6800–6816.
110. S. T. Smale, *Nature Immunol.* **2011,** *12*, 689–694.
111. M. S. Hayden, S. Ghosh, *Genes & Dev* **2012,** *26*, 203–234.
112. V. Brabec, J. Kasparkova, H. Kostrhunova, N. P. Farrell, *Sci. Rep*. **2016** *6***,** 28474.
113. D. Fink, S. Nebel, S. Aebi, S. H. Zhang, B. Cenni, A. Nehmé, R. D. Christen, S. B. Howell, *Cancer Res,* **1996**, *56*, 4881–4886.
114. P. Perego, L. Gatti, C. Caserini, R. Supino, D. Colangelo, R. Leone, S. Spinelli, N. Farrell, F. Zunino, *J. Inorg. Biochem*. **1999**, *77,* 59–64.
115. L. Orlandi, G. Colella, A. Bearzatto, G. Abolafio, C. Manzotti, M. G. Daidone, N. Zaffaroni, *Eur. J. Cancer,* **2001**, *37*, 649–659.
116. L. Gatti, G. L. Beretta, N. Carenini, F. Zunino, P. Perego, *Cell. Mol. Life Sci.* **2004**, *61*, 973–981.

117. L. Gatti, R. Supino, P. Perego, C. Caserini, N. Carenini, S. C. Righetti, V. Zuco, F. Zunino, *Cell Death Differ.* **2002**, *9*, 1352–1359.
118. T. Shingu, V. C. Chumbalkar, H.-S. Gwak, K. Keishi Fujiwara, K. Seiji Kondo, N. Farrell, O. Bögler, *Neuro-Oncology* **2010**, *12*, 1269–1277.
119. V. R. Menon, E. J. Peterson, K. Valerie, N. P. Farrell, L. F. Povirk, *Biochem. Pharmacol.* **2013,** *86*, 1708–1720.
120. S. Komeda, Y. Qu, J. B. Mangrum, A. Hegmans, L. D. Williams, N. P. Farrell. *Inorg. Chim. Acta* **2016**, *452*, 25–33.

3

Platinum(IV) Prodrugs

V. Venkatesh and Peter J. Sadler

Department of Chemistry, University of Warwick, Coventry CV4 7AL, UK
<venka7@gmail.com>
<P.J.Sadler@warwick.ac.uk>

ABSTRACT 70
1. INTRODUCTION 70
    1.1. Design Strategy 71
    1.2. Synthesis 72
    1.3. Characterization 73
    1.4. Redox Reactions 73
    1.5. Biological Activity 74
    1.6. Molecular Pharmacology and Toxicology 75
2. INTERACTIONS WITH BIOMOLECULES 77
    2.1. Serum Proteins 77
        2.1.1. Human Serum Albumin 77
    2.2. DNA 78
    2.3. Small Biomolecules 78
        2.3.1. Glutathione 78
        2.3.2. L-Methionine 79
        2.3.3. Ascorbic Acid 79
3. DESIGN FEATURES FOR ANTICANCER COMPLEXES 80
    3.1. Targeted Delivery 80
        3.1.1. Integrin-Targeting Pt(IV) Complexes 80
        3.1.2. Pt(IV) Complexes Targeting Glucose Transporters 84
    3.2. Synergistic Action 85
    3.3. Fluorescent Probes 86
4. PHOTOACTIVATABLE COMPLEXES 88
    4.1. Diiodido Platinum(IV) Complexes 88
    4.2. Diazido Platinum(IV) Complexes 89

Metal Ions in Life Sciences, Volume 18 Edited by Astrid Sigel, Helmut Sigel, Eva Freisinger, and Roland K. O. Sigel

https://doi.org/10.1515/9783110470734-003

5. NANO MATERIALS FOR DRUG DELIVERY 92
5.1. Metallic Nanoparticles 92
5.2. Polymeric Nanoparticles 94
5.2.1. Non-covalent Encapsulation of Pt(IV) Prodrugs 94
5.2.2. Covalent Functionalization with Pt(IV) Prodrugs 95
5.3. Carbon-Based Materials 96
5.4. Supramolecular Motifs 98
5.5. Upconversion Nanoparticles 99
6. CONCLUDING REMARKS 101
ACKNOWLEDGMENTS 102
ABBREVIATIONS 102
REFERENCES 103

Abstract: This chapter is an overview of recent progress in the design of Pt(IV) prodrugs. These kinetically-inert octahedral prodrugs can be reduced in cancer cells to active square-planar Pt(II) complexes, for example by intracellular reducing agents such as glutathione or by photoexcitation. The additional axial ligands in Pt(IV) complexes which are released on reduction, allow bioactive molecules to be delivered which can act synergistically with Pt(II) in killing cancer cells, or act as targeting vectors, allow attachment to polymer and nanoparticle delivery systems, or labelling with fluorescent probes. Pt(IV) prodrugs have yet to be approved for clinical use, although some offer the promise of increased efficacy and reduced side effects.

Keywords: nanoparticles · photoactivation · Pt(IV) prodrugs · targeted delivery · upconversion nanoparticles

1. INTRODUCTION

The serendipitous discovery of the antitumor activity of *cis*-diamminedichloridoplatinum(II) (cisplatin) by Barnett Rosenberg in the 1960s is a milestone in the area of medicinal inorganic chemistry [1]. Two more platinum compounds (carboplatin and oxaliplatin) have since been approved by the FDA for clinical use world-wide, and three (nedaplatin, lobaplatin, and heptaplatin), for regional use in Japan, China, and Korea, respectively [2].

The mode of action of cisplatin is mainly due to targeting nuclear DNA after entering cells either by active (via the copper transporter Ctr1) or passive transport [3, 4]. The chloride concentration drops from about 104 mM outside cells to 23 mM in the cytoplasm, and even lower, ca. 4 mM, in the nucleus, resulting in hydrolysis and formation of more reactive platinum(II) aqua complexes. These aqua species react readily with biomolecules in cells, including the nucleophilic N7 nitrogen of purine nucleobases (G and A). Intrastrand GG DNA cross-links especially can inhibit transcription [5]. Binding of cisplatin to other cellular targets especially cysteine and methionine sulfur in peptides (glutathione) and proteins, also occurs [6], and although less widely studied than nucleobase adducts, may be important for understanding the systemic toxicity of cisplatin and resistance to the drug.

One approach to reducing the toxic side-effects of cisplatin is the use of platinum(IV) complexes as prodrugs [7, 8]. Octahedral low-spin $5d^6$ platinum(IV)

complexes are much more kinetically inert than square-planar $5d^8$ platinum(II) complexes. This difference can allow delivery of the intact drug ('prodrug') with fewer side reactions before the target site is reached. Platinum(IV) complexes are likely to be stable under the highly acidic conditions in the stomach and therefore suitable for oral administration [9]. Also with 6 ligands, there are more possibilities for structural variations with Pt(IV) compared to Pt(II). For example, the axial ligands (so-called, although more than one axis could be defined as such depending on the symmetry) present in Pt(IV) complexes can be modified to improve the pharmacokinetics of the drug by tuning the reduction potential, lipophilicity, bioactivity [10], and targeting ability [11, 12]. In this chapter we describe recent progress on the rational design of platinum(IV) complexes as prodrugs for cancer therapy.

1.1. Design Strategy

As shown in Figure 1, Pt(IV) complexes often contain a non-leaving ligand L, a nitrogen donor ligand (am(m)ine, pyridine), which does not undergo any intracellular transformation and is retained in the final Pt(II)-DNA adduct. L is also crucial for determining the biological activity of the complex [13–15]. The leaving ligand X (Cl, I) can undergo aquation/activation allowing reaction with purine bases in DNA.

The axial ligands are typically hydroxide or chloride, which are lost on reaction of the complexes with biological reductants (e.g., glutathione, ascorbic acid) or external reductants. The axial hydroxido ligands can be carboxylated to attach

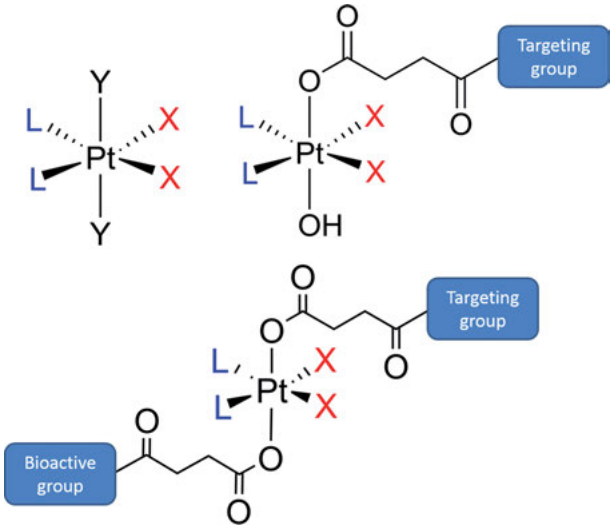

Figure 1. Design strategy for platinum(IV) prodrugs (L = non-leaving ligand, X = leaving ligand, Y = OH, Cl, RCO_2).

targeting groups, bioactive ligands (e.g. drugs and enzyme inhibitors), or both. This approach has been used to attach Pt complexes to the surface of nanoparticles for selective internalization using the enhanced permeability and retention (EPR) effect and further stimuli-responsive delivery to the target site [16].

1.2. Synthesis

Examples of oxidants used for the synthesis of *trans* Pt(IV) complexes are shown in Figure 2. Typically the synthesis involves reaction of Pt(II) complexes with hydrogen peroxide or chlorine [17, 18] in a 2-electron oxidative-addition reaction.

Mechanistic studies with H_2O_2, carried out in the presence of ^{18}O-labelled water, have revealed that only one hydroxido ligand comes from H_2O_2. The second comes from solvent water [19]. This finding is important if Pt(IV) compounds are synthesized in coordinating solvents, for example if H_2O_2 is used as the oxidant in methanol, *trans* hydroxido-methoxido Pt(IV) complexes can be formed [20]. When such oxidations are carried out in the presence of carboxylic acids, the product formed (mono- or dicarboxylato complex) is determined by the pK_a of the acid [21]. Hypervalent iodine species are known to be as strong

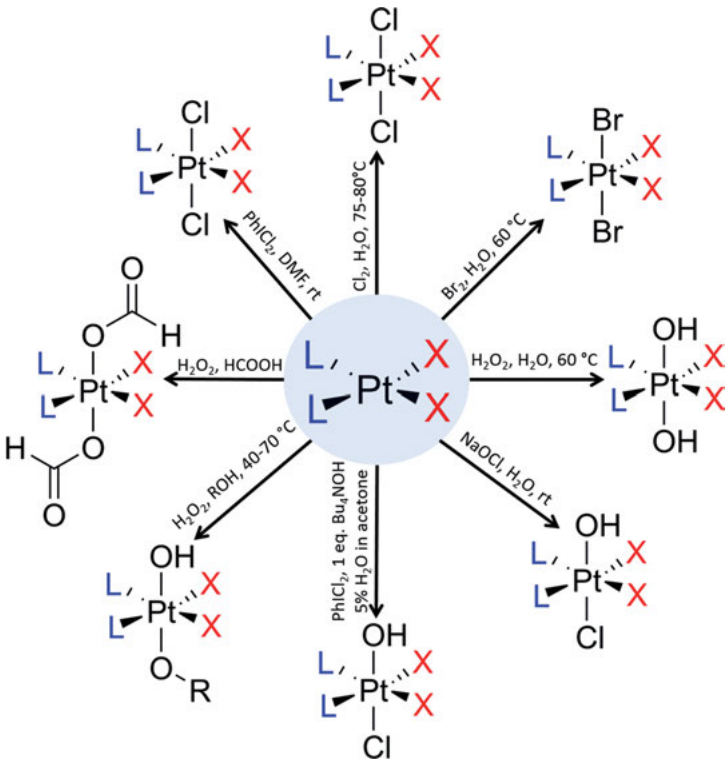

Figure 2. Synthesis of Pt(IV) complexes from Pt(II) precursors.

oxidizing agents in organic synthesis. The oxidation of Pt(II) complexes with $PhICl_2$ results in *trans* dichlorido Pt(IV) complexes [22, 23]. Pt(IV) complexes with axial carboxylato ligands have been prepared by reacting dihydroxido Pt(IV) complexes with corresponding anhydrides or acyl chlorides in various solvents (e.g., DMF, DMSO, acetonitrile) at 50–80 °C for 6–24 h. Axial carboxylato ligands in the axial positions can be used for conjugation to bioactive molecules and targeting groups [24].

1.3. Characterization

Platinum(IV) complexes can be characterized by various analytical techniques, including NMR, mass spectrometry, FTIR, UV/Vis spectroscopy, and X-ray crystallography. Often a combination of techniques is used depending on whether samples are solutions or solids. Care has to be taken to check that Pt(IV) is not reduced by the solvent, and especially with Pt(II) that ligands are not substituted by solvent (e.g., DMSO). Platinum complexes may also be photoactive and exposure to light can also be a problem.

^{195}Pt (33.7 % natural abundance) is an NMR-active I = 1/2 nucleus with similar sensitivity to ^{13}C, but a much wider chemical shift range of ca. 15,000 ppm. Pt(IV) resonances tend to have low-field shifts relative to Pt(II). In view of its high stability, $[PtCl_6]^{2-}$ is a common ^{195}Pt chemical shift reference ($\delta = 0$ ppm). ^{195}Pt NMR resonances usually broaden as complexes increase in MW and also broaden at higher observation frequencies [25]. The presence of Pt in complexes is often evident from studies of ^{1}H, ^{13}C, ^{15}N or ^{31}P (I = 1/2) nuclei in ligands. They can give rise to one- to four-bond ^{195}Pt couplings, resulting in the appearance of 1 : 4 : 1 peak intensity patterns with the outer lines being the ^{195}Pt satellites. These satellites are sharper for Pt(IV) complexes compared to Pt(II) due to less broadening by chemical shift anisotropy relaxation [25].

Recent studies have illustrated the potential of FTIR for characterizing Pt anticancer complexes and their derivatives [26]. UV/Vis spectroscopy provides valuable information about the charge-transfer and other transitions in Pt(IV) complexes [27]. Fluorescent probes designed recently can distinguish Pt(IV) and Pt(II) species inside cancer cells, particularly useful for understanding the reduction of Pt(IV) complexes [28, 29].

1.4. Redox Reactions

The anticancer activity of Pt(IV) complexes is usually attributed to their reduction to Pt(II) products which bind to DNA. The ease of reduction is therefore important for the biological activity of the complex, and usually assumed to involve intracellular or extracellular reductants such as glutathione, thiol groups of proteins, and ascorbic acid. Reduction of Pt(IV) to Pt(II) is an irreversible two-electron process with loss of two ligands (often referred to as the axial ligands, but in practice various combinations can be lost). The rate of reduction

Table 1. Reduction (half-wave) potentials and reduction rates for Pt(IV) complexes (1 mM in 0.1 M KCl, pH = 7) with various axial ligands reported by Choi et al. [30].

Complexes	Reduction potential (Ep in mV)	Rate of reduction k ($M^{-1}s^{-1}$)
$[Pt(en)(OH)_2Cl_2]$	–884	0
$[Pt(en)(OCOCH_3)_2Cl_2]$	–546	0.54
$[Pt(en)Cl_4]$	–160	164
$[Pt(en)(OCOCF_3)_2Cl_2]$	0	209

of Pt(IV) complexes depends upon both the axial and equatorial ligands [30]. Strongly electron-withdrawing axial groups increase the reduction rate, in the order: $OH < OCOCH_3 < Cl < OCOCF_3$ (Table 1).

Bulkier axial and equatorial ligands also enhance the reduction rate. For example, ascorbic acid does not reduce $[Pt(en)(OH)_2Cl_2]$, but readily reduces $[Pt(ipa)_2(OH)_2Cl_2]$ (en = ethylenediamine, ipa = isopropylamine) due to the presence of the bulky isopropylamine ligands. Faster reduction rates for complexes with similar equatorial ligands appear to correlate with higher cytotoxic activity [30]. The reduction of *trans,cis*-$[Pt(en)(OH)_2I_2]$ by glutathione results in a chelate ring-opened Pt(II) complex, the reaction proceeding through the removal of an iodide ligand by glutathione (GSH) as the sulfenyl iodide. The sulfenyl iodide may react with another molecule of GSH to produce GSSG and free I^-. Free GSH or I^- further react with ring-opened Pt(II) species to form $[\{Pt(en)(\mu\text{-SR})\}_2]^{2+}$ and $[Pt(en)I_2]$ [31].

Gibson et al. [32] have studied the reduction of *cis,trans,cis*-$[PtCl_2(OCOCH_3)_2(NH_3)_2]$ in the presence of three different cancer cell lines. The rate of reduction follows the order: A2780cisR (cisplatin-resistant ovarian) > A2780 (ovarian) > HT29 (colon). Interestingly small molecule reductants are not involved in the reduction, rather cellular components with MW >3000 [32]. They showed that 4 products are formed from the reduction of *cis,cis,trans*-$[PtCl_2(^{15}NH_3)(NH_2R)(OOC^{13}CH_3)_2]$ (R = H, cyclohexyl or isopropyl) with potential intracellular reductants such as glutathione, ascorbate, cytochrome *c*, and NADH involving loss of two axial ligands (acetate), one axial (acetate) and one equatorial (chloride) ligand, or two equatorial (chloride) ligands [33].

1.5. Biological Activity

Low-spin $5d^6$ Pt(IV) complexes are relatively inert to substitution reactions hence their reactions with biological nucleophiles are very slow. This increases the circulation lifetime of the Pt(IV) complexes in the blood stream. The reduction of Pt(IV) complexes to biologically active square-planar Pt(II) complexes provides a strategy for release and delivery of biologically-active ligands. Examples of Pt(IV) complexes that have entered clinical trials are tetraplatin, satraplatin, and iproplatin (Figure 3).

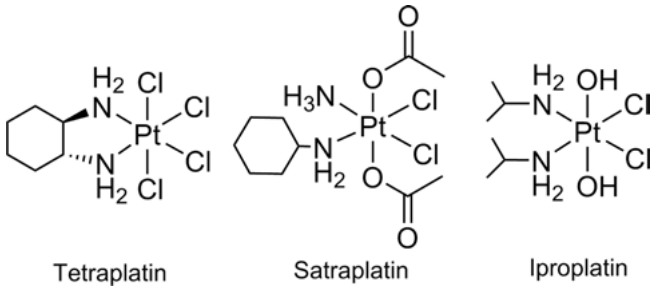

Figure 3. Platinum(IV) complexes that have undergone clinical trials.

The preclinical studies of tetraplatin were encouraging, but in phase I it showed severe neurotoxicity [34]. Kelland et al. reported that satraplatin was 840-fold more active than cisplatin *in vitro* [35]. Phase III trials did not reflect this activity. The higher activity *in vitro* could be due to high cellular uptake of the active drug. The complex may be reduced i*n vivo* before reaching its target. Similarly, iproplatin also showed disappointing activity in phase II and III trials. However, Pt(IV) complexes still possess potential as anticancer agents. Some maintain potency against spheroids indicating effectiveness against multicellular resistance (MCR) and additionally, the hypoxic environment in cancer cells provides a reducing environment which improves the efficacy of such prodrugs [36, 37]. The pharmacological activity of Pt(IV) complexes can also be improved by appropriate choice of the axial ligands, which can be vectors for specific cell receptors, e.g., folate or integrin receptors, used for attachment to nanoparticle delivery vehicles, or for delivery of bioactive ligands such as drugs or enzyme inhibitors.

1.6. Molecular Pharmacology and Toxicology

Platinum drugs can enter cells by passive diffusion, and as recently discovered for cisplatin, by active transport via the copper transporter hCtr1 [38]. Two copper exporter proteins ATP7A and ATP7B may be involved in efflux of platinum drugs, and over-expression of these proteins in ovarian cancer cells results in resistance to cisplatin [39]. Other transporters include the organic cationic transporter (OCT), and multidrug and toxin extrusion (MATE) protein. In cells, cisplatin readily aquates to form mono- and bis-aqua and less reactive hydroxido adducts. The aqua adducts are particularly active towards many biological nucleophiles. Sulfur groups of Cys and Met residues in amino acids, peptides (especially glutathione), and proteins are targets for Pt(II) drugs. Strong Pt–S bonds are usually thought to inactivate the drugs. Figure 4 depicts some biological transformations of Pt(II) and Pt(IV) drugs in cells.

The final adducts of cisplatin, carboplatin, and oxaliplatin with DNA are similar, but the lower reactivity of the chelated complexes leads to fewer DNA ad-

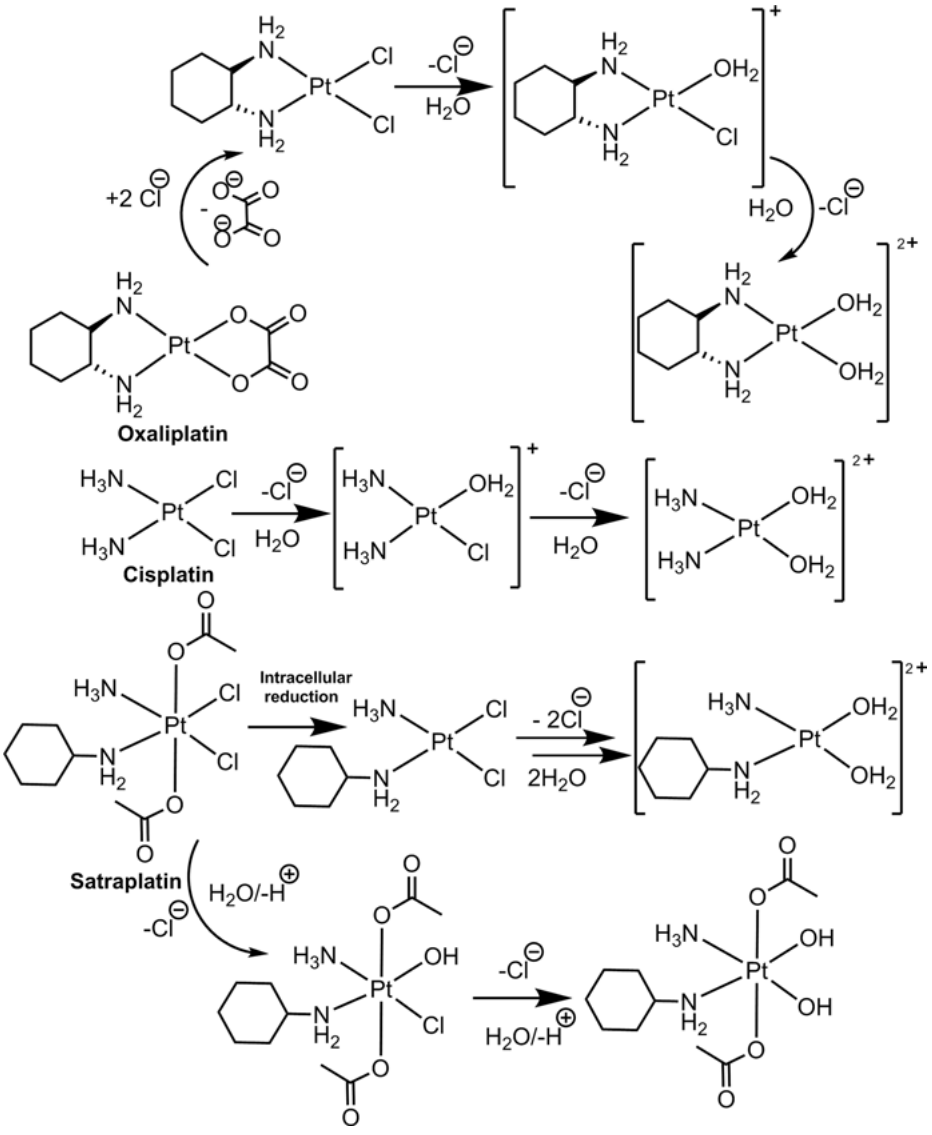

Figure 4. Biotransformations of Pt(II) and Pt(IV) drugs.

ducts compared to cisplatin. Also the presence of the bulky diaminocyclohexyl ligand in oxaliplatin leads to differences in the conformational change induced in DNA and subsequent protein recognition of platinated cross-links [40]. The Pt(IV) complex satraplatin exhibits activity by a slightly different mechanistic pathway. It is believed to enter cells through passive diffusion and undergo activation first by reduction to Pt(II), followed by binding to DNA, and secondly by metabolism to different Pt(IV) complexes as shown in Figure 4, which can then bind to DNA. *In vitro* studies suggest that satraplatin is not only very active,

but also reacts with DNA much faster than cisplatin, the increased activity *in vitro* is mainly due to the formation of reactive oxygen species which further induce necrosis in cancer cells [41].

2. INTERACTIONS WITH BIOMOLECULES

2.1. Serum Proteins

2.1.1. Human Serum Albumin

The interaction of Pt anticancer drugs with serum proteins plays an important role in drug accumulation, transportation, distribution, metabolism, activity, and toxicity. Human serum albumin (HSA; 66.5 kDa) is the most abundant protein in blood serum (ca. 0.6 mM) and consists of three similar domains (I, II, and III), each of which has two subdomains. Under physiological conditions it adopts a largely helical conformation. Albumin contains 585 amino acids, with 17 disulfide bonds, one free Cys (Cys-34), 6 Met, and 16 His residues that are all potentially strong Pt binding sites, although not all readily accessible (e.g., Cys-34 is in a crevice) [42].

Monofunctional adducts of cisplatin with Met and Cys-34 and the S,N-chelation of surface-exposed Met-298 have been proposed based on ^{1}H and ^{15}N NMR data [43]. Reactions of the photoactivatable complex *trans,cis*-$[PtI_2(OH)_2(en)]$ with human serum albumin have been monitored by UV-Vis and NMR spectroscopy. The Pt(IV)-I ligand-to-metal charge transfer (LMCT) band drastically reduced in intensity after 24 h reaction with albumin, but there was no reaction when Cys-34 was blocked indicating involvement of the thiol group. The mechanism of reaction appears to involve attack of an iodido ligand on the sulfur of Cys-34 resulting in a sulfenyl iodide Cys-SI which further undergoes hydrolysis to form the sulfenic acid Cys-SOH. The Pt(II) complex formed further reacts with albumin, but with chlorido instead of iodido ligands such a reaction was not observed [44].

Kowol et al. have synthesized a maleimide-functionalized Pt(IV) complex to target HSA [45], known to accumulate in tumor tissues by endocytosis and the EPR effect [46, 47]. Recently, Lippard et al. [48] designed Pt(IV)-prodrugs containing axial ligands with different aliphatic chain lengths (C2 to C16) to mimic fatty acids and studied their interaction with human serum albumin. They utilized the advantage of non-covalent association between the aliphatic chain of the Pt(IV) prodrug with HSA for transporting the prodrug in the blood stream. Quenching of the fluorescence of Trp-214 showed that the Pt prodrug with C16 aliphatic chains has the highest binding affinity ($K_a = 1.04 \times 10^6\,M^{-1}$) towards HSA. Computational studies suggested that the prodrug is buried inside the protein [48].

Shi et al. [49] reported the synthesis of a Pt(IV)-HSA conjugate that avoids premature reduction of Pt(IV) in the extracellular environment. They suggested that the specific anticancer activity of the Pt(IV)-HSA conjugate towards cancer cells was due to release of the active Pt(II) analogue in the acidic and hypoxic tumor environment [49].

2.2. DNA

Platinum(IV) complexes are thought to bind strongly to DNA only after forming Pt(II) by reaction with biological reductants. Platinum(II) preferentially binds to guanine over adenine in DNA, and binding to guanine is stabilized by H-bonding interactions between the exocyclic 6-oxo group of guanine and the ammine group of cisplatin, but adenine forms weaker H-bonds [50].

Binding of Pt(II) to DNA results in a number of structurally different adducts, including intrastrand cross-links, interstrand cross-links, N,O chelation of guanine and DNA-Pt-protein cross-links (DPCLs) [51]. Cisplatin forms ca. 65 % 1,2-d(GpG), 25 % 1,2-d(ApG) intrastrand cross-links and nearly 1–3 % interstrand cross-links and monofunctional adducts [52]. In contrast, transplatin does not form 1,2 intrastrand cross-links due to steric constraints. These results suggest the importance of 1,2 intrastrand cross-links for the anticancer activity of cisplatin. However, the $[Pt(hmp)Cl_2]$ complex (hmp = homopiperazine) preferentially forms interstrand cross-links and yet exhibits potent cytotoxicity against cancer cells [53]. Iproplatin initially appeared to induce strand breakage of closed circular PM2-DNA [54]. However, Dabrowiak et al. observed the presence of one molecule of H_2O_2 per iproplatin molecule in the crystal lattice. It appears that this H_2O_2 caused the DNA cleavage, and not iproplatin itself [55]. Brabec et al. reported that DNA binding of iproplatin and oxoplatin requires high concentrations of Pt(IV) and long reaction times (10 % of Pt bound after 12 d) [56, 57]. The *in vitro* binding studies carried out by Blatter et al. clearly showed that neither iproplatin nor oxoplatin bind to PM2-DNA until a reducing agent is added and Pt(II) is formed [58].

2.3. Small Biomolecules

2.3.1. Glutathione

Glutathione (γ-L-glutamyl-L-cysteinyl-glycine, GSH) is an antioxidant tripeptide present in cells at millimolar concentrations. The presence of the thiol group of cysteine allows it to act as an antioxidant by directly reacting with reactive oxygen species or xenobiotic electrophiles. The thiol group of GSH is readily oxidized (E_P = –240 mV) to the disulfide (GSSG) under biological conditions. The reduction of Pt(IV) complexes can proceed via halide-bridged electron transfer with no observable intermediate [59]. The presence of GSH (10 μM to 100 μM) increased the anticancer activity of tetraplatin (10 μM) against cisplatin-resistant L1210 leukemia cells, due to the reduction of Pt(IV) to Pt(II) and binding to DNA [60]. The concentration of GSH is crucial for its cytotoxicity, an increase in GSH concentration (100 μM) resulted in lower cytotoxicity. At high GSH concentrations, GSH binds to the Pt(II) product thereby interfering with its binding to DNA [60]. In the absence of GSH, the Pt(II)- (salmon sperm) DNA adducts were minimal, but after the addition of GSH (10 μM–1 mM), substantial amounts of Pt(II)-DNA adducts formed. The reduction of tetraplatin by GSH is a prerequisite for the anticancer activity.

Often cancer cells that are resistant to Pt(II) and Pt(IV) complexes have elevated levels of GSH [61], therefore it appears that GSH plays a crucial role in enhancing the cellular resistance to Pt(II) and Pt(IV) complexes. Pendyala et al. [62] investigated the relationship between intracellular GSH concentration and cytotoxicity of both Pt(II) (cisplatin, carboplatin, and oxaliplatin) and Pt(IV) (iproplatin and tetraplatin) complexes. The correlation is significant for iproplatin and tetraplatin, but not for Pt(II) [62]. Satraplatin (JM216) was administered to cell lines with varying intracellular GSH concentrations. Cell lines that expressed higher concentrations of GSH produced JM118, a Pt(II) biotransformation product of JM216, whereas cell lines that expressed lower levels of GSH gave rise to Pt(IV) biotransformation products [63]. *Trans,trans,trans*-$[PtCl_2(OH)_2(c\text{-}C_6H_{11}NH_2)(NH_3)]$ (JM335) is reduced by GSH to *trans,trans*-$[Pt(OH)_2(c\text{-}C_6H_{11}NH_2)(NH_3)]$, but no trace of *trans,trans*-$[PtCl_2(c\text{-}C_6H_{11}NH_2)(NH_3)]$ is observed. Under similar reaction conditions, the isomer of JM335, *cis,trans,cis*-$[PtCl_2(OH)_2(c\text{-}C_6H_{11}NH_2)(NH_3)]$ (JM149) did not undergo reduction. Thus, the presence of chlorido ligands in *trans* positions appears to favor the reduction of the Pt(IV) complexes by glutathione [64].

2.3.2. L-Methionine

The thioether L-methionine is an essential amino acid present in human blood, and in many peptides, proteins, and in S-adenosyl methionine (SAM). Ribosomal protein synthesis is usually initiated with an N-terminal Met residue. The interaction of methionine with Pt(IV) complexes in water can result in the formation of Pt(II) analogues and methionine sulfoxide [MeS(O)R]. The reduction is believed to take place via halide-bridged one-electron reduction. The short-lived intermediate, [MeS(X)R], hydrolyzes immediately to give [MeS(O)R] [65]. The reduction of JM216 (*cis,trans,cis*-$[PtCl_2(OCOCH_3)_2(NH_3)_2]$) with methionine results in the formation of *cis*-$[PtCl_2(NH_3)_2]$. Reduction proceeds through an acetate ligand, but when methionine is in excess it can replace the labile chlorido ligands to form methionine-Pt(II) adducts [66].

2.3.3. Ascorbic Acid

Ascorbic acid (vitamin C) is a small-molecule antioxidant present in mammalian cells at micromolar (or higher) concentration, often taken as a dietary supplement. It acts as a reductant and is involved in many important biological processes such as collagen formation and enzyme cycling. At physiological pH it is present as the ascorbate monoanion (pK_a ca. 3.8). Its reaction with Pt(IV) complex is a two-electron reduction process resulting in the formation of Pt(II) complexes.

The reduction of Pt(IV) complexes by ascorbate can take place by either inner-sphere or outer-sphere mechanisms. Elding and coworkers [67] reported that the reduction of *trans,trans,trans*-$[Pt(cha)(OCOCH_3)_2NH_3(Cl)_2]$ (JM576) is $3\times$ faster than its isomer *trans,cis,cis*-$[Pt(cha)(OCOCH_3)_2NH_3(Cl)_2]$ (JM216). The

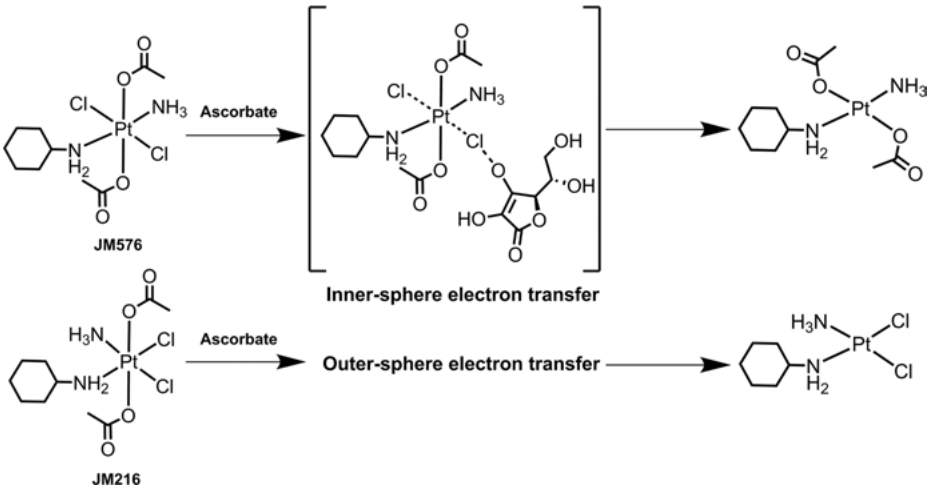

Figure 5. Reduction of *trans,trans,trans*-[Pt(cha)$(OCOCH_3)_2NH_3(Cl)_2$] and *trans,cis,cis*-[Pt(cha)$(OCOCH_3)_2NH_3(Cl)_2$] by ascorbate; the upper chloride-bridged mechanism is described as inner-sphere [67].

faster reduction of JM576 is due to inner-sphere electron transfer between *trans* chlorido ligands and ascorbate, whereas JM216 forms outer-sphere adducts with ascorbate resulting in slower reduction (Figure 5).

3. DESIGN FEATURES FOR ANTICANCER COMPLEXES

3.1. Targeted Delivery

3.1.1. Integrin-Targeting Pt(IV) Complexes

The aim of targeted chemotherapy is to increase the amount of drug reaching the tumor site, thereby reducing side reactions with normal healthy cells. This can be achieved by selectively targeting molecules that are over-expressed by cancer cells. Angiogenesis is an important biological process required for the development of new blood vessels, which is also crucial for tumor cell growth, survival, and metastasis. In case of tumor-induced angiogenesis, transmembrane receptors such as integrins ($\alpha_v\beta_3$ and $\alpha_v\beta_5$) and the surface protein aminopeptidase (APN) are highly expressed. Both integrins and APN recognize peptides containing RGD (Arg-Gly-Asp) and NGR (Asn-Gly-Arg) sequences with very high affinity. In this regard, Lippard et al. have synthesized Pt(IV) complexes conjugated with RGD and NGR motifs [68]. A series of mono- and difunctional Pt(IV) complexes appended with RGD, NGR, cyclic-CRGDC, and cyclic-RGDfK have been prepared (Figure 6) and their activity studied towards cancer cell lines known to express $\alpha_v\beta_3/\alpha_v\beta_5$ integrins.

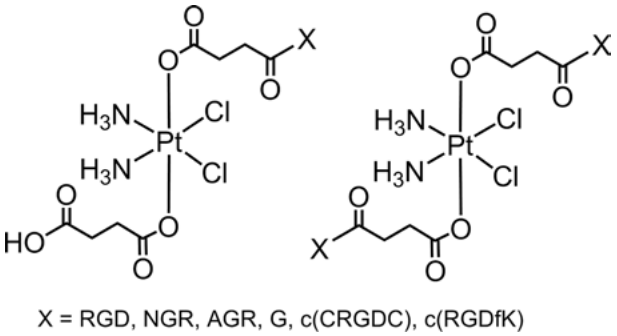

Figure 6. Pt(IV) complexes of cisplatin with conjugated peptides attached to the axial positions.

In vitro studies on endothelial and human cancer cell lines show that RGD-conjugated Pt(IV) complexes exhibit potent cytotoxicity when compared with non-targeted Pt(IV) complexes. NGR-conjugated Pt(IV) complexes are less toxic than RGD-conjugated Pt(IV) complexes, but show better activity when compared with non-specific Pt(IV)-peptide conjugates.

Marchan et al. designed Pt(IV) complexes of picoplatin containing monomeric [Pt-c(RGDfK)] and tetrameric [Pt-RAFT-c(RGDfK)$_4$] RGD peptides [69] (Figure 7). The activities of these complexes were determined against SK-MEL-28 melanoma cells that express high levels of $\alpha_v\beta_3$ and $\alpha_v\beta_5$ integrins. To probe the selectivity of these complexes, CAPAN-1 pancreatic cancer cells and fibroblast 1BR3G cells were tested as negative controls. The uptake directly correlated with integrin expression and RGD-containing Pt(IV) complex. The accumulation of Pt in SK-MEL-28 cell lines was higher than in CAPAN-1. Importantly the tetrameric [Pt-RAFT-c(RGDfK)$_4$] complex displayed higher uptake when compared with monomeric [Pt-c(RGDfK)].

The monomeric complex [Pt-c(RGDfK)] is 2.4-fold more cytotoxic than picoplatin, whereas the tetrameric complex [Pt-RAFT-c(RGDfK)$_4$] exhibits a 20-fold increase in cytotoxicity. These studies illustrate the effectiveness of targeting peptide conjugates for selective internalization, uptake, and cytotoxicity. The same strategy has been used for photoactivatable diazido Pt(IV) complexes having an integrin-recognizing peptide c(RGDfK) appended in an axial position [70].

The RGD peptide targets cancer cells selectively, and the complex is then activated only when irradiated with particular wavelengths of light (Figure 8). This strategy should minimize the systemic toxicity of the complex. The photocytotoxicity of the complex was determined for SK-MEL-28 cell lines that express both $\alpha_v\beta_3$ and $\alpha_v\beta_5$ integrins in high levels and the DU-145 human prostate carcinoma cell line which expresses $\alpha_v\beta_5$ to a similar level, but expresses considerably low levels of $\alpha_v\beta_3$ integrin. The photocytotoxicity against DU-145 was 4-fold lower than for SK-MEL-28 cells, which suggests a significant role for the $\alpha_v\beta_3$ integrin receptor in complex internalization. Uptake studies further supported this observation.

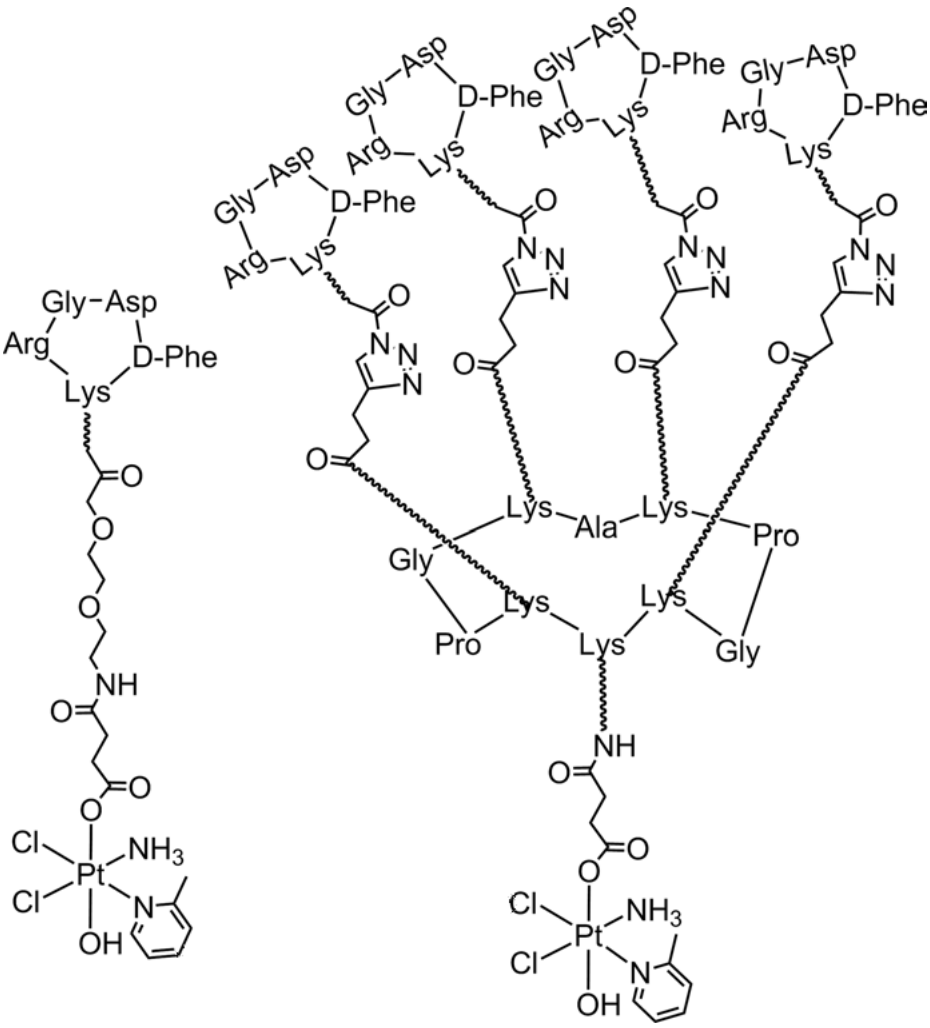

Figure 7. Molecular structures of monomeric [Pt-c(RGDfK)] and tetrameric [Pt-RAFT-c(RGDfK)$_4$] complexes.

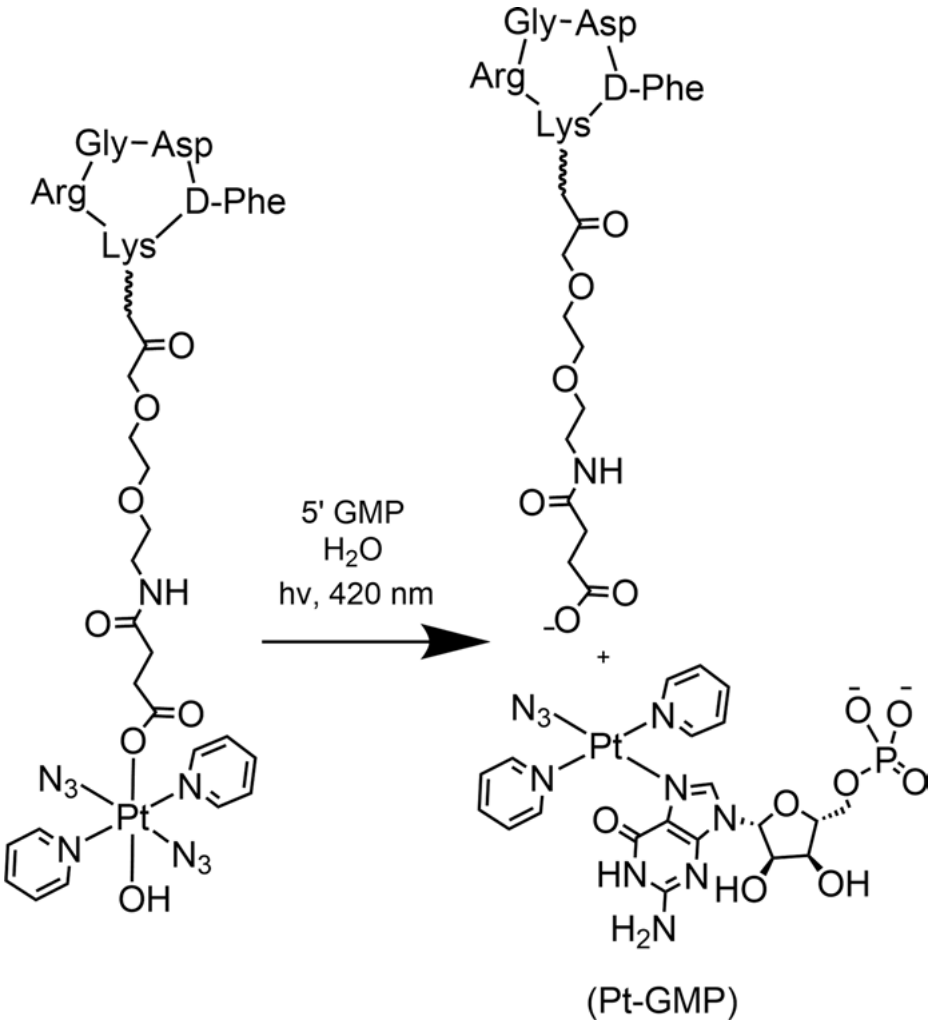

Figure 8. Photo-reaction of c(RGDfK)-appended diazido Pt(IV) complex with 5′-GMP.

3.1.2. Pt(IV) Complexes Targeting Glucose Transporters

Glucose-platinum conjugates are an interesting class of prodrugs for targeting glucose transporters that are over-expressed in cancer cells. Glucose transporters such as GLUT1, GLUT2, GLUT3, GLUT12, SGLT1–2 are over-expressed in different types of cancer cells, especially GLUT1 (ovarian, esophageal, pancreatic, breast, brain, renal, lung, cutaneous, colorectal, endometrial, and cervical). Recently, Lippard et al. [71, 72] synthesized a series of positional isomers of glucose-Pt conjugates and studied their binding specificity with GLUT1, cell uptake, and cytotoxicity. C1α and C2-substituted conjugates showed potent cytotoxicity against DU145 cells; other conjugates were less cytotoxic. Uptake studies in the presence and absence of the GLUT1 inhibitor cytochalasin B showed that the C2 glucose-Pt conjugate is specifically taken up by the GLUT1 transporter and exhibits potent cytotoxicity against a breast cancer mouse model that over-expresses GLUT1 [71, 72].

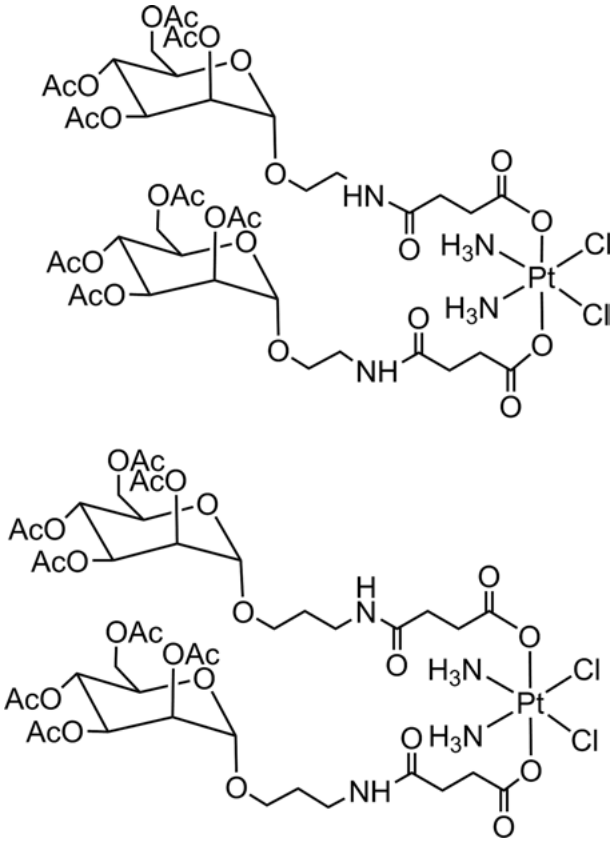

Figure 9. Pt(IV)-mannose conjugates active against prostate cancer cells (LNCaP) reported by Wang et al. [73]

Pt(IV) conjugates of glucose, mannose (Figure 9), and rhamnose exhibit significant activity against prostate cancer cells [73]. Pt(II)-GMP adducts were observed only in the presence of ascorbic acid, indicating the importance of intracellular reductants for the activity of the Pt(IV)-mannose conjugate. The platinated DNA content was much higher for mannose-Pt(IV) conjugate in HeLa cells, when compared with cisplatin and oxaliplatin. This result signifies high cellular uptake of the mannose-Pt(IV) conjugate (Figure 9) followed by intracellular reduction and the increased anticancer activity [73].

3.2. Synergistic Action

Synergistic action is one way of increasing the pharmacological activity of Pt(IV) complexes by designing the axial ligands appropriately. The axial ligands can be antiproliferative agents or bioactive molecules that enhance the activity of platinum drugs. Kelland et al. found that increasing the number of carbon atoms in the axial position increases cell accumulation and enhances the cytotoxic activity *in vitro* [74]. Tolan et al. reported that Pt(IV) complexes with mono- and bisindole derivatives in axial positions have increased uptake of Pt and higher reactive oxygen species levels resulting in loss of mitochondrial membrane potential and apoptosis [75].

Bioactive ligands such as small molecule inhibitors have been appended in the axial position to target different DNA repair proteins and enzymes. Anti-inflammatory drugs such as ibuprofen and indomethacin appended to the axial

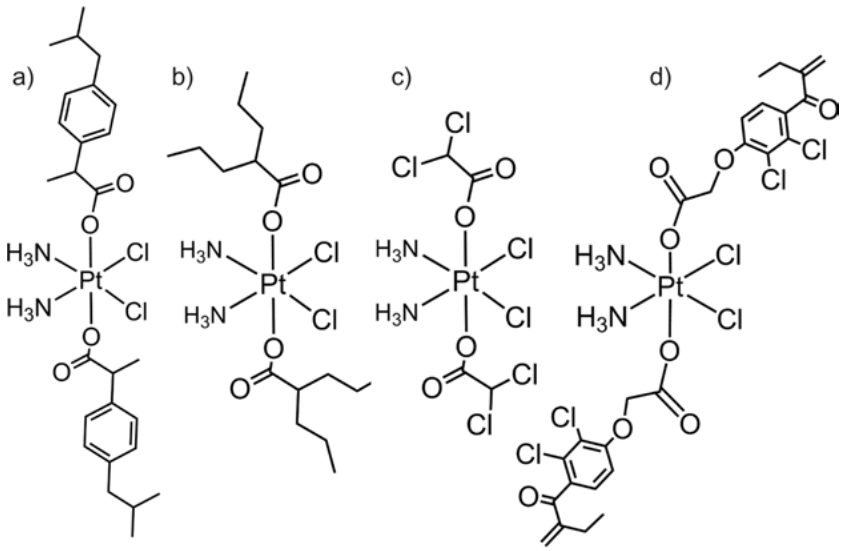

Figure 10. Pt(IV) complexes with bioactive axial ligands: (**a**) ibuprofen, (**b**) valproate, (**c**) mitaplatin, and (**d**) ethacraplatin.

position of cisplatin (Figure 10) increase the anticancer efficacy by inhibiting the COX-2 enzyme known to be involved in tumorigenesis and drug resistance [76, 77]. Dyson et al. designed Pt(IV) complexes with axial ethacrynic acid to target selectively cytosolic glutathione S-transferase (GST) that catalyzes the conjugation of glutathione to xenobiotic substrates [78, 79].

A similar strategy was followed by Dhar and Lippard who incorporated dichloroacetate ligands in the axial positions of cisplatin (mitaplatin) to target the mitochondrial membrane potential that triggers release of cytochrome *c* and induces signalling pathways leading to apoptosis [80]. Barnes, Kutikov, and Lippard also designed a Pt(IV) complex based on cisplatin with two axial estrogens. The estrogens induce the overexpression of HMGB1 proteins which bind to the minor grove of bent platinated-DNA adducts and protects them from nucleotide repair proteins. This improves the anticancer activity of the compound [81].

Shen et al. and Alessio et al. reported Pt(IV) complexes with axial valproato ligands that exhibit histone deacetylase (HDAC) inhibitory activity and are 50-fold more potent than cisplatin in various cancer cell lines [82, 83]. However, there is a debate whether the activity is due to higher cellular uptake or HDAC inhibitory activity, because the IC_{50} value of valproate is in the millimolar range.

3.3. Fluorescent Probes

Hambley and coworkers designed cisplatin analogues containing coumarin (C120 and C151) fluorophores in their non-leaving position (Figure 11a,b) [84]. They observed that the fluorescence emission was quenched after complexation; when the Pt(II) complex was oxidized to its corresponding Pt(IV) analogue, this further diminished its fluorescence intensity. They followed the reduction of Pt(IV) inside A2780 cells by confocal microscopy. Strong fluorescence signified the reduction of Pt(IV) to Pt(II) in cells, but the distribution of Pt was different for the Pt(II) and Pt(IV) complexes. This indicates that the reduction takes place after the uptake of Pt(IV).

Later Wilson and Lippard designed the dansyl Pt(II) and Pt(IV) complexes shown in Figure 11c,d. The quantum yield of Pt(II) decreased from 27 % to 1.6 % after oxidation to Pt(IV). They proposed that this drastic change in the fluorescence intensity will be useful for understanding the reduction of platinum prodrugs in live cells [22]. Recently, a targeted theranostic Pt(IV) prodrug was reported by Yuan et al. [86], a Pt(IV) complex containing cRGD for targeting and luminogen for aggregation-induced emission (AIE) in its axial positions. The prodrug is highly emissive after entering cells due to intracellular reduction [85]. Ang et al. reported a post-labelling strategy to study the intracellular distribution of platinum complexes [29]. They designed a non-fluorescent probe by coupling rhodamine B with diethyldithiocarbamate (Rho-DDTC) (Figure 12). This probe selectively binds to Pt(II) species *via* diethyldithiocarbamate. Labilization of the *trans* ligand facilitates reaction with the spirolactam motif and concomitant turn-on fluorescence. The turn-on fluorescence of this probe is useful for detecting Pt(II) species with *cis*-$[PtA_2X_2]$ analogues. Pt(IV) complexes do not appear to

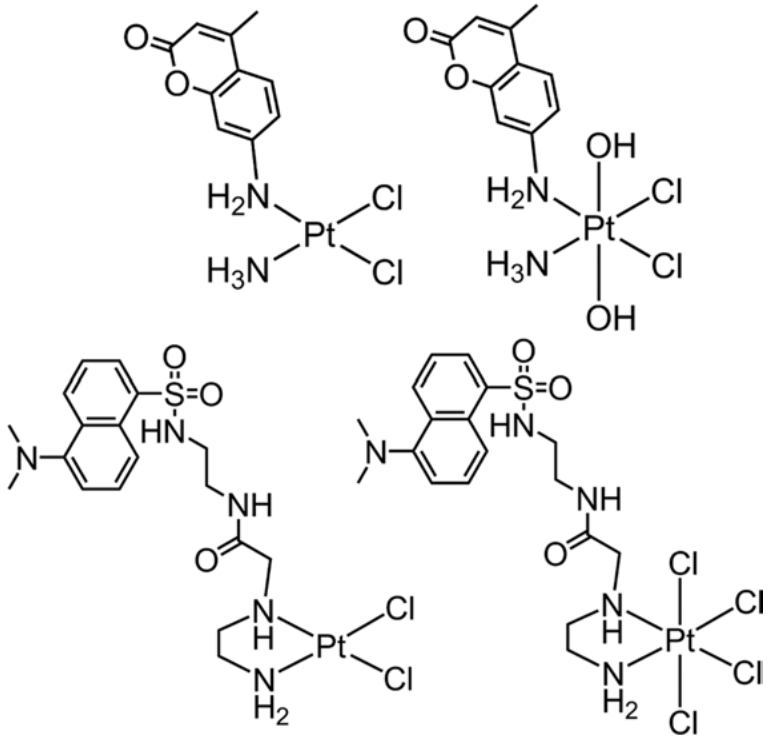

Figure 11. Fluorescent tags appended to Pt(II) and Pt(IV) complexes.

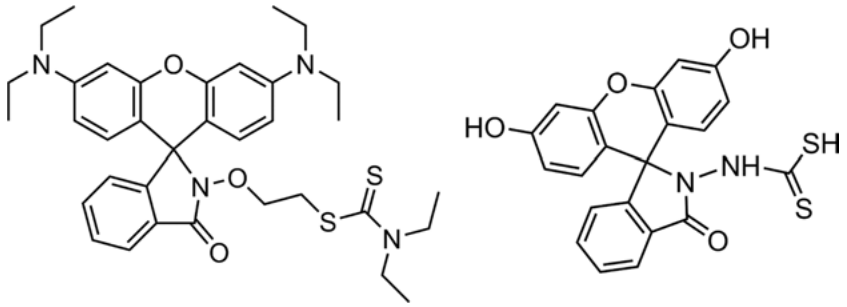

Figure 12. Rhodamine B and fluorescein-appended dithiocarbamate and dithocarbamic acid probes for detection of Pt(II) species in live cells.

turn-on Rho-DDTC fluorescence. This probe can be utilized to study further the reduction of Pt(IV) complexes after cell internalization.

Recently, New et al. designed a fluorescent probe that selectively senses monofunctional Pt(II) complexes [28] by coupling fluorescein with dithiocarbamic acid (Figure 12b). In the case of the bi-functional adduct, π-π stacking with the fluorescein moiety leads to fluorescence quenching.

4. PHOTOACTIVATABLE COMPLEXES

Platinum(IV) complexes have potential as prodrugs for photoactivatable chemotherapy (PACT). This strategy is attractive due to its spatial and temporal control over the drug activation and specific targeting ability. An advantage of PACT is that it leaves normal cells unaffected, so it is a potentially safer form of treatment compared with radiotherapy, surgery, and other conventional chemotherapy. The advantage of using PACT in cancer therapy over photodynamic therapy (PDT) is that PDT requires oxygen for its activity (converts ground state triplet oxygen to excited state singlet oxygen which kills cells), whereas cancer cells are often deprived of oxygen (hypoxic). Two classes of photoactivatable Pt(IV) complexes have been widely studied: diiodido-Pt(IV) complexes and diazido-Pt(IV) complexes.

4.1. Diiodido Platinum(IV) Complexes

Bednarski et al. designed the photoactivatable diiodido-Pt(IV) anticancer complex *trans,cis*-[$PtCl_2I_2$(en)] containing ethylenediamine as a non-leaving ligand to avoid photodimerization [86]. The photoreduction of *trans,cis*-[$PtCl_2I_2$(en)] was monitored by the decrease in intensity of the iodide-to-Pt(IV) LMCT band. However, unexpectedly this complex showed similar DNA binding ability in the dark as in the light, which could be due to facile intracellular reduction by GSH

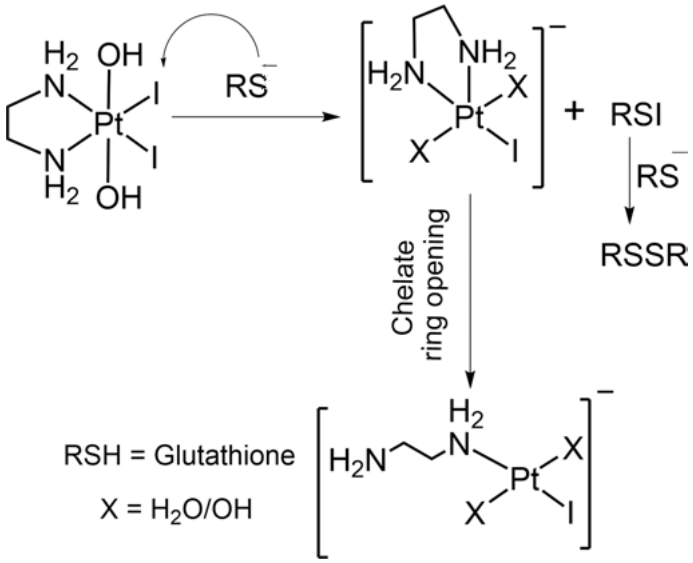

Figure 13. Proposed mechanism for the formation of the chelate-ring-opened Pt(II) complex when glutathione reacts with the photoactive complex *trans,cis*-[$Pt(OH)_2I_2$(en)].

(Figure 13). Replacement of the chloride ligands by acetates improved the dark stability of the complex [87].

Irradiation of *trans,cis*-[$Pt(OAc)_2I_2(en)$] and calf thymus DNA with UVA at 375 nm gave rise to substantial DNA platination, but under similar conditions *trans,cis*-[$Pt(OH)_2I_2(en)$] did not. Hence, reduction of Pt(IV) to Pt(II) is important for platinated DNA adduct formation. The *in vitro* cytotoxicity of diiodido-Pt(IV) complexes against TCCSUP bladder cancer cells increased after irradiation, but the IC_{50} values were similar in the dark and in the light. In order to understand the dark cytotoxicities of diiodido-Pt(IV) complexes, reactions of *trans,cis*-[$Pt(OH)_2I_2(en)$] with glutathione were studied [88]; unexpectedly they form chelate ring-opened Pt(II) complexes at physiological pH. The complex also forms Pt-DNA adducts in the presence of GSH much faster than [$PtI_2(en)$]. Diiodido-Pt(IV) complexes form >90 % Pt-DNA adducts in the presence GSH (2 mol equiv) after 24 h at 37 °C, whereas the dichlorido-Pt(IV) complex does not react with DNA in the presence of GSH [89].

4.2. Diazido Platinum(IV) Complexes

The first photochemical reductive elimination reaction for *trans*-$[Pt(CN)_4(N_3)_2]^{2-}$ was reported by Vogler et al. in 1978 [90]. Irradiation of this complex with UVA results in the formation of azidyl radicals with concomitant two-electron reduction to $[Pt(CN)_4]^{2-}$. They proposed that unstable azidyl radicals react readily with solvent molecules to produce N_2. Diazido-Pt(IV) complexes have interesting anticancer activity. The X-ray crystal structures of diazido-Pt(IV) cisplatin analogues of *cis,cis,trans*-$[Pt(NH_3)_2(N_3)_2(OH)_2]$ and *cis,trans*-$[Pt(en)(N_3)_2(OH)_2]$ have been reported [91] (Figure 14). Unlike diiodido-Pt(IV) complexes, diazido-Pt(IV) complexes show very good dark stability. They do not react with 5′-GMP or d(GpG) in the dark over a period of one week at 25 °C. Irradiation with UVA or visible light (λ_{irr} = 457.9 nm) results in formation of Pt(II) species that readily react with N7 of 5′-GMP and d(GpG). The photodecomposition pathways can be monitored by NMR. ^{14}N NMR is more useful than ^{15}N NMR since azide ligands have no coupled protons and so the intensities of their ^{15}N resonances cannot be enhanced by polarization transfer. However, the strongly-shielded ^{14}N resonance from the coordinated azide (N_α) is very broad and difficult to detect, whereas N_β is remarkably sharp [92, 93]. Photolysis of *cis,cis,trans*-$[Pt(NH_3)_2(N_3)_2(OH)_2]$ [94] gives rise

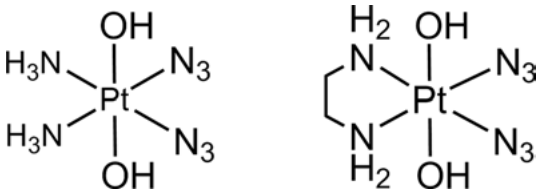

Figure 14. Photoactivatable *cis* diazido-Pt(IV) complexes.

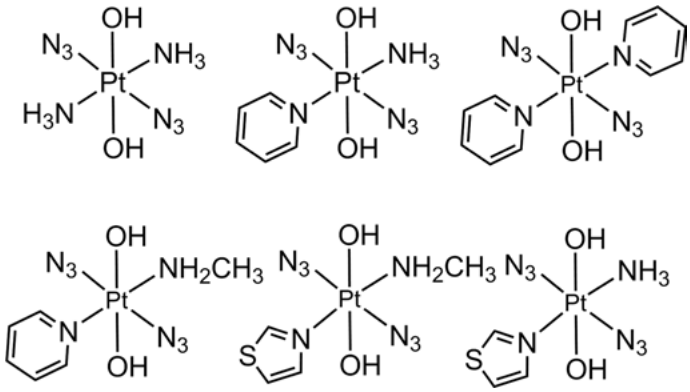

Figure 15. Photoactivatable *trans* diazido-Pt(IV) complexes with different non-leaving ligands.

to azide in phosphate buffer, N_2 under acidic aqueous conditions, and ammonia and O_2 at higher pH. These photodecomposition products along with Pt(II) species could contribute to the different mechanism of action of *cis* diazido-Pt(IV) complexes.

On irridiation with visible light, *cis,trans*-$[Pt(en)(N_3)_2(OH)_2]$ forms cross-links with d(GpG) much faster than cisplatin [95]. Thus the interaction of diazido-Pt(IV) complexes with DNA is different from cisplatin. Under dark conditions these complexes are non-toxic, but after irradiation they are equally toxic to cisplatin-resistant 5637 human bladder cancer cells. After light irradiation the morphology of bladder cancer cells changed drastically; disintegration of cell nuclei was observed [96].

Diazido-Pt(IV) complexes having *trans* diazido ligands exhibit different electronic properties compared with their *cis* isomers. The $N_3 \rightarrow Pt$ LMCT band of *trans,trans,trans*-$[Pt(N_3)_2(OH)_2(NH_3)_2]$ shifts towards the visible region compared with its *cis* isomer [97].

Excitation with longer wavelength light can allow deeper penetration into tissues. Current clinical use of photodynamic therapy uses red light, although shorter wavelength yellow, green, and blue light might be useful for surface cancers such as bladder and esophageal. The photocytotoxicity of diazido-Pt(IV) complexes can also be varied by changing the non-leaving ligands (Figure 15). When mixed amine ligands such as pyridine, piperidine, piperazine, 4-picoline, isopropylamine, methylamine, and thiazole are used, the photocytotoxicites increase drastically [98]. TDDFT calculations have revealed that the non-leaving ligands can play important roles in increasing absorption at higher wavelengths, for example hydroquinoline ligands form hydrogen bonds with axial –OH ligands and shift the absorption towards the red region [99]. The anticancer activity of *trans,trans,trans*-$[Pt(N_3)_2(OH)_2(py)(NH_3)]$ towards various cell lines has been studied (HL60, OE19, A2780, and A2780cis). There is potent photocytotoxicity against HL60 cells, but no apoptosis, indicating a different mechanism compared to cisplatin [100]. In general these diazido-Pt(IV) complexes do not undergo hydrolysis and

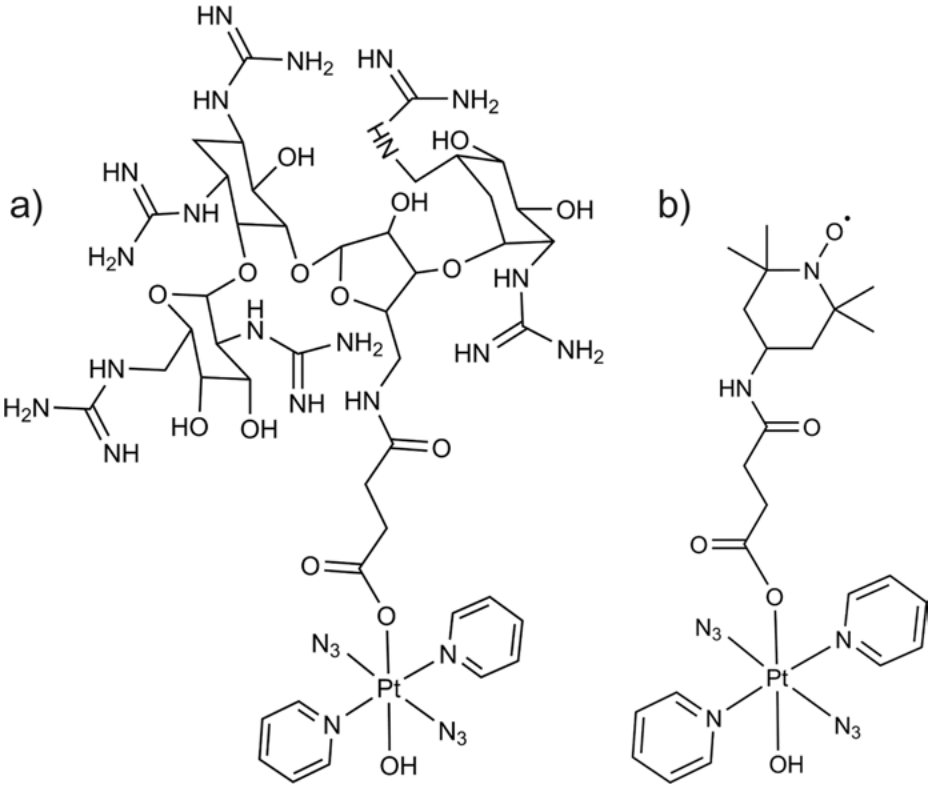

Figure 16. Photoactivatable *trans* diazido-Pt(IV) complexes with bioactive axial ligands.

reduction in the dark [101], but in the presence of UVA readily form cytotoxic photolysis products and do not show cross resistance with cisplatin.

The photo-induced reaction of *trans,trans,trans*-[$Pt(N_3)_2(OH)_2(MA)(py)$] with 5'-GMP involves formation of azidyl radicals, free azide, N_2, and singlet oxygen [102]. The cytotoxic action of diazido-Pt(IV) complexes may result not only from Pt(II) but also from these additional reactive species produced during photolysis. An interesting finding is the ability of the natural amino acid L-tryptophan (L-Trp) to quench the azidyl radicals formed on photolysis of *trans,trans,trans*-[$Pt(N_3)_2(OH)_2(py)_2$]. L-Trp (at 0.5 mM) can even protect A2780 ovarian cancer cells from the cytotoxic effects of this complex [103]. This quenching may be the result of electron transfer from tryptophan to azidyl radicals, and such effects might be used to modulate the activity of the photochemotherapeutic diazido-Pt(IV) complexes in cells.

The axial ligands can be used for targeting *trans* diazido-Pt(IV) complexes. For example, guanidinoneomycin has been appended in the axial position of *trans,trans,trans*-[$Pt(N_3)_2(OH)(OR)(py)_2$] as a carboxylate derivative (Figure 16a) to target RNA selectively [104]. This conjugate exhibits similar photocytotoxicity

to that of its parent compound against SK-MEL-28 melanoma cells, but is less photocytoxic to DU-145 human prostate cells.

Similarly, a stable free radical TEMPO (2,2,6,6-tetramethylpiperidine 1-oxyl) has been tethered in the axial position (Figure 16b). The photocytotoxicity of the conjugate increased by 1.2 × against A2780 ovarian cancer cells compared with its parent analogue, probably due to the antioxidant properties of TEMPO [105].

5. NANO MATERIALS FOR DRUG DELIVERY

5.1. Metallic Nanoparticles

Gold nanoparticles (AuNPs) are attractive drug delivery vehicles because of their high biocompatibility, low toxicity, non-immunogenicity, and high tissue permeability. Lippard et al. [106] have designed a Pt(IV) analogue of cisplatin with a tethered succinate group in an axial position. They functionalized AuNPs with thiolated 28-mer oligonucleotides having a terminal dodecyl amine and conjugated to the Pt(IV) prodrug *cis,cis,trans*-$[Pt(NH_3)_2Cl_2(OH)(OOCCH_2CH_2CO_2H]$ using amide coupling [109]. Pt-DNA-AuNP constructs are internalized in cells and reduced by intracellular reductants resulting in the release of an active Pt(II) analogue that forms 1,2-d(GpG) intrastrand cross-links with DNA. Most importantly the construct showed high antiproliferative activity against different cancer cell lines and was more effective than cisplatin. In another study, Shi et al. designed a Pt(IV) complex with an axial adamantyl unit and attached it to β-cyclodextrin-modified gold nanoparticles using β-cyclodextrin and adamantane host-guest interactions [107] (Figure 17). Clustering of the prodrug-loaded AuNP nanoparticles was observed in the nuclear region of SK-N-SH neuroblastoma cells. The *in vitro* toxicity of this compound was low compared with cisplatin, suggesting that the Pt(IV) prodrug is not completely reduced to the cytotoxic Pt(II) analogue.

Liu and coworkers have engineered gold nanorods (GNRs) for delivery of platinum anticancer drugs [108] by PEGylation to increase the drug circulation time in the blood stream, and conjugated to Pt(IV) prodrugs using EDC coupling. Pt(IV) functionalized GNRs display high cellular uptake and exhibit potent cytotoxicity against cancer cell lines. Most notably Pt-PEG-GNRs are not affected by cellular resistance which is a commonly encountered problem with platinum-based drugs. The uptake of Pt-PEG-GNRs is not affected by low-level expression of the copper transporter Ctr1, nor higher concentrations of glutathione and metallothionein.

Quantum dots (QDs) are semiconductor nanomaterials which possess interesting electronic properties that vary with the size of the particles. Mareque-Rivas and coworkers have reported the reduction of the Pt(IV) complex $[PtCl_4(bpy)]$ (bpy = 2,2′-bipyridine) to Pt(II) by CdSe-ZnS QDs in the presence of visible light [109] (Figure 18). Even in the absence of covalent attachment, the reduction of the Pt(IV) complex was efficient. They believe that this strategy can be utilized to activate other photoactivatable anticancer complexes as well. Later they

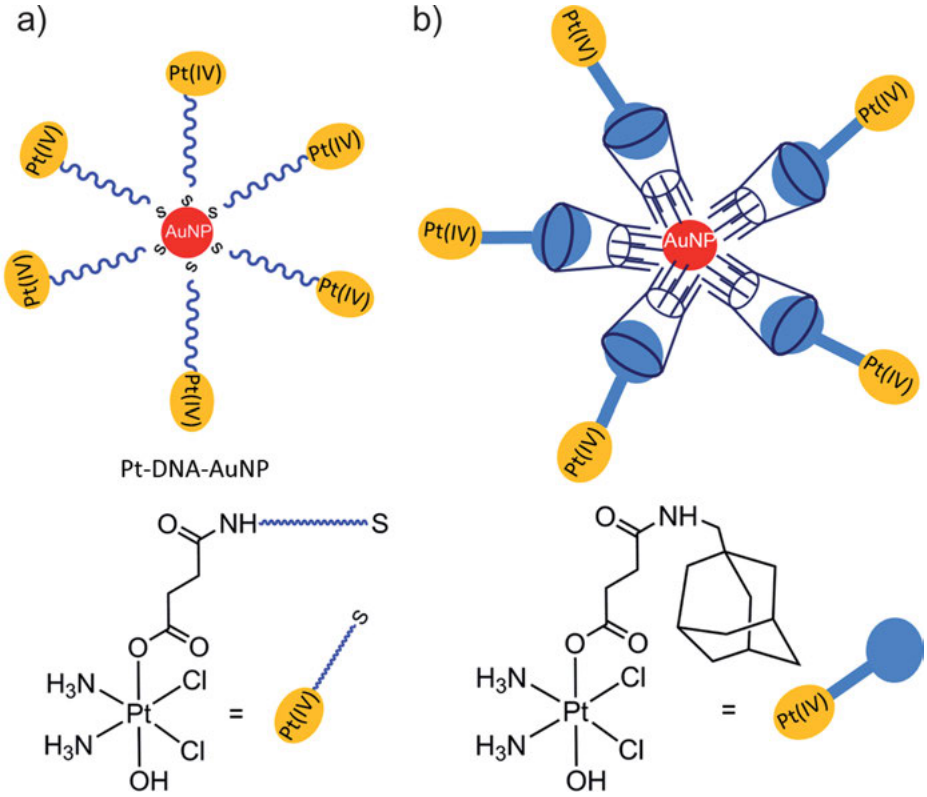

Figure 17. (**a**) Pt-DNA-AuNP construct, (**b**) Pt(IV) prodrug attached to AuNPs using host-guest interaction between β-cyclodextrin and adamantane units.

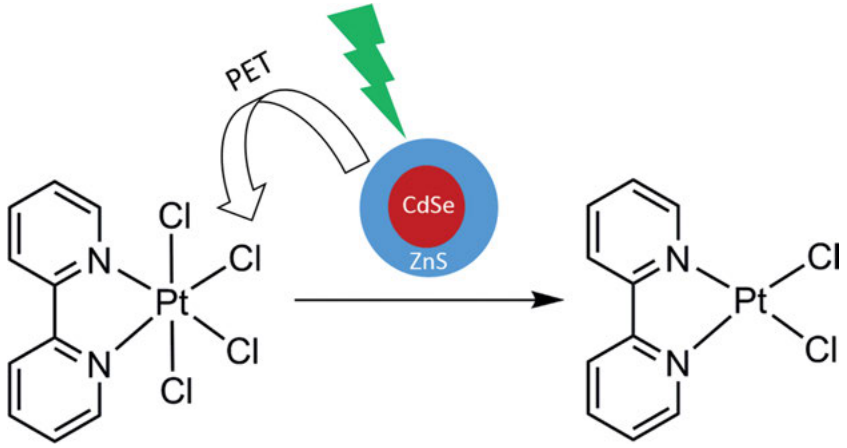

Figure 18. Visible light-induced electron transfer from CdSe-ZnS QDs to $[PtCl_4(bpy)]$.

designed micelles filled with QDs that react with *fac*-$[^{99m}Tc(OH_2)_3(CO)_3]^+$ to give a bimodal single photon-emission-computed tomography (SPECT) optical probe, which, on irradiation with visible light, generates cytotoxic Pt(II) complexes from inert Pt(IV) complexes [110].

Encapsulation of iron oxide nanoparticles (IONPs) with FITC-modified gelatin using hydrophobic-hydrophobic interactions has been reported by Cheng et al. [111]. The presence of a free amine group on gelatin was utilized to conjugate a Pt(IV) prodrug covalently. The construct shows good anticancer activity against MCF-7 cells, mainly due to the reduction of Pt(IV) prodrug to cytotoxic Pt(II) analogues intracellularly, and are potential candidates for drug delivery, MRI contrast, and fluorescence-sensing in cancer therapy.

5.2. Polymeric Nanoparticles

Polymeric nanoparticles have been extensively explored as drug carriers for Pt(IV) prodrugs. They are often formed from amphiphilic block co-polymers which contain a hydrophobic head and a hydrophilic tail. In water, the hydrophobic regions cluster to form a core with the hydrophilic portion exposed to water. Pt(IV) prodrugs can be loaded into polymeric nanoparticles either by encapsulation in the hydrophobic core or covalent conjugation on the backbone of the polymeric chain.

5.2.1. Non-covalent Encapsulation of Pt(IV) Prodrugs

The co-polymer poly(lactic-co-glycolic acid)-block-poly(ethylene glycol) (PLGA-PEG) has been extensively studied as a drug carrier, where PLGA and PEG act as hydrophobic and hydrophilic parts, respectively. The properties and assembly of these nanoparticles can be tuned by changing the lactic acid/glycolic acid ratio which leads to different PLGA block sizes. Both PLGA and PEG have been declared by the FDA as safe delivery vehicles.

PLGA-PEG-COOH nanoparticles have been used to encapsulate the hydrophobic hexanoate-bearing Pt(IV) prodrug *cis,cis,trans*-$[Pt(NH_3)_2Cl_2(OOCCH_2CH_2CH_2CH_2CH_3)_2]$. The free carboxylic acid group on the polymer has been conjugated to a targeting RNA aptamer that specifically recognizes prostate-specific membrane antigen (PSMA) [112]. PSMA is highly expressed in prostate cancer cells, so this construct can be used to treat prostate cancer mainly in the metastatic and hormone-refractory forms. The Pt(IV) prodrug-loaded construct gave rise to substantial reduction in tumor size in mice injected with LNCaP cells to form a subcutaneous xenograft. Prolonged blood circulation time, PSMA targeting ability, and the enhanced permeability and retention effect all appear to contribute to the observed high activity of this construct. Increasing the length of the polymethylene chain of the axial alkyl carboxylate ligand in *cis,cis,trans*-$[Pt(NH_3)_2Cl_2(OOC(CH_2)_nCH_3)_2]$ increases the loading of the Pt(IV) prodrug and leads to aggregation of these particles [113]. Different functionaliza-

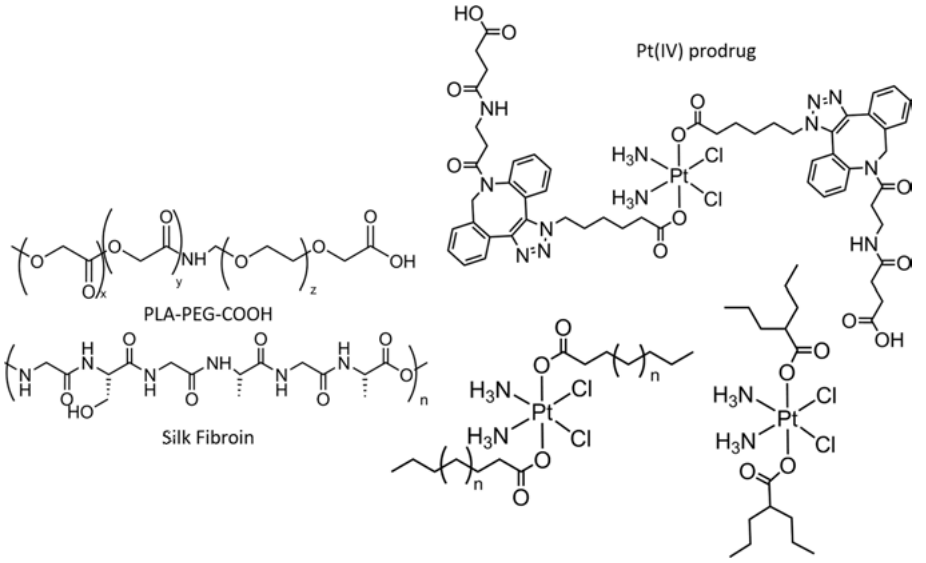

Figure 19. Polymers and Pt(IV) prodrugs which have been used for nanoencapsulation [118].

tion of the Pt(IV) complex can be achieved using azide-alkyne click reactions. Copper-free click chemistry has the advantage of not requiring ascorbate which might reduce Pt(IV) prodrugs readily. The Pt(IV) prodrug was tethered with an axial azide and reacted with azadibenzocyclooctyne (ADIBO) [114, 115]. The increased lipophilicity of the clicked conjugate allowed encapsulation in nanoparticles with a very high loading of the Pt(IV) prodrug (Figure 19). The polymer backbone was modified with positively-charged lipophilic triphenylphosphonium groups that can target mitochondria. This construct was 17 times more potent towards neuroblastoma cells than cisplatin.

Instead of synthetic polymers, natural polymers such as silk fibroin can be used as carriers for Pt(IV) prodrugs [116]. The axial ligands in Pt(IV) complexes not only control the hydrophobicity of the complexes, but also possess biological activity when released. The Pt(IV) complex with, for example, axial valproate (VAAP, an antiepileptic drug) ligands has increased hydrophobicity, facilitates encapsulation inside polymeric nanoparticles, and at the same time it acts as a histone deacetylase inhibitor when released. This dual-thread complex potentiates the anticancer activity [117].

5.2.2. Covalent Functionalization with Pt(IV) Prodrugs

Zhang et al. have reported the covalent functionalization of a Pt(IV) prodrug containing axial levulinate ligands with hydrazine-terminated poly(ethylene glycol)-block-poly(L-lactic acid) (PLA-PEG) [118]. The delivery of the platinum complex from this conjugate can be tuned under acidic conditions due to the

acid lability of the hydrazone linkage. This conjugate was more active towards ovarian cancer cells than cisplatin. Commonly Pt(IV) complexes with succinate axial ligands are coupled with hydroxyl or ammine terminated polymer chains via amide or ester bond formation. mPEG-PLA-OH was conjugated with succinate ligands of *cis,cis,trans*-$[Pt(NH_3)_2Cl_2(OOCCH_2CH_2COOH)_2]$ which forms micelles in aqueous solution and undergoes thermo-reversible hydrogel formation at 37 °C [119]. This conjugate releases cisplatin in a controlled manner and is more active than cisplatin itself.

In another strategy, two different polymer chains have been covalently functionalized with two different anticancer drugs to make composite nanoparticles. Jing and coworkers conjugated daunorubicin with the pendant carboxyl group of biodegradable methoxyl-poly-(ethylene glycol)-block-poly(lactide-co-2-methyl-2-carboxyl-propylene carbonate) (P1). P1 was treated with ethanolamine to convert the carboxylic acid to a terminal alcohol (P2). Then this was conjugated with the axial carboxylate of the succinato derivative of oxidized dihydroxidooxaliplatin. These two polymers having similar polymer backbones co-assemble to micelles. This conjugate releases oxaliplatin in reducing environments and daunorubicin during hydrolysis [120]. It reduces the systemic toxicity and increases the efficacy due to synergetic effects when compared with the combination of these two drugs without polymer functionalization *in vitro* and *in vivo*. They further conjugated a cisplatin prodrug and paclitaxel to polymeric chains by using a similar strategy to make composite nanoparticles [121].

A Pt(IV) prodrug of cisplatin with axial dichloroacetate (DCA) and succinate ligands has been prepared. The succinate arm was used to conjugate with methoxyl-poly(ethylene glycol)-block-poly(ε-caprolactone)-block-poly(L-lysine) (MPEG-b-PCL-b-PLL) and the DCA ligand targets mitochondria. This multifunctional Pt(IV) hybrid is highly active against SKOV-3 human ovarian cancer cells when compared with its Pt(IV) precursors [122].

Photoactivatable Pt(IV) complexes containing *cis* azide ligands conjugated with polymers are stable in the dark, but after irradiation with UVA release cytotoxic Pt(II) species. A polymer nanoparticle conjugate with *cis,trans*-$[Pt(DACH)(N_3)_2(OH)(OOCCH_2CH_2CO_2H)]$ injected intratumorally in a xenograft model of murine hepatocarcinoma and irradiated with UVA for 1 h resulted in reduction in tumor growth [123].

In the aforementioned strategies, Pt(IV) prodrugs are buried inside polymer nanoparticles. Polymeric nanoparticles with free succinate arms on the surface conjugated with *cis,cis,trans*-$[Pt(NH_3)_2Cl_2(OH)_2]$ show an initial burst and then a slow sustained release of the platinum drug [124].

5.3. Carbon-Based Materials

Carbon nanotubes have been extensively studied as drug carriers. Lippard and coworkers attached SWCNTs to the Pt(IV) prodrug *cis,cis,trans*-$[Pt(NH_3)_2Cl_2(OEt)(OOCCH_2CH_2COOH)]$ [125]. The SWCNTs were functionalized with phospholipid-PEG-NH_2 through non-covalent interaction between SWCNTs and

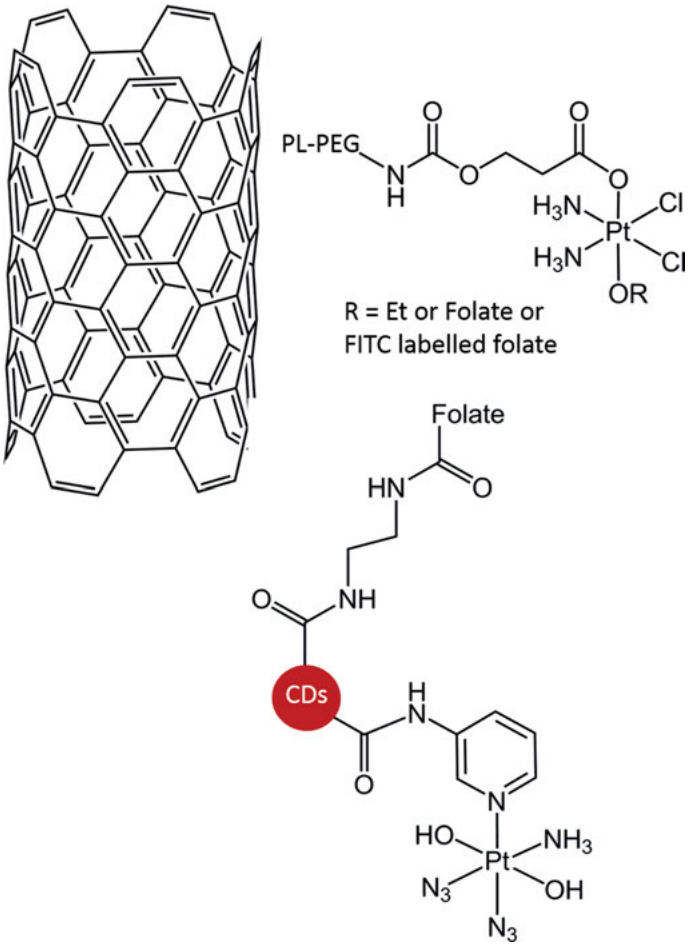

Figure 20. (**a**) Non-covalent attachment of SWCNT with the Pt(IV) prodrug, (**b**) folate and Pt(IV) prodrug functionalized carbon dots (CD).

phospholipid. A PEG spacer containing a free amine was covalently conjugated with the carboxylic acid group of the Pt(IV) prodrug. Co-tethered fluorescein-based fluorophores revealed that this conjugate was highly localized in the nucleus and cytosol when compared with the Pt(IV) prodrug and cisplatin. The conjugate exhibited potent toxicity against the testicular carcinoma cell line NTera-2. Incorporation of an axial folate derivative in the Pt(IV) prodrug *cis,cis,trans*-$[Pt(NH_3)_2Cl_2(OOCCH_2CH_2COOH)(OOCCH_2CH_2CONH\text{-}PEG\text{-}FA)]$ functionalized with SWCNT-PL-PEG-NH_2 provides specific targeting to cancer cells that overexpress folate receptors (FR+). Fluorescence microscopy imaging using a fluorescein isothiocyanate (FITC)-labelled folate derivative (Figure 20) on the surface of the SWCNTs showed high accumulation of this conjugate on FR(+) KB cells when compared with FR(–) NTera-2 cells [126].

In addition to surface functionalization, the internal cavity of nanotubes has been investigated for drug loading and delivery applications. MWCNTs have larger inner diameters than SWCNTs and are preferred for loading the hydrophobic cisplatin prodrug *cis,cis,trans*-$[Pt(NH_3)_2Cl_2(OOCC_6H_5)_2]$ by nanoextraction.

This construct releases Pt in the presence of a reducing agent. The activity is improved when the surface is functionalized with a rhodamine dye that targets mitochondria. *In vivo* studies in mice showed that this construct releases lower levels of platinum to the liver and kidney compared to cisplatin, but accumulation in the lungs increased [127]. A dual threat Pt(IV) complex was prepared by coupling the amine group of doxorubicin with *cis,cis,trans*-$[Pt(NH_3)_2Cl_2(OOCC_6H_5)(OOCCH_2CH_2COOH)]$. The conjugate is highly hydrophobic and readily encapsulated in MWCNTs. The surface of the nanotubes has been conjugated with integrin-targeting c(RGDfK) peptide to target cancer cells. During the reduction, this conjugate releases the two chemotherapeutic drugs doxorubicin and cisplatin simultaneously [128].

Carbon nanoparticles are attracting interest due to their striking photophysical properties and ease of preparation [129,130]. Liu and coworkers [131] have synthesized carboxylic acid functionalized carbon nanoparticles conjugated with *cis,trans,cis*-$[Pt(N_3)_2(OH)_2(NH_3)(3\text{-}NH_2py)]$ for targeting; folic acid was also conjugated to the nanoparticles via an ethylenediamine linker. Microscopy showed that functionalization does not change the shape of the particles. Irradiation of this construct resulted in formation of Pt(II) species, not only via excitation of the platinum center, but also via excitation of carbon nanoparticles through photo-induced electron transfer [131].

5.4. Supramolecular Motifs

Nanoscale coordination polymers (NCPs) have been prepared from Pt(IV) prodrugs containing two succinate pendant arms. The reaction of Tb(III) with *cis,cis,trans*-$[Pt(NH_3)_2Cl_2(OOCCH_2CH_2COOH)_2]$ results in a cross-linked coordination polymer which can be coated with silyl-derivatized c(RGDfK) to target cancer cells that overexpress integrin. Microscopy shows that this construct self-assembles into nanoparticles with cytotoxicity selective towards HT-29 colon cancer cells which overexpress $\alpha_v\beta_3$ integrin compared to MCF-7 breast cancer cells which do not [132]. Platinum(IV) prodrugs with pendant phosphonate ligands treated with Zn(II) ions also give rise to coordination polymers. PEGylation (phospholipids, cholesterol, and PEGylated phospholipids) avoids premature drug release before the NCPs reach the target by the EPR effect. Fluorescently-labelled analogues of this construct allow the internalization process to be studied by fluorescence microscopy. *In vitro* studies carried out with different inhibitors showed that cell internalization proceeds via endocytosis. Pharmacokinetic studies show a 40-fold increase in blood circulation time of this construct compared with parent drugs [133] (Figure 21).

Post-synthetic modification has also been used to design iron-carboxylate metal organic frameworks (MOF) for imaging and delivery of platinum complexes.

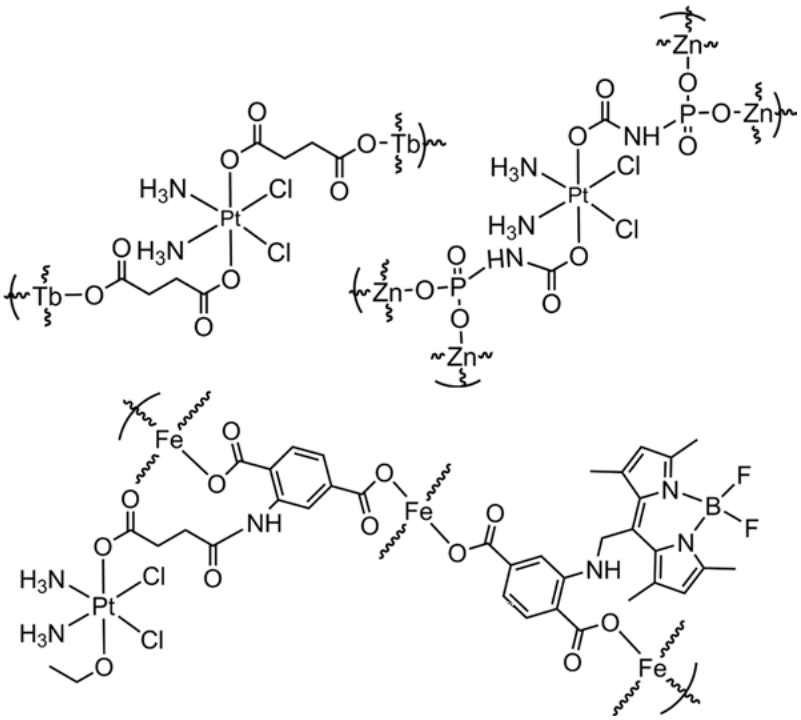

Figure 21. Axial functionalized Pt(IV) complexes for designing polymeric coordination frameworks.

2-Aminoterephthalic acid attached to BODIPY and the Pt(IV) prodrug *cis,cis,trans*-$[Pt(NH_3)_2Cl_2(OEt)(OOCCH_2CH_2COOH)]$ yields a MOF on treatment with an iron salt, which after coating with SiO_2, yields a core-shell nanostructure. The potency of this construct is slightly less than cisplatin towards HT-29 cells, but is increased on functionalization of the silica surface with c(RGDfK) [134].

Supramolecular cages have been investigated for the delivery of platinum anticancer drugs. Reaction of dichloro(ethylenediamine)Pt(II) with 2,4,6-tris(2-pyridyl)-s-triazine results in the formation of a supramolecular cage, in which Pt occupies the vertices of an octahedron and triazine ligands are present in four faces of the polyhedron. The remaining four faces can encapsulate *cis,cis,trans*-$[PtCl_2(NH_3)_2(OCONHC_{10}H_{15})(OOCCH_2CH_2COOH)]$ via the axial adamantyl unit. The free succinate arm is exposed to solvent, which increases water solubility and acts as a handle for further functionalization with bioactive molecules or targeting groups [135].

5.5. Upconversion Nanoparticles

Upconversion nanoparticles (UCNPs) are an interesting class of nanomaterials for converting low energy into high-energy photons. They are generally made

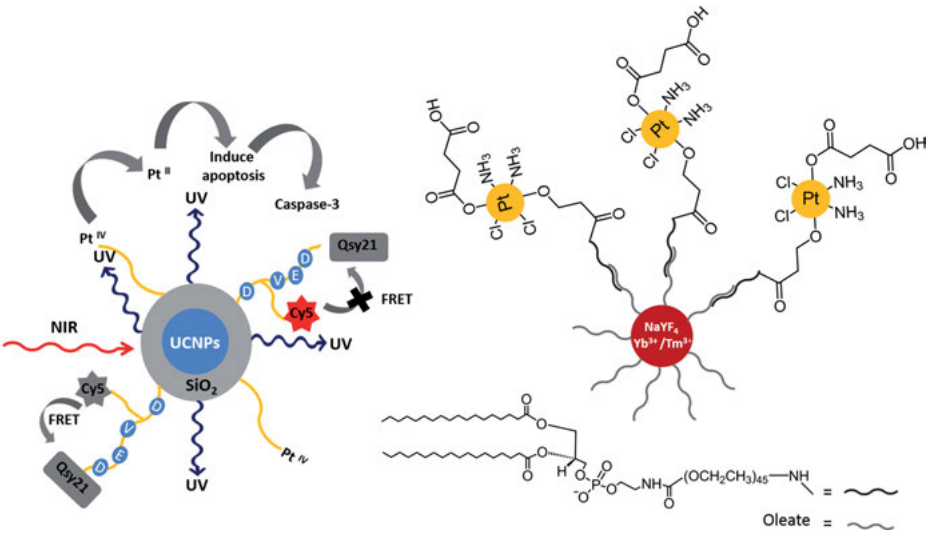

Figure 22. Pt(IV)-functionalized upconversion nanoparticles for applications in NIR-triggered drug delivery.

up of an inorganic host material such as YF_3 doped with Ln^{3+} ions. Several mechanisms have been proposed to explain the upconversion processes such as excited state absorbance (ESA), energy transfer upconversion (ETU), photon avalanche (PA), cooperative sensitization upconversion (CSU), and cross relaxation (CR) [136]. Upconversion nanoparticles have advantages such as easy surface functionalization, multi-color luminescence, low cytotoxicity, and an ability to convert deep-penetrating NIR radiation into high energy UV/Vis light for drug release with spatial and temporal control. UCNPs therefore have potential applications in light-activated drug delivery systems (PDT and PACT).

Min et al. [137] have reported the NIR-mediated delivery of antitumor platinum complexes from the surface of silica-coated UCNPs. They functionalized the surface of UCNPs@SiO_2 with a photoactivatable Pt(IV) prodrug and an apoptosis-sensing peptide. The synthesis was carried out by reacting amine-functionalized UCNPs@SiO_2 with *trans,trans,trans*-[$Pt(N_3)_2(OH)(OCOCH_2CH_2COONHS)(Py)_2$]. Prior to this, the surface of the UCNPs was modified with an oligo(ethyl glycol) ($dPEG_6$) linker containing a maleimide group which facilitates the reaction with a thiol group present in the sensing peptide. After irradiating the Pt(IV) prodrug-functionalized UCNPs with a 980 nm infrared laser the cytotoxic platinum(II) complex was released. The anticancer activity of the Pt(IV) probe UCNPs@SiO_2 was tested against cisplatin-sensitive A2780 and resistant A2780cis human ovarian cancer cells using the MTT assay. The Pt(IV) probe UCNPs@SiO_2 is not cytotoxic but becomes cytotoxic after irradiation, which increases with increasing light exposure time. Pt(IV) probe UCNPs@SiO_2 nanoparticles are significantly active against cisplatin-resistant A2780 cell lines. The sensing peptide probe, Cy5-acp-CGDEV-

DAK-Qsy21 on the surface of Pt-UCNPs@SiO_2 showed weak fluorescence because of FRET, but after irradiation, Pt(IV) species are reduced to cytotoxic Pt(II) species which induce apoptosis, further activate caspase-3 and disrupt the FRET process by moving the Qsy21 non-fluorescent diarylrhodamine quencher chromophore away from Cy5 leading to significant fluorescence emission from Cy5. This system has potential as a real-time tumor marker to evaluate the anticancer activity at the cellular level [137].

In an another example, Ruggiero et al. reported the synthesis and photoactivation of Pt(IV)-conjugated Tm-doped UCNPs [138]. They coupled *cis,cis,trans*-$[Pt(NH_3)_2(Cl)_2(O_2CCH_2CH_2CO_2H)_2]$ to the surface of $NaYF_4$:Yb^{3+}/Tm^{3+} nanocrystals. To improve the biocompatibility, it was further functionalized with PEGylated phospholipid DSPE-PEG(2000). They followed the photoactivation of Pt(IV) functionalized $NaYF_4$:Yb^{3+}/Tm^{3+} particles by ^1H NMR spectroscopy, and subsequent photo-reduction of Pt(IV) to Pt(II) was monitored by XPS (X-ray photoelectron spectroscopy).

Perfahl et al. have reported the synthesis and photoactivation of diiodido-Pt(IV) complexes coupled to UCNPs [139]. They used two strategies to attach diiodido-Pt(IV) complexes to UCNPs (Yb, Er- and Yb,Tm-doped β-$NaGdF_4$). The first involved covalent conjugation of succinate appended diiodido-Pt(IV) complexes to amine-functionalized UCNPs. The second involved the exchange of oleate by the carboxylate of diiodido-Pt(IV) carboxylato complexes. When 980 nm NIR laser radiation of was used to activate the diiodido-Pt(IV) complexes, the stability of the complexes was little affected. In contrast, irradiation of diiodido-Pt(IV) complexes attached to UCNPs with 980 nm laser irradiation resulted in the loss of the ligand-to-metal charge-transfer band and release of Pt(II) complexes which then bind strongly to calf-thymus DNA (ct-DNA). The release of platinum was faster in the case of covalently conjugated UCNPs compared with carboxylate-attached UCNPs. After irradiation with NIR, the UCNPs-Pt conjugates and constructs showed significant toxicity towards human leukemia HL60 cells.

6. CONCLUDING REMARKS

This chapter summarizes recent studies on the synthesis, characterization, redox properties and biological activity of Pt(IV) prodrugs. The ease of synthesis by oxidative addition to Pt(II) precursors and incorporation of functional groups, targeting groups, and bioactive ligands into one or both axial positions, gives rise to many families of complexes both as small molecules, polymers and larger nanoparticles, with a wealth of potential applications. In particular the use of relatively inert Pt(IV) prodrugs which are activated near target sites either by chemical reduction, by light, or heat, might avoid systemic toxicity and unwanted side effects commonly seen for Pt(II) drugs. Some Pt(IV) pro-drugs have been on clinical trials, but, so far, have not been demonstrated to have advantages over Pt(II) drugs. However, we can expect more Pt(IV) produgs to enter clinical trials in the future.

This field is stimulating fundamental studies on the mechanisms of ligand substitution and reduction of Pt(IV) complexes, both chemical and photophysical. The challenge of understanding the activation and targeting of Pt(IV) prodrugs in biological cells in the complicated network of dynamic intracellular pathways and feedback loops, which often operate far from thermodynamic equilibrium, is a major one for the future.

ACKNOWLEDGMENTS

We thank the Royal Society (Newton International Fellowship for VV), ERC (grant no 247450), MRC (grant no. G0701062) and EPSRC (grant no. EP/G006792) for their support for our work in this area and members of COST Action CM1105 for stimulating discussions.

ABBREVIATIONS

AuNP	gold nanoparticles
BODIPY	4,4-difluoro-4-bora-3a,4a-diaza-s-indacene
bpy	2,2′-bipyridine
cha	cyclohexylamine
CSU	cooperative sensitization upconversion
Cy5	cyanine 5
DMF	dimethylformamide
DMSO	dimethylsulfoxide
EDC	1-ethyl-3-(3-dimethylaminopropyl)carbodiimide
en	ethylenediamine = ethane-1,2-diamine
EPR	enhanced permeability and retention effect
FA	folic acid
FDA	US Food and Drug Administration
FITC	fluoroscein isothiocyanate
FR	folate receptor
FRET	Förster resonance energy transfer
FTIR	Fourier transform-infrared
GSH	glutathione
5′-GMP	guanosine 5′-monophosphate
GNR	gold nanorod
HSA	human serum albumin
IC_{50}	half maximal inhibitory concentration
LMCT	ligand-to-metal charge-transfer
MA	methylamine
MRI	magnetic resonance imaging
MTT	3-(4,5-dimethylthiazol-2-yl)-2,5-diphenyltetrazolium bromide
MW	molecular weight

MWCNT	multiwall carbon nanotubes
NADH	nicotinamide adenine dinucleotide reduced
NCP	nanoscale coordination polymer
NIR	near infrared
NMR	nuclear magnetic resonance
PA	photon avalanche
PACT	photoactivatable chemotherapy
PDT	photodynamic therapy
PEG	poly(ethylene glycol)
PL	polylysine
PLA	poly(L-lactic acid)
PLGA	poly(lactic-co-glycolic acid)
PSMA	prostate-specific membrane antigen
py	pyridine
QD	quantum dot
rt	room temperature
SWCNT	single-walled carbon nanotubes
TDDFT	time-dependent density functional theory
TEMPO	2,2,6,6-tetramethylpiperidine 1-oxyl
UCNP	upconversion nanoparticle

REFERENCES

1. B. Rosenberg, L. VanCamp, J. E. Trosko, V. H. Mansour, *Nature* **1969**, *222*, 385–386.
2. N. J. Wheate, S. Walker, G. E. Craig, R. Oun, *Dalton Trans.* **2010**, *39*, 8113–8127.
3. R. Safaei, K. Katano, G. Samimi, W. Naerdemann, J. L. Stevenson, M. Rochdi, S. B. Howell, *Cancer Chemother. Pharmacol*., **2004**, *53*, 239–246.
4. D. P. Gately, S. B. Howell, *Br. J. Cancer* **1993**, *67*, 1171–1176.
5. R. C. Todd, S. J. Lippard, *Metallomics* **2009**, *1*, 280–291.
6. T. Zimmermann, M. Zeizinger, J. V. Burda, *J. Inorg. Biochem.* **2005**, *99*, 2184–2196.
7. E. Wexselblatt, D. Gibson*, J. Inorg. Biochem*. **2012**, *117*, 220–229.
8. D. Gibson, *Dalton Trans.* **2016**, *45*, 12983–12991.
9. *Platinum Met. Rev.* **1999**, *43*(2), 61.
10. S. G. Awuah, Y. R. Zheng, P. M. Bruno, M. T. Hemann, S. J. Lippard, *J. Am. Chem. Soc.* **2015**, *137*, 14854–14857.
11. J. Kasparkova, H. Kostrhunova, O. Novakova, R. Krikavova, J. Vanco, Z. Travnicek, V. Brabec, *Angew. Chem. Int. Ed*. **2015**, *54*, 14478 –14482.
12. A. Gandioso, E. Shaili, A. Massaguer, G. Artigas, A. Gonzalez-Canto, J. A. Woods, P. J. Sadler, V. Marchan, *Chem. Commun*., **2015**, *51*, 9169–9172.
13. B. Spingler, D. A. Whittington, S. J. Lippard, *Inorg. Chem*. **2001**, *40*, 5596–5602.
14. A. P. Silverman, W. Bu, S. M. Cohen, S. J. Lippard, *J. Biol. Chem*. **2002**, *277*, 49743–49749.
15. K. S. Lovejoy, R. C. Todd, S. Zhang, M. S. McCormick, J. A. D'Aquino, J. T. Reardon, A. Sancar, K. M. Giacomini, S. J. Lippard, *Proc. Natl. Acad. Sci. USA* **2008**, *105*, 8902–8907.
16. S. Dhara , F. X. Gu, R. Langer, O. C. Farokhzad, S. J. Lippard, *Proc. Natl. Acad. Sci. USA* **2008**, *105*, 17356–17361.

17. T. S. Chung, Y. M. Na, S. W. Kang, O.-S. Jung, Y.-A. Lee, *Transition Met. Chem*. **2005**, *30*, 541–545.
18. G. B. Kauffman, G. Slusarczuk, S. Kirschner, *Inorg. Synth*. **1963**, *7*, 236–238.
19. S. O. Dunham, R. D. Larsen, E. H. Abbott, *Inorg. Chem*. **1993**, *32*, 2049–2055.
20. Y.-A. Lee, O.-S. Jung, *Bull. Chem. Soc. Jpn*. **2002**, *75*, 1533–1537.
21. T. C. Johnstone, J. J. Wilson, S. J. Lippard*, Inorg. Chem*. **2013**, *52*, 12234–12249.
22. J. J. Wilson, S. J. Lippard, *Inorg. Chim. Acta* **2012**, *389*, 77–84.
23. J. J. Wilson, S. J. Lippard, *Polyhedron* **2013**, *58*, 71–78.
24. J. J. Wilson, S. J. Lippard, *Chem. Rev*. **2014**, *114*, 4470–4495.
25. S. J. Berners-Price, L. Ronconi, P. J. Sadler, *Prog. Nucl. Magn. Reson. Spectrosc*. **2006**, *49*, 65–98.
26. R. R. Vernooij, T. Joshi, E. Shaili, M. Kubeil, D. R. T. Appadoo, E. I. Izgorodina, B. Graham, P. J. Sadler, B. R. Wood, L. Spiccia, *Inorg. Chem*. **2016**, *55*, 5983–5992.
27. F. S. Mackay, J. A. Woods, P. Heringova, J. Kasparkova, A. M. Pizarro, S. A. Moggach, S. Parsons, V. Brabec, P. J. Sadler, *Proc. Natl. Acad. Sci. USA*, **2007**, *104*, 20743–20748.
28. C. Shen, B. D. W. Harris, L. J. Dawson, K. A. Charles, T. W. Hambley, E. J. New, *Chem. Commun*. **2015**, *51*, 6312–6314.
29. D. Montagner, S. Q.Yap, W. H. Ang, *Angew. Chem. Int. Ed.* **2013**, *52*, 11785 –11789.
30. S. Choi, C. Filotto, M. Bisanzo, S. Delaney, D. Lagasee, J. L. Whitworth, A. Jusko, C. Li, N. A. Wood, J. Willingham, A. Schwenker, K. Spaulding, *Inorg. Chem*. **1998**, *37*, 2500–2504.
31. N. A. Kratochwil, Z. Guo, P. del. S. Murdoch, J. A. Parkinson, P. J. Bednarski, P. J. Sadler, *J. Am. Chem. Soc*. **1998**, *120*, 8253–8254.
32. A. Nemirovski, Y. Kasherman, Y. Tzaraf, D. Gibson, *J. Med. Chem*. **2007**, *50*, 5554–5556.
33. A. Nemirovski, I. Vinograd, K. Takrouri, A. Mijovilovich, A. Rompel, D. Gibson, *Chem. Commun*. **2010**, *46*, 1842–1844.
34. T. J. O'Rourke, G. R. Weiss, P. New, H. A. Burris, G. Rodriguez, J. Eckhardt, J. Hardy, J. G. Kuhn, S. Fields, G. M. Clark, D. D. Von Hoff, *Anticancer Drugs* **1994***, 5,* 520–526.
35. L. R. Kelland, B. A. Murrer, G. Abel, C. M. Giandomenico, P. Mistry, K. R. Harrap, *Cancer Res.* **1992**, *52*, 822–828.
36. M. D. Hall, C. Martin, D. J. P. Ferguson, R. M. Phillips, T. W. Hambley, R. Callaghan, *Biochem. Pharmacol*. **2004**, *67*, 17–30.
37. H. R. Mellor, S. Snelling, M. D. Hall, S. Modok, M. Jaffar, T. W. Hambley, R. Callaghan, *Biochem. Pharmacol.* **2005**, *70*, 1137–1146.
38. X. Lin, T. Okuda, A. Holzer, S. B. Howell, *Mol. Pharmacol*. **2002**, *62*, 1154–1159.
39. M. Komatsu, T. Sumizawa, M. Mutoh, Z. S. Chen, K. Terada, T. Furukawa, X. L. Yang, H. Gao, N. Miura, T. Sugiyama, S. Akiyama*, Cancer Res.* **2000**, *60*, 1312–1316.
40. C. P. Saris, P. J. van de Vaart, R. C. Rietbroek, F. A. Blommaert, *Carcinogenesis* **1996**, *17*, 2763–2769.
41. F. I. Raynaud, P. Mistry, A. Donaghue, G. K. Poon, L. R. Kelland, C. F. Barnard, B. A. Murrer, K. R. Harrap, *Cancer Chemother. Pharmacol*. **1996**, *38*, 155–162.
42. T. Yotsuyanagi, N. Ohta, T. Futo, S. Ito, D. Chen, K. Ikeda, *Chem. Pharm. Bull*. **1991**, *39*, 3003–3006.
43. A. I. Ivanov, J. Christodoulou, J. A. Parkinson, K. J. Barnham, A. Tucker, J. Woodrow, P. J. Sadler, *J. Biol. Chem*. **1998**, *273*, 14721–14730.
44. N. A. Kratochwil, A. I. Ivanov, M. Patriarca, J. A. Parkinson, A. M. Gouldsworthy, P. D. S. Murdoch, P. J. Sadler*, J. Am. Chem. Soc*. **1999**, *121*, 8193–8203.

45. V. Pichler, J. Mayr, P. Heffeter, O. Dömötör, É. A. Enyedy, G. Hermann, D. Groza, G. Köllensperger, M. Galanksi, W. Berger, B. K. Keppler, C. R. Kowol, *Chem. Commun*. **2013**, *49*, 2249–2251.
46. D. F Baban, L. W. Seymour, *Adv. Drug Delivery Rev.* **1998**, *34*,109–119.
47. E. Frei, *Diabetol. Metab. Syndr.* **2011**, *3*, DOI: 10.1186/1758–5996–3-11
48. Y. R. Zheng, K. Suntharalingam, T. C. Johnstone, H. Yoo, W. Lin, J. G. Brooks, S. J. Lippard, *J. Am. Chem. Soc.* **2014**, *136*, 8790–8798.
49. H. Shi, Q.Cheng, S. Yuan, X. Ding, Y. Liu, *Chem. Eur. J.* **2015**, *21*, 16547–16554.
50. B. Chiavarino, M. E. Crestoni, S. Fornarini, D. Scuderi, J.-Y. Salpin, *J. Am. Chem. Soc.* **2013**, *135*, 1445–1455.
51. S. E. Sherman, S. J. Lippard, *Chem. Rev.* **1987**, *87*, 1153–1181.
52. A. M. J. Fichtinger-Schepman, J. L. van der Veer, J. H. J. den Hartog, P. H. M. Lohman, J. Reedijk, *Biochemistry* **1985**, *24*, 707–713.
53. M. S. Ali, E. Longoria Jr., T. O. Ely, K. H. Whitmire, A. R. Khokhar, *Polyhedron* **2006**, *25*, 2065–2071.
54. S. Mong, D. C. Eubanks, A. W. Prestayko, S. T. Crooke, *Biochemistry* **1982**, *21*, 3174–3179.
55. J. F. Vollano, E. E. Blatter, J. C. Dabrowiak, *J. Am. Chem. Soc.* **1984**,*106*, 2732–2733.
56. O. Vrana, V. Brabec, V. Kleinwachter, *Anti-Cancer Drug Des.* **1986**, *1*, 95–109.
57. V. Brabec, O. Vrana, V. Kleinwachter, *Stud. Biophys.***1986**, *114*, 199–207.
58. E. E. Blatter, J. F. Vollano, B. S. Krishnan, J. C. Dabrowiak, *Biochemistry* **1984**, *23*, 4817–4820.
59. W. K. Wilmarth, Y. -T. Fanchiang, J. E. Byrd, *Coord. Chem. Rev.* **1983**, *51*, 141–153.
60. Y. Kido, A. R. Khokhar, Z. H. Siddik, *Biochem Pharmacol*. **1994**, *47*, 1635–1642.
61. K. Chvalova, V. Brabec, J. Kasparkova, *Nucleic Acids Res.* **2007**, *35*, 1812–1821.
62. L. Pendyala, P. J. Creaven, R. Perez, J. R. Zdanowicz, D. Raghavan, *Cancer Chemother. Pharmacol*. **1995**, *36*, 271–278.
63. F. I. Raynaud, D. E. Odell, L. R. Kelland, *Br. J. Cancer* **1996**, *74*, 380–386.
64. K. Lemma, T. Shi, L. I. Elding, *Inorg. Chem*. **2000**, *39*, 1728–1734.
65. T. Shi, J. Berglund, L. I. Elding, *J. Chem. Soc. Dalton Trans.* **1997**, 2073–2078.
66. L. Chen, P. F. Lee, J. D. Ranford, J. J. Vittal, S. Y. Wong, *J. Chem. Soc. Dalton Trans.* **1999**, 1209–1212.
67. K. Lemma, A. M. Sargeson, L. I. Elding, *J. Chem. Soc. Dalton* **2000**, 1167–1172.
68. S. Mukhopadhyay, C. M. Barnés, A. Haskel, S. M. Short, K. R. Barnes, S. J. Lippard, *Bioconjugate Chem.* **2008**, *19*, 39–49.
69. A. Massaguer, A. Gonzalez-Canto, E. Escribano, S. Barrabes, G. Artigas, V. Moreno, V. Marchan, *Dalton Trans.* **2015**, *44*, 202–212.
70. A. Gandioso, E. Shaili, A. Massaguer, G. Artigas, A. Gonzalez-Canto, J. A. Woods, P. J. Sadler, V. Marchan, *Chem. Commun*., **2015**, *51*, 9169–9172.
71. M. Patra, S. G. Awuah, S. J. Lippard, *J. Am. Chem. Soc.* **2016**, *138*, 12541–12551.
72. M. Patra, T. C. Johnstone, K. Suntharalingam, S. J. Lippard, *Angew. Chem., Int. Ed*. **2016**, 55, 2550–2554.
73. J. Ma, Q. Wang, X. Yang, W. Hao, Z. Huang, J. Zhang, X. Wang, P. G. Wang, *Dalton Trans.* **2016**, *45*, 11830–11838.
74. L. R. Kelland, B. A. Murrer, G. Abel, C. M. Giandomenico, P. Mistry, K. R. Harrap, *Cancer Res.* **1992**, *52*, 822–828.
75. D. Tolan, V. Gandin, L. Morrison, A. El-Nahas, C. Marzano, D. Montagner, A. Erxleben, *Sci. Rep.* **2016,** *11*, 6:29367.
76. W. Neumann, B. C. Crews, L. J. Marnett, E. Hey-Hawkins, *ChemMedChem* **2015**, *9*, 1150–1153.
77. W. Neumann, B. C. Crews, M. B. Sarosi, C. M. Daniel, K. Ghebreselasie, M. S. Scholz, L. J. Marnett, E. Hey-Hawkins, *ChemMedChem* **2015**, *10*, 183–192.

78. W. H. Ang, I. Khalaila, C. S. Allardyce, L. Juillerat-Jeanneret, P. J. Dyson, *J. Am. Chem. Soc.* **2005**, *127*, 1382–1383.
79. W. H. Ang, S. Pilet, R. Scopelliti, F. Bussy, L. Juillerat-Jeanneret, P. J. Dyson, *J. Med. Chem.* **2005**, *48*, 8060–8069.
80. S. Dhar, S. J. Lippard, *Proc. Natl. Acad. Sci. USA* **2009**, *106*, 22199–22204.
81. K. R. Barnes, A. Kutikov, S. J. Lippard, *Chem. Biol*. **2004**, *11*, 557–564.
82. J. Yang, X. Sun, W. Mao, M. Sui, J. Tang, Y. Shen, *Mol. Pharmaceutics* **2012**, *9*, 2793–2800.
83. M. Alessio, I. Zanellato, I. Bonarrigo, E. Gabano, M. Ravera, D. Osella, *J. Inorg. Biochem*. **2013**, *129*, 52–57.
84. E. J. New, R. Duan, J. Z. Zhang, T. W. Hambley, *Dalton Trans.* **2009**, 3092–3101.
85. Y. Yuan, Y. Chen, B. Z. Tang, B. Liu, *Chem. Commun*. **2014**, *50*, 3868–3870.
86. N. A. Kratochwil, P. J. Bednarski, H. Mrozek, A. Vogler, J. K. Nagle, *Anti-Cancer Drug Des.* **1996**, *11*, 155–171.
87. N. A. Kratochwil, M. Zabel, K.-J. Range, P. J. Bednarski, *J. Med. Chem*. **1996**, *39*, 2499–2507.
88. N. A. Kratochwil, Z. Guo, P. S. Murdoch, J. A. Parkinson, P. J. Bednarski, P. J. Sadler, *J. Am. Chem. Soc*. **1998**, *120*, 8253–8254.
89. N. A. Kratochwil, P. J. Bednarski, *Arch. Pharm. Pharm. Med. Chem.* **1999**, *332*, 279–285.
90. A. Vogler, A. Kern, J. Huttermann, *Angew. Chem. Int. Ed*. **1978**, *17*, 524–525.
91. P. Müller, B. Schröder, J. A. Parkinson, N. A. Kratochwil, R. A. Coxall, A. Parkin, S. Parsons, P. J. Sadler, *Angew. Chem. Int. Ed*. **2003**, *42*, 335–339.
92. N. J. Farrer, P. Gierth, P. J. Sadler, *Chem. Eur. J.* **2011**, *17*, 12059–12066.
93. K. Sutter, J. Autschbach, *J. Am. Chem. Soc.* **2012**, *134*, 13374–13385.
94. L. Ronconi, A. M. Pizarro, R. J. McQuitty, P. J. Sadler, *Chem. Eur. J.* **2011**, *17*, 12051 – 12058.
95. J. Kasparkova, F. S. Mackay, V. Brabec, P. J. Sadler, *J. Biol. Inorg. Chem.* **2003**, *8*, 741–745.
96. P. J. Bednarski, R. Grunert, M. Zielzki, A. Wellner, F. S. Mackay, P. J. Sadler, *Chemistry & Biology* **2006**, *13*, 61–67.
97. F. S. Mackay, J. A. Woods, H. Moseley, J. Ferguson, A. Dawson, S. Parsons, P. J. Sadler, *Chem. Eur. J.* **2006**, *12*, 3155–3161.
98. Y. Zhao, J. A. Woods, N. J. Farrer, K. S. Robinson, J. Pracharova, J. Kasparkova, O. Novakova, H. Li, L. Salassa, A. M. Pizarro, G. J. Clarkson, L. Song, V. Brabec, P. J. Sadler, *Chem. Eur. J.* **2013**, *19*, 9578 – 9591.
99. H.-C. Tai, Y. Zhao, N. J. Farrer, A. E. Anastasi, G. Clarkson, P. J. Sadler, R. J. Deeth, *Chem. Eur. J.* **2012**, *18*, 10630 – 10642.
100. A. F. Westendorf, J. A. Woods, K. Korpis, N. J. Farrer, L. Salassa, K. Robinson, V. Appleyard, K. Murray, R. Grunert, A. M. Thompson, P. J. Sadler, P. J. Bednarski, *Mol. Cancer Ther.* **2012**, *11*, 1894–1904.
101. A. F. Westendorf, A. Bodtke, P. J. Bednarski, *Dalton Trans.* **2011**, *40*, 5342–5351.
102. Y. Zhao, N. J. Farrer, H. Li, J. S. Butler, R. J. McQuitty, A. Habtemariam, F. Wang, P. J. Sadler, *Angew. Chem. Int. Ed*. **2013**, *52*, 13633 –13637.
103. J. S. Butler, J. A. Woods, N. J. Farrer, M. E. Newton, P. J. Sadler, *J. Am. Chem. Soc.* **2012**, *134*, 16508–16511.
104. E. Shaili, M. F. Giménez, S. R Astor, A. Gandioso, L. Sandín, C. G. Vélez, A. Massaguer, G. J. Clarkson, J. A Woods, P. J Sadler, V. Marchán, *Chem. Eur. J.* **2015**, *21*, 18474 –18486.
105. V. Venkatesh, C. J. Wedge, I. R. Canelón, A. Habtemariama, P. J. Sadler, *Dalton Trans.* **2016**, *45*, 13034–13037.

106. S. Dhar, W. L. Daniel, D. A. Giljohann, C. A. Mirkin, S. J. Lippard, *J. Am. Chem. Soc*. **2009**, *131*, 14652–14653.
107. Y. Shi, J. Goodisman, J. C. Dabrowiak, *Inorg. Chem*. **2013**, *52*, 9418–9426.
108. Y. Min, C. Mao, D. Xu, J. Wang, Y. Liu, *Chem. Commun*. **2010**, *46*, 8424–8426.
109. N. G. Blanco, C. R. Maldonado, J. C. Mareque-Rivas, *Chem. Commun*. **2009**, 5257–5259.
110. C. R. Maldonado, N. Gomez-Blanco, M. Jauregui-Osoro, V. G. Brunton, L. Yate, J. C. Mareque-Rivas, *Chem. Commun*. **2013**, *49*, 3985–3987.
111. Z. Cheng, Y. Dai, X. Kang, C. Li, S. Huang, H. Lian, Z. Hou, P. Ma, J. Lin, *Biomaterials* **2014**, *35*, 6359–6368.
112. R. E. Reiter, Z. Gu, T. Watabe, G. Thomas, K. Szigeti, E. Davis, M. Wahl, S. Nisitani, J. Yamashiro, M. M. Le Beau, M. Loda, O. N. Witte, *Proc. Natl. Acad. Sci. USA* **1998**, *95*, 1735–1740.
113. S. Dhar, N. Kolishetti, S. J. Lippard, O. C. Farokhzad, *Proc. Natl. Acad. Sci. USA* **2011**, *108*, 1850–1855.
114. S. Marrache, R. K. Pathak, S. Dhar, *Proc. Natl. Acad. Sci. USA* **2014**, *111*, 10444–10449.
115. T. C. Johnstone, K. Suntharalingam, S. J. Lippard, *Chem. Rev*. **2016**, *116*, 3436–3486.
116. A. A. Lozano-Perez, A. L. Gil, S. A. Perez, N. Cutillas, H. Meyer, M. Pedreño, S. D. Aznar-Cervantes, C. Janiak, J. L. Cenis, J. Ruiz, *Dalton Trans*. **2015**, *44*, 13513–13521.
117. C.-T. Lin, H.-C. Lai, H.-Y. Lee, W.-H. Lin, C.-C. Chang, T.-Y. Chu, Y.-W. Lin, K.-D. Lee, M.-H. Yu, *Cancer Sci*. **2008**, *99*, 1218–1226.
118. S. Aryal, C.-M. J. Hu, L. Zhang, *ACS Nano* **2010**, *4*, 251–258.
119. W. Shen, J. Luan, L. Cao, J. Sun, L. Yu, J. Ding, *Biomacromolecules* **2015**, *16*, 105–115.
120. H. Xiao, W. Li, R. Qi, L. Yan, R. Wang, S. Liu, Y. Zheng, Z. Xie, Y. Huang, X. Jing, *J. Controlled Release* **2012**, *163*, 304–314.
121. H. Xiao, H. Song, Q. Yang, H. Cai, R. Qi, L. Yan, S. Liu, Y. Zheng, Y. Huang, T. Liu, X. Jing, *Biomaterials* **2012**, *33*, 6507–6519.
122. H. Xiao, L. Yan, Y. Zhang, R. Qi, W. Li, R. Wang, S. Liu, Y. Huang, Y. Li, X. Jing, *Chem. Commun*. **2012**, *48*, 10730–10732.
123. R. Du, H. Xiao, G. Guo, B. Jiang, X. Yan, W. Li, X. Yang, Y. Zhang, Y. Li, X. Jing, *Colloids Surf. B* **2014**, *123*, 734–741.
124. Y. Mi, J. Zhao, S.-S. Feng, *Int. J. Pharm*. **2012**, *438*, 98–106.
125. R. P. Feazell, N. Nakayama-Ratchford, H. Dai, S. J. Lippard, *J. Am. Chem. Soc*. **2007**, *129*, 8438–8439.
126. S. Dhar, Z. Liu, J. Thomale, H. Dai, S. J. Lippard, *J. Am. Chem. Soc*. **2008**, *130*, 11467–11476.
127. J. Li, S. Q. Yap, C. F. Chin, Q. Tian, S. L. Yoong, G. Pastorin, W. H. Ang, *Chem. Sci.* **2012**, *3*, 2083–2087.
128. C. F. Chin, S. Q. Yap, J. Li, G. Pastorin, W. H. Ang, *Chem. Sci*. **2014**, *5*, 2265–2270.
129. S. Sahu, B. Behera, T. K. Maiti, S. Mohapatra, *Chem. Commun*. **2012**, *48*, 8835–8837.
130. H. Liu, T. Ye, C. Mao, *Angew. Chem. Int. Ed*. **2007**, *46*, 6473–6475.
131. X.-D. Yang, H.-J. Xiang, L. An, S.-P. Yang, J.-G. Liu, *New J. Chem*. **2015**, *39*, 800–804.
132. W. J. Rieter, K. M. Pott, K. M. L. Taylor, W. Lin, *J. Am. Chem. Soc*. **2008**, *130*, 11584–11585.
133. D. Liu, C. Poon, K. Lu, C. He, W. Lin, *Nat. Commun*. **2014**, *5*, 4182.
134. K. M. L. Taylor-Pashow, J. Della Rocca, Z. Xie, S. Tran, W. Lin, *J. Am. Chem. Soc*. **2009**, *131*, 14261–14263.
135. Y.-R. Zheng, K. Suntharalingam, T. C. Johnstone, S. J. Lippard, *Chem. Sci*. **2015**, *6*, 1189–1193.

136. J. Chen, J. X. Zhao, *Sensors* **2012**, *12*, 2414–2435.
137. Y. Min, J. Li, F. Liu, E. K. L. Yeow, B. Xing, *Angew. Chem. Int. Ed*. **2013**, *53*, 1012–1016.
138. E. Ruggiero, J. Hernandez-Gil, J. C. Mareque-Rivasab, L. Salassa, *Chem. Commun*. **2015**, *51*, 2091–2094.
139. S. Perfahl, M. M. Natile, H. S. Mohamad, C. A. Helm, C. Schulzke, G. Natile, P. J. Bednarski, *Mol. Pharm.* **2016**, *13*, 2346–2362.

4

Metalloglycomics

Nicholas P. Farrell, [1,2] ***Anil K. Gorle,*** [2]
Erica J. Peterson, [1] ***and Susan J. Berners-Price*** [2]

[1]Department of Chemistry, Virginia Commonwealth University,
Richmond, VA 23284–2006, USA
<npfarrell@vcu.edu>

[2]Institute for Glycomics, Griffith University, Gold Coast Campus,
Southport, Queensland 4222, Australia
<s.berners-price@griffith.edu.au>

ABSTRACT 110
1. INTRODUCTION. METALLOGLYCOMICS, HEPARIN, AND HEPARAN SULFATE 110
2. STRUCTURE AND CONFORMATION OF HEPARIN AND HEPARAN SULFATE 112
   2.1. Heparin and Heparan Sulfate Binding to Proteins 114
   2.2. Heparin and Heparan Sulfate as Enzyme Substrates 118
3. INTERACTION OF METAL IONS WITH GLYCOSAMINOGLYCANS 118
4. INTERACTION OF COORDINATION COMPOUNDS WITH GLYCOSAMINOGLYCANS 121
   4.1. Platinum Anticancer Agents. Covalent Bond Formation 122
   4.2. Platinum Anticancer Agents. Non-Covalent Interactions and Sulfate Cluster Binding 125
      4.2.1. Non-Covalent Heparan Sulfate Interactions. Sulfate Cluster Binding and Metalloshielding 126
5. CONSEQUENCES OF HIGH-AFFINITY HEPARAN SULFATE BINDING 128
   5.1. Sulfate Group Protection 128
   5.2. Heparan Sulfate as Receptor for Cellular Accumulation of Polynuclear Platinum 129

Metal Ions in Life Sciences, Volume 18 Edited by Astrid Sigel, Helmut Sigel, Eva Freisinger, and Roland K. O. Sigel

https://doi.org/10.1515/9783110470734-004

5.3. Inhibition of Function of Heparan Sulfate 130
5.3.1. Heparanase Cleavage Inhibition 131
5.3.2. Growth Factor Binding Inhibition 131
6. USE OF METAL COMPLEXES IN HEPARIN ANALYSIS 134
7. CONCLUSIONS AND OUTLOOK 135
ACKNOWLEDGMENTS 135
ABBREVIATIONS AND DEFINITIONS 135
REFERENCES 136

Abstract: Glycosaminoglycans (GAGs) such as heparin and heparan sulfate (HS) are large complex carbohydrate molecules that bind to a wide variety of proteins and exercise important physiological and pathological processes. This chapter focuses on the concept of metalloglycomics and reviews the structure and conformation of GAGs and the role of various metal ions during the interaction of GAGs with their biological partners such as proteins and enzymes. The use of metal complexes in heparin analysis is discussed. Cleavage of heparan sulfate proteoglycans (HSPGs) by the enzyme heparanase modulates tumor-related events including angiogenesis, cell invasion, metastasis, and inflammation. HS is identified as a ligand receptor for polynuclear platinum complexes (PPCs) defining a new mechanism of cellular accumulation for platinum drugs with implications for tumor selectivity. The covalent and noncovalent interaction of PPCs with GAGs and the functional consequences of strong binding with HS are explained in detail. Sulfate cluster anchoring shields the sulfates from recognition by charged protein residues preventing the exercise of the HS-enzyme/protein function, such as growth factor recognition and the activity of heparanase on HS. The cellular consequences are inhibition of invasion and angiogenesis. Metalloglycomics is a potentially rich new area of endeavor for bioinorganic chemists to study the relevance of intrinsic metal ions in heparin/HS-protein interactions and for development of new compounds for therapeutic, analytical, and imaging applications.

Keywords: heparan sulfate · heparin · proteoglycans · metal ions · platinum anticancer drugs

1. INTRODUCTION. METALLOGLYCOMICS, HEPARIN, AND HEPARAN SULFATE

This chapter introduces the concept of metalloglycomics – the study of the interaction of metal ions and coordination compounds with biologically relevant oligosaccharides and, in particular, glycosaminoglycans and proteoglycans. Glycomics itself is a very broad scientific discipline elucidating the diverse array of structure and function of glycans in biological systems [1–3]. Sugars are considered the most abundant class of organic molecules on earth and, taking the varying complexity into consideration, are the third major class of biomolecules after proteins and nucleic acids. Glycans are unbranched anionic polysaccharides found as large structural units or protein and lipid conjugates of varying size. The glycosaminoglycans (GAGs) are linear polysaccharides composed of repeating disaccharide units of alternating uronic acid and hexosamine residues. When conjugated with proteins, the proteoglycans are found in connective tissue with critical functions in cellular adhesion and migration. In the extracellular matrix proteoglycans form large complexes, both to other proteoglycans, to hyaluronan (an unsulfated GAG), and to fibrous matrix proteins such as collagen, affecting

the activity and stability of proteins and signaling molecules within the matrix. Individual functions of proteoglycans can be attributed to either the protein core or the attached GAG chain.

Heparin is a sulfated glycosaminoglycan with numerous important biological activities associated with its interaction with diverse proteins, including growth factors, proteases, lipid-binding proteins, and adhesion proteins [4, 5]. Heparin is widely used as an anticoagulant drug based on its ability to accelerate the rate at which antithrombin inhibits serine proteases in the blood coagulation cascade. The discovery and use of heparin for treatment of thrombosis in humans has been an iconic and important medical discovery with a lasting impact on health as well as being a billion-dollar industry [3, 4]. Endogenous human heparin is found exclusively in a subset of mast cells where it may function as a means of immunological protection [4, 6]. During their biosynthesis, heparin chains are attached to a unique core protein, serglycin, found only in mast cells and some hematopoietic cells. Sequential processing eventually produces small (ca. 15–20 kDa) polysaccharide chains of GAG heparin. The vast majority of the chemical and physical properties of heparin are related to GAG structure or sequence and conformation as well as molecular weight and charge density. Heparin has the highest negative charge density of any known biological macromolecule because of its high content of negatively charged sulfate and carboxylate groups – the average heparin disaccharide contains 2.7 sulfate groups.

Heparan sulfate (HS) (or heparan sulfate glycosaminoglycans (HSGAGs)) is ubiquitously expressed on the surfaces of animal cells and as a component of extracellular matrices and basement membranes [4, 7]. HS is structurally related to heparin but has a more varied structure with overall less sulfate substitution but with sequences of low or high sulfation. Heparin, which is widely available due to its anti-coagulant use, is often used as a model compound for HS. Present at the cell–tissue–organ interface, HSGAGs exert crucial regulatory roles in normal physiological processes such as embryogenesis, as well as in pathophysiological conditions, including the processes of tumor onset and progression [7]. HS is found *in vivo* attached to various core protein conjugates, heparan sulfate proteoglycans (HSPGs). The principal cell surface HSPGs are the syndecans (integral membrane proteins) and glypicans (GPI-anchored proteins). Basement membrane proteoglycans include perlecans, agrin, and collagen Type XVIII [7]. HS, as with heparin, interacts with many important proteins regulating a range of biological activities including cell proliferation, inflammation, angiogenesis, viral infectivity, and development [4, 7]. Other structurally discrete oligosaccharides include chondroitin, dermatan and keratan sulfates which each have their own distinct biological activities [8–10]. The intriguing heterogeneity of these biomolecules may be realistically related to the exercise of specific biological functions and requires a full understanding of their interactions at the molecular level to elucidate their importance.

2. STRUCTURE AND CONFORMATION OF HEPARIN AND HEPARAN SULFATE

Both HS and heparin are alternating copolymers of glucosamine with both iduronic and glucoronate-containing sequences which may be variably substituted at the *O*-sulfate, *N*-sulfate, and *N*-acetyl positions. The primary receptors for many heparin/HS-protein interactions are the sulfate groups and protein recognition is affected by substitution pattern, molecular shape, and internal mobility [11, 12]. A combination of solution-state NMR, fiber diffraction and crystallographic data, as well as molecular modelling, has defined the standard single-stranded helical nature of heparin (Figure 1).

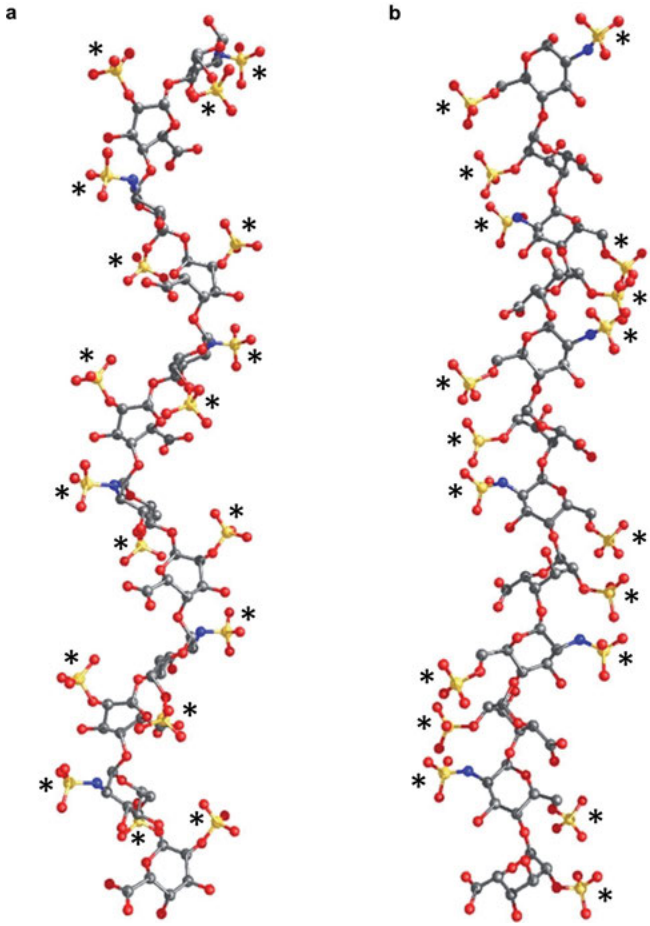

Figure 1. NMR-derived solution structure of the heparin dodecamer (PDB 1HPN) where all IdoA(2S) residues are either in $^{2}S_{0}$ conformation (**a**) or in $^{1}C_{4}$ conformation (**b**) [11, 12]. Sulfate groups in both the conformers are indicated by asterisks.

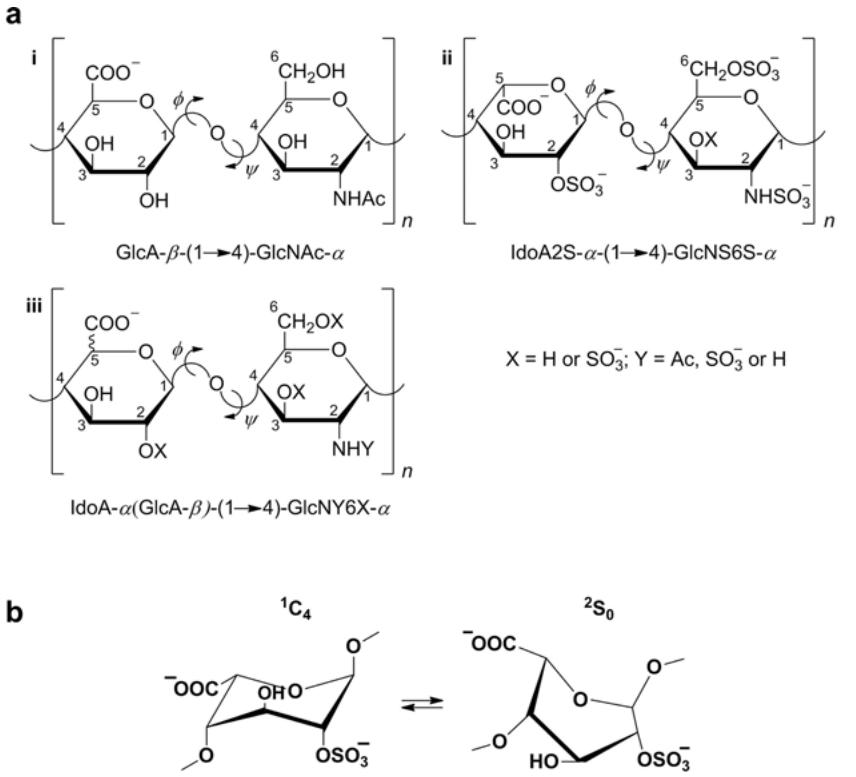

Figure 2. (**a**) Major repeating disaccharide unit of (i) heparan sulfate; (ii) heparin; and (iii) variable repeating disaccharide unit of heparin and heparan sulfate. Φ and ψ denote glycosidic torsion angles. (**b**) Equilibrium between the two major conformations found in IdoA(2S) residues of heparin and heparan sulfate.

In detail, HS sequences consist of repeating 1 → 4 linked disaccharide units of uronic acid and D-glucosamine, where uronic acid is either D-glucouronate (GlcA) or its C5 epimer, L-iduronate (IdoA), and D-glucosamine is either *N*-sulfoglucosamine (GlcNS) or *N*-acetylglucosamine (GlcNAc). The HS sequences are modified by *O*-sulfation at the 2-*O* position of uronic acid and the 6-*O* and 3-*O* positions of D-glucosamine residues (Figure 2a).

The extreme structural diversity of HS is a result of variable distribution of the above residues and presence/absence of sulfate groups along the polysaccharide chains. HS sequences are structurally related to heparin polysaccharides and the main structural differences between heparin and HS are: (i) the major uronic acid residues in heparin are mainly IdoA units, whereas in HS they are mainly GlcA residues with a substantial amount of IdoA residues; (ii) The D-glucosamine residues in heparin are mainly *N*-sulfated (GlcNS) whereas in HS they are *N*-acetylated (GlcNAc); (iii) 70–80 % repeating disaccharide units of heparin are IdoA(2S)-GlcNS(6S), whereas in HS 40–60 % of disaccharide units are GlcA-GlcNS/NAc. These structural differences make heparin more sulfated and more

negatively charged than HS [4, 13]. The HS backbone typically contains 50–400 monosaccharide units and has a much higher average molecular weight (ca. 50 kDa) than that of heparin (ca. 20 kDa) [4, 11, 14].

Much information on heparin and HS structure has been obtained from studies on small site-specifically modified polysaccharides. Analysis of the conformations of monosaccharide units of free heparin/HS indicates that glucosamine residues irrespective of substitution at the *N* and *O* positions prefer $^4C_1$ chair conformation [15, 16]. Much attention has been focused on the conformationally flexible iduronic acid residue (IdoA(2S)) of HS/heparin which can potentially adopt both the $^1C_4$ chair and $^2S_0$ skew boat conformations (Figure 2b) [17–19]. This type of conformational flexibility is not common in oligosaccharide structures, where flexibility is generally associated with the rotational freedom around the glycosidic linkages. Extensive NMR and molecular mechanic studies on heparin show that the equilibrium between the $^1C_4$ and $^2S_0$ forms and the contribution of the conformers to the equilibrium is dependent on the sulfation substitution and structures of the adjacent monosaccharide units [16]. For example, the ratio of $^1C_4$ and $^2S_0$ conformers of IdoA(2S) in heparin is 60 : 40 whereas in the antithrombin-binding sequence, Fondaparinux (FPX, see Figure 3), which contains a trisulfated glucosamine adjacent to IdoA(2S), the ratio of $^1C_4$ and $^2S_0$ conformers is 40 : 60 [17]. Importantly, when HS fragments bind to their biological receptors, IdoA(2S) adopts the most favorable conformation depending on the receptor.

NMR and density functional theory (DFT) on a trisaccharide from heparin repeating sequence has been studied where the central iduronic acid residue is again in either the $^1C_4$ or $^2S_0$ conformation [20]. These studies report detailed analysis of coupling constants and the optimized structures obtained showed differences in geometry at the glycosidic linkages, and in the formation of intramolecular hydrogen bonds for the conformers. Combined with circular dichroism, NMR spectroscopy, and molecular modeling, as well as DFT, are increasingly useful in interpreting the mechanism of action of GAGs and in drug design [21–23].

2.1. Heparin and Heparan Sulfate Binding to Proteins

HS sequences bind to a wide range of proteins, growth factors, and enzymes and influence their cellular processes [4, 6, 14, 24]. A full description of these interactions is simply beyond the scope of this review but two well-studied examples of specific interest are interactions with the plasma protein antithrombin-III (AT) and growth factors such as fibroblast growth factor (FGF) and its receptor (FGFR). Conformational and chemical factors such as torsion angles around glycosidic linkages and the conformation of the critical IdoA(2S) residues, the presence and distribution of sulfate groups and associated cation effects, are all parameters intimately involved in protein recognition.

The anticoagulant effect of heparin is manifested through its interaction with the plasma protein antithrombin-III. The structural requirements for heparin binding to AT, as shown in Figure 3, have been elucidated based on the crystal structures of FPX with AT [25]. The crystal structure of FPX bound to thrombo-

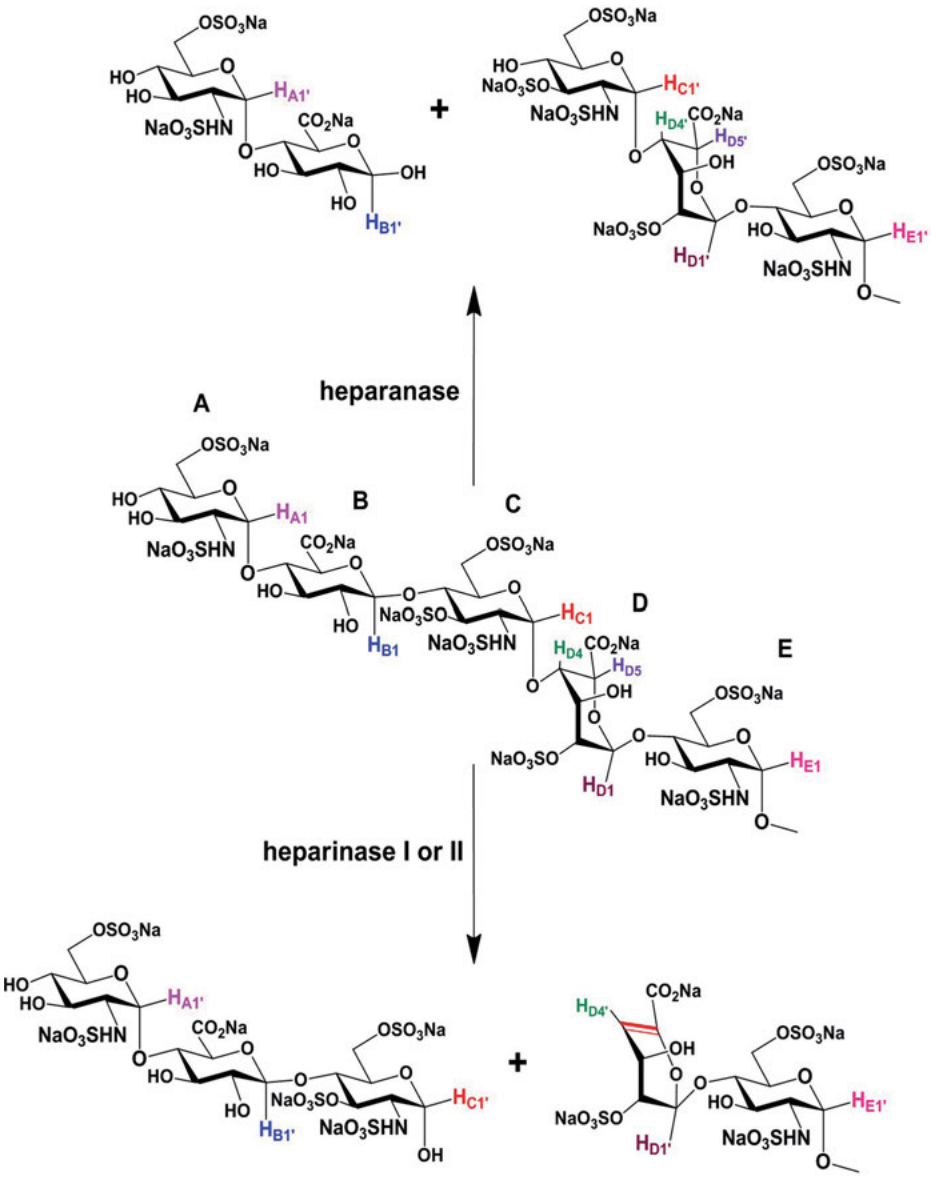

Figure 3. Structure of Fondaparinux (FPX), a highly-sulfated heparin mimetic used as an antithrombotic agent. The pentasaccharide incorporates the essential structural features required for heparin binding to the plasma protein antithrombin-III. Cleavage patterns of FPX by human (heparanase) and bacterial (heparinase I or II) enzymes are illustrated (see Section 2.2).

spondin-1 (TSPN-1) also delineated similar binding features [26]. Fondaparinux (Arixtra) (Figure 3) is the highly sulfated synthetic glycosaminoglycan-based fragment GlcNS(6S)-GlcA-GlcNS(3S)(6S)-IdoA(2S)-GlcNS(6S) that has been used clinically as an antithrombotic agent since the 1940s [27].

Structure-activity relationships for a series of related pentasaccharides varying the number and positions of the carboxylate and sulfate residues have also confirmed these essential features and the importance of a pentasaccharide sequence for binding [28]. Removal of the 3-*O*-sulfate in the central ring (C) of FPX decreases binding affinity to AT by approximately four orders of magnitude.

The solution structure of FPX, combined with DFT calculations, has been resolved [29]. NMR studies on FPX bound to AT showed that the protein drives the conformation of IdoA(2S) to a skew boat ($^2S_0$) form and also induces a conformational change in the geometry around the glycosidic linkages [30]. The examination of NOEs in the NMR structure confirmed that FPX-AT interaction is also mediated through strong arginine-sulfate interactions [31–33]. Studies involving heparin oligosaccharides differing in length and sulfation pattern have also revealed similar behavior of IdoA residues. NMR and simulation studies on a heparin octasaccharide in the presence and absence of AT showed that nonsulfated IdoA residues of heparin exist in the $^2S_0$ conformation in the absence of AT and in the $^1C_4$ conformation when bound to AT [34].

The prototypical example of HSGAG–protein interactions is the family of fibroblast growth factors (FGFs) [35, 36]. FGFs are intimately involved in development processes including cell proliferation, differentiation, and angiogenesis [35, 36], and bind with high affinity to four distinct but related transmembrane tyrosine kinase receptors (FGFR1 – FGFR4). Cell membrane HS protects FGFs from denaturation and proteolytic degradation and the presence of HS stabilizes binding of FGF to its cognate tyrosine kinase signaling receptors (FGFRs). A wealth of evidence supports a critical role of aberrant growth factor receptor signaling in cancer, including overexpression, activating mutations and amplifications of both the growth factors and receptors [35–37]. The basic structure of the FGF–FGFR complex comprises two receptor molecules, two FGFs and one heparan sulfate proteoglycan (HSPG) chain. *Trans*-autophosphorylation of FGFRs at intracellular tyrosine residues results in the activation of the Ras/mitogen-activated protein kinase and/or phosphoinositide 3-kinases (PI3K)/Akt signaling networks [38]. In general, increased stimulation of receptor tyrosine kinases (RTKs) by growth factors is associated with the development and metastatic spread of cancerous cells [39].

The crystal structure of heparin-derived tetra- and hexasaccharides bound to the basic fibroblast growth factor (bFGF or FGF-2) showed that the heparin structure could be approximated as a helical polymer [40]. The binding of both molecules was similar with contacts on the FGF-2 surfaces including asparagine, arginine, lysine, and glutamine residues. Both substrates overlap in the tetrasaccharide-binding region, identified therefore as a high-affinity binding site occupied by a sulfate group [40, 41] (Figure 4).

No significant conformational changes occur in the peptide suggesting that heparin primarily serves to situate components of the FGF signal transduction

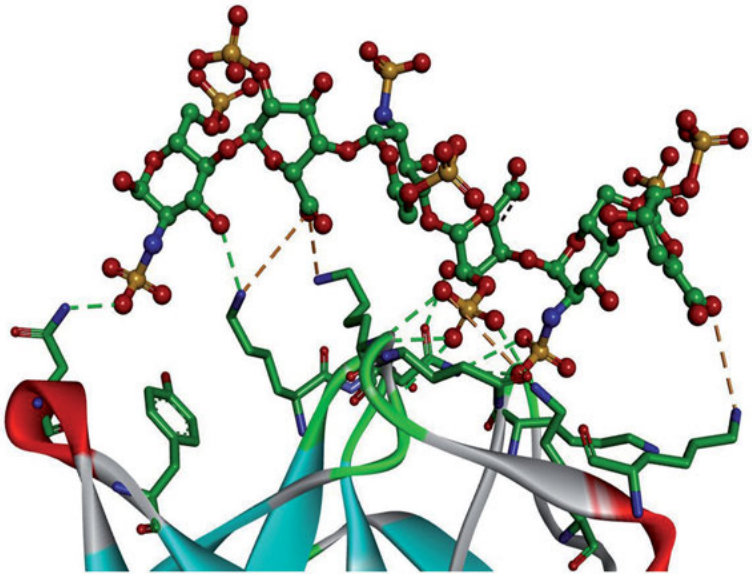

Figure 4. Crystal structure of heparin hexasaccharide bound with basic fibroblast growth factor (bFGF), PDB code 1BFC [40]. Interactions between the sulfate groups of heparin hexasaccharide (shown in ball and stick) and the basic residues (shown in sticks) of bFGF (shown in ribbons) are highlighted. The figure was prepared using Discovery Studio Visualizer 2016.

pathway. In the hexasaccharide, one of the two IdoA(2S) residues of the hexasaccharide adopts the $^{1}C_{4}$ conformation and the other is in $^{2}S_{0}$ conformation [40]. The requirement for sulfate binding is of great interest and varies amongst growth factors – FGF-2 requires the 2-*O*-sulfate but not the 6-*O*-sulfate for heparin binding, whereas FGF-1 requires both [41]. There is significant diversity in the structural features so far elucidated for heparin/HS-growth factor structures including in some cases the absence of sulfate groups [41]. The different requirements and responses of the FGF family to HS are central to understanding the details of signal transduction pathways and effects of chain length, sulfation pattern and HS conformation are all important and have been documented [42]. The minimal structural requirements for FGF-2 binding to heparin and HS oligosaccharides have been studied by NMR spectroscopy [43, 44]. The non-6-*O*-sulfated tetrasaccharide GlcNS-IdoA(2S)-GlcNS-IdoA(2S)(OPr) (where Pr = propyl) is the shortest HSGAG sequence that binds to FGF-2 and, in contrast to the crystal structure, both IdoA(2S) residues adopt chair $^{1}C_{4}$ conformation upon FGF-2 binding to obtain the best molecular fit [43]. Overall, for our purposes in discussing how metal ions and metal complexes affect these interactions, the conformational plurality of IdoA(2S) and the accommodation of ensuing sulfation patterns are critical to providing binding specificity. Finally, the crystal structure of the fibroblast growth factor receptor ectodomain bound to a heparin

decasaccharide shows the importance of sulfate groups in stabilizing the ternary FGF1-FGFR2-heparin complex [45].

2.2. Heparin and Heparan Sulfate as Enzyme Substrates

The biosynthesis of GAG chains mostly takes place in the Golgi apparatus [4]. A series of sulfotransferases using mainly 3′-phosphoadenosine-5′-phosphosulfate (PAPS) as sulfate donor are responsible for the sulfation of the oligosaccharide moieties. The structural variability of the heparin/HS chain is due in part to the incomplete nature of the biosynthetic modifications. The human sulfatases Sulf 1 and Sulf 2 are two closely related cell surface-associated enzymes which selectively remove the 6-*O*-sulfate group from glucosamine residues, affecting the composition and function of the glycosoaminoglycans [46, 47]. These enzymes are readily detectable in normal tissues, but undetectable in a large number of breast and other cancer cell lines [46, 47].

Heparin and HSPGs are cleaved at glycosidic bonds by mammalian and bacterial enzymes. There are three major bacterial heparinases which are enzymatically lyases and act by an eliminative mechanism. Degradation in bacteria is important as a carbon source and *in vitro* also leads to biologically active oligosaccharides with significant clinical and pharmaceutical implications. The mammalian heparanase is an *endo*-β-glucoronidase which cleaves heparan sulfate [48]. The hydrolase activity is thus formally distinct from the lyases. The cleavage patterns are illustrated in Figure 3, using Fondaparinux as an example. In the mammalian case, degradation releases angiogenic and growth factors leading to tumor cell migration, growth, and angiogenesis. Heparanase overexpression is associated with tumor progression in many human cancers and there is significant correlation between metastatic potential and heparanase activity [46, 47, 49, 50].

3. INTERACTION OF METAL IONS WITH GLYCOSAMINOGLYCANS

The highly anionic nature of heparin and HS means they are associated *in vivo* with physiologically relevant cations, in much the same way as nucleic acids. Biological functions involve binding and release of cations, whether as small ions or basic peptides and proteins, affecting the biomolecule conformation. Using atomic absorption and spectrophotometry, an overall trend for heparin-metal affinity and number of binding sites was deduced as $Mn^{2+} > Cu^{2+} > Ca^{2+} > Zn^{2+} > Co^{2+} > Na^{+} > Mg^{2+} > Fe^{3+} > Ni^{2+} > Al^{3+} > Sr^{2+}$ with the trend in number of binding sites being opposite compared to K_a [51]. The conformation of uronic acid IdoA(2S) residues is sensitive to the identity of adjacent residues and their substitution patterns in heparin and heparin fragments [52]. The glycosidic linkage geometry is also influenced by altered substitution pattern. Synchrotron radiation circular dichroism (SRCD) spectroscopy, which is sensitive to

uronic acid conformation, has been applied to examine the effect of metal ions on conformation of modified disaccharides containing one IdoA(2S) unit and a linked modified monosaccharide. Almost all disaccharide/cation combinations resulted in unique spectra suggesting that, in considering conformation and flexibility of the disaccharide, the contribution of the metal ion must be considered − the sequence alone does not define conformation or flexibility for this class of molecule [52]. Coupled with NMR studies, the conformations of the Na^+ and Cu^{2+} forms differed. The K^+ and Cu^{2+} forms of the modified heparin derivative, which contains 2-de-*O*-sulfated iduronate linked with glucosamine (IdoA(2OH)-GlcNS(6S)) as the predominant structure, supported FGF2-FGFR tyrosine kinase signaling, a result not attributable to the free cations themselves. Possible explanations are that the bound ion is involved in formation of the signaling complex when intimately involved with the heparin fragment, or that an active conformation is formed in this manner. In contrast, altering the cation from Na^+ to Cu^{2+} with an *N*-acetyl-enriched heparin resulted in inhibition of the FGF1-FGFR signaling pathway in a cell-based BaF3 assay [53].

Cu^{2+} ions show a strong selectivity for specific sequences in heparin binding with initial coordination including the carboxylic acid group, the ring oxygen of the iduronate-2-*O*-sulfate, the glycosidic oxygen between this residue and its neighboring glucosamine and the 6-*O*-sulfate group. Titration of Cu(II) ions into a solution of heparin indicated that the initial binding phase was complete by 15–20 Cu(II) ions per chain; thereafter the ions bound in a non-specific mode [54, 55]. Electron paramagnetic resonance studies suggested a tetragonal arrangement of the binding site in heparin and an octahedral coordination sphere in the *N*-acetylated heparin [54]. The strong binding of Cu^{2+} has been used to detect GAGs by capillary electrophoresis in an analytical application [56].

Angiogenesis is promoted by Cu^{2+} although its full role still needs to be elucidated [57, 58]. Relevant to this understanding is that growth factors are copper-dependent, with a slightly higher affinity for FGF-1 compared to FGF-2 [54, 59]. The vascular endothelial growth factor VEGF-A has its activity modulated by Cu^{2+} and spectroscopic studies of VEGF fragments (VEGF73–101 and VEGF84–101) indicated binding of the metal to three histidine residues with high affinity. These sequences represent specific recognition sites within the VEGF receptor and the conformational changes on the longer fragment interfered with the VEGFR recognition [60]. Certainly, the interplay between heparin binding, growth factors, and angiogenesis could be exploited to develop copper-based therapies specifically affecting signaling pathways [61].

The subtle changes in conformation resulting from M^{n+} binding and its effects on protein recognition is also seen with Zn^{2+}, where a Zn^{2+}-HS complex destabilizes lysozyme with alteration of conformation [62]. Hen lysozyme is a model amyloid-forming protein and it has been suggested that M-HS complexes such as Zn^{2+}, which is abundant in brain, may provide alternative folding routes for proteins.

Surface plasmon resonance (SPR) has also been utilized in defining the role of metal-heparin binding and its effects on growth factor and growth factor receptor recognition [63]. When studying heparin–protein interactions by SPR, heparin is

preferentially immobilized onto the sensor chip rather than the protein because this more closely mimics natural biological systems where HS is found at the cell surface as a proteoglycan and binds to target proteins [64, 65]. Metal ions showed a greater effect on HS-FGF1 interaction than on heparin-FGF1 and most of the effects were considered concentration-dependent. FGF1 binding to HS/heparin was reduced at 10 μM of Ca^{2+} and Mg^{2+} and also Fe^{3+} [63]. FGF1 binding was unaffected by Zn^{2+} at 10 μM, but was dramatically reduced at higher concentrations. At physiological lower/upper limit concentrations the effects of most individual metal ions with the exception of Cu^{2+} and to some extent Fe^{3+} were minimal [63].

NMR Spectroscopy. The diversity in molecular arrangements and dynamics displayed by glycans renders traditional NMR strategies, employed for proteins and nucleic acids, insufficient [23]. Because of the unique properties of glycans, structural studies often require the adoption of a different repertoire of tailor-made experiments and protocols. Experiments using isotopic labeling may overcome spectral overlap and raise sensitivity. Multinuclear NMR studies have also been useful in studying metal ion-heparin interactions. ^{1}H and ^{23}Na NMR spectroscopy indicated that Na^{+}, Ca^{2+}, and Mg^{2+} interacted at low pH with the carboxylic acid form of heparin by long-range electrostatic interactions [66]. At higher pH and consequent deprotonation of the carboxylic acid there is a site-specific contribution to the binding of Ca^{2+}, Zn^{2+}, and La^{3+}. The release of heparin-associated Na^{+} in the presence of competing cations can be studied by ^{23}Na NMR spectroscopy and the results also suggested site-specific binding for Ca^{2+} and Zn^{2+}, but not Mg^{2+}.

Measurements of NMR relaxation rates of ^{23}Na, ^{39}K, ^{25}Mg, and ^{43}Ca ions with bovine nasal cartilage proteoglycans and hog mucosal heparin suggested that relaxation rates were determined predominantly by polymer concentration and charge density – heparin bound the monovalent and divalent cations to a much greater extent than the proteoglycans [67].

Mass Spectrometry. Defined sequence heparin oligomers provide a level of simplification suitable for electrophoresis in conjunction with electrospray ionization mass spectrometry (ESI-MS) and tandem mass spectrometry and is increasingly being deployed in sequencing studies [68]. The formation of glycosidic bond cleavages from GAG ions is balanced against that of competing processes, both for low and high charge states. For low charge states, losses of SO_3 result in the most abundant product ions in the tandem mass spectra [68]. For higher charge states, losses of equivalents of H_2SO_4 from the precursor ion and from product ions derived from scission of glycosidic bonds represent unproductive fragmentation channels with respect to the useful information available from the tandem mass spectra. Ion mobility mass spectrometry has shown that various metal ions such as Na^{+} and Ca^{2+} induce a conformational contraction in a heparin octasaccharide structure [69]. The number of metal ion adducts, the ionic radii, and the ionic valence of metal ions all contribute to the contraction and conformational change. There was little difference in the measurements of conformational change measured in the gas phase with those from solution measurements [52, 66]. The binding of successive metal ions to the octasaccharide results

in a decreased collisional cross-section (CCS) of the metal ion coordinated octasaccharide. There are no general differences observed in the calculated CCSs of sodium ion-adducted *versus* potassium ion-adducted octasaccharide when more than one metal ion is present. An increased number of metal ion adducts may bind more free sulfate groups or carboxylates that would otherwise experience charge–charge repulsion, thus generating a more compact conformational change compared to fewer metal ion adducts. The effects of transition metal ions (Mn^{2+}, Fe^{2+}, Co^{2+}, and Ni^{2+}) on CCSs of heparin octasaccharide showed similar trends with decreased CCSs upon successive additions of metal ions. However, the greatest difference observed for transition metal ions occurred at the singly metal ion bound form, i.e., the cobalt adduct differed from one nickel adduct by 13 $Å^2$ [69].

The case of Ca^{2+} as a physiologically relevant cation is also an interesting one. The binding preferences in solution for Ca^{2+} have been delineated and show similarities to those found crystallographically in heparin-Ca-protein complexes such as annexin proteins [70–72]. The carboxylate groups of the idouronate residue and the *N*-sulfate and 6-*O*-sulfate of GlcNS are essential for Ca^{2+} binding. Conformation and sulfate selectivity are affected – the sulfate at position 2 of IdoA(2S) in a synthetic hexasaccharide is not essential for binding but specific binding is similar to heparin, whereas Ca^{2+} binds more weakly when the substrates lack the 6-*O*-sulfate of glucosamine [70, 71]. The iduronate residues adopt the $^1C_4$ conformation upon coordination.

The negative charge arising from GAG sulfation will be modified by counter-ion condensation, strictly analogous to other natural polyelectrolytes such as DNA. Counter-ion condensation and release may also play a role in GAG-protein binding [73–75]. Electrophoretic mobility measurements have confirmed counter-ion condensation but electropherograms of native heparin are naturally quite complex due to the heterogeneity of heparin and the corresponding lack of uniformity of sulfation patterns. The truncated electropherogram for native heparin is best explained by a limiting effective charged density arising from counter-ion condensation. A theoretical treatment for polyelectrolyte end effects shows the reduced counter-ion condensation, i.e., larger effective charges for short chains. In addition to the end segments, junctions separating regions of different charge densities could lead to diminishing counter-ion condensation, and this effect could be more pronounced for heparin due to its higher degree of heterogeneity [74].

In sum, M-heparin binding plays diverse roles in affecting conformational change, sulfate binding, and condensation. These structural changes are intimately related to the exercise of biological function of heparin and HS and these consequences are worthy of further detailed study.

4. INTERACTION OF COORDINATION COMPOUNDS WITH GLYCOSAMINOGLYCANS

The role of endogenous metal ions in heparin and HS structure and modulation of their function, allied to analogies with nucleic acids, suggests that the oligosac-

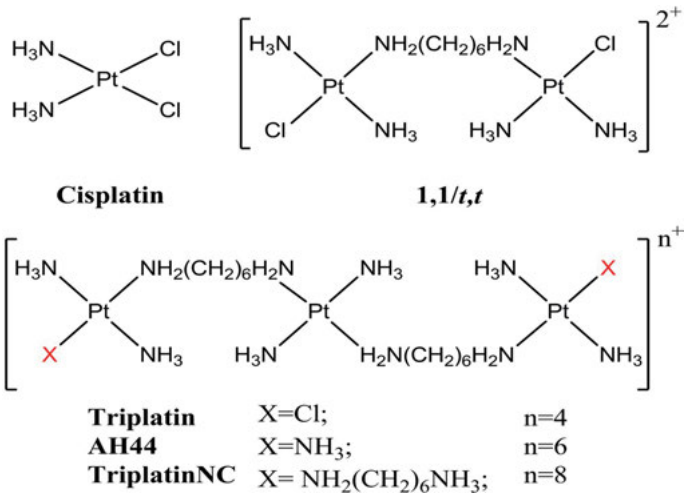

Figure 5. Structures of cisplatin and glycan-interacting polynuclear platinum complexes (PPCs). Where **X** = Cl, covalent bond-forming interactions are possible. AH44 and TriplatinNC bind in "non-covalent" manner. The total charge on the molecule is dictated by **X**.

charides are obvious templates for study with coordination compounds. As suggested first by us with respect to polynuclear platinum complexes (PPCs, Figure 5) [75], the study of defined coordination compounds with oligosaccharides has rich and multiple applications in this new area of endeavor in the field of bioinorganic chemistry distinct from protein and DNA/RNA interactions. Extending from aquated metal ions as discussed above, the inherent ability to alter oxidation state, coordination number and geometry, as well as substitution lability of coordinated ligands allows study of a wide variety of structural types to examine effects of structure and function on the "heparin/HS interactome" [37]. The glycan-coordinating moieties available are the oxygen donor atoms of the hard carboxylate and sulfate bases. Binding preferences therefore will not be the same for the donor atoms most commonly considered in DNA and proteins – the *N*-heterocycle purine and pyrimidine atoms and the *N*-histidine donors and thioether and thiol/thiolate *S*-donors of proteins. The interplay and application of hard and soft acid–base concepts can be expected to produce new patterns of metal ion binding with respect to selectivity and kinetic and thermodynamic stability. Further, electrostatic and hydrogen-bonding interactions should provide opportunities for "non-covalent" interactions as has also been formalized on DNA and proteins.

4.1. Platinum Anticancer Agents. Covalent Bond Formation

The binding of *cis*-$[PtCl_2(NH_3)_2]$, cisplatin, to heparin has been reported with a decrease in pH accompanying binding; however, the source and integrity of the

coordination compound is not clear [76]. A formulation for polyethylene glycol (PEG)-coated liposomes containing a cationic lipid, 3,5-dipentadecyloxybenzamidine hydrochloride (TRX-20), preferentially bind certain chrondroitin sulfate (CS) chains which are expressed on the surface of highly metastatic tumor cells [77]. When TRX-20 liposomes were loaded with cisplatin, they effectively killed the CS-expressing cells *in vitro*, and also markedly suppressed the liver metastasis of a high CS-expressing tumor, LM8G5, *in vivo*, increasing the survival time of the tumor-bearing mice [77]. Sustained release of active platinum species has also been observed from nanocomplexes of aquated cisplatin and pluronic-conjugated heparin [78]. The nanoconjugate showed good loading capacity and slower profile release whilst maintaining good cytotoxicity in NCI-H460 lung cancer cells [78]. Some glycoproteins can participate in DNA-protein cross-links induced by the action of cisplatin [79]. The nephrotoxicity of cisplatin is diminished upon conjugation with chondroitin sulfates [80, 81]. NMR and UV-visible spectroscopic studies indicated the necessity for aquation of the cisplatin prior to binding and ^{195}Pt NMR spectroscopy showed the presence of intact cisplatin even after 19 h – the chemical shifts of new products were consistent with *O*-donors suggesting binding through the carboxylate or sulfate moieties [82].

These latter results raise the question of the nature and strength of covalent binding given that the proposed carboxylate and sulfate oxygen binding sites are considered weak ligands for platinum. The seminal early ^{15}N and ^{195}Pt NMR studies of Appleton and coworkers characterized the binding of platinum(II)aqua complexes with simple anions such as phosphate, acetate, and sulfate [83]. More recently, {^{1}H,^{15}N} HSQC NMR studies have been used to investigate the aquation reactions of platinum drugs in the presence of simple anions [84]. For cisplatin, only the reaction with phosphate has been studied in detail and the reactions that ensue with the various aquated forms of cisplatin are complex [85]. In a reaction of ^{15}N-cisplatin with a 4.5-fold excess of phosphate (pH 5.9) more than seven aquated and phosphate-bound species were observed at equilibrium [85].

For the dinuclear platinum complex [{*trans*-$PtCl(NH_3)_2$}$_2$μ-$H_2N(CH_2)_6NH_2$]$^{2+}$ (1,1/*t*,*t*, Figure 5) aquation reactions have been carried out in the presence of 15 mM acetate, phosphate, and sulfate under identical conditions (298 K, pH 5.4), allowing for a direct comparison of the binding of these weak ligands [86, 87]. Figure 6 shows a representative {^{1}H,^{15}N} HSQC NMR spectrum from the reaction with sulfate and the derived rate and equilibrium constants for the different reactions are summarized in Table 1.

While there is some variation in the aquation rates of the Pt-Cl bond in the presence of the various anions, the rate constant for sulfate displacement of the aqua ligand (k_L) is approximately three times higher than that of acetate and phosphate, while for the reverse ligation reaction (k_{-L}) the rate constant for sulfate is more than an order of magnitude higher. The differences in k_L may reflect the higher negative charge of the sulfate. These results also suggest that a sulfate-bound platinum species is kinetically labile due to the high rate constant for the reverse reaction. The results are relevant for two reasons – firstly, inorganic sulfate (SO_4^{2-}) is the fourth most abundant anion in human plasma with

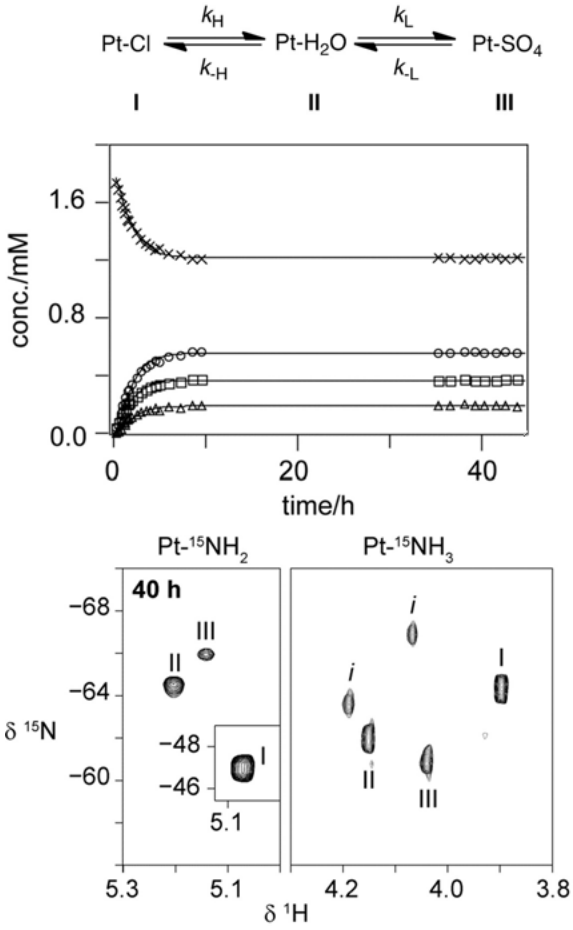

Figure 6. {^{1}H,^{15}N} HSQC NMR spectrum of ^{15}N-1,1/*t*,*t* in 15 mM sulfate (pH 5.4, 298K) at equilibrium (40 h). The plot shows the time dependence of the species observed and the rate constants derived from the kinetic model are shown in Table 1. Adapted with permission from [87]; copyright 2010 American Chemical Society.

Table 1. Rate and equilibrium constants for the aquation of 1,1/*t*,*t* (Figure 5) in 15mM phosphate, acetate, and sulfate.[a] The kinetic model is shown in Figure 6.

1,1/t,t	**Phosphate**	**Acetate**	**Sulfate**
k_H (10^{-5} s^{-1})	2.49 ± 0.04	1.83 ± 0.03	3.85 ± 0.05
k_{-H} (M^{-1} s^{-1})	0.40 ± 0.01	0.262 ± 0.009	0.229 ± 0.04
k_L (M^{-1} s^{-1})	0.0086 ± 0.0002	0.0086 ± 0.0001	0.025 ± 0.004
k_{-L} (M^{-1} s^{-1})	3.9 ± 0.1	0.56 ± 0.02	70 ± 10
pK_1	4.21 ± 0.02	4.16 ± 0.02	3.77 ± 0.01
pK_2	–2.34 ± 0.02	–3.19 ± 0.02	–1.6 ± 0.1

[a] Adapted with permission from [87]; copyright 2010 American Chemical Society.

concentrations reported to be 0.3 to 0.4 mM and is itself involved in a wide variety of metabolic and cellular processes [88, 89]. A full description of platinum cellular chemistry should include reactions with apparently "weak" anions such as sulfate and carbonate because of their high concentration [90, 91]. Secondly, the specific interactions with sulfate are relevant to the role of HS as receptor for cellular accumulation of polynuclear platinum complexes (see Section 5.2).

4.2. Platinum Anticancer Agents. Non-Covalent Interactions and Sulfate Cluster Binding

It is clear from studies on Pt-DNA interactions that "pre-association" or non-covalent interactions on the biomolecule is an important feature of the mechanism prior to occurrence of Pt-DNA covalent bond formation and may be visualized by NMR and other spectroscopic methods. In broad terms, the intercalation of a wide class of Ru(polypyridyl) complexes on DNA and stabilization of Z-form DNA by $[Co(NH_3)_6]^{3+}$ are mediated purely by electrostatic and H-bonding contributions. A further relevant example is that of polynuclear platinum complexes (Figure 5), a discrete set of platinum-based anticancer agents whose design and development was predicated on the hypothesis that altering modes of DNA binding and producing structurally distinct Pt-DNA adducts would over-

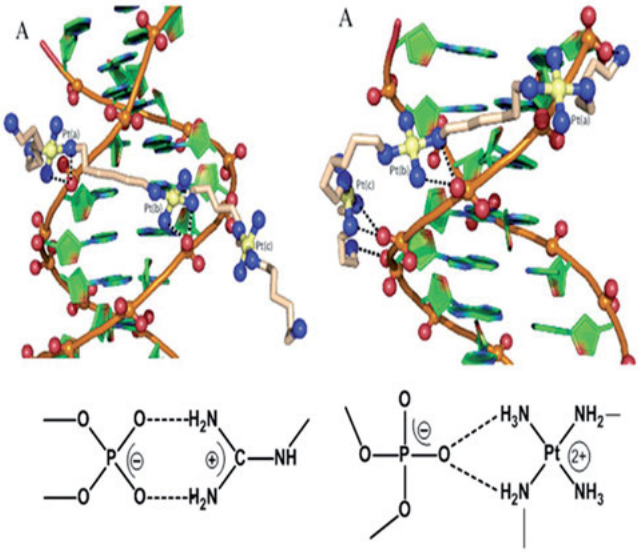

Figure 7. Structure of TriplatinNC complexed to the Dickerson-Drew dodecamer (NDB 2DYW) showing backbone tracking and groove spanning. Comparison of arginine fork (left) and phosphate clamp (right). Adapted with permission from [94]; copyright 2006 American Chemical Society.

come DNA repair-related resistance to the clinical drug. Proof of the success of this approach is given by the entry of Triplatin (BBR3464) to Phase II clinical trials, the only non-cisplatin analog to be introduced to humans. The clinical studies and mechanistic work on DNA has been extensively reviewed [92, 93]. A companion ctehapter discusses the properties of the Pt-DNA adducts formed by PPCs (see Chapter 2).

Replacement of Pt-Cl by substitution-inert ligands such as NH_3 or the "dangling" amine, $-H_2N(CH_2)_nNH_3^+$, gives substitution-inert analogs which are unreactive toward sulfur nucleophiles, thus enhancing metabolic stability, and also allows study of "non-covalent' contributions in the absence of Pt-biomolecule bond formation. The X-ray crystal structure of the Dickerson-Drew dodecamer (DDD, $[d(CGCGAATTCGCG)]_2$) with the non-covalent TriplatinNC showed a new mode of ligand-DNA recognition distinct from the conventional modes of intercalation and groove binding (PDB entry 2DYW). Hydrogen bonding with phosphate oxygens results in either backbone tracking or groove spanning through formation of "phosphate clamps" where the square-planar tetraam(m)ine Pt(II) coordination units all form bidentate N-O-N complexes with phosphate oxygen (OP) atoms (Figure 7) [94].

The generality of the motif was confirmed by a second crystal and molecular structure with AH44, that is with $L = NH_3$ (6+) instead of $-NH_2(CH_2)_6NH_3^+$ (8+) (see Figure 5) [95]. The phosphate clamp is analogous to that of the guanidino group of arginine which shows an analogous, but attenuated clamping ability in which two OP atoms form a clamp-like structure, the arginine fork (Figure 7) [94]. 2D and $\{^1H, ^{15}N\}$ HSQC NMR studies also confirmed the presence of the phosphate clamp in solution [96].

4.2.1. Non-Covalent Heparan Sulfate Interactions. Sulfate Cluster Binding and Metalloshielding

The discovery of the phosphate clamp as a biologically relevant binding motif immediately suggested analogies with the isostructural sulfate. Using a model compound *trans*-$[Pt(NH_3)_2(NH_2CH_3)_2]^{2+}$, the free energy of interaction (E_{int}) for isolated sulfate and phosphate interactions were compared [97]. The interaction in water with an isolated sulfate monoester is not significantly favorable and indeed inherently weaker than that of phosphate. These results can be explained by the fact that the negative charge is more dispersed on a sulfate monoester because of delocalization involving three non-ester oxygen atoms compared to the phosphate diester with only two non-ester oxygen atoms. In both cases, the interactions were not significantly different from a model methylguanidinium interaction, used as a model for the arginine fork.

The identity and conformation of the sugar and the number and positions of sulfation make GAGs highly complex systems, with significantly more variability than DNA, also with respect to non-bond-forming interactions. To examine the strength of sulfate binding in heparin and heparan sulfate, the binding of a simple coordination unit $[Pt(NH_3)_4]^{2+}$ to a [GlcNS(6S)-IdoA(2S)-GlcNS(6S)] trisac-

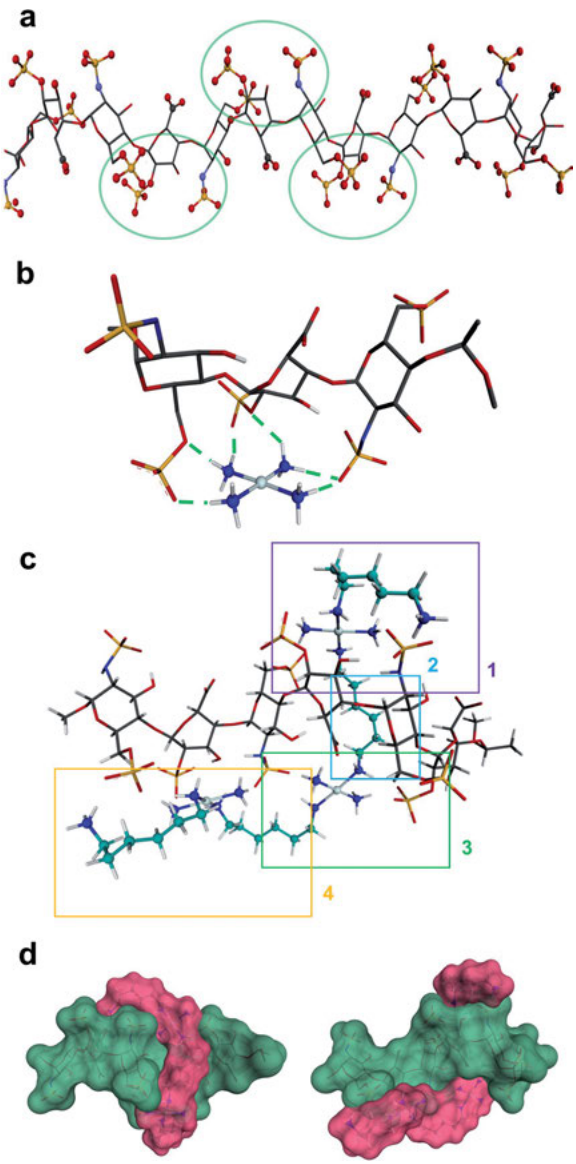

Figure 8. Sulfate cluster anchoring as a model for PPC-HS interactions. (**a**) Structure of the heparin dodecamer comprising dimers of IdoA(2S) and GlcNS(6S) where the iduronic acid residues are in the $^{2}S_{0}$ conformation (1HPN). The green circles represent areas of negatively charged sulfate and carboxylate clustering. (**b**) The optimized structure of the trimer cluster [GlcNS(6S)-IdoA(2S)-GlcNS(6S)] modeled with the simple Pt-tetrammine $[Pt(NH_3)_4]^{2+}$. (**c**) Optimized structure of TriplatinNC with a heparin hexamer $[IdoA(2S)\text{-}GlcNS(6S)]_3$. Sections 1, 3, and 4 show regions of sulfate clamp interactions while Section 2 shows van der Waals contacts between sugar and diamine backbones. (d) Surface maps (two views) showing the relationship of TriplatinNC (magenta) to the heparin hexamer (green). Adapted from [97] with permission from the Royal Society of Chemistry.

charide heparin fragment was examined (Figure 8) [97]. The fragment, which has also been used for NMR and DFT applications [20, 21], was derived from the NMR-derived structure of heparin. The structure of heparin is approximated by a ribbon with a cluster of sulfates and carboxylates on the edges and hydroxyl and sugar ring oxygens positioned on the surfaces between these negatively charged groups. The optimized structure now shows regions of clustering with interactions of the $[Pt(NH_3)_4]^{2+}$ units with multiple sulfate and carboxylate moieties (Figure 8b). This binding produces a more extended hydrogen-bonding network along the face of the cluster. Superimposition of the optimized structure of the association complex with the optimized structure of the free heparin trimer, shows no major conformational changes and the E_{int} is –53 kcal mol^{-1} [97].

Extension of these results to TriplatinNC, using now a derived heparin hexamer to account for the larger charge and longer length of the trinuclear species, again shows a similar pattern of sulfate clustering but with an even greater E_{int} of –250 kcal/mol (Figure 8c and d). These results help explain some of our earlier observations on PPC-HS interactions (see below, Section 5.2) and also allow us to predict the consequences of strong PPC-HS binding on the function of the biomolecule. Sulfate cluster binding is by its nature delocalized but will result in neutralization of the sulfate charge and further physically protect the sulfate groups from their receptors. The biological consequences of masking or *metallo-shielding* of the essential sulfate residues will, *a priori*, affect protein recognition in strict analogy to inhibition of protein-DNA interactions upon formation of Pt(M)-DNA adducts.

5. CONSEQUENCES OF HIGH-AFFINITY HEPARAN SULFATE BINDING

5.1. Sulfate Group Protection

The sulfated moieties on octasaccharides are quite labile and the mass spectrum of free octasaccharide shows a series of peaks corresponding to SO_3 (commonly denominated as sulfate) loss [68, 69]. The mass spectrum under the same conditions of the 1 : 1 adducts formed with representative PPCs show little loss compared to free polymer and protection from sulfate loss is also seen at increasing energies. The interaction is by its nature non-covalent and the stabilization is dependent on the charge of the PPC with TriplatinNC especially effective with a difference of up to 7 of a total of 10 sulfate groups protected *versus* free oligosaccharide (Figure 9). No, or very little, cleavage of the glycosidic backbone was apparent even at high voltages and the results are entirely consistent with PPC binding introducing a large charge in a localized area and, with the increased stability toward dissociation, verify the complexation with sulfate moieties in preference to elsewhere on the glycosidic backbone [75].

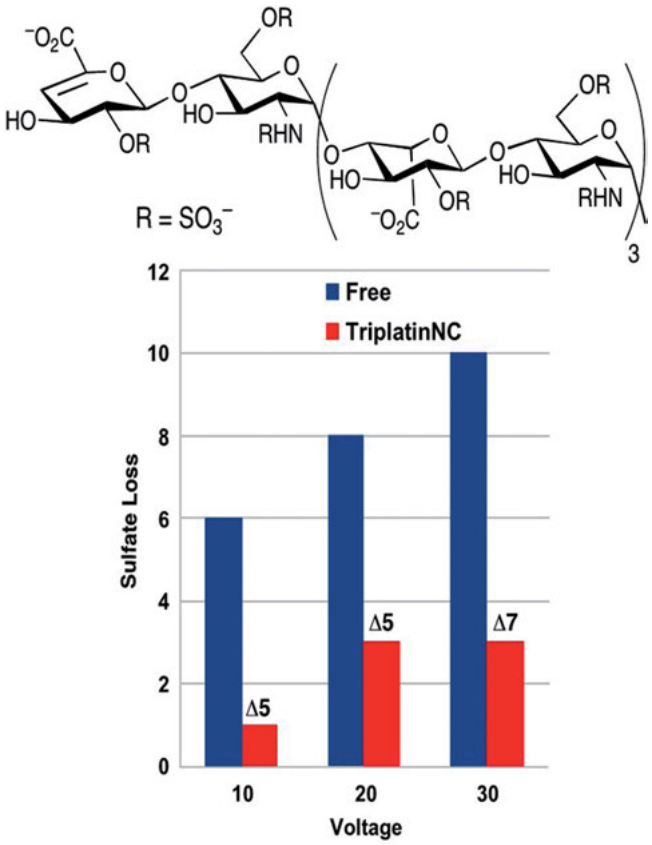

Fogure 9. TriplatinNC protects against sulfate elimination in an octasaccharide (dp8). Δn is the difference in sulfate loss between free and adducted dp8. Adapted from [75] with permission from the Royal Society of Chemistry.

5.2. Heparan Sulfate as Receptor for Cellular Accumulation of Polynuclear Platinum

PPCs, especially those containing a central charged/H-bonding capacity, are accumulated to a significantly greater extent than neutral compounds [98, 99]. The cellular accumulation is higher than for cisplatin and actually increases with charge, a perhaps paradoxical situation for Pt. Natural and synthetic polycationic peptides, especially containing the poly(arginine) motif, are efficiently taken up by cells and also facilitate cellular accumulation of a host of molecules [100]. HSPGs were confirmed as the cellular receptors for polyarginines using TAMRA-R_9, (a nonaarginine peptide (R_9) coupled to the TAMRA fluorescent label 5-(6)-carboxytetramethylrhodamine) in wild-type (wt) and mutant (lacking HS or HS/chondroitin sulfate) Chinese hamster ovary (CHO) cells [101, 102]. Fluorescence microscopy and flow cytometry showed that PPCs, but not neutral cis-

Table 2. Enhancement of TriplatinNC cytotoxicity in transformed mast cells.[a]

Mast Cell Line	(IC_{50}, μM)		
	Triplatin	**TriplatinNC**	**Cisplatin**
BMMC(primary)	0.004	1.79	0.27
P815(transformed)	0.27	0.41	0.82
PDMC(transformed)	0.04	0.3	0.96

[a] IC_{50} (μM) is the concentration required to kill 50 % of cells by apoptosis as measured by propidium iodide staining. BMMC: bone marrow mast cell. PDMC: peritoneal derived mast cells. Adapted with permission from [98]: A. L. Harris, J. J. Ryan, N. P. Farrell (2006) Biological Consequences of Trinuclear Platinum Complexes: Comparison of [{*trans*-$PtCl(NH_3)_2$}$_2$μ-(*trans*-$Pt(NH_3)_2(H_2N(CH_2)_6NH_2)_2$)]$^{4+}$ (BBR3464) with Its Noncovalent Congeners, *Mol. Pharmacol. 69*:666–672.

platin or oxaliplatin, blocked the cellular entry of TAMRA-R_9 in CHO cells [103]. Accumulation of TriplatinNC in mutant CHO-pgsD-677 (lacking HS), and CHO-pgsA (lacking HS and chondroitin sulfate) cells decreased relative to wt CHO. Apoptosis and growth inhibition assays paralleled the effect of mutant cells on accumulation, as shown for TriplatinNC. We conclude that PPCs inhibit the polyarginine binding and that HSPG-receptor mediated interactions are an important mechanism for their internalization.

Tumor Selectivity. This is a completely new mechanism of cellular accumulation for platinum drugs with important implications for tumor selectivity, since proteoglycans are expressed 2 to 3 times more in many tumor cells lines [104]. Strict comparisons are hard to find but it is relevant that transformed P815 mast cells were more selective for PPC uptake than their bone marrow progenitor-derived mast cells (BMMCs) [98, 99]. Cytotoxicity, especially for TriplatinNC, was also enhanced in the tumor cells [98] (see Table 2).

Scanning the literature confirmed that P815 mastocytoma cells produced significant amounts of chondroitin-4-sulfate rather than the normal heparin, suggesting the possibility of a role for glycans in this "promotion" of the cytotoxicity [105]. Thus, the cellular accumulation can be analyzed now in a new context, i.e., extracellular HS receptors. A recent study showed polyarginine-R8, with a charge similar to TriplatinNC, accumulates to high levels in wt CHO-K1 tumors compared to GAG-deficient pgsA-745 tumors *in vivo* [106].

5.3. Inhibition of Function of Heparan Sulfate

Interactions between HS and enzymes and extracellular proteins mediate the patho-physiological processes of tumor growth and metastasis. Metalloshielding could act on many of these processes, and two relevant examples with the chemical features and their biological consequences are as outlined in Figure 10. Again, these concepts are in complete analogy to inhibition of protein binding on metal-modified DNA.

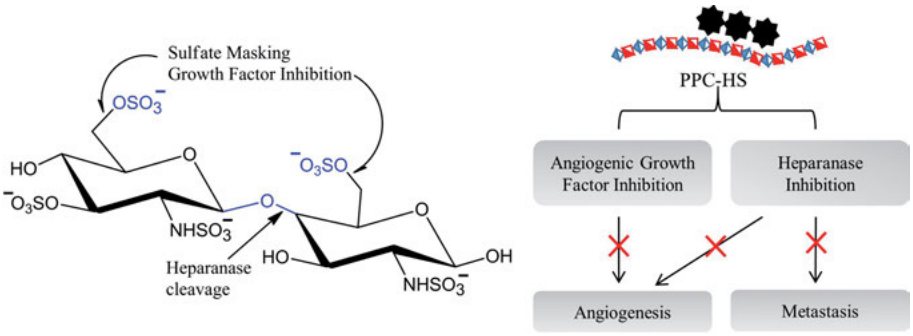

Figure 10. Potential chemical approaches to inhibition of HS-associated enzyme and protein recognition and activation through sulfate masking.

5.3.1. Heparanase Cleavage Inhibition

Glycans are acted upon by two related enzymes, the bacterial heparinase and the mammalian heparanase. The relevance of heparanase cleavage of substrate HS to tumor growth and metastasis has been outlined in Section 2.2. To examine the efficacy of metalloshielding in blocking heparinase and heparanase action on HS-containing proteoglycans we used the sulfated pentasaccharide, Fondaparinux as a model HS-like substrate. FPX is a substrate for both bacterial heparinases and human heparanase and has been used in assay development for screening the efficiency and kinetics of potential heparanase inhibitors [48, 107, 108]. FPX is an ideal substrate for mechanistic studies because it is homogeneous, has low molecular weight and, with a single point of cleavage either by heparinase or heparanase, leads to the formation of only two products (see Figure 3). The course of FPX hydrolysis can conveniently be determined by ^{1}H NMR spectroscopy as the anomeric protons are sensitive reporters of the cleavage reaction by both heparanase and the bacterial heparinases [48, 97, 107, 109]. Figure 11a shows that 1 : 1 stoichiometric ratios of TriplatinNC:FPX very effectively inhibit enzymatic cleavage [97]. Modifying a colorimetric assay, pre-incubation of FPX with PPCs effectively inhibited its cleavage by bacterial heparinase (Figure 11b). The inhibition was as effective as a polyarginine control whereas cisplatin had little or no effect [75]. In both cases, Triplatin itself is also effective suggesting a contribution to the binding by the expected weak interactions of Pt-sulfate bonds.

5.3.2. Growth Factor Binding Inhibition

HS-binding protects growth factors and cytokines from denaturation and proteolytic degradation, provides a matrix-bound or cell-surface reservoir for cells and is essential for the activation of cell signaling receptors (see Section 2.1 and Figure 12). Incubation of varying concentrations of Triplatin and TriplatinNC with biotinylated HS directly inhibited FGF-2 binding, whereas cisplatin is completely inef-

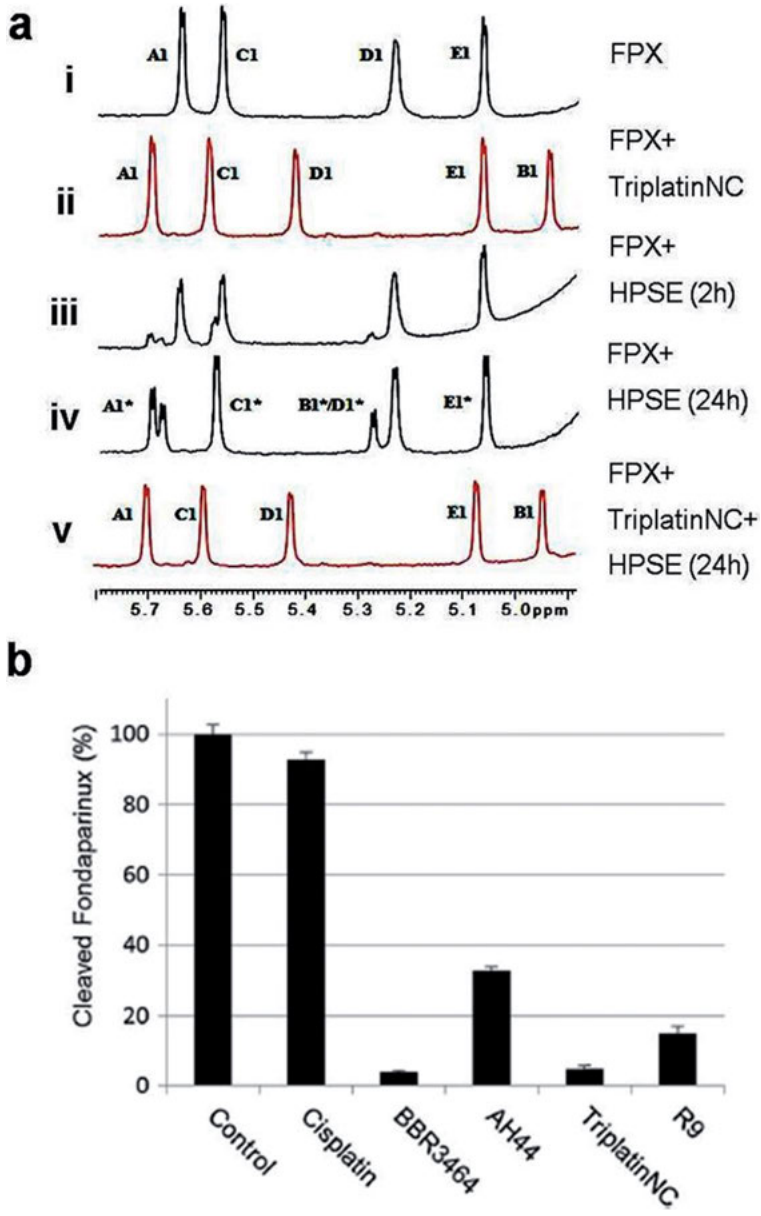

Figure 11. Blockage of heparinase and heparanase activity by PPCs. (**a**) ^{1}H NMR assay: Incubation of FPX with human heparanase (HPSE) confirmed the expected cleavage of FPX (i → iii → iv; see Figure 3 for assignment of anomeric protons). In the presence of one equivalent of TriplatinNC FPX cleavage by the enzyme was completely inhibited and significant shifts are immediately seen in the anomeric protons of FPX (i → ii). (**b**) Colorimetric assay: Inhibition of heparinase I FPX cleavage (3 h incubation) by polynuclear platinum complexes and the arginine-rich R_9 protein (1 : 3 stoichiometry). Adapted from (a) [97] and (b) [75] with permission from the Royal Society of Chemistry.

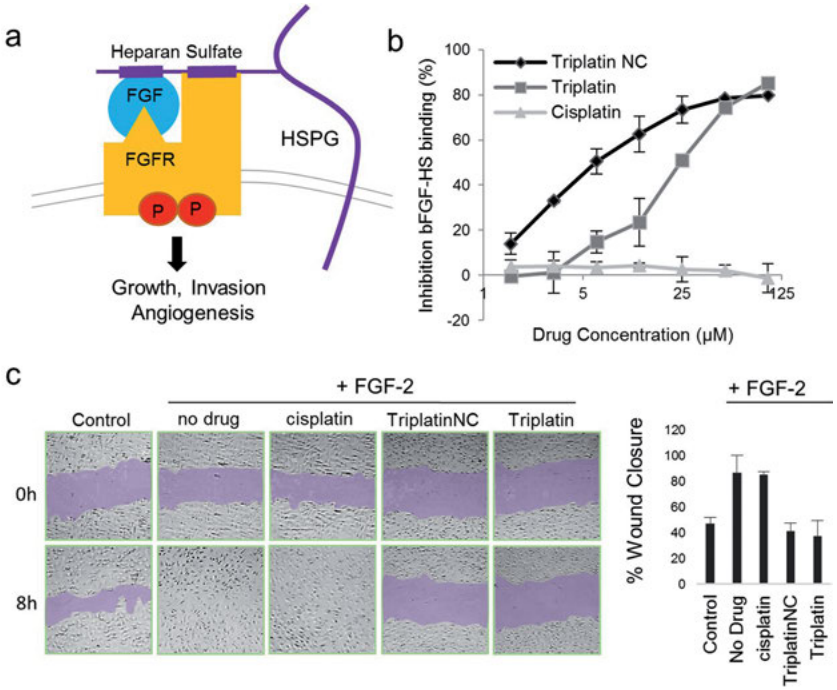

Figure 12. Inhibition of HS-protein interactions. (**a**) Growth signaling occurs when a growth factor (GF) binds and activates a cell surface receptor tyrosine kinase (FGFR). This interaction is facilitated by growth factor binding to heparan sulfate proteoglycans (HSPGs) forming stable high-affinity ternary complexes with FGFRs. (**b**) PPCs inhibit FGF-2 binding to heparan sulfate. (**c**) PPCs at sub-cytotoxic concentrations but not cisplatin inhibit FGF-2-induced migration of human umbilical vein epithelial cells (HUVECs). Adapted from [97] with permission from the Royal Society of Chemistry.

fective (Figure 12b). The biological consequence of this inhibition may be measured in many ways and is exemplified by the wound healing assay, which measures directional migration of cells in a monolayer after a scratch or 'wound' is inflicted [110]. Upon addition of 2 μM cisplatin, Triplatin, or TriplatinNC to monolayers of scratched confluent human umbilical vein epithelial cells (HUVECs), only the PPCs inhibited growth factor induced migration (Figure 12c). The drug concentration used was well below the cytotoxic level for this short exposure time [97].

The systematic extension of this proof-of-concept work was extended to inhibition of kinase signaling pathways where TriplatinNC can inhibit FGF-2 -induced accumulation of phospho-S6 ribosomal protein (pS6) in HCT116 colon cancer cells.

Finally, the end-point of heparanase and growth factor inhibition will be inhibition of cell invasion, angiogenesis, and metastasis. Proof-of-principle that Triplatin and TriplatinNC are effective antiangiogenic compounds has been obtained using the rat aortic ring assay [97].

6. USE OF METAL COMPLEXES IN HEPARIN ANALYSIS

The formation of a Cu^{2+}-heparin complex is sufficiently strong to allow detection of heparin as low as 10 ng by capillary electrophoresis [56]. Ruthenium red is a polycationic stain used to visualize acid polysaccharides on the outer surface of cells. Ruthenium red staining followed by electron microscopic analysis was used to demonstrate the presence of an external glycoprotein layer surrounding the spore of both *Bacillus anthracis* and *Bacillus subtilis* [111]. An early study used the fluorescent properties of $[Ru(bipy)_3]^{2+}$ to detect heparin and HS [112]. Accurate measurements of heparin concentration is important in health-related applications. The minimum content of heparin detected by fluorescence was 25–50 ng. Two to six disaccharide units are bound by each $[Ru(bipy)_3]^{2+}$ and Scatchard analysis gave $K_d = 8.56 \times 10^{-5}$ M for one Ru complex binding site. The assay was further used to detect heparinase activity and determine its substrate specificity [113]. Modification of the Ru fluorophore to $[Ru(phen)_2(dppz\text{-}idzo)]^{2+}$ (dppz-idzo = dipyrido-[3,2-*a*:2′,3′-*c*] phenazine-imidazolone) allowed development of a "switch-on" assay for heparin, with a significant fluorescence enhancement of the Ru complex upon binding, which can be used in biological media such as fetal bovine serum [114]. Molecular modelling combined with fluorescence and UV absorption studies showed good fluorescence selectivity towards heparin over analogs, such as chondroitin 4-sulfate or hyaluronic acid, which have lower charge density [78]. Quantification of heparin is in the range 0.01–4.87 U mL^{-1}. Notably, due to high DNA affinity, the assay should be used in DNA-free biological systems.

The fluorescent and photo-activating properties of Ru-polypyridyl complexes has found novel use in analyzing the abundance and degree of sulfation of HS in the development of hepatocellular carcinoma and to evaluate HS-growth factor interactions [115]. Use of $[Ru(bipy)_2(dppz)]^{2+}$ in this case is used as a photocatalyst to induce radical depolymerization of HS, analogous to observed radical photo-cleavage of DNA [115, 116]. This allows for more sensitive read-out and applications in hepatocellular carcinoma (HCC) HepG2 cells, changes between the activity of sulfatase 2 (HSulf 2) in regulating FGF2-induced cell proliferation, and the abundance, degree of sulfation and growth factor binding of HS can be observed. This method has also been applied to analyze clinical tissue samples of HCC.

A biferroceylene thiol conjugate assembled on a gold surface has been used to detect and quantify heparin and chondroitin sulfate in aqueous buffer by cyclic voltammetry and was also shown to function in a blood plasma sample. Controlled binding and release of heparin could be achieved by switching the BFD-SAM (= biferrocenylene thiol conjugate self-assembled monolayer) between the monocationic and neutral state [117]. An early paper used the binding of $[Co(NH_3)_6]^{3+}$ to chondroitin sulfate to calculate the amount of anionic sulfate [118].

7. CONCLUSIONS AND OUTLOOK

In this contribution, we summarize for the first time the relevance of metal ion binding to oligosaccharides and especially glycosoaminoglycans. As befits a highly anionic biomolecule, intrinsic $[M(aqua)]^{n+}$ interactions play an important part in stabilization and conformation of the sugar backbone. Extension to defined coordination compounds with the inherent ability to alter oxidation state, coordination number, and geometry, as well as substitution lability of coordinated ligands allows for the study of a wide variety of structural types to examine effects of structure and function on the heparin/HS interactome. As exemplified by the polynuclear platinum example, these studies lead to new targets and new patterns of biological activity, including the potential for selectivity in tumor uptake. The comparison with double-stranded DNA is relevant given the helical nature of both biomolecules.

Glycoscience is generally considered to be less developed than that of nucleic acids and proteins, in part due to the heterogeneity and variability in glycan structure. Metalloglycomics is a potentially rich area of endeavor for bioinorganic chemists to study the relevance of intrinsic metal ions in heparin/heparan sulfate-protein interactions and for development of new compounds for therapeutic, analytical, and imaging applications. Bioinorganic chemistry can play an important role as the science and understanding of glycomics advances, and investment of research effort into this hitherto little developed area is likely to be rewarding in a truly interdisciplinary manner.

ACKNOWLEDGMENTS

NF acknowledges support through The National Institutes of Health (RO1 CA78754) and The Massey Cancer Center (P30 CA016059). This work was supported by The Australian Research Council (DP150100308). We sincerely thank Professor Mark von Itzstein for his enthusiastic support for our work and for helpful discussions.

ABBREVIATIONS AND DEFINITIONS

AT	antithrombin-III
BMMC	bone marrow-derived mast cells
CCS	collisional cross sections
CHO	Chinese hamster ovary cells
CS	chondroitin sulfate
DFT	density functional theory
FGF	fibroblast growth factors
FGFR	fibroblast growth factor receptor
FPX	Fondaparinux (Arixtra)

GAGs	glycosaminoglycans
GlcA	D-glucuronate
GlcNAc	*N*-acetylated D-glucosamine
GlcNS	*N*-sulfated D-glucosamine
GlcNS(6S)	6-*O*-sulfated, *N*-sulfated D-glucosamine
GlcNS(3S)(6S)	3-*O*-sulfated, 6-*O*-sulfated, *N*-sulfated D-glucosamine
GPI	glycosylphosphatidylinositol
HS	heparan sulfate
HSPG	heparan sulfate proteoglycan
HSQC	heteronuclear single quantum correlation
IdoA	L-iduronate
IdoA(2S)	2-*O*-sulfated L-iduronate
NMR	nuclear magnetic resonance
NOE	nuclear Overhauser effect
phen	1,10-phenanthroline
PPCs	polynuclear platinum complexes
SPR	surface plasmon resonance
UV	ultraviolet
VEGF	vascular endothelial growth factor

REFERENCES

1. *Essentials of Glycobiology*, 2nd Ed., Eds A. Varki, R. D. Cummings, J. D. Esko, H. H. Freeze, P. Stanley, C. R. Bertozzi, G. W. Hart, M. E. Etzler, Cold Spring Harbor Laboratory Press, Cold Spring Harbor, NY, 2009.
2. R. D. Cummings, J. M. Pierce, *Chem. Biol.* **2014**, *21*, 1–15.
3. J. E. Hudak, C. R. Bertozzi, *Chem. Biol.* **2014**, *21*, 16–37.
4. I. Capila, R. J. Linhardt, *Angew. Chem. Intl. Ed*. **2002** *41*, 390–412.
5. D. E. Humphries, G. W. Wong, D. S. Friend, M. F. Gurish, W.-T. Qiu, C. Huang, A. H. Sharpe, R. L. Stevens *Nature* **1999**, *400*, 769–772.
6. M. C. Menenghetti, A. J. Hughes, T. R. Rudd, H. B. Nader, A. K. Powell, E. A. Yates, M. A. Lima, *J. R. Soc. Interface* **2015**, *12*:20150589.
7. R. Sasiekharan, Z. Shriver, G. Venkataraman, U. Narayanasami, *Nature Rev. Cancer* **2002**, *2*, 521–528.
8. N. K. Karamanos, G. N. Tzanakakis, *Curr. Opin. Pharmacol.* **2012**, *12*, 220–222.
9. N. Afratis, C. Gialeli, D. Nikitovic, T. Tsegenidis, E. Karousou, A .D. Theocharis, M. S. Pavão, G. N. Tzanakakis, N. K. Karamanos, *FEBS Journal* **2012**, *279*, 1177–1197.
10. S. Yamada, K. Sugahara, *Curr. Drug Discov. Technol.* **2008**, *5*, 289–301.
11. B. Mulloy, M. J. Forster, *Glycobiology* **2000**, *10*, 1147–1156.
12. B. Mulloy, D. T. Crane, A. F. Drake, D. B. Davies, *Biochem. J.* **1997**, *328*, 51–61.
13. D. Wardrop, D. Keeling, *Br. J. Haematol.* **2008**, *141*, 757–763.
14. N. S. Gandhi, R. L. Mancera, *Chem. Biol. Drug. Des.* **2008**, *72*, 455–482.
15. U. R. Desai, H.-M. Wang, T. R. Kelly, R. J. Linhardt, *Carbohydr. Res.* **1993**, *241*, 249–259.
16. E. A. Yates, F. Santini, M. Guerrini, A. Naggi, G. Torri, B. Casu, *Carbohydr. Res.* **1996**, *294*, 15–27.
17. D. R. Ferro, A. Provasoli, M. Ragazzi, G. Torri, B. Casu, G. Gatti, J. C. Jacquinet, P. Sinay, M. Petitou, J. Choay, *J. Am. Chem. Soc.* **1986**, *108*, 6773–6778.

18. D. R. Ferro, A. Provasoli, M. Ragazzi, B. Casu, G. Torri, V. Bossennec, B. Perly, P. Sinaÿ, M. Petitou, J. Choay, *Carbohydr. Res.* **1990**, *195*, 157–167.
19. E. A. Yates, C. J. Terry, C. Rees, T. R. Rudd, L. Duchesne, M. A. Skidomore, R. Levy, N. T. K. Thanh, R. J. Nichols, D. T. Clarke, D. G. Fernig, *Biochem. Soc. Trans.* **2006**, *34*, 427–430.
20. M. Hricovini, P.-A. Driguez, O. L. Malkina, *J. Phys. Chem. B* **2014**, *118*, 11931–11942.
21. M. Hricovini, *J. Phys. Chem. B* **2011**, *115*, 1503–1511.
22. T. R. Rudd, E. A. Yates, M. Hricovini, *Curr. Med. Chem*. **2009**, *16*, 4750–4766.
23. M. D. Battistel, H. F. Azurmendi, Y. Bingwu, D .I. Freedberg, *Prog. Nuclear Mag. Res. Spectr.* **2014**, *79*, 48–68.
24. J. Kreuger, D. Spillmann, J.-P. Li, U. Lindahl, *J. Cell Biol.* **2006**, *174*, 323–327.
25. D. J. D. Johnson, W. Li, T. E. Adams, J. A. Huntington, *EMBO J.* **2006**, *25*, 2029–2037.
26. K. Tan, M. Duquette, J.-H. Liu, R. Zhang, A. Joachimiak, J.-H Wang, J. Lawler, *Structure* **2006**, *14*, 33–42.
27. M. Petitou, C. A. A. van Boeckel, *Angew. Chem. Inter. Ed.* **2004**, *43*, 3118–3133.
28. M. Petitou, P. Duchaussoy, P. A. Driguez, G. Jaurand, J. P. Herault, J.-C. Lormeau, C. A. A. van Boeckel, J.-M. Herbert, *Angew. Chem. Int. Ed.* **1998**, *37*, 3009–3014.
29. M. Hricovini, *J. Phys. Chem. B* **2015**, *119*, 12397–12409.
30. M. Hricovini, M. Guerrini, A. Bisio, G. Torri, M. Petitou, B. Casu, *Biochem J.* **2001**, *359*, 265–272.
31. U. Desai, R. Swanson, S. C. Bock, I. Bjork, S. T. Olson, *J. Biol. Chem.* **2000**, *275*, 18976–18984.
32. V. Arocas, S. C. Bock, S. T. Olson, I. Björk, *Biochemistry* **1999**, *38*, 10196–10204.
33. M. Petitou, J.-C. Lormeau, J. Choay, *Eur. J. Biochem*. **1985**, *176*, 637–640.
34. M. Guerrini, S. Guglieri, D. Beccati, G. Torri, C. Viskov, P. Mourier, *Biochem. J.* **2006**, *399*, 191–198.
35. M. Guerrini, M. Hricovíni, G. Torri, *Curr. Pharm. Des.* **2007**, *13*, 2045–2056.
36. J. Wesche, K. Haglund, E. M. Haugsten, *Biochem. J.* **2011**, *437*, 199–213.
37. P. Chiodelli, A. Bugatti, C. Urbinati and M. Rusnati, *Molecules* **2015**, *20*, 6342–6388.
38. J. H. Dey, F. Bianchi, J. Voshol, D. Bonenfant, E. J. Oakeley, N. E. Hynes, *Cancer Res.* **2010**, *70*, 4151–4162.
39. M. Koziczak, T. Holbro, N. E. Hynes, *Oncogene* **2004**, *23*, 3501–3508.
40. S. Faham, R. E. Hileman, J. R. Fromm, R. J. Linhardt, D. C. Rees, *Science* **1996**, *271*, 1116–1120.
41. S. Faham, R. J. Linhardt, D. C. Rees, *Curr. Opin. Struct. Biol*.**1998**, *8*, 578–586.
42. S. Guimond, M. Maccarana, B. B. Olwin, U. Lindahl, A. C. Rapraeger, *J. Biol. Chem.* **1993**, *268*, 23906–23914.
43. S. Guglier, M. Hricovíni, R. Raman, L. Polito, G. Torri, B. Casu, R. Sasisekharan, M. Guerrini, *Biochemistry* **2008**, *47*, 13862–13869.
44. R. Raman, G. Venkataraman, S. Ernst, V. Sasisekharan, R. Sasisekharan, *Proc. Natl. Acad. Sci. USA* **2003**, *100*, 2357–2362.
45. L. Pellegrini, D. F. Burke, F. von Delft, B. Mulloy, T. L. Blundell, *Nature* **2000**, *407*, 1029–1034.
46. E. Hammond, A. Khurana, V. Shridhar, K. Dredge, *Front. Oncol.* **2014**, *4*, 1–15.
47. A. M. Gomes, M. P. Stelling, M. S. G. Pavão, *BioMed Res. Int.* **2013**, *2013* 1–11.
48. J. C. Wilson, A. E. Laloo, S. Singh and V. Ferro, *Biochem. Biophys. Res. Commun.* **2014**, *443*, 185–188.
49. C. Pisano, I. Vlodavsky, N. Ilan and F. Zunino, *Biochem. Pharmacol.* **2014**, *89*, 12–19.
50. F. Levy-Adam, N. Ilan, I. Vlodavsky, *Sem. Cancer Biol*. **2010**, *20*, 153–160.

51. I. Stevic, N. Parmar N. Paredes L. R. Berry, A. K. Chan, *Cell Biochem. Biophys.* **2011**, *59*,171–178.
52. T. R. Rudd, S. E. Guimond, M. A. Skidmore, L. Duchesne, M. Guerrini, G. Torri, C. Cosentino, A. Brown, D. T. Clarke, J. E. Turnbull, D. G. Fernig, E. A. Yates, *Glycobiology* **2007**, *17*, 983–993.
53. S. E. Guimond, T. R. Rudd, M. A. Skidmore, A. Ori, D. Gaudesi, C. Cosentino, M. Guerrini, R. Edge, D. Collison, E. McInnes, G. Torri, J. E. Turnbull, D. G. Fernig, E. A. Yates, *Biochemistry* **2009**, *48*, 4772–4779.
54. T. R. Rudd, M. A. Skidmore, S. E. Guimond, M. Guerrini, C. Cosentino, R. Edge, A. Brown, D. T. Clarke, G. Torri, J. E. Turnbull, R. J. Nichols, D. G. Fernig, E. A. Yates, *Carbohydr. Res.* **2008**, *343*, 2184–2193.
55. K. J. Murphy, N. McLay, A. D. Pye, *J. Am. Chem. Soc*. **2008**, *130*, 12435–12444.
56. T. Toida, R. J. Linhardt, *Electrophoresis* **1996**, *17*, 341–346.
57. H. Xie, Y. J. Kang, *Curr. Med. Chem*. **2009**, *16*, 1304–1314.
58. L. D. D'Andrea, A. Romanelli, R. Di Stasi, C. Pedone, *Dalton Trans.* **2010**, *39*, 7625–7636.
59. K. W. Hung, T. K. S. Kurnar, K. M. Kathir, P. Xu, F. Ni, H. H. Ji, M. C. Chen, C. C. Yang, F. P. Lin, I. M. Chiu, C. Yu, C. *Biochemistry* **2005**, *44,* 15787–15798.
60. G. Grasso, A. M. Santoro, A. Magri, D. La Mendola, M. F. Tomasello, S. Zimbone, E. Rizzarelli, *J. Inorg. Biochem*. **2016**, *159*, 149–158.
61. J. Folkman, R. Langer, R. J. Lindhardt, C. Haudenshild, S. Taylor, *Science* **1983**, *221*, 719–725.
62. A. J. Hughes, R. Hussain, C. Cosentino, M. Guerrini, G. Siligardi, E. A. Yates, T. R. Rudd, *Biochem. Biophys. Res. Comm*. **2012**, *425*, 794–799.
63. F. Zhang, X. Liang, J. M. Beaudet, Y. Lee and R. J. Linhardt. *J. Biom. Tech. Res.* **2014**, *1*, 6000101.
64. R. I. W. Osmond, W. C. Kett, S. E. Skett, D. R. Coombe, *Anal. Biochem*. **2002**, *310*, 199–207.
65. S. Cochran, C. P. Li, V. Ferro, *Glycocong. J.* **2009**, *26*, 577–587.
66. D. L. Rabenstein, J. M. Robert, J. Peng, *Carbohydr. Res.* **1995**, *278*, 239–256.
67. L. Lerner, D. A. Torchia, *J. Biol. Chem*. **1986**, *261*, 12706–12714.
68. E. F. Naggar, C. E. Costello, J. Zaia, *J. Am. Soc. Mass Spectrom*. **2004**, *15*, 1534–1544.
69. Y. Seo, M. R. Schenauer, J. A. Leary, *Inter. J. Mass Spectrom*. **2011**, *303*, 191–198.
70. F. Chevalier, R. Lucas, J. Angulo, M. Martin-Lomas, P. M. Nieto, *Carbohydr. Res.* **2004**, *339*, 975–983.
71. F. Chevalier, J. Angulo, R. Lucas, P. M. Nieto, M. Martin-Lomas, *Eur. J. Org. Chem.* **2002**, *14,* 2367–2376.
72. C. Shao, F. Zhang, M. M. Kemp, R. J. Linhardt, D. M. Waisman, J. F. Head, B. A. Seaton, *J. Biol. Chem*. **2006**, *281*, 31689–31695.
73. G. S. Manning, *Macromolecules* **2008**, *41*, 6217–6227.
74. B. B. Minsky, A. Atmuri, I. A. Kaltashov, P. L. Dubin, *Biomacromolecules* **2013**, *14*, 1113–1121.
75. J. B. Mangrum, B. J. Engelmann, E. J. Peterson, J. J. Ryan, S. J. Berners-Price, N. P. Farrell, *Chem. Commun.* **2014**, *50,* 4056–4058.
76. D. Grant, W. F. Long, F. B. Williamson, *Biochem. Soc. Trans.* **1996**, *24*, 204S.
77. C. M. Lee, T. Tanaka, T. Murai, M. Kondo, J. Kimura, W. Su, T. Kitagawa, T. Ito, H. Matsuda and M. Miyasaka, *Cancer Res.* **2002**, *62*, 4282–4288.
78. N. A. Tong, T. P. Nguyen, N. Cuu Khoa, N. Q. Tran, *J. Biomater. Sci. Polym*. **2016**, *27*, 709–720.
79. A. Kreślak, A. Lipińska, *Gen. Physiol. Biophys.* **2002**, *21*, 267–276.
80. J. S. Zhang, T. Imai, A. Suenaga, M. Otagiri, **2002**, *Int. J. Pharm*. *240*, 23–31.
81. J. S. Zhang, T. Imai, M. Otagiri, *Arch. Toxicol*. **2000**, *74*, 300–307.

82. J. S. Zhang, M. Anraku, D. Kadowaki, T. Imai, A. Suenaga, A. Odani, M. Otagiri, *Carbohydr. Res.* **2011**, *346*, 631–637.
83. T. G. Appleton, J. R. Hall, S. F. Ralph, C. S. M. Thompson, *Inorg. Chem.* **1984**, *23*, 3521–3525.
84. S. J. Berners-Price, L. Ronconi, P. J. Sadler, *Prog. Nucl. Magn. Reson. Spectr.* **2006**, *49*, 65–98.
85. M. S. Davies, S. J. Berners-Price, T. W. Hambley, *Inorg. Chem.* **2000**, *39*, 5603–5613.
86. J. Zhang, D. S. Thomas, M. S. Davies, S. J. Berners-Price, N. Farrell, *J. Biol. Inorg. Chem.* **2005**, *10*, 652–666.
87. R. A. Ruhayel, B. Corry, C. Braun, D. S. Thomas, S. J. Berners-Price, N. P. Farrell, *Inorg. Chem.* **2010**, *49*, 10815–10819.
88. E. L. Becker, H. O. Heinemann, K. Igaraski, J. E. Hodler, H. Gershberg, *J. Clin. Invest.* **1960**, *39*, 1909–1913.
89. K. R. Krijgsheld, E. Scholtens, G. J. Mulder, *Comp. Biochem. Physiol.* **1980**, *67A 683–686*.
90. A. Binter, J. Goodisman, J. C. Dabrowiak, *J. Inorg. Biochem*. **2006**, *100*, 1219–1224.
91. A. J. Di Pasqua, C. R. Centerwall, D. J. Kerwood, J. C. Dabrowiak, *Inorg. Chem*. **2009**, *48*, 1192–1197.
92. N. P. Farrell, *Chem. Soc. Rev.* **2015**, *44*, 8773–8785.
93. N. P. Farrell, *Drugs of The Future* **2012**, *37*, 795–806.
94. S. Komeda, T. Moulaei, K. K. Woods, M. Chikuma, N. P. Farrell, L. D. Williams, *J. Am. Chem. Soc.* **2006**, *128*, 16092–16103.
95. S. Komeda, T. Moulaei, M. Chikuma, A. Odani, R. Kipping, N. P. Farrell, L. D. Williams, *Nucleic Acids Res.* **2011**, *39*, 325–336.
96. Y. Qu, R. Kipping, N. P. Farrell, *Dalton Trans.* **2015**, *44*, 3563–3572.
97. E. J. Peterson, A. G. Daniel, S. J. Katner, L. Bohlmann, C-W. Chang, A. Bezos, C. R. Parish, M. von Itzstein, S. J. Berners-Price, N. P. Farrell, *Chem. Sci*. **2017** ***8***, 241–252.
98. A. L. Harris, J. J. Ryan, N. P. Farrell, *Mol. Pharmacol.* **2006**, *69*, 666–672.
99. A. L. Harris, X. Yang, A. Hegmans, L. Povirk, J. J. Ryan, L. Kelland, N. P. Farrell, *Inorg. Chem*. **2005,** *44*, 9598–9600.
100. S. M. Fuchs, R. T. Raines, *Biochemistry* **2004**, *43*, 2438–2444.
101. S. M. Fuchs, R. T. Raines, *Cell Mol. Life Sci.* **2006**, *63*, 1819–1822.
102. M. Belting, *Trends Biochem. Sci.* **2003**, *28*, 145–151.
103. H. Silva, F. Frézard, E. J. Peterson, P. Kabolizadeh, J. J. Ryan, N. P. Farrell, *Mol. Pharmaceutics* **2012**, *9*, 1795–1802.
104. M. M. Fuster, J. D. Esko, *Nature Reviews* **2005**, *5*, 526–542.
105. R. G. Lewis, A. F. Spenser, J. E. Silbert, *Biochem. J.* **1973**, *134*, 455–463.
106. Y. Kawaguchi, T. Takeuchi, K. Kuwata, J. Chiba, Y. Hatanaka, I. Nakase, S. Futaki, *Bioconjugate Chem.* **2016,** *27*, 1119–1130.
107. L. Bohlmann, C. Chang, I. Beacham, M. von Itzstein, *ChemBioChem* **2015**, ***16***, 1205–1211.
108. E. Hammond, C. P. Li, V. Ferro, *Anal. Biochem.* **2010**, *396*, 112–116.
109. G. Torri, B. Casu, G. Gatti, M. Petitou, J. Choay, J. C. Jacquinet, P. Sinay, *Biochem. Biophys. Res. Commun.* **1985**, *128*, 134–140.
110. W H. Zhao, H. Liu, Y. Chen, X. Xin, J. Li, Y. Hou, Z. Zhang, X. Zhang, C. Xie, M. Geng, J. Ding, *Cancer Res.* **2006**, *66*, 8779–8787.
111. A. Ziegler, J. Seelig, *Biophys. J.* **2008**, *94*, 2142–2149.
112. L. N. Waller, N. Fox, K. F. Fox, A. Fox, R. L. Price, *J. Microbiol. Methods* **2004**, *58*, 23–30.
113. G. I. Rozenberg, J. Espada, L. L. de Cidre, A. M. Eiján, J. C. Calvo, G. E. Bertolesi, *Electrophoresis* **2001**, *22*, 3–11.

114. T.-T. Cheng, J.-L. Yao, X. Gao, W. Sun, S. Shi, T.-M. Yao, *Analyst* **2013**, *138*, 3483–3489.
115. Y. Yu, H. Li, Y. Yang, Y. Ding, Z. Wang, G. Li, *Anal. Chem*. **2016**, *88*, 12287–12293.
116. X.-W. Liu, J.-L. Wu, Y.-D. Chen, L. Li, D.-S. Zhang, *Inorg. Chim. Acta* **2011**, *379*, 1–6.
117. K. Chen, M. Schmittel, *Analyst* **2013**, *138*, 2405–2410.
118. S. M. Bykchov, V. N. Kharlamova, *Bull. Exper. Biol. Med.* **1974**, *78*, 28–31.

5

The Deceptively Similar Ruthenium(III) Drug Candidates KP1019 and NAMI-A Have Different Actions. What Did We Learn in the Past 30 Years?

Enzo Alessio [1] ***and Luigi Messori*** [2]

[1]Department of Chemical and Pharmaceutical Sciences, University of Trieste, Via L. Giorgieri 1, I-34127 Trieste, Italy
<alessi@units.it>

[2]Department of Chemistry 'Ugo Schiff', University of Florence, Via della Lastruccia 3–13, I-50019 Sesto Fiorentino, Italy
<luigi.messori@unifi.it>

ABSTRACT 142
1. INTRODUCTION 142
    1.1. History 144
2. COMPARISON OF NAMI-A AND KP1019 145
    2.1. Clinical Investigations 145
        2.1.1. NAMI-A 145
        2.1.2. KP1019 and KP1339 147
    2.2. Chemical Features and Chemical Behavior in Solution 147
        2.2.1. NAMI-A 147
        2.2.2. KP1019 and KP1339 148
    2.3. *In Vivo* Results: Animal Tests and Biodistribution 149
        2.3.1. NAMI-A 149
        2.3.2. KP1019 and KP1339 149
    2.4. *In Vitro* Results: Cytotoxicity 150
        2.4.1. NAMI-A 150
        2.4.2. KP1019 and KP1339 150

Metal Ions in Life Sciences, Volume 18 Edited by Astrid Sigel, Helmut Sigel, Eva Freisinger, and Roland K. O. Sigel

https://doi.org/10.1515/9783110470734-005

Met. Ions Life Sci. **2018**, *18*, 141–170

2.5. Transport Mechanisms in the Blood and Binding to Serum Proteins 151
2.5.1. KP1019 151
2.5.2. NAMI-A 154
2.6. Cellular Uptake and Intracellular Distribution 154
2.6.1. NAMI-A versus KP1019/1339 155
2.7. Interactions with DNA 156
2.7.1. NAMI-A versus KP1019 156
2.8. Interactions with Proteins 158
2.8.1. NAMI-A 158
2.8.2. KP1019 160
2.9. Cellular Effects and Cellular Death Mechanisms 160
2.9.1. NAMI-A 161
2.9.2. KP1019 and KP1339 162
2.10. Hypotheses on the Mechanisms of Action 163
2.10.1. NAMI-A 163
2.10.2. KP1019 and KP1339 163
3. CONCLUSIONS AND OUTLOOK 164
ACKNOWLEDGMENTS 165
ABBREVIATIONS AND DEFINITIONS 165
REFERENCES 166

Abstract: The general interest in anticancer metal-based drugs and some encouraging pharmacological results obtained at the beginning of the investigations on innovative Ru-based drugs triggered a lot of attention on NAMI-A and KP1019, the two Ru(III) coordination compounds that are the subject of this review. This great attention led to a considerable amount of scientific results and, more importantly, to their eventual admission into clinical trials. Both complexes share a relatively low systemic toxicity that allows reaching rather high dosages, comparable to those of carboplatin. Soon it became evident that NAMI-A and KP1019, in spite of their structural similarity, manifest very distinct chemical and biological properties. The pharmacological performances qualified KP1019 mainly as a cytotoxic drug for the treatment of platinum-resistant colorectal cancers, whereas NAMI-A gained the reputation of a potential anticancer drug with negligible effects on the primary tumor but a pronounced ability to affect metastases. We believe that a strictly comparative exam of NAMI-A and KP1019, based on the substantial body of studies accomplished since their discovery almost 30 years ago, might be an useful exercise, both for assessing the state of the art in terms of biological and clinical profiles, and of the inherent mechanisms, and for envisaging possible future developments in the light of past achievements.

Keywords: anticancer · antimetastatic · clinical study · protein binding · ruthenium · uptake

1. INTRODUCTION

As demonstrated by the graph reported in Figure 1, the number of studies on ruthenium anticancer compounds has been increasing constantly since the early 80's of last century. At that time the focus was almost exclusively on Pt drugs. The fact that two structurally similar Ru(III) coordination compounds, known as

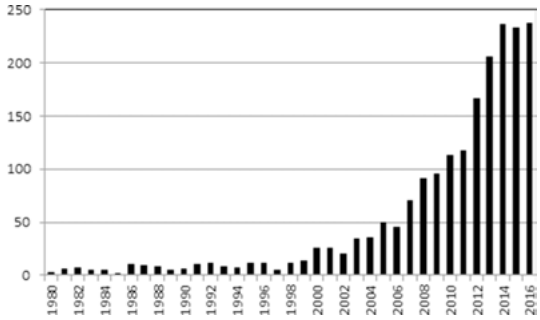

Figure 1. Number of publications per year (according to Scopus®, Jan. 2017) that contain either in the title, abstract or keywords at least one of the following terms ruthenium & anticancer, or ruthenium & antitumor, or ruthenium & cytotoxic, or ruthenium & cytotoxicity.

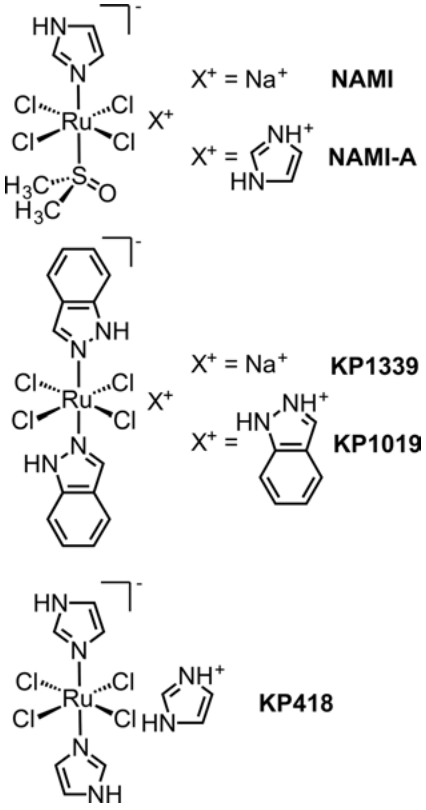

Figure 2. Schematic structures of the Ru(III) anticancer drug candidates subject of this work. KP1019 is sometimes also called FFC14, or FFC14a, or FFC14A. The sodium salt of KP1019, besides KP1339, is also called KP-1339, or NKP1339, or – more recently – IT-139. In the early days, the imidazole complex KP418 was called ICR.

NAMI-A and KP1019 [NAMI-A = (ImH)[*trans*-$RuCl_4$(dmso-S)(Im)], Im = imidazole; KP1019 = (IndH)[*trans*-$RuCl_4(Ind)_2$], Ind = indazole, Figure 2], reached the stage of clinical investigation on human beings, thus opening the way to new expectations, greatly contributed to the growth of interest on this topic.

This chapter aims to summarize and compare the main features of these two ruthenium drug candidates almost 30 years after their discovery, highlighting the similarities as well as the – often unexpected – differences, ending up with the current understanding of their mechanisms of action. Several previous review articles focused on KP1019 [1–3] or NAMI-A [4–10] or dealing with both [11–19] (and other Ru compounds) can be found in the literature.

1.1. History

Soon after the discovery by Barnett Rosenberg and coworkers that some simple Pt(II) coordination compounds are endowed with a potent anticancer activity, compounds based on different metals started to be investigated in this respect as well. Pioneering work on Ru complexes was performed by Clarke and coworkers who investigated simple Ru(III) chloro-ammine compounds, such as *fac*-$[RuCl_3(NH_3)_3]$ and *cis*-$[RuCl_2(NH_3)_4]Cl$ [20], in which the influence of cisplatin is quite evident. With similar motivations, as early as 1977, Mestroni, Sava et al. investigated the anticancer properties of *cis*-$RuCl_2(dmso)_4$ (dmso = dimethylsulfoxide) [21]: similarly to cisplatin, this complex is neutral and has two *cis* chlorides (the presumed leaving ligands); in addition, dmso was expected to facilitate the diffusion of the complex through the cell membrane.

However, the real break-through in ruthenium anticancer compounds occurred in 1986 when Keppler et al. reported for the first time the antitumor activity of the water-soluble anionic Ru(III) complex imidazolium *trans*-bis-imidazole tetrachlororuthenate(III), (ImH)[*trans*-$RuCl_4(Im)_2$] (Im = imidazole), later labeled KP418 (Figure 2), against P388 leukemia and the B16 melanoma in BDF_1 mice [22]. The tumor-inhibiting effect was comparable or better than that of cyclophosphamide, cisplatin, or 5-fluorouracil used as positive reference compounds. Most importantly, one year later, Keppler and coworkers reported that KP418 is considerably effective, in a dose-dependent manner, against the growth of AMMN-induced colorectal adenocarcinoma in SD rats [23]. Comparable results, with a tumor growth inhibition exceeding 90 %, were later obtained with the less toxic indazole (Ind) analogue, HInd[*trans*-$RuCl_4(Ind)_2$] (KP1019, Figure 2) [24]. Notably, this tumor model – that mimics very closely the human situation – is not sensitive to clinically established antineoplastic agents, including cisplatin, with the exception of the 5-fluorouracil/leucovorin combination therapy, which shows moderate activity. For example, whereas KP1019 at the optimum dose of 13 mg/kg reached a T/C value of 27 % (T/C = ratio of increases in mean tumor volume of treated and control groups) combined with 0 % mortality, the standard therapy of 5-fluorouracil and leucovorin resulted in a moderate antitumor activity (T/C = 45 %) accompanied by a very high mortality (33 %) [25].

The exciting results reported by Keppler and coworkers eventually led to the development, in the early 90's, of the compound known as NAMI-A. Mestroni and Alessio first prepared the Ru(III)-dmso intermediate X[*trans*-$RuCl_4$(dmso-$S)_2$] ($X^+ = (dmso)_2H^+$, Na^+, NH_4^+) that has an obvious structural similarity with the anticancer active *trans*-azole Ru(III) complexes (KP-type compounds) described above [26]. Even though itself unsuited for biological tests owing to its high lability, Na[*trans*-$RuCl_4$(dmso-$S)_2$] turned out to be an excellent precursor for compounds of the general formula Na[*trans*-$RuCl_4$(dmso-S)(L)] (where $L = NH_3$, azole or pyridine) that showed improved stability in aqueous solution [27, 28]. Tests performed by Sava and coworkers on solid metastasizing tumors in mice evidenced that these compounds (as well as the less soluble neutral derivatives of formula *mer*-$RuCl_3(dmso)_2(L)$) induced a remarkable reduction of lung metastasis formation, significantly greater than the unimpressive reduction of primary tumor growth [29, 30]. The antimetastatic effect was more pronounced with low doses given daily than with large doses given with drug-free intervals. From these early studies the well water-soluble imidazole complex Na[*trans*-$RuCl_4$(dmso-S)(Im)] (NAMI, Figure 2) was selected for further investigations. NAMI was later replaced by the corresponding imidazolium salt, (ImH)[*trans*-$RuCl_4$(dmso-S)(Im)], called NAMI-A, that has improved preparation, stability in the solid state and analytical profile, while maintaining a good solubility in water [31].

Quite remarkably, both the KP-type and the NAMI-A-type compounds did not go through the usual pre-screening of *in vitro* cytotoxicity against cancer cell lines, but were investigated immediately on animal models. This unusual procedure was instrumental to their further developments: in fact, neither one of these structurally similar Ru(III) complexes is particularly cytotoxic (see also below) [32].

2. COMPARISON OF NAMI-A AND KP1019

2.1. Clinical Investigations

We decided to start this comparative report from the end of the story because we believe that the results of a clinical investigation are "*the real thing*". The clinical study, besides being the aim and the justification of all the work previously done on the drug candidate, provides a wealth of precious information, often unpredictable and unrelated to the preclinical studies, and – most importantly – determines the fate of the compound. A phase I is a dose-escalation (i.e., dose-finding) and pharmacokinetic study performed on tumor patients without further established therapeutic options. Conversely, a phase II study is aimed to establish the efficacy of the drug candidate against selected tumors.

2.1.1. NAMI-A

NAMI-A was the first ruthenium drug candidate to be tested on humans [33]. In 1999, after extensive preclinical studies, a phase I study was performed at the

National Cancer Institute of Amsterdam (NKI). Twenty-four adult patients, with different types of solid tumors, were treated at 12 dose levels (2.4–500 mg/m^2/day). NAMI-A, was given as an intravenous (i. v.) infusion (3 h) for 5 consecutive days every 3 weeks. Hematological toxicity was negligible. Mild and completely reversible renal toxicity was observed at the highest doses. Nausea, vomiting, and diarrhea were significant but treatable. At 400 mg/m^2/day painful blisters started to develop on fingers and toes, and became very persistent at higher doses. Owing to this unprecedented and dose-limiting form of toxicity, the advised dose for further testing of NAMI-A according to this schedule was 300 mg/m^2/day. At this dose level the toxicity, mainly in the form of general malaise and mild nausea and vomiting, was mild to moderate. Overall, the toxicity profile of NAMI-A was quite different from that of the platinum anticancer drugs. In blood, ruthenium was found to be largely bound to proteins. As a consequence, the total body retention of Ru was longer than expected from the preclinical studies [34].

Even though partial or complete responses were not obtained, disease stabilization was observed in heavily pretreated patients with advanced non-small cell lung cancer (NSCLC) and one of them had stable disease for 21 weeks. This result, together with the excellent activity shown by NAMI-A against lung metastases in mice models (see above Section 1.1), suggested NSCLC as the target disease for a phase II study. In addition, since gemcitabine + cisplatin regimens are widely used for first-line treatment of NSCLC [35], it was decided to use a similar combination with NAMI-A replacing cisplatin.

Thus, after very promising preclinical tests, in 2008–2011 a phase I/II combination study of NAMI-A + gemcitabine was carried out at NKI on 32 patients with advanced NSCLC [36]. In the phase I of the study dose-escalation of NAMI-A was initially performed in a 28 day cycle (3 h i. v. infusion on days 1, 8, and 15), later amended into a 21 day cycle (days 1 and 8) due to frequent neutropenic dose interruptions in the third week when the NAMI-A dose was increased. Gemcitabine was given at the typical dose of 1 g/m^2 on each day subsequent to the administration of NAMI-A. The maximal tolerable dose (MTD) of NAMI-A was found to be 300 mg/m^2 in the 28 day cycle and 450 mg/m^2 in the 21 day cycle. A further increase to 600 mg/m^2 induced dose-limiting toxicity (DLT) in the form of the already mentioned blisters. In addition to the common terminology criteria (CTC) grade 2–4 neutropenia and anemia, at the highest doses, the main non-hematological adverse events were elevated liver enzymes, transient creatinine elevation, renal toxicity, constipation, and fatigue.

In the phase II of the study, 15 patients were treated with the previously established MTD of NAMI-A (450 mg/m^2 in the 21 day cycle) for assessing the antitumor activity according to the response evaluation criteria in solid tumors (RECIST) [37]. Since the efficacy of the treatment (1 case of partial remission and 10 patients with stable disease for at least 6–8 weeks) was lower than expected for gemcitabine alone, the further expansion of the phase II cohort with additional patients was not pursued. Overall, the combination of NAMI-A with gemcitabine was only moderately tolerated by patients and experienced as very exhausting mainly because of the quite severe nausea, vomiting, and diarrhea. The treatment was declared to be "*insufficiently effective for further use*" [36].

2.1.2. KP1019 and KP1339

A small-scale phase I investigation was performed with KP1019 on eight patients with advanced solid tumors [2, 38]. The complex, that was actually reconstituted from the sodium salt and Ind·HCl in a 1 : 1.1 ratio for stabilizing the infusion solution, was given i.v. twice weekly over 3 weeks. It was overall very well tolerated in the investigated dose range (total doses from 25 to 600 mg) and only mild toxicity was observed [39]. Disease stabilization for 8–10 weeks, unrelated to the dose, was observed for five out of six evaluable patients. Even though the DLT was not reached, the relatively low solubility of KP1019 did not allow further dose escalation (too large volume of infusion solution required). For this reason, an additional full-scale phase I study was performed with the ca. 35-fold more soluble sodium derivative Na[*trans*-$RuCl_4(Ind)_2$] (KP1339, Figure 2), obtained from KP1019 in a two-step cation exchange via the tetramethylammonium salt [40]. In this investigation 34 patients were treated at 9 dose levels (20–780 mg/m^2/day) in a 28 day cycle (i.v. infusion on days 1, 8, and 15) [3]. In general, only minor side effects were observed. Grade 2–3 nausea, accompanied by increased creatinine levels, was found to be DLT at the highest dose. No MTD was reported. Seven patients, with different types of tumors (including 2 cases of NSCLC), experienced stable disease (SD) up to 88 weeks, and partial response (PR) was observed in one patient with a neuroendocrine tumor.

Very recently, the outcome of a new phase I clinical study performed in the US with KP1339 (now called IT-139) was published [41]. The study, that employed the same dose levels and treatment schedule as the previous one (see above), concerned 46 patients. The MTD was established to be 625 mg/m^2. Also the tolerability and safety profile were similar to those already established. In particular, no significant neurotoxicity and dose-limiting hematological toxicity were found, thus making KP1339 suitable for combination therapies. Overall, the complex showed a modest antitumor activity; however, 3 of the 5 patients with carcinoid neuroendocrine tumors had disease control (two SDs and one PR). The authors, also on the basis of independent *in vitro* studies [42, 43], state that the mechanism of action of KP1339 involves the targeting of the endoplasmic reticulum chaperone protein GRP78, whose levels are highly increased in several cancers in response to stress (see also below Section 2.9.2). The decrease of GRP78 levels leads to increased vulnerability and apoptosis of tumor cells.

2.2. Chemical Features and Chemical Behavior in Solution

2.2.1. NAMI-A

NAMI-A is perfectly stable in the solid state, whereas in aqueous solution it undergoes strongly pH-dependent hydrolytic processes [5, 6, 44, 45]. At 37 °C and physiological conditions (phosphate buffer, pH 7.4, NaCl 0.9 %), the parent complex disappears from the solution within ca. 15 min due to rapid chloride and dmso hydrolysis, leading to the formation of dark-green uncharacterized

poly-oxo species and eventually to a black precipitate. A similar behavior was observed for NAMI-A-type complexes [46], and for [dmtpH][*trans*-$RuCl_4$(dmso-S)(dmtp)] (dmtp = 5,7-dimethyl[1,2,4]triazolo[1,5-a]pyrimidine). The first hydrolysis product of this latter complex, the neutral species [*mer*-$RuCl_3(H_2O)$(dmso-S)(dmtp)], was isolated and characterized [47]. On the contrary, NAMI-A is remarkably more stable at mildly acidic pH (3.0–6.0) and in pure water (pH ca. 5.5), where only slow dmso hydrolysis occurs. For this reason, NAMI-A was administered to patients dissolved in physiological saline made slightly acidic by the citric acid contained in the formulation of the drug [33]. Interestingly, NAMI-A-type complexes bearing azole ligands that are less basic than imidazole, such as pyrazole and thiazole, are more stable than NAMI-A in slightly acidic aqueous solution [48].

The presence in the coordination sphere of the moderate π-acceptor dmso-S gives to NAMI-A-type complexes a relatively high reduction potential [28, 49, 50]. For example, NAMI-A ($E°$ +235 mV versus NHE) at pH 7.4 and 25 °C is quantitatively and instantaneously reduced to the corresponding dianionic Ru(II) species [*trans*-$RuCl_4$(dmso-S)(Im)]$^{2-}$ by the addition of stoichiometric amounts of biologically relevant reducing agents, such as ascorbic acid (AsH, 11–79 μM in blood plasma) and glutathione (GSH, 0.5–10 mM inside the cell) [49, 51].

2.2.2. KP1019 and KP1339

KP1019 is stable in the solid state and has a rather moderate solubility in water where, however, it is sufficiently stable for administration by infusion. In fact, in aqueous solution at 25ºC, slow exchange of one chloride ligand for water (ca. 2 % per hour) occurs [52], generating the corresponding neutral complex *mer,trans*-$RuCl_3(Ind)_2(OH_2)$ that has been isolated and structurally characterized [53]. Similarly to NAMI-A, KP1019 hydrolyzes much faster upon increasing the pH: at 37ºC the half-life of the complex is 5.4 h in phosphate buffer at pH 6.0, whereas it is less than 0.5 h at pH 7.4, where release of the indazole ligands also occurs [52]. The formation of a precipitate within minutes from fresh solutions of KP1019, dependent on concentration, pH, and temperature, is often reported [52, 54].

In phosphate buffer, at pH 7, KP1019 has a lower redox potential compared to NAMI-A ($E°$ = +30 mV versus NHE, measured on the more soluble sodium salt KP1339) [50]. Keppler and coworkers demonstrated that both ascorbic acid and glutathione are capable of reducing the *trans*-$[RuCl_4(Ind)_2]^-$ anion even though at a slower rate compared to NAMI-A: in phosphate-buffered solution, complete reduction of KP1019 required from minutes (AsH) to hours (GSH), even at KP1019:GSH or AsH = 1 : 2 [55]. In parallel, the precipitation of uncharacterized species was observed.

2.3. *In Vivo* Results: Animal Tests and Biodistribution

2.3.1. NAMI-A

As mentioned already, NAMI-A was firstly tested on mice [29, 30] and was found to prevent the development and growth of metastases generated by several solid tumor models, both in the lungs (Lewis lung carcinoma, MCa mammary carcinoma, TS/A mammary carcinoma, B16 melanoma, and H460M2, a human NSCLC xenotransplanted into nude mice) and in the brain (P388 leukemia) [46, 56–60]. The reduction of the number (from 40 to 100 %) and weight (from 70 to 100 %) of metastases led to a significant prolongation of the survival time of the treated mice, and even to cures when combined with the surgical removal of the primary neoplasm [6, 61]. The activity of NAMI-A was peculiarly selective towards metastasis, as no significant inhibition of primary tumor growth was observed. This difference cannot be ascribed to the pharmacokinetics of the complex. In fact, when mice bearing MCa mammary carcinoma were given NAMI-A through intraperitoneal (i.p.) injection, ruthenium concentration in the lungs (comparable to that in the liver and kidneys) was ca. 2–3 times higher than in the solid tumor [49].

A similar ruthenium uptake by primary tumor and host tissues was found in mice bearing Lewis lung carcinoma and treated i.p. with NAMI-A [62]. However, when NAMI-A was injected directly into the tumor mass, the reduction of the primary tumor growth was still modest compared to that of lung metastases even though ruthenium concentration in the solid tumor was ca. one order of magnitude higher than in the lungs (where the concentration was similar to that obtained with i.p. treatment) [61, 63]. It was also found that the decrease of ruthenium level from the lungs, liver, and kidneys is remarkably slower than from the primary tumor, suggesting a stronger binding and persistence in those tissues [63].

2.3.2. KP1019 and KP1339

KP1019 was originally found to be highly active, with a tumor volume reduction up to 95 %, in an autochthonous colorectal carcinoma of the rat that is platinum-resistant and resembles colon cancer of humans (comparable histological appearance and behavior toward chemotherapeutics) [1, 24, 25, 64]. In addition, KP1019 was tested *in vitro* against more than 50 primary tumors explanted from humans: in this highly predictive model, the complex afforded a positive response rate higher than 80 % [65].

The time-dependent tissue distribution of KP1339 (given i.v.) in non-tumor bearing BALB/c nude mice was recently determined [66]. The highest (and comparable) Ru concentrations were found in the liver, lungs, kidneys, and – surprisingly – in the thymus, followed by spleen and colon (ca. 50 % less). Consistent with the trend of total Ru in blood plasma, the peak levels in the mentioned tissues were found 1–6 h after administration and decreased slowly with time, with the exception of the spleen where the highest amount was found 24 h post injection.

The antimetastatic ability of KP1019 was also assessed. Treatment of mice bearing the MCa mammary carcinoma with KP1019 at two dose levels was moderately active in reducing the primary tumor but ineffective in reducing the development of lung metastases [67].

2.4. *In Vitro* Results: Cytotoxicity

2.4.1. NAMI-A

Since the beginning of their development, Sava and coworkers demonstrated that NAMI- and NAMI-A-type complexes have – in general – a negligible cytotoxicity, that is unrelated to their antimetastatic activity [68]. More lipophilic complexes, such as Na[*trans*-$RuCl_4$(TMSO)(Iq)] (TMSO = tetramethylenesulfoxide; Iq = isoquinoline), showed significant cytotoxicity *in vitro* but negligible antimetastatic activity *in vivo* [68]. The substantial lack of cytotoxicity for NAMI-A was later confirmed by other studies [57]. For example, it was shown that NAMI-A is, on average, more than 1000 times less cytotoxic than cisplatin against several tumor cell lines [69], and when tested in the 60-cell line panel of NCI for *in vitro* anticancer drug screening it showed no activity [9]. However, in an indirect test performed on mice bearing Lewis lung carcinoma, NAMI-A was found to target primarily tumor cells endowed with metastatic ability within the primary tumor (see also below Section 2.10.1) [70]. Finally, we and others recently found that – unexpectedly – NAMI-A is strongly cytotoxic (even at low μM concentrations) against several leukemia cell lines, both myeloid and lymphoid, an activity apparently related to the selective inhibition of KCa 3.1 channels (see below) [71].

2.4.2. KP1019 and KP1339

KP1019 is moderately cytotoxic *in vitro*. For example, when tested against a panel of chemo-sensitive cell lines and their chemo-resistant sublines IC_{50} in the range 50–180 μM were found [72]. When compared in several cancer cell lines with its sodium salt KP1339, KP1019 tended to be moderately more cytotoxic (mean IC_{50} 93.1 μM for KP1019 versus 115.1 μM for KP1319) [73]. Nevertheless, the significant correlation of the cytotoxicity profiles suggests that they share similar modes of action. Interestingly, for both compounds no correlation between total cellular drug uptake and cytotoxicity was found [73]. Both KP1019 and KP1339 were moderately cytotoxic (30–95 μM) – but more than cisplatin and etoposide – in colorectal carcinoma cells (SW480 and HT29) upon short-term exposure (24 h) and induced apoptosis predominantly by the intrinsic mitochondrial pathway. However, upon long-term exposure (72 h), cisplatin and etoposide became much more effective than the two Ru compounds [74]. Of particular interest, in view of the results described above for NAMI-A, is the recently reported NCI screening against a 60-cell line panel in which KP1019 showed high response rates in the leukemia cell subpanel [66].

More recently, KP1339 was investigated in more realistic three-dimensional cell culture systems (cancer cell spheroids), where it resulted less cytotoxic compared to conventional two-dimensional cultures (e.g., for HCT116 cells, the IC_{50} was 136 $\pm$ 27 in the 2D model versus 244 $\pm$ 14 in the 3D model) [75]. Similar IC_{50} values were obtained in hypoxic as well as non-hypoxic spheroids, in contrast with the often invoked "activation-by-reduction" hypothesis, according to which Ru(III) compounds serve as pro-drugs and are activated in the hypoxic environment of the solid tumors [3, 10].

2.5. Transport Mechanisms in the Blood and Binding to Serum Proteins

Transport of anticancer ruthenium drugs in the blood stream is an issue that has attracted a lot of attention in the scientific community since the very first studies. Interest in serum proteins, in particular transferrin, was primarily dictated by the consideration that Ru(III) is believed to mimic quite closely the chemical behavior of Fe(III), leading to the concept that the physiological transport mechanisms of iron (the so called "*transferrin route*") might be exploited by non-physiological ruthenium species as a smart way to enter cells, according to a "Trojan horse" strategy [76–78]. In addition, this kind of uptake mechanism seemed particularly attractive for a prospective anticancer drug as cancer cells usually require a far larger amount of iron than healthy cells to fulfil their increased metabolic needs and express – accordingly – a greater number of transferrin receptors [76–78]. Thus, if proved true [10], the transferrin-mediated uptake could impart some degree of selectivity to ruthenium drugs for the high iron demanding cancer cells. The studies, initially focused on the interactions with serum transferrin, were subsequently extended to the major serum protein, i.e., serum albumin. A critical description of the main achievements in this area is given below. It should be noted that the meaningful translation of the *in vitro* findings into mechanistic hypotheses is hampered by remarkable difficulties: (i) it is hard to know the precise nature of the ruthenium species, derived from either complex, that serum proteins will meet *in vivo*, not to mention their concentration; (ii) in the case of transferrin it is similarly difficult to establish the role of naturally abundant Fe(III); (iii) the competition with other biological components is usually not considered; (iv) the release step has been much less investigated.

2.5.1. KP1019

A pioneering study by Kratz et al., published in 1994 [79], first explored the interactions of KP1019 and its imidazole counterpart KP418 with human serum transferrin, in the iron-free apo form (apoTf). Clear evidence for adduct formation was gained, mainly through a joint spectroscopic and chromatographic approach. KP1019 was found to react with apoTf much faster than KP418. Protein binding completely prevented the formation of its insoluble degradation prod-

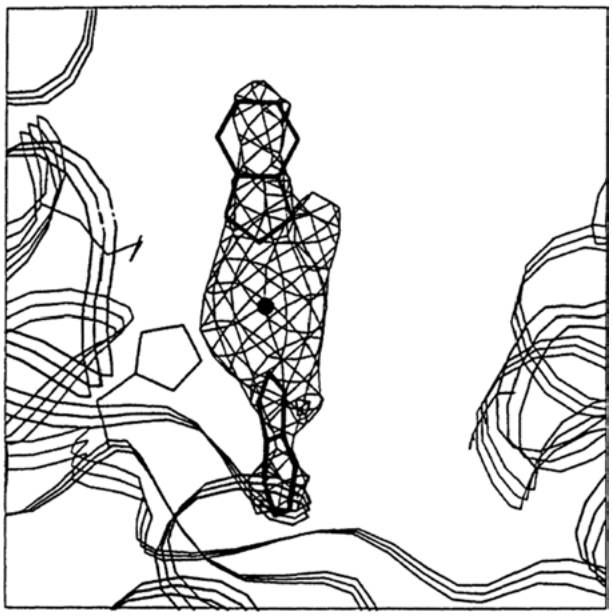

Figure 3. Difference electron density map for KP1019 in the N-terminal site of human apolactoferrin showing that the two indazole ligands are likely retained. The Ru atom binds to His253 and the nearby side chain of Lys301 may help stabilize the binding. Reproduced from [80] with permission; copyright 1994 Hindawi.

ucts that build up in a physiological environment as a consequence of aquation and oligomerization processes (see above Section 2.2.2). This study was quickly supported by structural results describing the nature of the formed metallodrug/protein adducts. Crystallographic investigations were conducted on apo-lactoferrin, a protein that is very similar – both structurally and functionally – to transferrin, for its greater tendency to form crystals suitable for X-ray diffraction measurements. The structure of the adduct of KP1019 with apo-lactoferrin, though solved at relatively low resolution, contributed to elucidate the nature of the occurring interactions [80, 81]. Indeed, a Ru fragment coordinated to a His residue in the iron-binding site of lactoferrin, i.e., His253, was unambiguously detected. Notably, the ruthenium center seems to conserve its two axial indazole ligands whereas losing the chloride ligands (Figure 3).

In the following years, the group of Keppler performed several additional studies on the KP1019/apoTf system and, more in general, on KP1019 binding to serum proteins in the blood but no conclusive evidence was obtained on the actual relevance of the proposed "Tf-shuttle mechanism" [82–87].

Conversely, in substantial agreement with the pharmacokinetic results of the clinical investigations, it was found that a large amount of KP1019 binds rapidly to human serum albumin (HSA), by far the most abundant protein in the plasma (ca. 600 μM, whereas the concentration of transferrin (HSTf) is ca. 15–20 times lower); as a consequence, the percentage of KP1019 associated to transferrin

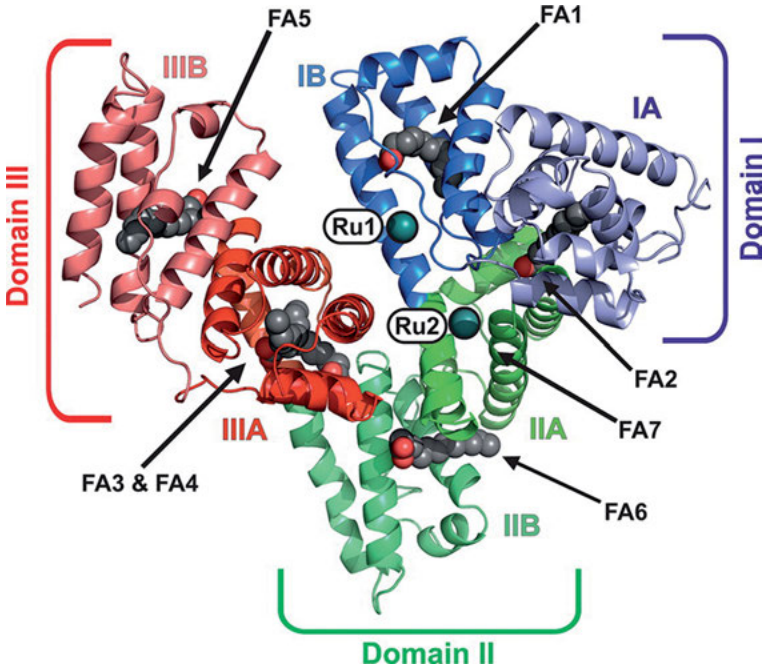

Figure 4. Overall structure of HSA-Myr-KP1339 (PDB ID 5IFO) (Myr = Myrystate). The structure is shown as a cartoon with every domain/subdomain being differently colored and labeled (domain I, blue; domain II, green; domain III, red). The bound metal centers are represented as deep teal spheres and labeled as Ru1 and Ru2, respectively. The seven FAs (fatty acids) bound to HSA are labeled as FA1–7 with bound FAs being displayed as sphere chains (aliphatic chain, grey spheres; carboxylate oxygens, red spheres). Reproduced from [88] with permission; copyright 2016 American Chemical Society.

turned out to be – at best – only a very small fraction of total administered KP1019. This finding further renders the mechanism centered on transferrin less probable and/or less relevant [85–87].

As a corollary to these controversial and sometimes conflicting results, the recent perspective paper by Keppler and coworkers, published in *Chemical Science*, states that the hypothesis of an uptake mechanism based on transferrin for KP1019/KP1339 remains problematic, much debated, and yet not validated [3]. Very recently, the group of Keppler also reported the crystal structure of the adduct formed between KP1019 and HSA [88]. Unambiguous evidence was gained for the binding of two naked Ru ions to histidine residues 146 and 242, which are both located within the well-known hydrophobic binding pockets of albumin (Figure 4). In this case evidence is offered for the dissociation of both indazole ligands from the ruthenium center. By virtue of these findings it was also suggested that HSA, rather than HSTf, could truly serve as a transporter for ruthenium drugs; some selectivity for solid tumor masses might be the consequence of the so-called enhanced permeability and retention (EPR) effect [89].

2.5.2. NAMI-A

Fewer investigations were carried out on the reactions of NAMI-A with serum proteins [90–92]. Studies conducted on the purified proteins indicated that NAMI-A, upon aquation, is able to bind tightly both HSTf and HSA, forming a number of stable adducts at various Ru/protein molar ratios [92]. Similarly to KP1019, it was also shown that binding to serum proteins prevents the aggregation phenomena of NAMI-A typically observed in test-tube experiments. Consistently, *in vivo* studies revealed that a large amount of injected NAMI-A binds rapidly to serum proteins, in particular serum albumin [93]. Yet, poor evidence has been obtained on the hypothesis that these adducts may retain the biological and pharmacological properties of the parent metal complex; this issue is still highly debated. Indeed, whereas the first indications favored the view that NAMI-A upon binding to albumin loses, to a large extent or even completely, its biological and pharmacological properties [92], more recently evidence has been gathered that the adducts formed between NAMI-A and HSA are still able to produce important pharmacological effects at the cellular level potentially linked to its antimetastatic activity, such as increased cell adhesion to the substrate, reduced cell motility and decreased ability of cells to penetrate into collagen gels [94, 95].

Further relevant contributions to the understanding of the interactions of KP1019 and NAMI-A with serum proteins have come from the groups of Lay, Walsby, and Harris, using a variety of spectroscopic methods, in particular XAS, ESR, and ENDOR [96–100]. Both Ru compounds were shown to bind very rapidly to HSA in a noncovalent manner, followed by coordination to protein side chains after ligand exchange. In addition, and again in contrast with the so-called "activation-by-reduction" hypothesis [10], independent ESR and XAS measurements could establish that ruthenium in the adducts predominantly remains in the oxidation state $+3$.

2.6. Cellular Uptake and Intracellular Distribution

Recently, research has moved to consider more extensively and more in depth the effects that putative anticancer ruthenium drugs produce on treated cancer cells, beyond the mere determination of their cytotoxic actions. In this frame Ru cellular uptake and intracellular distribution are topics with relevant mechanistic implications. Indeed, it is reasonable to assume that ruthenium drugs will produce their biological and cytotoxic effects maximally in those cellular compartments where the local concentration of Ru is highest. At the same time, it is important to establish whether the intracellular distribution of Ru is roughly uniform or specific sites are instead present, with a high local Ru concentration. The availability of metal-selective analytical techniques of continuously increasing sensitivity and spatial resolution, such as AAS, ICP-MS, XAS, or X-ray fluorescence, allows today a precise quantitative determination of the metal content in the cells and in the various sub-cellular compartments. These bioanalytical

approaches have been applied in several occasions to both NAMI-A and KP1019 during the past 15 years, through a number of studies [101–103]. The numerous bioanalytical reports that are now available on the uptake and distribution of Ru drugs in cellular models are on the whole rather fragmentary and sometimes conflicting, often dependent on the applied experimental settings; yet, from a careful and critical analysis of the available results, some general trends may be drawn with notable mechanistic implications as illustrated below.

In general, it should be taken into account that the results – in particular the early ones – might be biased by the fact that less attention was paid to separate intracellular ruthenium from ruthenium attached on the cell membrane making the term "intracellular" at least questionable. In addition, as evidenced by Keppler and coworkers [104], protocols using cell lysis in the culture plate that do not include corrections of adsorption effects can produce artefacts to an extent comparable with the actual cellular content. Finally, when biological samples are submitted to relatively harsh extraction/analytical procedures, including chemical/enzymatic treatments (developed for the more robust Pt adducts) prior to performing the metal detection, it should not be forgotten that loss of Ru may occur, leading to an underestimate of ruthenium amounts.

2.6.1. NAMI-A versus KP1019/1339

Several analytical determinations of ruthenium uptake in cancer cells treated with NAMI-A were first performed in the group of Sava in Trieste already in the late 90's. They were mainly based on GFAAS measurements and comprehensively described in a paper which appeared in 2002 [101]. In that paper, the uptake of NAMI-A by KB cells *in vitro* was compared with the effects on the cell cycle phase distribution. It was found that the uptake of ruthenium is proportional to the concentration of NAMI-A in the medium but is significant only for concentrations larger than 100 μM; in addition, the Ru uptake turned out to be higher when cells were incubated in PBS (phosphate-buffered saline) compared to MEM (minimum essential media), stressing the importance of the applied solution conditions [105]. The effect of temperature on Ru uptake was consistent with an active transport mechanism. In turn, the effects of NAMI-A on cell cycle distribution were strictly correlated to ruthenium uptake by tumor cells but not to its extracellular concentration.

Subsequently, a paper by Schellens and coworkers confirmed the relatively low uptake of NAMI-A in four human tumor cell lines (see also below Section 2.7.1) [69].

Similarly, the uptake of KP1019 and KP1339 was analyzed in depth in the group of Keppler [74]. It was shown that both complexes are efficiently taken up into cancer cells: notably a 100 μM ruthenium(III) complex concentration in the growth medium led to the uptake of 120–160 ng ruthenium per 10^6 cells within 30 min. Both KP1019 and KP1339 induced apoptosis in SW480 and HT29 cells predominantly by the intrinsic mitochondrial pathway as indicated by loss of mitochondrial membrane potential.

More recently, the cellular uptake of NAMI-A was investigated in direct comparison to KP1019 in human liver cancer cells by Ru K-edge X-ray absorption spectroscopy. Very remarkably, the cellular uptake of KP1019 was approximately 20-fold higher than that of NAMI-A under the same solution conditions; however, it was also observed that the uptake of the former complex is drastically reduced after aging in cell-culture media, suggesting that the parent complex KP1019 is taken up by cells mostly through passive diffusion [96].

In another, nearly simultaneous, study by Harris and coworkers [102], X-ray fluorescence imaging was exploited to reveal the intracellular distribution of Ru in single human cells treated with KP1019; evidence was obtained that Ru is localized both in the cytosol and in the nuclear region. In stark contrast, Ru could not be visualized in cells treated with NAMI-A under the same conditions, indicating that NAMI-A is not internalized and supporting the concept that its activity is mainly exerted through a membrane-interaction mechanism. These findings are in substantial agreement with independent results obtained by Groessl et al. [103].

On the whole, the above described results highlight a striking difference in the cellular uptake and intracellular distribution behavior for NAMI-A compared to KP1019: NAMI-A, at variance with KP1019, has a poor ability to enter the cytosol; as a consequence, ruthenium associated to cells is mostly located at the membrane level. In any case, the amount of Ru capable of reaching the cell nucleus and binding to DNA is small even for KP1019, and far smaller than for classical Pt drugs.

2.7. Interactions with DNA

As the field of anticancer metal based drugs has been largely dominated by the success of Pt drugs and by the so called “DNA paradigm” to explain their mode of action, subsequent studies on other non-Pt anticancer metal drugs invariantly started from the assumption that DNA might similarly represent the primary biomolecular target. So, even in the case of ruthenium drugs, several investigations were directed at analyzing their interactions with a variety of DNA [73, 74, 106, 107] – and also RNA [108] – molecules, even in the absence of solid evidence proving their importance as targets. The main studies in the field are summarized below.

2.7.1. NAMI-A versus KP1019

An important and comprehensive study analyzing the interactions of NAMI-A and KP1019 with DNA molecules in a cell free medium was contributed by the group of Brabec in 2001 [106]. The modifications of natural DNA produced by these ruthenium(III) compounds were characterized by a battery of biophysical methods including DNA binding studies by atomic absorption spectroscopy, inhibition of restriction endonucleases, mapping of DNA adducts by transcription

assay, interstrand cross-linking quantitation employing gel electrophoresis under denaturing conditions, DNA unwinding studied by gel electrophoresis, circular dichroism analysis of the B→Z transition in DNA, and DNA melting curves measured by absorption spectrophotometry. Overall, results indicated that the two Ru compounds are able to coordinate irreversibly to DNA; however, their DNA binding mode appears to be profoundly different from that of cisplatin.

NAMI-A binds to DNA *in vitro* considerably faster than KP1019 and also cisplatin, in accord with its greater kinetic reactivity; it also forms bifunctional intrastrand adducts on double-helical DNA that are capable of terminating RNA synthesis *in vitro*, while the capability of KP1019 to form such adducts is markedly lower. Even though the binding of both NAMI-A and KP1019 affects the DNA structure, the conformational changes induced by ruthenium drugs are usually smaller than those of platinum drugs, resulting in a less severe DNA damage. It was proposed that the altered DNA binding mode of ruthenium drugs in comparison with cisplatin might be an important factor responsible for their lower cytostatic activity in tumor cells.

A subsequent paper by Schellens et al. [69] explored the cytotoxicity, intracellular accumulation, and DNA adduct formation of NAMI-A *in vitro* in comparison to cisplatin in four distinct human tumor cell lines: IGROV-1, 2008, MCF-7, and T47D. The cytotoxicity of cisplatin correlated well to both intracellular platinum accumulation and DNA binding, whereas that of NAMI-A (on average ca. 1000 times lower than cisplatin) was only related to DNA binding and not to intracellular ruthenium accumulation. Ruthenium intracellular accumulation and DNA binding were about 4.8 and 42 times smaller than those of cisplatin. The low binding of NAMI-A to cellular DNA could not simply be explained by a lower capacity to bind DNA because the absolute level of binding *in vitro* to calf thymus DNA was the same for NAMI-A and cisplatin. The lower cytotoxicity of NAMI-A versus cisplatin may be explained, at least in part, by its reduced reactivity to DNA in intact cells.

A more recent study has appeared on the same topics based on the use of advanced mass spectrometry methods [107]. Specifically, the binding of KP1019 and NAMI-A towards different double-stranded oligonucleotides was probed by electrospray ionization mass spectrometry and compared with that of the platinum drugs cisplatin, carboplatin, and oxaliplatin. Notably, the extent of adduct formation decreased in the following order: cisplatin > oxaliplatin > NAMI-A > KP1019. The binding sites of these metallodrugs on the oligonucleotides were elucidated using top-down tandem mass spectrometry, highlighting in all cases a strong preference for guanine residues.

Further insight into the interactions of Ru drugs with DNA and their relevance comes from the above-mentioned clinical study on NAMI-A [33]. It is worth reminding that no Ru-GG and -AG adduct could be detected in DNA extracted from white blood cells (WBCs) of treated patients, even at the highest applied doses (see above Section 2.1.1); this offers a further indication that DNA is a unlikely target for Ru drugs; however, the lack of detectable Ru-GG and -AG adducts might arise from the fact that such adducts, being less robust than the Pt-DNA adducts, do not survive the extraction/analytical procedures.

2.8. Interactions with Proteins

The interactions of NAMI-A and KP1019 with proteins have been investigated intensely and repeatedly for various reasons. As already pointed out, early studies showed that both ruthenium drugs interact tightly with serum proteins (see above Section 2.5); in addition, the growing evidence that DNA is an unlikely target for Ru drugs (compared to Pt drugs) further prompted researchers to characterize their interactions with a variety of cellular proteins as targets.

A few recent studies were specifically aimed to model, at the atomic level, the interactions of a few putative Ru drugs with standard proteins. These studies, mainly based on a combined X-ray diffraction and ESI-MS approach, elucidated the nature of the occurring interactions and the general mode of Ru binding (so called "*protein ruthenation*"). These aspects are treated exhaustively and competently in a recent structural review by Merlino [109], to which the reader is referred; we will consider here just a few key aspects emerging from those investigations.

2.8.1. NAMI-A

The interactions of NAMI-A with the model proteins lysozyme [110] and carbonic anhydrase [111] have been analyzed in depth and now there is sufficient evidence to illustrate the underlying modes of interaction.

In the case of lysozyme, the X-ray structure shows that NAMI-A behaves as an "ultimate prodrug" [10], losing all its original ligands during the soaking process: the resulting naked ruthenium ions interact with the protein through formation of coordinative bonds to the carboxylate groups of two distinct aspartate residues, i.e., Asp101 and Asp119 (Figure 5).

Similar results were obtained upon solving the crystal structure of the adduct formed between NAMI-A and carbonic anhydrase. Again, a naked ruthenium ion was detected coordinatively bound to the protein; however, in this latter case, the ruthenium ion coordinates to the imidazole group of a solvent-exposed histidine, i.e., His64 (Figure 6).

Also the NAMI-A-type complex having pyridine instead of imidazole, nicknamed AziRu, manifests a similar mode of interaction with model proteins [112]. These aspects are comparatively examined in a recent review paper by Montesarchio et al. [113].

Based on the results illustrated above, we can state that the mechanism of protein ruthenation induced by NAMI-A type compounds has been satisfactorily clarified at the molecular level in various proteins, and seems to be largely conserved. Typically, degradation of the Ru(III) complex anion proceeds completely so that a naked ruthenium ion is eventually bound to the protein at selected side chains, mainly the imidazole group of histidine or the carboxylate group of Asp or Glu.

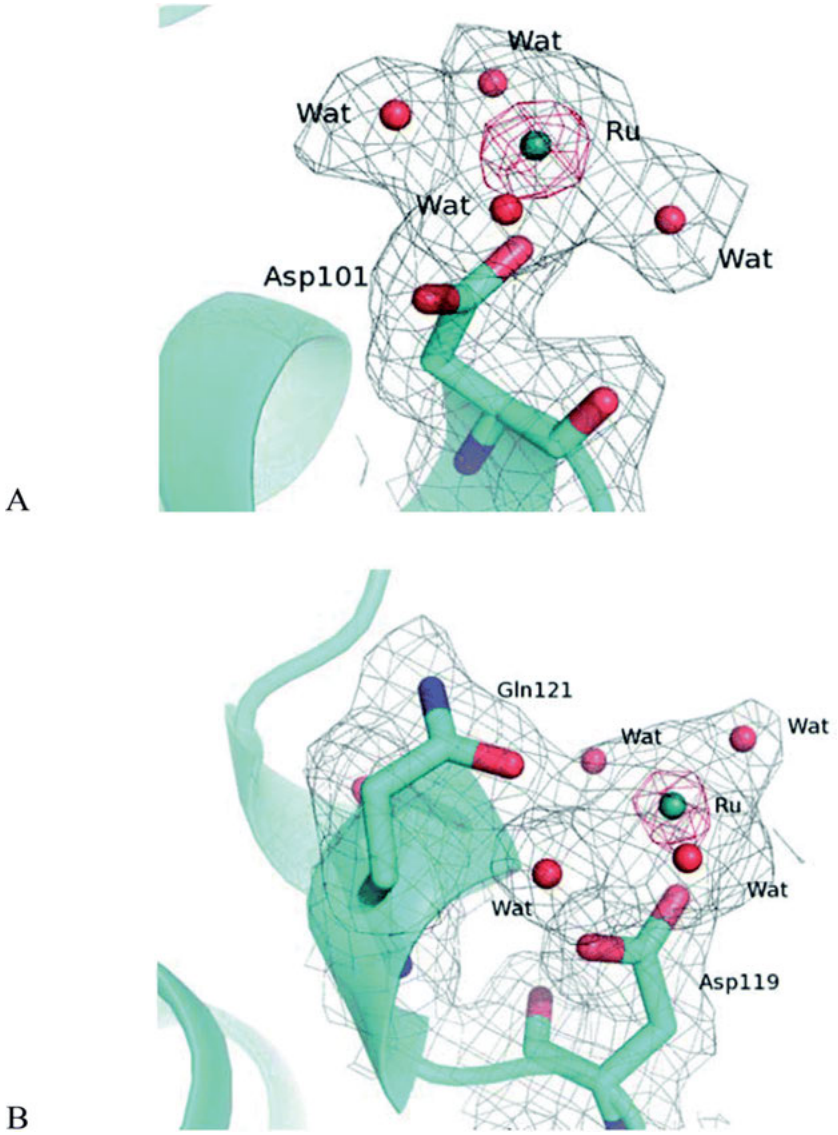

Figure 5. The adduct of NAMI-A with HEWL (= hen egg white lysozyme). $2F_o-F_c$ electron density maps contoured at 0.5 σ level (gray) and 2.0 σ level (red) showing the Ru ions bound to HEWL. The red peak shows the electron-rich Ru atom. The lack of definition of the axial ligand is probably due to rotational disorder. (**A**) Ru binding site close to Asp101. (**B**) Ru binding site close to Asp119. Reproduced from [110] with permission of the Royal Society of Chemistry.

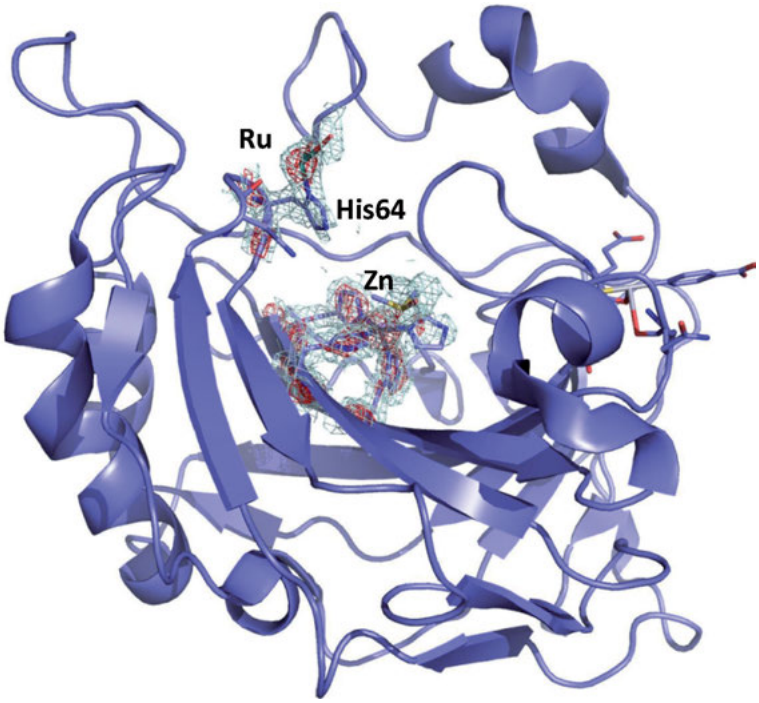

Figure 6. The adduct of NAMI-A with hCAII (= human carbonic anhydrase II). $2F_o - F_c$ electron density map contoured at 1σ level showing the ruthenium ion bound to the hCAII residue His64. Reproduced from [109] with permission; copyright 2016 Elsevier.

2.8.2. KP1019

Unfortunately, recent work devoted at investigating the interactions of KP1019 with model proteins failed to afford good quality crystals and the respective high-resolution crystal structures. Therefore, the best structural models for protein metalation by KP1019 are still those deriving from the relatively low resolution crystal structure of the apo-lactoferrin adduct and from the more recent crystal structure of the HSA adducts, previously commented. However, these structural studies have been corroborated and partially validated by a few spectroscopic studies in solution mainly carried out by the groups of Walsby and Harris [54, 97–100]. Notably KP1019 – at variance with NAMI-A and in accordance with its greater inertness – seems capable to retain, at least in part, its heterocyclic ligands upon protein binding [114].

2.9. Cellular Effects and Cellular Death Mechanisms

During the last two decades several studies explored, on a larger scale but still through targeted approaches, the effects that either NAMI-A or KP1019 produce

at the cellular level in treated cancer cells trying to highlight the most meaningful and relevant alterations. As pointed out above, these two Ru drugs show a quite distinct biological profile; accordingly, the mentioned studies were generally focused on specific cellular processes in dependence on the investigated drug. In other words, as KP1019 possesses the frank profile of a cytotoxic drug, the respective cellular studies were mainly devoted to characterize the induction of apoptosis and the inherent mechanisms of cell death; at variance, being NAMI-A – predominantly – a non-cytotoxic agent, studies mainly examined its effects on other cellular aspects such as the interactions with typical membrane proteins, e.g., integrins, the effects on cell motility and cell adhesion, on ion channels, on the cytoskeleton, and so on.

Only very recently the cellular effects produced by these Ru drugs were analyzed through untargeted approaches – either on a genome-wide or a proteome-wide level – with the help of the emerging "omics" technologies. While not entering here into the details, the multiple facets and the intrinsic complexity of these cellular investigations, we try to describe a few aspects that seem to us particularly relevant.

2.9.1. NAMI-A

As stated above, NAMI-A shows in most cases a non-cytotoxic profile with IC_{50} values usually greater than 500 μM. This implies that cells treated with NAMI-A – at the concentrations usually applied for the *in vivo* and *in vitro* studies – do not manifest evident signs of sufferance or damage and remain viable. This is the reason why studies on cell death and apoptosis induced by this compound are virtually missing as those processes only occur at unrealistically high drug concentrations, except for a few leukemia cell lines [71]. Accordingly, other strategies need to be exploited to reveal the cellular alterations induced by NAMI-A with an emphasis on those that are mediated by membrane interactions. Most of these studies mainly concerned the analysis on the effects produced on cell adhesion and migration, on the cytoskeleton, on cell motility and so on. Particularly relevant is a recent study by Sava and coworkers where the effects of NAMI-A on adhesion and migration are described in depth [115]; in particular this study reports that NAMI-A affects two important steps of the tumor metastatic progression of colorectal cancer, i.e., adhesion and migration of the tumor cells on the extracellular matrix proteins. The fibronectin receptor α5β1 integrin is likely involved in mediating these actions.

"Omics" technologies started to be exploited to characterize the cellular effects of NAMI-A. In 2013 a study appeared, which described the proteomic alterations produced by NAMI-A in A2780 human ovarian cancer cells [116]; it was found that the compound, at a concentration of 50 μM over 24 h exposure, induced on the whole relatively few proteomic alterations. Omega-amidase (NIT2), thymidylate kinase (TMK), histidine triad nucleotide-binding protein 1 (HINT1), serine threonine protein phosphatase subunit b (PP2A), peptidyl-prolyl *cis-trans* isomerase D (PPID), elongation factor 1-delta (EF1D), cathepsin D (CATD), peroxiredoxin-1 (PRDX1), protein S100-A4 (S10A4), and prefoldin

subunit 3 (PFD3) were the proteins that showed an appreciable upregulation upon NAMI-A treatment while DNA polymerase epsilon subunit 3 (POLE3) was markedly downregulated [116].

More recently, the group of Sava analyzed the transcriptomic changes caused by NAMI-A [117]. The genes differentially expressed upon treatment with NAMI-A were identified through whole-transcriptome analysis and RNA-sequencing in the metastatic MDA-MB-231 mammary carcinoma cells, in comparison to the non-tumorigenic HBL-100 mammary gland cells. NAMI-A treatment rapidly induced a relevant but transient up-regulation of a few genes. The observed changes in gene expression profoundly differ between MDA-MB-231 and HBL-100 cells, highlighting the large selectivity of the NAMI-A induced transcriptional perturbations in the invasive rather than in the non-tumorigenic phenotype. The transcriptional response, in the invasive MDA-MB-231 cells, comprises a set of early-response transcription factors and reveals a pharmacological signature in substantial agreement with the NAMI-A behavior as a metastasis inhibitor involving cell cycle regulation and ECM (extra-cellular matrix) remodeling. Globally, the results of this study underscore the role of some transcription factors that crucially affect the expression and activity of many downstream genes and proteins fundamentally involved in the functional effects of NAMI-A [117].

2.9.2. KP1019 and KP1339

Cellular studies carried out on KP1019 have followed a more classical course as they primarily concerned the detailed description of cancer cell death and the investigation of the underlying mechanisms. Those studies were mainly contributed by the group of Keppler ([3] and refs therein). It emerges that KP1019 is able to induce apoptotic death of cancer cells. The most credited mechanisms are summarized in a recent paper [118]. It is proposed that the biological activity of KP1339 is mostly mediated by overproduction of reactive oxygen species (ROS). ROS lead to Nrf2 activation, which in turn triggers antioxidant response gene transcription. GRP78 down-regulation on the protein level suggests endoplasmic reticulum (ER) associated protein degradation (ERAD) as a mode of action [42, 43]. Another important part for the mode of action is ER stress, as different factors are highly upregulated on the protein level. For example PERK, a transmembrane receptor which is released by GRP78 when the ER is disturbed, is upregulated and phosphorylated. EIF2α is phosphorylated, which leads to an inhibition of CAP-dependent translation and other stress responses. The transcription factor CHOP (DDIT3), which promotes ER stress-dependent apoptosis, is time- and concentration-dependently upregulated. Finally, cytotoxicity tests revealed that inhibition of ER stress leads to decreased cytotoxic effects of KP1339, which highlights the involvement of this mechanism in the mode of action [118].

At variance with NAMI-A, to the best of our knowledge, no complete proteomic or transcriptomic studies have been carried out on KP1019/1339 and related KP-type compounds.

2.10. Hypotheses on the Mechanisms of Action

It is somehow frustrating to admit that, despite the numerous investigations carried out so far, the precise mechanisms of action of NAMI-A and KP1019 are still largely unknown. The striking difference compared to Pt anticancer drugs, for which the (main) mechanism of action could be drafted – at least broadly – since the early studies, has to be found in the greater lability of the two Ru coordination compounds. The relatively fast aquation processes and ligand-exchange reactions generate several species that, while diffusing through the different biological compartments (blood serum, extracellular matrix, cell surface, cell interior …) can react with a variety of biological components leading to a manifold of effects.

Nevertheless, even within this rather uncertain framework, on the ground of the conspicuous number of available mechanistic studies, we may formulate some reasonable hypotheses concerning their likely modes of action.

2.10.1. NAMI-A

The activity of NAMI-A seems to be the result of concurrent mechanisms that, contrary to the original expectations, apparently do not involve nuclear DNA [9, 14]. Sava and coworkers demonstrated years ago, through an indirect experiment, that NAMI-A selectively affects tumor cells with metastatic ability within the primary tumor (Lewis lung carcinoma) [59]. Cells harvested from the primary tumor of mice treated with NAMI-A at the normal dose active on metastases, when transplanted into healthy mice, showed no change in primary tumor development, but a significant reduction in the formation of spontaneous lung metastases. This finding suggested that the treatment with NAMI-A had depleted the primary tumor of the clone of cells endowed with metastasizing ability. Several *in vitro* investigations on different cancer cell lines by the groups of Sava [58, 59, 115, 119, 120] and Lay [94] confirmed the capability of NAMI-A to affect significantly tumor cells with metastatic ability by interfering – at sub-cytotoxic and physiologically relevant Ru concentrations – with important steps of the tumor metastatic progression. In fact, by virtue of its fast ligand-exchange kinetics, NAMI-A is not significantly internalized by cells but rather binds to collagens of the extracellular matrix and to cell surface integrins, thus leading to increased adhesion and reduced invasiveness of cancer cells.

If these results are consistent with the capability of NAMI-A of inhibiting the growth of new metastases, its activity against already grown metastases is perhaps more reasonably attributable to its anti-angiogenic properties, confirmed in the chick chorioallantoic membrane and in the rabbit eye cornea model [121, 122].

2.10.2. KP1019 and KP1339

The overall experimental evidence collected for KP1019 suggests a different mechanism of action. First of all, the relatively slower extracellular degradation

and higher lipophilicity of KP1019 compared to NAMI-A allow enhanced cellular uptake, most likely by passive diffusion. Accordingly, the *in vivo* activity of KP1019 on primary tumor growth is predominantly due to direct cytotoxic effects on tumor cells. In other words, KP1019 seems to behave as a classical cytotoxic drug, even though the mechanism leading to cell damage and death is unclear. The most recent and credited interpretations on the molecular mechanism of KP1339 tend to rule out a direct DNA damage as the main determinant of its cytotoxic action. In contrast, the mechanism appears to be centered on strong interactions with cytosol proteins leading to ROS overproduction, oxidative and ER stress. Eventually, this cellular damage triggers apoptosis through a mitochondrial pathway [118].

On the other hand, there are controversial findings on the anti-metastatic ability of KP1019. Despite the inactivity found *in vivo* in the MCa tumor model, KP1019 revealed some anti-invasive activity in monolayer cultures of breast cancer cell lines, causing significant reduction of cell migration and invasion [67]. However, KP1339 was later found to have no anti-invasive activity, neither in the spheroid model nor in the trans-well assay in the cell line HT1080 [75].

3. CONCLUSIONS AND OUTLOOK

The most surprising aspect of NAMI-A and KP1019 is that, despite their obvious structural similarity, they have so markedly different macroscopic pharmacological activities: KP1019 behaves rather as a classical anticancer compound (with the great advantage of being active also against platinum-resistant tumors), whereas NAMI-A has a more unconventional activity that affects the metastases and not the primary tumor.

A question spontaneously arises: is such difference in activity caused by an intrinsic chemical feature, i.e., the different axial ligands in the two Ru(III) anions, or is it mainly ascribable to the distinct kinetics that such different ligands entail? Both complexes have relatively fast ligand-exchange kinetics, with NAMI-A being more labile than KP1019. Since a great deal of experimental evidence indicates that, under *in vivo* conditions, both compounds are very likely to lose also the axial ligands, generating eventually the naked Ru ion, the culprit seems to be found mainly in the complex intertwining of chemical and diffusional kinetics (see above).

A recent comparative study performed by the group of Harris [100] in multicellular spheroids of SH-SY5Y human neuroblastoma cells of various diameters (50–800 μm) supported this vision showing that, also in this *in vitro* model of a solid tumor, NAMI-A and KP1019 behave differently. A detailed XANES investigation (performed 24 h after treatment of the spheroids with the compounds) indicated that the speciation of NAMI-A did not change significantly as hypoxia levels of the spheroids increased, whereas the fate of Ru from KP1019 was greatly affected by the level of hypoxia. Given that NAMI-A is more labile and more easily reduced than KP1019, this result suggests that the chemical

transformation (i.e., speciation) of NAMI-A had already come to an end *before* the collection of the Ru K-edge data started [100].

The complex *in vivo* chemistry of these two simple Ru(III) compounds is a two-edged sword. On the one hand, the absence of clear identified target(s) (e.g., DNA) and activity markers – not surprising given their very complex speciation processes – is affecting negatively their development [9]. Indeed, even though NAMI-A and KP1019 are relatively safe, their clinical development, after the initial progress, is now apparently lagging behind. On the other hand, in the 30 years after their discovery, the scientific community has acquired a good general knowledge of the behaviors and features of both KP-type and NAMI-A-type complexes. We learned that relatively small changes in the axial ligands of these anionic species lead, in a complex series of cascade events, to remarkably different pharmacological effects. Thus, it might be rewarding to re-examine these two classes of complexes: perhaps – in the light of our current knowledge – novel and different drug candidates might emerge.

Finally, it is worth noting that the exploration of nanoparticle formulations of both NAMI-A and KP1019 just started [123, 124]. This approach, through a careful optimization of a few physico-chemical parameters, offers the chance to improve the stability of the resulting nano constructs and optimize their ability to target cancer tissues, thus opening a new and truly exciting frontier for the development of these Ru drugs.

ACKNOWLEDGMENTS

The authors are grateful to Beneficentia Stiftung for continued financial support. E. A. gratefully acknowledges the University of Trieste for the research grant "Finanziamento di Ateneo per progetti di ricerca scientifica – FRA 2015". L. M. acknowledges CIRCMSB, Ente CRF, ITT (Istituto Toscano Tumori) and AIRC.

ABBREVIATIONS AND DEFINITIONS

AAS	atomic absorption spectroscopy
AMMN	acetoxymethylmethylnitrosamine
apoTf	apo-transferrin
AsH	ascorbic acid
DLT	dose limiting toxicity
dmso	dimethylsulfoxide
dmtp	5,7-dimethyl[1,2,4]triazolo[1,5a]pyrimidine
ENDOR	electron nuclear double resonance spectroscopy
ER	endoplasmic reticulum
ESI-MS	electrospray ionization mass spectrometry
ESR	electron spin resonance
GFAAS	graphite furnace atomic absorption spectroscopy

GSH	glutathione
HSA	human serum albumin
HSTf	human serum transferrin
ICP-MS	inductively coupled plasma mass spectrometry
Im	imidazole
Ind	indazole
i.p.	intraperitoneal
i.v.	intravenous
MTD	maximal tolerable dose
NAMI	sodium *trans*-[tetrachloro(dimethylsulfoxide)(imidazole) ruthenate(III)]
NAMI-A	imidazolium *trans*-[tetrachloro(dimethylsulfoxide)(imidazole) ruthenate(III)]
NKI	National Cancer Institute of Amsterdam
NSCLC	non-small cell lung cancer
KP418	imidazolium *trans*-[tetrachlorobis(imidazole)ruthenate(III)]
KP1019	indazolium *trans*-[tetrachlorobis(indazole)ruthenate(III)]
KP1339	sodium *trans*-[tetrachlorobis(indazole)ruthenate(III)]
PR	partial response
ROS	reactive oxygen species
SD	stable disease
XAS	X-ray absorption spectroscopy

REFERENCES

1. B. K. Keppler, K.-G. Lipponer, B. Stenzel, F. Kratz, in *Metal Complexes in Cancer Chemotherapy*, Ed. B. K. Keppler, VCH, Weinheim, **1993**, pp. 187–220.
2. C. G. Hartinger, M. A. Jakupec, S. Zorbas-Seifried, M. Groessl, A. Egger, W. Berger, H. Zorbas, P. J. Dyson, B. K. Keppler, *Chem. Biodiversity* **2008**, *5*, 2140–2155.
3. R. Trondl, P. Heffeter, C. R. Kowol, M. A. Jakupec, W. Berger, B. K. Keppler, *Chem. Sci.* **2014**, *5*, 2925–2932.
4. G. Mestroni, E. Alessio, G. Sava, S. Pacor, M. Coluccia, in *Metal Complexes in Cancer Chemotherapy*, Ed. B. K. Keppler, VCH, Weinheim, **1993**, pp. 157–185.
5. G. Mestroni, E. Alessio, G. Sava, S. Pacor, M. Coluccia, A. Boccarelli, *Met. Based Drugs* **1994**, *1*, 41–63.
6. E. Alessio, G. Mestroni, A. Bergamo, G. Sava, Vol. 42 of *Metal Ions in Biological Systems,* Eds. A. Sigel, H. Sigel, M. Dekker, New York, **2004**, pp. 323–351.
7. E. Alessio, G. Mestroni, A. Bergamo, G. Sava, *Curr. Topics Med. Chem.*, **2004**, *4*, 1525–1535.
8. I. Bratsos, S. Jedner, T. Gianferrara, E. Alessio, *Chimia* **2007**, *61*, 692–697.
9. A. Bergamo, G. Sava, *Chem. Soc. Rev.* **2015**, *44*, 8818–8835.
10. E. Alessio, *Eur. J. Inorg. Chem.* **2017**, 1549–1560.
11. G. Sava, A. Bergamo, *Int. J. Oncol.* **2000**, *17*, 353–365.
12. I. Kostova, *Curr. Med. Chem.* **2006**, *13*, 1085–1107.
13. M. A. Jakupec, M. Galanski, V. B. Arion, C. G. Hartinger, B. K. Keppler, *Dalton Trans.* **2008**, 183–194.
14. A. Levina, A. Mitra, P. A. Lay, *Metallomics* **2009**, *1*, 458–470.

15. E. S. Antonarakis, A. Emadi, *Cancer Chemother. Pharmacol.* **2010**, *66*,1–9.
16. I. Bratsos, T. Gianferrara, E. Alessio, C. G. Hartinger, M. A. Jakupec, B. K. Keppler, in *Bioinorganic Medicinal Chemistry*, Ed. E. Alessio, Wiley-VCH, Weinheim, **2011**, pp. 151–174.
17. G. Sava, A. Bergamo, P. J. Dyson, *Dalton Trans.* **2011**, *40*, 9069–9075.
18. A. Bergamo, C. Gaiddon, J. H. M. Schellens, J. H. Beijnen, G. Sava, *J. Inorg. Biochem.* **2012**, *106*, 90–99.
19. S. Medici, M. Peana, V. M. Nurchi, J. I. Lachowicz, G. Crisponi, M. A. Zoroddu, *Coord. Chem. Rev.* **2015**, *284*, 329–350.
20. M. J. Clarke, Vol. 11 of *Metal Ions in Biological Systems*; Eds. A. Sigel, H. Sigel, M. Dekker, New York, **1980**, pp. 231–283.
21. T. Giraldi, G. Sava, G. Bertoli, G. Mestroni, G. Zassinovich, *Cancer Res.* **1977**, *37*, 2662–2666.
22. B. K. Keppler, W. Rupp, *J. Cancer Res. Clin. Oncol.* **1986**, *111*, 166–168.
23. F. T. Garzon, M. R. Berger, B. K. Keppler, D. Schmähl, *Cancer Chemother. Pharmacol.* **1987**, *19*, 347–349.
24. M. R. Berger, F. T. Garzon, B. K. Keppler, D. Schmähl, *Anticancer Res.* **1989**, *9*, 761–765.
25. M. H. Seelig, M. R. Berger, B. K. Keppler, *J. Cancer Res. Clin. Oncol.* **1992** *118*, 195–200.
26. E. Alessio, G. Balducci, M. Calligaris, G. Costa, W. M. Attia, G. Mestroni, *Inorg. Chem.* **1991**, *30*, 609–618.
27. E. Alessio, G. Mestroni, S. Pacor, G. Sava, S. Spinelli, *International Patent* **1990**, WO90/13553.
28. E. Alessio, G. Balducci, A. Lutman, G. Mestroni, M. Calligaris, W. M. Attia, *Inorg. Chim. Acta* **1993**, *203*, 205–217.
29. G. Sava, S. Pacor, G. Mestroni, E. Alessio, *Clin. Exp. Metastasis* **1992**, *10*, 273–280.
30. G. Sava, S. Pacor, G. Mestroni, E. Alessio, *Anti-Cancer Drugs* **1992**, *3*, 25–31.
31. G. Mestroni, E. Alessio, G. Sava, *International Patent* **1998**, WO 98/00431, PCT C F 7, 15.
32. A. Galeano, M. R. Berger, B. K. Keppler, *Arzneimittel-Forschung/Drug Res.* **1992**, *42*, 821–824.
33. J. M. Rademaker-Lakhai, D. van den Bongard, D. Pluil, J. H. Beijnen, J. H. M. Schellens, *Clin. Cancer Res.* **2004**, *10*, 3717–3727.
34. M. Cocchietto, G. Sava, *Pharmacol. Toxicol.* **2000**, *87*, 193–197.
35. J. Jassem, M. Krzakowski, K. Roszkowski, R. Ramlau, J. M. Słomiński, A. Szczęsna, K. Krawczyk, B. Możejko-Pastewka, J. Lis, K. Miracki, *Lung Cancer* **2002**, *35*, 73–79.
36. S. Leijen, S. A. Burgers, P. Baas, D. Pluim, M. Tibben, E. van Werkhoven, E. Alessio, G. Sava, J. H. Beijnen, J. H. M. Schellens, *Invest. New Drugs* **2015**, *33*, 201–214.
37. P. Therasse, S. G. Arbuck, E. A. Eisenhauer, J. Wanders, R. S. Kaplan, L. Rubinstein, J. Verweij, G. M. Van, A. T. van Oosterom, M. C. Christian, S. G. Gwyther, *J. Natl. Cancer Inst.* **2000**, *92*, 205–216.
38. C. G. Hartinger, S. Zorbas-Seifried, M. A. Jakupec, B. Kynast, H. Zorbas, B. K. Keppler, *J. Inorg. Biochem.* **2006**, *100*, 891–904.
39. M. M. Henke, H. Richly, A. Drescher, M. Grubert, D. Alex, D. Thyssen, U. Jaehde, M. E. Scheulen, R. A. Hilger, *Int. J. Clin. Pharmacol. Ther.* **2009**, *47*, 58–60.
40. W. Peti, T. Pieper, M. Sommer, B. K. Keppler, G. Giester, *Eur. J. Inorg. Chem.* **1999**, 1551–1555.
41. H. A. Burris, S. Bakewell, J. C. Bendell, J. Infante, S. F. Jones, D. R. Spigel, G. J. Weiss, R. K. Ramanathan, A. Ogden, D. Von Hoff, *ESMO Open* **2016**, 1:e000154.
42. M. M. Lizardo, J. J. Morrow, T. E. Miller, E. S. Hong, L. Ren, A. Mendoza, C. H. Halsey, P. C. Scacheri, L. J. Helman, C. Khanna, *Neoplasia* **2016**, *18*, 699–710.

43. J. B. Gifford, W. Huang, A. E. Zeleniak, A. Hindoyan, H. Wu, T. R. Donahue, R. Hill, *Mol. Cancer Ther.* **2016**, *15*, 1043–1052.
44. M. Bouma, B. Nuijen, M. T. Jansen, G. Sava, A. Flaibani, A. Bult, J. H. Beijnen, *Int. J. Pharm.* **2002**, *248*, 239–246.
45. M. Bacac, A. C. G. Hotze, K. van der Schilden, J. G. Haasnoot, S. Pacor, E. Alessio, G. Sava, J. Reedijk, *J. Inorg. Biochem.* **2004**, *98*, 402–412.
46. M. Groessl, E. Reisner, C. G. Hartinger, R. Eichinger, O. Semenova, A. R. Timerbaev, M. A. Jakupec, V. B. Arion, B. K. Keppler, *J. Med. Chem.* **2007**, *50*, 2185–2193.
47. A. H. Velders, A. Bergamo, E. Alessio, E. Zangrando, J. G. Haasnoot, C. Casarsa, M. Cocchietto, S. Zorzet, G. Sava, *J. Med. Chem.* **2004**, *47*, 1110–1121.
48. A. Bergamo, B. Gava, E. Alessio, G. Mestroni, B. Serli, M. Cocchietto, S. Zorzet, G. Sava, *Int. J. Oncol.* **2002**, *21*, 1331–1338.
49. G. Sava, A. Bergamo, S. Zorzet, B. Gava, C. Casarsa, M. Cocchietto, A. Furlani, V. Scarcia, B. Serli, E. Iengo, E. Alessio, G. Mestroni, *Eur. J. Cancer* **2002**, *38*, 427–435.
50. E. Reisner, V. B. Arion, M. F. C. Guedes da Silva, R. Lichtenecker, A. Eichinger, B. K. Keppler, V. Yu. Kukushkin, A. J. L. Pombeiro, *Inorg. Chem.* **2004**, *43*, 7083–7093.
51. M. Brindell, D. Piotrowska, A. A. Shoukry, G. Stochel, R. van Eldik, *J. Biol. Inorg. Chem.* **2007**, *12*, 809–818.
52. A. Küng, T. Pieper, R. Wissiack, E. Rosenberg, B. K. Keppler, *J. Biol. Inorg. Chem.* **2001**, *6*, 292–299.
53. B. Cebrian-Losantos, E. Reisner, C. R. Kowol, A. Roller, S. Shova, V. B. Arion, B. K. Keppler, *Inorg. Chem.* **2008**, *47*, 6513–6523.
54. N. Cetinbas, M. I. Webb, J. A. Dubland, C. J. Walsby, *J. Biol. Inorg. Chem.* **2010**, *15*, 131–145.
55. P. Schluga, C. G. Hartinger, A. Egger, E. Reisner, M. Galanski, M. A. Jakupec, B. K. Keppler, *Dalton Trans.* **2006**, 1796–1802.
56. G. Sava, I. Capozzi, K. Clerici, R. Gagliardi, E. Alessio, G. Mestroni, *Clin. Exp. Metastasis* **1998**, *16*, 371–379.
57. A. Bergamo, R. Gagliardi, V. Scarcia, A. Furlani, E. Alessio, G. Mestroni, G. Sava, *J. Pharmacol. Exp. Ther.* **1999**, *289*, 559–564.
58. B. Gava, S. Zorzet, P. Spessotto, M. Cocchietto, G. Sava, *J. Pharmacol. Exp. Ther.* **2006**, *317*, 284–291.
59. G. Sava, S. Zorzet, C. Turrin, F. Vita, M. R. Soranzo, G. Zabucchi, M. Cocchietto, A. Bergamo, S. DiGiovine, G. Pezzoni, L. Sartor, S. Garbisa, *Clin. Cancer Res.* **2003**, *9*, 1898–1905.
60. M. Coluccia, G. Sava, G. Salerno, A. Bergamo, S. Pacor, G. Mestroni, E. Alessio, *Met. Based Drugs* **1995**, *2*, 195–199.
61. A. Bergamo, G. Sava, *Dalton Trans.* **2007**, 1267–1272.
62. S. Zorzet, A. Bergamo, M. Cocchietto, A. Sorc, B. Gava, E. Alessio, E. Iengo, G. Sava, *J. Pharmacol. Exp. Ther.* **2000**, *295*, 927–933.
63. S. Pacor, S. Zorzet, M. Cocchietto, M. Bacac, M. Vadori, C. Turrin, B. Gava, A. Castellarin, G. Sava, *J. Pharmacol. Exp. Ther.* **2004**, *310*, 737–744.
64. B. K. Keppler, M. Henn, U. M. Juhl, M. R. Berger, R. Niebl, F. E. Wagner, *Prog. Clin. Biochem. Med.* **1989**, *10*, 41–69.
65. T. Pieper, K. Borsky, B. K. Keppler, *Top. Biol. Inorg. Chem*. **1999**, *1*, 171–199.
66. A. K. Bytzek, G. Koellensperger, B. K. Keppler, C. G. Hartinger, *J. Inorg. Biochem.* **2016**, *160*, 250–255.
67. A. Bergamo, A. Masi, M. A. Jakupec, B. K. Keppler, G. Sava, *Met. Based Drugs* **2009**, 681270.
68. G. Sava, S. Pacor, A. Bergamo, M. Cocchietto, G. Mestroni, E. Alessio, *Chem. Biol. Interactions* **1995**, *95*, 109–126.

69. D. Pluim, R. C. A. M. van Waardenburg, J. H. Beijnen, J. H. M. Schellens, *Cancer Chemother. Pharmacol.* **2004**, *54*, 71–78.
70. G. Sava, I. Capozzi, K Clerici, G. Gagliardi, E. Alessio, G. Mestroni *Clin. Exp. Metastasis.* **1998**, *16*, 371–379.
71. S. Pillozzi, L. Gasparoli, M. Stefanini, M. Ristori, M. D'Amico, E. Alessio, F. Scaletti, A. Becchetti, A. Arcangeli, L. Messori, *Dalton Trans.* **2014**, *43*, 12150–12155.
72. P. Heffeter, M. Pongratz, E. Steiner, P. Chiba, M. A. Jakupec, L. Elbling, B. Marian, W. Körner, F. Sevelda, M. Micksche, B. K. Keppler, W. Berger, *J. Pharmacol. Exp. Ther.* **2005**, *312*, 281–289.
73. P. Heffeter, K. Böck, B. Atil, M. A. R. Hoda, W. Körner, C. Bartel, U. Jungwirth, B. K. Keppler, M. Micksche, W. Berger, G. Koellensperger, *J. Biol. Inorg. Chem.* **2010**, *15*, 737–748.
74. S. Kapitza, M. Pongratz, M. A. Jakupec, P. Heffeter, W. Berger, L. Lackinger, B. K. Keppler, B. Marian, *J. Cancer Res. Clin. Oncol.* **2005**, *131*, 101–110.
75. E. Schreiber-Brynzak, E. Klapproth, C. Unger, I. Lichtscheidl-Schultz, S. Goeschl, S. Schweighofer, R. Trondl, H. Dolznig, M. A. Jakupec, B. K. Keppler, *Invest. New Drugs* **2015**, *33*, 835–847.
76. A. N. Luck, A. B. Mason, *Adv. Drug Deliv. Rev.* **2013**, *65*, 1012–1019.
77. F. Kratz, U. Beyer, *Drug Deliv.* **1998**, *5*, 281–299.
78. T. R. Daniels, E. Bernabeu, J. A. Rodríguez, S. Patel, M. Kozman, D. A. Chiappetta, E. Holler, J. Y. Ljubimova, G. Helguera, M. L. Penichet, *Biochim. Biophys. Acta*. **2012**, *1820*, 291–317.
79. F. Kratz , M. Hartmann, B. K. Keppler, L. Messori, *J. Biol. Chem.* **1994**, *269*, 2581–2588.
80. F. Kratz, B. K. Keppler, L. Messori, C. A. Smith, E. N. Baker, *Met. Based Drugs* **1994**, *1*, 169–173.
81. C. A. Smith, A. J. Sutherland-Smith, B. K. Keppler, F. Kratz, E. N. Baker, *J. Biol. Inorg. Chem.* **1996**, *1*, 424–431.
82. K. Połeć-Pawlak, J. K. Abramski, J. Ferenc, L. S. Foteeva, A. R. Timerbaev, B. K. Keppler, M. Jarosz, *J. Chromatog. A* **2008**, *1192*, 323–326.
83. C. G. Hartinger, S. Hann, G. Koellensperger, M. Sulyok, M. Groessl, A. R. Timerbaev, A. V. Rudnev, G. Stingeder, B. K. Keppler, *Int. J. Clin. Pharmacol. Ther.* **2005**, *43*, 583–585.
84. M. Pongratz, P. Schluga, M. A. Jakupec, V. B. Arion, C. G. Hartinger, G. Allmaier, B. K. Keppler, *J. Anal. Atom. Spectrom.* **2004**, *19*, 46–51.
85. O. Dömötör, C. G. Hartinger, A. K. Bytzek, T. Kiss, B. K. Keppler, E. Enyedy, *J. Biol. Inorg. Chem.* **2013**, *18*, 9–17.
86. M. Sulyok, S. Hann, C. G. Hartinger, B. K. Keppler, G. Stingeder, G. Koellensperger, *J. Anal. At. Spectrom.* **2005**, 20, 856–863.
87. M. Groessl, C. G. Hartinger, K. Polec-Pawlak, M. Jarosz, B. K. Keppler, *Electrophoresis* **2008**, *29*, 2224–2232.
88. A. Bijelic, S. Theiner, B. K. Keppler, A. Rompel, *J. Med. Chem.* **2016**, 59, 5894–5903.
89. H. Yin, L. Liao, J. Fang, *JSM Clin. Oncol. Res.* **2014**, *2*, 1010–1014.
90. L. Messori, F. Kratz, E. Alessio,. *Met. Based Drugs.* **1996**, *3*, 1–9.
91. L. Messori, P. Orioli, D. Vullo, E. Alessio, E. Iengo, *Eur. J. Biochem.* **2000**, *267*, 1206–1213.
92. A. Bergamo, L. Messori, F. Piccioli, M. Cocchietto, G. Sava, *Invest. New Drugs* **2003**, *21*, 401–411.
93. I. Khalaila, A. Bergamo, F. Bussy, G. Sava, P. J. Dyson, *Int. J. Oncol.* **2006**, *29*, 261–268.
94. M. Liu, Z. J. Lim, Y. Y. Gwee, A. Levina, P. A. Lay, *Angew. Chem. Int. Ed. Engl.* **2010**, *49*, 1661–1664.

95. V. Novohradský, A. Bergamo, M. Cocchietto, J. Zajac, V. Brabec, G. Mestroni, G. Sava, *Dalton Trans.* **2015** , *44*, 1905–1913.
96. A. Levina, J. B. Aitken, Y. Y. Gwee, Z. J. Lim, M. Liu, A. M. Singharay, P. F. Wong, P. A. Lay, *Chem. Eur. J.* **2013**, *19*, 3609–3619.
97. M. I. Webb, C. J. Walsby, *Dalton Trans.* **2011**, *40*, 1322–1331.
98. M. I. Webb, C. J. Walsby, *Metallomics* **2013**, *5*, 1624–1633.
99. M. I. Webb, C. J. Walsby, *Dalton Trans.* **2015**, *44*, 17482–17493.
100. G. K. Gransbury, P. Kappen, C. J. Glover, J. N. Hughes, A. Levina, P. A. Lay, I. F. Musgrave, H. H. Harris, *Metallomics* **2016**, *8*, 762–773.
101. F. Frausin, M. Cocchietto, A. Bergamo, V. Scarcia, A. Furlani, G. Sava, *Cancer Chemother. Pharmacol*. **2002**, *50*,405–411.
102. J. B. Aitken, S. Antony, C. M. Weekley, B. Lai, L. Spiccia, H. H. Harris, *Metallomics* **2012**, *4*, 1051–1056.
103. M. Groessl, O. Zava, P. J. Dyson, *Metallomics* **2011**, *3*, 591–599.
104. A. E. Egger, C. Rappel, M. A. Jakupec, C. G. Hartinger, P. Heffeter, B. K. Keppler, *J. Anal. At. Spectrom.* **2009**, *24*, 51–61.
105. A. Levina, D. C. Crans, P. A. Lay, *Coord. Chem. Rev.*, **2017**, *352*, 473–498.
106. J. Malina, O. Novakova, B. K. Keppler, E. Alessio, V. Brabec, *J. Biol. Inorg. Chem.* **2001**, *6*, 435–445.
107. M. Groessl, Y. O. Tsybin, C. G. Hartinger, B. K. Keppler, P. J. Dyson, *J. Biol. Inorg. Chem.* **2010**, *15*, 677–688.
108. A. A. Hostetter, M. L. Miranda, V. J. DeRose, K. L. McFarlane Holman, *J. Biol. Inorg. Chem*. **2011**, *16*, 1177–1185.
109. A. Merlino, *Coord. Chem. Rev.* **2016**, *326*, 111–134.
110. L. Messori, A. Merlino, *Dalton Trans.* **2014**, *43*, 6128–6131.
111. A. Casini, C. Temperini, C. Gabbiani, C. T. Supuran, L. Messori, *ChemMedChem* **2010**, *5*, 1989–1994.
112. A. Vergara, G. D'Errico, D. Montesarchio, G. Mangiapia, L. Paduano, A. Merlino, *Inorg. Chem.* **2013**, *52*. 4157–4159.
113. C. Riccardi, D. Musumeci, C. Irace, L. Paduano, D. Montesarchio, *Eur. J. Org. Chem.* **2017**, 1100–1119.
114. S. Antony, J. B. Aitken, S. Vogt, B. Lai, T. Brown, L. Spiccia, H. H. Harris, *J. Biol. Inorg. Chem.* **2013**, *18*, 845–853.
115. C. Pelillo, H. Mollica, J. A. Eble, J. Grosche, L. Herzog, B. Codan, G. Sava, A. Bergamo, *J. Inorg. Biochem.* **2016**, *160*, 225–235.
116. F. Guidi, A. Modesti, I. Landini, S. Nobili, E. Mini, L. Bini, M. Puglia, A. Casini, P. J. Dyson, C. Gabbiani, L. Messori, *J. Inorg. Biochem*. **2013**, *118*, 94–99.
117. A. Bergamo, M. Gerdol, M. Lucafò, C. Pelillo, M. Battaglia, A. Pallavicini, G. Sava, *Metallomics.* **2015**, *7*, 1439–1450.
118. L. S. Flocke, R. Trondl, M. A. Jakupec, B. K. Keppler, *Invest. New Drugs* **2016**, *34*, 261–268.
119. G. Sava, F. Frausin, M. Cocchietto, F. Vita, E. Podda, P. Spessotto, A. Furlani, V. Scarcia, G. Zabucchi, *Eur. J. Cancer* **2004**, *40*, 1383–1396.
120. C. Casarsa, M. T. Mischis, G. Sava, *J. Inorg. Biochem.* **2004**, *98*, 1648–1654.
121. A. Vacca, M. Bruno, A. Boccarelli, M. Coluccia, D. Ribatti, A. Bergamo, S. Garbisa, L. Sartor, G. Sava, *Br. J. Cancer* **2002**, *86*, 993–998.
122. L. Morbidelli, S. Donnini, S. Filippi, L. Messori, F. Piccioli, P. Orioli, G. Sava, M. Ziche, *Br. J. Cancer* **2003**, *88*, 1484–1491.
123. B. M. Blunden, A. Rawal, H. Lu, M. H. Stenzel, *Macromolecules* **2014**, *47*, 1646–1655.
124. B. Fischer, P. Heffeter, K. Kryeziu, L. Gille, S. M. Meier, W. Berger, C. R. Kowol, B. K. Keppler, *Dalton Trans.* **2014**, *43*, 1096–1104.

6

Multinuclear Organometallic Ruthenium-Arene Complexes for Cancer Therapy

Maria V. Babak and Wee Han Ang

Department of Chemistry, National University of Singapore,
3 Science Drive 2, 117543, Singapore
<phamari@nus.edu.sg>, <chmawh@nus.edu.sg>

ABSTRACT 172
1. INTRODUCTION 172
2. HOMOLEPTIC DINUCLEAR COMPLEXES 174
   2.1. Direct Conjugation via Linkers 174
   2.2. Bridging via Chalcogenato-Donor Ligands 176
   2.3. Functional Bridging Ligands 178
3. HOMOLEPTIC TRINUCLEAR AND TETRANUCLEAR COMPLEXES 178
   3.1. Rigid Metallacrowns and Clusters 179
   3.2. Trinuclear and Tetranuclear Complexes with Flexible Linkers 180
4. POLYNUCLEAR RUTHENIUM-ARENE CAGES 181
   4.1. Tetranuclear Metallarectangles 181
   4.2. Hexanuclear Metallaprisms 183
   4.3. Octanuclear Metallacubes 185
5. HETERONUCLEAR RUTHENIUM-ARENE COMPLEXES 186
   5.1. Dinuclear Ru(arene)-Ti Complexes 186
   5.2. Dinuclear Ru(arene)-Pt Complexes 187
   5.3. Ru(arene)-Au Complexes 188
   5.4. Ru(arene)-Fe and Ru(arene)-Co Complexes 189
   5.5. Dinuclear Ru(arene)-Sn Complexes 190
   5.6. Ru(arene) Complexes Conjugated to Carboranes 191
   5.7. Ru(arene) Complexes Conjugated to Other Metals 191
6. CONCLUSIONS 192

Metal Ions in Life Sciences, Volume 18 Edited by Astrid Sigel, Helmut Sigel, Eva Freisinger, and Roland K. O. Sigel

https://doi.org/10.1515/9783110470734-006

ACKNOWLEDGMENTS 193
ABBREVIATIONS 193
REFERENCES 194

Abstract: There has been much recent interest in the development of therapeutic transition metal-based complexes in part fueled by the clinical success of the platinum(II) anticancer drug, cisplatin. Yet known platinum drugs are limited by their high toxicity, severe side-effects, and incidences of drug resistance. Organometallic ruthenium-arene complexes have risen to prominence as a pharmacophore due to the success of other ruthenium drug candidates in clinical trials. In this chapter, we highlight higher order multinuclear ruthenium-arene complexes and their respective investigations as chemotherapeutic agents. We discuss their unique structural properties and the associated biochemical evaluation in the context of anticancer drug design. We also review the structural considerations for the design of these scaffolds and new therapeutic applications that are uncovered for this class of complexes.

Keywords: arene ligands · cancer therapy · heterometallic complexes · multinuclear complexes · ruthenium

1. INTRODUCTION

The current paradigm of drug discovery research is largely driven by the development of organic molecules as pharmacophores. Because these are constructed from carbon-based backbones, there is a limit to the structural complexity of scaffolds that can be produced from essentially sp^2 and sp^3 carbon atoms and other low valent main group elements. Indeed, out of the 24 million organic molecules registered under the Chemical Abstract Service registry, half could be classified into only 143 unique motifs [1]. Analysis of the 5000 compounds in the Comprehensive Medicine Chemistry database for their topological diversity revealed that half belong to only 32 shape classifications [2]. New molecular entities are needed to fill this broad and potentially valuable unexplored chemical space.

Inorganic molecules can fill this gap by enabling new structural topologies and reactivities [3]. A classic example is the Pt^{II} drug *cisplatin* (Figure 1) which is structurally distinct from organic scaffolds and capable of covalent DNA-Pt bonding, resulting in anticancer efficacies [4, 5]. Inorganic scaffolds based on transition metals can have tunable electrochemical and photophysical properties for targeted interactions with specific biomolecules. Following the clinical success of cisplatin since the discovery of its antitumoral activities in 1965, there has been intensive research to discover inorganic molecules that can interfere with the development, progression, and metastasis of cancer [6–10]. Buoyed by promising results of Ru^{III} drug candidates in clinical trials, an interest arose in half-sandwiched Ru^{II}-arene complexes for cancer therapy.

Ru(arene) complexes are valuable structural scaffolds for the development of anticancer agents because of their stability, accessibility by conventional synthetic routes, and well-established pharmacological parameters including solubility and lipophilicity. Ru(arene) complexes are almost exclusively low spin d^6 Ru^{II} species, preferentially with an octahedral geometry. The arene ligand is facially-

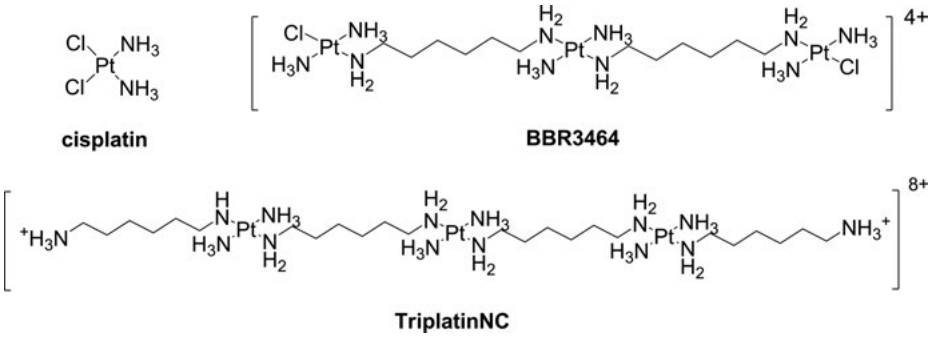

Figure 1. Molecular structures of cisplatin and multinuclear Pt complexes in clinical trials.

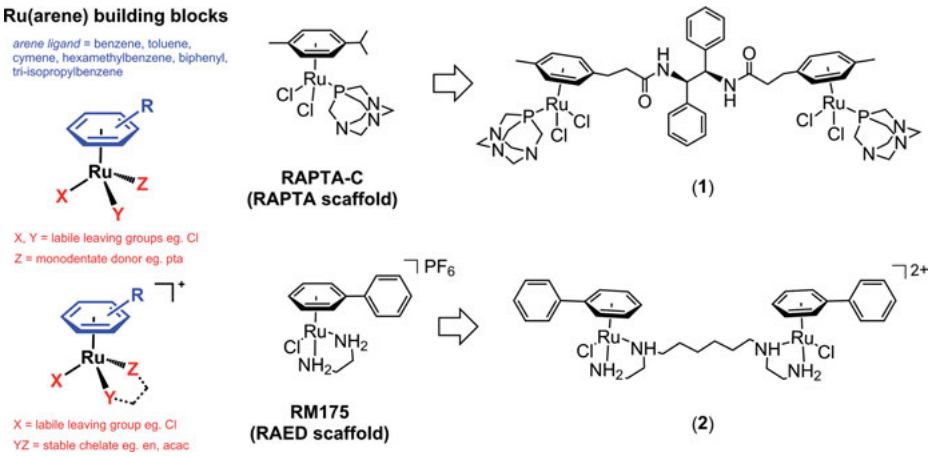

Figure 2. Ru(arene) as building blocks for multinuclear complexes.

bound onto 3 of these coordination sites, leaving the other 3 sites for ligand binding, giving thus rise to the characteristic 3-legged piano-stool structure (Figure 2). Mononuclear Ru(arene) complexes have therapeutic properties against cancer *in vitro* and *in vivo* [11–17], therefore research groups began exploiting these potentially therapeutic entities for higher-order multinuclear Ru(arene) complexes.

The strategy to modify the action modes and enhance the therapeutic properties of complexes by engineering multinuclear and heteronuclear scaffolds is well-proven. It is based on the hypothesis that new modes of anticancer activity may arise from synergistic interactions of the different metal-based moieties with the intended target. These interactions can be fine-tuned through design and variation of the linker length between the fragments. Metal-based fragments in polynuclear complexes give rise to long-range rather than short-range interactions typical of their mononuclear congeners. The interest in multinuclear metal-

based anticancer compounds is motivated in part by the trinuclear Pt^{II} complex BBR3464, and subsequently by TriplatinNC, which both entered Phase II clinical trials but were eventually abandoned (Figure 1) [18, 19]. BBR3464 acted via DNA interstrand crosslinking through electrostatic and covalent binding, and these crosslinks inhibited the intracellular repair machinery, demonstrating also a remarkable *in vitro* activity against cisplatin-resistant cell lines [18, 19]. TriplatinNC cannot bind covalently to DNA, since the chloride ligands were replaced with "dangling amine arms". However, it could H-bond efficiently with the phosphate backbone giving a "phosphate clamp" and it was highly efficacious against various cancer cell lines [20]. These highly-active polynuclear Pt species suggested that charge neutrality and direct Pt-DNA bond formation were not necessarily prerequisites for anticancer activity. This observation led to a shift in thinking on the principles governing the design of metal-based anticancer complexes. We review the application of this multinuclearity concept regarding the development of anticancer Ru(arene) complexes.

2. HOMOLEPTIC DINUCLEAR COMPLEXES

2.1. Direct Conjugation via Linkers

One strategy is to directly link mononuclear Ru(arene) complexes with established anticancer modalities within a homonuclear dileptic platform. Dyson et al. and Sadler et al. developed such homonuclear dileptic complexes based on (η^6-arene)Ru(pta)Cl_2 (RAPTA) and [(η^6-arene)Ru(en)Cl]PF_6 (RAED) scaffolds, respectively (Figure 2) [14, 21, 22]. RAPTA fragments were connected by short and inflexible 1,2-diphenylethylenediamine (DPEN) linkers through functionalized arene ligands, resulting in the formation of rigid structures **1** that resisted racemization (Figure 2). The stereochemical configuration of the linkers affected the conformations of resulting binuclear RAPTA complexes. The use of *(R,R)*- or *(S,S)*-DPEN resulted in dileptic complexes with "closed" conformations, while *(R,S)*-DPEN yielded an "open-form" complex with RAPTA components directed away from each other. Dinuclear complexes with the "closed" conformation, incorporating *(R,R)*- or *(S,S)*-DPEN linkers, demonstrated improved cytotoxicities compared to the "open-form". The authors hypothesized that these conformation-dependent activities may be attributed to the ability of "closed" dinuclear complexes to more readily form cross-links with their biological targets [23]. In contrast, two RAED units were conjugated together by a relatively long and flexible 1,6-diaminohexane linker between two ethylenediamine (en) ligands to allow for the facile epimerization of Ru and N stereocenters (complex **2**, Figure 2). The stereoconfigurations at the Ru^{II} center were not rigidly fixed and could be changed dynamically upon binding to DNA, its intended target. DNA cross-linking experiments showed that the dinuclear RAED complex formed both inter- and intra-strand crosslinks [22] due to its ability to conformationally adapt to the flexible DNA structure, thereby achieving improved DNA recognition.

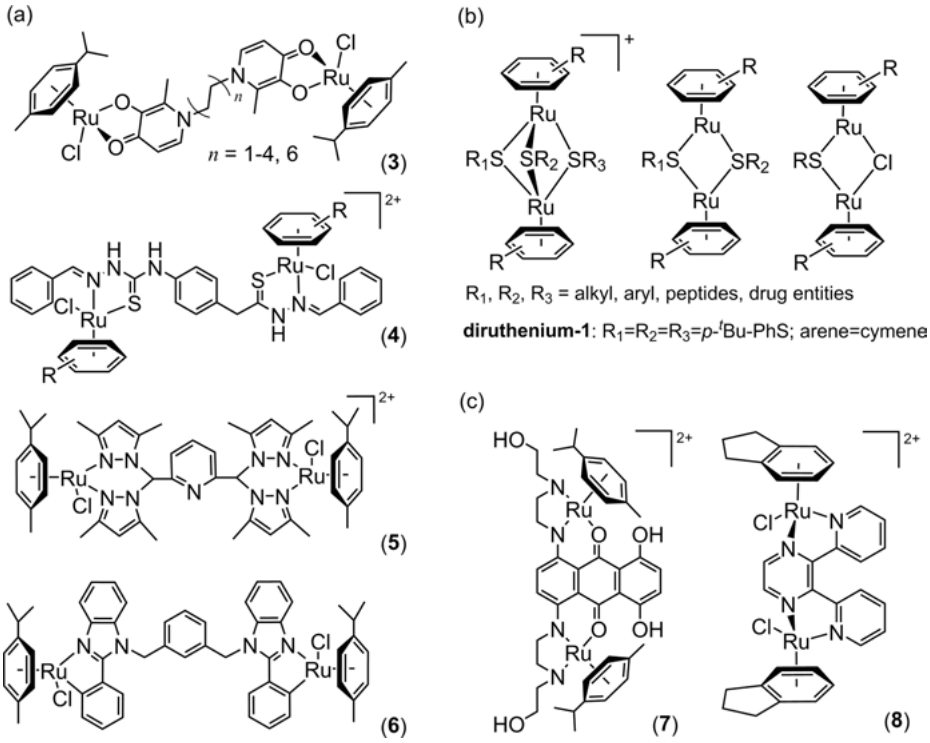

Figure 3. Homonuclear dinuclear Ru(arene) complexes investigated for cancer therapy.

Keppler et al. developed a class of homodinuclear Ru(arene) compounds **3** using maltol-derived ligands connected by the alkyl chains of various lengths (Figure 3a) [24–27]. The choice of the maltol-derived ligands was based on their versatile synthetic chemistry and the possibility of tuning pharmacological parameters by modifying the structure of the pyridinone moiety. All dinuclear Ru(arene) complexes were considerably more cytotoxic than their mononuclear analogues indicating a synergistic effect of the two Ru^{II} units. Cytotoxicities of the complexes were strongly dependent on the length of the aliphatic spacer and the lipophilicity of the metal complexes, as reflected by their octanol-water partition coefficient (Log*P*) values, with complexes with short and inflexible linkers exhibiting only moderate cytotoxicities in a micromolar range. Intriguingly, with the dodecane spacer ($n = 6$), the Ru(arene) complex demonstrated nanomolar activity with a distinctly different mode of DNA binding, as evidenced by circular dichroism and plasmid DNA unwinding experiments. The authors suggested that the complex mediated the formation of DNA-protein ternary complexes, leading to the development of irreparable "suicide" lesions [28].

Maltolato-bridged complexes were only moderately active when the Ru(arene) units were tightly bound and not spatially separated. Similarly, dinuclear Ru(arene) complexes with dithiosemicarbazone bridges **4** revealed marginal effects on

the esophageal cancer cell line WHCO1 and significant decrease in activities compared to the free uncoordinated thiosemicarbazone ligand (Figure 3a) [29]. Dinuclear arene(Ru) complexes with the α,α,α′,α′-tetra(pyrazol-1-yl)-2,6-lutidine ligand **5** [30] and doubly-cyclometallated Ru(arene) complexes **6** [31] also exhibited moderate cytotoxicities with IC_{50} values in the range of 5–60 μM in various cancer cell lines (Figure 3a). However, their activities were markedly higher than the activity of corresponding phenylbenzimidazole-based ligands. The most active complex **6** in the doubly-cyclometallated series was subjected to gene expression analyses and demonstrated a reduction of RPS21 expression, known to play a role in tumor progression. Furthermore, treated THP-1 monocytes secreted 7 cytokines (IFNγ, IL-1α, EGF, Eotaxin-3, IL-10, TGF-β and IL-17α) in 3-fold excess compared to untreated control indicative of an immunogenic response, as well as release of angiogenic vascular endothelial growth factor (VEGF) at 8.2-fold excess versus control. The authors theorized that **6** could act directly on the cancer growth via RPS21 reduction as well as promoting secretion of cytotoxic cytokines from immune cells.

2.2. Bridging via Chalcogenato-Donor Ligands

Stable $[(\eta^6\text{-arene})Ru(\mu\text{-SR})_{2-x}(\mu\text{-Cl})_xRu(\eta^6\text{-arene})]$ (x = 0, 1) or $[(\eta^6\text{-arene})Ru(\mu\text{-SR})_3Ru(\eta^6\text{-arene})]^+$ complexes (where R = alkyl, aryl) with thiolate and halide ligands bridging 2 Ru(arene) moieties have been extensively investigated as potential anticancer complexes (Figure 3b) [32]. This is primarily because the syntheses and chemical transformations of thiolate-bridged dinuclear Ru(arene) compounds are well-established and it is possible to control the reaction conditions to access mixed thiolate/halide complexes with different thiol bridges. This class of dinuclear Ru(arene) complexes is typically less reactive toward substitution reactions and resists hydrolysis. In particular, triply-bridged dinuclear Ru(arene)-thiolate complexes, by virtue of their inert Ru-S bonding framework and the absence of potential coordination sites on both Ru centers, would yield modes of action distinct from classical alkylating agents such as cisplatin that involved direct covalent bonding.

Furrer, Suess-Fink, et al. synthesized a library of thiolato-bridged Ru(arene) complexes and investigated their anticancer properties [32]. The novel compounds demonstrated high cytotoxicities in cancer cell lines and the activity of the complexes was shown to be dependent on the nature and lipophilicity of the arene and thiol ligands, as well as the electronic influence of their substituents. The Ru^{II} centers did not have a considerable impact on the activity of the complexes. In contrast, the nature and number of chalcogenato bridges was an important determinant in cytotoxicities and complexes with thiol bridges were more active when compared to those containing selenolato and tellurolato bridges [33]. Whereas the activity of the mono- and dithiolato complexes was comparable, trithiolato complexes were considerably more cytotoxic, which was related to the differences in the cellular uptake, stability, and reactivity towards biomolecules. Ru(arene)-trithiolate complexes were stable towards hydrolysis and reac-

tions with DNA and amino acids (except for cysteine), while mono- and dithiolate complexes were markedly more reactive, indicating inverse correlation between reactivity and cytotoxicity.

One notable trithiolato compound, **diruthenium-1** $[(\eta^6\text{-cymene})_2Ru_2(\mu\text{-}S\text{-}p\text{-}C_6H_4\text{-}^tBu)_3]Cl$ (Figure 3b) demonstrated remarkable cytotoxicity in both A2780 and A2780cisR cell lines (IC_{50} < 30 nM) and is amongst the most cytotoxic Ru(arene) complexes ever reported [34–36]. Because thiolato-bridged complexes were originally designed as catalysts [35], their catalytic properties could be at least partially involved in their mode of action. Cell-free experiments showed that Ru(arene)-trithiolate complexes were capable of efficient catalytic oxidation of the major intracellular reducing agent glutathione (GSH) to GSSG and the cause of intracellular increase of reactive oxygen species (ROS), since glutathione was an effective ROS scavenger.

Diruthenium-1 generated a burst of ROS in MCF-7 cells only after 30 min of treatment. ROS formation might be related to the mitochondrial dysfunction since it inhibited mitochondrial respiration and caused the disruption of mitochondrial membrane. It was suggested that the complex affected aerobic metabolism in cancer cells, which was supported by the increase in lactate production accompanied by a decrease in ATP levels. Unexpectedly, during the incubation of MCF-7 cells with diruthenium-1, intracellular levels of both reduced (GSH) and oxidized (GSSG) glutathione decreased, indicating that catalytic oxidation of glutathione might not be causal of the ROS burst. Further studies also established that its cytotoxic effects could be related to its ability to arrest cell cycle at the G2/M checkpoint which could cause the accumulation of unrepaired DNA lesions [36]. *In vivo* using a classical mouse model, the complex significantly prolonged the survival rate of tumor-bearing mice and inhibition of tumor regrowth. Despite the encouraging results, its maximum tolerated dose was significantly lower than that of cisplatin due to its low solubility and high toxicity [35].

To address these limitations, mixed Ru(arene)-thiolate complexes with functionalized peptide ligands were designed to improve targeting and uptake [37]. The peptides were conjugated onto the Ru(arene)-thiolate scaffold in 2 steps: firstly, thiophenol and α-chloroacetyl functional groups were installed onto the scaffold and peptide, respectively, then the thioether linkage was formed using the thiophenol nucleophilic group. Three peptides were evaluated: *cyclo*[Lys(ClAc)-Arg-Gly-Asp-*D*-Phe] to target $\alpha_v\beta_3$ integrin receptors typically overexpressed in cancer cells and, octaarginine and octalysine as self-penetrating peptides for enhanced cell penetration (Figure 3b). The conjugates were highly water-soluble but exhibited lower levels of anticancer efficacies, common for metal-peptide conjugates. Several Ru(arene)-thiolate complexes were also conjugated to the nitrogen mustard chlorambucil, which acted via interstrand DNA cross-linking, to realise a two-pronged bifunctional drug strategy. While these chlorambucil conjugates were cytotoxic in A2780 and A2780cisR cells at nanomolar concentration ranges and inhibited tumor growth *in vivo*, there was also a significant increase in systemic toxicities. Furthermore, their low catalytic activities and DNA binding potentials did not corroborate the expected cooperative mode of actions. Thus far, diruthenium-1 remained the most promising and efficacious anticancer candidate amongst thiolato-bridged Ru(arene) complexes studied.

2.3. Functional Bridging Ligands

Biologically-active compounds have been coordinated to mononuclear Ru(arene) scaffolds in order to tune, modify, and modulate their modes of action or to improve pharmacological properties such as cellular uptake. There are few dinuclear Ru(arene) examples because such ligands are comparatively rare. Navarro and Barrea et al. reported a dinuclear Ru(cymene) complex **7** bridged by a known cytotoxic chemotherapeutic agent mitoxantrone (Figure 3c) [38]. The Ru(arene)-mitoxantrone complex was active against ovarian cancer cell lines A2780 and A2780cisR but not to the levels of uncoordinated mitoxantrone. Attachment of Ru(cymene) fragments did not alter considerably the ability of mitoxantrone to intercalate DNA which is its primary target. However, ^{1}H NMR experiments suggested that the conjugate was capable of other modes of reactivity through its Ru(arene) fragments, particularly with both S- (cysteine, glutathione) and N-donor (histidine) biomolecules. Intriguingly, the Ru(arene)-mitoxantrone complex inhibited the protease activities of cathepsin B and D, unlike mitoxantrone, and could be construed as a dual-target complex with new modes of activities.

Several authors investigated the dinuclear Ru complexes with luminescent properties, which could be used either as a visualization tool or photoactivation. Bodio and Casini et al. explored antiproliferative properties of the dinuclear Ru compound **8**, where a Ru(arene) fragment was linked to different luminescent Ru^{II}(polypyridine) entities; however, both complexes showed poor or no activity in A2780, A2780cisR, and A549 cell lines [39].

Several authors investigated the dinuclear Ru complexes with luminescent properties, which could be used either as a visualization tool or photoactivation. Bodio and Casini et al. explored the antiproliferative properties of a dinuclear Ru compound, where a Ru(arene) fragment was linked to different luminescent Ru^{II}(polypyridine) entities; however, both complexes showed poor or no activity in A2780, A2780cisR, and A549 cell lines [39].

Sadler et al. prepared the dinuclear Ru(arene) complex **8** with bischelating pyrazine as the bridge which form monofunctional Ru-DNA adducts that slightly block RNA polymerase activities (Figure 3c) [40]. The pyrazine ligand acted to modulate the luminescent properties of the dinuclear complex which could release the indane ligand to form highly reactive Ru intermediates upon UV irradiation at 360 nm. DNA crosslinking was significantly enhanced upon irradiation and the subsequent RuDNA adducts formed were potent transcription inhibitors. The authors noted that photoactivation of metal-based complexes could produce types of metal-DNA crosslinks not possible with direct covalent binding.

3. HOMOLEPTIC TRINUCLEAR AND TETRANUCLEAR COMPLEXES

Trinuclear Ru(arene) anticancer compounds are considerably less developed as compared to their dinuclear counterparts. Three Ru(arene) fragments can be

conjugated by small and inflexible linkers, giving rise to robust cyclic or cluster compounds, where three moieties are forced to act in close proximity. Alternatively, they can be connected by branched and flexible linkers, enabling flexibility and conformational adjustment of each Ru unit.

3.1. Rigid Metallacrowns and Clusters

One of the earlier trinuclear Ru(arene) metallacycles was developed by Severin et al. who investigated the self-assembly reaction of Ru(arene) complexes containing 3-hydroxy-2-pyridone ligands (Figure 4a). Addition of a weak base triggered a diastereoselective reaction that resulted in the formation of the stable [12]-metallacrown-3 complex **9** with each 3-hydroxy-2-pyridone ligands bridging 2 Ru(arene) moieties in a trimeric arrangement [41]. These complexes also exhibit pH-dependent reactivity and convert from trimeric at pH = 7 to monomeric form at pH ≤4. The authors hypothesized that such metallacycles may dissociate into mononuclear Ru(arene) complexes within an acidic tumor microenvironment while staying intact in healthy tissue, and that this pH-dependent dissociation phenomena could be harnessed for therapy [42]. While these trinuclear Ru(arene) complexes showed selectivity toward cancer cells (A2780 and A2780cisR ovarian carcinoma) compared to normal tissue (VS79 and GS78 vaginal myofibroblasts primary culture), further investigations were not warranted due to the marginal efficacies.

A different approach was taken by Therrien et al. who developed several trinuclear and tetranuclear Ru(arene) clusters with improved stability for prolonged blood circulation (Figure 4a) [43]. Whereas tetranuclear Ru(arene) clusters **11**

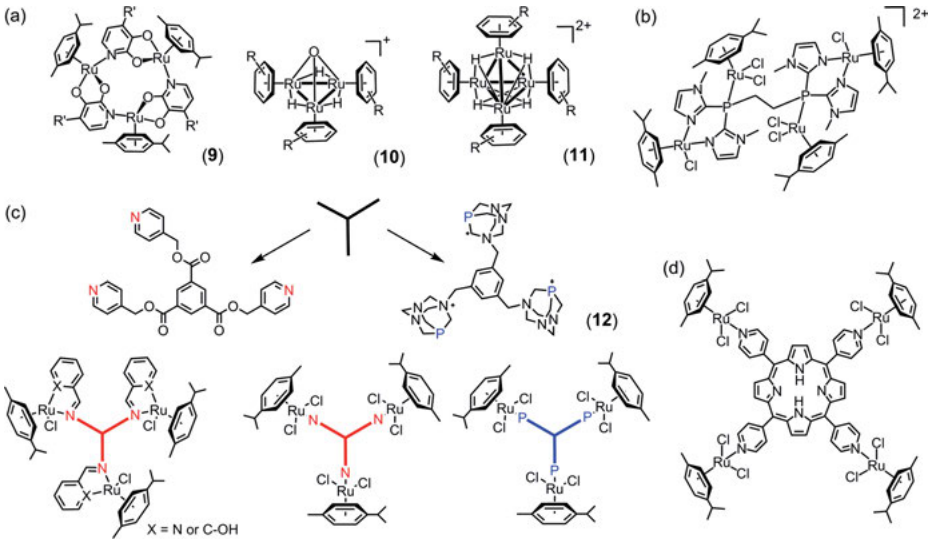

Figure 4. Examples of tri- and tetranuclear Ru(arene) complexes.

lacked efficacies against A2780 and A2780cisR cancer cell lines, the trinuclear derivatives **10** exhibited activities in the low micromolar ranges. Such differences were explained by the formation of a hydrophobic pocket within trinuclear clusters, which could be involved in supramolecular recognition processes with biomolecular aryl functional groups.

3.2. Trinuclear and Tetranuclear Complexes with Flexible Linkers

Increased nuclearity can also be achieved using flexible multitopic ligands with several coordination sites in a classical linker strategy. A novel tetranuclear Ru(arene) complex was prepared using 1,2-bis(di-*N*-methylimidazol-2-ylphosphino)ethane with the objective of increasing hydrophilicity and improving aqueous solubility [44]. The ditopic ligand coordinated Ru(arene) monovalently via the P-atom and divalently on the imidazole motif *via* a *N,N'*-chelate in 2 distinct coordination modes, giving rise to the tetranuclear Ru(arene) structure (Figure 4b). This compound exhibited marginal cytotoxicities (>100 μM) in HCT116, Huh7, H4IIE, and A2780 cell lines and was not further pursued.

The effects of the flexible linker ligands on the anticancer activity of polynuclear Ru(arene) compounds have been extensively investigated by Smith et al. using mono-, di- and trinuclear Ru(arene) complexes with polyester ligands (Figure 4c) [45, 46]. The highly lipophilic and flexible polyester bridges enhanced the cellular uptake of the complexes and allowed the investigated Ru(arene) construct to structurally adapt to the target biomolecules. This class of complexes demonstrated cytotoxicity in micromolar concentration ranges with selectivity towards A2780 and A2780cisR cancer cells over human fibroblast skin cell line KMST-6 and human embryonic kidney cell line HEK293. In particular trinuclear Ru(arene) compounds were significantly more active than their corresponding ligands and precursors, even after accounting for the presence of 3 Ru(arene) motifs, suggesting synergism between the Ru(arene) fragments. A series with Ru(arene) complexes **12** bridged by a tritopic ligand containing 3 alkylated pta ligands was subsequently investigated but they only exhibited moderate antiproliferative activity in the WHCO1 esophageal cancer cell line [47].

Besides flexible linking ligands, Ru(arene) motifs have also been coordinated to rigid porphyrin scaffolds with the objective of modulating the solubilities and lipophilicities of the ligands, and consequently changing cellular uptake parameters. For example, the coordination of 4 Ru(cymene) units significantly improved the water solubility of the tetrapyridylporphyrin ligand (Figure 4d). The resultant tetranuclear Ru(arene) complex showed only moderate cytotoxicity (>50 μM) in human melanoma Me300 cells [48], but its activity was markedly enhanced upon exposure to light (λ_{ex}: 652 nm). This enhancement of cytotoxicity can be explained by photosensitizing properties of porphyrins, which produce cytotoxic $^1O_2$ species upon irradiation. In this strategy, conjugation of porphyrins with Ru(arene) increased the hydrophilicity of the resulting compounds and fa-

cilitated the internalization of the complexes into cancer cells, while leaving the luminescence properties of the porphyrin ligand intact.

4. POLYNUCLEAR RUTHENIUM-ARENE CAGES

Ru(arene) moieties can be linked using multitopic ligands to generate three-dimensional structures and networks. These macromolecular 3D-architectures could be designed to penetrate and be taken up by "leaky" cancer cells that are permeable to large and non-natural molecules. Supramolecular structures can be engineered using a combination of Ru(arene) scaffolds with organic spacers. The general strategy is to employ the Ru(arene) fragments as corner building blocks, with organic spacers constituting the more complex structural elements, by taking advantage of their pseudo-tetrahedral geometry. In addition, by using a ditopic bridging ligand with bis-chelating donor ligands to bind 2 Ru(arene) fragments, it is also possible to generate *syn*-coordinating dinuclear Ru(arene) "molecular clips" as synthons for more complex supramolecular architectures. The arene can also serve as a handle to tune the lipophilicities of the supramolecular complex.

4.1. Tetranuclear Metallarectangles

Tetranuclear Ru(arene) metallorectangles can be prepared from a combination of dinuclear Ru(arene) clips with linear polypyridyl connectors. These dinuclear Ru(arene) clips are constituted by 2 Ru(arene) moieties bridged by ditopic bis-chelating OO∩OO, NN∩NN and NO∩NO ligands (Figure 5) [49, 50]. The Ru(arene)-thiolate compounds described earlier can also serve as molecular clips [51]. A supramolecular assembly between the Ru(arene) clips and linear poly-pyridyl spacers is usually initiated by vacating the remaining coordination site on Ru, e.g., through halide extraction by silver salts, to form the stable and robust

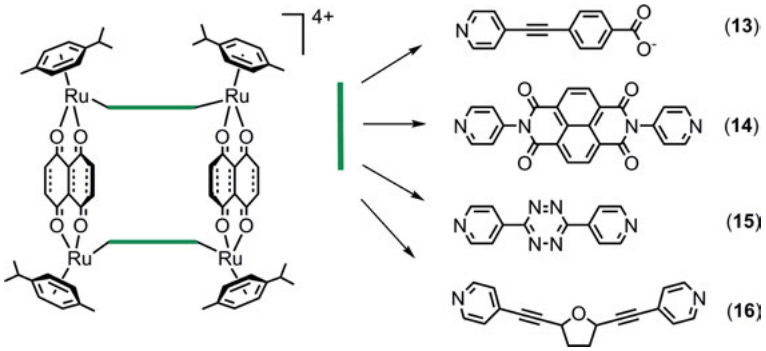

Figure 5. Examples of tetranuclear Ru(arene) metallarectangles.

metallarectangles. The size of the final tetranuclear Ru(arene) metallarectangle assembly is defined by the spacer length as well as the size of the bridging ligand [49]. Incorporation of longer linkers into metallacages have been correlated with higher anticancer activity although it has not been established why [52]. With a few exceptions, these Ru(arene) metallacages demonstrated higher cytotoxicities than their molecular clips and ditopic ligands [53].

Barea and Navarro et al. [53, 54] investigated the DNA-binding properties of several tetranuclear Ru(arene) metallarectangles and demonstrated their exceptional stabilities in aqueous media, even in the presence of mononucleotides and S-donor ligands. In contrast, the constituent Ru(arene) molecular clips were highly reactive towards nucleophiles such as AMP and GMP. DNA binding assays and atomic force microscopy indicated that the investigated metallarectangles induced significant conformational changes in the double strand DNA, presumably from supramolecular interactions. The authors hypothesized that the metallarectangles were interacting at the major groove of the DNA giving rise to the observed DNA distortion [53, 54].

Kang and Chi et al. [55] prepared asymmetric metallarectangles, where dinuclear Ru(arene) clips were connected by pyridyl-carboxylate ligands in a "head-to-tail" manner, and investigated their ability to induce apoptotic cell death. Amongst the complexes found to induce apoptotic cell death *in vitro*, metallarectangle **13** (Figure 5) was subjected to the hollow-fiber assay *in vivo* using fibers loaded with AGS gastric cancer cells that were implanted into nude mice at intraperitoneal and subcutaneous sites. After a treatment period of 5 days, cancer cell growth was inhibited by 33 % and 8 % at the intraperitoneal and subcutaneous sites, respectively [55]. Similarly, symmetric metallarectangles with naphthalene [56], tetrazine- and furan-derived [57] dipyridyl linkers inhibited up to 23 % and 8.5 % of HCT15 colon cancer cells grown in hollow fibers implanted at intraperitoneal and subcutaneous sites, respectively. In comparison, cisplatin inhibited cancer cell growth up to 38 % and 10 % under similar conditions. The low inhibitory activity at subcutaneous sites was related to the oral application of compounds and inefficient drug delivery. Metallarectangle **14** (Figure 5) was further investigated compared against HCT15 cell line and its multidrug-resistant HCT15/CL02 variant, and found to be equipotent against both cell lines, suggesting that it can bypass multidrug resistance. In comparison, the topoisomerase II inhibitor (Topo II) doxorubicin was 20 times less effective in HCT15/CL02 cells. Lastly, complexes **15** and **16** (Figure 5) were shown to significantly increase the number of autophagic vacuoles at low concentrations (0–5 μM), suggesting that their anticancer activity was directly related to the induction of autophagic cell death [57]. Taken together, these evidences point to a structural dependency of metallarectangles on its anticancer profile which cannot be readily controlled via ligand tuning and coordination.

In a separate approach, long organic spacers, e.g., 2,6-bis(*N*-(4-pyridyl)carbamoyl)-pyridine or 3,6-bis(pyridin-3-ylethynyl)phenanthrene yielded large and highly stable tetranuclear Ru(arene) complexes with bowl-shaped structures. These "metallabowls" did not lead to improved cytotoxic activity as compared to the earlier metallarectangles but gene expression analysis indicated that they

were able to increase expression of colorectal cancer suppressors, namely APC and p53 genes [58]. These complexes also induced autophagic vacuoles formation in AGS cells, as well as concentration-dependent apoptotic cell death. This was consistent with p62 upregulation as well as LC3-I to LC3-III conversion, indicative of autophagic flux. To conclude, tetranuclear metallacages exerted high anticancer activities via different mechanisms of actions but the structure-mechanism relationships remained unclear. However, the ability of metallacages of different structures to induce both autophagy and apoptotic cell death maybe be a distinctive mechanistic feature for further investigations [59].

4.2. Hexanuclear Metallaprisms

Hexanuclear Ru(arene) metallaprisms can be constituted from 3 Ru(arene) molecular clips and 2 triazine-pyridinyl organic spacers with 3 pyridinyl groups positioned in a trigonal planar arrangement (Figure 6). These metallaprisms are characterized by an accessible hydrophobic cavity, sandwiched between the two organic spacers, whose size could be adjusted by changing the size of the Ru(arene) molecular clips. Ru(arene) metallaprisms can interact directly with protein biomolecules via electrostatic interactions and induce structural changes to the bound protein or cause their precipitation. They can also initiate catalytic oxidation of ascorbic acid, cysteine, and glutathione, which might at least partially explain their cytotoxicity. Stang and Chi et al. have shown that hexanuclear

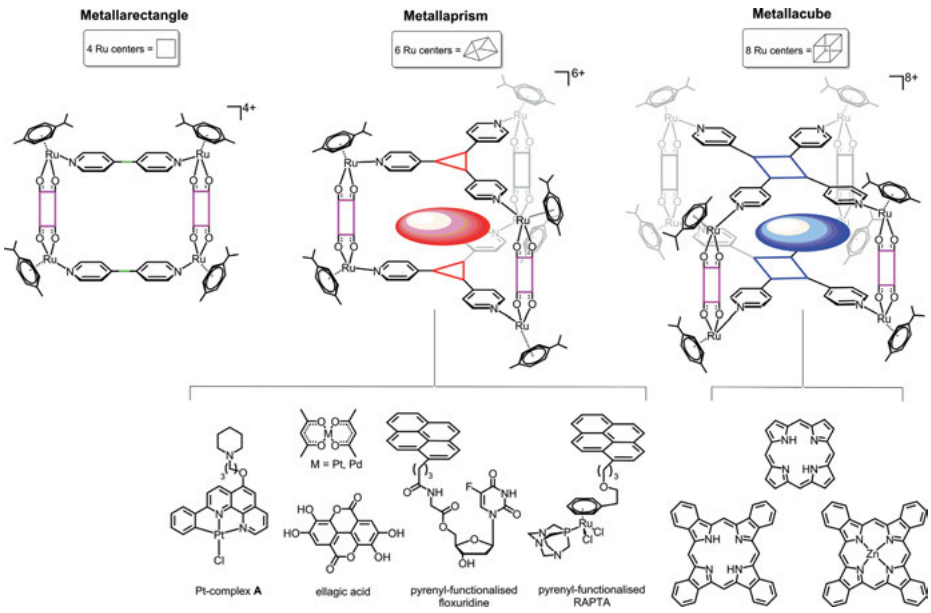

Figure 6. General strategy for polynuclear Ru(arene) constructs.

Ru(arene) metallaprisms can directly induce apoptotic cell death through G1 phase cell cycle arrest [60].

Intriguingly, the anticancer activity of metallaprisms may be further enhanced by the encapsulation of other molecules inside the cavity in a host-guest arrangement. These stable carceplex complexes can release their payload upon cell entry or remain intact, acting as a drug delivery agent, by tuning the coordination chemistry of the Ru(arene) motif [61]. Therrien et al. developed cationic and water-soluble hexanuclear Ru(arene) metallaprisms, which were large enough to encapsulate different guests, including planar aromatic molecules [50, 62], porphyrins [63], and pyrenyl derivatives [62, 64–66]. The encapsulation significantly improved the cytotoxicity of the host-guest system compared to empty metallaprisms. Attempts were made to encapsulate biologically-relevant compounds such as the anticancer drug cisplatin into the cavity of the metallaprisms [64, 67, 68]. However, the highly hydrophilic cisplatin could not be contained stably within the hydrophobic cavity. As a proof-of-concept, the authors showed that hydrophobic square-planar Pt and Pd acetylacetonate (acac) complexes could be stably entrapped and delivered intracellularly to cancer cells using the metallaprisms as a carrier.

More recently, Kang and Chi et al. [69] showed that the natural phenol antioxidant ellagic acid can also be directly encapsulated into the Ru(arene) metallaprism using this approach. Ellagic acid is poorly taken up by cells due to its hydrophilic character but it can be readily encapsulated into Ru(arene) metallaprisms due to its extended planar ring structure. Encapsulation of the ellagic acid into hexanuclear Ru(arene) metallaprisms resulted in improved uptake and increased cytotoxicities *in vitro*, but altered mechanisms of action at the molecular level which may limit its future applications [69].

As an extension to this strategy, Therrien et al. [70] conjugated hydrophilic payloads to pyrenyl functionalized groups for encapsulation by the Ru(arene) metallaprisms. By virtue of the strong π-π interactions between the pyrenyl functional groups and the triazine ligand in the hydrophobic cavity, the hydrophilic payloads could be readily tethered to the metallaprisms. Furthermore, when encapsulated, fluorescence arising from the pyrenyl functional group was significantly quenched; thus the payload release could be investigated by monitoring fluorescence turn-on of the pyrenyl group [70]. Thus far, the authors have investigated several potential compounds, including RAPTA, floxuridine, and cyclometallated Pt complex **A**, as drug payload using this strategy (Figure 6) [66]. For RAPTA and floxuridine, the metallaprism conjugate containing the tethered drug motifs led to significant enhancement in cytotoxicity and the improved activities were corroborated by increased uptake of the payloads monitored by fluorescence turn-on [65]. The fluorescence turn-on property was further exploited to determine the cellular localization of **A**. Using this strategy, the authors were able to establish the intracellular release of **A**, its localization to the nucleus as well as to investigate possible interactions with various DNA topologies [68].

This strategy was further extended using large dendrimers containing terminal pyrenyl moieties. Pitto-Barry et al. employed hydrophobic poly(arylester)cyanobiphenyl and poly(benzylether) dendrimers conjugated to pyrene as the scaffold and assembled hexanuclear Ru(arene) metallaprisms around the pyrenyl groups

[71–73]. Consequently, the pyrene moieties were effectively encapsulated within the metallaprisms thereby forming a highly stable amphiphilic macromolecular [dendrimer⊂prism]$^{6+}$ complex [71, 72]. With increased incorporation of the pyrenyl moiety in the higher dendrimer generations, a marked reduction in solubility as well as metallaprism encapsulation was observed, due to increased steric encumbrance and diminished access for encapsulation. The macromolecular complex exhibited improved solubility and micromolar-submicromolar activity against A2780 and A2780cisR cell lines, compared to free Ru(arene) metallaprisms. Subsequently, the authors also prepared a series of water-soluble pyrenyl-functionalized bis-MPA dendrimers with different end groups and carried out encapsulation by the Ru(arene) metallaprisms [73]. This allowed the comparison of the cytotoxicities between free and encapsulated dendrimers. In keeping with the earlier systems, the combined macromolecular complex was more efficacious compared to both the free dendrimers and metallaprisms, indicating the important role of the cationic cages.

4.3. Octanuclear Metallacubes

Release of the guest molecules from the cavity of Ru(arene) metallaprisms is not necessarily predicated on the rupture of the carceplex. The unobstructed passage of the guest molecule through the cavity aperture is preferred because it enables the most efficient release of the cargo. Therefore, octanuclear Ru(arene) metallacubes with larger cavities are developed to provide room to encapsulate larger photosensitizing agents, namely porphyrins and phtalocyanins, as guest molecules (Figure 6). Photosensitizers are important components of photodynamic therapy (PDT) and have been successfully applied for the treatment of melanomas. Despite the high therapeutic efficacies of PDT, arising from their high selectivities and precise photo-delivery, PDT photosensitizers are generally poorly soluble in water and can produce painful skin lesions arising from off-target phototoxicity on healthy tissue.

Therrien et al. encapsulated porphyrin into hexanuclear metallaprisms with different portal sizes, as well as larger octanuclear metallacubes (Figure 6) [50, 63]. The phototoxicity of loaded metallacages was strongly dependent on the efficiency of payload release, which can be monitored by fluorescence turn-on measurements. The authors discovered that phototoxicity was minimized when the photosensitizer was encapsulated, and phototoxicity was activated only upon release from encapsulation. Therefore, the metallacages served as an effective shield against adventitious photoactivation. More recently, the strategy was extended to phtalocyanins encapsulated in octanuclear Ru(arene) metallacubes since phtalocyanins could be activated in the red or near-infrared region, which would have better tissue-penetrating properties [63].

5. HETERONUCLEAR RUTHENIUM-ARENE COMPLEXES

An emerging approach entails the combination of Ru(arene) with other therapeutic metal fragments to produce multifunctional heterometallic complexes that can harness the therapeutic properties of both metallic entities. Instead of administering a mixture of the two individual mononuclear complexes, a rationally-designed heteronuclear complex would benefit from the synchronous delivery of both therapeutic entities at the target site and may display more favorable pharmacological profiles since their biological fate can be controlled. Conjugation of Pt and Au anticancer drugs with other metallic fragments have resulted in improved stability, solubility, and lower toxicity *in vivo* [74–80]. Examples of heteronuclear Ru(arene) complexes are still scarce (Figure 7).

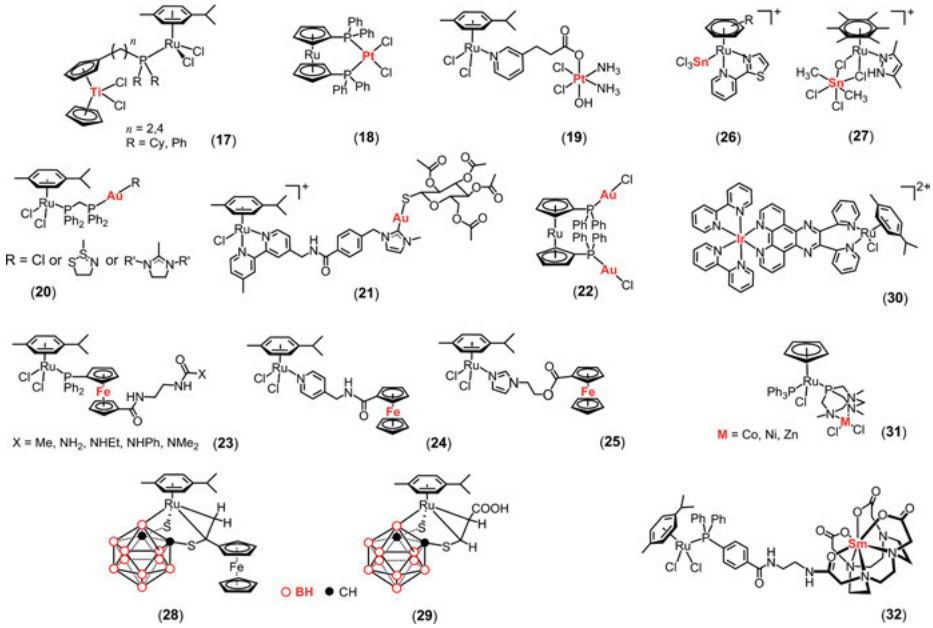

Figure 7. Examples of heteronuclear Ru(arene) complexes.

5.1. Dinuclear Ru(arene)-Ti Complexes

One of the first examples of heterometallic Ru(arene) complexes with anticancer properties was reported by Casini and Picquet et al. [81]. The authors prepared a series of titanocene-Ru(arene) complexes and investigated their structure-activity relationships. The choice of titanocene as a building block for heterometallic complexes was based on the appealing biological properties of Ti-based compounds [82, 83]. Budotitane was the first non-Pt compound that was clinically

evaluated but was prematurely terminated due to formulation issues [84, 85]. Titanocene dichloride exhibited excellent anticancer properties both *in vitro* and *in vivo*, but its development was hindered by its high nephrotoxicity [86, 87]. The authors explored the combination of a lowly toxic Ru(arene) fragment conjugated to titanocene dichloride **17** (Figure 7) [81]. While most Ru(arene) complexes interacted preferentially with protein biomolecules, titanocene dichloride was expected to act via DNA-binding; thus, the separate biological targets could give rise to synergistic effects. The resultant heteronuclear Ru(arene)-titanocene conjugate was highly cytotoxic *in vitro*, more than 20-fold more active than its constituent titanocene and Ru(arene) fragments, even in cisplatin-resistant cell lines. The authors hypothesized that the lack of cross-resistance arose from its ability to efficiently inhibit cathepsin B, associated with chemoresistance and metastases, since both Ti and Ru centers can compete for cysteine-binding at the active site of cathepsin B. In keeping with dinuclear Ru(arene) complexes, incorporation of longer spacers resulted in an increased cytotoxicity and improved cathepsin B inhibition.

5.2. Dinuclear Ru(arene)-Pt Complexes

The FDA-approved Pt-based anticancer drugs cisplatin and its analogues exert their cytotoxic effects *via* DNA damage, which can give rise to Pt-DNA adducts that efficiently inhibit replication and transcription. Failure to reverse stalled transcription through repair pathways triggers cellular apoptosis which forms the basis for the anticancer activity for Pt drugs [88–93]. Development of "ruthplatins" is therefore an interesting proposition as it combines Ru with a proven therapeutic entity and may lead to new modes of activity. One of the earlier attempts was reported by Darkwa and Elmroth et al. and involved a *cis*-platinum(II) chloride fragment with substituted bis(diphenylphosphino)-ruthenocenes **18** (Figure 7) but the resultant complexes were not sufficiently stable to be tested *in vitro* [94]. Recently, Zhu et al. developed a novel series of multifunctional Ru(arene)-Pt(IV) complexes which employed the *cis*,*cis*,*trans*-diammine-dichloridobiscarboxylatoplatinum(IV) complex **19** (Figure 7) as a cisplatin-prodrug [95]. The Ru(arene) moiety was conjugated via 3-pyridinepropionate to the axial position of the Pt(IV) fragment, and the ligand would be released from Pt(IV) by intracellular chemical reduction with the concomitant formation of cisplatin. The evaluated heteronuclear Ru(arene)-Pt(IV) complex was stable in aqueous solutions and exhibited remarkable cytotoxicities in the low micromolar to nanomolar range against a panel of cancer cell lines, including the highly resistant triple-negative breast cancer. They also exhibited high selectivity towards cancerous cells over healthy fibroblast cells. The heteronuclear complex **19** induced apoptosis *in vitro* and inhibited DNA synthesis, in keeping with cisplatin. However, the authors also found that by incorporating a Ru(arene) fragment, the complex exhibited increased antimigratory properties as it inhibited wound closure in a wound-healing assay to comparable levels of the known antimetastatic agent sunitinib [95]. In contrast, the mononuclear Ru(arene) analogue and

its 1:1 mixture with cisplatin demonstrated only weak inhibition of the wound closure.

Dinuclear Ru(arene) clips can be conjugated with Pt^{II}-diethynyldipyridyl ligands to form Ru(arene)-Pt metallarectangles *via* the self-assembly coordination process [96]. The novel heteronuclear Ru(arene)-Pt metallarectangles demonstrated a distinctly different electrochemical behavior from homonuclear Ru(arene) metallarectangles. Ru-Pt rectangles displayed two reversible reduction waves, one of which was attributed to Ru reduction and another wave was arising from Pt. The heteronuclear metallarectangles exhibited low micromolar activity against SK-hep-1, HeLa, HCT-15, and AGS cancer cell lines and were more cytotoxic than structurally-similar homonuclear Ru(arene) metallarectangles. The increased cytotoxicity was ascribed to their larger cavity size and metal-ligand interactions but the role of Pt was not investigated.

5.3. Ru(arene)-Au Complexes

Gold-based drugs have been widely used for the treatment of rheumatoid arthritis but also demonstrated promising anticancer properties *in vitro* and *in vivo* [97, 98]. In particular, the Au^{I}-phosphine antiarthritis drug auranofin has been extensively investigated and displays reproducibly high levels of anticancer activity *in vivo* [99]. The antitumor effects of Au^{I}-phosphine compounds is not entirely understood, but there is evidence that they occur via direct cytotoxic action, involving mitochondria targeting and induction of apoptotic cell death. As with most Ru(arene) complexes, DNA is not their primary target [100–102]. Furthermore, cisplatin-resistant cell lines are hypersensitive to Au^{I}-phosphine compounds and heteronuclear Ru(arene)-Au complexes can be employed to overcome cisplatin-based drug resistance.

The general approach for this class of complexes is to introduce a linker ligand which can bind both Au^{I} and Ru(arene) as a σ-donor/π-acceptor. While Au^{I} is limited by the availability of coordination sites, binding to Ru(arene) can be further stabilized *via* chelation. Messori et al. prepared a range of heteronuclear Ru(arene)-Au complexes **20** (Figure 7), where the (η^6-cymene)$RuCl_2$ fragment was linked to various Au^{I} moieties *via* 1,1-bis(diphenyl-phosphino)methane (dppm) [103, 104]. Notably, the heterobimetallic complexes with Au^{I}-NHC (*N*-heterocyclic carbenes) were significantly more cytotoxic than their monometallic analogues and their mixtures. The authors reported that the heteronuclear Ru(arene)-Au complexes did not bind DNA but were highly reactive toward protein models, particularly RNAse. Protein-binding was achieved through the disruption of the heteronuclear complex with the release of naked metals and their subsequent coordination to the biomolecules. The Ru(arene)-Au complexes also inhibited cathepsin B and thioredoxin reductase (TrxR) enzymatic activity, known targets of their Ru(arene) and Au^{I} fragments, respectively. Notably, the heteronuclear complex was markedly more active in the inhibition of capthesin B and TrxR than either their constituent mononuclear Ru(arene) and Au(I) complexes.

Casini and Bodio et al. extended this approach by linking Au-NHC to Ru(arene) using a sterically-encumbered bipyridyl-benzoate ligand to yield **21** to introduce sufficient spatial separation between the fragments [105]. The antiproliferative activities were too low to warrant further investigations. Darkwa and Elmroth et al. also prepared trinuclear Au^{I}-Ru^{II}-Au^{I} complex **22** using 1,1′-bis(diphenylphosphino)ruthenocene to bridge 2 Au^{I}-Cl fragments [94]. While these trinuclear complexes displayed cytotoxicities in the micromolar concentration range against the HeLa cell line *in vitro*, their mechanism of action was not investigated.

5.4. Ru(arene)-Fe and Ru(arene)-Co Complexes

Ferrocene (Fc) is an excellent building block for heterometallic complexes due to its specific geometry and high stability in the nonoxidant media [106]. It is also well-known that ferrocene undergoes reversible one-electron oxidation to form the cytotoxic ferricenium radical cation (Cp_2Fe^+), which readily interacts with a variety of free radicals, biologically important electron donors and other nucleophiles. The reverse reaction, where the ferricenium radical cation is reduced back to metallocene, can be also carried out in cells by $NADH^+$ or various metalloproteins. The conjugation of ferrocene derivatives with Ru(arene) fragments can result in efficacious heteronuclear complexes capable of inducing reactive oxygen species in cancer cells.

Ferrocene can be easily derivatized and various functional groups can be added to either or both cyclopentadienyl groups [107]. This strategy has been widely employed to access various Ru(arene)-ferrocene compounds *via* diphenylphosphino (**23**) [108, 109], imidazole (**24**) [110], and pyridinyl-functionalized ligands (**25**) (Figure 7) [110–112]. Coordination of ferrocene-pyridinyl ligands to Ru(arene) did not affect the one-electron reversible oxidation of ferrocene [109, 111], but Ru redox potential was affected by the number of alkyl substituents attached to the arene ring. The authors concluded that there was no clear correlation between the cytotoxicity of Ru(arene)-Fc complexes and their electrochemical behavior. All complexes demonstrated marginal to moderate antiproliferative activity in the micromolar concentration range *in vitro* and the trinuclear compounds Fc-Ru(arene)-Fc were slightly more cytotoxic than their dinuclear analogues [110, 111]. First- and second-generation dendrimers containing heteronuclear Ru(arene)-Fc pendants had been prepared and studied but results were not encouraging [112, 113].

Cobalt-based compounds hold great promise as anticancer agents, mainly due to the ability of Co^{III} and Co^{II} to induce ROS in cancer cells [114]. Co^{III} complexes can be used as prodrugs for bioreduction and selective targeting of malignant tissues [115]. Co sandwich complexes are similar to ferrocene in terms of stability and solubility and they can be readily derivatized [116–118]. However, there are very few examples of anticancer cobalt sandwich complexes in the literature [119]. Kim, Kang, Chi, et al. utilized a coordination-driven self-assembly to prepare heteronuclear Ru(arene) metallacages with cobalt sandwich do-

nors [120]. While the monometallic Co^{III} sandwich complex did not show any activity on HCT-15, SK-hep-1 and AGS cell lines (>100 μM), insertion of the Co^{III} sandwich unit into Ru(arene) metallarectangles resulted in drastic improvement of cytotoxicities (up to 5 μM). Intriguingly, depending on the structure of the Ru(arene)-Co metallarectangles, different types of cell death were induced in AGS cells. For Ru(arene)-Co metallarectangles containing short linker motifs, such as oxalato- and napthaquinone-derived bridges, autophagic cell death was induced. This was evidenced by the upregulation of LC3-I and LC3-III in Western blot experiments, common markers of autophagy, as well as by the formation of autophagic acidic vacuoles observed *via* fluorescent bioimaging. In contrast, metallarectangles with larger naphtacenedione-derived linkers did not cause a marked induction of autophagy, but significantly reduced induction of the main apoptotic marker caspase-3/7 suggesting decreased apoptotic activities. It should also be noted that homonuclear Ru(arene) metallarectangles were demonstrated to induce autophagic and apoptotic cell death but the role of cobalt fragments was not well understood.

5.5. Dinuclear Ru(arene)-Sn Complexes

Tin-based anticancer compounds are not widely studied but organotin compounds have been shown to be highly cytotoxic *in vitro*, but to lower levels compared to Pt complexes [121–123]. In addition, Sn-based compounds do not typically exhibit cross-resistance with Pt drugs. Heteronuclear Ru(arene)-Sn^{II} complexes **26** (Figure 7) containing formal Ru^{II}-Sn^{II} bonds were prepared from Ru(arene) complexes containing the pyTz ligand via the insertion of $SnCl_2$ into the Ru-Cl bond [124]. These complexes showed only moderate cytotoxicity in A2780 and A2780cisR cell lines *in vitro* and were markedly less toxic than cisplatin, but their resistance factors were lower than that of cisplatin.

Tabassum et al. prepared Ru(arene)-Sn^{IV} complex **27** (Figure 7) with the 3,5-dimethylpyrazole ligand and bridging chlorido ligands between Ru and Sn fragments, which was cytotoxic in the low micromolar concentration range in HeLa and HepG2 cancer cells [125]. The heteronuclear complex interacted with DNA not via covalent binding or intercalation, but via binding at the minor groove through electrostatic interactions between the phosphate backbone and the Sn^{IV} fragment. The complex was able to induce single-strand cleavage of plasmid DNA, leading to relaxation and unwinding of the supercoiled DNA. This cleavage activity was demonstrated to be related to the formation of $^1O_2$, $OH^{\cdot}$, and $O_2^{\cdot-}$ species, supportive of the oxidative cleavage pathway. The authors further examined the interactions of the Ru(arene)-Sn^{IV} complex against the DNA remodeling enzyme topoisomerase I (Topo I), an established biological target for cancer chemotherapy, since minor groove binders such as the clinical drug camptothecin are known Topo I inhibitors. Encouragingly, the Ru(arene)-Sn^{IV} complex was a potent Topo I inhibitor and the authors postulated that the complex acts by preventing Topo I from binding to target DNA strand [126, 127].

5.6. Ru(arene) Complexes Conjugated to Carboranes

Polyhedral boron compounds are widely known for their use in boron neutron capture therapy (BNCT) for cancer [128]. This therapy is based on the nuclear reaction that occurs between two non-toxic species, low energy thermal neutrons, and the non-radioactive stable isotope ^{10}B. The neutron capture reaction gives rise to energetic (^{4}He) alpha-particles and ^{7}Li nuclei, which dissipate their kinetic energy in malignant tissues, thereby killing cancer cells with precision. The advantages of using polyhedral boron compounds for BNCT are related to their stability, low toxicity, and high nuclearity [129]. Yan et al. developed Ru(arene)-complexes with 1,2-dicarba-*closo*-dodecaborane ligands **28** (Figure 7) that were cytotoxic to HCC827 human lung cancer, SMMC-7721 hepatocellular carcinoma, and non-cancerous HELF cell embryonic lung fibroblasts at low micromolar concentration [130–132]. Intriguingly, when the Fc moiety was substituted with a carboxylic group, cytotoxicity against the non-cancerous HELF cells was abrogated while efficacies against the cancer cells were retained. The heteronuclear Ru(arene)-carborane complex **29** (Figure 7) induced apoptosis in HCC827 cells *in vitro* [131]. When the complex was tested against nude mice bearing HCC827 xenograft *in vivo* at a dose of 100 μmol/kg administered every two days for 20 days, the tumor size decreased 10 times compared to the control mice group [131]. Biopsy of the treated xenografts was in agreement with the results of the *in vitro* experiments, showing upregulated cleaved caspases 8, 9, and 3, as well as cleaved PARP, indicating the ability of Ru(arene)-carborane complex to induce apoptosis both *in vitro* and *in vivo*.

Barry and Sadler et al. reported the encapsulation of a highly hydrophobic 16-electron Ru(cymene)-carborane complex in water-soluble Pluronuic® core-shell micelles [133, 134]. The cytotoxicity of the micelles with the encapsulated Ru complex was assessed by a MTT assay in A2780 and A2780cisR cell lines [134] and healthy fibroblasts MRC5 [133] and were compared to the cytotoxicity of the free complex and micelles. Whereas Pluronic® micelles were devoid of any cytotoxicity, the encapsulated Ru(arene)-carborane complex showed a remarkable cytotoxicity in A2780 and A2780cisR cells in a submicromolar concentration range. Upon encapsulation, its activity decreased by 40-fold; however the selectivity towards cancer cells over normal healthy cells and cellular accumulation increased, ensuring high ^{10}B uptake. Unfortunately, boron neutron capture therapy (BNCT) experiments indicated that there was only a slight increase of cytotoxicities between the free and the encapsulated Ru complex in A2780 cells bombarded by thermal neutrons [134]. Therefore, while physical encapsulation improved solubility and cellular accumulation, the Ru(arene) macromolecules did not increase its sensitivity to BNCT conditions.

5.7. Ru(arene) Complexes Conjugated to Other Metals

Organoiridium compounds are commonly used for photocatalysis and in material chemistry [135]. Catalytically-active organometallic Ir^{III} complexes can con-

vert NADH to NAD^+ via hydride transfer, thereby interfering with NADH-mediated cell signaling pathways [135]. Cyclometalated Ir^{III} complexes are effective photosensitizers for photodynamic therapy due to the production of singlet oxygen. Kim and Patra et al. combined Ru(arene) with cyclometalated Ir^{III} fragments **30** (Figure 7) via the polypyridyl-based ligand 2,3-di(pyridin-2-yl)pyrazino[2,3-*f*][1,10] phenanthroline. The resulting complex exhibited cytotoxicity in the low micromolar concentration range in a number of cancer cell lines [136]. The heteronuclear complex induced autophagy via the formation of acidic vacuoles which was validated by the upregulation of LC3-III, beclin-1, and atg5 protein markers in Western blot experiments. Biological properties of the mononuclear fragments were not assessed and therefore, the advantages of bridging monometallic moieties into a heterobimetallic complex cannot be identified.

Romerosa et al. developed a series of heteronuclear complexes $[CpRuCl(PPh_3)(\mu\text{-dmoPTA-1}\kappa P\text{:}2\kappa^2 N,N'\text{-M(acac-}\kappa^2 O,O')_2)]^+$ **31** (Figure 7) where M = Co, Ni, and Zn [137]. The dmoPTA is structurally-related to the PTA ligand used in RAPTA complexes but with terminal *N*,*N*'-methyl groups instead of the *N*,*N*'-methylene bridge that would complete the adamantane-like scaffold. In keeping with PTA, dmoPTA is stable, imparts good aqueous solubility, and binds Ru(arene) via the P-atom. However, dmoPTA is also capable of *N*,*N*'-chelation – a property that the authors utilized to bind the $M(acac)_2$ fragment. The heteronuclear complexes exhibited micromolar and submicromolar cytotoxicity in HBL-100, T-47D, SW1573, HeLa, and WiDr cancer cells lines and are amongst the most cytotoxic heterobimetallic complexes reported so far. However, the monometallic Ru-HdmoPTA analogue displayed similar cytotoxicities, indicating the defining role of this fragment in the biological activity of the complexes.

Ru(arene) complexes can also be linked to radionuclides, giving rise to theranostic compounds. Campello and Bodio et al. used a 1,4,7,10-tetraaza-cyclododecane-1,4,7,10-tetraacetic acid (DOTA)-derived ligand for coordination with the Ru(cymene) fragment and subsequent complexation with $^{153}Sm^{III}$ within the DOTA cage [138]. The resultant Ru(cymene)-^{153}Sm complex **32** (Figure 7) was highly water-soluble and efficacious against A2780cisR cell lines *in vitro* for at least two times. The complex did not cause acute toxicity in CD-1 mice *in vivo*, was not taken up by soft tissues, such as muscle, spleen, heart, lung, and stomach, and was quickly excreted to kidney and liver.

6. CONCLUSIONS

In this chapter, we discussed the use of the Ru(arene) scaffold as a building block for multinuclear structures and scaffolds. By leveraging on its stability, synthetic accessibility, and unique structural characteristics, it is possible to rationally develop a diversity of complex Ru(arene) frameworks with tailored attributes that can be exploited for cancer therapy. Many of these structures are not possible *via* conventional organic building blocks. This review has also uncovered the wide spectrum of unusual therapeutic applications of multinuclear

Ru(arene) structures including their promising use as delivery agents with a protective shield for photodynamic therapy agents. In this continuing quest to fight cancer, particularly against highly resistant ones, that cannot be treated with classical drugs such as cisplatin, we can expect even more focus and research toward uncovering new Ru(arene) structures to fill the chemical space as chemotherapeutic agents.

ACKNOWLEDGMENTS

The authors acknowledge financial support from the National University of Singapore and the Singapore Ministry of Education (R143-000-680-114 to W.H.A).

ABBREVIATIONS

acac	acetylacetonate
AMP	adenosine 5′-monophosphate
bis-MPA	2,2-bis(hydroxymethyl)propionic acid
Cp	cyclopentadienyl
cymene	1-methyl-4-(propan-2-yl)benzene
EGF	epidermal growth factor
EPR	enhanced permeability and retention
Fc	ferrocene
FDA	Food and Drug Administration
GMP	guanosine 5′-monophosphate
GSH	glutathione
GSSG	oxidized glutathione
IC_{50}	half-maximal inhibitory concentration
IFNγ	interferon gamma
IL	interleukin
LC3-I, LC3-III	light chain subunits
NADH	nicotinamide adenine dinucleotide reduced
NHC	*N*-heterocyclic carbenes
PARP	poly-ADP ribose polymerase
PEMA	polyethylmetacrylate
pta	1,3,5-triaza-7-phosphaadamantane
pyTz	2-(pyridine-2-yl)thiazole
RAED	$[(\eta^6\text{-arene})Ru(en)Cl]PF_6$
RAPTA	$(\eta^6\text{-arene})Ru(pta)Cl_2$
RPS2	ribosomal protein S2
TGF-β	transforming growth factor beta
Topo	topoisomerase

REFERENCES

1. A. H. Lipkus, Q. Yuan, K. A. Lucas, S. A. Funk, W. F. Bartelt, III, R. J. Schenck, A. J. Trippe, *J. Org. Chem.* **2008**, *73*, 4443–4451.
2. G. W. Bemis, M. A. Murcko, *J. Med. Chem.* **1996**, *39*, 2887–2893.
3. E. Meggers, *Curr. Opin. Chem. Biol.* **2007**, *11*, 287–292.
4. B. Lippert, Ed., *Cisplatin: Chemistry and Biochemistry of a Leading Anticancer Drug*, Verlag Helvetica Chimica Acta-Wiley, Zürich, **1999**.
5. A. W. Prestayko, S. T. Crooke, S. K. Carter, Es, *Cisplatin: Current Status and New Developments*, Academic Press, New York, **1980**.
6. K. B. Garbutcheon-Singh, M. P. Grant, B. W. Harper, A. M. Krause-Heuer, M. Manohar, N. Orkey, J. R. Aldrich-Wright, *Curr. Top. Med. Chem.* **2011**, *11*, 521–542.
7. M. J. Hannon, *Pure Appl. Chem.* **2007**, *79*, 2243–2261.
8. C. G. Hartinger, P. J. Dyson, *Chem. Soc. Rev.* **2009**, *38*, 391–401.
9. G. Gasser, I. Ott, N. Metzler-Nolte, *J. Med. Chem.* **2011**, *54*, 3–25.
10. N. P. E. Barry, P. J. Sadler, *Pure Appl. Chem.* **2014**, *86*, 1897–1910.
11. M. Melchart, P. J. Sadler, in *Bioorganometallics: Biomolecules, Labeling, Medicine*, Ed. G. Jaouen, Wiley-VCH Verlag GmbH & Co. KGaA, Weinheim, Germany, **2006**, pp. 39–64.
12. Y. K. Yan, M. Melchart, A. Habtemariam, P. J. Sadler, *Chem. Commun.* **2005**, 4764–4776.
13. S. J. Dougan, P. J. Sadler, *Chimia* **2007**, *61*, 704–715.
14. B. S. Murray, M. V. Babak, C. G. Hartinger, P. J. Dyson, *Coord. Chem. Rev.* **2016**, *306*, 86–114.
15. W. H. Ang, P. J. Dyson, *Eur. J. Inorg. Chem.* **2006**, 4003–4018.
16. W.-H. Ang, A. Casini, G. Sava, P. J. Dyson, *J. Organomet. Chem.* **2011**, *696*, 989–998.
17. A. A. Nazarov, C. G. Hartinger, P. J. Dyson, *J. Organomet. Chem.* **2014**, *751*, 251–260.
18. J. B. Mangrum, N. P. Farrell, *Chem. Commun.* **2010**, *46*, 6640–6650.
19. A. Hegmans, S. J. Berners-Price, M. S. Davies, D. S. Thomas, A. S. Humphreys, N. Farrell, *J. Am. Chem. Soc.* **2004**, *126*, 2166–2180.
20. S. Komeda, T. Moulaei, M. Chikuma, A. Odani, R. Kipping, N. P. Farrell, L. D. Williams, *Nucleic Acids Res.* **2011**, *39*, 325–336.
21. Z. Adhireksan, G. E. Davey, P. Campomanes, M. Groessl, C. M. Clavel, H. Yu, A. A. Nazarov, C. H. F. Yeo, W. H. Ang, P. Droge, U. Rothlisberger, P. J. Dyson, C. A. Davey, *Nat. Commun.* **2014**, *5*, 4462; doi: 10.1038/ncomms4462.
22. H. Chen, J. A. Parkinson, O. Novakova, J. Bella, F. Wang, A. Dawson, R. Gould, S. Parsons, V. Brabec, P. J. Sadler, *Proc. Natl. Acad. Sci. USA* **2003**, *100*, 14623–14628.
23. B. S. Murray, L. Menin, R. Scopelliti, P. J. Dyson, *Chem. Sci.* **2014**, *5*, 2536–2545.
24. M. G. Mendoza-Ferri, C. G. Hartinger, M. A. Mendoza, M. Groessl, A. E. Egger, R. E. Eichinger, J. B. Mangrum, N. P. Farrell, M. Maruszak, P. J. Bednarski, F. Klein, M. A. Jakupec, A. A. Nazarov, K. Severin, B. K. Keppler, *J. Med. Chem.* **2009**, *52*, 916–925.
25. M.-G. Mendoza-Ferri, C. G. Hartinger, R. E. Eichinger, N. Stolyarova, K. Severin, M. A. Jakupec, A. A. Nazarov, B. K. Keppler, *Organometallics* **2008**, *27*, 2405–2407.
26. M. G. Mendoza-Ferri, C. G. Hartinger, A. A. Nazarov, R. E. Eichinger, M. A. Jakupec, K. Severin, B. K. Keppler, *Organometallics* **2009**, *28*, 6260–6265.
27. M. G. Mendoza-Ferri, C. G. Hartinger, A. A. Nazarov, W. Kandioller, K. Severin, B. K. Keppler, *Appl. Organomet. Chem.* **2008**, *22*, 326–332.
28. O. Novakova, A. A. Nazarov, C. G. Hartinger, B. K. Keppler, V. Brabec, *Biochem. Pharmacol.* **2009**, *77*, 364–374.

29. T. Stringer, B. Therrien, D. T. Hendricks, H. Guzgay, G. S. Smith, *Inorg. Chem. Commun.* **2011**, *14*, 956–960.
30. S. K. Tripathy, R. K. Surada, R. K. Manne, S. M. Mobin, M. K. Santra, S. Patra, *Dalton Trans.* **2013**, *42*, 14081–14091.
31. P. Elumalai, Y. J. Jeong, D. W. Park, D. H. Kim, H. Kim, S. C. Kang, K.-W. Chi, *Dalton Trans.* **2016**, *45*, 6667–6673.
32. J. Furrer, G. Suess-Fink, *Coord. Chem. Rev.* **2016**, *309*, 36–50.
33. J. P. Johnpeter, G. Gupta, J. M. Kumar, G. Srinivas, N. Nagesh, B. Therrien, *Inorg. Chem.* **2013**, *52*, 13663–13673.
34. F. Giannini, J. Furrer, A.-F. Ibao, G. Suess-Fink, B. Therrien, O. Zava, M. Baquie, P. J. Dyson, P. Stepnicka, *J. Biol. Inorg. Chem.* **2012**, *17*, 951–960.
35. P. Tomsik, D. Muthna, M. Rezacova, S. Micuda, J. Cmielova, M. Hroch, R. Endlicher, Z. Cervinkova, E. Rudolf, S. Hann, D. Stibal, B. Therrien, G. Suess-Fink, *J. Organomet. Chem.* **2015**, *782*, 42–51.
36. A. Koceva-Chyla, K. Matczak, M. P. Hikisz, M. K. Durka, M. K. Kochel, G. Suess-Fink, J. Furrer, K. Kowalski, *ChemMedChem* **2016**, *11*, 2171–2187.
37. F. Giannini, M. Bartoloni, L. E. H. Paul, G. Suess-Fink, J.-L. Reymond, J. Furrer, *MedChemComm* **2015**, *6*, 347–350.
38. S. Rojas, E. Quartapelle-Procopio, F. J. Carmona, M. A. Romero, J. A. R. Navarro, E. Barea, *J. Mater. Chem. B* **2014**, *2*, 2473–2477.
39. M. Wenzel, A. de Almeida, E. Bigaeva, P. Kavanagh, M. Picquet, P. Le Gendre, E. Bodio, A. Casini, *Inorg. Chem.* **2016**, *55*, 2544–2557.
40. S. W. Magennis, A. Habtemariam, O. Novakova, J. B. Henry, S. Meier, S. Parsons, I. D. H. Oswald, V. Brabec, P. J. Sadler, *Inorg. Chem.* **2007**, *46*, 5059–5068.
41. H. Piotrowski, G. Hilt, A. Schulz, P. Mayer, K. Polborn, K. Severin, *Chem. Eur. J.* **2001**, *7*, 3196–3208.
42. W. H. Ang, Z. Grote, R. Scopelliti, L. Juillerat-Jeanneret, K. Severin, P. J. Dyson, *J. Organomet. Chem.* **2009**, *694*, 968–972.
43. B. Therrien, W. H. Ang, F. Cherioux, L. Vieille-Petit, L. Juillerat-Jeanneret, G. Suess-Fink, P. J. Dyson, *J. Cluster Sci.* **2007**, *18*, 741–752.
44. A. L. Noffke, M. Bongartz, W. Waetjen, P. Boehler, B. Spingler, P. C. Kunz, *J. Organomet. Chem.* **2011**, *696*, 1096–1101.
45. A. R. Burgoyne, B. C. E. Makhubela, M. Meyer, G. S. Smith, *Eur. J. Inorg. Chem.* **2015**, *2015*, 1433–1444.
46. P. Chellan, K. M. Land, A. Shokar, A. Au, S. H. An, D. Taylor, P. J. Smith, T. Riedel, P. J. Dyson, K. Chibale, G. S. Smith, *Dalton Trans.* **2014**, *43*, 513–526.
47. A. R. Burgoyne, C. H. Kaschula, M. I. Parker, G. S. Smith, *Eur. J. Inorg. Chem.* **2016**, *2016*, 1267–1273.
48. F. Schmitt, P. Govindaswamy, G. Suess-Fink, W. H. Ang, P. J. Dyson, L. Juillerat-Jeanneret, B. Therrien, *J. Med. Chem.* **2008**, *51*, 1811–1816.
49. N. P. E. Barry, F. Edafe, B. Therrien, *Dalton Trans.* **2011**, *40*, 7172–7180.
50. A. Garci, J.-P. Mbakidi, V. Chaleix, V. Sol, E. Orhan, B. Therrien, *Organometallics* **2015**, *34*, 4138–4146.
51. M. A. Furrer, A. Garci, E. Denoyelle-Di-Muro, P. Trouillas, F. Giannini, J. Furrer, C. M. Clavel, P. J. Dyson, G. Suess-Fink, B. Therrien, *Chem. Eur. J.* **2013**, *19*, 3198–3203.
52. V. Vajpayee, Y. H. Song, Y. J. Yang, S. C. Kang, H. Kim, I. S. Kim, M. Wang, P. J. Stang, K.-W. Chi, *Organometallics* **2011**, *30*, 3242–3245.
53. F. Linares, E. Q. Procopio, M. A. Galindo, M. A. Romero, J. A. R. Navarro, E. Barea, *CrystEngComm* **2010**, *12*, 2343–2346.
54. F. Linares, M. A. Galindo, S. Galli, M. Angustias Romero, J. A. R. Navarro, E. Barea, *Inorg. Chem.* **2009**, *48*, 7413–7420.

55. H. Jung, A. Dubey, H. J. Koo, V. Vajpayee, T. R. Cook, H. Kim, S. C. Kang, P. J. Stang, K.-W. Chi, *Chem. Eur. J.* **2013**, *19*, 6709–6717.
56. A. Dubey, J. W. Min, H. J. Koo, H. Kim, T. R. Cook, S. C. Kang, P. J. Stang, K.-W. Chi, *Chem. Eur. J.* **2013**, *19*, 11622–11628.
57. A. Dubey, Y. J. Jeong, J. H. Jo, S. Woo, D. H. Kim, H. Kim, S. C. Kang, P. J. Stang, K.-W. Chi, *Organometallics* **2015**, *34*, 4507–4514.
58. A. Mishra, Y. J. Jeong, J.-H. Jo, S. C. Kang, M. S. Lah, K.-W. Chi, *ChemBioChem* **2014**, *15*, 695–700.
59. I. Kim, Y. H. Song, N. Singh, Y. J. Jeong, J. E. Kwon, H. Kim, Y. M. Cho, S. C. Kang, K.-W. Chi, *Int. J. Nanomed.* **2015**, *10*, 143–153.
60. V. Vajpayee, Y. J. Yang, S. C. Kang, H. Kim, I. S. Kim, M. Wang, P. J. Stang, K.-W. Chi, *Chem. Commun.* **2011**, *47*, 5184–5186.
61. N. P. E. Barry, O. Zava, P. J. Dyson, B. Therrien, *Chem. Eur. J.* **2011**, *17*, 9669–9677.
62. J. Mattsson, O. Zava, A. K. Renfrew, Y. Sei, K. Yamaguchi, P. J. Dyson, B. Therrien, *Dalton Trans.* **2010**, *39*, 8248–8255.
63. F. Schmitt, J. Freudenreich, N. P. E. Barry, L. Juillerat-Jeanneret, G. Suss-Fink, B. Therrien, *J. Am. Chem. Soc.* **2012**, *134*, 754–757.
64. N. P. E. Barry, O. Zava, W. Wu, J. Zhao, B. Therrien, *Inorg. Chem. Commun.* **2012**, *18*, 25–28.
65. J. W. Yi, N. P. E. Barry, M. A. Furrer, O. Zava, P. J. Dyson, B. Therrien, B. H. Kim, *Bioconjugate Chem.* **2012**, *23*, 461–471.
66. M. A. Furrer, F. Schmitt, M. Wiederkehr, L. Juillerat-Jeanneret, B. Therrien, *Dalton Trans.* **2012**, *41*, 7201–7211.
67. B. Therrien, G. Suess-Fink, P. Govindaswamy, A. K. Renfrew, P. J. Dyson, *Angew. Chem. Int. Ed.* **2008**, *47*, 3773–3776.
68. K. Suntharalingam, A. Leczkowska, M. A. Furrer, Y. Wu, M. K. Kuimova, B. Therrien, A. J. P. White, R. Vilar, *Chem. Eur. J.* **2012**, *18*, 16277–16282.
69. A. Dubey, D. W. Park, J. E. Kwon, Y. J. Jeong, T. Kim, I. Kim, S. C. Kang, K.-W. Chi, *Int. J. Nanomed.* **2015**, *10*, 227–240.
70. O. Zava, J. Mattsson, B. Therrien, P. J. Dyson, *Chem. – Eur. J.* **2010**, *16*, 1428–1431.
71. A. Pitto-Barry, N. P. E. Barry, O. Zava, R. Deschenaux, P. J. Dyson, B. Therrien, *Chem. Eur. J.* **2011**, *17*, 1966–1971.
72. A. Pitto-Barry, N. P. E. Barry, O. Zava, R. Deschenaux, B. Therrien, *Chem. Asian J.* **2011**, *6*, 1595–1603.
73. A. Pitto-Barry, O. Zava, P. J. Dyson, R. Deschenaux, B. Therrien, *Inorg. Chem.* **2012**, *51*, 7119–7124.
74. J. Fernandez-Gallardo, B. T. Elie, F. J. Sulzmaier, M. Sanau, J. W. Ramos, M. Contel, *Organometallics* **2014**, *33*, 6669–6681.
75. J. M. Fenton, M. Busse, L. M. Rendina, *Aust. J. Chem.* **2015**, *68*, 576–580.
76. A. Chandra, K. Singh, S. Singh, S. Sivakumar, A. K. Patra, *Dalton Trans.* **2016**, *45*, 494–497.
77. D. Nieto, A. M. Gonzalez-Vadillo, S. Bruna, C. J. Pastor, C. Rios-Luci, L. G. Leon, J. M. Padron, C. Navarro-Ranninger, I. Cuadrado, *Dalton Trans.* **2012**, *41*, 432–441.
78. J. F. Gonzalez-Pantoja, M. Stern, A. A. Jarzecki, E. Royo, E. Robles-Escajeda, A. Varela-Ramirez, R. J. Aguilera, M. Contel, *Inorg Chem* **2011**, *50*, 11099–11110.
79. M. P. Donzello, E. Viola, C. Ercolani, Z. Fu, D. Futur, K. M. Kadish, *Inorg. Chem.* **2012**, *51*, 12548–12559.
80. D. Nieto, S. Bruna, A. M. Gonzalez-Vadillo, J. Perles, F. Carrillo-Hermosilla, A. Antinolo, J. M. Padron, G. B. Plata, I. Cuadrado, *Organometallics* **2015**, *34*, 5407–5417.

81. F. Pelletier, V. Comte, A. Massard, M. Wenzel, S. Toulot, P. Richard, M. Picquet, P. Le Gendre, O. Zava, F. Edafe, A. Casini, P. J. Dyson, *J. Med. Chem.* **2010**, *53*, 6923–6933.
82. F. Caruso, M. Rossi, *Met. Ions Biol. Syst.* **2004**, *42*, 353–384.
83. F. Caruso, M. Rossi, *Mini-Rev. Med. Chem.* **2004**, *4*, 49–60.
84. B. K. Keppler, M. E. Heim, H. Flechtner, F. Wingen, B. L. Pool, *Arzneim.-Forsch.* **1989**, *39*, 706–709.
85. T. Schilling, K. B. Keppler, M. E. Heim, G. Niebch, H. Dietzfelbinger, J. Rastetter, A. R. Hanauske, *Invest. New Drugs* **1996**, *13*, 327–332.
86. A. Korfel, M. E. Scheulen, H.-J. Schmoll, O. Grundel, A. Harstrick, M. Knoche, L. M. Fels, M. Skorzec, F. Bach, J. Baumgart, G. Sass, S. Seeber, E. Thiel, W. E. Berdel, *Clin. Cancer Res.* **1998**, *4*, 2701–2708.
87. K. Mross, P. Robben-Bathe, L. Edler, J. Baumgart, W. E. Berdel, H. Fiebig, C. Unger, *Onkologie* **2000**, *23*, 576–579.
88. M. E. Hardie, H. W. Kava, V. Murray, *Curr. Pharm. Des.* **2016**, *22*, 6645–6664.
89. X. Shu, X. Xiong, J. Song, C. He, C. Yi, *Angew. Chem. Int. Ed.* **2016**, *55*, 14246–14249.
90. R. N. Bose, *Mini-Rev. Med. Chem.* **2002**, *2*, 103–111.
91. D. M. J. Lilley, *J. Biol. Inorg. Chem.* **1996**, *1*, 189–191.
92. A. Rebillard, D. Lagadic-Gossmann, M.-T. Dimanche-Boitrel, *Curr. Med. Chem.* **2008**, *15*, 2656–2663.
93. J. J. Roberts, R. J. Knox, F. Friedlos, D. A. Lydall, *Assoc. Int. Cancer Res. Symp.* **1986**, *4*, 29–64.
94. H. Bjelosevic, I. A. Guzei, L. C. Spencer, T. Persson, F. H. Kriel, R. Hewer, M. J. Nell, J. Gut, C. E. J. van Rensburg, P. J. Rosenthal, J. Coates, J. Darkwa, S. K. C. Elmroth, *J. Organomet. Chem.* **2012**, *720*, 52–59.
95. L. Ma, R. Ma, Z. Wang, S.-M. Yiu, G. Zhu, *Chem. Commun.* **2016**, *52*, 10735–10738.
96. V. Vajpayee, Y. H. Song, Y. J. Yang, S. C. Kang, T. R. Cook, D. W. Kim, M. S. Lah, I. S. Kim, M. Wang, P. J. Stang, K.-W. Chi, *Organometallics* **2011**, *30*, 6482–6489.
97. S. J. Berners-Price, A. Filipovska, *Metallomics* **2011**, *3*, 863–873.
98. C. Nardon, G. Boscutti, D. Fregona, *Anticancer Res.* **2014**, *34*, 487–492.
99. M. J. McKeage, L. Maharaj, S. J. Berners-Price, *Coord. Chem. Rev.* **2002**, *232*, 127–135.
100. A. Bindoli, M. P. Rigobello, G. Scutari, C. Gabbiani, A. Casini, L. Messori, *Coord. Chem. Rev.* **2009**, *253*, 1692–1707.
101. A. Casini, L. Messori, *Curr. Top. Med. Chem.* **2011**, *11*, 2647–2660.
102. C. Gabbiani, L. Messori, *Anti-Cancer Agents Med. Chem.* **2011**, *11*, 929–939.
103. L. Massai, J. Fernandez-Gallardo, A. Guerri, A. Arcangeli, S. Pillozzi, M. Contel, L. Messori, *Dalton Trans.* **2015**, *44*, 11067–11076.
104. J. Fernandez-Gallardo, B. T. Elie, M. Sanau, M. Contel, *Chem. Commun.* **2016**, *52*, 3155–3158.
105. B. Bertrand, A. Citta, I. L. Franken, M. Picquet, A. Folda, V. Scalcon, M. P. Rigobello, P. Le Gendre, A. Casini, E. Bodio, *J. Biol. Inorg. Chem.* **2015**, *20*, 1005–1020.
106. S. S. Braga, A. M. S. Silva, *Organometallics* **2013**, *32*, 5626–5639.
107. M. I. Bruce, *Organometal. Chem. Rev., Sect. B* **1972**, *10*, 75–122.
108. H. Charvatova, T. Riedel, I. Cisarova, P. J. Dyson, P. Stepnicka, *J. Organomet. Chem.* **2016**, *802*, 21–26.
109. J. Tauchman, G. Suess-Fink, P. Stepnicka, O. Zava, P. J. Dyson, *J. Organomet. Chem.* **2013**, *723*, 233–238.
110. M. Auzias, J. Gueniat, B. Therrien, G. Suess-Fink, A. K. Renfrew, P. J. Dyson, *J. Organomet. Chem.* **2009**, *694*, 855–861.

111. M. Auzias, B. Therrien, G. Suess-Fink, P. Stepnicka, W. H. Ang, P. J. Dyson, *Inorg. Chem.* **2008**, *47*, 578–583.
112. P. Govender, T. Riedel, P. J. Dyson, G. S. Smith, *Dalton Trans.* **2016**, *45*, 9529–9539.
113. P. Govender, H. Lemmerhirt, A. T. Hutton, B. Therrien, P. J. Bednarski, G. S. Smith, *Organometallics* **2014**, *33*, 5535–5545.
114. C. R. Munteanu, K. Suntharalingam, *Dalton Trans.* **2015**, *44*, 13796–13808.
115. M. C. Heffern, N. Yamamoto, R. J. Holbrook, A. L. Eckermann, T. J. Meade, *Curr. Opin. Chem. Biol.* **2013**, *17*, 189–196.
116. A. R. Kudinov, E. V. Mutseneck, D. A. Loginov, *Coord. Chem. Rev.* **2004**, *248*, 571–585.
117. D. A. Loginov, E. V. Mutsenek, Z. A. Starikova, E. A. Petrovskaya, A. R. Kudinov, *Russ. Chem. Bull.* **2014**, *63*, 2290–2298.
118. D. A. Loginov, A. A. Pronin, L. S. Shul'pina, E. V. Mutseneck, Z. A. Starikova, P. V. Petrovskii, A. R. Kudinov, *Russ. Chem. Bull.* **2008**, *57*, 546–551.
119. K. Nikitin, Y. Ortin, H. Muller-Bunz, M.-A. Plamont, G. Jaouen, A. Vessieres, M. J. McGlinchey, *J. Organomet. Chem.* **2010**, *695*, 595–608.
120. N. Singh, S. Jang, J.-H. Jo, D. H. Kim, D. W. Park, I. Kim, H. Kim, S. C. Kang, K.-W. Chi, *Chem. Eur. J.* **2016**, *22*, 16157–16164.
121. T. S. B. Baul, D. Dutta, D. de Vos, H. Hopfl, Pooja, P. Singh, *Curr. Top. Med. Chem.* **2012**, *12*, 2810–2826.
122. F. Arjmand, S. Parveen, S. Tabassum, C. Pettinari, *Inorg. Chim. Acta* **2014**, *423*, 26–37.
123. S. Tabassum, C. Pettinari, *J. Organomet. Chem.* **2006**, *691*, 1761–1766.
124. M. Gras, B. Therrien, G. Suess-Fink, A. Casini, F. Edafe, P. J. Dyson, *J. Organomet. Chem.* **2010**, *695*, 1119–1125.
125. R. A. Khan, A. Asim, R. Kakkar, D. Gupta, V. Bagchi, F. Arjmand, S. Tabassum, *Organometallics* **2013**, *32*, 2546–2551.
126. R. A. Khan, S. Yadav, Z. Hussain, F. Arjmand, S. Tabassum, *Dalton Trans.* **2014**, *43*, 2534–2548.
127. S. Tabassum, A. Asim, R. A. Khan, Z. Hussain, S. Srivastav, S. Srikrishna, F. Arjmand, *Dalton Trans.* **2013**, *42*, 16749–16761.
128. G. Calabrese, J. J. Nesnas, E. Barbu, D. Fatouros, J. Tsibouklis, *Drug Discov. Today* **2012**, *17*, 153–159.
129. I. B. Sivaev, V. V. Bregadze, *Eur. J. Inorg. Chem.* **2009**, 1433–1450.
130. D.-H. Wu, C.-H. Wu, Y.-Z. Li, D.-D. Guo, X.-M. Wang, H. Yan, *Dalton Trans.* **2009**, 285–290.
131. G. Zhang, C. Wu, H. Ye, H. Yan, X. Wang, *J. Nanobiotechnol.* **2011**, *9*, 6.
132. C.-H. Wu, D.-H. Wu, X. Liu, G. Guoyiqibayi, D.-D. Guo, G. Lv, X.-M. Wang, H. Yan, H. Jiang, Z.-H. Lu, *Inorg. Chem.* **2009**, *48*, 2352–2354.
133. N. P. E. Barry, A. Pitto-Barry, I. Romero-Canelon, J. Tran, J. J. Soldevila-Barreda, I. Hands-Portman, C. J. Smith, N. Kirby, A. P. Dove, R. K. O'Reilly, P. J. Sadler, *Faraday Discuss.* **2014**, *175*, 229–240.
134. I. Romero-Canelon, B. Phoenix, A. Pitto-Barry, J. Tran, J. J. Soldevila-Barreda, N. Kirby, S. Green, P. J. Sadler, N. P. E. Barry, *J. Organomet. Chem.* **2015**, *796*, 17–25.
135. Z. Liu, P. J. Sadler, *Acc. Chem. Res.* **2014**, *47*, 1174–1185.
136. S. K. Tripathy, U. De, N. Dehury, S. Pal, H. S. Kim, S. Patra, *Dalton Trans.* **2014**, *43*, 14546–14549.
137. M. Serrano-Ruiz, L. M. Aguilera-Saez, P. Lorenzo-Luis, J. M. Padron, A. Romerosa, *Dalton Trans.* **2013**, *42*, 11212–11219.
138. L. Adriaenssens, Q. Liu, F. Chaux-Picquet, S. Tasan, M. Picquet, F. Denat, P. Le Gendre, F. Marques, C. Fernandes, F. Mendes, L. Gano, M. P. C. Campello, E. Bodio, *ChemMedChem* **2014**, *9*, 1567–1573.

7

Medicinal Chemistry of Gold Anticancer Metallodrugs

Angela Casini, [1] ***Raymond Wai-Yin Sun,*** [2] ***and Ingo Ott*** [3]

[1]School of Chemistry, Cardiff University, Park Place, Cardiff CF10 3AT, United Kingdom
<casinia@cardiff.ac.uk>

[2]Guangzhou Lee & Man Technology Co. Ltd., Guangzhou, Guangdong, P. R. China and Department of Chemistry, Shantou University, Shantou, Guangdong, P. R. China
<rwysun@leemanchemical.com>

[3]Institute of Medicinal and Pharmaceutical Chemistry, Technische Universität Braunschweig, Beethovenstr. 55, D-38106 Braunschweig, Germany
<ingo.ott@tu-bs.de>

ABSTRACT 200
1. INTRODUCTION 200
2. CURRENT STATUS OF REGISTERED GOLD DRUGS 200
    2.1. Gold Complexes in the Therapy of Rheumatoid Arthritis 200
    2.2. New Therapeutic Applications for Gold Drugs 201
3. GOLD(I) ANTICANCER DRUGS 202
    3.1. Gold(I) Phosphane Complexes 202
    3.2. Oganometallic Gold(I) Complexes 203
4. GOLD(III) ANTICANCER DRUGS 205
    4.1. Gold(III) Complexes with Tetradentate Ligands 205
    4.2. Gold(III) Complexes with Tridentate Ligands 206
    4.3. Gold(III) Complexes with Bidentate Ligands 207
5. BIOLOGICAL FUNCTIONS OF GOLD COMPLEXES 208
    5.1. Interactions with Biological Targets 208
        5.1.1. Thioredoxin Reductases 209
        5.1.2. Aquaporins 210
6. GENERAL CONCLUSIONS 213

Metal Ions in Life Sciences, Volume 18 Edited by Astrid Sigel, Helmut Sigel, Eva Freisinger, and Roland K. O. Sigel

https://doi.org/10.1515/9783110470734-007

Met. Ions Life Sci. **2018**, *18*, 199–217

ACKNOWLEGMENTS 213
ABBREVIATIONS AND DEFINITIONS 214
REFERENCES 214

Abstract: Since ancient times gold and its complexes have been used as therapeutics against different diseases. In modern medicine gold drugs have been applied for the treatment of rheumatoid arthritis, however, recently other medical applications have come into the focus of inorganic medicinal chemistry. This chapter provides a non-comprehensive overview of key developments in the field of gold anticancer drugs. Exciting findings on gold(I) and gold(III) complexes as antitumor agents are summarized together with a discussion of relevant aspects of their modes of action.

Keywords: aquaporins · carbenes · dithiocarbamates · gold · metallodrugs · phosphanes · porphyrins · thioredoxin reductase

1. INTRODUCTION

Medicinal applications of gold and its complexes have a long history dating back thousands of years [1, 2]. For example, in ancient China the use of gold was related to the desire for longevity and has been found in very old recorded prescriptions [3]. The element was also important for medieval alchemy in Europe as exemplified by so called "Aurum potabile" medicines, which contained gold in potable form [4]. In 1890 the famous bacteriologist Robert Koch reported about antibacterial properties of gold salts against tuberculosis strains [5]. This finding has probably paved the way of gold-based drugs into modern medicine. In the 1920s the physician Jacques Forestier hypothesized that gold compounds could be used to treat rheumatoid arthritis since the manifestations of this disease were similar to those of tuberculosis [6]. His studies have led to application of the first gold-based drugs, such as aurothioglucose and gold sodium thiomalate, for the treatment of rheumatoid arthritis.

In 1972 Sutton and colleagues reported about the antiinflammatory properties of orally administrable gold complexes and from these studies the gold phosphane compound auranofin emerged, which is nowadays considered as the lead compound of gold metallodrugs [7]. For auranofin and many other gold complexes also strong effects against cancer cells have been reported. These findings have triggered major efforts in the inorganic medicinal chemistry community to develop new gold-based anticancer drugs. Although so far no new gold metallodrug has reached the drug market, a rich knowledge on the medicinal chemistry of such complexes has been established and current clinical trials with some of the existing gold drugs emphasize the feasibility of the drug design approach.

2. CURRENT STATUS OF REGISTERED GOLD DRUGS

2.1. Gold Complexes in the Therapy of Rheumatoid Arthritis

Rheumatoid arthritis is the most common inflammatory disease of the joints and can be characterized as a chronic autoimmune disorder. It primarily affects the

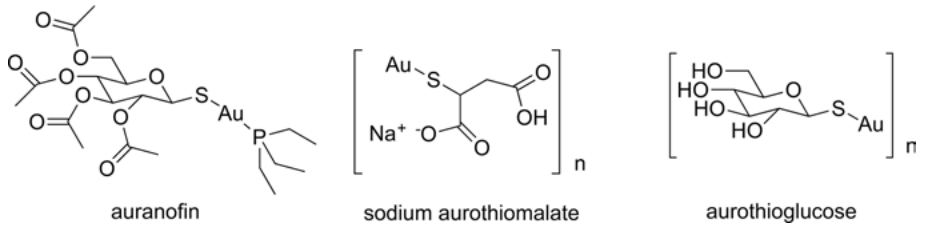

Figure 1. Examples of gold drugs. Sodium thiomalate and aurothioglucose are polymeric compounds.

joints but also other organs can be involved. There is currently no cure available and therapy focuses on the management of the disease and its symptoms, which can significantly affect the quality of life of the patients.

Several gold complexes have been applied to treat rheumatoid arthritis, the most frequently used are: aurothiomalate, aurothioglucose, and auranofin (see Figure 1). Whereas auranofin can be taken orally, the other gold complexes are adminstered by injection and are more effective [2, 8]. Gold drugs belong to the group of so called disease-modifiying antirheumatic drugs (DMARDs), which is a category of otherwise rather unrelated agents including the purine metabolism inhibitor methotrexate. The main purpose of DMARDs is to slow-down the progression of the chronic disease and to achieve a remission of the symptoms. Although gold-based therapy is effective, its relevance is decreasing based on the the fear of side effects, the requirement of strict patient monitoring, the lack of experience of physicians regarding the administration of the more complicated treatment procedure, and finally due to marketing strategies of pharmaceutical companies [8].

2.2. New Therapeutic Applications for Gold Drugs

Despite the decline in the application for the treatment of rheumatoid arthritis, there is a high interest in the development of gold metallodrugs for other indications. Certainly, this has been stimulated by the increasing knowledge on the modes of action of gold complexes as well as the global interest of the pharmaceutical industry in drug repurposing strategies. The cytotoxicity and *in vivo* antitumoral effects of auranofin had been noted in early reports [9, 10]. Besides this important medicinal application, gold complexes have also been studied successfully as antiinfective agents (antiparasitic, antibacterial, antiviral) [11].

A search for current clinical trials (www.clinicaltrials.gov) in March 2017 yielded several ongoing or recent studies for auranofin and aurothiomalate not related to rheumatoid arthritis. The conditions included several cancers or leukemia (e.g., lung cancer, recurrent ovarian epithelial cancer, chronic lymphocytic leukemia) and infectious diseases (e.g., amoebiasis, giardiasis, HIV).

3. GOLD(I) ANTICANCER DRUGS

Starting from the established gold(I) drugs, there have been substantial efforts in developing gold-based anticancer agents. In this section gold(I) phosphane complexes and gold(I) organometallics are reviewed as relevant types representing gold in the oxidation state +1.

3.1. Gold(I) Phosphane Complexes

The lead compound auranofin represents a neutral, linear two-coordinate gold phosphane complex with a thioglucose ligand. Phosphanes are good donor ligands and as such they are readily attached to gold(I). The successful development and the therapeutic efficacy of auranofin were most likely the deciding factors that have triggered ongoing efforts in developing metallodrugs based on a gold(I)(phosphane) partial structure. A structure-activity relationship study by Mirabelli and coworkers on a series of 63 complexes of the general type L-Au-X highlighted the importance of both the phosphane and thiosugar partial structures *in vitro* as well as *in vivo* [12]. Simple chlorido gold phosphane complexes such as ClAu(I)(triethylphosphane) (**1**) or ClAu(I)(triphenylphosphane) (**2**) (Figure 2) have demonstrated similar key features like auranofin, including strong cytotoxicity, antimitochondrial activity or thioredoxin reductase inhibition. The residues at the phosphorus atom likely affect gold bioavailability reflecting differences in lipophilicity. For example, complexes with the triphenylphosphane moiety showed a higher cellular uptake into cancer cells compared to the trialkyl analogues [13].

The gold phosphole complex GoPI (**3**) was found to be a highly efficient inhibitor of both glutathione reductase and thioredoxin reductase (TrxR). X-ray crystallography of glutathione reductase exposed to **3** confirmed that its ligands were replaced by cysteine residues of the enzyme [14]. Bischelating phosphanes such as **4** (Figure 2) are lipophilic cations, which have a long history in anticancer drug research. For **4** and related complexes lipophilicity was a crucial factor affecting cellular uptake, binding to plasma proteins and *in vivo* toxicity [15]. The higher kinetic stability of complexes with bischelating phosphanes is an important advantage. For **4** stability in the presence of serum and thiols was con-

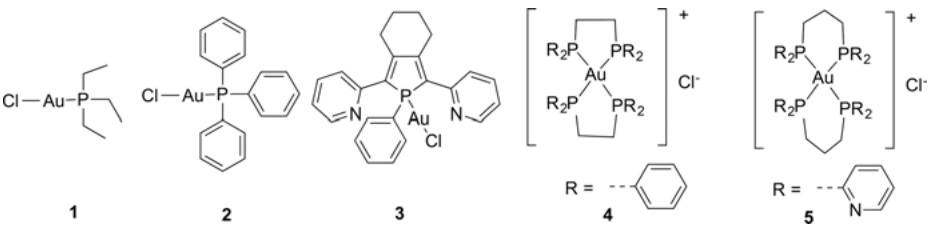

Figure 2. Selected examples of anticancer gold(I) phosphane complexes.

firmed and serum did not reduce the cytotoxicity of the complex. The compound also displayed promising activity *in vivo* [16]. Interestingly, for **4** and related complexes the presence of the phenyl groups at the phosphorus was of high relevance, and the biological activity was reduced or lost upon replacement with alkyl residues [17]. The lipophilic cationic character of bischelating phosphane gold(I) complexes can cause an accumulation inside mitochondria as a consequence of the higher membrane potential of these organelles. However, unspecific accumulation in mitochondria also might have caused toxic effects of **4** that prevented its further development [18].

The indicated problem could be solved by further structural optimization leading to the cationic **5** (Figure 2), which was reported to be selectively toxic in breast cancer cells and effectively inhibited TrxR activity. The gold(I) phosphane moiety has also been applied with (bio)conjugates and for the purpose of targeting. The underlying strategy is to link the cytotoxic gold partial structure with a component that itself carries biological activity and/or can be used to increase bioavailability. For example this can be achieved with peptide conjugates [19].

In conclusion, gold(I) phosphanes represent important anticancer-active moieties. Gold phosphane partial structures can also be found in many other types of gold drugs (e.g., gold alkynyl phosphane complexes, see below).

3.2. Oganometallic Gold(I) Complexes

In recent years organometallic gold complexes have attracted a high attention. This was certainly motivated by the increased stability of the metal-carbon bond that can be achieved, e.g., by using *N*-heterocyclic carbene (NHC) or alkynyl ligands, which are reviewed in this section. NHCs are strong σ-donor ligands that can be stably coordinated to a number of transition metals, including gold [20]. In the first essential reports on the exciting biological potential of gold(I) NHC complexes by Berner-Price and colleagues, cationic linear complexes with two NHC ligands (biscarbene complexes), such as **6** (Figure 3), were described to trigger strong antimitochondrial effects and to target protein selenols in preference to thiols [21, 22]. Importantly, **6** was able to inhibit TrxR activity in cells whereas no inhibition of glutathione reductase was noted [22]. Both TrxR inhibition and antimitochondrial effects, which have been identified in the early key reports, have been observed with many new gold(I) NHC complexes and can be considered as important contributors to their biological pattern. Taking these and the results from the protein crystallography studies with **3** [14] into account, gold(I) NHC chlorido complexes with a benzimidazole-derived NHC ligand were prepared by Ott et al. (see **7** in Figure 3 for an example) [23]. In these compounds the chlorido secondary ligand should be easily replaceable by thiol or selenol groups in the active site of TrxR and with this enable the design of very efficient inhibitors. In fact, a series of strong TrxR inhibitors could be obtained with this strategy and, importantly, the inhibition was selective if compared to glutathione reductase.

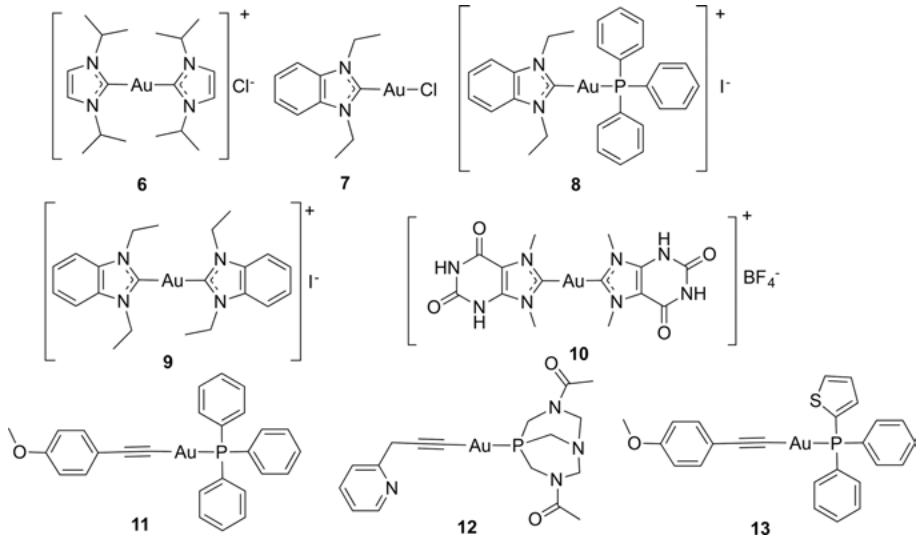

Figure 3. Selected examples of organometallic anticancer gold(I) complexes.

Complexes **8** and **9** represent derivatives of **7** (Figure 3), in which the anionic chloride ligand was replaced by triphenyl-phosphane or a second NHC ligand, respectively, leading to cationic species [24]. The calculated bond dissociation energies indicated a lower reactivity of the cationic complexes, and in fact they were less active TrxR inhibitors. However, the cellular uptake and trafficking into the mitochondria were increased for the cationic **8** and **9** and this resulted in higher overall cytotoxicity. Besides TrxR inhibition and antimitochondrial effects, also other cellular pathways were reported to be of high importance for the biological activity of gold(I) NHC complexes (see Section 5.1.1 for more details). Another very interesting example is the cationic biscarbene complex **10** reported by Casini et al. [25, 26]. Complex **10** contains two caffeine-derived NHC ligands and was found to be an efficient and selective G-quadruplex stabilizing agent. Importantly, **10** was shown to bind non-covalently to three distinct binding sites of a G-quadruplex structure [26].

The preference of gold(I) for a linear geometry together with the linearity of alkynes, which are good ligands due to their π-unsaturated nature, have made gold(I) alkynyl complexes useful organometallic tools with possible applications in material chemistry, supramolecular chemistry or luminescence [27]. Complex **11** (Figure 3) was one of the most active TrxR inhibitors out of a series of cytotoxic gold(I) triphenylphosphane complexes with structurally diverse alkynyl ligands reported by Ott et al. [28]. Interestingly, **11** triggered effective antiangiogenic effects in zebrafish embryos. Closer evaluation of the effects of **11** on cellular phosphorylation signaling showed an activation of the mitogen-activated protein kinases (MAPK) ERK1 and ERK2 (ERK: extracellular signal related kinase) as well as the chaperone HSP27 (heat shock protein 27) [29]. Administration of **11** *in vivo*, however, was problematic due to solubility issues, required

the development of a suitable formulation, and provided no tumor growth reduction so far. Further structural optimization of **11** was focused on an optimization of the phosphane ligands and led to its triethylphosphane anaologue as a probably better alternative for *in vivo* studies [29].

In this context the propargylthiol derivative **12** (Figure 3) with a solubility-enhancing phosphane ligand represents a very interesting development [30]. The complex led to an increase in the mean survival time and life expectancy in an athymic nude mice xenograft model. The tumor growth reduction was moderate and there was no acute toxicity. Another example, which showed good activity *in vivo* is **13** [31]. It was identified in a screening of various gold complexes, is an efficient TrxR inhibitor, and displayed highly promising results *in vivo*.

4. GOLD(III) ANTICANCER DRUGS

Due to the structural similarity to various platinum(II)-based anticancer drugs, gold(III) complexes have long been regarded as a class of effective anticancer therapeutics [32]. Nevertheless, the gold(III) ion under physiological condition is easily reduced to gold(I) or gold(0) (metallic gold). Thus, one major challenge for their medical development is the stability issue. By employing various tetra-, tri-, and bidentate ligands, numerous stable gold(III) complexes possessing anticancer properties have been identified in the last decade.

4.1. Gold(III) Complexes with Tetradentate Ligands

A stable gold(III) complex system, $[Au^{III}(porphyrin)]^+$, with a net cationic charge can be achieved by using the robust tetradentate porphyrinato ligand scaffold [33]. Che and coworkers have first reported in 2003 the anticancer properties of a gold(III) *meso*-tetraphenylporphyrin complex (gold-1a, **14**, Figure 4) [34]. *In vitro* and *in vivo* studies revealed that **14** is highly effective towards nasopharyngeal carcinoma (NPC) metastasis, and inhibits tumor growth of nude mice bearing colon cancer, neuroblastoma, melanoma, and cisplatin-resistant ovarian cancer [33]. Moreover, in 2013 Che, Sun, and coworkers have first identified its anticancer stem cells property [35].

The LD_{50} value (median lethal dose) of **14** was determined to be 6.8 mg/kg (effective anticancer dosage: ~3.0 mg/kg). One approach to reduce its toxicity is to employ drug carriers. Enhanced anticancer activities of **14** have been demonstrated by using polymeric encapsulating materials such as a mixture of gelatin and acacia [36], polyethylene glycol [37], and a type of organogold(III) supramolecular polymers [38]. Also, mesoporous silica nanoparticles for delivery of **14** with enhanced selectivity and apoptosis-inducing efficacy were employed [39].

An additional advantage for the medicinal development of the $[Au^{III}(porphyrin)]^+$ system is the ease in its structural modification. The anticancer studies of 25 gold(III) porphyrin complexes including some water-soluble

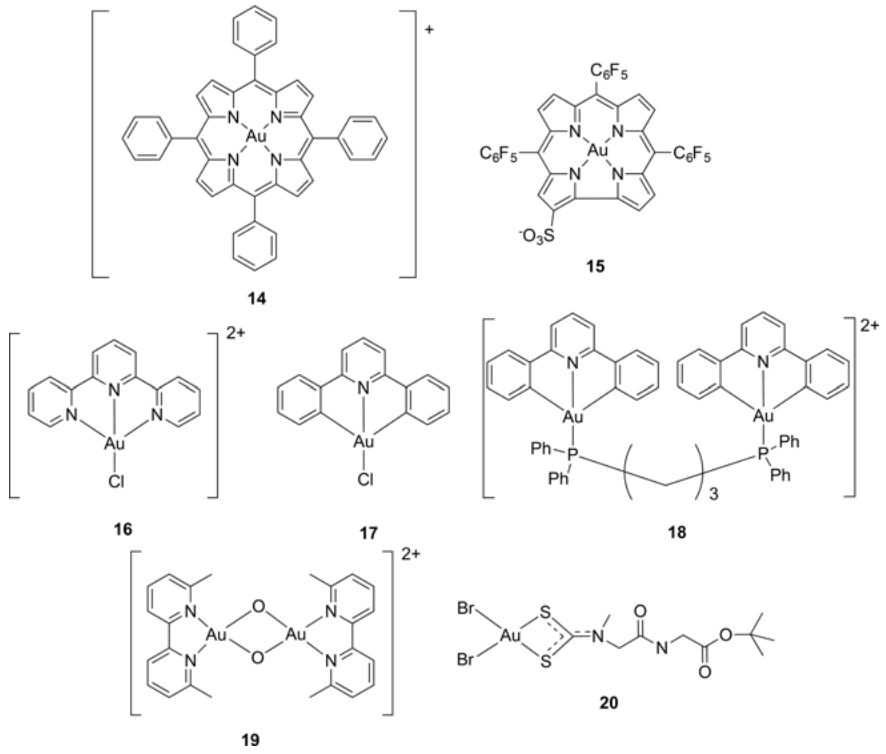

Figure 4. Selected examples of anticancer gold(III) complexes.

and asymmetrical analogs with a dynamic range of lipophilicity were reported [40]. Recently, Isab and coworkers reported the *in vitro* anticancer activities of gold(III) complexes of *meso*-1,2-di(1-naphthyl)-1,2-diaminoethane [41]. Sessler and coworkers have identified a series of new water-soluble gold(III) porphyrin complexes with cytotoxic IC_{50} values down to 9 μM toward a human ovarian cancer cell line in 2015 [42].

Other types of anticancer gold(III) complexes with tetradentate ligands have also been reported. A water-soluble gold(III) corrole complex (1-Au, **15**, Figure 4) was found to display promising cytostatic activity [43]. Cytotoxicity of gold(III) complexes with Schiff bases and bis(pyridyl)carboxamide ligands have previously been reported to exhibit comparable cytotoxicity to cisplatin [44]. Yet, a gold(III) complex containing cyclam (= 1,4,8,11-tetraazacyclotetradecane) was found to display a low cytotoxic activity towards a series of cancer cells, having IC_{50} values >100 μM [45].

4.2. Gold(III) Complexes with Tridentate Ligands

2,2′,2″-Terpyridine (terpy) is a typical tridentate ligand to stabilize a highly oxidizing metal center. The gold(III) complex of terpy **16** (Figure 4) has first been

reported by Lippard et al. in 1983 [46]. Che and coworkers in 1995 demonstrated its high binding affinity to calf thymus DNA [47], and in 2000, its promising *in vitro* anticancer activities have first been demonstrated by Messori and coworkers [45]. This gold(III) complex exhibited similar anticancer potency compared to that of the terpy ligand itself, suggestive of its ligand-mediated cytotoxic activity. Some other gold(III) complexes having tridentate terpy or aminoquinoline ligands have been reported [48] and four gold(III) complexes with terpy ligands showed higher cytotoxicity than cisplatin against various cancer cell lines [49].

An organogold(III) complex of 6-(1,1-dimethylbenzyl)-2,2'-bipyridine) (Au-bipy^c, **17**; Figure 4) showed potent anticancer activities *in vitro* [50]. A proteomic approach including the use of 2D gel electrophoresis separation and subsequent mass spectrometry identification has been launched in order to elucidate its action mechanisms in A2780 human ovarian cancer cells [51].

The anticancer activities of various gold(III) cyclometalated gold(III) complexes $[Au^{III}(C\hat{}N\hat{}C)L]^+$ (wherein HC^N^CH = 2,6-diphenylpyridine; L = an auxiliary ligand) was reported [52]. These complexes are stable in aqueous solutions containing glutathione. With triphenylphosphane as the auxiliary ligand, $[Au^{III}(C\hat{}N\hat{}C)L]^+$ was found to display cytotoxic activity towards different cancer cell lines with IC_{50} values down to ~4 μM. By using different bidentate bis(diphenylphosphane)C_n ligands (wherein C_n = saturated hydrocarbon linker with n = 1 to 6), gold(III) complexes of $[Au_2^{III}(C\hat{}N\hat{}C)_2(\mu\text{-bis(diphenylphosphane)}C_n)]^{2+}$ could be obtained. Notably, a dinuclear gold(III) phosphane complex $[(C\hat{}N\hat{}C)_2Au_2(\mu\text{-dppp})](CF_3SO_3)_2$ [Au3, **18** wherein dppp = bis(diphenylphosphino)propane] displayed a promising inhibition on tumor growth *in vivo*, and exerted low sub-chronic toxicities in beagle dogs [53].

Since 2006, Messori and coworkers have reported that various binuclear gold(III)-oxo complexes (e.g., Auoxo-6, **19**) were anticancer active and display a high cancer cell selectivity [54]. Another binuclear gold(III)-oxo complex (namely Auoxo3) has been studied for the interaction with the protein lysozyme [55]. The gold(III) metal center would undergo reduction and produce reactive gold(I) species, which are capable to bind with the protein and hence, form relatively stable derivatives.

4.3. Gold(III) Complexes with Bidentate Ligands

Since the first identification of the anticancer properties in 2005 [56], various gold(III) dithiocarbamato derivatives have been developed during the past ten years [57]. Some dithiocarbamate complexes containing amino acids or oligopeptides have been reported to display promising anticancer properties. Several gold(III) dithiocarbamato peptidomimetics were developed as promising anticancer agents against human breast neoplasia (e.g., **20**; Figure 4) [58]. These complexes show an improved chemotherapeutic index and therapeutic spectrum, and some of them are highly active towards human MDA-MB-231 xenografts. Very recently, various gold(III) pyrrolidinedithiocarbamato complexes have been reported as promising anticancer agents [59]. It was found that the bromido

derivative was more effective than the chlorido one in terms of IC_{50} values to the cancer cells.

Target-selective micelles for bombesin receptors to encapsulate the gold(III) dithiocarbamato complexes were prepared by developing some sterically-stabilized micelles having phospholipids as delivery systems [60]. Incorporation in micelle composition of a low amount of the peptide derivative containing a bombesin peptide does not change the size of the micelles. Their cancer-targeting properties were confirmed by using PC-3 cells overexpressing the GRP/bombesin receptors.

Casini and coworkers have reported the use of some anticancer gold(III) complexes to achieve inhibition of membrane water/glycerol channels of aquaporin proteins [61]. Various gold(III) complexes bearing nitrogen donor ligands including 1,10-phenanthroline, 2,2′-bipyridine, 4,4′-dimethyl-2,2′-bipyridine, and 4,4′-diamino-2,2′-bipyridine have been evaluated in human red blood cells expressing AQP1 and AQP3, which are responsible for water and glycerol movement, respectively.

Che and coworkers have developed various gold(III) complexes containing NHC ligands to be used as effective thiol "switch-on" fluorescent probes [62]. Some of them displayed promising *in vivo* anticancer properties. Another new class of gold(III) carbene complexes containing various bidentate C-deprotonated C^N and *cis*-chelating bis-NHC ligands has been synthesized [63]. These complexes displayed an inhibition on deubiquitinase UCHL3 with an IC_{50} value of 0.15 μM. Gold(III) complexes with dithiocarbamate ligands, $[Au^{III}(C^N)(R_2NCS_2)]^+$ (where HC^N = 2-phenylpyridine), were found to display significant inhibition on deubiquitinases, and high selective cytotoxicity towards breast cancer cells [64]. Also various gold(III) allenylidene compounds with phosphorescence properties were developed [65]. These complexes are readily self-assembled to form nanostructures in solution and display cytotoxicity towards cancer cells.

5. BIOLOGICAL FUNCTIONS OF GOLD COMPLEXES

5.1. Interactions with Biological Targets

Numerous research efforts have been directed to the understanding of the cytotoxic activity and related mode of action of cytotoxic gold-based complexes, as well as to the identification of their preferential "protein targets", as it is increasingly evident that, at variance with cisplatin [66], DNA is not the unique or major target for such compounds [67, 68]. In fact, although some gold(I) phosphane complexes were documented to interact with DNA or DNA polymerases, several subsequent studies strongly suggested that mitochondria and pathways of oxidative phosphorylation are the primary intracellular targets [69]. As an example, auranofin was reported to inhibit mitochondrial functions, to stimulate the release of cytochrome *c* and to induce apoptosis. In general, since their discovery as antiproliferative agents, various experiments on cancer cells revealed a variety of effects of gold compounds on cellular metabolism, including a high increase

of ROS formation and reduced mitochondrial activity, finally resulting in apoptotic cell death.

Notably, in the case of Au(I) complexes, most of these effects could be attributed to the strong and selective inhibition of the seleno-enzyme TrxR [70] as discussed in previous sections. In the case of Au(III) complexes, other proteins have emerged as putative pharmacological targets, including zinc-finger proteins [71–74], membrane water and glycerol channels (aquaporins), protein deubiquitinases [64], the proteasome [75], as well as other cancer-related enzymes. In this context, this section focuses only on the widely investigated TrxRs and on the most novel aquaporin targets, and includes a summary of representative studies on such systems. The reader is referred to other relevant literature for a more comprehensive overview on the topic [33, 76, 77].

5.1.1. Thioredoxin Reductases

TrxRs are homodimeric flavoproteins of the cellular antioxidant system which maintain a reducing environment by transmitting the electron flux from nicotinamide adenine dinucleotide phosphate (reduced) generated by the pentose phosphate pathway to thioredoxins (Trxs). The latter are a group of small (10- to 12-kD) and widely distributed redox active peptides that have a conserved -Trp-Cys-Gly-Pro-Cys-Lys- catalytic site that undergoes reversible oxidation and reduction of the two Cys residues [78]. The thioredoxin system is involved in the redox control of different signaling pathways and regulates crucial cell functions such as viability and proliferation [79]. Moreover, Trx expression is increased in several human primary cancers [80]. Accordingly, both Trx and TrxR might be considered as suitable targets for the development of new anticancer agents, since their inhibition leads to accumulation of H_2O_2 and reduces the capacity of one of the most important antioxidant systems in cancer cells to counteract ROS-mediated damage [81].

Belonging to the pyridine nucleotide-disulfide oxidoreductase family such as glutathione reductase, lipoamide dehydrogenase, and trypanothione reductase, TrxRs form homodimers and each subunit contains a redox-active catalytic active site containing a selenocysteine and a bound flavin adenine dinucleotide molecule. The selenocysteine redox center is located on a flexible arm, solvent-exposed and reactive towards electrophilic agents [82], where it constitutes an optimal target for the development of selective enzyme inhibitors, including gold-based complexes [83] with high affinity for selenol groups.

Within this framework, in the last years, a number of Au(I) complexes, both coordination and organometallics, have been reported for their TrxR inhibition properties, including auranofin [84]. Interestingly, recent studies have demonstrated a strong and selective TrxR inhibition by different families of Au(I) NHC complexes [85, 86], as initially reported by Berners-Price et al. in 2008 [22]. In cancer cells, this effect resulted in a general imbalance of the metabolism, including mitochondrial activity, leading to apoptotic cell death [87].

Notably, in 2014 Ott, Wölfl, and coworkers performed a detailed investigation of the biological activity of the selected Au(I) NHC complex **8** (see Figure 3)

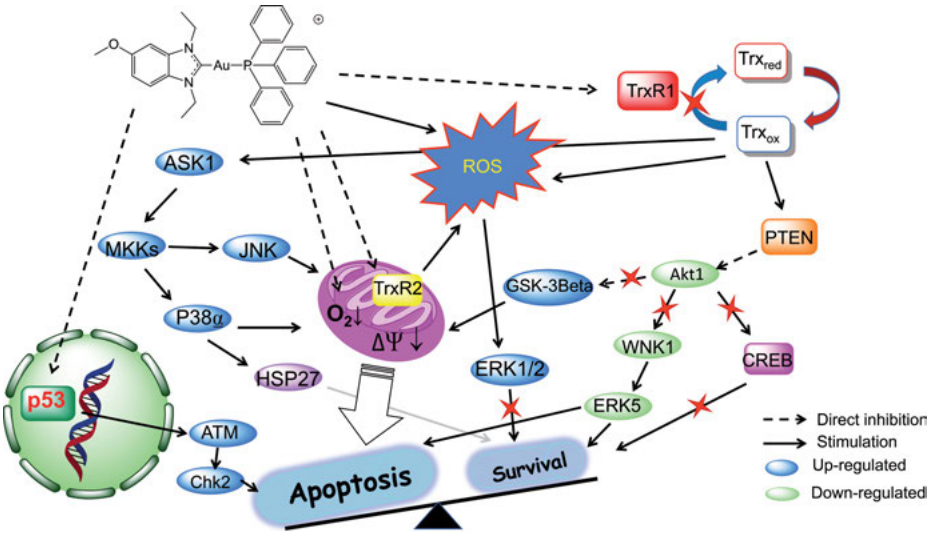

Figure 5. Signaling model underlying cell death pathways induced by a gold(I) NHC complex. Partly adapted from [88].

with a strong cytotoxic potential [88]. In summary, the reported results showed that the compound induces apoptosis in cancer cells targeting at least three different pathways, namely (i) inhibition of TrxR, (ii) direct inhibition of the mitochondrial respiratory chain, and (iii) indirect DNA damage. The ensemble of such alterations resulted in potent programmed cell death.

Specifically, the study made use of ELISA microarray analysis of signal transduction pathways combined to immunoblot assays, which revealed time-dependent up-regulation of pro-apoptotic signaling proteins, including p38 and JNK, whereas pro-survival signals directly linked to the Trx system were down-regulated [88]. Moreover, the analysis of cellular metabolism and morphological changes in cancer cells were investigated by a real-time biosensor chip, measuring pH changes and oxygen consumption, as well as cellular impedance. The obtained results pointed towards mitochondria as key targets for the gold compound, due to immediate inhibition of oxygen consumption in cancer cells upon drug treatment, as well as to cell shifts in the energy metabolism leading to switching to glycolysis from oxidative phosphorylation, mirrored by an increase in acidification rates [88]. Furthermore, the gold compound markedly increased ROS production, most likely due to TrxR inhibition. The overall cellular effects induced by the Au(I) NHC complex are summarized in Figure 5. Notably, similar effects were observed in the case of cancer cells treated with auranofin [88].

5.1.2. Aquaporins

Aquaporins (AQPs), members of a superfamily of transmembrane channel proteins, are ubiquitous in all domains of life, and can be functionally categorized

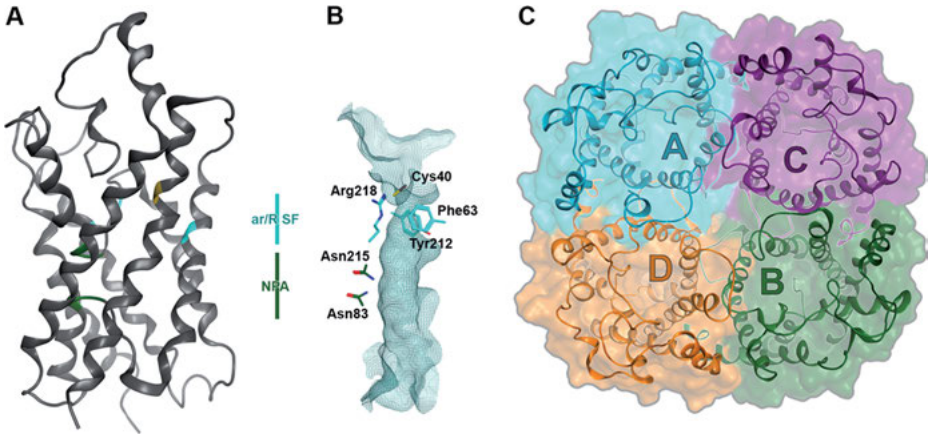

Figure 6. Predicted structure of a human AQP3 monomer. (**A**) Ribbon representation and (**B**) surface representation. Amino acid side chains are shown in stick representation the amino acids of the ar/R selectivity filter are in cyan; green represents the residues in the NPA region (ribbon representation is green for the whole NPA region and only representative Asn residues are displayed); Cys40, crucial for inhibition by gold complexes, is in pink (yellow for the S atom). (**C**) AQP3 tetramer, top view. The figures were generated with the Molecular Operating Environment (MOE), 2012.10, Chemical Computing Group Inc. (Montreal, QC, Canada).

into two major subgroups: (i) orthodox aquaporins, which are water-selective channels, and (ii) aquaglyceroporins, allowing permeation of water but also of non-polar solutes, such as glycerol and other polyols, urea, the reactive oxygen species hydrogen peroxide, as well as ammonia, gases, and metalloids. In mammals, the 13 aquaporin isoforms identified so far (AQP0–12) are expressed in a wide range of tissues and are involved in different biological functions [89].

AQPs share a common protein fold, with the typical six membrane-spanning helices surrounding the 20-Å-long and 3- to 4-Å-wide amphipathic channel, plus two half-helices with their positive, N-terminal ends located at the center of the protein and their C-terminal ends pointing towards the intracellular side of the membrane [90]. The selectivity of AQPs' transport of specific solutes is guaranteed by the presence of two constriction sites (Figure 6): (i) an aromatic/arginine selectivity filter (ar/R SF) near the periplasmic/extracellular entrance, that determines the size of molecules allowed to pass through and provides distinguishing features that identify the subfamilies, and (ii) a second constriction site composed of two conserved asparagine-proline-alanine (NPA) sequence motifs, located at the N-terminal ends of the two half-helices, at the center of the channel. In humans, functional aquaporins are organized in a tetrameric structure.

Due to their numerous roles in physiology, these proteins are essential membrane transporters involved in crucial metabolic processes and expressed in almost all tissues. Specifically, the 'aquaglyceroporins' regulate glycerol content in epidermal, fat, and other tissues, and appear to be involved in skin hydration, cell proliferation, carcinogenesis, and fat metabolism [91]. The functional signifi-

cance of glycerol transport by aquaglyceroporins has been the subject of several studies. For example, the relationship between aquaglyceroporin expression and cancer development has been reported, as well as a correlation with obesity.

With the aim to validate the hypotheses on the various roles of AQPs in health and disease, in addition to genetic approaches, the use of inhibitors to unravel aquaporin function and to develop new therapies holds great promise. However, so far no reported AQP inhibitors are good candidates for clinical development due to insufficient isoform selectivity and toxicity [92]. Within this context, Casini, Soveral, et al. have reported on the potent and selective inhibition of human AQP3 by a series of square planar gold(III) coordination compounds with nitrogen-donor ligands in human red blood cells (hRBC), using a stopped-flow technique [61, 93]. Interestingly, the compounds were able to potently inhibit glycerol transport in hRBC through hAQP3, while not having a significant effect on water transport, through the orthodox water channel human AQP1. The most effective inhibitor of the series, Auphen ($[Au(phen)Cl_2]Cl$, phen = 1,10-phenanthroline), was observed to have an IC_{50} in the low micromolar range (0.8 ± 0.08 μM). Notably, Auphen was far more potent than the mercurial benchmark inhibitor $HgCl_2$. It is also worth mentioning that coordination compounds with gold in a different oxidation state, namely Au(I), such as aurothioglucose and auranofin, were not able to inhibit either AQP1 or AQP3.

In order to gain insight into the mechanism of AQP3 inhibition by gold compounds, molecular modelling studies were undertaken and a homology model of hAQP3 was built, and used to further disclose the possible gold binding sites inside of the hAQP3 channel [93]. Since gold has a high affinity for binding to sulfur, the mechanism of inhibition of Auphen and analogues in hAQP3 is possibly based on the ability of Au(III) to interact with sulfur-donor groups of proteins such as the thiolate of cysteine or the thioether of methionine residues. In human AQP3, only the thiol group of Cys40 located just above the ar/R SF (see Figure 6) inside the protein channel is accessible for gold binding from the extracellular side. Therefore, this residue was proposed as a likely candidate for binding to gold(III) complexes via a direct Au-thiol bond [93]. According to the hypothesized mechanism of inhibition, the bound metal complex causes steric blockage of the pore, hindering the passage of glycerol and water through hAQP3. Notably, such a mechanism was supported by further site-directed mutagenesis studies, where mutation of Cys40 to Ser40 significantly decreased the inhibitory effects of Auphen [94].

Noteworthy, molecular dynamics (MD) approaches have recently been used to investigate the binding of Hg^{2+} ions to human AQP3 in order to gain further insight concerning the mechanisms of AQP inhibition by mercurial compounds [95]. Overall, such *in silico* approach suggests that the coordination environment of Hg^{2+} ions is determinant for the inhibition of the AQP3 water/glycerol flux, since it may induce major conformational changes in the protein structure leading to pore closure [95]. These findings were relevant also in the case of AQP3 inhibition by gold complexes studied by MD [96], supporting a mechanism whereby the closure of the pore is not due to steric blockage, but by conformational changes in the protein structure upon metal binding.

Interestingly, as human AQP3 has been shown to have a role in cell proliferation and migration and to be overexpressed in different cancer types [91], its possible role in cancer progression has been speculated. However, so far no clear mechanism unravelling the interplay between AQPs and cell proliferation has emerged, and new experiments designed specifically to address these challenging research questions are necessary. Thus, to investigate this hypothesis, the capacity of the Au(III) compounds of inhibiting selected AQP isoforms in cancer cells may be certainly exploited [94]. Notably, preliminary data showed that the antiproliferative effects exerted by Auphen in various cancerous and non-tumorigenic cells were proportional to the expression levels of AQP3 [94].

6. GENERAL CONCLUSIONS

The medical use of gold and its complexes has a long tradition and currently some gold(I) complexes are used as antirheumatic agents. The potential of the known gold drugs as anticancer agents has also been known for several decades and there have been substantial efforts in the development of gold-based antitumor drugs. Regarding gold(I) complexes, compounds with phosphane ligands and organometallics have been most frequently investigated.

Very promising effects, which can be modulated by optimization of the coordinated ligand structures, have been observed *in vitro* and *in vivo*. For gold(III) complexes, reduction to gold(0/I) under physiological conditions has to be considered. Stable complexes can be generated using different types of bi-, tri-, and tetradentate ligand systems and their high efficacy has been demonstrated *in vitro* and *in vivo*. Various mechanisms of action have been identified for gold drugs. Although some complexes were reported to interact with DNA, this biomolecule does not appear to be a general molecular target for gold species. Pathways and targets related to mitochondria and the Trx/TrxR system are more likely the key players in gold pharmacology. Furthermore, various other relevant targets have been identified. Among those are the membrane transporters aquaporins, which are very likely anticancer drug targets.

Current clinical trials evaluate the potential of approved gold drugs for cancer chemotherapy. Whereas these trials are additionally motivated by aspects of drug repurposing, the outcome of the studies might facilitate the translation of new gold metallodrugs into therapeutic application.

ACKNOWLEGMENTS

R. W.-Y. S. acknowledges the support from the Guangdong Natural Science Foundation Project (2016A030313064). I. O. acknowledges support by Deutsche Forschungsgemeinschaft (DFG, project OT338/7-1).

ABBREVIATIONS AND DEFINITIONS

AQPs	aquaporins
hRBC	human red blood cells
IC_{50}	half maximal inhibitory concentration
LD_{50}	median lethal dose
MD	molecular dynamics
NHC	N-heterocyclic carbene
ROS	reactive oxygen species
Trx	thioredoxin
TrxR	thioredoxin reductase

REFERENCES

1. S. J. Berners-Price, *Gold-Based Therapeutic Agents: A New Perspective*, in *Bioinorganic Medicinal Chemistry*, Ed. E. Alessio, Wiley-VCH Verlag GmbH, Weinheim, **2011**, 197–221.
2. W. F. Kean, I. R. L. Kean, *Inflammopharmacol*. **2008**, *16*, 112–125.
3. H. Zhao, Y. Ning, *Gold Bull.* **2001**, *34*, 24–29.
4. G. J. Higby, *Gold Bull.* **1982**, *15*, 130–140.
5. R. Koch, in Verhandlungen des X. Internationalen Medizinischen Kongresses, Bd. I., Berlin 1890, Verlag August Hirschwald, Berlin, 1891.
6. W. F. Kean, F. Forestier, Y. Kassam, W. W. Buchanan, P. J. Rooney, *Semin. Arthritis Rheumat.* **1985**, *14*, 180–186.
7. B. M. Sutton, E. McGusty, D. T. Waltz, M. J. Di Mattino, *J. Med. Chem.* **1972**, *15,* 1095–1098.
8. R. Rau, *Goldtherapie der rheumatoiden Arthritis*, UNI-MED Verlag AG, **2005**, ISBN 3–89599–820–6.
9. T. M. Simon, D. H. Kunishima, G. J. Vibert, A. Lorber, *Cancer* **1979**, *44*, 1965–1975.
10. C. K. Mirabelli, R. K. Johnson, C. M. Sung, L. Faucette, K. Muirhead, S. T. Crooke, *Cancer Res.* **1985**, *45*, 32–39.
11. J. M. Madeira, D. L. Gibson, W. F. Kean, A. Klegeris, *Inflammopharmacol.* **2012**, *20*, 297–306.
12. C. K. Mirabelli, R. K. Johnson, D. T. Hill, L. F. Faucette, G. R. Girard, G. Y. Kuo, C. M. Sung, S. T. Crooke, *J. Med. Chem.* **1986**, *29*, 218–223.
13. H. Scheffler, Y. You, I. Ott, *Polyhedron* **2010**, *29*, 66–69.
14. S. Urig, K. Fritz-Wolf, R. Reau, C. Herold-Mende, K. Toth, E. Davioud-Charvet, K. Becker, *Angew. Chem. Int. Ed.* **2006**, *45*, 1881–1886.
15. M. J. McKeague, S. J. Berners-Price, P. Galettis, R. J. Bowen, W. Brouwer, L. Ding, L. Zhuang, B. C. Baguley, *Cancer Chemother. Pharmacol.* **2000**, *46*, 343–350.
16. S. J. Berners-Price, C. K. Mirabelli, R. K. Johnson, M. R. Mattern, F. L. McCabe, L. F. Faucette, C.-M. Sung, S.-M. Mong, P. J. Sadler, S. T. Crooke, *Cancer Res.* **1986**, *46*, 5486–5493.
17. S. J. Berners-Price, G. R. Girard, D. T. Hill, B. M. Sutton, J. S. Jarrett, L. F. Faucette, R. K. Johnson, C. K. Mirabelli, P. J. Sadler, *J. Med. Chem.* **1990**, *33*, 1386–1392.
18. S. J. Berners-Price, P. J. Barnard, in *Ligand Design in Medicinal Chemistry*, Ed. T. Storr, John Wiley & Sons, Ltd., **2014**, 227–256.
19. S. D. Köster, H. Alborzinia, S. Can, I. Kitanovic, S. Wölfl, R. Rubbiani, I. Ott, P. Riesterer, A. Prokop, K. Merz, N. Metzler-Nolte, *Chem. Sci.* **2012**, *3*, 2062–2072.

20. M. N. Hopkinson, C. Richter, M. Schedler, F. Glorius *Nature* **2014**, *510*, 485–496.
21. M. V. Baker, P. J. Barnard, S. J. Berners-Price, S. K. Brayshaw, J. L. Hickey, B. W. Skelton, A. H. White, *Dalton Trans.* **2004**, 3708–3715.
22. J. L. Hickey, R. A. Ruhayel, P. J. Barnard, M. V. Baker, S. J. Berners-Price, A. Filipovska *J. Am. Chem. Soc.* **2008**, *130*, 12570–12571.
23. R. Rubbiani, I. Kitanovic, H. Alborzinia, S. Can, Kitanovic A., L. A. Onambele, M. Stefanopoulou, Y. Geldmacher, W. S. Sheldrick, G. Wolber, A. Prokop, S. Wölfl, I. Ott, *J. Med. Chem.* **2010**, *53*, 8608–8618.
24. R. Rubbiani, S. Can, I. Kitanovic, H. Alborzinia, M. Stefanopoulou, M. Kokoschka, S. Mönchgesang, W. S. Sheldrick, S. Wölfl, I. Ott, *J. Med. Chem.* **2011**, *54*, 86468–657.
25. B. Bertrand, L. Stefan, M. Pirrotta, D. Monchaud, E. Bodio, P. Richard, P. Le Gendre, E. Warmerdam, M. H. De Jager, G. M. M. Groothuis, M. Picquet, A. Casini, *Inorg. Chem.* **2014**, *53*, 2296–2303.
26. C. Bazzicalupi, M. Ferraroni, F. Papi, L. Massai, B. Bertrand, L. Messori, P. Gratteri, A. Casini, *Angew. Chem. Int. Ed.* **2016**, *55*, 42564–4259.
27. J. C. Lima, L. Rodriguez, *Chem. Soc. Rev.* **2011**, *40*, 5442–5446.
28. A. Meyer, C. P. Bagowski, M. Kokoschka, M. Stefanpoulou, H. Alborzinia, S. Can, D. H. Vlecken, W. S. Sheldrick, S. Wölfl, I. Ott, *Angew. Chem. Int. Ed.* **2012**, *51*, 8895–8899.
29. V. Andermark, K. Göke, M. Kokoschka, M. A. Abu el Maaty, C. T. Lum, T. Zou, R. W.-Y. Sun, E. Aguilo, L. Oehninger, L. Rodriguez, H. Bunjes, S. Wölfl, C. M. Che, I. Ott, *J. Inorg. Biochem.* **2016**, 160, 140–148.
30. E. García-Moreno, A. Tomás, E. Atrián-Blasco, S. Gascón, E. Romanos, J. Rodriguez-Yoldi, E. Cerrada, M. Laguna, *Dalton Trans.* **2016**, *45*, 2462–2475.
31. D. Zhang, Z. Xu, J. Yuan, Y.-X. Zhao, Z.-Y. Qiao, Y.-J. Gao, G.-A. Yu, J. Li, H. Wang, *J. Med. Chem.* **2014**, *57*, 8132–8139.
32. C. F. Shaw III, *Chem. Rev.* **1999**, *99*, 2589–2600.
33. T. Zou, C. T. Lum, C.-N. Lok, J.-J. Zhang, C.-M. Che, *Chem. Soc. Rev.* **2015**, *44*, 8786–8801.
34. C.-M. Che, R. W.-Y. Sun, W.-Y. Yu, C.-B. Ko, N. Zhu, H. Sun, *Chem. Commun.* **2003**, 1718–1719.
35. C. T. Lum, A. S.-T. Wong, M. C. M. Lin, C.-M. Che, R. W.-Y. Sun, *Chem. Commun.* **2013**, *49*, 4364–4366.
36. J. J. Yan, R. W.-Y. Sun, P. Wu, M. C. M. Lin, A. S.-C. Chan, C.-M. Che, *Dalton Trans.* **2009**, *39*, 7700–7705.
37. P. Lee, R. Zhang, V. Li, X. Liu, R. W.-Y. Sun, C.-M. Che, K. K.-Y. Wong, *Int. J. Nanomed.* **2012**, *7*, 731–737.
38. J.-J. Zhang, W. Lu, R. W.-Y. Sun, C.-M. Che, *Angew. Chem. Int. Ed.*, **2012**, *51*, 4882–4886.
39. L. He, T. Chen, Y. You, H. Hu, W. Zheng, W.-L. Kwong, T. Zou, C.-M. Che, *Angew. Chem. Int. Ed.* **2014**, *53*, 12532–12536.
40. R. W.-Y. Sun, C. K.-L. Li, D.-L. Ma, J. J. Yan, C.-N. Lok, C.-H. Leung, N. Zhu, C.-M. Che, *Chem. Eur. J.* **2010**, *16*, 3097–3113.
41. M. Altaf, S. Ahmad, A.-N. Kawde, N. Baig, A. Alawad, S. Altuwaijri, H. Stoeckli-Evans, A. A. Isab, *New J. Chem.* **2016**, *40*, 8288–8295.
42. A. D. Lammer, M. E. Cook, J. L. Sessler, *J. Porphyrins Phthalocyanines* **2015**, *19*, 398–403.
43. R. D. Teo, H. B. Gray, P. Lim, J. Termini, E. Domeshek, Z. Gross, *Chem. Commun.* **2014**, *50*, 13789–13792.
44. R. W.-Y. Sun, C.-M. Che, *Coord. Chem. Rev.* **2009**, *253*, 1682–1691.
45. L. Messori, F. Abbate, G. Marcon, P. Orioli, M. Fontani, E. Mini, T. Mazzei, S. Carotti, T. O'Connell, P. Zanello, *J. Med. Chem.* **2000**, *43*, 3541–3548.

46. L. S. Hollis, S. J. Lippard, *J. Am. Chem. Soc.* **1983**, *105*, 4293–4299.
47. H.-Q. Liu, T.-C. Cheung, S.-M. Peng, C.-M. Che, *Chem. Commun.* **1995**, 1787–1788.
48. X. Wang, Z. Guo, *Dalton Trans.* **2008**, 1521–1532.
49. P. Shi, Q, Jiang, Y. Zhao, Y. Zhang, J. Lin, L. Lin, J. Ding, Z. Guo, *J. Biol. Inorg. Chem.* **2006**, *11*, 745–752.
50. G. Marcon, S. Carotti, M. Coronello, L. Messori, E. Mini, P. Orioli, T. Mazzei, M. A. Cinellu, G. Minghetti, *J. Med. Chem.* **2002**, *45*, 1672–1677.
51. T. Gamberi, L. Massai, F. Magherini, I. Landini, T. Fiaschi, F. Scaletti, C. Gabbiani, L. Bianchi, L. Bini, S. Nobili, G. Perrone, E. Mini, L. Messori, A. Modesti, *J. Proteomics* **2014**, *103*, 103–120.
52. C. K.-L. Li, R. W.-Y. Sun, S. C.-F. Kui, N. Zhu, C.-M. Che, *Chem. Eur. J.* **2006**, *12*, 5253–5266.
53. R. W.-Y. Sun, C.-N. Lok, T. T.-H. Fong, C. K.-L. Li, Z. F. Yang, T. Zou, A. F.-M. Siu, C.-M. Che, *Chem. Sci.* **2013**, *4*, 1979–1988.
54. S. Nobili, E. Mini, I. Landini, C. Gabbiani, A. Casini, L. Messori, *Med. Res. Rev.* **2010**, *30*, 550–580.
55. I. R. Krauss, L. Messori, M. A. Cinellu, D. Marasco, R. Sirignano, A. Merlino, *Dalton Trans.* **2014**, *43*, 17483–17488.
56. L. Giovagnini, L. Ronconi, D. Aldinucci, D. Lorenzon, S. Sitran, D. Fregona, *J. Med. Chem.* **2005**, *48*, 1588–1595.
57. L. Ronconi, D. Aldinucci, Q. P. Dou, D. Fregona, *Anticancer Agents Med. Chem.* **2010**, *10*, 283–292.
58. C. Nardon, M. S. Sara, H. Yang, J. Zuo, D. Fregona, Q. P. Dou. *PLoS One* **2014**, *9*, e84248.
59. C. Nardon, F. Chiara, L. Brustolin, A. Gambalunga, F. Ciscato, A. Rasola, A. Trevisan, D. Fregona, *ChemistryOpen* **2015**, *4*, 183–191.
60. P. Ringhieri, R. Iannitti, C. Nardon, R. Palumbo, D. Fregona, G. Morelli, A. Accardo, *Int. J. Pharm.* **2014**, *473*, 194–202.
61. A. P. Martins, C. Ciancetta, A. de Almeida, A. Marrone, N. Re, G. Soveral, A. Casini, *ChemMedChem* **2013**, *8*, 1086–1092.
62. T. Zou, C. T. Lum, S. S.-Y. Chui, C.-M. Che, *Angew. Chem. Int. Ed.* **2013**, *52*, 2930–2933.
63. F. F. Hung, W.-P. To, J.-J. Zhang, W.-Y. Wong, C.-M. Che, *Chem. Eur. J.* **2014**, *20*, 8604–8614.
64. J.-J. Zhang, K.-M. Ng, C.-N. Lok, R. W.-Y. Sun, C.-M. Che, *Chem. Commun.* **2013**, *49*, 5153–5155.
65. X.-S. Xiao, W.-L. Kwong, X. Guan, C. Yang, W. Lu, C.-M. Che, *Chem. Eur. J.* **2013**, *19*, 9457–9462.
66. R. C. Todd, S. J. Lippard, *Metallomics* **2009**, *1*, 280–291.
67. A. Casini, C. Hartinger, C. Gabbiani, E. Mini, P. J. Dyson, B. K. Keppler, L. Messori, *J. Inorg. Biochem.* **2008**, *102*, 564–575.
68. P. C. A. Bruijnincx, P. J. Sadler, *Curr. Opin. Chem. Biol.* **2008**, *12*, 197–206.
69. P. J. Barnard, S. J. Berners-Price, *Coord. Chem. Rev.* **2007**, *251*, 1889–1902.
70. S. J. Berners-Price, A. Filipovska, *Metallomics* **2011**, *3*, 863–873.
71. F. Mendes, M. Groessl, A. A. Nazarov, Y. O. Tsybin, G. Sava, I. Santos, P. J. Dyson, A. Casini, *J. Med. Chem.* **2011**, *54*, 2196–2206.
72. U. A. Laskay, C. Garino, Y. O. Tsybin, L. Salassa, A. Casini, *Chem. Commun.* **2015**, *51*, 1612–1615.
73. A. Jacques, C. Lebrun, A. Casini, I. Kieffer, O. Proux, J. M. Latour, O. Seneque, *Inorg. Chem.* **2015**, *54*, 4104–4113.
74. A. Citta, V. Scalcon, P. Gobel, B. Bertrand, M. Wenzel, A. Folda, M. P. Rigobello, E. Meggers, A. Casini, *RSC Adv.* **2016**, *6*, 79147–79152.

75. E. M. Nagy, L. Ronconi, C. Nardon, D. Fregona, *Mini-Rev. Med. Chem.* **2012**, *12*, 1216–1229.
76. W. Liu, R. Gust, *Coord. Chem. Rev.* **2016**, *329*, 191–213.
77. C. Nardon, G. Boscutti, D. Fregona, *Anticancer Res.* **2014**, *34*, 487–492.
78. M. Matsui, M. Oshima, H. Oshima, K. Takaku, T. Maruyama, J. Yodoi, M. M. Taketo, *Develop. Biol.* **1996**, *178*, 179–185.
79. S. Lee, S. M. Kim, R. T. Lee, *Antioxid. Redox Signal.* **2013**, *18*, 1165–1207.
80. H. Nakamura, J. Bai, Y. Nishinaka, S. Ueda, T. Sasada, G. Ohshio, M. Imamura, A. Takabayashi, Y. Yamaoka, J. Yodoi, *Cancer Detect. Prevent.* **1999**, *24*, 53–60.
81. S. Urig, K. Becker, *Semin. Cancer Biol.* **2006**, *16*, 452–465.
82. S. Gromer, J. Wissing, D. Behne, K. Ashman, R. H. Schirmer, L. Flohe, K. Becker, *Biochem. J.* **1998**, *332*, 591–592.
83. A. Bindoli, M. P. Rigobello, G. Scutari, C. Gabbiani, A. Casini, L. Messori, *Coord. Chem. Rev.* **2009**, *253*, 1692–1707.
84. M. P. Rigobello, L. Messori, G. Marcon, M. A. Cinellu, M. Bragadin, A. Folda, G. Scutari, A. Bindoli, *J. Inorg. Biochem.* **2004**, *98*, 1634–1641.
85. B. Bertrand, A. Casini, *Dalton Trans.* **2014**, *43*, 4209–4219.
86. A. Citta, E. Schuh, F. Mohr, A. Folda, M. L. Massimino, A. Bindoli, A. Casini, M. P. Rigobello, *Metallomics* **2013**, 1006–1015.
87. L. Oehninger, R. Rubbiani, I. Ott, *Dalton Trans.* **2013**, *42*, 3269–3284.
88. P. Holenya, S. Can, R. Rubbiani, H. Alborzinia, A. Junger, X. Cheng, I. Ott, S. Wölfl, *Metallomics* **2014**, *6*, 1591–1601.
89. *Aquaporins in Health and Disease: New Molecular Targets for Drug Discovery*, Eds G. Soveral, S. Nielsen, A. Casini, CRC Press, Taylor & Francis Group, 2016.
90. L. S. King, D. Kozono, P. Agre, *Nature Rev. Mol. Cell Biol.* **2004**, *5*, 687–698.
91. A. de Almeida, G. Soveral, A. Casini, *MedChemComm* **2014**, *5*, 1444–1453.
92. G. Soveral, A. Casini, *Expert Opin. Ther. Pat.* **2016**, 1–14.
93. A. P. Martins, A. Marrone, A. Ciancetta, A. Galan Cobo, M. Echevarria, T. F. Moura, N. Re, A. Casini, G. Soveral, *PLoS One* **2012**, *7*, e37435.
94. A. Serna, A. Galan-Cobo, C. Rodrigues, I. Sanchez-Gomar, J. J. Toledo-Aral, T. F. Moura, A. Casini, G. Soveral, M. Echevarria, *J. Cell. Physiol.* **2014**, *229*, 1787–1801.
95. A. Spinello, A. de Almeida, A. Casini, G. Barone, *J. Inorg. Biochem.* **2016**, *160*, 78–84.
96. A. De Almeida, A. F. Mosca, D. Wragg, M. Wenzel, P. Kavanagh, G. Barone, S. Leoni, G. Soveral, A. Casini, *Chem. Commun*. **2017,** *27*, 3830–3833.

8

Coordination Complexes of Titanium(IV) for Anticancer Therapy

Edit Y. Tshuva and Maya Miller

Institute of Chemistry, The Hebrew University of Jerusalem, Jerusalem 9190401, Israel
<edit.tshuva@mail.huji.ac.il>

ABSTRACT 219
1. INTRODUCTION 220
2. CYCLOPENTADIENYL-BASED COMPLEXES 221
   2.1. Titanocene Dichloride – Pros and Cons 221
   2.2. Leading Cyclopentadienyl-Based Derivatives 222
   2.3. Mechanistic Insights 226
3. BUDOTITANE AND RELATED DIKETONATO COMPLEXES 227
4. COMPLEXES OF PHENOLATO LIGANDS 230
   4.1. $LTiX_2$-Type Complexes 230
   4.2. Complexes of Reduced Lability 233
   4.3. Mechanistic Insights 236
5. CONLUSIONS AND OUTLOOK 237
ACKNOWLEDGMENTS 240
ABBREVIATIONS AND DEFINITIONS 240
REFERENCES 240

Abstract: Titanium(IV) coordination complexes represent attractive alternatives to platinum-based anticancer drugs. The advantage of the titanium metal lies in its low toxicity, and the hydrolysis of titanium(IV) coordination complexes in biological water-based environment to the safe and inert titanium dioxide is an enormous benefit. On the other hand, the rapid hydrolysis of titanium(IV) complexes in biological environment and their rich aquatic chemistry hampered the exploration and the development of effective compounds.

Titanium(IV) complexes were the first to enter clinical trials for cancer treatment following the success of platinum-based chemotherapy, with the pioneering compounds titanocene dichloride and budotitane. Despite the high efficacy and low toxicity observed *in vivo*, the com-

Metal Ions in Life Sciences, Volume 18 Edited by Astrid Sigel, Helmut Sigel, Eva Freisinger, and Roland K. O. Sigel

https://doi.org/10.1515/9783110470734-008

pounds failed the trials due to insufficient efficacy to toxicity ratio and formulation complications. The rapid hydrolysis of the complexes led to formation of multiple undefined aggregates and difficulties in isolating and identifying the particular active species and its precise cellular target. Numerous derivatives with different labile ligands or substitutions on the inert ones contributed to improve the complex anticancer features, and the best ones were comparable with, and occasionally better than cisplatin. Hydrolytic stability was improved in some cases but remained challenging. The following generation of phenolato-based complexes that came three decades later exhibited high activity and markedly improved stability, where no dissociation was observed for weeks in biological solutions. Complexes of no labile ligands whatsoever that remain intact in solution demonstrated *in vitro* and *in vivo* efficacy, with no signs of toxicity to the treated animals. Mechanistic insights gained for the different complexes analyzed include, among others, possible interaction with DNA and induction of apoptosis. Such complexes are highly promising for future exploration and clinical development.

Keywords: anticancer · cytotoxicity · metallodrugs · non-platinum · titanium(IV)

1. INTRODUCTION

Cancer diseases of more than 100 different kinds represent a major cause of human deaths worldwide, with more than 10 million new cases diagnosed each year. Cancer research spans across numerous directions and fields, from diagnosis to unique approaches to therapy and drug delivery. Much progress was achieved in recent years with novel therapeutic methodologies, such as immunotherapy [1] and precision (personalized) medicine [2]. Nevertheless, such approaches, although considered relatively selective and effective, may be applied only for specific cases and are very limited to particular cancer types and populations. The vast majority of cancer cases thus still relies on chemotherapy for attempted treatment, and will surely continue to do so for many years to come. As the main limitations of classical chemotherapy are the severe side effects accompanying the drug efficacy, developing highly potent chemotherapeutics of reduced side effects, effective toward a relatively wide range of cancer types, is of essence.

Cisplatin [3], as a landmark of metallodrugs-based chemotherapy for cancer, is discussed elsewhere in this book, along with its closely related Pt-based derivatives. The success of cisplatin in the clinic, along with its drawbacks relating mainly to resistance development and severe toxicity, opened a new research direction that explores complexes of other transition metals as potential anticancer therapeutics [4–22]. Complexes of Ru, Cu, Au, V, Ga, and others were investigated, some showing promising results, as discussed in other chapters. The first metal reaching clinical trials following the platinum compounds is Ti, with the two pioneering derivatives titanocene dichloride [23, 24] and budotitane [25, 26] (Figure 1) [27–31].

Titanium is relatively abundant in the earth crust in the oxidation state +IV and as a first row transition element it is relatively labile. Still, identified natural roles of titanium in biological organisms are lacking [32]. A reasonable explanation relies on the complex aquatic chemistry of titanium. Titanium(IV) coordination complexes in water solutions mostly readily hydrolyze due to the high affinity of the electron-poor d^0 hard metal to hard O-based ligands. Formation of O-

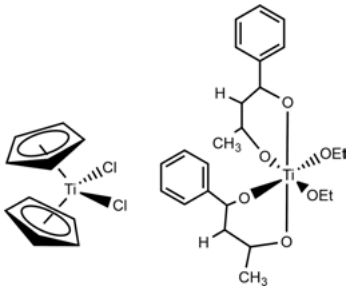

Figure 1. Titanocene dichloride (left) and budotitane (right).

bridged aggregates normally leads to the final thermodynamic product titanium dioxide. Nevertheless, titanium is considered a bio-friendly non-toxic metal, with some historical mentioning of therapeutic activity, including toward tumors [8]. Titanium dioxide often appears in food products, as well as various cosmetic products and drugs, and thus Ti is often detected in the human body and can reach various organs [8]. It is thus reasonable to base the design of new therapeutics on metal coordination complexes that after hydrolysis in the human body should yield a non-toxic product that can hopefully leave the body through normal function. And still, the rich hydrolytic chemistry of titanium(IV) coordination complexes remains an issue to resolve, as the formation of unidentified aggregates in the biological environment is disadvantageous for controllable transport of the active species and mechanistic elucidation. In this review we will discuss the main classes of titanium(IV) coordination complexes studied for anticancer therapy, their advantages and disadvantages, and future perspectives. The anticancer related reactivity and drug delivery of Ti-based nano-materials is discussed elsewhere and will not be covered herein [33].

2. CYCLOPENTADIENYL-BASED COMPLEXES

2.1. Titanocene Dichloride – Pros and Cons

Titanocene dichloride is one of several metallocenes that have shown promising anticancer features [34–40], as firstly reported by Köpf-Mayer and coworkers in 1979 [41]. Efficacy was detected in mice models toward Ehrlich ascites tumors [41–47], colon carcinoma [48, 49], lung adenocarcinoma, and small cell lung carcinoma [50], gastrointestinal carcinomas [51], leukemia [52], ovarian carcinoma [53, 54], renal carcinoma [55], and more [49, 56–58]. Tumor size often decreased by more than 50 %, with up to 100 % survival of the treated animals. Titanocene dichloride was also effective on cells resistant to cisplatin [59–63], establishing an advantage over the platinum parent complex. Importantly, the biggest advantage of the titanium metal was manifested by the relatively mild toxicity observed *in vivo* [42, 59, 64–68]. Some indications of liver damage were detected

following a single injection through concentration increase of related enzymes, along with decrease in glucose levels, but return to normal values after several days implied a reversible condition [64]. No renal impairment was observed after administration of LD_{50} doses [68], and some postperiotonic symptoms were also manageable through pH control [42]. Some teratogenic effects on embryos were also noted [69, 70]. Most notably, nephro- and gastrotoxicity were markedly reduced relative to those of cisplatin detected in control animals [64, 65]. Pharmacokinetic studies pointed to titanium build-up in the liver and intestine, with no changes of titanium level in the brain relative to untreated control animals [71].

The promising results obtained with titanocene dichloride encouraged its entry to clinical trials. Phase I trials with patients suffering from various cancer types revealed limited efficiency, with dose-limiting toxicities being reversible high levels of creatinine and bilirubin, nephrotoxicity or liver toxicity [72–75]. Additional toxicities detected included hepatic toxicity, emetic toxicity, with side effects of fatigue, hypokalemia, diarrhea, nausea, and metallic taste. Phase II trials were conducted at 270 mg/m^2 every three weeks with patients suffering from advanced renal cell carcinoma [76] and metastatic breast cancers [77]. Although the former showed mild side effects, the latter suffered from various gastrointestinal, neurological, haptic and renal-related side effects. Nevertheless, the effectiveness of the treatment was limited in both cases, implying no real advantage for the use of titanocene dichloride as drug for these cancer conditions. The compound thus failed the trials due to an overall insufficient activity/toxicity ratio.

The contrast between the promising results obtained for titanocene dichloride *in vivo* and the disappointing ones obtained in clinical trials, on one hand demonstrates the enormous potential of the highly potent titanium complexes, but on the other, reflect the differences among biological systems. Although these differences may be associated to numerous biological parameters, one distinct feature of the titanium complexes stands out as a possible contributor to failure in clinical trials, especially when compared to the clinically effective platinum complexes: The rapid hydrolysis of the titanium complexes under physiological conditions to multiple species, which surely occurs more extensively in a bigger biological system, is likely to produce many products that are not all active, leading to an unfavorable activity-to-toxicity ratio. Studies on the hydrolysis of titanocene dichloride [78–83] indeed pointed to rapid loss of the labile chloride ligands, within seconds to minutes (more rapid and extensive than that observed for cisplatin) [78], followed by hydrolysis of the cyclopentadienyl (Cp) ligands as well to give multiple species. Some solubility difficulties also affected the hydrolysis rate [84]. It thus became clear that hydrolysis of titanium complexes for anticancer application is an obstacle to overcome, which encouraged the investigation of related compounds of various substitutions.

2.2. Leading Cyclopentadienyl-Based Derivatives

Derivatives of titanocene dichloride were studied extensively for anticancer applications. Both substitution of the labile chloride ligands and substituted Cp

rings were investigated [85]. Most substitutions of the labile ligands with other monoanionic groups such as CO, Br, F, and more, did not significantly improve the complex anticancer features [50, 57, 86–88], although some higher activity was reported specifically for fluorinated compounds [89, 90], and carboxylate [50, 86, 87, 91, 92] and oximato [93] complexes, which also often presented enhanced solubility. Some derivatives, including ionic ones with improved solubility, also exhibited *in vivo* efficacy [57, 58, 94–98]. An additional schisandrol-bound complex showed improved stability and solubility [99]. Moreover, substitution of the labile ligands with chelating agents were also investigated [95, 97, 100–103], which often contributed to improved cytotoxicity and stability. It is noteworthy that IC_{50} values obtained for these titanocene derivatives were mostly higher than those of cisplatin studied as control. Nevertheless, improved activity *in vitro* was achieved relative to the titanocene dichloride parent compound, which had been more effective *in vivo* than *in vitro* [55, 104, 105].

More significant influence of the complex anticancer features was obtained through substitutions on the more inert Cp rings [106]. Numerous substitutions were investigated, from simple alkylations to complex cyclic derivatizations. Impact was achieved on cytotoxic activity *in vitro* and efficacy *in vivo*, and on solubility and stability in water and other relevant solutions. The different substitutions often affected the complex symmetry, and hence the chirality, which was relevant to the number of stereoisomers present in solution.

Methylation on the Cp had a minor influence on the complex performance. Although slightly improving the hydrolytic stability, no significant change in cytotoxicity was observed [79, 82]. In contrast, more hydrophilic units such as carboxy or charged amino units contributed to somewhat improved cytotoxicity on particular lines, with activity also toward cisplatin-resistant lines, although the activity was generally lower than that of cisplatin toward cisplatin-sensitive lines [87, 107–113]. Increasing further the steric bulk of the Cp substituent in a series of chiral (racemic) *ansa*-titanocene complexes mostly affected solubility, depending on the total hydrophilicity of the entire group [114–119]. Nevertheless, improved IC_{50} values relative to titanocene dichloride could be obtained, although still generally worse than those obtained for cisplatin [115–118, 120–126]. Representative examples are presented in Figure 2. For instance, the *ansa*-titanocene complex known as "titanocene X" was particularly effective, also *in vivo*, increasing the survival of treated mice inoculated with Ehrlich ascites tumor [127].

Another large series of complexes investigated included substituted benzyl or related aromatic moieties on one or two of the Cp rings, to give achiral complexes, lacking the disadvantage of two enantiomers present in solution [110, 118, 122, 128–148]. Representative examples are presented in Figure 3a. Improvements in the complex potency were certainly noticeable. One leading derivative is titanocene Y, which showed activity comparable to that of cisplatin as well as *in vivo* efficacy [129, 130, 149–157]. Its oxali derivative also presented high efficacy *in vitro* and *in vivo* [158, 159]. Additionally, a recent study compared among two enantiomers of a complex with chiral substituted rings, showing some enantioselectivity, supporting a chiral target/s along the cytotoxicity pathway (Figure 3a, bottom right) [160].

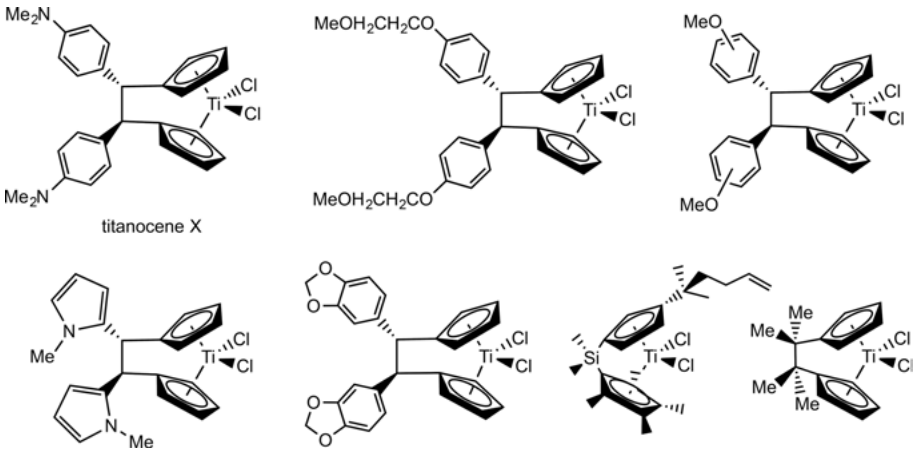

Figure 2. Representative bridged titanocene dichloride derivatives analyzed for cytotoxicity.

Overall, although solubility improvement was achieved for some derivatives, most did not exhibit significant improvement in hydrolytic stability [118, 132, 148]. Another set of compounds aimed at improving this character includes derivatives with an additional coordinating amino arm; the added donor was proposed to improve stability of the presumed active species and also enhanced solubility [136, 161–164]. Such compounds showed good cytotoxicities also on cisplatin-resistant cell lines [113]. The best compounds of this advanced series have demonstrated activities comparable to those of cisplatin. An example of a leading soluble complex of this series with activity in the micromolar range is presented in Figure 3b [165]. Notably, attempts to add separate coordinating ligands, such as amino acids, although often improving solubility, did not afford particularly stable complexes as such ligands dissociated fairly rapidly [166]. Another approach to enhance hydrolytic stability involved linking a Cp substituent to one of the labile groups, thus affording a chelating ligand [103, 148, 167]. An example is presented in Figure 3c.

A marked improvement of cytotoxicity was interestingly achieved through the covalent combination with a second metal center in heterodinuclear Ti/Au, Ru, Pd, or Pt complexes (or heterotrinuclear ones with two added metal centers, Figure 4) [168–173]. These complexes showed an activity comparable with, and even higher than, that of cisplatin, also toward cells that are cisplatin-resistant, with notable improvement relative to the mononuclear analogues. *In vivo* efficacy was also detected. The stability of these complexes was often greater as well.

Another approach to improve solubility and often also stability involves incorporation of the titanocene compound into polymeric material for controlled delivery [174–180]. For example, grafting functionalized titanocene into nanostructured-silica enabled high activity toward several cell lines, while inhibiting hydrolysis processes. The activity varied among the different derivatives, in good correlation with their reactivity when administered directly, implying little influ-

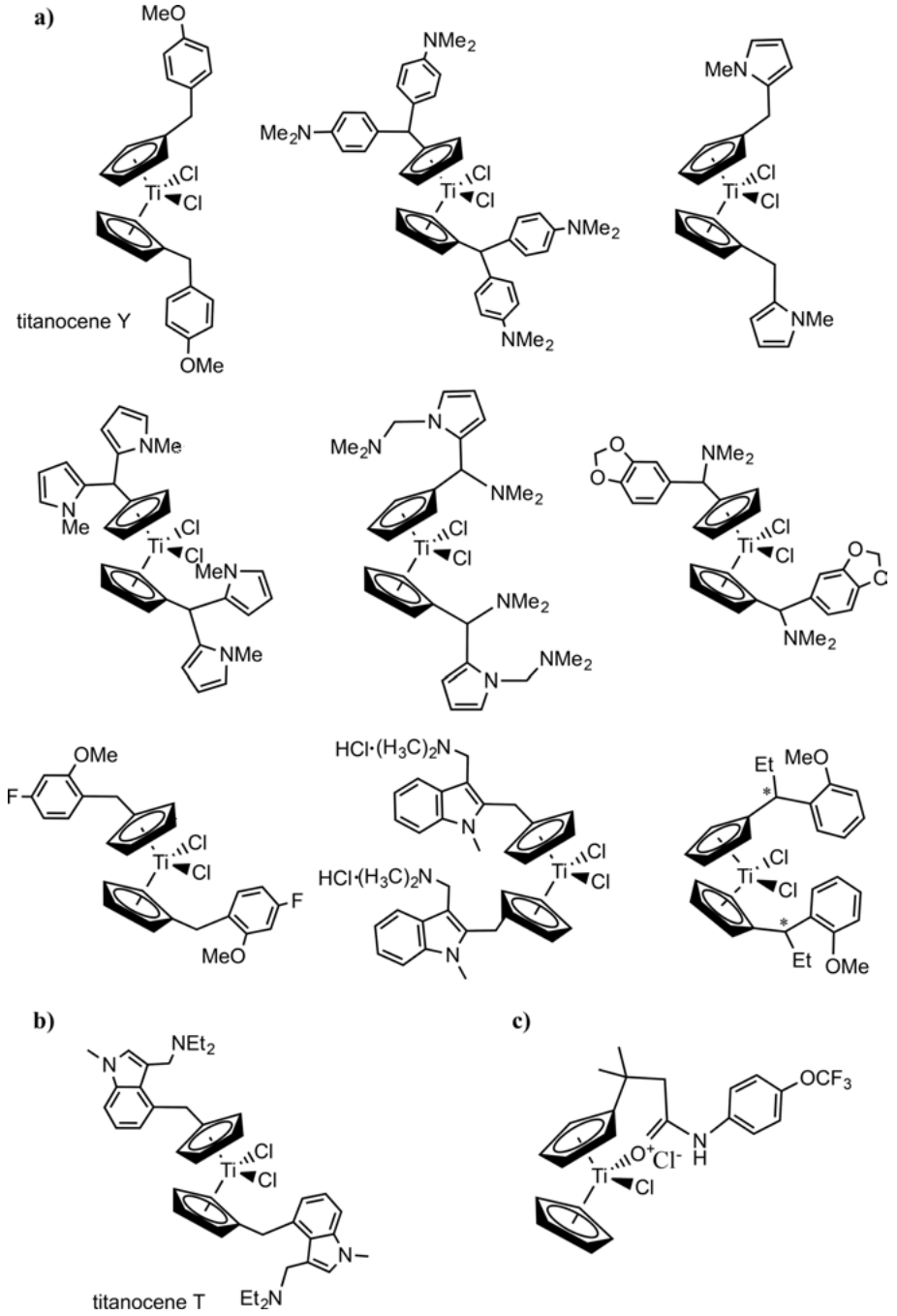

Figure 3. Representative aryl-substituted titanocene dichloride derivatives analyzed for cytotoxicity (**a**) with various substitutions; (**b**) with added amino coordination for added stability; (**c**) with aryl substitution bridged to a labile ligand for added stability.

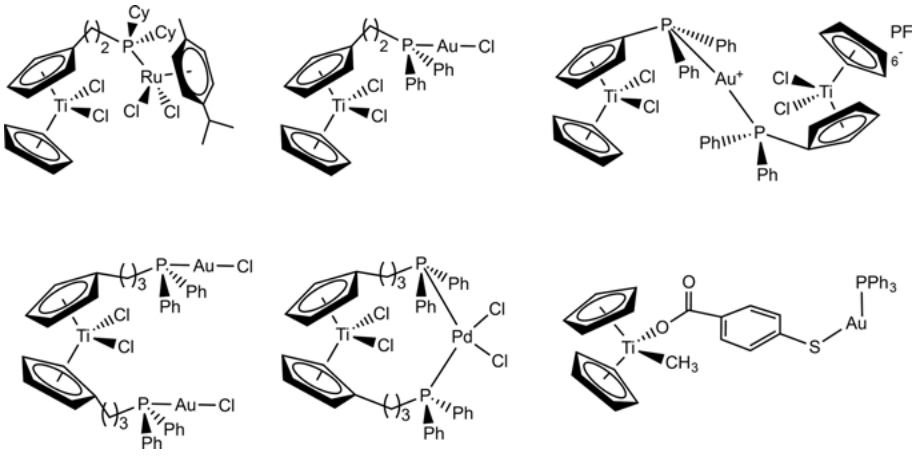

Figure 4. Representative heterodi- or trinuclear complexes of titanocene dichloride derivatives covalently linked to a different metal center(s), analyzed for cytotoxicity.

ence of the polymer on the activity pattern. Another interesting study aimed at improving selective delivery involved functionalizing the titanocenes with steroidal esters, to enable recognition by specific receptors on the cell membrane surface [181]. High activities were recorded especially on hormone-dependent cell types.

It is thus evident that a massive amount of work has been conducted with this family of Cp-based anticancer complexes. Interestingly, it is difficult to draw a clear correlation between specific structural parameters and particular impacts, as these were variable among the series tested. Some obvious conclusions are that hydrophilicity improves water solubility, chelation increases hydrolytic stability, and steric bulk impact depends on the particular group and its location. Nevertheless, among the many derivatives investigated, improvements in antitumor features were certainly achieved relative to the parent compound titanocene dichloride, mostly in *in vitro* activity and solubility, and lesser with hydrolytic stability. Activity is generally observed also for cells resistant to cisplatin, and *in vivo* studies do not point to significant toxicity, exemplifying the advantage of the titanium metal. Nonetheless, it appears that perhaps due to the remaining hydrolytic instability issue, and lack of substantial mechanistic knowledge, no additional clinical trials took place for titanocene derivatives.

2.3. Mechanistic Insights

Several mechanistic studies were conducted for titanocene dichloride as well as some Cp-substituted derivatives, to shed light on their mode of operation. A detailed tutorial review on the topic, gathering mechanistic information of various titanium(IV) complexes was recently reported [182], and thus the mechanistic insights gained will be described here in brief. As naturally all first compari-

sons were to the parent compound cisplatin, binding to DNA was considered. Early sub-cellular distribution analyses indeed pointed to the entry of the Ti to the cell and therein to the nuclei [183–187]. It was also found that titanocene dichloride can interfere with the metabolism of nucleic acids [188, 189]. Follow-up work by different methodologies also for additional derivatives supported the interaction of the titanium(IV) complex with nucleotides and DNA, where stability plays an important role [52, 60, 81, 87, 91, 148, 149, 190–206].

Related studies implied on interruption to cell cycle and induction of apoptotic pathways, often along with upregulation of related proteins such as p53 and activation of caspases [60, 89, 114, 154, 171, 174, 192, 207, 208]; this was also supported by gene expression analyses [193, 209], although some newer derivatives studied recently pointed to an alternative mechanism not involving cell cycle arrest or DNA breaks [160]. Alternative mechanisms suggested influence of kinase proteins [160, 172, 210], inhibition to topoisomerase I and II [145, 211], and other possible enzymes [8, 172, 212]. Accordingly, antiangiogeneic activity was recorded for some specific derivatives [128, 150, 159, 212, 215]. An enhancement of antiproliferative activity was also observed in estrogen receptor positive cells [216], suggesting a "hormone-like" behavior. Altogether, the different possible pathways identified and variation among derivatives imply that more than a single mode of action is possible for titanium(IV) complexes, which themselves may also operate differently [182].

Additional mechanistic investigations addressed the issue of delivery into cells. Accessibility is obviously an important issue for any synthetic drug, and the change of administrating solvent alone had a marked impact on reactivity [84]. Several studies pointed to binding of Ti to the human serum protein transferrin, as a competitor of the natural substrate Fe [217–229]; the protein thus may deliver the metal into cells, predominantly to cancer cells due to enhanced levels of transferrin receptors on the cell surface. Interaction with albumin has also been proposed when considering the role of serum proteins [157, 230–233]. It is thus obvious that drug delivery and targeting is a critical issue to address in any future studies of anticancer metallodrugs, as for any designed therapeutics.

3. BUDOTITANE AND RELATED DIKETONATO COMPLEXES

The anticancer activity of diketonato complexes (Figure 5a) was discovered shortly after that of titanocene dichloride [234–240]. The halogenated compounds (Figure 5a, X = Cl, Br, F) were tested first and showed efficacy on leukemia and other mice models. Consequently, the related ethoxylated derivatives showed somewhat enhanced efficacy on colon tumors, more significantly decreasing tumor size and animal mortality. The activity reported was greater than that of fluorouracil, commonly applied for treatment of colon cancer conditions. Interestingly, here as well, the reported toxicity was relatively minor, with the only toxological observation being abscess-forming bronchopneumonia, and minor liver and nephrotoxicity. Binding to DNA was also observed [241].

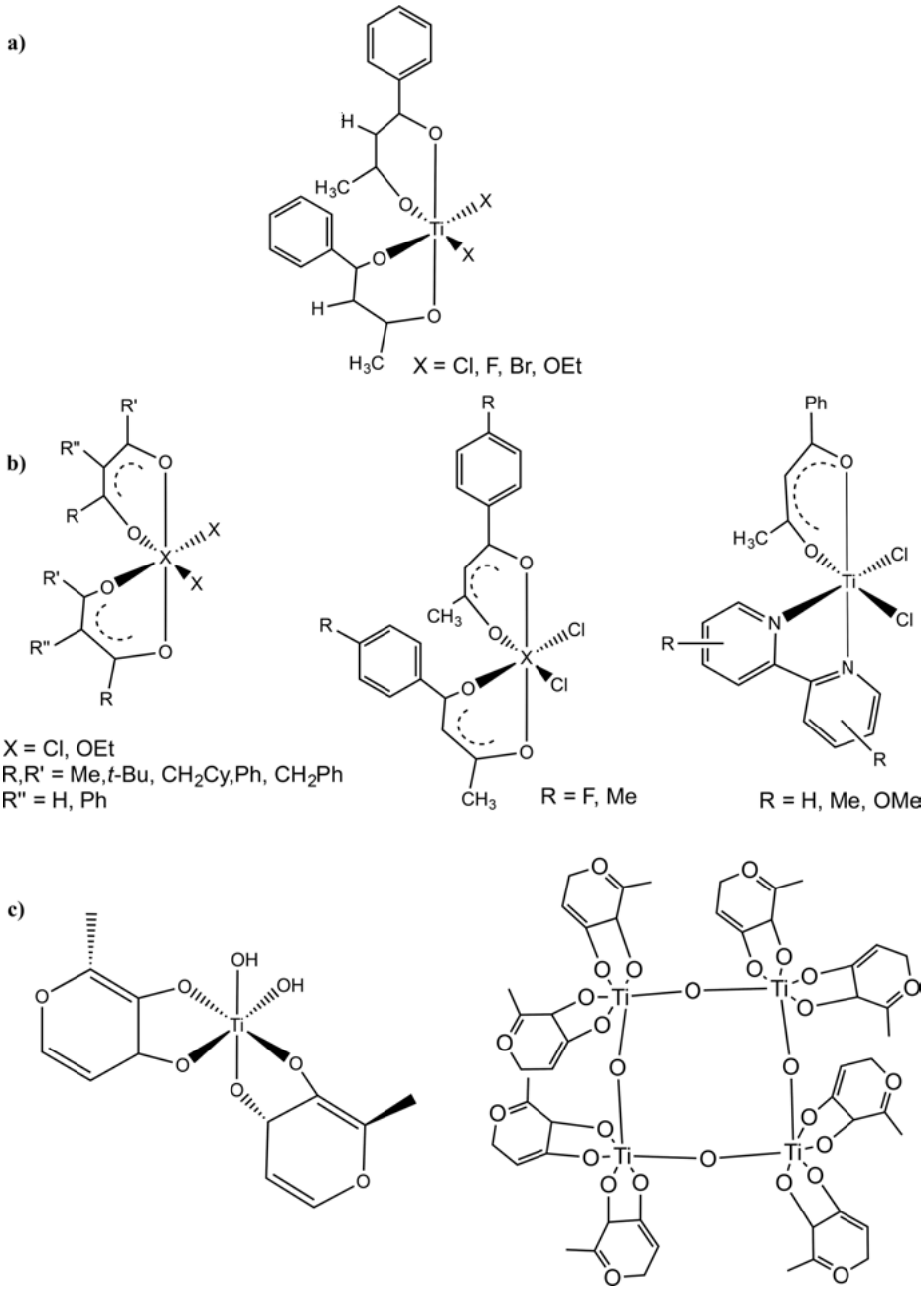

Figure 5. Budotitane and related diketonato Ti(IV) complexes analyzed for cytotoxicity; (**a**) with different labile ligands; (**b**) with different/altered diketonato systems; (**c**) maltolato-based derivatives.

The positive results observed *in vivo* with budotitane led to phase I clinical trials [239, 240, 242]. The tolerated dose was determined as 230 mg/m^3 and the limiting toxicity was identified as cardiac arrhythmia with mild hepatoxicity. Nevertheless, as observed with titanocene dichloride, tumor response was minor.

Structure-activity relationship studies included derivatives with not only different labile groups (Figure 5a), but also different substitutions on the aromatic rings and on the diketonato skeleton, as well as monodiketonato Ti(III) complexes (Figure 5b) [238, 243–247]. The labile ligands mostly did not impact strongly the antitumor features, asymmetry in the diketonato was favourable for increasing activity, and the larger planarity afforded by the phenyl substitution improved efficacy, presumably by enhancing DNA intercalating interactions [238, 244, 248].

One marked challenge encountered with this family of compounds relates to their aqueous chemistry and speciation. The variety of possible isomers and their relevance to the antitumor features of the compounds were investigated [238, 249–251]. Most active compounds adopt the *cis* configuration in solution, for which different isomers may exist in equilibrium. Interestingly, some of the isomers are chiral, rendering two enantiomers in solution. The hydrolytic instability of these compounds leads to relatively rapid loss of the labile ligands to form oxo-bridged products and increase further the number of species present in solution [238, 249, 250, 252].

Moving from Cl to OEt as the labile group enhances somewhat the stability, as well as replacing both with a chelating agent [251], but nonetheless, stability and accessibility of the active species remain a challenge. Interestingly, some polynuclear oxo-bridged partial hydrolysis products of these compounds showed themselves a degree of cytotoxicity and *in vivo* efficacy when encapsulated in liposome [253, 254]. Related complexes of maltolato ligands (Figure 5c) [111, 255] were also investigated, which featured enhanced stability but also yielded polynuclear oxo-bridged products at physiological pH. This product itself showed high stability as manifested by its reluctance to transfer Ti(IV) to apotransferrin unlike related titanocene derivatives (see above), and still featured cytotoxic activity.

It is thus obvious that the diketonato complexes join the titanocene compounds in establishing the high potency of titanium complexes for cancer treatment. The strong points remain the high efficacy *in vivo* and mild side effects in treated animals, where the weakness lies in the hydrolytic instability and formulation difficulties and multiple possible isomeric species. Additional titanium(IV) complexes of different amino and alkoxo ligands presented in recent years were tested for anticancer applications, some showed cytotoxicity features, but mostly without marked enhancement of hydrolytic stability [256–264]. On the other hand, slight activity was reported for triazine complexes of high stability [265]. The following generation of compounds therefore had to address the hydrolytic stability issue for highly active complexes and provide more water resistant and controllable anticancer titanium agents.

4. COMPLEXES OF PHENOLATO LIGANDS

In 2007 a new generation of titanium complexes was introduced [266], based on phenolato chelating polydentate ligands. As the main remaining drawback of the previously known titanium(IV) complexes was their hydrolytic instability and undefined chemistry in aqueous biological environment, the main aim was to design ligand systems with higher denticity and strong Ti–O coordination. The strong titanium(IV) phenolato binding offers increased resistance toward formation of O-bridged species upon interaction with water. The first group of compounds tested was of the type $LTiX_2$, L being a tetradentate dianionic chelating ligand and X being a labile monoanionic monodentate group, to resemble the structural motif of both titanocene dichloride and budotitane, as well as that of cisplatin. Later studies evinced, in accordance with the reactivity of polynuclear diketonato complexes (see above), that such labile ligands are not essential for the cellular operation of the complexes, thus governing a new ligand design as described below.

4.1. $LTiX_2$-Type Complexes

The first group of phenolato titanium(IV) complexes for cancer treatment included "salan" type ligands and two *cis* labile alkoxo ligands (Figure 6). The C_2 symmetrical complexes were each obtained as a single (racemic) geometrical isomer. Complexes of this type demonstrated *in vitro* activity toward various cancer cell lines, including those resistant to cisplatin and MDR (multi-drug resistant), with IC_{50} values in the low micromolar range [266–270]. In some *in vitro* studies, synergism with cisplatin was observed [271]. Importantly, negligible activity was detected on non-cancerous primary murine cells [269]. Consequently, *in vivo* efficacy was also established [272, 273], with consistently no signs of toxicity to treated animals, as also demonstrated on zebrafish embryos showing no reduction in viability following treatment [274]. Interestingly, the activity of some derivatives was comparable with, and occasionally higher than that of cisplatin, and higher than those of previously known parent titanium complexes such as titanocene dichloride [274]. Notably, the hydrolytic stability of such complexes was markedly higher than those of the previously known compounds of Cp and diketonato ligands. The higher stability is probably a result of strong

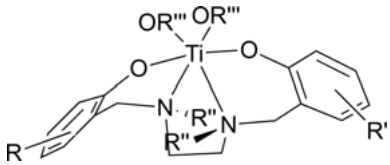

Figure 6. "Salan" type diaminobis(phenolato) $LTiX_2$-type complexes analyzed for cytotoxicity.

chelating binding of the bis(phenolato) ligand. Additionally, the choice of alkoxy labile groups versus halides contributed to enhanced stability. In the presence of water, these complexes undergo hydrolysis of the labile X groups within a few hours/days, to give defined polynuclear oxo-bridged clusters, which are themselves stable for weeks in water [267, 275].

Structure-activity investigations of cytotoxic salan-type complexes included numerous derivatives, showing a strong influence of ligand structure on the complex performance [267, 275–280]. When analyzing the impact of substitution on the main inert salan ligands, the following insights were gained: (a) *ortho* halogenation generally increased hydrolytic stability; (b) N-methylation versus NH increased stability; (c) steric bulk reduced cytotoxicity. Asymmetrical complexes enabled fine-tuning of ligand properties to often obtain higher activity than that of both symmetrical analogues [278]. Replacing the ethylenediamino bridge with homo/piperazine had little effect [276], while the phenylenediamine moiety dramatically decreased the hydrolytic stability [281]. When looking into the effect of the labile ligands, as observed with previous complexes, no great impact on cytotoxicity was observed when analyzing different monoanionic alkoxo ligands, except for their influence on the overall steric bulk [279] and solubility of the complex [282]. Nonetheless, replacing the two labile ligands with a chelating group increased the hydrolytic stability of the complex as expected, often maintaining cytotoxicity features (see below in Section 4.2) [267, 276, 283–285].

A profound stereochemical study was performed on the chiral $LTiX_2$-type phenolato anticancer complexes (Figure 7a) [286–289]. Having a symmetry of C_2, these complexes are present in solution as a mixture of enantiomers, similarly to budotitane and some *ansa*-titanocene derivatives (see above). Ligand-to-metal chiral induction enabled isolation of pure enantiomers in high chemical and enantiomeric purity. The activity of the two enantiomers was therefore compared, and analyzed with respect to the racemic mixture. Specific derivatives showed different activity of the two enantiomers, while for others the activity of the two enantiomers was similar. Interestingly, for most compounds analyzed, the activity of the pure enantiomers was markedly different from that of the racemic mixture, which could not be explained as an additive effect of both enantiomers operating in an unrelated fashion, nor by a competitive mechanism. It was thus proposed that different active diastereomers form when starting from an optically pure compound or from a racemate. Indeed, the dinuclear hydrolysis products forming from the optically pure compound and its racemate were crystallographically characterized as different diastereomers (Figure 7b), supporting their possible participation as active species. This observation questioned the necessity of the labile ligands, especially as the stereochemistry of chiral (*sec*-butoxide) labile ligands did not influence the complex performance.

Another group of $LTiX_2$-type complexes of a different geometrical structure analyzed for antitumor applications is based on "salen" ligands [290, 291]. Unlike the salan derivatives, featuring *cis* labile ligands that may enable chelate binding to a biological target, salen complexes possess *trans* labile ligands due to the planarity of the tetradentate ligand, wrapping around the metal center equatorially (Figure 8a). Bulky labile ligands further contributed to the pure isolation

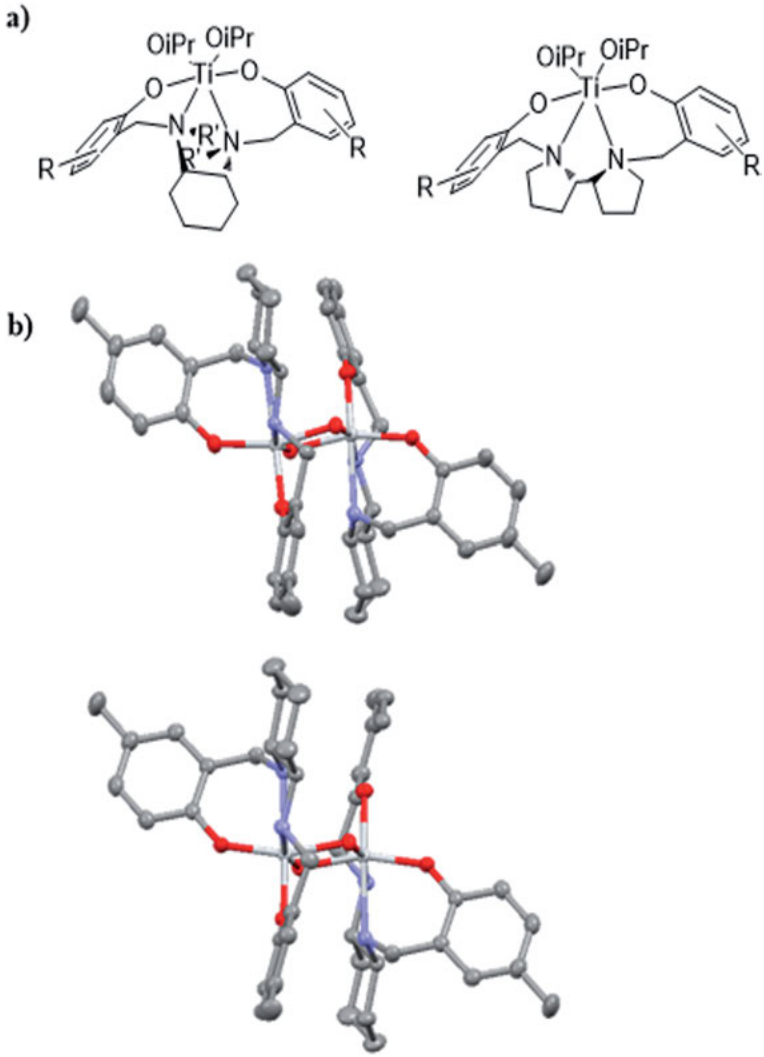

Figure 7. Chiral "salan"-type phenolato complexes; (**a**) complexes analyzed as pure enantiomers; (**b**) the homo chiral dimeric hydrolysis product of an optically pure "salan"-titanium(IV) complex (top) and the corresponding hetero-chiral product of the racemate (bottom). This figure was prepared from the CCDC data base (856889 and 856888, see [289]).

of the *trans* complexes. Interestingly, these *trans* complexes demonstrated high cytotoxicity and hydrolytic stability comparable to that of the corresponding salan counterparts. This provides another clue to the insignificance of the labile ligands and their specific orientation. A follow-up study with "salalen"-type complexes that are half salan-half salen hybrids (Figure 8b) of a third geometrical structure (*cis* labile ligands and *cis* phenolato donors) provided complexes with

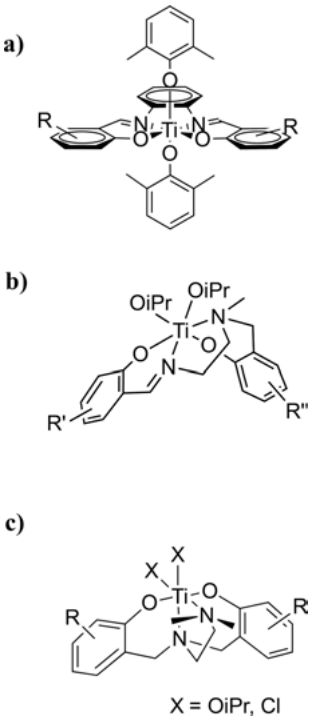

Figure 8. Other $LTiX_2$-type phenolato complexes; (**a**) "salen"; (**b**) "salalen"; (**c**) complexes with branched connectivity.

high cytotoxicity, yet low hydrolytic stability, probably due to their rigid structure [292].

A related ligand system that was explored included the donor atoms in a branched rather than sequential connectivity, where one amine donor is located on a side arm (Figure 8c) [293, 294]. Complexes of this type exhibited marked cytotoxicity but reduced stability, probably due to weaker coordination of the side arm amine donor.

The observations with the $LTiX_2$-type phenolato complexes discussed above suggested that the labile ligands are not essential for reactivity, and being the first to hydrolyze, they reduce the overall hydrolytic stability of the complexes. This was consistent with the activity observed earlier for the hydrolysis products of diketonato complexes (see above). This conclusion prompt the analysis of various more inert titanium(IV) complexes lacking particularly labile groups for anticancer applications.

4.2. Complexes of Reduced Lability

As described above, the $LTiX_2$-type complexes undergo hydrolysis of the labile ligands to give inert oxo-bridged clusters within a few hours; and yet they show

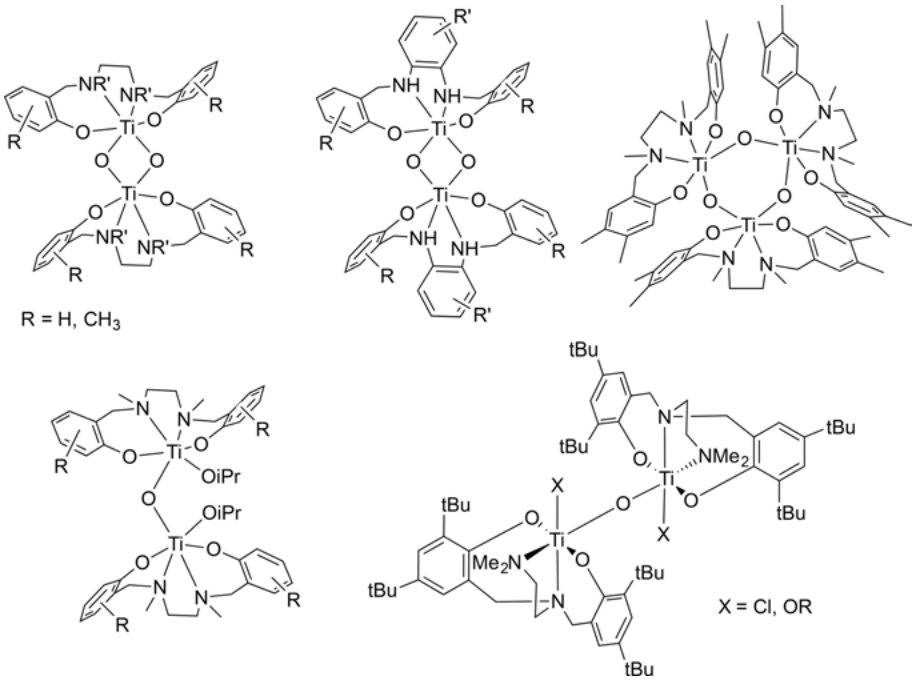

Figure 9. Oxo-bridged polynuclear hydrolysis products of $LTiX_2$-type Ti(IV) phenolato complexes analyzed for cytotoxicity.

cytotoxicity following incubation in cells for up to three days. Therefore, the hydrolysis products were suspected as the active species, as is also supported by the studies on diketonato-based clusters (see above).

Although some early studies with defined bulky trimers and dimers showed no activity [267, 275, 277], later studies with smaller dimers and other clusters formulated into nano-particles showed marked cytotoxicity (Figure 9) [261, 293, 295–297]. This observation confirmed that large steric bulk has a negative effect on cytotoxicity, and thus formulations improve solubility and facilitate cellular penetration [295], emphasizing the importance of biological accessibility. It thus became obvious that labile groups are not required of active titanium(IV) complexes, giving rise to a new structural design of octahedral inert complexes.

One group of more inert compounds consists of complexes of one bis(phenolato) tetradentate ligand and an additional chelating ligand (Figure 10a) [267, 276, 283–285, 292]. Such complexes demonstrated higher hydrolytic stability, and some also possessed efficacy both *in vitro* and *in vivo*. Substitution on this chelating ligand had some impact on hydrolytic stability depending on its electronic character. Switching the phenolato to softer thiophenolato donors hampered the stability as expected. Other complexes reported included a pentacoordinate ligand and one added labile group (Figure 10b); these bulky complexes again demonstrated enhanced stability relative to their bis(isopropoxo) counterparts, and mild cytotoxicity often depending on formulations [292, 297].

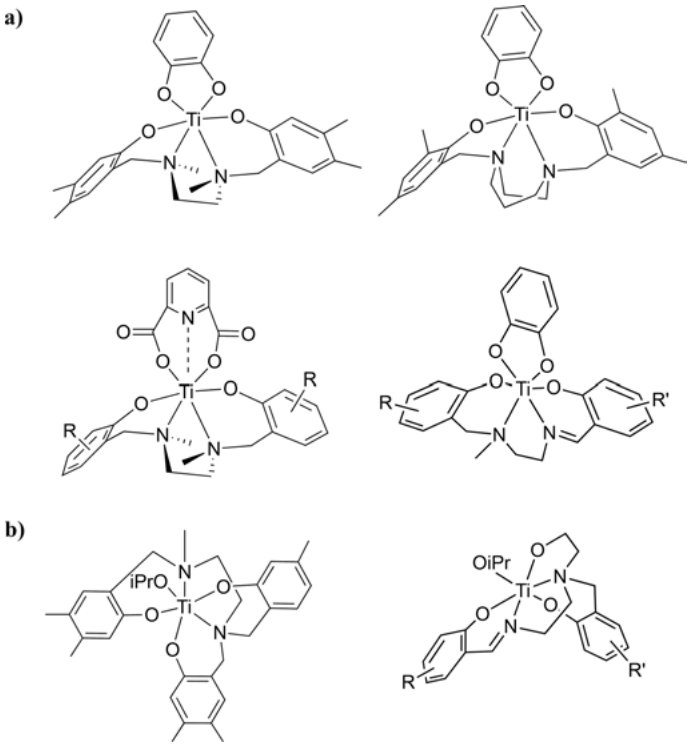

Figure 10. LTiX-type phenolato complexes analyzed for cytotoxicity: (**a**) diamino-bis(phenolato) bis-chelate complexes (X is a chelating ligand); (**b**) diaminotris(phenolato) complexes (X is a monodentate labile ligand).

Another set of octahedral complexes includes a single chelating hexadentate ligand and no other groups of reduced lability whatsoever. Tetrakis(phenolato) complexes showed very high hydrolytic stability along with high activity *in vitro* and *in vivo*, but again only when formulated (Figure 11a) [295, 297, 298]. No reactivity was mostly observed when the complexes were administered directly, reflecting their large steric bulk and inaccessibility. A related complex investigated includes in the hexadentate ligand system with two phenolato and two carboxylato covalent donors in addition to the two coordinative amines (Figure 11b) [262, 299]. As the carboxylato ligand binds more weakly to the titanium(IV) center relative to the phenolato donors, such complexes may release the ligand more readily, often forming oxo compounds [257]. Nevertheless, in this chelating system, the anionic complex obtained after only partial hydrolysis at neutral pH exhibited marked cytotoxicity toward some cell lines. It was suggested that being a transferrin mimic, Fe(III) binding by the free ligand contributes to the activity by depleting iron concentration. Negligible activity was recorded for the related Fe(III) and Ga(III) complexes [299], emphasizing the importance of the titanium(IV) metal.

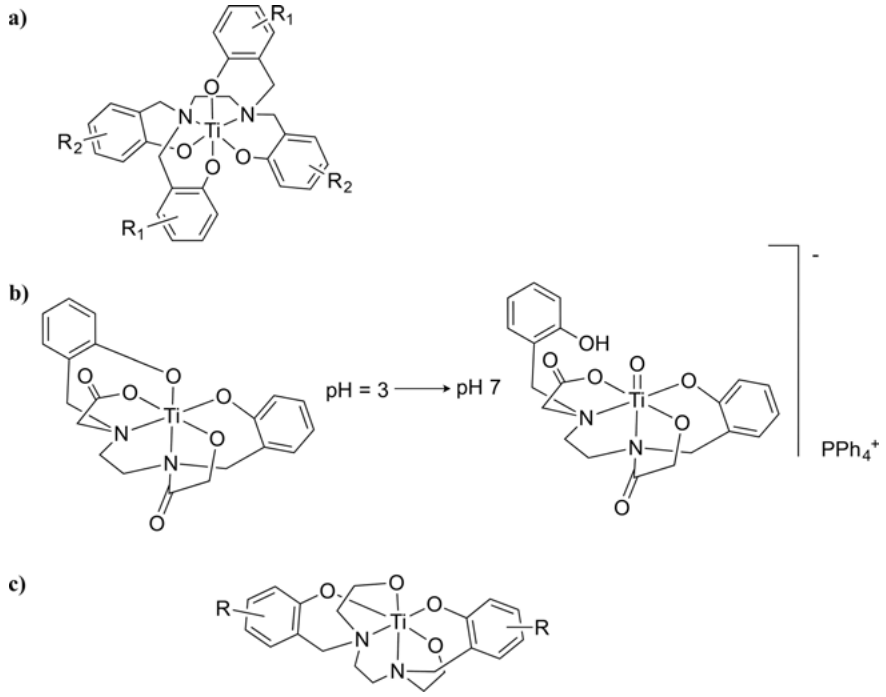

Figure 11. Phenolato complexes of hexadentate ligands analyzed for cytotoxicity: (**a**) diaminotetrakis(phenolato) LTi-type complexes, (**b**) an oxo diaminophenolatobis(carboxylato) LTiO-type complex, and (**c**) diaminobis(phenolato)-bis(alkoxo) LTi-type complexes.

A combination of high activity, stability, and accessibility was recently achieved with a new family of complexes based on the bis(phenolato)-bis(alkoxo) hexadentate ligand system (Figure 11c) [300]. These complexes exhibited *in vitro* activity toward many cell lines, as also established by the NCI-60 program with average GI_{50} of 4.7 $\pm$ 2 μM. Activity was obtained also toward lines resistant to cisplatin and MDR. *In vivo* studies on murine models showed good efficacy and no signs of toxicity to the treated animals, as also supported by a degree of selectivity to cancer lines versus fibroblast cells. These complexes were active without formulations, and are stable for weeks in biological environments.

4.3. Mechanistic Insights

Mechanistic studies on various phenolato titanium(IV) complexes was consistent with cancer selectivity and induction of apoptotic pathways accompanied by cell cycle arrest [269, 273, 300–302]. Additionally, build-up of proteins relevant to apoptosis such as p53 was observed, along with activation of caspases. Bio-distribution studies were conducted in comparison to Cp-based complexes, and more

effective cellular accumulation was detected, as well as gradual accumulation in both the nuclei and mitochondria [274, 303]. Reduced binding to macromolecules such as DNA and albumin compared with those recorded for the Cp-based derivatives supported the notion that not all titanium complexes necessarily operate by identical mechanisms. The involvement of serum proteins in titanium(IV) transfer from this group of compounds remains enigmatic [262, 274, 303, 304]. Additional mechanistic information can be found on a recently published detailed tutorial review [182].

5. CONLUSIONS AND OUTLOOK

Clearly, titanium(IV) complexes bear an enormous potential for cancer treatment. The numerous complexes investigated throughout more than thirty years of research enabled fine-tuning of complex properties to produce complexes often even more potent than cisplatin toward many cell lines. The activity range of the complexes is wide, as is also established by the NCI-60 program screening close to sixty lines (with average activity higher for Ti than for Pt, Figure 12) with activity also towards lines resistant to cisplatin or MDR. In fact, no reports on titanium resistance exist to date. The titanium complexes have also been consistently active *in vivo* against many different murine models. Most importantly, the advantage in using the bio-friendly metal titanium over platinum or other heavy metals have been confirmed: no signs of toxicity to the treated animals is mostly recorded in *in vivo* studies, as was also supported by selectivity to cancer cells over primary murine healthy cells, zebrafish embryos, or human fibroblasts. This of course could potentially represent another major breakthrough in anticancer chemotherapy, which is normally heavily toxic.

Nevertheless, the early complexes, which indeed had shown reduced toxicity *in vivo*, have failed the clinical trials due to limiting toxicity in human subjects. The rapid undefined hydrolysis processes to give multiple species, not all necessarily active, required increasing unfavorably the doses for treatment. The advanced titanium complexes have resolved this issue; they are not only highly active, generally as high as any previously reported titanium or other metal (including platinum) complex, but they also demonstrate tremendous stability in water and biological environments, without any signs of decomposition for days and weeks. It is thus now confirmed: highly effective AND hydrolytically stable complexes can be produced based on the generally SAFE metal titanium(IV).

After achieving what appears to be all the desired qualities in the advanced titanium(IV) complexes to produce potentially effective, selective, and stable titanium-based drugs, the one main thing missing is understanding their mode of action [182], and the source of the unique and enigmatic combination of wide effectiveness – and yet – cancer selectivity and safety. The high stability and inertness of the advanced highly active compounds raises new dilemmas on possible modes of action and binding to the biological target – if not through labile ligand hydrolysis as occurs for cisplatin. When gathering the mechanistic insights gained throughout the years on different titanium(IV) complexes, many different

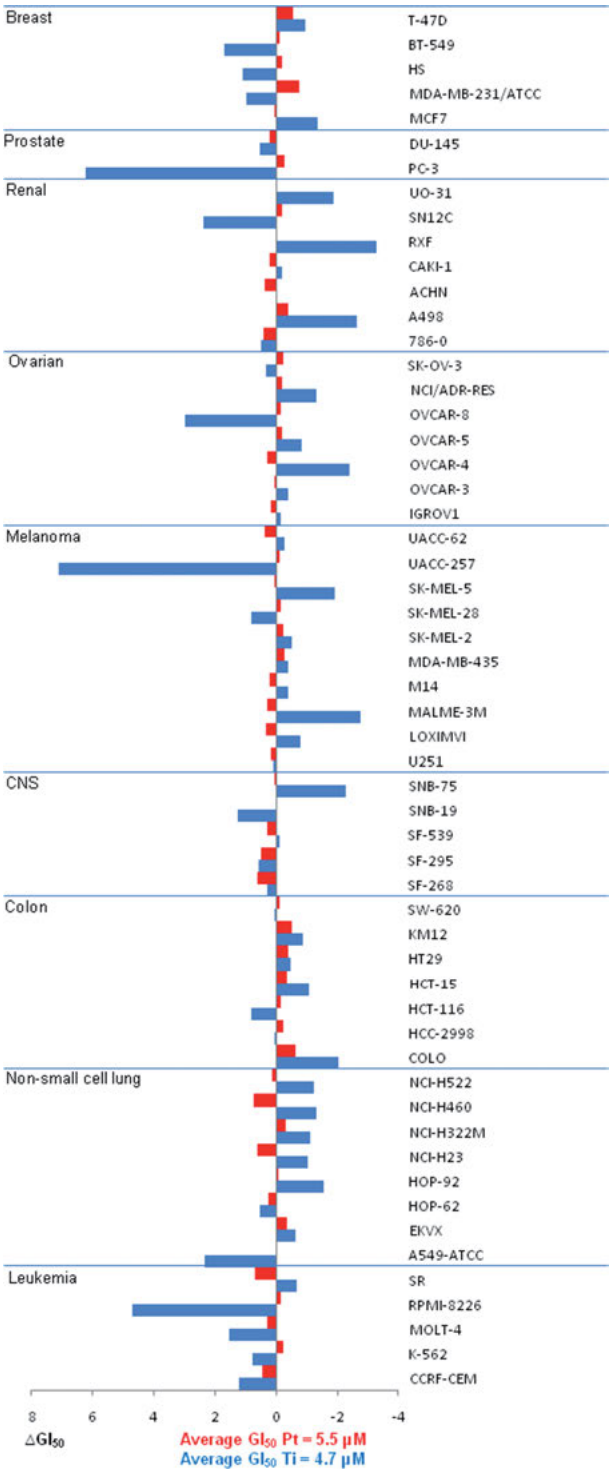

possible pathways were suggested; possible binding to DNA as well as possible binding to proteins and enzymes; possible interruption of cell cycle and induction of apoptosis by different pathways; possible antiangiogenetic effects in addition to cellular cytotoxicity; these various observations may infect more than a single mode of operation, as well as possible varieties of modes occurring among the different derivatives studied.

Nevertheless, one conclusion stands out – the mechanism of titanium complexes is probably different from that of cisplatin. This can also be deduced by the different resistance patterns, as well as the different cell relative sensitivity as reflected in the NCI-60 results (Figure 12) [300, 305]. For instance, some particular lines of non-small-lung, melanoma, and renal cancers are relatively sensitive to an advanced titanium(IV) complex while being relatively resistant to cisplatin. These differences provide an enormous opportunity to extend treatments to additional cancer conditions. Moreover, the different mechanism implied by these differences, as also established by the COMPARE analysis, is highly advantageous for combination therapies, as confirmed by early combination studies *in vitro*. Moreover, looking at the different sensitivity pattern (Figure 12), it appears that the difference in cell response among the different lines is wider for Ti than for Pt, implying involvement of specific cellular pathways that may vary among different cells. All of the above raise even further the great promise of the titanium complexes for use in the clinic, and the leading ones will hopefully enter clinical trials sooner rather than later.

To conclude, the future holds great promise for titanium(IV) anticancer coordination complexes. Greater efforts should be placed on full elucidation of the mechanism of action, and identification of the exact cellular target/s, which should also accelerate clinical development. Additional combinations with known drugs with the lines identified as most sensitive should be explored, both *in vitro* and *in vivo*. Moreover, combinations with other types of treatment such as immunotherapy should also offer many benefits. And last, specific targeting of the active titanium(IV) compounds to the cancer cell by various methodologies, known and yet unknown, should expand ever more the merit of the titanium(IV) anticancer coordination complexes. Finally, if one dares to dream even farther, after obtaining a complex of the oxophilic titanium(IV) metal stable for weeks in water, and given the positive results observed for TiO_2-based nanoparticles [33], perhaps the utopia of an oral administration of a safe and effective titanium(IV) anticancer coordination drug is not beyond reach.

Figure 12. Comparison of the relative sensitivity of ca. 60 human cancer cell lines of the NCI-60 panel to cisplatin (red) vs. an advanced titanium(IV) complex (blue). The average GI_{50} of each compound (higher average activity of titanium 4.7 versus 5.5 μM) was calibrated as zero; ΔGI_{50} (*x*-axis) for each line equals to [GI_{50} for the particular line] minus [average GI_{50}]; thus, positive values indicate sensitivity lower than the average for each compound and negative values indicate particularly high sensitivity; the variation in activities obtained for the titanium relative to platinum among the lines implies added selectivity of titanium to specific lines. This figure was prepared from the NIH data base (NSC-783837, see also [300]).

ACKNOWLEDGMENTS

We thank all the scientists and students who have undertaken the work described herein to produce all the data, and the funding agencies enabling the research. Our lab acknowledges the European Research Council (ERC) for funding along the years. We also thank Prof. J. Hochman from the Hebrew University and his group for fruitful collaborations and various scientific discussions on cancer biology.

ABBREVIATIONS AND DEFINITIONS

Cp	η^5-C_5H_5; cyclopentadienyl = cyclopentadienide
GI_{50}	growth inhibition of 50 % cells
IC_{50}	inhibition concentration of 50 % cells
LD_{50}	lethal dose of 50 % sample tested
MDR	multi drug resistance / multi drug resistant
NCI-60	national cancer institute screen of 60 cell lines
OEt	ethoxy
OR	alkoxy

REFERENCES

1. I. Mellman, G. Coukos, G. Dranoff, *Nature* **2011**, *480*, 480–489.
2. I. S. Chan, G. S. Ginsburg, T. Kuhn, *Annu. Rev. Genomics Hum. Genet.* **2011**, *12*, 217–244.
3. S. Dilruba, G. V. Kalayda, *Cancer Chemother. Pharmacol.* **2016**, *77*, 1103–1124.
4. G. Kazantzis, *Environ. Health Perspect.* **1981**, *40*, 143–161.
5. P. Köpf-Maier, H. Köpf, *Chem. Rev.* **1987**, *87*, 1137–1152.
6. P. Köpf-Maier, *Eur. J. Clin. Pharmacol.* **1994**, *47*, 1–16.
7. M. Hartmann, B. K. Keppler, *Comments Inorg. Chem.* **1995**, *16*, 339–372.
8. C. W. Schwietert, J. P. McCue, *Coord. Chem. Rev.* **1999**, *184*, 67–89, and references therein.
9. F. Kratz, M. T. Schutte, *Cancer J.* **1998**, *11*, 60–67.
10. T. Pieper, K. Borsky, B. K. Keppler, in *Metallotherapeuticals I*, Vol. 1 of *Topics in Biological Inorganic Chemistry*, Eds. M. J. Clarke, P. J. Sadler, Springer, Berlin, Heidelberg, **1999**, pp. 171–199.
11. Z. Guo, P. J. Sadler, *Angew. Chem. Int. Ed.* **1999**, *38*, 1512–1531.
12. M. J. Clarke, F. Zhu, D. R. Frasca, *Chem. Rev.* **1999**, *99*, 2511–2533.
13. Z. Guo, P. J. Sadler, *Adv. Inorg. Chem.* **1999**, *49*, 183–306.
14. B. Desoize, *Anticancer Res.* **2004**, *24*, 1529–1544.
15. I. Ott, R. Gust, *Archiv der Pharmazie* **2007**, *340*, 117–126.
16. N. Muhammad, Z. Guo, *Curr. Opin. Chem. Biol.* **2014**, *19*, 144–153.
17. K. B. Garbutcheon-Singh, M. P. Grant, B. W. Harper, A. M. Krause-Heuer, M. Manohar, N. Orkey, J. R. Aldrich-Wright, *Curr. Top. Med. Chem.* **2011**, *11*, 521–542.
18. G. N. Kaluđerović, R. Paschke, *Curr. Med. Chem.* **2011**, *18*, 4738–4752.
19. D. B. Lovejoy, D. R. Richardson, *Exp. Opin. Invest. Drugs* **2000**, *9*, 1257–1270.

20. A. M. Pizarro, A. Habtemariam, P. J. Sadler, *Med. Organomet. Chem.* **2010**, *32*, 21–56.
21. I. Kostova, *Anti-Cancer Age. Med. Chem.* **2009**, *9*, 827–842.
22. K. Sakai, Y. Yamane, *Jap. J. Toxicol. Environ. Health* **1990**, *36*, 181–200.
23. P. Köpf-Maier, H. Köpf, in *Metal Compounds in Cancer Therapy*, Ed. S. P. Fricker, Springer Netherlands, Dordrecht, **1994**, pp. 109–146.
24. S. Grabowski, H. Köpf, *Eur. J. Med. Chem.* **1984**, *19*, 347–352.
25. B. K. Keppler, M. E. Heim, *Drug Future* **1988**, *13*, 637–652.
26. B. K. Keppler, C. Friesen, H. Vongerichten, in *Metal Complexes in Cancer Chemotherapy,* Ed. B. K. Keppler, Verlag Chemie VCH, Weinheim **1993**, 187–220.
27. E. Meléndez, *Crit. Rev. Oncol. Hematol.* **2002**, *42*, 309–315.
28. F. Caruso, M. Rossi, in *Metal Complexes in Tumor Diagnosis and as Anticancer Agents,* Vol. 42 of *Metal Ions in Biological Systems,* Eds. A. Sigel, H. Sigel, Marcel Dekker, Inc., New York, **2004**, pp. 353–353.
29. F. Caruso, M. Rossi, *Mini-Rev. Med. Chem.* **2004**, *4*, 49–60.
30. F. Caruso, M. Rossi, C. Pettinari, *Expert Opin. Ther. Pat.* **2001**, *11*, 969–979.
31. P. J. Sadler*, Adv. Inorg. Chem.*, **1991**, *36,* 1–48.
32. K. M. Buettner, A. M. Valentine, *Chem. Rev.* **2012**, *112*, 1863–1881.
33. Q. Wang, J. Y. Huang, H. Q. Li, Z. Chen, A. Z. J. Zhao, Y. Wang, K. Q. Zhang, H. T. Sun, S. S. Al-Deyab, Y. K. Lai, *Int. J. Nanomedicine* **2016**, *11*, 4816–4834.
34. L. Y. Kuo, A. H. Liu, T. J. Marks, *Met. Ions Biol. Syst.* **1996**, *33*, 53–85.
35. P. Köpf-Maier, H. Köpf, in *Bioinorganic Chemistry*, Vol. 70 of *Structure and Bonding,* Springer, Berlin, Heidelberg, **1988**, pp. 103–185.
36. P. Köpf-Maier, in *Ruthenium and Other Non-Platinum Metal Complexes in Cancer Chemotherapy*, Vol. 10 of *Progress in Clinical Biochemistry and Medicine*, Eds. E. Baulieu, D. T. Forman, M. Ingelman-Sundberg, L. Jaenicke, J. A. Kellen, Y. Nagai, G. F. Springer, L. Träger, L. Will-Shahab, J. L. Wittliff, Springer, Berlin, Heidelberg, **1989**, pp. 151–184.
37. G. Gasser, I. Ott, N. Metzler-Nolte, *J. Med. Chem.* **2011**, *54*, 3–25.
38. P. Köpf-Maier, H. Köpf, *Met. Based Antitumor Drugs* **1988**, 55–102.
39. P. Köpf-Maier, H. Köpf, *Drug Future* **1986**, *11*, 297–319.
40. P. Köpf-Maier, H. Köpf, *ACS Symp. Series* **1983**, *209*, 315–333.
41. H. Köpf, P. Köpf-Maier, *Angew. Chem. Int. Ed.* **1979**, *18*, 477–478.
42. P. Köpf-Maier, B. Hesse, R. Voigtländer, H. Köpf, *J. Cancer Res. Clin. Oncol.* **1980**, *97*, 31–39.
43. P. Köpf-Maier, B. Hesse, H. Köpf, *J. Cancer Res. Clin. Oncol.* **1980**, *96*, 43–51.
44. P. Tarillion, G. Taubert, H. Nenning, *Mutat. Res. Genet. Toxicol. Environ. Mutag.* **1997**, *389*, 213–218.
45. M. C. Valadares, S. I. Klein, S. Zyngier, M. L. S. Queiroz, *Int. J. Immunopharmacol.* **1998**, *20*, 573–581.
46. M. C. Valadares, S. I. Klein, A. M. A. Guaraldo, M. L. S. Queiroz, *Eur. J. Pharmacol.* **2003**, *473*, 191–196.
47. P. Köpf-Maier, W. Wagner, E. Liss, *J. Cancer Res. Clin. Oncol.* **1981**, *102*, 21–30.
48. P. Köpf-Maier, A. Moormann, H. Köpf, *Eur. J. Cancer Clin. Oncol.* **1985**, *21*, 853–857.
49. P. Köpf-Maier, H. Köpf, *Arzneimittelforschung* **1987**, *37*, 532–534.
50. P. Köpf-Maier, *J. Cancer Res. Clin. Oncol.* **1987**, *113*, 342–348.
51. P. Köpf-Maier, *Cancer Chemother. Pharmacol.* **1989**, *24*, 23–27.
52. P. Köpf-Maier, W. Wagner, B. Hesse, H. Köpf, *Eur. J. Cancer* **1981**, *17*, 665–669.
53. C. Villena-Heinsen, M. Friedrich, A. K. Ertan, C. Farnhammer, W. Schmidt, *Anti-Cancer Drugs* **1998**, *9*, 557–563.

54. M. Friedrich, C. Villena-Heinsen, C. Farnhammer, W. Schmidt, *Eur. J. Gynaecol. Oncol.* **1998**, *19*, 333–337.
55. P. Köpf-Maier, *Anticancer Res.* **1999**, *19*, 493–504.
56. M. M. Harding, G. Mokdsi, *Curr. Med. Chem.* **2000**, *7*, 1289–1303.
57. P. Köpf-Maier, F. Preiss, T. Marx, T. Klapötke, H. Köpf, *Anticancer Res.* **1986**, *6*, 33–37.
58. P. Köpf-Maier, H. Köpf, *Anticancer Res.* **1986**, *6*, 227–233.
59. A. Harstrick, H. J. Schmoll, H. Poliwoda, G. Sass, Y. Rustum, *Eur. J. Cancer* **1993**, *29*, 1000–1002.
60. C. Christodoulou, A. Eliopoulos, L. Young, L. Hodgkins, D. Ferry, D. Kerr, *Br. J. Cancer* **1998**, *77*, 2088–2097.
61. C. M. Kurbacher, P. Mallmann, J. A. Kurbacher, G. Sass, P. E. Andreotti, A. Rahmun, H. Hübner, D. Krebs, *Anticancer Res.* **1994**, *14*, 1961–1965.
62. C. M. Kurbacher, W. Nagel, P. Mallmann, J. A. Kurbacher, G. Sass, H. Hübner, P. E. Andreotti, D. Krebs, *Anticancer Res.* **1994**, *14*, 1529–1533.
63. C. M. Kurbacher, H. W. Bruckner, P. E. Andreotti, J. A. Kurbacher, G. Sa, D. Krebs, *Anti-Cancer Drugs* **1995**, *6,* 697–704.
64. P. Köpf-Maier, S. Gerlach, *J. Cancer Res. Clin. Oncol.* **1986**, *111*, 243–247.
65. D. P. Fairlie, M. W. Whitehouse, J. A. Broomhead, *Chem. Biol. Interact.* **1987**, *61*, 277–291.
66. P. Köpf-Maier, P. Erkenswick, *Toxicology* **1984**, *33*, 171–181.
67. P. Köpf-Maier, S. Gerlach, *Anticancer Res.* **1986**, *6*, 235–240.
68. P. Köpf-Maier, P. Funke-Kaiser, *Toxicology* **1986**, *38*, 81–90.
69. P. Köpf-Maier, *Toxicology* **1985**, *37*, 111–116.
70. P. Köpf-Maier, U. Brauchle, A. Heussler, *Toxicology* **1988**, *48*, 253–260.
71. P. Köpf-Maier, U. Brauchle, A. Henssler, *Toxicology* **1988**, *51*, 291–298.
72. A. Korfel, M. E. Scheulen, H. J. Schmoll, O. Gründel, A. Harstrick, M. Knoche, L. M. Fels, M. Skorzec, F. Bach, J. Baumgart, G. Sass, S. Seeber, E. Thiel, W. E. Berdel, *Clin. Cancer Res.* **1998**, *4*, 2701–2708.
73. C. V. Christodoulou, D. R. Ferry, D. W. Fyfe, A. Young, J. Doran, T. M. T. Sheehan, A. Eliopoulos, K. Hale, J. Baumgart, G. Sass, D. J. Kerr, *J. Clin. Oncol.* **1998**, 276–279.
74. K. Mross, P. Robben-Bathe, L. Edler, J. Baumgart, W. E. Berdel, H. Fiebig, C. Unger, *Onkologie* **2000**, *23*, 576–579.
75. W. Berdel, H. Schmoll, M. Scheulen, *Onkologie* **1993**, *16*, R172.
76. G. Lümmen, H. Sperling, H. Luboldt, T. Otto, H. Rübben, *Cancer Chemother. Pharmacol.* **1998**, *42*, 415–417.
77. N. Kröger, U. R. Kleeberg, K. Mross, L. Edler, D. K. Hossfeld, *Oncol. Res. Treat.* **2000**, *23*, 60–62.
78. J. H. Toney, T. J. Marks, *J. Am. Chem. Soc.* **1985**, *107*, 947–953.
79. G. Mokdsi, M. M. Harding, *J. Organomet. Chem.* **1998**, *565*, 29–35.
80. H. Wittrisch, H. P. Schröer, J. Vogt, C. Vogt, *Electrophoresis* **1998**, *19*, 3012–3017.
81. E. Meléndez, M. a. Marrero, C. Rivera, E. Hernández, A. Segal, *Inorg. Chim. Acta* **2000**, *298*, 178–186.
82. F. Palacios, P. Royo, R. Serrano, J. L. Balcázar, I. Fonseca, F. Florencio, *J. Organomet. Chem.* **1989**, *375*, 51–58.
83. G. Mokdsi, M. M. Harding, *Met. Based Drugs* **1998**, *5*, 207–215.
84. M. Ravera, C. Cassino, E. Monti, M. Gariboldi, D. Osella, *J. Inorg. Biochem.* **2005**, *99*, 2264–2269.
85. P. Manohari Abeysinghe, M. M. Harding, *Dalton Trans.*, **2007**, *32*, 3474–3482.
86. R. Hernández, J. Méndez, J. Lamboy, M. Torres, F. R. Román, E. Meléndez, *Toxicology in Vitro* **2010**, *24*, 178–183.

87. G. N. Kaluđerović, V. Tayurskaya, R. Paschke, S. Prashar, M. Fajardo, S. Gómez-Ruiz, *Appl. Organomet. Chem.* **2010**, *24*, 656–662.
88. R. Meyer, S. Brink, C. E. J. Van Rensburg, G. K. Jooné, H. Görls, S. Lotz, *J. Organomet. Chem.* **2005,** *690,* 117–125 .
89. L. Koubkova, R. Vyzula, J. Karban, J. Pinkas, E. Ondrouskova, B. Vojtesek, R. Hrstka, *Invest. New Drugs* **2015**, *33*, 1123–1132.
90. S. Eger, T. A. Immel, J. Claffey, H. Müller-Bunz, M. Tacke, U. Groth, T. Huhn, *Inorg. Chem.* **2010**, *49*, 1292–1294.
91. J. Ceballos-Torres, M. J. Caballero-Rodríguez, S. Prashar, R. Paschke, D. Steinborn, G. N. Kaluđerović, S. Gómez-Ruiz, *J. Organomet. Chem.* **2012**, *716*, 201–207.
92. S. Gómez-Ruiz, B. Gallego, Ž. Žižak, E. Hey-Hawkins, Z. D. Juranić, G. N. Kaluđerović, *Polyhedron* **2010**, *29*, 354–360.
93. I. De La Cueva-Alique, L. Muñoz-Moreno, Y. Benabdelouahab, B. T. Elie, M. A. El Amrani, M. E. G. Mosquera, M. Contel, A. M. Bajo, T. Cuenca, E. Royo, *J. Inorg. Biochem.* **2016,** *156,* 22–34.
94. P. Köpf-Maier, S. Grabowski, J. Liegener, H. Köpf, *Inorg. Chim. Acta* **1985**, *108*, 99–103.
95. P. Köpf-Maier, T. Klapötke, H. Köpf, *Inorg. Chim. Acta* **1988**, *153*, 119–122.
96. P. Köpf-Maier, T. Klapötke, *Arzneimittelforschung* **1989**, *39*, 488–490.
97. P. Köpf-Maier, E. Neuse, T. Klapötke, H. Köpf, *Cancer Chemother. Pharmacol.* **1989**, *24*, 23–27.
98. P. Köpf-Maier, I. C. Tornieporth-Oetting, *BioMetals* **1996**, *9*, 267–271.
99. A. Gmeiner, K. Effenberger-Neidnicht, M. Zoldakova, R. Schobert, *Appl. Organomet. Chem.* **2011**, *25*, 117–120.
100. S. Gómez-Ruiz, T. P. Stanojković, G. N. Kaluđerović, *Appl. Organomet. Chem.* **2012**, *26*, 383–389.
101. J. Claffey, A. Deally, B. Gleeson, S. Patil, M. Tacke, *Appl. Organomet. Chem.* **2010**, *24,* 675–679.
102. T. A. Immel, J. T. Martin, C. J. Duer, U. Groth, T. Huhn, *J. Inorg. Biochem.* **2010,** *104*, 863–867.
103. L. M. Gao, J. Matta, A. L. Rheingold, E. Meléndez, *J. Organomet. Chem.* **2009**, *694*, 4134–4139.
104. P. Köpf-Maier, W. Wagner, H. Köpf, *Cancer Chemother. Pharmacol.* **1981**, *5*, 237–241.
105. V. J. Moebus, R. Stein, D. G. Kieback, I. B. Runnebaum, G. Sass, R. Kreienberg, *Anticancer Res.* **1997**, *17*, 815–821.
106. K. Strohfeldt, M. Tacke, *Chem. Soc. Rev.* **2008**, *37*, 1174–1187.
107. J. R. Boyles, M. C. Baird, B. G. Campling, N. Jain, *J. Inorg. Biochem.* **2001**, *84*, 159–162.
108. O. R. Allen, L. Croll, A. L. Gott, R. J. Knox, P. C. McGowan, *Organometallics* **2004**, *23*, 288–292.
109. P. W. Causey, M. C. Baird, S. P. C. Cole, *Organometallics* **2004**, *23*, 4486–4494.
110. G. D. Potter, M. C. Baird, M. Chan, S. P. C. Cole, *Inorg. Chem. Commun.* **2006**, *9*, 1114–1116.
111. R. N. Hernández, J. Lamboy, L. M. Gao, J. Matta, F. R. Román, E. Meléndez, *J. Biol. Inorg. Chem.* **2008**, *13*, 685–692.
112. S. Gómez-Ruiz, G. N. Kaluđerović, Ž. Žižak, I. Besu, Z. D. Juranić, S. Prashar, M. Fajardo, *J. Organomet. Chem.* **2009**, *694*, 1981–1987.
113. G. D. Potter, M. C. Baird, S. P. C. Cole, *J, Organo. Chem.***2010**, *692*, 3508–3518.
114. S. Mijatović, M. Bulatović, M. Mojić, S. Stošić-Grujičić, D. Miljković, D. Maksimović-Ivanić, S. Gómez-Ruiz, J. Pinkas, M. Horáček, G. N. Kaluđerović, *J. Organomet. Chem.* **2014**, *751,*361–367.

115. M. Tacke, L. T. Allen, L. Cuffe, W. M. Gallagher, Y. Lou, O. Mendoza, H. Müller-Bunz, F. J. K. Rehmann, N. Sweeney, *J. Organomet. Chem.* **2004**, *689*, 2242–2249.
116. M. Tacke, L. P. Cuffe, W. M. Gallagher, Y. Lou, O. Mendoza, H. Müller-Bunz, F. J. K. Rehmann, N. Sweeney, *J. Inorg. Biochem.* **2004**, *98*, 1987–1994.
117. F. J. K. Rehmann, A. J. Rous, O. Mendoza, N. J. Sweeney, K. Strohfeldt, W. M. Gallagher, M. Tacke, *Polyhedron* **2005**, *24*, 1250–1255.
118. K. Strohfeldt, H. Müller-Bunz, C. Pampillón, N. J. Sweeney, M. Tacke, *Eur. J. Inorg. Chem.* **2006**, 4621–4628.
119. W. Kahl, N. Klouras, G. Hermann, H. Köpf, *Eur. J. Med. Chem.* **1981**, *16*, 275–281.
120. F. J. K. Rehmann, L. P. Cuffe, O. Mendoza, D. K. Rai, N. Sweeney, K. Strohfeldt, W. M. Gallagher, M. Tacke, *Appl. Organomet. Chem.* **2005**, *19*, 293–300.
121. G. Kelter, N. J. Sweeney, K. Strohfeldt, H.-H. Fiebig, M. Tacke, M. Tacke, *Anti-Cancer Drugs* **2005**, *16*, 1091–1098.
122. N. J. Sweeney, J. Claffey, H. Müller-Bunz, C. Pampillón, K. Strohfeldt, M. Tacke, *Appl. Organomet. Chem.* **2007**, *21*, 57–65.
123. O. Oberschmidt, A. R. Hanauske, F.J. K. Rehmann, K. Strohfeldt, N. Sweeney, M. Tacke, *Anti-Cancer Drugs* **2005**, *16*, 1071–1073.
124. M. Tacke, M. Hogan, J. Claffey, C. Pampillón, *Med. Chem.* **2008**, *4*, 91–99.
125. S. Gómez-Ruiz, G. N. Kaluđerović, D. Polo-Cerón, S. Prashar, M. Fajardo, Ž. Žižak, Z. D. Juranić, T. J. Sabo, *Inorg. Chem. Commun.* **2007**, *10*, 748–752.
126. S. Gómez-Ruiz, G. N. Kaluđerović, S. Prashar, D. Polo-Cerón, M. Fajardo, Ž. Žižak, T. J. Sabo, Z. D. Juranić, *J. Inorg. Biochem.* **2008**, *102*, 1558–1570.
127. M. C. Valadares, A. L. Ramos, F. J. K. Rehmann, N. J. Sweeney, K. Strohfeldt, M. Tacke, M. L. S. Queiroz, *Eur. J. Pharmacol.* **2006**, *534*, 264–270.
128. M. Hogan, M. Tacke, *Top, Organomet. Chem.* **2010**, *32*, 119–140.
129. N. J. Sweeney, O. Mendoza, H. Müller-Bunz, C. Pampillón, F. J. K. Rehmann, K. Strohfeldt, M. Tacke, *J. Organomet. Chem.* **2005**, *690*, 4537–4544.
130. I. Fichtner, C. Pampillón, N. J. Sweeney, K. Strohfeldt, M. Tacke, *Anti-Cancer Drugs* **2006**, *17*, 333–336.
131. C. Pampillón, O. Mendoza, N. J. Sweeney, K. Strohfeldt, M. Tacke, *Polyhedron* **2006**, *25*, 2101–2108.
132. N. Sweeney, W. M. Gallagher, H. Müller-Bunz, C. Pampillón, K. Strohfeldt, M. Tacke, *J. Inorg. Biochem.* **2006**, *100*, 1479–1486.
133. C. Pampillón, N. J. Sweeney, K. Strohfeldt, M. Tacke, *Inorg. Chim. Acta* **2006**, *359*, 3969–3975.
134. C. Pampillón, J. Claffey, M. Hogan, M. Tacke, *Z. Anorg. Allg. Chem.* **2007**, *633*, 1695–1700.
135. C. Pampillón, N. J. Sweeney, K. Strohfeldt, M. Tacke, *J. Organomet. Chem.* **2007**, *692*, 2153–2159.
136. M. Hogan, J. Cotter, J. Claffey, B. Gleeson, D. Wallis, D. O. Shea, M. Tacke, *Helv. Chim. Acta* **2008**, *91*, 1787–1797.
137. J. Claffey, M. Hogan, H. Müller-Bunz, C. Pampillón, M. Tacke, *J. Organomet. Chem.* **2008**, *693*, 526–536.
138. C. Pampillón, J. Claffey, K. Strohfeldt, M. Tacke, *Eur. J. Med. Chem.* **2008**, *43*, 122–128.
139. C. Pampillón, J. Claffey, M. Hogan, M. Tacke, *BioMetals* **2008**, *21*, 197–204.
140. J. Claffey, B. Gleeson, M. Hogan, H. Müller-Bunz, D. Wallis, M. Tacke, *Eur. J. Inorg. Chem.* **2008**, 4074–4082.
141. A. Deally, J. Claffey, B. Gleeson, M. Hogan, H. Müller-Bunz, S. Patil, D. F. O'Shea, M. Tacke, *Organometallics* **2010**, *29*, 1032–1040.
142. A. Deally, J. Claffey, B. Gleeson, M. Hogan, H. Müller-Bunz, S. Patil, D. F. O'Shea, M. Tacke, *Polyhedron* **2010**, *29*, 2445–2453.

143. J. Claffey, H. Müller-Bunz, M. Tacke, *J. Organomet. Chem.* **2010**, *695*, 2105–2117.
144. M. Cini, T. D. Bradshaw, W. Lewis, S. Woodward, *Eur. J. Org. Chem.* **2013**, 3997–4007.
145. A. Chimento, C. Saturnino, D. Iacopetta, R. Mazzotta, A. Caruso, M. R. Plutino, A. Mariconda, A. Ramunno, M. S. Sinicropi, V. Pezzi, P. Longo, *Bioorg. Med. Chem.* **2015**, *23*, 7302–7312.
146. J. Ceballos-Torres, S. Gómez-Ruiz, G. N. Kaluđerović, M. Fajardo, R. Paschke, S. Prashar, *J. Organomet. Chem.* **2012**, *700*, 188–193.
147. J. Ceballos-Torres, I. Del Hierro, S. Prashar, M. Fajardo, S. Mijatović, D. Maksimović-Ivanić, G. N. Kalucrossed D Signerović, S. Gómez-Ruiz, *J. Organomet. Chem.* **2014**, *769*, 46–57.
148. J. Ceballos-Torres, S. Prashar, M. Fajardo, A. Chicca, J. Gertsch, A. B. Pinar, S. Gómez-Ruiz, *Organometallics* **2015**, *34*, 2522–2532.
149. R. A. Hilger, D. Alex, A. Deally, B. Gleeson, M. Tacke, *Lett. Drug Des. Discov.* **2011**, *8*, 904–910.
150. I. Fichtner, D. Behrens, J. Claffey, A. Deally, B. Gleeson, S. Patil, H. Weber, M. Tacke, *Lett. Drug Des. Discov.* **2011**, *8*, 302–307.
151. M. Hogan, B. Gleeson, M. Tacke, *Lett. Drug Des. Discov.* **2010**, *7*, 310–317.
152. J. Claffey, A. Deally, B. Gleeson, M. Hogan, L. M. Menedez, H. Müller-Bunz, S. Patil, D. Wallis, M. Tacke, *Metallomics* **2009**, *1*, 511–517.
153. C. M. Dowling, J. Claffey, S. Cuffe, I. Fichtner, C. Pampillón, N. J. Sweeney, K. Strohfeldt, R. W. G. Watson, M. Tacke, *Lett. Drug Des. Discov.* **2008**, *5*, 141–144.
154. J. H. Bannon, I. Fichtner, A. O'Neill, C. Pampillón, N. J. Sweeney, K. Strohfeldt, R. W. Watson, M. Tacke, M. M. Mc Gee, *Br. J. Cancer* **2007**, *97*, 1234–1241.
155. P. Beckhove, O. Oberschmidt, A. R. Hanauske, C. Pampillón, V. Schirrmacher, N. J. Sweeney, K. Strohfeldt, M. Tacke, *Anti-Cancer Drugs* **2007**, *18*, 311–315.
156. O. Oberschmidt, A. R. Hanauske, C. Pampillón , N. J. Sweeney, K. Strohfeldt, M. Tacke, *Anti-Cancer Drugs* **2007**, *18*, 317–321.
157. A. Vessières, M. A. Plamont, C. Cabestaing, J. Claffey, S. Dieckmann, M. Hogan, H. Müller-Bunz, K. Strohfeldt, M. Tacke, *J. Organomet. Chem.* **2009**, *694*, 874–879.
158. J. Claffey, M. Hogan, H. Müller-Bunz, C. Pampillón, M. Tacke, *ChemMedChem* **2008**, *3*, 729–731.
159. I. Fichtner, D. Behrens, J. Claffey, B. Gleeson, M. Hogan, D. Wallis, H. Weber, M. Tacke, *Lett. Drug Des. Discov.* **2008**, *5*, 489–493.
160. M. Cini, S. Woodward, T. D. Bradshaw, *Metallomics* **2016**, *8*, 286–297.
161. G. D. Potter, M. C. Baird, S. P. C. Cole, *J. Organomet. Chem.* **2007**, *692*, 3508–3518.
162. M. Hogan, J. Claffey, C. Pampillón, R. W. G. Watson, M. Tacke, *Organometallics* **2007**, *26*, 2501–2506.
163. T. Hickey, J. Claffey, E. Fitzpatrick, M. Hogan, C. Pampillón, M. Tacke, *Invest. New Drugs* **2007**, *25*, 425–433.
164. C. Pampillón, J. Claffey, M. Hogan, K. Strohfeldt, M. Tacke, *Transition Met. Chem.* **2007**, *32*, 434–441.
165. W. Walther, I. Fichtner, A. Deally, M. Hogan, M. Tacke, *Lett. Drug Des. Discov.* **2013**, *10*, 375–381.
166. Y. Pérez, V. López, L. Rivera-Rivera, A. Cardona, E. Meléndez, *J. Biol. Inorg. Chem.* **2005**, *10*, 94–104.
167. A. Gansäuer, I. Winkler, D. Worgull, T. Lauterbach, D. Franke, A. Selig, L. Wagner, A. Prokop, *Chem. Eur. J.* **2008**, *14*, 4160–4163.
168. M. Wenzel, B. Bertrand, M. J. Eymin, V. Comte, J. A. Harvey, P. Richard, M. Groessl, O. Zava, H. Amrouche, P. D. Harvey, P. Le Gendre, M. Picquet, A. Casini, *Inorg. Chem.* **2011**, *50*, 9472–9480.

169. J. F. González-Pantoja, M. Stern, A. A. Jarzecki, E. Royo, E. Robles-Escajeda, A. Varela-Ramírez, R. J. Aguilera, M. Contel, *Inorg. Chem.* **2011**, *50*, 11099–11110.
170. F. Pelletier, V. Comte, A. Massard, M. Wenzel, S. Toulot, P. Richard, M. Picquet, P. Le Gendre, O. Zava, F. Edafe, A. Casini, P. J. Dyson, *J. Med. Chem.* **2010**, *53*, 6923–6933.
171. J. Fernández-Gallardo, B. T. Elie, T. Sadhukha, S. Prabha, M. Saná, S. A. Rotenberg, J. W. Ramos, M. A. Contel, *Chem. Sci.* **2015**, *6*, 5269–5283.
172. J. Fernández-Gallardo, B. T. Elie, F. J. Sulzmaier, M. Sanaú, J. W. Ramos, M. Contel, *Organometallics* **2014**, *33*, 6669–6681.
173. Y. F. Mui, J. Fernández-Gallardo, B. T. Elie, A. Gubran, I. Maluenda, M. Sanaú, O. Navarro, M. A. Contel, *Organometallics* **2016**, *35*, 1218–1227.
174. J. Ceballos-Torres, P. Virag, M. Cenariu, S. Prashar, M. Fajardo, E. Fischer-Fodor, S. Gómez-Ruiz, *Chem. Eur. J.* **2014**, *20*, 10811–10828.
175. A. García-Peñas, S. Gómez-Ruiz, D. Pérez-Quintanilla, R. Paschke, I. Sierra, S. Prashar, I. Del Hierro, G. N. Kalucrossed D Signerović, *J. Inorg. Biochem.* **2012**, *106*, 100–110.
176. G. N. Kaluđerović, D. Pérez-Quintanilla, Z. Zizak, Z. D. Juranić, S. Gómez-Ruiz, *Dalton Trans.* **2010**, *39*, 2597–2608.
177. G. N. Kaluđerović, D. Pérez-Quintanilla, I. Sierra, S. Prashar, I. D. Hierro, Ž. Žižak, Z. D. Juranić, M. Fajardo, S. Gómez-Ruiz, *J. Mater. Chem.* **2010**, *20*, 806–806.
178. D. Pérez-Quintanilla, S. Gómez-Ruiz, Ž. Žižak, I. Sierra, S. Prashar, I. Del Hierro, M. Fajardo, Z. D. Juranic, G. N. Kaluđerović, *Chem. Eur. J.* **2009**, *15*, 5588–5597.
179. D. P. Buck, P. M. Abeysinghe, C. Cullinane, A. I. Day, J. G. Collins, M. M. Harding, *Dalton Trans.* **2008**, *2*, 2328–2334.
180. C. E. Carraher Jr., M. R. Roner, K. Shahi, Y. Ashida, G. Barot, *J. Polym. Mater.* **2007**, *24*, 357–369.
181. L. M. Gao, J. L. Vera, J. Matta, E. Meléndez, *J. Biol. Inorg. Chem.* **2010**, *15*, 851–859.
182. C. Melchior, T. Bradshaw, S. Woodward, *Chem. Soc. Rev.* **2017**, *46*, 1040–1051.
183. P. Köpf-Maier, R. Martin, *Virchows Archiv B* **1989**, *57*, 213–222.
184. P. Köpf-Maier, *J. Struct. Biol.* **1990**, *105*, 35–45.
185. P. Kopfmaier, D. Krahl, *Naturwissenschaften,* **1981**, *68*, 273–274.
186. P. Köpf-Maier, D. Krahl, *Chem. Biol. Interact.* **1983**, *44*, 317–328.
187. J. B. Waern, H. H. Harris, B. Lai, Z. Cai, M. M. Harding, C. T. Dillon, *J. Biol. Inorg. Chem.* **2005**, *10*, 443.
188. P. Köpf-Maier, W. Wagner, H. Köpf, *Naturwissenschaften* **1981**, *68*, 272–273.
189. P. Köpf-Maier, H. Köpf, *Naturwissenschaften* **1980**, *67*, 415–416.
190. A. L. Beauchamp, D. Cozak, A. Mardhy, *Inorg. Chim. Acta* **1984**, *92*, 191–197.
191. M. Guo, Z. Guo, P. Sadler, *J. Biol. Inorg. Chem.* **2001**, *6*, 698–707.
192. S. Cuffe, C. M. Dowling, J. Claffey, C. Pampillón, M. Hogan, J. M. Fitzpatrick, M. P. Carty, M. Tacke, R. W. G. Watson, *Prostate* **2011**, *71*, 111–124.
193. U. Olszewski, J. Claffey, M. Hogan, M. Tacke, R. Zeillinger, P. J. Bednarski, G. Hamilton, *Invest. New Drugs* **2011**, *29*, 607–614.
194. A. L. Beauchamp, F. Belanger-Gariepy, A. Mardhy, D. Cozak, *Inorg. Chim. Acta* **1986**, *124*, L23–L24.
195. D. Cozak, A. Mardhy, M. J. Olivier, A. L. Beauchamp, *Inorg. Chem.* **1986**, *25*, 2600–2606.
196. G. Pneumatikakis, A. Yannopoulos, J. Markopoulos, *Inorg. Chim. Acta* **1988**, *151*, 125–128.
197. J. H. Murray, M. M. Harding, *J. Med. Chem.* **1994**, *37*, 1936–1941.
198. Z. Zhang, P. Yang, M. Guo, H. Wang, *J. Inorg. Biochem.* **1996**, *63*, 183–190.
199. Z. Zhang, P. Yang, M. Guo, *Transition Met. Chem.* **1996**, *21*, 322–326.

200. J. L. Vera, F. R. Román, E. Meléndez, *Anal. Bioanal. Chem.* **2004**, *379*, 399–403.
201. M. Mascini, G. Bagni, M. L. D. Pietro, M. Ravera, S. Baracco, D. Osella, *BioMetals* **2006**, *19*, 409–418.
202. M. Tacke, *Lett. Drug Des. Discov.* **2008**, *5*, 332–335.
203. P. Yang, M. Guo, *Met. Based Drugs* **1998**, *5*, 41–58.
204. C. Rivera, E. Meléndez, in *Metal Ions in Biology and Medicine*, Vol. 6, John Libbey, 1998, **2000**, pp. 580–584.
205. P. Yang, M. Guo, *Coord. Chem. Rev.* **1999**, *185–186*, 189–211.
206. M. L. McLaughlin, J. M. Cronan, T. R. Schaller, R. D. Snelling, *J. Am. Chem. Soc.* **1990**, *112*, 8949–8952.
207. K. O'Connor, C. Gill, M. Tacke, F. J. K. Rehmann, K. Strohfeldt, N. Sweeney, J. M. Fitzpatrick, R. W. G. Watson, *Apoptosis* **2006**, *11*, 1205–1214.
208. P. Köpf-Maier, W. Wagner, E. Liss, *J. Cancer Res. Clin. Oncol.* **1983**, *106*, 44–52.
209. U. Olszewski, G. Hamilton, *Anti-Cancer Age. Med. Chem.* **2010**, *10*, 302–311.
210. U. Olszewski, a. Deally, M. Tacke, G. Hamilton, *Neoplasia* **2012**, *14*, 813–822.
211. G. Mokdsi, M. M. Harding, *J. Inorg. Biochem.* **2001**, *83*, 205–209.
212. M. Pavlaki, K. Debeli, I. E. Triantaphyllidou, N. Klouras, E. Giannopoulou, A. J. Aletras, *J. Biol. Inorg. Chem.* **2009**, *14*, 947–957.
213. H. Weber, J. Claffey, M. Hogan, C. Pampillón, M. Tacke, *Toxicology in Vitro* **2008**, *22*, 531–534.
214. M. Bastaki, E. Missirlis, N. Klouras, G. Karakiulakis, M. E. Maragoudakis, *Eur. J. Pharmacol.* **1994**, *251*, 263–269.
215. M. E. Maragoudakis, P. Peristeris, E. Missirlis, A. Aletras, P. Andriopoulou, G. Haralabopoulos, *Ann. N. Y. Acad. Sci.* **1994**, *732*, 280–293.
216. A. Vessieres, S. Top, W. Beck, E. Hillard, G. Jaouen, *Dalton Trans.* **2005**, 529–541.
217. H. Sun, H. Li, R. A. Weir, P. J. Sadler, *Angew. Chem. Int. Ed.* **1998**, *37*, 1577–1579.
218. L. Messori, P. Orioli, V. Banholzer, I. Pais, P. Zatta, *FEBS Lett.* **1999**, *442*, 157–161.
219. M. L. Guo, P. J. Sadler, *Dalton Trans.* **2000**, 7–9.
220. M. Guo, H. Sun, H. J. McArdle, L. Gambling, P. J. Sadler, *Biochemistry* **2000**, *39*, 10023–10033.
221. L. M. Gao, R. Hernández, J. Matta, E. Meléndez, *J. Biol. Inorg. Chem.* **2007**, *12*, 959–967.
222. C. J. P. Siburt, E. M. Lin, S. J. Brandt, A. D. Tinoco, A. M. Valentine, A. L. Crumbliss, *J. Inorg. Biochem.* **2010**, *104*, 1006–1009.
223. M. Guo, H. Sun, S. Bihari, J. A. Parkinson, R. O. Gould, S. Parsons, P. J. Sadler, *Inorg. Chem.* **2000**, *39*, 206–215.
224. A. D. Tinoco, A. M. Valentine, *J. Am. Chem. Soc.* **2005**, *127*, 11218–11219.
225. A. D. Tinoco, C. D. Incarvito, A. M. Valentine, *J. Am. Chem. Soc.* **2007**, *129*, 3444–3454.
226. A. Sarmiento-González, J. R. Encinar, A. M. Cantarero-Roldán, J. M. Marchante-Gayón, A. Sanz-Medel, *Anal. Chem.* **2008**, *80*, 8702–8711.
227. M. Shen, J. Wang, M. Yang, G. Li, *Electrochem. Commun.* **2011**, *13*, 114–116.
228. K. M. Buettner, R. C. Snoeberger Iii, V. S. Batista, A. M. Valentine, *Dalton Trans.* **2011**, *40*, 9580–9580.
229. J. B. Vincent, S. Love, *Biochem. Biophys. Acta-General Sub.*, **2012**, *1820*, 362–378.
230. S. W. Sarsam, D. R. Nutt, K. Strohfeldt, K. A. Watson, *Metallomics* **2011**, *3*, 152–161.
231. A. D. Tinoco, E. V. Eames, C. D. Incarvito, A. M. Valentine, *Inorg. Chem.* **2008**, *47*, 8380.
232. M. Ravera, E. Gabano, S. Baracco, D. Osella, *Inorg. Chim. Acta* **2009**, *362*, 1303–1306.
233. G. Lally, A. Deally, F. Hackenberg, S. J. Quinn, M. Tacke, *Lett. Drug Des. Discov.* **2013**, *10*, 675.

234. B. K. Keppler, M. R. Berger, M. E. Heimt, *Cancer Treat. Rev.* **1990**, *17*, 261–277.
235. B. K. Keppler, M. Hartmann, *Met. Based Drugs* **1994**, *1*, 145–149.
236. H. J. Keller, B. Keppler, D. Schmähl, *J. Cancer Res. Clin. Oncol.* **1983**, *105*, 109–110.
237. H. Bischoffl, M. R. Berger, B. K. Keppler, D. Schmähl, *J. Cancer Res. Clin. Oncol.* **1987**, *113*, 446–450.
238. B. K. Keppler, C. Friesen, H. G. Moritz, H. Vongerichten, E. Vogel, in *Bioinorganic Chemistry*, Vol. 78 of *Structure and Bonding*, Springer, Berlin, Heidelberg, **1991**, pp. 97–127.
239. B. K. Keppler, M. E. Heim, H. Flechtner, F. Wingen, B. L. Pool, *Arzneimittelforschung* **1989**, *39*, 706–709.
240. M. E. Heim, H. Flechtner, B. K. Keppler, in *Ruthenium and Other Non-Platinum Metal Complexes in Cancer Chemotherapy,* Eds. E. Baulieu, D. T. Forman, M. Ingelman-Sundberg, L. Jaenicke, J. A. Kellen, Y. Nagai, G. F. Springer, L. Träger, L. Will-Shahab, J. L. Wittliff, Springer, Berlin, Heidelberg, **1989**, pp. 217–223.
241. T. J. Einhäuser, B. Keppler, *J. Inorg. Biochem.* **1993**, *51*, 434.
242. T. Schilling, K. B. Keppler, M. E. Heim, G. Niebch, H. Dietzfelbinger, J. Rastetter, A. R. Hanauske, *Invest. New Drugs* **1996**, *13,* 327–332.
243. R. M. Lord, J. J. Mannion, A. J. Hebden, A. E. Nako, B. D. Crossley, M. W. McMullon, F. D. Janeway, R. M. Phillips, P. C. McGowan, *ChemMedChem* **2014**, *9*, 1136–1139.
244. N. Kumar, R. Kaushal, A. Chaudhary, S. Arora, P. Awasthi, *Med. Chem. Res.* **2014**, *23*, 3897–3906.
245. H. J. Keller, B. Keppler, D. Schmähl, *Arzneimittelforschung* **1982**, *32*, 806–807.
246. B. K. Keppler, D. Schmähl, *Arzneimittelforschung* **1986**, *36*, 1822–1828.
247. B. K. Keppler, A. Diez, V. Seifried, *Arzneimittelforschung* **1985**, *35*, 1832–1836.
248. S. Frühauf, W. J. Zeller, *Cancer Research* **1991**, *51*, 2943–2948.
249. P. Comba, H. Jakob, B. Nuber, B. K. Keppler, *Inorg. Chem.* **1994**, *33*, 3396–3400.
250. E. Dubler, R. Buschmann, H. W. Schmalle, *J. Inorg. Biochem.* **2003**, *95*, 97–104.
251. A. Kuhn, T. A. Tsotetsi, A. Muller, J. Conradie, *Inorg. Chim. Acta* **2009**, *362*, 3088–3096.
252. F. Caruso, C. Pettinari, F. Marchetti, P. Natanti, C. Phillips, J. Tanski, M. Rossi, *Inorg. Chem.* **2007**, *46*, 7553–7560.
253. F. Caruso, M. Rossi, C. Opazo, C. Pettinari, *Bioinorg. Chem. Appl.* **2005**, *3*, 317–329.
254. F. Caruso, M. Rossi, J. Tanski, R. Sartori, R. Sariego, S. Moya, S. Diez, E. Navarrete, A. Cingolani, F. Marchetti, C. Pettinari, *J. Med. Chem.* **2000**, *43*, 3665–3670.
255. J. L. Lamboy, A. Pasquale, A. L. Rheingold, E. Meléndez, *Inorg. Chim. Acta* **2007**, *360*, 2115–2120.
256. A. Obeid, A. El-Shekeil, S. Al-Aghbari, J. Al-Shabi, *J. Coord. Chem.* **2012**, *65*, 2762–2770.
257. M. Shavit, E. Y. Tshuva, *Eur. J. Inorg. Chem.* **2008**, 1467–1474.
258. C. M. Manna, M. Shavit, E. Y. Tshuva, *J. Organomet. Chem.* **2008**, *693*, 3947–3950.
259. K. Nehra, R. Kaushal, S. Arora, D. Kaur, *Russ. J. Gen. Chem.* **2016**, *86*, 1070–3632.
260. F. Shabani, S. J. Bozorghi, M. Sheykhpoor, *J. Chem. Soc. Pak.* **2015**, *37*, 1135–1142.
261. A. Rajini, A. K. Adepu, S. Chirra, N. Venkatathri, *RSC Adv.* **2015**, *5*, 87713–87722.
262. A. D. Tinoco, H. R. Thomas, C. D. Incarvito, A. Saghatelian, A. M. Valentine, *PNAS* **2012**, *109*, 5016–5021.
263. E. A. Williamson, T. J. Boyle, R. Raymond, J. Farrington, C. Verschraegen, M. Shaheen, R. Hromas, *Invest. New Drugs* **2012**, *30*, 114–120.
264. T. Hermon, E. Y. Tshuva, *J. Org. Chem.* **2008**, *73*, 5953–5958.
265. M. Shavit, D. Peri, A. Melman, E. Y. Tshuva, *J. Biol. Inorg. Chem.* **2007**, *12*, 825–830.

266. M. Shavit, D. Peri, C. M. Manna, J. S. Alexander, E. Y. Tshuva, *J. Am. Chem. Soc.* **2007**, *129*, 12098–12099.
267. D. Peri, S. Meker, M. Shavit, E. Y. Tshuva, *Chem. Eur. J.* **2009**, *15*, 2403–2415.
268. E. Y. Tshuva, J. A. Ashenhurst, *Eur. J. Inorg. Chem.* **2009**, 2203–2218.
269. C. M. Manna, O. Braitbard, E. Weiss, J. Hochman, E. Y. Tshuva, *ChemMedChem* **2012**, *7*, 703–708.
270. E. Y. Tshuva, D. Peri, *Coord. Chem. Rev.* **2009**, *253*, 2098–2115.
271. N. Ganot, B. Redko, G. Gellerman, E. Y. Tshuva, *RSC Adv.* **2015**, *5*, 7874–7879.
272. T. A. Immel, U. Groth, T. Huhn, P. Öhlschläger, *PLoS ONE* **2011**, *6*, e17869.
273. M. Miller, O. Braitbard, J. Hochman, E. Y. Tshuva, *J. Inorg. Biochem.* **2016**, *163*, 250–257.
274. J. Schur, C. M. Manna, A. Deally, R. W. Koester, M. Tacke, E. Y. Tshuva, I. Ott, *Chem. Commun.* **2013**, *49*, 4785–4787.
275. D. Peri, S. Meker, C. M. Manna, E. Y. Tshuva, *Inorg. Chem.* **2011**, *50*, 1030–1038.
276. S. L. Hancock, R. Gati, M. F. Mahon, E. Y. Tshuva, M. D. Jones, *Dalton Trans.* **2014**, *43*, 1380–1385.
277. S. Meker, C. M. Manna, D. Peri, E. Y. Tshuva, *Dalton Trans.* **2011**, *40*, 9802–9809.
278. H. Glasner, E. Y. Tshuva, *J. Am. Chem. Soc.* **2011**, *133*, 16812–16814.
279. T. A. Immel, U. Groth, T. Huhn, *Chem. Eur. J.* **2010**, *16*, 2775–2789.
280. H. Glasner, E. Y. Tshuva, *Inorg. Chem.* **2014**, *53*, 3170–3176.
281. H. Glasner, E. Y. Tshuva, *Inorg. Chem. Commun.* **2015**, *53*, 31–33.
282. H. Glasner, S. Meker, E. Y. Tshuva, *J. Organomet. Chem.* **2015**, *788*, 33–35.
283. M. Gruetzke, T. Zhao, T. A. Immel, T. Huhn, *Inorg. Chem.* **2015**, *54*, 6697–6706.
284. T. Zhao, M. Grützke, K. H. Götz, T. Druzhenko, T. Huhn, *Dalton Trans.* **2015**, *44*, 16475–16485.
285. T. A. Immel, M. Gruzke, A.-K. Spae, U. Groth, P. Hlschlaer, T. Huhn, *Chem. Commun.* **2012**, *48*, 5790–5792.
286. C. M. Manna, E. Y. Tshuva, *Dalton Trans.* **2010**, *39*, 1182–1184.
287. M. Miller, E. Y. Tshuva, *Eur. J. Inorg. Chem.* **2014**, 1485–1491.
288. C. M. Manna, G. Armony, E. Y. Tshuva, *Chem. Eur. J.* **2011**, 14094–14103.
289. C. M. Manna, G. Armony, E. Y. Tshuva, *Inorg. Chem.* **2011**, *50*, 10284–10291.
290. A. Tzubery, E. Y. Tshuva, *Inorg. Chem.* **2011**, *50*, 7946–7948.
291. A. Tzubery, E. Y. Tshuva, *Inorg. Chem.* **2012**, *51*, 1796–1804.
292. A. Tzubery, E. Y. Tshuva, *Eur. J. Inorg. Chem.* **2017**, 1695–1705.
293. S. Barroso, A. M. Coelho, S. Gómez-Ruiz, M. J. Calhorda, Z. Žižak, G. N. Kaluđerović, A. M. Martins, *Dalton Trans.* **2015**, *44*, 2497–2497.
294. D. Peri, C. M. Manna, M. Shavit, E. Y. Tshuva, *Eur. J. Inorg. Chem.* **2011**, 4896–4900.
295. S. Meker, K. Margulis-Goshen, E. Weiss, O. Braitbard, J. Hochman, S. Magdassi, E. Y. Tshuva, *ChemMedChem* **2014**, *9*, 1294–1298.
296. T. A. Immel, M. Grützke, E. Batroff, U. Groth, T. Huhn, *J. Inorg. Biochem.* **2012**, *106*, 68–75.
297. S. Meker, K. Margulis-Goshen, E. Weiss, S. Magdassi, E. Y. Tshuva, *Angew. Chem. Int. Ed.* **2012**, *51*, 10515–10517.
298. S. Meker, O. Braitbard, K. Margulis-Goshen, S. Magdassi, J. Hochman, E. Y. Tshuva, *Molecules* **2015**, *20*, 18526–18538.
299. T. B. Parks, Y. M. Cruz, A. D. Tinoco, *Inorg. Chem.* **2014**, *53*, 1743–1749.
300. S. Meker, O. Braitbard, M. D. Hall, J. Hochman, E. Y. Tshuva, *Chem. Eur. J.* **2016**, *22*, 9986–9995.
301. T. A. Immel, M. Debiak, U. Groth, A. Bürkle, T. Huhn, *Chem Med Chem* **2009**, *4*, 738–741.

302. T. Pesch, H. Schuhwerk, P. Wyrsch, T. Immel, W. Dirks, A. Bürkle, T. Huhn, S. Beneke, *BMC Cancer* **2016**, *16*, 469–469.
303. J. Schur, C. M. Manna, A. Tshuva, I. Ott, *Metallodrugs* **2014**, *1*, 1–9.
304. A. D. Tinoco, E. V. Eames, A. M. Valentine, *J. Am. Chem. Soc.* **2008**, *130*, 2262–2270.
305. https://dtp.cancer.gov/discovery development/nci-60/methodolo-gy.html

9

Health Benefits of Vanadium and Its Potential as an Anticancer Agent

Debbie C. Crans, [1*] ***Lining Yang,*** [1,2] ***Allison Haase,*** [1] ***and Xiaogai Yang*** [3]

[1]Department Chemistry and Cell and Molecular Biology, Colorado State University, Fort Collins, CO 80523, USA
<debbie.crans@colostate.edu>

[2]College of Pharmacy, Xi'an Medical University, Xi'an, Shaanxi 710021, China

[3]Department of Chemical Biology, School of Pharmaceutical Sciences, Peking University, Beijing 100191, China

ABSTRACT 252
1. INTRODUCTION: VANADIUM-CONTAINING COMPOUNDS INDUCE BIOLOGICAL ACTIONS 252
2. APPLICATIONS OF VANADIUM COMPOUNDS IN HUMAN STUDIES 254
   2.1. Vanadium-Based Compounds in Clinical Trials 254
   2.2. Vanadium Compounds as Nutritional Additives 258
3. BIOLOGICAL CHEMISTRY OF VANADIUM 258
   3.1. Vanadium Salts and Their Speciation 259
   3.2. Organic Vanadium Compounds 261
4. THE ANTICANCER EFFECTS OF VANADIUM COMPOUNDS 262
5. VANADIUM-CONTAINING DRUGS IN CONTEXT OF OTHER DISEASES 265
   5.1. Comparison of Anticancer Vanadium and Other Anticancer Compounds 265
   5.2. Linking Treatments of Cancer to Treatments of Diabetes 266
6. VANADIUM-BASED DRUGS AND ADDITIVES AND THEIR FORMULATION 267
7. CONCLUSIONS AND OUTLOOK 272

Metal Ions in Life Sciences, Volume 18 Edited by Astrid Sigel, Helmut Sigel, Eva Freisinger, and Roland K. O. Sigel

https://doi.org/10.1515/9783110470734-009

Met. Ions Life Sci. **2018**, *18*, 251–279

ACKNOWLEDGMENTS 273
ABBREVIATIONS 273
REFERENCES 274

Abstract: Vanadium compounds have been known to have beneficial therapeutic properties since the turn of the century, but it was not until 1965 when it was discovered that those effects could be extended to treating cancer. Some vanadium compounds can combat common markers of cancer, which include metabolic processes that are important to initiating and developing the phenotypes of cancer. It is appropriate to consider vanadium as a treatment option due to the similarities in some of the metabolic pathways utilized by both diabetes and cancer and therefore is among the few drugs that are effective against more than one disease. The development of vanadium compounds as protein phosphatase inhibitors for the treatment of diabetes may be useful for potential applications as an anticancer agent. Furthermore, the ability of vanadium to redox cycle is also important for biological properties and is involved in the pathways of reactive oxygen species. Early agents including vanadocene and peroxovanadium compounds have been investigated in detail, and the results can be used to gain a better understanding of how some vanadium compounds are modifying the metabolic pathways potentially developing cancer. Considering the importance of coordination chemistry to biological responses, it is likely that proper consideration of compound formulation will improve the efficacy of the drug. Future development of vanadium-based drugs should include consideration of drug formulation at earlier stages of drug development.

Keywords: anticancer agents · formulation · nutritional additives · protein phosphatase inhibitor · vanadate · vanadium · vanadyl sulfate

1. INTRODUCTION: VANADIUM-CONTAINING COMPOUNDS INDUCE BIOLOGICAL ACTIONS

Vanadium compounds have been known to have desirable biological properties such as normalizing elevated blood glucose levels for more than a century [1–4], and for many years, several sources of vanadium have been available as nutritional supplements as single additives or as a component of vitamin supplements such as Centrum® [5]. Recently, a large human study involving approximately 1,500 human patients has shown that low levels of vanadium in their diet are protective against the development of a metabolic disease such as diabetes [6]. The biological properties reported include a range of effects on signal transduction, and redox states in the cell. Specifically, vanadium compounds are inhibitors of numerous important biological processes such as phosphorylation processes [7–16], and some cell cycling events [17, 18] which carry the markers of cancer [19–22]. These beneficial properties have led to the suggested therapeutic use of vanadium compounds against several diseases, the most prominently investigated being diabetes [7, 23–32], cancer [20–22, 33, 34], and other infectious diseases [5, 11, 2, 22, 35–44]. Here in this review, we selected studies carried out with vanadium compounds with the objective of evaluating their potential uses as anticancer agents.

The beneficial properties of vanadium salts have been explored by chemists and life scientists for several decades [45–49]. Early studies focused on developing potent compounds that surpass the effects of simple vanadium salts, such as sodium, potassium, and ammonium vanadate and vanadyl sulfate [36, 48, 50–56].

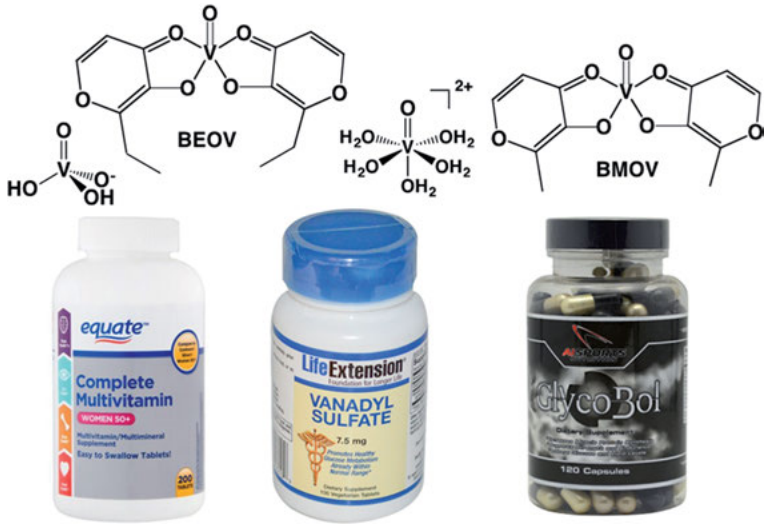

Figure 1. Bis(ethylmaltolato)oxovanadium(IV) (BEOV) is the compound that underwent clinical trial Phase 1 and 2 [23, 24]. The negatively charged anion vanadate forms in solutions from $NaVO_3$ and Na_3VO_4. A cationic form, formed from $VOSO_4$, contains vanadium(IV). Finally, bismaltolatooxovanadium(IV) (BMOV) is now a standard vanadium compound used for comparison of other compounds. All these forms are available to the public.

There are seven simple vanadium salts, three of which are historically used in medicine. Two of these compounds are in oxidation state five – sodium orthovanadate (Na_3VO_4) and sodium metavanadate ($NaVO_3$) – while vanadyl sulfate ($VOSO_4$) is in oxidation state IV [10, 41, 44, 57–69]. In Figure 1 we show vanadate ($H_2VO_4^-$) that forms upon dissolution of both Na_3VO_4 and $NaVO_3$ at physiological pH. However, an additional vanadium compound containing an organic ligand, bis(ethylmaltolato)oxovanadium(IV) (BEOV, Figure 1), was also subjected to clinical trials as an antidiabetic agent [24, 24, 55]. This compound is still being considered for use as a weight loss compound and its analog bismaltolatooxovanadium(IV) (BMOV, Figure 1) is already available to the public as a nutritional additive. Although it may appear that access to these compounds as nutritional additives is irrelevant with regard to cancer, the fact that the public can access these compounds means that they can take these compounds to potentially prevent disease.

Over the past few decades, hundreds of new vanadium compounds have been prepared and tested for their biological effects. Most of them have only been tested in a variety of different cell assays [68, 70] or for their inhibition of some specifically isolated enzyme preparations [11, 12, 68, 71–73]. However, many promising compounds were selected for animal studies, where the ultimate objective was to demonstrate that the compounds have sufficiently low toxicity with suitable efficacy so that the compounds may be safely and effectively used for therapeutic purposes [25]. One disease of interest for which vanadium com-

pounds have been found to be effective against is diabetes. Since diabetes is sometimes characterized as an autoimmune or metabolic disease with which the patients live for many years, the low toxicity of potential drugs is a particularly stringent requirement. Furthermore, the therapeutic index of vanadium compounds is small, partially contributing to the fact that the vanadium compounds in clinical trials have not made it to the clinic [23, 55, 72, 83]. In the case of life-threatening diseases such as cancer, a higher level of toxicity can be tolerated if there are no better treatment options.

In the past, drug discovery has generally been focused on a single disease by a hypothesis-driven targeted screening or by a target-agnostic phenotypic screening. However, links between diseases have been emerging through increasing evidence that commonalities in etiology or pathology exist. Specifically, reported epidemiological investigations suggest that incidence of pancreatic, liver, and endometrial cancers are associated with diabetes even though the molecular mechanisms and links have not yet been fully understood [74, 75]. Recent studies have shown much potential and new insight into the mechanistic aspects of how the vanadium compounds act and some of these studies will be summarized below.

2. APPLICATIONS OF VANADIUM COMPOUNDS IN HUMAN STUDIES

2.1. Vanadium-Based Compounds in Clinical Trials

Before drugs can be administered to the public, many studies are required to assure the safety and non-toxicity of the compound to human beings [20–25]. Research often starts with studies in cell culture, although some scientists prefer to advance to animal studies as rapidly as possible, as in the case of vanadium compounds [55]. For these compounds the cell studies are not as informative as with other drugs because these drugs appear to be sensitive to as of yet unidentified organismic responses and the regulatory mechanisms of the cell. Due to space limitations we refer the readers to other reviews and original literature with regard to studies of vanadium compounds in cell and animal model systems [20–25, 76].

Studies in human beings are referred to as clinical trials, and there are 3 such studies required before the data obtained ensure the guarantee for safety of the compound to be sold to the public [23–25, 77, 80]. The first clinical trial, also known as Phase 1, involves studies with normal human beings to show that the drug under investigation is not toxic.

The second trial is a study in which humans suffering from a disease such as diabetes or cancer are tested for compound efficacy and whether there are undesirable side-effects at the doses needed to observe beneficial effects. It is at this stage that appropriate concentrations of the drug are established on a small group of human beings (see Table 1). Successful completion of Phase 2 clinical trials brings the study to Phase 3, which is the main study with a larger number of

Table 1. Clinical studies investigating toxicity of and responses to different types of vanadium[a]

V compound	Subjects	Total number male / fem	Study purpose	Toxicity side effects	Pharmaco-kinetic data	Dose / duration	Route and Other Info	Ref.
$NaVO_3$	Healthy males		PK		87.6 % Fecal and 12.4 % urine excrete	12.5 mg/d; 12 d	Oral	[79]
Na_3VO_4	Healthy males	2 total (2m)	PK	Vomiting; diarrhea; salivation	10 % Fecal and 90 % urine excrete	18, 24 mg/wk; 6 in 1 wk	i. v.	[4]
$(NH_4)_2VO$-(tar)	Healthy humans	12 total (9m / 3f)	Toxicity	Upper abdominal pain; anorexia; nausea; weight loss; green tongue; pharyngitis		75–125 mg/d; 6 months	Oral	[45]
Ammonium vanadyl tartrate	Healthy humans	6 total 1m / 5f	Toxicity	Diarrhea; cramping		25100 mg/d; 45–68 days	Oral	[80]
$NaVO_3$	IDDM and NIDDM humans	10 total 7m / 3f	IDDM and NIDDM	Vomiting; diarrhea; salivation		125 mg/d; 2 wks	Oral	[59]
$VOSO_4$	NIDDM humans	7 total 6m / 1f	NIDDM	Diarrhea; abdom. cramps; nausea; stool discolored		100 mg/d; 3 wks	Oral	[81]
$VOSO_4$	NIDDM humans	6 total (4m / 2f)	NIDDM	Body weight	V in plasma 73.3 μg/L during treat; 22.4 μg/L after 2 wks	100 mg/d; 3 wks	Oral body weight, Hb and He reduction	[82]
$VOSO_4$	NIDDM humans	8 total (4m / 4f)	NIDDM	Diarrhea; abdom. cramp; flatulence; nausea	blood conc. during treat: 1.7 + 0.7 μmol/L		Half-life 18 h	[64]

V compound	Subjects	Total number male / fem	Study purpose	Toxicity side effects	Pharmaco-kinetic data	Dose / duration	Route and Other Info	Ref.
$VOSO_4$	WT athletes	31 total (23m / 8f)	WT athletes	None		0.5 mg/kg/d; 12 wks	Oral	[65]
$VOSO_4$	NIDDM humans	16 total (11m / 5f)	NIDDM	Diarrhea; abdom. cramp	See[b]	75, 150, 300 mg/d; 6wks	Oral	[83]
$VOSO_4$	NIDDM humans	11 total (7m / 4f)	Diabetes	Diarrhea; abdom. discomfort		150 mg/d; 6 wks	Oral	[42]
$VOSO_4$	Healthy humans	7 total (5m / 2f)	Toxicity	Flatulence; abdom. cramp; nausea; diarrhea; stool discolored		100 mg /d; 8 d	Oral	[66]
V albumin	Healthy males	5 total (5m)	PK		Tzero time conc. 31 d; 52 % urinary excre-tion	47.6 μg 1 d	i. v. half-life: 1.2 h, 26 h, and 10 d	[84]
BEOV	Healthy humans	40 total	Diabetes PK		Tmax: 0.8–3.5 h	10, 25, 35, 60, 90 mg	Oral half-life 45.1–63.5 h	[24]
$VOSO_4$	Healthy humans	40 total	Diabetes PK		Tmax: 6.0 h	50 mg	Oral half-life 59.2 h	[24]
$VOSO_4$	NIDDM humans	16 total (11m / 5f)	Seeking active V-pool		One compartment open model		Nonlinear response	[67]

From diet	Healthy humans	1,598 total[c] 796 healthy	Compare plasma V levels and T2D	None	Plasma level in subjects 1.2 μg/L	V plasma level inversely associated with diabetes	[6]
From diet	Diabetic humans	1,598 total[c]; 802 new diagnosed T2D	Compare plasma V levels and T2D	None	Plasma level in subjects 1.0 μg/L	V plasma levels inversely associated with diabetes	[6]

Hb = hemoglobin; He = hematocrit; IDDM = insulin-dependent diabetes mellitus or type 1 diabetes; m/f = male/female; NIDDM = non–insulin-dependent diabetes mellitus or type 2 diabetes; PK = pharmacokinetics; T2D = type 2 diabetes; $VOSO_4$ = vanadyl sulfate; wk = week; WT = weight trainer

[a] For more detailed information we refer the readers to the original literature and an earlier review [35].

[b] Peak plasma V: 16.0(5.1), 83.6(44.0), 284.5(146.3) ng/mL; peak urine V: 0.094(0.05), 0.280(0.25), 1.21(0.87) mg/mL/24 h; 1 % urinary excretion.

[c] Patients were from the Chinese Han ethnicity.

patients with either diabetes or cancer to test the concentrations determined in Phase 1 and 2. Various vanadium compounds have been investigated in many trials, and a summary of human studies done are given in Table 1 [4, 6, 24, 42, 45, 59, 65–67, 78–84].

A set of Phase 1 and Phase 2 clinical trials that were carried out in the early 2000's and reported in 2006 involved the bis(ethylmaltolato)oxovanadium(IV) compound (BEOV) which is the ethyl derivative of bismaltolatooxovanadium(IV) (BMOV) that is commonly used as a standard to compare biological activity [24]. Unfortunately, these compounds (Figure 1) went off patent at September 30, 2011, and thus, future studies being carried out with BEOV were terminated due to lack of financial incentive [23, 24, 77]. However, in reviewing the literature, it is surprising that most of these human studies with vanadium have focused on diabetes because there are reports of the anticancer properties of vanadium compounds dating back to the 1950's.

2.2. Vanadium Compounds as Nutritional Additives

Although no vanadium compound has been approved for therapeutic use against diabetes, cancer or any other disease, several of them are available as nutritional supplements. These agents are used to control blood glucose levels and are taken by diabetics and bodybuilders. The forms of vanadium commercially available include vanadate and bismaltolatooxovanadium(IV), however, the most common vanadium-based material sold by far is $VOSO_4$, vanadyl sulfate. Further details are given in Section 6, where we list a number of different sources for $VOSO_4$. These nutritional supplements must adhere to the regulations by the Food and Drug Administration. Generally, the compounds need to appear on a "food safety list" and are not considered to be harmful before they can be sold as nutritional additives [85, 86].

As shown in Figure 1, there are several sources of vanadium compounds to supplement ones diet. Public access to these compounds allows people to treat themselves, and recognition of this fact was responsible for funding by the National Institutes of Health as mandated by Congress, to investigate the impact of vanadium salts in humans (see Table 1) [59, 67, 78, 81]. However, it was not tested for its effectiveness against cancer, presumably because the link between cancer and diabetes was not established at the time [18, 74].

3. BIOLOGICAL CHEMISTRY OF VANADIUM

Multiple reviews of the chemistry of vanadium, its salts, and organic vanadium compounds exist [7, 20, 26, 29, 44, 47, 57, 76, 87–91], in which a range of properties are generally described. The differences between vanadium compounds are highlighted based on the solution chemistry of vanadium in different oxidation states. Furthermore, biological studies generally involve vanadium in oxidation

states III, IV, and V that have been reported in biological systems, although vanadium can exist in 8 different oxidation states. These studies are limited by the stability of vanadium and generally focus on the properties of vanadium in solution [92–94].

Vanadium salts available as nutritional additives are usually in tablet form, regardless of the active ingredient. Upon digestion of these tablets, the active form of vanadium will be solubilized as the tablet travels from the mouth to the stomach and through the digestive tract. Animal studies are often carried out by administration of the vanadium compounds in drinking water or in food, and the forms of vanadium are dependent upon the method of administration [25]. The effects of the vehicle material that carries the vanadium compounds is usually not investigated [70].

3.1. Vanadium Salts and Their Speciation

The three most common forms of vanadium listed in the Introduction are Na_3VO_4, $NaVO_3$, and $VOSO_4$. There are four additional commercially available sources of vanadium, including sodium decavanadate ($Na_6V_{10}O_{28}$), vanadium pentoxide (V_2O_5), vanadyl dichloride ($VOCl_{2)}$, and vanadium(III) chloride (VCl_3). $Na_6V_{10}O_{28}$ and V_2O_5 contain V(V), $VOCl_2$ V(IV), and VCl_3 V(III). V_2O_5 is different than the others in that this material is a powder and any contact of this material with water will convert it to vanadate [95]. Because it is produced and used industrially, a chronic inhalation bioassay of V_2O_5 and its hydrolysis products by the National Toxicology Program produced evidence of treatment-related lung tumors in both male and female B6C3F1 mice [96]. The Environmental Protection Agency (EPA) has carried out a risk assessment and toxicological review of the material [96–100]. In contrast, $VOCl_2$ and VCl_3 are used much less frequently, mostly in research studies. The oxometallate decavanadate ($Na_6V_{10}O_{28}$) has been used more frequently in research studies, and animal studies with the sodium derivative and other salts of decavanadate have been reported to have antidiabetic effects [101–104].

The properties of vanadium in solution are often described by the Pourbaix diagram shown in Figure 2 [29, 91]. This figure shows what the nature of a solution of a vanadium salt is when placed under the conditions of a particular pH and redox environment. Because the figure is based on an aqueous solution, the stability of water is indicated by broken lines. Because the speciation is of most interest when water is stable, we are most interested in the speciation in the region between those broken lines. If the focus is on the properties of vanadium compounds under normal biological conditions and the conditions of the blood stream, the pH would be near 7.4 and the redox potential near -0.3 V, which is very different compared to the conditions of the stomach where the pH ranges from 2 to 4. Because the dissolution of a tablet is very different depending on its environment, one should consider the spectrum of reactivity, and the likely interconversion between oxidation states IV and V [29, 76].

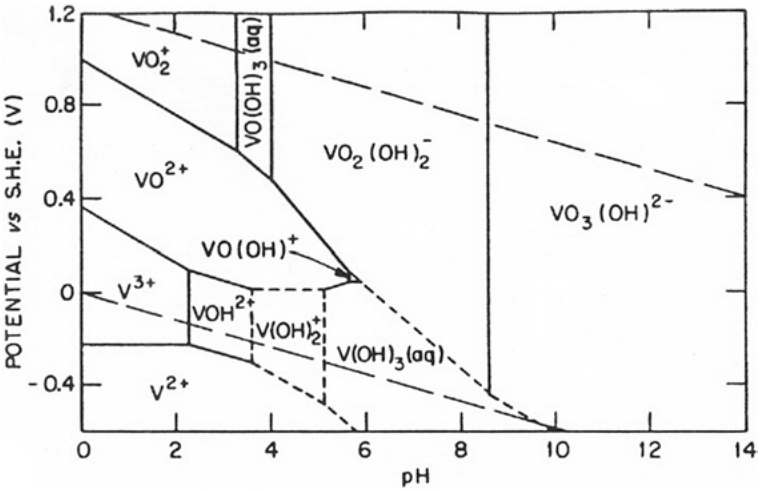

Figure 2. A Pourbaix diagram of vanadium in dependence on pH and potential is shown. Reproduced with permission from [91]; copyright 1976 John Wiley & Sons.

Each oxidation state exhibits interconversions that are strongly linked to the pH of the system [29, 76]. Vanadium(V) is the form of vanadium where the speciation is best understood, in part because it can readily be observed by ^{51}V NMR spectroscopy. Vanadate ($H_2VO_4^-$) is a structural and electronic analog of phosphate ($H_2PO_4^-$). Spectroscopic studies of vanadate have demonstrated that the specific form of vanadium(V) includes mono-, di-, tetra-, penta-, and decanuclear oxovanadate species [93, 94, 105]. These studies, in combination with biological studies, have documented that certain vanadium species are responsible for the observed biological effects. Under physiological conditions and at the low concentrations, the mononuclear species ($H_2VO_4^-/HVO_4^-$) is likely to predominate unless the vanadium compound is associated with a protein or another ligand system that will support an oligomeric form [58]. However, oligomeric species can also exist without coordination if the vanadium is compartmentalized so that the effective concentration will be higher, thus supporting vanadium species of higher nuclearity [106].

Vanadium(IV) is the form of vanadium that is directly compatible with the reducing environment in the blood and in cells. The fundamental unit is the $V{=}O^{2+}$ cation and Figure 1 shows the hydrated species likely to form in aqueous solution [47, 107]. This form readily dimerizes or polymerizes and is known to be able to replace cations such as Zn^{2+}. This species is the form that exists in dissolved $VOSO_4$. Vanadium in oxidation state III was until recently believed to rarely form in biological systems other than in tunicates (sea squirts) [108–110]. However, it was recognized that vanadium(III) can form by oxidation of ascorbate which may only be observable using high field EPR spectroscopy [111, 112] and not the X-band EPR spectroscopy that is commonly used.

3.2. Organic Vanadium Compounds

The term 'organic vanadium compounds' is generally used for compounds that contains both vanadium and organic ligands. Thus, this class of species includes both organometallic compounds and coordination complexes. The former group includes compounds containing cyclopentadienyl ligands, and the simple analog, vanadocene dichloride (Figure 3), was one of the first vanadium compounds that was reported having anticancer properties [13, 20, 113, 114].

The second class of species, the coordination complexes, do not contain a covalent V–C bond, but only ionic bonds instead. Examples of both complexes are also shown in Figure 3 [13, 20, 114–116]. Coordination complexes form readily in aqueous solution between a ligand (such as HMHCPE) and a vanadium ion,

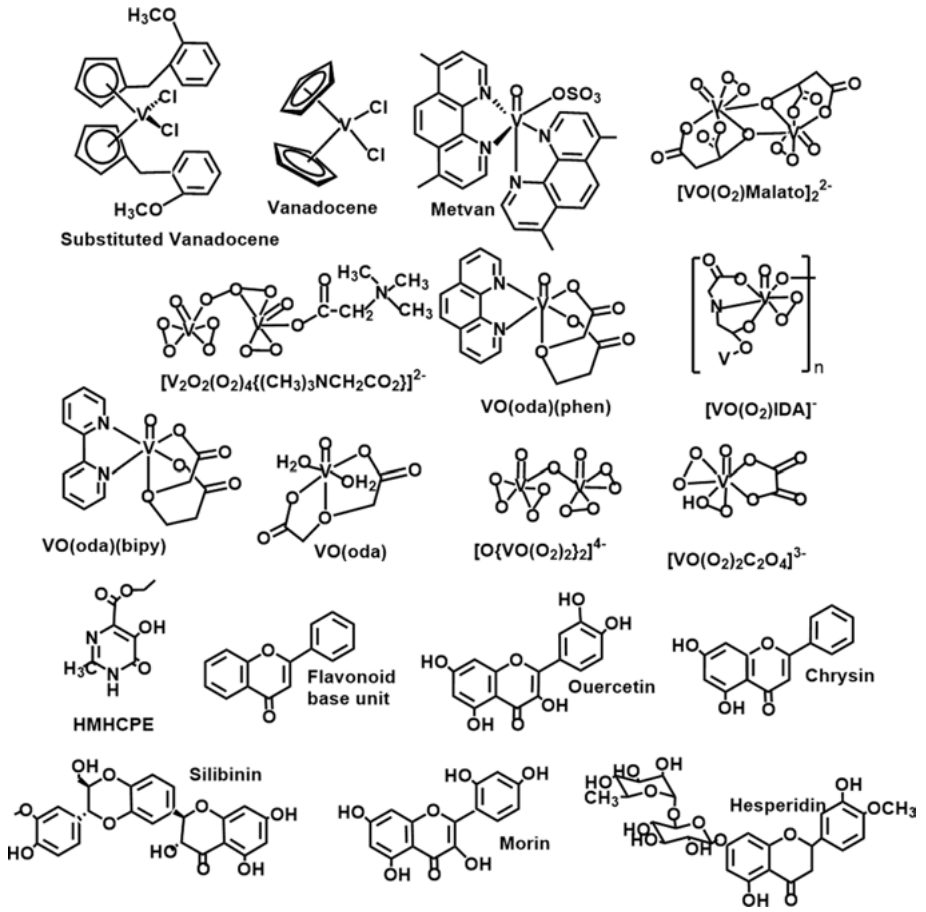

Figure 3. A range of different vanadium compounds and some active ligands, which when mixed with a vanadium salt resulted in a material containing ligand and vanadium with favorable anticarcinogenic properties.

however, most of these complexes also undergo ligand exchange which sometimes results in the formation of more than one species. Although this lability may give the impression that the compounds are difficult to work with, such lability is in fact a general property of many transition metal ions and their complexes. More importantly, it has been suggested that this lability may be key to the biological effects reported for some of the vanadium compounds [23–29, 76, 77, 117].

4. THE ANTICANCER EFFECTS OF VANADIUM COMPOUNDS

The "hallmarks" of cancer include sustaining proliferative signaling, resisting cell death, evading growth suppressors, evading immune destruction, enabling replicative immortality, inducing angiogenesis, activating invasion and metastasis, and reprogramming of energy metabolism [20, 118]. These important targets include inducing metabolic aberrations and disturbances in energy production, disorders in the structure and function of the mitochondria [119, 120] and changes in the reactive oxygen species (ROS) levels, production, and metabolism [8, 121]. The keen ability of vanadium compounds to become involved in cellular processes linked to molecular events in cancer makes them particularly able to suppress growth and decrease the spread of tumors. In a general sense, this is done via the vanadium compound by (a) inhibiting tumor cell proliferation and inducing apoptosis and (b) limiting invasion and the metastatic potential of neoplastic cells [20]. In the following section, the mechanistic studies carried out recently with $VO(acac)_2$ will be summarized to illustrate how advanced the area has become [18]. But, due to space limitations, this area cannot be reviewed comprehensively, the reader should refer to the original literature and other reviews [19–22, 48, 97–100].

Vanadate and $VO(acac)_2$ have shown promise, exhibiting an antiproliferative effect through inducing G2/M cell cycle arrest and elevating the levels of ROS in a human pancreatic cancer cell line (AsPC-1) [18]. Both these vanadium compounds activated the PI3K/AKT and MAPK/ERK signaling pathways in a dose- and time-dependent manner and their proposed mode of action is depicted in Figure 4. These mechanistic studies explored the nature of the ROS effects and were found to sustain the MAPK/ERK activation and be responsible for the G2/M cell cycle arrest. The ROS level plateaued after activation and was consistent with an intracellular feedback loop controlling the elevated ROS level induced by vanadate or $VO(acac)_2$. While the ROS level plateaued, the glutathione content increased and expression level of the antioxidant enzymes remained unchanged. Therefore, it was concluded that the vanadium compounds can be regarded as a novel class of anticancer drugs acting through the activation of the MAPK/ERK pathway. The present results provided a proof-of-concept that vanadium compounds have the potential as both antidiabetic and antipancreatic cancer agents to prevent or treat patients suffering from both diabetes and cancer [18, 122].

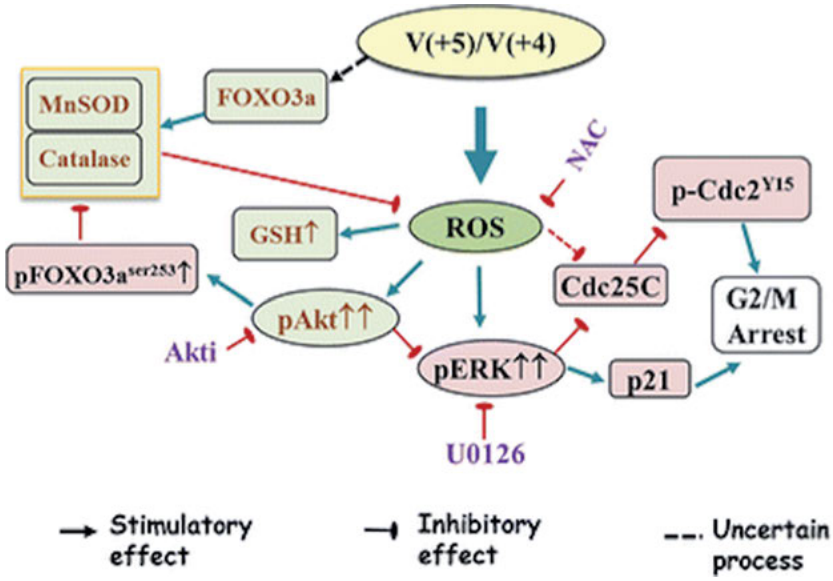

Figure 4. Scheme summarizing the possible mechanisms underlying $VO(acac)_2$ and vanadate-induced G2/M cell cycle arrest in AsPC-1 cells. The two vanadium compounds exhibited an antiproliferative effect through inducing G2/M cell cycle arrest. Both vanadium compounds increase the ROS levels in the cells. Simultaneously, the induced activation of both PI3K/AKT and MAPK/ERK signaling pathways in a dose- and time-dependent manner, which could be counteracted with the antioxidant N-acetylcysteine. Reproduced with permission from [18]; copyright 2016 Springer Publishing Company.

When the insulin-like properties of vanadium compounds were initially discovered, it was surprising that a small oxometallate could have the same effects as the 51-amino acid insulin peptide [123–125]. The mode of action of vanadium compounds is often described as poorly defined, although it is commonly accepted that some of the biological effects of vanadium compounds are due to the inhibition of phosphatases [77, 123, 126, 127]. Interaction of phosphatases with vanadate are generally very potent [77, 123, 126, 128, 129]. Most organic ligands coordinated to vanadium dissociate once the complex interacts with protein tyrosine phosphatases, but the affinity will change with the type of phosphatase, and in one report a vanadate peptide bound to protein tyrosine phosphatase 1B has been crystallographically characterized [126, 130, 131].

Vanadium compounds are also generally believed to lose the organic ligand before binding to transferrin [132] and other proteins [133] at the low concentrations found under physiological conditions. Interactions with transferrin are selective but vary with oxidation states which, when combined with the ability of vanadium compounds to undergo redox chemistry, provide several alternative avenues to also exert their action in addition to phosphatase inhibition [128, 129, 132, 133]. The alternative modes of action generally include modification of the

cellular redox state, vanadium recycling, and ROS formation [124, 134] as well as interactions with transferrin and other proteins [34, 132, 133].

Compounds with promising antitumor properties are shown in Figure 3 and include intact vanadium compounds as well as ligands that have been reported to form complexes with vanadium exhibiting promising antitumor properties in solution. In addition to the simple salts and other species two vanadocenes are seen in Figure 3 which represent the first-class vanadium compounds that were reported to have anticancer properties [13, 36, 113, 135–137]. These organometallic compounds have limited stability in aqueous environment. Titananocene [114] was investigated in Phase 1 clinical trial, but it was not continued to Phase 2, therefore vanadocene remains the most promising metallocene [138]. Mechanistic studies are important because they demonstrate that these compounds have a mode of action distinct from the Pt-based anticancer agents, and thus have effects on cells resistant to Pt-based drugs [13, 114, 136].

Peroxovanadium compounds, also shown in Figure 3, are reactive vanadium compounds which were found to have anticarcinogenic effects in cell culture studies [36, 48]. This class of compounds has unique chemical properties in several aspects, which affect its biological and medicinal applications [88]. First, the peroxo group is unique among vanadium compounds because of the three-membered peroxo ring, the structure of which is different than anything else in chemistry and biology [52, 88, 139–141]. Second, the three-membered peroxovanadium species supports reactivity involving ROS radical formation, and as such is tied to ROS-types of metabolic processing in the cell [15, 43, 52, 88, 139–144]. This is particularly important because these vanadium compounds undergo reactions with H_2O_2 or with superoxide, both of which can form in small amounts under some biological conditions, and thus, this class of compounds could form in cells. Third, the stability of most of these complexes is limited, which is a serious problem, because if they are to be used for oral administration, strategies must be developed to stabilize them [52, 88, 139–141]. To date, there are no reports of studies with these compounds in animals, presumably because such studies would show extensive oxidative damage of the digestive tract when the vanadium compound is administered orally. Fourth, this compound belongs to the first class of compounds that showed a dramatic enhancement of the effects of vanadium on activation of insulin receptors [124, 141]. This report documented that it was the complex that yielded the response because it surpassed the effects of the salts alone. These findings caused a surge in applications of this class of compounds, and the early results obtained with it fueled studies for several decades including a focus on applications for the treatment of cancer [17, 19–22, 33, 34, 145]. Creative compound designs of many different types have been reported, including a class of binary and ternary V-peroxide-betaine compounds with a built-in transporter peptide as part of the complex [146, 147].

Simple coordination complexes have also been investigated and found to have anticarcinogenic potential; representative examples are shown in Figure 3 as VO(oda)(bipy), VO(oda), VO(oda)(phen), and Metvan [17, 33, 148]. These complexes are formed *in situ*, and their stoichiometry can vary. However, for complexes formed from ligands with these types of functionalities, mainly 1 : 1 or

1 : 2 complexes are anticipated (although other forms are possible). Most of these results are based on cell culture and *in vitro* studies, although some have been carried out in animal studies. Often the interactions of these compounds were investigated with isolated DNA and the results can be found in other reviews and the original literature [17, 33, 148]. Recent studies with flavonoids and their vanadium complexes have demonstrated much potential as anticancer agents [33, 145, 149–151]. These species are less readily characterized because they do not form simple complexes that can be isolated in crystalline form. However, the activity of the compounds is promising with the best candidates being vanadium complexes with silibinin and quercetin, and the effects are supported by the flavonoid ligands that often have activity by themselves.

Finally, there have been many studies with simple salts. The salts may seem to be the simplest class of vanadium materials to study. However, the fact that vanadium salts readily undergo both hydrolytic and redox processes under the conditions of the biological studies makes studies with the simple salts some of the most complex studies to interpret. Specifically [67], $VOSO_4$ is the most commonly used control, but it is not innocuous in the many different biological systems investigated (cells, animals or human beings). However, because $VOSO_4$ undergoes several reactions under biological conditions, it becomes difficult to assign specific effects to the salt. Therefore, meaningful interpretations of studies with $VOSO_4$ must be subject to consider the method of delivery. Although considerations are made in some studies, the effect of the biological system on the chemistry is often not analyzed or discussed [24, 67].

A novel effect of vanadium compounds has been reported on oncolytic viruses, that is, viruses that prefer to attack cancer cells, and has much potential in cancer treatment. Oncolytic viruses are an emerging class of anticancer bio-therapeutics that induce antitumor immunity through selective replication in tumor cells [152]. Recently it was reported that a synergetic strategy, which boosts the therapeutic efficacy of oncolytic viruses, is combining their activity with immunomodulating small molecules, i.e., protein tyrosine-phosphatase inhibitors such as vanadium compounds [153]. We found that vanadium compounds could enhance oncolytic viruses' infection *in vitro* and *ex vivo* in resistant tumor cell lines. Furthermore, vanadium compounds increased the anticarcinogenic efficacy when being administrated in combination with oncolytic viruses in several syngeneic tumor models. This new combination of treatment with both the oncovirus and the vanadium compound offers new avenues for the development of improved immunotherapy strategies to combat cancer [152, 153].

5. VANADIUM-CONTAINING DRUGS IN CONTEXT OF OTHER DISEASES

5.1. Comparison of Anticancer Vanadium and Other Anticancer Compounds

Cisplatin and other Pt-based drugs are among the most successful anticancer drugs and are still a major part of the anticancer drugs administered in the clinic

[60, 154–162]. The further development of Pt-drugs was done to change the mode of administration to oral, which lowers toxicity and can reduce drug resistance. To evaluate the effectiveness of vanadium compounds, their effects are often compared to cisplatin, and the fact that the vanadium compounds are effective toward cell lines that are Pt-resistant is important. The differences between the anticancer activities of vanadium and platinum compounds are related to their fundamental chemical differences. Pt compounds can hydrolyze when entering cells, the degree to which this occurs is much less than vanadium compounds that are generally believed to dissociate while entering cells or organelles [60, 154–162]. Although Pt(IV) compounds are known to be reduced in cellular environments, the Pt(II) compounds less readily undergo redox processes [60, 154–162], whereas vanadium in oxidation states IV and V readily go through a redox cycle [1, 29, 47]. These facts support the possibility that the vanadium compounds are more likely to be involved in ROS processes than the Pt-compounds.

There are many other reports of metal-containing compounds with anticancer properties [9, 43, 114, 163–165]. These compounds range from ruthenium-based systems that already have been in clinical trials [166, 167] to titanium compounds that are potent phosphatase inhibitors [168], and to the controversies revolving around the chromium-based additives that have been Ames test-positive [33, 169–172].

5.2. Linking Treatments of Cancer to Treatments of Diabetes

Antidiabetic drugs have been reported to both increase and decrease cancer risks, although the role of hyperglycemia and the effects of diabetic medications on cancer risks remain controversial [122]. Insulin and insulin-like growth factor-1 may exert both metabolic and mitogenic effects on cancer initiation and/or progression at both the receptor and post-receptor levels [74, 173]. In addition, adding insulin to mediums containing high concentrations of glucose can activate the PI3K-AKT-mTOR pathway leading to the increased proliferation of cancer cells [174]. Furthermore, cancer risk is increased by insulin, insulin analogues, and secretagogues that cause hyperinsulinemia through an increase of insulin secretion [175]. In contrast, metformin, a biguanide, is known to reduce cancer risk by stimulation of AMPK and its upstream tumor suppressor protein regulator LKB1, in addition to reducing glucose and insulin levels [176]. The PI3K-AKT signaling pathway is well-known for its central role in survival, cell proliferation, growth, protein synthesis, and glucose metabolism. Inhibiting these vital components will cause side effects including hyperglycemia and glucose intolerance [177]. Development of AKT and PI3K inhibitors that are iso-form specific and do not perturb the metabolic function or pathway would represent a new approach to inhibitors [122]. Another possibility is to develop a drug inhibiting tumor proliferation without affecting metabolic function.

Vanadium compounds are known to have a range of effects on cellular and animal systems and as such have potential as a new type of therapeutic agent [19–22]. Generally they exhibit insulin-like effects including lowering blood glu-

cose levels, stimulation of glucose uptake, and activation of glycogen synthase as well as inhibition of lipolysis in diabetic rats or adipocytes [23, 25, 178–180]. Several studies also indicated that they enhance neurogenesis or exert neuroprotective effects in several animal models [181]. The multi-pathway effects of vanadium compounds may make them unique among current available treatments, and as a class these compounds have great potential to exert both preventive and therapeutic effects on patients with more than one disease. Further studies are needed to capitalize on the therapeutic potential of such drugs with the possibility to act on several diseases and to minimize potential side effects.

More studies are necessary before vanadium-based anticancer agents will be ready for use in the clinic. However, it is important to recognize that many vanadium-containing nutritional additives are already used by the public, and thus permission for clinical trials studies should be more readily obtained. Based on the current knowledge of the coordination chemistry of vanadium, it seems appropriate that a holistic approach to future drug development should include drug formulation strategies and that such an approach would significantly improve the chances of success of future drug candidates.

6. VANADIUM-BASED DRUGS AND ADDITIVES AND THEIR FORMULATION

Many different forms of vanadyl sulfate are commercially available as shown in Figure 5, created from various images of the $VOSO_4$ supplements found online. The bottles shown reflect the number of different preparations and formulations of vanadyl sulfate-containing supplements. It is interesting to note that, as shown in Table 2, the formulations of $VOSO_4$ vary significantly depending on the brand and the company selling the compound. Regardless of the amounts of $VOSO_4$ per tablet, the recommended dose of administration is generally 1–2 tablets and implies that the different formulations provide different efficacy of the vanadium (see Table 2 below for a more detailed description).

It will be difficult to keep the vanadium compounds from interacting with the metabolites occurring under physiological conditions once the compound has been administered. It is therefore to be expected that the compounds co-administered with $VOSO_4$ will play a key role for the distribution and processing of vanadium. The different formulations of $VOSO_4$ shown in Figure 5 will deliver the vanadium(IV) cation in a different manner. This means that vanadium(IV) will have different abilities to redox cycle, form vanadium(V) and the vanadate anion as well as to react with other metabolites and form coordination compounds. In other words, the fundamental coordination chemistry of vanadium(IV) will be important for the efficacy of $VOSO_4$. It has been recognized for some time now that the ligands are likely to be important to the delivery of vanadium to its target [182, 183].

The number of different formulations listed in Table 2 underline the wide variety of materials used for administration of $VOSO_4$. The different additives include nutrients, metabolites, traditional formulation compounds and thus undoubtedly

Table 2. Forms of vanadyl sulfate available in 2016–2017. Name, total vanadium, formulation material, and use.

Supplement name V source	V compound/ mg	Total V/mg	Formulation Material (nutrients are bolded)	Suggested use
Douglas Lab-Vanadyl Sulfate	7.5	1.46	Cellulose, stearic acid, magnesium stearate, and silica	Support blood sugar and cholesterol levels
Life-Extension-Vanadyl Sulfate	7.5	1.5	$Ca_3(PO_4)_2$, microcrystalline cellulose, stearic acid, vegetable stearate, croscarmellose sodium, film coating	Tissue sensitivity and glucose metabolism
Olympianlabs-Vanadyl Sulfate[a]	20	4.7[a]	**Niacin**, vegetarian capsule (HPMC), rice flour, microcrystalline cellulose (plant fiber), silicon dioxide, ascorbyl palmitate	Maintain healthy blood sugar levels
Olympian Labs-Vanadyl Plus[a]	10	2.35[a]	**Niacin**, chromium (picolinate, chromax®), microcrystalline cellulose (plant fiber), rice flour, magnesium stearate, silica	Support healthy blood sugar levels and endurance
Country life-Vanadyl Sulfate	5	0.975	Cellulose (capsule shell), cellulose, magnesium stearate, silica	Support glucose and lipid metabolism
Dee cee Labs-Vanadyl Sulfate[a]	10	2.35[a]	$Ca_3(PO_4)_2$, cellulose, vegetable stearic acid, croscarmellose sodium, silica, vegetable magnesium stearate	Lowers blood sugar levels
Ultimate nutrition-Vanadyl Sulfate	10	2.35[a]	Lactose, microcrystalline cellulose, croscarmellose sodium, stearic acid, magnesium stearate, SiO_2	General supplement
Vitamin shoppe-Vanadyl Sulfate[b]	2	0.47[a]	$Ca_3(PO_4)_2$, microcrystalline cellulose, stearic acid, magnesium stearate, croscarmellose sodium, hydroxypropyl methylcellulose, polyethylene glycol	Glucose metabolism
Source naturals-Vanadyl Sulfate	10	2	Microcrystalline cellulose, stearic acid, and colloidal SiO_2	Maintain blood sugar level
Puritan's pride-Vanadyl Sulfate	10	2.35[a]	$Ca_3(PO_4)_2$, vegetable cellulose, vegetable stearic acid, silica, vegetable magnesium stearate	Reduces cholesterol, health supplement

Nutrakey Vanadyl Sulfate	10	2.35[a]	Gelatin, rice flour	Blood sugar regulation
Vitamin research-Vanadyl Sulfate [b]	50	10	Microcrystalline cellulose, hydroxypropylmethylcellulose	Hormone and blood sugar metabolism
FNX-Daily-V Women's Vanadyl Sulfate	1	0.235[a]	**Vitamin A, C, D, K1, B1, B2, B6, niacin**, calcium (Ca_3Cit_2), KI, MgO, zinc gluconate, iron citrate, selenium methionate, copper (gluconate 10 %), $MnSO_4$, chromium (from albion chelavite), boron (from albion amino acid complex), dong quai root, red clover, PABA, *Cimicifuga racemosa L*. root, vegetarian and microcrystalline cellulose, silica magnesium stearate	General supplement
Wonder Labs-Vanadyl Sulfate	10	2.35[a]	$Ca_3(PO_4)_2$, vegetable cellulose, vegetable stearic acid, silica, vegetable magnesium stearate	Maintain a healthy blood sugar level
GNC-Mega Men® 50 Plus One Daily Vanadyl Sulfate	0.01		MgO, **vitamin A, C, D, E, K, B6, and B12, thiamin mononitrate (vitamin B1), riboflavin (vitamin B2), niacin (as niacinamide), folic acid**, biotin, pantothenic acid (as calcium d-pantothenate), $CaCO_3$, $Ca_3(PO_4)_2$, KI, ZnO, Na_2SeO_3, Cu_2O, $MnSO_4$, chromium, boron, and molybdenum (hydrolyzed protein chelate), KCl Gingko Biloba leaf extract, phosphatidyl serine, choline bitartrate, inositol, Lutemax 2020™ Lutein, zeaxanthin isomers, pumpkin seed meal (*Cucurbita pepo/maxima*), *Serenoa repens* extract, lycopene, SiO_2, $SnCl_2$, Ni_2SO_4, cellulose, TiO_2, vegetable acetoglycerides, caramel color, ethyl vanillin	Men's health
Bricker Labs-vig-Vtriple strength Vanadyl Sulfate	30	7.05[a]	Taurine, selenium, chromium, niacin, gelatin, microcrystalline cellulose	Insulin response supports glucose metabolism

Supplement name V source	V compound/ mg	Total V/mg	Formulation Material (nutrients are bolded)	Suggested use
GNC-Preventive Nutrition® Healthy Blood Sugar Formula Vanadyl Sulfate	0.05	0.012	**Thiamin mononitrate (vitamin B1), riboflavin (vitamin B2), vitamin B6 (pyridoxine HCl and pyridoxal-5-phosphate) and B12 (as cyanocobalamin), biotin,** ZnO, chromium hydrolyzed protein chelate, fermented soybean extract, *Cinnamomum zeylanicum* extract, *Momordica charantia* powder, alpha lipoic acid (R-ALA), *Acacia catechu* wood and bark extract, *Scutellaria baicalensis* extract, resVida® trans-Resveratrol, Lutemax 2020™ Lutein, zeaxanthin, cellulose, $Ca_3(PO_4)_2$	Support the specific health needs of women
GNC Women's Ultra Mega One Daily Vanadyl Sulfate	0.01		Choline bitartrate, inositol, Lutemax 2020™ Lutein, zeaxanthin isomers, cranberry fruit concentrate, boron (as hydrolyzed protein chelate), $SnCl_2$, Ni_2SO_4	Brain and memory support
Priority One Vitamins-VanaTrace Vanadyl Sulfate	50	10	Rice chelate, vegetarian capsule	Support blood glucose levels
Metabolic Maintenance-Metabolic X[c]	50	0.5	**Vitamin C**, chromium, *Gymnema silvestre* leaf extract, Cin-nulin PF, Banaba leaf extract, vegetarian cellulose capsule	Maintain energy, intensity, endurance
Natural Sport-Cinnamon Vanadyl Chromium	10		**Vitamin C**, cinnamon, chromium, bay leaf, clove, cellulose, silica and stearic acid	Glucose support
Vitamin World-Vanadyl Sulfate	10	2.35[a]	Calcium phosphate, vegetable cellulose, vegetable stearic acid, contains <2 % of silica, vegetable magnesium stearate.	Exercise supplement
Futurebiotics-Colloidal Chromium Vanadium	0.089		$CrCl_3$, vanadyl sulfate, deionized water, potassium sorbate, hydrogen chloride	General supplement and carbohydrate metabolism

Source naturals-Vanadium with Chromium	1	Vanadium (as bisglycinatooxovanadium), chromium GTF (as polynicotinate [ChromeMate®]), microcrystalline cellulose and stearic acid	Help maintain blood sugar levels (already normal)
Kal-Trace Minerals Vanadyl Sulfate	0.03	**Vitamin B12 (cyanocobalamin)**, KI, selenomethionine, copper gluconate, zinc, manganese, chromium, molybdenum, and boron as glycinate complexes, inland sea mineral concentrate, parsley leaf, alfalfa juice powder, aloe vera gel concentrate, watercress leaf, spinach leaf, cellulose, stearic acid, silica and magnesium stearate	Prevent vitamin and mineral deficiencies and help to protect against or manage certain diseases
Kal-Vanadyl Complex	10	**Vitamin C (as ascorbic acid),** chromium picolinate, *Cinnamomum verum* bark, *Laurus nobilus* leaf, *Syzgium aromaticum* flower, cellulose, silica and stearic acid	Dietary supplement
Piping Rock-Ultra Vanadyl Complex	10	**Niacin USP (vitamin B3**), chromium picolinate, $Ca_3(PO_4)_2$, dicalcium phosphate, vegetable stearic acid and magnesium stearate, croscarmellose sodium, silica	Support glucose levels
Ai Sports GlycoBol BMOV (Bis-malto-oxovanadium)		**Na-R-ALA, glycobol, Trigonella seed isolate (standardized to 10 % 4-hydroxyisoleucine), Phellodendron extract (standard 90 % berberine), cinnamon bark 20 : 1 extract (standard 16 % flavonoids)**, gelatin (capsule), maltodextrin, Candurin Silver Fine, Red #40, FD&C Blue #1, FD&C Yellow #5	Insulin mimetic supplement

BMOV = bismaltolatooxovanadium(IV); BEOV = bis(ethylmaltolato)oxovanadium(IV); PABA = 4-aminobenzoic acid: GTF = glucose tolerance factor: ALA = alpha lipoic acid; USP = United States Pharmacopoeia – tested for purity; HPMC = hydroxy, propyl, methyl, and cellulose

[a] Supplier does not indicate V-content so the calculated amount is based on $VOSO_4 \cdot 3\,H_2O$.

[b] No longer commercially available as of 2017.

[c] Requires 2 capsules per day vanadium (as vanadium glycinate)

Figure 5. Different bottles of vanadyl sulfate supplements obtained from the internet. Each bottle is prepared using different formulations, commercially available diet supplements and their vanadium content. Reproduced with permission from [163]; copyright 2016 Elsevier.

there is a large difference in how vanadium is being delivered. Considering that these nutritional additives are used, and many of them sold in food stores, there are many options available for the public to access these compounds. We conclude that how these different vanadium complexes form and are processed is likely to be important for the efficacy of these nutritional additives and we expect that some of these supplements work much better than others.

Considering that the importance of the delivery of $VOSO_4$ is not generally investigated in the literature [23, 24, 67], there is a need for data showing the effects of coordination chemistry for its biological activities. An understanding of the mode of processing and action of vanadium compounds as well as of other metal-containing nutritional additives would facilitate further drug development.

7. CONCLUSIONS AND OUTLOOK

The studies of vanadium compounds with anticancer properties have come a long way since the first studies with vanadocene dichloride and the discovery of its anticancer properties in 1965 [184]. Many different classes of vanadium

compounds have been investigated since these first studies and many different biological systems have been used. Recently, there has been an effort to develop new model systems that avoid using animal cancer models [33, 185]. Considering the problems associated with animal studies such model studies could be helpful at the initial stages of compound testing, however, it is critical that the data obtained before a compound is being considered for clinical trials include consideration of the formulation, as it can make a dramatic difference.

Links between diseases have been emerging through increasing evidence that commonalities exist in etiology or pathology [74]. Therefore, we no longer recommend an exclusive focus on single disease treatments, as is supported by reports of epidemiological investigations suggesting that incidence of pancreatic, liver, and endometrial cancers are associated with diabetes [75]. Searching for multi-disease targeting drugs provides a unique approach for the discovery of new medicines to treat, prevent or delay the onset of more than one type of disease, or take advantage of the advances developed for one disease in the treatment of a second one [74]. Vanadium compounds with their specific (sub)cellular biomolecular interactions emerge with an outstanding potential in the quest for identifying selective and specific interactions leading to vanadium compound-induced demise of cancer cells [20].

Finally, we suggest a new promising effect of vanadium compounds involving oncolytic viruses and their potential for treating cancer [153]. The strategy is based on the boost of therapeutic efficacy of oncolytic viruses by combining their activity with immuno-modulating small molecules, protein tyrosine phosphatase inhibitors, such as vanadium compounds. The infection of oncolytic viruses *in vitro* and *ex vivo* in resistant tumor cell lines was enhanced by vanadium compounds. This newly discovered tumor-reducing effect of vanadium-based compounds offers new avenues for the development of improved immunotherapeutic strategies to combat cancer.

ACKNOWLEDGMENTS

DCC thanks the Arthur Cope foundation managed by the American Chemical Society for funding. XG Yang thanks the National Natural Science Foundation of China (Grant No. 21171011 and 21671009).

ABBREVIATIONS

acac	acetylacetonato
bipy	2,2′-bipyridine
HMHCPE	2-methyl-3H-5-hydroxy-6-carboxy-4-pyrimidinone ethyl ester
IDA	iminodiacetic acid
Metvan	bis(4,7-dimethyl-1,10-phenanthroline)sulfatooxovanadium(IV)
oda	oxydiacetate

phen	1,10-phenenthroline
ROS	reactive oxygen species
tar	tartrate

REFERENCES

1. B. Lyonnet, S. Martz, E. Martin, *La Presse Méd.* **1899**, *1*, 191–192.
2. C. E. Lewis, *Am. Med. Assoc. Arch. Ind. Health* **1959**, *19*, 497–503.
3. A. Morinville, D. Maysinger, A. Shaver, *Trends. Pharmacol. Sci.* **1998**, *19*, 452–460.
4. N. L. Kent, R. A. McCance, *Biochem. J.* **1941**, *35*, 837–844.
5. K. Gruzewska, A. Michno, T. Pawelczyk, H. Bielarczyk, *J. Physiol. Pharmacol.* **2014**, *65*, 603–611.
6. X. Wang, T. Sun, J. Liu, Z. Shan, Y. Jin, S. Chen, W. Bao, F. B. Hu, L. Liu, *Am. J. Epidemiol.* **2014**, *180*, 378–384.
7. D. Rehder, *Angew. Chem. Int. Ed.* **1991**, *30*, 148–167.
8. Z. Zhang, C. Huang, J. Li, S. S. Leonard, R. Lanciotti, L. Butterworth, X. Shi, *Arch. Biochem. Biophys.* **2001**, *392*, 311–320.
9. L. P. Lu, M. L. Zhu, *Anti-Cancer Agents Med. Chem.* **2011**, *11*, 164–171.
10. M. A. Zoroddu, M. Fruianu, R. Dallocchio, A. Masia, *Biometals* **1996**, *9*, 91–97.
11. J. Aubrecht, R. Narla, P, J. Stanek, F. Uckun, *Toxicol. Appl. Pharmacol.* **1999**, *154*, 228–235.
12. O. J. D'Cruz, Y. Dong, F. M. Uckun, *Anticancer Drugs* **2000**, *11*, 849–858.
13. C. S. Navara, A. Benyumov, A. Vassilev, R. K. Narla, P. Ghosh, F. M. Uckun, *Anticancer Drugs* **2001**, *12*, 369–376.
14. P. K. Wilmsen, D. S. Spada, M. Salvador, *J. Agric. Food Chem.* **2005**, *53*, 4757–4761.
15. P. K. Sasmal, R. Majumdar, R. R. Dighe, A. R. Chakravarty, *Dalton Trans.* **2010**, *39*, 2147–2158.
16. D. C. Crans, C. M. Simone, A. K. Saha, R. H. Glew, *Biochem. Biophys. Res. Commun.* **1989**, *165*, 246–250.
17. I. León, N. Butenko, A. Di Virgilio, C. Muglia, E. Baran, I. Cavaco, S. Etcheverry, *J. Inorg. Biochem.* **2014**, *134*, 106–117.
18. J.-X. Wu, Y. H. Hong, X. G. Yang, *J. Biol. Inorg. Chem.* **2016**, *21*, 1–11.
19. A. Bishayee, A. Waghray, M. A. Patel, M. Chatterjee, *Cancer Lett.* **2010**, *294*, 1–12.
20. E. Kioseoglou, S. Petanidis, C. Gabriel, A. Salifoglou, *Coord. Chem. Rev.* **2015**, *301*, 87–105.
21. A. M. Evangelou, *Crit. Rev. Oncol. Hematol.* **2002**, *42*, 249–265.
22. J. C. Pessoa, S. Etcheverry, D. Gambino, *Coord. Chem. Rev.* **2015**, *301–302*, 24–48.
23. K. H. Thompson, J. Lichter, C. LeBel, M. C. Scaife, J. H. McNeill, C. Orvig, *J. Inorg. Biochem.* **2009**, *103*, 554–558.
24. K. H. Thompson, C. Orvig, *J. Inorg. Biochem* **2006**, *100*, 1925–1935.
25. G. R. Willsky, L.-H. Chi, M. Godzala, III, P. J. Kostyniak, J. J. Smee, A. M. Trujillo, J. A. Alfano, W. Ding, Z. Hu, D. C. Crans, *Coord. Chem. Rev.* **2011**, *255*, 2258–2269.
26. D. C. Crans, A. M. Trujillo, P. S. Pharazyn, M. D. Cohen, *Coord. Chem. Rev.* **2011**, *255*, 2178–2192.
27. D. C. Crans, S. Schoeberl, E. Gaidamauskas, B. Baruah, D. A. Roess, *J. Biol. Inorg. Chem.* **2011**, *16*, 961–972.
28. X. G. Yang, X. D. Yang, L. Yuan, K. Wang, D. C. Crans, *Pharm. Res.* **2004**, *21*, 1026–1033.
29. D. C. Crans, J. J. Smee, E. Gaidamauskas, L. Q. Yang, *Chem. Rev.* **2004**, *104*, 849–902.

30. D. Rehder, *Inorg. Chem. Comm.* **2003**, *6*, 604–617.
31. D. Rehder, *Coord. Chem. Rev.* **1999**, *182*, 297–322.
32. D. Rehder, J. C. Pessoa, C. Geraldes, M. Castro, T. Kabanos, T. Kiss, B. Meier, G. Micera, L. Pettersson, M. Rangel, A. Salifoglou, I. Turel, D. R. Wang, *J. Biol. Inorg. Chem.* **2002**, *7*, 384–396.
33. I. León, J. Cadavid-Vargas, A. Di Virgilio, S. Etcheverry, *Curr. Med. Chem.* **2017**, *24*, 112–148.
34. U. Jungwirth, C. R. Kowoi, B. K. Keppler, C. G. Hartinger, W. Berger, P. Heffeter, *Antioxid. Redox Signal.* **2011**, *15*, 1086–1127.
35. A. Bishayee, A. Waghray, M. A. Patel, M. Chatterjee, *Cancer Lett.* **2010**, *294*, 1–12.
36. P. Köpf-Maier, *Met. Complexes Cancer Chemother.* **1993**, 259–296.
37. Y. Dong, R. K. Narla, E. Sudbeck, F. M. Uckun, *J. Inorg. Biochem.* **2000**, *78*, 321–330.
38. F. Chen, V. Vallyathan, V. Castranova, X. Shi, *Mol. Cell. Biochem.* **2001**, *222*, 183–188.
39. D. Mustafi, B. Peng, S. Foxley, M. Makinen, G. Karczmar, M. Zamora, J. Ejnik, H. Martin, *J. Biol. Inorg. Chem.* **2009**, *14*, 1187–1197.
40. Y. Shechter, *Diabetes* **1990**, *39*, 1–5.
41. N. Cohen, M. Halberstam, P. Shlimovich, C. J. Chang, H. Shamoon, L. Rossetti, *J. Clin. Invest.* **1995**, *95*, 2501–2509.
42. K. Cusi, S. Cukier, R. A. DeFronzo, M. Torres, F. M. Puchulu, J. C. P. Redondo, *J. Clin. Endocrinol. Metab.* **2001**, *86*, 1410–1417.
43. T.-T. Liu, Y.-J. Liu, Q. Wang, X.-G. Yang, K. Wang, *J. Biol. Inorg. Chem.* **2012**, *17*, 311–320.
44. D. Rehder, *Future Med. Chem.* **2012**, *4*, 1823–1837.
45. J. Somerville, B. Davies, *Am. Heart J.* **1962**, *64*, 54–56.
46. N. D. Chasteen, R. J. DeKoch, B. L. Rogers, M. W. Hanna, *J. Am. Chem. Soc.* **1973**, *95*, 1301–1309.
47. N. D. Chasteen, in "*The Biochemistry of Vanadium*", *Structure and Bonding*, Eds. M. J. Clarke, J. B. Goodenough, J. A. Ibers, C. K. Jørgensen, D. M. P. Mingos, J. B. Neilands, G. A. Palmer, D. Reinen, P. J. Sadler, R. Weiss, R. J. P. Williams, Springer-Verlag, New York, 1983, Vol. 53, pp. 105–138.
48. C. Djordjevic, G. L. Wampler, *J. Inorg. Biochem.* **1985**, *25*, 51–55.
49. N. D. Chasteen, E. M. Lord, H. J. Thompson, J. K. Grady, *Biochim. Biophys. Acta* **1986**, *884*, 84–92.
50. I.-B. Svensson, R. Stomberg, *Acta Chem. Scand.* **1971**, *25*, 898–910.
51. D. Begin, F. W. B. Einstein, J. Field, *Inorg. Chem.* **1975**, *14,* 1785–1790.
52. C. Djordjevic, S. A. Craig, E. Sinn, *Inorg. Chem.* **1985**, *24*, 1281–1283.
53. W. Priebsch, D. Rehder, *Inorg. Chem.* **1990**, *29*, 3013–3019.
54. M. Helena, S. F. Teixeira, J. C. Pessoa, L. F. V. Boas, *Polyhedron* **1992**, *11*, 697–708.
55. J. H. McNeill, V. G. Yuen, H. R. Hoveyda, C. Orvig, *J. Med. Chem.* **1992**, *35*, 1489–1491.
56. P. Caravan, L. Gelmini, N. Glover, F. G. Herring, H. L. Li, J. H. McNeill, S. J. Rettig, I. A. Setyawati, E. Shuter, Y. Sun, A. S. Tracey, V. G. Yuen, C. Orvig, *J. Am. Chem. Soc.* **1995**, *117*, 12759–12770.
57. L. V. Vilas Boas, J. Costa Pessoa, in *Comprehensive Coordination Chemistry. The Synthesis, Reactions, Properties and Applications of Coordination Compounds*, Eds. G. Wilkinson, R. D. Gillard, J. A. McCleverty, Pergamon Press, New York, 1987, Vol. 3, pp. 453–583.
58. D. C. Crans, R. L. Bunch, L. A. Theisen, *J. Am. Chem. Soc* **1989**, *111*, 7597–7607.
59. A. B. Goldfine, D. C. Simonson, F. Folli, M. E. Patti, C. R. Kahn, *J. Clin. Endocrinol. Metab.* **1995**, *80*, 3311–3320.

60. M. Aureliano, D. C. Crans, *J. Inorg. Biochem.* **2009**, *103*, 536–546.
61. D. C. Crans, B. Baruah, A. Ross, N. E. Levinger, *Coord. Chem. Rev.* **2009**, *253*, 2178–2185.
62. A. Chatkon, P. B. Chatterjee, M. A. Sedgwick, K. J. Haller, D. C. Crans, *Eur. J. Inorg. Chem.* **2013**, 1859–1868.
63. A. Chatkon, A. Barres, N. Samart, S. E. Boyle, K. J. Haller, D. C. Crans, *Inorg. Chim. Acta.* **2014**, *420*, 85–91.
64. G. Boden, X. Chen, J. Ruiz, G. D. V. van Rossum, S. Turco, *Metabolism* **1996**, *45*, 1130–1135.
65. J. P. Fawcett, S. J. Farquhar, T. Thou, B. I. Shand, *Pharmacol. Toxicol.* **1997**, *80*, 202–206.
66. R. L. P. G. Jentjens, A. E. Jeukendrup, *Int. J. Sport Nutr. Exercise Metab.* **2002**, *12*, 470–479.
67. G. R. Willsky, K. Halvorsen, M. E. Godzala, III, L.-H. Chi, M. J. Most, P. Kaszynski, D. C. Crans, A. B. Goldfine, P. J. Kostyniak, *Metallomics* **2013**, *5*, 1491–1502.
68. A. Bordbar, L. Creagh, F. Mohammadi, C. Haynes, C. Orvig, *J. Biol. Inorg. Chem.* **2009**, *103*, 643–647.
69. H. Sakurai, K. Fujii, H. Watanabe, H. Tamura, *Biochem. Biophys. Res. Commun.* **1995**, *214*, 1095–1099.
70. A. Levina, D. C. Crans, P. Lay, *Coord. Chem. Rev.* **2017**, *352*, 473–498.
71. M. Žižić, M. Živić, I. Spasojevic, J. Bogdanovic Pristov, M. Stanić, T. Cvetic-Antic, J. Zakrzewska, *Res. Microbiol.* **2013**, *164*, 61–69.
72. V. Conte, B. Floris, P. Galloni, A. Silvagni, *Pure Appl. Chem.* **2005**, *77*, 1575–1581.
73. J. J. Boruah, D. Kalita, S. P. Das, S. Paul, N. S. Islam, *Inorg. Chem.* **2011**, *50*, 8046–8062.
74. X.-G. Yang, K. Wang, *Curr. Top. Med. Chem.* **2016**, *16*, 675–676.
75. P. Vigneri, F. Frasca, L. Sciacca, G. Pandini, R. Vigneri, *Endocr.-Relat. Cancer* **2009**, *16*, 1103–1123.
76. D. C. Crans, *Pure Appl. Chem.* **2005**, *77*, 1497–1527.
77. D. C. Crans, *J. Org. Chem.* **2015**, *80*, 11899–11915.
78. G. R. Willsky, A. B. Goldfine, P. J. Kostyniak, J. H. McNeill, L. Q. Yang, H. R. Khan, D. C. Crans, *J. Inorg. Biochem.* **2001**, *85*, 33–42.
79. F. Proescher, H. A. Seil, *Am. J. Syph.* **1917**, *1*, 347–405.
80. E. G. Dimond, J. Caravaca, A. Benchimol, *Am. J. Clin. Nutr.* **1963**, *12*, 49–53.
81. M. Halberstam, N. Cohen, P. Shlimovich, L. Rossetti, H. Shamoon, *Diabetes* **1996**, *45*, 659–666.
82. M. D. Cohen, M. Sisco, C. Prophete, L.-c. Chen, J. T. Zelikoff, A. J. Ghio, J. D. Stonehuerner, J. J. Smee, A. A. Holder, D. C. Crans, *J. Immunotoxicol.* **2007**, *4*, 49–60.
83. A. B. Goldfine, M.-E. Patti, L. Zuberi, B. J. Goldstein, R. LeBlanc, E. J. Landaker, Z. Y. Jiang, G. R. Willsky, C. R. Kahn, *Metabolism* **2000**, *49*, 400–410.
84. G. Heinemann, B. Fichtl, W. Vogt, *Br. J. Clin. Pharmacol.* **2003**, *55*, 241–245.
85. M. McBane, *Ill-health Canada: Promoting Food and Drug Company Profits ahead of Safety*, Canadian Centre for Policy Alternatives, Ottawa, ON, 2005, pp. 131 p.
86. R. B. Kreider, C. D. Wilborn, L. Taylor, B. Campbell, A. L. Almada, R. Collins, M. Cooke, C. P. Earnest, M. Greenwood, D. S. Kalman, C. M. Kerksick, S. M. Kleiner, B. Leutholtz, H. Lopez, L. M. Lowery, R. Mendel, A. Smith, M. Spano, R. Wildman, D. S. Willoughby, T. N. Ziegenfuss, J. Antonio, *J. Int. Soc. Sports Nutr.* **2010**, *7*, 1–43.
87. A. Butler, in *Vanadium in Biological Systems: Physiology and Biochemistry*, Ed. N. D. Chasteen, Kluwer Academic Publishers, Boston, 1990, pp. 25–50.
88. A. Butler, M. J. Clague, G. Meister, *Chem. Rev.* **1994**, *94*, 625–638.

89. D. C. Crans, K. A. Woll, K. Prusinskas, M. D. Johnson, E. Norkus, *Inorg. Chem.* **2013**, *52*, 12262–12275.
90. T. Kiss, T. Jakusch, D. Hollender, A. Dornyei, E. A. Enyedy, J. C. Pessoa, H. Sakurai, A. Sanz-Medel, *Coord. Chem. Rev.* **2008**, *252*, 1153–1162.
91. C. F. J. Baes, Jr., R. E. Mesmer, *The Hydrolysis of Cations*, John Wiley & Sons, New York, 1976, pp. 193–210.
92. J. Krakowiak, D. Lundberg, I. Persson, *Inorg. Chem.* **2012**, *51*, 9598–9609.
93. L. Pettersson, I. Andersson, B. Hedman, *Chem. Scrip.* **1985**, *25*, 309–317.
94. L. Pettersson, B. Hedman, I. Andersson, N. Ingri, *Chem. Scrip.* **1983**, *22*, 254–264.
95. A. Al-Qatati, F. L. Fontes, B. G. Barisas, D. Zhang, D. A. Roess, D. C. Crans, *Dalton Trans.* **2013**, *42*, 11912–11920.
96. T. B. Starr, J. A. MacGregor, *Regul. Toxicol. Pharmacol.* **2014**, *69*, 333–337.
97. M. B. Black, D. E. Dodd, P. D. McMullen, S. Pendse, J. A. MacGregor, B. B. Gollapudi, M. E. Andersen, *Regul. Toxicol. Pharmacol.* **2015**, *73*, 339–347.
98. M. G. Manjanatha, S. D. Shelton, L. Haber, B. Gollapudi, J. A. MacGregor, N. Rajendran, M. M. Moore, *Mutat. Res.-Genet. Toxicol. Environ. Mutag.* **2015**, *789*, 46–52.
99. N. Rajendran, J. C. Seagrave, L. M. Plunkett, J. A. MacGregor, *Inhalation Toxicol.* **2016**, *28*, 618–628.
100. M. Banda, K. L. Mckim, L. T. Haber, J. A. MacGregor, B. B. Gollapudi, B. L. Parsons, *Mutat. Res.-Genet. Toxicol. Environ. Mutag.* **2015**, *789*, 53–60.
101. M. J. Pereira, E. Carvalho, J. W. Eriksson, D. C. Crans, M. Aureliano, *J. Inorg. Biochem.* **2009**, *103*, 1687–1692.
102. E. Gonzalez Vergara, S. Trevino Mora, V. E. Sarmiento Ortega, E. Sanchez Lara, I. Sanchez Lombardo, A. D. Diaz Fonseca, J. A. F. Flores Hernandez, A. R. Perez Benitez, E. M. Brambila Colombres, in "Pharmaceutical Composition of Metformin Decavanadate for Prevention and Treatment of Metabolic Syndrome, Obesity, and Diabetes", Mexican Patent No. MX 2015003461 Diabetes. Benemerita Universidad Autonoma de Puebla, Mex. 2016.
103. S. Trevino, E. Brambila-Colombres, D. Velazquez-Vazquez, E. Sanchez-Lara, E. Gonzalez-Vergara, A. Diaz-Fonseca, J. A. Flores-Hernandez, A. Perez-Benitez, *Oxid. Med. Cell. Longev.* **2016**, *2016*, 60–75.
104. S. Trevino, E. Sanchez-Lara, V. E. Sarmiento-Ortega, I. Sanchez-Lombardo, J. A. Flores-Hernandez, A. Perez-Benitez, E. Brambila-Colombres, E. Gonzalez-Vergara, *J. Inorg. Biochem.* **2015**, *147*, 85–92.
105. D. C. Crans, C. D. Rithner, L. A. Theisen, *J. Am. Chem. Soc.* **1990**, *112*, 2901–2908.
106. P. B. Chatterjee, O. Goncharov-Zapata, L. L. Quinn, G. Hou, H. Hamaed, R. W. Schurko, T. Polenova, D. C. Crans, *Inorg. Chem.* **2011**, *50*, 9794–9803.
107. D. C. Crans, B. Zhang, E. Gaidamauskas, A. D. Keramidas, G. R. Willsky, C. R. Roberts, *Inorg. Chem.* **2010**, *49*, 4245–4256.
108. P. Buglyó, D. C. Crans, E. M. Nagy, R. L. Lindo, L. Q. Yang, J. J. Smee, W. Z. Jin, L. H. Chi, M. E. Godzala, G. R. Willsky, *Inorg. Chem.* **2005**, *44*, 5416–5427.
109. M. Melchior, S. Rettig, B. Liboiron, K. Thompson, V. Yuen, J. McNeil, C. Orvig, *Inorg. Chem.* **2009**, *40*, 4686–4690.
110. H. Michibata, T. Uyama, K. Kanamori, in *The Biology of Ascididans*, Eds H. Sawada, H. Yokosawa, C. C. Lambert, Springer Japan, Tokyo, 2001, pp. 363–373.
111. J. Krzystek, A. Ozarowski, J. Telser, D. C. Crans, *Coord. Chem. Rev.* **2015**, *301*, 123–133.
112. A. A. Holder, P. Taylor, A. R. Magnusen, E. T. Moffett, K. Meyer, Y. Hong, S. E. Ramsdale, M. Gordon, J. Stubbs, L. A. Seymour, D. Acharya, R. T. Weber, P. F. Smith, G. C. Dismukes, P. Ji, L. Menocal, F. Bai, J. L. Williams, D. M. Cropek, W. L. Jarrett, *Dalton Trans.* **2013**, *42*, 11881–11899.

113. B. Gleeson, J. Claffey, A. Deally, M. Hogan, L. M. M. Méndez, H. Müller-Bunz, S. Patil, D. Wallis, M. Tacke, *Eur. J. Inorg. Chem.* **2009**, *2009*, 2804–2810.
114. I. Kostova, *Anti-Cancer Agents Med. Chem.* **2009**, *9*, 827–842.
115. H. Faneca, V. Figueiredo, I. Tomaz, G. Gonçalves, F. Avecilla, M. P. de Lima, C. F. Geraldes, J. C. Pessoa, M. M. C. Castro, *J. Inorg. Biochem.* **2009**, *103*, 601–608.
116. I. Correia, S. Roy, C. Matos, S. Borovic, N. Butenko, I. Cavaco, F. Marques, J. Lorenzo, A. Rodriguez, V. Moreno, J. C. Pessoa, *J. Inorg. Biochem.* **2015**, *147*, 134–146.
117. K. H. Thompson, C. Orvig, *Met. Ions Biol. Syst.* **2004**, *41*, 221–252.
118. D. Hanahan, R. A. Weinberg, *Cell* **2011**, *144*, 646–674.
119. T. N. Seyfried, R. E. Flores, A. M. Poff, D. P. D'Agostino, *Carcinogenesis* **2014**, *35*, 515–527.
120. K. O. Alfarouk, A. K. Muddathir, M. E. A. Shayoub, *Cancers* **2011**, *3*, 408–414.
121. K. M. Holmstrøm, T. Finkel, *Nat. Rev. Mol. Cell Biol.* **2014**, *15*, 411–421.
122. X.-G. Yang, K. Wang, *Curr. Topics Med. Chem.* **2016**, *16*, 675–676.
123. M. J. Gresser, A. S. Tracey, P. J. Stankiewicz, *Adv. Prot. Phosphatases* **1987**, *4*, 35–57.
124. B. I. Posner, A. Shaver, I. G. Fantus, in *New Antidiabetic Drugs*, Eds C. J. Bailey, P. R. Flatt, Smith-Gordon, London, 1990, pp. 107–118.
125. C. Cuncic, N. Detich, D. Ethier, A. S. Tracey, M. J. Gresser, C. Ramachandran, *J. Biol. Inorg. Chem.* **1999**, *4*, 354–359.
126. C. C. McLauchlan, B. J. Peters, G. R. Willsky, D. C. Crans, *Coord. Chem. Rev.* **2015**, *301–302*, 163–199.
127. G. Huyer, S. Liu, J. Kelly, J. Moffat, P. Payette, B. Kennedy, G. Tsaprailis, M. J. Gresser, C. Ramachandran, *J. Biol. Chem.* **1997**, *272*, 843–851.
128. Y. L. Guo, B. B. Kang, J. R. Williamson, *J. Biol. Chem.* **1998**, *273*, 10362–10366.
129. N. H. Guo, H. C. Krutzsch, J. K. Inman, D. D. Roberts, *Cancer Res.* **1997**, *57*, 1735–1742.
130. T. A. S. Brandao, A. C. Hengge, S. J. Johnson, *J. Biol. Chem.* **2010**, *285*, 15874–15883.
131. T. A. S. Brandão, S. J. Johnson, A. C. Hengge, *Arch. Biochem. Biophys.* **2012**, *525*, 53–59.
132. J. C. Pessoa, I. Tomaz, *Curr. Med. Chem.* **2010**, *17*, 3701–3738.
133. N. D. Chasteen, in *Metal Ions in Biological Systems*, Eds. H. Sigel, A. Sigel, Marcel Dekker, Inc., New York, 1995, Vol. 31, pp. 231–248.
134. C. J. Band, B. I. Posner, V. Dumas, J.-O. Contreres, *Mol. Endo.* **1997**, *11*, 1899–1910.
135. R. K. Narla, Y. Dong, P. Ghosh, K. Thoen, F. M. Uckun, *Drugs Future.* **2000**, *25*, 1053–1068.
136. J. Vinklárek, I. Pavlík, Z. Cernosek, *Met. Based Drugs* **1997**, *4*, 207–219.
137. J. R. Vinklárek, J. Honzíček, J. Holubová, *Inorg. Chim. Acta.* **2004**, *357*, 3765–3769.
138. P. Ghosh, O. J. D'Cruz, R. K. Narla, F. M. Uckun, *Clin. Cancer Res.* **2000**, *6*, 1536–1545.
139. C. Djordjevic, M. Lee-Renslo, E. Sinn, *Inorg. Chim. Acta* **1995**, *233*, 97–102.
140. V. S. Sergienko, *Kristallografiya* **2004**, *49*, 401–426.
141. A. Shaver, J. B. Ng, D. A. Hall, B. I. Posner, *Mol. Cell. Biochem.* **1995**, *153*, 5–15.
142. S. Petanidis, E. Kioseoglou, M. Hadzopoulou-Cladaras, A. Salifoglou, *Cancer Lett.* **2013**, *335*, 387–396.
143. P. K. Sasmal, S. Saha, R. Majumdar, S. De, R. R. Dighe, A. R. Chakravarty, *Dalton Trans.* **2010**, *39*, 2147.
144. M. Sam, H. Hwang Jung, G. Chanfreau, M. Abu-Omar Mahdi, *Inorg. Chem.* **2004**, *43*, 8447–8455.
145. S. Etcheverry, E. Ferrer, L. Naso, J. Rivadeneira, V. Salinas, P. Williams, *J. Biol. Inorg. Chem.* **2008**, *13*, 435–447.

146. C. Gabriel, E. Kioseoglou, J. Venetis, V. Psycharis, A. Raptopoulou, A. Terzis, G. Voylatzis, M. Bertmer, C. Mateescu, A. Salifoglou, *Inorg. Chem.* **2012**, *51*, 6056–6069.
147. C. Gabriel, M. Kaliva, J. Venetis, P. Baran, I. Rodriquez-Escudero, G. Voylatzis, A. Salifoglou, *Inorg. Chem.* **2009**, *48*, 476–487.
148. I. E. León, S. B. Etcheverry, B. S. Parajón-Costa, E. J. Baran, *Biol. Trace. Elem. Res.* **2012**, *147*, 403–407.
149. I. León, J. Cadavid-Vargas, I. Tiscornia, V. Porro, S. Castelli, P. Katkar, A. Desideri, M. Bollati-Fogolin, S. Etcheverry, *J. Biol. Inorg. Chem.* **2015**, *20*, 1175–1191.
150. I. E. Leon, V. Porro, V. A. Di, L. G. Naso, P. A. Williams, M. Bollati-Fogolín, S. B. Etcheverry, *J. Biol. Inorg. Chem.* **2014**, *19*, 59.
151. I. E. Leon, V. A. Di, V. Porro, C. I. Muglia, L. G. Naso, P. A. Williams, M. Bollatifogolin, S. B. Etcheverry, *Dalton Trans.* **2013**, *42*, 11868–11880.
152. C. S. Ilkow, S. L. Swift, J. C. Bell, J.-S. Diallo, *PLoS Pathog.* **2014**, *10*, e1003836.
153. D. C. Crans, M. Selman, J.-S. Diallo, *J. Biol. Inorg. Chem.* **2017**, *22 (Suppl 1)*, S164.
154. A. H. Calvert, D. R. Newell, L. A. Gumbrell, S. Oreilly, M. Burnell, F. E. Boxall, Z. H. Siddik, I. R. Judson, M. E. Gore, E. Wiltshaw, *J. Clin. Oncol.* **1989**, *7*, 1748–1756.
155. T. Boulikas, M. Vougiouka, *Oncol. Rep.* **2003**, *10*, 1663–1682.
156. I. Arany, R. L. Safirstein, *Semin. Nephrol.* **2003**, *23*, 460–464.
157. R. A. Alderden, M. D. Hall, T. W. Hambley, *J. Chem. Educ.* **2006**, *83*, 728–734.
158. R. R. Barefoot, *J. Chromatogr. B* **2001**, *751*, 205–211.
159. S. E. Sherman, S. J. Lippard, *Chem. Rev.* **1987**, *87*, 1153–1181.
160. D. Wang, S. J. Lippard, *Nat. Rev. Drug Discov.* **2005**, *4*, 307–320.
161. N. Farrell, *Met. Ions Biol. Syst.* **1996**, *32*, 603–639.
162. J. Reedijk, *Chem. Commun.* **1996**, 801–806.
163. K. A. Doucette, K. N. Hassell, D. C. Crans, *J. Inorg. Biochem.* **2016**, *165*, 56–70.
164. I. Zwolak, H. Zaporowska, *Cell Biol. Toxicol.* **2012**, *28*, 31–46.
165. P. C. A. Bruijnincx, P. J. Sadler, *Curr. Opin. Chem. Biol.* **2008**, *12*, 197–206.
166. Y. K. Yan, M. Melchart, A. Habtemariam, P. J. Sadler, *Chem. Commun.* **2005**, 4764–4776.
167. H. M. Chen, J. A. Parkinson, S. Parsons, R. A. Coxall, R. O. Gould, P. J. Sadler, *J. Am. Chem. Soc* **2002**, *124*, 3064–3082.
168. T. E. Thingholm, M. R. Larsen, C. R. Ingrell, M. Kassem, O. N. Jensen, *J. Proteome Res.* **2008**, *7*, 3304–3313.
169. J. C. Codina, C. Pereztorrente, A. Perezgarcia, F. M. Cazorla, A. Devicente, *Arch. Environ. Contam. Toxicol.* **1995**, *29*, 260–265.
170. K. Szyba, M. C. Golonka, K. Gasiorowski, J. Urban, *Biometals* **1992**, *5*, 157–161.
171. M. Shara, T. Yasmin, A. E. Kincaid, A. L. Limpach, J. Bartz, K. A. Brenneman, A. Chatterjee, M. Bagchi, S. J. Stohs, D. Bagchi, *J. Inorg. Biochem.* **2005**, *99*, 2161–2183.
172. P. A. White, J. B. Rasmussen, *Environ. Mol. Mutag.* **1996**, *27*, 270–305.
173. P. Jacob, T. A. Chowdhury, *Quart. J. Med.* **2015**, *108*, 443–448.
174. R. G. Jones, C. B. Thompson, *Genes Dev.* **2009**, *23*, 537–548.
175. L. Grimaldi-Bensouda, M. Marty, M. Pollak, D. Cameron, M. Riddle, B. Charbonnel, A. H. Barnett, P. Boffetta, J. F. Boivin, M. Evans, M. Rossignol, J. Benichou, L. Abenhaim, *Lancet* **2010**, *376*, 769–770.
176. I. Pernicova, M. Korbonits, *Nat. Rev. Endocrinol.* **2014**, *10*, 143–156.
177. T. A. Yap, M. D. Garrett, M. I. Walton, F. Raynaud, J. S. de Bono, P. Workman, *Curr. Opin. Pharmacol.* **2008**, *8*, 393–412.
178. J.-C. Liu, Y. Yu, G. Wang, K. Wang, X.-G. Yang, *Metallomics* **2013**, *5*, 813–820.
179. H. Ou, L. Yan, D. Mustafi, M. W. Makinen, M. J. Brady, *J. Biol. Inorg. Chem.* **2005**, *10*, 874–886.
180. L. Gao, Y. Niu, W. Liu, M. Xie, X. Liu, Z. Chen, L. Li, *Clin. Chim. Acta* **2008**, *388*, 89–94.

181. N. Shioda, T. Ishigami, F. Han, S. Moriguchi, M. Shibuya, Y. Iwabuchi, K. Fukunaga, *Neuroscience* **2007**, *148*, 221–229.
182. B. A. Reul, S. S. Amin, J. P. Buchet, L. N. Ongemba, D. C. Crans, S. M. Brichard, *Br. J. Pharmacol.* **1999**, *126*, 467–477.
183. I. Osinska-Krolicka, H. Podsiadly, K. Bukietynska, M. Zemanek-Zboch, D. Nowak, K. Suchoszek-Lukaniuk, M. Malicka-Blaszkiewicz, *J. Inorg. Biochem.* **2004**, *98*, 2087–2098.
184. J. Kieler, A. Gromek, N. I. Nissen, *Acta Chir. Scand. Suppl.* **1965**, *343*, 154–164.
185. W. R. Wilson, M. P. Hay, *Nature Rev.* **2011**, *11*, 393–410.

10

Gallium Complexes as Anticancer Drugs

Christopher R. Chitambar

Department of Medicine, Hematology & Oncology Division, Medical College of Wisconsin,
9200 W. Wisconsin Avenue, Milwaukee, WI 53226, USA
<cchitamb@mcw.edu>

ABSTRACT 282
1. HISTORY 282
2. CHEMISTRY 283
3. GALLIUM-BASED AGENTS IN CLINICAL USE. PHARMACOLOGY AND EFFICACY 283
   3.1. Background 283
   3.2. Gallium Nitrate 284
   3.3. Gallium Maltolate 286
   3.4 Tris(8-quinolinolato)gallium(III) (KP46, FFC11) 287
4. CELLULAR HANDLING OF GALLIUM 288
   4.1. Transport and Cellular Uptake 288
   4.2. Intracellular Trafficking 290
5. ANTINEOPLASTIC MECHANISM OF CLINICALLY USED GALLIUM COMPOUNDS 290
   5.1. Inhibition of Cellular Iron Uptake and Cell Proliferation 291
   5.2. Inhibition of Iron-Dependent Ribonucleotide Reductase 291
   5.3. Action on the Mitochondria and Induction of Apoptosis 292
   5.4. Action of Tris(8-quinolinolato)gallium(III) on the Cytoskeleton 293
6. GALLIUM COMPOUNDS IN PRECLINICAL DEVELOPMENT 294
   6.1. Gallium Pyridine and Gallium Phenolate 294
   6.2. Gallium Thiosemicarbazones 295
   6.3. Gallium-Pyridoxal Isonicotinyl Hydrazone 295
   6.4. Gallium Complexes with Azole Ligands 295

Metal Ions in Life Sciences, Volume 18 Edited by Astrid Sigel, Helmut Sigel, Eva Freisinger, and Roland K. O. Sigel

https://doi.org/10.1515/9783110470734-010

6.5. Bi- and Tetranuclear Gallium(III) Complexes with Heterocyclic Thiolato Ligands and Dinuclear Gallium Carboxylate Complexes 296
6.6. Gallium-Corroles 296
7. SUMMARY AND OUTLOOK 296
ACKNOWLEDGMENTS 297
ABBREVIATIONS 297
REFERENCES 297

Abstract: Clinical trials have shown gallium nitrate, a group 13 (formerly IIIa) metal salt, to have antineoplastic activity against non-Hodgkin's lymphoma and urothelial cancers. Interest in gallium as a metal with anticancer properties emerged when it was discovered that ^{67}Ga(III) citrate injected in tumor-bearing animals localized to sites of tumor. Animal studies showed non-radioactive gallium nitrate to inhibit the growth of implanted solid tumors. Following further evaluation of its efficacy and toxicity in animals, gallium nitrate, $Ga(NO_3)_3$, was designated an investigational drug by the National Cancer Institute (USA) and advanced to Phase 1 and 2 clinical trials.

Gallium(III) shares certain chemical characteristics with iron(III) which enable it to interact with iron-binding proteins and disrupt iron-dependent tumor cell growth. Gallium's mechanisms of action include the inhibition of cellular iron uptake and disruption of intracellular iron homeostasis, these effects result in inhibition of ribonucleotide reductase and mitochondrial function, and changes in the expression in proteins of iron transport and storage. Whereas the growth-inhibitory effects of gallium become apparent after 24 to 48 hours of incubation of cells, an increase in intracellular reactive oxygen species (ROS) is seen with 1 to 4 hours of incubation. Gallium-induced ROS consequently triggers the upregulation of metallothionein and hemoxygenase-1 genes.

Beyond the first generation of gallium salts such as gallium nitrate and gallium chloride, a new generation of gallium-ligand complexes such as tris(8-quinolinolato)gallium(III) (KP46) and gallium maltolate has emerged. These agents are being evaluated in the clinic while other ligands for gallium are in preclinical development. These newer agents appear to possess greater antitumor efficacy and a broader spectrum of antineoplastic activity than the earlier generation of gallium compounds.

Keywords: cancer therapeutics · gallium · iron · mitochondria · ribonucleotide reductase

1. HISTORY

Gallium exists in the earth's crust at a concentration of 5–15 mg/kg and is obtained as a byproduct of extraction of aluminum and zinc ores. It was discovered in 1875 by the French chemist Paul-Emile Lecoq de Boisbaudran who noted gallium as a new element with two distinct violet bands on spectroscopy. Prior to its discovery, however, gallium's existence had been predicted by the Russian chemist Dimitri Mendeleev who termed it eka-aluminum, as he felt it would be located on the periodic table below aluminum. However, it was found as a trace element in zinc sulfide rather than aluminum. Although the origin of the name gallium appears to have been in honor of France (Gallia), it is possible that the name originated from "gallus", Latin for Lecoq (meaning rooster), the name of its discoverer.

2. CHEMISTRY

Gallium is a group 13 (formerly IIIA) metal with the atomic number 31 in the periodic table of elements. It possesses a silvery white color and has a melting point of 28.7646° (85.5763 °F). As a result, it can attain a near liquid state at room temperature and can transition from solid to liquid when held in the hand. Certain chemical properties of gallium are shared with iron(III). For example, the octahedral ionic radius for Ga^{3+} is 0.620 Å while that for high spin Fe^{3+} is 0.645 Å and the tetrahedral ionic radius is 0.47 Å and 0.49 Å for Ga^{3+} and Fe^{3+}, respectively. The electron affinity and ionization potential values for Ga^{3+} are 30.71 eV and 64 eV, respectively, while for high spin Fe^{3+} they are 30.65 eV and 54.8 eV, respectively [1]. Gallium undergoes hydrolysis to yield a mixture of gallium hydroxides of $Ga(OH)_{11}^{8-}$) and $Ga(OH)_3$ at pH ~4 , and a mixture of $Ga(OH)_3$ and $Ga(OH)_4^-$ at the physiologic pH 7.4 [2].

3. GALLIUM-BASED AGENTS IN CLINICAL USE. PHARMACOLOGY AND EFFICACY

3.1. Background

The potential of gallium as a therapeutic agent was suggested in 1931 by Levaditi et al. who reported the eradication of syphilis in rabbits and trypanosoma evansi in mice by gallium tartrate [3]. Years later, the discovery that radiogallium (^{67}Ga) injected intravenously would localize in tumors in animals sparked interest in developing ^{67}Ga citrate as a tumor imaging agent in patients. For several decades to follow, ^{67}Ga scanning was used as a diagnostic tool in the clinic to detect occult tumors or residual viable tumors following treatment [4]. Although more contemporary imaging approaches such as positron emission tomography (PET) scans have largely replaced the ^{67}Ga scan, ^{68}Ga-labeled pharmaceuticals are in development as advanced tools for tumor imaging [5, 6].

Not surprisingly, the ability of ^{67}Ga to concentrate in certain cancers *in vivo* stimulated interest in the effects of non-radioactive gallium on malignant cells. To investigate this, Hart and Adamson compared the antitumor activities of the group 13 metal salts of aluminum, gallium, indium, and thallium in a rodent tumor-bearing model [7]. Their results showed gallium nitrate to be the most effective of these metal salts in inhibiting the growth of three of the four malignant rodent tumors inoculated in animals. Following further preclinical studies to define the antineoplastic activity and toxicity in different animal models, gallium nitrate was designated an investigation drug (NSC 15200) by the National Cancer Institute (NCI, USA) and entered clinical trials. During the same period, Collery et al. in France explored the activity of oral gallium chloride in solid tumors and demonstrated its antineoplastic potential [8, 9]. However, the amount of gallium that could be absorbed from oral gallium chloride was found to be therapeutically insufficient. In contrast, gallium nitrate, administered intravenously displayed

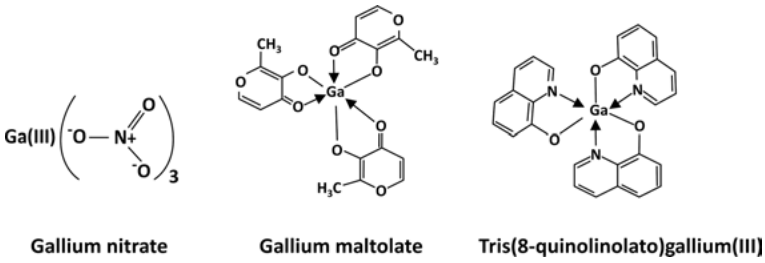

Figure 1. Chemical structures of gallium compounds that have been evaluated in the clinic for cancer treatment.

meaningful antineoplastic activity in Phase 1 and Phase 2 trials [10, 11]; it thus remains the standard against which newer gallium-based agents must be compared. This section will focus on gallium nitrate, gallium maltolate, and tris(8-quinolinolato)gallium(III) (KP46) as these gallium compounds have advanced to the clinic. Their chemical structures are shown in Figure 1.

3.2. Gallium Nitrate

As the first gallium compound to gain approval for clinical use by the Food and Drug Administration (FDA), gallium nitrate has been extensively studied for its antineoplastic efficacy and toxicity in humans [10]. Interestingly, the drug was approved in the early 1990s not as an anticancer agent, but for the treatment of cancer-associated hypercalcemia [12]. During its evaluation as an antineoplastic agent, gallium nitrate was found to interact with bone metabolism and lower calcium levels in the blood [12]. This prompted several trials of gallium nitrate in patients with cancer and metabolic bone disease which confirmed its ability to inhibit bone resorption and lower pathologically elevated blood calcium levels [12]. These trials led to the FDA approval of gallium nitrate as a drug for the treatment of malignancy-associated hypercalcemia. With regard to its activity as an anticancer drug, extensive Phase 2 clinical trials were conducted to explore the antineoplastic activity of gallium nitrate in chronic lymphocytic leukemia, Hodgkin's lymphoma, and non-Hodgkin's lymphoma, and in sarcoma, breast, bladder, renal, melanoma, prostate, lung, ovarian, and cervical cancers. Of these malignancies, gallium nitrate was found to have antineoplastic activity primarily against advanced bladder cancer and non-Hodgkin's lymphoma [11, 13, 14], and hence, subsequent clinical trials of this drug focused on these latter malignancies.

In Phase 2 trials of gallium nitrate in lymphoma and bladder cancer, significant responses to treatment were reported in patients whose tumors had relapsed or failed to respond to conventional chemotherapy (reviewed in references [13–15])]. In these studies, patients treated with gallium nitrate had cancers that progressed or failed to respond to conventional chemotherapeutic drugs. Complete and partial responses to gallium nitrate were seen in approximately 35–40 % of patients

with non-Hodgkin's lymphoma. In other studies, 18–22 % of patients with advanced bladder cancer responded to treatment with gallium nitrate.

A limited number of clinical trials investigated combinations of gallium nitrate with other chemotherapeutic agents in patients with bladder cancer or non-Hodgkin's lymphoma and confirmed that gallium nitrate could be safely combined with other drugs with a good clinical outcome [11, 13, 14]. An important consideration in the use of gallium nitrate is that it does not suppress the production of white blood cells or platelets. It can therefore be used to treat patients with low blood counts or can be combined with other antineoplastic agents without exacerbating their myelosuppressive effects. This is a major advantage of gallium nitrate since the majority of cytotoxic chemotherapeutic agents can suppress hematopoiesis.

Gallium nitrate must be administered intravenously to patients as its bioavailability is poor when taken orally. Pharmacokinetic studies of gallium nitrate given as an intravenous infusion over 30 minutes demonstrated that it is excreted primarily through the kidney, with a biphasic excretion pattern showing a T½ α of 8.3–26 minutes and a T½ β of 6.3–196 hours [16]. The latter slower excretion phase likely reflects gallium bound to transferrin (Tf) in the circulation. By 24 and 48 hours following its intravenous administration, 69 % and 91 % of the administered gallium dose was excreted in the urine [16]. In another study, the pharmacokinetics of gallium nitrate following its brief intravenous administration at 3 dose levels (500, 750, and 900 mg/m^2) showed biphasic serum gallium disappearance curves with a T½ α of 87 minutes and T½ β of 24.5 hours. Here, approximately 65 % of the infused gallium was recovered in the urine during the first 24 hours; half of this amount appeared in the urine within the first 4 hours after injection [17].

Due to dose-limiting renal toxicity encountered with high-dose gallium nitrate infusions, subsequent studies were conducted using a lower dose of gallium nitrate (200–300 mg/m^2/day) administered by intravenous infusion continuously over 24 hours for 5–7 days. Under these conditions, at a dose of 200 mg/m^2/day, mean steady-state plasma levels of gallium were achieved by 2–3 days with urinary excretion approximately matching the daily dose of the drug [18]. Plasma gallium concentration during steady state infusion at this dose level ranged from 0.9–1.9 μg/mL. Four days after cessation of treatment, it was 0.45–0.7 μg/mL. The advantage of administering gallium nitrate by continuous infusion is that the drug is better tolerated and patients receive a greater amount of gallium over time when compared with the brief infusion schedule [18]. Moreover, continuous infusion of gallium nitrate appears to be more efficacious than a brief infusion and, for this reason, continuous infusion of gallium nitrate for 5–7 days has been the recommended method of drug administration. However, the continuous intravenous gallium nitrate is cumbersome as it requires that the drug be administered in the hospital or as an outpatient through a pump device. Alternative treatment schedules that are more acceptable to patients should be explored.

At this time, gallium nitrate is no longer being marketed because the company manufacturing the drug closed for reasons unrelated to the drug. However, considerable information on the potential antineoplastic activity of gallium has been

generated through preclinical and clinical investigations of gallium nitrate. As a result, a number of new compounds have emerged that consist of gallium bound to more complex ligands. In preclinical studies, these agents appear to be more effective than gallium nitrate in inhibiting the proliferation of cancer cells at lower gallium concentrations; however, their superiority to gallium nitrate in the clinic remains to be determined. Two of the new generation gallium formulations that have advanced to clinical evaluation are tris(3-hydroxy-2-methyl-4*H*-pyran-4 onato)gallium(III) (gallium maltolate) and tris(8-quinolinolato)gallium(III) (KP46) (Figure 1).

3.3. Gallium Maltolate

This compound contains a central gallium atom bound to three maltol [tris(3-hydroxy-2methyl-pyrone)] ligands in a propeller-like arrangement (Figure 1) [19]; it is fashioned after ferric maltol, an oral iron formulation used to treat iron deficiency anemia [20, 21]. Indeed, gallium maltolate has shown good bioavailability in animal and human studies [19] where serum gallium levels of 0.115 and 0.569 μg/mL have been reported following a single oral dose of 100–500 mg of gallium maltolate. This is comparable to gallium blood levels reported with gallium nitrate administered by continuous intravenous infusion. The mechanism of gastrointestinal uptake of gallium maltolate is not well understood. While gallium maltolate may bear semblance to ferric maltolate, the absorption of the latter compound requires the initial reduction of ferric iron to ferrous iron in the gut [22]. Since gallium(III) is not reduced to gallium(II), it appears unlikely that the mechanism of gastrointestinal uptake of gallium maltolate is similar to that of ferric maltol. While the process by which gallium crosses the gastrointestinal mucosa remains to be elucidated, it is known that the majority of gallium appearing in the blood following oral administration of gallium maltolate is bound to Tf, the transport protein for iron in the circulation [23]. A better understanding of the gastrointestinal uptake of gallium maltolate is relevant as it may suggest strategies to enhance the oral bioavailability and antineoplastic activity of this drug.

As an antitumor agent, gallium maltolate has been shown to inhibit the proliferation of lymphoma and hepatocellular cancer cell lines *in vitro* at gallium concentrations that are significantly lower than that of gallium nitrate, thus indicating that it may have greater efficacy as a therapeutic agent [24, 25]. An additional important distinction between gallium nitrate and gallium maltolate is that lymphoma cell lines with acquired or intrinsic resistance to the growth-inhibitory effects of gallium nitrate remain sensitive to growth inhibition by gallium maltolate [24]. The development of drug resistance to chemotherapeutic agents remains one of the major obstacles to the successful treatment of cancer. Therefore, the lack of tumor cross-resistance between gallium nitrate and gallium maltolate has important therapeutic implications.

In vivo studies to explore the antitumor activity of gallium maltolate have been conducted in a mouse tumor model of cutaneous T-cell lymphoma and in an

animal model of human glioblastoma xenografts inoculated into a rat brain [26, 27]. In both these animal models, gallium maltolate displayed significant antineoplastic activity. Regarding glioblastoma, it is known that most conventional chemotherapeutic drugs lack efficacy against brain tumors mainly due to their inability to cross the blood brain barrier. Therefore, the ability of gallium maltolate to inhibit the growth of glioblastoma in an animal brain tumor model has important implications for its advancement to clinical trials for the treatment of brain tumors.

Although clinical trials of gallium maltolate in cancer have yet to be developed, Bernstein, et al. reported a patient with advanced hepatocellular cancer who experienced a significant response to treatment with oral gallium maltolate; here, the treatment for 2 months resulted in a marked reduction in tumor-related pain, improvement in abnormal liver function, blood tests, and a shrinkage in the size of viable tumor as measured by computerized axial tomography imaging [28]. A ^{67}Ga scan prior to treatment demonstrated uptake of radiogallium by the patient's liver cancer, indicating that the tumor was very likely to take up gallium maltolate. No adverse side-effects were experienced by the patient with this treatment [28]. Such case reports are important to note as they form the basis for advancing gallium maltolate to more comprehensive clinical trials.

Although not within the scope of this chapter, it should be noted that gallium maltolate has also been shown to be effective against certain microorganisms in animal models of infection. Its mechanism of antimicrobial action relates to gallium's interference with iron utilization by pathogenic microorganisms. The application of gallium compounds as antibiotics has been reviewed elsewhere [29, 30].

3.4 Tris(8-quinolinolato)gallium(III) (KP46, FFC11)

This compound was developed by virtue of the strong metal chelating properties of 8-quinolinol to form tris(8-quinolinolato)gallium(III) [31]. The drug is an oral compound with a high thermodynamic stability (log β_3 40.7). Based on its aqueous solubility of 3.5 x 10^{-5} M, KP46 is thought to cross the gastrointestinal epithelium and enter the bloodstream intact [32]. Kinetic studies of KP46 solution in water or in physiologic buffers show that 50 % of the drug is chemically stable for several hours. Calculations based on a plasma model suggest that KP46 may remain intact in the circulation for a while even in the presence of physiologic concentrations of Tf [32]. This is in contrast to gallium maltolate where gallium is found in the circulation bound to Tf after the drug has been absorbed through the gastrointestinal tract [23]. Preclinical studies have shown that the *in vitro* IC_{50} of KP46 is <5 μM in cancer cell lines representative of lung, ovarian, breast, and colon cancers and melanoma [32]. Pharmacokinetic studies of KP46 administered to healthy Swiss mice as a single oral dose established LD_{50} values of KP46 as 2870 mg/kg (410 mg Ga^{3+}) and 2370 mg/kg (339 mg Ga^{3+}/kg) for male and female animals, respectively. A KP46 dose of 62.5 mg/kg/day administered orally for two weeks was established as a well-tolerated dose for animal studies [33]. Gallium distribution in tissues was shown to be highest in bone, followed by the

liver, spleen, and kidneys, respectively [33]. These studies led to further evaluation of KP46 *in vivo* where its antineoplastic activity was demonstrated in a rat tumor model inoculated with Walker carcinosarcoma 256 cells.

The pharmacokinetics and side effects of KP46 were examined in a small Phase 1 study of 7 patients. Single oral dosing schedules of 30 mg/m^2 to 480 mg/m^2 produced peak serum gallium concentrations of 15.3 μg/mL and 62.7 μg/mL, respectively, with corresponding T½ of 53.5 and 121.5 hours, respectively [34]. In this study, 3 of 4 patients with renal cancer who had progressive disease at the time of entry into the study attained stabilization of their tumors. One patient achieved a partial response after the second cycle of treatment. The authors concluded that further Phase 2 studies of KP46 were warranted in renal cancer [34]. However, further clinical trials of KP46 in cancer patients have not been reported to date. Studies are in progress to enhance the oral bioavailability of KP46 using lipiodol emulsions [35]. This approach may improve the gastrointestinal uptake of KP46 and enhance its clinical antitumor activity.

4. CELLULAR HANDLING OF GALLIUM

4.1. Transport and Cellular Uptake

Gallium has no known physiological function in the human body; however, some of its chemical similarities with iron enable it to interact with proteins that transport, store, and utilize iron for a variety of important cellular functions. Hence, an appreciation of iron metabolism is relevant to understanding some of the mechanisms of gallium's antineoplastic activity. Iron in the blood circulates bound to Tf, an 80 kD protein with two iron-binding sites each located at the amino and carboxyl terminals of the molecule. Physiologically, approximately one-third of Tf in the blood is occupied by iron. Thus, Tf may exist in forms that are referred to as apoTf (devoid of iron), monoferric Tf, or diferric Tf. Iron is taken up by cells by the binding of Tf-iron to Tf receptors (TfRs) present on cell surfaces. This receptor-ligand interaction triggers endocytosis of the iron-Tf-TfR complex and its translocation to an acidic endosome in the cytoplasm where ferric iron is released from Tf. ApoTf-TfR cycles back to the cell surface where apoTf is released from the receptor and becomes available to bind iron. Iron exits the endosome through divalent metal transporter1 (DMT1) after it is reduced to iron(II) by a ferrireductase. In the cytoplasm, iron can be found in a putative "pool" from where it travels (presumably bound to low-molecular-weight molecules) to cellular compartments to support the function of a number of iron-containing proteins.

The initial entry of gallium into malignant cells follows steps that are similar to iron. Early studies demonstrated that similar to ^{59}Fe, ^{67}Ga uptake by myeloma cell lines *in vitro* could be enhanced by the addition of exogenous Tf to the culture medium [36]. These similarities between ^{59}Fe and ^{67}Ga uptake suggested that there was a shared transport system for both metals. In support of this was the finding that over 99 % of radiogallium injected into the blood was bound to

Tf while being transported to target sites in the body [37]. Subsequent studies showed that the uptake of ^{67}Ga by HL60 cells *in vitro* and by athymic mice bearing a human malignant melanoma could be inhibited by monoclonal antibodies to the Tf receptor antibody [38, 39]. Thus, the role of Tf and the TfR in ^{67}Ga uptake by malignant cells *in vitro* and *in vivo* is supported by these and a number of other studies. Beyond this though, it should be noted that both iron and gallium may also be taken up by certain cells through mechanisms that are independent of the TfR and that each metal may stimulate the Tf-independent uptake of the other metal. While this may suggest that both metals share the same Tf-independent transport system, it is difficult to reconcile. Tf-independent iron uptake involves the initial reduction of Fe(III) to Fe(II) by a ferrireductase [40]. In contrast, Ga(III) is not readily reduced to Ga(II), suggesting that a different mechanism is involved in its Tf-independent uptake.

The relevance of the Tf-TfR iron transport system to the therapeutic application of non-radioactive gallium compounds becomes obvious when it is considered that approximately one-third of Tf in the blood is physiologically bound to iron. Hence, two thirds of Tf not occupied by iron are available to bind other metals. Harris and Pecoraro have shown that gallium binds with high avidity to Tf, albeit with a binding constant lower than that of iron [41]. These studies indicate that akin to iron, stable, non-radioactive gallium in the blood should bind to Tf and be taken up by cancer cells that express high levels of TfR. However, the extent of gallium binding to Tf is influenced by its aqueous chemistry. Studies by Hacht showed that gallium undergoes hydrolysis to the hydroxides $Ga(OH)_4^-$ and $Ga(OH)_3$ at pH 4, and $Ga(OH)_3$ and $Ga(OH)_{11}^{8-}$ at physiologic pH [2]. At concentrations up to 50 μM, 95 % of gallium in the blood is bound to Tf; however, at higher gallium concentrations in the blood, it's binding to Tf decreases resulting in the formation of $[Ga(OH)_4^-]$ [1]. These Tf and gallium interactions are relevant to the therapeutic application of gallium where the primary objective is to target Tf-Ga complexes to TfRs that are highly expressed on lymphoma, bladder cancer, and other malignancies [42–44]. Thus, the pharmacokinetics of gallium and its antitumor activity and toxicities following a short intravenous administration at high concentrations (as was used in the Phase 1 clinical trials of gallium nitrate) are likely to be different from when it is administered by continuous infusion at a lower dose or by daily oral intake. Though not proven, it is possible that gallium hydroxides rather than Tf-Ga are the primary gallium species in the circulation responsible for some of the toxicities, such as renal dysfunction, encountered with gallium nitrate.

It is relevant to note that cancer cells may be surrounded by areas of inflammation and infection and that ^{67}Ga may concentrate in such non-tumorous sites [45]. In these situations, ^{67}Ga may be found bound to lactoferrin [46], an iron-binding protein present in neutrophils, or be taken up by microorganisms via siderophores secreted by them to acquire iron from the extracellular environment [47]. In addition, malignant cells may produce Tf as an autocrine factor in an attempt to acquire iron for their growth [48, 49]. Tf secreted by such tumors could bind extracellular gallium and further enhance its cellular uptake.

4.2. Intracellular Trafficking

The targeting of Tf-Ga to TfR-bearing cancers and its uptake by TfR-mediated endocytosis is the first step in gallium's antitumor action. Subsequent steps in the intracellular trafficking of gallium are less well understood. Gallium taken up by TfRs appears to locate initially in an acidic endosomal compartment. This is suggested by the observation that blockade of endosomal acidification results in a decrease in the cellular incorporation of ^{67}Ga [50]. Whereas Tf-Fe and Tf-Ga appear to collocate in the same endosome, studies by Illing et al. suggest that in contrast to iron, DMT1 is unlikely to facilitate the transport of gallium out of the endosome [51]. This raises the question as to how gallium transits from the endosome to the cytoplasm. A role for involvement of the lysosome in this process is suggested by early studies which showed that following its injection into rats bearing hepatoma, ^{67}Ga concentrated in microsomes and lysosomes in the tumor cells [52–54].

Other studies demonstrated that ^{67}Ga concentrated in metabolically active tumors and identified a 45 kD gallium-binding protein in rat hepatoma cells [55, 56]. It is possible therefore, that Tf-Ga in the acidic endosome is routed to the lysosome and released from there to the cytoplasm. Further studies will be needed to clarify this matter. Within the cell, gallium can be found in a "pool" presumably bound to low-molecular-weight complexes that transport it to various compartments [57]. The nature of these gallium-binding molecules is not known, but since gallium can form complexes with citrate, nucleotides, and other compounds *in vitro* [58, 59], such molecules are candidates for being intracellular gallium transporters. In an equilibrium dialysis chamber *in vitro,* ATP can transfer ^{67}Ga across membranes from Tf to ferritin, a shell-shaped iron storage protein in cells. This finding lends support to the notion that nucleotides may transport gallium in cells [58]. With regard to ferritin, however, iron entry into the ferritin shell requires reduction of Fe(III) to Fe(II); since gallium is not reduced to Ga(II), it is likely that gallium binds to the external surface of the molecule rather than entering it.

5. ANTINEOPLASTIC MECHANISM OF CLINICALLY USED GALLIUM COMPOUNDS

While many of the mechanisms of antineoplastic activity of the early generation of gallium compounds relate to its interaction with iron-dependent processes, the mechanisms of action of the newer gallium compounds, especially those with more complex ligands, are only partly understood. Early studies showed that gallium nitrate inhibited DNA polymerases, but this effect was insufficient to explain its antitumor activity [60]. Berggren et al. reported that gallium nitrate inhibited tyrosine phosphatase; however, as this could not be linked to its cytotoxicity, it was not considered to be relevant to its mechanism of antitumor activity [61]. These studies were conducted prior to our present knowledge of the

myriad of cell signaling pathways that exist; further studies of the action of gallium on signaling pathways may yield new information. Gallium(III) was also shown to inhibit magnesium-dependent ATPase by competing with Mg(II) [62] and block tubulin polymerization in a cell-free assay [63]; both these actions could contribute to its cytotoxicity.

5.1. Inhibition of Cellular Iron Uptake and Cell Proliferation

Early studies showed that the cellular uptake of ^{59}Fe-Tf and the proliferation of leukemic and other malignant cells *in vitro* could be inhibited by Tf-Ga or gallium nitrate in a dose-dependent manner [64]. This effect of gallium on cellular iron uptake results from competitive inhibition of Tf-Fe binding to TfRs by Tf-Ga and interference with endosomal acidification by Ga; the latter impairs the dissociation of Fe from Tf-Fe [64]. In this way, Tf-Ga produces a state of cellular iron deprivation, which, in turn, diminishes the activity of iron-dependent proteins involved in cell proliferation and viability. In addition, inhibition of cellular iron uptake by Tf-Ga blocks hemoglobin production in murine erythroleukemia cells, an effect that is independent of gallium's action on cell proliferation [65].

The inhibitory effects of Tf-Ga on cellular proliferation and hemoglobin production can be reversed by the addition of Tf-Fe, iron salts, or hemin thus indicating that cellular iron deprivation plays an important role in gallium's mechanisms of action. Consistent with a gallium-induced decrease in cellular iron, HL60 cells incubated with Tf-Ga display an increase in TfR mRNA and protein [66]. Gallium's disruption of cellular iron homeostasis *in vitro* is relevant to its mechanisms of action *in vivo*. Patients treated with gallium nitrate often develop a microcytic hypochromic anemia associated with elevated free erythrocyte protoporphyrin levels; these findings are characteristic of iron-deficiency anemia [67].

5.2. Inhibition of Iron-Dependent Ribonucleotide Reductase

The synthesis for deoxyribonucleoside diphosphates (dNDPs) from ribonucleoside disphosphates (NDPs) depends on the activity of ribonucleotide reductase (RR), a rate-limiting enzyme for DNA synthesis [68–70]. RR is a heterodimer that consists of M1 and M2 subunits that are products of different genes and are expressed during different phases of the cell cycle. The RRM2 subunit increases as cells enter the S-phase [71, 72]; it contains a binuclear iron center and a tyrosyl free radical, both of which are essential for its activity [73]. Since the RRM2 protein has a relatively rapid turn-over with a half-life of 3 hours [72], proliferating cells require a steady supply of iron to maintain the activity of newly synthesized RRM2 and DNA synthesis [74]. The need for iron for RR activity is reflected by the increase in TfRs seen as cells increase their rate of proliferation [75].

Tf-Ga and gallium nitrate have been shown to inhibit the iron-dependent activity of RR through two distinct mechanisms. The first involves inhibition of cellu-

lar iron uptake resulting in insufficient intracellular iron to support RRM2 activity while the second is a direct inhibitory effect of gallium on enzyme activity. In support of the first mechanism are studies that show that human HL60 leukemia cells incubated with Tf-Ga for 6–24 hours displayed a diminution in the RRM2 tyrosyl radical signal on EPR spectroscopy; this was accompanied by a decrease in dNTP pools [76]. These findings are consistent with a loss in RRM2 activity. Gallium-induced loss of the tyrosyl radical signal was abrogated by coincubation of cells with hemin as the source of iron [76]. In other studies, lysates of L1210 leukemia cells incubated with gallium nitrate for 18 hours showed a complete loss of the tyrosyl radical signal on EPR spectroscopy [77]. However, this signal was regenerated to normal levels within 10 minutes by the addition of ferrous ammonium sulfate to the cell lysate [77]. These findings indicate that the loss of RRM2 activity in gallium-treated cells is not due to a decrease in RRM2 protein but rather to the presence of an RRM2 protein that has been rendered functionally inactive by the lack of an iron center (apoR2).

The second mechanism by which gallium inhibits RR is unrelated to its action on cellular iron uptake and involves a direct action of the metal on RR. The direct inhibition of gallium nitrate to the cell-free enzyme assay, inhibited the enzymatic activity of CDP and ADP reductase [78]. Enzyme kinetic analysis indicated that gallium blocked CDP and ADP reductase activity by competitive inhibition of substrate-enzyme interaction [78]. Since nucleosides can bind to gallium [79], the inhibition of RR activity by gallium can likely be explained by the formation of Ga-nucleotides which compete with endogenous ADP or CDP for binding to RR.

5.3. Action on the Mitochondria and Induction of Apoptosis

The ability of gallium to target iron-containing proteins has important implications for its potential to act on iron-sulfur (Fe-S)-containing proteins in the mitochondria. These proteins include aconitase in the citric acid cycle and Fe-S proteins in the mitochondrial electron transport chain (ETC). In lymphoma cells, gallium maltolate was shown to reduce mitochondrial oxygen consumption rate in a dose-dependent manner [26]. Incubation of human leukemic CCRF-CEM with gallium maltolate for 2 hours resulted in an increase in intracellular reactive oxygen species (ROS) which was blocked by mitoquinone, a mitochondria-targeted antioxidant [24]. The latter indicates that ROS produced in gallium-treated cells originates from the mitochondria. Cellular glutathione (GSH) levels decreased within 1 hour of incubation of cells with gallium nitrate, consistent with an increase in oxidative stress [80]. As it is known that chemical inhibition of ETC complexes I, II, or III result in increased production of superoxide in cells, it is reasonable to speculate that the Fe-S-containing proteins of one or more of ETC complexes are likewise disrupted by gallium. However, further research will be needed to define gallium's precise site of action on the mitochondria.

ROS generated by cells exposed to gallium nitrate were shown to trigger an increase in the synthesis of metallothionein-2A and heme oxygenase-1, felt to be

an early cytoprotective response [80]. That this was secondary to ROS was supported by the demonstration that the addition of the antioxidant N-acetyl cysteine (NAC) to cells blocked gallium-induced ROS production and the rise in MT-2A and HO-1 levels. Further evidence that this was a cytoprotective response to gallium was that abrogation of ROS by NAC blocked the increase in MT-2A and HO-1 and enhanced the cytotoxicity of gallium nitrate [80]. MT-2A upregulation secondary to gallium-induced ROS production was associated with a shift in the intracellular zinc pool and an increase of metal transcription factor-1 binding to metal response elements on the promoter region of the metallothionein gene [80, 81]. HO-1 upregulation following gallium-induced ROS production occurred through an increase in phosphorylation of p38 mitogen-activated protein kinase and activation of Nrf-2, a regulator of HO-1 gene transcription [80].

Given that the initial biologic response to gallium nitrate exposure is one of cytoprotection, a model of gallium's mechanism of action emerges in which cell death is triggered only after these cytoprotective responses have been overcome. According to this model, cells with a low capacity to generate a cytoprotective response might be more sensitive to the cytotoxicity of gallium than cells capable of generating a strong protective response. Apoptosis is triggered with the activation of Bax and its translocation to the mitochondria resulting in a loss of mitochondrial membrane potential and the release of cytochrome *c* from the mitochondria to the cytoplasm. The latter step leads to downstream activation of executioner caspases and apoptotic cell death.

With regard to KP46, recent studies have broadened our understanding of the antineoplastic mechanisms of this gallium compound. Using a panel of cell lines with wild-type, null, or mutant p53, Gogna et al. showed that KP46 induced intracellular calcium release; this generated ROS and triggered both p53-dependent apoptosis through the intrinsic mitochondrial pathway and p53-dependent apoptosis through the extrinsic FAS-mediated pathway [82]. KP-46 induced calcium release stabilized the p53-p300 complex resulting in increased p53 gene expression with downstream activation of pro-apoptotic genes. In their studies, MCF-7 and HepG2 cell lines with wild-type p53 were more sensitive to KP46 than cell lines with mutant or null p53 (PC3 and H1299 cells, respectively) [82]. The impact of p53 on the cytotoxicity of KP46 can be contrasted with other studies which showed that the p53 mutant WTK1 lymphoma cell line was resistant to growth inhibition by gallium nitrate but was not resistant to growth inhibition by gallium maltolate [24]. This illustrates that gallium compounds differ in their spectrum and mechanisms of antineoplastic activity. Whereas KP46-induced Bax activation results from changes in calcium signaling, it needs to be determined whether a similar sequence of events occurs with the activation of Bax by gallium nitrate and gallium maltolate.

5.4. Action of Tris(8-quinolinolato)gallium(III) on the Cytoskeleton

Recent studies by Jungwirth et al. showed that the mechanisms of KP46-induced cell death in colon and lung cancer cells included alterations in cytoskeletal pro-

teins involved in cell adhesion and contraction [83]. These changes in cells occurred within 24 hours of incubation with KP46 and were different from classic p53-dependent, caspase-mediated cell death. The investigators showed that within 6 hours of exposure to KP46, cells displayed a downregulation of integrin-β1 and its focal adhesion-specific binding partner talin. It was suggested that the non-lysosomal protease calpain played a role in mediating these effects since the calpain inhibitor PD150606 diminished KP46-mediated integrin destabilization and the induction of cell death [83]. These *in vitro* findings were confirmed in a human colon cancer xenograft model in SCID mice, where KP46 reduced tumor growth and membrane localization of integrin-β1 was shown to be reduced in the viable tumor remaining after KP46 treatment [83].

6. GALLIUM COMPOUNDS IN PRECLINICAL DEVELOPMENT

In addition to the gallium compounds described above, a number of gallium complexes with preclinical antitumor activity have been reported. These agents remain to be further investigated to determine whether they have potential for evaluation in clinic trials.

6.1. Gallium Pyridine and Gallium Phenolate

Gallium complexes with 2-methyl-pyridine and 2-methyl-phenolate groups attached to a secondary amine are of particular interest as some of them have displayed *in vivo* antitumor activity in a rodent model. Shakya et al. [84] synthesized 5 novel gallium(III) complexes described as $[Ga^{III}(Lx)^{2-}]ClO_4$, where Lx is a negatively-charged ligand containing 2-methylpyridine and 2-methylphenolate groups attached to a secondary amine [84]. The phenol moiety of these complexes has substituents (X) that encompass the electron-withdrawing and electron-donating methoxy (complex 1), nitro (complex 2), chloro (complex 3), bromo (complex 4), and iodo (complex 5) groups [84]. Whereas complex 1 displayed an IC_{50} of 245.4 μM in BE(2)-C neuroblastoma cells *in vitro,* complexes 2–5 displayed the greatest apoptosis-inducing activity (IC_{50} 13.3–23.8 μM) [84]. Chen et al. demonstrated that these complexes had antineoplastic activity in prostate cancer cell lines *in vitro* and in human prostate cancer xenografts in a rodent tumor model *in vivo* [85]. The greatest level of apoptosis in PC-3 prostate cell lines *in vitro* was induced by complex 5 which also inhibited the growth of PC-3 prostate cancer cell xenografts in nude mice by 66 % [85]. Tumor extracts from mice treated with complex 5 showed an increase in ubiquitinated proteins, an accumulation of p27 (a proteasomal target protein), a decrease in proteasomal chymotrypsin activity, and an induction of apoptosis [85]. Thus, these gallium complexes displayed a novel mechanism of action that has potential clinical application since other proteasome inhibitor drugs are being used in the clinic for the treatment of hematologic malignancies.

6.2. Gallium Thiosemicarbazones

Early studies demonstrated that many α-*(N)*-heterocyclic carboxaldehyde thiosemicarbazones are capable of chelating metals and have significant antitumor activity [86]. The iron complexes of these thiosemicarbazones are 3- to 6-fold more potent than the free ligand in inhibiting ribonucleotide reductase [87]. The synthesis of gallium(III) complexes of different 2-acetylpyridine thiosemicarbazones was reported by Kratz et al. [88]; while others demonstrated the antitumor activity of gallium complexes with 2-acetylpyridine ^{4}N-dimethylthiosemicarbazone in SW480 (colon adenocarcinoma), SK-B-3 (breast adenocarcinoma), and 41-M (ovarian cancer) cell lines *in vitro* [89]. The coordination of gallium to 2-pyridineformamide thiosemicarbazones greatly increased their ability to induce apoptosis in glioblastoma cell lines *in vitro* [90]. In these studies, the coordination of gallium to these thiosemicarbazones increased their cytotoxicity by 15- to 37-fold in RT2 glioblastoma cells with wild-type p53 and by 7- to 36-fold in T98 glioblastoma cells with mutant p53.

The thiosemicarbazone 3-aminopyridine-2-carboxyaldehyde thiosemicarbazone (3-AP, Triapine) has been in Phase 1 and 2 clinical trials [91]; it has been shown to enhance the response to radiation therapy in cervical cancer [92]. The ability of gallium to potentiate the anti-proliferative action of 3-AP was shown in studies that compared the effects of iron and gallium complexes of 3-AP on ribonucleotide reductase and tumor cell proliferation *in vitro* and demonstrated that the cytotoxicity of this thiosemicarbazone was enhanced by gallium but weakened by iron [93].

6.3. Gallium-Pyridoxal Isonicotinyl Hydrazone

Pyridoxal isonicotinyl hydrazone (PIH) and its analogues are lipophilic iron chelators that can inhibit the proliferation of a variety of malignant cells *in vitro* [94, 95]. Importantly, PIH can also deliver iron to cells to support cell growth and function [96] and can thus bind and transport gallium into cells. Ga-PIH enters cells by a transferrin-independent route and displays greater cytotoxicity than PIH alone [94, 97, 98].

6.4. Gallium Complexes with Azole Ligands

The synthesis of gallium complexes of 2,1,3-benzothiadiazole, 1,2,3-benzotriazole, and 1-methyl-4,5-diphenylimidazole has been described by Zanias et al. [99]. These compounds inhibit the proliferation of breast, ovarian, cervical, and colon tumor cell lines *in vitro* [99].

6.5. Bi- and Tetranuclear Gallium(III) Complexes with Heterocyclic Thiolato Ligands and Dinuclear Gallium Carboxylate Complexes

A variety of these complexes have been reported to display cytotoxicity against solid tumor cell lines *in vitro* [100, 101]. The gallium thiolato ligand complexes were shown to bind to fish sperm DNA and display greater cytotoxicity in malignant cell lines than in fibroblast cells [101].

6.6. Gallium-Corroles

Gallium forms complexes with corroles; the latter are macrocyclic molecules related to porphyrins and other aromatic macrocycles [102]. The derivatives of gallium(III) tris(pentafluorophenyl)corrole, 1[Gatpfc)], with sulfonic or carboxylic acids have shown high cytotoxicity in the NCI60 panel of solid tumor cell lines which include melanoma, breast, ovarian, and prostate cancers [103]. Gallium-corroles are taken up rapidly by cells and emit intense fluorescence which enables them to be tracked in cells by confocal microscopy [103]. I*n vitro* studies with these gallium-containing agents show promise and further evaluation of their antineoplastic activity in relevant animal tumor models is awaited.

7. SUMMARY AND OUTLOOK

The antineoplastic activity of gallium nitrate was recognized over 3 decades ago and several clinical trials have confirmed its activity in patients with lymphoma and bladder cancer. Since then, new generations of gallium-containing agents have emerged that show promise in preclinical studies. The ability of gallium to disrupt critical iron-dependent processes in malignant cells distinguishes its mechanisms of action from that of other drugs. This makes gallium-based agents effective against tumors that have developed resistance to conventional therapies.

The newer gallium agents display greater efficacy and a broader spectrum of antitumor activity than the older gallium nitrate. Importantly, the development of gallium formulations such as gallium maltolate and KP46 that have oral bioavailability has been an important advance in gallium therapeutics; these preparations are more acceptable to patients than formulations that must be administered by the parenteral route. Several other novel gallium-ligands in early preclinical development have been reported. For these agents to be advanced to the clinic, they need further evaluation of their antitumor efficacy and toxicity in animal tumor models.

Future directions in this field should also focus on understanding the intracellular pathways targeted by gallium compounds. Knowledge of tumor markers (proteins or genetic mutations) that predict tumor sensitivity or resistance to

gallium compounds would have important clinical application since it would help to identify patients likely to respond to treatment with these drugs.

ACKNOWLEDGMENTS

This work was supported by a grant from the Greater Milwaukee Foundation and by the Thomas A. and Lorraine M. Rosenberg Award for Translational Cancer Research from the Froedtert Hospital Foundation and the Medical College of Wisconsin Cancer Center.

ABBREVIATIONS

ADP	adenosine 5′-diphosphate
ATP	adenosine 5′-triphosphate
CDP	cytidine 5′-diphosphate
DMT-1	divalent metal transporter 1
dNTP	2-deoxynucleoside 5′-triphosphate
ETC	electron transport chain
FAS	apoptosis stimulating fragment
HO-1	heme oxygenase 1
IC_{50}	half maximal inhibitory concentration
KP46/FFC11	tris(8-quinolinato)gallium(III)
MT-2A	metallothionein-2A
ROS	reactive oxygen species
RR	ribonucleotide reductase
Tf	transferrin
TfR	transferrin receptor

REFERENCES

1. L. R. Bernstein, *Pharmacol. Rev.* **1998**, *50*, 665–682.
2. B. Hacht, *Bull. Korean Chem. Soc.* **2008**, *29*, 372–376.
3. C. B. J. Levadidti, V. Tchertkoff, A. Vaisman. *C. R. Hebd. Seances Acad. Sci. Se. D. S. Di. Sci. Nat.* **1931**, *192*, 1142–1143.
4. D. Front, R. Bar-Shalom, R. Epelbaum, N. Haim, M. W. Ben-Arush, M. Ben-Shahar, M. Gorenberg, U. Kleinhaus, S. Parmett, G. M. Kolodny, O. Israel, *J. Nucl. Med.* **1993**, *34*, 2101–2104.
5. M. U. Khan, S. Khan, S. El-Refaie, Z. Win, D. Rubello, A. Al-Nahhas, *Eur. J. Surg. Oncol.* **2009**, *35*, 561–567.
6. A. Al-Nahhas, Z. Win, T. Szyszko, A. Singh, C. Nanni, S. Fanti, D. Rubello, *Anticancer Res.* **2007**, *27*, 4087–4094.
7. M. M. Hart, R. H. Adamson, *Proc. Natl. Acad. Sci. USA* **1971**, *68*, 1623–1626.
8. P. Collery, H. Millart, D. Lamiable, R. Vistelle, P. Rinjard, G. Tran, B. Gourdier, C. Cossart, J. C. Bouana, C. Pechery, J. C. Etienne, H. Choisy, J. M. Dubois de Montreynaud, *Anticancer Res.* **1989**, *9*, 353–356.

9. P. Collery, M. Morel, B. Desoize, H. Millart, D. Perdu, A. Prevost, H. Vallerand, C. Pechery, H. Choisy, J. C. Etienne, *Anticancer Res.* **1991**, *11*, 1529–1532.
10. B. J. Foster, K. Clagett-Carr, D. Hoth, B. Leyland-Jones, *Cancer Treat. Rep.* **1988**, *70*, 1311–1319.
11. D. J. Straus, *Semin. Oncol.* **2003**, *30*, 25–33.
12. P. A. Todd, A. Fitton, *Drugs* **1991**, *42*, 261–273.
13. L. Einhorn. *Semin. Oncol.* **2003**, *30*, 34–41.
14. C. R. Chitambar, *Expert. Opin. Investig. Drugs* **2004**, *13*, 531–541.
15. C. R. Chitambar, *Curr. Opin. Oncol.* **2004**, *16*, 547–552.
16. D. P. Kelsen, N. Alcock, S. Yeh, J. Brown, C. Young, *Cancer* **1980**, *46*, 2009–2013.
17. I. H. Krakoff, R. A. Newman, R. S. Goldberg, *Cancer* **1979**, *44*, 1722–1727.
18. R. P. Warrell, Jr., C. J. Coonley, D. J. Straus, C. W. Young, *Cancer* **1983**, *51*, 1982–1987.
19. L. R. Bernstein, T. Tanner, C. Godfrey, B. Noll, *Metal-Based Drugs* **2000**, *7*, 33–47.
20. S. M. Kelsey, D. R. Blake, R. C. Hider, C. N. Gutteridge, A. C. Newland, *Clin. Lab Haematol.* **1989**, *11*, 287–288.
21. C. Gasche, T. Ahmad, Z. Tulassay, D. C. Baumgart, B. Bokemeyer, C. Buning, S. Howaldt, A. Stallmach, *Inflamm. Bowel. Dis.* **2015**, *21*, 579–588.
22. J. M. Piepmeier, N. Rabidou, S. C. Schold, Jr., A. J. Bitonti, N. J. Prakash, T. L. Bush, *Cancer Res.* **1996**, *56*, 359–361.
23. K. P. Allamneni, R. B. Burns, D. J. Gray, F. H. Valone, L. R. Bucalo, S. P. Sreedharan, *Proc. Am. Assoc. Cancer Res.* **2004**, 45:230 (abstract 1013).
24. C. R. Chitambar, D. P. Purpi, J. Woodliff, M. Yang, J. P. Wereley, *J. Pharmacol. Exp. Ther.* **2007**, *322*, 1228–1236.
25. M. S. Chua, L. R. Bernstein, R. Li, S. K. So, *Anticancer Res.* **2006**, *26*, 1739–1743.
26. X. Wu, T. W. Wang, G. M. Lessmann, J. Saleh, X. Liu, C. R. Chitambar, S. T. Hwang, *J. Invest Dermatol.* **2014**, *135*, 877–844.
27. M. Al-Gizawiy, J. P. Wereley, K. M. Schmaind, C. R. Chitambar, *Neuro Oncol.* **2016**, *18,* vi63–vi64 (Abstr.).
28. L. R. Bernstein, J. J. M. van der Hoeven, R. O. Boer, *Anti-cancer Agents Med. Chem.* **2011**, *11*, 585–590.
29. A. Rangel-Vega, L. R. Bernstein, E. A. Mandujano-Tinoco, S. J. Garcia-Contreras, R. Garcia-Contreras, *Front Microbiol.* **2015**, *6*, 282.
30. A. B. Kelson, M. Carnevali, V. Truong-Le, *Curr. Opin. Pharmacol.* **2013**, *13*, 707–716.
31. P. Collery, M. A. Jakupec, B. Kynast, B. K. Keppler, *Preclinical and Early Clinical Development of the Oral Gallium Complex KP46 (FFC11)*, in *Metal Ions in Biology and Medicine*, Eds M. C. Alpoim, P. V. Morais, M. A. Santos, L. Cristovao, J. A. Centeno, P. Collery, John Libbey Eurotext, Paris, 2006, 9:521–524.
32. A. R. Timerbaev, *Metallomics.* **2009**, *1*, 193–198.
33. P. Collery, J. L. Domingo, B. K. Keppler, *Anticancer Res.* **1996**, *16*, 687–692.
34. R. D. Hofheinz, C. Dittrich, M. A. Jakupec, A. Drescher, U. Jaehde, M. Gneist, K. N. Graf von Keyserlingk, B. K. Keppler, A. Hochhaus, *Int. J. Clin. Pharmacol. Ther.* **2005**, *43*, 590–591.
35. B. C. Losantos, I. Pashkunova-Martic, N. Kandler, B. Keppler. *Curr. Drug Deliv.* **2016**,
36. A. W. Harris, R. G. Sephton, *Cancer Res.* **1977**, *37*, 3634–3638.
37. S. R. Vallabhajosula, J. F. Harwig, J. K. Siemsen, W. Wolf, *J. Nucl. Med.* **1980**, *21*, 650–656.
38. C. R. Chitambar, Z. Zivkovic, *Cancer Res.* **1987**, *47*, 3929–3934.
39. S. M. Chan, P. B. Hoffer, P. Duray, *J. Nucl. Med.* **1987**, *28*, 1303–1307.

40. R. S. Inman, M. M. Coughlin, M. Wessling-Resnick, *Biochemistry* **1994**, *33*, 11850–11857.
41. W. R. Harris, V. L. Pecoraro, *Biochemistry* **1983**, *22*, 292–299.
42. K. C. Gatter, G. Brown, I. S. Trowbridge, R. E. Woolston, D. Y. Mason. *J. Clin. Pathol.* **1983**, *36*, 539–545.
43. F. Nejmeddine, M. Raphael, A. Martin, G. Le Roux, J. L. Moretti, N. Caillat-Vigneron, *J. Nucl. Med.* **1999**, *40*, 40–45.
44. I. Basar, A. Ayhan, K. Bircan, A. Ergen, C. Tasar, *Br. J. Urol.* **1991**, *67*, 165–168.
45. C. J. Palestro, *Semin. Nucl. Med.* **1994**, *24*, 128–141.
46. W. R. Harris, *Biochemistry* **1986**, *25*, 803–808.
47. R. Saha, N. Saha, R. S. Donofrio, L. L. Bestervelt, *J. Basic Microbiol.* **2013**, *53*, 303–317.
48. H. Tanoguchi, M. Tachibana, M. Murai, *Br. J. Cancer* **1997**, *76*, 1262–1270.
49. L. E. Shapiro, N. Wagner, *In Vitro Cell Dev. Biol.* **1989**, *25*, 650–654.
50. C. R. Chitambar, Z. Zivkovic-Gilgenbach, *Cancer Res.* **1990**, *50*, 1484–1487.
51. A. C. Illing, A. Shawki, C. L. Cunningham, B. Mackenzie, *J. Biol. Chem.* **2012**, *287*, 30485–30496.
52. E. Aulbert, U. Haubold, *Nucl. Med.* **1974**, *13*, 72–84.
53. P. A. G. Hammersley, M. N. Cauchi, D. M. Taylor, *Cancer Res.* **1975**, *35*, ll54–ll58.
54. D. H. Brown, B. L. Byrd, J. E. Carlton, D. C. Swartzendruber, R. L. Hayes, *Cancer Res.* **1976**, *36*, 956–963.
55. R. L. Hayes, J. E. Carlton, *Cancer Res.* **1973**, *33*, 3265–3272.
56. D. Lawless, D. H. Brown, K. F. Hubner, S. P. Colyer, J. E. Carlton, R. L. Hayes, *Cancer Res.* **1978**, *34*, 4440–4444.
57. N. P. Davies, Y. S. Rahmanto, C. R. Chitambar, D. R. Richardson, *J. Pharmacol. Exp. Ther.* **2006**, *317*, 153–162.
58. R. E. Weiner, G. J. Schreiber, P. B. Hoffer, *J. Nucl. Med.* **1983**, *24*, 608–614.
59. A. W. Harris, A. E. Martell, *Inorg. Chem.* **1976**, *15*, 713–720.
60. T. P. Waalkes, K. Sanders, R. G. Smith, R. H. Adamson, *Cancer Res.* **1974**, *34*, 385–391.
61. M. M. Berggren, L. A. Burns, R. T. Abraham, G. Powis, *Cancer Res.* **1993**, *53*, 1862–1866.
62. L. J. Anghileri, J. Robert, *Magnesium-Bulletin* **1982**, *2*, 197–200.
63. E. M. Perchellet, J. B. Ladesich, P. Collery, J. P. Perchellet, *Anticancer Drugs* **1999**, *10*, 477–488.
64. C. R. Chitambar, P. A. Seligman, *J. Clin. Invest.* **1986**, *78*, 1538–1546.
65. C. R. Chitambar, Z. Zivkovic, *Blood* **1987**, *69*, 144–149.
66. R. U. Haq, C. R. Chitambar, *Biochem. J.* **1993**, *294*, 873–877.
67. P. A. Seligman, E. D. Crawford, *J. Natl. Cancer Inst.* **1991**, *83*, 1582–1584.
68. L. Thelander, P. Reichard, *Ann. Rev. Biochem.* **1979**, *48*, 133–158.
69. J. G. Cory, *Role of Ribonucleotide Reductase in Cell Division*, in *Inhibitors of Ribonucleoside Diphosphate Reductase Activity*, Eds J. G. Cory, A. H. Cory, Pergamon Press, New York, 1989, 1–16.
70. Y. Aye, M. Li, M. J. Long, R. S. Weiss, *Oncogene* **2014**, *34*, 2011–2021.
71. Y. Engstrom, S. Eriksson, I. Jildevik, S. Skog, L. Thelander, B. Tribukait, *J. Biol. Chem.* **1985**, *260*, 9114–9116.
72. S. Eriksson, A. Gräslund, S. Skog, L. Thelander, B. Tribukait, *J. Biol. Chem.* **1984**, *259*, 11695–11700.
73. A. Gräslund, M. Sahlin, B.-M. Sjöberg, *Environ. Health Perspect.* **1985**, *64*, 139–149.
74. S. Nyholm, G. J. Mann, A. G. Johansson, R. J. Bergeron, A. Gräslund, L. Thelander, *J. Biol. Chem.* **1993**, *268*, 26200–26205.

75. E. Pelosi, U. Testa, F. Louache, P. Thomopoulos, G. Salvo, P. Samoggia, C. Peschle, *J. Biol. Chem.* **1986**, *261*, 3036–3042.
76. C. R. Chitambar, W. G. Matthaeus, W. E. Antholine, K. Graff, W. J. O'Brien, *Blood* **1988**, *72*, 1930–1936.
77. J. Narasimhan, W. E. Antholine, C. R. Chitambar, *Biochem. Pharmacol.* **1992**, *44*, 2403–2408.
78. C. R. Chitambar, J. Narasimhan, J. Guy, D. S. Sem, W. J. O'Brien, *Cancer Res.* **1991**, *51*, 6199–6201.
79. L. G. Marzilli, B. de Castro, J. P. Caradonna, R. C. Stewart, C. P. Van Vuuren, *J. Am. Chem. Soc.* **1980**, *102*, 916–924.
80. M. Yang, C. R. Chitambar, *Free Radic. Biol. Med.* **2008**, *45*, 763–772.
81. M. Yang, S. H. Kroft, C. R. Chitambar, *Mol. Cancer Ther.* **2007**, *6*, 633–643.
82. R. Gogna, E. Madan, B. Keppler, U. Pati, *Br. J. Pharmacol.* **2012**, *166*, 617–636.
83. U. Jungwirth, J. Gojo, T. Tuder, G. Walko, M. Holcmann, T. Schofl, K. Nowikovsky, N. Wilfinger, S. Schoonhoven, C. R. Kowol, R. Lemmens-Gruber, P. Heffeter, B. K. Keppler, W. Berger, *Mol. Cancer Ther.* **2014**, *13*, 2436–2449.
84. R. Shakya, F. Peng, J. Liu, M. J. Heeg, C. N. Verani, *Inorg. Chem.* **2006**, *45*, 6263–6268.
85. D. Chen, M. Frezza, R. Shakya, Q. C. Cui, V. Milacic, C. N. Verani, Q. P. Dou, *Cancer Res.* **2007**, *67*, 9258–9265.
86. E. C. Moore, A. C. Sartorelli, *The Inhibition of Ribonucleotide Reductase by a-(N)-Heterocyclic Carboxaldehyde Thiosemicarbazones*, in *Inhibitors of Ribonucleoside Diphosphate Reductase Activity*, Eds J. G. Cory, A. H. Cory, Pergamon Press, New York, 1989, 203–215.
87. L. A. Saryan, E. Ankel, C. Krishnamurti, D. H. Petering, H. Elford, *J. Med. Chem.* **1979**, *22*, 1218–1221.
88. F. Kratz, B. Nuber, J. Weis, B. K. Keppler, *Synth. React. Inorg. Met.-Org. Chem.* **1991**, *21*, 1601–1615.
89. V. B. Arion, M. A. Jakupec, M. Galanski, P. Unfried, B. K. Keppler, *J. Inorg. Biochem.* **2002**, *91*, 298–305.
90. I. C. Mendes, M. A. Soares, R. G. Dos Santos, C. Pinheiro, H. Beraldo, *Eur. J. Med. Chem.* **2009**, *44*, 1870–1877.
91. J. Murren, M. Modiano, C. Clairmont, P. Lambert, N. Savaraj, T. Doyle, M. Sznol, *Clin. Cancer Res.* **2003**, *9*, 4092–4100.
92. C. A. Kunos, S. Waggoner, V. von Gruenigen, E. Eldermire, J. Pink, A. Dowlati, T. J. Kinsella, *Clin. Cancer Res.* **2010**, *16*, 1298–1306.
93. C. R. Kowol, R. Berger, R. Eichinger, A. Roller, M. A. Jakupec, P. P. Schmidt, V. B. Arion, B. K. Keppler, *J. Med. Chem.* **2007**, *50*, 1254–1265.
94. D. R. Richardson, E. H. Tran, P. Ponka, *Blood* **1995**, *86*, 4295–4306.
95. D. R. Richardson, K. Milnes, *Blood* **1997**, *89*, 3025–3038.
96. W. Landschulz, I. Thesleff, P. Ekblom, *J. Cell Biol.* **1984**, *98*, 596–601.
97. G. M. Knorr, C. R. Chitambar, *Anticancer Res.* **1998**, *18*, 1733–1738.
98. C. R. Chitambar, P. Boon, J. P. Wereley, *Clin. Cancer Res.* **1996**, *2*, 1009–1015.
99. S. Zanias, G. S. Papaefstathiou, C. P. Raptopoulou, K. T. Papazisis, V. Vala, D. Zambouli, A. H. Kortsaris, D. A. Kyriakidis, T. F. Zafiropoulos, *Bioinorg. Chem. Appl.* 2010, *2010*, pii: 168030. doi: 10.1155/*2010*/168030.
100. M. R. Kaluderovic, S. Gomez-Ruiz, B. Gallego, E. Hey-Hawkins, R. Paschke, G. N. Kaluderovic, *Eur. J. Med. Chem.* **2010**, *45*, 519–525.
101. B. Gallego, M. R. Kaluderovic, H. Kommera, R. Paschke, E. Hey-Hawkins, T. W. Remmerbach, G. N. Kaluderovic, S. Gomez-Ruiz, *Invest. New Drugs* **2011**, *29*, 932–944.

102. J. Bendix, I. J. Dmochowski, H. B. Gray, A. Mahammed, L. Simkhovich, Z. Gross, *Angew. Chem. Int. Ed Engl.* **2000**, *39*, 4048–4051.
103. M. Pribisko, J. Palmer, R. H. Grubbs, H. B. Gray, J. Termini, P. Lim, *Proc. Natl. Acad. Sci. USA* **2016**, *113*, E2258–E2266.

11

Non-covalent Metallo-Drugs: Using Shape to Target DNA and RNA Junctions and Other Nucleic Acid Structures

Lucia Cardo and Michael J. Hannon

School of Chemistry, University of Birmingham, Edgbaston, Birmingham, B15 2TT, UK
<l.cardo@bham.ac.uk>
<m.j.hannon@bham.ac.uk>

Dedicated to the late Professor Mark Rodger, colleague, collaborator and friend: a gentle man and a fine intellect.

ABSTRACT 304
1. INTRODUCTION 304
2. METALLO-CYLINDERS 304
   2.1. Design and Binding to Polymeric DNAs 304
   2.2. Three-Way Junction DNA Binding 306
   2.3. Recognition of RNA Structures 308
   2.4. Binding to Forks and Bulges 308
   2.5. Binding to Tetraplex DNAs 309
   2.6. Biological Effects of Cylinders 309
3. OTHER SUPRAMOLECULAR DESIGNS AND THEIR TARGETS 310
   3.1. Mononuclear Agents 310
   3.2. Flexicates 312
   3.3. Other Helicates and Dinuclear Supramolecular Complexes 315
   3.4. Squares, Boxes, and Cubes Targeting G-Quadruplex 317
4. CONCLUDING REMARKS AND FUTURE DIRECTIONS 319
ACKNOWLEDGMENTS 320
ABBREVIATIONS AND DEFINITIONS 320
REFERENCES 321

Metal Ions in Life Sciences, Volume 18 Edited by Astrid Sigel, Helmut Sigel, Eva Freisinger, and Roland K. O. Sigel

https://doi.org/10.1515/9783110470734-011

Met. Ions Life Sci. **2018**, *18*, 303–324

Abstract: The most effective class of anticancer drugs in clinical use are the platins which act by binding to duplex B-DNA. Yet duplex DNA is not DNA in its active form, and many other structures are formed in cells; for example, Y-shaped fork structures are involved in DNA replication and transcription and 4-way junctions with DNA repair. In this chapter we explore how large, cationic metallo-supramolecular structures can be used to bind to these less common, yet active, nucleic acid structures.

Keywords: DNA/RNA non-covalent recognition · helicates · metallo-supramolecular chemistry · nucleic acid junctions · unusual nucleic acids

1. INTRODUCTION

In the 1960s three important modes of binding to duplex DNA were characterized: metal coordination to heteroatoms in the DNA bases; intercalation of planar aromatics between the base pairs; and minor groove binding by crescent shaped molecules [1–4]. These gave rise to the potent anticancer drugs cisplatin [2] and doxorubicin [5], which have been crucial in curing patients since the 1970s. Minor groove DNA binders are used as antiviral, antiparasitic, and anticancer agents [4].

The Watson-Crick DNA duplex, which is the target of these drugs, is the most common form of DNA inside humans, but many other structures are present including 3- and 4-way junctions, tetraplexes, left-handed Z-DNA, i-motifs, and forks. These structures are often found during DNA processing or modification, in small amounts but with very different structures from B-DNA. Binding them could achieve DNA specificity through structure recognition as opposed to the traditional approach of seeking sequence specificity. In this review we explore binding to such less common DNA structures, in particular by metallo-supramolecular compounds.

2. METALLO-CYLINDERS

2.1. Design and Binding to Polymeric DNAs

At the center of investigations into DNA recognition by supramolecular drugs have been the cylinder compounds developed in our laboratory. The cylinders are dinuclear triple-helical compounds which are prepared in a single pot from commercial reagents; a pyridyl-aldehyde, a diamine, and an octahedral metal (usually iron(II)) (Figure 1) [6]. Three ligand strands wrap around two metals, resulting in a roughly cylindrical tetracation approximately 2 nm in length and 1 nm in diameter. As a triple helical metal complex it follows on from the innovative work of early supramolecular chemists Lehn [7, 8] and Sauvage [9], Constable [10], and Williams [11]. The cylinders can be prepared quickly (compared to previous designs), and thus attention can turn to their properties, not just their preparation.

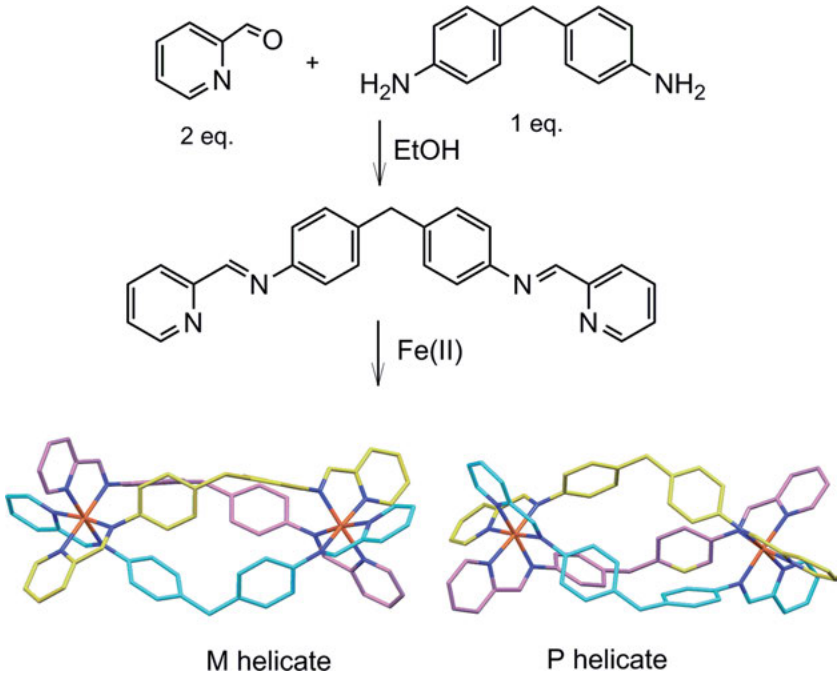

Figure 1. Preparation of a triple-helical metallo-supramolecular cylinder [6], obtained as a racemic mixture of M (left handed, CSD JETVIO) and P (right handed, CSD NITBIB) enantiomers.

The cylinders also differ from earlier helicates in another way. The Lehn and Sauvage helicate systems comprise bipyridine ligands linked by flexible alkyl or alkylether chains and these introduce flexibility (or floppiness) into the helical structure. By contrast in the cylinder, the rings of the diphenylmethane 'spacer' are face-edge π-stacked onto the rings in the other strands (two groups of three rings) and this imparts a stiffness right along the length of the structure. The term 'cylinder' serves to highlight this feature though the compounds are also formally 'triple-helicates'.

As a tetracation, some interaction with DNA (even just an electrostatic charge quenching) is anticipated and indeed Schoentjes and Lehn [12], had explored their copper(I) double-helicates (created from bipyridines linked by alkylethers) and shown an interaction with plasmid DNA in gel electrophoresis and inhibition of some restriction enzymes. What was intriguing about the cylinder was that the size and shape is similar to a peptide alpha-helix and that structure is frequently used by proteins to bind the DNA major groove (e.g., zinc fingers). While many zinc fingers span 3–4 base pairs, the cylinder is slightly longer and should stretch across 5 base pairs.

The 'parent' iron(II) cylinder has excellent water solubility and binds strongly to calf thymus DNA, displacing other DNA binders such as ethidium bromide and Hoechst [13, 14]. Its binding constant is greater than 10^7 M^{-1} at 20 mM

sodium chloride. The circular dichroism spectrum shows that a B-DNA conformation is retained. Flow linear dichroism and AFM show that the cylinder causes dramatic intramolecular coiling, winding the DNA into ball-like structures [14]. The AFM images imply that the coiling seems to start at an end of DNA [14]. By contrast, traditional polyamine condensation of DNA creates very different looped structures. The linear dichroism also reveals that the cylinder is orientated on the DNA, with insertion or intercalation precluded and groove binding most likely.

Helicates are inherently chiral because of their twisting: the M enantiomer ($\Lambda\Lambda$ at the metal centers) is a left-handed helix and the P enantiomer ($\Delta\Delta$) is right handed. The two enantiomers are separated on cellulose columns eluting with aqueous sodium chloride solution [15, 16]. The surface of cellulose is known to have chiral grooves, where the M enantiomer binds less strongly and elutes first. Both enantiomers bind strongly and coil DNA, and are oriented similarly on the DNA, however, the M enantiomer coils more aggressively [17]. Both enantiomers also unwind DNA, with the M enantiomer again having a greater effect [18, 19] and footprinting studies imply some preference for alternating purine-pyrimidine sequences [18].

The cylinder structure can be readily modified. Methyl groups at the ends of the cylinder (at the 5-pyridyl position) have only minor effects on the DNA binding and coiling, but if they point out of the cylinder (from the 3-pyridyl position) they reduce the DNA coiling [20]. This implies that the cylinder binds DNA through its body and sides not its ends. Molecular dynamics simulations also show this with the cylinder lying in the major groove and then partially pushed out when methyls are added at the 3-pyridyl position [21, 22]. Replacing the central CH_2 group with an S or O atom does not change the cylinder structure, DNA affinity or coiling ability [23]. Similarly, changing the central metal has little effect and the iron(II), nickel(II), and ruthenium(II) cylinders have analogous DNA binding [24, 25]. The ruthenium cylinders can photo-cleave DNA by a singlet oxygen mechanism (UV or visible light). The single strand breaks are formed within alternating purine-pyrimidine tracts reflecting observations that the iron cylinder binds at such tracts [25]. These changes show that the external shape and size of the cylinder is key to its binding.

Introducing three Gly-Gly-Ser tripeptides to each end of the cylinder makes it a longer structure and this reduces the DNA coiling [26]. Introducing arginines at the ends increases the charge but also controls the cylinder helicity: the L-arginine induces P helicity while D-arginine induces M [27]. The D-arg (M) cylinder is the more aggressive coiling agent but despite its higher charge, does not coil more aggressively than the unsubstituted cylinder [28].

2.2. Three-Way Junction DNA Binding

Crystallization of the cylinder with a DNA hexamer revealed an unexpected binding mode. The cylinder is not in the groove of a duplex DNA but rather is bound to the heart of a DNA 3-way junction [29]. The 6 DNA bases (3 pairs) at the

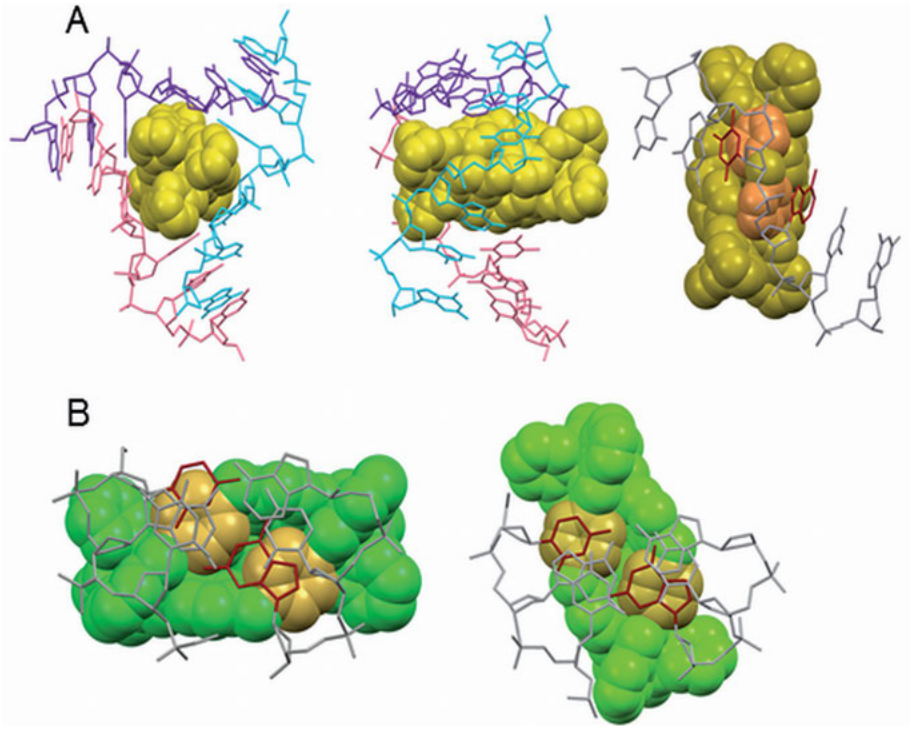

Figure 2. (**A**) End and side views of the cylinder bound at the heart of a DNA 3-way junction, together with a view showing how the DNA bases (A and T) stack onto the phenylene rings (PDB 2ET0) [29]. (**B**) Views of M (left) and P (right) cylinder stacking onto the ends of duplexes, highlighting how the DNA bases (G and C) stack onto the phenylene rings (PDB 3I1D) [30].

junction point are π-stacked onto the 6 phenylene rings of the central core of the cylinder (Figure 2). In the different crystal structures obtained, the M enantiomer is always the one in this junction [29, 30]. The cylinder's structure is the same as that when it is crystallized in the absence of DNA [6, 16, 29] and the DNA structure closely resembles the structure of a DNA 3-way junction (3WJ) in complex with a protein. They seem to be perfectly complementary structures.

The self-complementary palindromic DNA used can potentially form any 'n'-way junction structure (duplex, 3-way, 4-way, 5-way, etc). In this case the cylinder has selected the 3-way junction demonstrating a preference for the 3-way junction over a duplex DNA. Given the excellent fit this is unsurprising. The same result is seen also in solution by NMR [31] and gel electrophoresis [32], which demonstrated binding to a wider range of DNA 3-way junctions too. Both M and P cylinders bind DNA 3-way junctions, with the M enantiomer binding more strongly. The M and P arginine cylinders also both stabilize the 3WJ with the M helix stabilizing more [27].

This binding is remarkable and unprecedented. The cylinder inserts into the heart of the DNA and forms π-stacking interactions with the bases. It could be

classed as a new form of intercalation but it does not involve the DNA having to open up as the cavity is inherent in the 3WJ and it is the recognition of that cavity. A second DNA binding mode is also observed, in which two cylinder phenylene rings stack onto the surface of the two bases at the end of the DNA duplex [29, 30]. Each of these cylinders binds to three duplexes forming a 'non-covalent' DNA 3-way junction and linking the DNA into a 3-dimensional mesh.

3-way junctions are rare in genomic DNA (being mainly associated with triplet repeat expansion diseases such as Huntington's) [33]. It seems likely therefore that on genomic DNA, in the absence of available 3WJs, most cylinders are in the major groove of the duplex.

2.3. Recognition of RNA Structures

The cylinder can also bind to RNA 3-way junctions in a similar fashion (Figure 3) [34]. The M enantiomer is again in the heart of the junction with extensive π-stacking between the 6 central phenylene rings from the cylinder and the 6 RNA bases at the junction point. As in the DNA 3WJ crystal structure, further cylinders stack onto the ends of the A-duplex RNA arms, forming non-covalent 3-way junctions. Gel studies indicate that both M and P enantiomers have a similar stabilizing effect on the RNA 3WJ [34]. Competition experiments indicate that the binding constant to both DNA and RNA 3WJs is similar.

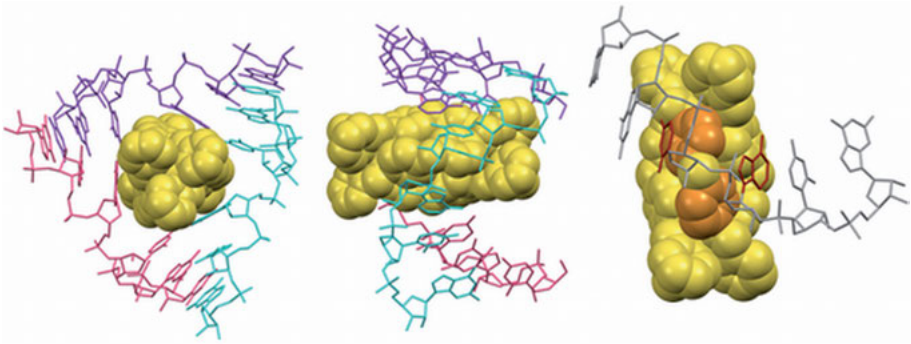

Figure 3. End and side views of the cylinder bound at the heart of a RNA 3-way junction, together with a view showing how the DNA bases (A and U) stack onto the phenylene rings. Cylinder can enter and leave the 3WJ structure to exchange between DNA and RNA 3WJs (PDB 4JIY) [34].

2.4. Binding to Forks and Bulges

DNA 3WJs are part of a broader group of Y-shaped DNA structures and some of these are much more common than 3WJs, for example replication and tran-

scription forks which have a Y-shape and 4 DNA bases at their junction point available to stack onto the surface of the cylinder. Gel electrophoresis studies have shown that the cylinder can also bind to forks. DNA bulges are formed when one strand in a duplex has extra unpaired bases and this causes a kink in the DNA axis [35]. The result is a Y-shape like structure that also has the potential to bind the cylinder.

Gel studies have confirmed that the cylinder can bind to different bulge structures, with 3-base bulges preferred [36]. DNA and RNA bulges are often a site of protein binding. As a relevant example, the HIV RNA genome contains a 3-base bulge in its trans activation response (TAR) region which needs to be recognized by a transactivator (TAT) protein for viral replication to proceed [37]. The cylinder can bind to this bulge and prevent the formation of a TAR-TAT adduct [38]. Excitingly, we have recently demonstrated that this can be used to switch off HIV viral replication in viable mammalian cells [39].

2.5. Binding to Tetraplex DNAs

It has been reported that the P enantiomer of the nickel(II) cylinder can interact with tetra-stranded DNA [40] binding to quadruplexes in which a loop of unpaired bases is located above the tetra-guanine surface. There appears to be some preference for TTA over TTT in the loops [41–43], which is perhaps consistent with the bases stacking onto the cylinder. While the P enantiomer stabilizes this quadruplex sequence, the M enantiomer does not. The structure of the quadruplexes varies with conditions and hybrid structures are possible to which both M and P appear to bind [40]. As with duplex DNA, introduction of methyl groups at the ends of the cylinder has little effect on the DNA binding. Adding methyl groups to the sides of the cylinder increases the DNA binding to the M enantiomer [44]. Most recently the M enantiomer has been proposed to bind to a left-handed quadruplex DNA [45]. There have been no structures of these cylinder-quadruplex complexes so the precise molecular recognition remains unclear. Elongated cylinders with an extra phenyl ring in the spacer have a higher quadruplex binding constant (around 10^6 M^{-1}) [46].

2.6. Biological Effects of Cylinders

The cylinders enter cells quickly and enter the nucleus as demonstrated by their ability to displace Hoechst 33258 from nuclear DNA in live cells [47]. The iron(II) cylinder inhibits cancer cell growth in culture and is a powerful cytostatic in breast T47D, ovarian SKOV-3, and leukemia HL60 cancer cells at low micromolar concentrations [47]. The cells arrest in the G0/G1 phase of the cell cycle, and at higher doses they enter apoptosis. Although it reaches the nuclear DNA, the cylinder does not cause mutagenicity or strand breaks. This contrasts with cisplatin that damages DNA, and it highlights the potential of this different binding mode.

In cell cultures the amount of cylinder present, rather than the concentration defines its activity [48] and this suggests that cells take up and concentrate the cylinder within them. The cylinder is active in MDA-MB231 breast and SKOV-3 ovarian cancer cell lines over 72 h, but its activity declines at longer time points: incubation times of 96, 120, and 144 h did not increase cytotoxicity. The arginine cylinders show similar cytotoxicity to the parent cylinder [27] while the ruthenium cylinder (as its hexafluorophosphate salt) is active against breast cancer cell lines, but not in ovarian SKOV-3 cells [24].

To assess the impact of cylinders on DNA processing we used the polymerase chain reaction (PCR) as an *in vitro* model DNA replication process [49]. PCR has similarities to mammalian DNA replication but involves elevated temperatures. The ruthenium cylinder prevented the Taq polymerase from binding to DNA and inhibited PCR at low micromolar concentrations (<2 μM). Transcription of plasmids by RNA polymerase is also inhibited *in vitro* by both M and P iron(II) cylinders at low micromolar concentrations [19]. The cylinders also inhibit the action of topoisomerase I at low micromolar concentrations apparently by inhibiting the re-ligation step of the nicked structure. The nicked structure provides a potential fork-like structure for the cylinder to bind. The iron(II) cylinder is 10-fold less effective at inhibiting DNase I and restriction endonucleases which bind and cleave double-stranded DNA.

Bacterial cells also represent a potential target for the cylinder. The cylinder acts as a bactericidal (rather than bacteriostatic) agent against Gram-positive *B. subtilis* and Gram-negative *E. coli* [50]. It stains bacterial DNA purple (the color of iron(II) cylinder) and kills the bacteria within 2 minutes. The cylinder's activity against cancer cells, bacteria, and viruses shows the potential of using a supramolecular compound to bind nucleic acid structures.

3. OTHER SUPRAMOLECULAR DESIGNS AND THEIR TARGETS

3.1. Mononuclear Agents

Monchaud has explored different compounds, both with and without metals, as possible DNA 3-way junction binders. A 1,4,7-triazacyclononane ligand bearing quinoline side arms (TACN-Q, Figure 4A) binds the DNA 3WJ but not duplex DNA [51, 52]. The experiments are conducted in the presence of lithium cations (90 mM) and the binding species may be a lithium complex. However, when transition metals are coordinated, the complexes bind less strongly to the 3WJ. The coordination of the transition metals causes the ligand to fold up reducing the π-surfaces available to bind the junction. Telaude-Fichou, Monchaud, and coworkers also explored the 3WJ binding of some azacryptands (Figure 4B) [53]. The compounds have a cylinder-like structure, with three aromatic π-surfaces, to interact with the base pairs of nucleic acids. They bind triplet repeat expansion DNA [53, 54], and some bind G quadruplex DNA [53, 55] though

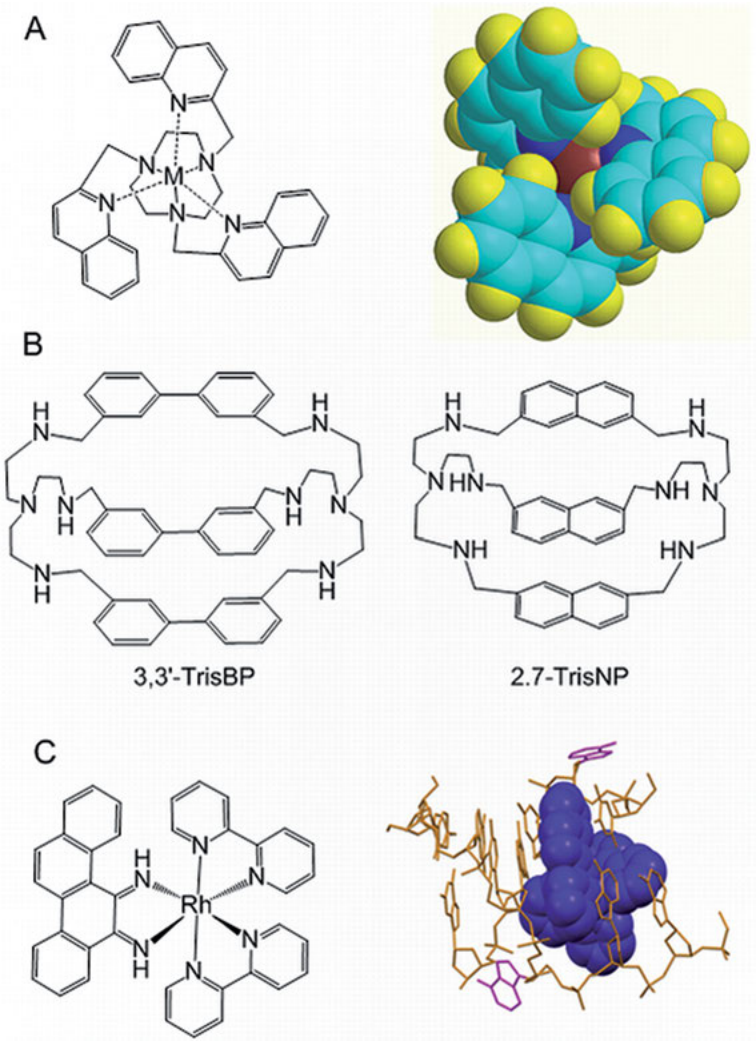

Figure 4. Developed by Monchaud and coworkers [51, 52]: (**A**) The mono-nuclear TACN-Q compound (CSD IQIWOW) [51]; (**B**) cylinder-like azacryptands with DNA 3WJ binding properties [53]. (**C**) The rhodium chrysi compound of Barton [56]. At the right: insertion of the chrysi ligand (blue) into a DNA bulge with two flipped out adenines (pink) (PDB 2O1I).

the 3WJ is preferred. The cryptands and TACN-Q show low micromolar cytotoxicity in B16 cells.

The mononuclear rhodium(III) compound Δ-$[Rh(bpy)_2(chrysi)]^{3+}$ of Barton et al. [56] target mismatches where two opposing bases are expelled from the DNA core. The 'chrysi' ligand is wider than traditional intercalators and thus favors larger sites (Figure 4C). The crystal structure of this compound binding

to DNA (shown in blue in Figure 4C) shows the chrysi ligand inserted from the minor groove. The compound can also bind to duplex DNA though the mismatch is the preferred site [56].

3.2. Flexicates

The control of chirality of metal-based helicates is a significant aspect for their use as nucleic acid binders and a variety of different strategies have been used to separate the enantiomers: chiral chromatography [16, 57], crystallization [8], chiral counter anions [58, 59], placing stereo centers in the ligand backbone [60, 61] or periphery [27], and light-induced isomerization [62].

Scott and coworkers have explored diastereoisomerically pure di-Fe(II) and di-Zn(II) triple stranded helicates based on bidentate pyridylimine ligands incorporating chiral centers in the spacer or periphery (Figure 5) [63]. Ligand L1 is related to the bis-pyridylimine ligand employed for cylinders, while in ligand L2 the chirality is attached to the ends. The stereo-centers induce the handedness of the resultant helicates (structure in Figure 5) just as the arginines did for the cylinders. Although the design is related to the cylinders, these helicates contain aliphatic linkers and in that sense have similarity to the original Lehn helicates with their more flexible structure. Scott calls them 'flexicates'.

The flexicates bind to long B-DNAs (ct-DNA, poly(dA-dT)$_2$, poly(dG-dC)$_2$ and plasmids), preferring AT-rich regions [63, 64]. Δ and Λ1a bind twice as strongly as Δ and Λ2a/b, which themselves do not stabilize DNA enough to affect its melting temperature. It is proposed that 1a flexicates (Figure 5) bind to B-DNA, presumably in a groove, whilst the interaction with other flexicates is mainly electrostatic ion pairing. This was further confirmed by atomic force microscopy studies where 2a flexicates did not promote any DNA coiling effect but only some strand aggregation. The 1a flexicate induces intramolecular coiling and aggregations at high loading. This suggests that phenyl groups in the linker are key components in DNA binding helicates, perhaps because they provide opportunity for face-face and edge-face π-stacking interactions with nucleobases. In all the spectroscopic experiments, Λ (M) flexicates exhibit higher affinity for B-DNA than Δ (P), reflecting the same trend as the cylinders [17].

The affinity of flexicates for non-conventional DNA structures was also explored. Variation of DNA melting temperatures (ΔT_m) of Y and T-shaped three way junctions (3WJ), four way junctions (4WJ), and bulge motifs were measured in the presence of 1a, 2a, and 2b [64, 65]. The highest ΔT_m values were again observed when employing 1a flexicates, and Y-shaped 3WJ were the motifs better stabilized by these complexes (ΔT_m 20 and 18 °C with Λ1a and Δ1a, respectively) with the M flexicate exerting the greater effect. Also in this case there is a general trend of Λ1a stabilizing non-canonical nucleic acid structures better than Δ1a and this was further confirmed by electrophoretic mobility shift assay. Flexicates 2a/b also stabilized Y-shaped 3WJ, although ΔT_m values were lower than those measured with 1a. Compounds 2a/b did not stabilize other motifs tested; the only exception was observed by electrophoretic mobility shift assays

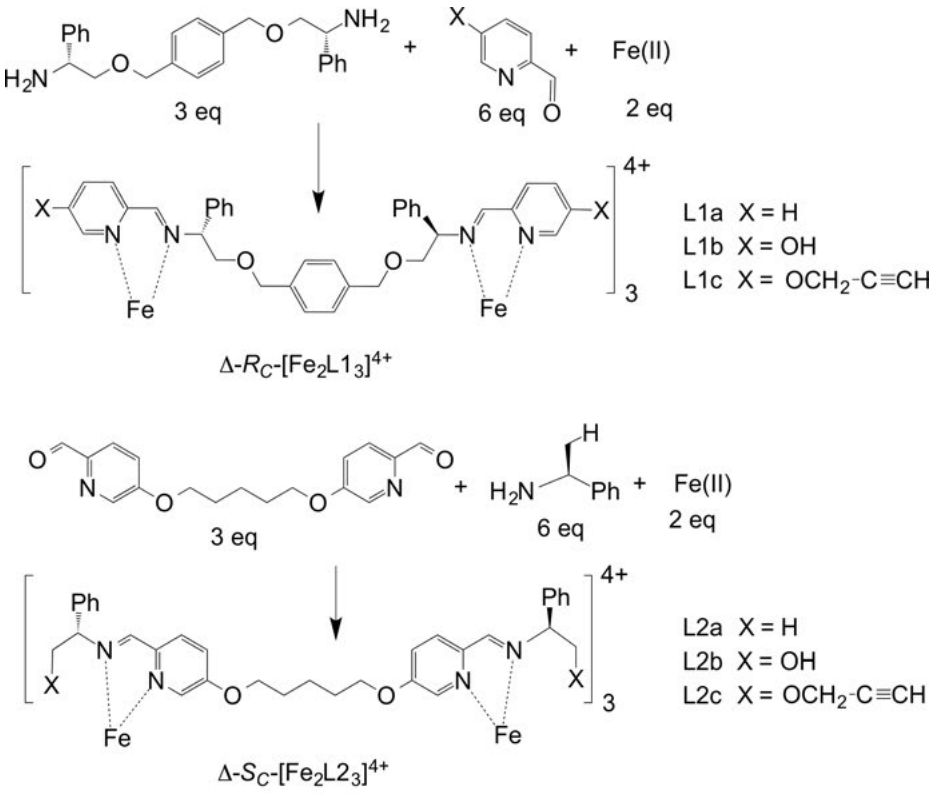

Flexicate employed for DNA binding and biological activity studies:

Δ and Λ-$[Fe_2L1a_3]Cl_4$ (Δ1a and Λ1a)
Δ and Λ-$[Fe_2L2a_3]Cl_4$ (Δ2a and Λ2a)
Δ and Λ-$[Fe_2L2b_3]Cl_4$ (Δ2b and Λ2b)

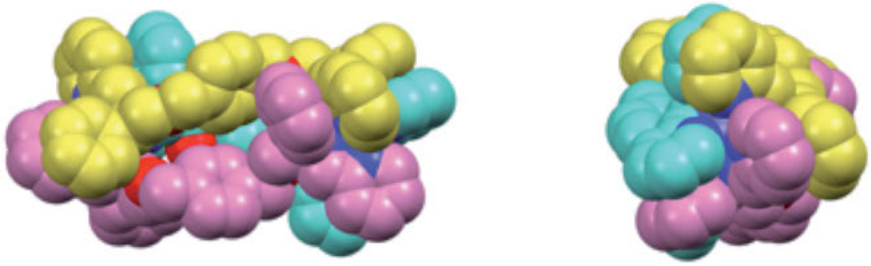

Figure 5. The 'one pot' synthesis of two sets of di-Fe(II) flexicates employing two different optically pure ligands L1 (above) and L2 (below). ClO_4^- and Cl^- were both employed as counter anions. The water soluble Δ and Λ-$[Fe_2L1a_3]Cl_4$, Δ and Λ-$[Fe_2L2a_3]Cl_4$, Δ and Λ-$[Fe_2L2b_3]Cl_4$ flexicates (indicated in the legend on the right) were investigated for their nucleic acid binding and biological activity. Bottom: a side and end view of L1-based flexicate (CSD PAHTID) [63].

Table 1. Antimicrobial activity (minimum inhibitory concentration, MIC) and cytotoxicity in cancer cell lines (IC_{50}) of flexicates.

Antimicrobial activity MIC (μg/mL)			**Cytotoxicity in cancer cell lines IC_{50} (μM (esd))**			
	***S. aureus* (Gram +)**	***E. coli* (Gram –)**	**MCF7**	**A2780**	**A2780cis**	**HCT116 $p53^{+/+}$**
Λ1a	8	4	3.7 (0.1)	4.8 (0.1)	2.2 (0.1)	1.7 (1.0)
Δ1a	8	8	2.9 (0.8)	3.7 (0.1)	2.4 (0.1)	0.6 (0.3)
Λ2a	64	32	5.5 (0.5)	3.3 (0.1)	7.3 (0.3)	0.6 (0.1)
Δ2a	64	>128	10.2 (0.2)	3.5 (0.1)	14.4 (0.4)	0.9 (0.1)
Λ2b	>128	>128	6.1 (0.2)	4.3 (0.0)	12.7 (0.0)	0.6 (0.1)
Δ2a	>128	>128	8.3 (0.2)	3.1 (0.1)	18.2 (0.1)	0.6 (0.1)

esd = estimated standard deviations
Data collected from [63, 64].

(run at lower temperatures compared to ΔT_m measurements), where a preferred binding of Λ2a/b to T-shaped 3WJs was observed, whilst Δ2a/b do not form any adduct with these nucleic acids.

The 1a flexicates also exhibited a stabilizing effect on 4WJ and bulge motifs, although 2- to 4-fold lower than their effect on Y-shaped 3WJ [64]. The interaction affinity for DNA bulges depends on bulge size: 3 nucleotides bulges are better stabilized than 2 or 1 nucleotide bulges; handedness does not appear to play a role. With smaller bulges, 1a forms 2 : 1 adducts with Λ1a more effective than Δ1a [65]. Binding of flexicate 1a to the TAR RNA sequence was also investigated. Melting temperature and gel experiments suggest that both diastereoisomers stabilizes TAR and Λ1a is more efficient than Δ1a [65]. The ΔT_m values (4–6 °C) indicate that they stabilize TAR RNA less than the Fe(II) cylinders (11–12 °C) [38].

Both Δ and Λ diastereoisomers of 1a flexicate displayed both antimicrobial activity and cytotoxicity against several cancer cell lines, including the cisplatin-resistant A2780cis and most of the assays *in cellulo* display a minor trend where Λ is more effective than Δ ([63–64], data summarized in Table 1). Flexicates 2a/b were also included in the same biological assays, showing definitely less potential as antimicrobial compounds, but still cytotoxicity in cancer cell lines.

Further derivatives of 2a have been prepared and also show poor or absent B-DNA-binding and low antimicrobial activity but good cytotoxicity [66]. The fact that both 1a and 2a flexicates show cytotoxic properties in cell lines, but only 1a binds well to nucleic acids suggests that there must be other biological targets for these compounds: 2a and derivatives most probably affect different cellular events. Indeed Scott et al. [64] have recently proposed that DNA is not the target of helicates, and this is certainly true of his flexicates which lack the large accessible oriented aromatic surfaces on their external surfaces that are seen in the cylinders and azacryptands and which are crucial to their unique forms of DNA recognition. It does however raise the question of what other targets or processes flexicates might be interfering with.

3.3. Other Helicates and Dinuclear Supramolecular Complexes

Other helical dinuclear supramolecular architectures have also been used to target DNA. Crowley and coworkers created libraries of helicates, using copper(I)-catalyzed 'click' reactions to prepare bidentate 2-pyridyl-1,2,3-triazole ligands (L_{triaz}) (Figure 6A) [67–69]. They obtained several $[Fe_2(L_{triaz})_3]^{4+}$ racemic helicates with spacers (a) or (f), and achiral ΛΔ-mesocates architectures with spacers (b) to (d) [67]. Molecular docking studies suggest that $[Fe_2(L_{triaz})_3]^{4+}$ compounds can bind in the B-DNA major groove. However, poor complex sta-

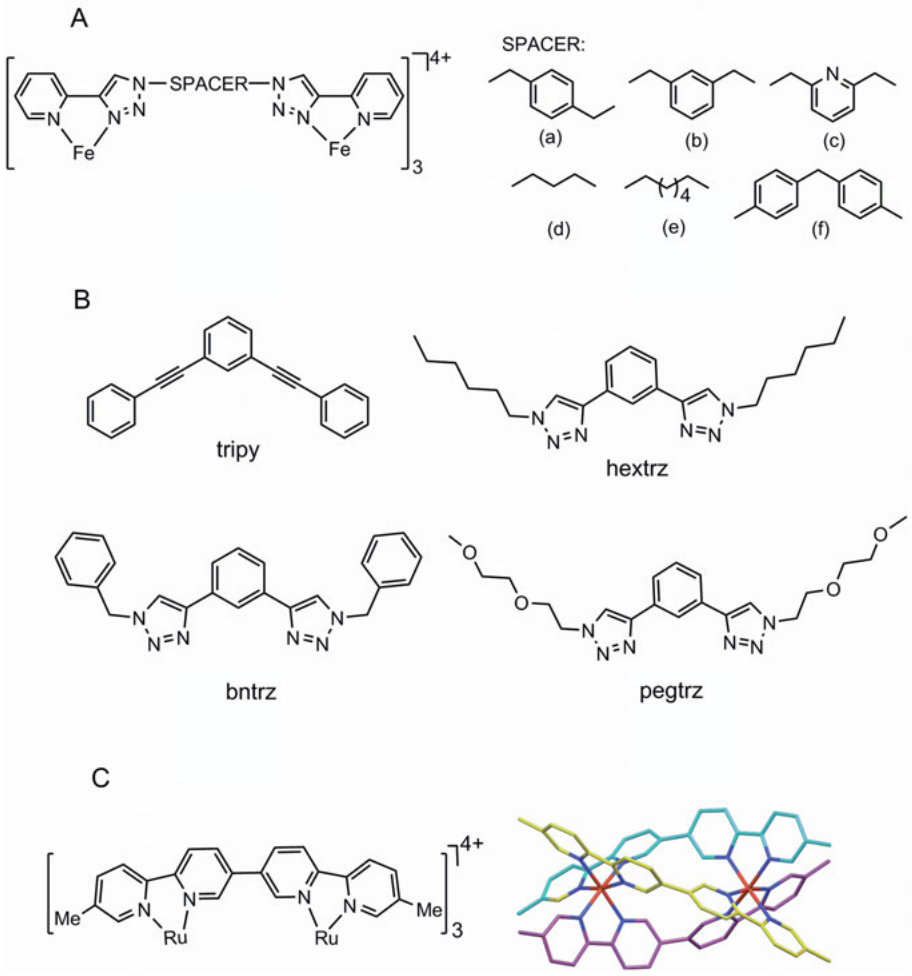

Figure 6. Crowley's compounds: (**A**) Fe(II) triple-stranded helicates employing 2-pyridyl-1,2,3-triazole ligands (L_{triaz}) [67] and (**B**) ligands employed for $[Pd_2L_4]^{4+}$ complexes [70, 71]. (**C**) Tetra-cationic di-Ru(II) triple-stranded helicate $[Ru_2Lq_3]^{4+}$ by Lindoy and coworkers [72] (molecular structure on the right) (CSD TOMROD)).

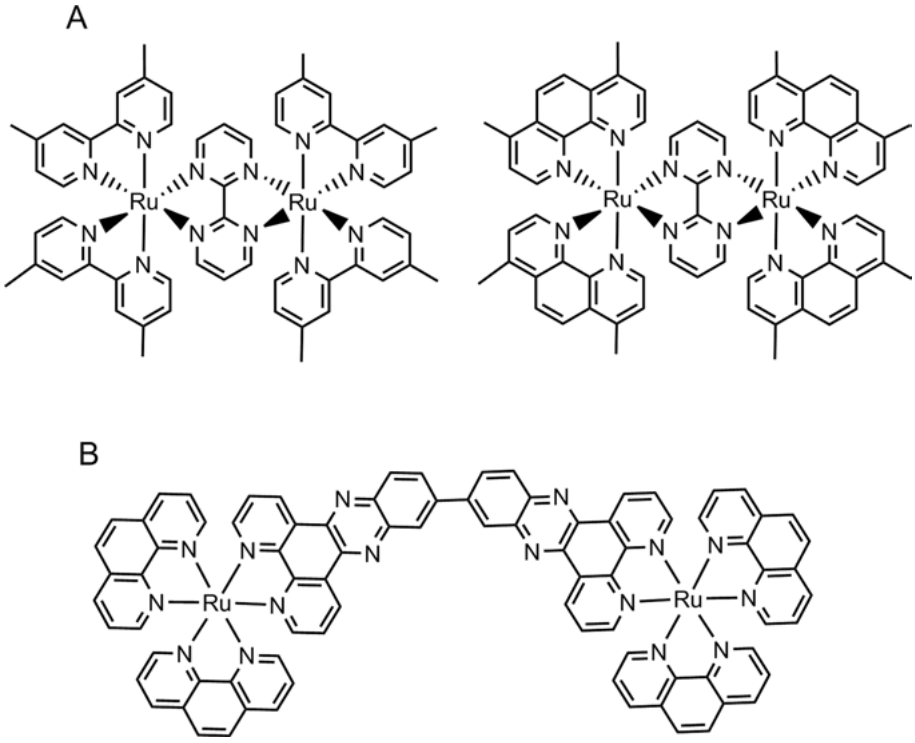

Figure 7. (**A**) Tetra-cationic di-Ru(II) assemblies $[\{Ru(Me_2bpy)_2\}_2(\mu\text{-bpm})]^{4+}$ (left) and $[\{Ru(phen)_2\}_2(\mu\text{-bpm})]^{4+}$ (right) as bulge binders investigated by Keene, Collins et al. [78, 79]. (**B**) The threading intercalators of Lincoln, Nordén et al. [85].

bility prevented extended biological studies. The analogous Co(III) compounds ($[Co_2(L_{\mathbf{triaz}})_3]^{6+}$) [68], have improved stability, but do not have antimicrobial activity perhaps because the high charge of these complexes (6+) does not allow bacterial membrane penetration. Related ligands (Figure 6B) were used to achieve di-Pd(II) tetra-stranded helicates [70, 71] which have high cytotoxicity against cancer cell lines. $[Pd_2(L_{\mathbf{hextrz}})_4]^{4+}$ is the most active (IC_{50} values below 8 μM) although the biological target of these complexes is uncertain.

Lindoy's $[Ru_2Lq_3]^{4+}$ triple-stranded helicate uses three 3,5‴-dimethyl-2,6′;3′ 5″;2″6‴-quaterpyridine ligands (Lq) to coordinate two octahedral ruthenium centers (Figure 6C) [72]. The M and P enantiomers were separated by C-25 Sephadex chromatography using (–)-O,O'-dibenzoyl-L-tartaric acid. The helicate is different from the cylinders because all the aryl rings (coordinated pyridines) present their edges (not faces) to the outside of the structure. DNA affinity chromatography showed the P enantiomer to have the highest DNA binding. Dinuclear double-stranded helicates are formed when copper(I) or silver(I) coordinate to 6,6‴-dimethyl-2,2′;6′,2″;6″2‴-quaterpyridine and also present their ring edges to the outside of the structure [73]. Docking studies suggested that these helicates could bind in a B-DNA groove, but likely via the aromatic faces

exposed at their ends. The complexes bind only weakly to DNA, competing poorly with ethidium bromide. They are active against T-47D, HaCat, and HeLa cell lines, and the silver complexes are the more cytotoxic. The counterions affect the cytotoxicity having an up to 3-fold effect.

Keene, Collins, and coworkers have studied a range of di-ruthenium supramolecular assemblies as nucleic acid binders and antimicrobial agents [74–78]. For example, $[\{Ru(Me_2bpy)_2\}_2(\mu\text{-bpm})]^{4+}$ (Figure 7A, left) binds the self-complimentary tridecanucleotide $d(CCG\mathbf{A}GAATTCCGG)_2$ containing a one-nucleotide bulge motif (the adenine in bold) [79, 80]. The ΔΔ enantiomer of the complex strongly binds to the bulge, whilst *meso*-ΛΔ binds only weakly. The complex also binds to the analogous RNA bulged sequence [81, 82]. When the Me_2bpy ligands are replaced with phen (Figure 7A, right) the *meso* isomer ΔΛ becomes the better binder [83]. Similar di-ruthenium compounds, where the internal linker is a larger poly-aromatic tetrapyrido-phenazine unit (tpphz), have been investigated by Thomas, Williamson, Félix, and coworkers as possible G4 binders ([77, 84] and references therein), indicating the versatility of this class of supramolecular assemblies.

Lincoln, Nordén et al. have also explored di-ruthenium bis-diimine complexes linked by an intercalating system (Figure 7B) [85]. These agents intercalate and thread through the DNA placing one metal center in the major groove and the other in the minor groove. Coll, Lincoln, and coworkers obtained a crystal structure of the ΔΔ enantiomer of this molecule bound to the hexameric oligonucleotide used in the 3WJ cylinder studies [86]. The bridging ligand threads through the DNA duplex pushing out an AT pair giving a binding similar to the mismatch binders. The other end of the bridging ligand binds to a second duplex. This brings two different duplexes together forming a type of non-covalent 4-way junction.

3.4. Squares, Boxes, and Cubes Targeting G-Quadruplex

G-quadruplex (G4) motifs are very important and widely studied targets for anticancer drug development because of their key role in inhibiting the telomerase enzyme (overexpressed in cancer cells) and affecting the transcription of some oncogenes. A large number of synthetic compounds, including metal-based complexes, have been synthesized and screened for G4 binding. These have been described in several excellent reviews (including Chapter 12 by Vilar in this book) [87–89]. Herein we only highlight representative examples in which metallo-supramolecular chemistry was employed as a tool to design new compounds aiming to improve selectivity toward G4 motifs over duplex DNA [90].

Porphyrin-based compounds are known to have strong affinity for G4 structures, although low selectivity as they also bind to duplex DNA. Therrien and coworkers employed arene ruthenium complexes as bridging blocks able to connect two porphyrin units and create octa-ruthenium supramolecular cubes (Figure 8A) [91]. The concept is that these cubes are too large to insert into DNA [92–94]. The G4 binding of these compounds was investigated by thiazole orange

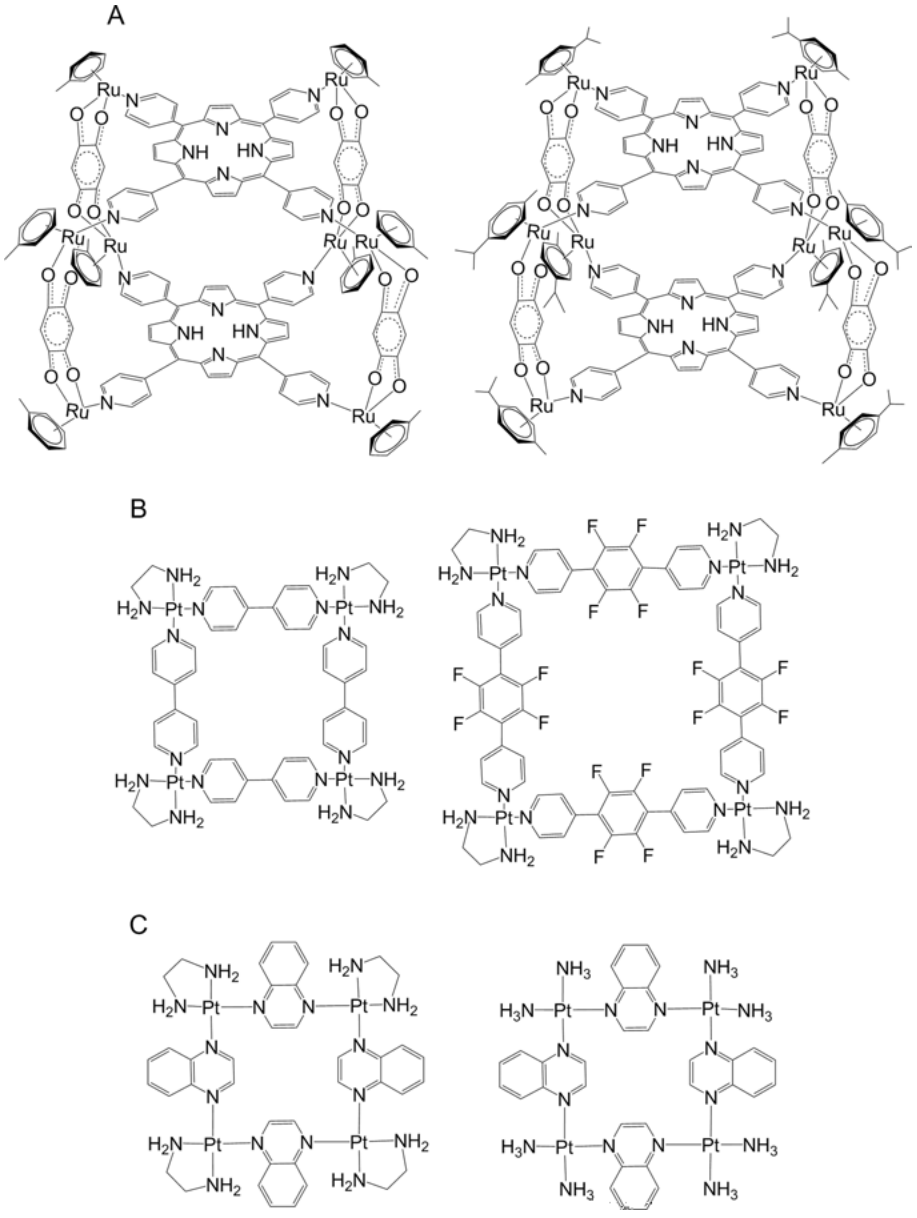

Figure 8. (**A**) Examples of porphyrin-based octa-ruthenium metallo-supramolecular cubes, by Therrien and coworkers [92]. (**B**) Fujita's compounds [96] employed by Sleiman and coworkers [95] (left) and Moreno's compound [99] with improved solubility (right). (**C**) Mao's compounds with improved selectivity [100].

(TO) fluorescence intercalation displacement (FID) and by surface plasmon resonance. The supramolecular cubes have high quadruplex affinity (DC_{50} between 0.1 and 0.7 μM) with two types of G4 motifs (*htelo* and *c-myc*), however the selectivity over duplex DNA was rather modest (between 2- and 4-fold), probably because of the high charge of these supramolecular cubes.

Sleiman and coworkers [95] have studied the G4 binding of multi-nuclear supramolecular square architectures, previously developed by Fujita [96, 97] and Stang [98]. Quadruplex stabilization was tested by FRET melting assays, revealing a high binding affinity (ΔT_m 34.5 °C) comparable with that displayed by other known G4 binders [95]. Again the selectivity is not remarkable (about 3-fold higher affinity for G4 over DNA duplex). Nevertheless, telomeric repeat amplification protocol (TRAP) assays indicated that this tetra-Pt square is among the strongest telomerase inhibitors (IC_{50} of 0.2 μM). In an earlier work Moreno and coworkers improved the solubility of this class of supramolecular squares by introducing a 1,4-bis(4-pyridyl)tetrafluorobenzene linker (Figure 8B, right) [99] and demonstrated that both the new complex and parent Fujita square [96, 97] displayed high cytotoxicity in HL-60 cell lines (IC_{50} around 3–5 μM).

Recognizing the potential of tetra-platinum squares as G4 binders, Mao and coworkers explored different derivatives and whether changing the organic linker between the Pt centers could influence binding selectivity [87]. For example, $[Pt(en)(quinoxaline)]_4(NO_3)_8$ and $[Pt(NH_3)_2(quinoxaline)]_4(NO_3)_8$ (Figure 8C, left and right, respectively) display binding affinity with *htelo* G4 similar to that observed by Sleiman when employing Fujita's $[Pt(en)(4,4'\text{-dipyridyl})]_4^{8+}$ (ΔT_m 32–33 °C by FRET melting assay), but their selectivity over other G4 motifs and duplex DNA is remarkably improved (ΔT_m is 3–6 °C and 1 °C with *c-myc* and dsDNA, respectively) [100]. Mao's compounds show high inhibition of human telomerase (IC_{50} 1.1 μM) and antiproliferative activity in A546/cisR cells (IC_{50} 6.5 μM). This study suggests that the selectivity of tetra-Pt squares can be improved by changing the organic linker and consequently the spatial configuration of the square and the set of π-π-stacking interactions.

Recently, Terenzi and coworkers reported further examples of how Pt(II)-directed self-assembly of supramolecular boxes allows the development of libraries of compounds where sizes, electrostatic charge, and set of non-covalent interactions can be tuned in order to improve selectivity toward G4 motifs and biological activity [101, 102].

4. CONCLUDING REMARKS AND FUTURE DIRECTIONS

The compounds described herein show the potential ability of metallo-supramolecular compounds to bind unusual nucleic acid structures in a shape-specific fashion. As our understanding improves of how and when different DNA and RNA structures inside cells, so will the potential of such agents as unique drugs become more apparent. Size, charge, and precise shape are the key to recognize different motifs and thus their activity. There are many possible directions that

this field could take but it is already clear that this new area of nucleic acid shape recognition is one of enormous potential.

ACKNOWLEDGMENTS

Our studies in this field have benefited from some great collaborators, who have brought their own skills and expertise to the challenge of studying DNA and RNA recognitions by cylinders. We thank them and our research team past and present for all their contributions and for helping to establish this exciting field of research.

ABBREVIATIONS AND DEFINITIONS

A	adenine residue in DNA/RNA
AFM	atomic force microscopy
bntrz	4,4′-benzene-1,3-diylbis(1-benzyl-1*H*-1,2,3-triazole)
bpm	2,2′-bipyrimidine
bpy	2,2′-bipyridine
chrysi	5,6-chrysenequinone diimine
dA	2′-deoxyadenosine residue
dC	2′-deoxycytidine residue
DC_{50}	concentration required to decrease fluorescence by 50 %
dG	2′-deoxyguanosine residue
dT	2′-deoxythymidine residue
en	ethylenediamine = 1,4-diazabutane
FID	fluorescence intercalation displacement
FRET	Förster resonance energy transfer
G4	guanosine quadruplex
hextrz	4,4′-benzene-1,3-diylbis(1-hexyl-1H-1,2,3-triazole)
Hoechst	family of bis-benzimide-based fluorescent dyes to stain DNA
IC_{50}	half maximal inhibitory concentration
Lq	quaterpyridine ligand
M enantiomer ($\Lambda\Lambda$)	left-handed helix of a helicate
Me_2bpy	4,4′-dimethyl-2,2′-bipyridine
P enantiomer ($\Delta\Delta$)	right-handed helix of a helicate
PCR	polymerase chain reaction
pegtrz	(1,3-bis(1-(2-(2-methoxyethoxy)ethyl)-1*H*-1,2,3-triazol-4-yl)benzene)
phen	1,10-phenanthroline
T	thymine residue in DNA/RNA
TACN	1,4,7-triazacyclononane ligand
TACN-Q	TACN with a quinoline side arm

TAR	trans activation response element
TAT	trans activator protein
T_m	melting temperature
TO	thiazole orange
tpphz	poly-aromatic tetrapyrido-phenazine unit
TRAP	telomeric repeat amplification protocol
triaz	triazole ligand
tripy	2,6-bis(pyridin-3-ylethynyl)pyridine
2,7-TrisNP	1,4,8,11,14,18,23,27-octaaza-6,16,25(2,7)-trinaphthalenabicyclo-[9.9.9]nonacosaphane
3,3′-TrisBP	1,4,9,12,15,20,25,30-octaaza-6,7,17,18,27,28(1,3)-hexabenzenabicyclo[10.10.10]dotriacontaphane
3WJ	3-way junction of DNA/RNA

REFERENCES

1. M. J. Hannon, *Chem. Soc. Rev.* **2007**, *36*, 280–295.
2. B. Rosenberg, L. Vancamp, T. Krigas, *Nature* **1965**, *205*, 698–699.
3. L. S. Lerman, *J. Mol. Biol.* **1961**, 18–30.
4. S. Puyo, D. Montaudon, P. Pourquier, *Crit. Rev. Oncol. Hemat.* **2014**, *89*, 43–61.
5. W. A. Denny, *Anti-Cancer Drug Des.* **1989**, *4*, 241–263.
6. M. J. Hannon, C. L. Painting, A. Jackson, J. Hamblin, W. Errington, *Chem. Commun.* **1997**, 1807–1808.
7. T. M. Garrett, U. Koert, J. M. Lehn, A. Rigault, D. Meyer, J. Fischer, *J. Chem. Soc. Chem. Comm.* **1990**, 557–558.
8. R. Kramer, J. M. Lehn, A. Decian, J. Fischer, *Angew. Chem. Int. Edit.* **1993**, *32*, 703–706.
9. C. O. Dietrich-Buchecker, J. P. Sauvage, J. P. Kintzinger, P. Maltese, C. Pascard, J. Guilhem, *New J. Chem.* **1992**, *16*, 931–942.
10. E. C. Constable, M. J. Hannon, D. A. Tocher, *Angew. Chem. Int. Edit.* **1992**, *31*, 230–232.
11. A. F. Williams, C. Piguet, G. Bernardinelli, *Angew. Chem. Int. Edit.* **1991**, *30*, 1490–1492.
12. B. Schoentjes, J. M. Lehn, *Helv. Chim. Acta* **1995**, *78*, 1–12.
13. M. Hannon, I. Meistermann, C. J. Isaac, A. Rodger, V. Moreno, M. J. Prieto, E. Sletten, E. Moldrheim, *J. Inorg. Biochem.* **2001**, *86*, 56–56.
14. M. J. Hannon, V. Moreno, M. J. Prieto, E. Moldrheim, E. Sletten, I. Meistermann, C. J. Isaac, K. J. Sanders, A. Rodger, *Angew. Chem. Int. Edit.* **2001**, *40*, 880–884.
15. M. J. Hannon, I. Meistermann, C. J. Isaac, C. Blomme, J. R. Aldrich-Wright, A. Rodger, *Chem. Commun.* **2001**, 1078–1079.
16. J. M. C. A. Kerckhoffs, J. C. Peberdy, I. Meistermann, L. J. Childs, C. J. Isaac, C. R. Pearmund, V. Reudegger, S. Khalid, N. W. Alcock, M. J. Hannon, A. Rodger, *Dalton Trans.* **2007**, 734–742.
17. I. Meistermann, V. Moreno, M. J. Prieto, E. Moldrheim, E. Sletten, S. Khalid, P. M. Rodger, J. C. Peberdy, C. J. Isaac, A. Rodger, M. J. Hannon, *Proc. Natl. Acad. Sci. USA* **2002**, *99*, 5069–5074.
18. J. Malina, M. J. Hannon, V. Brabec, *Nucleic Acids Res.* **2008**, *36*, 3630–3638.
19. J. Malina, M. J. Hannon, V. Brabec, *Chem. Eur. J.* **2015**, *21*, 11189–11195.

20. J. C. Peberdy, J. Malina, S. Khalid, M. J. Hannon, A. Rodger, *J. Inorg. Biochem.* **2007**, *101*, 1937–1945.
21. S. Khalid, M. J. Hannon, A. Rodger, P. M. Rodger, *Chem. Eur. J.* **2006**, *12*, 3493–3506.
22. S. Khalid, M. J. Hannon, A. Rodger, P. M. Rodger, *J. Mol. Graph. Model.* **2007**, *25*, 794–800.
23. Y. Parajo, J. Malina, I. Meistermann, G. J. Clarkson, M. Pascu, A. Rodger, M. J. Hannon, P. Lincoln, *Dalton Trans.* **2009**, 4868–4874.
24. G. I. Pascu, A. C. G. Hotze, C. Sanchez-Cano, B. M. Kariuki, M. J. Hannon, *Angew. Chem. Int. Edit.* **2007**, *46*, 4374–4378.
25. J. Malina, M. J. Hannon, V. Brabec, *Chem. Eur. J.* **2008**, *14*, 10408–10414.
26. L. Cardo, M. J. Hannon, *Inorg. Chim. Acta* **2009**, *362*, 784–792.
27. L. Cardo, V. Sadovnikova, S. Phongtongpasuk, N. J. Hodges, M. J. Hannon, *Chem. Commun.* **2011**, *47*, 6575–6577.
28. L. Cardo, PhD Thesis, University of Birmingham, **2010**, 126–150.
29. A. Oleksi, A. G. Blanco, R. Boer, I. Uson, J. Aymami, A. Rodger, M. J. Hannon, M. Coll, *Angew. Chem. Int. Edit.* **2006**, *45*, 1227–1231.
30. D. R. Boer, J. M. C. A. Kerckhoffs, Y. Parajo, M. Pascu, I. Uson, P. Lincoln, M. J. Hannon, M. Coll, *Angew. Chem. Int. Edit.* **2010**, *49*, 2336–2339.
31. L. Cerasino, M. J. Hannon, E. Sletten, *Inorg. Chem.* **2007**, *46*, 6245–6251.
32. J. Malina, M. J. Hannon, V. Brabec, *Chem. Eur. J.* **2007**, *13*, 3871–3877.
33. R. R. Sinden, *Nature* **2001**, *411*, 757–758.
34. S. Phongtongpasuk, S. Paulus, J. Schnabl, R. K. O. Sigel, B. Spingler, M. J. Hannon, E. Freisinger, *Angew. Chem. Int. Edit.* **2013**, *52*, 11513–11516.
35. F. A. Gollmick, M. Lorenz, U. Dornberger, J. von Langen, S. Diekmann, H. Fritzsche, *Nucleic Acids Res.* **2002**, *30*, 2669–2677.
36. J. Malina, M. J. Hannon, V. Brabec, *FEBS J.* **2014**, *281*, 987–997.
37. S. Bannwarth, A. Gatignol, *Curr. HIV Res.* **2005**, *3*, 61–71.
38. J. Malina, M. J. Hannon, V. Brabec, *Scientific Reports* **2016**, *6*, Article: 29674. DOI:10.1038/srep29674.
39. L. Cardo, I. Nawroth, P. J. Cail, J. A. McKeating, M. J. Hannon, manuscript submitted.
40. H. J. Yu, X. H. Wang, M. L. Fu, J. S. Ren, X. G. Qu, *Nucleic Acids Res.* **2008**, *36*, 5695–5703.
41. H. J. Yu, C. Q. Zhao, Y. Chen, M. L. Fu, J. S. Ren, X. G. Qu, *J. Med. Chem.* **2010**, *53*, 492–498.
42. C. Q. Zhao, J. Geng, L. Y. Feng, J. S. Ren, X. G. Qu, *Chem. Eur. J.* **2011**, *17*, 8209–8215.
43. J. S. Wang, Y. Chen, J. S. Ren, C. Q. Zhao, X. G. Qu, *Nucleic Acids Res.* **2014**, *42*, 3792–3802.
44. B. L. Xu, C. Q. Zhao, Y. Chen, H. Tateishi-Karimata, J. S. Ren, N. Sugimoto, X. G. Qu, *Chem. Eur. J.* **2014**, *20*, 16467–16472.
45. A. D. Zhao, C. Q. Zhao, J. S. Ren, X. G. Qu, *Chem. Commun.* **2016**, *52*, 1365–1368.
46. X. X. Xu, J. J. Na, F. F. Bao, W. Zhou, C. Y. Pang, Z. J. Li, Z. G. Gu, *Spectrochim. Acta A* **2014**, *124*, 21–29.
47. A. C. G. Hotze, N. J. Hodges, R. E. Hayden, C. Sanchez-Cano, C. Paines, N. Male, M. K. Tse, C. M. Bunce, J. K. Chipman, M. J. Hannon, *Chem. Biol.* **2008**, *15*, 1258–1267.
48. A. J. Pope, C. Bruce, B. Kysela, M. J. Hannon, *Dalton Trans.* **2010**, *39*, 2772–2774.
49. C. Ducani, A. Leczkowska, N. J. Hodges, M. J. Hannon, *Angew. Chem. Int. Edit.* **2010**, *49*, 8942–8945.

50. A. D. Richards, A. Rodger, M. J. Hannon, A. Bolhuis, *Int. J. Antimicrob. Agents* **2009**, *33*, 469–472.
51. S. Vuong, L. Stefan, P. Lejault, Y. Rousselin, F. Denat, D. Monchaud, *Biochimie* **2012**, *94*, 442–450.
52. L. Stefan, B. Bertrand, P. Richard, P. Le Gendre, F. Denat, M. Picquet, D. Monchaud, *ChemBioChem* **2012**, *13*, 1905–1912.
53. J. Novotna, A. Laguerre, A. Granzhan, M. Pirrotta, M. P. Teulade-Fichou, D. Monchaud, *Org. Biomol. Chem.* **2015**, *13*, 215–222.
54. S. Amrane, A. De Cian, F. Rosu, M. Kaiser, E. De Pauw, M. P. Teulade-Fichou, J. L. Mergny, *ChemBioChem* **2008**, *9*, 1229–1234.
55. D. Monchaud, A. Granzhan, N. Saettel, A. Guédin, J. L. Mergny, M. P. Teulade-Fichou, *J. Nucleic Acids* **2010**, *2010*, Article ID 525862.
56. V. C. Pierre, J. T. Kaiser, J. K. Barton, *Proc. Natl. Acad. Sci. USA* **2007**, *104*, 429–434.
57. N. C. Fletcher, R. T. Brown, A. P. Doherty, *Inorg. Chem.* **2006**, *45*, 6132–6134.
58. R. M. Yeh, K. N. Raymond, *Inorg. Chem.* **2006**, *45*, 1130–1139.
59. T. Haino, H. Shio, R. Takano, Y. Fukazawa, *Chem. Commun.* **2009**, 2481–2483.
60. O. Mamula, A. von Zelewsky, *Coord. Chem. Rev.* **2003**, *242*, 87–95.
61. S. E. Howson, P. Scott, *Dalton Trans.* **2011**, *40*, 10268–10277.
62. D. P. Zhao, T. van Leeuwen, J. L. Cheng, B. L. Feringa, *Nat. Chem.* **2017**, *9*, 250–256.
63. S. E. Howson, A. Bolhuis, V. Brabec, G. J. Clarkson, J. Malina, A. Rodger, P. Scott, *Nat. Chem.* **2012**, *4*, 31–36.
64. V. Brabec, S. E. Howson, R. A. Kaner, R. M. Lord, J. Malina, R. M. Phillips, Q. M. A. Abdallah, P. C. McGowan, A. Rodger, P. Scott, *Chem. Sci.* **2013**, *4*, 4407–4416.
65. J. Malina, P. Scott, V. Brabec, *Dalton Trans.* **2015**, *44*, 14656–14665.
66. R. A. Kaner, S. J. Allison, A. D. Faulkner, R. M. Phillips, D. I. Roper, S. L. Shepherd, D. H. Simpson, N. R. Waterfield, P. Scott, *Chem. Sci.* **2016**, *7*, 951–958.
67. S. K. Vellas, J. E. M. Lewis, M. Shankar, A. Sagatova, J. D. A. Tyndall, B. C. Monk, C. M. Fitchett, L. R. Hanton, J. D. Crowley, *Molecules* **2013**, *18*, 6383–6407.
68. R. A. S. Vasdev, D. Preston, S. O. Scottwell, H. J. L. Brooks, J. D. Crowley, M. P. Schramm, *Molecules* **2016**, *21,* 1548. DOI:103390/molecules21111548.
69. S. V. Kumar, W. K. C. Lo, H. J. L. Brooks, J. D. Crowley, *Inorg. Chim. Acta* **2015**, *425*, 1–6.
70. J. E. M. Lewis, J. D. Crowley, *Supramol. Chem.* **2014**, *26*, 173–181.
71. S. M. McNeill, D. Preston, J. E. M. Lewis, A. Robert, K. Knerr-Rupp, D. O. Graham, J. R. Wright, G. I. Giles, J. D. Crowley, *Dalton Trans.* **2015**, *44*, 11129–11136.
72. C. R. K. Glasson, G. V. Meehan, J. K. Clegg, L. F. Lindoy, J. A. Smith, F. R. Keene, C. Motti, *Chem. Eur. J.* **2008**, *14*, 10535–10538.
73. A. Adamski, M. A. Fik, M. Kubicki, Z. Hnatejko, D. Gurda, A. Fedoruk-Wyszomirska, E. Wyszko, D. Kruszka, Z. Dutkiewicz, V. Patroniak, *New J. Chem.* **2016**, *40*, 7943–7957.
74. F. F. Li, J. G. Collins, F. R. Keene, *Chem. Soc. Rev.* **2015**, *44*, 2529–2542.
75. M. Pandrala, F. F. Li, M. Feterl, Y. Mulyana, J. M. Warner, L. Wallace, F. R. Keene, J. G. Collins, *Dalton Trans.* **2013**, *42*, 4686–4694.
76. F. R. Keene, J. A. Smith, J. G. Collins, *Coord. Chem. Rev.* **2009**, *253*, 2021–2035.
77. M. R. Gill, J. A. Thomas, *Chem. Soc. Rev.* **2012**, *41*, 3179–3192.
78. F. R. Keene, *Dalton Trans.* **2011**, *40*, 2405–2418.
79. B. T. Patterson, J. G. Collins, F. M. Foley, F. R. Keene, *Dalton Trans.* **2002**, 4343–4350.
80. J. A. Smith, J. G. Collins, B. T. Patterson, F. R. Keene, *Dalton Trans.* **2004**, 1277–1283.

81. C. B. Spillane, J. A. Smith, D. P. Buck, J. G. Collins, F. R. Keene, *Dalton Trans.* **2007**, 5290–5296.
82. D. P. Buck, C. B. Spillane, J. G. Collins, F. R. Keene, *Mol. Biosyst.* **2008**, *4*, 851–854.
83. J. L. Morgan, D. P. Buck, A. G. Turley, J. G. Collins, F. R. Keene, *Inorg. Chim. Acta* **2006**, *359*, 888–898.
84. T. Wilson, P. J. Costa, V. Felix, M. P. Williamson, J. A. Thomas, *J. Med. Chem.* **2013**, *56*, 8674–8683.
85. F. Westerlund, P. Nordell, B. Norden, P. Lincoln, *J. Phys. Chem. B* **2007**, *111*, 9132–9137.
86. D. R. Boer, L. S. Wu, P. Lincoln, M. Coll, *Angew. Chem. Int. Edit.* **2014**, *53*, 1949–1952.
87. Q. Cao, Y. Li, E. Freisinger, P. Z. Qin, R. K. O. Sigel, Z. W. Mao, *Inorg. Chem. Frontiers* **2017**, *4*, 10–32.
88. R. Hansel-Hertsch, M. Di Antonio, S. Balasubramanian, *Nature Rev. Mol. Cell Biol.* **2017**, *18*, 279–284.
89. S. Neidle, *J. Med. Chem.* **2016**, *59*, 5987–6011.
90. T. R. Cook, V. Vajpayee, M. H. Lee, P. J. Stang, K. W. Chi, *Acc. Chem. Res.* **2013**, *46*, 2464–2474.
91. B. Therrien, *Eur. J. Inorg. Chem.* **2009**, 2445–2453.
92. N. P. E. Barry, N. H. Abd Karim, R. Vilar, B. Therrien, *Dalton. Trans.* **2009**, 10717–10719.
93. N. P. E. Barry, O. Zava, P. J. Dyson, B. Therrien, *Aust. J. Chem.* **2010**, *63*, 1529–1537.
94. N. P. E. Barry, O. Zava, J. Furrer, P. J. Dyson, B. Therrien, *Dalton Trans.* **2010**, *39*, 5272–5277.
95. R. Kieltyka, P. Englebienne, J. Fakhoury, C. Autexier, N. Moitessier, H. F. Sleiman, *J. Am. Chem. Soc.* **2008**, *130*, 10040–10041.
96. M. Fujita, J. Yazaki, K. Ogura, *J. Am. Chem. Soc.* **1990**, *112*, 5645–5647.
97. M. Fujita, M. Tominaga, A. Hori, B. Therrien, *Acc. Chem. Res.* **2005**, *38*, 369–378.
98. P. J. Stang, B. Olenyuk, *Angew. Chem. Int. Edit.* **1996**, *35*, 732–736.
99. M. Mounir, J. Lorenzo, M. Ferrer, M. J. Prieto, O. Rossell, F. X. Aviles, V. Moreno, *J. Inorg. Biochem.* **2007**, *101*, 660–666.
100. X. H. Zheng, H. Y. Chen, M. L. Tong, L. N. Ji, Z. W. Mao, *Chem. Commun.* **2012**, *48*, 7607–7609.
101. O. Domarco, D. Lotsch, J. Schreiber, C. Dinhof, S. Van Schoonhoven, M. D. Garcia, C. Peinador, B. K. Keppler, W. Berger, A. Terenzi, *Dalton Trans.* **2017**, *46*, 329–332.
102. A. Terenzi, C. Ducani, V. Blanco, L. Zerzankova, A. F. Westendorf, C. Peinador, J. M. Quintela, P. J. Bednarski, G. Barone, M. J. Hannon, *Chem. Eur. J.* **2012**, *18*, 10983–10990.

12

Nucleic Acid Quadruplexes and Metallo-Drugs

Ramon Vilar

Department of Chemistry, Imperial College London, London SW7 2AZ, UK
<r.vilar@imperial.ac.uk>

ABSTRACT 325
1. INTRODUCTION 326
2. G-QUADRUPLEXES AND THEIR BIOLOGICAL ROLES 327
   2.1. G-Quadruplex DNA and RNA and Their Proposed Biological Roles 327
   2.2. G-Quadruplexes as Drug Targets 328
3. METAL COMPLEXES AS G-QUADRUPLEX BINDERS 328
   3.1. Metal Complexes that Bind via Non-covalent Interactions 329
      3.1.1. Planar Complexes Based on Macrocycles 329
      3.1.2. Planar Complexes with Acyclic Polydentate Ligands 331
      3.1.3. Octahedral Complexes and Supramolecular Metallo-Assemblies 335
   3.2. Direct Coordination of the Metal to G-Quadruplexes 338
4. METAL-BASED OPTICAL PROBES FOR G-QUADRUPLEXES 338
5. BIOLOGICAL ACTIVITY OF METAL-BASED G-QUADRUPLEX BINDERS 340
   5.1. Metallo-Binders that Target Telomeric G4 340
   5.2. Metallo-Binders that Target Gene Promoters 343
6. CONCLUDING REMARKS AND FUTURE DIRECTIONS 344
ACKNOWLEDGMENTS 344
ABBREVIATIONS 344
REFERENCES 345

Abstract: Guanine-rich sequences of DNA can readily fold into tetra-stranded helical assemblies known as G-quadruplexes (G4s). It has been proposed that these structures play important biological roles in transcription, translation, replication, and telomere maintenance.

Metal Ions in Life Sciences, Volume 18 Edited by Astrid Sigel, Helmut Sigel, Eva Freisinger, and Roland K. O. Sigel

https://doi.org/10.1515/9783110470734-012

Therefore, over the past 20 years they have been investigated as potential drug targets for small molecules including metal complexes. This chapter provides an overview of the different classes of metal complexes as G4-binders and discusses the application of these species as optical probes for G-quadruplexes as well as metallo-drugs.

Keywords: cancer · DNA · metallo-drugs · oncogene · optical probes · quadruplex · RNA · telomere

1. INTRODUCTION

It has been known for several decades that guanines (G) can self-assemble into molecular squares (known as G-tetrads) via hydrogen-bonding interactions between the Watson-Crick edge of each guanine and the Hoogsteen edge of its neighbor (Figure 1a). Similarly, guanine-rich oligonucleotides can follow an analogous hydrogen-bonding pattern to assemble under physiological conditions into tetra-stranded helical structures known as G-quadruplexes (G4). These assemblies can be intermolecular, where either two or four G-rich oligonucleotide strands assemble, or intramolecular, where a single strand with several G-runs folds into a stable G-quadruplex structure [1] (Figure 1).

Spectroscopic and structural studies have shown that these G-quadruplexes are stabilized by physiological concentrations of alkali metal cations (such as Na^+ and K^+), which display electrostatic interactions with the carbonyl groups of the guanines. In recent years, several studies have provided substantial evidence showing that G4 DNA and RNA structures form *in vivo* and may play important biological roles in replication, transcription, translation, and telomere maintenance [2, 3]. Because of their proposed biological relevance, G4s have been identified as potential drug targets, in particular for cancer [4, 5]. Consequently, a large number of molecules have been developed with the aim of binding and stabilizing G4s and in doing so display some pharmacological effect.

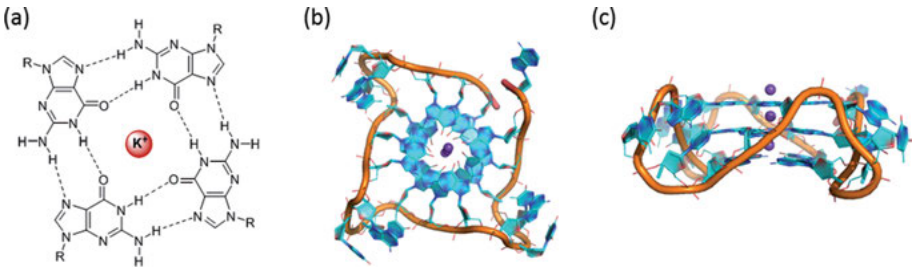

Figure 1. G-quadruplex DNA. (**a**) Schematic representation of the G-tetrad formed by hydrogen-bonding interactions between the Watson-Crick edge of each guanine and the Hoogsteen edge of its neighbor; (**b**) and (**c**) two views of the X-ray crystal structure of an intramolecular G-quadruplex DNA formed from a single oligonucleotide strand (PDB 1KF1) [1]. Figure generated with PyMol.

2. G-QUADRUPLEXES AND THEIR BIOLOGICAL ROLES

2.1. G-Quadruplex DNA and RNA and Their Proposed Biological Roles

Several excellent reviews discussing in detail the proposed biological roles and evidence for G4 formation *in vivo* have been previously published [2, 3, 6]. Therefore, herein only a brief description will be provided. Direct evidence that G-quadruplexes could form in cells was provided in 2001 by Plückthun et al. who reported a high-affinity antibody against the telomeric G4 DNA structure and showed that these structures are present in the nucleus of the ciliate *Stylonychia lemmae* [7]. More recently, Balasubramanian et al. engineered high-affinity antibodies that detected foci of G4 DNA in mammalian cells using immunofluorescent staining [8]. On the other hand, a number of small-molecule optical probes (some based on metal complexes as discussed below) have been used to study G4 structures in living cells [9–11].

The highest abundance of G4s is in telomeric DNA at the ends of chromosomes. In humans, the telomere is composed of hundreds of TTAGGG repeats that end in a single-stranded overhang of around 100–200 nucleobases [12]. Under physiological conditions this single-stranded sequence can readily fold into G-quadruplex structures since it is not constrained by the complementary DNA strand. The proposed biological roles of telomeric G4s include tethering chromatids together during meiosis as well as facilitating the alignment of strand ends during recombination.

In addition to the human telomere, bioinformatic studies based on the assumption that G4 structures could fold from sequences of the type $G_{3–5}X_n$ $G_{3–5}X_o$ $G_{3–5}X_p$ $G_{3–5}$ (with loops X_n, X_o, X_p being between 1 and 7 bases long) showed that in the human genome there are ca. 350,000 putative G4-forming sequences [13, 14]. More recent bioinformatics studies (allowing for longer loops) have predicted an even higher number of putative G4-forming sequences [15]. In addition to these bioinformatic predictions, a recent experimental high-throughput G4-sequencing identified over 700,000 distinct G4 structures in the human genome [16]. Interestingly, the G4 structures predicted by both bioinformatics and sequencing studies are not randomly distributed, but rather are concentrated in gene promoters (ca. in 50 %). Therefore, it has been hypothesized that the formation of G4 structures in these promoters may be a biological mechanism of regulating transcription. In 2016 Balasubramanian et al. reported a study showing the prevalence of G4s in human chromatin using an immunoprecipitation technique. This, combined with RNA sequencing, revealed ca. 10,000 sequences that form G4s under cellular conditions – which interestingly are mainly located in promoters and 5'-untranslated regions (5'-UTR) of genes [17].

RNA can also fold into G4 structures *in vitro*. Interestingly, bioinformatic studies have shown that putative quadruplex structures are significantly conserved and enriched in various regulatory elements including the 5'-UTR regions of mRNAs [18]. A computational search of all annotated 5'-UTRs of the human transcriptome, identified approximately 3000 5'-UTRs that contained putative

G4 structures, including several proto-oncogenes [19]. Therefore, it has been proposed that the G4 RNA structures may play a regulatory role in translation [20]. However, a recent study using reverse transcriptase stop assays and chemical footprinting showed that, while G4 RNA structures form readily *in vitro* and are stable, in mammalian cells they are unfolded by helicases and therefore the number of G4 RNAs *in vivo* is significantly less than initially predicted [21].

2.2. G-Quadruplexes as Drug Targets

Since G-quadruplexes have been implicated in several essential biological roles, they have been proposed as drug targets. Consequently, there has been great interest in developing small molecules that can bind, template and/or stabilize G-quadruplexes. Several excellent reviews have been published in this area and the reader is directed to these publications [3, 4, 22, 23].

Initially, most molecules designed to interact with G-quadruplexes where based on purely organic compounds, more specifically on polyaromatic systems featuring positive charges – e.g., with protonatable amine substituents – to increase their water solubility and DNA affinity. In 1997 Hurley, Neidle, and coworkers published a landmark study in which they demonstrated that a di-substituted 2,6-diamidoanthraquinone could bind to G-quadruplex DNA from the human telomeric sequence $[TTAGGG]_n$ in preference to other DNA topologies [24]. They also showed that the compound was able to inhibit the activity of telomerase, a reverse transcriptase overexpressed in most human cancer cells but not in normal somatic cells. This study set the basis for the development of several other polyaromatic molecules designed to target G-quadruplex DNA. While initial studies mainly focused on G4-mediated telomerase inhibition, recent investigations have shown that the effects caused by G4 binders are more complex. In particular, it has become increasingly evident that targeting G4s with small molecules can cause DNA damage to susceptible cancer cells [23].

Bioinformatic and experimental studies have identified that a large proportion of G4-forming sequences are located in promoters of oncogenes. Consequently, it has been proposed that G4 formation in these regions can regulate gene transcription and therefore G4s in oncogene (e.g., *c-myc*, *KRAS*, *kit*, *BCL2)* promoters have been proposed as drug targets [4, 5].

3. METAL COMPLEXES AS G-QUADRUPLEX BINDERS

Metal complexes have a number of features that make them particularly suitable as G4 DNA binders and therefore as potential drugs [25]. A metal ion coordinated to planar aromatic ligands withdraws electron density from the organic framework increasing its ability to display π-π stacking interactions with the guanine tetrad. Furthermore, coordinated metals can provide a positive charge to the

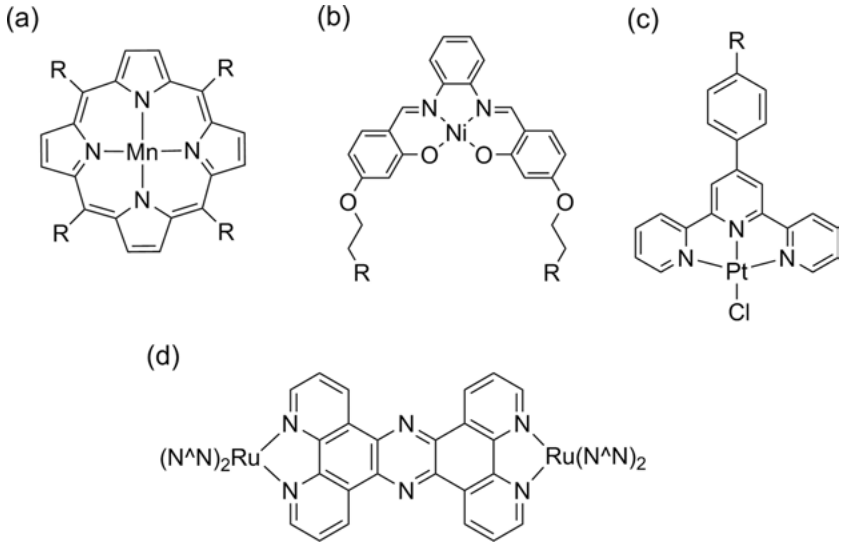

Figure 2. Chemical structures of the first classes of metal complexes to be reported as G-quadruplex binders (**a**) metal porphyrins; (**b**) metal salphens; (**c**) metal terpyridines; (**d**) di-ruthenium complex.

entire complex and take the position that would normally be occupied by K^+ at the external G-tetrad of a G4 structure. While the metal plays largely a structural role in most G4 binders, there are also examples where it interacts directly with G4s by electrostatic interactions or direct coordination with nucleobases [25, 26]. The first examples of G-quadruplex binders based on metal complexes were reported in the 2000s. These included square planar or square-based pyramidal metal complexes with porphyrins [27–30], salphens [31, 32], and terpyridines [33], as well as octahedral Ru^{II}-polypyridyl complexes [34] (Figure 2). Since these pioneering studies, there have been hundreds of reports of metal complexes as G4 binders [25, 26, 35].

3.1. Metal Complexes that Bind via Non-covalent Interactions

3.1.1. Planar Complexes Based on Macrocycles

Porphyrins and other poly-aromatic macrocycles have been widely studied as G4 DNA binders due to their well-matched size and symmetry with the G-tetrad. Indeed, metalloporphyrins were the first reported examples of metal-based G4 DNA binders (see Figure 3) [27, 29]. They predominantly bind via π-π stacking interactions on top of the G-tetrads at the termini of the quadruplexes. While the interaction of unsubstituted hemin porphyrins with G4 DNA structures has been reported, metalloporphyrins featuring cationic meso substituents have shown to be better G4 DNA binders since they can display electrostatic interac-

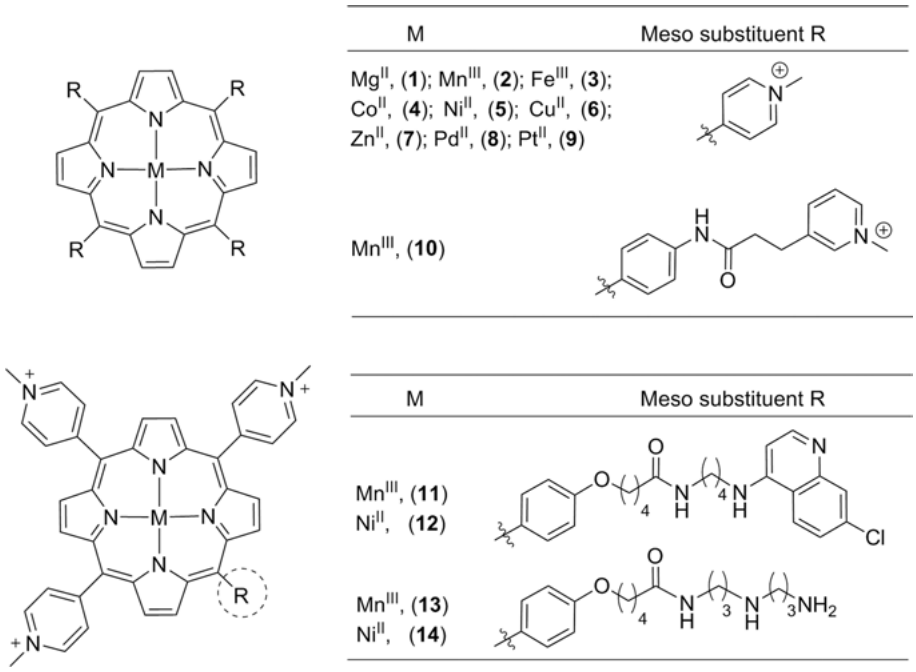

Figure 3. Representative examples of G4 binders based on metal-porphyrin complexes.

tions with the negatively charged phosphate backbone of DNA. In addition, the presence of the metal ion in the corresponding metalloporphyrins has been proposed to engage in further electrostatic interactions with G4 DNA. The nature of both the metal center and the meso substituents on the porphyrin are key parameters in determining the affinity and selectivity of the resulting metal complexes.

Many of the metalloporphyrins studied as G4 DNA binders (e.g., **1**–**9**) are based on the well-known tetra-(*N*-methyl-4-pyridyl)porphyrin (TMPyP4) ligand (Figure 3). Complexes with a square planar geometry (e.g. with Cu^{II}) or square-based pyramidal geometry (e.g., with Zn^{II}) [27, 36] have high affinities towards G4 DNA structures. This is due to the ability of the planar face(s) to stack on top of the G-tetrad. On the other hand, complexes with an octahedral geometry would not be expected to be good G-quadruplex binders. Interestingly, some octahedral complexes such as Mn-TMPyP4 with two axial water ligands coordinated to Mn^{III} also have high affinity toward G4 DNA. Indeed, the manganese(III)-porphyrin **10** reported by Meunier, Pratviel et al. has been shown to have a 1000-fold selectivity for G4 over duplex DNA [37].

Another class of macrocycles that have been reported to be good G4 binders are phthalocyanines (Figure 4) [38-40] that have a large planar π system well suited to interact with the G-tetrad. Amongst the best examples of this family are the guanidinium-substituted phtalocyanine zinc(II) complexes (**15–17**) report-

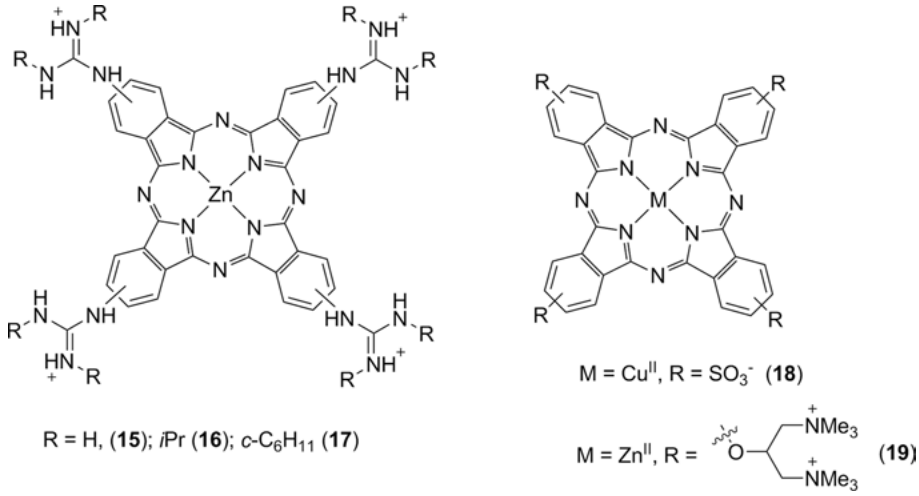

Figure 4. Representative examples of G4 binders based on metal-phthalocyanine complexes.

ed by Luedtke et al., which have a very high affinity for a range of G-quadruplexes including human telomeric (HTelo) and *c-myc* DNA [38].

3.1.2. Planar Complexes with Acyclic Polydentate Ligands

The first examples of metal salphen complexes as G4 binders were reported by Vilar et al. in 2006 [31]. The relative ease of synthesis and structural flexibility of these compounds makes them an ideal scaffold to generate libraries of compounds (Figure 5) and study their DNA binding properties. The geometry, size, and electronic properties of these complexes can be readily modified by changing the metal center (e.g., square-planar with Ni^{II}, Cu^{II}, and Pt^{II}, square-base pyramidal with V=O or distorted trigonal bipyramidal with Zn^{II}), or the nature and position of the substituents on the salphen ligand. This has led to a large number of compounds being reported with affinities towards G4-DNA (mainly HTelo and *c-myc*) ranging between 10^3 and 10^7 M^{-1} and with various levels of selectivity over duplex DNA [32, 41–47]. More recently, di-nuclear complexes where two nickel-salphen units are linked via polyethylene glycol spacers have been shown to have higher selectivity for dimeric G4 over monomeric G4 structures [48].

The end-stacking binding mode of this type of binders was confirmed by two X-ray crystal structures of metal-salphens (**23** and **24**) bound to a parallel bimolecular quadruplex (Figure 6) [41]. The corresponding metal center (either Ni^{II} or Cu^{II}) is positioned almost in line with the channel formed by the K^+ ions bound to the G4 structure. This confirmed the initial design principle that a metal complex would be better suited to interact with G4s than purely organic species.

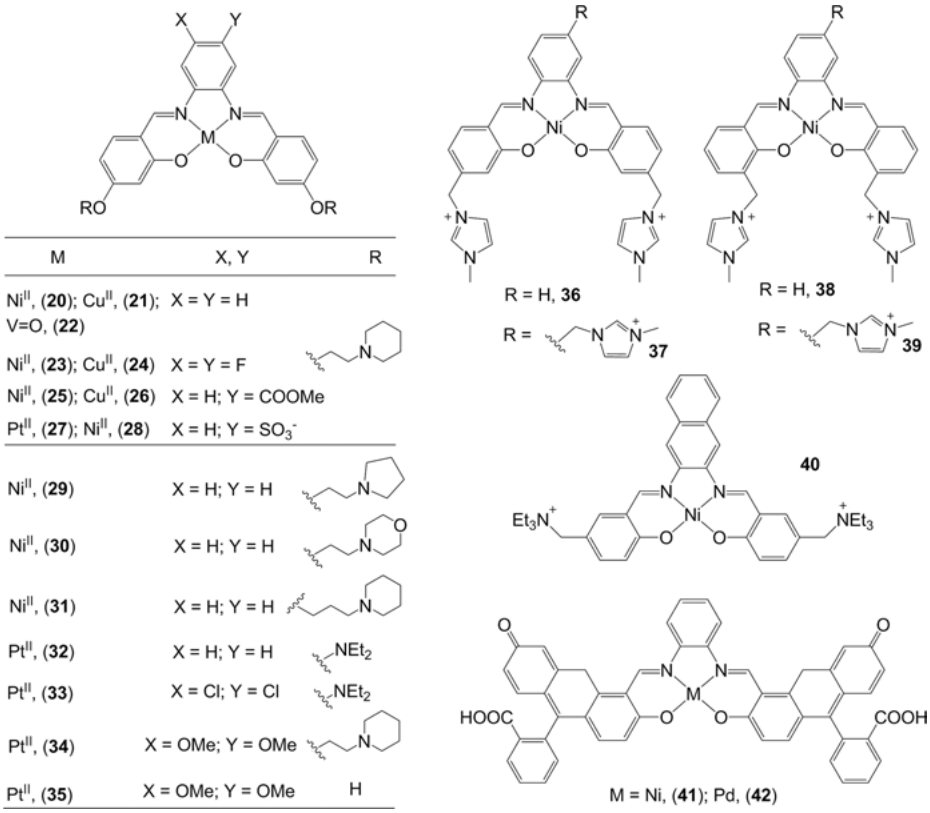

Figure 5. Representative examples of G4 binders based on metal-salphen complexes.

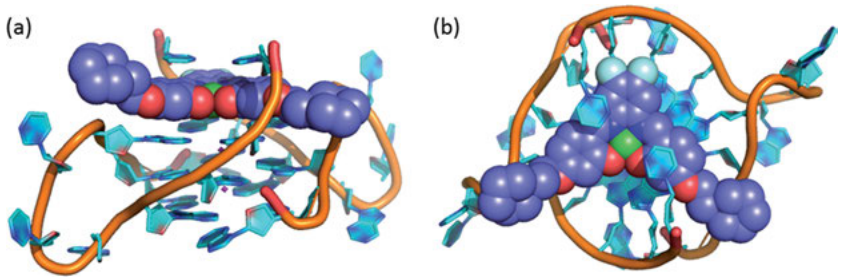

Figure 6. Two views of the X-ray crystal structure of Ni-salphen bound to G4 DNA. Figure generated from PDB 3QSC [42] using PyMol.

Another important family of G4 binders are metal complexes coordinated to tripyridyl ligands. Metal terpyridines were first reported as G4 binders in 2007 by Teulade-Fichou et al. in a study showing that the geometry of the resulting complex dictated its affinity and selectivity for G4 DNA [33]. It was shown that

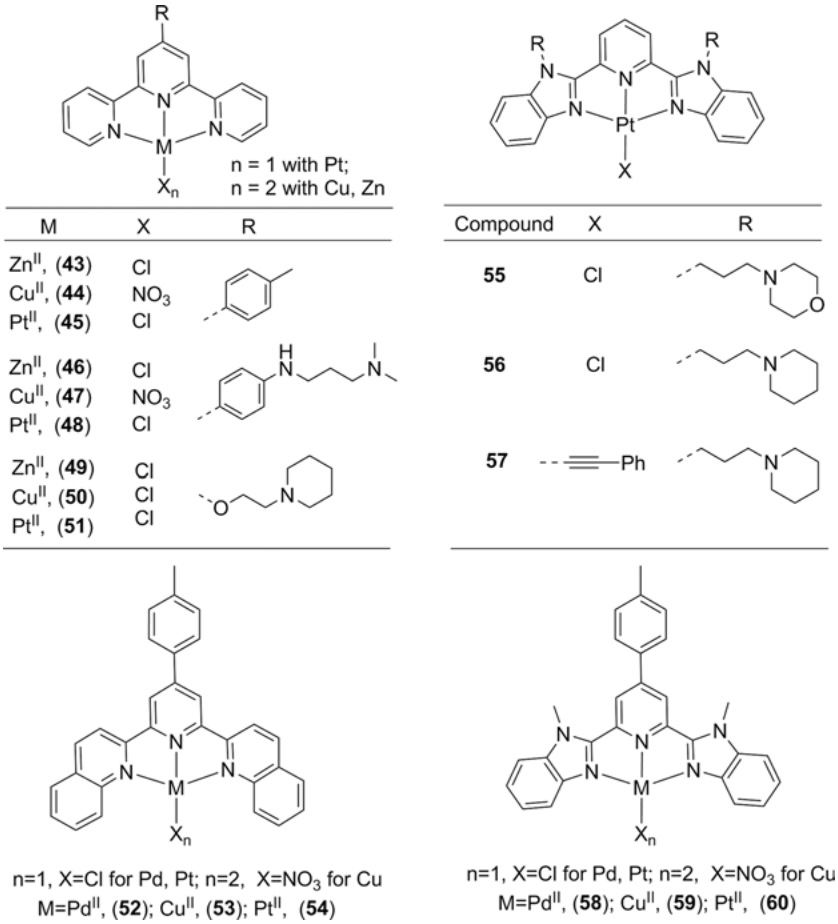

Figure 7. Examples of G4 binders based on metal complexes with tripyridyl ligands.

G4 binding of terpyridine complexes with Cu^{II}, Pt^{II}, Zn^{II} and Ru^{III} (Figure 7) differed greatly, and only those complexes with at least one accessible planar surface to engage in effective π-π stacking with the G-tetrad, bind well to G-quadruplexes. Analogous observations have been reported by other groups using different terpyridines (Figure 7) [49, 50] that have confirmed that the best G4 DNA binders are those with a square-planar geometry and therefore most subsequent studies have focused on complexes with Pt^{II}.

While metal-terpyridines interact with the G-tetrad via π-π stacking interactions, over time they can also display direct coordination of the metal center with bases present in the loops of the G4 structure (e.g., adenines present in the loop of HTelo G4). Interestingly, extending the aromatic surface of the terpyridine (**54**) retains the complex's high affinity for G4 but prevents metalation [51]. More recently, a combined NMR and gel electrophoresis analysis has provided further evidence that **45** binds to *c-myc* G4 DNA via a combination of π-π stacking and direct

coordination [52]. It has also been shown that Pd^{II} complexes with terpyridines and analogous tridentate ligands (Figure 7) often have higher affinities for G4 DNA than the Pt^{II} counterparts [53]. This is due to the Pd^{II} center having a higher propensity to coordinate to bases in the G4 loops than Pt^{II}.

Several other metal complexes with substituted terpyridines have been studied as G-quadruplex DNA binders. This includes photoactivatable Pt^{II}-terpyridines with the ability to bind to G4 DNA via non-covalent interactions, platination and photo-crosslinking [54] as well as Pt^{II}- and Cu^{II}-terpyridine complexes with an anthracene moiety added to the terpyridine ligand [55]. There have also been reports of Pt^{II}-terpyridine complexes where the fourth coordination position on the metal center is occupied by an alkynyl ligand yielding compounds with high affinity for HTelo and *c-myc* G4-DNA [56]. Che et al. have reported a series of luminescent Pt^{II} complexes coordinated to tridentate ligands (e.g., **55–57**) as good *c-myc* G4 binders (see Section 4) [57].

Metal-terpyridines have been functionalized with a second coordinating ligand to yield bi-metallic complexes with very high affinity towards G4 DNA [58, 59]. In addition to these bi-metallic complexes, di-Pt^{II} complexes have also been reported where two Pt^{II}-terpyridine units are linked via alkyl spacers [60]. Some of these complexes displayed high affinity for *c-myc* G4 DNA that is retained even in the presence of a 600-fold excess of competing duplex DNA.

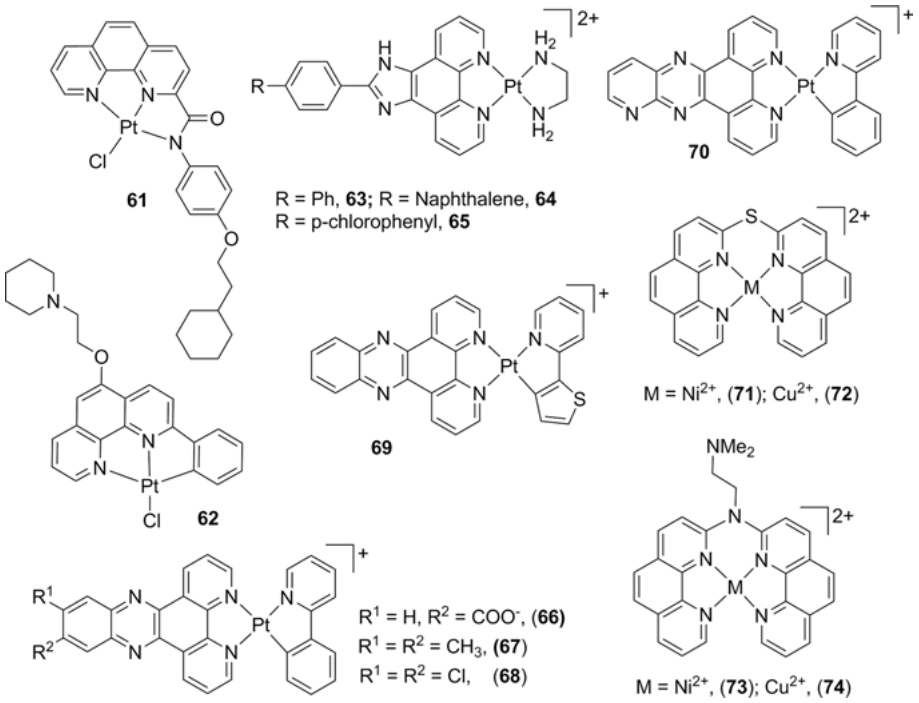

Figure 8. Examples of G4 binders based on square planar complexes with phenanthroline derivatives.

Several other complexes with polypyridyl ligands – mainly based on phenanthroline derivatives – have been studied as G4 DNA binders (Figure 8). Vilar et al. reported that Pt^{II} complexes **61** and **62** had good affinity and selectivity for G4 HTelo DNA; **61** displayed telomerase inhibition activity [61] while **62** was used for cellular imaging [62] (see Sections 4 and 5). Sleiman et al. reported a series of Pt^{II} phenylphenanthroimidazole complexes (**63–65**) with high affinity for G4 DNA [63, 64]. Molecular modelling studies showed that the complexes can efficiently interact with the G-tetrad via π-π stacking interactions. Che and coworkers reported a series of Pt^{II} complexes containing dipyridophenazine (dppz) and C-deprotonated 2-phenylpyridine ligands (**66–70**); complex **66** showed to have high affinity (ca. 10^7 M^{-1}) for G4 HTelo DNA and displayed a large increase in emission intensity (293-fold) upon binding [65]. On the other hand, Sissi et al. reported that the –S or –NR bridged phenanthroline complexes **71–74** can stabilize the melting temperature of G4 DNA by up to 30 °C – while the free ligand did not show significant binding affinity to G4 [66].

3.1.3. Octahedral Complexes and Supramolecular Metallo-Assemblies

The complexes discussed in the previous section are square planar (or square-based pyramidal) and therefore in most cases the metal is located within the unit that stacks on top of the G-tetrads. In this section we will discuss G4 binders with octahedral geometries containing ligands that have a large planar aromatic surface for efficient π-π stacking interactions with the G-tetrad. In these cases the metal center is normally located on the side of the G-tetrad rather than forming part of the π-π stacking unit – which is similar to what is observed when octahedral metal complexes intercalate into duplex DNA. Thomas et al. reported in 2006 that the di-ruthenium complexes **75** and **76** (Figure 9) interact with both calf thymus (CT) DNA and with HTelo G-quadruplex DNA [34]. These complexes displayed an increase in emission intensity upon binding to DNA (2.5 higher when interacting with G4 than with CT-DNA), a blue-shift and different emission lifetimes when bound to each of the two topologies (with longer lifetimes when bound to G4 DNA). A subsequent study with **75** showed that its ΛΛ isomer has a ca. 40-times higher affinity for HTelo G4 DNA than the ΔΔ isomer. In this study, the binding mode of the compound to G4 DNA was also investigated by NMR spectroscopy and molecular dynamics calculations [67]. These studies established that **75** binds to both ends of the G4 structure and that the ΛΛ isomer (but not the ΔΔ isomer) fits well under the diagonal loop (Figure 10) providing a structural rational for the differences in G4 DNA affinity between the two stereoisomers.

Following these first reports, several octahedral ruthenium complexes have been reported as good G4 binders (Figure 9) [68–72]. In most cases, they also exhibit a fluorescence 'switch-on' effect making them attractive scaffolds for the development of DNA optical probes (see below).

Although the vast majority of octahedral G4 binders are based on Ru^{II} complexes, some examples with Ir^{III} have also been reported (Figure 9) [73–75]. Sleiman et al. showed that complexes with the general formula $[Ir(ppy)_2(N^{\wedge}N)]^+$

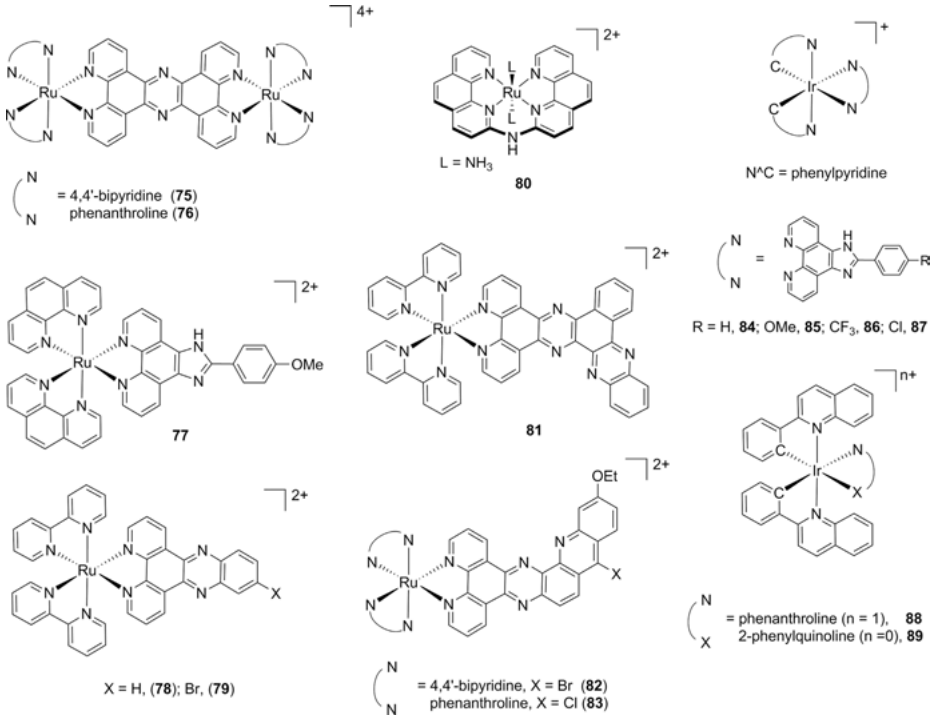

Figure 9. Representative examples of G4 binders based on octahedral mono- and di-metal complexes.

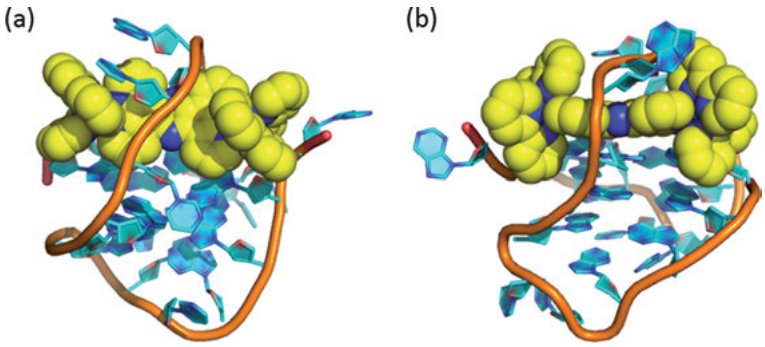

Figure 10. Structure of the di-Ru complex ΛΛ**-75** bound to G4 DNA. The structure (top view, (**a**) and side view (**b**)) shows how the ΛΛ isomer of complex **75** threads through the loop and the G-tetrad. Figure generated from PDB 2MCO [67] using PyMol.

(where ppy = 2-phenylpyridinato and N^N = derivatives of phenylimidazole phenanthrolines – e.g., complexes **84–87**) bind to HTelo G4 DNA with low micromolar affinities [73]. Several other octahedral iridium(III) complexes such as **88** and **89**

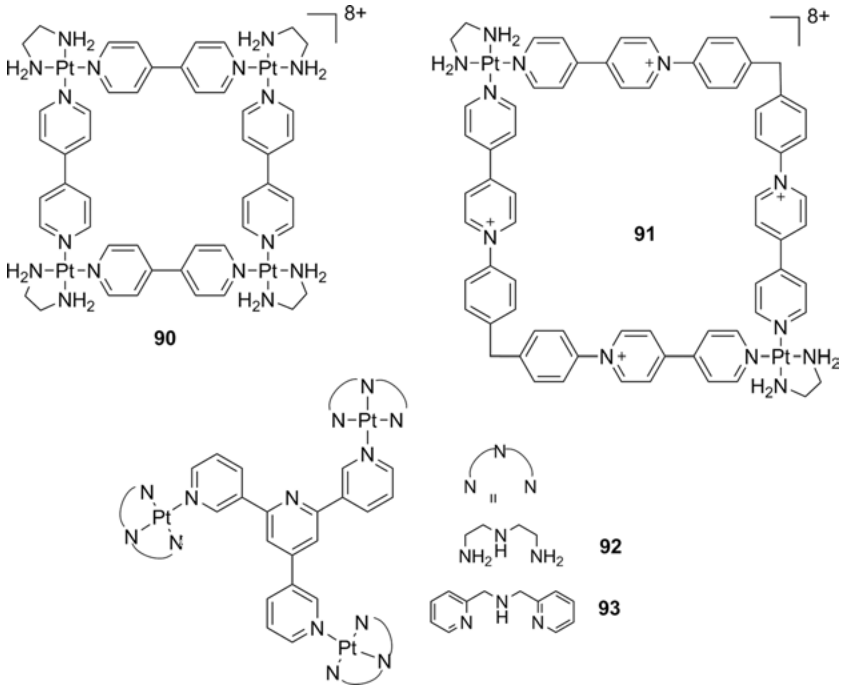

Figure 11. Examples of poly-nuclear assemblies that have been studied as G4 DNA binders.

(Figure 9) have been reported by Ma, Leung, and coworkers as G-quadruplex DNA binders [74, 76].

Another class of non-planar systems that can display excellent G-quadruplex binding properties, are supramolecular metallo-assemblies. In 2008 Sleiman et al. reported the first example of this type of systems as G4 DNA binder [77]. It was shown that the Pt^{II}-square **90** has a high binding affinity towards the HTelo G4 DNA. Molecular modelling studies suggested that this metallo-assembly interacts with G4 DNA thanks to the square arrangement of the bipyridyl bridging ligands, the high electrostatic charge of the assembly and the hydrogen bonding interactions between the ethylendiamine ligands (coordinated to each Pt^{II} center) and the phosphate backbone of DNA. Following this study, several other supramolecular metallo-assemblies including cubes [78], helicates [79], rectangles [80], and other squares [81–83] have been reported as good G4 DNA binders.

In a different approach, Mao et al. have reported that the tri-platinum(II) complexes **92** and **93** (as well as di-Pt^{II} analogues) have high affinity for HTelo G4 DNA over duplex DNA and, more interestingly, over other G4 structures such as *c-myc* and *BCL2* [84–86].

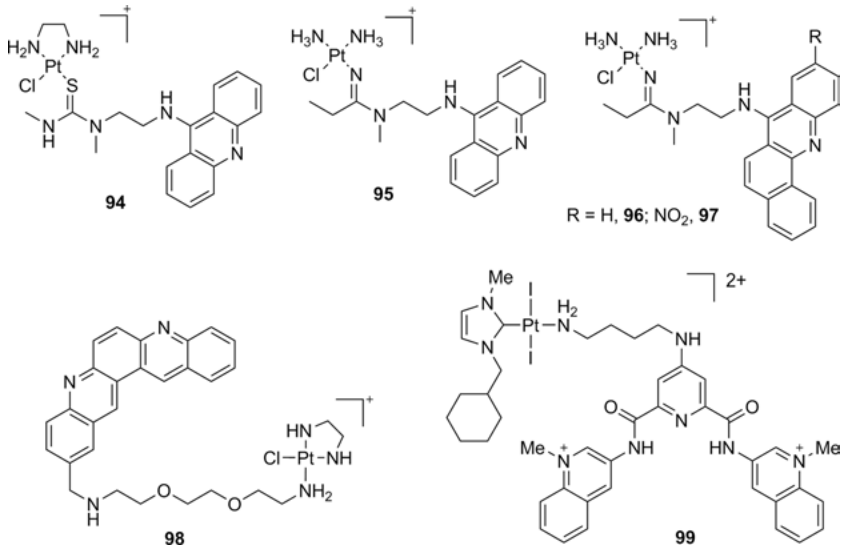

Figure 12. Examples of complexes that interact with G4 DNA via a combined π-stacking and coordination binding mode.

3.2. Direct Coordination of the Metal to G-Quadruplexes

It is also possible for metal complexes to interact with G4 structures via direct coordination between the metal center and nucleobases. As has already been mentioned above, some Pt^{II} and Pd^{II} terpyridine complexes interact with G4 DNA, not only via π-π stacking, but also by direct coordination [51, 53]. Other examples of complexes that metallate G4 DNA are based on a dual binding mode, namely a polyaromatic unit designed to interact with the G-tetrad via π-π stacking linked to a platinum(II) complex able to coordinate to nucleobases (Figure 12).

Bierbach and coworkers have reported a series of complexes (**94–97**) using this approach and showed that they have higher kinetic preference for platination at adenine (N7 site) over guanine [87–89]. Bombard et al. have reported other complexes that platinate G4 DNA [90, 91], for example **99** which binds preferentially and irreversibly to G4 HTelo DNA. Interestingly, this complex also showed a different binding profile than the unsubstitued Pt-NHC unit indicating that the pyridodicarboxamide is important in directing the complex to the G4 structure [91].

4. METAL-BASED OPTICAL PROBES FOR G-QUADRUPLEXES

The luminescence of several metal complexes (mainly with Pt^{II} and Ru^{II}) has been exploited to develop optical probes to detect and visualize G4s. This con-

tributes significantly to the development of potential metallo-drugs since it allows the study of G4 binding *in vitro*, and establishes cellular uptake and localization of the complexes. The general area of optical probes for G-quadruplexes has been previously reviewed by Luedtke et al. [92] and Teulade-Fichou et al. [93].

Most G4 optical probes based on metal complexes, are switch-on probes, namely compounds that have low or no emission under physiological conditions and upon interaction with DNA their emission intensity increases. The Ru^{II} compounds **75** and **76** were the first examples of metal complexes used as *in vitro* switch-on probes for G-quadruplexes [34]. In addition to displaying an increase in emission intensity upon DNA binding, these complexes also showed a blue-shift and a different emission lifetime when bound to G4 as compared to dsDNA. A confocal microscopy study using breast cancer MCF-7 cells, showed that complex **76** is cell-permeable, localizes in the nucleus, and binds to DNA [10]. Furthermore, lambda stacking experiments (i.e., measuring emission intensity across a range of wavelengths with a single excitation wavelength) showed two different emission maxima at ca. 680 and 630 nm in cells corresponding to approximately the same values observed *in vitro* for duplex DNA and G4 DNA. Following these initial studies by Thomas [10, 34], most Ru^{II} complexes reported to date as G4 DNA binders have been shown to be switch-on probes displaying a range of selectivities for G4 versus duplex DNA. While most studies have only focussed on *in vitro* studies [69, 94, 95], the cellular uptake and localization of some of these Ru^{II} complexes have also been investigated [68, 72, 96]. For example, Monchaud et al. have reported that complexes **82** and **83** display up to 330-fold luminescence enhancement upon interaction with G4 DNA [72]. This study also showed that complex **82** is cell-permeable (using melanoma B16F10 cell line) staining the nucleoli and perinuclear cytoplasmic foci.

More recently, octahedral Ir^{III} cyclometallated complexes have also been shown to act as switch-on probes for G4 DNA. For example, upon binding to HTelo G4 DNA, complexes **84–89** displayed enhanced luminescence with the best complex displaying a 53-fold increase as well as a 42 nm blue-shift. Interestingly, this switch-on effect was not observed with duplex or single-stranded DNA [73]. The switch-on effect displayed by **88** when bound to G4 DNA has been successfully employed as a luminescent test for hepatitis C virus NS3 helicase activity [74].

Pt^{II} complexes are the other large class of compounds that have been studied as switch-on optical probes for G4 DNA. Examples of this type of probes include Pt^{II} complexes **66–69** coordinated to dipyridophenazine ligands [65], **62** coordinated to a substituted phenanthroline [62] and several Pt^{II}-salphen complexes (e.g., **27** and **32–35**) [42, 46]. The platinum-dipyridophenazine derivatives show significant increase in their photoluminescence upon G4 DNA binding (ca. 290-fold for **66**) as well as telomerase inhibition activity (see below). Although most Pt^{II}-based optical probes for G4 DNA have been studied *in vitro* via emission spectroscopy, a number of complexes have also been investigated in cells. For example, **62**, which has a 1000-fold higher affinity for *c-myc* and HTelo G4 than for duplex DNA, was investigated both *in vitro* and in cells [62]. Although the

complex is not taken up by cells (osteosarcoma U2OS) on its own, when encapsulated inside a ruthenium supramolecular cage known to act as 'transporter', it is readily internalized and a significant proportion of **62** stains the cell nucleus as shown by confocal microscopy. Interestingly, while this probe interacts with DNA it does not co-localize with DAPI (a duplex DNA minor groove binder) suggesting that it might be preferentially binding to alternative DNA topologies.

Two studies have shown that metal-salphen complexes are cell permeable and localize in the nucleus. The first of these studies showed that **27** has higher affinity for G4 DNA than for duplex DNA and upon binding its emission is switched on [42]. Confocal microscopy studies with HeLa cells incubated with **27** showed that the complex is cell-permeable and localizes in the nucleus (with some distinct nucleoli staining). In the second study, Ni^{II} and Pd^{II} salphen complexes (**41** and **42**) were made emissive by introducing fluorescein as part of the ligand's backbone [43]. These complexes were incubated with cancer cells HEK 293T and A549 and confocal microscopy studies showed that they are cell-permeable and accumulate in the nucleus and mitochondria.

Luedtke et al. reported that the Zn^{II}-phthalocyanine **16** is an excellent G4 binder and can be used as optical probe [38]. This complex displays a ca. 200-fold increase in its photoluminescence upon interaction with G4 structures and a selectivity of ca. 5000-fold higher for G4 (*c-myc*) than for CT-DNA. In addition, confocal microscopy also showed that **16** is taken up by a wide range of live cells including HeLa, MCF7, B16F10, SH-SY5Y, *E. coli* BL-21, and SK-Mel-28. Interestingly, the cellular localization of this probe was significantly different to that of well-established duplex DNA probes suggesting that its cellular target could be non-canonical DNA structures.

5. BIOLOGICAL ACTIVITY OF METAL-BASED G-QUADRUPLEX BINDERS

As has been discussed in the preceding sections there are now many metal complexes that display excellent *in vitro* affinity for G-quadruplexes as well as good selectivity over duplex DNA. In some cases, cellular studies with the corresponding complexes have been performed to establish their biological activity. However, to date there is still very little direct evidence linking the targeting of G4s by metal complexes with their observed cellular effects (e.g., cytotoxicity against cancer cell lines). The following two sections discuss a selection of complexes that have been shown to bind either HTelo DNA or oncogene promoters *in vitro* and for which biological studies have shown the potential of these complexes as metallo-drugs.

5.1. Metallo-Binders that Target Telomeric G4

As explained in Section 2.2, the stabilization of G4 structures in telomeric DNA has been shown to inhibit the activity of telomerase (which is overexpressed in

more than 85 % of cancer cells). The telomerase repeat amplification protocol (TRAP) assay is a cell-free method that is extensively used to assess the inhibition of telomerase by G4 binders. However, it is important to note that the original TRAP assay often overestimates the activity of compounds as telomerase inhibitors since it does not account for the possible inhibition of the polymerase used in the assay by the compounds under study. Some protocols such as the TRAP-LIG [97] and TRAP-G4 [98] assays have been subsequently reported which overcome some of the problems of the original method.

Several of the studies reporting EC_{50} values for telomerase, have been aimed at establishing a structure activity relation (SAR) for the complexes under investigation and correlate the G4 binding properties of the compounds with their ability to inhibit telomerase. Some of the parameters that have been investigated are metal geometry, overall charge of the complex and the number and nature of the ligand substituents. For example, in 2001 Hurley et al. studied a wide range of substituted porphyrins including TMPyP4 complexes with Ni^{II}, Pd^{II}, Pt^{II}, Co^{II}, Cu^{II}, Mn^{III}, Fe^{III}, and Mg^{II} [27]. Using a cell-free primer extension assay, the study suggested that those complexes with an unhindered face for stacking were better inhibitors. Thus, the square planar Cu^{II} and square-based pyramidal Zn^{II} complexes displayed 75 % and 88 % inhibition, respectively, at 25 μM, while octahedral complexes such as those with Mg^{II} and Mn^{III} showed lower activity (42 and 37 %, respectively). However, the SAR with some of the other metal complexes was not as straightforward since the octahedral Fe^{III} complex showed reasonably high inhibition at 67 %. Three subsequent studies by Pratviel et al. showed that Mn^{III} and Ni^{II} complexes with substituted TMPyP4 porphyrins, such as **10** and **12**, also had telomerase inhibitory activity at low μM concentrations ($EC_{50} = 0.6$ for **10** using the TRAP assay) [28, 30, 37]. Similarly, metallo-phthalocyanines were shown to inhibit telomerase with EC_{50} of 2.1 μM [99].

The other large family of complexes for which telomerase inhibition data has been reported are metal-salphens. The Ni^{II} and Cu^{II} complexes **20**, **23** and **24** have EC_{50} values of 11.7, 19.2, and 3.6 μM, respectively (with the modified TRAP-LIG assay), however, there was no clear correlation between these values and the affinity of the complexes for G4 HTelo DNA [41]. In this work, it was also shown that **20**, **23**, and **24** are significantly cytotoxic (IC_{50} values between 0.8 and 6.4 μM) against several cancer cell lines including MCS7, A549, RCC4, and Mia-PaCa-2, although they also showed to be active against the non-cancer cell line WI38. On the other hand, **41** (with a much larger π-aromatic system) displayed high telomerase inhibition activity with an EC_{50} of 0.9 μM using the TRAP-LIG assay [43]. Interestingly, this complex showed to have poor cytotoxicity on HEK 293T and HeLa in the short-term (72 h), however, a long-term viability assay (15 day) showed the complex to be cytotoxic. Similarly, the imidazolium-substituted nickel-salphen complexes **36–39** have good affinity for G4 Htelo DNA and display high telomerase inhibition; in particular, **39** with the imidazolium substituents in ortho position displays excellent inhibition towards telomerase with an EC_{50} value of 70 nM (using the TRAP-G4) [44].

Telomerase inhibition studies with several Pt^{II} complexes coordinated to derivatives of phenanthrolines have also been reported. **61** was the first of this series

of compounds to be investigated as telomerase inhibitor showing a modest EC_{50} of 49.5 μM (using the TRAP-LIG assay); in contrast, the uncoordinated ligand did not show significant activity ($EC_{50} > 200$ μM) highlighting the importance of the metal center in the telomerase-inhibition activity [61]. On the other hand, the Pt^{II} complex **63** is a potent inhibitor of telomerase *in vitro* (100 % inhibition at 50 μM using the TRAP-LIG assay) [64], it inhibits the seeding capacity of A549 lung cancer cells and decreases the average telomere length of A549 cells over time [100].

Octahedral complexes have also been shown to be telomerase inhibitors. For example, the enantiomerically pure Λ-**77** complex (with much higher G4 DNA affinity than the Δ-**77** isomer) inhibits telomerase in a dose-response fashion (with concentrations between 1 and 32 μM) while the Δ-**77** enantiomer is a poor telomerase inhibitor [68]. The antiproliferative properties of both Λ- and Δ-**77** were investigated using the MTT assay against various cancer cell lines (i.e., HepG2, A549, HeLa, and SW62) and mouse fibroblast (NIH/3T3), showing that Λ-**77** is generally more cytotoxic than Δ-**77**, and particularly against cancer cells (IC_{50} between 4.4 and 32 μM). On the other hand, the molecular square **90** showed to be very active as telomerase inhibitor with $EC_{50} = 0.2$ μM (using a modified version of the original TRAP assay) [77].

While significant telomerase inhibition data has now been reported for many G4 binders, no clear SAR has emerged encompassing all the complexes. As indicated above, part of the problem is the differences in how the TRAP assay is performed as well as the fact that potentially more than one effect – not only telomerase inhibition – is being measured in this assay. It has also become evident that the interplay between telomerase, telomeric DNA, and telomere-binding proteins (such as POT1 and TRF2) in cells is very complex. Therefore, the effects of G4-binding compounds in telomere biology is expected to be far more complex than what the cell-free TRAP assay unveils. Some studies with metal complexes have already been carried out towards this aim. For example Pratviel et al. have shown that a Ni^{II}-porphyrin with four phenyl guanidinium substituents, has high *in vitro* affinity for telomeric G4 DNA, is able to displace hPOT1 from telomeres, and has a moderate antiproliferative effect on A549 cells [101]. On the other hand, Bombard et al. reported detailed cellular studies with the platinating complex **99** using the ovarian cancer A2780 and A2780cis cell lines, which are sensitive and resistant to the antitumor drug cisplatin, respectively [91]. The complex was shown to have good cellular permeability and IC_{50} values of 8 and 15 μM for these cell lines, respectively. One of the key findings of this study was that **99** induces a significant loss of TRF2 (a protein that is essential for telomere maintenance) from telomeres. Interestingly, the displacement of TRF2 by this compound was significantly higher than any of its individual components suggesting an important synergistic effect between the coordinating Pt^{II} moiety and the G4-DNA binding group of the conjugate.

One of the observed consequences of G4 stabilization by small molecules is an increase in DNA damage and some studies with metal complexes have explored this approach. For example, the Pt-terpyridine complex **48**, which has high affinity for G4 HTelo DNA, has been shown to enhance the sensitivity to

ionizing radiation of human glioblastoma (SF763 and SF767) and non-small cell lung cancer (A549 and H1299) cells [102]. This complex displayed sub-μM antiproliferative properties against these cancer cell lines and, when non-toxic concentrations of the complex were used, radiosensensitization of all cell lines was observed. It was proposed that this effect might by due to DNA damage induced by **48**, especially in the telomeric region – although it cannot be excluded that the observed effects are due to the interaction of the compound with other G4-forming regions such as those found in promoters of oncogenes. In a different study, Mao et al. have shown that the tri-Pt complexes **92** and **93** have a high affinity and selectivity for G4 HTelo DNA *in vitro* and inhibit telomerase (using the TRAP assay) [86]. The effects of these complexes on cells were investigated showing that they have comparable cytotoxicity to cisplatin not only in telomerase-positive cancer cells (HeLa, A549, and HTC75) but also in telomerase-negative ALT cells (SAOS2, U2OS, and VA13). While these observations would not be consistent with the inhibition of telomerase in cells, the complexes display a strong telomeric DNA damage response in HeLa cells resulting in telomere dysfunction and cell senescence.

The selective cleavage of telomeric DNA is another potential approach for anticancer agents. Recently, Yu, Han, and Cowan showed that a Cu^{II} complex attached to acridine, binds selectively to HTelo G4 DNA structures (over duplex DNA) and cleaves it irreversibly – in preference to HTelo DNA folded in different structures [103]. The complex also showed to induce senescence and apoptosis in breast cancer cells (MCF7), as well as shortening of the telomere after 7 days treatment.

5.2. Metallo-Binders that Target Gene Promoters

As discussed in Section 2.2, stabilizing G4s in oncogene promoters could lead to downregulation of the corresponding gene and therefore provide a new target for the development of anticancer agents [4]. Luedtke et al. showed that the Zn^{II}-phthalocyanine **16** localizes in the cell nucleus (see Section 4) and also downregulates *c-myc* expression [38]. Addition of a non-cytotoxic concentration (1 μM) of this complex to neuroblastoma cells (SH-SY5Y) followed by a quantitative reverse transcription-polymerase chain reaction (qRT-PCR) analysis, showed a time-dependent decrease in *c-myc* expression (up to threefold).

Two other studies reported that the Pt^{II}-salphen and Pt^{II}-benzimidazole complexes **32–35** and **55–57**, respectively [46, 57], have a high affinity for *c-myc* G4 structures. The levels of *c-myc* mRNA from hepatocarcinoma cells (HepG2) were determined after they had been incubated with different doses of the compounds under study. It was shown that some of these complexes induced a significant decrease in the levels of *c-myc* mRNA (determined by RT-PCR rather than the more accurate qRT-PCR), with **55** being one of the most potent complexes (IC_{50} of ca. 17 μM).

The Pt^{II} assembly **91** has high affinity towards *c-kit* and *BCL2* G4 structures (although it also has high affinity towards dsDNA) [82]. mRNA levels of *c-*

kit and *BCL2* were determined by qRT-PCR after treating cancer cells (VM-1 melanoma cells for *c-kit* and MCF-7 breast cancer cells for *BCL2*) with **91**. For both these genes, a significant reduction on mRNA levels was observed after 24-hour incubation with **91**.

An unusual metal-mediated upregulation of *c-myc* has been recently reported by Vázquez, Mascareñas et al. [104]. When the complex $[Ru(terpy)(bpy)Cl]^+$ was added to the *c-myc* sequence $d[TTGAG_3TG_3TAG_3TG_3TA_3]$ in 100 mM KCl (to form the G4) and irradiated ($\lambda = 455$ nm), the clean formation of a mono-adduct between $[Ru(terpy)(bpy)]^{2+}$ and *c-myc* was observed. It was also determined that the metallation occurs exclusively in the first guanine of the sequence, which is not involved in the G4 structure. Prompted by this observation, they investigated whether the complex could regulate the expression of *c-myc* when added to cells (HeLa and Vero). Surprisingly, they observed an increase in the amount of *c-myc* mRNA (measured by qRT-PCR) rather than a downregulation as has been observed in most cases when small molecules interact with the *c-myc* promoter.

6. CONCLUDING REMARKS AND FUTURE DIRECTIONS

Since the first reports in the early 2000s that metal complexes can be effective G-quadruplex binders, the field has expanded rapidly. Several families of compounds ranging from planar mono-metallic complexes to multi-metallic supramolecular assemblies have been successfully developed as G4 binders. Some of them have been used as optical probes (both *in vitro* and in cells) while others have shown to be cytotoxic.

Unveiling the exact biomolecular target(s) of metal complexes and therefore establishing whether they indeed bind to G4s in cells, is a challenging and exciting problem that will likely be the main focus of future research in this area. This will require the development of metal complexes with much higher selectivity for G4 DNA, better biocompatibility, and useful functionalities (such as optical properties).

ACKNOWLEDGMENTS

The author thanks EPSRC and BBSRC for financial support and all coworkers, past and present, for their input and stimulating discussions.

ABBREVIATIONS

ALT	alternative lengthening of telomeres
bpy	bipyridine
BCL2	B-cell lymphoma-2

CT-DNA	calf thymus DNA
DAPI	4′,6-diamidino-2-phenylindole
dppz	dipyridophenazine
EC_{50}	half maximal effective concentration
G4	guanine quadruplex
HTelo	human telomeric
IC_{50}	half maximal inhibitory concentration
KRAS	Kirsten rat sarcoma
MTT	3-(4,5-dimethylthiazol-2-yl)-2,5-diphenyltetrazolium bromide
NHC	*N*-heterocyclic carbene
POT1	protection of telomeres protein 1
ppy	2-phenylpyridinato
qRT-PCR	quantitative reverse transcription-polymerase chain reaction
SAR	structure-activity relationship
terpy	terpyridine
TMPyP4	tetra-(N-methyl-4-pyridyl)porphyrin
TRAP	telomerase repeat amplification protocol
TRAP-LIG	a modified telomerase repeat amplification protocol (TRAP) that accounts for possible inhibition of polymerase by the ligand being tested
TRF2	telomeric repeat-binding factor 2
5′-UTR	5’-untranslated region

REFERENCES

1. G. N. Parkinson, M. P. H. Lee, S. Neidle, *Nature* **2002**, *417*, 876–880.
2. D. Rhodes, H. J. Lipps, *Nucleic Acids Res.* **2015**, *43*, 8627–8637.
3. R. Hansel-Hertsch, M. Di Antonio, S. Balasubramanian, *Nat. Rev. Mol. Cell Biol.* **2017**, *18*, 279–284.
4. S. Balasubramanian, L. H. Hurley, S. Neidle, *Nat. Rev. Drug Discovery* **2011**, *10*, 261–275.
5. S. Neidle, *J. Med. Chem.* **2016**, *59*, 5987–6011.
6. P. Murat, S. Balasubramanian, *Curr. Opin. Genet. Dev.* **2014**, *25*, 22–29.
7. C. Schaffitzel, I. Berger, J. Postberg, J. Hanes, H. J. Lipps, A. Plückthun, *Proc. Natl. Acad. Sci. USA* **2001**, *98*, 8572–8577.
8. G. Biffi, D. Tannahill, J. McCafferty, S. Balasubramanian, *Nat. Chem.* **2013**, *5*, 182–186.
9. A. Shivalingam, M. A. Izquierdo, A. L. Marois, A. Vysniauskas, K. Suhling, M. K. Kuimova, R. Vilar, *Nat. Commun.* **2015**, *6*, 8178.
10. M. R. Gill, J. Garcia-Lara, S. J. Foster, C. Smythe, G. Battaglia, J. A. Thomas, *Nat. Chem.* **2009**, *1*, 662–667.
11. W.-C. Huang, T.-Y. Tseng, Y.-T. Chen, C.-C. Chang, Z.-F. Wang, C.-L. Wang, T.-N. Hsu, P.-T. Li, C.-T. Chen, J.-J. Lin, P.-J. Lou, T.-C. Chang, *Nucleic Acids Res.* **2015**, *43*, 10102–10113.
12. W. E. Wright, V. M. Tesmer, K. E. Huffman, S. D. Levene, J. W. Shay, *Genes Dev.* **1997**, *11*, 2801–2809.
13. A. K. Todd, M. Johnston, S. Neidle, *Nucleic Acids Res.* **2005**, *33*, 2901–2907.

14. J. L. Huppert, S. Balasubramanian, *Nucleic Acids Res.* **2005**, *33*, 2908–2916.
15. A. Bedrat, J.-L. Mergny, L. Lacroix, *Nucleic Acids Res.* **2016**, *44*, 1746–1759.
16. S. Chambers Vicki, G. Marsico, M. Boutell Jonathan, P. Smith Geoffrey, M. Di Antonio, S. Balasubramanian, *Nat. Biotechnol.* **2015**, *33*, 877–881.
17. R. Hansel-Hertsch, D. Beraldi, S. V. Lensing, G. Marsico, K. Zyner, A. Parry, M. Di Antonio, J. Pike, H. Kimura, M. Narita, D. Tannahill, S. Balasubramanian, *Nat. Genet.* **2016**, *48*, 1267–1272.
18. J.-D. Beaudoin, J.-P. Perreault, *Nucleic Acids Res.* **2010**, *38*, 7022–7036.
19. J. L. Huppert, A. Bugaut, S. Kumari, S. Balasubramanian, *Nucleic Acids Res.* **2008**, *36*, 6260–6268.
20. S. Kumari, A. Bugaut, J. L. Huppert, S. Balasubramanian, *Nat. Chem. Biol.* **2007**, *3*, 218–221.
21. J. U. Guo, D. P. Bartel, *Science* **2016**, *353*, 1382.
22. S. A. Ohnmacht, S. Neidle, *Bioorg. Med. Chem. Lett.* **2014**, *24*, 2602–2612.
23. S. Neidle, *Nature Reviews Chemistry* **2017**, *1*, 10.
24. D. Sun, B. Thompson, B. E. Cathers, M. Salazar, S. M. Kerwin, J. O. Trent, T. C. Jenkins, S. Neidle, L. H. Hurley, *J. Med. Chem.* **1997**, *40*, 2113–2116.
25. N. Georgiades Savvas, H. Abd Karim Nurul, K. Suntharalingam, R. Vilar, *Angew. Chem. Int. Ed. Engl.* **2010**, *49*, 4020–4034.
26. Q. Cao, Y. Li, E. Freisinger, P. Z. Qin, R. K. O. Sigel, Z.-W. Mao, *Inorg. Chem. Front.* **2017**, *4*, 10–32.
27. D.-F. Shi, R. T. Wheelhouse, D. Sun, L. H. Hurley, *J. Med. Chem.* **2001**, *44*, 4509–4523.
28. A. Maraval, S. Franco, C. Vialas, G. Pratviel, M. A. Blasco, B. Meunier, *Org. Biomol. Chem.* **2003**, *1*, 921–927.
29. L. R. Keating, V. A. Szalai, *Biochemistry* **2004**, *43*, 15891–15900.
30. I. M. Dixon, F. Lopez, J.-P. Esteve, A. M. Tejera, M. A. Blasco, G. Pratviel, B. Meunier, *ChemBioChem* **2005**, *6*, 123–132.
31. J. E. Reed, A. A. Arnal, S. Neidle, R. Vilar, *J. Am. Chem. Soc.* **2006**, *128*, 5992–5993.
32. A. Arola-Arnal, J. Benet-Buchholz, S. Neidle, R. Vilar, *Inorg. Chem.* **2008**, *47*, 11910–11919.
33. H. Bertrand, D. Monchaud, A. De Cian, R. Guillot, J.-L. Mergny, M.-P. Teulade-Fichou, *Org. Biomol. Chem.* **2007**, *5*, 2555–2559.
34. C. Rajput, R. Rutkaite, L. Swanson, I. Haq, J. A. Thomas, *Chem. Eur. J.* **2006**, *12*, 4611–4619.
35. S. F. Ralph, *Curr. Top. Med. Chem.* **2011**, *11*, 572–590.
36. A. J. Bhattacharjee, K. Ahluwalia, S. Taylor, O. Jin, J. M. Nicoludis, R. Buscaglia, J. Brad Chaires, D. J. P. Kornfilt, D. G. S. Marquardt, L. A. Yatsunyk, *Biochimie* **2011**, *93*, 1297–1309.
37. I. M. Dixon, F. Lopez, A. M. Tejera, J.-P. Esteve, M. A. Blasco, G. Pratviel, B. Meunier, *J. Am. Chem. Soc.* **2007**, *129*, 1502–1503.
38. J. Alzeer, B. R. Vummidi, P. J. C. Roth, N. W. Luedtke, *Angew. Chem., Int. Ed.* **2009**, *48*, 9362–9365.
39. J. Alzeer, N. W. Luedtke, *Biochemistry* **2010**, *49*, 4339–4348.
40. L. Ren, A. Zhang, J. Huang, P. Wang, X. Weng, L. Zhang, F. Liang, Z. Tan, X. Zhou, *ChemBioChem* **2007**, *8*, 775–780.
41. N. H. Campbell, N. H. A. Karim, G. N. Parkinson, M. Gunaratnam, V. Petrucci, A. K. Todd, R. Vilar, S. Neidle, *J. Med. Chem.* **2012**, *55*, 209–222.
42. N. H. Abd Karim, O. Mendoza, A. Shivalingam, A. J. Thompson, S. Ghosh, M. K. Kuimova, R. Vilar, *RSC Adv.* **2014**, *4*, 3355–3363.
43. A. Ali, M. Kamra, S. Roy, K. Muniyappa, S. Bhattacharya, *Bioconjugate Chem.* **2017**, *28*, 341–352.

44. L. Lecarme, E. Prado, A. De Rache, M.-L. Nicolau-Travers, G. Gellon, J. Dejeu, T. Lavergne, H. Jamet, D. Gomez, J.-L. Mergny, E. Defrancq, O. Jarjayes, F. Thomas, *ChemMedChem* **2016**, *11*, 1133–1136.
45. K. J. Davis, C. Richardson, J. L. Beck, B. M. Knowles, A. Guedin, J.–L. Mergny, A. C. Willis, S. F. Ralph, *Dalton Trans.* **2015**, *44*, 3136–3150.
46. P. Wu, D.-L. Ma, C.-H. Leung, S.-C. Yan, N. Zhu, R. Abagyan, C.-M. Che, *Chem. Eur. J.* **2009**, *15*, 13008–13021.
47. A. Ali, M. Kamra, S. Roy, K. Muniyappa, S. Bhattacharya, *Chem. Asian J.* **2016**, *11*, 2542–2554.
48. C.-Q. Zhou, T.-C. Liao, Z.-Q. Li, J. Gonzalez-Garcia, M. Reynolds, M. Zou, R. Vilar, *Chem. Eur. J.* **2017**, *23*, 4713–4722.
49. K. Suntharalingam, A. J. P. White, R. Vilar, *Inorg. Chem.* **2009**, *48*, 9427–9435.
50. J.-T. Wang, Y. Li, J.-H. Tan, L.-N. Ji, Z.-W. Mao, *Dalton Trans.* **2011**, *40*, 564–566.
51. H. Bertrand, S. Bombard, D. Monchaud, E. Talbot, A. Guedin, J.-L. Mergny, R. Grunert, P. J. Bednarski, M.-P. Teulade-Fichou, *Org. Biomol. Chem.* **2009**, *7*, 2864–2871.
52. M. Trajkovski, E. Morel, F. Hamon, S. Bombard, M.-P. Teulade-Fichou, J. Plavec, *Chem. Eur. J.* **2015**, *21*, 7798–7807.
53. E. Largy, F. Hamon, F. Rosu, V. Gabelica, E. De Pauw, A. Guedin, J.-L. Mergny, M.-P. Teulade-Fichou, *Chem. Eur. J.* **2011**, *17*, 13274–13283.
54. E. Morel, F. Poyer, L. Vaslin, S. Bombard, M.-P. Teulade-Fichou, *Inorg. Chim. Acta* **2016**, *452*, 152–158.
55. S. Gama, I. Rodrigues, F. Mendes, I. C. Santos, E. Gabano, B. Klejevskaja, J. Gonzalez-Garcia, M. Ravera, R. Vilar, A. Paulo, *J. Inorg. Biochem.* **2016**, *160*, 275–286.
56. Z. Ou, Z. Feng, G. Liu, Y. Chen, Y. Gao, Y. Li, X. Wang, *Chem. Lett.* **2015**, *44*, 425–427.
57. P. Wang, C.-H. Leung, D.-L. Ma, S.-C. Yan, C.-M. Che, *Chem. Eur. J.* **2010**, *16*, 6900–6911.
58. V. S. Stafford, K. Suntharalingam, A. Shivalingam, A. J. P. White, D. J. Mann, R. Vilar, *Dalton Trans.* **2015**, *44*, 3686–3700.
59. K. Suntharalingam, A. J. P. White, R. Vilar, *Inorg. Chem.* **2010**, *49*, 8371–8380.
60. D. L. Ang, B. W. J. Harper, L. Cubo, O. Mendoza, R. Vilar, J. Aldrich-Wright, *Chem. Eur. J.* **2016**, *22*, 2317–2325.
61. J. E. Reed, S. Neidle, R. Vilar, *Chem. Commun.* **2007**, 4366–4368.
62. K. Suntharalingam, A. Leczkowska, M. A. Furrer, Y. Wu, M. K. Kuimova, B. Therrien, A. J. P. White, R. Vilar, *Chem. Eur. J.* **2012**, *18*, 16277–16282.
63. R. Kieltyka, J. Fakhoury, N. Moitessier, H. F. Sleiman, *Chem. Eur. J.* **2008**, *14*, 1145–1154.
64. K. J. Castor, J. Mancini, J. Fakhoury, N. Weill, R. Kieltyka, P. Englebienne, N. Avakyan, A. Mittermaier, C. Autexier, N. Moitessier, H. F. Sleiman, *ChemMedChem* **2012**, *7*, 85–94.
65. D.-L. Ma, C.-M. Che, S.-C. Yan, *J. Am. Chem. Soc.* **2009**, *131*, 1835–1846.
66. S. Bianco, C. Musetti, A. Waldeck, S. Sparapani, J. D. Seitz, A. P. Krapcho, M. Palumbo, C. Sissi, *Dalton Trans.* **2010**, *39*, 5833–5841.
67. T. Wilson, P. J. Costa, V. Felix, M. P. Williamson, J. A. Thomas, *J. Med. Chem.* **2013**, *56*, 8674–8683.
68. D. Sun, Y. Liu, D. Liu, R. Zhang, X. Yang, J. Liu, *Chem. Eur. J.* **2012**, *18*, 4285–4295.
69. G.-L. Liao, X. Chen, L.-N. Ji, H. Chao, *Chem. Commun.* **2012**, *48*, 10781–10783.
70. E. Wachter, D. Moya, E. C. Glazer, *ACS Comb. Sci.* **2017**, *19*, 85–95.
71. L. He, X. Chen, Z. Meng, J. Wang, K. Tian, T. Li, F. Shao, *Chem. Commun.* **2016**, *52*, 8095–8098.

72. D. Saadallah, M. Bellakhal, S. Amor, J.-F. Lefebvre, M. Chavarot-Kerlidou, I. Baussanne, C. Moucheron, M. Demeunynck, D. Monchaud, *Chem. Eur. J.* **2017**, *23*, 4967–4972.
73. K. J. Castor, K. L. Metera, U. M. Tefashe, C. J. Serpell, J. Mauzeroll, H. F. Sleiman, *Inorg. Chem.* **2015**, *54*, 6958–6967.
74. K.-H. Leung, H.-Z. He, B. He, H.-J. Zhong, S. Lin, Y.-T. Wang, D.-L. Ma, C.-H. Leung, *Chem. Sci.* **2015**, *6*, 2166–2171.
75. M. Wang, Z. Mao, T.-S. Kang, C.-Y. Wong, J.-L. Mergny, C.-H. Leung, D.-L. Ma, *Chem. Sci.* **2016**, *7*, 2516–2523.
76. S. Lin, L. Lu, T.-S. Kang, J.-L. Mergny, C.-H. Leung, D.-L. Ma, *Anal. Chem.* **2016**, *88*, 10290–10295.
77. R. Kieltyka, P. Englebienne, J. Fakhoury, C. Autexier, N. Moitessier, H. F. Sleiman, *J. Am. Chem. Soc.* **2008**, *130*, 10040–10041.
78. N. P. E. Barry, N. H. Abd Karim, R. Vilar, B. Therrien, *Dalton Trans.* **2009**, 10717–10719.
79. H. Yu, X. Wang, M. Fu, J. Ren, X. Qu, *Nucleic Acids Res.* **2008**, *36*, 5695–5703.
80. S. Ghosh, O. Mendoza, L. Cubo, F. Rosu, V. Gabelica, A. J. P. White, R. Vilar, *Chem. Eur. J.* **2014**, *20*, 4772–4779.
81. X.-H. Zheng, H.-Y. Chen, M.-L. Tong, L.-N. Ji, Z.-W. Mao, *Chem. Commun.* **2012**, *48*, 7607–7609.
82. O. Domarco, D. Lotsch, J. Schreiber, C. Dinhof, S. Van Schoonhoven, M. D. Garcia, C. Peinador, B. K. Keppler, W. Berger, A. Terenzi, *Dalton Trans.* **2017**, *46*, 329–332.
83. X.-H. Zheng, Y.-F. Zhong, C.-P. Tan, L.-N. Ji, Z.-W. Mao, *Dalton Trans.* **2012**, *41*, 11807–11812.
84. C.-X. Xu, Y.-X. Zheng, X.-H. Zheng, Q. Hu, Y. Zhao, L.-N. Ji, Z.-W. Mao, *Sci. Rep.* **2013**, *3*, 2060.
85. C.-X. Xu, Y. Shen, Q. Hu, Y.-X. Zheng, Q. Cao, P. Z. Qin, Y. Zhao, L.-N. Ji, Z.-W. Mao, *Chem. Asian J.* **2014**, *9*, 2519–2526.
86. X.-H. Zheng, G. Mu, Y.-F. Zhong, T.-P. Zhang, Q. Cao, L.-N. Ji, Y. Zhao, Z.-W. Mao, *Chem. Commun.* **2016**, *52*, 14101–14104.
87. L. Rao, U. Bierbach, *J. Am. Chem. Soc.* **2007**, *129*, 15764–15765.
88. L. Rao, J. D. Dworkin, W. E. Nell, U. Bierbach, *J. Phys. Chem. B* **2011**, *115*, 13701–13712.
89. A. J. Pickard, F. Liu, T. F. Bartenstein, L. G. Haines, K. E. Levine, G. L. Kucera, U. Bierbach, *Chem. Eur. J.* **2014**, *20*, 16174–16187.
90. E. Gabano, S. Gama, F. Mendes, M. B. Gariboldi, E. Monti, S. Bombard, S. Bianco, M. Ravera, *J. Biol. Inorg. Chem.* **2013**, *18*, 791–801.
91. J.-F. Betzer, F. Nuter, M. Chtchigrovsky, F. Hamon, G. Kellermann, S. Ali, M.-A. Calmejane, S. Roque, J. Poupon, T. Cresteil, M.-P. Teulade-Fichou, A. Marinetti, S. Bombard, *Bioconjugate Chem.* **2016**, *27*, 1456–1470.
92. B. R. Vummidi, J. Alzeer, N. W. Luedtke, *ChemBioChem* **2013**, *14*, 540–558.
93. E. Largy, A. Granzhan, F. Hamon, D. Verga, M.-P. Teulade-Fichou, *Top. Curr. Chem.* **2013**, *330*, 111–178.
94. S. Shi, J. Zhao, X. Geng, T. Yao, H. Huang, T. Liu, L. Zheng, Z. Li, D. Yang, L. Ji, *Dalton Trans.* **2010**, *39*, 2490–2493.
95. E. Wachter, D. Moya, S. Parkin, E. C. Glazer, *Chem. Eur. J.* **2016**, *22*, 550–559.
96. Q. Yu, Y. Liu, C. Wang, D. Sun, X. Yang, Y. Liu, J. Liu, *PLoS One* **2012**, *7*, e50902.
97. J. Reed, M. Gunaratnam, M. Beltran, A. P. Reszka, R. Vilar, S. Neidle, *Anal. Biochem.* **2008**, *380*, 99–105.
98. D. Gomez, J.-L. Mergny, J.-F. Riou, *Cancer Res.* **2002**, *62*, 3365–3368.
99. H. Yaku, T. Murashima, D. Miyoshi, N. Sugimoto, *J. Phys. Chem. B* **2014**, *118*, 2605–2614.

100. J. Mancini, P. Rousseau, K. J. Castor, H. F. Sleiman, C. Autexier, *Biochimie* **2016**, *121*, 287–297.
101. L. Sabater, M.-L. Nicolau-Travers, A. De Rache, E. Prado, J. Dejeu, O. Bombarde, J. Lacroix, P. Calsou, E. Defrancq, J.-L. Mergny, D. Gomez, G. Pratviel, *J. Biol. Inorg. Chem.* **2015**, *20*, 729–738.
102. P. Merle, M. Gueugneau, M.-P. Teulade-Fichou, M. Muller-Barthelemy, S. Amiard, E. Chautard, C. Guetta, V. Dedieu, Y. Communal, J.-L. Mergny, M. Gallego, C. White, P. Verrelle, A. Tchirkov, *Sci. Rep.* **2015**, *5*, 16255.
103. Z. Yu, M. Han, J. A. Cowan, *Angew. Chem., Int. Ed.* **2015**, *54*, 1901–1905.
104. J. Rodriguez, J. Mosquera, J. R. Couceiro, M. E. Vázquez, J. L. Mascareñas, *Angew. Chem., Int. Ed.* **2016**, *55*, 15615–15618.

13

Antitumor Metallodrugs that Target Proteins

Matthew P. Sullivan, [*] ***Hannah U. Holtkamp,*** [*] ***and Christian G. Hartinger***

[*]*these authors contributed equally to this work*

School of Chemical Sciences, University of Auckland,
Private Bag 92019, 1142 Auckland, New Zealand
<c.hartinger@auckland.ac.nz>

ABSTRACT 352
1. INTRODUCTION 352
2. ANTICANCER METALLODRUGS THAT TARGET CARRIER PROTEINS 354
   2.1. Transferrin. Metallodrugs Targeting the Iron Binding Site 355
   2.2. Albumin. Exploiting the Enhanced Permeability and Retention Effect 356
      2.2.1. Metallodrugs Reacting at the Metal Center with Human Serum Albumin after Administration 357
      2.2.2. Covalent Modification of Human Serum Albumin with Pharmacophores 358
      2.2.3. Non-covalent Human Serum Albumin-Targeting Metallodrugs 360
   2.3. Proteins and the Cellular Accumulation of Metallodrugs 360
      2.3.1. Copper-Binding Proteins and Cisplatin Transport 360
      2.3.2. Conjugation of Metallodrugs with Sugar Ligands 361
      2.3.3. Other Carrier Proteins as Targets 362
3. SELECTED CANCER-RELATED PROTEINS AS TARGETS 362
   3.1. Kinase Inhibitors 362
   3.2. Estrogen Receptor Targeting Metallodrugs 364
   3.3. The (Seleno)cysteine-Containing Proteins Thioredoxin Reductase and Cathepsin B 365

Metal Ions in Life Sciences, Volume 18 Edited by Astrid Sigel, Helmut Sigel, Eva Freisinger, and Roland K. O. Sigel

https://doi.org/10.1515/9783110470734-013

3.4. Topoisomerase. Metal-Based Inhibitors and Poisons 367
3.5. Matrix Metalloproteinases as Targets for Metallodrugs 368
3.6. Glutathione *S*-Transferase. Targeting the Defense Mechanism of Tumor Cells 368
3.7. Anti-inflammatory Drug-Inspired Anticancer Agents to Target Cyclooxygenases 369
3.8. Histone Deacetylase Inhibitors 370
3.9. Ribonucleotide Reductase as a Drug Target. Substitution of the Iron Center and Ligand Development 371
3.10. Other Proteins Targeted with Metal-Based Anticancer Agents 372
4. NON-CONVENTIONAL PROTEIN TARGETS FOR ANTICANCER METALLODRUGS 373
4.1. Protein versus DNA Binding. The Nucleosome Core Particle 373
4.2. At the Interface of Proteins: Disrupting Protein–Protein Interactions 374
5. MODERN BIOANALYTICAL METHODS 375
6. CONCLUDING REMARKS AND FUTURE DIRECTIONS 376
ACKNOWLEDGMENTS 377
ABBREVIATIONS 377
REFERENCES 379

Abstract: Anticancer platinum-based drugs are widely used in the treatment of a variety of tumorigenic diseases. They have been identified to target DNA and thereby induce apoptosis in cancer cells. Their reactivity to biomolecules other than DNA has often been associated with side effects that many cancer patients experience during chemotherapy. The development of metal compounds that target proteins rather than DNA has the potential to overcome or at least reduce the disadvantages of commonly used chemotherapeutics. Many exciting new metal complexes with novel modes of action have been reported and their anticancer activity was linked to selective protein interaction that may lead to improved accumulation in the tumor, higher selectivity and/or enhanced antiproliferative efficacy. The development of new lead structures requires bioanalytical methods to confirm the hypothesized modes of action or identify new, previously unexplored biological targets and pathways. We have selected original developments for review in this chapter and highlighted compounds on track toward clinical application.

Keywords: bioanalytical chemistry · drug targets · metal-based anticancer drugs · metallomics · protein inhibitors · protein interaction · proteomics

1. INTRODUCTION

Metallodrugs have been extensively used for the treatment and diagnosis of different diseases [1–3]. The inherent properties of metal ions can cause them to undergo ligand exchange reactions to form covalent bonds with donor atoms found in biological molecules. Such interactions for example with DNA are essential for the anticancer activity of cisplatin (and analogous Pt complexes; Figure 1) and lead to structural changes in DNA and eventually the induction of apoptosis [4–7]. At the same time, covalent binding to proteins was considered to

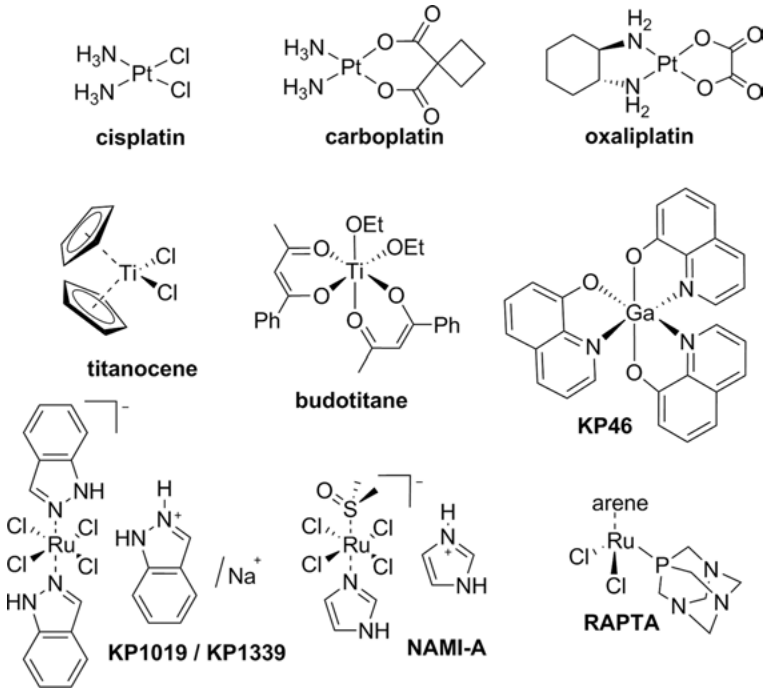

Figure 1. Chemical structures of representative Pt, Ru, Ti, and Ga anticancer drugs (arene = η^6-*p*-cymene [cym], η^6-toluene, η^6-biphenyl).

contribute to the side effects observed for Pt-based chemotherapy and possibly deactivation [8]. The widely studied and clinically investigated complexes based on Ru or Ga, i.e., KP1019/NKP-1339 and NAMI-A or KP46 [tris(8-oxyquinolinato)gallium(III) (Figure 1) and tris(maltolato)gallium(III)], respectively, demonstrate the difference in properties for Pt and other metal complexes [2, 8]. Complexes based on the latter metal centers have been shown to rely on blood serum protein binding already after administration, whether covalent or hydrophobic, to exhibit their selective anticancer activity [9, 10].

With increasing knowledge about the proteome and the role of proteins in cancer progression and metastasis, metallodrugs have been designed to target proteins involved in these processes. By forming either covalent bonds, delivering selective inhibitors or providing a structural scaffold in inhibitor design, efficient protein-targeting coordination and organometallic compounds have been designed, some of which are the best in class [11].

The design of protein-binding metallodrugs has gone hand in hand with the development of advanced analytical techniques to characterize the adducts formed, as well as studies on the impact on biological systems [12]. Major advances have been made in the visualization of the distribution of especially non-endogenous metals in biological systems as well as in the structural characterization of metal–biomolecule adducts and target identification in highly complex

biological matrices [12–14]. These methods have already made major contributions to metallodrug development and will surely enable more streamlined drug development programs in the future.

In this chapter, we review some of the most important and original developments in protein-targeting anticancer metallodrug design and studies that support the design concept, especially with a focus on their primary protein interaction, although down-stream effects on protein expression is beyond the scope of this chapter. Many of these drug lead structures have the potential to advance to clinical studies, progress facilitated by the use and advancement of modern analytical technology. Analytical advances have been a major driving force, and will be summarized and discussed at the end of the chapter.

2. ANTICANCER METALLODRUGS THAT TARGET CARRIER PROTEINS

Metal complexes are known to undergo ligand exchange reactions in the presence of biological molecules, such as amino acids and DNA building blocks. This reactivity can be exploited to form bioconjugates after administration into the human body either orally or intravenously [15]. Once the metallodrugs reach the blood, they may interact with the main components of blood serum, often the serum proteins human serum albumin (HSA) and transferrin (Tf). These proteins transport hormones, fatty acids, and other essential components throughout the body and have also been associated with the transportation of pharmaceuticals. In addition, as metallodrugs undergo ligand exchange reactions, these proteins may act as reservoirs and provide a means for drug delivery into tumors through the enhanced permeability and retention (EPR) effect or receptor-mediated endocytosis [4, 8]. The EPR effect is related to an increased permeability of leaky blood vessels around quickly growing tumors towards proteins and other macromolecules [16–19], such as micelles, nanotubes, and nanoparticles, all of which have been established to be efficacious in delivering pharmacophores [20–27].

Transport mediated by serum proteins has been extensively researched in the development of metal-based drugs [8]. It has often been suggested that the binding of drugs to proteins causes deactivation or side effects [4, 28]. However, in the case of metallodrugs the loading of the pharmacophore onto serum proteins has been seen positively and suggested to contribute to reducing toxicity through improved accumulation in tumor tissue [15, 29]. Even in clinical trials, lower side effects of cisplatin–protein conjugates have been reported than observed for the free drug while maintaining the pharmacophore's antitumor activity [29]. Initial investigations assumed that the chemical properties of anticancer-active metal ions similar to those of Fe could help exploit Tf-mediated endocytosis through interaction with Tf at the Fe binding sites.

Recently, new approaches have been considered including the use of selective linkers which covalently conjugate the metallodrug toward the carrier protein after intravenous administration [30, 31], bind non-covalently to hydrophobic

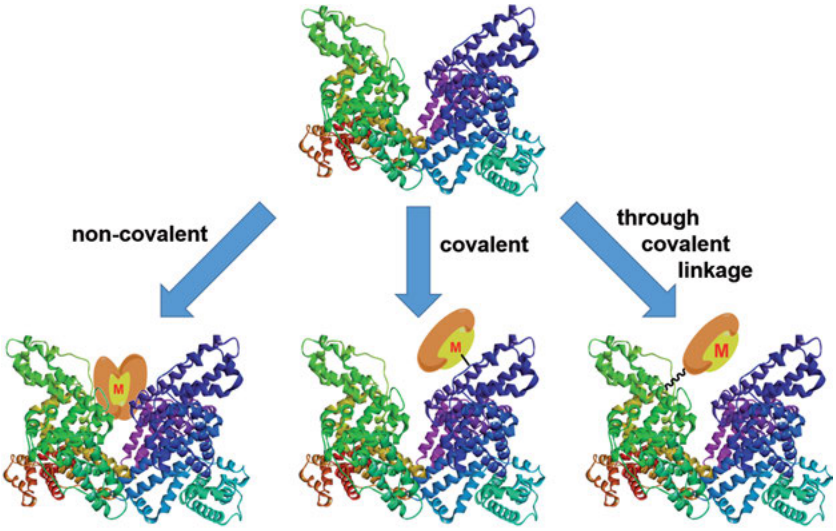

Figure 2. Proteins as carriers for metal-based anticancer agents coordination of the metal center to the protein, non-covalent/hydrophobic interaction and (cleavable) linkers as a means for drugs targeted to carrier proteins.

areas of proteins [10, 32] or even direct conjugation prior to administration has been suggested (Figure 2) [33–35].

2.1. Transferrin. Metallodrugs Targeting the Iron Binding Site

Iron is an essential element in the body and absorbed from the intestine. It enters the circulatory system and binds to Tf, which delivers it into cells by receptor-mediated endocytosis [36]. Instead of Fe, other metal ions have been shown to bind strongly to the same binding sites in Tf. As tumors grow rapidly, they have a higher demand for Fe and an overexpression of Tf receptors on the cell surface is initiated. The binding of metal ions other than Fe could be exploited in a Trojan horse approach, allowing for selective accumulation of metal-based cytotoxins in tumor cells. This was the design hypothesis for Ru, Ga, and Ti anticancer compounds, which also show high affinity to the Fe binding sites of Tf [37]. While not designed to interact with serum proteins, cisplatin has been shown to extensively bind to serum proteins after intravenous administration, particularly Tf and HSA [38], but the role of these cisplatin-serum protein adducts in the mode of action is still a matter of debate, although there have been promising clinical trials with these adducts [29].

Ru anticancer agents are now regarded as the most probable metallodrugs to join Pt drugs in clinical use. Towards the end of the last century, the Ru(III) anticancer agents KP1019 and NAMI-A (Figure 1) were developed and they entered clinical trials early in the 2000's. They bind effectively to serum proteins

and their low toxicity was thought to be related to their superior accumulation in tumor tissue. In addition, the activation by reduction hypothesis suggests that they are reduced inside cells to more reactive Ru(II) species, adding another level of selectivity for these compounds [39, 40].

Indeed, clinical trials for both NAMI-A and KP1019, and later KP1339 (Figure 1), demonstrated their low general toxicity. These results were not unexpected as preclinical studies supported the hypothesis that Tf binding would facilitate transfer into cancer cells. For example, mass spectrometry (MS) and circular dichroism (CD) spectroscopy indicated that the loading of KP1019 on Tf increases the concentration of Ru in the cells, which was however dependent on the Fe loading of Tf [41]. The binding of KP1019 to lactoferrin as a homologue to Tf, was characterized crystallographically with the Ru fragment bound to the Fe binding site [42]. One of the chlorido ligands of KP1019 was shown to undergo a ligand exchange reaction with His253 and Lys301 stabilizing the interaction. The reaction was also monitored in solution using size exclusion chromatography (SEC), which demonstrated that KP1019 rapidly binds to Tf through an intermediate in the presence of bicarbonate as the counter anion. However, pharmacokinetic studies accompanying the clinical trials, revealed preference for HSA over Tf [43], which was also confirmed in an *in vivo* mouse model [44]. Similarly to the bis(indazole)Ru complexes, NAMI-A binding to Tf was also studied [45, 46] and the binding rate was found influenced by the type of azole ligand bound to the Ru center [45].

In an analogous manner to the Ru compounds, Ti anticancer agents have been suggested to bind to Tf [47] and the binding constant found for Ti(IV) is even higher than that of Fe(III) [37]. In particular, titanocene dichloride (Figure 1) was widely studied and reached clinical trials in the 1990's but it failed in phase II, as no improvement over other treatments was observed [48, 49]. The disadvantage of titanocene dichloride is that it hydrolyzes quickly in aqueous solution resulting in the loss of the cyclopentadienyl ligands [50, 51].

Ga(III) shares a similar ionic radius and Tf binding constant as Fe(III) [37]. Therefore, it was hypothesized that Ga(III) compounds may interact with Tf and its cell uptake is Tf-mediated [52–54]. With these favorable properties in mind, numerous Ga compounds have been developed. The first generation Ga compounds included $Ga(NO_3)_3$ and $GaCl_3$ which showed promising anticancer properties [55–57]. The low bioavailability of these simple Ga salts resulted in the preparation of the Ga coordination compounds KP46 (Figure 1) and tris(maltolato)gallium(III), which recently underwent clinical trials [58]. KP46 was found to bind to Tf selectively, even in the presence of a large excess of HSA, as is found in human blood serum [59].

2.2. Albumin. Exploiting the Enhanced Permeability and Retention Effect

HSA plays a variety of roles in the body. Importantly, it transports many drugs including aspirin, ibuprofen, and warfarin and it has a major effect on the half-

life of these drugs [60]. Recently, the FDA approved Abraxane as a drug carrier anticancer medicine based on albumin which is loaded with paclitaxel [61, 62]. This also shows its potential for the delivery of metal complexes mediated by the EPR effect. Moreover, HSA can be very selectively functionalized on its single free L-cysteine residue (Cys34) [63], or covalently loaded through reactions with other amino acid side chains.

2.2.1. Metallodrugs Reacting at the Metal Center with Human Serum Albumin after Administration

HSA was theorized as a major route for metallodrug detoxification, however, research on cisplatin incubated with HSA and Tf prior to administration, indicated that the drug conjugates still showed anticancer activity in clinical trials [15, 29]. Cisplatin binds to HSA preferentially at solvent-exposed cysteine and methionine residues [64, 65]. This was confirmed by 2D nuclear magnetic resonance (NMR) spectroscopy, using ^{15}N-labeled platinum ammine complexes. It was demonstrated that cisplatin binds primarily to Met298 and forms an *S*,*N*-macrochelate with the support of an *N*-donor amino acid side chain [65]. More recently, the binding site was characterized crystallographically and Met298 was found platinated among other His and Met residues (Figure 3).

Employing a bottom-up MS approach on the reaction of cisplatin with recombinant HSA (rHSA) allowed the identification of bifunctional cisplatin–rHSA adducts [66]. Cisplatin formed inter-domain crosslinks between His67 of domain I and His247 of domain II, which blocks the Zn binding site. This means that cisplatin may compete for this binding site, interfering with the zinc homeostasis and explains side effects such as hyperzincuria and hypozincemia observed in patients treated with cisplatin.

As mentioned in Section 2.1, Ru compounds such as KP1019 were developed on the premise that they use Tf-mediated endocytosis as their mechanism to

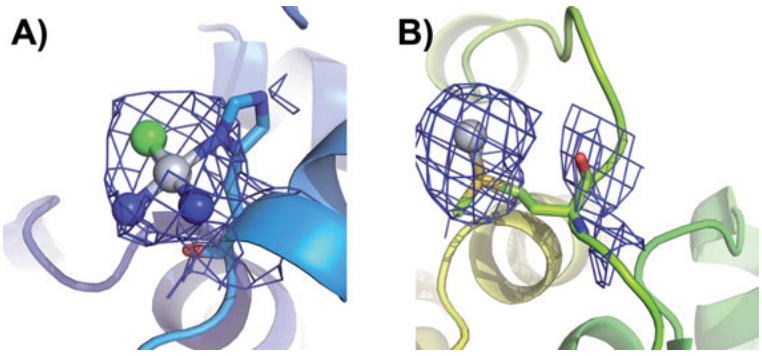

Figure 3. Details of binding sites found for cisplatin on HSA. (**A**) His105, (**B**) Met298. This figure was prepared from PDB ID 4S1Y [65].

accumulate in cells. However, the amount found bound to HSA was much higher than for Tf [43]. Electron paramagnetic resonance was used to show that the Ru compound initially binds non-covalently to HSA but over time, a coordination bond is formed [9]. In contrast, the reaction to Tf was found to be very slow and only to occur through ligand exchange reactions.

X-ray absorption spectroscopy allowed for the determination of the oxidation state of the Ru drugs and the atom they are interacting with on the protein through comparison of the edge energies with model complexes [67]. The data suggests the formation of Ru(III)–S bonds on HSA and Tf, as well as on collagen, the latter most likely being the reason for the antimetastatic activity of Ru complexes. When KP1019 was reacted with HSA, crystallography studies allowed the detection of the complex coordinated to His146 and His242 in the hydrophobic pocket of HSA [68]. This clearly demonstrates that more than one analytical method is required to obtain a complete understanding of the full picture and that the analysis conditions must be chosen carefully.

2.2.2. *Covalent Modification of Human Serum Albumin with Pharmacophores*

Since many biological drugs based on proteins may cause an immune response [69], the functionalization of proteins in blood stream seems to be an attractive feature to overcome such undesired effects. HSA, as the most abundant serum protein, has been considered an attractive target for this purpose [70] because of the low immunotoxicity, elongated half-life of the pharmacophore in blood serum and increased tumor accumulation. This strategy has resulted in the clinical approval of Abraxene, i.e., HSA loaded with paclitaxel and the conjugate being administered to the patient [61, 62]. Furthermore, INNO-206, the 6-maleimidocaproyl hydrazone derivative of doxorubicin, was tested in clinical trials and found well tolerated after rapid reaction in the bloodstream with Cys34 of HSA [71]. The amino acid side chains or termini offer potential sites for functionalization and different conjugation strategies have been explored [72]. Several metallodrugs bearing functional groups for covalent binding to the protein, not involving the metal pharmacophore, have been designed and tested as anticancer agents.

The high reactivity of maleimide functional groups to Cys34 of HSA has been used to conjugate metallodrugs covalently to HSA. To the best of our knowledge,

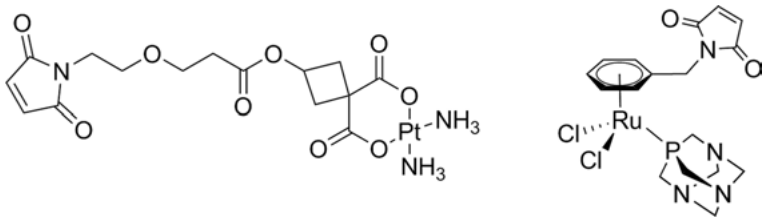

Figure 4. Chemical structures of Pt and Ru (Mal-RAPTA) compounds designed to covalently functionalize HSA.

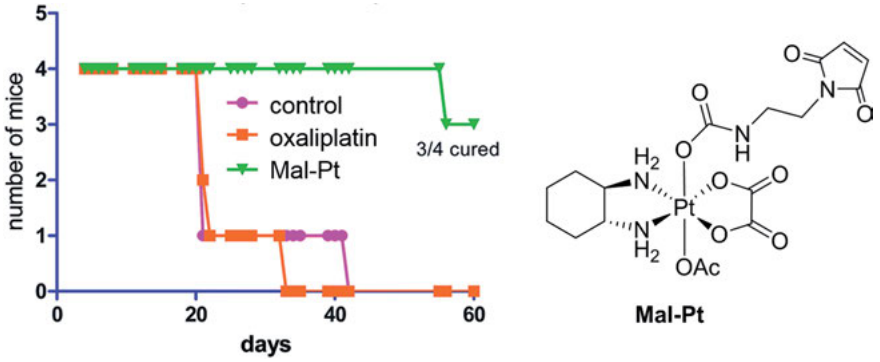

Figure 5. Survival of female BALB/c mice upon treatment with Mal-Pt as compared to treatment with oxaliplatin and an untreated control group. Adapted from [81], published under a Creative Commons 3.0 license by The Royal Society of Chemistry.

Kratz et al. were the first to introduce maleimide functionalization in metallodrug research [30, 31]. They designed carboplatin-based complexes (Figure 4, left) where the bidentate cyclobutane-1,1-dicarboxylic acid (CBDA) ligand was modified with a maleimide-functionalized linker intended to covalently link to HSA post intravenous administration. The advantage of the maleimide functional group over other linkers [15, 73] is that once delivered into the tumor tissue no acid sensitive or enzymatically degradable bond is required as instead the platinum fragment is released from the CBDA ligand via hydrolysis. The derivative featuring a (1*R*,2*R*)-cyclohexanediamine ligand as found in oxaliplatin instead of the ammine ligands of carboplatin, was found to be the most potent in *in vitro* assays [30, 31]. However, the conjugation to HSA lowered the cytotoxic activity significantly. When studied *in vivo* in mouse models, the advantage of HSA conjugation became apparent and resulted in equal or higher activity of the carboplatin analogues than found for carboplatin [30].

We applied the same strategy more recently to organoruthenium(II) complexes where the arene group of RAPTA-C, i.e., [Ru(cym)(1,3,5-triaza-7-phosphatricyclo[3.3.1.1]decane)Cl_2], an antimetastatic compound [16, 74], was modified to incorporate a maleimide moiety (Mal-RAPTA; Figure 4) [74, 75]. When designing Mal-RAPTA the maleimide was introduced at the arene, as arene functionalization was shown to have a smaller impact on the biological activity as opposed to modifying the PTA co-ligand [76]. We extended this concept by using maleimide-functionalized *N*-donor co-ligands, such as indazole, which is also found in the pharmacophore of KP1019 and KP1339 [77]. The Ru(arene) compounds with such ligands exhibited potent anticancer activity while maintaining a similar reactivity with biological thiols as Mal-RAPTA. In contrast, introducing the maleimide group in a pyridinecarbothioamide bidentate ligand scaffold, resulted in non-cytotoxic organometallic compounds [78].

Following this concept resulted in the preparation of symmetrically bis-maleimide substituted Pt(IV) anticancer agents [79]. Following the activation-by-reduction hypothesis, Pt(IV) is reduced in the reductive tumor environment to

Pt(II) and the complex is converted from an octahedral geometry to square-planar under the release of the axial ligands [80]. Therefore, the functionalization of the axial ligands with maleimide allows for accumulation in the tumor and release of the metal center through reduction. The compounds reacted quickly with biological thiols and *in vivo* studies revealed a reduction of the tumor volume by more than 50 % in BALB/c mice. In a similar approach, the maleimide-bearing Pt(IV) complex Mal-Pt (Figure 5) resulted in a significant increase of survival *in vivo* [81]. Surprisingly, the survival was gender-dependent with female mice responding better than male mice.

2.2.3. Non-covalent Human Serum Albumin-Targeting Metallodrugs

HSA is known for its ability to carry many different organic compound classes through the bloodstream, for example, bilirubin, warfarin, fatty acids, and others would bind to HSA non-covalently [82]. The advantage of non-covalent HSA binders is that no bonds need to be broken in order to release the cytotoxin from the carrier. Conversely, this also limits the access to selective release mechanisms as found for Pt(IV).

In an elegant approach, Lippard and coworkers asymmetrically functionalized octahedral Pt(IV)-based cisplatin prodrugs in axial position with aliphatic tails which resulted in a molecule with amphiphilic structure resembling a fatty acid [32]. This structural feature enabled the efficient interaction with HSA and activation by reduction leads to the formation of cisplatin to kill the tumor cells. The most potent compound was found to form a 1 : 1 adduct with HSA by binding deep beneath the protein surface, which reduces the reduction rate of Pt(IV) to Pt(II). However, reduction also changes the lipophilicity of the compound, which allows for release of the cytotoxin, i.e., cisplatin.

2.3. Proteins and the Cellular Accumulation of Metallodrugs

2.3.1. Copper-Binding Proteins and Cisplatin Transport

Cell surface receptor proteins are proteins that are embedded in the membranes of cells and represent suitable targets for anticancer drugs [83]. For a long time the standard paradigm for cisplatin cellular uptake centered around passive diffusion, while more recently the role of transporters has been explored [6]. Cisplatin was found to interact with Met1 of the copper transporter protein CTR1 [84], which is responsible for the transfer to the copper chaperone protein ATOX1 [85]. Inductively-coupled plasma-atomic emission spectroscopy (ICP-AES) analysis showed that stoichiometric binding between cisplatin and ATOX1 occurred and X-ray crystallographic data analysis gave insight into the binding sites [86]. On monomeric ATOX1 the Pt(II) ion was coordinated to the protein through the thiols of Cys12 and Cys15 and the amide nitrogen of Cys12. However, in a dimeric ATOX1 structure, the Pt retained the ammines while crosslink-

ing the Cys15 residues of two ATOX1 monomers. Solution and in-cell NMR spectroscopy showed that initially an ATOX1–Pt(ammine)$_2$ is formed while longer reaction times result in protein dimerization and loss of the ammines [87].

2.3.2. Conjugation of Metallodrugs with Sugar Ligands

Cancer cells are highly energy-dependent for rapid growth and replication (Warburg effect) [88]. As they rely on glycolysis for energy generation when they grow rapidly, glucose transporters (GLUT) are often overexpressed in cancer cells. This has led to the design of metallodrugs linked to sugar-based vectors. Different conjugation strategies have been explored that include coordination through *N* donors, the introduction of linkers, *O* donor-based ligand systems facilitating the release of cytotoxins, macromolecular compounds, *P* donor ligands, etc. [89]. Such ligands were coordinated to metal centers such as Pt, Au, and Ru.

Significant increases in the life spans of tumor-bearing mice were found for several drug candidates. For example, [$PtCl_2$(benzyl 3,4-diamino-3,4-dideoxy-β-L-arabinopyranoside)] (Figure 6, left) gave a lifespan increase of 390 % versus control in an S180 *in vivo* model at a dose of 10 mg/kg [90]. Because of the analogy of the 6-membered pyranose ring, other sugar compounds were designed to resemble oxaliplatin [91]. However, the cytotoxicity was lower than for oxaliplatin, though still comparable to that of carboplatin. This may be a result of the more hydrophilic nature of sugar compounds [91]. However, more recently highly cytotoxic Pt(II) complexes resembling oxaliplatin were reported where the sugar moiety was introduced *via* functionalization of a malonato ligand, as found in carboplatin, and conveying the complexes greater stability [92]. Studies on the cellular uptake of the compound type in the presence and absence of a GLUT1 inhibitor suggested the involvement of this transporter and may provide a means for selectivity.

With the advent of organometallic anticancer agents, several organoruthenium compounds were reported featuring sugar phosphite ligands and resembling the

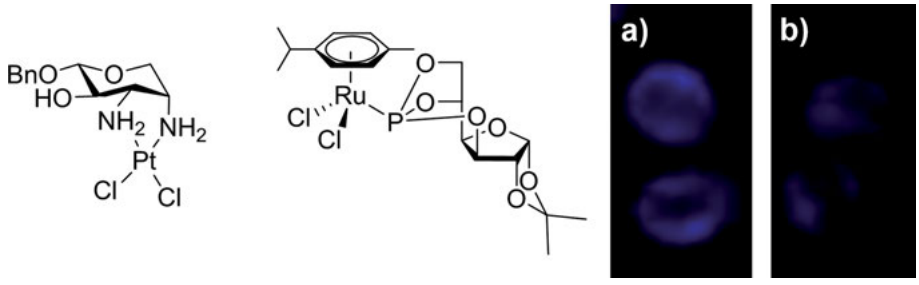

Figure 6. Chemical structures of anticancer-active Pt (left) and Ru (center) metal complexes functionalized with sugar residues. Right: The localization of a fluorescent probe based on the organoruthenium compound shown in the center (**a**) as compared to a RAPTA analogue (**b**). Reproduced from [96] with permission; copyright 2012 American Chemical Society.

structure of RAPTA compounds [93–97]. Though the sugar moiety did not improve the cellular accumulation of the Ru species as compared to an anthracene-modified RAPTA analogue (Figure 6, right), this may have actually been masked by the high lipophilicity of the compounds.

2.3.3. Other Carrier Proteins as Targets

Several other carrier proteins have been targeted, directly – by conjugation to a substrate to be taken up into the cell – or indirectly – by blocking the function of a transporter – with both cases resulting in growth inhibition of cancer cells. For example, several Au-containing peptidomimetics were developed to inhibit the PEPT1 and PEPT2 receptors [98], which transport tripeptides into the cell. Remarkably, these Au-peptidomimetics showed no cross-resistance with cisplatin and were shown to inhibit tumor cell proliferation and proven to be cytotoxic at lower IC_{50} values than cisplatin.

P-glycoprotein 1 (Pgp) and multidrug resistance protein 1 (MRP1) are proteins involved in the efflux of foreign substances resulting in drug resistance [99]. Modified phenoxazine and anthracene-based multidrug resistance modulator ligands were attached to a Ru(cym) fragment [100]. Once coordinated to Ru(II) accelerated uptake was achieved for the most active compound bearing an anthracene group which was also shown to result in increased Pgp inhibitory activity and cytotoxicity.

Single-walled carbon nanotubes (SWCNT) are effective carriers of cargo across cell membranes using clathrin-mediated endocytosis [101]. These SWCNT allow for the delivery of the $Pt(NH_3)_2Cl_2(OEt)$ moiety into the cell which can be reduced in the hypoxic environment to a Pt(II) cisplatin analogue [102]. It was determined by AAS that the Pt(II) can readily diffuse throughout the cell, while the SWCNT remains inside the endosome. Importantly, for drug delivery the cytotoxicity of the Pt complex increases more than 100-fold when the complex is attached to the surface of the functionalized SWCNTs.

3. SELECTED CANCER-RELATED PROTEINS AS TARGETS

Initially, metallodrug research focused on the "DNA paradigm" which relies on the principle of metallodrugs directly damaging DNA [103]. However, recently it has become evident that metallodrugs exert their effect also through DNA-independent mechanisms and it is important to understand their modes of action at the molecular level.

3.1. Kinase Inhibitors

Kinases are central for the regulation of most cellular functions and have become popular targets for drug discovery [104], including metal-based compounds fea-

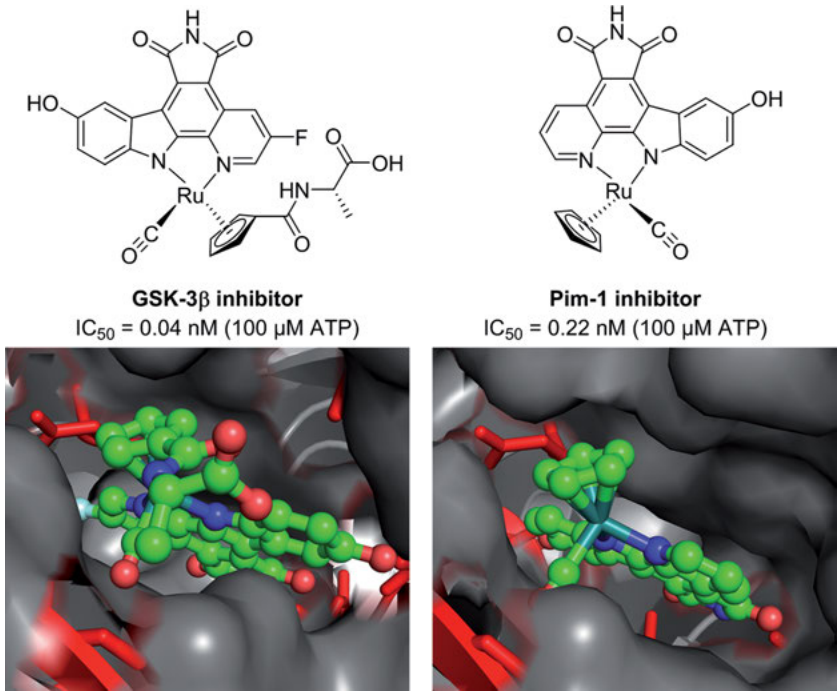

Figure 7. Examples of half-sandwich complexes that inhibit the kinases GSK-3β [113] and Pim-1 [111]. This figure was prepared from PDB IDs 2JLD and 2BZI, respectively.

turing, e.g., Pt, Ir, Ru, and Os metal centers [105–107]. Inspired by staurosporine, a well-known kinase inhibitor featuring a carbohydrate in its structure and competing for the ATP binding site, Meggers et al. designed inhibitors with organometallic moieties in the place of the sugar residue [105]. With the introduction of the organometallic moiety a significant increase in selectivity for any of the more than 500 kinases encoded in the human genome was obtained as compared to staurosporine [108].

Meggers and coworkers co-crystallized several kinases with organometallic inhibitors bound to the ATP-binding site (Figure 7) [109–115]. Variation of the structure in terms of substitution pattern of the organic components, the metal center, and the chirality allowed for an efficient way to obtain selectivity for different kinases [116]. For example, efficient inhibition of the kinase Pim-1 was achieved with a Ru complex bearing an L-alanine-substituted cyclopentadienyl (Cp) ligand (Figure 7, left) while the *S*-enantiomer of a related Ru complex not substituted at the Cp bound effectively to GSK-3β (Figure 7, right). Pim-1 is overexpressed in human prostate cancer cells [117], and GSK-3 has been considered a potential drug target for diabetes, cancer, and other diseases [118]. Interestingly, the nature of the metal center seems to play a minor role, supporting the notion that in this case the metal center has a merely structural role to position the ligands to ideally match the binding pocket [105, 111, 112].

The Pim-1 inhibitor shown in Figure 7, also known as DW2, inhibits GSK-3β, although to a lesser extent than Pim-1 [111]. Its enantiomer DW1 was a slightly more effective GSK-3 enzyme inhibitor and this mirrored findings in *in vitro* anticancer activity assays in 1205Lu melanoma cells but it showed limited activity in melanoma cells with p53 mutations [119]. Importantly, the enantiomeric mixture was as effective as DW1 against 1205Lu cells and the murine double minute proteins *m*DM-2 and -4 were downregulated.

In 1990, *in silico* studies highlighted that paullones may act as cyclin-dependent kinase (CDK) inhibitors as CDKs are known to regulate the cell cycle [120]. Paullones showed poor aqueous solubility and low bioavailability [121–124]. Arion et al. explored the effect of metal coordination on the antiproliferative effects and the solubility upon functionalizing paullones to become efficient metal binders [125–128]. Ru and Os complexes showed cytotoxicities in the low μM range independent of the metal center and inhibited DNA synthesis. At low concentrations cell cycle arrest occurred mainly in the G_0/G_1 phase while at higher concentrations apoptotic cell death was observed [125, 126, 128]. Similarly, by coordinating Ru(cym) or Os(cym) to established CDK inhibitors, they aimed for synergistic effects between the organic moiety and the metal center [129]. All compounds inhibited CDKs and were more effective against CDK2/cyclin E than CDK1/cyclin B.

A series of other organometallic compounds were tested on their CDK inhibitory activity, using a novel electrochemical assay [130–132]. Both pyridone [130, 132] and flavone [131] complexes were discovered to inhibit CDK2/cyclin A protein kinase and revealed potent activity of some Ru and Os complexes, similar to roscovitine used as a positive control.

B-Raf is a serine/threonine-protein kinase, which is mutated in several cancer types [133], and has attracted attention as a drug target. In an attempt to identify an organometallic inhibitor, a library of compounds structurally related to DW1 was screened and the carboxylic acid functionalized inhibitor CS292 was identified as a lead. A co-crystal structure showed that CS292 binds in the ATP pocket as a competitive inhibitor with high nM levels of inhibition.

3.2. Estrogen Receptor Targeting Metallodrugs

One of the most extensively studied classes of organometallic anticancer agents are the ferrocifens (Figure 8) [49, 134, 135], a class of compounds derived from tamoxifen in which one of the phenyl rings was replaced with ferrocene. Tamoxifen is a commonly applied breast cancer drug which selectively targets the estrogen receptor (ER) and is given to patients with estrogen receptor-positive [ER(+)] breast cancer. Several ferrocene derivatives of this drug were developed, which possess the unusual feature of being antiproliferative on both hormone-dependent and hormone-independent breast cancer cells in the low μM range [135]. The introduction of the ferrocene moiety did not impair their ability to bind to ERα and ERβ. Their mode of action seems to be strongly related to the redox properties of ferrocene, resulting in the formation of reactive oxygen

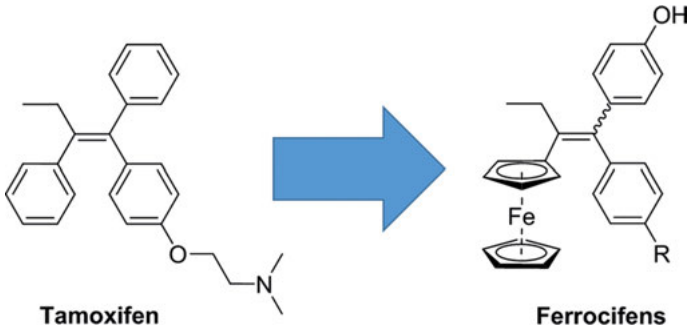

Figure 8. From tamoxifen to the ferrocifen compound class developed by Jaouen, Vessières, and Top [135].

species (ROS) and quinone methide formation. The design concept used to create the ferrocifens led to the development of numerous other compounds including anti-androgens [136], sugar nucleoside analogues [137], and many more [135].

Lippard et al. tethered estrogen to Pt(IV)-based cisplatin precursors via the axial ligands [138]. This compound class was designed to sensitize ER(+) breast cancer cells to cisplatin, as the treatment of cells with estrogen improved the cytotoxicity of cisplatin [139]. Upon cellular reduction estradiol was released from the Pt(IV) complex, which induces the upregulation of high-mobility group (HMG) domain protein HMGB1, a protein that shields platinated DNA from nucleotide excision repair (NER) [138]. However, the *in vitro* studies revealed only a marginal difference in ER(+) cells as compared to ER(–) ones.

3.3. The (Seleno)cysteine-Containing Proteins Thioredoxin Reductase and Cathepsin B

The selenocysteine-containing enzyme thioredoxin reductase (TrxR) is critical for maintaining the cellular redox state – inhibition of both cytosolic and mitochondrial thioredoxin reductase can shift the redox balance [140] – and linked to tumor proliferation [141]. The cysteine protease cathepsin B (CatB) was shown to be upregulated in premalignant cells, and is involved in the migration and invasion during tumor metastasis [142, 143]. Their (seleno)cysteine residues can be targeted by metal complexes as they often have high affinity for soft donors.

Auranofin is used in the treatment of rheumatoid arthritis [144] and has also been evaluated for the treatment of cancer as well as other Au(I) and Au(III) complexes [145]. The anticancer activity of auranofin has been attributed to mitochondrial TrxR inactivation [140]. Its antiproliferative activity was found to be higher than that of cisplatin, particularly in cisplatin-resistant cells. A variety of other Au compounds displayed low μM cytotoxicity and were suggested to target TrxR [146–148]. The mitochondrial TrxR inhibitory activity was much more pro-

nounced than that of cisplatin but the parent compound auranofin was an order of magnitude more active [147]. Au compounds with a variety of oxidation states and ligands showed selective inhibition against the cytosolic form of TrxR while not suppressing mitochondrial function [148].

Interestingly, an octahedral Ru(III) compound structurally related to KP1019 with 2-amino-5-methylthiazole replacing the indazole ligands, showed selective inhibition against the cytosolic form of TrxR as compared to mitochondrial TrxR [149]. On the other hand, RAPTA complexes were shown to inhibit TrxR but to a lesser extent than CatB [103]. A strong influence of the nature and the substituents on the arene ring was found, as well as some impact of the denticity of the leaving group to allow for coordination to Cys or SeCys in the protein.

A wide variety of other complexes was studied. For example, a series of Au(I)- and Pt(II)-phosphole compounds were shown to be highly potent TrxR inhibitors, with a Au(I) phosphole complex reaching an IC_{50} value of <1 nM [150]. Using TrxR mutants allowed for the identification of selenocysteine as the target site for the compounds. Moreover, the compounds showed pronounced activity over the glioblastoma drug carmustine in glioblastoma cells, a tumor type notoriously hard to treat. The TrxR binding site of (terpyridine)Pt(II) complexes, which inhibit TrxR at concentrations as small as ~60 nM while displaying low μM inhibition against HeLa cells, was identified by matrix assisted laser desorption/ionization (MALDI)-MS and X-ray crystallography as sulfur atoms of the GCCG motif on the surface of TrxR [151].

N-Heterocyclic carbene (NHC) compounds are extensively used in chemical catalysis, but Au, Ag, Ru, Pt, and other metal complexes have only recently been introduced in medicinal chemistry [152]. Some Au-based NHC anticancer agents were shown to induce mitochondrial permeability and alter mitochondrial biochemistry, and they were suggested to also interact with TrxR. For related Ru(arene)(NHC) complexes, one of the key biological targets was shown to be TrxR and they were also potent inhibitors of CatB [152]. CatB inhibitory activity was also observed for organoruthenium–sugar complexes [97]. The most active derivative (Figure 6, center) showed similar potency as structurally related, antimetastatic RAPTA compounds [103].

In order to exploit the properties of Ru and Au complexes in a single molecule, Messori et al. reported bimetallic ruthenogold compounds [153]. They found that the compounds inhibited CatB although at fairly high concentrations. In *in vitro* anticancer activity assays, the bimetallic compounds showed greater selectivity for cancer cell lines over normal cells and significantly higher activity than monoruthenium compounds included in the assays but lower potency than a Au compound. In contrast, several Re compounds were shown to be much more potent CatB inhibitors than the bimetallic compounds mentioned before [154]. In fact they showed significant selectivity for CatB over CatK, which is involved in osteoporosis and metastasis. Some of the Re compounds showed low nM reversible inhibition. As observed for many metal complexes, small alterations in the ligands surrounding the Re center affected the biological activity of these compounds.

3.4. Topoisomerase. Metal-Based Inhibitors and Poisons

Several types of topoisomerases have been identified in human cells and especially topoisomerase I and II have been considered as promising targets for anticancer drugs [155]. They have a variety of functions, including the breaking and rejoining of DNA strands and both poisons – interfering with the DNA–topoisomerase complex formation – and inhibitors have been developed as anticancer agents.

Using a DNA intercalator is one way to poison the DNA–topoisomerase complex. Terpyridine complexes are known for their DNA intercalating ability. Therefore it is not surprising that TrxR-inhibiting (terpyridine)Pt(II) complexes (see Section 3.3) were also shown to inhibit topoisomerase I and IIα in the low μM range, similar to that of the established inhibitors camptothecin and etoposide, respectively [151].

In a multitargeted approach, i.e., using more than one bioactive component in a single molecule, we introduced flavonols as ligands to Ru(arene) complexes [131, 156]. Flavones are known topoisomerase inhibitors and the combination with a metal center increased the inhibitory activity (Figure 9). However, this did not impact the cytotoxicity of the compounds but the potency correlated in general with the inhibitory activity of the enzyme. The cytotoxicity of the compound class was dependent on the substitution pattern of the flavonol ligand, with in particular ortho-suasbstituted compounds showing the lowest activity possibly because of loss of the planarity of the ligand [157].

Many other classes of compounds have been explored for their topoisomerase inhibitory activity. Kou et al. studied the impact of the chirality of octahedral Ru coordination compounds featuring anthraquinone moieties on the topoisomerase inhibitory activity [158]. The compounds were shown to inhibit both topoisomerase I and II to similar extents, while structurally related compounds were commonly selective for topoisomerase II. Their strong ability to intercalate into DNA may be beneficial for their enzyme inhibitory activity.

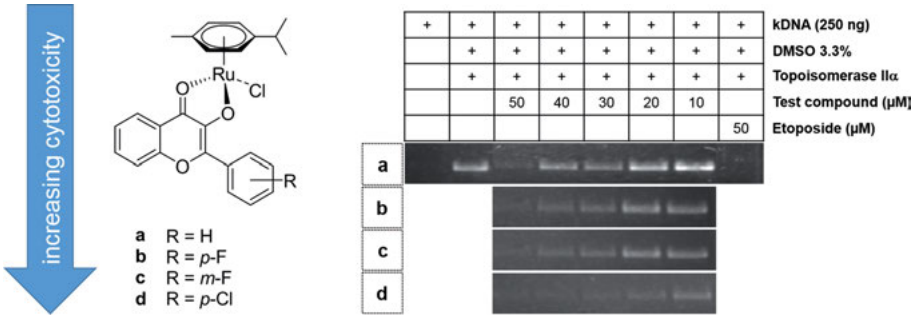

Figure 9. Correlation between topoisomerase IIα inhibitory activity and cytotoxic potency. Adapted from [131] with permission; copyright 2012 American Chemical Society.

3.5. Matrix Metalloproteinases as Targets for Metallodrugs

Matrix metalloproteinases (MMPs) are an important class of the protease family involved in the degradation of a number of extracellular proteins. Many classes of inhibitors have been developed which target MMPs, which usually contain a chelating group that binds to the catalytic Zn ion [159].

In an attempt to exploit tumor hypoxia and thereby labilize a Co(III) complex by reduction to Co(II), a Co(III) complex carrying the MMP inhibitor marimastat was designed [160]. Marimastat would be able to exhibit its mode of action more selectively as it would be released in the tumor. In an *in vitro* assay, when tested under non-reducing conditions, the complexation resulted in decreased MMP-9 inhibitory activity as compared to marimastat. However, *in vivo* the complex showed more potent tumor growth inhibition than marimistat, while increasing the metastatic potential. A related Fe(salen) compound which is more labile than the Co(III) complex, was a more potent MMP-9 inhibitor in the same assay [161].

Pt(II) complexes of diethyl[(methylsulfinyl)methyl]phosphonate have also been investigated as MMP inhibitors, inspired by the inhibitory properties of bisphosphonates. They were found to be low μM inhibitors of MMP-3, -9, and -12 but do not inhibit MMP-2 [162].

Although many more MMP inhibitors are known, it is interesting to note that RAED [Ru(η^6-biphenyl)(1,2-ethylenediamine)Cl]$^+$, which is at an advanced preclinical development stage, was shown to reduce the growth of primary as well as secondary tumors by inhibiting the detachment of MDA-MB-231 due to interference with the formation of MMP-2 as an alternative mechanism involving MMPs [163].

3.6. Glutathione *S*-Transferase. Targeting the Defense Mechanism of Tumor Cells

Glutathione *S*-transferase (GST) is often found in solid tumors, and the gene is upregulated upon exposure to antitumor drugs as it is part of the defense system of the cell against xenobiotics [164]. The inhibition of different GST isoenzymes has become a popular anticancer drug target and ethacrynic acid (EA; Figure 10) was found especially potent. EA interacts with different GSTs and inhibits them to varying extents [165].

Dyson et al. [164] developed the Pt(IV)–EA complex ethacraplatin (Figure 10). It can undergo reduction in the reductive milieu of the tumor and release EA that will target GST. The inhibition of GST weakens the defense of the cell against the released Pt fragment which targets DNA [164]. Ethacraplatin was in all cell lines investigated more potent than cisplatin [164] and reversed cisplatin resistance in MCF7 cells which overexpress a GST enzyme [166]. In A549 cells the activity of GST was only 22.6 % compared to the control upon treatment with ethacraplatin, while cisplatin and EA treatment reduced it only to 63.6 and 78.5 %, respectively [164]. Ethacraplatin was also a more potent inhibitor of the

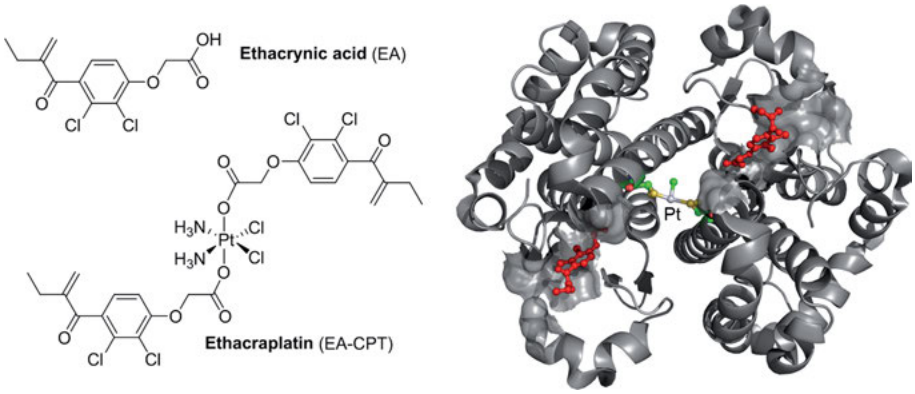

Figure 10. Chemical structures of ethacrynic acid and ethacraplatin. Crystal structure of a GST P1–1 dimer with the Pt center found at the interface of the dimer and EA at the H-sites. This figure was prepared from PDB ID 3N9J [167].

isolated enzyme than EA. In a crystal structure of GST P1–1 obtained after treatment with ethacraplatin, the reduced Pt center, as shown by XANES, was found at the interface of the protein dimer and EA at the H-sites (Figure 10) [167]. Molecular modelling studies suggested initial coordination and reduction of the Pt center at the interface and diffusion of the EA residues to their binding sites.

A similar strategy resulted in the preparation of metal(arene) and NAMI-analogous inhibitors of GST [168]. For the arene compounds two design strategies were employed – in one case the arene ligand was tethered to EA [169], while in another approach the arene ligand remained unmodified and EA was coordinated to the metal center through imidazole, pyridine or phosphine residues [168, 170]. In the case of the arene-modified compounds, the Ru center was found to be able to access the Cys101 residues at the dimer interface upon productively binding the EA unit at the H-site [169].

Interestingly, the RAED compound class was also found to inhibit GST [171]. Their inhibitory potency depended on the arene ligand with the Ru(cym) derivative being most potent. Bottom-up MS revealed binding of the metal complex to *S*-donors of Met and Cys residues, and in case of Cys residues an oxidation of the thiolates to sulfonates was observed.

3.7. Anti-inflammatory Drug-Inspired Anticancer Agents to Target Cyclooxygenases

Cyclooxygenases (COX) have been detected in numerous solid tumors although expressed to varying extents and they catalyze the initial step in the production of prostaglandins, for example, in inflammatory reactions [172]. The non-steroidal anti-inflammatory (NSAID) drug aspirin (acetylsalicylic acid) irreversibly

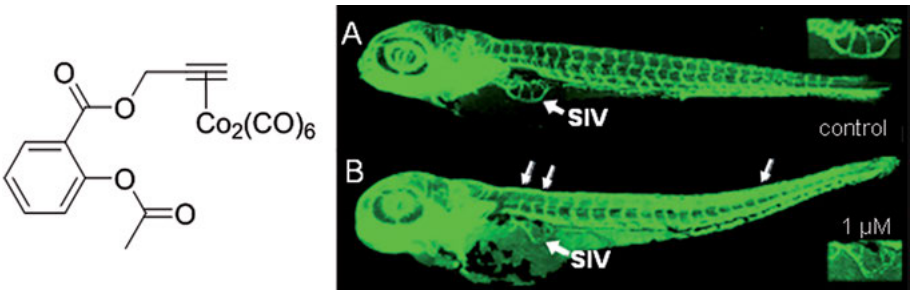

Figure 11. Chemical structure of Co-ASS and its effect on the blood vessel formation in zebrafish embryos. (**A**) Aspirin-treated and (**B**) Co-ASS-treated embryos at 4 days post fertilization and the subintestinal vein (SIV) indicated and shown in the inset. The white arrows indicate damaged or missing dorsal longitudinal anastomotic vessels. Reproduced from [174] with permission; copyright 2009 Wiley-VCH.

inhibits COX-1 and modifies the enzymatic activity of COX-2, which has been suggested as a target for cancer chemotherapy.

A series of metal-based COX inhibitors were reported that were inspired by the structures of NSAIDs. For example, the bis-Co complex Co-ASS features a 2-propynyl-functionalized aspirin which acts as an η^2 ligand bridging the two Co centers in the $Co_2(CO)_6$ moiety. Co-ASS was the most cytotoxic compound of a series of related structures as well as the strongest inhibitor of COX-1 and -2 [173]. While the observed antiangiogenic activity (Figure 11) could be related to downstream effects of COX inhibition, COX-independent biological activity was also revealed [174]. Analogous $Ru_3(CO)_9$, $Fe_3(CO)_9$, and $Co_4(CO)_{10}$ complexes and ferrocene derivatives showed slightly reduced antiproliferative potency in breast and colon cancer cell lines [175]. In general, the compounds were more potent COX-2 inhibitors than COX-1 but the biological activity may not be directly dependent on COX inhibition.

Other widely used NSAIDs are found in the oxicam family and meloxicam and piroxicam are widely used examples. Pt(II)-oxicam complexes were found highly cytotoxic in a series of cancer cell lines [176], while they were less active in intrinsically cisplatin-resistant cell lines. These Pt complexes reacted with model proteins, as confirmed in MS studies, but no COX inhibition was reported. Given the high number of donor atoms and therewith coordination sites, a series of organo-Ru, -Rh, and -Ir complexes were prepared but they demonstrated only modest cytotoxicity [177–179]. Docking studies with COX-2 for a series of derivatives suggested that they do not target COX-2 [178].

3.8. Histone Deacetylase Inhibitors

Histone deacetylases (HDAC) catalyze the removal of acetyl groups from DNA and thereby help regulate DNA expression [180]. HDAC was suggested as a

target for anticancer agents and vorinostat (SAHA) is a clinically used HDAC inhibitor (HDACi) that targets the catalytic Zn^{2+} ion of HDAC.

A series of metal-based SAHA derivatives were reported that were inspired by vorinostat and Cu, Fe, Pt, Ru, and other metal complexes have been proposed as SAHA delivery vehicles [181, 182]. For example, SAHA was functionalized with malonic acid to act as a bidentate ligand to a $Pt(NH_3)_2$ moiety and thereby resembling to some extent carboplatin. These compounds were designed to allow for bifunctional activity, i.e., DNA binding and HDAC inhibition [181]. Although they displayed lower HDAC inhibition than SAHA, the complex showed similar cytotoxicity to cisplatin while being more selective toward tumor cells. Belinostat, a SAHA-related HDAC inhibitor, was also modified with the cisplatin pharmacophore to result in more cytotoxic compounds in ovarian cancer cells [183].

In an approach similar to the modification of tamoxifen with ferrocene, Spencer et al. introduced a ferrocene moiety into SAHA [184]. The organometallics displayed nM and sub-nM HDAC inhibition with slight selectivity for class I over class IIA HDACs. All compounds showed low μM activity against breast cancer cells but there seems to be no direct correlation to the HDAC inhibition.

Mao and coworkers designed SAHA-based HDAC-targeted fluorescent Ru(II) polypyridyl complexes and analyzed their HDAC and cell growth inhibitory activity [185]. By comparing the compounds with structural analogues not bearing the SAHA group, they demonstrated lower cytotoxicity in cells. For the compounds substituted with SAHA, the HDAC inhibition correlated with their antiproliferative activity.

3.9. Ribonucleotide Reductase as a Drug Target. Substitution of the Iron Center and Ligand Development

Ribonucleotide reductase (RNR) is an important enzyme in the process of nucleotide synthesis, converting ribonucleotides into deoxyribonucleotides. Ga(III) anticancer agents inhibit RNR by replacing the redox active Fe(III) center in the active site with Ga(III) [54]. The Ga complexes tris(maltolato)Ga and KP46 were developed and evaluated in clinical trials following the early discovery of Ga salts being anticancer-active [58, 186].

Alternatively, a series of different ligand systems were studied on their RNR inhibitory activity, most notably thiosemicarbazones with a representative in clinical trials [187]. They were found to coordinate Fe and this may be linked to their antitumor activity. In a combination of both approaches, several Ga and Fe compounds bearing *N*-heterocyclic carboxaldehyde thiosemicarbazones were found to inhibit RNR [188]. A tyrosine free radical assay using electron paramagnetic resonance was developed to show the activity of mouse RNR. Both the ligand and Ga inhibit RNR and the resulting complex yielded a highly cytotoxic compound. Most of the biological effect was attributed to the thiosemicarbazone, however, the Ga center beneficially contributed to the cytotoxicity.

Similarly, thiosemicarbazone ligands functionalized with iminodiacetate groups were coordinated to Cu(II) [189]. Formation of the Cu complex increased the cytotoxicity of the ligands and microscale thermophoresis revealed RNR binding affinity with K_D values in the low μM range. Both the ligand and Cu complex studied efficiently destroyed the tyrosyl radical in mouse RNR2.

3.10. Other Proteins Targeted with Metal-Based Anticancer Agents

A significant number of other proteins have been targeted with metal-based anticancer agents, often by the combination of bioactive ligands coordinated to metal centers. This reflects clearly the current trend in metallodrug research moving away from DNA as a target.

As mentioned in Section 2, the functionalization of drugs with sugar derivatives may help their accumulation in tumor cells [89]. However, sugar homeostasis may also be targeted rather than aiming for increased uptake of sugar-derived complexes. A viable target for this approach is hexokinase, a membrane-bound mitochondrial protein that phosphorylates hexoses. It can be inhibited with lonidamine which reduces aerobic glycolysis in cancer cells but not in normal cells [190]. Lonidamine was conjugated to a Ru(cym) fragment and promisingly showed a synergistic effect with superior cytotoxicity in human glioblastoma cells compared to lonidamine [191].

Inhibitors of epidermal growth factor receptors (EGFR) have been identified as promising anticancer agents and the clinically used gefitinib and erlotinib were inspiration for the preparation of a Co(III) complex carrying the pharmacophore [192]. Upon reduction of Co(III) to Co(II) in hypoxic tissue conditions the EGFR inhibitor was released which resulted in potent anticancer activity *in vitro* and *in vivo*.

Nucleotide excision repair (NER) is an important DNA repair mechanism in the cell involved in detoxification of Pt–DNA adducts. The Pt(IV) prodrug NERi–Pt(IV) (Figure 12) was rationally designed with dual action, i.e., it causes DNA damage while simultaneously inhibiting NER through an inhibitor released upon reduction [193]. NERi–Pt(IV) showed improved cytotoxicity over cisplatin and was more active in cells than cisplatin co-administered with the organic NER inhibitor. A higher proportion of GG-Pt adducts was detected for this compound as compared to cisplatin (Figure 12), indicating a weakened defense system of the cells.

Na/K-ATPase is an example of an enzyme overexpressed in some tumor cells, such as in apoptosis-resistant glioblastoma cells, while it is reduced in others [194]. Au(III) coordination and organometallic compounds were shown to be potent inhibitors of Na/K-ATPase as well as displaying antiproliferative properties [195]. Each compound interacted with the ATPase in a slightly different modality, which is dependent upon their structure and ultimately caused conformation changes to the protein. Under physiological conditions, Au complexes bind more strongly to Na/K-ATPase than cisplatin [195–197]. This shows that

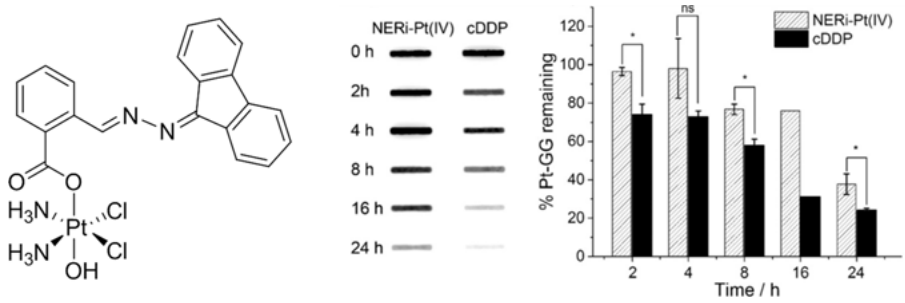

Figure 12. Chemical structure of NERi–Pt(IV), a NER inhibitor conjugated to a cisplatin-releasing Pt(IV) prodrug. Electrophoretic study indicating Pt–GG intrastrand crosslink levels after treatment with NERi–Pt(IV) and cisplatin (cDDP). Reproduced from [193] with permission; copyright 2016 Wiley-VCH.

Na/K-ATPase may be a relevant target for Au(III) complexes and may be involved in their modes of action.

4. NON-CONVENTIONAL PROTEIN TARGETS FOR ANTICANCER METALLODRUGS

4.1. Protein versus DNA Binding. The Nucleosome Core Particle

The molecular target of cisplatin has been established as DNA [198], however, side reactions with other biomolecules may occur and have been linked to its side effects (compare Section 1). Nowadays, more and more metal-based compounds are designed to specifically target proteins over DNA to achieve more selective anticancer activity. The nucleosome core particle (NCP) represents an ideal model with biological relevance to study the preference for DNA or protein coordination, as it consists of double-stranded DNA and histone proteins and has been studied extensively crystallographically.

While cisplatin was shown to bind to N7 of guanine residues and bifunctional crosslinks formed in a stepwise manner [199], RAPTA and other metal(arene) compounds were found at the histone proteins [200, 201]. In contrast, RAED-C, [(cym)Ru(1,2-ethylenediamine)Cl](PF_6), a compound with activity in cisplatin-resistant tumor models [202], was found attached mainly to DNA [200, 201]. While RAPTA-C has a bulky PTA ligand which creates unfavorable steric interactions with the DNA, computational results show that RAED-C–DNA binding has a lower transition state and adduct energy. These studies suggest that the two compounds are electronically very similar and that the uniqueness arises in structural features. These results were mirrored by NCP crystal structures with Ru adducts from RAED-C binding at similar binding sites on DNA to those of cisplatin. However, RAED only forms monofunctional adducts which results in

a subtler distortion of the DNA. SEC–ICP-MS showed that ~71 % of RAED-C is bound to DNA while ~85 % of RAPTA-C reacts with the histone core [200, 201].

4.2. At the Interface of Proteins: Disrupting Protein–Protein Interactions

There is considerable interest in the use of organometallic compounds containing transition metals as scaffolds for the design of potent inhibitors of pharmacologically-important molecular targets. In particular, Ir compounds are valued for their tunable chemical and biological reactivity and the Ir(III) metal center provides kinetic inertness. Leung, Ma et al. [203] investigated the use of Ir complexes for the inhibition of protein–protein interactions to trigger apoptosis. An Ir complex was developed as a selective Jumonji domain-containing protein 2 (JMJD2) inhibitor over other JMJDs, affecting histone methylation levels in A549 cells [203]. It was shown to decrease the JMJD2D−H3K9me3 interaction in A549 cells and increased levels of apoptosis protein markers were detected in A549 cells.

Inactivation of the p53 transcription factor has been associated with tumorigenesis [204]. Human double minute 2 protein (*h*DM2) binds to and regulates p53 which causes proteasomal p53 degradation [205]. Novel organoiridium(III) complexes were found to block the interaction of p53/*h*DM2 in an *in vitro* assay (Figure 13) [206]. The Ir complex exhibited anti-proliferative activity and induced apoptosis in cancer cells at low μM concentrations.

Similarly, chalcoplatin consists of a p53 activator coordinated to a Pt(IV) center [207]. The ligand used was a chalcone that is known to disrupt the p53–*m*DM2 interaction through binding to the p53 binding site of *m*DM2. In this approach cells were aimed to be sensitized for cisplatin through the activation of p53, and cisplatin would be delivered as the reduction product of the prodrug chalcoplatin. Indeed, the compound showed greater levels of cytotoxicity com-

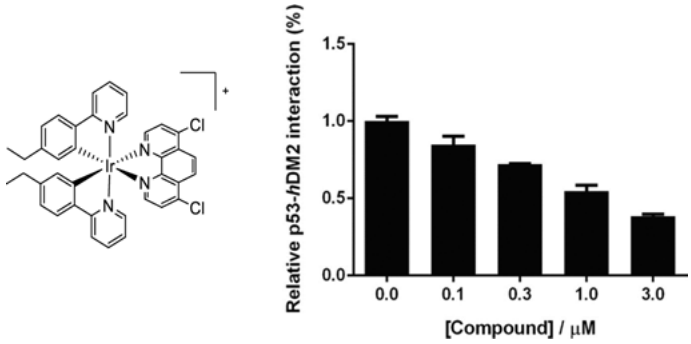

Figure 13. Chemical structure of an organoiridium compound which inhibits the interaction of p53/*h*DM2 in A375 cells. Adapted from [206], published under a Creative Commons 3.0 license by Impact Journals.

pared to cisplatin in p53 wild-type cells but not in p53 null cells, and was in general equally or more active than co-administered cisplatin and chalcone. These similar levels of inhibition in the p53 null cell lines highlighted the dual targeting ability of these complexes, while it also forms cytotoxic Pt–DNA adducts.

5. MODERN BIOANALYTICAL METHODS

With the emergence of protein-targeted anticancer agents, the number of analytical methods used to characterize their modes of action has significantly increased [8, 208–210]. While DNA functionalization can be straightforwardly quantified by element-specific methods after isolation of DNA from cells, protein binding and, in particular, the characterization of the binding site is more challenging. This often requires the combination of more than one method and careful sample preparation to avoid any shifts in equilibria (Figure 14).

Many of the early investigations into the protein binding of metallodrugs were conducted with blood serum proteins, in particular HSA and Tf (compare Section 2). The methods used were relatively simple separation methods, often SEC and capillary electrophoresis. With the advent of more advanced analytical techniques, their hyphenation to mass spectrometers has emerged as a powerful and sensitive method of analysis for metal drugs. The advances especially in MS technology have enabled access to the study of various '-omics' that previously have been too complex to study [14, 211]. Moreover, due to the presence of

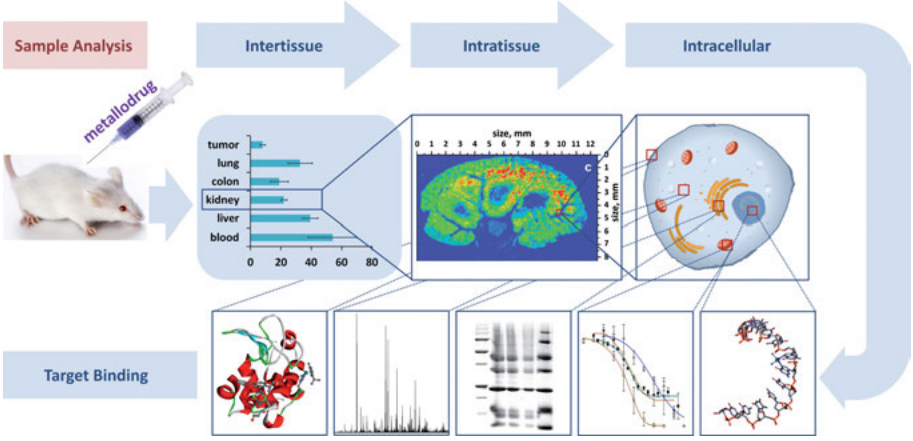

Figure 14. From inter-tissue distribution to the structural characterization of metallodrug–biomolecule adducts. Parts of the figure were adapted from [209] with permission from The Royal Society of Chemistry. The LA-ICP-MS picture was adapted from [218] with permission; copyright 2011 American Chemical Society. The other parts of the figure were constructed from original data.

metals in the structures of the developed drugs, element-specific methods can be used which are very specific and often very sensitive.

One of the most frequently used element-specific methods is ICP-MS, which is based on the atomization and ionization of elements and especially well-suited for the analysis of non-endogenic transition metal ions in biological samples, such as the ones often used in metallodrug research [212]. Importantly ICP-MS can also be hyphenated to laser ablation (LA), which gives access to spatial elemental distribution maps at around 5 μm resolution. Bioimaging techniques allow for the visualization of metal-based drug distribution within organs, tissue, and cells. In order to get more detailed results, especially for cell organelle distributions, nanoSIMS (nano-scale secondary ion-MS) is the method of choice [212]. This allows delineating the area of accumulation in the cell and can be complemented by other imaging methodologies such as lower resolution but molecular information-providing MALDI-MS, or X-ray fluorescence microscopy [212].

In the last decade proteomic methods have been introduced into the field using methods such as gel electrophoresis for the separation of an entire cell's proteome to the blood serum proteins, which can then be analyzed with LA-ICP-MS for metal distribution [213–215]. Even offline comparison of the relative protein expression levels of treated and untreated cells [211] will give a first indication of potential drug targets and their downstream effects. The introduction of proteomics methods has advanced the field from isolated target interaction studies using for example NMR, MS or X-ray diffraction methods. While such experiments with well-chosen biological targets still add significant value to drug development in terms of identification of likely reaction products, stoichiometry, and adduct types, moving closer to a real-life situation is advantageous. This has clearly been achieved by employing proteomics approaches such as multidimensional protein identification technology (MudPIT) [211, 216, 217] or drug pull-downs [14, 219] to identify the targets and/or binding sites of metal fragments to proteins.

These methods provide the basic information to understand the protein binding pattern of metallodrugs and therewith the development of the next generation of compounds with improved biological activity and more selective anticancer action.

6. CONCLUDING REMARKS AND FUTURE DIRECTIONS

For a long time the design paradigm for metal-based anticancer agents was inspired by the DNA binding ability of Pt drugs and, therewith, structures resembling the *cis* configured Pt(II) complexes dominated. However, in the last 20 years the design concept has very much shifted to the consideration of protein targets. The use of protein carriers for simple Ru(III), Ga(III), and Ti(IV) compounds, which reached clinical trials, gave an early indication that protein binding of metallodrugs may be beneficial in their modes of action. Unlike for organic drugs, the loading of metallodrugs onto serum proteins is not necessarily

disadvantageous, as both Tf and HSA, which have been most often studied for this purpose, may improve the accumulation of the cytotoxin in the tumor. Nowadays, this is often used by designing compounds that may bind to serum proteins covalently, non-covalently or through a flexible, often cleavable linker.

While serum protein binding may be advantageous for the transport of the drug, their modification is unlikely to contribute a cytotoxic effect. To achieve protein targeting and interfere with the biological function of the protein, a wide variety of compounds have been designed. The most common design principle used is the coordination of bioactive ligands (or derivatives) to a metal center aiming for a synergistic effect in so-called multitargeted compounds. Original contributions also include a combination with activation mechanisms, as in the case of Pt(IV) or Co(III) complexes which may undergo reduction in cancer cells. The reported Pt(IV) complexes often release cisplatin or analogues and an enzyme inhibitor that, for example, may knock out the cell's defense mechanism, allowing the Pt complex to be more effective.

The reported design concepts were accompanied by the development of new analytical methods while biological assays were used to validate the hypothesis. For a long time the field was dominated by the use of relatively simple separation methods, in the best case combined with mass spectrometric detection. More recently more advanced proteomic methods have been developed and adapted for the special needs of metal compounds and their specific chemical properties. The studies are often combined with experiments to elucidate the distribution of compounds, either in entire test animals or down to the spatial distribution in cells. All these efforts improve the understanding of the behavior of the developed metallodrugs and eventually will support their development to clinical trials.

ACKNOWLEDGMENTS

We thank the organizations and foundations that have supported our research efforts in this area, especially the University of Auckland (University of Auckland Doctoral Scholarship to H.H. and Frederick Douglas Brown Postgraduate Science Research Scholarship to M.P.S), the Royal Society of New Zealand and COST CM1105.

ABBREVIATIONS

AAS	atomic absorption spectroscopy
AES	atomic emission spectroscopy
ASS	acetyl salicylic acid
ATP	adenosine 5′-triphosphate
CatB	cathepsin B

CBDA	bidentate cyclobutane-1,1-dicarboxylic acid
CD	circular dichroism
cDDP	cisplatin
CDK	cyclin-dependent kinase
CE	capillary electrophoresis
COX	cyclooxygenases
Cp	cyclopentadienyl
cym	η^6-p-cymene
EA	ethacrynic acid
EGFR	epidermal growth factor receptor
EPR	enhanced permeability and retention
ER	estrogen receptor
FDA	Food and Drug Administration
GLUT	glucose transporters
GSK-3	glycogen synthase kinase 3
GST	glutathione S-transferase
HDAC	histone deacetylase
HDACi	histone deacetylase inhibitor
*h*DM	human double minute
HSA	human serum albumin
IC_{50}	50 % inhibitory concentration
ICP	inductively coupled plasma
KP1019/NKP-1339	indazolium/sodium *trans*-[tetrachloridobis(1H-indazole) ruthenate(III)]
KP46	[tris(8-oxyquinolinato)gallium(III)]
LA	laser ablation
MALDI	matrix-assisted laser desorption/ionization
MDA-MB-231	breast cancer cell line
*m*DM	murine double minute
MMP	matrix metalloproteinase
MRP1	multidrug resistance protein 1
MS	mass spectrometry
MudPIT	multidimensional protein identification technology
Na/K-ATPase	sodium-potassium adenosine triphosphatase
NAMI-A	new antitumor metastasis inhibitor [H_2imidazole][*trans*-$RuCl_4$(dimethyl sulfoxide)(imidazole)]
nanoSIMS	nanoscale secondary ion mass spectrometry
NCP	nucleosome core particle
NER	nucleotide excision repair
NHC	*N*-heterocyclic carbene
NMR	nuclear magnetic resonance
NSAID	non-steroidal anti-inflammatory drug
PEPT	peptide transporter
Pgp	P-glycoprotein 1
PTA	1,3,5-triaza-7-phosphatricyclo[3.3.1.1]decane
RAED	[Ru(arene)(1,2-ethylenediamine)Cl]$^+$

RAPTA	[Ru(arene)(1,3,5-triaza-7-phosphatricyclo[3.3.1.1]decane)Cl_2]
rHSA	recombinant human serum albumin
RNR	ribonucleotide reductase
ROS	reactive oxygen species
SAHA	suberoylanilide hydroxamic acid (vorinostat)
SEC	size exclusion chromatography
SWCNT	single-walled carbon nanotubes
Tf	transferrin
TrxR	thioredoxin reductase
XANES	X-ray absorption near edge structure

REFERENCES

1. C. S. Allardyce, P. J. Dyson, *Platinum Met. Rev.* **2001**, *45*, 62–69.
2. M. A. Jakupec, M. Galanski, V. B. Arion, C. G. Hartinger, B. K. Keppler, *Dalton Trans.* **2008**, 183–194.
3. C. Barnard, *Johnson Matthey Technol. Rev.* **2017**, *61*, 52–59.
4. J. Reedijk, *Chem. Rev.* **1999**, *99*, 2499–2510.
5. L. Kelland, *Nat. Rev. Cancer* **2007**, *7*, 573–584.
6. F. Arnesano, G. Natile, *Coord. Chem. Rev.* **2009**, *253*, 2070–2081.
7. N. P. E. Barry, P. J. Sadler, *Chem. Commun.* **2013**, *49*, 5106–5131.
8. A. R. Timerbaev, C. G. Hartinger, S. S. Aleksenko, B. K. Keppler, *Chem. Rev.* **2006**, *106*, 2224–2248.
9. N. Cetinbas, M. I. Webb, J. A. Dubland, C. J. Walsby, *J. Biol. Inorg. Chem.* **2010**, *15*, 131–145.
10. M. I. Webb, R. A. Chard, Y. M. Al-Jobory, M. R. Jones, E. W. Y. Wong, C. J. Walsby, *Inorg. Chem.* **2012**, *51*, 954–966.
11. S. P. Mulcahy, E. Meggers, *Top. Organomet. Chem.* **2010**, *32*, 141–153.
12. M. Groessl, P. J. Dyson, *Curr. Top. Med. Chem.* **2011**, *11*, 2632–2646.
13. J. S. Becker, A. Matusch, B. Wu, *Anal. Chim. Acta* **2014**, *835*, 1–18.
14. M. V. Babak, S. M. Meier, K. V. M. Huber, J. Reynisson, A. A. Legin, M. A. Jakupec, A. Roller, A. Stukalov, M. Gridling, K. L. Bennett, J. Colinge, W. Berger, P. J. Dyson, G. Superti-Furga, B. K. Keppler, C. G. Hartinger, *Chem. Sci.* **2015**, *6*, 2449–2456.
15. F. Kratz, *Expert Opin. Therap. Pat.* **2002**, *12*, 433–439.
16. C. S. Allardyce, P. J. Dyson, D. J. Ellis, S. L. Heath, *Chem. Commun.* **2001**, 1396–1397.
17. T. M. Allen, *Nat. Rev. Cancer* **2002**, *2*, 750–763.
18. D. Peer, J. M. Karp, S. Hong, O. C. Farokhzad, R. Margalit, R. Langer, *Nat. Nanotechnol.* **2007**, *2*, 751–760.
19. F. Kratz, *J. Controlled Release* **2008**, *132*, 171–183.
20. S. van Zutphen, J. Reedijk, *Coord. Chem. Rev.* **2005**, *249*, 2845–2853.
21. A. Ito, M. Shinkai, H. Honda, T. Kobayashi, *J. Biosci. Bioeng.* **2005**, *100*, 1–11.
22. C. Corot, P. Robert, J. Idée, M. Port, *Adv. Drug Delivery Rev.* **2006**, *58*, 1471–1504.
23. D. L. J. Thorek, A. K. Chen, J. Czupryna, A. Tsourkas, *Ann. Biomed. Eng.* **2006**, *34*, 23–38.
24. J. Xie, J. Huang, X. Li, S. Sun, X. Chen, *Curr. Med. Chem.* **2009**, *16*, 1278–1294.
25. H. Maeda, in *Drug Delivery in Oncology*, Eds F. Kratz, P. Senter, H. Steinhagen, Wiley-VCH, Weinheim, **2011**, pp. 65–84.

26. S. Sharifi, H. Seyednejad, S. Laurent, F. Atyabi, A. Saei, M. Mahmoudi, *Contrast Media Mol. Imaging* **2015**, *10*, 329–355.
27. W. A. Wani, S. Prashar, S. Shreaz, S. Gómez-Ruiz, *Coord. Chem. Rev.* **2016**, *312*, 67–98.
28. M. A. Jakupec, M. Galanski, B. K. Keppler, in *Rev. Physiol. Biochem. Pharmacol.*, Springer, Berlin, Heidelberg, **2003**, pp. 1–53.
29. J. D. Holding, W. E. Lindup, C. van Laer, G. C. Vreeburg, V. Schilling, J. A. Wilson, P. M. Stell, *Br. J. Clin. Pharmacol.* **1992**, *33*, 75–81.
30. A. Warnecke, I. Fichtner, D. Garmann, U. Jaehde, F. Kratz, *Bioconjug. Chem.* **2004**, *15*, 1349–1359.
31. D. Garmann, A. Warnecke, G. V. Kalayda, F. Kratz, U. Jaehde, *J. Controlled Release* **2008**, *131*, 100–106.
32. Y.-R. Zheng, K. Suntharalingam, T. C. Johnstone, H. Yoo, W. Lin, J. G. Brooks, S. J. Lippard, *J. Am. Chem. Soc.* **2014**, *136*, 8790–8798.
33. F. Kratz, I. Fichtner, A. Zhu, A. Craig, *Mol. Cancer Ther.* **2007**, *6*, A263-A263.
34. R. Graeser, N. Esser, H. Unger, I. Fichtner, A. Zhu, C. Unger, F. Kratz, *Invest. New Drugs* **2010**, *28*, 14–19.
35. F. Liu, J. Mu, B. Xing, *Curr. Pharm. Des.* **2015**, *21*, 1866–1888.
36. M. C. M. Chung, *Biochem. Educ.* **1984**, *12*, 146–154.
37. A. D. Tinoco, A. M. Valentine, *J. Am. Chem. Soc.* **2005**, *127*, 11218–11219.
38. A. V. Rudnev, S. S. Aleksenko, O. Semenova, C. G. Hartinger, A. R. Timerbaev, B. K. Keppler, *J. Sep. Sci.* **2005**, *28*, 121–127.
39. M. J. Clarke, S. Bitler, D. Rennert, M. Buchbinder, A. D. Kelman, *J. Inorg. Biochem.* **1980**, *12*, 79–87.
40. N. Graf, S. J. Lippard, *Adv. Drug Delivery Rev.* **2012**, *64*, 993–1004.
41. M. Pongratz, P. Schluga, M. A. Jakupec, V. B. Arion, C. G. Hartinger, G. Allmaier, B. K. Keppler, *J. Anal. At. Spectrom.* **2004**, *19*, 46–51.
42. F. Kratz, B. K. Keppler, L. Messori, C. Smith, E. N. Baker, *Met. Based Drugs* **1994**, *1*, 169–173.
43. M. Groessl, C. G. Hartinger, K. Polec-Pawlak, M. Jarosz, B. K. Keppler, *Electrophoresis* **2008**, *29*, 2224–2232.
44. A. K. Bytzek, G. Koellensperger, B. K. Keppler, C. G. Hartinger, *J. Inorg. Biochem.* **2016**, *160*, 250–255.
45. M. Groessl, E. Reisner, C. G. Hartinger, R. Eichinger, O. Semenova, A. R. Timerbaev, M. A. Jakupec, V. B. Arion, B. K. Keppler, *J. Med. Chem.* **2007**, *50*, 2185–2193.
46. K. Śpiewak, M. Brindell, *J. Biol. Inorg. Chem.* **2015**, *20*, 695–703.
47. M. Guo, H. Sun, H. J. McArdle, L. Gambling, P. J. Sadler, *Biochemistry* **2000**, *39*, 10023–10033.
48. P. Köpf-Maier, *Anticancer Res.* **1999**, *19*, 493–504.
49. C. G. Hartinger, P. J. Dyson, *Chem. Soc. Rev.* **2009**, *38*, 391–401.
50. J. H. Toney, T. J. Marks, *J. Am. Chem. Soc.* **1985**, *107*, 947–953.
51. E. Y. Tshuva, D. Peri, *Coord. Chem. Rev.* **2009**, *253*, 2098–2115.
52. W. R. Harris, V. L. Pecoraro, *Biochemistry* **1983**, *22*, 292–299.
53. E. J. Beatty, M. C. Cox, T. A. Frenkiel, G. Kubal, A. B. Mason, P. J. Sadler, R. C. Woodworth, *Metal Ions in Biology and Medicine. John Libbey Eurotext* **1994**, 315–320.
54. L. R. Bernstein, *Pharmacol. Rev.* **1998**, *50*, 665–682.
55. Y. Carpentier, F. Liautaud-Roger, F. Labbe, M. Loirette, P. Collery, P. Coninx, *Anticancer Res.* **1987**, *7*, 745–748.
56. L. Einhorn, *Semin. Oncol.* **2003**, *30*, 34–41.
57. C. R. Chitambar, *Expert Opin. Invest. Drugs* **2004**, *13*, 531–541.

58. C. R. Chitambar, *Future Med. Chem.* **2012**, *4*, 1257–1272.
59. M. Groessl, A. Bytzek, C. G. Hartinger, *Electrophoresis* **2009**, *30*, 2720–2727.
60. X. M. He, D. C. Carter, *Nature* **1992**, *358*, 209–215.
61. A. Z. Wang, R. Langer, O. C. Farokhzad, *Annu. Rev. Med.* **2012**, *63*, 185–198.
62. G. Pillai, *SOJ Pharm. Pharm. Sci.* **2014**, *1*, 13.
63. G. J. Quinlan, G. S. Martin, T. W. Evans, *Hepatology* **2005**, *41*, 1211–1219.
64. A. I. Ivanov, J. Christodoulou, J. A. Parkinson, K. J. Barnham, A. Tucker, J. Woodrow, P. J. Sadler, *J. Biol. Chem.* **1998**, *273*, 14721–14730.
65. G. Ferraro, L. Massai, L. Messori, A. Merlino, *Chem. Commun.* **2015**, *51*, 9436–9439.
66. W. Hu, Q. Luo, K. Wu, X. Li, F. Wang, Y. Chen, X. Ma, J. Wang, J. Liu, S. Xiong, P. J. Sadler, *Chem. Commun.* **2011**, *47*, 6006–6008.
67. A. Levina, J. B. Aitken, Y. Gwee, Z. Lim, M. Liu, A. M. Singharay, P. Wong, P. A. Lay, *Chem. Eur. J.* **2013**, *19*, 3609–3619.
68. A. Bijelic, S. Theiner, B. K. Keppler, A. Rompel, *J. Med. Chem.* **2016**, *59*, 5894–5903.
69. M. Baker, H. M. Reynolds, B. Lumicisi, C. J. Bryson, *Self/Nonself* **2010**, *1*, 314–322.
70. W. H. Ang, E. Daldini, L. Juillerat-Jeanneret, P. J. Dyson, *Inorg. Chem.* **2007**, *46*, 9048–9050.
71. F. Kratz, I. Fichtner, R. Graeser, *Invest. New Drugs* **2012**, *30*, 1743–1749.
72. C. D. Spicer, B. G. Davis, *Nat. Commun.* **2014**, *5*, 4740.
73. A. M. Mansour, J. Drevs, N. Esser, F. M. Hamada, O. A. Badary, C. Unger, I. Fichtner, F. Kratz, *Cancer Res.* **2003**, *63*, 4062–4066.
74. C. Scolaro, A. Bergamo, L. Brescacin, R. Delfino, M. Cocchietto, G. Laurenczy, T. J. Geldbach, G. Sava, P. J. Dyson, *J. Med. Chem.* **2005**, *48*, 4161–4171.
75. C. Scolaro, T. J. Geldbach, S. Rochat, A. Dorcier, C. Gossens, A. Bergamo, M. Cocchietto, I. Tavernelli, G. Sava, U. Rothlisberger, P. J. Dyson, *Organometallics* **2006**, *25*, 756–765.
76. M. Hanif, A. A. Nazarov, A. Legin, M. Groessl, V. B. Arion, M. A. Jakupec, Y. O. Tsybin, P. J. Dyson, B. K. Keppler, C. G. Hartinger, *Chem. Commun.* **2012**, *48*, 1475–1477.
77. S. Moon, M. Hanif, M. Kubanik, H. Holtkamp, T. Sohnel, S. M. F. Jamieson, C. G. Hartinger, *ChemPlusChem* **2015**, *80*, 231–236.
78. M. Hanif, S. Moon, M. P. Sullivan, S. Movassaghi, M. Kubanik, D. C. Goldstone, T. Söhnel, S. M. F. Jamieson, C. G. Hartinger, *J. Inorg. Biochem.* **2016**, *165*, 100–107.
79. V. Pichler, J. Mayr, P. Heffeter, O. Domotor, E. A. Enyedy, G. Hermann, D. Groza, G. Kollensperger, M. Galanksi, W. Berger, B. K. Keppler, C. R. Kowol, *Chem. Commun.* **2013**, *49*, 2249–2251.
80. T. C. Johnstone, K. Suntharalingam, S. J. Lippard, *Chem. Rev.* **2016**, *116*, 3436–3486.
81. J. Mayr, P. Heffeter, D. Groza, L. Galvez, G. Koellensperger, A. Roller, B. Alte, M. Haider, W. Berger, C. R. Kowol, B. K. Keppler, *Chem. Sci.* **2017**, *8*, 2241–2250.
82. O. Dömötör, C. G. Hartinger, A. K. Bytzek, T. Kiss, B. K. Keppler, E. A. Enyedy, *J. Biol. Inorg. Chem.* **2013**, *18*, 9–17.
83. J. P. Overington, B. Al-Lazikani, A. L. Hopkins, *Nat. Rev. Drug Discovery* **2006**, *5*, 993–996.
84. F. Arnesano, S. Scintilla, G. Natile, *Angew. Chem., Int. Ed.* **2007**, *46*, 9062–9064.
85. D. Kahra, M. Kovermann, P. Wittung-Stafshede, *Biophys. J.* **2016**, *110*, 95–102.
86. A. K. Boal, A. C. Rosenzweig, *J. Am. Chem. Soc.* **2009**, *131*, 14196–14197.
87. F. Arnesano, L. Banci, I. Bertini, I. C. Felli, M. Losacco, G. Natile, *J. Am. Chem. Soc.* **2011**, *133*, 18361–18369.
88. M. G. Vander Heiden, L. C. Cantley, C. B. Thompson, *Science* **2009**, *324*, 1029–1033.
89. C. G. Hartinger, A. A. Nazarov, S. M. Ashraf, P. J. Dyson, B. K. Keppler, *Curr. Med. Chem.* **2008**, *15*, 2574–2591.

90. T. Tsubomura, M. Ogawa, S. Yano, K. Kobayashi, T. Sakurai, S. Yoshikawa, *Inorg. Chem.* **1990**, *29*, 2622–2626.
91. I. Berger, A. A. Nazarov, C. G. Hartinger, M. Groessl, S.-M. Valiahdi, M. A. Jakupec, B. K. Keppler, *ChemMedChem* **2007**, *2*, 505–514.
92. M. Patra, T. C. Johnstone, K. Suntharalingam, S. J. Lippard, *Angew. Chem., Int. Ed.* **2016**, *55*, 2550–2554.
93. I. Berger, M. Hanif, A. A. Nazarov, C. G. Hartinger, R. O. John, M. L. Kuznetsov, M. Groessl, F. Schmitt, O. Zava, F. Biba, V. B. Arion, M. Galanski, M. A. Jakupec, L. Juillerat-Jeanneret, P. J. Dyson, B. K. Keppler, *Chem. Eur. J.* **2008**, *14*, 9046–9057.
94. M. Hanif, A. A. Nazarov, C. G. Hartinger, W. Kandioller, M. A. Jakupec, V. B. Arion, P. J. Dyson, B. K. Keppler, *Dalton Trans.* **2010**, *39*, 7345–7352.
95. M. Hanif, A. A. Nazarov, A. Legin, M. Groessl, V. B. Arion, M. A. Jakupec, Y. O. Tsybin, P. J. Dyson, B. K. Keppler, C. G. Hartinger, *Chem. Commun.* **2012**, *48*, 1475–1477.
96. A. A. Nazarov, J. Risse, W. H. Ang, F. Schmitt, O. Zava, A. Ruggi, M. Groessl, R. Scopelitti, L. Juillerat-Jeanneret, C. G. Hartinger, P. J. Dyson, *Inorg. Chem.* **2012**, *51*, 3633–3639.
97. M. Hanif, S. Meier, A. Nazarov, J. Risse, A. Legin, A. Casini, M. Jakupec, B. Keppler, C. Hartinger, *Front. Chem.* **2013**, *1*.
98. M. Negom Kouodom, L. Ronconi, M. Celegato, C. Nardon, L. Marchiò, Q. P. Dou, D. Aldinucci, F. Formaggio, D. Fregona, *J. Med. Chem.* **2012**, *55*, 2212–2226.
99. K. N. Thimmaiah, J. K. Horton, R. Seshadri, M. Israel, J. A. Houghton, F. C. Harwood, P. J. Houghton, *J. Med. Chem.* **1992**, *35*, 3358–3364.
100. C. A. Vock, W. H. Ang, C. Scolaro, A. D. Phillips, L. Lagopoulos, L. Juillerat-Jeanneret, G. Sava, R. Scopelliti, P. J. Dyson, *J. Med. Chem.* **2007**, *50*, 2166–2175.
101. L. Meng, X. Zhang, Q. Lu, Z. Fei, P. J. Dyson, *Biomaterials* **2012**, *33*, 1689–1698.
102. R. P. Feazell, N. Nakayama-Ratchford, H. Dai, S. J. Lippard, *J. Am. Chem. Soc.* **2007**, *129*, 8438–8439.
103. A. Casini, C. Gabbiani, F. Sorrentino, M. P. Rigobello, A. Bindoli, T. J. Geldbach, A. Marrone, N. Re, C. G. Hartinger, P. J. Dyson, L. Messori, *J. Med. Chem.* **2008**, *51*, 6773–6781.
104. P. Cohen, *Nat. Rev. Drug Discovery* **2002**, *1*, 309–315.
105. J. Maksimoska, D. S. Williams, G. E. Atilla-Gokcumen, K. S. Smalley, P. J. Carroll, R. D. Webster, P. Filippakopoulos, S. Knapp, M. Herlyn, E. Meggers, *Chem. Eur. J.* **2008**, *14*, 4816–4822.
106. L. Dvořák, I. Popa, P. Štarha, Z. Trávníček, *Eur. J. Inorg. Chem.* **2010**, *2010*, 3441–3448.
107. A. Wilbuer, D. H. Vlecken, D. J. Schmitz, K. Kräling, K. Harms, C. P. Bagowski, E. Meggers, *Angew. Chem., Int. Ed.* **2010**, *49*, 3839–3842.
108. E. Meggers, *Curr. Opin. Chem. Biol.* **2007**, *11*, 287–292.
109. D. S. Williams, G. E. Atilla, H. Bregman, A. Arzoumanian, P. S. Klein, E. Meggers, *Angew. Chem., Int. Ed. Engl.* **2005**, *44*, 1984–1987.
110. G. E. Atilla-Gokcumen, D. S. Williams, H. Bregman, N. Pagano, E. Meggers, *ChemBioChem* **2006**, *7*, 1443–1450.
111. J. E. Debreczeni, A. N. Bullock, G. E. Atilla, D. S. Williams, H. Bregman, S. Knapp, E. Meggers, *Angew. Chem., Int. Ed. Engl.* **2006**, *45*, 1580–1585.
112. J. Maksimoska, D. S. Williams, G. E. Atilla–Gokcumen, K. S. M. Smalley, P. J. Carroll, R. D. Webster, P. Filippakopoulos, S. Knapp, M. Herlyn, E. Meggers, *Chem. Eur. J.* **2008**, *14*, 4816–4822.
113. G. E. Atilla-Gokcumen, N. Pagano, C. Streu, J. Maksimoska, P. Filippakopoulos, S. Knapp, E. Meggers, *ChemBioChem* **2008**, *9*, 2933–2936.

114. P. Xie, C. Streu, J. Qin, H. Bregman, N. Pagano, E. Meggers, R. Marmorstein, *Biochemistry* **2009**, *48*, 5187–5198.
115. G. E. Atilla-Gokcumen, C. L. Di, E. Meggers, *J. Biol. Inorg. Chem.* **2011**, *16*, 45–50.
116. M. Dörr, E. Meggers, *Curr. Opin. Chem. Biol.* **2014**, *19*, 76–81.
117. A. Valdman, X. Fang, S.-T. Pang, P. Ekman, L. Egevad, *The Prostate* **2004**, *60*, 367–371.
118. S. Patel, J. I. M. Woodgett, *Cancer Cell* **2008**, *14*, 351–353.
119. K. S. M. Smalley, R. Contractor, N. K. Haass, A. N. Kulp, G. E. Atilla-Gokcumen, D. S. Williams, H. Bregman, K. T. Flaherty, M. S. Soengas, E. Meggers, M. Herlyn, *Cancer Res.* **2007**, *67*, 209–217.
120. D. W. Zaharevitz, R. Gussio, M. Leost, A. M. Senderowicz, T. Lahusen, C. Kunick, L. Meijer, E. A. Sausville, *Cancer Res.* **1999**, *59*, 2566–2569.
121. A. Dobrov, V. B. Arion, N. Kandler, W. Ginzinger, M. A. Jakupec, A. Rufińska, N. Graf von Keyserlingk, M. Galanski, C. Kowol, B. K. Keppler, *Inorg. Chem.* **2006**, *45*, 1945–1950.
122. W. F. Schmid, S. Zorbas-Seifried, R. O. John, V. B. Arion, M. A. Jakupec, A. Roller, M. Galanski, I. Chiorescu, H. Zorbas, B. K. Keppler, *Inorg. Chem.* **2007**, *46*, 3645–3656.
123. M. F. Primik, G. Mühlgassner, M. A. Jakupec, O. Zava, P. J. Dyson, V. B. Arion, B. K. Keppler, *Inorg. Chem.* **2010**, *49*, 302–311.
124. L. K. Filak, G. Mühlgassner, M. A. Jakupec, P. Heffeter, W. Berger, V. B. Arion, B. K. Keppler, *J. Biol. Inorg. Chem.* **2010**, *15*, 903–918.
125. W. F. Schmid, R. O. John, G. Mühlgassner, P. Heffeter, M. A. Jakupec, M. Galanski, W. Berger, V. B. Arion, B. K. Keppler, *J. Med. Chem.* **2007**, *50*, 6343–6355.
126. W. F. Schmid, R. O. John, V. B. Arion, M. A. Jakupec, B. K. Keppler, *Organometallics* **2007**, *26*, 6643–6652.
127. W. Ginzinger, V. B. Arion, G. Giester, M. Galanski, B. K. Keppler, *Cent. Eur. J. Chem.* **2008**, *6*, 340–346.
128. G. Mühlgassner, C. Bartel, W. F. Schmid, M. A. Jakupec, V. B. Arion, B. K. Keppler, *J. Inorg. Biochem.* **2012**, *116*, 180–187.
129. I. N. Stepanenko, M. S. Novak, G. Mühlgassner, A. Roller, M. Hejl, V. B. Arion, M. A. Jakupec, B. K. Keppler, *Inorg. Chem.* **2011**, *50*, 11715–11728.
130. M. Hanif, H. Henke, S. M. Meier, S. Martic, M. Labib, W. Kandioller, M. A. Jakupec, V. B. Arion, H. B. Kraatz, B. K. Keppler, C. G. Hartinger, *Inorg. Chem.* **2010**, *49*, 7953–7963.
131. A. Kurzwernhart, W. Kandioller, S. Bächler, C. Bartel, S. Martic, M. Buczkowska, G. Mühlgassner, M. A. Jakupec, H.-B. Kraatz, P. J. Bednarski, V. B. Arion, D. Marko, B. K. Keppler, C. G. Hartinger, *J. Med. Chem.* **2012**, *55*, 10512–10522.
132. M. Hanif, S. M. Meier, Z. Adhireksan, H. Henke, S. Martic, S. Movassaghi, M. Labib, W. Kandioller, S. M. F. Jamieson, M. Hejl, M. A. Jakupec, H.-B. Kraatz, C. A. Davey, B. K. Keppler, C. G. Hartinger, *ChemPlusChem* **2017**, *82*, 841–847.
133. P. Xie, C. Streu, J. Qin, H. Bregman, N. Pagano, E. Meggers, R. Marmorstein, *Biochemistry* **2009**, *48*, 5187–5198.
134. A. Nguyen, A. Vessières, E. A. Hillard, S. Top, P. Pigeon, G. Jaouen, *Chimia* **2007**, *61*, 716–724.
135. G. Jaouen, A. Vessières, S. Top, *Chem. Soc. Rev.* **2015**, *44*, 8802–8817.
136. D. Plazuk, A. Wieczorek, A. Blauz, B. Rychlik, *MedChemComm* **2012**, *3*, 498–501.
137. H. V. Nguyen, A. Sallustrau, J. Balzarini, M. R. Bedford, J. C. Eden, N. Georgousi, N. J. Hodges, J. Kedge, Y. Mehellou, C. Tselepis, J. H. R. Tucker, *J. Med. Chem.* **2014**, *57*, 5817–5822.
138. K. R. Barnes, A. Kutikov, S. J. Lippard, *Chem. Biol.* **2004**, *11*, 557–564.
139. Q. He, C. H. Liang, S. J. Lippard, *Proc. Natl. Acad. Sci.* **2000**, *97*, 5768–5772.

140. C. Marzano, V. Gandin, A. Folda, G. Scutari, A. Bindoli, M. P. Rigobello, *Free Radic. Biol. Med.* **2007**, *42*, 872–881.
141. S. Urig, K. Becker, *Seminars in Cancer Biology* **2006**, *16*, 452–465.
142. B. Sloane, J. Dunn, K. Honn, *Science* **1981**, *212*, 1151–1153.
143. B. F. Sloane, *Semin. Cancer Biol.* **1990**, *1*, 137–152.
144. C. F. Shaw, III, *Chem. Rev.* **1999**, *99*, 2589–2600.
145. P. J. Barnard, S. J. Berners-Price, *Coord. Chem. Rev.* **2007**, *251*, 1889–1902.
146. E. S. Arner, H. Nakamura, T. Sasada, J. Yodoi, A. Holmgren, G. Spyrou, *Free Radic. Biol. Med.* **2001**, *31*, 1170–1178.
147. M. Coronnello, E. Mini, B. Caciagli, M. A. Cinellu, A. Bindoli, C. Gabbiani, L. Messori, *J. Med. Chem.* **2005**, *48*, 6761–6765.
148. Y. Omata, M. Folan, M. Shaw, R. L. Messer, P. E. Lockwood, D. Hobbs, S. Bouillaguet, H. Sano, J. B. Lewis, J. C. Wataha, *Toxicol. in Vitro* **2006**, *20*, 882–890.
149. P. Mura, M. Camalli, A. Bindoli, F. Sorrentino, A. Casini, C. Gabbiani, M. Corsini, P. Zanello, M. P. Rigobello, L. Messori, *J. Med. Chem.* **2007**, *50*, 5871–5874.
150. S. Urig, K. Fritz-Wolf, R. Réau, C. Herold-Mende, K. Tóth, E. Davioud-Charvet, K. Becker, *Angew. Chem., Int. Ed.* **2006**, *45*, 1881–1886.
151. Y.-C. Lo, T.-P. Ko, W.-C. Su, T.-L. Su, A. H. J. Wang, *J. Inorg. Biochem.* **2009**, *103*, 1082–1092.
152. L. Oehninger, R. Rubbiani, I. Ott, *Dalton Trans.* **2013**, *42*, 3269–3284.
153. L. Massai, J. Fernandez-Gallardo, A. Guerri, A. Arcangeli, S. Pillozzi, M. Contel, L. Messori, *Dalton Trans.* **2015**, *44*, 11067–11076.
154. R. Mosi, I. R. Baird, J. Cox, V. Anastassov, B. Cameron, R. T. Skerlj, S. P. Fricker, *J. Med. Chem.* **2006**, *49*, 5262–5272.
155. T.-K. Li, L. F. Liu, *Annu. Rev. Pharmacol. Toxicol.* **2001**, *41*, 53–77.
156. J.-P. Monserrat, K. N. Tiwari, L. Quentin, P. Pigeon, G. Jaouen, A. Vessières, G. G. Chabot, E. A. Hillard, *J. Organomet. Chem.* **2013**, *734*, 78–85.
157. M. Kubanik, J. K. Y. Tu, T. Söhnel, M. Hejl, M. A. Jakupec, W. Kandioller, B. K. Keppler, C. G. Hartinger, *Metallodrugs* **2015**, *1*, 24–35.
158. J.-F. Kou, C. Qian, J.-Q. Wang, X. Chen, L.-L. Wang, H. Chao, L.-N. Ji, *J. Biol. Inorg. Chem.* **2012**, *17*, 81–96.
159. R. Visse, H. Nagase, *Circ. Res.* **2003**, *92*, 827–839.
160. T. W. Failes, C. Cullinane, C. I. Diakos, N. Yamamoto, J. G. Lyons, T. W. Hambley, *Chem. Eur. J.* **2007**, *13*, 2974–2982.
161. T. W. Failes, T. W. Hambley, *J. Inorg. Biochem.* **2007**, *101*, 396–403.
162. R. Sasanelli, A. Boccarelli, D. Giordano, M. Laforgia, F. Arnesano, G. Natile, C. Cardellicchio, M. A. M. Capozzi, M. Coluccia, *J. Med. Chem.* **2007**, *50*, 3434–3441.
163. A. Bergamo, A. Masi, A. F. A. Peacock, A. Habtemariam, P. J. Sadler, G. Sava, *J. Inorg. Biochem.* **2010**, *104*, 79–86.
164. W. H. Ang, I. Khalaila, C. S. Allardyce, L. Juillerat-Jeanneret, P. J. Dyson, *J. Am. Chem. Soc.* **2005**, *127*, 1382–1383.
165. H.-W. Lo, F. Ali-Osman, *Curr. Opin. Pharmacol.* **2007**, *7*, 367–374.
166. K. Johansson, M. Ito, C. M. S. Schophuizen, S. Mathew Thengumtharayil, V. D. Heuser, J. Zhang, M. Shimoji, M. Vahter, W. H. Ang, P. J. Dyson, A. Shibata, S. Shuto, Y. Ito, H. Abe, R. Morgenstern, *Mol. Pharmaceutics* **2011**, *8*, 1698–1708.
167. L. J. Parker, L. C. Italiano, C. J. Morton, N. C. Hancock, D. B. Ascher, J. B. Aitken, H. H. Harris, P. Campomanes, U. Rothlisberger, A. De Luca, M. Lo Bello, W. H. Ang, P. J. Dyson, M. W. Parker, *Chem. Eur. J.* **2011**, *17*, 7806–7816.
168. G. Agonigi, T. Riedel, S. Zacchini, E. Păunescu, G. Pampaloni, N. Bartalucci, P. J. Dyson, F. Marchetti, *Inorg. Chem.* **2015**, *54*, 6504–6512.
169. W. H. Ang, L. J. Parker, A. De Luca, L. Juillerat-Jeanneret, C. J. Morton, M. Lo Bello, M. W. Parker, P. J. Dyson, *Angew. Chem., Int. Ed.* **2009**, *48*, 3854–3857.

170. W. H. Ang, A. De Luca, C. Chapuis-Bernasconi, L. Juillerat-Jeanneret, M. Lo Bello, P. J. Dyson, *ChemMedChem* **2007**, *2*, 1799–1806.
171. Y. Lin, Y. Huang, W. Zheng, F. Wang, A. Habtemariam, Q. Luo, X. Li, K. Wu, P. J. Sadler, S. Xiong, *J. Inorg. Biochem.* **2013**, *128*, 77–84.
172. J. B. Meric, S. Rottey, K. Olaussen, J. C. Soria, D. Khayat, O. Rixe, J. P. Spano, *Crit. Rev. Oncol. Hematol.* **2006**, *59*, 51–64.
173. I. Ott, K. Schmidt, B. Kircher, P. Schumacher, T. Wiglenda, R. Gust, *J. Med. Chem.* **2005**, *48*, 622–629.
174. I. Ott, B. Kircher, C. P. Bagowski, D. H. W. Vlecken, E. B. Ott, J. Will, K. Bensdorf, W. S. Sheldrick, R. Gust, *Angew. Chem., Int. Ed.* **2009**, *48*, 1160–1163.
175. G. Rubner, K. Bensdorf, A. Wellner, B. Kircher, S. Bergemann, I. Ott, R. Gust, *J. Med. Chem.* **2010**, *53*, 6889–6898.
176. G. Tamasi, M. Casolaro, A. Magnani, A. Sega, L. Chiasserini, L. Messori, C. Gabbiani, S. M. Valiahdi, M. A. Jakupec, B. K. Keppler, M. B. Hursthouse, R. Cini, *J. Inorg. Biochem.* **2010**, *104*, 799–814.
177. M. U. Raja, J. Tauchman, B. Therrien, G. Süss-Fink, T. Riedel, P. J. Dyson, *Inorg. Chim. Acta* **2014**, *409, Part B*, 479–483.
178. F. Aman, M. Hanif, W. A. Siddiqui, A. Ashraf, L. K. Filak, J. Reynisson, T. Söhnel, S. M. F. Jamieson, C. G. Hartinger, *Organometallics* **2014**, *33*, 5546–5553.
179. F. Aman, M. Hanif, M. Kubanik, A. Ashraf, T. Soehnel, S. Jamieson, W. Siddiqui, C. Hartinger, *Chem. Eur. J.* **2017**, *23*, 4893–4902.
180. M. Paris, M. Porcelloni, M. Binaschi, D. Fattori, *J. Med. Chem.* **2008**, *51*, 1505–1529.
181. D. Griffith, M. P. Morgan, C. J. Marmion, *Chem. Commun.* **2009**, 6735–6737.
182. D. M. Griffith, B. Szőcs, T. Keogh, K. Y. Suponitsky, E. Farkas, P. Buglyó, C. J. Marmion, *J. Inorg. Biochem.* **2011**, *105*, 763–769.
183. J. P. Parker, H. Nimir, D. M. Griffith, B. Duff, A. J. Chubb, M. P. Brennan, M. P. Morgan, D. A. Egan, C. J. Marmion, *J. Inorg. Biochem.* **2013**, *124*, 70–77.
184. J. Spencer, J. Amin, M. Wang, G. Packham, S. S. S. Alwi, G. J. Tizzard, S. J. Coles, R. M. Paranal, J. E. Bradner, T. D. Heightman, *ACS Med. Chem. Lett.* **2011**, *2*, 358–362.
185. R.-R. Ye, Z.-F. Ke, C.-P. Tan, L. He, L.-N. Ji, Z.-W. Mao, *Chem. Eur. J.* **2013**, *19*, 10160–10169.
186. M. A. Jakupec, B. K. Keppler, *Curr. Top. Med. Chem.* **2004**, *4*, 1575–1583.
187. Y. Yu, D. S. Kalinowski, Z. Kovacevic, A. R. Siafakas, P. J. Jansson, C. Stefani, D. B. Lovejoy, P. C. Sharpe, P. V. Bernhardt, D. R. Richardson, *J. Med. Chem.* **2009**, *52*, 5271–5294.
188. C. R. Kowol, R. Berger, R. Eichinger, A. Roller, M. A. Jakupec, P. P. Schmidt, V. B. Arion, B. K. Keppler, *J. Med. Chem.* **2007**, *50*, 1254–1265.
189. M. F. Zaltariov, M. Hammerstad, H. J. Arabshahi, K. Jovanović, K. W. Richter, M. Cazacu, S. Shova, M. Balan, N. H. Andersen, S. Radulović, J. Reynisson, K. K. Andersson, V. B. Arion, *Inorg. Chem.* **2017**.
190. A. Floridi, M. G. Paggi, M. L. Marcante, B. Silvestrini, A. Caputo, C. de Martino, *JNCI, J. Natl. Cancer Inst.* **1981**, *66*, 497–499.
191. A. A. Nazarov, D. Gardini, M. Baquie, L. Juillerat-Jeanneret, T. P. Serkova, E. P. Shevtsova, R. Scopelliti, P. J. Dyson, *Dalton Trans.* **2013**, *42*, 2347–2350.
192. C. Karnthaler-Benbakka, D. Groza, K. Kryeziu, V. Pichler, A. Roller, W. Berger, P. Heffeter, C. R. Kowol, *Angew. Chem., Int. Ed.* **2014**, *53*, 12930–12935.
193. Z. Wang, Z. Xu, G. Zhu, *Angew. Chem., Int. Ed.* **2016**, *55*, 15564–15568.
194. D. G. Garcia, H. C. d. Castro-Faria-Neto, C. I. d. Silva, K. F. C. d. Souza e Souza, C. F. Gonçalves-de-Albuquerque, A. R. Silva, L. M. d. F. d. Amorim, A. S. Freire, R. E. Santelli, L. P. Diniz, F. C. A. Gomes, M. V. d. C. Faria, P. Burth, *Mol. Cancer* **2015**, *14*, 105.

195. A. M. Bondzic, G. Janjic, M. D. Dramicanin, L. Messori, L. Massai, T. Parac-Vogt, V. Vasic, *Metallomics* **2017**, *9*, 292–300.
196. J. F. Neault, A. Benkirane, H. Malonga, H. A. Tajmir-Riahi, *J. Inorg. Biochem.* **2001**, *86*, 603–609.
197. M. Huličiak, J. Vacek, M. Šebela, E. Orolinová, J. Znaleziona, M. Havlíková, M. Kubala, *Biochem. Pharmacol.* **2012**, *83*, 1507–1513.
198. A. T. Yarnell, S. Oh, D. Reinberg, S. J. Lippard, *J. Biol. Chem.* **2001**, *276*, 25736–25741.
199. D. P. Bancroft, C. A. Lepre, S. J. Lippard, *J. Am. Chem. Soc.* **1990**, *112*, 6860–6871.
200. B. Wu, M. S. Ong, M. Groessl, Z. Adhireksan, C. G. Hartinger, P. J. Dyson, C. A. Davey, *Chem. Eur. J.* **2011**, *17*, 3562–3566.
201. Z. Adhireksan, G. E. Davey, P. Campomanes, M. Groessl, C. M. Clavel, H. Yu, A. A. Nazarov, C. H. Yeo, W. H. Ang, P. Droge, U. Rothlisberger, P. J. Dyson, C. A. Davey, *Nat. Commun.* **2014**, *5*, 3462.
202. R. E. Morris, R. E. Aird, S. Murdoch Pdel, H. Chen, J. Cummings, N. D. Hughes, S. Parsons, A. Parkin, G. Boyd, D. I. Jodrell, P. J. Sadler, *J. Med. Chem.* **2001**, *44*, 3616–3621.
203. L.-J. Liu, L. Lu, H.-J. Zhong, B. He, D. W. J. Kwong, D.-L. Ma, C.-H. Leung, *J. Med. Chem.* **2015**, *58*, 6697–6703.
204. B. Vogelstein, D. Lane, A. J. Levine, *Nature* **2000**, *408*, 307–310.
205. S. P. Deb, *Mol. Cancer Res.* **2004**, *1*, 1009.
206. L.-J. Liu, B. He, J. A. Miles, W. Wang, Z. Mao, W. I. Che, J.-J. Lu, X.-P. Chen, A. J. Wilson, D.-L. Ma, C.-H. Leung, *Oncotarget* **2016**, *7*, 13965–13975.
207. L. Ma, R. Ma, Y. Wang, X. Zhu, J. Zhang, H. C. Chan, X. Chen, W. Zhang, S.-K. Chiu, G. Zhu, *Chem. Commun.* **2015**, *51*, 6301–6304.
208. A. Levina, D. C. Crans, P. A. Lay, *Coord. Chem. Rev.* **2017**, *352*, 473–498.
209. C. G. Hartinger, M. Groessl, S. M. Meier, A. Casini, P. J. Dyson, *Chem. Soc. Rev.* **2013**, *42*, 6186–6199.
210. H. Sun, Z.-F. Chai, *Annu. Rep. Prog. Chem., Sect. A, Inorg. Chem.* **2010**, *106*, 20–38.
211. D. A. Wolters, M. P. Washburn, J. R. Yates, *Anal. Chem.* **2001**, *73*, 5683–5690.
212. R. F. S. Lee, S. Theiner, A. Meibom, G. Koellensperger, B. K. Keppler, P. J. Dyson, *Metallomics* **2017**, *9*, 365–381.
213. S. F. Durrant, *J. Anal. At. Spectrom.* **1999**, *14*, 1385–1403.
214. M. S. Jimenez, M. T. Gomez, L. Rodriguez, L. Martinez, J. R. Castillo, *Anal. Bioanal. Chem.* **2009**, *393*, 699–707.
215. M. S. Jiménez, L. Rodriguez, M. T. Gomez, J. R. Castillo, *Talanta* **2010**, *81*, 241–247.
216. A. J. Link, J. Eng, D. M. Schieltz, E. Carmack, G. J. Mize, D. R. Morris, B. M. Garvik, J. R. Yates, *Nat. Biotechnol.* **1999**, *17*, 676–682.
217. M. P. Washburn, D. Wolters, J. R. Yates, *Nat. Biotechnol.* **2001**, *19*, 242–247.
218. E. Moreno-Gordaliza, C. Giesen, A. Lázaro, D. Esteban-Fernández, B. Humanes, B. Cañas, U. Panne, A. Tejedor, N. Jakubowski, M. M. Gómez-Gómez, *Anal. Chem.* **2011**, *83*, 7933–7940.
219. S. M. Meier, D. Kreutz, L. Winter, M. H. M. Klose, K. Cseh, T. Weiss, A. Bileck, B. Alte, J. C. Mader, S. Jana, A. Chatterjee, A. Bhattacharyya, M. Hejl, M. A. Jakupec, P. Heffeter, W. Berger, C. G. Hartinger, B. K. Keppler, G. Wiche, C. Gerner, *Angew. Chem.*, *Int. Ed.* **2017**, *56*, 8267–8271.

14

Metallointercalators and Metalloinsertors: Structural Requirements for DNA Recognition and Anticancer Activity

Ulrich Schatzschneider

Institut für Anorganische Chemie, Julius-Maximilians-Universität Würzburg,
Am Hubland, D-97074 Würzburg, Germany
<ulrich.schatzschneider@uni-wuerzburg.de>

ABSTRACT 388
1. INTRODUCTION 388
2. THE BASICS: NUCLEIC ACID STRUCTURE AND ENZYMATIC PROCESSING 389
   2.1. Bases, Nucleosides, Nucleotides, and Nucleic Acids 389
   2.2. Standard and Non-Standard DNA Structures 391
   2.3. Major and Minor Groove 392
   2.4. Chromatin Structure 393
   2.5. Enzymatic DNA Processing and Modification of Chromatin 393
3. ANALYTICAL METHODS TO STUDY METAL COMPLEX-DNA INTERACTIONS 394
   3.1. Optical Spectroscopy 394
   3.2. Viscosity Measurements 395
   3.3. Other Methods 395
4. METALLOINTERCALATORS 396
   4.1. Ruthenium Polypyridyl Complexes 396
   4.2. Ruthenium Arene Complexes 408
   4.3. Other Metal Complexes 411
5. METALLOINSERTORS 413
   5.1. DNA Mismatches, Mismatch Repair Systems, and Cancer 413
   5.2. Rhodium Metalloinsertors 414
   5.3. Other Metal Complexes 422

Metal Ions in Life Sciences, Volume 18 Edited by Astrid Sigel, Helmut Sigel, Eva Freisinger, and Roland K. O. Sigel

https://doi.org/10.1515/9783110470734-014

Met. Ions Life Sci. **2018**, *18*, 387–435

6. CONCLUDING REMARKS AND FUTURE DIRECTIONS 426
ABBREVIATIONS AND DEFINITIONS 427
REFERENCES 430

Abstract: As the carrier of the inheritable information in cells, DNA has been the target of metal complexes for over 40 years. In this chapter, the focus will be on non-covalent recognition of the highly structured DNA surface by substitutionally inert metal complexes capable of either sliding in between the normal base pairs as metallointercalators or flipping out thermodynamically destabilized mispaired nucleobases as metalloinsertors. While most of the compounds discussed are based on ruthenium(II) and rhodium(III) due to their stable octahedral coordination environment and low-spin $4d^6$ electronic configuration, most recent developments of alternative metal complexes, based on both transition metals and main group elements, will also be highlighted. A particular focus of the coverage is on structural data from X-ray structure analysis, which now provides details of the interaction at unprecedented details and will enable development of novel DNA binding probes for fundamental studies as well as new anticancer drug candidates.

Keywords: DNA · metallointercalators · metalloinsertors · mismatches · rhodium · ruthenium

1. INTRODUCTION

DNA as the central carrier of information in living systems has been targeted by metal complexes for more than four decades. In addition to covalent binding to the backbone phosphate groups and, in particular, exposed nitrogen atoms of the nucleobases, the study of non-covalent interactions with the highly structured DNA surface has emerged as a very important line of research. This is motivated both by the search for fundamental tools to probe DNA structure and dynamics, but also for the development of novel chemotherapeutic approaches in anticancer treatment.

Requirements are a substitutionally inert metal center to obtain compounds stable under physiological conditions, and a proper design of the outer ligand periphery for selective interaction with the functional groups exposed on the DNA surface, by a combination of sterics-based shape recognition and weak non-covalent interactions. Two different major binding modes have emerged in recent years.

On one hand, metallointercalators incorporate ligands with an extended aromatic surface area able to gain access to the DNA base stack by sliding in between the nucleobase pairs without further disturbance of the overall π-stack, but with distortion of the sugar-phosphate backbone and regular helical structure. Further binding specificity of these "extra base pairs" can be achieved by variation of the coligand periphery.

On the other hand, metalloinsertors flip out a thermodynamically destabilized base pair, for example at mismatched sites not involving the canonical Watson-Crick pairs, and then insert an extended aromatic ligand instead of the mispaired nucleobases.

After a short recapitulation of the basic features of the DNA double helix and its organization into chromatin as well as common analytical methods to investi-

gate metal complex binding to DNA, this chapter will focus on recent structural data, mostly from X-ray structure analysis that has become available during the last couple of years, which showcases the wide variety of metal complex binding to both matched and mismatched oligonucleotides, and will also highlight the latest developments in multifunctional metallointercalators and metalloinsertors, with a particular focus on reports where bioactivity data has also become available. The literature survey is mostly restricted to new results published within the last five years, with publications covered from approximately 2012 until early 2017.

2. THE BASICS: NUCLEIC ACID STRUCTURE AND ENZYMATIC PROCESSING

2.1. Bases, Nucleosides, Nucleotides, and Nucleic Acids

The DNA double helix is one of the most iconic structures in science and the carrier of inheritable information of all organisms, with the exception of retro- and riboviruses, which utilize RNA instead. Although composed of only four basic building blocks, it exhibits a diverse range of structural features which can be specifically recognized by metal complexes in a variety of binding modes.

The central repeat unit of the DNA backbone is the nucleotide, which is composed of the cyclic furanoside sugar β-D-2′-deoxyribose, which is phosphorylated in the 5′-position and functionalized at C1′ via a β-glycosidic C-N bond to either a purine or pyrimidine heterocycle [1]. In contrast, the term nucleoside refers to the non-phosphorylated combination of deoxyribose sugar and nucleobase, while the free bases have a hydrogen atom in position 9 for the purines or position 1 for the pyrimidines, respectively (Figure 1).

The phosphate group in nucleotides undergoes a facile monodeprotonation already at a low pH, although the pK_a value is not easily accessible, but for the second hydroxy group, a pK_a of 6.6–6.7 was determined for all nucleotides, which thus exist in the monoanionic form under physiological conditions [1].

With regard to the atomic labeling scheme, a prime symbol indicates positions in the ribose moiety while nucleobase atom indicators are non-primed. The free bases are usually indicated by three-letter codes Ade, Gua, Cyt, and Thy while nucleotides are refered to by capital one-letter codes A, G, C, and T, with a preceeding letter “d” to indicate the deoxyribose form. In RNA, thymine is replaced by uracil with letter codes Ura and U for the nucleobase and nucleotide, respectively (Figure 1).

The nucleotides are linked by 3′,5′-phosphodiester bonds to form oligonucleotides. The base sequence is written from left to right with single-letter codes refering to a 5′-to-3′ chain direction while graphical representations are either from top to bottom or left to right in the same 5′-to-3′ arrangement. Phosphate groups are indicated with a letter “p” but this is often omitted for convenience. A homopolymer composed of deoxyadenylate repeat units is abbreviated as poly(dA) while heteropolymers with a well-defined alternating structure, for example of deoxyadenylate and deoxythymidylate, are indicated as poly(dA-dT).

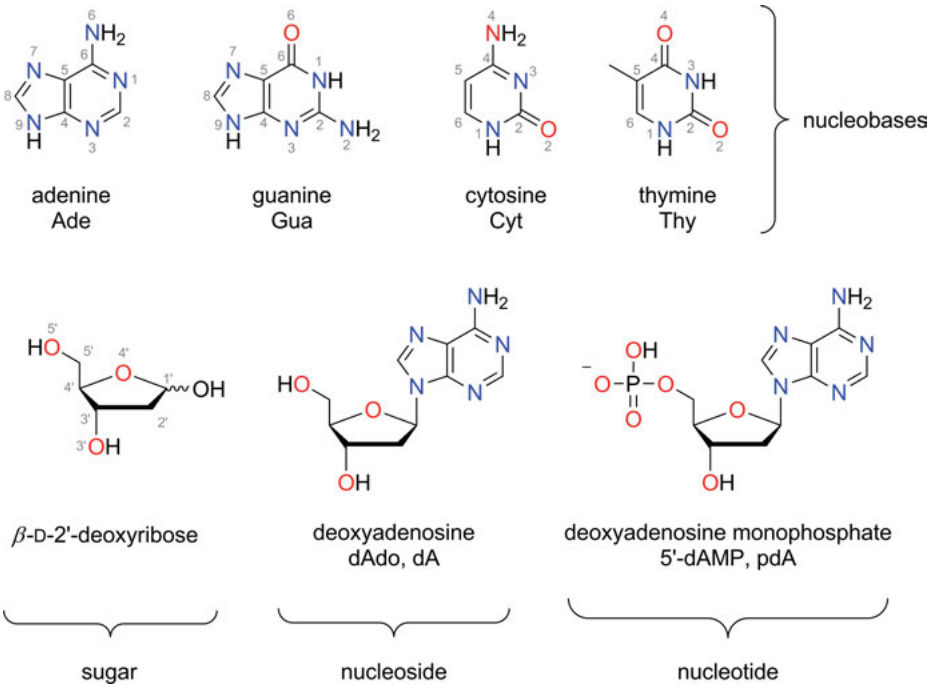

Figure 1. Structure and atomic labeling scheme for the deoxyribose sugar, the four DNA nucleobases, and the adenine-based nucleoside and nucleotide.

If there is a random distribution of the building blocks over the chain, this is instead indicated by a comma as in poly(dA,dT).

While the aromatic nucleobases are planar, this is not the case with the (deoxy)ribose sugar and the sugar-phosphate backbone. Torsion angles along the sequence of atoms P → O(5′) → C(5′) → C(4′) and so on are indicated in alphabetic order by greek symbols α, β, γ, ... The torsion angles in the sugar are given as ν_0 to ν_4 and the orientation of the base relative to the sugar by χ. The five-membered furanose ring assumes either an "envelope" (E) form with four atoms in plane and the fifth out of plane, or a "twist" (T) form with two atoms displaced in opposite directions relative to a plane defined by the other three atoms [1]. Furthermore, the nucleobase can either be oriented in a way that the larger part of the heterocycle (the six-membered ring in the purines or the O(2) in the pyrimidines) points away from the sugar or overlaps with its five-membered ring. The former orientation is called *anti* while the latter is labeled as *syn*. Finally, different orientations of O(5′) due to rotation along the C(4′)-C(5′) bond can give rise to additional conformational flexibility.

2.2. Standard and Non-Standard DNA Structures

Due to the complementary hydrogen-bonding ability of the A and T as well as G and C nucleotides, these form purine-pyrimidine base pairs held together by A(N6):T(O4) and T(N3):A(N1) interactions in the former and G(N1):C(N3), G(N2):C(O2), and C(N4):G(O6) bonds in the latter case if properly oriented relative to each other. In this notation, the donor atom is given first followed by the acceptor atom. Usually, two different complementary oligonucleotides form a dimeric structure, but "self-interaction" is also possible in so-called hairpins if there are matching sequences on a single oligonucleotide. However, this treatment will be restricted to oligonucleotide duplexes.

These are composed of a core of hydrogen-bonded nucleobase pairs which are stacked on top of each other while two antiparallel strands of the sugar-phosphate backbone with a 5′→3′ and 3′→5′ alignment run along the outer rim of the base stack. Several different parameters characterize the relative orientation of the nucleobase pairs and the alignment of the backbone. The pitch of the helix is the distance along the backbone to complete one turn, while the pitch height is the number of nucleotides in one turn, and the unit height defines the translation along the helix axis per base pair. Finally, the unit twist is the angle between one nucleotide and either of its nearest neighbors. Although the distance between the two sugar C(1′) atoms of a hydrogen-bonded nucleobase pair is about the same for the A:T and G:C base pairs, these are usually not centered along the axis of the helix, but displaced outwards, and additionally tilted from an orientation exactly perpendicular to the helix axis. A small propeller twist is also possible in paired nucleobases, with a perfect coplanar arrangement not a strict requirement [1].

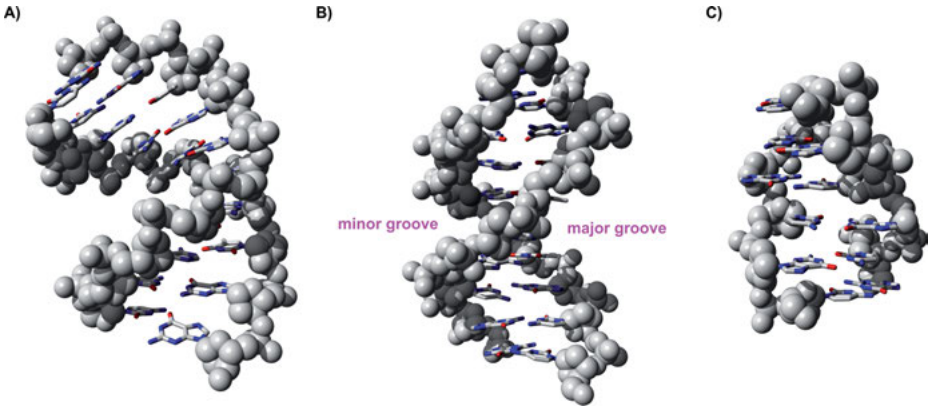

Figure 2. Crystal structures of A-, B-, and Z-DNA (from left to right) with the sugar-phosphate backbone shown as grey spheres and the nucleobases as sticks (carbon grey, nitrogen: blue, oxygen: red). All solvent water molecules as well as counterions have been removed for clarity and hydrogen atoms are not shown. The two grooves are labelled accordingly. The figure was prepared with Yasara and PovRay from the PDB entries 1ZF8, 1ZF0, and 3P4J, respectively [2, 3].

Different structural types of DNA have been characterized over the last decades, most of them by single crystal X-ray diffraction. The standard form assumed by native DNA is a right-handed helix called B-DNA with a pitch of 33.8 Å and 10 nucleobase pairs per full turn, and thus an axial rise per residue of 3.38 Å (Figure 2B). However, depending on the sequence context, variation of the salt concentration in the crystallization buffer, and the nature of the cations present, other structures such as A- and Z-DNA are also observed (Figure 2A+C) [1–3].

2.3. Major and Minor Groove

Due to the abovementioned deviation of the base pairs from the central helix axis, the outer envelope of the double helix is not a smooth cylinder, but exhibits two indentations of different depth and width called grooves (Figure 2B). The metrical parameters of these grooves as well as the nucleobase functional groups exposed at their bottom are key recognition elements which can be used to guide metal complexes to particular sites in an oligonucleotide duplex.

The minor groove is defined by the O(2) atoms of the pyrimidine bases and the N(3) centers of the purines, while the major groove is lined by N(6) and O(4) from the A:T base pair as well as O(6) and N(4) of the G:C nucleobases (Figure 3). At 11.7 *vs.* 5.7 Å, the major groove in B-DNA is about twice as wide as the minor one while the depth shows only a slight variation, with 7.5 Å for the minor and 8.5 Å for the major groove [1]. Interestingly, in the alternative A-DNA form (Figure 2A), the "minor" groove at 11.0 Å is wider than the "major" one with 2.7 Å and there are also much more pronounced differences in the depth, at 2.8 Å *vs.* 13.5 Å for minor and major groove, respectively.

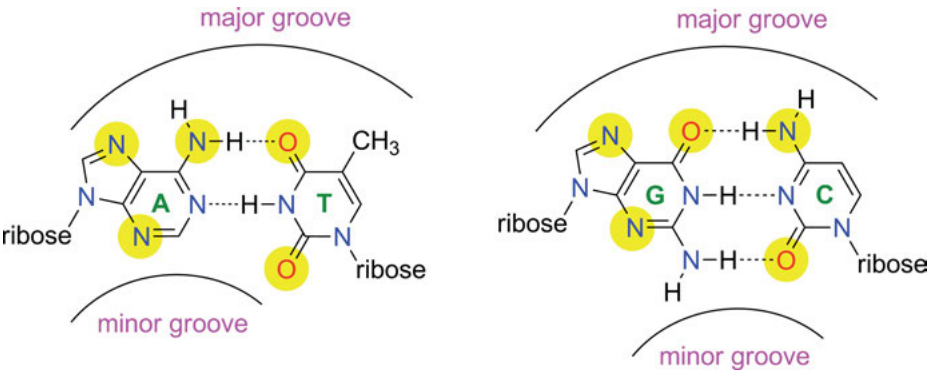

Figure 3. Structures of the A:T and G:C nucleobase pairs with hydrogen bonds indicated as dashed lines and functional groups exposed in the major and minor groove highlighted by yellow circles.

2.4. Chromatin Structure

While the primary building blocks and structure of the DNA double helix is the same for all branches of life, the localization and organization of the genome is different for prokaryotic *vs.* eukaryotic organisms. Prokaryotes only contain a single set of DNA, usually packed in a circular, double-stranded structure called nucleoid. Since there is only one copy of each gene, these organisms are haploid. Their chromosomal DNA is sometimes supplemented by additional circular pieces of DNA called plasmids, which can also be transferred between cells.

In contrast, the DNA of eukaryotes is localized in a special membrane-enclosed compartment, the nucleus, and consists of several linear pieces of double-stranded DNA. Furthermore, eukaryotes are typically diploid, and thus contain two copies of each gene on a pair of chromosomes, 46 of them in the case of humans. Importantly, the eukaryotic DNA is normally tightly packed around a class of basic proteins called histones, with five sub-types H1, H2A, H2B, H3, and H4 identified [4]. A high content of lysine or arginine is present in all histones for charge compensation of the negatively charged sugar-phosphate backbone of the DNA. About 147 base pairs are wrapped around a heterooctamer of two copies each of H2A, H2B, H3, and H4 called the nucleosome, while the linker histone H1 stabilizes DNA between the nucleosome particles.

2.5. Enzymatic DNA Processing and Modification of Chromatin

Histones are post-translationally modified by acetylation, methylation, phosphorylation, poly-ADP-ribosylation, and, in the case of H2A and H2B, ubiquitylation, among others [4–7]. The attachment and removal of these covalent modifiers has important implications in the control of replication and transcription. Methylation occurs at the ε-amino groups of particular lysines and arginines in H3 and H4. In contrast, acetylation can be assigned to two different types of modification. While that of the amino group in *N*-terminal serine residues in H1, H2A, and H4 is also irreversible, some of the lysine ε-amino functionalities in H2A, H2B, H3, and H4 can be acetylated in a reversible fashion. Histone phosphorylation, on the other hand, takes place at specific serine and threonine hydroxy groups in histone H1, is reversible, and coupled to certain events in the cell cycle. Finally, ubiquitylation takes place at Lys119 of histone H2a via a glycine dipeptide [8].

Importantly, these covalent histone modifications are a major contributor to the regulation of accessibility and function of eukaryotic DNA since the "histone code" can be read by several enzymes [8]. In particular, the interplay of histone acetyltransferases (HATs) and histone deacetylases (HDACs) in the transfer of an acetyl group to and from the ε-amino groups of lysine side chains is implicated in transcriptional control. Changes in histone modification are associated with genomic instability, chromosome segregation defects, and cancer. Consequently, a number of metal complexes have been designed and explored as HDAC inhibitors [9–11].

3. ANALYTICAL METHODS TO STUDY METAL COMPLEX-DNA INTERACTIONS

3.1. Optical Spectroscopy

The most straightforward methods to investigate metal complex-DNA interactions commonly available in a chemical or biological laboratory, are based on optical spectroscopy, and involve the measurement of changes in the optical absorption or emission profile of metal complexes in the presence and absence of duplex DNA, usually either short synthetic oligonucleotides or isolates of genomic DNA with a random sequence, such as calf-thymus DNA (CT DNA). Many metal complexes show intense absorption bands in the UV/Vis spectral range, usually due to charge transfer transitions involving π-orbitals of extended (hetero)aromatic ligands. When these interact with the π-stack of the nucleobase pairs, electronic coupling results in an increase of delocalization. The associated decrease of the HOMO-LUMO gap results in a red (bathochromic) shift of the metal-associated absorption bands in the DNA-bound state compared to the free complex in solution. Although less easy to rationalize, this is often also accompanied with an overall decrease of the band intensity (hypochromic effect). In particular, a plot of hypochromicity *vs.* the DNA-to-metal complex concentration ratio should show a saturation behavior upon addition of increasing amounts of DNA. From a fit to this plot, the intrinsic DNA binding constant K_B can be determined [12, 13]. *However, it is vital to note that this method only provides information on the strength of the association of the metal complex with the DNA, but not on the binding mode.* Thus, from such "DNA titrations", it is not possible to distinguish binding in the major or minor groove from intercalation or insertion. Or, to put it another way, while a DNA intercalator is expected to show a bathochromic and hypochromic effect in the presence of a duplex oligonucleotide, not all compounds showing this effect are necessarily intercalators [14].

Alternatively, changes in the emission quantum yield and/or excited state lifetime can be utilized to determine the binding constant by fluorescence spectroscopy. While many metal complexes are non-emissive in aqueous solution, with quenching usually assigned to hydrogen bonding of water to heteroatom sites, a tight association of such compounds with the DNA double helix can give rise to an increase in emission, if part of the complex is shielded from interactions with water due to the local hydrophobic environment in the DNA base stack.

Furthermore, if the compound of interest is non-emissive even under these conditions, the so-called ethidium bromide (EtBr) displacement assay can be utilized, in which the organic phenanthridine dye EtBr is expelled from the DNA double helix by a metal complex with a higher binding constant, which results in quenching of the emission of the EtBr released. *However, even though EtBr is well-established to bind in an intercalative fashion, the molecule which displaces it does not necessarily have to be an intercalator itself, since the only requirement is that it binds to DNA more tightly than EtBr.* Thus, this assay also provides information only on the strength of the interaction, but not on the binding mode.

Finally, CD spectroscopy is sensitive to conformational changes of the chiral right-handed double helix of B-DNA, as induced, for example, by metal complex binding. Its typical spectroscopic signature shows a negative band at 245 nm due to the helicity of the DNA duplex and a positive one at 275 nm due to base stacking [15]. In addition, induced CD signals can be detected in the spectral range of MLCT bands, if a metal complex probe is tightly associated with the DNA and thus exposed to its local chiral environment [16]. Interestingly, enantiomer separation of DNA-binding metal complexes has also been achieved by HPLC using chiral stationary phases [17].

3.2. Viscosity Measurements

For an unambiguous demonstration of an intercalative binding mode, methods are required which are sensitive to the contour length of the DNA, since metallointercalators act like "additional base pairs" and their binding results in a significant stiffening and increase of the contour length of the DNA. In contrast, groove binders usually allow the DNA to "coil up" around the molecule and thus decrease the hydrodynamic radius. If this effect is sufficiently pronounced, it can be determined by the measurement of the viscosity of DNA duplex solutions in the presence and absence of a metal complex [18]. Metallointercalators will lead to increased viscosity, although often less pronounced than the effect observed for ethidium bromide, which should always be included in any study as a positive control, while groove binding results in a decrease of the viscosity.

3.3. Other Methods

An insight in the energetics of the DNA binding of metal complexes is provided by thermal melting studies of duplex DNA in the absence and presence of probe molecules as well as isothermal titration calorimetry (ITC) [19, 20]. Covalent modifications and DNA strand breaks are revealed by gel electrophoresis, which can also be used for footprinting experiments to detect metal complex or protein binding sites. Higher levels of DNA organisation such as metal complex-induced aggregation is visualized for example by atomic force microscopy (AFM) [21], or, utilizing the high electron density of transition metal centers, by transmission electron microscopy (TEM) [22].

Finally, detailed structural insights in the interaction of metal complexes at atomic resolution are provided by NMR or single crystal X-ray structure analysis. In recent years, also some high-level theoretical studies have be utilized to investigate DNA binding of metal-based probes in the absence of structural information [23–25].

4. METALLOINTERCALATORS

4.1. Ruthenium Polypyridyl Complexes

More than 50 years ago, it was recognized that planar aromatic molecules such as 9-aminoacridine or ethidium bromide bind to duplex DNA by intercalation. This binding mode is characterized by the intercalating molecule sliding in between the nucleobase pairs without further disturbance of the overall π-stack but distortion of the sugar-phosphate backbone and regular helical structure [1]. Two stages of the binding process can be distinguished, an initial fast diffusion-controlled interaction with the outer parts of the double helix, followed by a slower access to the DNA base stack.

Possibly inspired by some structural similarity between the acridine dyes and square-planar platinum complexes such as $[PtCl(terpy)]^+$, in 1974, Lippard reported on the binding of $[Pt(SCH_2CH_2OH)(terpy)]^+$, with chloride replaced by the more tightly coordinated 2-hydroxyethanethiolate ligand, to calf thymus DNA [26]. A binding constant of $K = 1.2 \times 10^6$ M^{-1} was determined by UV/Vis titration and the specific viscosity was found to increase with increasing amounts of metal complex added to the CT DNA. In this publication, the term "metallointercalation" was introduced to the literature for the first time [26].

While such planar metal complexes exhibit a rather high affinity for duplex DNA, an enantioselective recognition of the chiral DNA duplex is not possible due to the presence of a plane of symmetry. However, in 1982, Barton reported on the intercalative binding of $[Zn(phen)_3]^{2+}$ to circular pM2 DNA and found an optical enrichment of one of the two enantiomers upon dialysis of CT DNA against a racemic mixture of $[Zn(phen)_3]^{2+}$ [27]. Although zinc(II) complexes are not inert against ligand dissociation, a half-live for racemization of 10 d at 4 °C was determined for $[Zn(phen)_3]^{2+}$. Consequently, the focus shifted to substitutionally more stable $[Ru(phen)_3]^{2+}$, which was obtained in enantiomerically pure Δ- and Λ-form by repeated diastereomeric recrystallization in the presence of antimony D-tartrate. Interestingly, a chiral discrimination was also observed in the DNA binding affinity [28, 29]. With a right-handed propeller-like structure, Δ-$[Ru(phen)_3]^{2+}$ was found to exhibit a stronger binding to the right-handed B-DNA helix than the corresponding Λ-enantiomer, in which the two non-intercalating phenanthroline ligands clash with the phosphate backbone. Indeed, NMR experiments later demonstrated a minor groove binding of the compound, although the intercalative interaction was questioned [30]. Since then, several thousand publications have appeared on the interaction of ruthenium polypyridyl complexes with DNA and their potential biological activity. The most notable of these is possibly the discovery of $[Ru(bpy)_2(dppz)]^{2+}$ as a fluorescent switch-on intercalative probe for duplex DNA [31, 32] (Figure 4).

While the complex itself is not luminescent in aqueous solution at 10 μM in the absence of DNA, the addition of 100 μM poly[d(GC)·d(GC)] resulted in an enhancement of the emission by a factor of about 10000 for both B- and Z-form DNA, while only a much weaker emission was observed for a related A-form duplex [31]. Detailed spectroscopic studies, for example with time-resolved infra-

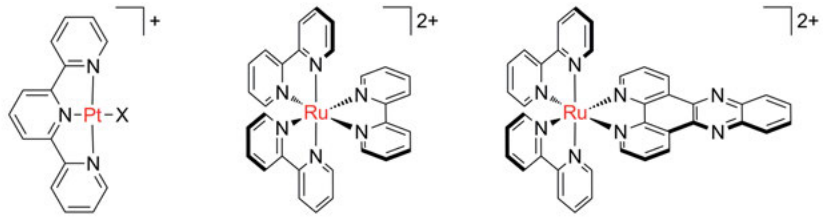

$[PtX(terpy)]^+$
X = Cl, SCH_2CH_2OH

$[Ru(bpy)_3]^{2+}$

$[Ru(bpy)_2(dppz)]^{2+}$

Figure 4. Structures of prototypical DNA metallointercalators $[PtX(terpy)]^+$, $[Ru(bpy)_3]^{2+}$, and $[Ru(bpy)_2(dppz)]^{2+}$.

red spectroscopy (TRIR), on this as well as closely related compounds have since then helped to identifiy the relevant emissive "bright" and non-emissive "dark" states [33] and the differences between the Δ- and Λ-isomers in the chiral environment of the DNA double helix [34, 35]. The influence of ionic strength, temperature, and DNA sequence and conformational context has also been studied [36]. More recently, even *in cellulo* studies have been carried out in HepG2 cells with localized pump-probe spectroscopy and demonstrated that $[Ru(bpy)_2(dppz)]^{2+}$ also intercalates to nuclear DNA in living cells [37]. Additional insight in the nature of the dark and emissive states also came from TDDFT calculations [38].

Due to the immense number of reports in the field, the following section will mostly be focused on compounds for which the DNA binding mode has been established at atomic resolution using X-ray structure analysis, which show particularly promising or unusual biological activity, or exhibit unusual structural motifs that have emerged only during the last 5 to 6 years. For the reminder of the work, the reader is directed at excellent recent reviews for example by Barton et al. [39–42], Thomas et al. [43, 44], Liu and Sadler [45], Aldrich-Wright et al. [46], Chao et al. [32], and Cardin et al. [47].

Although NMR spectroscopy has regularly been applied to investigate the binding mode of metal complexes to duplex DNA [30, 48–50], a distinct analysis of all interactions usually requires structural data from X-ray crystallography. This is a formidable task since the formation of suitable crystals depends to a large degree on the use of a proper oligonucleotide sequence and usually requires a lot of screening of different conditions and additives. Thus, while the structure of a rhodium complex bound to a short synthetic duplex DNA was already reported in 2000 (see Section 4.3) [51], it took another decade until Cardin and coworkers in 2011 finally reported on the structure determination of an intercalating ruthenium(II) dipyridophenazine (dppz) complex bound to a 10mer duplex DNA at 1.1 Ångström resolution [52]. Instead of the bpy and phen coligands otherwise often utilized in metallintercalators, the title compound of this study, $[Ru(tap)_2(dppz)]^{2+}$, incorporates electron-deficient 1,4,5,8-tetraazaphenanthrene (tap) coligands to increase the oxidation potential of the excited state to facilitate direct guanine oxidation and covalent adduct formation with DNA. The oligonu-

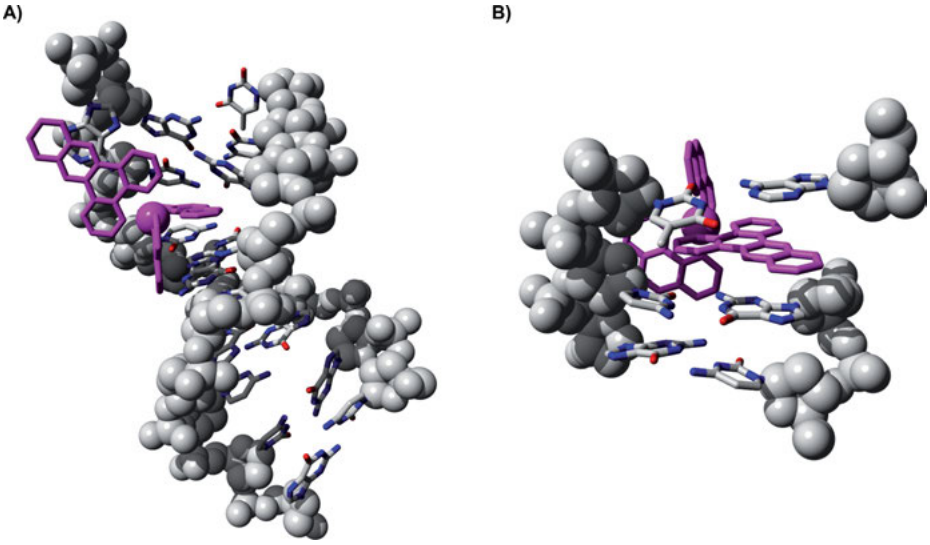

Figure 5. Crystal structure of $[Ru(tap)_2(dppz)]^{2+}$ non-covalently bound to $d(TCGGCGCCGA)_2$ showing the two different binding sites (**A**) with one tap ligand semi-intercalated at the G3-G4 step and (**B**) the dppz ligand intercalated from the minor groove between G9 and A10, but with the terminal residue A10 flipped out and interacting with another duplex in the crystal lattice. The figure was prepared with Yasara and PovRay from the PDB entry 3QRN [52].

cleotide chosen was a self-complementary decamer $d(TCGGCGCCGA)_2$ known to form both standard B-DNA and Holliday junctions and the Λ-enantiomer of $[Ru(tap)_2(dppz)]^{2+}$ was used in the crystallization study [52] (Figure 5).

The structure contained four molecules of $[Ru(tap)_2(dppz)]^{2+}$ non-covalently bound to the oligonucleotide duplex in two different binding modes, in pair-wise relation due to symmetry. While one binding site incorporated a tap ligand semi-intercalated at the G3-G4 step (Figure 5A), the second binding site was occupied by a dppz ligand intercalated from the minor groove between G9 and A10, but with the terminal residue A10 flipped out and interacting with another duplex in the crystal lattice (Figure 5B) [52]. Very recently, the effect of photoexcitation of this system at 400 nm was studied with time-resolved IR spectroscopy on the picosecond to microsecond timescale on crushed microcrystals of material previously investigated by X-ray structure analysis [53]. Interestingly, new transient absorption bands resulting from the electronically excited state as well as ground state bleaching could clearly be distinguished for the metal complex *vs.* nucleobase vibrations. Even in the absence of direct DNA excitation, the C=O stretches of cytosine and guanine at 1645 and 1680 cm^{-1}, respectively, as well as the guanine and adenine ring vibrations at 1580 and 1620 cm^{-1} experienced a pronounced decrease in intensity already at 20 ps post-excitation, indicative of changes in the charge distribution in the vicinity [53]. The photophysical properties of $[Ru(tap)_2(dppz)]^{2+}$ bound to short oligonucleotides also showed an enan-

tiomeric discrimination, in which particularly the Λ-enantiomer was very sensitive to the base sequence context [54]. Interestingly, the degree of hydration was also found to have a profound influence on the structure of such ruthenium dppz complex adducts with duplex oligonucleotides [55].

Next to appear in the literature was the crystal structure of the Δ-enantiomer of the prototypical "ligth-switch" complex $[Ru(bpy)_2(dppz)]^{2+}$ bound to a 12mer oligonucleotide duplex $d(CGGAAATTACCG)_2$ incorporating two AA mismatches. Interestingly, although the Ru dppz moiety is generally assumed to bind in an intercalative fashion, the structural analysis revealed a mix of metallointercalation and metalloinsertion binding modes on the same duplex (see Section 5.3) [56].

In contrast, the Λ-enantiomer of the closely related $[Ru(phen)_2(dppz)]^{2+}$ was found to bind to $d(CCGGTACCGG)_2$ from the minor groove [57]. Three molecules of the Ru complex are intercalated, two in symmetry-equivalent positions at each end of the duplex, and the third one in the center at T_5A_6 (Figure 6). In each case, the dppz ligand is positioned deep inside the nucleobase stack in a prototypical example of a symmetrical perpendicular intercalative mode, with the ruthenium center displaced from the helix axis by about 5 Å, and the distal part of the dppz ligand protruding into the opposite major groove. The enantiomeric specificity of this binding mode was traced back to interactions with the sugar H(4′) and nucleobase H(2) of the adenosine residue in the center of the duplex, which are in close contact to one of the phen ligands. No curvature of the duplex is induced at the intercalation site, but the local base pair experiences a twist of about 40°. In contrast, in $d(CCGGATCCGG)_2$, in which the position of the central thymine and adenine nucleobases is reversed, only the two terminal binding sites are occupied while there is no intercalation at the central A_5T_6 position [57].

In subsequent work, the effect of substitution in the distal part of the dppz ligand, in particular the 11-position, was investigated. Crystals of Λ-$[Ru(tap)_2(11\text{-Cl-dppz})]^{2+}$ bound to the $d(TCGGCGCCGA)_2$ already utilized in the initial work on the dppz parent complex [52] diffracted to 1.0 Å resolution with only one ruthenium dppz moiety bound to the duplex [58]. Interestingly, the racemic mixture of the metal complex in the form of the chloride salt was used in the crystallization mixture, but only the Λ-enantiomer was found to bind. While the overall structure is similar to that reported in [52], the presence of the chloride substituent on the dppz ligand creates an element of asymmetry and consequently, there are two different orientations of the ligand in a 66/34 ratio. Again, the intercalation of the dppz ligand is very deep and consequently the chloride atom in the 11-position is exposed in the major groove on the opposite side of the duplex [58]. The effect of other substituents on the dppz ligand was also investigated by crystallization of $[Ru(tap)_2(10\text{-}CH_3\text{-dppz})]^{2+}$, $[Ru(tap)_2(11\text{-}CH_3\text{-dppz})]^{2+}$, $[Ru(tap)_2(10,12\text{-}CH_3\text{-dppz})]^{2+}$, and $[Ru(tap)_2(11,12\text{-}CH_3\text{-dppz})]^{2+}$ with $d(TCGGCGCCGA)_2$ [59]. With the exception of the orientation of the methyl group(s), the overall structure of the DNA adducts was essentially identical to the ones previously reported. Only the Λ-enantiomer crystallized from the racemic mixture of the metal complexes [52]. In the case of the 10-methyl-dipyridophenazine ($10\text{-}CH_3$-dppz) ligand, the substituent is exclusively positioned in the major groove and oriented towards the pyrimidine in the intercalation site.

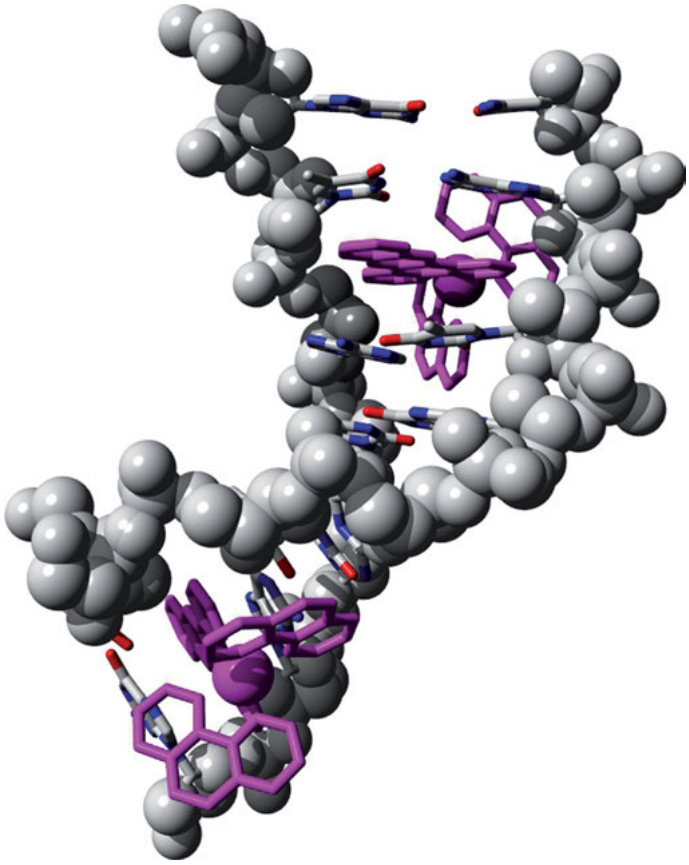

Figure 6. Crystal structure of $[Ru(phen)_2(dppz)]^{2+}$ non-covalently bound to $d(CCGGTACCGG)_2$ from the minor groove showing the two different binding sites in symmetry-equivalent positions at each end of the duplex (shown at the bottom) and the third one in the center at T_5A_6 (shown at the top). The figure was prepared with Yasara and PovRay from the PDB entry 3U38 [57].

The 11-substituted isomer, on the other hand, has the methyl group pointing away from the major groove and towards the purine nucleobase. In the 10,12-disubstituted complex, only one orientation for the methyl groups is observed, with the 10-methyl group in the major groove of the pyrimidine side and the 12-methyl substituent pointing away from the groove on the purine part. This structure is essentially a superposition of the 10- and 11-monosubstituted complexes [59]. Interestingly, none of the methyl groups in these three structures protrude into the major groove opposite to the intercalation site. Only in $[Ru(tap)_2(11,12\text{-}CH_3\text{-}dppz)]^{2+}$, there is one methyl functionality, that in the 11-position, directed outward and the other one toward to the purine base.

Further insights in the structural discrimination between the two enantiomers of $[Ru(phen)_2(dppz)]^{2+}$ came from a co-crystallization study of the racemic met-

al complex with $d(ATGCAT)_2$. Interestingly, no crystals could be obtained upon incubation of the pure enantiomers with this hexameric duplex, indicating a very rare case of enantiomeric cooperative binding [60]. In the asymmetric unit, one molecule each of Δ- and Λ-$[Ru(phen)_2(dppz)]^{2+}$ is bound to the oligonucleotide duplex, with the Δ-enantiomer at T_2G_3 and the Λ-enantiomer at C_4A_5. Both complex units are intercalated from the minor groove and again, the distal part of the dppz ligand extends into the opposite major groove. However, due to subtle differences in the orientation, there is no further interaction of this part of the complex in the Λ-enantiomer, but for the Δ-enantiomer, one of the phenazine nitrogen atoms is hydrogen-bonded to an ordered solvent water molecule, which makes further contact to the carbonyl O atom of the G_3 residue [60]. Overall, binding of the Δ-enantiomer was found to be favored due to a shorter Ru-P distance, which leads to a stronger electrostatic interaction between the cationic metal complex and the negatively charged sugar-phosphate backbone and a higher DNA twist angle.

However, the crystal structure of a matched duplex only incorporating the single enantiomer Δ-$[Ru(phen)_2(dppz)]^{2+}$ was obtained using $d(TCGGCGCCGA)_2$ [61]. Two distinct binding modes were observed. In the first one, termed "end-capping", the dppz ligand stacks on the C_2-G_9 base pair while the nucleobases T_1 and A_{10} are flipped out. The other binding mode is characterized by a semi-intercalation of one of the phenanthroline coligands between the G_3G_4:C_7C_8 base pairs in the minor groove, which induces a significant kink in the duplex to each side [61]. Thus, the dppz ligand in the Δ-enantiomer of $[Ru(phen)_2(dppz)]^{2+}$ is not able to intercalate into duplex DNA and instead the complex switches to semi-intercalation of a phen coligand or stacks to a destabilized end of the duplex.

To further probe the influence of the base sequence context on the intercalative binding mode, very recently, the binding of Λ-$[Ru(N\hat{}N)_2(dppz^{R,R})]^{2+}$ with N^N = bpy, phen, and the dppz ligand either carrying R = H or CH_3 in the 11- and 12-position to d((5BrC)GGC/GCCG) was investigated with X-ray crystallography [62]. At the central 5′-CG-3′ position, a canted intercalation was observed from the minor groove in which the long axis of the dppz ligand is displaced relative to the vectors of the base pair hydrogen bonds by 44° on one and 90° on the other side. Interestingly, no crystals were obtained when using non-brominated DNA, which again highlights the extreme importance of the base sequence context on the success (or failure) of crystallization attempts [62]. In contrast, the variation of bpy *vs.* phen or substitution at the distal part of the dppz ligand had only a marginal effect on the resulting structures. Overall, however, the intercalation at the 5′-CG-3′ step is more shallow than at the 5′-TA-3′ one, which could also contribute to differences observed in the photophysical properties of closely related compounds.

While the structures discussed above now give a fairly good picture of the binding preference of the different enantiomers of mononuclear metallointercalators, very little is known to date about the binding of dinuclear complexes at atomic resolution. However, recently, a so-called "threading" intercalator $[(phen)_2Ru(\mu\text{-bidppz})Ru(phen)_2]^{4+}$ with bidppz = 11,11′-bis(dipyrido[3,2-*a*:2′,3′-*c*]phenazinyl) was cocrystallized with $d(CGTACG)_2$ (Figure 7) [63, 64]. The

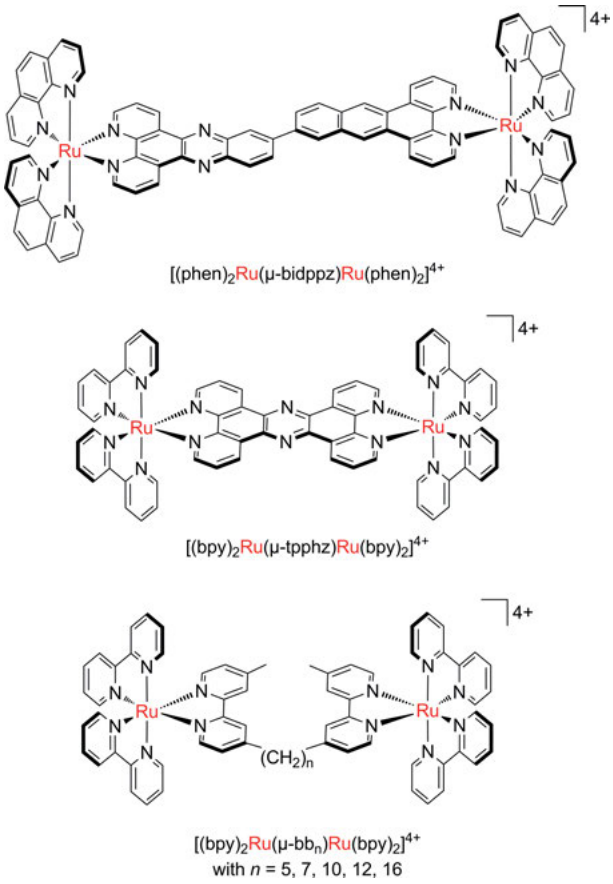

Figure 7. Structures of the bis-intercalators $[(phen)_2Ru(\mu\text{-bidppz})Ru(phen)_2]^{4+}$, $[(bpy)_2Ru(\mu\text{-tpphz})Ru(bpy)_2]^{4+}$, and $[(bpy)_2Ru(\mu\text{-bb}_n)Ru(bpy)_2]^{4+}$ with $n = 5, 7, 10, 12, 16$.

bidppz ligand extends through the double helix while the two $Ru(phen)_2$ "end groups" of the dumbbell-shaped molecule are positioned in opposite grooves on the oligonucleotide and result in a kinetic trapping of the metal complex. This is reminiscent of small-molecule rotaxanes, in which the DNA duplex takes the role of the macrocyclic "wheel" (Latin *rota*) while the metal complex serves as the axle. Consequently, the dissociation half-life was estimated to be 38 h at 37 °C. However, since the central AT base pair is extruded from the duplex to accommodate the metal complex, the binding mode is actually more correctly described as metalloinsertion (see Sections 5.2 and 5.3) and not metallointercalation, but notably takes place at a fully matched site [63]. In addition, for the metal complex to bind, a transient bubble has to form in the base pair stack to allow one of the $Ru(phen)_2$ moieties to traverse the duplex.

Interestingly, an NMR study of the binding of the bpy analogue of the above complex with $d(CGCGAATTCGCG)_2$ did not provide any evidence for interca-

lation or insertion and this system seems to assume a surface-bound state [65]. Another threading intercalator, $[(bpy)_2Ru(\mu\text{-tpphz})Ru(bpy)_2]^{4+}$ with tpphz = tetrapyrido[3,2-*a*:2′,3′-*c*:3",2"-*h*:2‴,3‴-*j*]phenazine (Figure 7) showed efficient two-photo absorption and was utilized in phosphorescent lifetime imaging microscopy (PLIM) of the metal complex distribution in cells, which eliminates background autofluorescence of biomolecules, since their excited state lifetime in the pico- to low nanosecond range is lower than that of the metal probes, which emit on the hundreds of nanoseconds to microsecond timescale [66]. More flexible linkers have also been utilized in the construction of bisintercalators (Figure 7), for example by Williams et al. [67] and Keene et al. [68]. The latter group also reported selective bulge recognition by a much more rigid bisintercalator based on 4,6-bis(2-pyridyl)pyrimidine (dppm) or 2,2′-bipyrimidine (bpym) bridging two $[Ru(phen)_2]^{2+}$ moieties [69–71].

Curiously, upon crystallization of $[Ru(bpy)_2(dppzCl_2)]Cl_2$, with $dppzCl_2$ = 7,8-dichloro-dipyrido[3,2-*a*:2′,3′-*c*]phenazine, the complex itself in the solid state also assumes a continuous left-handed double helical arrangement of non-covalently bound Ru complex building blocks, in which the $Ru(bpy)_2$ groups line the outer helical backbone while the dppz ligands point towards the center of the helix [72]. These structures have a stunning similarity to the classical nucleic acid double helices, for example, that of DNA.

Since co-crystal structures of metallointercalators with duplex DNA are still far from routine to obtain, theoretical chemists have also utilized computational methods to explore the binding of metal complexes to DNA [23, 73]. However, many of these studies, in particular when not applied by true experts in the field, are mere docking attempts which are often hampered by improper use of computational tools that are, for example, not able to handle the presence of the metal center or deal with the mix of weak interactions that characterize duplex-metal complex binding. For meaningful results, a mix of force-field molecular dynamics (MD) and hybrid quantum-classical (QM/MM) MD simulations is usually required, which are very demanding with respect to computational resources. For example, Vargiu and Magistrato first optimized the geometries of Δ-$[Ru(bpy)_2(dppz)]^{2+}$ and Δ-$[Ru(bpy)_2(eilatin)]^{2+}$ with the CPMD package and a plane-wave basis set. These were then utilized in classical all-atom MD simulations performed on a 12mer oligonucleotide duplex [24]. The simulation was run in the presence of explicit water molecules and sodium cations were added for charge neutrality. The whole system had a size of 15000–25000 atoms, which is a formidable task.

Finally, equilibrium conformations taken from these MD simulations were taken as input for higher level QM/MM MD calculations, in which the metal complex was treated at the QM level while the duplex, water, and cations are modeled with MM [24]. Environmental effects on the photophysical properties of prototypical $[Ru(bpy)_2(dppz)]^{2+}$ were also investigated using time-dependent DFT [74]. Such advanced methodology allowed to obtain reliable deintercalation energetics and showed that the main energetic factor is the disruption of π-π-stacking between the dppz ligand and the nucleobases flanking the binding site [25].

While Ru dppz complexes have featured prominently among the published metallointercalators, other ruthenium(II)-coligand combinations have also been ex-

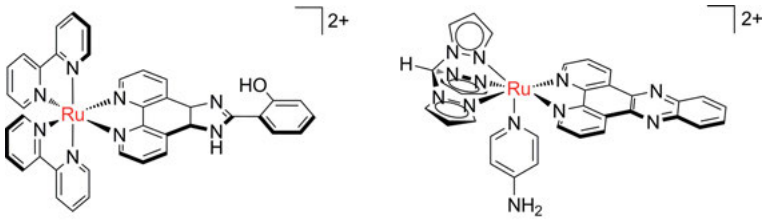

Figure 8. Structures of two non-classical ruthenium(II) metallointercalators based on hpip = 2-(2-hydroxyphenyl)imidazo[4,5-*f*][1,10]phenanthroline instead of dppz as the intercalating moiety or a mix of tri-, bi-, and monodentate ligands instead of three bidentate ones.

plored in great detail. For example, there is a wide range of compounds based on a $Ru(bpy)_2$ moiety with the octahedral coordination sphere of the metal center completed by derivatives of 1*H*imidazo[4,5*f*][1,10]phenanthroline substituted in the 2-position (Figure 8) [75–77]. More elaborate ligands have also enabled access to complexes such as $[Ru(phen)_2(dipytap)]^{2+}$ with dipytap = 2,3-di-2-pyridinylpyrazino[2,3-*f*]quinoxaline, which acts as a NIR light switch probe for DNA with the emission centered between 680–860 nm [78]. Alternative ligand systems include 2,3-dihydro-1,4-dioxino[2,3-*f*]-1,10-phenanthroline (dop) or 2,3-dihydro-1,4-dioxino[2,3-*f*]-2,9-dimethyl-1,10-phenanthroline (dmdop) [79]. Furthermore, a combination of bi- and monodentate ligands has been used, for example in $[Ru(bpy)_2(imid)_2]^{2+}$, with imid = imidazole or N-methylimidazole [80].

While most DNA metallointercalators are based on a combination of a bidentate intercalating ligand and a $[Ru(N\hat{}N)_2]^{2+}$ "cap", with N^N usually either 2,2-bipyridine (bpy), 1,10-phenanthroline (phen), or a closely related analogue thereof, sometimes also a combination of a tridentate facial and a monodentate ligand has been utilized to complete the octahedral coordination sphere of the ruthenium(II) center. Interestingly, $[Ru(tpm)(4amp)(dppz)]^{2+}$ with tpm = tris(pyrazolyl)methane and 4amp = 4-aminomethylpyridine, for example, showed a temperature-dependent variation of the DNA binding mode (Figure 8). While it is groove-binding at room temperature, it switches to an intercalative interaction at 10 °C, and shows the expected light-switch effect [81].

The study of the biological activity of ruthenium(II) polypyridyl complexes dates back more than 60 years, when Dwyer et al. reported on the enzyme inhibition, antibacterial activity, and toxicity on mice of $[Ru(bpy)_3]I_2$, $[Ru(phen)_3](ClO_4)_2$, and $[Ru(terpy)_2]X_2$ with X = I, ClO_4, along with some cobalt(III), nickel(II), iron(II), and osmium(II) complexes [82, 83]. In a series of $[Ru(bpy)_2(N\hat{}N)]Cl_2$ complexes in which the aromatic surface area of the N^N ligand (= bpy, phen, dpq, dppz, dppn) systematically increased, the cytotoxicity on HT-29 and MCF-7 human cancers cells strongly depended on the nature of the coligand and IC_{50} values generally decreased with increased size of the ligand [84]. The biological potency was correlated with increased intracellular ruthenium accumulation, as determined by graphite furnace atomic absorption spectroscopy (GF-AAS). Inter-

estingly, however, quasi-continuous monitoring of oxygen consumption, extracellular acidification rate, and changes in cellular morphology and adhesion properties by a chip-based sensor systems of HT-29 cells exposed to the compounds for 48 h gave indications of large variability in the underlying mechanism of action. While the dppn complex led to a steady decrease of the standard cell impedance as a measure of cell adhesion, which did not recover even when supply of the compound was stopped, the other complexes resulted in much slower and different response. This was taken as an indication of a membrane interaction for $[Ru(bpy)_2(dppn)]Cl_2$, in contrast to DNA binding generally assumed as the major mode of activity for such compounds [84].

Thus, cellular uptake and intracellular localization are important parameters which determine the biological mode of action of a given compound and therefore, extreme caution should be exercized when transferring the results of cell-free assays to *in vitro* studies. For example, Glazer and coworkers investigated the biological activity of $[Ru(dpp)_3]^{2+}$ with dpp = 4,7-diphenyl-1,10-phenanthroline (bathophenanthroline) and $[Ru(dpp^{SO3,SO3})_3]^{4-}$, the latter incorporating the dpp ligand modified with sulfonate groups in the *para*-position of the phenyl groups [85]. While the photophysical properties of the two compounds were essentially identical, the tetraanionic complex was inactive in the dark on A549 human alveolar adenocarcinoma cells but showed high light-triggered cytotoxicity. The dicationic compound, on the other hand, showed significant toxicity already in the absence of illumination, which was attributed to the different intracellular distribution. While the dpp parent compound with the positive charge was taken up by the mitochondria, as demonstrated by flow cytometry and fluorescence microscopy, the anionic complex was also internalized, but remained in the cytosol [85].

Variation of the functional group in the 11-position of dppz in $[Ru(bpy)_2(dppz^R)](PF_6)_2$ also led to distinct differences in biological activity on MRC-5 and HeLa cells, with IC_{50} values from low micromolar to essentially inactive [86]. In addition to such single substituents on the dppz ligand, the effect of annelated rings has also been explored [87]. A systematic variation of the steric and electrostatic contributions to the DNA binding of $[Ru(bpy)_2(dppz)]^{2+}$ by subsequent addition of carboxylate and ester pendant groups revealed that a decrease of the electrostatic potential led to better duplex specificity over single-strand interaction [88]. The overall complex charge can also be modulated by exchange of one 2,2′-bipyridine ligand to 2-phenylpyridine (ppy). In a series of $[Ru(bpy)(ppy)(N\hat{}N)]^{+}$ complexes with different bidentate coligands, the octanol/water partition coefficient log *P* was systematically higher for these compounds relative to their $[Ru(bpy)_2(N\hat{}N)]^{2+}$ congeners and the latter also showed significantly lower cytotoxic potential (>100 μM) compared to <10 μM for the ppy compounds [89]. A similar line of investigation was followed by Gaiddon and coworkers, who studied uptake, intracellular distribution, and biological activity of $[Ru(phen)_2(ppy)]^{+}$, which also has a reduced charge due to the C^N-chelating 2-phenylpyridine ligand [90]. Submicromolar IC_{50} values were determined on human glioblastoma cells, a particularly aggressive and invasive form of cancer, and uptake investigated with confocal fluorescence microscopy based on the inherent emission profile of the

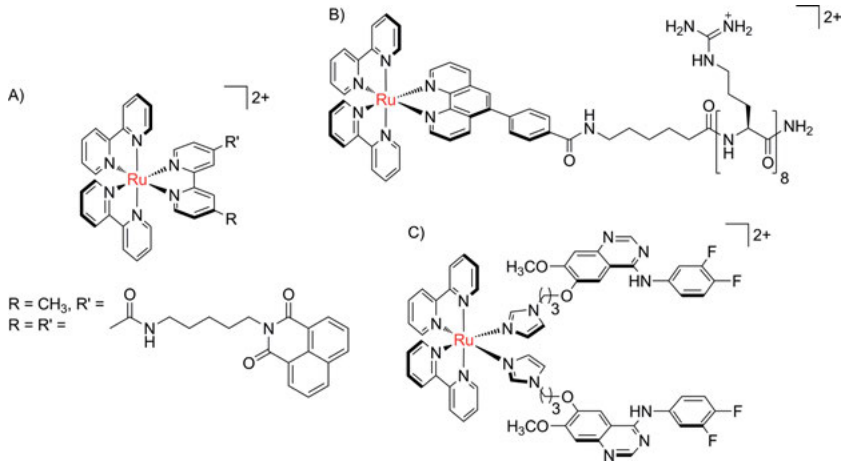

Figure 9. Structures of three ruthenium(II) polypyridyl complexes functionalized with various bioaffinity groups, including (**A**) naphthalimide, (**B**) a poly(arginine) peptide, and (**C**) a 4-anilinoquinazoline drug.

metal complexes. Other researchers have also explored related compounds, but incorporated more bulky coligands [91].

Beyond simple variation of the charge, introduction of functional groups capable of DNA interactions by themselves to the outer ligand periphery of ruthenium metallointercalators has also led to very interesting effects. For example, compounds incorporating either one or two 1,8-naphthalimide pendant groups to one of the bpy ligands of $[Ru(bpy)_3]^{2+}$ resulted in pronounced changes in the binding mode (Figure 9A). While in the mono-functionalized compound, the ruthenium core was found to be closely associated with the DNA duplex, it is displaced from the DNA backbone in the bis-functionalized compound in a "negative allosteric effect", which also had a significant influence on the photoinduced cleavage of plasmid DNA and dark/light cytotoxicity on HeLa cells [92]. Other DNA intercalating groups, such as anthracenyl, have also been introduced to the periphery of ruthenium polypyridyl complexes to study the differential binding preference of the metal complex fragment *vs.* organic intercalator [93, 94].

Various bio(macro)molecules have also been conjugated to the ruthenium polypyridyl core structure to control the cellular uptake and intracellular distribution as well as specific targeting of malignant cells. For example, Keyes and coworkers used a 1,10-phenanthroline ligand modified in the 5-position with a benzoic acid group or a related 4-substituted 2,2′-bipyridine to couple various peptide carriers to a $[Ru(bpy)_2]^{2+}$ or $[Ru(bpy)(dppz)]^{2+}$ core [95]. The polypeptide sequences attached in this way included non-targeted cell-penetrating peptide (CPP) Arg_8, the nuclear localizing sequence (NLS), and an endoplasmic reticulum (ER)-directing 16mer polypeptide also known as penetratin (Figure 9B). The light-switch capability was retained in $[Ru(bpy)(bpy^{NLS})(dppz)]^{2+}$ and while the unconjugated parent complex was unable to cross the plasma

membrane of living HeLa cells, the penetratin- and Arg_8-functionalized complexes showed rapid intracellular accumulation. While the non-specific Arg_8 compound was widely distributed in the cytoplasm but not the nucleus, the penetratin conjugate showed selective localization in the ER after an extended period of incubation, as expected. The NLS-modified dppz complex showed much slower uptake kinetics. At short incubation times (6 h), it was mostly associated with membrane structures, while after 24 h, it was found to bind to the DNA, presumably *via* the dppz intercalator [72]. Both chromosomes and ribosomes could be visualized at high resolution using STED microscopy, with the latter assumed to be revealed due to Ru dppz binding to RNA mismatches within the ribosome. Even the phase of cell division could be determined in this way.

In another approach to dual-functional bioactive ruthenium complexes, the $[Ru(bpy)_2]^{2+}$ and $[Ru(phen)_2]^{2+}$ moieties were functionalized with 4-anilinoquinazoline derivatives incorporating an imidazole ligand *via* a variable-length alkyl linker (Figure 9C) [96]. These pharmacophores are known to inhibit the epidermal growth factor receptor (EGFR), a transmembrane glycoprotein involved in cell growth and apopotosis as well as cell differentiation and migration. As such, EGFR inhibitors are implicated as antitumor agents with reduced cytotoxicity. Interestingly, one of the compounds, incorporating two 4-anilinoquinazoline ligands and a long alkyl linker, showed an EGFR inhibitory activity in the mid-nanomolar range that is comparable to gefitinib, a tyrosine kinase inhibitor in clinical use against some forms of breast and lung cancer [96]. Low to mid-micromolar IC_{50} values were determined on a range of cancer cells lines, although the potency appeared to be more or less independent of EGF stimulation and was comparable for the metal complexes *vs.* ligands.

An interesting alternative is the modification of the ligand periphery by "click" reactions. For example, the group of Rau reported on $[Ru(bpy^{tBu,tBu})_2(bpy^{triazolate,triazolate})]^{2+}$, in which the triazolate-functionalized bpy derivative is accessible by azide-alkyne cycloaddition of aryl and benzyl azides to bis-alkyne-substituted 2,2′-bipyridine (Figure 10A) [97].

In addition to increased receptivity to growth factors, cancer cells are also characterized by a high demand for energy. Since glucose is the most important cellular source of energy, and glucose transporters are often upregulated in malignant cells, metal-glucose conjugates have actively been explored as novel experimental anticancer agents. For example, Bonnet and coworkers coordinated a thioether glucose derivative, either in the D- or L-form, to a $[Ru(dppz)(terpy)]^{2+}$ moiety *via* sulfur coordination (Figure 10B) [98]. The assessment of the biological activity on A549 and MCF-7 human cancer cells in the absence and presence of blue light (454 nm) revealed a significant decrease in the IC_{50} values (and thus, higher anticancer activity) upon photoactivation, from mid-micromolar in the dark incubated samples to nanomolar in the illuminated ones. Notably, while the photocytotoxicity was independent of the choice of the glucose enantiomer, the dark activity was somewhat higher for the D- *vs.* the L-form [98].

Finally, to potentiate the biological activity of the ruthenium(II) polypyridyl moiety, $[Ru(terpy)_2]^{2+}$ was decorated in one of the 4′-positions with a *N*-(pyridylmethyl)-4-aminophenyl moiety which acts as a bidentate chelator for

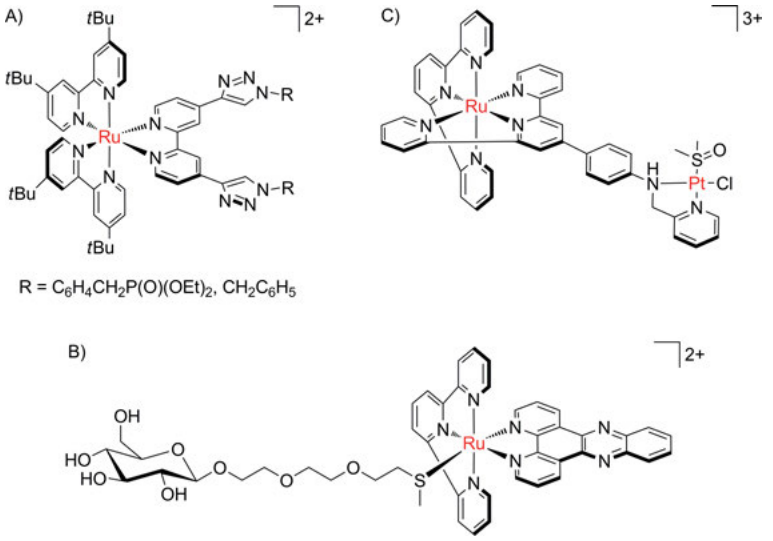

Figure 10. Structures of ruthenium(II) polypyridyl complexes (**A**) prepared by azide-alkyne cycloaddition formation of triazolate groups in the ligand periphery, (**B**) a thioglucose-tethered Ru(dppz) metallointercalator for targeting the energy metabolism of cancer cells, and (**C**) a dual-functional Ru(II)-Pt(II) anticancer drug candidate.

$[PtCl(\kappa S\text{-dmso})]^+$ (Figure 10C) [99]. Compared to the non-platinated ruthenium complex and $[PtCl(\kappa S\text{-dmso})(2\text{-(aminomethyl)pyridine})]^+$ also investigated for comparison, the IC_{50} values determined for A2780 human cancer cells were about one order of magnitude lower for the Ru/Pt heterodimetallic compound, which was also able to break the resistance against cisplatin in the related A2780cis cell line, although the potency on the responsive cells was about 10-fold lower compared to cisplatin (30 *vs.* 3 μM) [99].

4.2. Ruthenium Arene Complexes

In addition to the common $[Ru(bpy)_3]^{2+}$ motif, a range of organometallic ruthenium(II) complexes with an arene capping ligand have also been utilized as metallointercalating compounds. One of the prototypical compounds is $[RuCl(\eta^6\text{-benzene})(en)]^+$ (Figure 11), which was reported by Sadler and coworkers in 2002 [100]. Since then, the arene coligand, bidentate chelator, and monodentate ligand have been extensively varied [45, 101], with particular contributions also from the groups of Dyson, Hartinger, Keppler, and others. In addition to extended arene ligands to replace the benzene, in particular dppz "hybrid" complexes have attracted considerable attention, in which the known intercalating dipyridophenazine ligand is combined with an organometallic ruthenium(II) fragment. Some 15 years ago, the group of W. S. Sheldrick reported on $[Ru(acMet)(hmb)(dppz)]^{2+}$ and related compounds (Figure 11). In addition

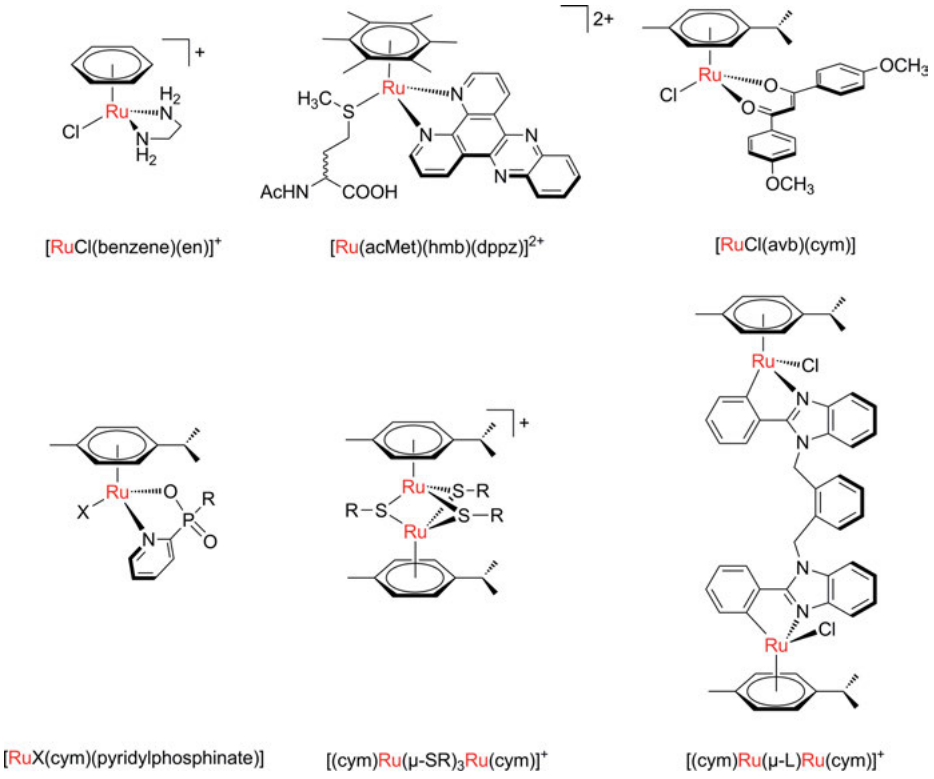

Figure 11. Structures of selected mono- and dinuclear ruthenium(II) arene complexes investigated for their biological activity and DNA binding affinity.

to detailed DNA binding studies, the interaction with the $d(GTCGAC)_2$ oligonucleotide duplex was studied with NOESY NMR and revealed a possible side-on intercalation between G_1T_2/C_6A_5 [102]. In a subsequent study, the analogous Cp^* rhodium and iridium complexes were also investigated [103]. The work was then extended to *in vitro* cell viability studies. In a series of compounds of general formula $[Ru(\kappa S\text{-dmso})(hmb)(N\text{^}N)]^{2+}$ with increasing aromatic surface area of N^N = dpq, dppz, dppn, again a side-on intercalation to duplex DNA was determined and the IC_{50} values on MCF-7 and HT-29 human cancer cells were found to decrease with increasing ligand size. For the dppn complex, low- to mid-nanomolar activity was determined, which correlated well with increased intracellular accumulation [104]. A similar trend was observed in a related series of $Cp^*Rh(III)$ compounds, with the most active compound again exhibiting nanomolar IC_{50} values [105].

A wide variety of other bidentate chelators has also been introduced to the $[Ru(\eta^6\text{-arene})]$ moiety, often inspired by biomolecules or established pharmacophores. For example, Dyson and coworkers replaced the N^N chelator by avobenzone (avb), an oil-soluble UVA filter (Figure 11). This compound, commonly employed in the formulation of sunscreens and cosmetics, incorporates a pro-

pane-1,3-dione moiety akin to acetylacetone (acac) and acts as an O^O chelator [106]. In biological screens, mid- to low micromolar IC_{50} values and breaking of cisplatin resistance were observed. The same group also applied the naphthalimide tagging described above for the classical ruthenium metallointercalators to a $[RuCl_2(\eta^6\text{-arene})(pta)]$ compound, in which the pendant organic intercalator was attached to the arene *via* an alkyl linker of variable length, which resulted in a significant increase in activity relative to the parent complex [107].

A wide range of other X^Y chelating groups in particular with X,Y = C, N, and O has also been introduced to the ruthenium(II) arene core [108], with far too many compounds to be comprehensively discussed here [109–112]. However, other heteroelements have been much less explored in this context to date. Only very recently, for example, Walton and coworkers reported on a series of 25 pyridylphosphinate complexes of the general structure [MX(arene)(N^O)] with M = Ru, Rh, Ir, Os, arene = *para*-cymene, benzene, and pentamethylcyclopentadiene, and X = Cl, I (Figure 11) [113]. While the ruthenium(II) chlorido complexes were inactive, some of the $Cp^*Ir(III)$ compounds exhibited mid-micromolar IC_{50} values on the lung carcinoma H460 cell line. The nature of the anionic ligand (chlorido *vs.* iodido) turned out to be important, with the latter compounds more active than the former ones, while the effect of iridium replacement by rhodium was negligible [113].

Although usually restricted to the realm of organic chemistry, the group of Ang recently reported the application of a new combinatorial approach to bioactive ruthenium(II) arene Schiff base complexes [114]. The dimeric ruthenium complex $[RuCl(\mu\text{-}Cl)(arene)]_2$ incorporating five different arene ligands was mixed in D_2O or DMSO/D_2O with substitued anilines (6 different compounds) and derivatives of 2-pyridinecarboxaldehde (15 derivatives) for *in situ* formation of the chelating iminopyridine in a 96-well format. At total of 450 new complexes were prepared this way and screened for cytotoxicity on A2780 ovarian cancer cells. A plot of the cell viability *vs.* hydrophobicity index, number of hydrogen-bond donor and acceptor groups, and molecular weight revealed that the biological activity was highest for strongly hydrophobic compounds with no more than 1–2 donor or acceptor groups and a molecular weight in the range of 500–650 Da [114].

In addition to the mononuclear compounds described above, also a number of homobimetallic organometal compounds has been tested for their biological activity. In particular, bridging of the Ru(arene) core by substituted thiolate ligands resulted in highly active complexes of the general formula $[(cym)Ru(\mu\text{-}SC_6H_4R)_3Ru(cym)]^+$ (Figure 11). Some of the most potent compounds exhibit IC_{50} values as low as 30 nM [115] while generally, the cytotoxicity increases in the order $[RuCl(\mu\text{-}Cl)(\mu\text{-}SR)RuCl] < [RuCl(\mu\text{-}SR)_2RuCl] < [Ru(\mu\text{-}SR)_3Ru]$ [116]. Larger linker systems which combine two C^N binding pockets on a 1,2-phenylene core have also been explored (Figure 11) but did not result in significantly higher biological activity compared to cisplatin [117].

Structural data on the DNA binding of organometallic ruthenium arene complexes is extremely rare. However, Davey, Dyson, and coworkers managed to co-crystallize $[RuCl(\eta^6\text{-tha})(en)]^+$ with tha = 5,8,9,10-tetrahydroanthracene with the nucleosome core particle (NCP), which is composed of a 145 base pair stretch

of double-stranded DNA and the histone octamer, as discussed in Section 2.5 [118]. Three main binding sites were identified, two in the major and one in the minor groove. The Ru(arene)(en) moiety was found to coordinate to the N7 nitrogen atom of guanine at the 5′-site of an AGG sequence. Substantial helix deformation results in an unusual mode of intercalation of the tha ligand, which prefers to insert between the A and G bases, as opposed to GG [118].

4.3. Other Metal Complexes

While a number of Cp^* rhodium(III) and iridium(III) complexes show properties closely related to their arene ruthenium(II) congeners [105, 119–123], only a relatively limited number of other metals has been explored as metallointercalating agents. A prerequisite is a very slow ligand exchange, as for example in octahedral chromium(III) complexes. Thus, Wheeler and Kane-Maguire reported on the DNA binding affinity of $[Cr(bpy)_2(dppz)]^{3+}$ and related compounds (Figure 12), which differ from their ruthenium(II) congeners by the +3 charge and the open-shell electronic configuration of the $3d^3$ chromium(III) center, which results in complications with NMR studies due to the paramagnetic nature of the compounds [124–129].

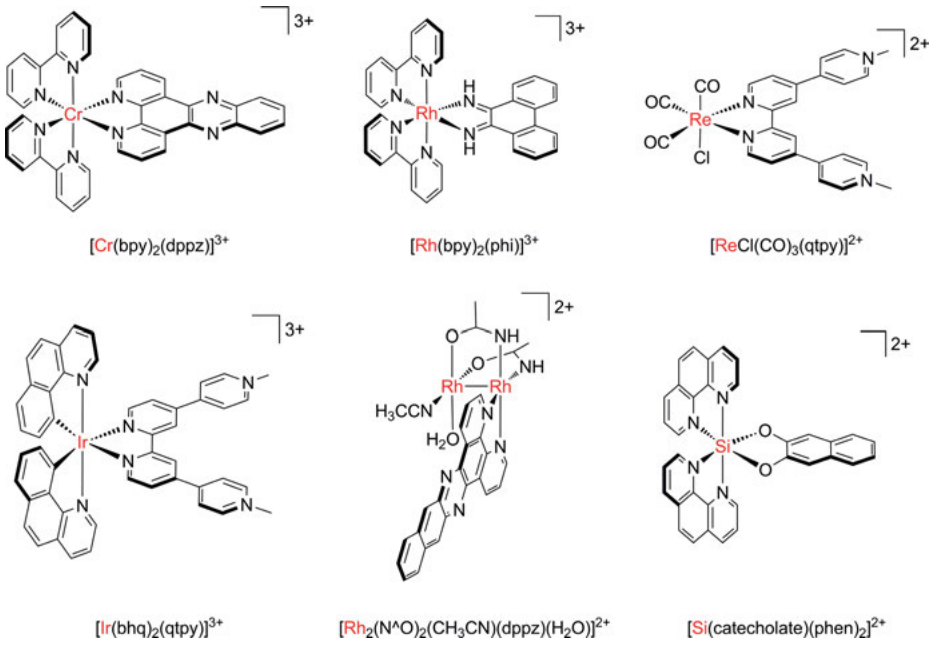

Figure 12. Structures of DNA metallointercalators not based on ruthenium(II). In addition to mononuclear chromium(III), rhodium(III), rhenium(I), and iridium(III) complexes, also homodinculear rhodium(II,II) compounds and main-group element systems based on octahedral silicon(IV) have been reported.

A similar stability is exhibited by rhodium(III) complexes, which however have a closed-shell $4d^6$ electronic configuration, and thus are easier to investigate using standard spectroscopic techniques based on NMR. The group of Barton prepared a wide range of such compounds based on the 9,10-phenanthrenediimine (phi) ligand coordinated to a rhodium(III) center, with the octahedral coordination sphere completed by either four monodentate ligands as in $[Rh(NH_3)_4(phi)]^{3+}$, two bidentate ligands as in $[Rh(en)_2(phi)]^{3+}$ and $[Rh(bpy)_2(phi)]^{3+}$ (Figure 12), or one tetradentate ligand, for example in complexes such as $[Rh(tren)(phi)]^{3+}$, $[Rh([12]aneN_4)(phi)]^{3+}$ and $[Rh([12]aneS_4)(phi)]^{3+}$ [130–132]. In addition, bis-9,10-phenanthrenediimine complexes such as $[Rh(phi)_2(phen)]^{3+}$ have also been explored for their ability to inhibit DNA transcription *in vitro* [133] and in addition to rhodium(III), tris-heteroleptic iridium(III) phenanthrenediimine compounds such as $[Ir(bpy)(phen)(phi)]^{3+}$ have also been explored [134]. Finally, the mode of intercalation of a rhodium(III) complex with a linear tetradentate ligand $[Rh(Me_2trien)(phi)]^{3+}$ with Me_2trien = 2*R*,9*R*-diamino-4,7,-diazadecane into the 8mer DNA duplex $d(G(dIU)TGCAAC)_2$ was revealed by X-ray structure analysis at high resolution [51]. The compound was found to bind from the major groove between the nucleobases of the central TG/CA sequence due to hydrogen bonding interaction of the terminal amino groups of the Me_2trien ligand with the guanine O(6) atoms and hydrophobic interaction between the methyl groups on the ligand and the thymine.

The introduction of charged functional groups to the ligand periphery of a DNA-binding metal complex is another interesting means to tune the interaction. In addition to some rhenium(I) tricarbonyl complexes $[ReCl(CO)_3(qtpy^{CH3,CH3})]^{2+}$ with qtpy = 2,2′:4,4″:4′,4‴-quaterpyridyl dimethylated in the 4″- and 4‴-positions, Thomas and coworkers also reported on the corresponding iridium(III) cyclometalated compounds $[Ir(bhq)(qtpy^{CH3,CH3})]^{3+}$ with bhq = benzo[*h*]quinoline [135]. Although sharing the same large bidentate ligand, the rhenium compounds showed classical intercalation into DNA, while the iridium complexes act as groove binders (Figure 12). Bimetallic complexes have also been constructed based on metal centers other than ruthenium. For example, C. Turro and coworkers reported on a dirhodium(II,II) complex with an extended dppn ligand (Figure 12), which interacts with DNA in a semi-intercalative way while still undergoing light-triggered ligand exchange and singlet oxygen production [136].

Finally, the group of Meggers demonstrated that transition metal centers are not a strict requirement for the construction of DNA-intercalating octahedral compounds. Starting from silicon(IV)iodide, $[Si(phen)_2I_2]$ was prepared and further reacted with an 1,2-arenediol, giving rise to $[Si(phen)_2(arenediolate)](PF_6)_2$ (Figure 12). Using a combination of UV melting curves and CD spectroscopy, it was shown that these compounds exhibit DNA binding constants in the range of 10^6 M^{-1}, which compares favorably with prototypical ruthenium(II) metallointercalators such as $[Ru(bpy)_2(dppz)]^{2+}$ [137].

5. METALLOINSERTORS

5.1. DNA Mismatches, Mismatch Repair Systems, and Cancer

DNA replication by polymerase enzymes is a highly accurate process with an overall error rate of only about 1 in 10^{10} [138]. However, it does not proceed with complete fidelity. At some instances, about 1 in 10^5 times, nucleotides are incorporated into the newly synthesized DNA strand which are not complementary in the Watson-Crick sense and do not form the canonical AT and GC base pairs, which alters the genetic code if they are not immediately removed. Eight different base pair mismatches can form, which are characterized as either transition mismatches (the purine-pyrimidine pairs GT and AC) or transversion mismatches, composed of purine-purine (AA, GG, and GA) and pyrimidine-pyrimidine (TT, CC, and TC) mispairs. These have different thermodynamic stability, which depends on the hydrogen-bonding pattern, but also the sequence context in which they occur, in particular the nature of the directly adjacent base pairs. The following order of stability has been determined for the different (mis)pairs: CC ≤ AC ≤ TC < AA ≤ TT < GA ≤ GT < GG < AT < GC [139, 140]. The stability also influences the ability to detect and remove a particular mismatch, with the least stable CC mismatch refractory to methyl-directed mismatch repair (see below) [141].

Two mechanisms are operative in cells to eliminate incorrectly paired nucleotides. Firstly, DNA polymerases have an inherent $3' \rightarrow 5'$ proofreading exonuclease function able to detect, excise, and correct mismatches directly during the replication process. In addition, there is also a post-replicative correction mechanism for DNA polymerization errors which is called mismatch repair (MMR). Together, these two systems are critical to maintain overall genetic integrity. Consequently, inheritable defects in DNA repair systems, including MMR, are associated with an increased susceptibility to develop certain types of cancer such as hereditary nonpolyposis colorectal cancer (HNPCC), also called Lynch syndrome [142].

In recent years, a detailed picture of the enzymes involved in bacterial as well as eukaryotic MMR has emerged and in 2015, Paul Modrich was awarded the Nobel Prize in Chemistry together with Tomas Lindahl and Aziz Sancar for the elucidation of the role of DNA methylation in the direction of the MMR system [143]. In addition to a comprehensive understanding of the natural mechanisms of mismatch repair, over the last two decades, there has also been significant research directed at the development of small-molecule probes to detect mismatches in genomic DNA. In the following section, such metal-based mismatch-recognizing compounds will be discussed in detail, with a particular focus on the most common rhodium-based systems.

However, it is worth a first look at the mechanism by which the natural MMR system recognizes misincorporated nucleotides [141, 144–147]. In bacteria such as *E. coli*, the MMR system is composed of the repair proteins MutS, MutL, MutH, and MutU (UvrD), encoded in the *mut* ("mutator") genes. Among those, MutS recognizes base/base mismatches as well as short insertion or deletion loops

(IDLs) up to four nucleotides long in an ATP-dependent process. Under consumption of additional ATP, MutL then translates this signal to MutH, which utilizes the transiently unmethylated state of the newly synthesized DNA daughter strand to distinguish it from the methylated template strand. The Mg^{2+}-dependent endonuclease function of MutH then introduces a single-strand break in the unmethylated strand of a hemimethylated d(GATC) sequence in the 5′ position to G, which triggers the removal of the mispaired nucleotide. Since the strand-differentiation signal can be located more than one kilobase (kb) away in either direction from the site of the mismatch, this set of repair enzymes is also called the "long-patch" system [148]. Finally, MutL is also required to direct the helicase MutU to the site of the nick, which starts DNA unwinding and removal of the nascent strand by the exonucleases RecJ, ExoVII, ExoI, or ExoX. Ultimately, DNA polymerase III and DNA ligase fill the resulting singled-stranded DNA gap again, which is transiently protected by single-strand binding protein (SSB). In contrast, eukaryotic MMR is more complex and involves multiple homologs of MutS and MutL which are active as heterodimers [149], while the *E. coli* systems operate as homodimers. In addition, in mammalian cells, the MMR complex seems to rely on close association with the DNA polymerase at the replication fork for strand discrimination [150, 151].

5.2. Rhodium Metalloinsertors

The first report of a metal complex specifically targeting a base pair mismatch was published 25 years ago when Chow and Barton investigated the interaction of the coordinatively saturated and substitutionally inert octahedral rhodium(III) complex $[Rh(dpp)_3]^{3+}$ with dpp = 4,7-diphenyl-1,10-phenanthroline (Figure 13) with double-helical RNA from yeast tRNA, 5S rRNA, and synthetic model "microhelices" containing G-U mismatches using photoinduced strand cleavage upon 313 nm UV excitation. Specific cleavage was consistently observed at the nucleotide on the 3′-side of the wobble-paired U, regardless of the nucleotide composition at that site or the flanking base pairs, and assigned to the shape-selective binding of the rhodium complex [152].

While $[Rh(dpp)_3]^{3+}$ was only shown to recognize G-U mispairs, the scope of base pair mismatches that can be targeted was significantly expanded with the introduction of $[Rh(bpy)_2(chrysi)]^{3+}$ by Jackson and Barton in 1997 [153]. This complex is derived from the 9,10-phenanthrendiimine (phi) metallointercalators described in Section 4.3 but incorporates the 5,6-chrysenediimine (chrysi) ligand (Figure 13), which has an expanded aromatic surface area due to the additional annelated benzene ring. Interestingly, the chrysi ligand was not directly introduced to the rhodium center, but generated by reaction in the metal coordination sphere from condensation of 5,6-chrysenequinone with $[Rh(bpy)_2(NH_3)_2]^{3+}$ [154]. In contrast to $[Rh(dpp)_3]^{3+}$, mismatch recognition in this case is not based on shape-selective binding but rather exploits the thermodynamic destabilization of a mispaired site relative to canonical double-helical DNA (see Section 5.1). It is assumed that in contrast to phi, the chrysi ligand is too large to gain access

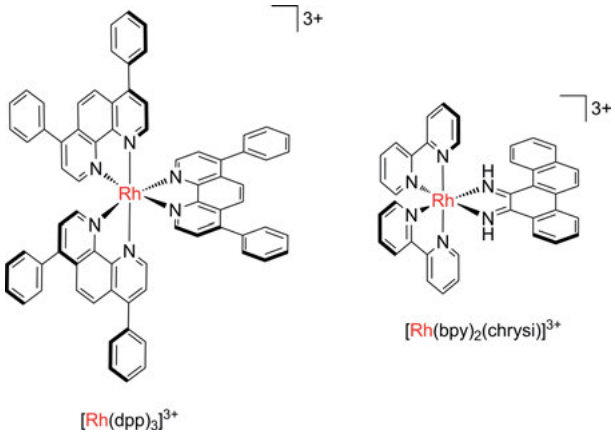

Figure 13. Structures of $[Rh(dpp)_3]^{3+}$, the first mistmatch-binding metal complex described (left) and $[Rh(bpy)_2(chrysi)]^{3+}$, the most thoroughly investigated metalloinsertor reported so far (right).

to the standard DNA base stack by intercalation but local perturbations at a base pair mismatch might allow it to bind there. The complex is able to reveal five of the eight mispairs possible, but with different efficiency and photocleavage pattern. The least stable CC mismatch showed the strongest cleavage and exhibits the 3′-scission pattern already described above. The other two pyrimidine-pyrimidine mispairs TT and TC are also revealed this way, albeit with somewhat lower efficiency. Of the pyrimidine-purine mismatches, only the CA pair is recognized, but shows a pattern different from the other three, with prominent cleavage at the mispaired C and neighboring the base on the 3′-side of the mismatch. The complex also binds the AA purine-purine mispair with a distinctive cleavage pattern at the base 3′ to the mismatch site and somewhat lower degree of scission at the AA mispair itself. Interestingly, the cleavage efficiency differs between the Δ- and Λ-enantiomers and also depends on the orientation and sequence context of the mismatch. In contrast, the more stable guanine-containing GA, GT, and GG mispairs are not recognized well by this compound [155]. Interestingly, the selectivity of $[Rh(bpy)_2(chrysi)]^{3+}$ was high enough to reveal a single CC mismatch in a 2725 bp linearized plasmid DNA double helix [156]. In addition, the complex is also able to recognize two other common DNA defects, abasic sites, which result from cleavage of the glycosidic bond, and single base bulges formed by replication errors [157, 158].

The precise mode of binding of $[Rh(bpy)_2(chrysi)]^{3+}$ to mismatched duplex DNA was then elucidated by a combination of solution NMR and single crystal X-ray diffraction studies. NOESY experiments on the interaction of the rhodium(III) complex with a synthetic 9mer oligonucleotide duplex incorporating a central CC mismatch showed that the chrysi ligand is deeply inserted in the DNA at the site of the mismatch from the minor groove while the two cytosine bases are ejected from the double helix to the opposite major groove. In contrast,

the flanking well-matched base pairs retain their standard hydrogen-bonding pattern and all sugar moieties are in the original conformation [159]. Finally, the X-ray crystal structure of $[Rh(bpy)_2(chrysi)]^{3+}$ bound to a 12mer palindromic oligonucleotide duplex incorporating an AC mismatch at 1.1 Å resolution was solved by Pierre, Kaiser, and Barton in 2007 [160]. Similar to the CC mismatch previously investigated by NMR, in this case, the chrysi ligand was again found to be inserted from the minor groove with both mispaired nucleobases ejected from the base stack, A to the minor groove and C to the major groove, although the structure also incorporated a second metal complex intercalated at a matched site from the major groove [160].

Another X-ray diffraction study on $[Rh(bpy)_2(chrysi)]^{3+}$ binding to the AA mismatch in a 12mer duplex otherwise similar to the one described above also displayed the same metallointercalation mode of interaction from the minor groove (Figure 14) [161]. A recent force-field and QM/MM molecular dynamics study confirmed these results and provided further insight in the energetics of the interaction, where the differential selectivity of the rhodium(III) chrysi complex toward distinct mismatches was correlated to their thermodynamic stability in free DNA *vs.* the corresponding insertion adduct [24]. Thus, while the *metallointercalators* described in Section 4 gain access to the DNA base stack between two well-matched base pairs, usually from the major groove, and π-stack to adjacent base pairs resulting in an increase of the contour length of the double helix, the *metalloinsertors* presented in this section bind from the minor groove and eject the mispaired bases from the oligonucleotide duplex without an increase in base pair rise, acting as π-stacking replacements [40, 162].

Since an accumulation of mismatches due to defects in the cellular MMR system is associated with certain types of cancer, the rhodium(III) chrysi moiety has, in recent years, also been modified with a range of additional DNA recognition and cleavage elements for potential applications in anticancer chemotherapy. The first such system was investigated by Schatzschneider and Barton [163], who reported on a tris-heteroleptic rhodium(III) complex with an octahedral ligand sphere composed of a chrysi, phen, and 4,4′-unsymmetrically substituted bpy ligand incorporating one methyl and one 7-aminoheptyl group. The latter was conjugated using EDAC-mediated coupling to a modified chlorambucil moiety (Figure 15A) [163]. This compound from the class of aniline mustards is used in the chemotherapy of chronic lymphocytic leukemia (CLL) as well as Hodgkin and non-Hodgkin lymphoma. Its activity is due to nucleobase alkylation resulting in monoadducts as well as interstrand crosslinks.

Using an electrophoretic mobility shift assay on a 17mer oligonucleotide duplex incorporating a central CC mismatch, the site of insertion of the Rh chrysi moiety was revealed by strand cleavage upon 442 nm photoactivation while the alkylation site became apparent in the autoradiogram after piperidine treatment. The primary alkylation was found to occur at a guanine four bases away from the CC mispair, which is consistent with the linker length and likely shielding of the G base directly next to the mismatch by the coligands [163]. Thus, the bifunctional metalloinsertor-alkylator conjugate is able to direct an alkylating anticancer agent to a mismatched site. The same Rh chrysi core with an aminoalkyl-

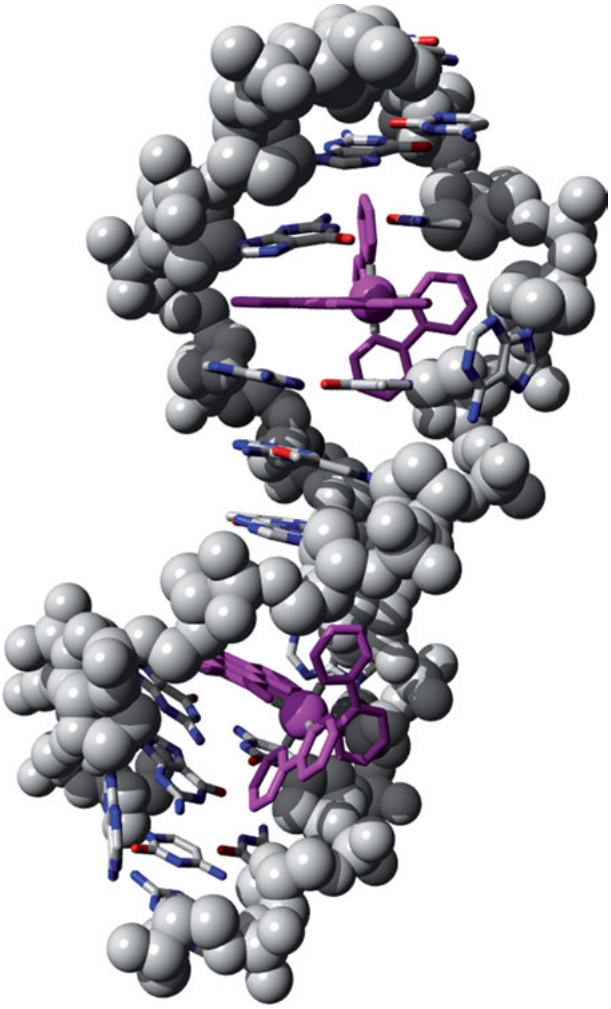

Figure 14. Crystal structure of $[Rh(bpy)_2(chrysi)]^{3+}$ non-covalently inserted to $d(CGGAAATTACCG)_2$ from the minor groove at the two AA mismatched sites with the flipped out adenine residues visible at the bottom left and center right. The figure was prepared with Yasara and PovRay from the PDB entry 3GSK [161].

modified bpy-coligand was also utilized in the construction of a metalloinsertor-cisplatin conjugate and platinum-mediated intra- and interstrand crosslinks were demonstrated by mass spectrometry (Figure 15B) [164]. An alternative footprinting method was based on Rh chrysi functionalization with a $[Cu(phen)_2]^+$ moiety by a similar linker strategy for oxidative cleavage of DNA near a mismatch site (Figure 15C) [165]. Upon addition of a reducing agent such as ascorbate, the copper(I) moiety promotes light-independent cleavage of the DNA backbone. The oligonucleotide scission was only observed in the presence of a CC mismatch

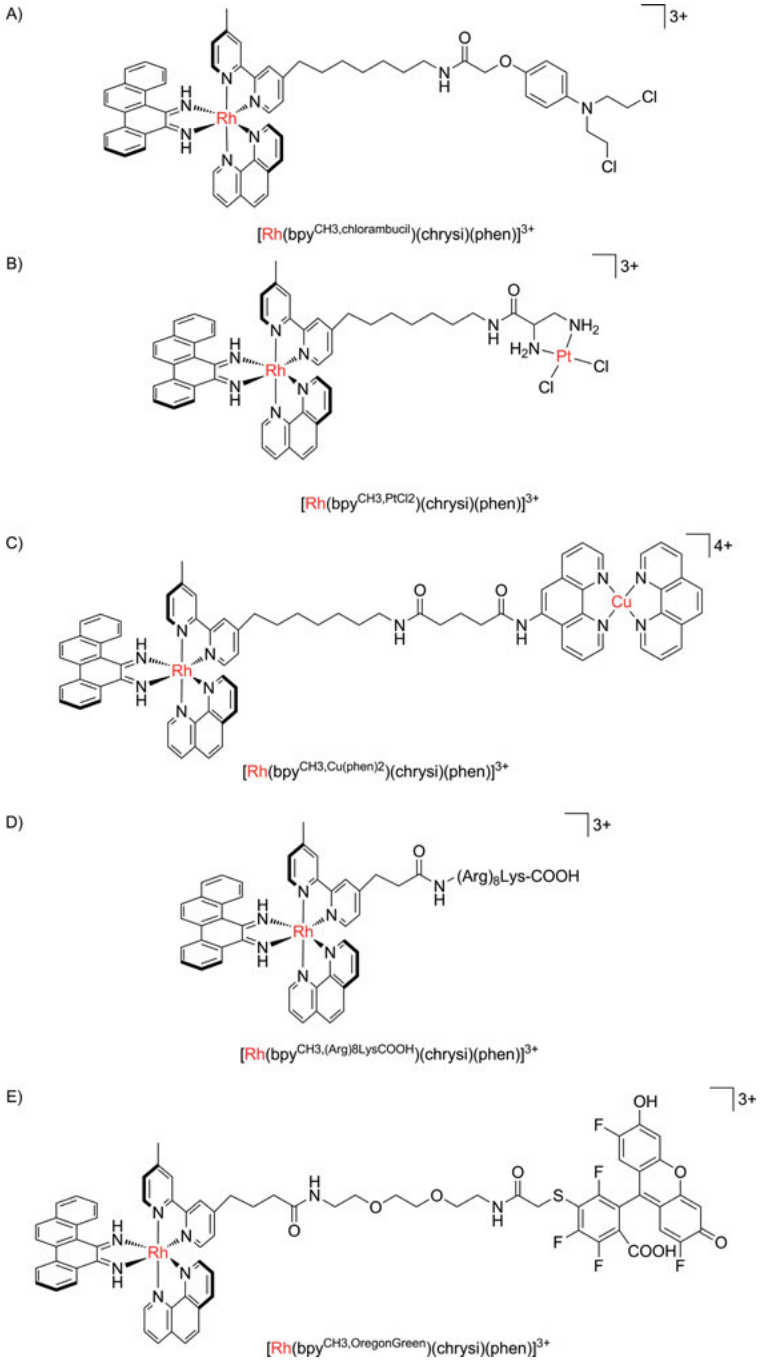

Figure 15. Structures of rhodium(III) chrysi metalloinsertors functionalized with (**A**) an aniline mustard, (**B**) cisplatin, (**C**) Cu(phen)$_2$ as well as (**D**) a cell-penetrating peptide (CPP), and (**E**) an Oregon Green fluorescent marker.

and occurred two or three bases away from the mispaired site, with both metals acting on the DNA from the minor groove.

While the studies described above were carried out on short synthetic oligonucleotides, it remained an open question whether the Rh chrysi metalloinsertor is also able to recognize mismatches *in vitro*. With a +3 charge due to the combination of a rhodium(III) center with neutral *N*,*N*-chelating ligands, cell uptake of these compounds is expected to be rather difficult. Therefore, Brunner and Barton used a HOBT/HBTU-mediated conjugation reaction to attach the nonapeptide (D-Arg)$_8$Lys to the pendant carboxy group of an alkyl-functionalized bpy ligand coordinated to a Rh chrysi core *via* the *N*-terminus using a Pbf/Mtt (= methyltrityl) protective group strategy (Figure 15D) [166]. In an alternative conjugation strategy, the Lys ε-amino group was used for coupling to the metalloinsertor outer ligand sphere which left the *N*-terminus of the (D-Arg)$_8$ peptide free for modification with an undecanoic acid-modified thiazole orange fluorescence marker. A fluorescein-modified rhodium complex as well as various controls were also synthesized. Using confocal flurescence microscopy, a significant uptake to the nuclei of HeLa cells was observed for the rhodium chrysi complex with the attached fluorescein moiety at 5 μM upon incubation for 60 min at 37 °C. Significant intracellular rhodium accumulation was also demonstrated by ICP-MS measurements of the metal content of HeLa cells for an independent demonstration of metalloinsertor uptake [166].

Since development of metalloinsertors showing an inherent change in emission upon binding to mispairs in DNA turned out to be difficult, an alternative access to such fluorescent mismatch probes was based on the conjugation of Oregon Green 514 to the rhodium chrysi moiety by the linker strategies described above (Figure 15E) [167]. In the presence of canonical DNA, the fluorescence of the conjugate is significantly quenched due to an intramolecular ion pairing mechanism. In contrast, the Oregon Green emission at 530 nm increased with increasing concentration of duplex oligonucleotide DNA incorporating a CC mismatch, in which the rhodium chrysi unit is shielded from interaction with the fluorophore by insertion into the double helix.

In addition to these modifications of the outer ligand sphere, the coligands on the rhodium chrysi core have also been widely varied in recent years. In particular, replacement of the two bpy ligands by 2-phenylpyridine (ppy) gave $[Rh(chrysi)(ppy)]^+$ with two *N*,*C*-chelators, resulting in a significantly reduced charge, down from +3 to +1. The compound was also able to recognize a CC mismatch, but photocleavage turned out to be much less efficient for the cyclometalated complex compared to the parent compound [168]. A flexible synthetic strategy with two subsequent 1,2-diketone condensation steps on $[Rh(phen)(NH_3)_4]^{3+}$ also gave access to tris-heteroleptic complexes such as $[Rh(chrysi)(phen)(phi)]^{3+}$ (Figure 16) and the robust coordination of bidentate chelators to the $4d^6$ low-spin rhodium(III) center allowed enantiomer separation with potassium antimonyl tartrate [154]. Even Rh chrysi complexes with monodentate ligands can be prepared starting from rhodium(III) hexaammine and one equivalent of chrysene-5,6-dione (Figure 16) [169].

While the preparation of tris-heteroleptic complexes such as $[Rh(chrysi)(bpy^{R,R'})(phen)]^{3+}$ with pendant functional groups on the bpy ligand is a cum-

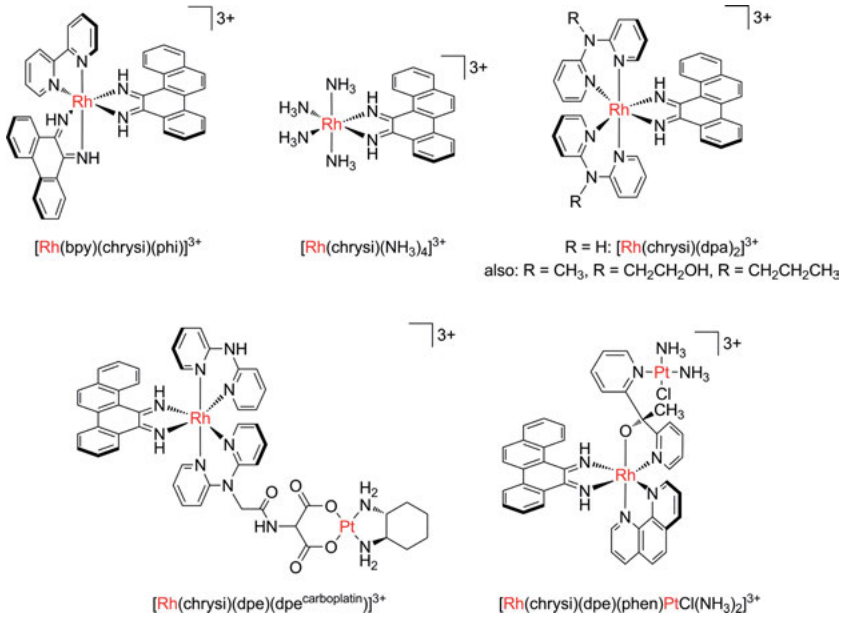

Figure 16. Structures of next-generation rhodium(III) chrysi metalloinsertors, showing the wide range of ligand functionalities that can be introduced, from trisheteroleptic complexes and simple amine ligands (top left) to use of di(pyridyl)amine (dpa) as an easy-to-functionalize symmetrically coordinated chelator (top right) and construction of heterobimetallic compounds combining a rhodium(III) metalloinsertor with a DNA-alkylating cisplatin or carboplatin moiety (bottom left and right).

bersome multi-step procedure [163], replacement of the bpy ligand by di(pyridyl)amine (dpa) offers a new handle for facile metalloinsertor functionalization by modification of the secondary amino group (Figure 16) [169]. However, compared to $[Rh(bpy)_2(chrysi)]^{3+}$, the binding affinity of $[Rh(dpa)_2(chrysi)]^{3+}$ to a CC mismatch was more than two orders of magnitude lower (K_D of 30 nM *vs.* 11 μM) and light-induced DNA cleavage important for footprinting applications is much reduced due to the presence of the amino group. Interestingly, some differential activity in the cell proliferation of mismatch repair-proficient *vs.* -deficient cell lines was observed for $[Rh(dpa)_2(chrysi)]^{3+}$ and some related metallointercalators, indicating that these compounds are possibly also able to recognize mispairs *in vitro* and trigger a biological response [169]. Significantly, the degree of inhibition of cell proliferation was found to correlate positively with the DNA mismatch binding affinity.

Further studies were then directed at the correlation of the intracellular rhodium content of MMR+/– cell lines exposed to $[Rh(bpy)_2(chrysi)]^{3+}$, $[Rh(dpa)_2(chrysi)]^{3+}$, and its methylated derivative with the cytotoxic potential determined with the MTT assay [170]. As determined by ICP-MS, the cellular uptake of the dpa complex was significantly higher than that of the analogous bpy compounds while no difference in intracellular rhodium content was found for the

mismatch repair-competent *vs.* -deficient cells within the accuracy of the experiment. However, the two dpa complexes showed somewhat higher cytotoxic activity on the MMR– cell line HCT116O compared to MMR+ HCT116N, which should lead to stronger mismatch accumulation in the former one. No such differential activity was observed in the MTT assay for $[Rh(bpy)_2(chrysi)]^{3+}$, though see [170]. Thus, the binding affinity of a metalloinsertor to a certain mismatch determined on isolated synthetic oligonucleotide duplexes is not a sufficient predictor for significant *in vitro* biological activity. This is due to the fact that on the way to the DNA target, the metal complex has to cross both the cellular and the nuclear membrane, and even highly efficient mismatch binders will not show any biological effect if they are unable to overcome these barriers. Therefore, any development of mismatch-targeting drug candidates has to optimize both mismatch-binding affinity and membrane permeability.

Interestingly, cell death induction by $[Rh(dpa)_2(chrysi)]^{3+}$ was *via* necrosis and not apoptosis [170]. Further studies were then aimed at modifications in the ligand periphery of the di(pyridyl)amine (dpa) ligand and indeed resulted in significant differences in nuclear *vs.* mitochondrial accumulation, as determined by ICP-MS [171]. Even small variations, such as substitution of propyl by 2-hydoxyethanol led to notable differences, indicating the great potential of these systems for tuning the biological properties. As an extension of this concept, di(pyridyl)glycine was coordinated to $[Rh(chrysi)(dpa)(NH_3)_2]^{3+}$, replacing the two ammine ligands, and the carboxylate group then coupled to diethyl aminomalonate using HATU as the activation reagent. Following base-mediated ester hydrolysis, a platinum(II) moiety was introduced by reaction with $[Pt(dach)(H_2O)_2]SO_4$, resulting in a metalloinsertor-carboplatin conjugate (Figure 16) [172]. Competition experiments with $[Rh(bpy)_2(chrysi)]^{3+}$ showed that the bimetallic complex retains the CC mismatch binding ability. The appearance of bands with reduced mobility in gel electrophoretic analysis of DNA binding indicated oligonucleotide binding through the platinum center, which was further substantiated by dimethyl sulfate footprinting. Thus, the Rh/Pt compounds acts as a dual-functional inserter-covalent binder. A low micromolar IC_{50} value of 9 μM was determined for the conjugate with the MTT assay and showed improved cytotoxic activity compared to cisplatin and oxaliplatin, which had IC_{50} values of 30 and 28 μM, respectively [172]. ICP-MS allowed the monitoring of the cellular accumulation of the Rh/Pt complex, which however decreased with increasing incubation time, indicative of a potential efflux mechanism operating on the compound or its decomposition products.

The mechanism of cell death was dependent on caspase, which indicates an apoptotic process. Apparently, the consequences of DNA platination dominate here over the effect of the non-covalent rhodium mismatch binding. In 2012, the group of Barton then published the most extensive study of mismatch binding affinity and nuclear accumulation in a series of 10 rhodium chrysi metalloinsertors, which also included the introduction of 1,1-di(pyridyl)ethanol (dpe) as an additional ancillary ligand [173]. Initially, the binding mode of dpe was incorrectly assumed to be *via* the two pyridyl groups in a *N,N*-chelating fashion. However, a more recent X-ray crystal structure showed that the ligand is in fact coordinat-

ed by only one pyridyl moiety as well as the deprotonated hydroxy group and dpe thus acts as a *N,O*-chelator (Figure 16) [174].

Some of the complexes showed significant differentiation between the MMR+ and MMR− cell lines, which interestingly was most pronounced for the tetrammine complex $[Rh(NH_3)_4(phzi)]^{3+}$. Although no IC_{50} values were reported, clear cyotoxic effects were observed in particular on the mismatch repair-deficient cell line HCT116O at about 5–20 μM for most complexes. ICP-MS analysis of the nuclear and mitochondrial rhodium content as well as whole-cell accumulation showed highly variable behavior, indicative of a range of different uptake mechanisms operative. Interestingly, with a few exceptions, cell-selective activity on the MMR+/– cell lines was correlated with low mitochondrial uptake. This suggests the nuclear DNA as the main target of the metalloinsertors [173].

Most recently, the discovery of *N,O*-binding of the 1,1-di(pyridyl)ethanol (dpe) ligand in $[Rh(chrysi)(dpe)(phen)]^{3+}$, with the second pendant pyridyl moiety not coordinated, opened the way for the synthesis of another heterobimetallic Rh/Pt complex, in which the abovementioned compound was simply reacted with cisplatin in a 1 : 4 ratio, giving rise to $[Rh(chrysi)(dpe)PtCl(NH_3)_2(phen)]^{3+}$. In spite of this modification, the compound retained the CC mismatch binding affinity and DNA platination could be demonstrated by autoradiography by dimethylsulfate footprinting. In the MTT assay, low micromolar potency on the MMR− cell lines HCT116O were observed [175].

Thus, while initial studies of rhodium metalloinsertors were mostly focused on model studies of their mismatch-recognition ability on short synthetic oligonucleotide duplexes, in recent years, the research focus has shifted more towards *in vitro* investigation of the differential cytotoxic activity in mismatch repair-proficient *vs.* -deficient cell lines [40]. More detailed structure-activity relationships will likely be required to establish the key molecular features to enable high mismatch binding affinity and efficient cellular and nuclear accumulation in a single molecule. How the mismatch binding of the metal complex is then recognized in cells and translated into a biological signal ultimately leading to cell death has to be elucidated in future research [139, 162].

5.3. Other Metal Complexes

While DNA mismatch recognition has been dominated by octahedral rhodium(III) complexes due to the interesting properties of systems based on the extended chrysenediimine ligand [40, 162], some ruthenium(II) and cobalt(III) compounds were also demonstrated to bind to mispaired nucleobases over the last decade. In line with the observation that sterically demanding ligands with an extended aromatic surface area can only access the DNA double helix at thermodynamically destabilized mismatched sites, derivatives of the classical $[Ru(bpy)_2(dppz)]^{2+}$ metallointercalator were prepared in which the dppz ligand was replaced by other polycyclic heteroaromatics, which however often present significant challenges in synthesis.

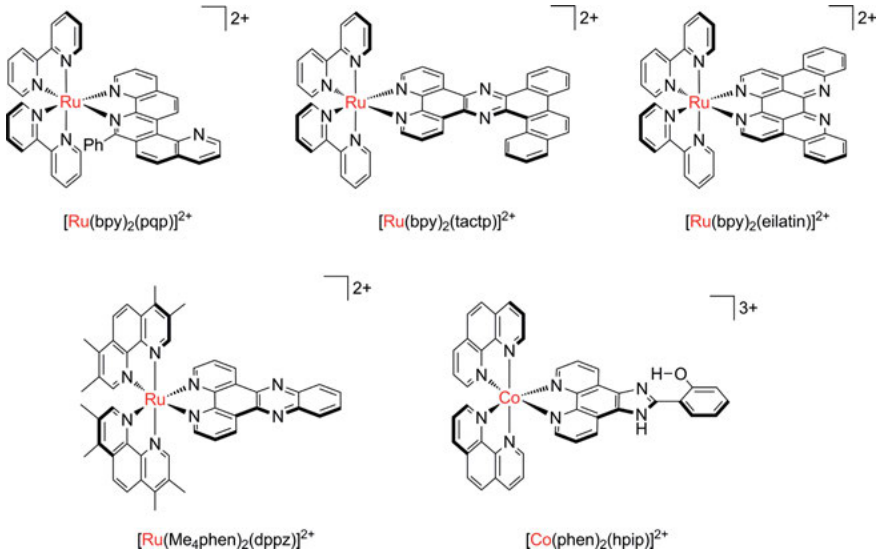

Figure 17. Structural variation of the ligand periphery in ruthenium(II) and cobalt(III) metalloinsertors to achieve good mismatch recognition properties and luminscence reporting of the mismatch binding.

The first such report utilized 6-phenylquino[8,7*k*][1,8]phenanthroline (pqp) as well as 4,5,9,18-tetraazachryseno[9,10*b*]triphenylene (tactp) as a substitute for dppz (Figure 17) [176]. While pqp can be viewed as a hybrid of 1,10-phenanthroline and quinoline sharing one edge, the tactp ligand is prepared by condensation of 5,6-chrysenequinone and 5,6-diamino-1,10-phenanthroline. Interestingly, $[Ru(bpy)_2(tactp)]^{2+}$, easily prepared from $[RuCl_2(bpy)_2]$ and the tactp ligand, turned out to be emissive in aqueous solution with the maximum centered at 610 nm and showed an increase in luminescence by one order of magnitude upon addition of DNA. The excited-state lifetime also more than doubled for the bound *vs.* free form (1230 *vs.* 480 ns, respectively). Using singlet oxygen sensitization by the Ru(II) complex as well as DNase I footprinting, the complex was shown to recognize a CC mismatch with significant affinity ($K_b = 8 \times 10^5\ M^{-1}$) [176]. Similar binding was found for the pqp analogue, which was not emissive under the conditions studied. A problem of these compounds that emerged during the studies, however, is their tendency to aggregate in aqueous solution, possibly due to stacking interactions of the rather hydrophobic ligands with extended aromatic π-systems, which led to concentration-dependent optical properties and quenching.

Interestingly, natural products can also serve as a source of ligands for the preparation of mismatch-binding metalloinsertors. For example, marine alkaloids from tunicates based on pyrido[2,3,4*kl*]acridine were shown to have substantial biological activity and incorporate a bpy/phen-type chelator motif. In spite of the complicated structure composed of seven annelated benzene and pyridine rings, one of these compounds, eilatin (dibenzo[*b*,*j*]dipyrido[4,3,2-*de*:2′,3′,4′-*gh*]-

[1,10]phenanthroline), named after its site of discovery in the Gulf of Eilat, could easily be synthesized from 1,2-benzoquinone and tryptamine [177] and was found to selectively coordinate to $[RuCl_2(bpy)_2]$ under chloride displacement with the bipyridine side (called "head-on") due to steric restrictions in the biquinoline face [178, 179]. In competitive DNA photocleavage studies of $[Ru(bpy)_2(eilatin)]^{2+}$ (Figure 17), the eilatin complex was able to recognize a CC mispair with a binding constant in the range of 2×10^6 M^{-1}, but selectivity for matched *vs.* mismatched DNA was lower than that of the benchmark compound $[Rh(bpy)_2(chrysi)]^{3+}$ [180]. Thus, an increased aromatic surface area of a metalloinsertor ligand does not guarantee a more specific binding at a mismatched site or, as the authors put it: "bulky is good, but bulkier is not necessarily better." This is attributed to the fact that the extended ligand surface is also able to intercalate at canonical matched duplex DNA.

A highly desirable target of metalloinsertor design is the development of luminescent probes which indicate mismatch binding by substantial changes in their emissive behavior. Two strategies were recently explored along these lines, the modification of the distal part of the dppz ligand in $[Ru(bpy)_2(dppz)]^{2+}$ to increase its steric bulk and thus prevent binding at matched DNA while retaining the affinity for thermodynamically destabilized mismatches, and adaption of the chrysi ligand framework, well-established in the case of rhodium(III) metalloinsertors, to the field of ruthenium(II) complexes [181]. However, the diimine compounds were non-luminescent at room temperature, which is assigned to a quenching process involving the exchangeable imino protons, and complexes with functionalized dppz ligands did not show much enhanced luminescence properties compared to the $[Ru(bpy)_2(eilatin)]^{2+}$ parent compound. In contrast, a more successful strategy was based on the increase of the steric bulk of the coligands while retaining the dppz DNA binding element. Thus, $[Ru(Me_4phen)_2(dppz)]^{2+}$ was finally established as a mismatch-recognition "light-up" probe for base pair mismatches (Figure 17) [182].

The differentiation between matched and mismatched DNA is based on significantly (26-fold) higher binding towards the destabilized mispaired site as well as increased excited state emission lifetime when bound to the mismatch (160 ns *vs.* 35 ns when bound to matched DNA). Based on quenching experiments with $[Cu(phen)_2]^+$, a metalloinsertion interaction from the minor groove was deduced [182]. The emission intensity, however, was strongly dependent on the type of DNA lesion. Incubation of $[Ru(Me_4phen)_2(dppz)]^{2+}$ with a DNA hairpin incorporating a rather stable GG mismatch led to only negligible differences in luminescence efficiency compared to the Watson-Crick GC and AT base pairs, while 4–6 times higher emission was found for the CA and CC mispair. The highest luminescence increase was, however, associated with binding to an abasic site.

Quite surprising, even the "classical" metallointercalator $[Ru(bpy)_2(dppz)]^{2+}$ shows a dual-mode binding to DNA incorporating both matched and mismatched sites, as revealed in a recent X-ray crystal structure determination of the Δ-isomer bound to a 12mer palindromic oligonucleotide duplex including two AA mismatches [56]. The asymmetric unit was found to contain one DNA duplex with five bound ruthenium complexes in three different binding modes. At one end of

the duplex, a Ru dppz complex was involved in stacking interactions with the terminal Watson-Crick base pair, while two additional metal complexes were bound at matched sites in the usual intercalative fashion with an expansion of the oligonucleotide duplex. Interestingly, however, two more $[Ru(bpy)_2(dppz)]^{2+}$ units were bound to the mismatches *via* metalloinsertion, with the two mispaired adenosines ejected from the DNA duplex and the dppz ligand deeply inserted from the minor groove [56]. More recently, the light switch effect of $[Ru(bpy)_2(dppz)]^{2+}$ was even demonstrated for a 26mer RNA hair pin including a CA mismatch in the stem region. From luminescence and quenching studies, it was inferred that the binding is by insertion from the minor groove [183].

Since low-spin $3d^6$ cobalt(III) complexes exhibit a stability comparable to rhodium(III) and ruthenium(II) compounds, a very small number of such systems has also been explored for their mismatch-binding properties. For example, Yang and coworkers prepared $[Co(phen)_2(dpq)]^{3+}$ and $[Co(phen)_2(hpip)]^{3+}$ (Figure 17) and studied their binding to the hexameric oligonucleotide $d(GCGAGC)_2$ incorporating two sheared G-A mispairs by NMR spectroscopy [184, 185]. The complex with the less expansive dpq ligand was found to bind to the terminal GC moiety from two directions while the hpip compound intercalates between the central G and A base pairs from the minor groove. Thus, even though the oligonucleotide duplex features two neighboring GA mispairs, no evidence of base flipping indicative of metalloinsertion was found in this report [184].

All metalloinsertors described in this section so far are based on octahedral complexes of the group 8 and 9 metals Rh(III), Ru(II), and Co(III). Only very recently, the first report on square-planar late transition metal complexes capable of selective binding to mispaired DNA has appeared. In this work, Fung, Zou, and coworkers tested the hypothesis that out-of-plane bulky coligands in otherwise planar platinum(II) complexes might impose sufficient steric hindrance to direct these compounds to destabilized mismatched sites [20]. Two different classes of compounds were explored (Figure 18). The first series of general formula $[Pt(N\text{-}Y\text{-}X)(NHC^{R,R'})]^+$ with Y = C, X = N or Y = N, X = C was based on a either a 2,6-bis(pyridyl)benzene *N*,*C*,*N*-ligand or a 6-phenyl-2,2′-bipyridine *C*,*N*,*N*-chelator bound in a tridentate fashion to a square-planar platinum(II) center, with the fourth coordination site occupied by an *N*-heterocyclic carbene (NHC) ligand. Substituents of variable steric bulk such as *n*-butyl or benzyl were introduced to the NHC ligand, which was previously shown to adapt an almost perpendicular orientation relative to the plane of the tridentate chelator [186].

In addition, bis-carbene complexes with a methylene spacer between the two NHC groups were also prepared, giving rise to dinuclear complexes. The second class of compounds was also based on a platinum(II) center coordinated by 6-phenyl-2,2′-bipyridine, but two such groups were connected by bisphosphanes of variable linker lengths and substituents, to give rise to homobimetallic complexes of the general formula $[Pt(N\text{-}N\text{-}C)(R_2PCH_2PR_2Pt(N\text{-}N\text{-}C)]^{2+}$ (Figure 18) [20]. Generally, affinity for the CC mismatch increased with steric demand of the NHC ligand. However, there was a certain upper limit in bulkiness, beyond which the binding became less efficient again.

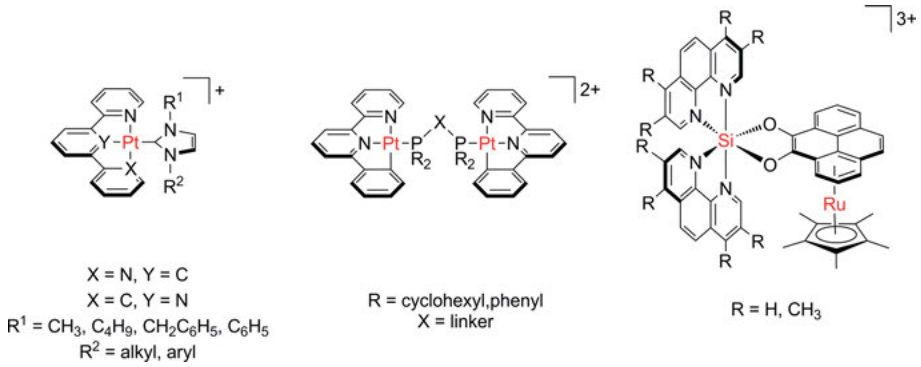

Figure 18. Structures of mononuclear as well as homo- and heterodinculear complexes based on platinum(II) and ruthenium(II)/silicon(IV) as alternative mismatch-sensitive metalloinsertors.

Finally, mismatch-binding compounds do not necessarily have to be based on a transition metal center, as demonstrated by recent work by Zhang, Meggers et al. [187], who prepared an octahedral silicon(IV) scaffold with a SiN_4O_2 coordination environment from two substituted 1,10-phenanthroline ligands and one *O*,*O*-chelating 4,5-pyrenediolate (Figure 18). For site-differentiation, one of the benzene rings in the pyrene moiety was then functionalized with a Cp^*Ru fragment by reaction with $[Ru(Cp^*)(CH_3CN)_3]PF_6$. The resulting heterobimetallic Ru/Si compound had a pronounced effect on the melting temperature of 19mer duplex DNA incorporating a central CC or CT mismatch ($\Delta T_M = 7.2\,^\circ C$) but did not affect the more stable CA mispair [187]. Such robust and hydrolytically stable octahedral silicon(IV) compounds might open the way to further exciting developments of main-group mismatch-recognizing systems.

Although rhodium(III) chrysi complexes have dominated the field of mismatch-binding agents so far, the recent results summarized above demonstrate that there is also considerable promise to explore the DNA recognition properties of other metal scaffolds, in particular with clever design of non-standard expanded aromatic ligands as well as sterically demanding coligands.

6. CONCLUDING REMARKS AND FUTURE DIRECTIONS

DNA metallointercalators have played a major role in bioinorganic chemistry from very early on and are possibly only surpassed in terms of attention by covalently binding metal complexes with a biological mode of action akin to cisplatin. In particular, the classical "light-switch" compound $[Ru(bpy)_2(dppz)]^{2+}$ with bpy = 2,2′-bipyridine and dppz = dipyrido[3,2-*a*;2′,3′-*c*]phenazine has been the inspiration for numerous derivatives over the last three decades. By now, the field has reached a very mature state and any new contributions need to go significantly beyond simple DNA titration experiments and cytotoxicity studies. In particular,

when developing potential anticancer drug candidates based on such lead structures, in addition to the obligatory DNA binding studies, the cellular uptake and intracellular distribution of any new compound should be carefully investigated, since the cell and nuclear membranes separate the DNA target from the extracellular environment and thus present formidable barriers for any metal complex.

Whether any metallointercalators will ever make it to clinical applications remains very questionable by now, also due to the fact that DNA is present in all cells and thus it is very difficult to differentiate between normal and malignant cells. Even though it seems unlikely now that these compounds will provide viable new drug candidates, they are nevertheless fascinating tools to probe DNA structure and dynamics. In particular, a number of recent X-ray crystal structures have provided an unprecedented insight in the wide range of binding modes and interactions, in particular when combined with ultrafast time-resolved spectroscopy. Bimetallic threading intercalators and novel metal-coligand combinations not explored much so far are also expected to provide the most interesting new results in the field.

In contrast, metalloinsertors capable of mismatch-detection in duplex DNA are so far restricted to only a very few classes of compounds and currently explored only by a very limited number of researchers. Since a high incidence of mispaired nucleobases as well as defects in mismatch repair systems are associated with certain forms of cancer, possibly this will allow for a better discrimination between normal and aberrant cells. Still, for all compounds acting on DNA, proper membrane passage has to be ensured for them to reach their intracellular target structure.

Even less studied than the binding of metal complexes to mismatched DNA is the interaction with non-genomic nucleic acids such as tRNA, mRNA, and rRNA. Combined with the latest spectroscopic and microscopic methods for metal complex detection in complex biological systems, fascinating new results can be expected for the future. Even if these should not pave the way to new clinical drug candidates, there is still much to explore in biological systems with the aid of metal-based nucleic acid-binding probes.

ABBREVIATIONS AND DEFINITIONS

[12aneN_4]	1,4,7,10-tetraazacyclododecane
[12aneS_4]	1,4,7,10-tetrathiacyclododecane
4amp	4-aminomethylpyridine
acac	acetylacetone
acMet	*N*-acetylmethionine
Ade	adenine
AFM	atomic force microscopy
Arg	arginine
ATP	adenosine 5′-triphosphate
avb	avobenzone (1-(4-*tert*-butylphenyl)-3-(4-methoxyphenyl)propane-1,3-dione)

bb_n	1,*n*-bis(4′-methyl-2,2′-biypridyl-4-yl)alkane
bhq	benzo[*h*]quinoline
bidppz	11,11′-bis(dipyrido[3,2-*a*:2′,3′-*c*]phenazinyl)
bp	base pair
bpy	2,2′-bipyridine
bpym	2,2′-bipyrimidine
CD	circular dichroism
chrysi	5,6-chrysenediimine
CLL	chronic lymphocytic leukemia
Cp^*	pentamethylcyclopentadienyl
CPMD	Car-Parrinello molecular dynamics
CPP	cell-penetrating peptide
CT DNA	calf-thymus DNA
cym	*para*-cymene
Cyt	cytosine
dach	1,2-diaminocyclohexane
DFT	density functional theory
dipytap	2,3-di-2-pyridinyl-pyrazino[2,3-*f*]quinoxaline
dmdop	2,3-dihydro-1,4-dioxino[2,3-*f*]-2,9-dimethyl-1,10-phenanthroline
dmso	dimethylsulfoxide
dop	2,3-dihydro-1,4-dioxino[2,3-*f*]-1,10-phenanthroline
dpa	di(pyridyl)amine
dpe	1,1-di(pyridyl)ethanol
dpp	4,7-diphenyl-1,10-phenanthroline, bathophenanthroline, bphen
dppm	4,6-bis(2-pyridyl)pyrimidine
dppn	4,5,9,16-tetraazadibenzo[*a*,*c*]naphthacene
dppz	dipyrido[3,2-*a*;2′,3′-*c*]phenazine
$dppzCl_2$	7,8-dichlorodipyrido[3,2-*a*;2′,3′-*c*]phenazine
dpq	dipyrido[3,2-*f*:20,30-*h*]quinoxaline
EDAC	1-ethyl-3-(3-dimethylaminopropyl)carbodiimide
EGFR	epidermal growth factor receptor
eilatin	dibenzo[*b*,*j*]dipyrido[4,3,2-*de*:2′,3′,4′-*gh*][1,10]phenanthroline
en	1,2-ethylenediamine
ER	endoplasmic reticulum
EtBr	ethidium bromide
GF-AAS	graphite furnace atomic absorption spectroscopy
Gua	guanine
HAT	histone acetyltransferase
HATU	*O*-(7-azabenzotriazol-1-yl)-1,1,3,3-tetramethyluronium hexafluorophosphate
HBTU	*O*-(2-(1*H*-benzotriazol-1-yl)-1,1,3,3-tetramethyluronium hexafluorophosphate
HDAC	histone deacetylase
hmb	hexamethylbenzene
HNPCC	hereditary nonpolyposis colorectal cancer
HOBT	hydroxybenzotriazole

HOMO	highest occupied molecular orbital
hpip	2-(2-hydroxyphenyl)imidazo[4,5-*f*][1,10]phenanthroline
HPLC	high-performance liquid chromatography
ICP-MS	inductively coupled plasma mass spectrometry
IC_{50}	half maximal inhibitory concentration
IDLs	insertion/deletion loops
ITC	isothermal titration calorimetry
LUMO	lowest unoccupied molecular orbital
Lys	lysine
MD	molecular dynamics
Me_2trien	2*R*,9*R*-diamino-4,7,-diazadecane
Me_4phen	3,4,7,8-tetramethyl-1,10-phenanthroline
MLCT	metal-to-ligand charge transfer
MM	molecular mechanics
MMR	mismatch repair
mRNA	messenger RNA
MTT	3-(4,5-dimethylthiazol-2-yl)-2,5-diphenyltetrazolium bromide
NCP	nucleosome core particle
NHC	*N*-heterocyclic carbene
NIR	near infrared
NLS	nuclear localizing sequence
NMR	nuclear magnetic resonance
NOESY	nuclear Overhauser effect spectroscopy
Pbf	2,2,4,6,7-pentamethyldihydrobenzofuran-5-sulfonyl
PDB	Protein Data Bank
phen	1,10-phenanthroline
phi	9,10-phenanthrenediimine
phzi	benzo[*a*]phenazine-5,6-quinonediimine
PLIM	phosphorescent liftetime imaging microscopy
ppy	2-phenylpyridine
pqp	6-phenylquino[8,7-*k*][1,8]phenanthroline
pta	1,3,5-triaza-7-phosphatricyclo[3.3.1.1.]decane
QM/MM	quantum mechanics/molecular mechanics
qtpy	2,2′:4,4″:4′,4‴-quaterpyridyl
rRNA	ribosomal RNA
SSB	single-strand binding protein
STED	stimulated emission depletion
tactp	4,5,9,18-tetraazachryseno[9,10-*b*]triphenylene
tap	1,4,5,8-tetraazaphenanthrene
TDDFT	time-dependent density functional theory
TEM	transmission electron microscopy
terpy	2,2′:6′,2″-terpyridine
tha	5,8,9,10-tetrahydroanthracene
Thy	thymine
tpm	tris(pyrazolyl)methane
tpphz	tetrapyrido[3,2-*a*:2′,3′-*c*:3",2"-*h*:2‴,3‴-*j*]phenazine

tren	tris(2-aminoethyl)amine
TRIR	time-resolved infrared spectroscopy
tRNA	transfer RNA
Ura	uracil
UV	ultraviolet
Vis	visible

REFERENCES

1. W. Saenger, *Principles of Nucleic Acid Structure*, Springer, New York, 1983.
2. F. A. Hays, A. Teegarden, Z. J. R. Jones, M. Harms, D. Raup, J. Watson, E. Cavaliere, P. S. Ho, *Proc. Nat. Acad. Sci.* **2005**, *102*, 7157–7162.
3. K. Brzezinski, A. Brzuszkiewicz, M. Dauter, M. Kubicki, M. Jaskolski, Z. Dauter, *Nucleic Acids Res.* **2011**, *39*, 6238–6248.
4. R. D. Kornberg, Y. Lorch, *Cell* **1999**, *98*, 285–294.
5. T. Jenuwein, C. D. Allis, *Science* **2001**, *293*, 1074–1080.
6. T. Kouzarides, *Cell* **2007**, *128*, 693–705.
7. S. B. Rothbart, B. D. Strahl, *Biochim. Biophys. Acta* **2014**, *1839*, 627–643.
8. A. J. Bannister, T. Kouzarides, *Cell Res.* **2011**, *21*, 381–395.
9. D. Griffith, M. P. Morgan, C. J. Marmion, *Chem. Commun.* **2009**, 6735–6737.
10. J. Spencer, J. Amin, M. D. Wang, G. Packham, S. S. S. Alwi, G. J. Tizzard, S. J. Coles, R. M. Paranal, J. E. Bradner, T. D. Heightman, *ACS Med. Chem. Lett.* **2011**, *2*, 358–362.
11. R.-R. Ye, C.-P. Tan, Y.-N. Lin, L.-N. Ji, Z.-W. Mao, *Chem. Commun.* **2015**, *51*, 8353–8356.
12. D. E. V. Schmechel, D. M. Crothers, *Biopolymers* **1971**, *10*, 463–480.
13. A. Wolfe, G. H. Shimer, T. Meehan, *Biochemistry* **1987**, *26*, 6392–6396.
14. S. Despax, F. C. Jia, M. Pfeffer, P. Hebraud, *Phys. Chem. Chem. Phys.* **2014**, *16*, 10491–10502.
15. S. Seeberg, C. Bischof, A. Loos, S. Braun, N. Jafarova, U. Schatzschneider, *J. Inorg. Biochem.* **2009**, *103*, 1126–1134.
16. A. K. F. Martensson, P. Lincoln, *Dalton Trans.* **2015**, *44*, 3604–3613.
17. Y. Shu, Z. S. Breitbach, M. K. Dissanayake, S. Perera, J. M. Aslan, N. Alatrash, F. M. MacDonnell, D. W. Armstrong, *Chirality* **2015**, *27*, 64–70.
18. G. Cohen, H. Eisenberg, *Biopolymers* **1969**, *8*, 45–55.
19. I. Haq, P. Lincoln, D. Suh, B. Nordén, B. Z. Chowdhry, J. B. Chaires, *J. Am. Chem. Soc.* **1995**, *117*, 4788–4796.
20. S. K. Fung, T. Zou, B. Cao, T. Chen, W.-P. To, C. Yang, C.-N. Lok, C.-M. Che, *Nature Comm.* **2016**, *7*, 10655.
21. M. J. Hannon, V. Moreno, M. J. Prieto, E. Moldrheim, E. Sletten, I. Meistermann, C. J. Isaac, K. J. Sanders, A. Rodger, *Angew. Chem. Int. Ed.* **2001**, *40*, 880–884.
22. A. Wragg, M. R. Gill, C. J. Hill, X. D. Su, A. Meijer, C. Smythe, J. A. Thomas, *Chem. Commun.* **2014**, *50*, 14494–14497.
23. S. Fantacci, F. De Angelis, A. Sgamellotti, A. Marrone, N. Re, *J. Am. Chem. Soc.* **2005**, *127*, 14144–14145.
24. A. V. Vargiu, A. Magistrato, *Inorg. Chem.* **2012**, *51*, 2046–2057.
25. D. Franco, A. V. Vargiu, A. Magistrato, *Inorg. Chem.* **2014**, *53*, 7999–8008.
26. K. W. Jennette, S. J. Lippard, G. A. Vassiliades, W. R. Bauer, *Proc. Nat. Acad. Sci. USA* **1974**, *71*, 3839–3843.

27. J. K. Barton, J. J. Dannenberg, A. L. Raphael, *J. Am. Chem. Soc.* **1982**, *104*, 4967–4969.
28. A. Yamagishi, *Chem. Commun.* **1983**, 572–573.
29. J. K. Barton, A. T. Danishhefsky, J. M. Goldberg, *J. Am. Chem. Soc.* **1984**, *106*, 2172–2176.
30. M. Eriksson, M. Leijon, C. Hiort, B. Norden, A. Graeslund, *J. Am. Chem. Soc.* **1992**, *114*, 4933–4934.
31. A. E. Friedman, J.-C. Chambron, J.-P. Sauvage, N. J. Turro, J. K. Barton, *J. Am. Chem. Soc.* **1990**, *112*, 4960–4962.
32. G. Li, L. Sun, L. Ji, H. Chao, *Dalton Trans.* **2016**, *45*, 13261–13276.
33. F. E. Poynton, J. P. Hall, P. M. Keane, C. Schwarz, I. V. Sazanovich, M. Towrie, T. Gunnlaugsson, C. J. Cardin, D. J. Cardin, S. J. Quinn, C. Long, J. M. Kelly, *Chem. Sci.* **2016**, *7*, 3075–3084.
34. A. McKinley, J. Andersson, P. Lincoln, E. M. Tuite, *Chem. Eur. J.* **2012**, *18*, 15142–15150.
35. J. Andersson, L. H. Fornander, M. Abrahamsson, E. Tuite, P. Nordell, P. Lincoln, *Inorg. Chem.* **2013**, *52*, 1151–1159.
36. A. W. McKinley, P. Lincoln, E. M. Tuite, *Dalton Trans.* **2013**, *42*, 4081–4090.
37. A. De la Cadena, D. Davydova, T. Tolstik, C. Reichardt, S. Shukla, D. Akimov, R. Heintzmann, J. Popp, B. Dietzek, *Sci. Rep.* **2016**, *6*, 9.
38. X. Gao, S. Shi, J. L. Yao, J. Zhao, T. M. Yao, *Dalton Trans.* **2015**, *44*, 19264–19274.
39. K. E. Erkkila, D. T. Odom, J. K. Barton, *Chem. Rev.* **1999**, *99*, 2777–2795.
40. B. M. Zeglis, V. C. Pierre, J. K. Barton, *Chem. Commun.* **2007**, 4565–4579.
41. C. A. Puckett, R. J. Ernst, J. K. Barton, *Dalton Trans.* **2010**, *39*, 1159–1170.
42. A. C. Komor, J. K. Barton, *Chem. Commun.* **2013**, *49*, 3617–3630.
43. C. Metcalfe, J. A. Thomas, *Chem. Soc. Rev.* **2003**, *32*, 215–224.
44. M. R. Gill, J. A. Thomas, *Chem. Soc. Rev.* **2012**, *41*, 3179–3192.
45. H.-K. Liu, P. J. Sadler, *Acc. Chem. Res.* **2011**, *44*, 349–359.
46. B. J. Pages, D. L. Ang, E. P. Wright, J. R. Aldrich-Wright, *Dalton Trans.* **2015**, *44*, 3505–3526.
47. J. M. Kelly, C. J. Cardin, S. J. Quinn, *Chem. Sci.* **2017**, *8*, 4705–4723.
48. C. M. Dupureur, J. K. Barton, *J. Am. Chem. Soc.* **1994**, *116*, 10286–10287.
49. J. G. Collins, A. D. Sleeman, J. R. Aldrich-Wright, I. D. Greguric, T. W. Hambley, *Inorg. Chem.* **1998**, *37*, 3133–3141.
50. A. Greguric, I. D. Greguric, T. W. Hambley, J. R. Aldrich-Wright, J. G. Collins, *Dalton Trans.* **2002**, 849–855.
51. C. L. Kielkopf, K. E. Erkkila, B. P. Hudson, J. K. Barton, D. C. Rees, *Nature Struct. Biol.* **2000**, *7*, 117–121.
52. J. P. Hall, K. O'Sullivan, A. Naseer, J. A. Smith, J. M. Kelly, C. J. Cardin, *Proc. Nat. Acad. Sci. USA* **2011**, *108*, 17610–17614.
53. J. P. Hall, F. E. Poynton, P. M. Keane, S. P. Gurung, J. A. Brazier, D. J. Cardin, G. Winter, T. Gunnlaugsson, I. V. Sazanovich, M. Towrie, C. J. Cardin, J. M. Kelly, S. J. Quinn, *Nature Chem.* **2015**, *7*, 961–967.
54. P. M. Keane, F. E. Poynton, J. P. Hall, I. P. Clark, I. V. Sazanovich, M. Towrie, T. Gunnlaugsson, S. J. Quinn, C. J. Cardin, J. M. Kelly, *J. Phys. Chem. Lett.* **2015**, *6*, 734–738.
55. J. P. Hall, J. Sanchez-Weatherby, C. Alberti, C. Hurtado Quimper, K. O'Sullivan, J. A. Brazier, G. Winter, T. Sorensen, J. M. Kelly, D. J. Cardin, C. J. Cardin, *J. Am. Chem. Soc.* **2014**, *135*, 17505–17512.
56. H. Song, J. T. Kaiser, J. K. Barton, *Nature Chem.* **2012**, *4*, 615–620.
57. H. Niyazi, J. P. Hall, K. O'Sullivan, G. Winter, T. Sorensen, J. M. Kelly, C. J. Cardin, *Nature Chem.* **2012**, *4*, 621–628.

58. J. P. Hall, H. Beer, K. Buchner, D. J. Cardin, C. J. Cardin, *Phil. Trans. R. Soc. A* **2013**, *371*, 20120525.
59. J. P. Hall, H. Beer, K. Buchner, D. J. Cardin, C. J. Cardin, *Organometallics* **2015**, *34*, 2481–2486.
60. J. P. Hall, D. Cook, S. Ruiz Morte, P. McIntyre, K. Buchner, H. Beer, D. J. Cardin, J. A. Brazier, G. Winter, J. M. Kelly, C. J. Cardin, *J. Am. Chem. Soc.* **2013**, *135*, 12652–12659.
61. J. P. Hall, P. M. Keane, H. Beer, K. Buchner, G. Winter, T. Sorensen, D. J. Cardin, J. A. Brazier, C. J. Cardin, *Nucleic Acids Res.* **2016**, *44*, 9472–9482.
62. J. P. Hall, S. P. Gurung, J. Henle, P. Poidl, J. Andersson, P. Lincoln, G. Winter, T. Sorensen, D. J. Cardin, J. A. Brazier, C. J. Cardin, *Chem. Eur. J.* **2017**, *23*, 4981–4985.
63. D. R. Boer, L. Wu, P. Lincoln, M. Coll, *Angew. Chem. Int. Ed.* **2014**, *53*, 1949–1952.
64. A. A. Almaqwashi, T. Paramanathan, P. Lincoln, I. Rouzina, F. Westerlund, M. C. Williams, *Nucleic Acids Res.* **2014**, *42*, 11634–11641.
65. L. S. Wu, A. Reymer, C. Persson, K. Kazimierczuk, T. Brown, P. Lincoln, B. Nordén, M. Billeter, *Chem. Eur. J.* **2013**, *19*, 5401–5410.
66. E. Baggaley, M. R. Gill, N. H. Green, D. Turton, I. V. Sazanovich, S. W. Botchway, C. Smythe, J. W. Haycock, J. A. Weinstein, J. A. Thomas, *Angew. Chem. Int. Ed.* **2014**, *53*, 3367–3371.
67. M. Bahira, M. J. McCauley, A. A. Almaqwashi, P. Lincoln, F. Westerlund, I. Rouzina, M. C. Williams, *Nucleic Acids Res.* **2015**, *43*, 8856–8867.
68. X. Li, A. K. Gorle, T. D. Ainsworth, K. Heimann, C. E. Woodward, J. G. Collins, R. Keene, *Dalton Trans.* **2015**, *44*, 3594–3603.
69. F. M. Foley, F. R. Keene, J. G. Collins, *Dalton Trans.* **2001**, 2968–2974.
70. B. T. Patterson, J. G. Collins, F. M. Foley, F. R. Keene, *Dalton Trans.* **2002**, 4343–4350.
71. J. L. Morgan, D. P. Buck, A. G. Turley, J. G. Collins, F. R. Keene, *J. Biol. Inorg. Chem.* **2006**, *11*, 824–834.
72. K. Van Hecke, T. Cardinaels, P. Nockemann, J. Jacobs, L. Vanpraet, T. N. Parac-Vogt, R. Van Deun, K. Binnemans, L. Van Meervelt, *Angew. Chem. Int. Ed.* **2014**, *53*, 8959–8962.
73. G. Palermo, A. Magistrato, T. Riedel, T. von Erlach, C. A. Davey, P. J. Dyson, U. Rothlisberger, *ChemMedChem* **2016**, *11*, 1199–1210.
74. T. Very, S. Despax, P. Hebraud, A. Monari, X. Assfeld, *Phys. Chem. Chem. Phys.* **2012**, *14*, 12496–12504.
75. Q.-L. Zhang, J.-H. Liu, J.-Z. Liu, P.-X. Zhang, X.-Z. Ren, Y. Liu, Y. Huang, L.-N. Ji, *J. Inorg. Biochem.* **2004**, *98*, 1405–1412.
76. T. Nandhini, K. R. Anju, V. M. Manikandamathavan, V. G. Vaidyanathan, B. U. Nair, *Dalton Trans.* **2015**, *44*, 9044–9051.
77. B. C. Poulsen, S. Estalayo-Adrian, S. Blasco, S. A. Bright, J. M. Kelly, D. C. Williams, T. Gunnlaugsson, *Dalton Trans.* **2016**, *45*, 18208–18220.
78. R. B. P. Elmes, J. A. Kitchen, D. C. Williams, T. Gunnlaugsson, *Dalton Trans.* **2012**, *41*, 6607–6610.
79. A. N. Hidayatullah, E. Wachter, D. K. Heidary, S. Parkin, E. C. Glazer, *Inorg. Chem.* **2014**, *53*, 10030–10032.
80. C. R. Cardoso, M. V. S. Lima, J. Cheleski, E. J. Peterson, T. Venancio, N. P. Farrell, R. M. Carlos, *J. Med. Chem.* **2014**, *57*, 4906–4915.
81. M. G. Walker, V. Gonzalez, E. Chekmeneva, J. A. Thomas, *Angew. Chem. Int. Ed.* **2012**, *51*, 12107–12110.
82. F. P. Dwyer, E. C. Gyarfas, W. P. Rogers, J. P. Koch, *Nature* **1952**, *170*, 190–191.
83. N. L. Kilah, E. Meggers, *Aust. J. Chem.* **2012**, *65*, 1325–1332.

84. U. Schatzschneider, J. Niesel, I. Ott, R. Gust, H. Alborzinia, S. Wölfl, *ChemMedChem* **2008**, *3*, 1104–1109.
85. M. Dickerson, Y. Sun, B. Howerton, E. C. Glazer, *Inorg. Chem.* **2014**, *53*, 10370–10377.
86. C. Mari, V. Pierroz, R. Rubbiani, M. Patra, J. Hess, B. Spingler, L. Oehninger, J. Schur, I. Ott, L. Salassa, S. Ferrari, G. Gasser, *Chem. Eur. J.* **2014**, *20*, 14421–14436.
87. S. M. Cloonan, R. B. P. Elmes, M. Erby, S. A. Bright, F. E. Poynton, D. E. Nolan, S. J. Quinn, T. Gunnlaugsson, D. C. Williams, *J. Med. Chem.* **2015**, *58*, 4494–4505.
88. C. M. Shade, R. D. Kennedy, J. L. Rouge, M. S. Rosen, M. X. Wang, S. E. Seo, D. J. Clingerman, C. A. Mirkin, *Chem. Eur. J.* **2015**, *21*, 10983–10987.
89. H. Y. Huang, P. Y. Zhang, H. M. Chen, L. N. Ji, H. Chao, *Chem. Eur. J.* **2015**, *21*, 715–725.
90. M. Klajner, C. Licona, L. Fetzer, P. Hebraud, G. Mellitzer, M. Pfeffer, S. Harlepp, C. Gaiddon, *Inorg. Chem.* **2014**, *53*, 5150–5158.
91. B. A. Albani, B. Pena, K. R. Dunbar, C. Turro, *Photochem. Photobiol. Sci.* **2014**, *13*, 272–280.
92. G. J. Ryan, F. E. Poynton, R. B. P. Elmes, M. Erby, D. C. Williams, S. J. Quinn, T. Gunnlaugsson, *Dalton Trans.* **2015**, *44*, 16332–16344.
93. F. D. Abreu, I. C. N. Diogenes, L. G. D. Lopes, E. H. S. Sousa, I. M. M. de Carvalho, *Inorg. Chim. Acta* **2016**, *439*, 92–99.
94. L. L. Zeng, Y. Chen, H. Y. Huang, J. Q. Wang, D. L. Zhao, L. N. Ji, H. Chao, *Chem. Eur. J.* **2015**, *21*, 15308–15319.
95. A. Byrne, C. S. Burke, T. E. Keyes, *Chem. Sci.* **2016**, *7*, 6551–6562.
96. J. Du, Y. Kang, Y. Zhao, W. Zheng, Y. Zhang, Y. Lin, Z. Y. Wang, Y. Y. Wang, Q. Luo, K. Wu, F. Y. Wang, *Inorg. Chem.* **2016**, *55*, 4595–4605.
97. M. Braumuller, M. Staniszewska, J. Guthmuller, S. Rau, *Eur. J. Inorg. Chem.* **2016**, 4958–4963.
98. L. N. Lameijer, S. L. Hopkins, T. G. Breve, S. H. C. Askes, S. Bonnet, *Chem. Eur. J.* **2016**, *22*, 18484–18491.
99. V. Ramu, M. R. Gill, P. J. Jarman, D. Turton, J. A. Thomas, A. Das, C. Smythe, *Chem. Eur. J.* **2015**, *21*, 9185–9197.
100. H. Chen, J. A. Parkinson, S. Parsons, R. A. Coxall, R. O. Gould, P. J. Sadler, *J. Am. Chem. Soc.* **2002**, *124*, 3064–3082.
101. M. Melchart, P. J. Sadler, in *Bioorganometallics*, Ed. G. Jaouen, Wiley-VCH, Weinheim, 2006, pp. 39–64.
102. A. Frodl, D. Herebian, W. S. Sheldrick, *Dalton Trans.* **2002**, 3664–3673.
103. D. Herebian, W. S. Sheldrick, *Dalton Trans.* **2002**, 966–974.
104. S. Schäfer, I. Ott, R. Gust, W. S. Sheldrick, *Eur. J. Inorg. Chem.* **2007**, 3034–3046.
105. M. A. Scharwitz, I. Ott, Y. Geldmacher, R. Gust, W. S. Sheldrick, *J. Organomet. Chem.* **2008**, *693*, 2299–2309.
106. R. Pettinari, F. Marchetti, A. Petrini, C. Pettinari, G. Lupidi, P. Smolenski, R. Scopelliti, T. Riedel, P. J. Dyson, *Organometallics* **2016**, *35*, 3734–3742.
107. K. J. Kilpin, C. M. Clavel, F. Edafe, P. J. Dyson, *Organometallics* **2012**, *31*, 7031–7039.
108. B. Biersack, *Mini-Rev. Med. Chem.* **2016**, *16*, 804–814.
109. Y. J. Chen, W. H. Lei, G. Y. Jiang, Y. J. Hou, C. Li, B. W. Zhang, Q. X. Zhou, X. S. Wang, *Dalton Trans.* **2014**, *43*, 15375–15384.
110. I. Ivanovic, K. K. Jovanovic, N. Gligorijevic, S. Radulovic, V. B. Arion, K. Sheweshein, Z. L. Tesic, S. Grguric-Sipka, *J. Organomet. Chem.* **2014**, *749*, 343–349.
111. S. Nikolic, L. Rangasamy, N. Gligorijevic, S. Arandelovic, S. Radulovic, G. Gasser, S. Grguric-Sipka, *J. Inorg. Biochem.* **2016**, *160*, 156–165.
112. R. K. Gupta, A. Kumar, R. P. Paitandi, R. S. Singh, S. Mukhopadhyay, S. P. Verma, P. Das, D. S. Pandey, *Dalton Trans.* **2016**, *45*, 7163–7177.

113. J. M. Cross, N. Gallagher, J. H. Gill, M. Jain, A. W. McNeillis, K. L. Rockley, F. H. Tscherny, N. J. Wirszycz, D. S. Yufit, J. W. Walton, *Dalton Trans.* **2016**, *45*, 12807–12813.
114. M. J. Chow, C. Licona, D. Y. Q. Wong, G. Pastorin, C. Gaiddon, W. H. Ang, *J. Med. Chem.* **2014**, *57*, 6043–6059.
115. A. Koceva-Chyla, K. Matczak, P. Hikisz, K. Durka, K. Kochel, G. Süss-Fink, J. Furrer, K. Kowalski, *ChemMedChem* **2016**, *11*, 2171–2187.
116. J. Furrer, G. Süss-Fink, *Coord. Chem. Rev.* **2016**, *309*, 36–50.
117. P. Elumalai, Y. J. Jeong, D. W. Park, D. H. Kim, H. Kim, S. C. Kang, K. W. Chi, *Dalton Trans.* **2016**, *45*, 6667–6673.
118. Z. Ma, G. Palermo, Z. Adhireksan, B. S. Murray, T. von Erlach, P. J. Dyson, U. Röthlisberger, C. A. Davey, *Angew. Chem. Int. Ed.* **2016**, *55*, 7441–7444.
119. M. A. Nazif, R. Rubbiani, H. Alborzinia, I. Kitanovic, S. Wolfl, I. Ott, W. S. Sheldrick, *Dalton Trans.* **2012**, *41*, 5587–5598.
120. R. Bieda, I. Ott, R. Gust, W. S. Sheldrick, *Eur. J. Inorg. Chem.* **2009**, 3821–3831.
121. S. Schäfer, W. S. Sheldrick, *J. Organomet. Chem.* **2007**, *692*, 1300–1309.
122. S. Gencaslan, W. S. Sheldrick, *Eur. J. Inorg. Chem.* **2005**, 3840–3849.
123. Y. Geldmacher, K. Splith, I. Kitanovic, H. Alborzinia, S. Can, R. Rubbiani, M. A. Nazif, P. Wefelmeier, A. Prokop, I. Ott, S. Wölfl, I. Neundorf, W. S. Sheldrick, *J. Biol. Inorg. Chem.* **2012**, *17*, 631–646.
124. R. T. Watson, N. Desai, J. Wildsmith, J. F. Wheeler, N. A. P. Kane-Maguire, *Inorg. Chem.* **1999**, *38*, 2683–2687.
125. K. D. Barker, B. R. Benoit, J. A. Bordelon, R. J. Davis, A. S. Delmas, O. V. Mytykh, J. T. Pettry, J. F. Wheeler, N. A. P. Kane-Maguire, *Inorg. Chim. Acta* **2001**, *322*, 74–78.
126. N. A. P. Kane-Maguire, J. F. Wheeler, *Coord. Chem. Rev.* **2001**, *211*, 145–162.
127. J. P. Schaeper, L. A. Nelsen, M. A. Shupe, b. J. Herbert, N. A. P. Kane-Maguire, J. F. Wheeler, *Electrophoresis* **2003**, *24*, 2704–2710.
128. E. G. Donnay, J. P. Schaeper, R. D. Brooksbank, J. L. Fox, R. G. Potts, R. M. Davidson, J. F. Wheeler, N. A. P. Kane-Maguire, *Inorg. Chim. Acta* **2007**, *360*, 3272–3280.
129. M. S. Vandiver, E. P. Bridges, R. L. Koon, A. N. Kinnaird, J. W. Glaeser, J. F. Campbell, C. J. Priedemann, W. T. Rosenblatt, B. J. Herbert, W. S.K., J. F. Wheeler, N. A. P. Kane-Maguire, *Inorg. Chem.* **2010**, *49*, 839–848.
130. A. H. Krotz, L. Y. Kuo, J. K. Barton, *Inorg. Chem.* **1993**, *32*, 5963–5974.
131. A. Sitlani, E. C. Long, A. M. Pyle, J. K. Barton, *J. Am. Chem. Soc.* **1992**, *114*, 2303–2312.
132. A. Sitlani, J. K. Barton, *Biochemistry* **1994**, *33*, 12100–12108.
133. P. K. L. Fu, C. Turro, *Chem. Commun.* **2001**, 279–280.
134. C. Stinner, M. D. Wightman, S. O. Kelley, M. G. Hill, J. K. Barton, *Inorg. Chem.* **2001**, *40*, 5245–5250.
135. H. Ahmad, A. Wragg, W. Cullen, C. Wombwell, A. Meijer, J. A. Thomas, *Chem. Eur. J.* **2014**, *20*, 3089–3096.
136. R. N. Akhimie, J. K. White, C. Turro, *Inorg. Chim. Acta* **2017**, *454*, 149–154.
137. Y. F. Xiang, C., T. Breiding, P. K. Sasmal, H. Liu, Q. Shen, K. Harms, L. Zhang, E. Meggers, *Chem. Commun.* **2012**, *48*, 7131–7133.
138. O. D. Schärer, *Angew. Chem. Int. Ed.* **2003**, *42*, 2946–2974.
139. A. Granzhan, N. Kotera, M.-P. Teulade-Fichou, *Chem. Soc. Rev.* **2014**, *43*, 3630–3665.
140. J. SantaLucia, D. Hicks, *Ann. Rev. Biophys. Biomol. Struct.* **2004**, *33*, 415–440.
141. P. Modrich, *Ann. Rev. Gen.* **1991**, *25*, 229–253.
142. H. T. Lynch, C. L. Snyder, T. G. Shaw, C. D. Heinen, M. P. Hitchins, *Nature Rev. Cancer* **2015**, *15*, 181–194.
143. P. Modrich, *Angew. Chem. Int. Ed.* **2016**, *55*, 8490–8501.

144. R. R. Iyer, A. Pluciennik, V. Burdett, P. Modrich, *Chem. Rev.* **2006**, *106*, 302–323.
145. T. A. Kunkel, D. A. Erie, *Ann. Rev. Biochem.* **2005**, *74*, 681–710.
146. J. Jiricny, *Nature Rev. Mol. Cell Biol.* **2006**, *7*, 335–346.
147. R. Fishel, *J. Biol. Chem.* **2015**, *290*, 26395–26403.
148. P. Modrich, R. Lahue, *Ann. Rev. Biochem.* **1996**, *65*, 101–133.
149. T. A. Kunkel, D. A. Erie, *Ann. Rev. Gen.* **2015**, *49*, 291–313.
150. A. B. Bürmeyer, S. M. Deschenes, S. M. Baker, R. M. Liskay, *Ann. Rev. Gen.* **1999**, *33*, 533–564.
151. B. D. Harfe, S. Jinks-Robertson, *Ann. Rev. Gen.* **2000**, *34*, 359–399.
152. C. S. Chow, J. K. Barton, *Biochemistry* **1992**, *31*, 5423–5429.
153. B. A. Jackson, J. K. Barton, *J. Am. Chem. Soc.* **1997**, *119*, 12986–12987.
154. H. Mürner, B. A. Jackson, J. K. Barton, *Inorg. Chem.* **1998**, *37*, 3007–3012.
155. B. A. Jackson, J. K. Barton, *Biochemistry* **2000**, *39*, 6176–6182.
156. B. A. Jackson, V. Y. Alekseyev, J. K. Barton, *Biochemistry* **1999**, *38*, 4655–4662.
157. B. M. Zeglis, J. A. Boland, J. K. Barton, *J. Am. Chem. Soc.* **2008**, *130*, 7530–7531.
158. B. M. Zeglis, J. A. Boland, J. K. Barton, *Biochemistry* **2009**, *48*, 839–849.
159. C. Cordier, V. C. Pierre, J. K. Barton, *J. Am. Chem. Soc.* **2007**, *129*, 12287–12295.
160. V. C. Pierre, J. T. Kaiser, J. K. Barton, *Proc. Nat. Acad. Sci. USA* **2007**, *104*, 429–434.
161. B. M. Zeglis, V. C. Pierre, J. T. Kaiser, J. K. Barton, *Biochemistry* **2009**, *48*, 4247–4253.
162. K. M. Boyle, J. K. Barton, *Inorg. Chim. Acta* **2016**, *452*, 3–11.
163. U. Schatzschneider, J. K. Barton, *J. Am. Chem. Soc.* **2004**, *126*, 8630–8631.
164. A. Petitjean, J. K. Barton, *J. Am. Chem. Soc.* **2004**, *126*, 14728–14729.
165. M. H. Lim, I. H. Lau, J. K. Barton, *Inorg. Chem.* **2007**, *46*, 9528.
166. J. Brunner, J. K. Barton, *Biochemistry* **2006**, *45*, 12295–12302.
167. B. M. Zeglis, J. K. Barton, *J. Am. Chem. Soc.* **2006**, *128*, 5654–5655.
168. J. L. Kisko, J. K. Barton, *Inorg. Chem.* **2000**, *39*, 4942–4949.
169. R. J. Ernst, H. Song, J. K. Barton, *J. Am. Chem. Soc.* **2009**, *131*, 2359–2366.
170. R. J. Ernst, A. C. Komor, J. K. Barton, *Biochemistry* **2011**, *50*, 10919–10928.
171. A. G. Weidmann, A. C. Komor, J. K. Barton, *Phil. Trans. R. Soc. A* **2013**, *371*, 20120117.
172. A. G. Weidmann, J. K. Barton, *Inorg. Chem.* **2014**, *53*, 7812–7814.
173. A. C. Komor, C. J. Schneider, A. G. Weidmann, J. K. Barton, *J. Am. Chem. Soc.* **2012**, *134*, 19223–19233.
174. A. C. Komor, J. K. Barton, *J. Am. Chem. Soc.* **2014**, *136*, 14160–14172.
175. A. G. Weidmann, J. K. Barton, *Inorg. Chem.* **2015**, *54*, 9626–9636.
176. E. Rüba, J. R. Hart, J. K. Barton, *Inorg. Chem.* **2004**, *43*, 4570–4578.
177. G. Gellerman, A. Rudi, Y. Kashman, *Tetrahedron* **1994**, *50*, 12959–12972.
178. A. Rudi, Y. Kashman, D. Gut, F. Lellouche, M. Kol, *Chem. Commun.* **1997**, 17–18.
179. D. Gut, A. Rudi, J. Kopilov, I. Goldberg, M. Kol, *J. Am. Chem. Soc.* **2002**, *124*, 5449–5456.
180. B. M. Zeglis, J. K. Barton, *Inorg. Chem.* **2008**, *47*, 6452–6457.
181. A. J. McConnell, M. H. Lim, E. D. Olmon, H. Song, E. E. Dervan, J. K. Barton, *Inorg. Chem.* **2012**, *51*, 12511–12520.
182. A. N. Boynton, L. Marcelis, J. K. Barton, *J. Am. Chem. Soc.* **2016**, *138*, 5020–5023.
183. A. J. McConnell, H. Song, J. K. Barton, *Inorg. Chem.* **2013**, *52*, 10131–10136.
184. H. Chen, P. Yang, C. Yuan, X. Pu, *Eur. J. Inorg. Chem.* **2005**, 3141–3148.
185. H. Chen, C. Dou, Y. Yu, H. Li, X. Xi, P. Yang, *J. Inorg. Biochem.* **2009**, *103*, 827–832.
186. R. W.-Y. Sun, A. L.-F. Chow, X.-H. Li, J. J. Yan, S. S.-Y. Chui, C.-M. Che, *Chem. Sci.* **2011**, *2*, 728–736.
187. C.-C. Fu, K. Harms, L. Zhang, E. Meggers, *Organometallics* **2014**, *33*, 3219–3222.

15

Iron and Its Role in Cancer Defense: A Double-Edged Sword

Frank Thévenod

Chair of Physiology, Pathophysiology & Toxicology and Center for Biomedical Education and Research (ZBAF), Department of Medicine Faculty of Health, Private University of Witten/Herdecke, D-58453 Witten, Germany
<frank.thevenod@uni-wh.de>

ABSTRACT 438
1. INTRODUCTION 438
2. SHORT OVERVIEW OF SYSTEMIC AND CELLULAR IRON HOMEOSTASIS 439
   2.1. Systemic Iron Homeostasis 439
   2.2. Cellular Iron Homeostasis 440
3. IRON AND CANCER FORMATION: "A PREDOMINANT FEATURE" 441
   3.1. Production of Reactive Oxygen Species and Induction of Oxidative Damage 441
   3.2. Dysregulation of Iron Homeostasis and Increased Tumor Growth 442
   3.3. Suppression of Cancer Immunity 444
4. IRON AND CANCER DEFENSE: "LONG LIVE THE DIFFERENCE" 444
   4.1. Effect of Hepcidin in Cancer Protection 444
   4.2. Function of Lipocalin-2/NGAL in Cancer Repression 445
      4.2.1. Prevention of Tumor Progression 445
      4.2.2. Promotion of Innate Immunity 447
   4.3. Lactoferrin as Anticancer Agent 448
   4.4. Contribution of Heme Oxygenase-1 to Cancer Defense 450
   4.5. Induction of Ferroptosis as Cancer Therapy 452
   4.6. Roles of Ferritin in Cancer Protection 453
   4.7. Functions of Iron-Sulfur Clusters in Cancer Defense 454

Metal Ions in Life Sciences, Volume 18 Edited by Astrid Sigel, Helmut Sigel, Eva Freisinger, and Roland K. O. Sigel

https://doi.org/10.1515/9783110470734-015

Met. Ions Life Sci. **2018**, *18*, 437–467

5. GENERAL CONCLUSIONS 456
ACKNOWLEDGMENTS 456
ABBREVIATIONS AND DEFINITIONS 456
REFERENCES 458

Abstract: Iron (Fe) is an essential metal, vital for biological functions, including electron transport, DNA synthesis, detoxification, and erythropoiesis that all contribute to metabolism, cell growth, and proliferation. Interactions between Fe and O_2 can result in the generation of reactive oxygen species (ROS), which is based on the ability of Fe to redox cycle. Excess Fe may cause oxidative damage with ensuing cell death, but DNA damage may also lead to permanent mutations. Hence Fe is carcinogenic and may initiate tumor formation and growth, and also nurture the tumor microenvironment and metastasis. However, Fe can also contribute to cancer defense. Fe may induce toxic ROS and/or initiate specific forms of cell death, including ferroptosis that will benefit cancer treatment. Furthermore, Fe-binding and Fe-regulatory proteins, such as hepcidin, lipocalin-2/NGAL, heme oxygenase-1, ferritin, and iron-sulfur clusters can display antitumor properties under specific conditions and in particular cancer types. In addition, the milk protein lactoferrin may synergize with other established anticancer agents in the prevention and therapy of cancer. Consequently, drugs that target Fe metabolism in tumors are promising candidates for the prevention and therapy of cancer, but consideration of context specificity (e.g., tumor type; systemic versus tumor microenvironment Fe homeostasis) is mandatory.

Keywords: cancer defense · carcinogenicity · heme oxygenase-1 · innate immunity · iron homeostasis · lactoferrin · lipocalin-2 · oxidative stress

1. INTRODUCTION

Iron (Fe) is crucial for many life processes and, once incorporated into appropriate proteins, in a variety of reactions [1]. These processes include cell growth and proliferation and also involve electron transport, DNA synthesis, and erythropoiesis. Fe mainly exists in two oxidation states: ferrous (Fe^{2+}) and ferric Fe (Fe^{3+}). The ability of Fe to be converted between these oxidation states through the acceptance or donation of an electron is a key factor in allowing it to perform a wide range of biological functions. Although Fe in the body is essential for O_2 transport, it is also crucial to understand that interactions between these two molecules may result in potentially damaging effects [2], namely the generation of reactive oxygen species (ROS), which is based on the ability of Fe to redox cycle through Fenton and Haber-Weiss chemistry (reviewed in [3]). Excess Fe is associated with toxicity and death because of its pro-oxidant effects but has also been associated with a number of diseases, and in particular the development of cancer [2]. However, Fe not only contributes to oncogenesis, it is also essential for maintaining the rapid growth rate of cancer cells that require for instance the Fe-dependent enzyme ribonucleotide reductase for DNA synthesis (see Section 2.1). Hence, altering Fe metabolism may be an effective strategy for both cancer prevention and cancer treatment.

Without disregarding the pro-mutagenic impact of Fe and its cancer promoting effects on growth, progression, and metastasis, in order to provide a more differentiated view of this complex topic, this review aims to highlight the fact that

under specific context-dependent conditions Fe as well as Fe-binding and/or -regulatory proteins display properties that may be beneficial in cancer prevention and/or defense. Hence, a more nuanced and careful evaluation of the literature on pro- and anticancer effects of Fe seemed necessary. This review summarizes recent knowledge on the role of Fe in cancer defense that complements other assessments on Fe stimulating cancer.

2. SHORT OVERVIEW OF SYSTEMIC AND CELLULAR IRON HOMEOSTASIS

2.1. Systemic Iron Homeostasis

Excellent recent reviews on systemic Fe homeostasis can be found elsewhere [4–6]. Fe is the major transition metal in the body and is mostly found in erythrocyte hemoglobin. Physiologically, Fe is also an essential component of various proteins involved in mitochondrial respiration (electron transport chain), metabolism and detoxification (cytochrome P450 enzymes), deoxyribonucleic acid (DNA) synthesis (ribonucleotide reductase), antioxidant defense (catalase), oxygen sensing (hypoxia-inducible factor (HIF) prolyl hydroxylases), and immune defense (myeloperoxidase) [7]. However, Fe can also be toxic due to the generation of damaging radicals through Fenton chemistry (see Section 3.1). Hence, systemic Fe homeostasis needs to be thoroughly controlled.

There is no known short-term mechanism of mammalian Fe excretion. Physiologically, Fe homeostasis is controlled by the amount of intestinal Fe absorption. Fe (~1mg) losses occur through shedding of Fe-laden intestinal enterocytes and are compensated by duodenal Fe absorption via two different pathways: While heme Fe uptake occurs via not yet clearly defined mechanisms (see [8, 9]), nonheme Fe is taken up by the proton-coupled divalent metal transporter 1 (DMT1/Nramp2/DCT1/SLC11A2) [10] after reduction of dietary Fe^{3+} to Fe^{2+} by duodenal cytochrome B (reviewed in [11]). Fe^{2+} is then carried by chaperones either to cytoplasmic ferritin for storage [12], or to the basolateral transporter ferroportin (FPN1/IREG1/MTP1/SLC40A1) [13–15] for delivery to the plasma. Efficient plasma export is mediated by members of a family of membrane-bound multicopper oxidases, e.g., hephaestin and/or ceruloplasmin [16–18], which convert effluxed Fe^{2+} to Fe^{3+}. In the plasma, Fe^{3+} mainly binds to the protein transferrin (Tf) as diferric Fe transferrin complex (Tf-$[Fe^{3+}]_2$). FPN1, which is the only known cellular Fe exporter, is post-translationally regulated by increased body Fe levels [19]. This occurs through stimulation of synthesis and release of the hepatic peptide hepcidin (see also Section 4.1), a master regulator of systemic Fe homeostasis, into the circulation that limits further intestinal absorption of dietary Fe and its release from cellular stores by decreasing cell surface levels of FPN1 (reviewed in [20]). Hepcidin binds to FPN1 in target cells, primarily enterocytes and macrophages, and to some extent hepatocytes, causing its phosphorylation, internalization, and subsequent lysosomal degradation. Hence, hepcidin negatively regulates both delivery of dietary Fe through the

enterocyte and Fe recycling through the reticuloendothelial (RE) system and macrophages, and consequently reduces Fe export into the plasma [21] (reviewed in [22]).

Free Fe is unsuitable for either plasma Fe transport (it would precipitate) or cytosolic Fe handling (it would damage the cellular environment) [23]. Hence Fe needs to be complexed with appropriate ligands. Plasma Fe transport to its sites of utilization mainly happens as Tf-bound Fe [24] (TBI), but Fe is also carried to a lesser extent by other serum proteins, e.g., albumin, ferritin (see Section 3.2), neutrophil gelatinase associated lipocalin (NGAL/24p3/lipocalin-2) (see Section 4.2.), possibly lactoferrin (see Section 4.3) and hepcidin (see Section 4.1). These latter forms of serum Fe – with the exception of ferritin – are termed non-Tf-bound Fe (NTBI) [23]. Normally, NTBI represents a minor portion of total serum Fe. Tf-bound Fe is mainly delivered to the bone marrow, where Fe is used to synthesize hemoglobin for red blood cells (RBCs). RBCs circulate for ~90 days before being degraded by macrophages of the RE system. Fe is released from catabolized heme and exported from the macrophage by FPN1, where it is loaded onto Tf in the blood circulation, in a process termed "Fe recycling", whereas excess Fe is stored in the liver (0.5–1g) (reviewed in [25]).

2.2. Cellular Iron Homeostasis

Fe assimilation by erythrocyte precursors and non-erythroid cells mainly occurs by receptor-mediated endocytosis (RME) of serum Tf-bound Fe^{3+} [26] that is mediated by the ubiquitous Tf receptor 1 (TfR1) [27, 28]. The acidic environment of the endosome favors the release of Fe from Tf, which remains bound to TfR1 and is subsequently recycled to the cell surface, where it participates in additional rounds of Fe uptake [29]. Endosomal Fe^{3+} is reduced to Fe^{2+} by oxidoreductases of the "Steap" (sixtransmembrane epithelial antigen of the prostate) protein family, namely Steap2 to Steap4 [30]. Fe^{2+} is transported out of the endosome into the cytosol by DMT1 [31].

In most cell types, Fe acquired during the Tf cycle is released into the cytosol and enters a "labile cytosolic Fe pool", i.e., a metabolically active pool of "loosely coordinated" chelatable and redox-active Fe^{2+} that represents a transient reservoir for Fe [32]. Several low-molecular-weight compounds are thought to operate as Fe chelators in this readily accessible Fe reservoir, such as citrate and phosphate, glutathione (GSH) [33], and "mammalian siderophores" (2,5-dihydroxybenzoic acid (DHBA) and catechol) [34, 35]. Cells use this Fe pool for (1) incorporation into prosthetic groups of Fe-dependent enzymes and proteins, (2) incorporation into heme (after transport across the mitochondrial membrane) and Fe-sulfur cluster biogenesis, and (3) storage in ferritin. The major Fe-utilizing cellular organelles are mitochondria that require Fe for the synthesis of heme and Fe-sulfur clusters in the mitochondrial matrix [36, 37]. In erythroid cells, Tf-derived Fe may be directly delivered to mitochondria through transient contact with endosomes (reviewed in [38]). DMT1 may be another mechanism for Fe^{2+} transfer across the outer mitochondrial membrane (OMM) [39]. Entry of Fe into

the mitochondrial matrix through the inner mitochondrial membrane (IMM) may require the SLC transporter mitoferrin-1 (also known as MFRN1/SLC25A37) [40]. Cells may eliminate excess intracellular Fe by secretion of Fe^{2+} via FPN1 or by secretion of heme through the feline leukemia virus, subgroup C, receptor [41]. Excess intracellular Fe may also be detoxified and stored in the cytosol by ferritin, which consists of 24 H (heavy) and L (light) subunits [42] (see Section 4.6). Shuttling of Fe to ferritin appears to be mediated by the poly-r(C)-binding protein 1 (PCBP1) family of chaperones [43]. To mobilize Fe, ferritin is degraded by recruitment of lysosomes and the proteasome (reviewed in [42]).

Like systemic Fe, cellular Fe homeostasis is also tightly regulated. In this case, regulation is achieved by a network of Fe-dependent proteins. Iron-regulatory proteins (IRP1; also known as aconitase 1) and IRP2 (also known as iron-responsive element binding protein 2) are the principal components of this Fe-regulatory network [44]. IRPs are cytosolic proteins that bind to iron-responsive elements (IREs), stem-loop structures found in either the 5' or 3' untranslated regions of mRNAs for proteins involved in Fe import (TfR1, DMT1), storage (ferritin [both heavy and light subunits]), and export (FPN1) [44]. Under conditions of Fe deficiency, IRPs bind to 5' IREs present in both ferritin and FPN1 mRNAs to repress their translation, and to 3' IREs in mRNAs of TfR1 and (presumably IRE-containing) DMT1 isoforms to stabilize them. Excess cytosolic Fe destabilizes IRP1 and IRP2, preventing them from binding to IREs, resulting in increased synthesis of ferritin and FPN1 and enhanced degradation of TfR1 and DMT1 mRNAs. By controlling the import, storage, and efflux of Fe, IRPs ensure that metabolic needs for Fe are met while minimizing the toxic effects of excess Fe.

3. IRON AND CANCER FORMATION: "A PREDOMINANT FEATURE"

3.1. Production of Reactive Oxygen Species and Induction of Oxidative Damage

Body Fe homeostasis needs to be tightly regulated because excess Fe is generally associated with toxicity since it induces the hydroxyl radical ($^{\cdot}OH$), a ROS formed via the Fenton reaction. Fe^{2+} interacts with O_2, which leads to the production of hydrogen peroxide (H_2O_2) to initiate the Fenton reaction. The Fenton reaction involves Fe^{2+} reacting with H_2O_2 to yield Fe^{3+}, a soluble $^{\cdot}OH$, and a hydroxide ion (OH^-). The hydroxyl radical can induce lipid peroxidation to yield lipid alkoxy ($RO^{\cdot}$) radicals − which is damaging to cell membranes −, more ROS and oxidative stress. Moreover, ROS such as superoxide anion (O_2^-) and H_2O_2 also play a role in the production of Fe-induced free radicals.

Fe and Fe derivatives (such as heme or Fe-sulfur [Fe-S] clusters) are essential for the function of ROS-producing enzymes such as nicotinamide adenine dinu-

cleotide phosphate hydride (NADPH) oxidases (NOXs) (involving heme), xanthine oxidase (involving Fe-S clusters), lipoxygenases (LOXs) (non-heme Fe^{3+}), cytochrome P450 enzymes (heme), and subunits of the mitochondrial electron transport chain (Fe-S clusters). Both Fe-dependent ROS-producing enzymes and "labile" Fe (see Section 2.2) are capable of directly catalyzing damaging free radical formation via Fenton chemistry and thereby contribute to ROS-dependent cell damage and death (reviewed in [45]).

3.2. Dysregulation of Iron Homeostasis and Increased Tumor Growth

Mechanisms how Fe may contribute to tumor induction or progression in clinical and nonclinical models have been reviewed extensively [2, 46–49]. Such mechanisms include oxidative DNA damage by Fe-catalyzed ROS production, alterations in gene expression consistent with increased Fe requirements in proliferating cells, as well as decreased immune surveillance against cancer (see Section 3.3).

Excess Fe is associated with DNA damage and promotion of oncogenesis, for instance in patients with hereditary hemochromatosis (Fe overload) who develop liver cancer because the liver is a major organ of Fe storage [50]. Other diseases with Fe overload may also increase the risk for cancer, such as β-thalassemia, with a greater incidence of hepatocellular carcinoma [51]. Fe may also promote the development of leukemia in transfusion-dependent patients with myelodysplastic syndrome [52]. Fe overload also contributes to cancer in the colon and breast tissues: Indeed, the intestinal epithelium is exposed to dietary Fe more than other tissues [53]; and, Fe and estrogen may work synergistically and contribute to the development of breast cancer [54]. An increase of DNA breaks was found in leukocytes obtained from rats chronically fed a diet containing excess Fe as well as after incubation of human leukocytes, primary colonocytes or preneoplastic colon adenoma cell lines with Fe [55, 56]. In non-neoplastic rat liver epithelial cells that were previously initiated with N-methyl-N-nitro-N-nitrosoguanidine (MNNG), ferric ammonium citrate enhanced neoplastic colony formation in a dose-dependent manner, but cell proliferation was reduced ~30 % at the Fe concentrations used [57].

In addition, the microenvironment may also play a role in promoting tumor growth by providing Fe to the tumor cells by tumor-associated macrophages that secrete ferritin [58] and by Fe released from erythrocytes and dead tumor cells [59]. Ferritin protects cancer cells from the Fe-induced generation of ROS thus increasing their resistance to chemotherapy (see Section 4.6). In tumor-associated macrophages, ferritin plays a role in maintaining a pro-tumorigenic (M2) program (reviewed in [60]) (see Section 4.2.2). Aside from its intracellular roles, serum (extracellular ferritin) can stimulate angiogenesis, immunosuppression, and proliferation through various signaling mechanisms [60]. Treatments that involve Fe depletion (e.g., Fe chelators), complemented by ROS reduction (e.g., activation of NF-E2-related factor-2 (Nrf2) pathways, antioxidants), may prevent the development of cancer in patients with Fe overload diseases (reviewed in [61, 62]).

In general, genes encoding proteins that increase intracellular Fe (TfR1, DMT1, and hepcidin) are upregulated in tumor cells, whilst those decreasing Fe levels (FPN-1, ferritin) are downregulated [63–66]. Furthermore, previous studies have shown that the proto-oncogene and proliferation gene c-myc may regulate the expression of TfR1 by directly binding to its promoter region, as well as by indirectly regulating IRP2 and ferritin [67, 68]. In line with these observations, the induction of the tumor suppressor p53 in lung and colorectal cancer (CRC) cell lines increases ferritin and decreases TfR1 protein levels [69], and p53 may induce cell cycle arrest via restricted availability of intracellular Fe to Fe-dependent enzymes (cyclin, cyclin-dependent kinases, ribonucleotide reductase) (reviewed in [70]).

Wingless-related integration site (Wnt) signaling results in the accumulation of β-catenin, which activates the T cell factor (TCF)-lymphoid enhancer factor (LEF) transcription factor complex to induce the expression of target genes, such as c-myc, cyclin D1, and the multidrug resistance P-glycoprotein pump ABCB1 that are involved in cell proliferation and survival [71]. Wnt signaling is regulated through a destruction complex composed of adenomatous polyposis coli (APC), axin, casein kinase 1, and glycogen synthase kinase 3β, which actively targets β-catenin for degradation. Some β-catenin is also sequestered from the destruction complex through an association with E-cadherin [71]. Because inactivating mutations in APC are an early event in CRC, and because alterations in Fe transporters have been observed in CRC tissue, the role of Fe in Wnt signaling has been studied with particular emphasis on proliferation of CRC cell lines [72]. Fe increased Wnt signaling and proliferation in cells with aberrant APC or β-catenin which suggested that the role of Fe is to regulate β-catenin. Hence, Fe may increase Wnt signaling and thereby exacerbate intestinal tumorigenesis, particularly in a background of APC mutations.

These cell culture observations were extended by experiments in $Apc^{min/+}$ mice [73], a model of intestinal cancer in which APC is inactivated. High levels of dietary Fe induced the proto-oncogene c-myc, TfR1, and DMT1 expression in intestinal polyps from $Apc^{min/+}$ mice, as well as in human adenomas and carcinomas, and accelerated tumor formation whereas low Fe levels reduced tumor formation. The stem cell compartment was particularly responsive to Fe manipulation. Further, dietary Fe, but not systemic Fe, was crucial to intestinal tumorigenesis [73]. Supporting the finding that dietary Fe increases cancer risk, Fe-enriched diets have similarly been shown to increase colorectal tumor incidence in a mouse model of colitis [53]. A high-Fe diet also enhanced proliferation and the formation of large adenomas in an azoxymethane-induced mouse model of colon cancer [74]. Conversely, low-Fe diets reduced the growth of colon cancer (as well as mammary adenocarcinoma and hepatoma) xenografts in mice [75]. But an opposite effect of Fe was observed in lymphoma cell lines with translocated copies of c-myc, where Fe inhibited proliferation via free radical-mediated DNA damage and downregulation of c-myc expression [76].

3.3. Suppression of Cancer Immunity

The interplay of Fe metabolism with the regulation of immune responses is complex and also context-dependent. Transfusional Fe overload leads to excessive Fe storage in macrophages and inhibits the immune system [77]. Hence, in macrophages, high intracellular Fe concentration can inhibit the interferon-γ (IFN-γ)-stimulated release of ROS and nitric oxide (NO) (reviewed in [78]), which are key effector pathways in innate immunity. In monocytes, Fe reduces surface expression of cell adhesion molecules such as intracellular cell adhesion molecule 1 (ICAM-1) and human leukocyte antigen (HLA)-DR, which are important in leukocyte migration, T-cell mediated killing and other T- and B-cell responses contributing to adaptive immunity [79]. In contrast, cell-mediated immunity can be enhanced by Fe. In T-lymphocytes, Fe reduces activation of the pro-apoptotic/antiproliferative IFN-γ/signal transducer and activator of transcription 1 (STAT1) pathway and favors the differentiation of T helper 1 (TH1) cells, which could promote cytotoxic antitumor responses [80].

4. IRON AND CANCER DEFENSE: "LONG LIVE THE DIFFERENCE"

4.1. Effect of Hepcidin in Cancer Protection

Fe efflux to the blood stream is physiologically controlled by hepcidin, an antimicrobial peptide and master hormonal regulator of systemic Fe metabolism [4, 20] (see Section 2.1). Hepcidin expression is predominantly modulated by Fe, inflammation, and erythropoiesis, as well as by other factors [4, 81, 82]. Increased serum or tissue Fe levels promote hepcidin induction via BMP/SMAD signaling. Inflammatory interleukin-6 (IL-6) triggers hepcidin induction via IL-6/STAT signaling in crosstalk with the BMP/SMAD pathway (reviewed in [83]). Activin B is another inflammatory cytokine that activates hepcidin via non-canonical BMP/SMAD signaling. Increased erythropoietic activity induced by erythropoietin leads to hepcidin suppression via erythroferrone and other cytokines, possibly by inhibiting BMP/SMAD signaling [83]. Genetic disorders of liver hepcidin expression contribute to Fe-related diseases. These disorders include various forms of hereditary hemochromatosis, which is associated with low hepcidin expression or function (reviewed in [84]) and genetic Fe-refractory Fe deficiency anemia, which is associated with high hepcidin levels and Fe deficit [85].

Hereditary hemochromatosis is a disorder of systemic Fe overload that is caused by hepcidin insufficiency and leads to hyperferremia and gradual Fe saturation of Tf so that NTBI increases which represents highly reactive forms of Fe. These pro-oxidant forms of Fe are ultimately diverted towards the liver hepatocytes, where they may promote oxidative damage [86] by generation of free radicals via Fenton chemistry (see Section 3.1). This subsequently causes damage to DNA, proteins, and membranes. The chronic Fe-driven damage of hepatocytes leads to fibrosis and long-term to hepatocellular carcinoma (HCC) [87].

Decreased liver tissue hepcidin under stress conditions, including HCC [88], is linked to activation of the rat sarcoma (Ras)/rapidly accelerated fibrosarcoma (RAF) mitogen-activated protein kinase (MAPK) and mechanistic target of rapamycin (mTOR) signaling that enhance cell proliferation and anabolic growth [89]. The latter study also showed that the RAF inhibitor sorafenib that is used for combined therapies of HCC [90] (in addition to its ability to induce ferroptosis; see Section 4.5) not only interferes with cancer cell proliferation and angiogenesis, but may also mediate Fe restriction for the growing tumor by inducing hepcidin expression [89]. But serum hepcidin can also be elevated in certain cancers (reviewed in [91]), and some cancer cells, such as breast, CRC, and prostate cancer cells synthesize higher amounts of hepcidin than their nonmalignant equivalents [65, 92, 93]. Hence, it has been suggested that the pro-oncogenic nature of hepcidin may be due to its ability to increase intracellular Fe content in tumor cells by inducing internalization and degradation of FPN1 [94, 95] (reviewed in [91]). In contrast, hepcidin levels have been shown to be influenced via a p53 response element in the hepcidin gene (*HAMP*) promoter [96]. Activation of p53 increased hepcidin expression, while silencing of p53 resulted in decreased hepcidin expression in human hepatoma cells. The authors hypothesized that hepcidin upregulation by p53 is part of a systemic defense mechanism against cancer, through Fe deprivation [96]. Hence, the role of hepcidin in cancer is complex and needs to be evaluated in the context of the type of cancer involved and the function of hepcidin in systemic versus cellular/local (i.e., cancer tissue) Fe homeostasis.

4.2. Function of Lipocalin-2/NGAL in Cancer Repression

4.2.1. Prevention of Tumor Progression

The lipocalin family comprises a group of over 20 small (160–180 amino acid residues) glycoproteins. The core structure of lipocalins consists of an eight-stranded antiparallel β-barrel forming a hydrophobic cavity that defines the "calyx", or cup-shaped ligand binding site capable of flexible ligand binding. Lipocalins are secreted by cells and perform a variety of important biological functions (reviewed in [97]). Lipocalin-2 (Lcn2) (also referred to as NGAL, neutrophil gelatinase-associated lipocalin or siderocalin in humans, in rodents neu-related lipocalin or 24p3) is a 24 kDa secreted protein that was first identified as part of the matrix metalloproteinase-9 (MMP-9; gelatinase-B)/NGAL complex in human neutrophils, where its binding to MMP-9 may accelerate MMP-9 activation or block its auto-degradation [98]. Lcn2 was found to be released by neutrophils at sites of infection and inflammation [99].

Lcn2 binds Fe^{3+} through association with bacterial hydrophobic catecholate-type ferric siderophores, such as enterobactin [100]. Hence, Lcn2 may play a role as an Fe^{3+}-siderophore sequestering protein in antibacterial innate immunity by blocking bacterial access to Fe, thereby decreasing susceptibility to bacterial infections [100, 101]. The interactions of Lcn2 with bacterial siderophores have

been very well characterized [102]. Lcn2 may also bind to mammalian counterparts of bacterial siderophores, such as DHBA and catechol [34, 35], thereby affecting Fe homeostasis of target cells and their survival and proliferation. Lcn2 may also stimulate growth and differentiation, and promote repair and regeneration of damaged epithelia (reviewed in [103]). Lcn2 may be cytoprotective through an antioxidative mode of action [104]. Lcn2 may modulate cell death or survival, depending on its Fe^{3+}-siderophore-loading [105]. When complexed with Fe^{3+} and one of its siderophores (holo-Lcn2), uptake of the molecule inhibits apoptosis by increasing intracellular Fe and decreasing Bcl-2 (B-cell lymphoma 2)-interacting mediator of cell death (Bim), a facilitator of apoptosis; conversely, the internalization of Fe-free Lcn2 (apo-Lcn2) leads to apoptosis, which is driven by Fe depletion and Bim upregulation [106]. Lcn2 is taken up by cells by RME via megalin (K_d ~60 nM) [107] or the 24p3/Lcn2 receptor "brain-type organic cation transporter" (SLC22A17) (K_d ~90 pM) [108].

In recent years, it has become apparent that Lcn2 is over-expressed in cancers of diverse origin and that it facilitates tumorigenesis by promoting survival, growth, and metastasis. Lcn2 has oncogenic potential by promoting epithelial-to-mesenchymal transition (EMT) that facilitates invasiveness and metastasis, in part by forming a complex with MMP-9 which increases its stability, by controlling Fe availability that stimulates cell survival, inflammation [109], and tumorigenesis (reviewed in [110–112]).

In striking contrast, a study by Hanai et al. [113] showed that introduction of Lcn2 (especially as holo-Lcn2) into Ras-transformed 4T1 mouse mammary tumor cells reversed EMT induced by the oncogene H-Ras, and blocked *in vivo* their aptitude for growth, invasiveness, and metastasis, as well as angiogenesis [113, 114]. This suggested that Lcn2 differentially regulates EMT and mesenchymal-to-epithelial transition (MET) in a cell context-dependent manner [113]. Some of the anticancer properties of Lcn2 in Ras-transformed 4T1 mouse mammary tumor cells were the consequence of its ability to inhibit HIF-1α-dependent expression of vascular endothelial growth factor (VEGF) [114]. These data were compatible with observations in cancer of the ovary [115]: Lcn2 expression was almost absent in normal ovaries, strongly present in well differentiated tumors, but weakly expressed in undifferentiated tumors. When EMT was induced by epidermic growth factor in ovarian tumor lines, Lcn2 expression was reduced, suggesting that Lcn2 may slow down development of more advanced grades of malignancy [115]. Similar observations were reported in pancreatic cancer [116]. Lcn2 reduced cell adhesion/invasion partly by suppressing focal adhesion kinase (FAK) activation/phosphorylation and partly inhibited angiogenesis by blocking VEGF production, both *in vitro* and *in vivo* [116]. An antimetastatic action of Lcn2 was also described for colon cancer [117]: In a subtype of particularly aggressive cell lines (KM12SM), Lcn2 expression was inversely correlated with metastasis, and the ectopic induction of Lcn2 inhibited invasion *in vitro* and the appearance of hepatic metastases *in vivo*, but without affecting growth and viability of tumor cells *in vitro* and *in vivo*. This study partly supports earlier work demonstrating high levels of Lcn2 expression in tissue but not in lymph node metastases from adenocarcinomas of the colon [99], and confirm the potential of NGAL as a possible antimetastatic agent.

Finally, $Apc^{min/+}$ intestinal tumorigenesis was investigated in an Lcn2-deficient background in mice [118]. Loss of Lcn2 increased tumor multiplicity specifically in the duodenum, suggesting a potential tumor-suppressive activity. Concurrently, however, Lcn2 increased the average small intestinal tumor size particularly in the distal small intestine. This suggests that the heterogeneous actions of Lcn2 may be (cancer) cell context-dependent and influenced by multiple mechanisms of action, e.g., Fe sequestration and complex formation with MMP9 promoting EMT and tumorigenesis, and inhibition of HIF-1α, FAK phosphorylation, and VEGF expression revealing its antineoplastic, antiangiogenic, and antimetastatic effects. In summary, although further knowledge of the receptors and signaling pathways mediating Lcn2 upregulation in aggressive cancers is necessary, Lcn2 is not only a useful diagnostic and prognostic biomarker of disease progression but also a promising target for cancer therapy in a cancer cell specific context.

4.2.2. Promotion of Innate Immunity

Macrophages are key players of innate immunity but also have a central role in Fe homeostasis. Due to their ability to phagocytose, in particular spleen and liver macrophages take up and degrade damaged or senescent erythrocytes and therefore represent a major source of available Fe in the body [119]. Macrophages are functionally heterogeneous, i.e., as M1- and M2-polarized macrophages, which allow them to adapt to changes in the microenvironment [120] and also determines Fe availability. M1-macrophages are pro-inflammatory, whereas M2-macrophages are antiinflammatory [121]. Due to their functional characteristics, macrophages have been further classified into host defense (M1), wound healing (M2a), and immune regulation (M2b/c) macrophages [122]. Consequently, macrophages contribute to different and even opposing biological functions [123]. M1-macrophages display an Fe-sequestering phenotype by optimizing Fe uptake and storage, and down-regulating Fe export in order to withdraw Fe from the microenvironment (and hence from invading pathogens) (reviewed in [124]). This makes M1-macrophages a major Fe storage site under inflammatory conditions. M1-macrophages express high levels of ferritin, DMT-1, and possibly apo-Lcn2, but low levels of TfR1 and FPN-1 (reviewed in [125]), thereby promoting Fe sequestration. In contrast, M2-macrophages rapidly release Fe to the local microenvironment [126], e.g., likely via FPN-1 and secretion of holo-Lcn2 and/or ferritin (see Section 4.6; also reviewed in [125]).

Lcn-2 is expressed in macrophages during infectious and inflammation-associated diseases [101]. Because the presence of immune cells, in particular macrophages, is also linked to chronic inflammatory conditions found in tumors, M1-polarized macrophages may exert antitumor activity by creating cancer-destructive inflammatory responses. Toll-like receptor (TLR)-signaling seems to be required for their antitumor activity [127] (reviewed in [128]). In patients with postoperative infections at the tumor site, spontaneous tumor regression has been described and consequently used for the therapy of bladder cancer by administering *Mycobacterium bovis bacillus* Calmette-Guérin (BCG) [129]. This likely occurs by activating TLR signaling and promoting the differentiation of

tumor infiltrating monocytes into M1-polarized macrophages. Accordingly, conditioned media of M1-polarized macrophages slow down colon cancer cell growth *in vitro* and *in vivo* [130]. Most importantly, secreted Lcn2 has been shown to promote the M1-macrophage phenotype in various tissues under inflammatory conditions [131–133]. Hence, it is possible that M1-macrophages in the tumor environment develop a Fe sequestration phenotype to attenuate tumor progression, similar to their pathogen-stimulated M1 counterparts, and that both TLR- and Lcn-2-dependent signaling contribute to differentiation into M1-macrophages.

In contrast, M2-macrophages may promote malignancy (reviewed in [125]).

4.3. Lactoferrin as Anticancer Agent

Lactoferrin (Lf) belongs to the Tf protein family and is a non-heme Fe binding glycoprotein with a molecular weight of 80 kDa that is found in bovine milk as well as in humans (reviewed in [134]). The structure of Lf consists of a single polypeptide chain which is folded into two lobes (reviewed in [134]). Each lobe can bind one Fe^{3+} ion in the presence of a carbonate ion that acts as a "synergistic anion". The carbonate ion can be protonated in acidic biological compartments and this helps to promote the release of Fe^{3+}, which is otherwise bound extremely tightly to the protein ($K_d \sim 10^{-20}$ mol/L). Hence, there are two forms of Lf, namely the Fe^{3+}-free (apo-Lf) and the Fe^{3+}-containing (holo-Lf) form. Although Tf and Lf share similar Fe^{3+}-binding properties, Lf does not appear to be important for Fe transport in the body [135]. Lf from human milk may play a role in providing Fe to newborns: Indeed, Lf receptor proteins have been discovered in the colon, which are capable of binding human (hLf) as well as bovine lactoferrin (bLf) [136, 137]. But studies with Lf-knockout mice have shown that Lf is not absolutely required as an Fe source for infants [135]. Lf is also abundant in neutrophils where it is stored in secretory granules (reviewed in [138]). Moreover, Lf is present in various other secreted body fluids, such as tears, saliva, sweat, as well as nasal and genital secretions and its biosynthesis can increase during bacterial infections. Consequently, it is now widely accepted that Lf belongs to the innate immune system [139].

Lf is known for its antibacterial, antifungal, antiviral, antioxidant, antiinflammatory, but also anticancerous properties [140]. Indeed, Lf and its proteolytic derivatives possess anticancer activities and their use in combination with other agents shows promising results (reviewed in [140, 141]). Currently, it is thought that bLf, hLf, and their derivatives may synergize with other established anticancer agents or delivery systems to combat cancer (reviewed in [142, 143]). Studies with various cancer cell lines, animal models, and clinical populations have been reported, all showing beneficial effects [144–147] (reviewed in [140, 148]). Of particular practical relevance is the observation that oral administration seems effective, which differs from practically all other therapeutic proteins, which require parenteral routes of administration to circumvent gastrointestinal (GI) proteolytic degradation. bLf is a relatively stable protein that can be active even

after crossing the GI tract as partially degraded fragments. These fragments, including bovine lactoferricin B, retain the receptor-binding regions of the protein as well as the anticancer active regions [149, 150] and can be internalized by specific Lf receptors in the apical membrane of enterocytes [136, 137]. Hence, some of the antimicrobial lactoferricin peptides have been used as anticancer agents, and occasionally this strategy has been successful in animal experiments [151]. Moreover, oral administration of bLf decreased colon carcinogenesis in azoxymethane-treated rats [152], 7,12-dimethylbenz(a)anthracene-induced hamster buccal carcinogenesis [153], or showed chemopreventive effects against esophagus and lung carcinogenesis in rats [154]. Additional *in vivo* data in mice suggested that bLf may enhance the effectiveness of chemotherapy of breast cancer [155]. The inhibition of tumor growth in animal studies has been attributed to the antiangiogenic and antiinflammatory functions of bLf [156].

Overall, these effects are thought to be mediated by stimulation of the immune response, by modulation of carcinogen-metabolizing enzymes, by modifying the redox profile in target organs, and/or by inhibiting angiogenesis. Yet, regulation of the immune function by Lf may be a key factor in the mechanisms of action involved in cancer prevention. Both innate and adaptive immunity have been implicated in the immune reaction elicited by Lf or its derivatives to combat cancer *in vivo*: Oral administration of bLf activates B- and T-cells and increases the effect of natural killer cells and macrophages, while the expression of IFN-γ, tumor necrosis factor alpha (TNF-α), caspase-1, and IL-18 increases (reviewed in [140]). In addition, Lf regulates multiple signaling pathways to convey cytotoxic effects on cancer cells. Both, bLf and hLf inhibit growth of cancer cells by inducing cell cycle arrest and/or mTOR signaling *in vitro* and *in vivo* [157, 158], while bovine lactoferricin B inhibits cell growth by triggering mitochondrial apoptosis and disrupting cell membranes [159, 160]. Lf and its derivatives inhibit the activity of Akt (protein kinase B), survivin and activate p21, p27, p38, and JNK and induce the release of caspase-8, caspase-3, and cytochrome *c* to induce apoptosis in cancer cells and cancer stem cells (reviewed in [140]). More recently, holo-bLf was shown to elicit apoptosis in breast cancer cell lines by inhibiting a plasma membrane vacuolar-type H^+-ATPase [161], whereas apo-bLf induced apoptosis in HeLa tumor cells by a mechanism involving ROS formation and GSH depletion [162]. The role of Fe in these processes remains unclear: Although Lf binds or releases Fe depending on its grade of Fe saturation, most anticancer effects of Lf may be unrelated to Fe since they can be mimicked by Lf fragments (see above) and its cytotoxic effects can be elicited equally well by apo- or holo-Lf [163].

Because of the convincing immunomodulatory, antiangiogenic, and pro-apoptotic effects of Lf *in vitro* and in animal experiments, a recombinant form of hLf was evaluated as a therapeutic agent for the treatment of human cancer in phase II and phase III clinical trials. In a randomized, double-blind, placebo-controlled study, administration of recombinant hLf extended survival by an average of 65 % in patients with advanced stage non-small cell lung carcinoma [164]. The same preparation was associated with marked improvements in overall survival when applied as an adjunct to standard chemotherapy in patients with newly

diagnosed lung cancer [165]. Furthermore, administration of bLf in a randomized placebo-controlled clinical trial setting had beneficial effects by blocking the growth of adenomatous colorectal polyps that often precede cancer development [166]. In conclusion, Lfs are attractive pharmaceutical drug candidates in clinical nutrition in the overall management of cancer (reviewed in [167]) whose application is so far not hampered by pro-carcinogenic effects. Yet, further studies are necessary to clarify the preventive and therapeutic roles of Lfs in malignancies.

4.4. Contribution of Heme Oxygenase-1 to Cancer Defense

Under oxidative stress, ROS are generated that may cause hemoproteins to release their prosthetic heme groups, producing free heme that can catalyze the production of additional free radicals through Fenton chemistry (see Section 3.1). The pro-oxidant effects of free heme can be avoided through a variety of mechanisms, including the rapid induction of heme oxygenase-1 (*HMOX1*) gene transcription and heme oxygenase-1 (HO-1) isoenzyme protein expression, which increases the rate of free heme catabolism, preventing it from inducing cell damage and death by apoptosis [168]. The rate of *HMOX1* transcription can be induced by heme as well as by a variety of stimuli that lead to ROS formation (reviewed in [169]), including Lcn2 [170]. Consequently, up-regulation of *HMOX1* serves as an adaptive mechanism to protect cells from oxidative damage during stress [171]. The *HMOX1* promoter contains DNA-responsive elements recognized by specific transcription factors activated in response to oxidative stress.

Under homeostasis transcription factors Bach1 (also known as FancJ or BRIP1)/small Maf dimers bind constitutively to stress-responsive elements (StRe) in the *HMOX1* promoter and inhibit *HMOX1* transcription. In response to oxidative stress, Bach1 is exported from the nucleus, ubiquitinated and degraded, thus eliminating transcriptional constraints. Oxidative stress also induces Kelch-like ECH-associated protein 1 (Keap1) ubiquitination-degradation, allowing the transcription factor Nrf2 to translocate into the nucleus. Nrf2/small Maf protein heterodimers bind to StRe and promote *HMOX1* transcription. Most likely the Bach1/Nrf2 transcriptional system interacts functionally with other transcription factors to regulate *HMOX1* transcription [169]. Nrf2 trans-activates many antioxidant proteins apart from HO-1, such as peroxiredoxin 1, catalase, GSH-dependent peroxidase (GPX), superoxide dismutase (SOD), thioredoxin, and proteins that enhance GSH synthesis and regeneration [172]. Hence, Nrf2 is one of the most important transcription factors that protect the organism against exogenous stressors and ROS damage (reviewed in [173]).

HO-1 catalyzes the oxidation of heme to biologically active products: carbon monoxide (CO), biliverdin, and Fe^{2+}. Biliverdin can be converted into the antioxidant bilirubin by biliverdin reductase (reviewed in [174]). Heme catabolism by HO-1 induces the expression of ferritin heavy chain (FtH) and controls in this manner the pro-oxidant activity of labile Fe, an effect which inhibits nuclear factor kappa B (NF-κB), thus limiting the transcription of pro-inflammatory

genes (reviewed in [168]). The CO produced through heme catabolism by HO-1 targets cytochrome *c* oxidase to produce a transient oxidative burst [175]. In addition, CO leads to the degradation of the p38 MAPK p38α isoforms, activating the antiapoptotic p38β isoform [176], which interacts functionally with NF-κB-dependent antiapoptotic A1 and cellular inhibitor of apoptosis protein-2 to suppress caspase activation and apoptosis (reviewed in [168]). Moreover, HO-1 induces expression of antiapoptotic Bcl-2 proteins through activation of the phosphatidylinositol-3-kinase signal transduction pathway, an effect that inhibits the mitochondrial intrinsic apoptotic cell death pathway [177, 178]. HO-1 and FtH also decrease the cellular pools of free heme and free Fe, respectively, an antioxidant effect that limits the extent of c-jun-N-terminal kinase activation [179], thus acting in a cytoprotective manner. Hence, HO-1 participates in maintaining cellular homeostasis and plays an important protective role in the tissues by reducing oxidative injury, attenuating the inflammatory response, inhibiting cell apoptosis, and regulating cell proliferation.

HO-1 involvement in cancer progression is well documented. HO-1 was shown to increase tumor cell proliferation and migration and prevent cancer cells from apoptosis and autophagy (for review see [180]). The regulation of blood vessel formation and the increase in the expression of pro-angiogenic factors are also regulated in an HO-1 dependent way in the context of tumor angiogenesis [181]. The positive correlation between the progression of tumors and increased HO-1 expression was noted for many tumors, including prostate cancer, renal cancer, glioma, melanoma, pancreatic cancer, Kaposi sarcoma, and others (for review see [182]). Recent studies also indicate a possible link between oncogenic mutations, including the leukemia fusion gene Bcr/Abl1, Ras, and c-myc signaling pathways, and HO-1 induction (reviewed in [183]).

However, a growing body of evidence indicates that HO-1 activation may also prevent carcinogenesis as well as the growth and metastasis of tumors. ROS are involved in both tumor initiation as well as in tumor progression, causing nucleic acid mutations. ROS scavenging through the Nrf2/HO-1-mediated induction of target genes may be protective against carcinogens and able to stop or delay the occurrence of malignancy, at least in some tumor types, due to Nrf2/HO-1-dependent antioxidant and genome-protecting activities. In agreement with that, HO-1 may protect healthy tissues against chemical induction of squamous cell carcinoma, but in already growing tumors HO-1 accelerates its progression toward more malignant forms [184]. Conversely, nuclear localization of HO-1 in human primary prostate carcinomas was shown to inhibit cell proliferation, migration, and invasion *in vitro* and to impair tumor growth *in vivo* [185]. In addition, HO-1 functions as an antiangiogenic factor in prostate carcinogenesis by repressing NF-κB signaling [186]. The transcription factor STAT3 (together with Akt) promotes development and metastasis of prostate cancer cells [187, 188]. HO-1 induction in tumor cells of the prostate abrogates STAT3 signaling by increasing HO-1/STAT3 complexing formation, thus enhancing cytoplasmic retention of STAT3 and subsequent inhibition of STAT3 signaling [189].

More recent studies extended these observations by demonstrating that HO-1 induction in prostate cancer cells increased E-cadherin and β-catenin levels, thus

favoring a less aggressive phenotype and further supporting its antitumoral function in prostate cancer [190]. Moreover, HO-1 appears to counteract tumor growth in non-small cell lung carcinoma [191], and in breast cancer it suppresses the invasive capacity of cells via MMP9 down-regulation [192].

Interestingly, exposure to the HO-1 product CO sensitized prostate cancer cells but not normal cells to chemotherapy, with growth arrest and apoptosis induced *in vivo* in part through mitotic catastrophe [193]; CO targeted mitochondria activity in these cells by transiently inducing an anti-Warburg effect, ultimately resulting in metabolic exhaustion. Furthermore, in human pancreatic cancer cells, CO significantly inhibited cell proliferation by decreasing Akt phosphorylation [194]. CO also inhibited tumor proliferation and microvascular density of xenotransplanted tumors and doubled the survival rates pointing to the potential chemoadjuvant/chemotherapeutic use of CO in pancreatic cancer [194].

In summary, HO-1 has a dual role by either promoting or preventing cancer, both in cancer development and progression, depending on the tumor type, and also via anti- versus pro-angiogenic signaling.

4.5. Induction of Ferroptosis as Cancer Therapy

Ferroptosis is an oxidative, Fe-dependent form of cell death that is distinct from other types of regulated cell death, such as apoptosis, necroptosis, and autophagic cell death at morphological, biochemical, and genetic levels [195]. It is likely that Fe-catalyzed production of specific ROS is mainly responsible for ferroptotic death, although Fe may also function as a cofactor for enzymes involved in ROS production [45]. Ferroptosis differs from apoptosis because it does not show chromatin condensation, nuclear fragmentation, plasma membrane blebbing, and caspase activation (reviewed in [196]). Ferroptosis is also distinct from autophagy because it does not form autophagosomes and lacks changes in microtubule-associated proteins 1A/1B light chain 3B (LC3). Unlike necrosis, ferroptosis does not display rapid depletion of ATP. Rather, ferroptosis is morphologically characterized by reduced mitochondrial size with increased membrane density, reduction or vanishing of mitochondria crista, and outer mitochondrial membrane rupture (reviewed in [196]). Ferroptosis is elicited by inactivation of cellular GSH-dependent antioxidant defenses, leading to the accumulation of damaging ROS derived from Fe metabolism and toxic lipid ROS (L-ROS) as well as depletion and peroxidation of polyunsaturated fatty acids (PUFAs) [197]. Mechanistically, ferroptosis may cause cell death through PUFA oxidation and fragmentation and membrane lipid damage, which may be sufficient to irreversibly permeabilize the plasma membrane (reviewed in [198]). Alternatively or in parallel, reactive lipid intermediates generated following PUFA oxidation could induce cell death by covalently modifying and inactivating essential intracellular proteins [198].

Ferroptosis can be induced by experimental compounds (e.g., erastin or Ras-selective lethal small molecule 3 (RSL3)) or clinical drugs (e.g., sorafenib) in cancer cells and certain normal cells (e.g., kidney tubule cells); class 1 inducers

(e.g., erastin, sorafenib) deplete GSH while class 2 inducers (e.g., RSL3) inhibit GPX4 function (reviewed in [196]). Ferroptosis can be pharmacologically inhibited by Fe chelators (e.g., deferoxamine and desferrioxamine mesylate) and lipid peroxidation inhibitors (e.g., ferrostatin-1, liproxstatin-1) by reducing cellular Fe uptake and limiting ROS production, respectively [195, 199]. GPX4 [200], heat shock protein beta-1 (HSPB1) [201], and Nrf2 [202] function as negative regulators of ferroptosis by reducing cellular Fe uptake and limiting ROS production, respectively. In contrast, NOX [195] and p53 (especially the acetylation-defective mutant p53) [203] act as positive regulators of ferroptosis by promoting ROS production and inhibiting expression of SLC7A11 (a key component of the system X_c^- cysteine/glutamate antiporter required for intracellular GSH synthesis).

HO-1 may have a context-dependent dual effect on ferroptosis: HO-1 inhibition prevented erastin-triggered ferroptotic cell death in cancer cells [204]. Furthermore, erastin increased protein and mRNA expression of HO-1 in HT1080 fibrosarcoma cells and fibroblasts and HO-1 expression increased ferroptotic cell death, possibly by increasing Fe-dependent lipid peroxidation [204]. On the other hand, the antioxidative transcriptional regulator Nrf2 that promotes transcription of genes encoding antioxidant proteins (including HO-1) had an antiferroptosis role in HCC [202]. Indeed, knockdown of Nrf2 and HO-1 accelerated erastin or sorafenib-induced ferroptosis in these cells.

In the context of cancer defense/therapy, ferroptosis may act as an endogenous tumor suppressive mechanism downstream of p53 (see above [203]). It is also conceivable to use small molecule activators of ferroptosis, such as erastin, to selectively eliminate cancer cells with mutations in the RAS-RAF-mitogen-activated protein kinase kinase (MEK)- extracellular-signal regulated kinase (ERK) pathway [200, 205]. Kidney and lymphoma cancer cells are more sensitive to erastin compared with cancer cells from other tissues (e.g., lung, colon, central nervous system, melanocytes, ovary, and breast) [200]. Erastin also enhances the impact of chemotherapeutic drugs (e.g., cisplatin, temozolomide, cytarabine, doxorubicin) in certain cancer cells [206–208]. *In vivo*, erastin and RSL3 prevented tumor growth in a xenograft model [200, 201]. Hence induction of ferroptosis by drugs, such as sorafenib (that is used as a treatment for advanced renal cell carcinoma, unresectable HCC, and thyroid cancer) holds great potential for cancer therapy.

4.6. Roles of Ferritin in Cancer Protection

Most cells store excess intracellular Fe in ferritin, where it can be safely sequestered from participation in ROS-generating reactions. Ferritin consists of 24 subunits surrounding a large cavity. The structure of ferritin is similar to a spherical shell enclosing a large cavity that holds up to 4500 Fe atoms in a safe, soluble, and bioavailable form (reviewed in [42, 209]). Ferritin interacts with Fe^{2+} to induce its oxidation and deposition in the cavity in a mineral form, a reaction that is catalyzed by a ferroxidase center. This antioxidant activity consumes Fe^{2+} and peroxides, and thereby prevents formation of toxic ROS via Fenton chemis-

try (see Section 3.1). Generally ferritin expression is regulated by Fe and by oxidative damage, and in mammals has a central role in the control of cellular Fe homeostasis (reviewed in [42, 209]). Ferritin is mostly cytosolic but is found also in mammalian mitochondria and nuclei. In mammals, cytosolic ferritins are composed of two subunit types, termed ferritin heavy (FtH) and ferritin light (FtL) chain subunits and they assemble in a tissue-specific manner that permits flexibility to adapt to cell needs. Ferritin is regulated by IRP1 and IRP2, which post-transcriptionally repress ferritin expression (see Section 2.2).

Several studies have demonstrated that increased intracellular ferritin expression is associated with proliferation, angiogenesis, immunosuppression, and Fe delivery in the context of cancer (reviewed in [60, 209]), but other studies suggest the contrary: Hence, c-myc that increases cell proliferation and transformation represses ferritin expression and stimulates IRP2 expression, which augments the labile Fe pool [67] (see also Section 3.2 for a discussion of the mechanisms involved). Similarly, the E1a oncogene found in adenovirus [210] and H-RAS [211, 212] repress ferritin as well. The effects of ferritin downregulation leading to increased proliferation and growth may be the consequence of an expansion of the labile Fe pool. Conversely, the tumor suppressor gene p53 may inactivate IRPs and increase ferritin expression resulting in a reduction of labile Fe and consequent growth arrest [69, 213] (see also Section 4.7). On the other hand, in human breast cancer cells, the micro RNA miR-200b was found to regulate FtH expression [214]: FtH was increased whereas miR-200b levels were decreased; reintroduction of miR-200b decreased FtH and sensitized cells to doxorubicin chemotherapy. Similarly, FtH small interfering RNAs increased sensitivity of glioma cells to the chemotherapeutic drug carmustine [215]. Both studies suggest that decreased ferritin increases the labile Fe pool in cancer cells and thereby sensitizes them to chemotherapy-induced apoptosis, possibly by increasing oxidative stress. Hence, ferritin may have a protective role in cancer development by preventing pre-cancerous cells from proliferating due to a reduction of the labile Fe pool. On the other hand, ferritin may protect cancer cells from (chemotherapy-induced) cell death by reducing oxidative stress.

4.7. Functions of Iron-Sulfur Clusters in Cancer Defense

Fe-S clusters are made up of Fe and sulfide centers and are co-factors of Fe-S proteins. Usually, Fe-S proteins harbor 2Fe-2S and/or 4Fe-4S clusters. The redox potential of Fe-S clusters varies from -500 mV to $+300$ mV so that they represent excellent electron donors/acceptors. In eukaryotic cells, Fe-S proteins are found in mitochondria, nuclei, and the cytosol where they function as electron carriers in redox reactions (reviewed in [216]). Fe-S clusters of numerous Fe-S proteins function as sensors of Fe or O_2, or operate in substrate binding/catalysis and gene expression regulation. In particular, they participate in various reactions including mitochondrial energy production, amino acid biosynthesis, tRNA modification, and several aspects of protein translation.

Biosynthesis of Fe-S clusters involves complex protein assembly systems which comprise scaffold proteins (including the mitochondrial Fe-S cluster-assembly enzyme (ISCU), a component of the Fe-S cluster scaffold), chaperones, electron transfer proteins, and cysteine desulfurases [217, 218]. Maturation of all cellular Fe-S proteins depends on the mitochondrial Fe-S cluster assembly machinery [218, 219]. Biogenesis of cytosolic and nuclear Fe-S proteins additionally requires a mitochondrial export system mediated by the ATP-binding cassette (ABC) transporter ABCB7 and a cytosolic Fe-S protein assembly (CIA) machinery [216]. The CIA supplies Fe-S clusters for cytosolic and nuclear proteins, including those involved in DNA replication and repair [216].

Several human diseases are associated with hereditary defects in Fe-S biogenesis, including Friedreich's ataxia, sideroblastic anemia, and cancer [217, 220]. For instance, succinate dehydrogenase (SDH; complex II in the mitochondrial respiratory chain) is made up of SDHA-D. Three Fe-S clusters are present in SDHB that facilitate transfer of electrons from the flavin adenine dinucleotide $FADH_2$ to ubiquinone. Mutations in SDH cause familial cancer syndromes (reviewed in [221]). An SDHB-deficient renal carcinoma cell line from a young patient displayed a SDHB mutation, which disrupted binding to the co-chaperone HSC20 causing rapid degradation of SDHB [222]. As a consequence succinate accumulated resulting in a metabolic shift to aerobic glycolysis that is typical for the Warburg effect observed in cancer tissues.

Furthermore, Fe-S cluster biogenesis is directly linked to nuclear genome stability. Instability arises when mitochondria develop defects in Fe-S cluster biogenesis (reviewed in [223]). Different nuclear DNA metabolism enzymes, such as DNA primases and DNA polymerases, ATP-dependent DNA helicases, and DNA glycosylases require a Fe-S cofactor to operate (reviewed in [216]). Defects in Fe-S cluster-containing DNA processing enzymes are implicated in cancer predisposition. Mutations in the human adenine DNA glycosylase MutY(H) cause MUTYH-associated polyposis that is an inherited autosomal recessive disease with a high predisposition to colorectal tumors due to the high level of oxidative damage in the colon and the role of MUTYH in repairing oxidative damage [224] (reviewed in [225]). Mutations in helicase XPD (xeroderma pigmentosum group D) lead to xeroderma pigmentosum (XP) and other diseases [226]. XP is a rare autosomal recessive disorder with sun sensitivity and ultraviolet radiation-induced skin cancer. XP mutants impact DNA and ATP-binding and helicase domain 1 and 2 conformational change. Mutations of Fanconi anemia complementation group J (FancJ; also known as Bach1 or BRIP1) DNA helicase initiate Fanconi anemia, a rare genetic disorder characterized by bone marrow failure and high risk of ovarian cancer [227]. Mutations of regulator of telomere elongation helicase 1 (RTEL1) are associated with dyskeratosis congenita, a rare inherited disorder characterized by bone marrow failure and cancer predisposition [228]. Mutations in ChlR1/DDX11, a DEAD/H DNA helicase that plays a role in sister chromatid cohesion, cause genome instability and are linked to the Warsaw breakage syndrome, which shows a combination of features of Fanconi anemia and Roberts syndrome [229], characterized by drug-induced chromosomal breakage and sister chromatid cohesion defects. Recently, a strong

association between mutations in replicative DNA polymerase pol ε and sporadic colorectal cancers and endometrial carcinomas has been found [230–233].

DNA damage-dependent activation of p53 may result in downstream induction of mitochondrial ISCU that mediates Fe-S cluster binding to IRP1. This causes increased FtH and decreased TfR1 expression resulting in a reduced labile Fe pool [213]. Decreased ISCU expression is found associated with p53 mutations in most human liver cancers, suggesting that p53-ISCU signaling controls Fe homeostasis and hepatocellular carcinogenesis [213] (see also Section 4.6). Hence, drugs that increase ISCU expression and hence, Fe-S cluster biogenesis and assembly could be part of a treatment strategy for cancers with altered Fe homeostasis [234].

5. GENERAL CONCLUSIONS

Most authors agree that excess Fe generally promotes oncogenesis and cancer progression. Yet, the picture is not as clear-cut as anticipated. Hence, whereas some Fe-binding and/or -regulatory proteins exhibit pro-tumorigenic effects under particular conditions they display antitumor properties under other circumstances, e.g., in the context of systemic versus local (i.e., cancer tissue) Fe homeostasis. Furthermore, Fe can induce specific forms of cell death, which may be beneficial to combat cancer (e.g., by inducing ferroptosis; see Section 4.5).

Remarkably, the milk protein lactoferrin, which belongs to the innate immune system, appears outstandingly promising in the prevention and therapy of certain types of cancer when combined with other established anticancer agents (see Section 4.3). Hence, a differentiated assessment of the pro- and anticancer effects of Fe, Fe-binding, and Fe-regulatory proteins seems mandatory. This is particularly necessary because most reviews on Fe and cancer have come to the conclusion that Fe is the culprit and they offer simple therapeutic solutions for a complex subject, namely the development of Fe chelators as antitumor agents. This review advocates caution and suggests differential and more specific therapeutic options to fight cancer in the context of Fe homeostasis.

ACKNOWLEDGMENTS

The author thanks Drs. Wing-Kee Lee and Natascha A. Wolff for valuable discussions and their scientific contributions to the topic of the review. Research in the laboratory is funded by The German Research Foundation (DFG) (grants FT345), BMBF Grant 01DN16039 and the Centre for Biomedical Education and Research (ZBAF) at the University of Witten/Herdecke.

ABBREVIATIONS AND DEFINITIONS

ABCB1	multidrug resistance P-glycoprotein
Akt	protein kinase B

APC	adenomatous polyposis coli
Apo-Lcn2	iron-free lipocalin-2/NGAL
Apo-Lf	iron-free lactoferrin
ATP	adenosine 5′-triphosphate
BCG	*Mycobacterium bovis bacillus* Calmette-Guérin
Bcl-2	B-cell lymphoma-2
Bim	Bcl-2-interacting mediator of cell death
bLf	bovine lactoferrin
CIA	cytosolic iron-sulfur protein assembly
CRC	colorectal cancer
DHBA	2,5-dihydroxybenzoic acid
DMT1	divalent metal transporter 1 (=Nramp2/DCT1/SLC11A2)
EMT	epithelial-to-mesenchymal transition
FAK	focal adhesion kinase
FPN1	ferroportin-1 (= IREG1/MTP1/SLC40A1)
FtH	ferritin heavy (H) chain
GPX	GSH-dependent peroxidase
GSH	glutathione
HCC	hepatocellular carcinoma
HIF	hypoxia-inducible factor
hLf	human lactoferrin
HMOX1	heme oxygenase (decycling) 1
HO-1	heme oxygenase 1
holo-Lcn2	iron-containing lipocalin-2/NGAL
holo-Lf	iron-containing lactoferrin
IFN- γ	interferon- γ
IL-6/-18	interleukin-6/-18
IRE	iron-responsive element
IRP	iron-regulatory protein
ISCU	iron-sulfur cluster assembly enzyme
JNK	c-Jun N-terminal kinase
Lcn2	lipocalin-2 (= 24p3)
Lf	lactoferrin
MAPK	mitogen-activated protein kinase
MET	mesenchymal-to-epithelial transition
MMP-9	matrix metalloproteinase-9
MNNG	N-methyl-N-nitro-N-nitrosoguanidine
mRNA	messenger RNA
mTOR	mechanistic target of rapamycin
NADPH	nicotinamide adenine dinucleotide phosphate hydride
NF-κB	nuclear factor kappa B
NGAL	lipocalin-2
NOX	NADPH oxidase
Nrf2	NF-E2-related factor-2
NTBI	non-transferrin-bound Fe
PUFA	polyunsaturated fatty acid

RAF	rapidly accelerated fibrosarcoma
RAS	rat fibrosarcoma
RBC	red blood cell
RE	reticuloendothelial
RME	receptor-mediated endocytosis
ROS	reactive oxygen species
RSL3	Ras-selective lethal small molecule 3
SDH	succinate dehydrogenase
STAT1/3	signal transducer and activator of transcription 1/3
Steap	sixtransmembrane epithelial antigen of the prostate
StRe	stress responsive elements
Tf	transferrin
TfR1	Tf receptor 1
TLR	toll-like receptor
tRNA	transfer RNA
VEGF	vascular endothelial growth factor
Wnt	wingless-related integration site
XP	xeroderma pigmentosum

REFERENCES

1. M. Arredondo, M. T. Nunez, *Mol. Aspects Med.* **2005**, *26*, 313–327.
2. S. Toyokuni, *Cancer Sci.* **2009**, *100*, 9–16.
3. B. Halliwell, J. M. Gutteridge, *Free Radicals in Biology and Medicine*, Oxford University Press, Oxford, New York, 1999, pp. 936.
4. T. Ganz, *Physiol. Rev.* **2013**, *93*, 1721–1741.
5. I. De Domenico, D. McVey Ward, J. Kaplan, *Nat. Rev. Mol. Cell Biol.* **2008**, *9*, 72–81.
6. K. Pantopoulos, S. K. Porwal, A. Tartakoff, L. Devireddy, *Biochemistry* **2012**, *51*, 5705–5724.
7. *Iron in Biochemistry and Medicine, II.*, Eds. A. Jacobs, M. Worwood, Academic Press, London, 1980, pp. 1–706.
8. M. Shayeghi, G. O. Latunde-Dada, J. S. Oakhill, A. H. Laftah, K. Takeuchi, N. Halliday, Y. Khan, A. Warley, F. E. McCann, R. C. Hider, D. M. Frazer, G. J. Anderson, C. D. Vulpe, R. J. Simpson, A. T. McKie, *Cell* **2005**, *122*, 789–801.
9. A. Rajagopal, A. U. Rao, J. Amigo, M. Tian, S. K. Upadhyay, C. Hall, S. Uhm, M. K. Mathew, M. D. Fleming, B. H. Paw, M. Krause, I. Hamza, *Nature* **2008**, *453*, 1127–1131.
10. H. Gunshin, B. Mackenzie, U. V. Berger, Y. Gunshin, M. F. Romero, W. F. Boron, S. Nussberger, J. L. Gollan, M. A. Hediger, *Nature* **1997**, *388*, 482–488.
11. D. J. Lane, D. H. Bae, A. M. Merlot, S. Sahni, D. R. Richardson, *Nutrients* **2015**, *7*, 2274–2296.
12. L. Vanoaica, D. Darshan, L. Richman, K. Schumann, L. C. Kuhn, *Cell Metab.* **2010**, *12*, 273–282.
13. S. Abboud, D. J. Haile, *J. Biol. Chem.* **2000**, *275*, 19906–19912.
14. A. Donovan, A. Brownlie, Y. Zhou, J. Shepard, S. J. Pratt, J. Moynihan, B. H. Paw, A. Drejer, B. Barut, A. Zapata, T. C. Law, C. Brugnara, S. E. Lux, G. S. Pinkus, J.

L. Pinkus, P. D. Kingsley, J. Palis, M. D. Fleming, N. C. Andrews, L. I. Zon, *Nature* **2000**, *403*, 776–781.
15. A. T. McKie, P. Marciani, A. Rolfs, K. Brennan, K. Wehr, D. Barrow, S. Miret, A. Bomford, T. J. Peters, F. Farzaneh, M. A. Hediger, M. W. Hentze, R. J. Simpson, *Mol. Cell* **2000**, *5*, 299–309.
16. Z. L. Harris, A. P. Durley, T. K. Man, J. D. Gitlin, *Proc. Natl. Acad. Sci. USA* **1999**, *96*, 10812–10817.
17. C. D. Vulpe, Y. M. Kuo, T. L. Murphy, L. Cowley, C. Askwith, N. Libina, J. Gitschier, G. J. Anderson, *Nat. Genet.* **1999**, *21*, 195–199.
18. S. Cherukuri, R. Potla, J. Sarkar, S. Nurko, Z. L. Harris, P. L. Fox, *Cell Metab.* **2005**, *2*, 309–319.
19. E. Ramos, L. Kautz, R. Rodriguez, M. Hansen, V. Gabayan, Y. Ginzburg, M. P. Roth, E. Nemeth, T. Ganz, *Hepatology* **2011**, *53*, 1333–1341.
20. T. Ganz, E. Nemeth, *Biochim. Biophys. Acta* **2012**, *1823*, 1434–1443.
21. E. Nemeth, M. S. Tuttle, J. Powelson, M. B. Vaughn, A. Donovan, D. M. Ward, T. Ganz, J. Kaplan, *Science* **2004**, *306*, 2090–2093.
22. H. Drakesmith, E. Nemeth, T. Ganz, *Cell Metab.* **2015**, *22*, 777–787.
23. P. Brissot, M. Ropert, C. Le Lan, O. Loreal, *Biochim. Biophys. Acta* **2012**, *1820*, 403–410.
24. B. J. Scott, A. R. Bradwell, *Clin. Chem.* **1983**, *29*, 629–633.
25. M. C. Linder, *Nutrients* **2013**, *5*, 4022–4050.
26. D. M. Frazer, G. J. Anderson, *Biofactors* **2014**, *40*, 206–214.
27. P. Aisen, *Int. J. Biochem. Cell Biol.* **2004**, *36*, 2137–2143.
28. J. E. Levy, O. Jin, Y. Fujiwara, F. Kuo, N. C. Andrews, *Nat. Genet.* **1999**, *21*, 396–399.
29. P. Ponka, C. Beaumont, D. R. Richardson, *Semin. Hematol.* **1998**, *35*, 35–54.
30. R. S. Ohgami, D. R. Campagna, A. McDonald, M. D. Fleming, *Blood* **2006**, *108*, 1388–1394.
31. M. D. Fleming, M. A. Romano, M. A. Su, L. M. Garrick, M. D. Garrick, N. C. Andrews, *Proc. Natl. Acad. Sci. USA* **1998**, *95*, 1148–1153.
32. W. Breuer, M. Shvartsman, Z. I. Cabantchik, *Int. J. Biochem. Cell Biol.* **2008**, *40*, 350–354.
33. R. C. Hider, X. L. Kong, *Biometals* **2011**, *24*, 1179–1187.
34. L. R. Devireddy, D. O. Hart, D. H. Goetz, M. R. Green, *Cell* **2010**, *141*, 1006–1017.
35. G. Bao, M. Clifton, T. M. Hoette, K. Mori, S. X. Deng, A. Qiu, M. Viltard, D. Williams, N. Paragas, T. Leete, R. Kulkarni, X. Li, B. Lee, A. Kalandadze, A. J. Ratner, J. C. Pizarro, K. M. Schmidt-Ott, D. W. Landry, K. N. Raymond, R. K. Strong, J. Barasch, *Nat. Chem. Biol.* **2010**, *6*, 602–609.
36. R. S. Ajioka, J. D. Phillips, J. P. Kushner, *Biochim. Biophys. Acta* **2006**, *1763*, 723–736.
37. R. Lill, B. Hoffmann, S. Molik, A. J. Pierik, N. Rietzschel, O. Stehling, M. A. Uzarska, H. Webert, C. Wilbrecht, U. Muhlenhoff, *Biochim. Biophys. Acta* **2012**, *1823*, 1491–1508.
38. D. R. Richardson, D. J. Lane, E. M. Becker, M. L. Huang, M. Whitnall, Y. Suryo Rahmanto, A. D. Sheftel, P. Ponka, *Proc. Natl. Acad. Sci. USA* **2010**, *107*, 10775–10782.
39. N. A. Wolff, A. J. Ghio, L. M. Garrick, M. D. Garrick, L. Zhao, R. A. Fenton, F. Thévenod, *FASEB J.* **2014**, *28*, 2134–2145.
40. G. C. Shaw, J. J. Cope, L. Li, K. Corson, C. Hersey, G. E. Ackermann, B. Gwynn, A. J. Lambert, R. A. Wingert, D. Traver, N. S. Trede, B. A. Barut, Y. Zhou, E. Minet, A. Donovan, A. Brownlie, R. Balzan, M. J. Weiss, L. L. Peters, J. Kaplan, L. I. Zon, B. H. Paw, *Nature* **2006**, *440*, 96–100.

41. S. B. Keel, R. T. Doty, Z. Yang, J. G. Quigley, J. Chen, S. Knoblaugh, P. D. Kingsley, I. De Domenico, M. B. Vaughn, J. Kaplan, J. Palis, J. L. Abkowitz, *Science* **2008**, *319*, 825–828.
42. D. Finazzi, P. Arosio, *Arch. Toxicol.* **2014**, *88*, 1787–1802.
43. S. Leidgens, K. Z. Bullough, H. Shi, F. Li, M. Shakoury-Elizeh, T. Yabe, P. Subramanian, E. Hsu, N. Natarajan, A. Nandal, T. L. Stemmler, C. C. Philpott, *J. Biol. Chem.* **2013**, *288*, 17791–17802.
44. L. C. Kuhn, *Metallomics* **2015**, *7*, 232–243.
45. S. J. Dixon, B. R. Stockwell, *Nat. Chem. Biol.* **2014**, *10*, 9–17.
46. S. V. Torti, F. M. Torti, *Nat. Rev. Cancer* **2013**, *13*, 342–355.
47. S. Okada, *Pathol. Int.* **1996**, *46*, 311–332.
48. E. D. Weinberg, *Eur. J. Cancer Prev.* **1996**, *5*, 19–36.
49. Y. Beguin, M. Aapro, H. Ludwig, L. Mizzen, A. Osterborg, *Crit. Rev. Oncol. Hematol.* **2014**, *89*, 1–15.
50. A. L. Fracanzani, D. Conte, M. Fraquelli, E. Taioli, M. Mattioli, A. Losco, S. Fargion, *Hepatology* **2001**, *33*, 647–651.
51. J. E. Maakaron, M. D. Cappellini, G. Graziadei, J. B. Ayache, A. T. Taher, *Ann. Hepatol.* **2013**, *12*, 142–146.
52. L. Malcovati, M. G. Porta, C. Pascutto, R. Invernizzi, M. Boni, E. Travaglino, F. Passamonti, L. Arcaini, M. Maffioli, P. Bernasconi, M. Lazzarino, M. Cazzola, *J. Clin. Oncol.* **2005**, *23*, 7594–7603.
53. D. N. Seril, J. Liao, K. L. Ho, A. Warsi, C. S. Yang, G. Y. Yang, *Dig. Dis. Sci.* **2002**, *47*, 1266–1278.
54. X. Huang, *Lancet Oncol.* **2008**, *9*, 803–807.
55. Y. Knobel, A. Weise, M. Glei, W. Sendt, U. Claussen, B. L. Pool-Zobel, *Food Chem. Toxicol.* **2007**, *45*, 804–811.
56. E. Park, M. Glei, Y. Knobel, B. L. Pool-Zobel, *Mutat. Res.* **2007**, *619*, 59–67.
57. D. J. Messner, K. V. Kowdley, *BMC Gastroenterol.* **2008**, *8*, 2.
58. A. A. Alkhateeb, B. Han, J. R. Connor, *Breast Cancer Res. Treat.* **2013**, *137*, 733–744.
59. I. Freitas, E. Boncompagni, R. Vaccarone, C. Fenoglio, S. Barni, G. F. Baronzio, *Anticancer Res.* **2007**, *27*, 3059–3065.
60. A. A. Alkhateeb, J. R. Connor, *Biochim. Biophys. Acta* **2013**, *1836*, 245–254.
61. L. M. Bystrom, S. Rivella, *Free Radic. Biol. Med.* **2015**, *79*, 337–342.
62. D. R. Richardson, D. S. Kalinowski, S. Lau, P. J. Jansson, D. B. Lovejoy, *Biochim. Biophys. Acta* **2009**, *1790*, 702–717.
63. M. J. Brookes, S. Hughes, F. E. Turner, G. Reynolds, N. Sharma, T. Ismail, G. Berx, A. T. McKie, N. Hotchin, G. J. Anderson, T. Iqbal, C. Tselepis, *Gut* **2006**, *55*, 1449–1460.
64. J. Boult, K. Roberts, M. J. Brookes, S. Hughes, J. P. Bury, S. S. Cross, G. J. Anderson, R. Spychal, T. Iqbal, C. Tselepis, *Clin. Cancer Res.* **2008**, *14*, 379–387.
65. Z. K. Pinnix, L. D. Miller, W. Wang, R. D'Agostino, Jr., T. Kute, M. C. Willingham, H. Hatcher, L. Tesfay, G. Sui, X. Di, S. V. Torti, F. M. Torti, *Sci. Transl. Med.* **2010**, *2*, 43ra56.
66. X. P. Jiang, R. L. Elliott, J. F. Head, *Anticancer Res.* **2010**, *30*, 759–765.
67. K. J. Wu, A. Polack, R. Dalla-Favera, *Science* **1999**, *283*, 676–679.
68. K. A. O'Donnell, D. Yu, K. I. Zeller, J. W. Kim, F. Racke, A. Thomas-Tikhonenko, C. V. Dang, *Mol. Cell Biol.* **2006**, *26*, 2373–2386.
69. F. Zhang, W. Wang, Y. Tsuji, S. V. Torti, F. M. Torti, *J. Biol. Chem.* **2008**, *283*, 33911–33918.
70. G. Weiss, *Biochim. Biophys. Acta* **2009**, *1790*, 682–693.
71. H. Clevers, *Cell* **2006**, *127*, 469–480.

72. M. J. Brookes, J. Boult, K. Roberts, B. T. Cooper, N. A. Hotchin, G. Matthews, T. Iqbal, C. Tselepis, *Oncogene* **2008**, *27*, 966–975.
73. S. Radulescu, M. J. Brookes, P. Salgueiro, R. A. Ridgway, E. McGhee, K. Anderson, S. J. Ford, D. H. Stones, T. H. Iqbal, C. Tselepis, O. J. Sansom, *Cell Rep.* **2012**, *2*, 270–282.
74. J. N. Ilsley, G. S. Belinsky, K. Guda, Q. Zhang, X. Huang, J. B. Blumberg, P. E. Milbury, L. J. Roberts, 2nd, R. G. Stevens, D. W. Rosenberg, *Nutr. Cancer* **2004**, *49*, 162–169.
75. H. W. Hann, M. W. Stahlhut, B. S. Blumberg, *Cancer Res.* **1988**, *48*, 4168–4170.
76. M. E. Habel, R. Lemieux, D. Jung, *J. Cell Physiol.* **2005**, *203*, 277–285.
77. S. Cunningham-Rundles, P. J. Giardina, R. W. Grady, C. Califano, P. McKenzie, M. De Sousa, *J. Infect. Dis.* **2000**, *182 Suppl. 1*, S115–121.
78. G. Weiss, *Eur. J. Clin. Invest.* **2002**, *32 Suppl. 1*, 70–78.
79. H. Oexle, A. Kaser, J. Most, R. Bellmann-Weiler, E. R. Werner, G. Werner-Felmayer, G. Weiss, *J. Leukoc. Biol.* **2003**, *74*, 287–294.
80. G. Regis, M. Bosticardo, L. Conti, S. De Angelis, D. Boselli, B. Tomaino, P. Bernabei, M. Giovarelli, F. Novelli, *Blood* **2005**, *105*, 3214–3221.
81. T. Ganz, E. Nemeth, *Nat. Rev. Immunol.* **2015**, *15*, 500–510.
82. C. Y. Wang, J. L. Babitt, *Curr. Opin. Hematol.* **2016**, *23*, 189–197.
83. G. Sebastiani, N. Wilkinson, K. Pantopoulos, *Front. Pharmacol.* **2016**, *7*, 160.
84. A. Pietrangelo, *Liver Int.* **2016**, *36 Suppl. 1*, 116–123.
85. K. E. Finberg, M. M. Heeney, D. R. Campagna, Y. Aydinok, H. A. Pearson, K. R. Hartman, M. M. Mayo, S. M. Samuel, J. J. Strouse, K. Markianos, N. C. Andrews, M. D. Fleming, *Nat. Genet.* **2008**, *40*, 569–571.
86. Z. I. Cabantchik, *Front. Pharmacol.* **2014**, *5*, 45.
87. A. Pietrangelo, *Semin. Liver Dis.* **1996**, *16*, 13–30.
88. U. Maegdefrau, S. Arndt, G. Kivorski, C. Hellerbrand, A. K. Bosserhoff, *Lab. Invest.* **2011**, *91*, 1615–1623.
89. K. Mleczko-Sanecka, F. Roche, A. R. da Silva, D. Call, F. D'Alessio, A. Ragab, P. E. Lapinski, R. Ummanni, U. Korf, C. Oakes, G. Damm, L. A. D'Alessandro, U. Klingmuller, P. D. King, M. Boutros, M. W. Hentze, M. U. Muckenthaler, *Blood* **2014**, *123*, 1574–1585.
90. J. M. Llovet, S. Ricci, V. Mazzaferro, P. Hilgard, E. Gane, J. F. Blanc, A. C. de Oliveira, A. Santoro, J. L. Raoul, A. Forner, M. Schwartz, C. Porta, S. Zeuzem, L. Bolondi, T. F. Greten, P. R. Galle, J. F. Seitz, I. Borbath, D. Haussinger, T. Giannaris, M. Shan, M. Moscovici, D. Voliotis, J. Bruix, S. I. S. Group, *New Engl. J. Med.* **2008**, *359*, 378–390.
91. D. H. Manz, N. L. Blanchette, B. T. Paul, F. M. Torti, S. V. Torti, *Ann. NY Acad. Sci.* **2016**, *1368*, 149–161.
92. L. Tesfay, K. A. Clausen, J. W. Kim, P. Hegde, X. Wang, L. D. Miller, Z. Deng, N. Blanchette, T. Arvedson, C. K. Miranti, J. L. Babitt, H. Y. Lin, D. M. Peehl, F. M. Torti, S. V. Torti, *Cancer Res.* **2015**, *75*, 2254–2263.
93. D. G. Ward, K. Roberts, M. J. Brookes, H. Joy, A. Martin, T. Ismail, R. Spychal, T. Iqbal, C. Tselepis, *World J. Gastroenterol.* **2008**, *14*, 1339–1345.
94. S. Zhang, Y. Chen, W. Guo, L. Yuan, D. Zhang, Y. Xu, E. Nemeth, T. Ganz, S. Liu, *Cell Signal* **2014**, *26*, 2539–2550.
95. W. Guo, S. Zhang, Y. Chen, D. Zhang, L. Yuan, H. Cong, S. Liu, *Acta Biochim. Biophys. Sin. (Shanghai)* **2015**, *47*, 703–715.
96. O. Weizer-Stern, K. Adamsky, O. Margalit, O. Ashur-Fabian, D. Givol, N. Amariglio, G. Rechavi, *Br. J. Haematol.* **2007**, *138*, 253–262.
97. D. R. Flower, *Biochem. J.* **1996**, *318*, 1–14.

98. L. Kjeldsen, A. H. Johnsen, H. Sengelov, N. Borregaard, *J. Biol. Chem.* **1993**, *268*, 10425–10432.
99. B. S. Nielsen, N. Borregaard, J. R. Bundgaard, S. Timshel, M. Sehested, L. Kjeldsen, *Gut* **1996**, *38*, 414–420.
100. D. H. Goetz, M. A. Holmes, N. Borregaard, M. E. Bluhm, K. N. Raymond, R. K. Strong, *Mol. Cell* **2002**, *10*, 1033–1043.
101. T. H. Flo, K. D. Smith, S. Sato, D. J. Rodriguez, M. A. Holmes, R. K. Strong, S. Akira, A. Aderem, *Nature* **2004**, *432*, 917–921.
102. R. J. Abergel, M. C. Clifton, J. C. Pizarro, J. A. Warner, D. K. Shuh, R. K. Strong, K. N. Raymond, *J. Am. Chem. Soc.* **2008**, *130*, 11524–11534.
103. K. M. Schmidt-Ott, K. Mori, J. Y. Li, A. Kalandadze, D. J. Cohen, P. Devarajan, J. Barasch, *J. Am. Soc. Nephrol.* **2007**, *18*, 407–413.
104. M. H. Roudkenar, R. Halabian, P. Bahmani, A. M. Roushandeh, Y. Kuwahara, M. Fukumoto, *Free Radic. Res.* **2011**, *45*, 810–819.
105. D. R. Richardson, *Cell* **2005**, *123*, 1175–1177.
106. L. R. Devireddy, C. Gazin, X. Zhu, M. R. Green, *Cell* **2005**, *123*, 1293–1305.
107. V. Hvidberg, C. Jacobsen, R. K. Strong, J. B. Cowland, S. K. Moestrup, N. Borregaard, *FEBS Lett.* **2005**, *579*, 773–777.
108. L. R. Devireddy, J. G. Teodoro, F. A. Richard, M. R. Green, *Science* **2001**, *293*, 829–834.
109. X. Xiao, B. S. Yeoh, P. Saha, R. A. Olvera, V. Singh, M. Vijay-Kumar, *Biometals* **2016**, *29*, 451–465.
110. D. Bolignano, V. Donato, A. Lacquaniti, M. R. Fazio, C. Bono, G. Coppolino, M. Buemi, *Cancer Lett.* **2010**, *288*, 10–16.
111. S. Candido, S. L. Abrams, L. S. Steelman, K. Lertpiriyapong, T. L. Fitzgerald, A. M. Martelli, L. Cocco, G. Montalto, M. Cervello, J. Polesel, M. Libra, J. A. McCubrey, *Biochim. Biophys. Acta* **2016**, *1863*, 438–448.
112. J. J. Rodvold, N. R. Mahadevan, M. Zanetti, *Cancer Lett.* **2012**, *316*, 132–138.
113. J. Hanai, T. Mammoto, P. Seth, K. Mori, S. A. Karumanchi, J. Barasch, V. P. Sukhatme, *J. Biol. Chem.* **2005**, *280*, 13641–13647.
114. S. Venkatesha, J. Hanai, P. Seth, S. A. Karumanchi, V. P. Sukhatme, *Mol. Cancer Res.* **2006**, *4*, 821–829.
115. R. Lim, N. Ahmed, N. Borregaard, C. Riley, R. Wafai, E. W. Thompson, M. A. Quinn, G. E. Rice, *Int. J. Cancer* **2007**, *120*, 2426–2434.
116. Z. Tong, A. B. Kunnumakkara, H. Wang, Y. Matsuo, P. Diagaradjane, K. B. Harikumar, V. Ramachandran, B. Sung, A. Chakraborty, R. S. Bresalier, C. Logsdon, B. B. Aggarwal, S. Krishnan, S. Guha, *Cancer Res.* **2008**, *68*, 6100–6108.
117. H. J. Lee, E. K. Lee, K. J. Lee, S. W. Hong, Y. Yoon, J. S. Kim, *Int. J. Cancer* **2006**, *118*, 2490–2497.
118. P. T. Reilly, W. L. Teo, M. J. Low, A. A. Amoyo-Brion, C. Dominguez-Brauer, A. J. Elia, T. Berger, G. Greicius, S. Pettersson, T. W. Mak, *Oncogene* **2013**, *32*, 1233–1239.
119. D. Z. de Back, E. B. Kostova, M. van Kraaij, T. K. van den Berg, R. van Bruggen, *Front. Physiol.* **2014**, *5*, 9.
120. R. D. Stout, C. Jiang, B. Matta, I. Tietzel, S. K. Watkins, J. Suttles, *J. Immunol.* **2005**, *175*, 342–349.
121. A. Mantovani, A. Sica, S. Sozzani, P. Allavena, A. Vecchi, M. Locati, *Trends Immunol.* **2004**, *25*, 677–686.
122. D. M. Mosser, J. P. Edwards, *Nat. Rev. Immunol.* **2008**, *8*, 958–969.
123. S. Gordon, F. O. Martinez, *Immunity* **2010**, *32*, 593–604.
124. M. Nairz, A. Schroll, T. Sonnweber, G. Weiss, *Cell Microbiol* **2010**, *12*, 1691–1702.
125. M. Jung, C. Mertens, B. Brune, *Immunobiology* **2015**, *220*, 295–304.

126. S. Recalcati, M. Locati, A. Marini, P. Santambrogio, F. Zaninotto, M. De Pizzol, L. Zammataro, D. Girelli, G. Cairo, *Eur. J. Immunol.* **2010**, *40*, 824–835.
127. F. Bellora, R. Castriconi, A. Dondero, A. Pessino, A. Nencioni, G. Liggieri, L. Moretta, A. Mantovani, A. Moretta, C. Bottino, *Eur. J. Immunol.* **2014**, *44*, 1814–1822.
128. S. Hallam, M. Escorcio-Correia, R. Soper, A. Schultheiss, T. Hagemann, *J. Pathol.* **2009**, *219*, 143–152.
129. H. LaRue, C. Ayari, A. Bergeron, Y. Fradet, *Nat. Rev. Urol.* **2013**, *10*, 537–545.
130. A. Engstrom, A. Erlandsson, D. Delbro, J. Wijkander, *Int. J. Oncol.* **2014**, *44*, 385–392.
131. E. Jang, S. Lee, J. H. Kim, J. H. Kim, J. W. Seo, W. H. Lee, K. Mori, K. Nakao, K. Suk, *FASEB J.* **2013**, *27*, 1176–1190.
132. L. Cheng, H. Xing, X. Mao, L. Li, X. Li, Q. Li, *Scand. J. Immunol.* **2015**, *81*, 31–38.
133. R. Oberoi, E. P. Bogalle, L. A. Matthes, H. Schuett, A. K. Koch, K. Grote, B. Schieffer, J. Schuett, M. Luchtefeld, *PLoS One* **2015**, *10*, e0137924.
134. H. J. Vogel, *Biochem. Cell Biol.* **2012**, *90*, 233–244.
135. P. P. Ward, M. Mendoza-Meneses, G. A. Cunningham, O. M. Conneely, *Mol. Cell Biol.* **2003**, *23*, 178–185.
136. Y. Takayama, R. Aoki, R. Uchida, A. Tajima, A. Aoki-Yoshida, *Biochem. Cell Biol.* **2017**, *95*, 57–63.
137. Y. A. Suzuki, K. Shin, B. Lonnerdal, *Biochemistry* **2001**, *40*, 15771–15779.
138. O. Levy, *J. Leukoc. Biol.* **2004**, *76*, 909–925.
139. D. Legrand, *Biochem. Cell Biol.* **2012**, *90*, 252–268.
140. Y. Zhang, C. F. Lima, L. R. Rodrigues, *Nutr. Rev.* **2014**, *72*, 763–773.
141. J. L. Gifford, H. N. Hunter, H. J. Vogel, *Cell Mol. Life Sci.* **2005**, *62*, 2588–2598.
142. J. A. Gibbons, R. K. Kanwar, J. R. Kanwar, *Front. Biosci. (Schol Ed)* **2011**, *3*, 1080–1088.
143. J. R. Kanwar, K. Roy, Y. Patel, S. F. Zhou, M. R. Singh, D. Singh, M. Nasir, R. Sehgal, A. Sehgal, R. S. Singh, S. Garg, R. K. Kanwar, *Molecules* **2015**, *20*, 9703–9731.
144. Q. Ye, Y. Zheng, S. Fan, Z. Qin, N. Li, A. Tang, F. Ai, X. Zhang, Y. Bian, W. Dang, J. Huang, M. Zhou, Y. Zhou, W. Xiong, Q. Yan, J. Ma, G. Li, *PLoS One* **2014**, *9*, e103298.
145. J. Zhang, T. Ling, H. Wu, K. Wang, *J. Oral Pathol. Med.* **2015**, *44*, 578–584.
146. V. F. Chekhun, I. V. Zalutskii, L. A. Naleskina, N. Y. Lukianova, T. M. Yalovenko, T. V. Borikun, S. O. Sobchenko, I. V. Semak, V. S. Lukashevich, *Exp. Oncol.* **2015**, *37*, 181–186.
147. L. A. Naleskina, N. Y. Lukianova, S. O. Sobchenko, D. M. Storchai, V. F. Chekhun, *Exp. Oncol.* **2016**, *38*, 181–186.
148. H. Tsuda, T. Kozu, G. Iinuma, Y. Ohashi, Y. Saito, D. Saito, T. Akasu, D. B. Alexander, M. Futakuchi, K. Fukamachi, J. Xu, T. Kakizoe, M. Iigo, *Biometals* **2010**, *23*, 399–409.
149. H. J. Vogel, D. J. Schibli, W. Jing, E. M. Lohmeier-Vogel, R. F. Epand, R. M. Epand, *Biochem. Cell Biol.* **2002**, *80*, 49–63.
150. V. A. Solarte, J. E. Rosas, Z. J. Rivera, M. L. Arango-Rodriguez, J. E. Garcia, J. P. Vernot, *Biomed. Res. Int.* **2015**, *2015*, 630179.
151. L. T. Eliassen, G. Berge, A. Leknessund, M. Wikman, I. Lindin, C. Lokke, F. Ponthan, J. I. Johnsen, B. Sveinbjornsson, P. Kogner, T. Flaegstad, O. Rekdal, *Int. J. Cancer* **2006**, *119*, 493–500.
152. H. Tsuda, K. Sekine, N. Takasuka, H. Toriyama-Baba, M. Iigo, *Biofactors* **2000**, *12*, 83–88.

153. K. V. Chandra Mohan, R. Kumaraguruparan, D. Prathiba, S. Nagini, *Nutrition* **2006**, *22*, 940–946.
154. Y. Ushida, K. Sekine, T. Kuhara, N. Takasuka, M. Iigo, M. Maeda, H. Tsuda, *Jpn. J. Cancer Res.* **1999**, *90*, 262–267.
155. X. Sun, R. Jiang, A. Przepiorski, S. Reddy, K. P. Palmano, G. W. Krissansen, *BMC Cancer* **2012**, *12*, 591.
156. Y. T. Tung, H. L. Chen, C. C. Yen, P. Y. Lee, H. C. Tsai, M. F. Lin, C. M. Chen, *J. Dairy Sci.* **2013**, *96*, 2095–2106.
157. Y. Zhang, A. Nicolau, C. F. Lima, L. R. Rodrigues, *Nutr. Cancer* **2014**, *66*, 1371–1385.
158. A. Arcella, M. A. Oliva, S. Staffieri, S. Aalberti, G. Grillea, M. Madonna, M. Bartolo, L. Pavone, F. Giangaspero, G. Cantore, A. Frati, *J. Neurosurg.* **2015**, *123*, 1026–1035.
159. J. S. Mader, A. Richardson, J. Salsman, D. Top, R. de Antueno, R. Duncan, D. W. Hoskin, *Exp. Cell Res.* **2007**, *313*, 2634–2650.
160. J. S. Mader, J. Salsman, D. M. Conrad, D. W. Hoskin, *Mol. Cancer Ther.* **2005**, *4*, 612–624.
161. C. S. Pereira, J. P. Guedes, M. Goncalves, L. Loureiro, L. Castro, H. Geros, L. R. Rodrigues, M. Corte-Real, *Oncotarget* **2016**, *7*, 62144–62158.
162. C. Luzi, F. Brisdelli, R. Iorio, A. Bozzi, V. Carnicelli, A. Di Giulio, A. R. Lizzi, *Cell Biochem. Funct.* **2017**, *35*, 33–41.
163. J. A. Gibbons, J. R. Kanwar, R. K. Kanwar, *BMC Cancer* **2015**, *15*, 425.
164. P. M. Parikh, A. Vaid, S. H. Advani, R. Digumarti, J. Madhavan, S. Nag, A. Bapna, J. S. Sekhon, S. Patil, P. M. Ismail, Y. Wang, A. Varadhachary, J. Zhu, R. Malik, *J. Clin. Oncol.* **2011**, *29*, 4129–4136.
165. R. Digumarti, Y. Wang, G. Raman, D. C. Doval, S. H. Advani, P. K. Julka, P. M. Parikh, S. Patil, S. Nag, J. Madhavan, A. Bapna, A. A. Ranade, A. Varadhachary, R. Malik, *J. Thorac. Oncol.* **2011**, *6*, 1098–1103.
166. T. Kozu, G. Iinuma, Y. Ohashi, Y. Saito, T. Akasu, D. Saito, D. B. Alexander, M. Iigo, T. Kakizoe, H. Tsuda, *Cancer Prev. Res. (Phila)* **2009**, *2*, 975–983.
167. H. Y. Chen, O. Mollstedt, M. H. Tsai, R. B. Kreider, *Curr. Med. Chem.* **2014**, *21*, 2424–2437.
168. R. Gozzelino, V. Jeney, M. P. Soares, *Annu. Rev. Pharmacol. Toxicol.* **2010**, *50*, 323–354.
169. J. Alam, J. L. Cook, *Am. J. Respir. Cell Mol. Biol.* **2007**, *36*, 166–174.
170. P. Bahmani, R. Halabian, M. Rouhbakhsh, A. M. Roushandeh, N. Masroori, M. Ebrahimi, A. Samadikuchaksaraei, M. A. Shokrgozar, M. H. Roudkenar, *Cell Stress Chaperones* **2010**, *15*, 395–403.
171. K. D. Poss, S. Tonegawa, *Proc. Natl. Acad. Sci. USA* **1997**, *94*, 10925–10930.
172. S. C. Lu, *Biochim. Biophys. Acta* **2013**, *1830*, 3143–3153.
173. R. Brigelius-Flohe, L. Flohe, *Antioxid. Redox Signal.* **2011**, *15*, 2335–2381.
174. J. Kapitulnik, M. D. Maines, *Trends Pharmacol. Sci.* **2009**, *30*, 129–137.
175. B. S. Zuckerbraun, B. Y. Chin, M. Bilban, J. C. d'Avila, J. Rao, T. R. Billiar, L. E. Otterbein, *FASEB J.* **2007**, *21*, 1099–1106.
176. G. Silva, A. Cunha, I. P. Gregoire, M. P. Seldon, M. P. Soares, *J. Immunol.* **2006**, *177*, 1894–1903.
177. X. Zhang, P. Shan, J. Alam, X. Y. Fu, P. J. Lee, *J. Biol. Chem.* **2005**, *280*, 8714–8721.
178. Y. L. Tang, Y. Tang, Y. C. Zhang, K. Qian, L. Shen, M. I. Phillips, *Hypertension* **2004**, *43*, 746–751.
179. D. Morse, S. E. Pischke, Z. Zhou, R. J. Davis, R. A. Flavell, T. Loop, S. L. Otterbein, L. E. Otterbein, A. M. Choi, *J. Biol. Chem.* **2003**, *278*, 36993–36998.
180. P. A. Dennery, *Antioxid. Redox Signal.* **2014**, *20*, 1743–1753.
181. A. Loboda, A. Jozkowicz, J. Dulak, *Vascul. Pharmacol.* **2015**, *74*, 11–22.
182. H. Was, J. Dulak, A. Jozkowicz, *Curr. Drug Targets* **2010**, *11*, 1551–1570.

183. A. Loboda, M. Damulewicz, E. Pyza, A. Jozkowicz, J. Dulak, *Cell Mol. Life Sci.* **2016**, *73*, 3221–3247.
184. H. Was, M. Sokolowska, A. Sierpniowska, P. Dominik, K. Skrzypek, B. Lackowska, A. Pratnicki, A. Grochot-Przeczek, H. Taha, J. Kotlinowski, M. Kozakowska, A. Mazan, W. Nowak, L. Muchova, L. Vitek, A. Ratajska, J. Dulak, A. Jozkowicz, *Free Radic. Biol. Med.* **2011**, *51*, 1717–1726.
185. G. Gueron, A. De Siervi, M. Ferrando, M. Salierno, P. De Luca, B. Elguero, R. Meiss, N. Navone, E. S. Vazquez, *Mol. Cancer Res.* **2009**, *7*, 1745–1755.
186. M. Ferrando, G. Gueron, B. Elguero, J. Giudice, A. Salles, F. C. Leskow, E. A. Jares-Erijman, L. Colombo, R. Meiss, N. Navone, A. De Siervi, E. Vazquez, *Angiogenesis* **2011**, *14*, 467–479.
187. J. Abdulghani, L. Gu, A. Dagvadorj, J. Lutz, B. Leiby, G. Bonuccelli, M. P. Lisanti, T. Zellweger, K. Alanen, T. Mirtti, T. Visakorpi, L. Bubendorf, M. T. Nevalainen, *Am. J. Pathol.* **2008**, *172*, 1717–1728.
188. J. M. Blando, S. Carbajal, E. Abel, L. Beltran, C. Conti, S. Fischer, J. DiGiovanni, *Neoplasia* **2011**, *13*, 254–265.
189. B. Elguero, G. Gueron, J. Giudice, M. A. Toscani, P. De Luca, F. Zalazar, F. Coluccio-Leskow, R. Meiss, N. Navone, A. De Siervi, E. Vazquez, *Neoplasia* **2012**, *14*, 1043–1056.
190. G. Gueron, J. Giudice, P. Valacco, A. Paez, B. Elguero, M. Toscani, F. Jaworski, F. C. Leskow, J. Cotignola, M. Marti, M. Binaghi, N. Navone, E. Vazquez, *Oncotarget* **2014**, *5*, 4087–4102.
191. K. Skrzypek, M. Tertil, S. Golda, M. Ciesla, K. Weglarczyk, G. Collet, A. Guichard, M. Kozakowska, J. Boczkowski, H. Was, T. Gil, J. Kuzdzal, L. Muchova, L. Vitek, A. Loboda, A. Jozkowicz, C. Kieda, J. Dulak, *Antioxid. Redox Signal.* **2013**, *19*, 644–660.
192. C. W. Lin, S. C. Shen, W. C. Hou, L. Y. Yang, Y. C. Chen, *Mol. Cancer Ther.* **2008**, *7*, 1195–1206.
193. B. Wegiel, D. Gallo, E. Csizmadia, C. Harris, J. Belcher, G. M. Vercellotti, N. Penacho, P. Seth, V. Sukhatme, A. Ahmed, P. P. Pandolfi, L. Helczynski, A. Bjartell, J. L. Persson, L. E. Otterbein, *Cancer Res.* **2013**, *73*, 7009–7021.
194. L. Vitek, H. Gbelcova, L. Muchova, K. Vanova, J. Zelenka, R. Konickova, J. Suk, M. Zadinova, Z. Knejzlik, S. Ahmad, T. Fujisawa, A. Ahmed, T. Ruml, *Dig. Liver Dis.* **2014**, *46*, 369–375.
195. S. J. Dixon, K. M. Lemberg, M. R. Lamprecht, R. Skouta, E. M. Zaitsev, C. E. Gleason, D. N. Patel, A. J. Bauer, A. M. Cantley, W. S. Yang, B. Morrison, 3rd, B. R. Stockwell, *Cell* **2012**, *149*, 1060–1072.
196. Y. Xie, W. Hou, X. Song, Y. Yu, J. Huang, X. Sun, R. Kang, D. Tang, *Cell Death Differ.* **2016**, *23*, 369–379.
197. W. S. Yang, K. J. Kim, M. M. Gaschler, M. Patel, M. S. Shchepinov, B. R. Stockwell, *Proc. Natl. Acad. Sci. USA* **2016**, *113*, E4966–4975.
198. J. Y. Cao, S. J. Dixon, *Cell. Mol. Life Sci.* **2016**, *73*, 2195–2209.
199. J. P. Friedmann Angeli, M. Schneider, B. Proneth, Y. Y. Tyurina, V. A. Tyurin, V. J. Hammond, N. Herbach, M. Aichler, A. Walch, E. Eggenhofer, D. Basavarajappa, O. Radmark, S. Kobayashi, T. Seibt, H. Beck, F. Neff, I. Esposito, R. Wanke, H. Forster, O. Yefremova, M. Heinrichmeyer, G. W. Bornkamm, E. K. Geissler, S. B. Thomas, B. R. Stockwell, V. B. O'Donnell, V. E. Kagan, J. A. Schick, M. Conrad, *Nat. Cell Biol.* **2014**, *16*, 1180–1191.
200. W. S. Yang, R. SriRamaratnam, M. E. Welsch, K. Shimada, R. Skouta, V. S. Viswanathan, J. H. Cheah, P. A. Clemons, A. F. Shamji, C. B. Clish, L. M. Brown, A. W. Girotti, V. W. Cornish, S. L. Schreiber, B. R. Stockwell, *Cell* **2014**, *156*, 317–331.

201. X. Sun, Z. Ou, M. Xie, R. Kang, Y. Fan, X. Niu, H. Wang, L. Cao, D. Tang, *Oncogene* **2015**, *34*, 5617–5625.
202. X. Sun, Z. Ou, R. Chen, X. Niu, D. Chen, R. Kang, D. Tang, *Hepatology* **2016**, *63*, 173–184.
203. L. Jiang, N. Kon, T. Li, S. J. Wang, T. Su, H. Hibshoosh, R. Baer, W. Gu, *Nature* **2015**, *520*, 57–62.
204. M. Y. Kwon, E. Park, S. J. Lee, S. W. Chung, *Oncotarget* **2015**, *6*, 24393–24403.
205. N. Yagoda, M. von Rechenberg, E. Zaganjor, A. J. Bauer, W. S. Yang, D. J. Fridman, A. J. Wolpaw, I. Smukste, J. M. Peltier, J. J. Boniface, R. Smith, S. L. Lessnick, S. Sahasrabudhe, B. R. Stockwell, *Nature* **2007**, *447*, 864–868.
206. H. Yamaguchi, J. L. Hsu, C. T. Chen, Y. N. Wang, M. C. Hsu, S. S. Chang, Y. Du, H. W. Ko, R. Herbst, M. C. Hung, *Clin. Cancer Res.* **2013**, *19*, 845–854.
207. L. Chen, X. Li, L. Liu, B. Yu, Y. Xue, Y. Liu, *Oncol. Rep.* **2015**, *33*, 1465–1474.
208. Y. Yu, Y. Xie, L. Cao, L. Yang, M. Yang, M. T. Lotze, H. J. Zeh, R. Kang, D. Tang, *Mol. Cell Oncol.* **2015**, *2*, e1054549.
209. P. Arosio, R. Ingrassia, P. Cavadini, *Biochim. Biophys. Acta* **2009**, *1790*, 589–599.
210. Y. Tsuji, E. Kwak, T. Saika, S. V. Torti, F. M. Torti, *J. Biol. Chem.* **1993**, *268*, 7270–7275.
211. O. Kakhlon, Y. Gruenbaum, Z. I. Cabantchik, *Biochem. Soc. Trans.* **2002**, *30*, 777–780.
212. O. Kakhlon, Y. Gruenbaum, Z. I. Cabantchik, *Biochem. J.* **2002**, *363*, 431–436.
213. Y. Funauchi, C. Tanikawa, P. H. Yi Lo, J. Mori, Y. Daigo, A. Takano, Y. Miyagi, A. Okawa, Y. Nakamura, K. Matsuda, *Sci. Rep.* **2015**, *5*, 16497.
214. S. I. Shpyleva, V. P. Tryndyak, O. Kovalchuk, A. Starlard-Davenport, V. F. Chekhun, F. A. Beland, I. P. Pogribny, *Breast Cancer Res. Treat.* **2011**, *126*, 63–71.
215. X. Liu, A. B. Madhankumar, B. Slagle-Webb, J. M. Sheehan, N. Surguladze, J. R. Connor, *Cancer Res.* **2011**, *71*, 2240–2249.
216. V. D. Paul, R. Lill, *Biochim. Biophys. Acta* **2015**, *1853*, 1528–1539.
217. N. Maio, T. A. Rouault, *Biochim. Biophys. Acta* **2015**, *1853*, 1493–1512.
218. R. Lill, *Nature* **2009**, *460*, 831–838.
219. L. K. Beilschmidt, H. M. Puccio, *Biochimie* **2014**, *100*, 48–60.
220. A. Sheftel, O. Stehling, R. Lill, *Trends Endocrinol. Metab.* **2010**, *21*, 302–314.
221. M. Yang, T. Soga, P. J. Pollard, *J. Clin. Invest.* **2013**, *123*, 3652–3658.
222. N. Saxena, N. Maio, D. R. Crooks, C. J. Ricketts, Y. Yang, M. H. Wei, T. W. Fan, A. N. Lane, C. Sourbier, A. Singh, J. K. Killian, P. S. Meltzer, C. D. Vocke, T. A. Rouault, W. M. Linehan, *J. Natl. Cancer Inst.* **2016**, *108* (1): djv287. doi: 10.1093/jnci/djv287.
223. J. O. Fuss, C. L. Tsai, J. P. Ishida, J. A. Tainer, *Biochim. Biophys. Acta* **2015**, *1853*, 1253–1271.
224. M. K. Brinkmeyer, S. S. David, *DNA Repair (Amst)* **2015**, *34*, 39–51.
225. F. Mazzei, A. Viel, M. Bignami, *Mutat. Res.* **2013**, *743–744*, 33–43.
226. J. J. DiGiovanna, K. H. Kraemer, *J. Invest. Dermatol.* **2012**, *132*, 785–796.
227. T. Rafnar, D. F. Gudbjartsson, P. Sulem, A. Jonasdottir, A. Sigurdsson, A. Jonasdottir, S. Besenbacher, P. Lundin, S. N. Stacey, J. Gudmundsson, O. T. Magnusson, L. le Roux, G. Orlygsdottir, H. T. Helgadottir, H. Johannsdottir, A. Gylfason, L. Tryggvadottir, J. G. Jonasson, A. de Juan, E. Ortega, J. M. Ramon-Cajal, M. D. Garcia-Prats, C. Mayordomo, A. Panadero, F. Rivera, K. K. Aben, A. M. van Altena, L. F. Massuger, M. Aavikko, P. M. Kujala, S. Staff, L. A. Aaltonen, K. Olafsdottir, J. Bjornsson, A. Kong, A. Salvarsdottir, H. Saemundsson, K. Olafsson, K. R. Benediktsdottir, J. Gulcher, G. Masson, L. A. Kiemeney, J. I. Mayordomo, U. Thorsteinsdottir, K. Stefansson, *Nat. Genet.* **2011**, *43*, 1104–1107.
228. B. J. Ballew, M. Yeager, K. Jacobs, N. Giri, J. Boland, L. Burdett, B. P. Alter, S. A. Savage, *Hum. Genet.* **2013**, *132*, 473–480.

229. P. van der Lelij, K. H. Chrzanowska, B. C. Godthelp, M. A. Rooimans, A. B. Oostra, M. Stumm, M. Z. Zdzienicka, H. Joenje, J. P. de Winter, *Am. J. Hum. Genet.* **2010**, *86*, 262–266.
230. D. P. Kane, P. V. Shcherbakova, *Cancer Res.* **2014**, *74*, 1895–1901.
231. N. Cancer Genome Atlas, *Nature* **2012**, *487*, 330–337.
232. D. N. Church, S. E. Briggs, C. Palles, E. Domingo, S. J. Kearsey, J. M. Grimes, M. Gorman, L. Martin, K. M. Howarth, S. V. Hodgson, N. Collaborators, K. Kaur, J. Taylor, I. P. Tomlinson, *Hum. Mol. Genet.* **2013**, *22*, 2820–2828.
233. N. Cancer Genome Atlas Research, C. Kandoth, N. Schultz, A. D. Cherniack, R. Akbani, Y. Liu, H. Shen, A. G. Robertson, I. Pashtan, R. Shen, C. C. Benz, C. Yau, P. W. Laird, L. Ding, W. Zhang, G. B. Mills, R. Kucherlapati, E. R. Mardis, D. A. Levine, *Nature* **2013**, *497*, 67–73.
234. J. M. Caron, J. M. Caron, *PLoS One* **2015**, *10*, e0141565.

16

Copper Complexes in Cancer Therapy

Delphine Denoyer, [1] ***Sharnel A. S. Clatworthy,*** [1] ***and Michael A. Cater*** [1,2,3]

[1]Centre for Cellular and Molecular Biology, School of Life and Environmental Sciences, Deakin University, Burwood, Victoria, Australia

[2]Department of Pathology, The University of Melbourne, Parkville, Victoria, Australia

[3]Rural Clinical School, The University of New South Wales, Port Macquarie, New South Wales, Australia

<m.cater@unsw.edu.au> or <mcater@unimelb.edu.au>

ABSTRACT 470
1. INTRODUCTION 470
2. REPURPOSING OLD COPPER COMPLEXES FOR CANCER TREATMENT 477
   2.1. Tetrathiomolybdate 477
      2.1.1. Biological Activity 477
      2.1.2. Clinical Trials for Cancer Treatment 480
   2.2. Clioquinol 482
      2.2.1. Mechanism of Anticancer Activity 482
      2.2.2. Therapeutic Applications for Cancer 484
   2.3. Disulfiram 485
      2.3.1. From Anti-Alcoholism Drug to Anticancer Agent 485
      2.3.2. Clinical Efficacy in Cancer Patients 487
3. EMERGING CLASSES OF COPPER COMPLEXES FOR CANCER TREATMENT 489
   3.1. Elesclomol 489
      3.1.1. Anticancer Properties 489
      3.1.2. Clinical Use for Cancer Treatment 490
   3.2. Copper Complexes of Thiosemicarbazones 491
      3.2.1. Bis(thiosemicarbazones) 491
      3.2.2. Other Thiosemicarbazones 494
4. GENERAL CONLUSIONS 496

Metal Ions in Life Sciences, Volume 18 Edited by Astrid Sigel, Helmut Sigel, Eva Freisinger, and Roland K. O. Sigel

https://doi.org/10.1515/9783110470734-016

ACKNOWLEDGMENTS 497
ABBREVIATIONS 497
REFERENCES 498

Abstract: Copper homeostasis is tightly regulated in both prokaryotic and eukaryotic cells to ensure sufficient amounts for cuproprotein biosynthesis, while limiting oxidative stress production and toxicity. Over the last century, copper complexes have been developed as antimicrobials and for treating diseases involving copper dyshomeostasis (e.g., Wilson's disease). There now exists a repertoire of copper complexes that can regulate bodily copper through a myriad of mechanisms. Furthermore, many copper complexes are now being appraised for a variety of therapeutic indications (e.g., Alzheimer's disease and amyotrophic lateral sclerosis) that require a range of copper-related pharmacological affects. Cancer therapy is also drawing considerable attention since copper has been recognized as a limiting factor for multiple aspects of cancer progression including growth, angiogenesis, and metastasis. Consequently, 'old copper complexes' (e.g., tetrathiomolybdate and clioquinol) have been repurposed for cancer therapy and have demonstrated anticancer activity *in vitro* and in preclinical models. Likewise, new tailor-made copper complexes have been designed based on structural and biological features ideal for their anticancer activity. Human clinical trials continue to evaluate the therapeutic efficacy of copper complexes as anticancer agents and considerable progress has been made in understanding their pharmacological requirements. In this chapter, we present a historical perspective on the main copper complexes that are currently being repurposed for cancer therapy and detail several of the more recently developed compounds that have emerged as promising anticancer agents. We further provide an overview of the known mechanisms of action, including molecular targets and we discuss associated clinical trials.

Keywords: cancer · chelator · clioquinol · copper · disulfiram · elesclomol · ionophore · tetrathiomolybdate · thiosemicarbazones

1. INTRODUCTION

Copper is an essential micronutrient required for fundamental biological processes in all organisms. Copper is a redox-active metal and has the ability to donate and accept electrons to shift between reduced (Cu^{+}) and oxidized (Cu^{2+}) states. This property allows copper to play an important biological role in oxidation-reduction (redox) reactions, by acting as a catalytic cofactor for the function of numerous critical enzymes. Additionally, copper is also required as a structural (allosteric) component for many important enzymes [1]. In humans, examples of prominent enzymes that require copper for their function include Cu/Zn superoxide dismutase (SOD) (free radical detoxification), cytochrome *c* oxidase (electron-transport enzyme involved in cellular respiration), ceruloplasmin (iron homeostasis by converting ferrous iron (Fe^{2+}) to ferric iron (Fe^{3+})), lysyl oxidase (LOX) (connective tissue synthesis), and tyrosinase (melanin synthesis) [1–4]. Nevertheless, ionic (free) copper can generate highly reactive oxygen species (ROS) due to being redox active and can cause damage to lipids, proteins, nucleic acids, and other biomolecules [1].

An excess of intracellular copper can become cytotoxic and therefore cells possess regulatory mechanisms to maintain copper homeostasis, including specific transporters for copper uptake, distribution, and efflux (e.g., CTR1 and

ATP7A/B) and small molecules for detoxification (e.g., glutathione and metallothioneins) [5]. The importance of copper homeostasis in humans is illustrated by the devastating consequences of two genetic disorders, Menkes and Wilson's (WD) diseases, which cause systemic copper deficiency or overload, respectively [6]. Classical Menkes disease is an X-linked recessive disorder and fatal to infant boys. Copper deficiency in Menkes disease causes a myriad of symptoms, including a failure to thrive, hypotonia, kinky hair (pili torti), deterioration of the nervous system, and severe intellectual disability [6]. WD is an autosomal recessive disorder characterized by profound accumulation of copper in the liver and several other organs (e.g., brain, kidney) with resulting toxicity (e.g., liver cirrhosis) [6]. For comprehensive information on mammalian copper homeostasis and associated diseases the reader is referred to the following reviews [5, 7, 8].

Recent evidence has established a strong connection between copper and both the development and progression of cancer. Preclinical studies have demonstrated that administering copper ($CuSO_4$) by oral gavage, or by supplying copper in drinking water, significantly enhanced cancer growth in rodent models of mammary tumor, pancreatic islet cell carcinoma, and $BRAF^{V600E}$-driven lung cancer [9–11]. Likewise, severe copper deficiency induced through a low copper diet diminished the immune system in mice and as a result cancer burden increased dramatically [12, 13]. Further studies have placed copper as a central modulator of normal and malignant angiogenesis, due to its ability to regulate many angiogenic responses. The formation of new blood vessels is essential to supply oxygen and nutrients to tumors larger than 1–2 millimeters [14]. The pro-angiogenic role of copper is mediated through various pathways including, but not limited to, improving growth and mobility of vascular endothelial cells [15–17], regulating the synthesis and secretion of pro-angiogenic mediators (e.g., fibroblast growth factors (FGFs), interleukin-1alpha (IL-1α), and vascular endothelial growth factor (VEGF)) and through binding directly to angiogenin (angiogenic growth factor) to enhance its activity [18–21]. Copper may also influence the capacity of cancer cells to invade surrounding tissues and to spread to distant organs (metastasis). For instance, the activities of both lysyl oxydase (LOX) and LOX-like proteins, which contribute to remodeling of the extracellular matrix and to establishing a pre-metastatic niche, are dependent on copper [2, 22]. More recently, the copper-dependent protein, Memo, was identified as a pro-metastatic mediator in breast cancer and served as a reliable prognostic marker for early distant metastases [23]. We recently reviewed in detail the importance of copper in cancer development and progression [5]. Recognizing that copper serves as a limiting factor for many facets of tumor progression has driven the development of copper complexes as therapeutics and many attractive anticancer strategies that target copper have emerged [5, 24–27].

Anticancer copper complexes can be classified into two main groups; copper chelators and copper ionophores. Copper chelators sequester copper ions from cells within the body and therefore aim to limit cancer progression by interfering with growth and malignant processes [24, 25]. Conversely, copper ionophores transport copper into cells increasing intracellular levels and exerting cytotoxic effects through a myriad of pathways [27, 28]. Many copper ionophores release

coordinated copper under the reductive intracellular environment, allowing copper to become bioavailable (exchangeable) and such compounds are usually more efficient at killing cancer cells [27, 29]. Many copper complexes have been used in the clinic for decades to treat other unrelated conditions (e.g., clioquinol and disulfiram for diarrhea and alcoholism, respectively), but since discovering their antiproliferative activities many have been repurposed as anticancer therapies. Concomitantly, structure-activity relationship studies have been performed on known copper complexes, allowing the development of new tailor-made analogues specific for cancer treatment (reviewed in [5, 26, 30]). Some of these analogues have enhanced anticancer activity, reduced toxicity toward normal cells/tissues, and more favorable pharmacokinetics in preclinical and/or clinical studies. We present below a historical perspective on the main copper complexes being repurposed (tetrathiomolybdate, clioquinol, and disulfiram) for cancer treatment and then discuss several of the newly developed compounds (elesclomol and thiosemicarbazones) that show promise as anticancer agents. The structures of these copper complexes are shown in Figure 1 and a summary of past and current human clinical trials evaluating their anticancer efficacy is tabulated (Table 1).

Figure 1. Chemical structures of (**A**) Tetrathiomolybdate (TM) and ATN-224 (bis-choline salt of tetrathiomolybdate); (**B**) Clioquinol (5-chloro-7-iodo-quinolin-8-ol); (**C**) Disulfiram (tetraethylthiuram disulfide) and its reduced form (DDTC; diethyldithiocarbamate); (**D**) Elesclomol [N-malonyl-bis(N-methyl-N-thiobenzoyl hydrazide)] and its neutral Cu(II)-elesclomol complex; (**E**) 1,2-Bis(thiosemicarbazones) and their neutral copper(II) complexes; (**F**) 3-AP (triapine); (**G**) Di-2-pyridylketone thiosemicarbazones (DpT series).

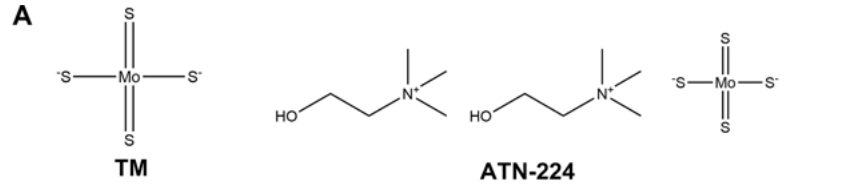

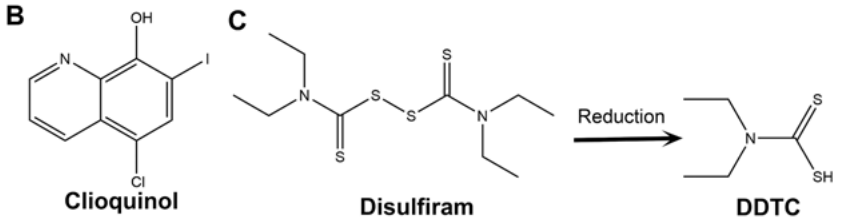

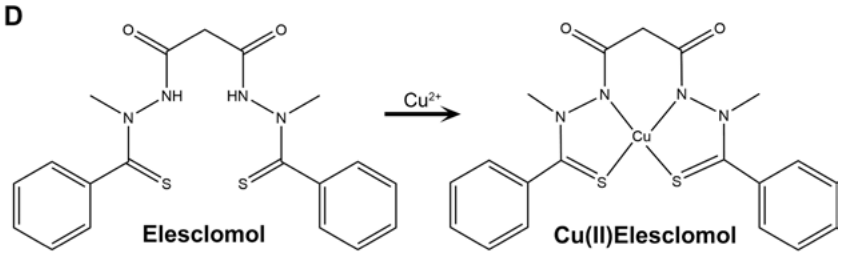

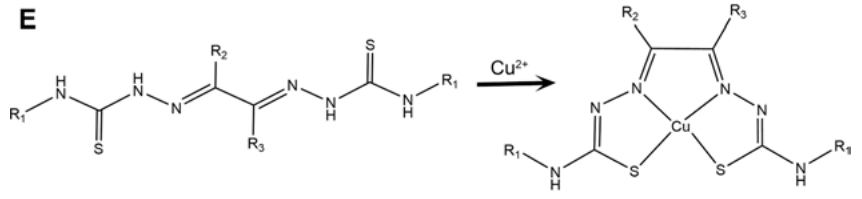

H_2kts and Cu(II)(kts) $R_1 = H$ $R_2 = H$ $R_3 = CH(CH_3)OC_2H_5$
H_2gtsm and Cu(II)(gtsm) $R_1 = CH_3$ $R_2 = H$ $R_3 = H$
H_2atsm and Cu(II)(atsm) $R_1 = CH_3$ $R_2 = CH_3$ $R_3 = CH_3$

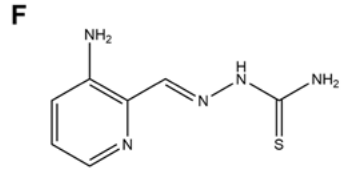

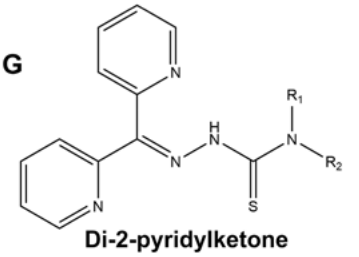

Dp44mT $R_1 = CH_3$ $R_2 = CH_3$
DpC $R_1 = CH_3$ R_2 = cyclohexyl

Table 1. Summary of clinical trials assessing the potential of copper complexes as anticancer treatments.

Compounds and treatments	Type(s) of cancer	Clinical trials	Results	Refs.
TM 90 to 120 mg/day Oral administration	Breast, colon, lung, pancreas and prostate cancers, melanoma, angiosarcoma, chondrosarcoma, hemangioendothelioma and nasopharyngeal and renal tumors	Phase I 18 patients	Only patients with minimal disease responded to TM therapy	[75]
TM 40 mg three times a day with meals and 60 mg at bedtime Oral administration	Advanced kidney cancer	Phase II 13 patients	31 % of patients achieved stable disease for >6 months (not significant when compared to no treatment)	[76]
TM	Asymptomatic hormone refractory prostate cancer	Phase II 16 patients	TM did not delay disease progression	[77]
ATN-224 30 mg/day or 300 mg/day within minutes after breakfast Oral administration	Biochemically recurrent hormone-naïve prostate cancer	Phase II n = 23 for dose-level 300 mg and n = 24 for 30 mg	Weak biological activity in low-dose ATN-224	[78]
TM as an adjuvant therapy 180 mg/day (40 mg with meals three times a day + 60 mg at bedtime) starting 4–6 weeks after surgery Oral administration	Malignant pleural mesothelioma	Phase II 30 high recurrence risk-patients	Time to progression doubled in stage I and II TM-treated patients	[80]
TM as an adjuvant therapy 180 mg/day (40 mg with meals three times a day + 60 mg at bedtime) given for 2 years as adjuvant treatment starting 4–6 weeks after chemoradiation followed by surgery Oral administration	Resectable oesophageal cancer	Phase II 69 high recurrence risk-patients	TM increased the 3-year recurrence-free survival and the 3-year overall survival	[81]

TM as an adjuvant therapy Induction: 180 mg/day Maintenance: 100 mg/day Oral administration	Stage II to IV breast cancer at high risk of relapse	Phase II 75 high recurrence risk patients	The relapse-free survival was 85 % at 10 months and 81 % at 5.6 years	[79][a]
180 mg/day TM (40 mg with meals three times a day + 60 mg at bedtime) + chemotherapy (IFL) Oral administration	Metastatic colorectal cancers	Phase I 24 patients	TM was well tolerated and had an anti-angiogenic effect. Study not powered to define treatment efficacy	[82]
TM + chemotherapy (carboplatin/pemetrexed)	Metastatic non-small cell lung cancer	Phase I Recruiting patients	Ongoing trial	NCT01837329[b]
Clioquinol Increasing doses twice daily Oral administration	Advanced hematologic malignancies	Phase I 11 patients	MTD: 1200 mg twice daily No clinical responses were observed	[115]
Surgery followed by chemotherapy ± DDTC 10 mg/kg once weekly for 9 months	Non-metastatic breast cancers but with high-risk of relapse	Phase II 64 patients	Overall survival at 6 years: 55 % in the placebo group vs 81 % in the DDTC-treated group Disease free survival: 55 % vs 76 % in the DDTC-group	[142]
DSF 250 mg twice a day for 3 months Oral administration	Metastatic melanoma	Phase I/II	The study has been completed but results are still unknown	NCT00256230[b]
DSF (250 mg once daily) + copper gluconate (2 to 6 mg daily)	Refractory malignancies (pancreatic, breast, colon, prostate and lung cancers and cutaneous and ocular melanoma)	Phase I 28 patients	DSF + copper gluconate at 6 mg/day was well tolerated No clinical responses by radiography	[225]
DSF (40 mg three times daily) + chemotherapy (cisplatin and vinorelbine)	Metastatic non-small cell lung cancer	Phase II 40 patients	DSF increased overall survival period DSF did not produce additional toxicity	[143]

Compounds and treatments	Type(s) of cancer	Clinical trials	Results	Refs.
DSF/copper combination + radiochemotherapy	Newly diagnosed glioblastoma multiform	Phase II	Ongoing trial	NCT01777919[b]
DSF 250 mg or 500 mg daily	Non-metastatic recurrent prostate cancer	Phase I	DSF was poorly tolerated No clinical benefits	[147]
Elesclomol (213 mg/m^2) + aclitaxel (80 mg/m^2) 1-hour intravenous infusion weekly	Stage IV metastatic melanoma	Phase II 81 patients	Elesclomol + paclitaxel increased progression-free survival compared to paclitaxel alone	[165]
Elesclomol (213 mg/m^2) + paclitaxel (80mg/m^2) administered weekly for 3 weeks of a 4-week cycle Intravenous administration	Metastatic melanoma	Phase III 651 chemo-naïve patients	Overall survival significantly lower in the elesclomol/ paclitaxel arm Serum LDH levels identified as a predictive biomarker of response to elesclomol	[166]
Triapine	Various cancer types	> 20 Phase I and II studies	Limited anti-tumor efficacy High toxicity	[207, 208]
DpC Dose-finding and pharmacokinetic study Oral administration	Advanced solid tumors	Phase I	Ongoing trial	NCT02688101[b]

TM = tetrathiomolybdate; DDTC = diethyldithiocarbamate; DSF = tetraethylthiuram disulfide (disulfiram); triapine = 3-aminopyridine-2-carboxaldehyde thiosemicarbazone; DpC = di-2-pyridylketone 4-cyclohexyl-4-methyl-3-thiosemicarbazone.

[a] http://meetinglibrary.asco.org/content/151971-156

[b] Clinical trial identifiers are from http://clinicaltrials.gov

2. REPURPOSING OLD COPPER COMPLEXES FOR CANCER TREATMENT

2.1. Tetrathiomolybdate

2.1.1. Biological Activity

Tetrathiomolybdate (TM, [MoS_4^{2-}]) is a highly specific copper chelator that was initially developed for the management of WD [31]. The discovery of TM occurred in the 1940's with the realization that excess dietary molybdate (MoO_4^{2-}) in ruminants induced copper deficiency; which resulted in a potentially fatal disorder called 'teart' pasture syndrome [32, 33]. Molybdate itself has negligible affinity for copper and it was later determined that the copper deficiency induced in ruminants was due to formation of TM, through the conversion of molybdates by sulfur present in their rumens [34, 35]. After discovering the copper-chelating property of TM, it was subsequently used effectively to treat copper poisoning in sheep, a common agricultural issue [36].

Although TM was initially being developed for the treatment of WD, it was superseded by two other copper chelators, trientine and penicillamine, which today remain first-line treatment options. However, trientine and penicillamine both cause dangerous side effects in a subset of WD patients who display severe (or acute) neurological manifestations [37–39]. Therefore, TM is currently being redeveloped for the treatment of these particular WD patients and has been shown in several clinical trials to be comparatively more effective and safer for copper clearance (reviewed in [39]). TM reacts with copper ions (Cu^+ and Cu^{2+}) and forms insoluble copper-molybdenum-sulfur clusters that are readily excreted from the body [39–41]. When administered with food, TM forms a tripartite complex with dietary copper and proteins, thereby preventing copper absorption by the gastrointestinal tract [42]. When administered alone, TM is absorbed into the bloodstream where it forms a non-toxic tripartite complex with albumin and blood copper [42]. Since the turn of the century, TM has also gained attention as a therapeutic inhibitor of angiogenesis for cancer therapy. Angiogenesis is controlled by the shifting balance between stimulating factors (e.g., angiogenin, vascular endothelial growth factor (VEGF), transforming growth factor β and basic fibroblast growth factor (bFGF)), regulatory cytokines (interleukin (IL)-1, 6, and 8) and inhibitors (e.g., angiostatin and endostatin) (reviewed in [43]).

Decades ago (1972), Folkman postulated that tumors larger than ~2 mm in diameter require their own blood supply in order to receive sufficient oxygen and nutrients to sustain growth [14]. Over the subsequent years, appreciation for the importance of malignant angiogenesis in cancer progression and a better understanding of its mediators, led to the development of angiogenic inhibitors for cancer therapy [14, 44]. One limitation however, is that these inhibitors often target a single angiogenic mediator leading to the occurrence of drug resistance. Given the importance of copper in many pro-angiogenic pathways, copper chelation may provide broad-spectrum inhibition of angiogenesis and hence, prove

better at impeding tumor growth longer term. The effectiveness of using copper chelation to block angiogenesis has been evaluated by many groups [16, 45–53]. Brewer and colleagues have amassed an immense body of work assessing the efficacy of TM in various mouse models of cancer [17, 54–58]. For example, TM treatment significantly impeded tumor growth by prohibiting angiogenesis in mouse models of subcutaneous squamous cell carcinoma, breast, prostate, lung, and head and neck cancers [17, 54–59]. More recently (2013), Ishida and colleagues demonstrated that TM delayed the onset of the angiogenic switch and reduced tumor growth in a transgenic mouse model that recapitulates the different steps of pancreatic neuroendocrine tumorigenesis [10]. Together, these studies demonstrated the promising cytostatic potential of TM and warrant further development.

The mechanism of action of TM as an anticancer agent has been attributed to its effects on numerous intra- and extracellular processes. In Figure 2, we show several of the better defined pathways targeted by TM. For instance, TM has been shown to inhibit the expression of the nuclear factor kappa B (NF-κB) transcription factor in breast cancer mouse models, resulting in decreased expression of five pro-angiogenic factors and cytokines (VEGF, bFGF, IL-1, IL-6, and IL-8) [17, 60]. Another prominent mode of action whereby TM blocks angiogenesis is through inhibition of SOD1, a cuproenzyme that catalyzes the conversion of superoxide to hydrogen peroxide. A reduction in SOD1 activity has been shown to induce vascular abnormalities (increased vasoconstriction and endothelial dysfunction) and impair angiogenesis [61]. SOD1 overexpression in mouse fibroblasts (NIH3T3) enhanced the generation of H_2O_2 [62] and markedly stimulated VEGF production, while SOD1 transgenic mice (overexpressed SOD1) had enhanced FGF-induced angiogenesis and tumor development [63]. TM and its second-generation analogue, ANT-224 (developed by Attenuon LLC), reduced SOD1 activity in mouse vascular endothelial cells and in an array of tumor cell lines [49, 64]. ATN-224 is the bis-choline salt of tetrathiomolybdate (instead of ammonium salt) and was developed to enhance compound stability, circumventing issues previously associated with TM administration to patients (e.g., poor stability in the body) [65]. Additionally, crystallographic and spectroscopic studies have revealed that TM forms extremely stable sulfur-bridged copper-molybdenum clusters with the copper chaperone ATOX1 [66]. These formed clusters suppressed copper incorporation into secreted cuproenzymes, including those involved in angiogenesis and metastasis, such as extracellular SOD and LOX, thereby inhibiting their activities [66]. TM can also reduce the expression of the ATP7A copper transporter, which is responsible for the delivery of copper to numerous intracellular and secreted cuproenzymes [66]. Conceivably, the ability of TM to interfere with copper transporters would have profound effects not only on angiogenesis, but also on cellular metabolism and proliferation, as many cuproproteins are involved in these processes. For example, TM has been demonstrated to reduce mitochondrial respiration by inhibiting the activity of copper-dependent cytochrome *c* oxidase, which increased oxygen availability, downregulated hypoxia-inducible factor 1α (HIF)-1α, and inhibited angiogenesis in models of ovarian, endometrial, and pancreatic cancers [10, 68]. Collectively,

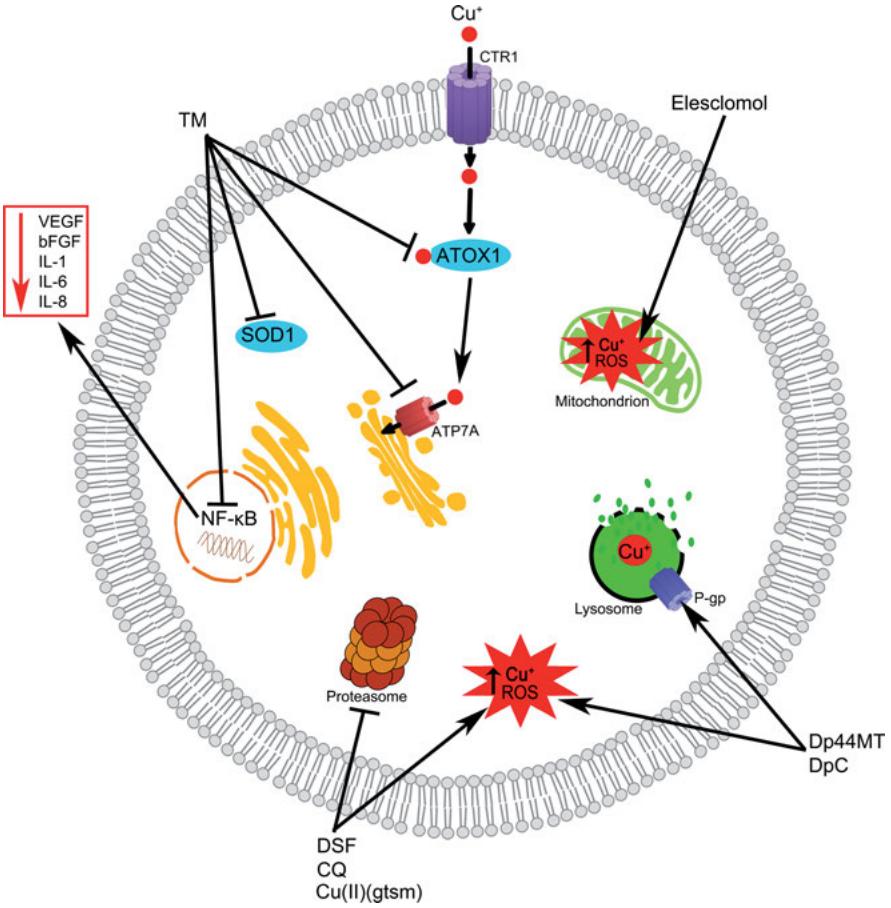

Figure 2. Summary of the main intracellular targets of the copper complexes.
(1) Tetrathiomolybdate (TM**)** is a strong copper chelator that inhibits angiogenesis by inhibiting the nuclear factor kappa B (NF-κB) transcription factor, resulting in decreased expression of five pro-angiogenic factors and cytokines (VEGF, bFGF, IL-1, IL-6, and IL-8). TM also impairs angiogenesis by inhibiting superoxide dismutase [Cu-Zn] (SOD1) activity, a regulator of vasoconstriction and endothelial function. TM can also target and suppress the copper chaperone ATOX1 and the copper-transporter ATP7A, which are responsible for the delivery of copper to intracellular and secreted cuproenzymes (e.g., LOX). **(2)** Cliquinol, disulfiram (DSF), and Cu(II)(gtsm) act as copper ionophores and increase intracellular bioavailable copper levels. All three copper ionophores cause intracellular ROS production and inhibit proteasomal activity in cancer cells, leading to apoptosis. DSF has also been shown to impede angiogenesis by inhibiting SOD1 activity (not shown). **(3)** Elesclomol is an ionophore that specifically increases copper levels in the mitochondria. At this site, copper dissociates from elesclomol causing ROS production disrupting the electron transport chain. **(4)** Dp44MT and DpC are copper ionophores that cause intracellular ROS production. Both copper ionophores also target the lysosome where membrane P-glycoprotein (P-gp) mediates their influx and sequestration. Dp44MT and DpC ultimately become trapped in lysosomes causing ROS production that damages membrane integrity.

these important studies shed light on potential mechanisms by which TM and its analogues suppress angiogenesis and therefore act as cytostatic agents.

There is also evidence that TM can help exert cytotoxic activity in addition to inhibition of angiogenesis. As previously mentioned, treating cells with TM can inhibit NF-κB expression [17] and high NF-κB expression has been implicated in resistance to apoptosis. Several studies have shown that suppressing NF-κB production with TM can restore cancer cell sensitivity to apoptosis, particularly when induced by chemotherapies [57, 69, 70]. TM has been shown to sensitize breast carcinoma cells (SUM149), human endometrial cancer cells (ECC-1, AN3CA, and KLE), and ovarian cancer cells (SKOV-3 and A2780) to chemotherapies including doxorubicin, fenretinide, 5-fluorouracil, and mitomycin C [57, 69, 70]. TM has also been shown to induce apoptosis in leukemic cells through inhibition of SOD1 [49]. Furthermore, cellular uptake of platinum-based chemotherapies (e.g., cisplatin) is mediated by the copper transporter CTR1 and low levels of this protein have been associated with poor clinical response in bladder [71, 72], non-small cell lung [73], and human ovarian cancers [74]. Given that both copper and platinum-based chemotherapies compete for the same transporter, lowering copper with TM can enhance chemotherapy uptake in cervical, ovarian, and breast cancer cells and sensitize them to apoptosis [66, 74]. Preclinical assessment of the TM/cisplatin combination in a transgenic mouse model of cervical carcinoma demonstrated increased cisplatin-DNA adduct levels, reduced angiogenesis, and improved therapeutic efficacy [74]. Importantly, the TM/cisplatin combination did not increase toxicity toward normal tissues. These findings provided a strong premise for conducting human clinical trials to evaluate the combination of TM and platinum-based chemotherapies for cancer treatment, as detailed in the next section.

2.1.2. Clinical Trials for Cancer Treatment

Promising preclinical studies prompted the investigation of TM in the clinic, both as a single agent and in combination with standard therapies. The first Phase I study evaluated TM as an anti-angiogenic agent and involved 18 patients with 11 different types of metastatic cancer (breast, colon, lung, pancreas, prostate, melanoma, angiosarcoma, chondrosarcoma, hemangioendothelioma, nasopharyngeal, and renal) [75]. These patients were orally administered TM at doses ranging from 90 to 120 mg/day. Counting 14 patients that were categorized as reaching a copper-depleted state (20 % serum ceruloplasmin activity), 5 individuals achieved stable disease for at least 3 months, 1 individual had progressive disease, but no one achieved disease regression [75]. It was concluded that patients with early metastatic or minimal disease responded to TM therapy, whereas patients with advanced metastases or bulky lesions were unresponsive [75].

Subsequently, TM was evaluated in a small-scale Phase II clinical trial on patients with advanced kidney cancer [76]. In this study, 13 patients were orally administered TM thrice daily at 40 mg and again once before bedtime at 60 mg [76]. While copper levels were depleted in all patients within 5 weeks of treatment, only 4 patients (31 %) achieved stable disease for >6 months, a result

that was not significantly different from observations without treatment [76]. Disappointing results were likewise obtained in Phase II clinical trials in patients with prostate cancer (recurrent hormone-naïve) treated with either TM or ATN-224 [77, 78]. In these trials, patients categorized as reaching a copper-depleted state (20 % serum ceruloplasmin activity) displayed unimpeded disease progression and with a clear lack of clinical activity the investigators discontinued the development of both TM and ATN-224 for prostate cancer therapy [77, 78]. In fact, despite providing confirmation that TM is relatively well tolerated, most clinical trials investigating the therapeutic efficacy of TM as a single anticancer agent have yielded disappointing results. What has become apparent is that treatment timing is paramount in achieving any clinical benefit with TM. Patients enrolled in many of the aforementioned trials had advanced cancer, whereas the most promising preclinical data were obtained in mouse models of small tumors, or of micro-metastases, before the angiogenic switch [10, 68].

Promising clinical results have been achieved using TM as an adjuvant therapy in highly recurrent cancer types, where no sign of metastases were seen at the time of surgery [79–81]. For example, malignant pleural mesothelioma progresses in 90–95 % of patients following surgical intervention. In a Phase II study involving 30 patients with malignant pleural mesothelioma, TM as an adjuvant therapy significantly improved the time to progression after surgery [80]. The time to progression doubled in stage I and II TM-treated patients compared to non-TM-treated patients (20 months versus 10 months, respectively), but a negligible difference was observed for patients with more advanced disease (stage III) [80]. In another Phase II trial involving 69 high recurrence risk patients with resectable esophageal cancer, TM was given for 2 years as adjuvant treatment after both surgery and chemoradiation [81]. The 3-year recurrence-free survival was 44 % (versus 32 % for non-TM-treated patients) and the 3-year overall survival was 45 % (versus 34 % for non-TM-treated patients), indicating that adjuvant TM treatment may be beneficial to esophageal cancer patients [81].

TM therapy also seems to keep stage II to IV breast cancer at high risk of relapse in check as reported in a Phase II clinical study from the Weill Cornell Medical College, New York [79]. In patients with no visible residual disease at the time of TM treatment, the relapse-free survival was 85 % at 10 months [79]. In a presentation at the 2015 American Society of Clinical Oncology (ASCO) annual meeting, the authors further reported that after a median follow-up period of 5.6 years, the progression-free survival rate for the 75 participants from the beginning of TM treatment was a staggering 81 % (http://meetinglibrary.asco.org/content/151971-156). Mechanistically, TM inhibited the formation of bone marrow-derived endothelial progenitor cells, which are recruited at the tumor site to mediate the angiogenic switch required for the progression of micro- to macro-metastases, thereby suppressed angiogenesis, promoted tumor dormancy, and ultimately prevented recurrence [79].

As mentioned above, TM or ATN-224 as single agents did not provide a survival benefit in patients with advanced solid tumors (breast, colon, lung, pancreas, kidney, and prostate cancers) [75–78]. However, there is compelling evidence that TM can sensitize cancer cells to certain chemotherapies [57, 69, 70, 74],

prompting clinical evaluation [82, 83]. The standard first-line therapy for metastatic colorectal cancer is a combination of irinotecan/5-fluorouracil/leucovorin (IFL). Investigators of a Phase I clinical study combining IFL and TM demonstrated patient tolerance, that the addition of TM did not compromise overall response rates, and that TM had an anti-angiogenic effect resulting from reduction of pro-angiogenic mediators including VEGF, bFGF, IL-6, and IL-8 [82]. This pilot trial involved 24 patients, but unfortunately did not define treatment efficacy [82]. A further small pilot study where 5 patients with ovarian cancer (platinum-resistant advanced epithelial cancer cells) were treated with carboplatin together with trientine, provided evidence that lowering bodily copper has the potential to overcome platinum resistance [83]. These patients were additionally treated with oral trientine (4 times daily with 500 mg) and 1 patient achieved remission, while 3 had stable disease. Platinum resistance also limits treatment options for metastatic non-small cell lung cancer and therefore combining TM with carboplatin/pemetrexed is currently being trialed.

2.2. Clioquinol

2.2.1. Mechanism of Anticancer Activity

Clioquinol (5-chloro-7-iodo-quinolin-8-ol) was initially synthesized as an antimicrobial agent and was used to treat a range of diseases such as shigellosis, diarrhea, and intestinal amebiasis [84–87]. The drug was used abundantly in the 1950s to 1970s, most commonly as a treatment for traveller's diarrhea, even though the mechanism by which clioquinol reduced symptoms was poorly understood [88]. However, prescribing clioquinol to treat gastrointestinal disorders was halted when over 10,000 patients manifesting with neurotoxic side effects were reported in Japan. Clioquinol induced subacute myelo-optic neuropathy (SMON) in these patients, causing the oral drug to be withdrawn from multiple countries' markets in 1980 [89]. Despite the potential risk, several countries continue to sell clioquinol as a topical treatment against fungal infections and to treat inflammatory skin disorders. Nonetheless, it should be noted that the cause/effect relationship of clioquinol and SMON was not established since several discrepancies between data collected at the time arose [90, 91]. Firstly, clioquinol was prescribed abundantly in Japan for 20 years before the SMON epidemic, with no adverse effects reported. In addition, many individuals diagnosed with SMON had not taken clioquinol in the 6 months prior to the onset of SMON symptoms. Finally, the effect of the drug was not seen in countries outside of Japan [91]. It has been postulated that the formation of a toxic byproduct during the production of clioquinol may have caused the neurotoxic effects [92].

Another report linked the combination of clioquinol and high exposure to metals from the environment as a potential cause of SMON symptoms [93]. In agreement with this idea, clioquinol can coordinate copper with high affinity and therefore the symptoms of SMON could have arisen from copper aberrations [93]. Interestingly, the discovery that clioquinol coordinates copper stimulated

research into its potential usefulness to dissociate amyloid plaques associated with Alzheimer's disease [94–96]. In a mouse model of Alzheimer's disease, clioquinol prevented the formation of amyloid plaques in the brain by redistributing copper away from amyloid and into neighboring neurons [94]. Note that copper is a known pathological cause of amyloid aggregation in Alzheimer's disease [94]. Clioquinol also displayed clinical benefit in some patients treated with increasing doses of the drug, given orally, over a 10-months period [96]. Importantly, two small trials in Sweden and in Australia conducted on 20 and 36 patients, respectively, showed no sign of toxicity in any of the Alzheimer's disease patients treated with clioquinol [95, 96].

The first study to evaluate the potential use of clioquinol as an anticancer therapeutic was conducted by Ding and colleagues in 2005, on the basis that clioquinol was a metal chelator [97]. These authors hypothesized that chelating copper and zinc with clioquinol would inactivate SOD1, which had previously emerged as a potential target for cancer therapy. Clioquinol induced apoptosis in eight different cancer cell lines and significantly impeded the growth of ovarian cancer xenografts (A2780 cells) in mice, but only weakly inactivated SOD1. It was subsequently shown that clioquinol is an ionophore rather than a chelator and its anticancer properties are contingent on its ability to transport metals into cancerous cells [97–100]. Copper is coordinated in a 1 : 2 ratio with clioquinol [101, 102].

Clioquinol was further shown to induce cytotoxicity in prostate cancer cells (LNCaP, C4–2B, DU145) both *in vitro* and *in vivo* [98, 103]. Daily treatment with clioquinol (10 mg/kg for 15 days) significantly impeded the growth of human prostate cancer xenografts (C4–2B cells) in mice [103]. In this study, clioquinol was used alone without additional copper, as the authors had previously identified that xenografts grown in various mouse models already possessed high levels of copper [104]. We, and others, have shown that copper ionophores that release their coordinated copper under the reductive intracellular environment (e.g., clioquinol, disulfiram, and Cu(II)(gtsm)) induce cancer cell apoptosis by inhibiting proteasomal chymotrypsin-like activity [28, 103, 105, 106]. Chen and colleagues identified that clioquinol specifically inhibits the 20S proteolytic core of the proteasome, subsequently increasing the amount of ubiquitinated proteins and the apoptosis regulator Bax [103]. Copper can directly regulate the stability and aggregation of ubiquitin [107] and likely ionophoric copper somehow occludes the proteasome by interfering with the ubiquitination process. Copper chelators (e.g., TM) and copper ionophores that retain their coordinated copper intracellularly (e.g., Cu(II)(atsm)), do not inhibit the proteasome [108].

Clioquinol has been shown to induce apoptosis in numerous types of cancers (e.g., prostate and breast cancers, leukemia and myeloma) by inhibiting the proteasome, in a process that is entirely copper-dependent [98, 108–110]. We have also shown in human prostate cancer cell lines that clioquinol significantly reduced the cytosolic amount of the X-linked inhibitor of apoptosis protein, perturbing its anti-apoptotic function [98]. Du and colleagues further demonstrated that clioquinol can also exacerbate the anticancer activity of macrophages, promoting their secretion of interleukins and cytokines, including tumor necrosis

factor α [111]. Clioquinol greatly potentiated the cytotoxicity of macrophages (RAW 264.7 cells) toward HeLa cells [111]. Most importantly, clioquinol can seemingly selectively target cancer cells without harming normal cells [108]. We have shown that clioquinol selectively killed prostate hyperplastic (BPH-1) and carcinoma (PC3, DU145, LNCaP) cells, whilst having a negligible effect on the viability of primary prostate epithelial cells [98]. Likewise, clioquinol is selectively toxic towards breast cancer cells (MDA-MB-231) and acute myeloid leukemia blasts when compared to their respective normal counterpart cells [108, 109]. By all accounts, there is a large therapeutic window between normal and cancerous cells when intracellular copper is forcibly increased (ionophoric copper), which is the premise for the development of copper ionophores as anticancer therapies.

2.2.2. Therapeutic Applications for Cancer

The potential use of clioquinol for the treatment of Alzheimer's disease motivated pharmacokinetic and metabolism studies (reviewed in [90]). In humans, the plasma concentration of clioquinol was dose-related and the half-life of the drug ranged from 11 to 14 hours [90, 112]. In addition, clioquinol is less metabolized to inactive conjugates in humans when compared to other species, such as mice, rats, rabbits or hamsters [113, 114]. Because clioquinol was thought to be associated with the development of SMON syndrome, toxicity studies were conducted across species [90, 112]. Neurotoxic symptoms appeared after the administration of high doses of clioquinol and were species-specific in occurrence. Species where there were higher concentrations of free serum clioquinol (dogs, monkeys, and humans) showed signs of neurotoxicity at lower doses than species that metabolized clioquinol (mice, rats, rabbits, and hamsters) more readily. Furthermore, the neurological side effects vary among human individuals, possibly due to differences in genetic background or drug metabolism [90, 112].

Despite the well-characterized anticancer activity of clioquinol across multiple preclinical studies [106], only one human clinical trial in cancer patients has been completed. The tolerance, and to a limited extent the efficacy, of oral clioquinol treatment on 11 patients with advanced hematologic malignancies was investigated in a Phase I trial [115]. The maximum tolerated dose was established at 1200 mg twice daily. Further analysis revealed that a slight and transient inhibition of the proteasome was detected in leukemic cells from only 2 patients, but no clinical response was observed [115]. These disappointing patient results were despite clioquinol reaching the serum concentration range (13–25 μmol) that was previously shown to inhibit proteasomal activity in leukemia and myeloma preclinical models [109]. The failure of clioquinol to elicit clinical activity was attributed to poor cellular uptake and did not apparently relate to administered dose [115]. However, one patient who had significantly higher serum clioquinol levels developed adverse side effects, including neuropathy. Since this clinical study, interest in clioquinol as an anticancer agent has somewhat waned, as further developmental and pharmacokinetic studies are required. Prana Biotechnology Ltd has generated clioquinol analogues with superior therapeutic properties for treating Alzheimer's disease and Huntington's diseases (e.g., PBT2). Most importantly,

these analogues show better pharmacokinetics, more readily cross the blood-brain barrier, and are well tolerated in human Alzheimer's disease and Huntington's disease patients (http://pranabio.com/). However, there has been no indication by the company that these analogues will be developed for cancer therapy.

2.3. Disulfiram

2.3.1. From Anti-Alcoholism Drug to Anticancer Agent

Disulfiram (tetraethylthiuram disulfide; DSF) was discovered by a Berlin chemist, M. Grodzki, in 1881 [116]. However, it was not until the 1920's that the compound was introduced into the rubber industry to accelerate the vulcanization of rubber [117]. In 1937, a physician in the American rubber industry reported that workers in the rubber plant noticed a link between working with DSF and adverse symptoms when ingesting alcohol [118]. Years later (1948), scientists from a pharmaceutical company in Copenhagen (Medicinalco) were self-dosing with DSF, testing for side effects and likewise reacted violently to alcohol consumption. In all cases, symptoms included nausea, headaches, vomiting, hypotension, and heart palpitations; essentially a terrible hangover. A clinician with experience in treating alcoholics, O. Martensen-Larsen, then initiated studies investigating the physiological actions of DSF, and subsequently its clinical efficacy as a drug treating alcoholism [119]. The final version of the compound was recrystallized with carbon tetrachloride and was marketed as an anti-alcoholism drug, trademarked 'Antabuse'. Antabuse was prescribed from 1949 in Denmark and Sweden and from 1951 in the United States, to help people quit drinking alcohol in conjunction with psychotherapy.

Ethanol is normally oxidized by the liver enzyme alcohol dehydrogenase to produce acetaldehyde and then acetaldehyde is quickly converted to harmless acetic acid by aldehyde dehydrogenase (ALDH). Subsequent studies have shown that DSF (Antabuse) competes with acetaldehyde for ALDH, leading to the accumulation of toxic acetaldehyde and consequently the symptoms of a hangover [120]. Characterization of DSF metabolism *in vivo* has demonstrated that upon administration, DSF is rapidly reduced to diethyldithiocarbamate (DDTC) and further methylated and oxidized to form methyl diethylthiocarbamoyl-sulfoxide (MeDTC-SO). It is believed that MeDTC-SO acts as the final inhibitor of ALDH, by chemically modifying cysteines in the active site of the enzyme [120]. MeDTC-SO directly inhibiting yeast and human ALDH has been demonstrated [121–124].

DSF gained attention as an anticancer compound in 1977, when a patients' case report, published by E. F. Lewison, presented staggering results about DSF being inadvertently used to treat a woman with advanced metastatic breast cancer [125]. Upon developing alcoholism, this patient with multiple breast cancer metastases (spine, ribs, and pelvis) halted anticancer therapies (radiation, hormone, and chemotherapy) and started DSF treatment. Over the following 10 years of taking DSF, a gradual yet complete resolution of all bone lesions was

observed. More recently, a female patient with stage IV ocular melanoma and liver metastases showed significantly reduced tumor volume during 53 continuous months of daily DSF treatment [126]. Note that in this case, zinc gluconate was also administered thrice daily (not concurrent with DSF), which is routinely used to prevent intestinal copper absorption in WD patients. Subsequently, there have been numerous *in vitro* and *in vivo* studies evaluating the therapeutic efficacy of DSF against multiple cancer types [105, 127, 128]. DSF has been shown to have two main pharmacological anticancer activities; it induces apoptosis through proteasomal inhibition and ROS production and can impede angiogenesis through multiple pathways. In human breast cancer cells (MDA-MB-231) DSF inhibited the chymotrypsin-like activity of purified 20S and 26S proteasomes, and subsequently induced apoptosis [105].

Similarly, mice bearing human breast cancer xenografts (MDA-MB-231 cells) and treated with DSF (50 mg/kg for 29 days) had significantly reduced tumor growth (74 %) attributed to decreased proteasomal activity and the accumulation of ubiquitinated proteins and apoptotic markers (e.g., Bax) [105]. Several other studies have also demonstrated that DSF inhibits the proteasome [28, 105, 129, 130]. A high-throughput screen of a chemical library including 2,000 compounds identified DSF as a therapeutic agent to inhibit proliferation and chymotrypsin-like proteasomal activity in glioma stem cells [129]. DSF and its metabolite DDTC, also inhibited chymotrypsin-like proteasomal activity and induced apoptosis in pancreatic cancer cells [130]. In all of the above cases, the ability of DSF to inhibit the proteasome, and thus to induce apoptosis, was shown to be entirely copper-dependent and could be exacerbated by adding exogenous copper. Note that copper coordination likely causes the reduction of DSF to produce two DDTC molecules, bridged together by a copper atom through the sulfur sites. However, the extent to which this occurs in medium, or indeed *in vivo*, has not been clearly demonstrated. For simplicity sake, we refer to the copper complex as being DSF.

We, and others, have shown that DSF acts as a copper ionophore and markedly increases intracellular copper levels [28, 131–133]. For example, DSF co-administered with copper increased intracellular copper levels 30-fold in inflammatory breast cancer cells (SUM149 and rSUM149) [131]. DSF alone can coordinate available milieu copper (e.g., medium copper) and increases intracellular copper concentrations more modestly [28, 132, 133]. We further demonstrated that copper can dissociate from DSF intracellularly and become bioavailable (exchangeable) [28]. Furthermore, copper ionophores with this biological property inhibited proteasomal activity [28] and generated considerable levels of intracellular ROS in cancer cells [133]. The ability of DSF to induce intracellular ROS has been shown in multiple cancer cell lines (e.g., melanoma, glioblastoma) and can be abrogated by co-treatment with antioxidants (e.g., N-acetyl-cysteine) or with strong copper chelation (e.g., TM) [128, 133–136]. Interestingly, abrogating ROS often averts the ability of DSF to induce cancer cell apoptosis, implying that ROS production may precede proteasomal inhibition. However, whether ROS and proteasomal inhibition are connected has not been investigated for any copper ionophore.

Another important anticancer activity of DSF is the ability to inhibit angiogenesis. DSF has been shown to perturb the formation of new blood vessels and significantly reduced tumor growth (≥ 60 %) in several angiogenesis-dependent xenograft mouse models (C6 glioma and Lewis lung carcinoma) [63]. The anti-angiogenic activity was attributed to the inhibition of SOD1 and a consequent increase in intracellular ROS in endothelial cells. These authors also demonstrated that copper enhanced the anti-angiogenic effects of DSF both *in vitro* and *in vivo* [63]. The ability of the DSF copper complex to inhibit angiogenesis by decreasing VEGF expression, and to concurrently reduce tumor growth, was further shown in a human glioblastoma xenograft mouse model (U87 cells) [137]. Additionally, DSF has been shown to down-regulate matrix metalloproteinases (MMP-9 and MMP-2) in human cancers (osteosarcoma, cervical and renal carcinomas) and endothelial cell lines (CL1–5, NTUB1, and HUVEC) [138, 139]. MMPs are responsible for extracellular matrix remodeling, which is required for endothelial cells to migrate and form new blood vessels. Together, these studies demonstrate that the combination of DSF and copper can inhibit angiogenesis, and therefore tumor growth and metastases, by interfering with critical regulatory components (e.g., SOD1, ROS, VEGF, and MMPs).

Several studies have also indicated that DSF may be suitable as an adjunct treatment to enhance the efficacy of certain conventional chemotherapies. The same property of DSF that makes it useful as an anti-alcoholism drug, its ability to block ALDH activity, may also have implications in the cancer treatment setting. ALDH is highly expressed in cancer stem cells, in particular in glioblastoma, breast and colon cancers and its activity is linked to enhanced tumorigenicity and resistance to chemotherapy *in vivo* [131]. Moreover, DSF can inhibit the activity of P-glycoprotein (P-gp), which can actively pump cytotoxic drugs out of cells. P-gp plays a major role in intrinsic and acquired multidrug resistance during chemotherapy [140]. DSF can directly target P-gp, preventing the protein from reaching maturation and thus can help to prevent drug resistance [141]. Human clinical trials evaluating the therapeutic efficacy of DSF as a direct and adjunct anticancer agent are discussed below.

2.3.2. Clinical Efficacy in Cancer Patients

Human clinical trials evaluating the efficacy of DSF as an anticancer agent were initiated given the promising preclinical and human patient case studies [125] and due to DSF being well tolerated by patients treated for alcoholism [119]. In 1993, DSF treatment was assessed in 64 patients at high-risk of relapse with non-metastatic breast cancer, in a placebo-controlled Phase II trial [142]. These patients initially underwent surgical resection, followed by fluorouracil, adriamycin, and cytoxan chemotherapy either with or without DDTC (10 mg/kg once weekly for 9 months), the active metabolite of DSF. The overall survival at 6 years was 81 % in the DDTC group versus 55 % for those treated with chemotherapy alone, indicating outcome improvement [142]. Additionally, a long-term Phase I/II trial (initiated in 2002) to evaluate DSF for the treatment of metastatic melanoma was recently completed, but the results are not available.

DSF had also been shown to potentiate certain chemotherapies in preclinical cancer models and accordingly is being trialed in combination therapies. A Phase II trial on 40 patients with metastatic non-small cell lung cancer assessed DSF administration (40 mg three times daily) in combination with standard chemotherapies with cisplatin and vinorelbine (2 cycles). Patients who additionally received DSF had a slight but significant increase in survival, when compared to patients taking the chemotherapies alone (10.0 versus 7.1 months) [143]. Furthermore, DSF did not produce additional side effects in these patients [143]. A further Phase II trial is about to commence to assess the DSF copper complex as an adjunct and concurrent chemotherapy in the treatment of patients with newly diagnosed glioblastoma multiforme (GBM). Analogous to many other cancer types, GBM shows a sub-population of ALDH overexpressing cancer stem cells, which constitute a source of recurrence [144]. ALDH overexpression has been shown to confer resistance for GBM to the first-line chemotherapy drug temozolomide and is further a reliable predictive marker for poor clinical outcome [145]. As previously discussed, DSF is a strong inhibitor of ALDH and according to the investigators' hypothesis, may make GBM more susceptible to temozolomide treatment and possibly reduce recurrence. Copper will be included with DSF in this trial to possibly enhance its cytotoxic effects through proteasome inhibition.

DSF was also identified in a screen for prostate cancer therapeutics and was subsequently evaluated in clinical trials on patients with non-metastatic recurrent prostate cancer [146, 147]. The investigators selected DSF on the basis that it inhibited DNA methyltransferases (DNMTs) in prostate cancer cell lines *in vitro*. DNMTs regulate the methylation of cytosines in gene promotor regions, which can lead to tumor suppressor gene silencing and promote cancer progression [147]. Several demethylating agents, including DNMT inhibitors (azacitidine and decitabine) are currently approved for treating myelodysplatic syndrome. Nevertheless, DSF failed to demonstrate clinical activity in the prostate cancer patients and appeared to weakly inhibit DNMT1 *in vivo*. Furthermore, DSF was toxic in these patients causing neuropathy (grade 3), diarrhea (grade 2), and fatigue (grade 2) and the investigators advised that DSF should not be further developed for this indication [147]. It should be noted that a high dose of apo-DSF was administered to these patients (500 mg daily) and that its pharmacokinetics in relation to copper was not evaluated.

The limited success of DSF in most clinical trials may relate to the drug's metabolism in the body. Once entering the blood, DSF is metabolized to produce DDTC and then further to diethyldithiomethylcarbamate and glucuronic acid [148, 149]. As mentioned previously, the DDTC copper complex is believed to be the active form and due to its turnover may be in insufficient concentrations to induce cancer cell death *in vivo*. There is now research effort into increasing the half-life of DSF in blood, by using either nanoparticles or liposomes to encapsulate for better delivery to cancer cells [150–152].

3. EMERGING CLASSES OF COPPER COMPLEXES FOR CANCER TREATMENT

3.1. Elesclomol

3.1.1. Anticancer Properties

In the early 1980s, the cell biologist Lan Bo Chen at Harvard Medical School gathered from around the world hundreds of thousands of chemical compounds that had not previously been evaluated as anticancer agents and conducted a mass drug screening on prostate cancer cells [153]. One compound obtained from the National Taras Shevchenko University of Kiev (Ukraine) stood out; elesclomol (N-malonyl-bis(N-methyl-N-thiobenzoyl hydrazide), STA-4783). It was the only compound that was active against cancer cells at concentrations in the nanomolar range, while seemingly not affecting normal cells. Investigations into the mechanism of action by which elesclomol induces cancer cell death revealed that copper played a central role [154–156]. In fact, the anticancer activity of elesclomol required the compound to coordinate copper and no other metal and could be inhibited with high-affinity copper chelators (e.g., TM) [155–157].

Elesclomol scavenges Cu^{2+} from the culture medium to form a 1 : 1 neutral Cu^{2+}-elesclomol complex, which is subsequently transported to the mitochondria where it disrupts the electron transport chain (ETC) [154, 156]. At the mitochondria, Cu^{2+} dissociates from the complex and the elesclomol ligand is subsequently effluxed from the cell, but it continues to shuttle more extracellular Cu^{2+} (reforms Cu(II)-elesclomol complexes) into the intracellular compartment (cycles in and out of cells) [156]. Furthermore, redox reduction of the dissociated Cu^{2+} to Cu^{+} induces mitochondrial ROS [158, 159]. Further evidence that elesclomol targets the mitochondria was provided by the demonstration that human melanoma cells lacking ETC activity are insensitive to elesclomol treatment [154, 160]. The elesclomol-induced ROS activates transcription factors that regulate oxidative stress responsive genes including heat shock proteins, metallothioneins, and cell survival proteins [159]. In accordance with elesclomol targeting the mitochondria, the use of yeast gene deletion mutants combined with gene-set enrichment analysis revealed that sensitivity to elesclomol is associated with genes involved in ETC, mitochondrial translation (mitochondrial ribosome subunits, translation factors, tRNAs, and mRNA splicing enzymes), mitochondrial copper homeostasis, and stress responses [154].

Elesclomol is selectively toxic towards many types of cancer cells *in vitro* and was found to enhance the efficacy of paclitaxel in human tumor xenograft models (M14 human melanoma and CT26 mouse colon carcinoma model) [161]. A large therapeutic window for the anticancer activity of elesclomol exists between leukemic cell lines (e.g., HL-60 cells; IC_{50} <100 nM) and normal peripheral blood mononuclear cells (IC_{50} >10 μM) [156]. However, despite both the normal and leukemic cells taking up elesclomol, only the cancerous cells accumulated copper, which resulted in increased ROS production especially in mitochondria [156]. Many different cancer cell types have been shown to harbor higher ROS levels and lower antioxidant capacity than normal cells [162].

Conceivably, an increase in ROS in cancer cells may be sufficient to reach a toxicity threshold and trigger apoptosis. We and many other groups have demonstrated that pro-oxidant ionophoric copper can cause the selective death of cancerous cells through ROS generation [162]. Elesclomol behaves in a similar manner. Consistently, depletion of the major cellular antioxidant glutathione sensitized leukemic cells (K562) to elesclomol, while pretreating an array of cancerous cell types (Hs294T melanoma, HSB2 T lymphoblast leukemia, and Ramos Burkitt's lymphoma B cells) with the antioxidant N-acetylcysteine abrogated elesclomol-induced apoptosis [155, 159]. However, unlike most other copper complexes, elesclomol selectively induces mitochondrial ROS to induce cancer cell death. Targeting the mitochondria represents a distinct and promising mode of action to kill cancer cells, in particular for melanoma, since this cancer type relies heavily on oxidative phosphorylation for enhanced metabolic requirements [160, 163].

However, one study has demonstrated non-mitochondrial components to the cytotoxic anticancer activity of elesclomol. Experiments performed with leukemic cells (K562) demonstrated that elesclomol caused an immediate cell cycle G0/G1 arrest, well before induction of death that occurred around 5 hours after treatment [158]. Elesclomol also produced DNA double-strand breaks and cells with a compromised ability to repair ROS-induced DNA damage were found to be more sensitive to elesclomol treatment [158]. Elesclomol was also found not to be a substrate for the ATP binding cassette-type efflux transporters (including P-gp), which are known mediators of cellular resistance to other copper complexes and conventional chemotherapies [158].

3.1.2. Clinical Use for Cancer Treatment

In 2000, to accelerate the translation of elesclomol into the clinic, Lan Bo Chen and Safi Bahcall co-founded a small biotechnology company named Synta Pharmaceuticals. A Phase I clinical trial on patients with refractory solid tumors determined the maximum tolerated dose, toxicity profile, and pharmacokinetics of elesclomol when used in combination with paclitaxel [164]. The elesclomol/paclitaxel combination was relatively well tolerated by patients with a toxicity profile similar to paclitaxel alone [164]. In a multi-center, double-blind, randomized Phase II study on 81 patients with stage IV metastatic melanoma, elesclomol in combination with paclitaxel significantly increased progression-free survival compared to paclitaxel alone (3.7 months versus 1.8 months, $p = 0.035$) [165]. Following this promising study, collaboration between Synta Pharmaceuticals and GlaxoSmithKline (GSK) allowed further development of elesclomol. In 2006, elesclomol received fast-track orphan drug designation from the U. S. Food and Drug Administration for the treatment of patients with metastatic melanoma. In 2007, a larger double blind randomized Phase III clinical trial of elesclomol in combination with paclitaxel in 651 chemo-naïve patients with metastatic melanoma was initiated (dubbed the SYMMETRY trial) [166]. Phase II trials were also planned in patients with other cancer types. However, in February 2009, all clinical trials with elesclomol were suspended since the overall survival

was found to be significantly lower in the elesclomol/paclitaxel arm than in the paclitaxel alone (control) arm (80 deaths versus 53 deaths, respectively) [166]. Subsequently, it was shown that patients with elevated lactate dehydrogenase (LDH) levels in their serum did not respond well to elesclomol. However, patients with low and/or normal LDH serum levels did have a significant improvement in median progression-free survival time.

In September 2010, the FDA gave approval to resume clinical development of elesclomol in a specific protocol that excluded patients with elevated LDH. As described in the previous section, elesclomol transports copper into mitochondria which subsequently induces ROS and disrupts ETC [154, 156]. Conceivably, tumor cells that rely more heavily on oxidative phosphorylation for their metabolic needs are likely to be more sensitive to elesclomol than cells that rely primarily on glycolysis [154, 160]. Since elevated serum levels of LDH reflect a tumor burden that substantially increased glycolysis, it is not so surprising that elesclomol did not provide benefit in patients with high LDH levels. Importantly, the SYMMETRY clinical trial established that serum LDH levels are a predictive biomarker of elesclomol treatment response, which may stratify patients in future clinical trials [166].

Currently, elesclomol is being evaluated in Phase I and II trials for the treatment of a broad range of cancer types including acute myeloid leukemia (NCT01280786), ovarian carcinoma (NCT00888615), prostate cancer (NCT00808418), soft tissue sarcoma (NCT00087997), and non-small cell lung cancer (NCT00088088) and the results of these trials are not yet known.

3.2. Copper Complexes of Thiosemicarbazones

Various thiosemicarbazones and bis(thiosemicarbazones) have the ability to coordinate metals (Cu^{2+}, $Fe^{2+/3+}$ or Zn^{2+}) resulting in the formation of lipophilic, neutral complexes. Their wide range of biological activities, many of which are attributed to their ability to coordinate and influence copper, are being redirected towards cancer treatments [27, 167]. Subtle differences in their structure (backbone substituents) dictate their cellular metabolism and can dramatically change their biological activity. Initially investigated as anticancer agents over 50 years ago, recent advances in understanding their copper chemistry and biological activities has renewed considerable interest in the development of thiosemicarbazones as cancer therapies.

3.2.1. Bis(thiosemicarbazones)

Several bis(thiosemicarbazones) and their copper complexes have shown considerable promise as anticancer therapeutics in preclinical studies but surprisingly, up until now, none have been tested in human clinical trials. In pioneer studies dating back to 1950s and 1960s, the potent anticancer efficacy of several bis(thiosemicarbazones) (glyoxal-bis(thiosemicarbazone) (H_2gts) and of 2-keto-3-

ethoxybutyraldehyde derivatives (H_2kts and H_2ktsm)) was demonstrated in Swiss mice harboring sarcoma-180 tumors and later in a number of other transplanted rodent tumor models [168–172]. These investigators suggested a role for copper in the mechanism of action and subsequently it was shown that removing copper from the diet of rats suppressed the inhibitory effect of H_2kts on tumor growth (Walker 256 carcinoma) [173]. Conversely, treating mice bearing sarcoma-180 tumors with the preformed H_2kts and copper complex (Cu(II)(kts)) increased their overall survival time (>40 % increased survival with 1.5 mg/kg Cu(II)(kts)), whereas $CuCl_2$ or H_2kts (ligand) treatments alone were ineffective [176, 177]. Additionally, coordinating the H_2kts ligand with other metals (e.g., Zn^{2+}, $Fe^{2+/3+}$, Ni^{2+}, and Ag^{+}) perturbed the anticancer activity [176, 177]. Subsequently, it has been shown that after Cu(II)(kts) enters cells the coordinated copper dissociates (Cu^{2+} reduces to Cu^{+}) under the intracellular reductive environment. Unexpectedly, the resultant ligand (H_2kts) can diffuse back out of the cell, re-coordinate copper (again forming Cu(II)(kts)) and cycle back across the plasma membrane [176, 178]. These properties renders several bis(thiosemicarbazones), those that continually cycle copper into cells, particularly toxic towards cancer cells [176, 178].

Our group assessed the therapeutic efficacy of two bis(thiosemicarbazonato) copper complexes, Cu(II)(gtsm) (glyoxalbis(N4-methylthiosemicarbazonato)Cu(II)) and Cu(II)(atsm) (diacetylbis-(N4-methylthiosemicarbazonato)Cu(II)) for the treatment of prostate cancer in the TRAMP mouse model [27]. Analogous to Cu(II)(kts), copper dissociates intracellularly from Cu(II)(gtsm) and the resultant intracellular H_2gtsm ligands (reduced Cu(II)(gtsm)) continue to redistribute copper into a bioavailable pool; possibly by cycling in and out of cells. TRAMP mice treated with Cu(II)(gtsm) (2.5 mg/kg/d) exhibited a significant reduction in prostate cancer burden ($\sim$70 %) and decreased disease severity (lesion grade) after 28 days of treatment, while treatment with Cu(II)(atsm) (30 mg/kg/d) was ineffective [28].

The anticancer activity of Cu(II)(gtsm) is dependent on the coordinated copper and the generation of intracellular ROS [28, 29, 133]. Sequestering copper with a strong chelator (e.g., TM), or increasing intracellular glutathione (the major antioxidant) levels by applying *N*-acetyl-L-cysteine, inhibited the anticancer activity of this complex [29]. We further demonstrated that increasing extracellular (media) copper concentrations enhanced the anticancer activity of Cu(II)(gtsm) and its ligand (H_2gtsm) was only toxic towards prostate cancer cells when in the presence of copper [28]. Importantly, Cu(II)(gtsm) was shown to selectively target and rapidly kill prostate cancer cells without harming normal prostate epithelial cells [28].

Our subsequent studies demonstrated that prostate cancer cells in comparison to normal prostate epithelial cells contain elevated ROS coupled with reduced glutathione-mediated antioxidant capacity; which together make them significantly more sensitive to pro-oxidant ionophoric copper [133]. Accordingly, copper ionophores that increase intracellular bioavailable copper, such as Cu(II)(gtsm), DSF, and clioquinol, generated toxic levels of intracellular ROS in prostate cancer cells but not in normal prostate epithelial cells [133]. However,

as previously mentioned, Cu(II)(gtsm) also inhibits the proteasome [28], another feature common to copper ionophores that increase intracellular bioavailable copper. The comparative importance of ROS production versus proteasome inhibition for the anticancer activity of Cu(II)(gtsm) has not been determined. Furthermore, it has been recently shown that Cu(II)(gtsm) causes cancer cell death, at least in part, by inducing lysosomal membrane permeabilization [29]. Therefore, further studies are required to delineate which targets are most important for the anticancer activity of Cu(II)(gtsm).

As previously mentioned, Cu(II)(atsm) was ineffective as a treatment for prostate cancer in the TRAMP mouse model [28]. However, Cu(II)(atsm) can only release its coordinated copper intracellularly under elevated reductive states, such as in hypoxic tissues [179]. Under such conditions, the dissociated copper is reduced (to Cu^{+}) and consequently the ligand (H_2atsm) becomes trapped within the cell(s) [27]. Many cancer types are hypoxic due to inadequate blood supply and this has been associated with aggressiveness, metastasis, and resistance to standard chemo- and radiotherapies (reviewed in [180]). The wider availability of the copper radioisotopes (copper-60, -61, -62, and -64) and advances in the field of radiolabelling (i.e., shorter synthesis times) have enabled the production of radiolabelled Cu(II)(atsm) for profiling hypoxic cancer lesions through positron emission tomography-computed tomography (PET/CT) [27]. The potential for Cu(II)(atsm) to be used as a hypoxia marker has been extensively evaluated both in preclinical and clinical studies [179, 181–187]. Small scale clinical studies using PET imaging with radiolabelled Cu(II)(atsm) (copper-60, copper-64 or copper-62), has enabled the identification of cancer patients that are likely to respond to chemotherapy or radiotherapy, in particular for lung, cervical, rectum and head and neck cancers [181, 182, 184, 188, 189].

Furthermore, Cu(II)(atsm) tumor uptake has been correlated with overexpression of hypoxic markers (e.g., hypoxia-inducible factor 1α) and poor clinical outcome in patients with cervical cancer [187]. In this particular study, the 4-year overall survival was 75 % for patients with non-hypoxic tumors and 33 % for patients with hypoxic tumors, indicating that Cu(II)(atsm) is a potential biomarker of malignant aggressive phenotypes [184]. Likewise, in 22 patients with glioma, Cu(II)(atsm) uptake correlated with tumor grades and was predictive of hypoxia-inducible factor 1α expression (92.3 % sensitivity and 88.9 % specificity) [190]. A Phase II clinical trial is ongoing to assess whether ^{64}Cu(atsm) PET scans can predict disease progression in cervical cancer patients undergoing treatment with cisplatin and radiation therapy. Chao and colleagues suggested that ^{60}Cu(atsm) PET images might guide intensity-modulated radiation therapy of head and neck cancer, as a novel approach to overcome tumor resistance associated with hypoxia [191].

The physical characteristics of copper-64 not only allow for its use as a PET radiotracer, but also as a therapeutic radioisotope, since it also decays by β^{-} emission and electron capture generating Auger electrons suitable for therapeutic applications. Auger electrons have a high linear energy-transfer and a short penetration range of 0.02–10 μm and therefore can produce toxic effects within targeted cells while sparing neighboring cells [192]. Providing that copper-64

localizes to the nucleus, Auger electrons produce more lethal DNA breaks than β^- particles, with this effect independent of oxygen concentration. Remarkably, radionuclide therapy with ^{64}Cu(atsm) in a hamster xenograft model of colon cancer (GW39 cells), significantly increased survival time by approximately 6-fold (one injection of 370 Mbq in animals bearing 7-day old tumors) [193]. A follow-up study using mice bearing mammary carcinoma xenografts (EMT6 cells) showed that combining ^{64}Cu(atsm) (74 Mbq dose) with daily administration of 2-deoxy-D-glucose (inhibits glycolysis) increased ^{64}Cu(atsm) tumor retention, inhibited tumor growth by approximately 60 % and significantly improved the survival rate by approximately 50 % compared to untreated mice, or mice treated with each compound alone [194]. Furthermore, in a mouse model of colon cancer (Colon-26), two systemic administrations of ^{64}Cu(atsm) (37 MBq dose) 7 days apart, inhibited tumor growth and the ability of the cancer to metastasize to lung [195]. The therapeutic effect was attributed to the fact that ^{64}Cu(atsm) preferentially accumulated in and reduced the number of CD133$^+$ cancer stem cells, which have been recognized as contributors to both therapy resistance and to tumor metastatic potential [195]. Clarifying the mechanism of action, McMillan and colleagues recently demonstrated that ^{64}Cu(atsm) does induce DNA damage via high linear energy-transfer Auger electrons [196].

One potential limitation of ^{64}Cu(atsm) is that tumor uptake may not always reflect hypoxia. Reduction of Cu(II)(atsm) involves NADH-cytochrome b5 reductase and NADPH-cytochrome P450 reductase [197]. Despite hypoxia enhancing these enzymatic reductions, Cu(II)(atsm) accumulation may not be a direct measurement of oxygen content, but rather of the intracellular concentration of reductants [197]. Additionally, the level of Cu(II)(atsm) retention is variable in different cell and cancer types [198, 199]. For instance, in human prostate cancer cell lines (e.g., PC-3, 22Rv1, LNCaP, and LAPC-4), high expression of fatty acid synthase (FAS), a protein that catalyzes fatty acid biosynthesis, is correlated with low intracellular Cu(II)(atsm) retention [200]. Accordingly, inhibiting FAS increased Cu(II)(atsm) accumulation in the prostate cancer cell lines [200]. Furthermore, *in vitro* and *in vivo* studies have demonstrated that Cu(II)(atsm) retention decreased (efflux increased) in cancer cells expressing high levels of the multidrug resistance P-gp protein [201]. These findings have important implication on the potential clinical use of ^{64}Cu(atsm) both as a hypoxic biomarker and as a therapeutic agent. Other analogues of Cu(II)(atsm) with greater selectivity for hypoxia are also being evaluated [202].

3.2.2. Other Thiosemicarbazones

In the search for potent metal complexes with anticancer properties, a number of α-(N)-heterocyclic thiosemicarbazones have been developed and evaluated. Among them, triapine (aka 3-AP) (3-aminopyridine-2-carboxaldehyde thiosemicarbazone) has been particularly well studied in preclinical models as a single agent, or in combination with cisplatin, doxorubicin or etoposide [203, 204]. Triapine is a strong inhibitor of ribonucleotide reductase (RNR), the enzyme that catalyzes the formation of deoxyribonucleotides from ribonucleotides for DNA

synthesis and repair [205, 206]. Therefore, RNR is ultimately required for cellular division and as such has become a target for cancer therapy. To date, triapine has been evaluated in over 20 clinical Phase I and II studies, but has demonstrated limited clinical activity and causes two serious side effects, the formation of methemoglobin and hypoxia [207, 208]. Both side effects are due to iron coordination, which is required for the anticancer activities of triapine through the generation of ROS, DNA damage, and ultimately cell death [209]. By contrast, the Ga^{3+} and the Zn^{2+} triapine complexes are relatively inert and Cu^{2+} inhibits triapine cytotoxic activity [209].

Further modification of the triapine structure, through structure-activity relationship studies, led to the development of several new series of thiosemicarbazones. These include the 2-pyridylketone thiosemicarbazones (DpT series), 2-benzoylpyridine thiosemicarbazones (BpT series) and the 2-acetylpyridine thiosemicarbazones (ApT series), which were selected for possessing more potent anticancer activity than triapine [210–212]. One of these compounds, Dp44mT (di-2-pyridylketone 4,4-dimethyl-3-thiosemicarbazone) emerged as the most promising first generation candidate and despite being structurally related to triapine had distinct biological activity [213]. In comparison to triapine, Dp44mT is ~47-fold more potent in cytotoxicity assays and greater than 16-fold more effective in the treatment of a mouse model bearing human lung carcinoma xenografts (DMS-53 cells) [213, 214]. Furthermore, Dp44mT has proven effective *in vivo* against several other aggressive cancer types (e.g., neuroepithelioma and melanoma) in mice, significantly inhibiting tumor growth and metastasis [213, 215]. Note, that the DpT series of thiosemicarbazones are thought to inhibit metastasis by up-regulating the expression of N-myc downstream regulated protein1; a metastasis suppressor protein [216–218].

Initially, the anticancer action of Dp44mT was thought to be similar to that of triapine and was attributed to the formation of a Fe^{3+} complex. Redox cycling of the triapine Fe^{3+} complex generates intracellular ROS, impedes the thiol-related antioxidant system (e.g., glutathione, thioredoxin, and glutaredoxin) and inhibits RNR through the modification of its disulfide bond [205, 206]. However, it was later demonstrated that copper plays a more important role in the anticancer activity of Dp44mT [210, 219]. In contrast to triapine where copper coordination abrogates its anticancer activity, the copper complex of Dp44mT possessed greater anticancer activity than its corresponding iron complex [210]. Dp44mT is a *bona fide* copper ionophore and consequently generates intracellular ROS, which can be abrogated by using strong copper chelation (e.g., TM) or by increasing intracellular antioxidant glutathione levels [219]. However, Dp44mT also targets the lysosome as part of its anticancer activity. The Dp44mT copper complex accumulates in lysosomes causing their membrane to permeabilize and the subsequent release of their contents into the cytosol. This sets off a cascade of events leading to cleavage and activation of the pro-apoptotic Bid protein and ultimately cell death [219]. Remarkably, Dp44mT is a P-gp substrate and P-gp located at the lysosome membrane influxes and increases sequestration of Dp44mT [220]. Dp44mT in the acidity (pH 5) of lysosomes becomes charged and trapped, and then it is thought that the coordinated copper causes ROS

that damages membrane integrity [220]. Usually P-gp substrates are rendered ineffective once sequestered into lysosomes, such as doxorubicin due to protonation, but the Dp44mT copper complex is instead potentiated [220]. The ability of Dp44mT to employ P-gp to enhance toxicity has major implications for both resisting and overcoming drug resistance. For instance, Dp44mT might be used in combination with doxorubicin to potentiate its anticancer activity, by causing the release of doxorubicin from lysosomes and therefore allowing it to reach its target, the nucleus [220].

Unfortunately, Dp44mT was found to induce cardiac fibrosis in mice and this prompted the development of second-generation DpT analogues, where the terminal H at N4 was replaced by an alkyl group [213, 214, 216]. Of these compounds, DpC (di-2-pyridylketone 4-cyclohexyl-4-methyl-3-thiosemicarbazone) was more potent and better tolerated than Dp44mT and does not cause either cardiac fibrosis or methemoglobin even when administered at high doses in mice [214, 216, 221]. Another advantage for DpC is that it can be administered orally without apparent toxicity, unlike Dp44mT which causes weight loss and cardiotoxicity when given orally at high doses [222]. In mice harboring either human lung (DMS-53 cells) or pancreatic (PANC-1 cells) xenografts, DpC potently inhibited cancer growth by greater than 80 % when compared to the vehicle control [214, 216]. In the pancreatic cancer model, the anticancer activity of DpC was found to be far superior to gemcitabine treatment, the current first-line chemotherapeutic for pancreatic cancer therapy [216]. DpC has better pharmacokinetics than Dp44mT and is retained in the body for considerably longer ($T_{1/2}$ = 1.7 h for Dp44mT versus 10.7 h for DpC) [223].

Importantly, analogous to what occurs with Dp44mT, high expression of P-gp in cancer cells increased the trapping of DpC in lysosomes potentiating its anticancer activity [224]. An independent study performed by the U. S. National Cancer Institute Developmental Therapeutics Program, revealed that DpC inhibited growth in 59 of 60 human cancer cell lines tested, with concentrations ranging from < 10 nM to 300 nM. Normal cells were shown to be refractory to DpC treatment (e.g., > 1000-fold for normal fibroblasts). DpC has been licensed by Oncochel Therapeutics LLC and entered Phase I clinical trial in 2016 (NCT02688101). Patients with advanced solid tumors will receive variable doses of DpC administered orally to determine the maximum tolerated dose and any change in patients' tumor size documented.

4. GENERAL CONLUSIONS

Considerable interest in developing copper complexes for cancer treatment has arisen from understanding of the importance of copper in cancer growth, malignant angiogenesis, and metastasis. Unfortunately, numerous 'very encouraging' preclinical studies have been countered with 'equally disappointing' human clinical trials. However, the few tantalizing clinical results where outcomes were improved, and our growing knowledge on the pharmacological activities of both 'old and new' copper complexes, provide a glimmer of optimism. Furthermore,

with recent advances in metallomics, in particular relating to mammalian copper homeostasis, we are now positioned to better develop and trial copper complexes as anticancer therapies. Indeed, exciting human clinical trials are underway (e.g., for TM and DpC), equipped with hard earned wisdom and more sophisticated ways to evaluate clinical efficacy. The newest paradigm is to develop anticancer agents that target multiple critical pathways in order to circumvent resistance and to improve therapeutic efficacy. Many copper complexes certainly fulfill this criterion. We eagerly await results from ongoing human trials that are assessing promising multi-target copper complexes, some repurposed (e.g., TM) and some newly designed (e.g., DpC).

ACKNOWLEDGMENTS

This study was funded by Movember through Prostate Cancer Foundation of Australia's Research Program (M. A. Cater), by the National Health and Medical Research Council of Australia (NHMRC) (M. A. Cater), and by a Medicine/Science CASS Foundation grant (D. Denoyer).

ABBREVIATIONS

ALDH	aldehyde dehydrogenase
ATN-224	tetrathiomolybdate bis-choline salt
ATOX1	antioxidant 1 copper chaperone
ATP	adenosine 5′-triphosphate
ATP7A/B	ATPase copper transporting A/B
BpT series	2-benzoylpyridine thiosemicarbazone class
CTR1	copper transporter 1
Cu(II)(atsm)	diacetylbis-[N4-methylthiosemicarbazonato]Cu(II)
Cu(II)(gtsm)	glyoxalbis[N4-methylthiosemicarbazonato]Cu(II)
DDTC	diethyldithiocarbamate
DNMT1	DNA methyltransferase 1
Dp44mT	di-2-pyridylketone 4,4-dimethyl-3-thiosemicarbazone
DpC	di-2-pyridylketone 4-cyclohexyl-4-methyl-3-thiosemicarbazone
DpT series	2-pyridylketone thiosemicarbazone class
DSF	disulfiram; tetraethylthiuram disulfate
ETC	electron transport chain
FGF	fibroblast growth factor
GBM	glioblastoma multiforme
H_2atsc	biacetyl-bis(4-pyrrolidinyl-3-thiosemicarbazone)
H_2btsc	benzil-bis(4-pyrrolidinyl-3-thiosemicarbazone)
H_2gts	glyoxal-bis(thiosemicarbazone)
H_2gtsc	glyoxal-bis(4-methyl-4-phenyl-3-thiosemicarbazone)

H2kts and H2ktsm	2-keto-3-ethoxybutyraldehyde derivatives
HUVEC	human umbilical vascular endothelial cell
IFL	irinotecan/ 5-fluorouracil/ leucovorin
IL-1α, -6, -8	interleukin-1alpha, -6, -8
LDH	lactate dehydrogenase
LOX	lysyl oxidase
MeDTC-SO	methyl diethylthiocarbamoyl-sulfoxide
MMP-2, -9	matrix metalloproteinases-2, -9
mRNA	messenger ribonucleic acid
NADH	nicotinamide adenine dinucleotide hydride
NADPH	reduced nicotinamide adenine dinucleotide phosphate
NF-κB	nuclear factor kappa B
PET	positron emission tomography
P-gp	P-glycoprotein
PrEC	primary prostate epithelial cells
RNR	ribonucleotide reductase
ROS	reactive oxygen species
SMON	subacute myelo-optic neuropathy
SOD	Cu/Zn superoxide dismutase
TM	tetrathiomolybdate
TRAMP	transgenic adenocarcinoma of mouse prostate
triapine	3-aminopyridine-2-carboxaldehyde thiosemicarbazone
tRNA	transfer ribonucleic acid
VEGF	vascular endothelial growth factor
WD	Wilson's disease

REFERENCES

1. M. Arredondo, M. T. Nunez, *Mol. Aspects Med.* **2005**, *26*, 313–327.
2. R. Bhuvanasundar, A. John, K. N. Sulochana, K. Coral, P. R. Deepa, V. Umashankar, *Bioinformation* **2014**, *10*, 406–412.
3. D. Horn, A. Barrientos, *IUBMB Life* **2008**, *60*, 421–429.
4. T. D. Rae, P. J. Schmidt, R. A. Pufahl, V. C. Culotta, T. V. O'Halloran, *Science* **1999**, *284*, 805–808.
5. D. Denoyer, S. Masaldan, S. La Fontaine, M. A. Cater, *Metallomics* **2015**, *7*, 1459–1476.
6. F. Tisato, C. Marzano, M. Porchia, M. Pellei, C. Santini, *Med. Res. Rev.* **2010**, *30*, 708–749.
7. E. Tokuda, Y. Furukawa, *Int. J. Mol. Sci.* **2016**, *17*, 636. DOI: 10.3390/ijms17050636.
8. S. Ayton, P. Lei, A. I. Bush, *Neurotherapeutics* **2015**, *12*, 109–120.
9. D. C. Brady, M. S. Crowe, M. L. Turski, G. A. Hobbs, X. Yao, A. Chaikuad, S. Knapp, K. Xiao, S. L. Campbell, D. J. Thiele, C. M. Counter, *Nature* **2014**, *509*, 492–496.
10. S. Ishida, P. Andreux, C. Poitry-Yamate, J. Auwerx, D. Hanahan, *Proc. Natl. Acad. Sci. USA* **2013**, *110*, 19507–19512.
11. D. Skrajnowska, B. Bobrowska-Korczak, A. Tokarz, S. Bialek, E. Jezierska, J. Makowska, *Biol. Trace Elem. Res.* **2013**, *156*, 271–278.
12. C. D. Davis, S. Newman, *Cancer Lett.* **2000**, *159*, 57–62.

13. O. A. Lukasewycz, J. R. Prohaska, *J. Natl. Cancer Inst.* **1982**, *69*, 489–493.
14. J. Folkman, *Ann. Surg.* **1972**, *175*, 409–416.
15. G. F. Hu, *J. Cell. Biochem.* **1998**, *69*, 326–335.
16. B. R. McAuslan, W. Reilly, *Exp. Cell Res.* **1980**, *130*, 147–157.
17. Q. Pan, C. G. Kleer, K. L. van Golen, J. Irani, K. M. Bottema, C. Bias, M. De Carvalho, E. A. Mesri, D. M. Robins, R. D. Dick, G. J. Brewer, S. D. Merajver, *Cancer Res.* **2002**, *62*, 4854–4859.
18. W. Feng, F. Ye, W. Xue, Z. Zhou, Y. J. Kang, *Mol. Pharmacol.* **2009**, *75*, 174–182.
19. L. Mandinov, A. Mandinova, S. Kyurkchiev, D. Kyurkchiev, I. Kehayov, V. Kolev, R. Soldi, C. Bagala, E. D. de Muinck, V. Lindner, M. J. Post, M. Simons, S. Bellum, I. Prudovsky, T. Maciag, *Proc. Natl. Acad. Sci. USA* **2003**, *100*, 6700–6705.
20. I. Prudovsky, C. Bagala, F. Tarantini, A. Mandinova, R. Soldi, S. Bellum, T. Maciag, *J. Cell Biol.* **2002**, *158*, 201–208.
21. F. Soncin, J. D. Guitton, T. Cartwright, J. Badet, *Biochem. Biophys. Res. Commun.* **1997**, *236*, 604–610.
22. H. Peinado, M. Del Carmen Iglesias-de la Cruz, D. Olmeda, K. Csiszar, K. S. Fong, S. Vega, M. A. Nieto, A. Cano, F. Portillo, *EMBO J.* **2005**, *24*, 3446–3458.
23. G. MacDonald, I. Nalvarte, T. Smirnova, M. Vecchi, N. Aceto, A. Dolemeyer, A. Frei, S. Lienhard, J. Wyckoff, D. Hess, J. Seebacher, J. J. Keusch, H. Gut, D. Salaun, G. Mazzarol, D. Disalvatore, M. Bentires-Alj, P. P. Di Fiore, A. Badache, N. E. Hynes, *Sci. Signaling* **2014**, *7*, ra56. DOI: 10.1126/scisignal.2004870.
24. V. Antoniades, A. Sioga, E. M. Dietrich, S. Meditskou, L. Ekonomou, K. Antoniades, *Med. Hypotheses* **2013**, 1159–1163.
25. V. L. Goodman, G. J. Brewer, S. D. Merajver, *Endocr.-Relat. Cancer* **2004**, *11*, 255–263.
26. K. C. Park, L. Fouani, P. J. Jansson, D. Wooi, S. Sahni, D. J. Lane, D. Palanimuthu, H. C. Lok, Z. Kovacevic, M. L. Huang, D. S. Kalinowski, D. R. Richardson, *Metallomics* **2016,** 874–886.
27. B. M. Paterson, P. S. Donnelly, *Chem. Soc. Rev.* **2011**, *40*, 3005–3018.
28. M. A. Cater, H. B. Pearson, K. Wolyniec, P. Klaver, M. Bilandzic, B. M. Paterson, A. I. Bush, P. O. Humbert, S. La Fontaine, P. S. Donnelly, Y. Haupt, *ACS Chem. Biol.* **2013**, *8*, 1621–1631.
29. C. Stefani, Z. Al-Eisawi, P. J. Jansson, D. S. Kalinowski, D. R. Richardson, *J. Inorg. Biochem.* **2015**, *152*, 20–37.
30. C. Santini, M. Pellei, V. Gandin, M. Porchia, F. Tisato, C. Marzano, *Chem. Rev.* **2014**, *114*, 815–862.
31. G. J. Brewer, P. Hedera, K. J. Kluin, M. Carlson, F. Askari, R. B. Dick, J. Sitterly, J. K. Fink, *Arch. Neurol. (Chicago)* **2003**, *60*, 379–385.
32. A. T. Dick, L. B. Bull, *Aust. Vet. J.* **1945**, *21*, 70–72.
33. W. S. Ferguson, A. H. Lewis, S. J. Watson, *Nature* **1938**, *3569*, 553.
34. A. T. Dick, D. W. Dewey, Gawthorne, *J. Agri. Sci.* **1975**, *85*, 567.
35. J. Mason, *Irish Veter. J.* **1990**, *43*, 18–21.
36. S. R. Gooneratne, J. M. Howell, J. M. Gawthorne, *Br. J. Nutr.* **1981**, *46*, 469–480.
37. G. J. Brewer, F. Askari, M. T. Lorincz, M. Carlson, M. Schilsky, K. J. Kluin, P. Hedera, P. Moretti, J. K. Fink, R. Tankanov, R. B. Dick, J. Sitterly, *Arch. Neurol. (Chicago)* **2006**, *63*, 521–527.
38. G. J. Brewer, C. A. Terry, A. M. Aisen, G. M. Hill, *Arch. Neurol.* **1987**, *44*, 490–493.
39. G. J. Brewer, *J. Trace Elem. Med. Biol.* **2014**, *28*, 372–378.
40. G. N. George, I. J. Pickering, H. H. Harris, J. Gailer, D. Klein, J. Lichtmannegger, K. H. Summer, *J. Am. Chem. Soc.* **2003**, *125*, 1704–1705.
41. Y. Ogra, H. Chikusa, K. T. Suzuki, *J. Inorg. Biochem.* **2000**, *78*, 123–128.
42. G. J. Brewer, *Exp. Biol. Med.* **2001**, *226*, 665–673.

43. P. Carmeliet, R. K. Jain, *Nature* **2011**, *473*, 298–307.
44. N. Ferrara, A. P. Adamis, *Nat. Rev. Drug Discovery* **2016**, *advance online publication*. DOI: 10.1038/nrd.2015.17.
45. S. Brem, A. M. Tsanaclis, D. Zagzag, *Neurosurgery* **1990**, *26*, 391–396.
46. S. S. Brem, D. Zagzag, A. M. Tsanaclis, S. Gately, M. P. Elkouby, S. E. Brien, *Am. J. Pathol.* **1990**, *137*, 1121–1142.
47. S. G. Elner, V. M. Elner, A. Yoshida, R. D. Dick, G. J. Brewer, *Invest. Ophthalmol. Visual Sci.* **2005**, *46*, 299–303.
48. P. M. Gullino, *Anticancer Res.* **1986**, *6*, 153–158.
49. J. C. Juarez, O. Betancourt, S. R. Pirie-Shepherd, X. Guan, M. L. Price, D. E. Shaw, A. P. Mazar, F. Doñate, *Clin. Cancer Res.* **2006**, *12*, 4974–4982.
50. A. Parke, P. Bhattacherjee, R. M. Palmer, N. R. Lazarus, *Am. J. Pathol.* **1988**, *130*, 173–178.
51. K. S. Raju, G. Alessandri, M. Ziche, P. M. Gullino, *J. Natl. Cancer Inst.* **1982**, *69*, 1183–1188.
52. J. Yoshii, H. Yoshiji, S. Kuriyama, Y. Ikenaka, R. Noguchi, H. Okuda, H. Tsujinoue, T. Nakatani, H. Kishida, D. Nakae, D. E. Gomez, M. S. De Lorenzo, A. M. Tejera, H. Fukui, *Int. J. Cancer* **2001**, *94*, 768–773.
53. M. Ziche, P. M. Gullino, *J. Natl. Cancer Inst.* **1982**, *69*, 483–487.
54. C. Cox, S. D. Merajver, S. Yoo, R. D. Dick, G. J. Brewer, J. S. Lee, T. N. Teknos, *Arch. Otolaryngol., Head Neck Surg.* **2003**, *129*, 781–785.
55. C. Cox, T. N. Teknos, M. Barrios, G. J. Brewer, R. D. Dick, S. D. Merajver, *Laryngoscope* **2001**, *111*, 696–701.
56. M. K. Khan, M. W. Miller, J. Taylor, N. K. Gill, R. D. Dick, K. Van Golen, G. J. Brewer, S. D. Merajver, *Neoplasia* **2002**, *4*, 164–170.
57. Q. Pan, L. W. Bao, C. G. Kleer, G. J. Brewer, S. D. Merajver, *Mol. Cancer Ther.* **2003**, *2*, 617–622.
58. K. L. van Golen, L. Bao, G. J. Brewer, K. J. Pienta, J. M. Kamradt, D. L. Livant, S. D. Merajver, *Neoplasia* **2002**, *4*, 373–379.
59. B. Hassouneh, M. Islam, T. Nagel, Q. Pan, S. D. Merajver, T. N. Teknos, *Mol. Cancer Ther.* **2007**, *6*, 1039–1045.
60. G. J. Brewer, *J. Trace Elem. Exper. Med.* **2003**, *16*, 191–199.
61. T. Fukai, M. Ushio-Fukai, *Antioxid. Redox Signaling* **2011**, *15*, 1583–1606.
62. J. Grzenkowicz-Wydra, J. Cisowski, J. Nakonieczna, A. Zarebski, N. Udilova, H. Nohl, A. Jozkowicz, A. Podhajska, J. Dulak, *Mol. Cell. Biochem.* **2004**, *264*, 169–181.
63. M. Marikovsky, N. Nevo, E. Vadai, C. Harris-Cerruti, *Int. J. Cancer* **2002**, *97*, 34–41.
64. S. A. Lowndes, H. V. Sheldon, S. Cai, J. M. Taylor, A. L. Harris, *Microvasc. Res.* **2009**, *77*, 314–326.
65. S. A. Lowndes, A. Adams, A. Timms, N. Fisher, J. Smythe, S. M. Watt, S. Joel, F. Donate, C. Hayward, S. Reich, M. Middleton, A. Mazar, A. L. Harris, *Clin. Cancer Res.* **2008**, *14*, 7526–7534.
66. H. M. Alvarez, Y. Xue, C. D. Robinson, M. A. Canalizo-Hernández, R. G. Marvin, R. A. Kelly, A. Mondragón, J. E. Penner-Hahn, T. V. O'Halloran, *Science* **2010**, *327*, 331–334.
67. C. L. Chisholm, H. Wang, A. H. Wong, G. Vazquez-Ortiz, W. Chen, X. Xu, C. X. Deng, *Oncotarget* **2016**, *7*, 84439–84452.
68. K. K. Kim, S. Abelman, N. Yano, J. R. Ribeiro, R. K. Singh, M. Tipping, R. G. Moore, *Sci. Rep.* **2015**, *5*, 14296. DOI: 14210.11038/srep14296.
69. K. K. Kim, N. M. Kawar, R. K. Singh, T. S. Lange, L. Brard, R. G. Moore, *Gynecol. Oncol.* **2011**, *122*, 183–189.
70. K. K. Kim, T. S. Lange, R. K. Singh, L. Brard, R. G. Moore, *BMC Cancer* **2012**, *12*, 1–10.

71. C. D. Landon, S. E. Benjamin, K. A. Ashcraft, M. W. Dewhirst, *Int. J. Hyperthermia* **2013**, *29*, 528–538.
72. D. Kilari, K. A. Iczkowski, C. Pandya, A. J. Robin, E. M. Messing, E. Guancial, E. S. Kim, *Anticancer Res.* **2016**, *36*, 495–501.
73. E. S. Kim, X. Tang, D. R. Peterson, D. Kilari, C. W. Chow, J. Fujimoto, N. Kalhor, S. G. Swisher, D. J. Stewart, Wistuba, II, Z. H. Siddik, *Lung Cancer* **2014**, *85*, 88–93.
74. S. Ishida, F. McCormick, K. Smith-McCune, D. Hanahan, *Cancer Cell* **2010**, *17*, 574–583.
75. G. J. Brewer, R. D. Dick, D. K. Grover, V. LeClaire, M. Tseng, M. Wicha, K. Pienta, B. G. Redman, T. Jahan, V. K. Sondak, M. Strawderman, G. LeCarpentier, S. D. Merajver, *Clin. Cancer Res.* **2000**, *6*, 1–10.
76. B. G. Redman, P. Esper, Q. Pan, R. L. Dunn, H. K. Hussain, T. Chenevert, G. J. Brewer, S. D. Merajver, *Clin. Cancer Res.* **2003**, *9*, 1666–1672.
77. N. L. Henry, R. Dunn, S. Merjaver, Q. Pan, K. J. Pienta, G. Brewer, D. C. Smith, *Oncology* **2006**, *71*, 168–175.
78. J. Lin, M. Zahurak, T. M. Beer, C. J. Ryan, G. Wilding, P. Mathew, M. Morris, J. A. Callahan, G. Gordon, S. D. Reich, M. A. Carducci, E. S. Antonarakis, *Urol. Oncol.* **2013**, *31*, 581–588.
79. S. Jain, J. Cohen, M. M. Ward, N. Kornhauser, E. Chuang, T. Cigler, A. Moore, D. Donovan, C. Lam, M. V. Cobham, S. Schneider, S. M. Hurtado Rúa, S. Benkert, C. Mathijsen Greenwood, R. Zelkowitz, J. D. Warren, M. E. Lane, V. Mittal, S. Rafii, L. T. Vahdat, *Ann. Oncol.* **2013**.
80. H. I. Pass, G. J. Brewer, R. Dick, M. Carbone, S. Merajver, *Ann. Thor. Surg.* **2008**, *86*, 383–390.
81. B. J. Schneider, J. S.-J. Lee, J. A. Hayman, A. C. Chang, M. B. Orringer, A. Pickens, C. C. Pan, S. D. Merajver, S. G. Urba, *Invest. New Drugs* **2012**, *31*, 435–442.
82. E. M. Gartner, K. A. Griffith, Q. Pan, G. J. Brewer, G. F. Henja, S. D. Merajver, M. M. Zalupski, *Invest. New Drugs* **2009**, *27*, 159–165.
83. S. Fu, A. Naing, C. Fu, M. T. Kuo, R. Kurzrock, *Mol. Cancer Ther.* **2012**, *11*, 1221–1225.
84. N. A. David, H. G. Johnstone, A. C. Reed, C. D. Leake, *J. Am. Med. Assoc.* **1933**, *100*, 1658–1661.
85. D. A. Richards, *Lancet* **1971**, *1*, 44–45.
86. W. Rohde, P. Mikelens, J. Jackson, J. Blackman, J. Whitcher, W. Levinson, *Antimicrob. Agents Chemother.* **1976**, *10*, 234–240.
87. R. B. Stoughton, *Arch. Dermatol.* **1970**, *101*, 160–166.
88. X. Mao, A. D. Schimmer, *Toxicol. Lett.* **2008**, *182*, 1–6.
89. T. Tsubaki, Y. Honma, M. Hoshi, *Lancet* **1971**, *297*, 696–697.
90. S. R. Bareggi, U. Cornelli, *CNS Neurosci. Ther.* **2012**, *18*, 41–46.
91. T. W. Meade, *Br. J. Prev. Soc. Med.* **1975**, *29*, 157–169.
92. L. Cahoon, *Nat. Med.* **2009**, *15*, 356–359.
93. H. Tjälve, *Med. Hypotheses* **1984**, *15*, 293–299.
94. R. A. Cherny, C. S. Atwood, M. E. Xilinas, D. N. Gray, W. D. Jones, C. A. McLean, K. J. Barnham, I. Volitakis, F. W. Fraser, Y.-S. Kim, X. Huang, L. E. Goldstein, R. D. Moir, J. T. Lim, K. Beyreuther, H. Zheng, R. E. Tanzi, C. L. Masters, A. I. Bush, *Neuron* **2001**, *30*, 665–676.
95. B. Regland, W. Lehmann, I. Abedini, K. Blennow, M. Jonsson, I. Karlsson, M. Sjogren, A. Wallin, M. Xilinas, C. G. Gottfries, *Dementia Geriatr. Cognit. Disord.* **2001**, *12*, 408–414.
96. C. W. Ritchie, A. I. Bush, A. Mackinnon, S. Macfarlane, M. Mastwyk, L. MacGregor, L. Kiers, R. Cherny, Q. X. Li, A. Tammer, D. Carrington, C. Mavros, I. Volitakis, M.

Xilinas, D. Ames, S. Davis, K. Beyreuther, R. E. Tanzi, C. L. Masters, *Arch. Neurol.* **2003**, *60*, 1685–1691.
97. W. Q. Ding, B. Liu, J. L. Vaught, H. Yamauchi, S. E. Lind, *Cancer Res.* **2005**, *65*, 3389–3395.
98. M. A. Cater, Y. Haupt, *Biochem. J.* **2011**, *436*, 481–491.
99. A. D. Schimmer, *Curr. Cancer Drug Targets* **2011**, *11*, 325–331.
100. A. R. White, T. Du, K. M. Laughton, I. Volitakis, R. A. Sharples, M. E. Xilinas, D. E. Hoke, R. M. Holsinger, G. Evin, R. A. Cherny, A. F. Hill, K. J. Barnham, Q. X. Li, A. I. Bush, C. L. Masters, *J. Biol. Chem.* **2006**, *281*, 17670–17680.
101. M. Di Vaira, C. Bazzicalupi, P. Orioli, L. Messori, B. Bruni, P. Zatta, *Inorg. Chem.* **2004**, *43*, 3795–3797.
102. M. J. Pushie, K. H. Nienaber, K. L. Summers, J. J. H. Cotelesage, O. Ponomarenko, H. K. Nichol, I. J. Pickering, G. N. George, *J. Inorg. Biochem.* **2014**, *133*, 50–56.
103. D. Chen, Q. C. Cui, H. Yang, R. A. Barrea, F. H. Sarkar, S. Sheng, B. Yan, G. P. V. Reddy, Q. P. Dou, *Cancer Res.* **2007**, *67*, 1636–1644.
104. R. A. Barrea, D. Chen, T. C. Irving, Q. P. Dou, *J. Cell. Biochem.* **2009**, *108*, 96–105.
105. D. Chen, Q. C. Cui, H. Yang, Q. P. Dou, *Cancer Res.* **2006**, *66*, 10425–10433.
106. Z. Zhang, H. Wang, M. Yan, H. Wang, C. Zhang, *Mol. Med. Rep.* **2017**, *15*, 3–11.
107. F. Arnesano, S. Scintilla, V. Calo, E. Bonfrate, C. Ingrosso, M. Losacco, T. Pellegrino, E. Rizzarelli, G. Natile, *PLoS One* **2009**, *4*, e7052. DOI: 7010.1371/journal.pone.0007052.
108. K. G. Daniel, D. Chen, S. Orlu, Q. C. Cui, F. R. Miller, Q. P. Dou, *Breast Cancer Res.* **2005**, *7*, R897–908.
109. X. Mao, X. Li, R. Sprangers, X. Wang, A. Venugopal, T. Wood, Y. Zhang, D. A. Kuntz, E. Coe, S. Trudel, D. Rose, R. A. Batey, L. E. Kay, A. D. Schimmer, *Leukemia* **2008**, *23*, 585–590.
110. S. Zhai, L. Yang, Q. C. Cui, Y. Sun, Q. P. Dou, B. Yan, *J. Biol. Inorg. Chem.* **2010**, *15*, 259–269.
111. T. Du, G. Filiz, A. Caragounis, P. J. Crouch, A. R. White, *J. Pharmacol. Exp. Ther.* **2008**, *324*, 360–367.
112. D. B. Jack, W. Riess, *J. Pharm. Sci.* **1973**, *62*, 1929–1932.
113. G. P. Bondiolotti, C. Pollera, R. Pirola, S. R. Bareggi, *J. Chromatogr. B: Anal. Technol. Biomed. Life Sci.* **2006**, *837*, 87–91.
114. C. Chen, K. Samejima, Z. Tamura, *Chem. Pharm. Bull.* **1976**, *24*, 97–101.
115. A. D. Schimmer, Y. Jitkova, M. Gronda, Z. Wang, J. Brandwein, C. Chen, V. Gupta, A. Schuh, K. Yee, J. Chen, S. Ackloo, T. Booth, S. Keays, M. D. Minden, *Clin. Lymphoma, Myeloma Leuk.* **2012**, *12*, 330–336.
116. M. Grodzki, *Ber. Dtsch. Chem. Ges.* **1881**, *14*, 2754–2758.
117. D. Twiss, S. A. Bazier, F. Thomas, *J. Soc. Chem. Ind.* **1922**, *41*, 81T–88T.
118. E. Williams, *J. Am. Med. Assoc.* **1937**, *109*, 1472–1473.
119. O. Martensen-Larsen, *Lancet* **1948**, *2*, 1004.
120. M. L. Shen, J. J. Lipsky, S. Naylor, *Biochem. Pharmacol.* **2000**, *60*, 947–953.
121. T. M. Kitson, *Biochem. Pharmacol.* **1983**, *213*, 551–554.
122. A. J. Tomlinson, K. L. Johnson, J. Lam-Holt, D. C. Mays, J. J. Lipsky, S. Naylor, *Biochem. Pharmacol.* **1997**, *54*, 1253–1260.
123. R. Vallari, R. Pietruszko, *Science* **1982**, *216*, 637–639.
124. K. A. Veverka, K. L. Johnson, D. C. Mays, J. J. Lipsky, S. Naylor, *Biochem. Pharmacol.* **1997**, *53*, 511–518.
125. E. F. Lewison, *Prog. Clin. Biol. Res.* **1977**, *12*, 47–53.
126. S. S. Brar, C. Grigg, K. S. Wilson, W. D. Holder, Jr., D. Dreau, C. Austin, M. Foster, A. J. Ghio, A. R. Whorton, G. W. Stowell, L. B. Whittall, R. R. Whittle, D. P. White, T. P. Kennedy, *Mol. Cancer Ther.* **2004**, *3*, 1049–1060.

127. D. Cen, D. Brayton, B. Shahandeh, F. L. Meyskens, P. J. Farmer, *J. Med. Chem.* **2004**, *47*, 6914–6920.
128. D. Cen, R. I. Gonzalez, J. A. Buckmeier, R. S. Kahlon, N. B. Tohidian, F. L. Meyskens, Jr., *Mol. Cancer Ther.* **2002**, *1*, 197–204.
129. P. Hothi, T. J. Martins, L. Chen, L. Deleyrolle, J.-G. Yoon, B. Reynolds, G. Foltz, *Oncotarget* **2012**, *3*, 1124–1136.
130. J. Han, L. Liu, X. Yue, J. Chang, W. Shi, Y. Hua, *Toxicol. Appl. Pharmacol.* **2013**, *273*, 477–483.
131. J. L. Allensworth, M. K. Evans, F. Bertucci, A. J. Aldrich, R. A. Festa, P. Finetti, N. T. Ueno, R. Safi, D. P. McDonnell, D. J. Thiele, S. Van Laere, G. R. Devi, *Mol. Oncol.* **2015**, *9*, 1155–1168.
132. J. Navratilova, P. Jungova, P. Vanhara, J. Preisler, V. Kanicky, J. Smarda, *Int. J. Mol. Med.* **2009**, *24*, 661–670.
133. D. Denoyer, H. B. Pearson, S. A. Clatworthy, Z. M. Smith, P. S. Francis, R. M. Llanos, I. Volitakis, W. A. Phillips, P. M. Meggyesy, S. Masaldan, M. A. Cater, *Oncotarget* **2016**, *7*, 37064–37080.
134. T. Chiba, E. Suzuki, K. Yuki, Y. Zen, M. Oshima, S. Miyagi, A. Saraya, S. Koide, T. Motoyama, S. Ogasawara, Y. Ooka, A. Tawada, T. Nakatsura, T. Hayashi, T. Yamashita, S. Kaneko, M. Miyazaki, A. Iwama, O. Yokosuka, *PLoS One* **2014**, *9*, e84807; doi: 84810.81371/journal.pone.0084807.
135. P. Liu, S. Brown, T. Goktug, P. Channathodiyil, V. Kannappan, J. P. Hugnot, P. O. Guichet, X. Bian, A. L. Armesilla, J. L. Darling, W. Wang, *Br. J. Cancer* **2012**, *107*, 1488–1497.
136. R. Safi, E. R. Nelson, S. K. Chitneni, K. J. Franz, D. J. George, M. R. Zalutsky, D. P. McDonnell, *Cancer Res.* **2014**, *74*, 5819–5831.
137. Y. Li, S.-Y. Fu, L.-H. Wang, F.-Y. Wang, N.-N. Wang, Q. Cao, Y.-T. Wang, J.-Y. Yang, C.-F. Wu, *Cancer Lett.* **2015**, *369*, 86–96.
138. S.-G. Shiah, Y.-R. Kao, F. Y.-H. Wu, C.-W. Wu, *Mol. Pharmacol.* **2003**, *64*, 1076–1084.
139. H. J. Cho, T. S. Lee, J. B. Park, K. K. Park, J. Y. Choe, D. I. Sin, Y. Y. Park, Y. S. Moon, K. G. Lee, J. H. Yeo, S. M. Han, Y. S. Cho, M. R. Choi, N. G. Park, Y. S. Lee, Y. C. Chang, *J. Biochem. Mol. Biol.* **2007**, *40*, 1069–1076.
140. S. V. Ambudkar, S. Dey, C. A. Hrycyna, M. Ramachandra, I. Pastan, M. M. Gottesman, *Annu. Rev. Pharmacol. Toxicol.* **1999**, *39*, 361–398.
141. T. W. Loo, D. M. Clarke, *J. Natl. Cancer Inst.* **2000**, *92*, 898–902.
142. P. Dufour, J. M. Lang, C. Giron, B. Duclos, P. Haehnel, D. Jaeck, J. M. Jung, F. Oberling, *Biotherapy* **1993**, *6*, 9–12.
143. H. Nechushtan, Y. Hamamreh, S. Nidal, M. Gotfried, A. Baron, Y. I. Shalev, B. Nisman, T. Peretz, N. Peylan-Ramu, *Oncologist* **2015**, *20*, 366–367.
144. M. Rasper, A. Schafer, G. Piontek, J. Teufel, G. Brockhoff, F. Ringel, S. Heindl, C. Zimmer, J. Schlegel, *Neuro-Oncology* **2010**, *12*, 1024–1033.
145. A. Schafer, J. Teufel, F. Ringel, M. Bettstetter, I. Hoepner, M. Rasper, J. Gempt, J. Koeritzer, F. Schmidt-Graf, B. Meyer, C. P. Beier, J. Schlegel, *Neuro-Oncology* **2012**, *14*, 1452–1464.
146. K. Iljin, K. Ketola, P. Vainio, P. Halonen, P. Kohonen, V. Fey, R. Grafstrom, M. Perala, O. Kallioniemi, *Clin. Cancer Res.* **2009**, *15*, 6070–6078.
147. M. T. Schweizer, J. Lin, A. Blackford, A. Bardia, S. King, A. J. Armstrong, M. A. Rudek, S. Yegnasubramanian, M. A. Carducci, *Prostate Cancer Prostatic Dis.* **2013**, *16*, 357–361.
148. J. Cobby, M. Mayersohn, S. Selliah, *Life Sci.* **1977**, *21*, 937–941.
149. B. Johansson, *Acta Psychiatr. Scand., Suppl.* **1992**, *369*, 15–26.
150. X. Duan, X. Jisheng, Y. Qi, Z. Zhiwen, Y. Haijun, M. Shirui, L. Yaping, *ACS Nano* **2013**, *7*, 2860–2871.

151. X. Duan, X. Jisheng, Y. Qi, Z. Zhiwen, Y. Haijun, M. Shirui, L. Yaping, *Nanotechnology* **2014**, *25*, 125102–125113.
152. P. Liu, Z. Wang, S. Brown, V. Kannappan, P. E. Tawari, W. Jiang, J. M. Irache, J. Z. Tang, A. L. Armesilla, J. L. Darling, X. Tang, W. Wang, *Oncotarget* **2014**, *5*, 7471–7485.
153. M. Gladwell, *The Treatment*, Houghton Mifflin Harcourt, Boston, 2011, pp. 384.
154. R. K. Blackman, K. Cheung-Ong, M. Gebbia, D. A. Proia, S. He, J. Kepros, A. Jonneaux, P. Marchetti, J. Kluza, P. E. Rao, Y. Wada, G. Giaever, C. Nislow, *PLoS One* **2012**, *7*, e29798; doi: 29710.21371/journal.pone.0029798.
155. B. B. Hasinoff, A. A. Yadav, D. Patel, X. Wu, *J. Inorg. Biochem.* **2014**, *137*, 22–30.
156. M. Nagai, N. H. Vo, L. Shin Ogawa, D. Chimmanamada, T. Inoue, J. Chu, B. C. Beaudette-Zlatanova, R. Lu, R. K. Blackman, J. Barsoum, K. Koya, Y. Wada, *Free Radical Biol. Med.* **2012**, *52*, 2142–2150.
157. A. A. Yadav, D. Patel, X. Wu, B. B. Hasinoff, *J. Inorg. Biochem.* **2013**, *126*, 1–6.
158. B. B. Hasinoff, X. Wu, A. A. Yadav, D. Patel, H. Zhang, D. S. Wang, Z. S. Chen, J. C. Yalowich, *Biochem. Pharmacol.* **2015**, *93*, 266–276.
159. J. R. Kirshner, S. He, V. Balasubramanyam, J. Kepros, C. Y. Yang, M. Zhang, Z. Du, J. Barsoum, J. Bertin, *Mol. Cancer Ther.* **2008**, *7*, 2319–2327.
160. M. Barbi de Moura, G. Vincent, S. L. Fayewicz, N. W. Bateman, B. L. Hood, M. Sun, J. Suhan, S. Duensing, Y. Yin, C. Sander, J. M. Kirkwood, D. Becker, T. P. Conrads, B. Van Houten, S. J. Moschos, *PLoS One* **2012**, *7*, e40690. DOI: 40610.41371/journal.pone.0040690.
161. K. Foley, J. Bertin, K. Chan, A. Hutchings, T. Inoue, J. Kirshner, T. Korbut, L. Li, R. Mihalek, P. Rao, J. Sang, D. Smith, N. Tatsuta, C. Zhang, D. Zhou, J. Barsoum, *Mol. Cancer Ther.* **2007**, *6*, A290.
162. Q. Kong, J. A. Beel, K. O. Lillehei, *Med. Hypotheses* **2000**, *55*, 29–35.
163. J. S. Modica-Napolitano, V. Weissig, *Int. J. Mol. Sci.* **2015**, *16*, 17394–17421.
164. A. Berkenblit, J. P. Eder, Jr., D. P. Ryan, M. V. Seiden, N. Tatsuta, M. L. Sherman, T. A. Dahl, B. J. Dezube, J. G. Supko, *Clin. Cancer Res.* **2007**, *13*, 584–590.
165. S. O'Day, R. Gonzalez, D. Lawson, R. Weber, L. Hutchins, C. Anderson, J. Haddad, S. Kong, A. Williams, E. Jacobson, *J. Clin. Oncol.* **2009**, *27*, 5452–5458.
166. S. J. O'Day, A. M. Eggermont, V. Chiarion-Sileni, R. Kefford, J. J. Grob, L. Mortier, C. Robert, J. Schachter, A. Testori, J. Mackiewicz, P. Friedlander, C. Garbe, S. Ugurel, F. Collichio, W. Guo, J. Lufkin, S. Bahcall, V. Vukovic, A. Hauschild, *J. Clin. Oncol.* **2013**, *31*, 1211–1218.
167. G. Pelosi, *The Open Crystallography Journal* **2010**, *3*, 16–28.
168. V. C. Barry, M. L. Conalty, J. F. O'Sullivan, *Cancer Res.* **1966**, *26*, 2165–2168.
169. F. A. French, B. L. Freedlander, *Cancer Res.* **1958**, *18*, 1290–1300.
170. F. A. French, B. L. Freedlander, *Cancer Res.* **1958**, *18*, 172–175.
171. F. A. French, B. L. Freedlander, E. J. Blanz, Jr., *Cancer Res.* **1961**, *21*, 343–348.
172. H. G. Petering, H. H. Buskirk, G. E. Underwood, *Cancer Res.* **1964**, *24*, 367–372.
173. H. G. Petering, H. H. Buskirk, J. A. Crim, *Cancer Res.* **1967**, *27*, 1115–1121.
174. B. A. Booth, A. C. Sartorelli, *Nature* **1966**, *210*, 104–105.
175. A. C. Sartorelli, B. A. Booth, *Cancer Res.* **1967**, *27*, 1614–1619.
176. B. A. Booth, A. C. Sartorelli, *Mol. Pharmacol.* **1967**, *3*, 290–302.
177. G. J. Van Giessen, H. G. Petering, *J. Med. Chem.* **1968**, *11*, 695–699.
178. J. A. Crim, H. G. Petering, *Cancer Res.* **1967**, *27*, 1278–1285.
179. J. L. J. Dearling, P. J. Blower, *Chem. Commun.* **1998**, 2531–2532.
180. J. M. Brown, *Cancer Res.* **1999**, *59*, 5863–5870.
181. F. Dehdashti, P. W. Grigsby, J. S. Lewis, R. Laforest, B. A. Siegel, M. J. Welch, *J. Nucl. Med.* **2008**, *49*, 201–205.

182. F. Dehdashti, M. A. Mintun, J. S. Lewis, J. Bradley, R. Govindan, R. Laforest, M. J. Welch, B. A. Siegel, *Eur. J. Nucl. Med. Mol. Imaging* **2003**, *30*, 844–850.
183. Y. Fujibayashi, H. Taniuchi, Y. Yonekura, H. Ohtani, J. Konishi, A. Yokoyama, *J. Nucl. Med.* **1997**, *38*, 1155–1160.
184. P. W. Grigsby, R. S. Malyapa, R. Higashikubo, J. K. Schwarz, M. J. Welch, P. C. Huettner, F. Dehdashti, *Mol. Imaging Biol.* **2007**, *9*, 278–283.
185. J. P. Holland, J. S. Lewis, F. Dehdashti, *Q. J. Nucl. Med. Mol. Imaging* **2009**, *53*, 193–200.
186. J. S. Lewis, D. W. McCarthy, T. J. McCarthy, Y. Fujibayashi, M. J. Welch, *J. Nucl. Med.* **1999**, *40*, 177–183.
187. A. L. Vavere, J. S. Lewis, *Dalton Trans.* **2007**, 4893–4902.
188. D. W. Dietz, F. Dehdashti, P. W. Grigsby, R. S. Malyapa, R. J. Myerson, J. Picus, J. Ritter, J. S. Lewis, M. J. Welch, B. A. Siegel, *Dis. Colon Rectum* **2008**, *51*, 1641–1648.
189. T. Tsujikawa, S. Asahi, M. Oh, Y. Sato, N. Narita, A. Makino, T. Mori, Y. Kiyono, T. Tsuchida, H. Kimura, S. Fujieda, H. Okazawa, *PLoS One* **2016**, *11*, e0155635. DOI: 0155610.0151371/journal.pone.0155635.
190. K. Tateishi, U. Tateishi, M. Sato, S. Yamanaka, H. Kanno, H. Murata, T. Inoue, N. Kawahara, *Am. J. Neuroradiol.* **2013**, *34*, 92–99.
191. K. S. Chao, W. R. Bosch, S. Mutic, J. S. Lewis, F. Dehdashti, M. A. Mintun, J. F. Dempsey, C. A. Perez, J. A. Purdy, M. J. Welch, *Int. J. Radiat. Oncol., Biol., Phys.* **2001**, *49*, 1171–1182.
192. S. J. Adelstein, *Am. J. Roentgenol.* **1993**, *160*, 707–713.
193. J. S. Lewis, R. Laforest, T. L. Buettner, S.-K. Song, Y. Fujibayashi, J. M. Connett, M. J. Welch, *Proc. Natl. Acad. Sci. USA* **2001**, *98*, 1206–1211.
194. R. L. Aft, J. S. Lewis, F. Zhang, J. Kim, M. J. Welch, *Cancer Res.* **2003**, *63*, 5496–5504.
195. Y. Yoshii, T. Furukawa, Y. Kiyono, R. Watanabe, T. Mori, H. Yoshii, T. Asai, H. Okazawa, M. J. Welch, Y. Fujibayashi, *Nucl. Med. Biol.* **2011**, *38*, 151–157.
196. D. D. McMillan, J. Maeda, J. J. Bell, M. D. Genet, G. Phoonswadi, K. A. Mann, S. L. Kraft, H. Kitamura, A. Fujimori, Y. Yoshii, T. Furukawa, Y. Fujibayashi, T. A. Kato, *J. Radiat. Res.* **2015**, *56*, 784–791.
197. A. Obata, E. Yoshimi, A. Waki, J. S. Lewis, N. Oyama, M. J. Welch, H. Saji, Y. Yonekura, Y. Fujibayashi, *Ann. Nucl. Med.* **2001**, *15*, 499–504.
198. A. R. Cowley, J. Davis, J. R. Dilworth, P. S. Donnelly, R. Dobson, A. Nightingale, J. M. Peach, B. Shore, D. Kerr, L. Seymour, *Chem. Commun.* **2005**, 845–847.
199. H. Yuan, T. Schroeder, J. E. Bowsher, L. W. Hedlund, T. Wong, M. W. Dewhirst, *J. Nucl. Med.* **2006**, *47*, 989–998.
200. A. L. Vavere, J. S. Lewis, *Nucl. Med. Biol.* **2008**, *35*, 273–279.
201. J. Liu, A. Hajibeigi, G. Ren, M. Lin, W. Siyambalapitiyage, Z. Liu, E. Simpson, R. W. Parkey, X. Sun, O. K. Oz, *J. Nucl. Med.* **2009**, *50*, 1332–1339.
202. P. McQuade, K. E. Martin, T. C. Castle, M. J. Went, P. J. Blower, M. J. Welch, J. S. Lewis, *Nucl. Med. Biol.* **2005**, *32*, 147–156.
203. M. C. Liu, T. S. Lin, A. C. Sartorelli, *J. Med. Chem.* **1992**, *35*, 3672–3677.
204. M. C. Liu, T. S. Lin, A. C. Sartorelli, *Prog. Med. Chem.* **1995**, *32*, 1–35.
205. R. A. Finch, M. Liu, S. P. Grill, W. C. Rose, R. Loomis, K. M. Vasquez, Y. Cheng, A. C. Sartorelli, *Biochem. Pharmacol.* **2000**, *59*, 983–991.
206. R. A. Finch, M. C. Liu, A. H. Cory, J. G. Cory, A. C. Sartorelli, *Adv. Enzyme Regul.* **1999**, *39*, 3–12.
207. J. J. Knox, S. J. Hotte, C. Kollmannsberger, E. Winquist, B. Fisher, E. A. Eisenhauer, *Invest. New Drugs* **2007**, *25*, 471–477.
208. B. Ma, B. C. Goh, E. H. Tan, K. C. Lam, R. Soo, S. S. Leong, L. Z. Wang, F. Mo, A. T. Chan, B. Zee, T. Mok, *Invest. New Drugs* **2008**, *26*, 169–173.

209. A. Popovic-Bijelic, C. R. Kowol, M. E. Lind, J. Luo, F. Himo, E. A. Enyedy, V. B. Arion, A. Graslund, *J. Inorg. Biochem.* **2011**, *105*, 1422–1431.
210. P. J. Jansson, P. C. Sharpe, P. V. Bernhardt, D. R. Richardson, *J. Med. Chem.* **2010**, *53*, 5759–5769.
211. D. S. Kalinowski, Y. Yu, P. C. Sharpe, M. Islam, Y. T. Liao, D. B. Lovejoy, N. Kumar, P. V. Bernhardt, D. R. Richardson, *J. Med. Chem.* **2007**, *50*, 3716–3729.
212. D. R. Richardson, P. C. Sharpe, D. B. Lovejoy, D. Senaratne, D. S. Kalinowski, M. Islam, P. V. Bernhardt, *J. Med. Chem.* **2006**, *49*, 6510–6521.
213. M. Whitnall, J. Howard, P. Ponka, D. R. Richardson, *Proc. Natl. Acad. Sci. USA* **2006**, *103*, 14901–14906.
214. D. B. Lovejoy, D. M. Sharp, N. Seebacher, P. Obeidy, T. Prichard, C. Stefani, M. T. Basha, P. C. Sharpe, P. J. Jansson, D. S. Kalinowski, P. V. Bernhardt, D. R. Richardson, *J. Med. Chem.* **2012**, *55*, 7230–7244.
215. J. Yuan, D. B. Lovejoy, D. R. Richardson, *Blood* **2004**, *104*, 1450–1458.
216. Z. Kovacevic, S. Chikhani, D. B. Lovejoy, D. R. Richardson, *Mol. Pharmacol.* **2011**, *80*, 598–609.
217. W. Liu, F. Xing, M. Iiizumi-Gairani, H. Okuda, M. Watabe, S. K. Pai, P. R. Pandey, S. Hirota, A. Kobayashi, Y. Y. Mo, K. Fukuda, Y. Li, K. Watabe, *EMBO Mol. Med.* **2012**, *4*, 93–108.
218. K. M. Dixon, G. Y. Lui, Z. Kovacevic, D. Zhang, M. Yao, Z. Chen, Q. Dong, S. J. Assinder, D. R. Richardson, *Br. J. Cancer* **2013**, *108*, 409–419.
219. D. B. Lovejoy, P. J. Jansson, U. T. Brunk, J. Wong, P. Ponka, D. R. Richardson, *Cancer Res.* **2011**, *71*, 5871–5880.
220. P. J. Jansson, T. Yamagishi, A. Arvind, N. Seebacher, E. Gutierrez, A. Stacy, S. Maleki, D. Sharp, S. Sahni, D. R. Richardson, *J. Biol. Chem.* **2015**, *290*, 9588–9603.
221. P. Quach, E. Gutierrez, M. T. Basha, D. S. Kalinowski, P. C. Sharpe, D. B. Lovejoy, P. V. Bernhardt, P. J. Jansson, D. R. Richardson, *Mol. Pharmacol.* **2012**, *82*, 105–114.
222. Y. Yu, Y. Suryo Rahmanto, D. R. Richardson, *Br. J. Pharmacol.* **2012**, *165*, 148–166.
223. V. Sestak, J. Stariat, J. Cermanova, E. Potuckova, J. Chladek, J. Roh, J. Bures, H. Jansova, P. Prusa, M. Sterba, S. Micuda, T. Simunek, D. S. Kalinowski, D. R. Richardson, P. Kovarikova, *Oncotarget* **2015**, *6*, 42411–42428.
224. N. A. Seebacher, D. J. Lane, P. J. Jansson, D. R. Richardson, *J. Biol. Chem.* **2016**, *291*, 3796–3820.
225. K. F. Grossmann, M. B. Blankenship, W. Akerley, M. C. Terrazas, K. M. Kosak, K. M. Boucher, S. S. Buys, K. Jones, T. L. Werner, N. Agarwal, J. Weis, S. Sharma, J. Ward, P. J. Shami, *Cancer Res.* **2011**, *71*, 1308–1308.

17

Targeting Zinc(II) Signalling to Prevent Cancer

Silvia Ziliotto, Olivia Ogle, and Kathryn M. Taylor

School of Pharmacy and Pharmaceutical Sciences, College of Biomedical Sciences, Cardiff University, Redwood Building, King Edward VIIth Avenue, Cardiff CF10 3NB, UK
<taylorkm@cardiff.ac.uk>

ABSTRACT 507
1. INTRODUCTION 508
2. ZINC HANDLING IN CELLS 508
   2.1. Long Term and Short Term Effects of Zinc in Cells 508
   2.2. Zinc Transporters and Intracellular Zinc Homeostasis 509
   2.3. Emergence of Zinc Signalling Mechanisms 512
3. ZINC IN CANCER 513
   3.1. Elevated Zinc Levels in Breast Cancer 513
   3.2. Zinc Involvement in Other Cancers 514
   3.3. ZIP Transporters in Cancer 515
4. ZINC SIGNALLING IN CANCER 518
   4.1. How Zinc Signalling Mechanisms Drive Cancer Growth 518
5. TARGETING ZINC SIGNALLING MECHANISMS IN CANCER 520
   5.1. Phosphorylated ZIP7 as a Cancer Biomarker 520
   5.2. ZIP7 as a Cancer Target 522
   5.3. ZIP6 and ZIP10 as Cancer Targets 522
6. GENERAL CONCLUSIONS 523
ACKNOWLEDGMENTS 523
ABBREVIATIONS AND DEFINITIONS 524
REFERENCES 524

Abstract: Zinc is an important element that is gaining momentum as a potential target for cancer therapy. In recent years zinc has been accepted as a second messenger that is now recognized to be able to activate many signalling pathways within a few minutes of an extracellular stimulus by release of zinc(II) from intracellular stores. One of the major effects of this

Metal Ions in Life Sciences, Volume 18 Edited by Astrid Sigel, Helmut Sigel, Eva Freisinger, and Roland K. O. Sigel

https://doi.org/10.1515/9783110470734-017

store release of zinc is to inhibit a multitude of tyrosine phosphatases which will prevent the inactivation of tyrosine kinases and hence, encourage further activation of tyrosine kinase-dependent signalling pathways. Most of these signalling pathways are not only known to be involved in driving aberrant cancer growth, they are usually the main driving force. All this data together now positions zinc and zinc signalling as potentially important new targets to prevent aggressive cancer growth.

Keywords: cancer · SLC39A · zinc · zinc signalling · zinc transporters · ZIP7 · ZIP6 · ZIP10

1. INTRODUCTION

Zinc(II) in biology is an emerging area. In fact, in recent years zinc has been demonstrated to play an important role in most physiological processes and has been designated to have an importance on a scale similar to that seen with calcium [1]. As zinc cannot traverse cellular membranes, it has to rely on the help of families of zinc transporters. Interestingly, many members of the SLC39A family of zinc influx transporters have been implicated in various diseases of late, and increasingly many cancers. For many years zinc has been known to be essential for cell growth and health and perhaps the increase of intracellular zinc by increased expression or activity of SLC39A transporters may be able to explain the link with cancer.

Here we aim to give a general introduction of how zinc works in cells, explaining the role of different zinc transporters before relating these to alterations on cancer growth and development. Additionally we address how discoveries concerning zinc transporters at the molecular level have provided potential new biomarkers and treatments for cancer.

2. ZINC HANDLING IN CELLS

2.1. Long Term and Short Term Effects of Zinc in Cells

Zinc in the human body is normally classified as free labile zinc, or protein-bound Zn(II). Most of the cytoplasmic zinc is bound to proteins with free zinc in nanomolar amount [2]. Zinc is an essential structural component of proteins such as transcription factors, and hence involved in RNA transcription and DNA synthesis [3]. The role of zinc in gene expression is also evident as zinc is required for more than 200 transcription factors [4]. Zinc is tightly bound to enzymes such as RNA polymerase [5], where it creates a link between histidine and cysteine domains in the polypeptide chain [6].

Apart from being essential as a structural component of proteins, zinc is also involved in cell signalling by regulating the activity of molecules such as protein kinases and phosphatases [7]. Zinc signalling involves the change of zinc concentrations which occurs in response to certain stimuli and can be either extracellular or intracellular. Extracellular zinc signalling has been widely investigated in

synaptic transmission where zinc has been demonstrated to act as a neuromodulator [1]. Intracellular zinc signalling necessitates the involvement of zinc transporters [8] to enable its transport across biological membranes and will be described in more detail below. Intracellular zinc signalling can be further divided into "fast" and "late" zinc signalling. The 'fast' signalling does not involve gene transcription [9], happens within minutes of a stimuli and provides a good demonstration of zinc acting as a second messenger [10]. In contrast, the "late" zinc signalling requires the expression of zinc transport proteins upon an external stimulus such as cytokines or lipopolysaccharide [11] and it therefore occurs within hours of the stimulus. The availability of zinc transport proteins is an important aspect of zinc homeostasis which needs to be tightly controlled in order for the zinc(II) to move between cellular compartments.

2.2. Zinc Transporters and Intracellular Zinc Homeostasis

Zinc cannot pass through membranes passively, hence its homeostasis relies on zinc transporter proteins which can be controlled by different mechanisms. There are two families of zinc transporters: the SLC30A (ZnT transporters) and SLC39A (ZIP transporters) [12]. While the ZnT transporters are zinc exporters as they transport zinc from the cytoplasm to the outside of cells or to the inside of intracellular stores, the members of the ZIP family are zinc importers as they transport zinc into the cytoplasm from outside the cell or from the intracellular stores [13].

ZnT transporters work as Zn^{2+}/H^{+} exchangers [14] and their family comprises 10 members that are divided into three subfamilies [15]. They all have six trans-

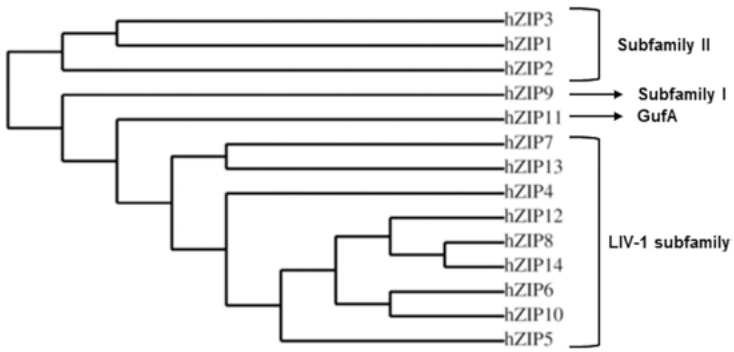

Figure 1. Phylogenetic tree of the human ZIP family (SLC39A) of zinc transporters. The human sequences of the ZIP family members have been processed in FASTA format and aligned using ClustalW5 tool (Swiss Institute of Bioinformatics). The analysis of the phylogenetic tree reveals that the ZIP family is divided into 4 main subfamilies: subfamily I (ZIP9), subfamily II (ZIP1, ZIP2, ZIP3), GufA (ZIP11), and LIV-1. The LIV-1 subfamily is the biggest of the family and it contains 9 members (ZIP4, ZIP5, ZIP6, ZIP7, ZIP8, ZIP10, ZIP12, ZIP13, ZIP14). The phylogenetic tree has been obtained using Phylogeny.fr web service [128].

Figure 2. Sequence alignment of the human LIV-1 family of ZIP transporters. The amino acid alignment shows the regions from the start of the transmembrane domains to the C-terminal end of the proteins and was performed using Clustal Omega within the EMBL-EBI framework [129].

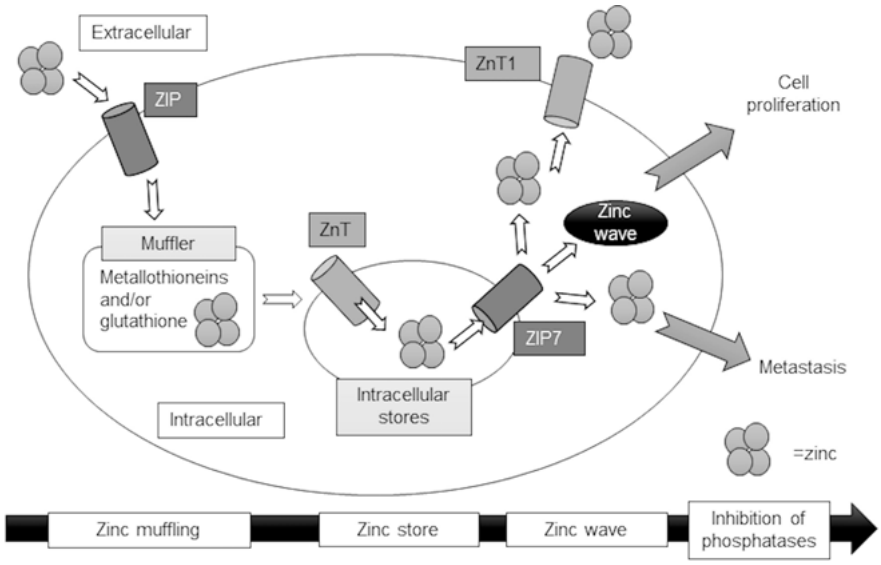

Figure 3. Intracellular zinc handling in cells. Zinc mobilization in cells has been described by a "muffler hypothesis" which involves proteins such metallothioneins and/or glutathione binding most of the cytoplasmic zinc as soon as zinc enters the cell. Zinc is then sequestered inside intracellular stores, probably by a ZnT transporter [23] and released into the cytoplasm following ZIP7 activation [98]. The "zinc wave" induced by ZIP7 activation is implicated in inhibition of phosphatases which lead to cell proliferation and metastasis [26].

membrane (TM) domains with both the N-terminal and C-terminal domains in the cytoplasm as well as a large cytoplasmic loop between TM IV and TM V [16]. Of all the ZnT transporters, only ZnT1 resides on the plasma membrane, whilst all the others are located on intracellular membranes [17].

The SLC39A family of zinc importers consists of 14 members divided into 4 subfamilies (Figure 1). The LIV-1 subfamily is the largest one, containing 9 members in total [18]. In recent years more evidence has accumulated showing how the aberrant expression of this family is implicated in a significant number of diseases, suggesting their important role in normal cell function. All the members of the SLC39A family are predicted to have eight transmembrane domains with an N- and C-terminal outside the cytoplasm and a large cytoplasmic loop (Figure 2). Most of the members of this family have a large number of histidine residues which are likely to be involved in the transport of zinc [18]. Moreover, the members of the LIV-1 subfamily have more histidine residues on the N-terminal domain and the extracellular loop between TM II and TM III, the exact role of which needs further characterization. The LIV-1 subfamily also contains an additional conserved motif in TM V.

This conserved motif HEXPHEXGD (where X stands for any amino acid) is similar to the consensus motif of the matrix metalloproteases that require zinc [18]. While most of the members of the LIV-1 subfamily reside on the plasma

membrane and transport zinc to the inside of cells, ZIP7 is situated on the endoplasmic reticulum membrane [19] and transports zinc from this store into the cytoplasm [20] and ZIP13 resides on Golgi membranes transporting zinc from this store [21].

The amount of labile free zinc inside the cells is in the region of low nanomolar amounts [2] because most of the cytoplasmic zinc is normally bound to proteins and in particular metallothioneins [12]. Metallothioneins are cysteine-rich proteins that play a pivotal role in zinc buffering and are also the main zinc supplier for redox reactions [22]. While the buffering reactions are necessary to maintain the cytosolic free zinc concentration in the order of picomolar under steady-state conditions, the muffling ones occur under non-steady state conditions [22]. The muffler hypothesis suggests that zinc entering the cells through a ZIP transporter is buffered in a muffler such as metallothioneins before being stored in internal compartments or removed from the cells, probably by a ZnT transporter. This mechanism is highly regulated by the ability of zinc to bind to these proteins [23] (Figure 3).

2.3. Emergence of Zinc Signalling Mechanisms

Zinc has a widespread role in cellular functions [24], and in particular for the function of several enzymes. In fact, it is estimated that almost 10 % of human genes contain zinc-binding motifs [25]. Its mobilization in cells has been described as a "zinc wave" [10], due to the rapid change of its concentrations in response to certain stimuli and the downstream effect followed by its release. This evidence was first seen in mast cells where zinc has a high affinity for the immunoglobin E receptor [10] resulting in zinc release from intracellular stores such as the endoplasmic reticulum. This zinc wave mechanism relies on calcium signalling and activation of mitogen-activated protein (MAP) kinase and it is responsible for the inhibition of a broad number of phosphatases [26]. The ability of zinc to inhibit phosphatases has a severe impact in all the pathways which require the activation of proteins such as tyrosine kinase receptors, normally involved in driving cancer or acquired resistance to treatments. In fact, the inhibition of phosphatases results in these pathways being continuously activated. In addition to phosphatase inhibition, zinc is involved in many other signalling molecules such as Ca/calmodulin-dependent protein kinase II, protein kinase C (PKC), and caspase 3 [27, 28]. For this reason, zinc is now considered a second messenger [10]. It is therefore important that zinc homeostasis is tightly controlled as both an excess and a deficiency can be harmful for human health [29]. For example, zinc deficiency has been associated with impaired growth [30] whereas a zinc excess can be toxic to cells [31] leading to apoptosis or programmed cell death [32].

Moreover, our group has been investigating for many years the role of zinc in driving anti-hormone resistance to endocrine treatment in estrogen receptor-positive breast cancer. The ability of zinc to inhibit phosphatases in these circumstances leads to the lack of inactivation of molecules such as Src, HER2 or

EGFR, which are known to be important drivers of the development of endocrine resistance in breast cancer [33]. We have indeed shown in previous studies how our model of tamoxifen-resistant breast cancer has a higher content of zinc [20] and increased expression of ZIP7 yet no other zinc transporters [34] suggesting a role for zinc in driving endocrine resistance. This will be described in more detail in Section 5.1.

3. ZINC IN CANCER

Zinc has been widely studied for many years for its role in human disease such as hypogonadism and dwarfism [35, 36], immune disorders [9], and neurodegeneration [37]. However, recent evidence suggests that it also has an important role in a variety of cancers.

The literature provides somewhat conflicting results regarding the levels of circulating zinc as a biomarker for cancer status. Serum and plasma zinc have been shown to be decreased in carcinomas of the head and neck [38], breast [39], lung [40], gastrointestinal tract [41], liver [42], gallbladder [43], and female reproductive system [44, 45]. Other studies have found increased circulating zinc in patients with breast, lung, stomach, or prostate cancer [46]. This conflict in results may be due in part to the different methods that were used to analyse the zinc. Further work is currently ongoing to try to establish a reliable marker of zinc status that can be used to examine further the relationship between zinc status and cancer states.

Zinc concentration has also been measured in hair, and shown to be decreased in patients with ovarian cancer [47] and lung cancer [48]. The results for these studies are less varied than the measurements in serum or plasma, though this is probably a reflection of the small sample size.

Arguably the most compelling evidence for the role of zinc in different cancers can be drawn from concentrations measured directly in tumor tissue, when compared with healthy tissue. The data appears to be less conflicting, and implicates the dysregulation of zinc as a second messenger, at a cellular level, as opposed to having a systemic role.

3.1. Elevated Zinc Levels in Breast Cancer

As described above, there is conflicting evidence about the circulating concentrations of zinc in breast cancer. While some studies have measured decreased serum zinc [47, 49, 50, 51], some have shown an increase [52], and others have shown that there is no difference at all [53]. Measurements from actual breast tumor tissue, however, consistently show significantly increased zinc compared to normal breast tissue [54], with the measured amount sometimes double that of benign breast tissue [55, 56], which itself has been shown to have an increased concentration [57]. It has been suggested that zinc could be a reliable biomarker

for breast cancer, as the concentration found in the tumor tissue correlates well to the histological malignancy grade [58].

Data regarding increased zinc concentrations in breast tumors can also be replicated experimentally *in vivo*. Commonly, N-methyl-N-nitrosourea (MNU) is used to induce mammary tumorigenesis in rats, and the resulting zinc concentration in the tumors is up to 19-fold increased when compared to zinc in the normal mammary tissue [59], regardless of dietary zinc intake.

Breast cancers are usually treated with anti-estrogens such as tamoxifen to reduce their growth. This treatment works well until the cancer develops resistance to tamoxifen, resulting in a more aggressive phenotype as a direct result of harnessing alternative signalling pathways such as EGFR and IGF-1R [33]. Our group has developed tamoxifen-resistant breast cancer cell lines [60] to investigate these aggressive mechanisms and have discovered that they have a two-fold increase in intracellular zinc as measured by the zinc dye Newport Green [20], implicating a role for the trace element in the development of the more aggressive phenotypes of the disease.

In parallel, increased expression of the heavy metal-binding protein, metallothionein (MT) has also been observed in breast cancer [55], further supporting the data which suggests there is more zinc in breast cancer tissue.

3.2. Zinc Involvement in Other Cancers

Zinc has a known role in male fertility, and sperm release and motility [61], and the prostate is a gland with one of the highest concentrations of zinc in the body [62]. Zinc measurements in prostate cancer appear to be in direct opposition to those observed in breast cancer; it is decreased in malignant prostate tissue compared to the healthy tissue [63]. Circulating zinc in these patients is also reduced, while patients with benign prostate disease have significantly elevated zinc [64].

The fact that zinc concentration in the prostate is significantly decreased in malignant prostate cancer is supportive of the data from many studies which suggests a chemo-protective role for zinc in the prostate. Zinc in this gland spares citrate from the citric acid cycle by inhibiting m-aconitase, allowing high amounts of citrate into the prostatic fluid [63]. Loss of this inhibitory effect causes oxidative phosphorylation, suggesting a protective role for zinc in the prostate. This is supported by zinc-deficient prostate epithelial cells having increased DNA damage. A further role for zinc in the prostate is the pro-apoptotic environment it produces [65]. Zinc directly induces bax-mediated mitochondrial cytochrome *c* release, activating the caspase cascade, ultimately leading to apoptotic cell death [66]. Zinc deficiency observed promotes cell survival by inhibiting apoptosis. While one study found a positive role for zinc supplementation in the prevention of prostate cancer [67], others have shown that a daily dose of over 100 mg for 10 years can double the chance of developing the disease [68], and a further study showed no association at all [69]. Clearly the role of zinc in prostate cancer is a complex one.

Like in prostate cancer, zinc has been shown to be significantly decreased in kidney carcinoma [54] which is perhaps a surprising result taken that zinc is not especially high in normal kidney. However, it does indicate that little is known yet about the effect of zinc levels on cancer and indeed the effect of cancer on zinc levels.

Some evidence suggests chemo-protective properties of zinc(II) in cancers [70] including those of colon, pancreas, esophageal, and head and neck [71, 72, 73] and the down-regulation of some DNA repair genes in zinc-depleted cells [74] which may be assumed to lead to cancer development. *In vivo* studies have shown that zinc supplementation prevents the development of cisplatinum- and melphalan-induced lung cancers in mice [75], 1,2-dimethylhydrazine-induced colon cancer in rats [76], and N-nitrosomethylbenzylamine (NMBA)-induced esophageal cancer in zinc-deficient rats [77]. It is interesting to speculate that lower serum zinc may be consistent with an increased requirement of cancer tissues for zinc but this theory is still currently unproven.

3.3. ZIP Transporters in Cancer

As we have described, there is much evidence to suggest that there is a link between zinc and cancer. One way to study zinc and the relevant signalling pathways that it can mobilize has been to look at the ZIP transporters in relation to cancer. Figure 4 demonstrates which ZIP transporters have been associated

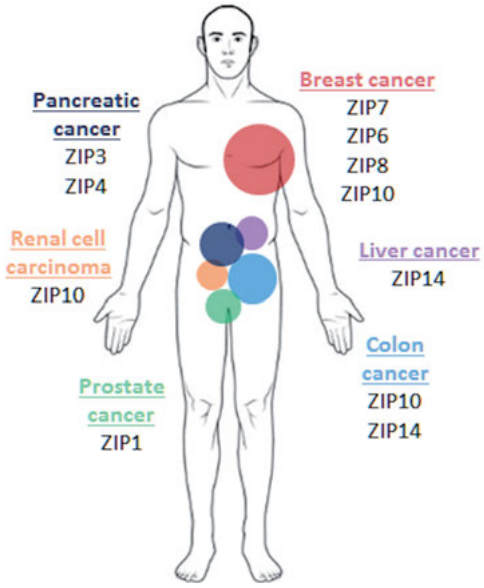

Figure 4. Schematic showing the members of the LIV-1 family of ZIP transporters and the different cancers in which they have been implicated.

with which different cancers. All the ZIP transporters currently linked to these cancers are members of the LIV-1 family of ZIP transporters.

We have previously demonstrated that ZIP7 and ZIP8 expression is elevated in anti-hormone resistant breast cancer models [34] suggesting a need for increased intracellular zinc. Additionally, we discovered that ZIP7 is one of the top 10 % genes overexpressed in breast cancers with poor clinical outcome [34], suggesting a role for ZIP7 in driving the aggressive growth of these cancers. ZIP7 is also positively correlated with the proliferation marker Ki67 in clinical breast cancer samples with lymph node involvement [34], confirming an association with the aggressive cells (Figure 5).

ZIP6 (also known as LIV-1) was originally discovered to be an estrogen-regulated gene associated with estrogen receptor-positive disease [78]. This association of ZIP6 with breast cancer was particularly important as ZIP6 was present in increased levels when the breast cancers were associated with metastatic spread to the lymph nodes [79]. The reliable association of ZIP6 with estrogen has made it a useful marker for estrogen receptor-positive luminal A breast cancer [80, 81]. Our investigations into ZIP6 function have revealed it to be causative in epithelial to mesenchymal transition [82], utilizing transcription factor Snail to produce loss of E-cadherin, causing cell rounding and detachment which is maintained in an anoikis-resistant manner. Elevated ZIP6 expression has also been linked to tumor size and degree of lymphatic infiltration in human pancreatic cancer cells [83] via the same mechanism as observed in breast cancer.

ZIP10, the closest paralogue to ZIP6 in the LIV-1 family of ZIP transporters [18, 84], has also been linked to invasive breast cancer [85]. Although ZIP10 has lower expression levels than ZIP6, it too has a positive correlation with the estrogen receptor [34]. ZIP10 over-expression has also been correlated to aggressiveness in renal cell carcinoma [86], and is one of the 7 genes upregulated in activated colon tumor cells.

ZIP4 is overexpressed in over 90 % of pancreatic adenocarcinomas. Experimental knockdown of ZIP4 using siRNA inhibits pancreatic tumor growth [87], and increases survival of mice with this disease. In hepatocellular carcinoma, ZIP4 has been linked to intracellular zinc accumulation, and progression through the cell cycle [88]. Furthermore, overexpression of ZIP4 results in increases in the expression of pro-metastatic genes MMP-2 and MMP-9, while decreasing expression of the pro-apoptotic genes caspase-3, caspase-9, and Bax [89].

Hepatocellular carcinoma [90] and colorectal cancer [91, 92] have both been linked to ZIP14, the latter identifying splice variants which have a role in the disease.

Much of the literature suggests a role for the LIV-1 family of ZIP transporters in different cancers, however, some of the other transporters have also been associated. ZIP1 is a known tumor suppressor gene in prostate cancer [93], and there is reduced expression in the peripheral zone of the prostate, the most common site of cancer. This explains the decreased levels of zinc observed in these patients, described earlier in this chapter. Additionally, ZIP1 overexpression reduces the metastatic ability of prostate cancer cells [94].

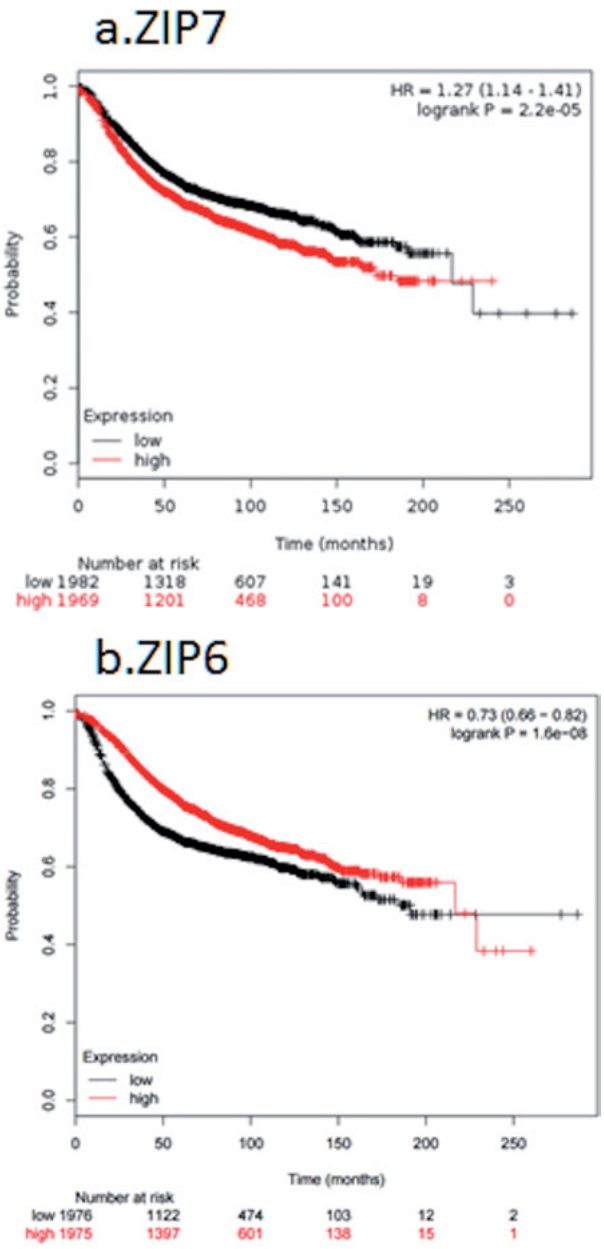

Figure 5. Kaplan-Meier plotter analysis of relationship between relapse free survival in a cohort of breast cancer patients following endocrine therapy or chemotherapy, and ZIP7 and ZIP6 expression. Increased ZIP7 decreases relapse free survival up to 10 years suggesting that it may be important in driving cancer growth (Figure 5a). In contrast, although there is no significant difference in relapse free survival for low or high ZIP6 values (Figure 5b), there is a suggestion that high levels of ZIP6 may be beneficial for as long as 8 years.

Another member of the ZIP subfamily I, ZIP3, has also been implicated in the early development of pancreatic adenocarcinoma. ZIP3 is significantly decreased in pancreatic intraepithelial neoplasia, thought to be the precancerous lesion which leads to adenocarcinoma [95]. This is coupled with the significant loss of zinc in both pre-cancerous and cancerous pancreatic tissue.

All this evidence together suggests a clear association of ZIP transporters and cancers. What remains to be elucidated is the exact signalling mechanisms that these transporters are involved in and whether they can be targeted as a potential cancer drug target.

4. ZINC SIGNALLING IN CANCER

We have demonstrated that there is a link between zinc, ZIP transporters, and cancer. The rest of this section will focus on zinc signalling as a second messenger downstream of ZIP transporters.

4.1. How Zinc Signalling Mechanisms Drive Cancer Growth

Zinc has been shown to activate receptor tyrosine kinases through the inhibition of phosphatase PTP1B [96, 97]. Given that this phosphatase has been linked with EGFR, IGF-1R, and Src, it is understandable how the increased zinc concentration in the TAMR cells leads to constitutively active cell proliferation pathways, and a more aggressive phenotype.

As described in Section 3, ZIP7 has been linked with breast cancer, and particularly anti-hormone resistant breast cancer. Our group demonstrated that ZIP7 is activated by phosphorylation of two adjacent serine residues (S275 and S276), present in the long cytoplasmic loop between TMD III and IV [98]. Phosphorylation triggers ZIP7-mediated release of zinc from intracellular stores, and activates downstream pathways including ERK1/2 and AKT, leading to cell proliferation and migration [20]. Casein kinase 2 (CK2) was identified as the kinase responsible for ZIP7 activation, which is itself involved in proliferation and oncogenesis [99].

MCF7-derived tamoxifen-resistant (TAMR) cells overexpress ZIP7, and demonstrate a more aggressive phenotype [100] than MCF7s. This highlights the potential of ZIP7 as a regulator of zinc-induced tumor progression. Zinc release from stores is responsible for activation of epidermal growth factor receptor (EGFR) [60], insulin growth factor receptor (IGF-1R) [101] and the non-receptor tyrosine kinase Src [20, 102] which is independently linked with aggressive cancer phenotypes [103]. Presence of ZIP7 siRNA prevents zinc-dependent activation of these pathways [20]. Clinically, agents which have been linked with poor outlook in breast cancer such as ki67, ErbB3, and STAT3, have been correlated to ZIP7 mRNA expression [34].

Given the data regarding the role of ZIP7 in aggressive, anti-hormone resistant breast cancer cells, it is possible that this zinc transporter could be used as a

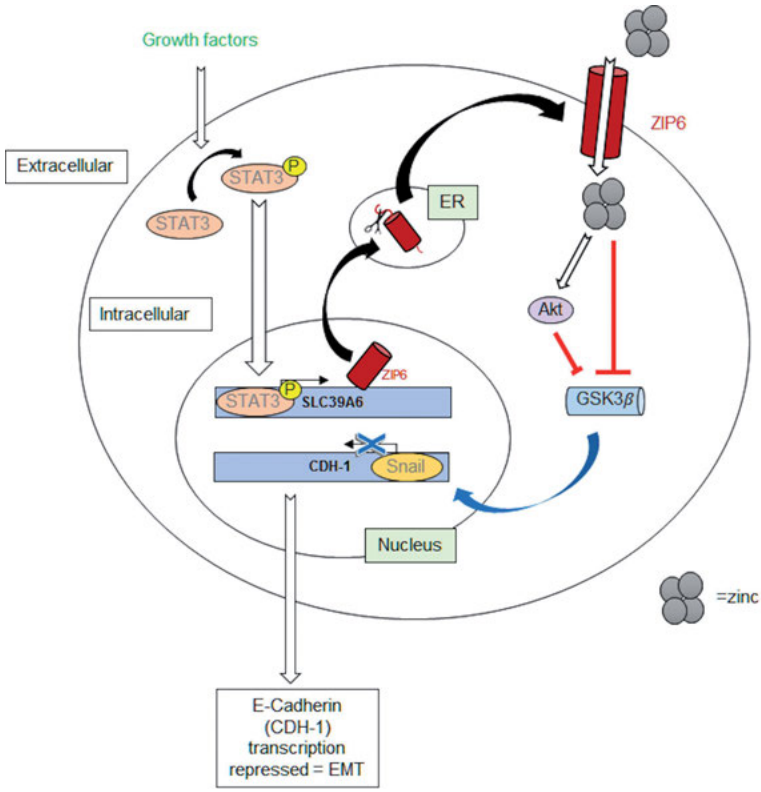

Figure 6. Schematic demonstrating the role of the STAT3/ZIP6 pathway in EMT. Transcriptional activation of ZIP6 by STAT3 causes zinc-dependent activation of Akt, and inhibition of GSK-3β. This causes nuclear retention of transcription factor Snail, and therefore repression of E-cadherin (CDH-1) transcription, leading to cell detachment and EMT.

target for treatment. Up to 40 % of estrogen receptor-positive breast cancers will become resistant to tamoxifen [104], highlighting the need for a new treatment in this cohort of patients. In addition, CK2 could also be a potential target because of its role in activating ZIP7. Previous work has shown the ability of the CK2 inhibitor 2-dimethylamino-4,5,6,7-tetrabromo-1H-benzimidazole (DMAT) to cause tamoxifen-resistant cells to die by apoptosis [105].

ZIP6 is expressed as a pro-protein, following transcriptional activation by STAT3 [82] which has a known role in metastasis in breast cancer [106]. Upon activation, ZIP6 is cleaved in the N-terminus, relocates from the endoplasmic reticulum to the plasma membrane, and allows zinc entry into the cell [107]. Zinc inhibits GSK-3β [108] and/or activation of Akt [109, 110] resulting in loss of E-cadherin gene expression [111], cell detachment and epithelial to mesenchymal transition (EMT), through nuclear retention of transcription factor Snail [82]. In addition, Snail is negatively regulated by GSK-3β-mediated phosphoryla-

tion, promoting nuclear export and degradation [112]. This pathway is demonstrated in the schematic Figure 6. This data is supported by the discovery that ZIP6 is required for EMT in zebrafish gastrulation, by promoting the nuclear localization of transcription factor Snail [113]. Furthermore, both STAT3 and Snail have a proven role in tumor progression, and STAT3 has a positive correlation with ZIP6 expression in breast cancer [34]. This mechanism is supported by the finding that ZIP6 in liver cancer cells has an inverse relationship with expression of E-cadherin [114].

ZIP10, the closest paralogue to ZIP6, is the only other ZIP transporter which contains a potential PEST cleavage site [115] in its N-terminus. ZIP10 and ZIP6 form a heteromer at the plasma membrane, and together they regulate cell migration and embryogenesis [84]. Furthermore, ZIP10 deficiency leads to overexpression of STAT3 and ZIP6, implicating a negative feedback loop to maintain the EMT process in these cells.

Zinc signalling through ZIP6 and STAT3 in breast cancer has similarities to ZIP4 and pancreatic cancer [116]. An increase in interleukin 6 (IL-6) activates STAT3, leading to cell proliferation and tumor progression.

5. TARGETING ZINC SIGNALLING MECHANISMS IN CANCER

The fact that a variety of zinc transporters have been implicated in various cancers does suggest that they may be a worthwhile cancer target. This is an emerging area of investigation as currently there is not much known about the function of individual zinc transporters and once more data is available then there will be new opportunities for targeting.

5.1. Phosphorylated ZIP7 as a Cancer Biomarker

ZIP7 is located on the endoplasmic reticulum membrane and is ubiquitously expressed [19], making it a gatekeeper of intracellular zinc release [117]. A recent study in our group has discovered that ZIP7 activation is due to the phosphorylation on two serine residues (S275 and S276) located in the long cytoplasmic loop between TM III and IV by protein kinase CK2 [98]. This study also confirmed that ZIP7 activation is immediately followed by activation of mitogen-activated protein kinase and tyrosine kinase signalling pathways, many of which have been implicated in cancer progression and therefore positioning CK2 and ZIP7 at a hub of zinc release [118]. Furthermore, all these activated kinases are targets of the phosphatases that zinc(II) is known to inhibit [26], potentially providing the mechanism of action.

As we mentioned above, our group has discovered that our unique model of tamoxifen-resistant breast cancer cells has increased expression of ZIP7 [34] along with a higher content of zinc [20]. Moreover, we have shown that treat-

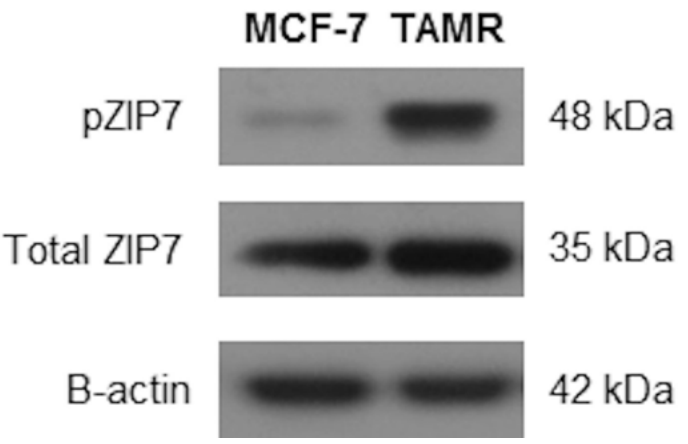

Figure 7. Increased activated ZIP7 in TAMR cells. Western blot analysis of MCF-7 and tamoxifen-resistant-MCF-7 (TAMR) derived cells using our unique anti-phospho ZIP7 antibody [119] reveals a significant increase of activated ZIP7 in the TAMR cells when compared to the total amount of ZIP7.

ment of these cells with exogenous zinc(II) leads to the activation of several pathways such as EGFR, IGF1-R, MAPK, Akt or Src, resulting in activation of tyrosine kinases, which explains the development of their more aggressive phenotype [20]. Interestingly, this mechanism relies on ZIP7 mediated zinc release from the endoplasmic reticulum which was demonstrated by the use of fluorescent zinc dyes such as Newport Green, Zinquin or Fluozin-3 [20, 98]. This ZIP7-mediated downstream pathway fits with the "zinc wave" mechanism explained above, as this effect was abolished when using siRNA directed against ZIP7 [20].

Furthermore, in our group we have generated other models of anti-hormone resistant breast cancer cells. We have MCF7-derived Faslodex resistant cells and also cells with long term resistance to tamoxifen and Faslodex, which represent additional acquired resistance to endocrine treatment in order to better reflect the variable clinical situation. By using our unique anti-phospho ZIP7 antibody (pZIP7), which only recognizes ZIP7 when phosphorylated on residues S275 and S276 [119], we have demonstrated that all these anti-hormone resistant breast cancer cells have increased activation of ZIP7, in particular in TAMR cells (Figure 7). This evidence would explain the development of their aggressive phenotype and their acquired resistance to the treatment whose mechanism is not yet fully understood. This discovery suggests that the use of activated ZIP7 may be a valuable biomarker for estrogen receptor-positive breast cancer and will help distinguish those cancers that develop resistance to current endocrine therapies, allowing for additional treatments. Furthermore, this ability of pZIP7 to act as a biomarker for aggressive cancers suggests that it may also be a worthwhile new target for therapy.

5.2. ZIP7 as a Cancer Target

The "zinc wave" mechanism which involves ZIP7 has several consequences in diseases such as cancer which relies on aberrant activation of many tyrosine kinases and that often show an increased level of zinc. This implicates ZIP7 as a potential target for inhibition of tyrosine kinases and their consequent downstream pathways in diseases such as cancer. ZIP7 has indeed been demonstrated to be one of the top 10 % genes to be overexpressed in cancers with poor prognosis [117]. Furthermore, in a recent study we have demonstrated that ZIP7-mediated zinc release is implicated in the activation of several pathways such as mTOR, PI3K-Akt, and MAPK, which are all involved in cell proliferation and cell survival [119].

The discovery that ZIP7 requires phosphorylation to be activated and release zinc, opens the door to further investigations targeting its activation. This involves the production of new agents that act as inhibitors of the signalling pathways induced by zinc which drives the aggressiveness of cancer. In particular, the discovery that ZIP7 activation is induced by protein kinase CK2 phosphorylation on S275 and S276 [98], suggests the use of CK2 inhibitors in order to prevent the zinc release from stores. Protein kinase CK2 is a ubiquitous serine/threonine kinase [120] which has several cellular targets and it has a known role in cell survival and proliferation [121]. CK2 levels are also raised in different cancers, suggesting its role as a potential target for treatment.

Taken together, the data suggests that both ZIP7 and CK2 play an important role in cell survival. In fact, targeting ZIP7-mediated zinc release in breast cancer has been shown to decrease invasion, signalling, and growth [20]. One specific CK2 inhibitor, called CX-4945, is under investigation in clinical trials [122] and it has been recently demonstrated to be a potential new treatment for leukemia [123] and glioblastoma [124]. Moreover, CK2 inhibitors have been shown to be beneficial in decreasing the viability of other cancer cells, such as prostate cancer and tamoxifen-resistant MCF-7 breast cancer cells [105]. In light of this data, targeting ZIP7-mediated zinc release could be beneficial in diseases such as anti-hormone resistant breast cancer, but also in other diseases which involve multiple signalling pathways that are kept continuously activated by the ability of zinc to inhibit phosphatases [26], and activate many other molecular signalling pathways [119].

5.3. ZIP6 and ZIP10 as Cancer Targets

ZIP6 was the first member of the LIV-1 subfamily to be discovered and it is known to be an estrogen-regulated gene [78] involved in metastatic breast cancer [79]. Furthermore, it is a marker of luminal A breast cancer [80] and is associated with STAT3 in breast cancer samples [34]. In a recent study we have demonstrated that ZIP6 is expressed as a pro-protein in the endoplasmic reticulum before being cleaved and relocated to the plasma membrane, where it can act as a zinc importer [82]. In particular, ZIP6 is enriched in the plasma membrane of migra-

tory cells and causative of an EMT mechanism and anoikis resistance [82]. The influx of zinc mediated by ZIP6 has been demonstrated to lead to the phosphorylation of GSK-3β, a kinase which is normally involved in the phosphorylation and inactivation of Snail, a transcription factor implicated in cell proliferation. In fact, the phosphorylation of GSK-3β induced by ZIP6-mediated zinc influx enables its inactivation, resulting in retention of Snail in the nucleus, where it acts as a repressor of E-cadherin, promoting cell rounding and detachment [82].

Figure 1 shows the phylogenetic tree of the LIV-1 subfamily demonstrating the close association of ZIP6 and ZIP10. Similar to ZIP6, ZIP10 is associated with metastatic breast cancer [85] and its expression and role in zinc homeostasis involves a STAT3 mechanism, suggesting that ZIP10 is also likely to be involved in cancer progression.

Furthermore, we have recently discovered that ZIP6 and ZIP10 form a heteromer [84], exemplifying a similar role for these two zinc transporters in cancer cells. Zinc is already known to be essential for the function of several cyclins and for cell cycle regulation [125] suggesting a role for zinc influx transporters in this process. Considering the association of both ZIP6 and ZIP10 with the process of EMT and metastatic cancer, there is now more evidence that targeting zinc transporters may be useful for preventing aberrant cell growth. Furthermore, since ZIP6 is able to cause cell rounding and detachment utilizing anoikis resistance it may be a valuable target to prevent metastasis from the original tumor. There is already evidence of an antibody-drug conjugate called SGN-LIV1A for targeting ZIP6 in metastatic breast cancer which is under clinical trials [126] that gives hope to a new concept of immune treatment for cancer.

6. GENERAL CONCLUSIONS

This is an exciting time in zinc(II) biology with new details of the molecular function of individual zinc transporters appearing on a regular basis. The more that is discovered about how these key molecules work the more chance we will have of finding new therapeutic targets for various cancers. Unfortunately, until there is a crystal structure for the SLC39A family of zinc transporters, it will be difficult to generate specific small-molecule inhibitors. However, progress is being made in this area with the recent discovery of the structure of the extracellular domain of ZIP4 [127] enabling potential inhibitors to be generated.

ACKNOWLEDGMENTS

This work was supported by a Wellcome Trust University Research Award [grant number 091991/Z/10/Z]. SZ is supported by Tenovus Cancer Care [grant number PhD2015/L31]. OO is supported by a PhD scholarship from the Life Sciences Research Network Wales. OO, SZ, and KMT are members of the European COST action ZINC-NET.

ABBREVIATIONS AND DEFINITIONS

Akt	protein kinase B
CK2	casein kinase 2
EGFR	epidermal growth factor receptor
EMT	epithelial to mesenchymal transition
ERK1/2	extracellular signal-regulated kinases 1/2
GSK-3β	glycogen synthase kinase 3β
HER2	human epidermal growth factor receptor 2
IGF1-R	insulin-like growth factor 1 receptor
IL-6	interleukin 6
MAPK	mitogen-activated protein kinase
MMP	matrix metalloproteinase
mRNA	messenger RNA
mTOR	mammalian target of rapamycin
PI3K	phosphoinositide 3-kinase
pZIP7	anti-phospho ZIP7
siRNA	small interfering RNA
Src	sarcoma-family kinase
STAT3	signal transducer and activator of transcription 3
TAMR	tamoxifen-resistant MCF-7 cells
TMD	transmembrane domain

REFERENCES

1. C. J. Frederickson, J. Y. Koh, A. I. Bush, *Nat. Rev. Neurosci.* **2005**, *6*, 449–462.
2. W. Maret, *Biometals* **2011**, *24*, 411–418.
3. A. S. Prasad, D. Oberleas, *J. Lab. Clin. Med.* **1974**, *83*, 634–639.
4. E. John, T. C. Laskow, W. J. Buchser, B. R. Pitt, P. H. Basse, L. H. Butterfield, P. Kalinski, M. T. Lotze, *J. Transl. Med.* **2010**, *8*, 118.
5. F. Y. Wu, W. J. Huang, R. B. Sinclair, L. Powers, *J. Biol. Chem.* **1992**, *267*, 25560–25567.
6. B. L. Vallee, D. S. Auld, *EXS* **1995**, *73*, 259–277.
7. H. Haase, W. Maret, *Exp. Cell Res.* **2003**, *291*, 289–298.
8. T. Hirano, M. Murakami, T. Fukada, K. Nishida, S. Yamasaki, T. Suzuki, *Adv. Immunol.* **2008**, *97*, 149–176.
9. H. Haase, L. Rink, *Annu. Rev. Nutr.* **2009**, *29*, 133–152.
10. S. Yamasaki, K. Sakata-Sogawa, A. Hasegawa, T. Suzuki, K. Kabu, E. Sato, T. Kurosaki, S. Yamashita, M. Tokunaga, K. Nishida, T. Hirano, *J. Cell Biol.* **2007**, *177*, 637–645.
11. T. Kambe, T. Tsuji, A. Hashimoto, N. Itsumura, *Physiol. Rev.* **2015**, *95*, 749–784.
12. L. A. Lichten, R. J. Cousins, *Annu. Rev. Nutr.* **2009**, *29*, 153–176.
13. T. Fukada, T. Kambe, *Metallomics* **2011**, *3*, 662–674.
14. E. Ohana, E. Hoch, C. Keasar, T. Kambe, O. Yifrach, M. Hershfinkel, I. Sekler, *J. Biol. Chem.* **2009**, *284*, 17677–17686.
15. L. Huang, S. Tepaamorndech, *Mol. Aspects Med.* **2013**, *34*, 548–560.
16. M. Seve, F. Chimienti, S. Devergnas, A. Favier, *BMC Genomics* **2004**, *5*, 32.

17. R. D. Palmiter, S. D. Findley, *EMBO J.* **1995**, *14*, 639–649.
18. K. M. Taylor, R. I. Nicholson, *Biochim. Biophys. Acta* **2003**, *1611*, 16–30.
19. K. M. Taylor, H. E. Morgan, A. Johnson, R. I. Nicholson, *Biochem. J.* **2004**, *377*, 131–139.
20. K. M. Taylor, P. Vichova, N. Jordan, S. Hiscox, R. Hendley, R. I. Nicholson, *Endocrinology* **2008**, *149*, 4912–4920.
21. T. Fukada, N. Civic, T. Furuichi, S. Shimoda, K. Mishima, H. Higashiyama, Y. Idaira, Y. Asada, H. Kitamura, S. Yamasaki, S. Hojyo, M. Nakayama, O. Ohara, H. Koseki, H. G. Dos Santos, L. Bonafe, R. Ha-Vinh, A. Zankl, S. Unger, M. E. Kraenzlin, J. S. Beckmann, I. Saito, C. Rivolta, S. Ikegawa, A. Superti-Furga, T. Hirano, *PloS One* **2008**, *3*, e3642.
22. R. A. Colvin, W. R. Holmes, C. P. Fontaine, W. Maret, *Metallomics* **2010**, *2*, 306–317.
23. R. A. Colvin, A. I. Bush, I. Volitakis, C. P. Fontaine, D. Thomas, K. Kikuchi, W. R. Holmes, *Am. J. Physiol. Cell Physiol.* **2008**, *294*, C726–742.
24. B. L. Vallee, K. H. Falchuk, *Physiol. Rev.* **1993**, *73*, 79–118.
25. A. Passerini, C. Andreini, S. Menchetti, A. Rosato, P. Frasconi, *BMC Bioinformatics* **2007**, *8*, 39.
26. H. Haase, W. Maret, *Biometals* **2005**, *18*, 333–338.
27. I. Lengyel, S. Fieuw-Makaroff, A. L. Hall, A. T. Sim, J. A. Rostas, P. R. Dunkley, *J. Neurochem.* **2000**, *75*, 594–605.
28. D. K. Perry, M. J. Smyth, H. R. Stennicke, G. S. Salvesen, P. Duriez, G. G. Poirier, Y. A. Hannun, *J. Biol. Chem.* **1997**, *272*, 18530–18533.
29. L. M. Plum, L. Rink, H. Haase, *Int. J. Environ. Res. Public Health* **2010**, *7*, 1342–1365.
30. A. S. Prasad, *Met. Ions Biol. Syst.* **2004**, *41*, 103–137.
31. J. E. Cummings, J. P. Kovacic, *J. Vet. Emerg. Crit. Care (San Antonio)* **2009**, *19*, 215–240.
32. P. J. Fraker, *J. Nutr.* **2005**, *135*, 359–362.
33. J. M. Knowlden, I. R. Hutcheson, D. Barrow, J. M. Gee, R. I. Nicholson, *Endocrinology* **2005**, *146*, 4609–4618.
34. K. M. Taylor, H. E. Morgan, K. Smart, N. M. Zahari, S. Pumford, I. O. Ellis, J. F. Robertson, R. I. Nicholson, *Mol. Med.* **2007**, *13*, 396–406.
35. J. A. Halsted, A. S. Prasad, *Isr. Med. J.* **1963**, *22*, 307–315.
36. K. H. Brown, J. M. Peerson, J. Rivera, L. H. Allen, *Am. J. Clin. Nutr.* **2002**, *75*, 1062–1071.
37. S. L. Sensi, P. Paoletti, A. I. Bush, I. Sekler, *Nat. Rev. Neurosci.* **2009**, *10*, 780–791.
38. J. Buntzel, F. Bruns, M. Glatzel, A. Garayev, R. Mucke, K. Kisters, U. Schafer, K. Schonekaes, O. Micke, *Anticancer Res.* **2007**, *27*, 1941–1943.
39. M. Kratochvilova, M. Raudenska, Z. Heger, L. Richtera, N. Cernei, V. Adam, P. Babula, M. Novakova, M. Masarik, J. Gumulec, *Prostate* **2017**.
40. N. Sattar, H. R. Scott, D. C. McMillan, D. Talwar, D. S. O'Reilly, G. S. Fell, *Nutr. Cancer* **1997**, *28*, 308–312.
41. A. Boz, O. Evliyaoglu, M. Yildirim, N. Erkan, B. Karaca, *Turk. J. Gastroenterol.* **2005**, *16*, 81–84.
42. M. Stepien, D. J. Hughes, S. Hybsier, C. Bamia, A. Tjonneland, K. Overvad, A. Affret, M. His, M. C. Boutron-Ruault, V. Katzke, T. Kuhn, K. Aleksandrova, A. Trichopoulou, P. Lagiou, P. Orfanos, D. Palli, S. Sieri, R. Tumino, F. Ricceri, S. Panico, H. B. Bueno-de-Mesquita, P. H. Peeters, E. Weiderpass, C. Lasheras, C. Bonet Bonet, E. Molina-Portillo, M. Dorronsoro, J. M. Huerta, A. Barricarte, B. Ohlsson, K. Sjoberg, M. Werner, D. Shungin, N. Wareham, K. T. Khaw, R. C. Travis, H. Freisling, A. J. Cross, L. Schomburg, M. Jenab, *Br. J. Cancer* **2017**, *116*, 688–696.
43. S. K. Gupta, S. P. Singh, V. K. Shukla, *J. Surg. Oncol.* **2005**, *91*, 204–208.

44. M. S. Naidu, A. N. Suryakar, S. C. Swami, R. V. Katkam, K. M. Kumbar, *Indian J. Clin. Biochem.* **2007**, *22*, 140–144.
45. H. Cunzhi, J. Jiexian, Z. Xianwen, G. Jingang, Z. Shumin, D. Lili, *Biol. Trace Elem. Res.* **2003**, *94*, 113–122.
46. S. A. Navarro Silvera, T. E. Rohan, *Cancer Causes Control* **2007**, *18*, 7–27.
47. A. U. Memon, T. G. Kazi, H. I. Afridi, M. K. Jamali, M. B. Arain, N. Jalbani, N. Syed, *Clin. Chim. Acta* **2007**, *379*, 66–70.
48. L. Piccinini, P. Borella, A. Bargellini, C. I. Medici, A. Zoboli, *Biol. Trace Elem. Res.* **1996**, *51*, 23–30.
49. M. J. Farquharson, A. Al-Ebraheem, K. Geraki, R. Leek, A. Jubb, A. L. Harris, *Physics in Medicine and Biology* **2009**, *54*, 4213–4223.
50. I. Yucel, F. Arpaci, A. Ozet, B. Doner, T. Karayilanoglu, A. Sayar, O. Berk, *Biol. Trace Elem. Res.* **1994**, *40*, 31–38.
51. S. K. Gupta, V. K. Shukla, M. P. Vaidya, S. K. Roy, S. Gupta, *J. Surg. Oncol.* **1991**, *46*, 178–181.
52. F. Cavallo, M. Gerber, E. Marubini, S. Richardson, A. Barbieri, A. Costa, A. DeCarli, H. Pujol, *Cancer* **1991**, *67*, 738–745.
53. A. S. Prasad, O. Kucuk, *Cancer Metastasis Rev.* **2002**, *21*, 291–295.
54. E. J. Margalioth, J. G. Schenker, M. Chevion, *Cancer* **1983**, *52*, 868–872.
55. R. Jin, B. Bay, P. Tan, B. K. Tan, *Oncol. Rep.* **1999**, *6*, 871–875.
56. P. M. Santoliquido, H. W. Southwick, J. H. Olwin, *Surg. Gynecol. Obstet.* **1976**, *142*, 65–70.
57. Y. Cui, S. Vogt, N. Olson, A. G. Glass, T. E. Rohan, *Cancer Epidemiol. Biomarkers Prev.* **2007**, *16*, 1682–1685.
58. D. Riesop, A. V. Hirner, P. Rusch, A. Bankfalvi, *J. Cancer Res. Clin. Oncol.* **2015**, *141*, 1321–1331.
59. W. Woo, Z. Xu, *Biol. Trace Elem. Res.* **2002**, *87*, 157–169.
60. J. M. Knowlden, I. R. Hutcheson, H. E. Jones, T. Madden, J. M. Gee, M. E. Harper, D. Barrow, A. E. Wakeling, R. I. Nicholson, *Endocrinology* **2003**, *144*, 1032–1044.
61. K. Yoshida, N. Kawano, M. Yoshiike, M. Yoshida, T. Iwamoto, M. Morisawa, *Mol. Hum. Reprod.* **2008**, *14*, 151–156.
62. V. Zaichick, T. V. Sviridova, S. V. Zaichick, *Int. Urol. Nephrol.* **1997**, *29*, 565–574.
63. L. C. Costello, R. B. Franklin, P. Feng, M. Tan, O. Bagasra, *Cancer Causes Control* **2005**, *16*, 901–915.
64. T. Goel, S. N. Sankhwar, *Scand. J. Urol. Nephrol.* **2006**, *40*, 108–112.
65. P. Feng, T. L. Li, Z. X. Guan, R. B. Franklin, L. C. Costello, *Prostate* **2002**, *52*, 311–318.
66. P. Feng, T. Li, Z. Guan, R. B. Franklin, L. C. Costello, *Mol. Cancer* **2008**, *7*, 25.
67. A. R. Kristal, J. L. Stanford, J. H. Cohen, K. Wicklund, R. E. Patterson, *Cancer Epidem. Biomarkers & Prevention* **1999**, *8*, 887–892.
68. M. F. Leitzmann, *J. Natl. Cancer Inst.* **2003**, *95*, 1004–1007.
69. E. T. Chang, M. Hedelin, H. O. Adami, H. Gronberg, K. A. Balter, *J. Natl. Cancer Inst.* **2004**, *96*, 1108; author reply 1108–1109.
70. A. S. Prasad, F. W. Beck, D. C. Snell, O. Kucuk, *Nutr. Cancer* **2009**, *61*, 879–887.
71. D. K. Dhawan, V. D. Chadha, *Indian J. Med. Res.* **2010**, *132*, 676–682.
72. E. Ho, *J. Nutr. Biochem.* **2004**, *15*, 572–578.
73. M. T. Leccia, M. J. Richard, A. Favier, J. C. Beani, *Biol. Trace Elem. Res.* **1999**, *69*, 177–190.
74. E. Ho, B. N. Ames, *Proc. Natl. Acad. Sci. USA* **2002**, *99*, 16770–16775.
75. M. Satoh, Y. Kondo, M. Mita, I. Nakagawa, A. Naganuma, N. Imura, *Cancer Res.* **1993**, *53*, 4767–4768.
76. V. Dani, A. Goel, K. Vaiphei, D. K. Dhawan, *Toxicol. Lett.* **2007**, *171*, 10–18.

77. L. Y. Fong, V. T. Nguyen, J. L. Farber, *J. Natl. Cancer Inst.* **2001**, *93*, 1525–1533.
78. D. L. Manning, R. A. McClelland, J. M. Gee, C. M. Chan, C. D. Green, R. W. Blamey, R. I. Nicholson, *Eur. J. Cancer* **1993**, *29A*, 1462–1468.
79. D. L. Manning, J. F. Robertson, I. O. Ellis, C. W. Elston, R. A. McClelland, J. M. Gee, R. J. Jones, C. D. Green, P. Cannon, R. W. Blamey, R. I. Nicholson, *Eur. J. Cancer* **1994**, *30A*, 675–678.
80. C. M. Perou, T. Sorlie, M. B. Eisen, M. van de Rijn, S. S. Jeffrey, C. A. Rees, J. R. Pollack, D. T. Ross, H. Johnsen, L. A. Akslen, O. Fluge, A. Pergamenschikov, C. Williams, S. X. Zhu, P. E. Lonning, A. L. Borresen-Dale, P. O. Brown, D. Botstein, *Nature* **2000**, *406*, 747–752.
81. S. Tozlu, I. Girault, S. Vacher, J. Vendrell, C. Andrieu, F. Spyratos, P. Cohen, R. Lidereau, I. Bieche, *Endocr. Relat. Cancer* **2006**, *13*, 1109–1120.
82. C. Hogstrand, P. Kille, M. L. Ackland, S. Hiscox, K. M. Taylor, *Biochem. J.* **2013**, *455*, 229–237.
83. J. Unno, K. Satoh, M. Hirota, A. Kanno, S. Hamada, H. Ito, A. Masamune, N. Tsukamoto, F. Motoi, S. Egawa, M. Unno, A. Horii, T. Shimosegawa, *Int. J. Oncol.* **2009**, *35*, 813–821.
84. K. M. Taylor, I. A. Muraina, D. Brethour, G. Schmitt-Ulms, T. Nimmanon, S. Ziliotto, P. Kille, C. Hogstrand, *Biochem. J.* **2016**, *473*, 2531–2544.
85. N. Kagara, N. Tanaka, S. Noguchi, T. Hirano, *Cancer Sci.* **2007**, *98*, 692–697.
86. D. Pal, U. Sharma, S. K. Singh, R. Prasad, *Gene* **2014**, *552*, 195–198.
87. M. Li, Y. Zhang, U. Bharadwaj, Q. J. Zhai, C. H. Ahern, W. E. Fisher, F. C. Brunicardi, C. D. Logsdon, C. Chen, Q. Yao, *Clin. Cancer Res.* **2009**, *15*, 5993–6001.
88. B. P. Weaver, Y. Zhang, S. Hiscox, G. L. Guo, U. Apte, K. M. Taylor, C. T. Sheline, L. Wang, G. K. Andrews, *PLoS One* **2010**, *5*.
89. C. Xu, M. B. Wallace, J. Yang, L. Jiang, Q. Zhai, Y. Zhang, C. Hong, Y. Chen, T. S. Frank, J. A. Stauffer, H. J. Asbun, M. Raimondo, T. A. Woodward, Z. Li, S. Guha, L. Zheng, M. Li, *Curr. Mol. Med.* **2014**, *14*, 309–315.
90. R. B. Franklin, B. A. Levy, J. Zou, N. Hanna, M. M. Desouki, O. Bagasra, L. A. Johnson, L. C. Costello, *J. Gastrointest. Cancer* **2012**, *43*, 249–257.
91. K. Thorsen, F. Mansilla, T. Schepeler, B. Oster, M. H. Rasmussen, L. Dyrskjot, R. Karni, M. Akerman, A. R. Krainer, S. Laurberg, C. L. Andersen, T. F. Orntoft, *Mol. Cell Proteomics* **2011**, *10*, M110 002998.
92. A. Sveen, A. C. Bakken, T. H. Agesen, G. E. Lind, A. Nesbakken, O. Nordgard, S. Brackmann, T. O. Rognum, R. A. Lothe, R. I. Skotheim, *Int. J. Cancer* **2012**, *131*, 1479–1485.
93. L. C. Costello, R. B. Franklin, *Mol. Cancer* **2006**, *5*, 17.
94. K. Golovine, P. Makhov, R. G. Uzzo, T. Shaw, D. Kunkle, V. M. Kolenko, *Clin. Cancer Res.* **2008**, *14*, 5376–5384.
95. L. C. Costello, J. Zou, M. M. Desouki, R. B. Franklin, *J. Gastrointest. Cancer* **2012**, *43*, 570–578.
96. E. Bellomo, A. Massarotti, C. Hogstrand, W. Maret, *Metallomics* **2014**, *6*, 1229–1239.
97. E. Bellomo, K. Birla Singh, A. Massarotti, C. Hogstrand, W. Maret, *Coord. Chem. Rev.* **2016**, *327–328*, 70–83.
98. K. M. Taylor, S. Hiscox, R. I. Nicholson, C. Hogstrand, P. Kille, *Sci. Signal* **2012**, *5*, ra11.
99. S. Tawfic, S. Yu, H. Wang, R. Faust, A. Davis, K. Ahmed, *Histol. Histopathol.* **2001**, *16*, 573–582.
100. S. Hiscox, L. Morgan, D. Barrow, C. Dutkowskil, A. Wakeling, R. I. Nicholson, *Clin. Exp. Metastasis* **2004**, *21*, 201–212.

101. H. E. Jones, L. Goddard, J. M. Gee, S. Hiscox, M. Rubini, D. Barrow, J. M. Knowlden, S. Williams, A. E. Wakeling, R. I. Nicholson, *Endocr. Relat. Cancer* **2004**, *11*, 793–814.
102. S. Hiscox, L. Morgan, T. P. Green, D. Barrow, J. Gee, R. I. Nicholson, *Breast Cancer Res. Treat.* **2006**, *97*, 263–274.
103. J. M. Summy, G. E. Gallick, *Clin. Cancer Res.* **2006**, *12*, 1398–1401.
104. A. Ring, M. Dowsett, *Endocr. Relat. Cancer* **2004**, *11*, 643–658.
105. C. W. Yde, T. Frogne, A. E. Lykkesfeldt, I. Fichtner, O. G. Issinger, J. Stenvang, *Cancer Lett.* **2007**, *256*, 229–237.
106. S. B. Pakala, S. K. Rayala, R. A. Wang, K. Ohshiro, P. Mudvari, S. D. Reddy, Y. Zheng, R. Pires, S. Casimiro, M. R. Pillai, L. Costa, R. Kumar, *Cancer Res.* **2013**, *73*, 3761–3770.
107. K. M. Taylor, S. Hiscox, R. I. Nicholson, *Trends Endocrinol. Metab.* **2004**, *15*, 461–463.
108. R. Ilouz, O. Kaidanovich, D. Gurwitz, H. Eldar-Finkelman, *Biochem. Biophys. Res. Commun.* **2002**, *295*, 102–106.
109. S. Lee, G. Chanoit, R. McIntosh, D. A. Zvara, Z. Xu, *Am. J. Physiol. Heart Circulat. Physiol.* **2009**, *297*, H569–575.
110. X. Tang, N. F. Shay, *J. Nutrit.* **2001**, *131*, 1414–1420.
111. H. Peinado, D. Olmeda, A. Cano, *Nat. Rev. Cancer* **2007**, *7*, 415–428.
112. B. P. Zhou, J. Deng, W. Xia, J. Xu, Y. M. Li, M. Gunduz, M. C. Hung, *Nature Cell Biol.* **2004**, *6*, 931–940.
113. S. Yamashita, C. Miyagi, T. Fukada, N. Kagara, Y. S. Che, T. Hirano, *Nature* **2004**, *429*, 298–302.
114. R. Shen, F. Xie, H. Shen, Q. liu, T. Zheng, X. Kou, D. Wang, J. Yang, *PLoS One* **2013**, *8*, e56542.
115. K. M. Taylor,d R. I. Nicholson, *Biochim. Biophys. Acta - Biomembranes* **2003**, *1611*, 16–30.
116. Y. Zhang, U. Bharadwaj, C. D. Logsdon, C. Chen, Q. Yao, M. Li, *Clin. Cancer Res.* **2010**, *16*, 1423–1430.
117. C. Hogstrand, P. Kille, R. I. Nicholson, K. M. Taylor, *Trends Mol. Med.* **2009**, *15*, 101–111.
118. K. M. Taylor, P. Kille, C. Hogstrand, *Cell Cycle* **2012**, *11*, 1863–1864.
119. T. Nimmanon, S. Ziliotto, S. Morris, L. Flanagan, K. M. Taylor, *Metallomics* **2017**.
120. K. Niefind, J. Raaf, O. G. Issinger, *Cell Mol. Life Sci.* **2009**, *66*, 1800–1816.
121. N. A. St-Denis, D. W. Litchfield, *Cell Mol. Life Sci.* **2009**, *66*, 1817–1829.
122. A. Siddiqui-Jain, D. Drygin, N. Streiner, P. Chua, F. Pierre, S. E. O'Brien, J. Bliesath, M. Omori, N. Huser, C. Ho, C. Proffitt, M. K. Schwaebe, D. M. Ryckman, W. G. Rice, K. Anderes, *Cancer Res.* **2010**, *70*, 10288–10298.
123. L. R. Martins, P. Lucio, A. Melao, I. Antunes, B. A. Cardoso, R. Stansfield, M. T. Bertilaccio, P. Ghia, D. Drygin, M. G. Silva, J. T. Barata, *Leukemia* **2014**, *28*, 179–182.
124. Y. Zheng, B. C. McFarland, D. Drygin, H. Yu, S. L. Bellis, H. Kim, M. Bredel, E. N. Benveniste, *Clin. Cancer Res.* **2013**, *19*, 6484–6494.
125. J. K. Chesters, L. Petrie, *J. Nutr. Biochem.* **1999**, *10*, 279–290.
126. D. Sussman, L. M. Smith, M. E. Anderson, S. Duniho, J. H. Hunter, H. Kostner, J. B. Miyamoto, A. Nesterova, L. Westendorf, H. A. Van Epps, N. Whiting, D. R. Benjamin, *Mol. Cancer Ther.* **2014**, *13*, 2991–3000.
127. T. Zhang, D. Sui, J. Hu, *Nat. Commun.* **2016**, *7*, 11979.
128. A. Dereeper, V. Guignon, G. Blanc, S. Audic, S. Buffet, F. Chevenet, J. F. Dufayard, S. Guindon, V. Lefort, M. Lescot, J. M. Claverie, O. Gascuel, *Nucl. Acids Res.* **2008**, *36*, W465–469.

129. W. Li, A. Cowley, M. Uludag, T. Gur, H. McWilliam, S. Squizzato, Y. M. Park, N. Buso, R. Lopez, *Nucl. Acids Res.* **2015**, *43*, W580–584.

Subject Index

A

AAS, *see* Atomic absorption spectroscopy
Abraxane, 357
N-Acetylglucosamine (GlcNAc), 113
Acetylsalicylic acid, *see* Aspirin
Acetyltransferases, 393
Acridines, 56, 343, 396, 423
Acute myeloid leukemia (NCT01280786), 484, 491
Adenocarcinoma, 29, 144, 221, 295, 405, 443, 446, 516, 518
AFM, *see* Atomic force microscopy
Albumin, *see* Human serum albumin
Alcoholism, 472, 485, 487
  anti-alcoholism drug, 485, 487
Aldehyde dehydrogenase (ALDH), 485, 487, 488
Alkanediamine linker, 46, 47
Aluminum(III), 118
Alzheimer's disease, 470, 483–485
Amino acids (*see also* individual names)
  biosynthesis, 454
R-2-Amino methyl pyrrolidine 1,1-cyclobutane dicarboxylate platinum(II), *see* Miboplatin
Anemia, 21, 146, 286, 291, 444, 455
  Fanconi's, 21, 22, 455
  sideroblastic, 455
Antabuse, 485
Anthraquinones, 56, 328, 367
Antiarthritis drug, 188
Antibacterial (agents), 200, 201, 404, 445, 448
Anticoagulant drug, 111, 114
Antidiabetic drugs, 253, 259, 262, 266
Antimetastatic effect, 61, 145, 150, 154, 187, 358, 359, 366, 446, 447
Antimicrobial agents, 287, 314, 316, 317, 444, 449, 482
Antineoplastic activity, 283–290, 293, 294, 296, 447
Antiparasitic agents, 201, 304
Antirheumatic drugs, 201
Antithrombin-III (AT), 114, 115
Antiviral agents, 201, 304, 448
Apoptosis (*see also* Cell death), 10, 22, 25–29, 60–62, 85, 86, 90, 100, 101, 130, 147, 150, 155, 161, 162, 164, 187, 191, 205, 208, 210, 220, 236, 238, 262, 292–295, 309, 343, 352, 372, 374, 421, 446, 449–452, 454, 479, 480, 483, 486, 490, 512, 514, 519
$[(\eta^6\text{-Arene})Ru(en)Cl]PF_6$ (RAED), 174, 368, 369, 373, 374
$(\eta^6\text{-Arene})Ru(pta)Cl_2$ (RAPTA), 174, 184, 192, 358, 359, 361, 362, 366, 373, 374
Arthritis, 188, 200–202, 365
Ascorbic acid, 71, 73, 74, 79, 85, 148, 183, 271
Aspirin (acetylsalicylic acid), 356, 369, 370
Atomic absorption spectroscopy (AAS), 118, 154–156, 362, 404
Atomic force microscopy (AFM), 57, 182, 306, 312, 395
ATOX1 (copper chaperone), 7, 8, 360, 361, 478, 479
ATPase, 291
  Na/K, 372, 373
ATP-binding cassette (ABC) transporter, 455
Auranofin, 188, 200–202, 209, 210, 212, 365, 366
Aurothioglucose, 200, 201, 212
Aurothiomalate, 201
Autoimmune disorder, 200, 254
Azidyl radical, 89, 91
Azolates, 55, 407, 408

Metal Ions in Life Sciences, Volume 18 Edited by Astrid Sigel, Helmut Sigel, Eva Freisinger, and Roland K. O. Sigel

https://doi.org/10.1515/9783110470734-018

B

Bacillus anthracis, 134
Bacillus subtilis, 134
Base excision repair (BER), 22
Basic fibroblast growth factor (bFGF), 116, 117, 477–479, 482
Bathophenanthroline (dpp), 405, 414, 415
BBR3464, *see* Triplatin
BEOV, *see* Bis(ethylmaltolato)oxovanadium(IV)
Bilirubin, 222, 360, 450
Biliverdin, 450
2,2′-Bipyridine (bpy), 54, 56, 92, 93, 207, 208, 305, 311, 316, 317, 343, 344, 396, 397, 399, 401–408, 411, 412, 414–417, 419–426
2,2-Bis aminomethyl-1,3-propandiol-N-N′ 1,1-cyclobutane dicarboxylate-O′,O′ platinum(II), *see* Zeniplatin
Bis(ethylmaltolato)oxovanadium(IV) (BEOV), 253, 256, 258, 271
Bismaltolatooxovanadium(IV) (BMOV), 253, 258, 271
Bis(thiosemicarbazones), 472, 491, 492
Bladder cancer, 3, 89, 90, 284, 285, 289, 296, 447, 480
Blood, 6, 10, 11, 13, 74, 77, 79, 80, 92, 94, 98, 134, 146, 148, 149, 151, 152, 163, 179, 255, 259, 260, 287–289, 353, 354, 356, 358, 360, 370, 375, 376, 444, 451, 471, 477, 487–489, 493
  calcium level, 284
  coagulation, 111
  copper in, 477
  gallium levels, 286, 289
  glucose levels, 252, 258, 266–271
  red cells, 208, 212, 440
  white cells, 157, 285
Blood-brain barrier, 287, 485
BMOV, *see* Bismaltolatooxovanadium(IV)
Bone, 284, 287, 485
  marrow, 440, 455
  marrow progenitor-derived mast cells (BMMCs), 130, 481
Boron neutron capture therapy (BNCT), 56, 191
Brain, 9, 11, 84, 119, 149, 222, 270, 287, 446, 471, 483
  -blood barrier, *see* Blood-brain barrier
  tumor, 149 287
Breast cancer, 222, 238, 310, 339, 343, 364, 365, 371, 442, 449, 452, 454, 471, 475, 478, 480, 481, 483–487, 512–523
  cells (MDA-MB-231), 24, 162, 207, 368, 484, 486
BTP-114 (cisplatin derivative), 30, 33
Budotitane, 186, 220, 221, 227–231

C

Calcium(II), 269–271, 284, 293, 508
  ^{43}Ca, 120
  signalling, 293, 512
Calf thymus DNA (CT-DNA), 89, 101, 157, 207, 305, 312, 335, 340, 394, 396
Calmodulin, 512
Calorimetry, 59, 395
Cancer (*see also* Carcinomas, Tumors, *and* individual names)
  biomarker, 520, 521, 447, 476, 491, 493, 494, 508, 513
  bladder, 3, 89, 90, 284, 285, 289, 296, 447, 480
  breast, *see* Breast cancer
  cervical, 84, 284, 295, 480, 487, 493
  colon, *see* Colon cancer
  colorectal, *see* Colorectal cancer
  esophageal, 3, 84, 90, 176, 180, 474, 481, 515
  head and neck, *see* Head and neck cancer
  kidney, 180, 453, 474, 480, 481, 515
  lung, 5, 123, 191, 201, 293, 341, 407, 450, 471, 475, 513
  neck, 3, 478, 493, 513, 515
  non-small cell lung, 8, 146, 149, 238, 239, 343, 449, 452, 475, 480, 482, 488, 491
  ovarian, *see* Ovarian cancer
  pancreatic, *see* Pancreatic cancer
  prostate, *see* Prostate cancer
  renal, *see* Renal cancer
  small cell lung, 3, 221
  stem cell, 32, 33, 205, 449, 487, 488, 494
  testicular, *see* Testicular cancer
Capillary electrophoresis, 119, 134, 375,
Carbon
  ^{13}C, 73, 74
  monoxide (CO), 450
  nanotubes, 96–98, 362
Carcinomas
  adeno-, *see* Adenocarcinoma
  breast, *see* Breast concer
  gallbladder, 513
  gastrointestinal, 221
  hepatocellular, *see* Hepatocellular carcinoma
  lung, *see* Lung carcinoma
  mammary, *see* Mammary carcinoma
  Walker 256, *see* Walker 256 carcinoma
Carbonic anhydrase, 158, 160
Carboplatin, 4, 5, 9, 12, 29, 30, 70, 75, 79, 157, 359, 361, 371, 420, 421, 475, 482, 520
Carboranes, 56, 191
Cardiotoxicity, 496
Caspases, 101, 190, 191, 227, 236, 293, 294, 421, 449, 451, 452, 512, 514, 516

Cathepsins
B (CatB), 178, 187, 188, 265, 365, 366
D, 161, 178
CD spectroscopy, 114, 118, 356, 157, 175, 306, 356, 395, 412
Cell(s)
cycle, 19, 21, 26–28, 61, 62, 155, 162, 177, 184, 227, 236, 238, 262, 263, 291, 309, 364, 393, 443, 449, 490, 516, 523
death, 6, 11, 19, 25, 29, 161, 162, 182–184, 188, 190, 209, 210, 262, 293, 294, 364, 421, 422, 438, 446, 451–454, 456, 488–490, 493, 495, 512, 514
leukemic, 490
metabolism, 208–210
migration, 118, 164, 520
stem, *see* Stem cells
Cellular iron homeostasis, 282, 291, 439–441
Ceruloplasmin, 439, 470, 480, 481
Cervical cancer, 284, 295, 493
Chaperones
copper (ATOX1), 7, 8, 360, 361, 478, 479
Checkpoint kinases, 26–28
Chemotherapy, 190, 213, 220, 284, 370, 416, 442, 449, 452, 454, 475, 476, 480, 485, 487, 488, 493, 517
photoactivatable (PACT), 88, 100
platinum-based, 4, 6, 8, 30, 31, 33, 80, 220, 353
5-Chloro-7-iodo-quinolin-8-ol, *see* Clioquinol
Chondroitin sulfate, 111, 123, 129, 130, 134
Chromatin, 17, 24, 26, 27, 327, 328, 388, 393, 452
Chromatography
chiral, 312
high performance liquid (HPLC), 15, 395
Sephadex, 316
size exclusion, 356
Chromium(III), 266, 268–271, 411
Chromosomes, 327, 393, 407
Chronic lymphocytic leukemia (CLL), 201, 284, 416
5,6-Chrysenediimine (chrysi), 311, 312, 414–422, 424, 426
Circular dichroism, *see* CD spectroscopy
cis-$[Pt(NH_3)_2Cl_2]$, *see* Cisplatin
cis-1,1-cyclobutane dicarboxylato(2R)-2-methyl-1,4-butanediamine platinum(II), *see* NK-121/C1-973, 4
cis-dichlorodiammineplatinum(II) (CDDP), *see* Cisplatin
cis-tetrachlorodiammineplatinum(IV), 3,
Cisplatin, 1–33, 45–51, 53, 55–62, 70, 74–79, 81, 85, 86, 89–92, 95–100, 122, 123, 126, 129–131, 133, 144, 146, 150, 157, 172–174, 176, 177, 182, 184, 187, 188, 190, 193, 205–208, 220–224, 226, 227, 230, 236–238, 265, 266, 304, 309, 314, 342, 343, 352, 354, 355, 357, 360, 362, 365, 366, 368, 370–375, 408, 410, 417, 418, 420–422, 426, 453, 475, 480, 488, 493, 494, 515
-DNA adduct, 19, 45, 480
resistance, 9, 10, 21, 22, 28, 32, 61, 368, 410
transport, 360–363, 377
Citrate, 269, 283, 290, 440, 442, 514
Clinical trials, 3, 4, 30, 57, 63, 74, 75, 101, 126, 172–174, 200, 201, 213, 220, 222, 226, 229, 237, 238, 253, 254, 258, 266, 267, 273, 283–285, 287–289, 295, 296, 354–357, 371, 376, 377, 449, 472, 474, 476, 477, 480, 487–491, 496, 497, 522, 523
Phase 1, 3, 75, 126, 145–147, 222, 229, 253, 254, 258, 264, 284, 288, 289, 295, 474–476, 480, 482, 487, 490, 491, 495, 496
Phase 2, 57, 222, 145, 146, 174, 254, 258, 264, 284, 288, 356, 449, 474–476, 480, 481, 487, 488, 490, 491, 493
Phase 3, 4, 75, 254, 449, 490
Clioquinol (5-chloro-7-iodo-quinolin-8-ol), 472, 475, 482–484, 492
Cobalt(II), 189, 190, 341, 368, 372
Cobalt(III), 189, 190, 316, 368, 372, 377, 404, 422, 423, 425
Colon cancer, 4, 12, 61, 74, 98, 133, 149, 182, 205, 221, 227, 238, 287, 293–295, 370, 442, 443, 446, 448, 449, 453, 455, 474, 475, 480, 481, 487, 489, 494, 515, 516
Colorectal cancer, 4, 10, 30, 149, 150, 161, 183, 413, 443, 456, 475, 482, 516
Confocal (flurescence) microscopy, 86, 296, 339, 340, 419
Copper
^{60}Cu, 493
^{64}Cu, 493, 494
deficiency, 471, 477
homeostasis, 8, 9, 470, 471, 489, 497
in blood, 477
-molybdenum clusters, 477
radioisotopes, 493
toxicity, 471, 472, 483
transporters (*see also* Transport of copper), 6–8, 478
Copper(I), 305, 315, 316, 417
Copper(II), 472
(atsm) (= diacetylbis-[N4-methylthiosemicarbazonato]CuII), 483, 492–494
(gtsm) (= glyoxalbis[N4-methylthiosemicarbazonato]CuII), 479, 483, 492, 493
(kts), 492
Cu/Zn superoxide dismutase (SOD), 450, 470, 478–480, 483, 487
Coumarin, 86
Covalent bonds, 122, 125, 176, 352, 353
Cyclin-dependent kinases (CDK), 27, 364, 443

1,1-Cyclobutane dicarboxylato-O′,O′ tetrahydro-4H pyran-4,4-dimethylamine-N′,N′ platinum(II), *see* Enloplatin
Cyclooxygenases (COX), 369, 370
Cyclopentadienyl (groups), 189, 221, 222, 261, 356, 363
Cytochrome *c,* 74, 86, 208, 293, 449, 514
  oxidase, 451, 470, 478
Cytokines, 28, 131, 176, 444, 477–479, 483, 509
Cytoskeleton, 161, 293
Cytotoxicity of
  cylinders, 310, 311, 314, 316, 317, 319
  G4, 340, 341, 343
  gallium, 290, 291, 293, 295, 296
  gold drugs, 201–208, 212
  photo-, 81, 90–92, 407
  platinum, 12, 26, 33, 44, 46, 53, 78, 79, 81, 84, 89, 90–92, 97, 100, 130, 157, 362, 365, 367, 372, 374
  ruthenium drugs, 145–147, 150, 157, 162, 177, 180, 183, 184, 186, 188, 189–192
  titanium drugs, 227–236, 238

D

Decavanadate ($Na_6V_{10}O_{28}$), 259
Deficiency of
  copper, 471, 477
  iron, 286, 441, 444
  zinc, 512, 514
Dehydrogenases
  aldehyde, *see* Aldehyde dehydrogenase
  lactate, 476, 491
Density functional theory (DFT), 90, 114, 116, 128, 397, 403
Deoxyribonucleoside diphosphates (dNDPs), 291
Diabetes, 252, 254, 256–258, 262, 266, 273, 363
Diammine[hydroxyacetato-O,O′]platinum(II), *see* Nedaplatin
Diazido-Pt(IV) complexes, 81, 83, 88–91
Dickerson-Drew dodecamer (DDD), 125, 126
Diethyldithiocarbamate (DDTC), 86, 87, 472, 475, 476, 485, 486–488
Differential scanning calorimetry, 59
Dihydroxidooxaliplatin, 96
Diketonato complexes, 227–230, 233, 234
1,2-Dimethylhydrazine, 515
Dinuclear complexes
  gallium, 296
  gold(II), 207, 224
  platinum, 46–57, 63, 123, 425
  ruthenium(II) (arene), 174–176, 178, 181, 182, 186–190, 408, 409
  supramolecular, 315, 316
1,2-Diphenylethylenediamine (DPEN), 174
4,7-Diphenyl-1,10-phenanthroline (dpp), 405, 414, 415
Dipyridophenazine (dppz), 134, 335, 396–409, 411, 422–426
Disaccharides, 110, 111, 113, 119, 134
Disease(s)
  Alzheimer's, 470, 483–485
  infectious, 201, 252, 447
  Menkes, 471
  -modifying antirheumatic drugs (DMARDs), 201
  Wilson's, 471
Disulfiram (tetraethylthiuram disulfide; DSF), 472, 475, 476, 479, 483, 485–488, 492
Dithiocarbamates, 86, 87, 207, 208, 472, 476, 485
Diethyldithiocarbamate (DDTC), 86, 87, 472, 475, 476, 485, 486–488
Divalent metal transporter1 (DMT1), 288, 290, 439–441, 443
DNA
  B-, 304, 306, 312, 315, 316, 392, 395, 396, 398
  c-myc, 331
  calf thymus (CT-), 89, 101, 157, 207, 305, 312, 335, 340, 394, 396
  -cisplatin adduct, 19, 45, 480
  coiling, 306, 312
  conformational changes, 52, 62
  cross-links, 17, 29, 51, 70, 174, 177, 178
  damage, 17, 22, 25–29, 53, 60, 157, 164, 187, 210, 328, 342, 343, 372, 438, 442, 443, 456, 490, 494, 495, 514
  duplex, 15, 16, 23, 24, 51, 54, 55, 304, 306, 307, 309, 310, 312, 317, 319, 330, 331, 334, 335, 337, 339, 340, 343, 394–397, 401, 403, 409, 415, 424, 426, 427
  G4, 326–339, 342–344
  inhibition of synthesis, 18, 50, 55, 62, 187, 364
  interactions, 56, 125, 128, 394, 406
  interstrand cross links, 78, 157, 174, 416, 417
  major groove, *see* Major groove
  minor groove, *see* Minor groove
  mismatches, 413, 420, 422
  Mismatch repair, *see* Mismatch repair
  photoinduced cleavage, 406, 414
  plasmid, 175, 190, 305, 406, 415
  polymerases, 18–20, 22, 25, 50, 162, 208, 290, 413, 414, 455, 456
  processing, 15, 304, 310, 393, 455
  recognition, 49, 126, 174, 304, 314, 416, 426
  repair, 2, 19, 22, 25, 26, 50, 55, 60, 85, 126, 304, 372, 413, 515
  ruthenium adducts, 178
  structures, 45, 57, 157, 174, 304, 307, 308, 312, 327, 329, 330, 340, 388, 391, 392, 427

synthesis, 18, 19, 21, 26, 48, 50, 62, 291, 364, 438, 439, 508
Z-, 45, 48, 304, 391, 392, 396
Dose-limiting toxicity (DLT), 30–32, 146, 147, 285
Doxorubicin, 98, 182, 304, 358, 453, 454, 480, 494, 496
Drug(s) (*see also* individual names)
antiarthritis, 188
antibacterial, 200, 201, 404, 445, 448
anticoagulant, 111, 114
antidiabetic, 253, 259, 262, 266
antimicrobial, 287, 314, 316, 317, 444, 449, 482
antiparasitic, 201, 304
antiviral, 201, 304, 448
carriers, 94, 96, 205, 357
design, 114, 200, 354
disease-modifying antirheumatic (DMARDs), 201
encapsulation, 94, 95, 184, 185, 191
gold, 200–213
metabolism, 484, 485, 488
non-steroidal anti-inflammatory (NSAID), 369, 370
platinum, *see* Platinum drugs *and* individual names
resistance, 14, 33, 86, 172, 182, 188, 266, 286, 362, 443, 477, 487, 494, 496
ruthenium (*see also* Ruthenium drugs *and* individual names), 142–165, 266, 358, 426
titanium, 219–238
Dwarfism, 513
Dyes, *see* individual names

E

EC_{50}, 341, 342
Ehrlich ascites tumor, 221, 223
Eilatin, 403, 423, 424
Electron microscopy, 395
Electron nuclear double resonance spectroscopy (ENDOR), 154
Electron paramagnetic resonance, 119, 154, 358, 371
high field, 260
Electron spin resonance, 154
Electron transport, 292, 438, 439, 442, 470, 479, 489, 491
Electrophoresis, 119, 134, 175
Electrospray ionization mass spectrometry (ESI-MS), 120, 157, 158
Elesclomol (N-malonyl-bis (N-methyl-N-thiobenzoyl hydrazide)), 440, 472, 476, 479, 489–491
Endocytosis, 77, 98, 288, 290, 354, 355, 357, 362, 440
Endonucleases, 22, 23, 156, 310, 414
Endoplasmic reticulum, 147, 162, 406, 512, 519–523
ENDOR, *see* Electron nuclear double resonance spectroscopy
Enhanced permeability and retention (EPR), 72, 94, 153, 354, 356
Enloplatin (1,1-cyclobutane dicarboxylato-O′,O′ tetrahydro-4H pyran-4,4-dimethylamine-N′,N′ platinum(II)), 4
Environmental Protection Agency (EPA), 259
Enzymes, *see* individual names
Epidermal growth factor receptors (EGFR), 372, 407, 513, 514, 518, 521
EPR, *see* Enhanced permeability and retention
Erlotinib, 372
Erythropoiesis, 438, 444
Escherichia coli (*E. coli*), 2, 18, 19, 310, 314, 340, 413, 414
ESI-MS, *see* Electrospray ionization mass spectrometry
Esophageal cancer, 3, 84, 90, 176, 180, 474, 481, 515
Estrogens, 86, 227, 364, 365, 442, 512, 514, 516, 519, 521, 522
Ethacraplatin, 85, 368, 369
Ethidium bromide (EtBr), 305, 317, 394–396
Ethylenediamine, 55, 74, 88, 98, 99, 174, 368, 373
1,2-diphenyl-, 174
Eukaryotes, 21, 393
Extracellular signal regulating kinases (ERK), 27, 28, 204, 262, 263, 453, 518

F

Fanconi's anemia, 21, 22, 455
Fatty acids, 77, 153, 354, 360, 452, 494
Fenretinide, 480
Fenton chemistry, 438, 439, 441, 442, 444, 450, 453
Ferricenium radical, 189
Ferrocene, 189, 364, 370, 371
Ferrocifens, 364, 365
Ferroportin, 439
Ferroptosis, 445, 452, 453, 456
Fe-S clusters, 292, 440–442, 454–456
2Fe-2S, 454
4Fe-4S, 454
Fibroblast growth factors (FGF), 114, 116–120, 133, 134, 471, 477–479, 482
Fibroblast growth factor receptor (FGFR), 114, 116, 118, 119, 133
Flexicates, 312–314

Fluorescein isothiocyanate (FITC), 94, 97
Fluorescence, 77, 86, 87, 94, 101, 134, 154, 184, 185, 187, 296, 335, 357, 394, 403, 419
probes, 73, 86, 87, 208, 361
intercalation displacement, 319
microscopy (imaging), 97, 98, 129, 376, 405
5-Fluorouracil, 4, 144, 227, 480, 482
Fluorophores, 86, 97, 134, 419
Fluozin-3, 521
Fondaparinux (FPX), 114–116, 131, 132
Food and Drug Administration (FDA), 3, 4, 70, 94, 258, 284, 490, 491
Force-field molecular dynamics, 403 416,
Förster resonance energy transfer (FRET), 101, 319
Fourier transform-infrared (FTIR), 73
Free radicals, 92, 189, 291, 371, 441–444, 450, 470
Friedreich's ataxia, 455

G

G-quadruplex (G4), 45, 53–55, 62, 204, 317, 319, 325–344, 398
cytotoxicity, *see* Cytotoxicity
binders (G4 binder), 317
DNA, 326–339, 342–344
G-tetrad, 326, 329, 330, 333, 335–338
Gallbladder carcinoma, 513
Gallium(II), 286
Gallium(III), 235, 282–296, 356, 371, 376, 495
^{67}Ga(III), 282, 283, 287, 288–290
carboxylate complexes, 296
corroles, 296
dinuclear complexes, 296
gallium chloride, 283
hydroxides, 283, 289
maltolate, 284, 286, 287, 292, 293, 296
nitrate, 283–286, 289–293, 296
phenolate, 294
pyridine, 294
-pyridoxal isonicotinyl hydrazone, 295
quinoline, 286, 287, 293, 353
thiosemicarbazones, 295
toxicity, 283–285
Gastrointestinal carcinoma, 221
Gefitinib, 372, 407
Gel electrophoresis, 157, 207, 305, 307, 309, 333, 376, 395
Gemcitabine, 146, 496
Gene promoters, 327, 340, 343
Genome, 60, 327, 363
Giardiasis, 201
Glioblastoma, 287, 295, 343, 366, 372, 405, 476, 486–488, 522
Glucosamines, 112–114, 118–121
N-acetyl- (GlcNAc), 113
Glucose, 202, 222, 252, 258, 266–271, 407, 408, 494
aurothio-, 200, 201, 212
blood levels, 252, 258, 266–271
metabolism, 266, 268–270
transporters (GLUT), 84, 361, 407
D-Glucuronate (GlcA), 113, 116
Glutathione (GSH), 14, 15, 31, 32, 52, 70, 71, 73–75, 78, 79, 86, 88, 89, 92, 148, 177, 178, 183, 202, 203, 207, 209, 262, 292, 368, 440, 449, 450, 452, 453, 471, 490, 492, 495, 511
reductase, 202, 203, 209
S-transferase (GST), 14, 86, 368, 369
Glycogen synthase kinase 3 (GSK-3β), 363, 364, 520, 523
Glycolysis, 25, 210, 361, 372, 455, 491, 494
Glycoproteins, 123, 134, 407, 445, 448
Glycosaminoglycans (GAG), 110, 111, 114, 116, 118–125, 130
Gold
Au(I), 188, 202–205, 207–210, 212, 213, 365, 366
Au(III), 205–209, 212, 213, 365, 372, 373
cytotoxicity, *see* Cytotoxicity
dinuclear gold(II) complexes, 207, 224
drugs, *see* individual names
nanoparticles (AuNPs), 92, 93
nanorods (GNRs), 92
organometallic complexes, 202–204, 209, 213
-phosphine, 188,
sodium thiomalate, 200
toxicity, 92, 206
Graphite furnace atomic absorption spectroscopy (GF-AAS), 155, 404
Growth factors, 28, 61, 111, 114, 116–120, 131, 133, 134, 176, 266, 407, 447, 471, 476–479, 482, 487

H

Hard and soft acid-base, 122
Head and neck cancer, 3, 478, 493, 513, 515
Helicates, 305, 306, 312, 314–316, 337
Heme oxygenase, 292, 293, 450–453
Heparan sulfate (HS), 110–118, 126, 129–131, 133, 135
glycosaminoglycans (HSGAGs), 111, 116, 117
proteoglycans (HSPGs), 111, 116, 118, 129, 130, 133
Heparanases, 115, 118, 131–133
Heparin, 110–123, 126–135

Hepatitis C virus, 339
Hepatocellular carcinoma, 96, 134, 191, 286, 287, 343, 442, 444, 456, 516
Hepatotoxicity of
  platinum, 31
  titanium drugs, 229
Hepcidin, 439, 440, 443–445
Heptaplatin ([propanedioato-O,O′][2-(1-methylethyl)-1,3-dioxolane-4,5-dimethanamine-N,N′]platinum(II)), 4, 5, 70
Hereditary hemochromatosis, 442, 444
N-Heterocyclic carbenes (NHC), 188, 189, 203, 204, 208–210, 338, 366, 425
Heteronuclear multiple quantum interference NMR spectroscopy (HSQC) {^{1}H,^{15}N}, 13, 58, 123, 124, 126
Heteronuclear ruthenium-arene complexes, 186–192
Hexasaccharides, 116, 117, 121
High field EPR spectroscopy, 260
High mobility group box proteins (HMGB), 23, 24, 48, 49, 52, 60, 365
High mobility group domain proteins (HMG), 24, 25, 30, 49, 55, 86, 365
High performance liquid chromatography (HPLC), 15, 395
High-resolution atomic force microscopy, 57
Histone acetyltransferases, 393
Histone deacetylases (HDACs), 86, 95, 370, 371, 393
Hodgkin's lymphoma, 284
  non-Hodgkin's, 284, 285, 416
Holliday junctions, 21, 45, 398
Homeostasis
  copper, 8, 9, 470, 471, 489, 497
  iron, 282, 291, 439–442, 445–447, 454, 456, 470
  sugar, 372
  zinc, 357, 509, 512, 523
Homoleptic
  dinuclear ruthenium-arene complexes, 174–178, 409
  tetranuclear ruthenium-arene complexes, 178–180
  trinuclear ruthenium-arene complexes, 178–180
Human
  bladder cancer, 90
  genome, 60, 327, 363
  glioblastoma cells, 287, 342, 372, 405, 487
  xenografts, *see* Xenografts
  umbilical vein epithelial cells (HUVECs), 133, 487
  immunodeficiency virus (HIV), 201, 309
Human serum albumin (HSA), 77, 152–154, 160, 354–360, 375, 377
Huntington's disease, 484, 485
Hybrid quantum-classical (QM/MM) molecular dynamics, 403
Hydrazine, 95, 515
Hydrogenase, *see* Dehydrogenase
Hydrogen bonding, 15, 16, 47, 57, 58, 90, 114, 122, 126, 136, 327, 391, 392, 394, 401, 410, 412, 413, 416
Hydrogen peroxide, 72, 78, 209, 264, 441, 478
Hydroxyl radical, 441
[2-Hydroxypropanoato-O1,O2][1,2-cyclobutanedimethanamine-N,N′]platinum(II), *see* Lobaplatin
Hypogonadism, 513
Hypoxia, 164, 368, 439, 478, 494, 495

I

IC_{50}, 55, 86, 89, 130, 150, 151, 161, 176, 177, 206–208, 212, 223, 230, 287, 294, 314, 316, 319, 341–343, 362, 366, 404, 405, 407–410, 421, 422, 489
ICP-AES, *see* Inductively-coupled plasma-atomic emission spectroscopy
ICP-MS, *see* Inductively coupled plasma mass spectrometry
L-Iduronate (IdoA), 112–114, 116–119, 121, 126, 127
(ImH)[*trans*-$RuCl_4$(dmso-S)(Im)], *see* NAMI-A
Imidazolium *trans*-bis-imidazole tetrachlororuthenate(III) (KP418), 143, 144, 151
Immune
  disorders, 200, 262, 513
  response, 358, 439, 442, 444, 447, 448, 449, 456, 471, 523
Immunofluorescent staining, 327
Immunotherapy, 220, 238, 265
Indazolium *trans*-[tetrachlorobis(indazole)ruthenate(III)] (KP1019), 142–166, 353, 355–359, 366
Inductively coupled plasma mass spectrometry (ICP-MS), 154, 374–376, 419–422
  laser ablation, 375, 376
Inductively-coupled plasma-atomic emission spectroscopy (ICP-AES), 360
Infectious diseases, 201, 252, 447
Infrared spectroscopy, 396, 398, 427
Inhalation bioassay, 259
Inhibition of
  DNA synthesis, 18, 50, 55, 62, 187, 364
  phosphatases, *see* Phosphatases
  telomerase, *see* Telomerase inhibition
Insulin, 257, 263, 264, 266, 269, 271, 518
Interleukins, 444, 471, 477, 483, 520
Interstrand cross-links, 15, 16, 18, 20, 21, 78, 157, 174, 416, 417
  {Pt,Pt}, 46, 48, 49, 51, 53, 56–58, 62

Intracellular trafficking, 290
Intrastrand cross-links, 15, 18, 20, 22–25, 33, 46–51, 78, 92, 373
Ionophores, 471, 479, 483, 484, 486, 492, 493, 495
Iproplatin, 74, 75, 78, 79
Iridium(III) complexes, 336, 374, 411, 412
Iron
  ^{59}Fe, 258, 291
  deficiency, 286, 441, 444
  homeostasis, 282, 291, 439–442, 445–447, 454, 456, 470
  metabolism, 288, 438, 444, 452
  oxide nanoparticles (IONPs), 94
  -regulatory proteins (IRP), 441, 443, 454, 456
  -sulfur clusters (Fe-S), 292, 440–442 454–456
  toxicity, 441
  transport, 440, 443, 448
Iron(II), 288, 304–306, 309, 310, 404
Iron(III), 118, 120, 151, 235, 282, 283, 289, 290, 341, 356, 368, 370, 371, 438–442, 445, 446, 448, 470, 495
Isothermal titration calorimetry (ITC), 395

J

JM216, 79, 80
JM576, 79, 80
c-Jun N-terminal kinase (JNK) 22, 27, 28, 210, 449

K

Kaposi sarcoma, 451
Ketonato complexes, 227–230, 233, 234
Kidney, 11, 12, 98, 149, 180, 192, 285, 288, 452, 471
  cancer, 180, 453, 474, 480, 481, 515
Kinases, 22, 26–29, 116, 119, 133, 161, 204, 227, 293, 363, 364, 451, 453, 508, 512, 518–522
  checkpoint, 26–28
  c-Jun N-terminal (JNK), 22, 27, 28, 210, 449
  cyclin-dependent (CDK), 27, 364, 443
  extracellular signal regulating (ERK), 27, 28, 204, 262, 263, 453, 518
  glycogen synthase (GSK-3β), 363, 364, 519, 520, 523
  inhibitors, 362, 363, 364, 407, 443, 446, 449
  mitogen activated protein (MAPK), 27, 28, 204, 262, 263, 445, 451, 521, 522
  phosphoinositide 3- (PI3K), 116, 262, 263, 266, 522
  protein (*see also* individual names), 27, 28, 364, 445, 449, 453, 508, 512, 520, 522
  serine/threonine-protein, 364, 522
  tyrosine, *see* Tyrosine kinase
KP-46, 293
KP418, *see* Imidazolium *trans*-bis-imidazole tetrachlororuthenate(III)
KP1019, *see* Indazolium *trans*-[tetrachlorobis (indazole)ruthenate(III)]

L

Lanthanum(III), 120
Lactate dehydrogenase (LDH), 476, 491
Lactoferrin (Lf), 152, 160, 289, 356, 440, 448–450, 456
Laser ablation ICP-MS, 375, 376
LD_{50}, 205, 222, 287
Leucovorin, 4, 144, 482
Leukemias, 3, 4, 78, 101, 144, 149, 150, 161, 201, 221, 227, 238, 284, 291, 292, 309, 416, 441, 442, 451, 483, 484, 490, 491, 522
  acute myeloid (NCT01280786), 484, 491
  chronic lymphocytic (CLL), 201, 284, 416
Leukemic cells (K562), 490
Lewis lung carcinoma, 149, 150, 163, 487
Linkage isomerization, 59
Lipid
  alkoxy radical, 441
  metabolism, 268
Lipocalins, 440, 445–448
Lipopolysaccharide, 509
Lithium
  ^{7}Li, 191
Lobaplatin ([2-Hydroxypropanoato-O1,O2][1,2-cyclobutanedimethanamine-N,N′]platinum(II)), 4, 5, 70
Lonidamine, 372
Luminescence, 100, 181, 204, 338, 339, 423–425
Lung carcinoma (or cancer), 3, 5, 8, 29, 30, 84, 98, 123, 145, 146, 149, 150, 163, 191, 192, 201, 221, 238, 259, 284, 287, 293, 341, 342, 407, 410, 443, 449, 450, 452, 453, 471, 474, 475, 478, 480, 481, 482, 487, 488, 491, 493, 494–496, 513, 515
Lymphomas, 29, 286, 289, 292, 293, 296, 443, 446, 453, 490
  Hodgkin's, 284
  non-Hodgkin's, 284, 285, 416
Lynch syndrome, 413
Lysyl oxidase (LOX), 470, 471, 478, 479

M

Macrocycles, 296, 329, 330
Macrophages, 439, 440, 442, 444, 447, 448, 483, 484

Magnesium(II), 118, 120, 291, 341, 414
^{25}Mg, 120
-dependent ATPase, 291
Major groove, 16, 58, 60, 182, 305, 306, 308, 315, 317, 392, 399, 400, 401, 412, 415, 416
Malate
aurothio-, 201
[N-Malonyl-bis (N-methyl-N-thiobenzoyl hydrazide)], *see* Elesclomol
Mammary carcinoma, 149, 150, 162, 443, 446, 471, 494, 514
Mannose, 84, 85
Manganese, 271, 330
Manganese(II), 118, 121
Manganese(III), 330, 341
MAPK, *see* Mitogen-activated protein kinase
Marimastat, 368
Mass spectrometry (MS), 73, 120, 157, 207, 356, 375, 377, 417
electrospray ionization (ESI-MS), 120, 157, 158
inductively coupled plasma mass spectrometry (ICP-MS), 154, 374–376, 419–422
nano-scale secondary ion (NanoSIMS), 376
tandem, 120, 157
Matrix metalloproteinases (MMPs), 368, 445–447, 452, 487, 511, 516
Maximal tolerable dose (MTD), 146, 147, 475
Mechanisms, 5–9, 11, 18–23, 26, 29, 30, 32, 33, 49, 55, 60, 77, 79, 80, 88, 90, 100, 102, 114, 118, 125, 130, 144, 147, 151–156, 158, 160–164, 183, 184, 189, 207, 212, 213, 227, 231, 237, 238, 254, 263, 286–294, 296, 306, 327, 357, 360, 362, 368–372, 377, 405, 413, 419, 421, 422, 439, 440, 442, 445, 447, 449, 450, 453, 454, 470, 478, 480, 482, 483, 489, 492, 494, 509, 512–514, 516, 518–523
Melanomas, 81, 92, 144, 149, 180, 185, 205, 238, 239, 284, 287, 289, 296, 339, 344, 364, 451, 474–476, 480, 486, 487, 489, 490, 495
Meloxicam, 370
Melphalan, 61, 515
Melting temperature, 54, 312, 314, 335, 426
Menkes disease, 471
Messenger RNA, *see* mRNA
Metabolism, 76, 77, 177, 438, 439, 455, 478, 484, 491
bone, 284
cellular, 208–210
drug, 484, 485, 488
energy, 262, 408
fat, 211
glucose, 266, 268–270
iron, 288, 438, 444, 452
lipid, 268
nucleic acid, 227
purine, 201
sugar, 269
L-Methionine, 15, 70, 79, 212, 271, 357
Metallacrowns, 179
Metallacubes, 185
Metallaprisms, 183–185
Metalloglycomics, 110–135
Metalloinsertors, 388, 389, 413–427
Metallointercalators, 388, 389, 395–416, 420, 426
Metallorectangles, 181
Metalloshielding, 126–128, 130, 131
Metallothionein, 282, 292, 293, 471, 489, 511–514
Metal transporters, *see* Transport(ers)
Metastasis (or metastatic), 80, 94, 116, 118, 123, 130, 131, 133, 145, 149, 150, 161–164, 172, 205, 262, 353, 365, 366, 368, 438, 446, 451, 471, 478, 493–495, 496, 511, 519, 523
anti- effect, 61, 145, 150, 154, 187, 358, 359, 366, 446, 447
breast cancer, 222, 480, 485, 516, 522, 523
colon cancer, 4, 475, 480, 482
lung cancer, 475, 480, 482, 488
melanoma, 475, 476, 480, 487, 490
Methylation, 223, 231, 374, 393, 413, 488
Methyltransferase, 488
Miboplatin (R-2-amino methyl pyrrolidine 1,1-cyclobutane dicarboxylate platinum(II)), 4
Microscopy
AFM, *see* Atomic force microscopy
confocal (flurescence), 86, 296, 340, 405, 419
fluorescence microscopy, 97, 98, 129, 376, 405, 419
high-resolution atomic force microscopy, 57
phosphorescent lifetime imaging microscopy (PLIM), 403
STED microscopy, 407
transmission electron microscopy (TEM), 395
Minor groove, 58, 59, 190, 304, 312, 317, 339, 392, 394, 396, 398–401, 411, 415–417, 419, 424, 425
Mismatch repair (MMR), 22, 32, 61, 413, 414, 416, 420–422, 427
Mitaplatin, 85, 86
Mitogen activated protein kinase (MAPK), 27, 28, 204, 262, 263, 445, 451, 521, 522
Mitomycin C, 480
Mitoxantrone, 178
MMR, *see* Mismatch repair
Molecular
dyamics, 54, 58, 212, 306, 335, 403, 416
modeling, 114
mRNA, 12, 19, 28, 32, 291, 327, 343, 344, 427, 441, 453, 489, 518
MTT assay, 100, 191, 342, 420–422

Multidimensional protein identification technology (MudPIT), 376
Multidrug and toxin extrusion proteins (MATEs), 6, 10–12, 75
Multidrug resistance (MDR), 182, 362, 443, 487, 494
  protein 1 (MRP1), 362
Mutagenicity, 2, 18, 33, 309
Mycobacterium bovis bacillus, 447

N

Na/K-ATPase, 372
NADH, *see* Nicotinamide adenine dinucleotide (reduced)
NAMI-A ((ImH)[*trans*-$RuCl_4$(dmso-S)(Im)]), 142–164, 353, 355, 356
Nanoparticles, 72, 75, 92–101, 165, 205, 239, 354, 488
Nanoscale coordination polymers, 98
Nano-scale secondary ion-MS (NanoSIMS), 376
Neck cancer, 3, 478, 493, 513, 515
Necrosis, 25, 61, 77, 421, 449, 452, 483
Nedaplatin (diammine[hydroxyacetato-O,O′] platinum(II)), 4, 5, 12, 70
Nephrotoxicity of
  platinum, 3, 11, 12, 31, 123
  ruthenium drugs, 187
  titanium drugs, 222, 227
NER, *see* Nucleotide excision repair
Neuroblastoma, 92, 95, 164, 205, 294, 343
Neurodegeneration, 513
Neuropathy, 30, 482, 484, 488
  peripheral, 30, 31
  subacute myelo-optic (SMON), 482, 484
Neurotoxicity of
  clioquinol, 484
  platinum, 30, 31, 75
Newport Green, 514, 521
Nickel(II), 118, 121, 306, 309, 331, 340–342, 404, 492
  sulfate, 269, 270
Nicotinamide adenine dinucleotide (reduced) (NADH), 74, 189, 192, 494
N-Nitrosomethylbenzylamine (NMBA), 515
Nitrogen
  ^{15}N, 73, 74, 123, 357
NKP1339, 143,
NMR, 13, 15, 48, 73, 112, 114, 116, 117, 119, 120, 123, 125, 128, 307, 333, 335, 357, 361, 376, 395–397, 402, 411, 412, 415, 416, 425
  ^{1}H, 77, 101, 120, 131, 132, 178
  ^{14}N, 89
  ^{15}N, 58, 77, 89, 123, 124
  ^{23}Na, 120
  NOESY, 409, 415
  ^{195}Pt NMR, 13, 73, 123
  ^{51}V NMR, 260
Non-covalent interactions, 63, 77, 94, 96, 97, 122, 125–128, 204, 308, 317, 319, 329, 334, 354, 355, 358, 360, 377, 388, 398, 400, 403, 417, 421
Non-Hodgkin lymphoma, 284, 285, 416
Non-small cell lung cancer, 8, 146, 147, 149, 238, 239, 343, 449, 452, 475, 480, 482, 488, 491
Non-steroidal anti-inflammatory drug (NSAID), 369, 370
Nuclear magnetic resonance, *see* NMR
Nuclear Overhauser effect spectroscopy (NOESY), 116, 409, 415
Nuclear transcription factor kappaB (NF-κB), 61, 450, 451, 478, 479, 480
Nucleases, 22, 23, 156, 310, 414
Nucleic acids (*see also* individual names), 53, 110, 118, 120, 121, 135, 227, 304–320, 470
  metabolism, 227
  mutation, 451
  structure, 389, 403
Nucleosides, 48, 292, 365, 389, 390
Nucleosome core particle (NCP), 17, 373, 410
Nucleotide(s), 15, 18, 20, 22, 23, 86, 161, 182, 227, 290, 292, 314, 317, 365, 371, 389–391, 413, 414
  excision repair (NER), 19, 20, 49, 365, 372
  oligo-, *see* Oligonucleotides
Nutritional additives, 252, 253, 258, 259, 267, 272

O

Octasaccharides, 455
Oligonucleotides, 48, 60, 92, 157, 326, 389, 391, 392, 394, 397–403, 409, 415–417, 419, 421, 422, 424, 425,
Oligosaccharide, 110, 111, 114, 116–118, 122, 128, 135
Oncogenes, 28, 317, 328, 340, 342, 343, 438, 442, 443, 446, 454, 456, 518
Oncolytic viruses, 265, 273
Optical probes, 94, 231, 232, 327, 335, 338–340, 344
Oregon Green, 418, 419
Organic cation transporters (OCT), 6, 7, 10–12, 75, 446
Organometallic complexes (*see also* individual names), 261, 264, 353, 359, 361, 363, 364, 371, 372, 374
  gold(I), 202–204, 209, 213
  ruthenium(II), 172–192, 408, 410
Osmium(II), 404

Ototoxicity of platinum, 11, 31
Ovarian cancer, 4, 30, 57, 61, 75, 91, 92, 96, 100, 161, 178, 205, 206, 207, 238, 310, 342, 371, 410, 455, 480, 482, 483, 491, 513
  xenografts (A2780 cells), 74, 86, 90–92, 100, 161, 177–180, 185, 190–192, 207, 314, 342, 408, 410, 480, 483
Oxaliplatin (*trans*-L-diaminocyclohexane oxalate platinum(II)), 1–33, 49, 63, 70, 75, 76, 79, 85, 96, 130, 157, 359, 361, 421
Oxicam, 370
Oxidases, 451, 470, 478
  lysyl, 470, 471, 478, 479
Oxidative
  cleavage, 417
  damage, 264, 292, 441, 442, 444, 450, 451, 454, 455
  phosphorylation, 208, 210, 490, 491, 514
  stress, 292, 441, 450, 454, 489
Oxygenases, 369, 370
  heme, 292, 293, 450–453

P

^{31}P, 73
p53 (tumor suppressor protein), 22, 25, 28–30, 32, 60–63, 183, 227, 236, 293–295, 314, 364, 374, 375, 443, 445, 453, 454, 456
Paclitaxel, 96, 357, 358, 476, 489–491
Palladium(II), 316, 334, 338, 340, 341
Pancreatic cancer, 81, 84, 254, 262, 273, 446, 451, 452, 471, 475, 478, 486, 516, 518, 520
PARP-1, *see* Poly(ADP-ribose)polymerase 1,
Penicillamine, 477
Pentasaccharides, 115, 116, 131
Peripheral neuropathy, 30, 31
Peroxovanadium, 264
P-glycoprotein 1 (Pgp), 362, 443, 479, 487
Pharmacokinetics, 57, 71, 98, 145, 149, 152, 222, 257, 285, 287–289, 356, 472, 476, 484, 485, 488, 490, 496
Pharmacology, 46, 75, 213, 283
Phenanthriplatin, 29
1,10-Phenanthroline (phen), 56, 134, 192, 208, 212, 316, 317, 334, 335, 339, 341, 396, 397, 399–406, 412, 414, 416–419, 422–426
  batho- (4,7-diphenyl-, dpp), 405, 414, 415
Phenolato titanium(IV) complexes, 230–236
2-Phenylpyridine (ppy), 208, 335, 336, 405, 419
Phosphanes, 200, 202–205, 207, 208, 213, 425
Phosphatases, 29, 161, 508, 512
  inhibition, 27, 161, 252, 263, 265, 266, 273, 290, 511, 512, 518, 520, 522
Phosphate buffer, 90, 147, 148, 155
Phosphodiester bond, 389
Phosphoinositide 3-kinases (PI3K), 116, 262, 263, 266, 522
Phosphorescent lifetime imaging microscopy (PLIM), 403
Phosphorylation, 22, 26–29, 116, 204, 208, 252, 293, 393, 439, 446, 447, 452, 518, 520, 522, 523
  oxidative, 208, 210, 490, 491, 514
Photoactivatable
  chemotherapy (PACT), 88, 100
  complex, 77, 81, 88–92, 96, 100, 334
Photoactivation, 101, 178, 185, 407, 416
Photocytotoxicity, 81, 90–92, 407
Photodynamic therapy (PDT), 88, 90, 185, 192, 193
Photoinduced cleavage of DNA, 406, 414
Phthalocyanines, 330, 331, 340, 341, 343
Picoplatin (*cis*-$PtCl_2(NH_3)$(2-mepyridine), 56, 81
Piroxicam, 370
Plasma levels of gallium, 285
Plasmid DNA, 175, 190, 305, 406, 415
Platinol, *see* Cisplatin
Platinum
  agents, *see* Toxicity of platinum agents
  -based, 4, 6, 8, 30, 31, 33, 80, 219, 220, 353
  cytotoxicity, *see* Cytotoxicity
  dinuclear complexes, 46–57, 63, 123, 425
  drugs, *see* individual names, e.g., Carboplatin, Cisplatin, Enloplatin, Ethacraplatin, Heptaplatin, Iproplatin, Lobaplatin, Miboplatin, Mitaplatin, Nedaplatin, Oxaliplatin, Phenanthriplatin, Picoplatin, Satraplatin, Tetraplatin, Zeniplatin
  hepatotoxicity of platinum, 31
  transport, 6–12, 31, 32, 360–363, 377
  trinuclear, 56, 57, 130
Platinum(II), 4, 46, 47, 49, 51–56, 71, 72–79, 85–92, 94, 96, 98, 99, 101, 126, 144, 172, 174, 188, 266, 319, 331, 333–343, 360–362, 366–368, 370, 376, 408
Platinum(IV), 70, 71–102, 187, 266, 359, 360, 362, 365, 368, 372–374, 377
  diazido complexes, 81, 83, 88–91
Poison, 367, 477
Poly(ADP-ribose)polymerase 1 (PARP-1), 25, 191
Polyethylene glycol (PEG), 92, 94–98, 100, 101, 123, 205, 268, 331
Polymerases, 17–19, 340
  chain reaction, 310, 343
  DNA, 18–20, 22, 25, 49, 50, 162, 208, 290, 310, 413, 414, 455, 456,
  poly(ADP-ribose)- (PARP), 25, 191
  RNA, 19, 49, 178, 310, 508
Polymeric nanoparticles, 94–96, 99, 205

Polynuclear
cluster, 231
diketonato complexes, 230
platinum complexes (PPC), 33, 43–64, 110, 122, 125–133, 135, 174
ruthenium-arene cages, 173, 180–183
titanium complexes, 229, 234
Polysaccharides, 110, 111, 113, 114, 134
Porphyrins, 180, 181, 184, 185, 205, 206, 291, 296, 317, 318, 329, 330, 341, 342
Positron emission tomography (PET), 283, 493
Potassium
^{39}K, 120
Pourbaix diagram, 259, 260
[Propanedioato-O,O′][2-(1-methylethyl)-1,3-dioxolane-4,5-dimethanamine-N,N′]platinum(II), *see* Heptaplatin
Prostaglandins, 369
Prostate cancer, 81, 84, 85, 92, 94, 238, 284, 294, 296, 363, 440, 445, 450–452, 474–476, 478, 480, 481, 483, 484, 488, 489, 491–494, 513–516, 522
Proteins (*see also* individual names)
glyco-, 123, 134, 362, 407, 443, 445, 448, 479, 487
high mobility group box (HMGB), 23, 24, 48, 49, 52, 60, 365
high mobility group domain (HMG), 24, 25, 30, 49, 55, 86, 365
interactions, 112, 116, 119, 133, 135, 354
iron-regulatory (IRP), 441, 443, 454, 456
kinases (*see also* individual names), 27, 28, 364, 445, 449, 453, 508, 512, 520, 522
multidrug and toxin extrusion (MATEs), 6, 10–12, 75
multidrug resistance (MRP1), 362
p53 (tumor suppressor protein), 22, 25, 28–30, 32, 60–63, 183, 227, 236, 293–295, 314, 364, 374, 375, 443, 445, 453, 454, 456
-protein interactions, 374, 375
TATA-binding (TBP), 25

Q

Quadruplex, *see* G-quadruplex
Quinoline, 310, 412, 423, 424
amino-, 207
gallium complexes, 286, 287, 293, 353
hydro-, 90
iso-, 150

R

Radicals
azidyl, 89, 91
ferricenium, 189
free, 92, 189, 291, 371, 441–444, 450, 470
hydroxyl, 441
lipid alkoxy, 441
tyrosyl, 292, 372
reactive oxygen species, 264
Radioisotope
copper, 493, 494
Rapamycin, 29, 445
RAPTA-C (Ru(cym)(1,3,5-triaza-7-phosphatricyclo[3.3.1.1]decane)Cl_2), 359, 373, 374
Reactive oxygen species (ROS), 77, 78, 85, 162, 177, 189, 211, 252, 262, 292, 364, 365, 438, 441, 442, 444, 449–453, 470, 479, 485–493, 495
Recombination (repair), 21, 51, 327
Red blood cells, 208, 212, 440
Redox
cycle (reaction), 73, 74, 267, 438, 495
potential, 23, 148, 189, 259, 264–267, 454
properties (state), 101, 209, 252, 259, 263–265, 364, 365, 371, 440, 449, 470, 489, 512
Reductases
glutathione, 202, 203, 209
ribonucleotide (RNR), 291, 295, 371, 372, 438, 439, 443, 494, 495
thioredoxin (TrxR), 188, 202, 209, 365
Renal
cancer (or carcinoma), 84, 221, 222, 238, 239, 284, 288, 451, 453, 455, 474, 480, 487, 516
damage, 3, 12, 31, 222, 289
toxicity, 11, 146, 285
Response evaluation criteria in solid tumors (RECIST), 146
Rhamnose, 85
Rhenium(I), 411, 412
Rheumatoid arthritis, 188, 200–202, 365
Rhodamin, 86, 87, 98, 101, 129
Rhodium(III), 245, 311, 397, 409, 410–426
Cp* complexes, 411
metalloinsertors, 414–426
Ribonucleotide reductase (RNR), 291, 295, 371, 372, 438, 439, 443, 494, 495
Ribosomes, 19, 29, 407, 489
Risk assessment, 259
RNA, 13, 18, 19, 29, 91, 94, 122, 156, 162, 389, 414, 425, 454, 508
junction, 304–319
mRNA (messenger), *see* mRNA
mismatch, 407
polymerases, 19, 49, 178, 310, 508
rRNA (ribosomal), 19, 24–26, 29, 414, 427
siRNA (small interfering), 10, 454, 516, 518, 521
structures, 308, 309, 314, 317–319, 326–328
synthesis, 25, 26, 56, 157
tRNA (transfer), *see* tRNA
RNAse, 188

Ru(cym)(1,3,5-triaza-7-phosphatricyclo[3.3.1.1] decane)Cl_2, *see* RAPTA-C
Ruthenium
cylinders, 306, 310
-DNA adducts, 178
metalloinsertors, 422, 423
Ruthenium(II), 174–176, 178, 189, 190, 306, 329, 335, 338, 339, 404
organometallic complexes, 172–192, 408, 410
intercalators, 396–411
Ruthenium(III), 142–166, 172, 333, 355–359, 366, 376, 426
Ruthenium(arene) compounds, 172–193, 366, 367, 408–412
[(η^6-arene)Ru(en)Cl]PF_6 (RAED), 174, 368, 369, 373, 374
(η^6-arene)Ru(pta)Cl_2 (RAPTA), 174, 184, 192, 358, 359, 361, 362, 366, 373, 374
cages, 173, 180–183
dinuclear, 174–176, 178, 181, 182, 186–190, 408, 409
heteronuclear, 186–192
Ru(arene)-Au, 188, 189
Ru(arene)-Co, 189, 190
Ru(arene)-Fe, 189
Ru(arene)-Pt, 187, 188
Ru(arene)-Sn, 190
Ru(arene)-thiolate, 177, 181
Ru(arene)-Ti, 186, 187
tetranuclear, 178–180
trinuclear, 178–180
Ruthenium complexes, 142, 156, 177, 316–318, 329, 335, 339, 359, 361, 366, 424, 425
polypyridyl, 396–399, 403, 404, 406–408
Ruthenium drugs (*see also* individual names), 142–165, 180, 183–192, 266, 358, 426
cytotoxicity, *see* Cytotoxicity
Ruthenium red, 134

S

Saccharides
di-, 110, 111, 113, 119, 134
hexa-, 116, 117, 121
lipopoly-, 509
octa-, 455
oligo-, 110, 111, 114, 116–118, 122, 128, 135
penta-, 115, 116, 131
poly-, 110, 111, 113, 114, 134
tetra-, 116, 117
tri-, 114
Salphens, 329, 331, 332, 339–341, 343
SAR, *see* Structure activity relation
Sarcomas (*see* also individual names), 3, 284, 288, 445
-180, 492
angio-, 474, 480
chondro-, 474, 480
fibro-, 445, 453
Kaposi, 451
osteo-, 340, 487
soft tissue, 491
Satraplatin, 74–76, 79
Serine/threonine-protein kinase, 364, 522
Serum albumin, *see* Human serum albumin
Sideroblastic anemia, 455
Siderophores, 289, 440, 445
bacterial, 445, 446
Signal transduction, 25–29, 116, 117, 210, 252, 451
Signaling (pathways or mechanisms), 22, 45, 61, 111, 116, 119, 131, 133, 192, 204, 209, 210, 262, 263, 266, 291, 293, 442–445, 447–449, 451, 452, 456
Silicon(IV), 268, 411, 412, 426
Silver(I), 181, 271, 316, 317
Single crystal X-ray diffraction, 13, 15, 392, 395, 415
Single photon-emission-computed tomography (SPECT), 94
Single-walled carbon nanotubes (SWCNT), 96–98, 362
Singlet oxygen, 88, 91, 192, 306, 412, 423
siRNA (small interfering), 10, 454, 516, 518, 521
Size exclusion chromatography, 356
SLC transporters, 8, 10, 11, 439, 441, 446, 453, 508, 509, 511, 523
Small cell lung cancer, 3, 221
Sodium
^{23}Na NMR, *see* NMR
decavanadate ($Na_6V_{10}O_{28}$), 259
metavanadate ($NaVO_3$), 253
orthovanadate (Na_3VO_4), 253
trans-[tetrachlorobis(indazole)ruthenate(III)] (KP1339), 142–164, 356, 359
Soft tissue sarcoma (NCT00087997), 491
Sorafenib, 445, 452, 453
Spermidine, 49, 50
Spermine, 50
π-Stacking, 54, 55, 87, 307–309, 312, 319, 328, 329, 331, 333, 335, 338, 339, 341, 395, 403, 416, 423, 425
STED microscopy, 407
Stem cells, 32, 33, 205, 443, 449, 486–488, 494
Stomach, 71, 192, 259, 513
Strontium(II), 118
Structure-activity relation (SAR), 341, 342
Stylonychia lemmae, 327
Subacute myelo-optic neuropathy (SMON), 482, 484
Sugar (*see also* individual names), 23, 48, 110, 126–128, 135, 202, 268–271, 361–363, 365, 366, 372, 388–390, 399, 416
homeostasis, 372

metabolism, 269
-phosphate backbone, 135, 388, 390, 391, 393, 396, 401
Sulfate
cluster, 125–128
chondroitin, 111, 123, 129, 130, 134
vanadyl ($VOSO_4$), 252, 253, 255–260, 265, 267, 268–272
N-Sulfoglucosamine (GlcNS), 113, 116, 117, 119, 121, 126, 127
Sulfotransferase, 118
Superoxide dismutase (SOD), 450
Cu/Zn, 470, 478–480, 483, 487
Supramolecular
cages, 99
cylinder, 305
dinuclear complexes, 315, 316
Surface plasmon resonance (SPR), 119, 319
SWCNT, *see* Single-walled carbon nanotubes
Synchrotron radiation circular dichroism (SRCD), 118
Synthesis,
amino acid bio-, 454
DNA, 18, 19, 21, 50, 55, 60, 187, 291, 364, 438, 439, 508
RNA, 25, 26, 56, 157
Systemic iron homeostasis, 439

T

Tamoxifen, 364, 365, 371, 513, 514, 518–522
Tandem mass spectrometry, 120, 157
TATA-binding proteins (TBP), 25
Telomerase inhibition, 54, 55, 317, 319, 328, 335, 339–343
Telomeres, 53, 326, 327, 341–343, 455
Telomeric repeat amplification protocol (TRAP), 319, 341–343
2,2′,2″-Terpyridine (terpy), 54, 55, 206, 207, 329, 332–334, 337, 342–44, 366, 367, 396, 397, 404, 407
Testicular cancer, 3, 5, 23, 32, 97
Tetraplatin, 74, 75, 78, 79
Tetrasaccharides, 116, 117
Tetrathiomolybdate, 472, 476, 477–479
β-Thalassemia, 442
Thiocarbamates
di-, 86, 87, 207, 208, 472, 476, 485
diethyldithio- (DDTC), 86, 87, 472, 475, 476, 485, 486–488
Thiocyanate, 94, 97
Thiolate, 14, 92, 122, 176, 177, 181, 212, 369, 396, 410
Thiols, 13, 31, 32, 54, 73, 77, 78, 100, 122, 134, 176, 202, 203, 205, 208, 359, 360, 495
Thiomalate, 200
Thiomolybdate, 472, 476–479
Thioredoxin, 450, 495
reductase (TrxR), 188, 202, 209, 365
Thiosemicarbazones, 175, 176, 295, 371, 472, 476, 491, 492, 494–496
bis-, 472, 491, 492
Thrombin, *see* Antithrombin
Thrombospondin-1 (TSPN-1), 115, 116
Thulium(III), 101
Time-resolved infrared spectroscopy (TRIR), 396, 398, 427
Tin(II), 190
Tin(IV), 190
Titanium
budotitane, 186, 220, 221, 227–231
cytotoxicity, *see* Cytotoxicity
dioxide, 221
drugs, 219–238
phenolato complexes, 230–236
polynuclear complexes, 229, 234
toxicity, 220–227, 230, 237
Titanium(IV), 219–239, 234, 356, 376
Titanocene
dichloride, 187, 220–227, 229–231, 256
-Ru(arene), 186
Tomography, 94
Topoisomerases, 45, 51
I (Topo I), 190, 227, 310, 367
II, 182, 227, 367
Toxic side effects, 3, 6, 7, 12, 30, 33, 70, 482
Toxicity (of)
cardiotoxicity, 496
copper, 471, 472, 483
cyto-, *see* Cytotoxicity
dose-limiting (DLT), 30–32, 146, 147, 285
gallium drugs, 283–285
gold complexes, 92, 206
hepatotoxicity of drugs, 31, 229
iron, 441
nephro-, *see* Nephrotoxicity
neuro-, *see* Neurotoxicity
oto-, 11, 17, 31
photocyto-, 81, 90–92, 407
platinum agents, 3, 4, 11, 13, 17, 30, 31, 33, 61, 70, 77, 97, 101
renal, 11, 146, 285
titanium drugs, 220–227, 230, 237
vanadium drugs, 253–256, 266
trans-L-diaminocyclohexane oxalate platinum(II), *see* Oxaliplatin
Transcription
factors (*see also* individual names), 61, 24, 25, 162, 163, 293, 374, 443, 450, 451, 478, 479, 489, 508, 516, 519, 520, 523
inhibition, 19, 25, 29, 70, 178, 187, 412, 450, 478, 479

Transferases
histone acetyl-, 393
glutathione *S*-, 14, 86, 368, 369
methyl-, 488
sulfo-, 118
Transferrin (Tf), 151, 152, 227, 229, 235, 263, 264, 285, 295, 354, 355, 439
Transmission electron microscopy (TEM), 395
Transport (of)
cisplatin, 360–363, 377
copper, 6–9, 70, 75, 77, 92, 471, 478–480, 483, 489, 491
electron, 292, 438, 439, 442, 470, 479, 489, 491
gallium, 288–290, 295
iron, 440–443, 446, 448
mechanisms, 11, 32, 151–155
platinum, 6–12, 31, 32
zinc, 508–513, 515–518, 520, 523
Transporters
ATP-binding cassette (ABC), 455
glucose (GLUT), 84, 361, 407
organic cation (OCT), 6, 7, 10–12, 75, 446
P-type, 6, 9
SLC, 8, 10, 11, 439, 441, 446, 453, 508, 509, 511, 523
ZIP family, 508–513, 515–523
Transmission electron microscopy (TEM), 395
TRAP assay, *see* Telomeric repeat amplification protocol
Trientine, 477, 482
Trinuclear platinum complexes, 56, 57, 130
Tripeptides, 78, 306, 362
Triplatin (BBR3464), 45, 46, 48–50, 56–63, 126, 130–133, 174
TriplatinNC, 122, 125–133, 174
Tris(maltolato)gallium(III), 353, 356, 371
Tris(8-oxyquinolinato)gallium(III) (KP1019), 142–164, 353, 355, 356–359, 366
Tris(8-quinolinolato)gallium(III) (KP46, FCC11), 353, 356, 371, 284, 286–288, 293, 294, 296
Trisaccharide, 114
tRNA, 414, 427, 454, 489
Tumor (*see also* individual names)
brain, 149, 287
Ehrlich ascites, 221, 223
growth, 29, 96, 130, 131, 144, 145, 149, 164, 177, 205, 207, 294, 368, 442, 449, 451–453, 478, 486, 487, 492, 495, 516
necrosis factor alpha (TNF-α), 28, 449, 483
suppressor gene, 454, 488, 516
suppressor protein p53, 25, 28–32, 60–62, 183, 227, 236, 266, 293–295, 314, 364, 374, 375, 443, 453, 454, 456
Tyrosine kinase, 116, 119, 133, 407, 508, 512, 518, 520–522
Tyrosyl radical, 292, 372

U

5′-Untranslated region (5′-UTR), 327, 441
Upconversion nanoparticles (UCNP), 99–101
Uracil, 4, 144, 227, 480, 482
Urine, 10, 11, 12, 255, 257, 269, 285
Urothelial cancers, 282
UV irradiation, 89, 91, 96, 178, 306, 414
UV/Vis, 73, 77, 100, 123, 134, 394, 396

V

Vanadate ($H_2VO_4^-$), 252, 253, 258–260, 262, 263, 267
deca- ($Na_6V_{10}O_{28}$), 259
meta- ($NaVO_3$), 253
ortho- (Na_3VO_4), 253
Vanadium
drug toxicity, 253–256, 266
pentoxide (V_2O_5), 259
peroxo-, 264
Vanadium(III), 259, 260
chloride (VCl_3), 259
Vanadium(IV), 251, 253, 256, 258, 260, 267, 271
Vanadyl
dichloride ($VOCl_{2)}$, 259
sulfate ($VOSO_4$), 252, 253, 255–260, 265, 267, 268–272
Vascular endothelial growth factor (VEGF), 61, 119, 176, 446, 447, 471, 476–479, 482, 487
Viscosity measurements, 395, 396
Virus
oncolytic, 265, 273
human immunodeficiency (HIV), 201, 309
Vitamin C, *see* Ascorbic acid

W

Walker 256 carcinoma, 288, 492
Warfarin, 356, 360
Watson-Crick, 304, 326, 388, 413, 424, 425
3-Way junction (3WJ), 306–308, 310–312, 314, 317
4-Way junction, 304, 307, 312, 314, 317
White blood cells, 157, 285
Wilson's disease, 471

X

Xenografts, 9, 60, 94, 453, 487, 489, 494
human breast cancer, 486
human colon cancer, 294, 443
human glioblastoma, 287, 487

human lung carcinoma (DMS-53 cells), 495, 496
human MDA-MB-231, 207
human pancreatic, 496
human prostate cancer (C4–2B cells), 294, 483
murine HCC827, 191
murine hepatocarcinoma, 96
nude mice, 205
ovarian cancer (A2780 cells), 74, 86, 90–92, 100, 161, 177–180, 185, 190–192, 207, 314, 342, 408, 410, 480, 483
X-ray
absorption near edge structure (XANES), 164, 369
absorption spectroscopy (XAS), 156, 358
crystal structures, 16, 326, 331, 332, 416, 421, 424, 427
crystallography, 73, 89, 126, 202, 360, 366, 397, 401
diffraction measurements, 13, 152, 158, 376, 392, 415, 416
fluorescense, 154, 156, 376
photoelectron spectroscopy (XPS), 101
Xeroderma pigmentosum, 21, 455

Y

Ytterbium(III), 101

Z

Z-DNA, 45, 48, 304, 391, 392, 396
Zeniplatin (2,2-bis aminomethyl-1,3-propandiol-N-N′ 1,1-cyclobutane dicarboxylate-O′,O′ platinum(II)), 4
Zinc(II), 118–120, 260, 330, 371, 396, 491, 492, 495, 508, 509, 515, 520, 521, 523
Cu/Zn superoxide dismutase (SOD), 450, 470, 479
deficiency, 512, 513
finger, 209, 305
gluconate, 269, 486
homeostasis, 357, 509, 512, 523
in cells, 508, 509
levels in cancer, 513–515
signalling, 507–523
transport, 508–513, 515–523
Zinquin, 521
ZIP family transporters, 508–513, 515–523